Jens Wittenburg

Kinematics

Theory and Applications

Springer

Kinematics

Jens Wittenburg

Kinematics

Theory and Applications

Springer

Jens Wittenburg
Institut für Technische Mechanik
Karlsruhe Institute of Technology (KIT)
Karlsruhe, Germany

ISBN 978-3-662-48486-9 ISBN 978-3-662-48487-6 (eBook)
DOI 10.1007/978-3-662-48487-6

Library of Congress Control Number: 2015951089

Springer Heidelberg New York Dordrecht London

Printed on acid-free paper

Springer-Verlag GmbH Berlin Heidelberg is part of Springer Science+Business Media (www.springer.com)

For Rosemarie

Preface

This book is devoted to the kinematics of the single rigid body and of systems of inter-connected rigid bodies. Engineers are confronted with an endless variety of systems ranging from simple planar mechanisms to robots, walking machines, prothetic devices, vehicles, stewart platforms, shaft couplings, gears etc. Subjects of kinematics are relationships between two and more positions, finite and infinitesimal displacements and continuous motions.

The book is intended for use as textbook in advanced courses on kinematics of mechanisms. It focuses on a solid theoretical foundation and on mathematical methods applicable to the solution of problems of very diverse nature. Applications are demonstrated in a large number of fully worked-out problems. In kinematics a wide variety of mathematical tools is applicable. The most important tools are vectors, tensors, matrices, complex numbers, quaternions, dual numbers, dual vectors, dual quaternions and elements of line geometry. Whereever possible vector equations are formulated instead of lengthy scalar coordinate equations. The principle of transference is applied to problems of very diverse nature.

The book has 19 chapters. Chapters 1 – 13, 16 and 18 are devoted to spatial kinematics and Chapts. 14, 15 and 17 to planar kinematics. In Chapt. 19 nonlinear dynamics equations of motion are formulated for general spatial mechanisms. Nearly one half of the book is dealing with position theory and the other half with motion.

Chapter 1 on *Finite rotation about a fixed point* introduces the direction cosine matrix, the similarity transformation, Euler and Bryan angles, Euler-Rodrigues parameters, quaternions, Cayley-Klein parameters, Rodrigues-, Euler- and Wiener vectors.

Subjects of Chapt. 2 on *Line geometry* are Plücker vectors with applications to the line of intersection of two planes, to lines intersecting four given lines, to the linear complex, to linear congruences and to ruled surfaces.

Chapter 3 on *Finite screw displacement* introduces the (4×4) transformation matrix for general rigid-body displacements, Chasles' and Halphen's

theorems and the screw triangle. Dual numbers and dual vectors lead to the principle of transference. This principle is applied to the composition and decomposition of finite and infinitesimal screw displacements and to determining the manifold of screw displacements effecting a prescribed line displacement.

In Chapt. 4 entitled *Degree of freedom of a mechanism* Grüblers formula is developed and illustrated by applications to various spatial mechanisms with or without overconstraint.

Chapter 5 is devoted to *Spatial closed kinematic chains* with a single independent and with six dependent joint variables. Such chains are basic elements of single-degree-of-freedom mechanisms. Efficient methods are developed for expressing the dependent variables in terms of the independent variable and of constant Denavit-Hartenberg parameters. As closure conditions Woernle-Lee equations and Lee's half-angle equations are formulated. For products of vectors in these equations a novel technique is developed. It is applied to ten mechanisms ranging from the RCCC mechanism with nine to the general 7R mechanism with twenty-one parameters. The final section is devoted to the inverse kinematics of serial 6-d.o.f. robots.

Chapter 6 entitled *Overconstrained mechanisms* starts with Bricard's theorem on single-loop-mechanisms with revolute joints. The technique developed in Chapt. 5 is applied to Bennett's 4R-mechanism, Goldberg's 5R-mechanism, to Bricard's 6R-mechanisms known as line-symmetric, plane-symmetric and trihedral mechanisms and to Dietmaier's 6R-mechanism. In addition, Steffen's mobile polyhedra, the Bricard-Borel mechanism, Bricard's hyperbolic mechanism, a cam mechanism and the HEUREKA octahedron are analyzed.

Chapter 7 is devoted to the position theory for the terminal body of spatial three-body chains with two revolute, prismatic or cylindrical joints.

Subject of Chapt. 8 is the direct kinematics of the *Stewart platform* of general geometry. Coordinate-free vector equations are formulated for the dual quaternion specifying the position of a platform The same problem is solved by elementary means for a Stuart platform with triangular geometry.

Chapter 9 entitled *Angular velocity, angular acceleration* is the first chapter devoted not to position theory, but to continuous motion. Key words are instantaneous screw axis, velocity screw, velocity and acceleration distribution in a rigid body, angular velocity of a body expressed in terms of positions and velocities of three points, novel formulas for striction point and distribution parameter of raccording axodes, strapdown inertial navigation, motion on curved surfaces, mecanum wheel.

In Chapt. 10 *Kinematic differential equations* are developed relating angular velocity to the time derivatives of direction cosines, Euler- and Bryan angles, Euler-Rodrigues parameters, Cayley-Klein parameters, Rodrigues parameters, Wiener parameters and the Euler vector.

Chapter 11 is devoted to *Kinematics of tree-structured systems* with joints of arbitrary nature. Positions, velocities and accelerations of bodies are expressed as functions of generalized joint variables and of their time derivatives. The structure of the tree is described by its path matrix with elements $+1$, -1 and zero.

Chapter 12 on *Screw systems* begins with the resultant of two general velocity screws, with the raccording hyperboloids of revolution associated with the relative motion of two bodies rotating about skew axes and with the analogy between force screw and velocity screw. The principle of virtual power leads to the concept of reciprocal screws. Screw systems reciprocal to first-order, second-order and third-order screw systems are investigated.

Chapter 13 on *Shaft couplings* starts with an analysis of Hooke's joint including the polhode and herpolhode cones of its cross-shaped central body. From the principle of transference results are obtained for a joint coupling skew axes. A simple formula is developed for the transmission ratio of a chain of series-connected Hooke's joints. Final sections are devoted to three classes of homokinetic shaft couplings and to an elementary analysis of the tripod joint.

In Chapt. 14 on *Displacements in a plane* complex numbers are used for describing translation, rotation about a point and reflection in a line and resultants of these three elementary displacements. Relationships between three and between four positions of a plane including Burmester's pole curve are studied. The last section is devoted to Heesch's work on tilings.

In Chapt. 15 on *Plane motion* the first part is devoted to centrodes and to the theorems of Burmester and Kennedy/Aronhold with a series of illustrative examples. Instantaneous centers of rotation and of acceleration, Bresse circles and normal poles are expressed in complex form. Curvature theory of plane trajectories leads to the Euler-Savary equation, the cubic of stationary curvature and to Ball's point. A short section on Holditch's theorem with applications is followed by the theory of trochoids in general and of cycloids in particular. An application of cycloids is demonstrated by the analysis of optimal dwell mechanisms. The final section is devoted to the problem of maneuvering a rectangle of maximum size in the space between two nonorthogonal straight lines and a point.

In Chapt. 16 entitled *Theory of gearing* the first part on gears with parallel axes has the key words analytical meshing conditions for calculating the tooth flank conjugate to a given flank, external and internal pin gears, curvature relationship for meshing tooth flanks, Camus' theorem, cycloidal gears, involute gearing, addendum modification, helicoidal gears. Subject of the final section is Giovanozzi's theory of general spatial involute gearing.

Chapter 17 on the *Planar four-bar* begins with sections on Grashof's condition, the transfer function relating input and output angles, classical and new formulas for stationary values of the transmission ratio, on four-bars for the transmission of forces (shears, prongs etc.) and on coupler curves

(Roberts-Tschebychev theorem, double points, cusps, symmetrical coupler curves). Two sections are devoted to applications of four-bars in planar robots and in Jeantaud's steering mechanism. For the former a simple position and velocity analysis is formulated. Final sections are devoted to Tschebychev's optimal straight-line approximations by coupler curves, to Peaucellier's inversor generating an exact straight line, to Burmester's four-position theory and to the trajectory of the composite system center of mass of a four-bar.

Chapter 18 on the *Spherical four-bar* has sections on the transfer function, on conditions analogous to Grashof's condition for the planar four-bar and on coupler curves (symmetry conditions, double points, cusps, number of points of intersection with a circle, stereographic projection). The chapter ends with the investigation of a spherical parallel robot.

In Chapt. 19 entitled *Dynamics of mechanisms* nonlinear differential equations of motion for spatial mechanisms are developed from the principle of virtual power. Equations for tree-structured systems are based on the kinematics formulation in Chapt. 11 . Equations for mechanisms with closed kinematic chains are obtained by incorporating additional kinematical constraint equations.

The author expresses his gratefulness to the following colleagues, research assistants and students who supported the development of this manuscript: Prof. Ljubomir Lilov / Kliment-Ochridsky Univ. Sofia (for his critical reading of parts of the manuscript and for contributing Eq.(1.181) and Sect. 9.10), Günther Stelzner (for fruitful discussions and contributions to Sect. 15.6), Andrey Shutovich (for contributing ideas to Chapt. 18 and for his critical reading of Chapt. 8) and Xu Tongsheng, Benjamin Rutschke, Andreas Funkhänel and Simon Fritz (for converting pencil-on-paper figures into data files). Last, but not least, I thank the Springer team for technical advice and for the patience in waiting for completion of the manuscript

Karlsruhe,
August 2015 *Jens Wittenburg*

Notation

Vectors are printed boldface: $\mathbf{r}$, $\boldsymbol{\omega}$.

Tensors are printed serif: Unit tensor I , dyad $\mathsf{D} = \mathbf{rr}$, inertia tensor $\mathsf{J} = \int_m (\mathbf{r}^2\mathsf{I} - \mathbf{rr})\,\mathrm{d}m$.

Products: $\boldsymbol{\omega}\cdot\mathbf{r}$, $\boldsymbol{\omega}\times\mathbf{r}$, $\mathsf{J}\cdot\boldsymbol{\omega}$.

Formulas: $\mathsf{I}\cdot\boldsymbol{\omega} \equiv \boldsymbol{\omega}$, $(\mathbf{n}\times\mathbf{r})\times\mathbf{n} = \mathbf{r} - \mathbf{nn}\cdot\mathbf{r} = (\mathsf{I} - \mathbf{nn})\cdot\mathbf{r}$ (unit vector $\mathbf{n}$) ,
$\int_m \mathbf{r}\times(\boldsymbol{\omega}\times\mathbf{r})\,\mathrm{d}m = \int_m (\mathbf{r}^2\mathsf{I} - \mathbf{rr})\,\mathrm{d}m\cdot\boldsymbol{\omega} = \mathsf{J}\cdot\boldsymbol{\omega}$ (angular momentum) ,
$\int_m (\boldsymbol{\omega}\times\mathbf{r})^2\,\mathrm{d}m = \boldsymbol{\omega}\cdot\int_m (\mathbf{r}^2\mathsf{I} - \mathbf{rr})\,\mathrm{d}m\cdot\boldsymbol{\omega} = \boldsymbol{\omega}\cdot\mathsf{J}\cdot\boldsymbol{\omega}$ (kinetic energy) ,
$\dot{\boldsymbol{\omega}}\times\mathbf{r} + \boldsymbol{\omega}\times(\boldsymbol{\omega}\times\mathbf{r}) = \dot{\boldsymbol{\omega}}\times\mathbf{r} + \boldsymbol{\omega}\,\boldsymbol{\omega}\cdot\mathbf{r} - \boldsymbol{\omega}^2\mathbf{r} = (\dot{\boldsymbol{\omega}}\times\mathsf{I} + \boldsymbol{\omega}\,\boldsymbol{\omega} - \boldsymbol{\omega}^2\,\mathsf{I})\cdot\mathbf{r}$ (acceleration) .

Matrices are underscored: $\underline{A}$, unit matrix $\underline{I}$. The transpose of $\underline{A}$ is $\underline{A}^T$.

A right-handed cartesian basis with unit basis vectors $\mathbf{e}_1, \mathbf{e}_2, \mathbf{e}_3$ is called basis $\underline{\mathbf{e}}$. This symbol $\underline{\mathbf{e}}$ denotes also the column matrix $[\,\mathbf{e}_1\ \mathbf{e}_2\ \mathbf{e}_3\,]^T$ of the three unit vectors.

The equation $\mathbf{r} = r_1\mathbf{e}_1 + r_2\mathbf{e}_2 + r_3\mathbf{e}_3$ defines the coordinates r_1 , r_2 , r_3 of a vector $\mathbf{r}$ in basis $\underline{\mathbf{e}}$ and the column matrix $\underline{r} = [\,r_1\ r_2\ r_3\,]^T$ of these coordinates. This matrix is not the vector since it is different in different bases. The relationship between vector and coordinate matrix is $\mathbf{r} = \underline{\mathbf{e}}^T\underline{r} = \underline{r}^T\underline{\mathbf{e}}$.

The coordinates $\omega_1, \omega_2, \omega_3$ of a vector $\boldsymbol{\omega}$ define the skew-symmetric matrix $\underline{\tilde{\omega}} = \begin{bmatrix} 0 & -\omega_3 & \omega_2 \\ \omega_3 & 0 & -\omega_1 \\ -\omega_2 & \omega_1 & 0 \end{bmatrix}$. If $\underline{r}$ is the column matrix of the coordinates of another vector $\mathbf{r}$ in the same reference basis, $\underline{\tilde{\omega}}\,\underline{r}$ is the column matrix of the coordinates of $\boldsymbol{\omega}\times\mathbf{r}$. Also $\underline{\tilde{\omega}}\,\underline{r} = -\underline{\tilde{r}}\,\underline{\omega}$.

Right-handed cartesian bases fixed on bodies $i = 0, 1, 2, \ldots$ are denoted $\underline{\mathbf{e}}^0$, $\underline{\mathbf{e}}^1$, $\underline{\mathbf{e}}^2$ etc. The coordinates of a vector $\mathbf{r}$ in basis $\underline{\mathbf{e}}^k$ are denoted r_1^k, r_2^k, r_3^k , and the column matrix of these coordinates is denoted $\underline{r}^k$. Whether r_1^2 is the square of some scalar r_1 or the first component of a vector $\mathbf{r}$ in basis $\underline{\mathbf{e}}^2$ is seen from the context.

Matrices with vectors as elements are boldface underscored: Basis $\underline{\mathbf{e}} = [\,\mathbf{e}_1\ \mathbf{e}_2\ \mathbf{e}_3\,]^T$, column matrix $\underline{\boldsymbol{\omega}} = [\,\boldsymbol{\omega}_1\ \ldots\boldsymbol{\omega}_n\,]^T$ of vectors $\boldsymbol{\omega}_1, \ldots, \boldsymbol{\omega}_n$.

Matrices with tensors as elements are serif underscored: Diagonal matrix $\underline{\mathsf{J}}$ of inertia tensors $\mathsf{J}_1 \ldots \mathsf{J}_n$.

The rule of ordinary matrix multiplication $(\underline{A}\,\underline{B})_{ij} = \sum_k A_{ik}B_{kj}$ is generalized for matrices with vectors and tensors as elements. Examples:
1. $\mathbf{r} = \underline{\mathbf{e}}^T\underline{r}$; 2. $\underline{\mathbf{e}}\cdot\underline{\mathbf{e}}^T = \underline{I}$; 3. $\underline{\mathbf{e}}^1\cdot\underline{\mathbf{e}}^{2\,T} = \left[\,\mathbf{e}_i^1\cdot\mathbf{e}_j^2\,\right]$ (direction cosine matrix) ; 4. $\mathbf{r}\cdot\underline{\mathbf{e}}\times\underline{\mathbf{e}}^T = \begin{bmatrix} 0 & r_3 & -r_2 \\ -r_3 & 0 & r_1 \\ r_2 & -r_1 & 0 \end{bmatrix} = -\underline{\tilde{r}}$; 5. $\underline{\mathsf{J}}\cdot\underline{\boldsymbol{\omega}} = [\,\mathsf{J}_1\cdot\boldsymbol{\omega}_1\ \ldots\ \mathsf{J}_n\cdot\boldsymbol{\omega}_n\,]^T$ (diagonal matrix $\underline{\mathsf{J}}$ of inertia tensors, column matrix $\underline{\boldsymbol{\omega}}$) .

Contents

Chapter 1
Rotation about a Fixed Point. Reflection in a Plane

Subject of this chapter are relationships between two positions of a rigid body with a fixed point. Note: Motions leading from one position to the other are not investigated. Consequently, terms such as velocity or angular velocity do not occur.
Literature: Rodrigues [25], Schoenflies [28], Klein/Müller [11], Meyer/ Mohrmann [17], Mises [19], Kuipers [14], Mayer [16], Murnaghan [23], Müller [20, 21, 22], Rooney [26], Altmann [1], Geradin/Park/Cardona [7], Angeles [2], Shuster [29], Kolve [13], Bronstein/Semendjajev/Musiol/Mühlig [5].

For describing positions two right-handed cartesian bases are defined. The origins of both bases coincide with the fixed point of the body. The basis with unit basis vectors $\mathbf{e}_i^1$ $(i = 1, 2, 3)$ serves as reference basis. The other basis with unit basis vectors $\mathbf{e}_i^2$ $(i = 1, 2, 3)$ is fixed on the body. It represents the body. The bases are denoted $\underline{\mathbf{e}}^1$ and $\underline{\mathbf{e}}^2$, respectively. The unit basis vectors of any right-handed cartesian basis $\underline{\mathbf{e}}$ satisfy the six orthonormality conditions

$$\mathbf{e}_i \cdot \mathbf{e}_j = \delta_{ij} \qquad (i, j = 1, 2, 3) \tag{1.1}$$

as well as the right-handedness condition

$$\mathbf{e}_1 \cdot \mathbf{e}_2 \times \mathbf{e}_3 = +1 \; . \tag{1.2}$$

The positions between which relationships are to be established are the so-called initial position in which $\underline{\mathbf{e}}^2$ coincides with $\underline{\mathbf{e}}^1$ and an arbitrary final position.

1.1 Direction Cosine Matrix

The unit basis vectors $\mathbf{e}_i^1$ and $\mathbf{e}_j^2$ $(i, j = 1, 2, 3)$ of the two bases define the altogether nine *direction cosines* $\mathbf{e}_i^1 \cdot \mathbf{e}_j^2 = \cos \sphericalangle (\mathbf{e}_i^1, \mathbf{e}_j^2)$ $(i, j = 1, 2, 3)$. They

J. Wittenburg, *Kinematics*, DOI 10.1007/978-3-662-48487-6_1

are abbreviated

$$a_{ij}^{12} = a_{ji}^{21} = \mathbf{e}_i^1 \cdot \mathbf{e}_j^2 \qquad (i,j = 1,2,3)\ . \tag{1.3}$$

These direction cosines are the coordinates of $\mathbf{e}_i^1$ $(i = 1,2,3)$ in $\underline{\mathbf{e}}^2$ as well as the coordinates of $\mathbf{e}_j^2$ $(j = 1,2,3)$ in $\underline{\mathbf{e}}^1$. Definition: The (3×3) *direction cosine matrix* $\underline{A}^{12}$ has in row i the coordinates of $\mathbf{e}_i^1$ $(i = 1,2,3)$ in $\underline{\mathbf{e}}^2$ and, consequently, in column j the coordinates of $\mathbf{e}_j^2$ $(j = 1,2,3)$ in $\underline{\mathbf{e}}^1$. The three equations

$$\mathbf{e}_i^1 = \sum_{j=1}^{3} a_{ij}^{12} \mathbf{e}_j^2 \qquad (i = 1,2,3) \tag{1.4}$$

are combined in matrix form in the equation

$$\underline{\mathbf{e}}^1 = \underline{A}^{12} \underline{\mathbf{e}}^2\ . \tag{1.5}$$

The symbols $\underline{\mathbf{e}}^1$ and $\underline{\mathbf{e}}^2$, until now simply the names of bases, denote the column matrices of the unit basis vectors: $\underline{\mathbf{e}}^1 = [\,\mathbf{e}_1^1\ \mathbf{e}_2^1\ \mathbf{e}_3^1\,]^T$, $\underline{\mathbf{e}}^2 = [\,\mathbf{e}_1^2\ \mathbf{e}_2^2\ \mathbf{e}_3^2\,]^T$. The exponent ^{T} denotes transposition. The use of boldface letters indicates that the elements of $\underline{\mathbf{e}}^1$ and $\underline{\mathbf{e}}^2$ are vectors. The matrix product $\underline{A}^{12}\underline{\mathbf{e}}^2$ is evaluated following the rule of ordinary matrix algebra, although one of the matrices has vectors as elements and the other scalars. For two matrices each having vectors as elements both the inner product (dot product) and the outer product (cross product) exist. Example: Scalar multiplication of (1.5) from the right by $\underline{\mathbf{e}}^{2^T}$ produces for the direction cosine matrix the explicit expression

$$\underline{A}^{12} = \underline{\mathbf{e}}^1 \cdot \underline{\mathbf{e}}^{2^T}\ . \tag{1.6}$$

This equation is the matrix form of the nine Eqs.(1.3).

The direction cosine matrix is the first mathematical quantity used for specifying the relationship between two positions. Other quantities are introduced later. In what follows, properties of the matrix are discussed. Since each row contains the coordinates of one of the unit basis vectors of $\underline{\mathbf{e}}^1$, the determinant of the matrix is the scalar triple product $\mathbf{e}_1^1 \cdot \mathbf{e}_2^1 \times \mathbf{e}_3^1$. According to (1.2) this equals $+1$. Hence

$$\det \underline{A}^{12} = +1\ . \tag{1.7}$$

The six orthonormality conditions (1.1) express the fact that the scalar product of any two rows i and j and also of any two columns i and j of $\underline{A}^{12}$ equals the Kronecker delta:

$$\sum_{k=1}^{3} a_{ik}^{12} a_{jk}^{12} = \delta_{ij}\ , \qquad \sum_{k=1}^{3} a_{ki}^{12} a_{kj}^{12} = \delta_{ij} \qquad (i,j = 1,2,3). \tag{1.8}$$

A matrix having these properties is called orthogonal matrix. Because of (1.8) the product $\underline{A}^{12}\underline{A}^{12^T}$ equals the unit matrix. Hence the matrix has the important property that its inverse equals its transpose:

$$(\underline{A}^{12})^{-1} = \underline{A}^{12^T} . \tag{1.9}$$

Definition: The *co-factor* of the element a_{ij}^{12} is $(-1)^{i+j}$ times the determinant of the (2×2)-submatrix of $\underline{A}^{12}$ left after deleting row i and column j. Because of the orthogonality of the matrix every element equals it own co-factor[1]. Omitting the upper indices ^{12} these identities can be written in the forms

$$\left.\begin{aligned} a_{ii} &= a_{jj}a_{kk} - a_{jk}a_{kj} ,\\ a_{jk} &= a_{ij}a_{ki} - a_{ii}a_{kj} ,\\ a_{kj} &= a_{ji}a_{ik} - a_{ii}a_{jk} \end{aligned}\right\} \quad (i,j,k = 1,2,3 \text{ cyclic}) . \tag{1.10}$$

With (1.9) the inverse of (1.5) is

$$\underline{\mathbf{e}}^2 = \underline{A}^{21}\underline{\mathbf{e}}^1 \quad \text{with} \quad \underline{A}^{21} = \underline{A}^{12^T} . \tag{1.11}$$

Let now $\mathbf{v}$ be an arbitrary vector (not necessarily the position vector of a point). In the bases $\underline{\mathbf{e}}^1$ and $\underline{\mathbf{e}}^2$ it has different coordinates v_i^1 and v_i^2, respectively $(i = 1,2,3)$:

$$\mathbf{v} = \sum_{i=1}^{3} v_i^1\mathbf{e}_i^1 = \sum_{i=1}^{3} v_i^2\mathbf{e}_i^2 . \tag{1.12}$$

The sums are written as matrix products. For this purpose the column matrices $\underline{v}^1 = [\, v_1^1\, v_2^1\, v_3^1\,]^T$ and $\underline{v}^2 = [\, v_1^2\, v_2^2\, v_3^2\,]^T$ of the coordinates of $\mathbf{v}$ in the two bases are defined. They are called coordinate matrices of $\mathbf{v}$ in $\underline{\mathbf{e}}^1$ and in $\underline{\mathbf{e}}^2$, respectively. It should be noted that the term *vector* is used for $\mathbf{v}$ and not as abbreviation for coordinate matrix. We also distinguish between the coordinate v_i and the component $v_i\mathbf{e}_i$ of a vector. A component is itself a vector, whereas a coordinate is a scalar.

In terms of coordinate matrices (1.12) has the form

$$\underline{\mathbf{e}}^{1^T}\underline{v}^1 = \underline{\mathbf{e}}^{2^T}\underline{v}^2 . \tag{1.13}$$

From (1.11) it follows that $\underline{\mathbf{e}}^{2^T} = \underline{\mathbf{e}}^{1^T}\underline{A}^{12}$. Substitution of this expression produces the equation $\underline{\mathbf{e}}^{1^T}\underline{v}^1 = \underline{\mathbf{e}}^{1^T}\underline{A}^{12}\underline{v}^2$ and, consequently,

$$\underline{v}^1 = \underline{A}^{12}\underline{v}^2 . \tag{1.14}$$

[1] Special case of the general formula $(\underline{A}^{-1})_{ij} = c_{ji}/\det\underline{A}$ valid for an arbitrary $(n\times n)$-matrix $\underline{A}$ (c_{ji} co-factor of the matrix element a_{ji})

More directly, this equation follows from the fact that the components of $\mathbf{v}$ are linear combinations of unit basis vectors. The equation is the rule by which vector coordinates are transformed from one basis into another. Because of this equation the direction cosine matrix is also called transformation matrix. The absolute value of a vector does not change under a transformation. Indeed, with both sets of coordinates the scalar product $\mathbf{v} \cdot \mathbf{v}$ is the same: $\underline{v}^{1\,T}\underline{v}^1 = \underline{v}^{2\,T}\underline{A}^{12\,T}\underline{A}^{12}\underline{v}^2 = \underline{v}^{2\,T}\underline{v}^2$.

Example: Let $\mathbf{r}$ and $\mathbf{r}^*$ be the position vectors of an arbitrary *body-fixed* point in the initial position and in the final position of basis $\underline{\mathbf{e}}^2$, respectively. The coordinate matrices $\underline{r}^{*1}$ in $\underline{\mathbf{e}}^1$ and $\underline{r}^{*2}$ in $\underline{\mathbf{e}}^2$ satisfy the equation $\underline{r}^{*1} = \underline{A}^{12}\underline{r}^{*2}$. However, since $\mathbf{r}^*$ coincides with $\mathbf{r}$, when $\underline{\mathbf{e}}^2$ coincides with $\underline{\mathbf{e}}^1$, also the identity $\underline{r}^1 = \underline{r}^{*2}$ is true. From this it follows that the coordinates of $\mathbf{r}^*$ and $\mathbf{r}$ in $\underline{\mathbf{e}}^1$ are related through the equation

$$\underline{r}^{*1} = \underline{A}^{12}\underline{r}^1 \ . \tag{1.15}$$

End of example.

Imagine in addition to the bases $\underline{\mathbf{e}}^1$ and $\underline{\mathbf{e}}^2$ a third basis $\underline{\mathbf{e}}^3$, i.e., a third position of the rigid body. Then three direction cosine matrices are defined by the equations

$$\underline{\mathbf{e}}^1 = \underline{A}^{13}\underline{\mathbf{e}}^3 \ , \qquad \underline{\mathbf{e}}^1 = \underline{A}^{12}\underline{\mathbf{e}}^2 \ , \qquad \underline{\mathbf{e}}^2 = \underline{A}^{23}\underline{\mathbf{e}}^3 \ . \tag{1.16}$$

The matrices are not independent. The last two equations establish the relationship $\underline{\mathbf{e}}^1 = \underline{A}^{12}\underline{A}^{23}\underline{\mathbf{e}}^3$. Comparison with the first equation yields

$$\underline{A}^{13} = \underline{A}^{12}\underline{A}^{23} \ . \tag{1.17}$$

This equation shows that orthogonal matrices constitute a group with respect to multiplication. They satisfy the four conditions: 1) The product of any two elements of the group is itself an element ($\underline{A}^{13}$ is an orthogonal matrix). 2) The product is associative. 3) There is a unit element, namely, the unit matrix. 4) For every element of the group the inverse element exists, namely, the transposed matrix. The group is denoted SO(3) with O for orthogonal.

Next, the eigenvalue problem $\underline{A}^{12}\underline{v} = \lambda\underline{v}$ or $(\underline{A}^{12} - \lambda\underline{I})\underline{v} = \underline{0}$ is investigated where $\underline{A}^{12}$ is an arbitrary direction cosine matrix. The equation is the transformation rule $\underline{A}^{12}\underline{v}^2 = \underline{v}^1$ in the special case $\underline{v}^1 = \lambda\underline{v}^2$. Since the absolute value of a vector does not change under a transformation, it can be predicted that all three eigenvalues have the absolute value one. The eigenvalues are the roots of the characteristic equation $\det(\underline{A}^{12} - \lambda\underline{I}) = 0$. Without the superscript of $\underline{A}^{12}$ this is the cubic equation

$$\begin{aligned} -\lambda^3 + \lambda^2 \operatorname{tr}\underline{A} - \lambda[(a_{11}a_{22} - a_{12}a_{21}) + (a_{22}a_{33} - a_{23}a_{32}) \\ +(a_{33}a_{11} - a_{31}a_{13})] + \det\underline{A} = 0 \ . \end{aligned} \tag{1.18}$$

According to (1.7) the free term is $+1$. Every expression in parentheses is the co-factor of one diagonal element of $\underline{A}^{12}$. According to the first Eq.(1.10) the co-factor is identical with the diagonal element. Consequently, the expression in square brackets represents the trace of the matrix. Thus, the equation reads

$$-\lambda^3 + \lambda^2 \operatorname{tr} \underline{A}^{12} - \lambda \operatorname{tr} \underline{A}^{12} + 1 = 0 \,. \tag{1.19}$$

It shows that every direction cosine matrix has the eigenvalue $\lambda = +1$. Division by $(\lambda - 1)$ produces for the other eigenvalues the quadratic equation $\lambda^2 - (\operatorname{tr} \underline{A}^{12} - 1)\lambda + 1 = 0$. It has the roots

$$\begin{aligned} \lambda_{2,3} &= \frac{\operatorname{tr} \underline{A}^{12} - 1}{2} \pm \mathrm{i} \sqrt{1 - \Big(\frac{\operatorname{tr} \underline{A}^{12} - 1}{2}\Big)^2} \\ &= \cos\varphi \pm \mathrm{i} \, \sin\varphi = \mathrm{e}^{\pm \mathrm{i}\,\varphi} \end{aligned} \tag{1.20}$$

with

$$\cos\varphi = \frac{\operatorname{tr} \underline{A}^{12} - 1}{2} \,. \tag{1.21}$$

If $\underline{A}^{12}$ is the unit matrix, it has the triple eigenvalue $+1$. In the case $\operatorname{tr} \underline{A}^{12} = -1$ it has the double eigenvalue $\lambda_{2,3} = -1$.

Let $\underline{n}$ be the normalized eigenvector associated with the eigenvalue $\lambda = +1$. It is calculated from the equations

$$(\underline{A}^{12} - \underline{I})\underline{n} = \underline{0} \,, \qquad n_1^2 + n_2^2 + n_3^2 = 1 \,. \tag{1.22}$$

This eigenvector $\underline{n}$ represents the coordinate matrix of a unit vector $\mathbf{n}$ which has identical coordinate matrices in the bases $\underline{\mathbf{e}}^1$ and $\underline{\mathbf{e}}^2$. Also this vector $\mathbf{n}$ is called eigenvector of $\underline{A}^{12}$.

Imagine that, starting from the initial position, the body-fixed basis $\underline{\mathbf{e}}^2$ is rotated about the eigenvector $\mathbf{n}$. The final position depends upon the rotation angle. Independent of the angle the vector $\mathbf{n}$ has identical coordinate matrices $\underline{n}^1 = \underline{n}^2 = \underline{n}$ in $\underline{\mathbf{e}}^1$ and in $\underline{\mathbf{e}}^2$. The existence of the eigenvector guarantees the existence of an angle which carries the basis from its initial position to the final position given by the matrix $\underline{A}^{12}$. Hence the

Theorem 1.1. (Euler) *The displacement of a body-fixed basis from an initial position* $\underline{\mathbf{e}}^1$ *to an arbitrary final position* $\underline{\mathbf{e}}^2$ *is achieved by a rotation through a certain angle about an axis which is fixed in both bases. The axis has the direction of the eigenvector associated with the eigenvalue* $\lambda = +1$ *of the direction cosine matrix* $\underline{A}^{12}$.

In Sect. 1.5 it is shown that the rotation angle in Euler's theorem is the angle φ in Eq.(1.20) for the eigenvalues λ_2 and λ_3. Euler's theorem guarantees that the direction cosine matrix $\underline{A}^{12}$ can be expressed in terms of the coordinates of its eigenvector $\mathbf{n}$ and of the rotation angle φ. This is the subject of Sect. 1.5.

The complex conjugate eigenvectors associated with the eigenvalues $\cos\varphi \pm$ i $\sin\varphi$ are determined at the end of Sect. 1.5 .

1.2 Similarity Transformation

Let $\underline{A}$ and $\underline{B}$ be arbitrary $(n \times n)$-matrices, $\underline{A}$ nonsingular. The transformation of $\underline{B}$ into the matrix

$$\underline{B}^* = \underline{A}\,\underline{B}\,\underline{A}^{-1} \tag{1.23}$$

is called similarity transformation of $\underline{B}$.

Theorem 1.2. *The matrices* $\underline{B}$ *and* $\underline{A}\,\underline{B}\,\underline{A}^{-1}$ *have identical characteristic polynomials and, therefore, identical eigenvalues and identical traces.*

Proof: The characteristic polynomial of $\underline{A}\,\underline{B}\,\underline{A}^{-1}$ is $\det(\underline{A}\,\underline{B}\,\underline{A}^{-1} - \lambda\underline{I}) = \det(\underline{A}\,\underline{B}\,\underline{A}^{-1} - \underline{A}\,\lambda\underline{I}\,\underline{A}^{-1}) = \det[\underline{A}\,(\underline{B} - \lambda\underline{I})\underline{A}^{-1}] = \det(\underline{B} - \lambda\underline{I}) = 0$ (the determinant of a product of matrices equals the product of the determinants of the factors). Since the trace is the sum of all eigenvalues, also the traces are identical. End of proof.

Theorem 1.3. *Let* $\underline{n}$ *and* $\underline{n}_B$ *be the eigenvectors of* $\underline{A}\,\underline{B}\,\underline{A}^{-1}$ *and of* $\underline{B}$, *respectively, associated with one and the same eigenvalue* λ *(arbitrary). They are related by the equation*

$$\underline{n} = \underline{A}\,\underline{n}_B\,. \tag{1.24}$$

Proof: By definition, $\underline{A}\,\underline{B}\,\underline{A}^{-1}\,\underline{n} = \lambda\underline{n}$ and $\underline{B}\,\underline{n}_\mathrm{B} = \lambda\underline{n}_\mathrm{B}$. With (1.24) the first equation is $\underline{A}\,\underline{B}\,\underline{A}^{-1}\underline{A}\,\underline{n}_\mathrm{B} = \lambda\underline{A}\,\underline{n}_\mathrm{B}$ or $\underline{B}\,\underline{n}_\mathrm{B} = \lambda\underline{n}_\mathrm{B}$. This is the second equation. End of proof.

Example: Let $\underline{A}^{12}$ be the direction cosine matrix relating the coordinates of vectors in two bases $\mathbf{e}^1$ and $\mathbf{e}^2$. Let, in particular, $\underline{a}^1$, $\underline{a}^2$ and $\underline{b}^1$, $\underline{b}^2$ be the coordinate matrices of two vectors $\mathbf{a}$ and $\mathbf{b}$, respectively, so that, for example, $\underline{b}^1 = \underline{A}^{12}\underline{b}^2$. The cross-product $\mathbf{a} \times \mathbf{b}$ has in the two bases the coordinate matrices $\tilde{\underline{a}}^1\underline{b}^1$ and $\tilde{\underline{a}}^2\underline{b}^2$ with the skew-symmetric matrices $\tilde{\underline{a}}^i = \begin{bmatrix} 0 & -a_3^i & a_2^i \\ a_3^i & 0 & -a_1^i \\ -a_2^i & a_1^i & 0 \end{bmatrix}$ $(i = 1, 2)$. Hence $\tilde{\underline{a}}^1\,\underline{b}^1 = \underline{A}^{12}\,\tilde{\underline{a}}^2\,\underline{b}^2$. On the right-hand side $\underline{b}^2 = \underline{A}^{12^T}\underline{b}^1$ is substituted. This results in the transformation formula

$$\tilde{\underline{a}}^1 = \underline{A}^{12}\,\tilde{\underline{a}}^2\,\underline{A}^{12^T}\,. \tag{1.25}$$

It is a similarity transformation. End of example.

1.3 Euler Angles

Calculations with nine direction cosines subject to six constraint equations are cumbersome. In the present section and in following sections the elements of the direction cosine matrix are formulated in various ways in terms of either three coordinates without constraint equations or in terms of four coordinates with one constraint equation. In the present section so-called Euler angles are introduced. The final position $\underline{\mathbf{e}}^2$ of the body-fixed basis is the result of three successive rotations (Fig. 1.1a). In the initial position prior to the first rotation the body-fixed basis coincides with $\underline{\mathbf{e}}^1$. The first rotation is carried out through an angle ψ about the axis $\mathbf{e}_3^1$ (in the usual right-handed sense). It carries the body-fixed basis into an intermediate position $\underline{\mathbf{e}}^{2''}$. The second rotation is carried out through an angle θ about the axis $\mathbf{e}_1^{2''}$. It carries the body-fixed basis into a new intermediate position $\underline{\mathbf{e}}^{2'}$. The third rotation is carried out through an angle ϕ about the axis $\mathbf{e}_3^{2'}$. It carries the body-fixed basis into the final position $\underline{\mathbf{e}}^2$. A characteristic feature of Euler angles is that the second and the third rotation are carried out about axes which are the result of the previous rotation (or rotations). Another characteristic feature is the sequence (3,1,3) of rotation axes.

The desired expression for the matrix $\underline{A}^{12}$ in terms of the three angles is obtained from the transformation Eqs.(1.5) for the individual rotations. Figure 1.1a yields the equations

$$\underline{\mathbf{e}}^1 = \underline{A}_\psi \underline{\mathbf{e}}^{2''} , \qquad \underline{\mathbf{e}}^{2''} = \underline{A}_\theta \underline{\mathbf{e}}^{2'} , \qquad \underline{\mathbf{e}}^{2'} = \underline{A}_\phi \underline{\mathbf{e}}^2 \tag{1.26}$$

with

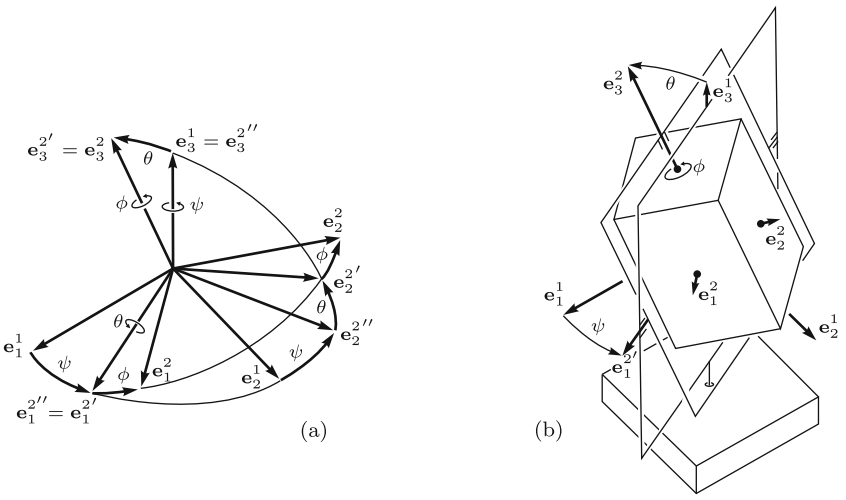

Fig. 1.1 Euler angles. Definition **(a)** and application in a two-gimbal suspension **(b)**

$$\underline{A}_\psi = \begin{bmatrix} \cos\psi & -\sin\psi & 0 \\ \sin\psi & \cos\psi & 0 \\ 0 & 0 & 1 \end{bmatrix}, \quad \underline{A}_\theta = \begin{bmatrix} 1 & 0 & 0 \\ 0 & \cos\theta & -\sin\theta \\ 0 & \sin\theta & \cos\theta \end{bmatrix},$$
$$\underline{A}_\phi = \begin{bmatrix} \cos\phi & -\sin\phi & 0 \\ \sin\phi & \cos\phi & 0 \\ 0 & 0 & 1 \end{bmatrix}. \tag{1.27}$$

From (1.26) it follows that $\underline{A}^{12} = \underline{A}_\psi \underline{A}_\theta \underline{A}_\phi$. When this is multiplied out and use is made of the abbreviations c_ψ, c_θ, c_ϕ for $\cos\psi$, $\cos\theta$, $\cos\phi$ and s_ψ, s_θ, s_ϕ for $\sin\psi$, $\sin\theta$, $\sin\phi$, the matrix is obtained in the form

$$\underline{A}^{12} = \begin{bmatrix} c_\psi c_\phi - s_\psi c_\theta s_\phi & -c_\psi s_\phi - s_\psi c_\theta c_\phi & s_\psi s_\theta \\ s_\psi c_\phi + c_\psi c_\theta s_\phi & -s_\psi s_\phi + c_\psi c_\theta c_\phi & -c_\psi s_\theta \\ s_\theta s_\phi & s_\theta c_\phi & c_\theta \end{bmatrix}. \tag{1.28}$$

The advantage of having only three coordinates and no constraint equation is paid for by the disadvantage that the direction cosines are complicated functions of the three coordinates. There is still another problem. Figure 1.1a shows that in the case $\theta = n\pi$ $(n = 0, \pm 1, \ldots)$ the axis of the third rotation coincides with the axis of the first rotation. This has the consequence that ψ and ϕ cannot be distinguished.

Euler angles can be illustrated by means of a rigid body in a two-gimbal suspension system (Fig. 1.1b). The bases $\underline{\mathbf{e}}^1$ and $\underline{\mathbf{e}}^2$ are attached to the material base and to the suspended body, respectively. The angles ψ, θ and ϕ are, in this order, the rotation angle of the outer gimbal relative to the material base, of the inner gimbal relative to the outer gimbal and of the body relative to the inner gimbal. With this device all three angles can be adjusted independently since the intermediate bases $\underline{\mathbf{e}}^{2''}$ and $\underline{\mathbf{e}}^{2'}$ are materially realized by the gimbals. For $\theta = n\pi$ $(n = 0, 1, \ldots)$ the planes of the gimbals coincide (gimbal lock).

Euler angles are ideally suited as position variables for the study of motions in which $\theta(t)$ is either exactly or approximately constant, whereas ψ and ϕ are (exactly or approximately) proportional to time, i.e., $\dot{\psi} \approx$ const and $\dot{\phi} \approx$ const. Euler angles are advantageous also whenever there exist two physically significant directions, one fixed in the reference basis $\underline{\mathbf{e}}^1$ and the other fixed in the body-fixed basis $\underline{\mathbf{e}}^2$. In such cases, $\mathbf{e}_3^1$ and $\mathbf{e}_3^2$ are given these directions so that θ is the angle between the two (as examples see Eqs.(10.10) and (10.83)). However, the use of Euler angles is not restricted to such special cases.

If the matrix $\underline{A}^{12}$ is given, the corresponding Euler angles are calculated from the equations

$$\left.\begin{array}{lll} \cos\theta = a_{33}^{12}\,, & \sin\theta = \sigma\sqrt{1-\cos^2\theta} & (\sigma = +1 \ \text{ or } \ -1)\,, \\ \cos\psi = -a_{23}^{12}/\sin\theta\,, & \sin\psi = a_{13}^{12}/\sin\theta\,, & \\ \cos\phi = \ \ a_{32}^{12}/\sin\theta\,, & \sin\phi = a_{31}^{12}/\sin\theta\,. & \end{array}\right\} \quad (1.29)$$

Let $(\psi\,,\,\theta\,,\,\phi)$ be the angles associated with $\sigma = +1$. The angles associated with $\sigma = -1$ are $(\pi+\psi\,,\,-\theta\,,\,\pi+\phi)$. Both triples produce one and the same final position of the basis $\underline{\mathbf{e}}^2$. Numerical difficulties arise when θ is close to one of the critical values $n\pi$ $(n = 0, 1, \ldots)$.

1.4 Bryan Angles

These angles are also referred to as Cardan angles. As before, the final position $\underline{\mathbf{e}}^2$ of the body-fixed basis is the result of three successive rotations (Fig. 1.2a). In the initial position prior to the first rotation the body-fixed basis coincides with $\underline{\mathbf{e}}^1$. The first rotation is carried out through an angle ϕ_1 about the axis $\mathbf{e}_1^1$. It carries the body-fixed basis into an intermediate position $\underline{\mathbf{e}}^{2''}$. The second rotation is carried out through an angle ϕ_2 about the axis $\mathbf{e}_2^{2''}$. It carries the body-fixed basis into a new intermediate position $\underline{\mathbf{e}}^{2'}$. The third rotation is carried out through an angle ϕ_3 about the axis $\mathbf{e}_3^{2'}$. It carries the body-fixed basis into the final position $\underline{\mathbf{e}}^2$. A characteristic feature of Bryan angles is the sequence (1,2,3) of rotation axes[2]. The desired expression for the matrix $\underline{A}^{12}$ is, again, the product of three matrices describing the individual rotations. Figure 1.2a shows that

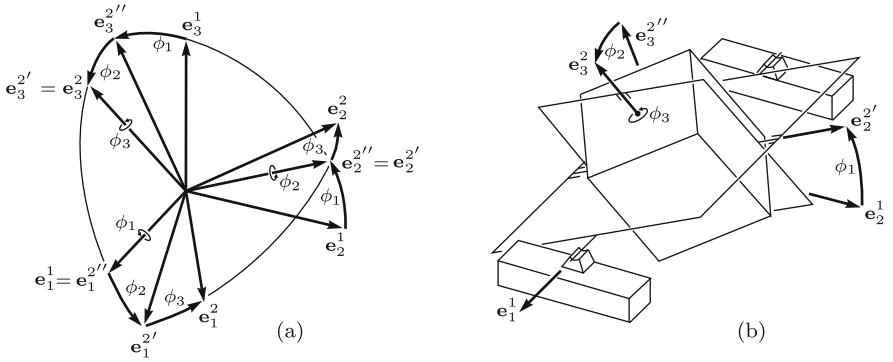

Fig. 1.2 Bryan angles. Definition **(a)** and application in a two-gimbal suspension **(b)**

[2] In contrast to Euler angles each of the three body-fixed basis vectors is axis of one of the three rotations. Other possible sequences of rotation axes for Bryan angles are (3,2,1) and the cyclic permutations (2,3,1), (3,1,2), (2,1,3) and (1,3,2). In Sect. 18.4 the sequence (3,2,1) is used

$$\underline{\mathbf{e}}^1 = \underline{A}_1 \underline{\mathbf{e}}^{2''} , \qquad \underline{\mathbf{e}}^{2''} = \underline{A}_2 \underline{\mathbf{e}}^{2'} , \qquad \underline{\mathbf{e}}^{2'} = \underline{A}_3 \underline{\mathbf{e}}^2 , \tag{1.30}$$

$$\underline{A}_1 = \begin{bmatrix} 1 & 0 & 0 \\ 0 & \cos\phi_1 & -\sin\phi_1 \\ 0 & \sin\phi_1 & \cos\phi_1 \end{bmatrix} , \quad \underline{A}_2 = \begin{bmatrix} \cos\phi_2 & 0 & \sin\phi_2 \\ 0 & 1 & 0 \\ -\sin\phi_2 & 0 & \cos\phi_2 \end{bmatrix} ,$$
$$\underline{A}_3 = \begin{bmatrix} \cos\phi_3 & -\sin\phi_3 & 0 \\ \sin\phi_3 & \cos\phi_3 & 0 \\ 0 & 0 & 1 \end{bmatrix} . \tag{1.31}$$

The desired matrix is $\underline{A}^{12} = \underline{A}_1 \underline{A}_2 \underline{A}_3$. When this is multiplied out and use is made of the abbreviations $c_i = \cos\phi_i$, $s_i = \sin\phi_i$ $(i = 1, 2, 3)$, the matrix has the form

$$\underline{A}^{12} = \begin{bmatrix} c_2 c_3 & -c_2 s_3 & s_2 \\ c_1 s_3 + s_1 s_2 c_3 & c_1 c_3 - s_1 s_2 s_3 & -s_1 c_2 \\ s_1 s_3 - c_1 s_2 c_3 & s_1 c_3 + c_1 s_2 s_3 & c_1 c_2 \end{bmatrix} . \tag{1.32}$$

Bryan angles, too, can be illustrated by means of a rigid body in a two-gimbal suspension system. The arrangement is shown in Fig. 1.2b . The bases $\underline{\mathbf{e}}^1$ and $\underline{\mathbf{e}}^2$ are attached to the material base and to the suspended body, respectively. The angles ϕ_1 , ϕ_2 and ϕ_3 are, in this order, the rotation angle of the outer gimbal relative to the material base, of the inner gimbal relative to the outer gimbal and of the body relative to the inner gimbal. The three angles can be adjusted independently since the intermediate bases $\underline{\mathbf{e}}^{2''}$ and $\underline{\mathbf{e}}^{2'}$ are materially realized by the gimbals. For $\phi_2 = 0$ the three rotation axes are mutually orthogonal. As with Euler angles there exists a critical case in which the axes of the first and of the third rotation coincide. It occurs if $\phi_2 = \pi/2 + n\pi$ $(n = 0, 1, \ldots)$.

In contrast to Euler angles linearization for small angles is possible. With $|\phi_i| \ll 1$ $(i = 1, 2, 3)$ $\sin\phi_i \approx \phi_i$, $\cos\phi_i \approx 1$ the matrix is

$$\underline{A}^{12} \approx \begin{bmatrix} 1 & -\phi_3 & \phi_2 \\ \phi_3 & 1 & -\phi_1 \\ -\phi_2 & \phi_1 & 1 \end{bmatrix} = \underline{I} + \underline{\tilde{\phi}} \qquad \text{with} \qquad \underline{\tilde{\phi}} = \begin{bmatrix} 0 & -\phi_3 & \phi_2 \\ \phi_3 & 0 & -\phi_1 \\ -\phi_2 & \phi_1 & 0 \end{bmatrix} . \tag{1.33}$$

The occurrence of the matrix $\underline{\tilde{\phi}}$ suggests to interpret ϕ_1 , ϕ_2 , ϕ_3 as coordinates of a *rotation vector* $\boldsymbol{\phi}$. In the linear approximation the coordinates are the same in both bases. Indeed, transformation, i.e., multiplication of the coordinate matrix $\underline{\phi} = [\,\phi_1 \;\; \phi_2 \;\; \phi_3\,]^T$ with $\underline{A}^{12}$, causes no change: $\underline{A}^{12}\underline{\phi} \approx (\underline{I} + \underline{\tilde{\phi}})\underline{\phi} = \underline{\phi}$. The rotation vector $\boldsymbol{\phi}$ is used as follows. Let $\mathbf{r}$ and $\mathbf{r}^*$ be the position vectors of an arbitrary body-fixed point before and after the small rotation, respectively. The coordinate matrices of these two vectors in $\underline{\mathbf{e}}^1$ satisfy (1.15): $\underline{r}^{*1} = \underline{A}^{12}\underline{r}^1 \approx (\underline{I} + \underline{\tilde{\phi}})\underline{r}^1 = \underline{r}^1 + \underline{\tilde{\phi}}\,\underline{r}^1$. This is the coordinate form of the vector equation

$$\mathbf{r}^* \approx \mathbf{r} + \boldsymbol{\phi} \times \mathbf{r} \qquad \text{(valid for small rotations only)} . \tag{1.34}$$

What follows, is not restricted to small angles. If the matrix $\underline{A}^{12}$ in (1.32) is given, the associated Bryan angles are calculated from the equations

$$\left.\begin{array}{lll} \sin\phi_2 = a_{13}^{12} , & \cos\phi_2 = \sigma\sqrt{1-\sin^2\phi_2} & (\sigma = +1 \ \text{ or } \ -1) , \\ \sin\phi_1 = -a_{23}^{12}/\cos\phi_2 , & \cos\phi_1 = a_{33}^{12}/\cos\phi_2 , & \\ \sin\phi_3 = -a_{12}^{12}/\cos\phi_2 , & \cos\phi_3 = a_{11}^{12}/\cos\phi_2 . & \end{array}\right\} \tag{1.35}$$

Numerical difficulties arise when ϕ_2 is close to one of the critical values $\pi/2 + n\pi$ $(n = 0, 1, \ldots)$. Let $(\phi_1 , \phi_2 , \phi_3)$ be the angles associated with $\sigma = +1$. The angles associated with $\sigma = -1$ are $(\pi + \phi_1 , \pi - \phi_2 , \pi + \phi_3)$. Both triples produce one and the same final position of the basis $\underline{\mathbf{e}}^2$.

The combination of (1.35) and (1.28) yields Bryan angles in terms of Euler angles. Conversely, the combination of (1.29) and (1.32) yields Euler angles in terms of Bryan angles.

1.5 Rotation Tensor

In this section Theorem 1.1 is taken up again: The displacement of a body-fixed basis from an initial position $\underline{\mathbf{e}}^1$ to an arbitrary final position $\underline{\mathbf{e}}^2$ is achieved by a rotation through a certain angle φ about the axis given by the eigenvector $\mathbf{n}$ which is associated with the eigenvalue $\lambda = +1$ of the direction cosine matrix $\underline{A}^{12}$. In what follows, the rotation is called rotation $(\mathbf{n}, \varphi)$. Note: The rotations $(\mathbf{n}, \varphi)$, $(-\mathbf{n}, -\varphi)$ and $(\mathbf{n}, \varphi + 2\pi)$ produce the same final position. For this reason, they are called equal. Now, the unit vector $\mathbf{n}$ and the angle φ of the rotation are prescribed. To be determined is the direction cosine matrix $\underline{A}^{12}$. In Fig. 1.3 the rotation is illustrated by its

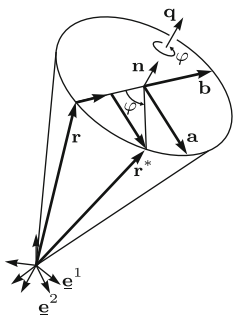

Fig. 1.3 Body-fixed vector in positions $\mathbf{r}$ before and $\mathbf{r}^*$ after the rotation $(\mathbf{n}, \varphi)$

effect on a body-fixed vector. Before the rotation the vector is in the position $\mathbf{r}$. The rotation $(\mathbf{n}, \varphi)$ carries it into the position $\mathbf{r}^*$. With the auxiliary vectors $\mathbf{a} = \mathbf{n} \times \mathbf{r}$ and $\mathbf{b} = \mathbf{n} \times \mathbf{a} = \mathbf{n} \times (\mathbf{n} \times \mathbf{r})$ the vector $\mathbf{r}^*$ is expressed in the form

$$\mathbf{r}^* = \mathbf{r} + (1 - \cos\varphi)\mathbf{b} + \sin\varphi\,\mathbf{a} \tag{1.36}$$

$$= \mathbf{r} + (1 - \cos\varphi)\mathbf{n} \times (\mathbf{n} \times \mathbf{r}) + \sin\varphi\,\mathbf{n} \times \mathbf{r} \tag{1.37}$$

$$= \cos\varphi\,\mathbf{r} + (1 - \cos\varphi)\mathbf{n}\mathbf{n} \cdot \mathbf{r} + \sin\varphi\,\mathbf{n} \times \mathbf{r}\,. \tag{1.38}$$

This has the form

$$\mathbf{r}^* = \mathsf{R}(\mathbf{n}, \varphi) \cdot \mathbf{r}\,. \tag{1.39}$$

The equation defines the *rotation tensor*

$$\mathsf{R}(\mathbf{n}, \varphi) = \cos\varphi\,\mathsf{I} + (1 - \cos\varphi)\mathbf{n}\mathbf{n} + \sin\varphi\,\mathbf{n} \times \mathsf{I} \qquad (\text{unit tensor } \mathsf{I})\,. \tag{1.40}$$

The inverse of the rotation $(\mathbf{n}, \varphi)$ is the rotation $(\mathbf{n}, -\varphi) = (-\mathbf{n}, \varphi)$. The rotation $(\mathbf{n}, \varphi)$ as well as the inverse rotation carries the axial vector $\mathbf{n}$ into itself. This is expressed by the identities

$$\mathsf{R}(\pm\mathbf{n}, \varphi) \cdot \mathbf{n} \equiv \mathbf{n}\,, \qquad \mathbf{n} \cdot \mathsf{R}(\pm\mathbf{n}, \varphi) \equiv \mathbf{n}\,. \tag{1.41}$$

The rotation tensor is symmetric if and only if $\sin\varphi = 0$, i.e., in the trivial case $\varphi = 0$ and in the case $\varphi = \pi$ which is of particular interest. This symmetric tensor is

$$\mathsf{R}(\mathbf{n}, \pm\pi) = 2\mathbf{n}\mathbf{n} - \mathsf{I}\,. \tag{1.42}$$

From Fig. 1.3 it is seen that a 180°-rotation about the line defined by $\mathbf{n}$ is equivalent to reflection in this line. Definition: A point P^* with position vector $\mathbf{r}^*$ is said to be the reflection of P (position vector $\mathbf{r}$) in a line if
- the line $\overline{\mathrm{PP}}^*$ intersects the reflecting line orthogonally
- the point of intersection is midpoint of $\overline{\mathrm{PP}}^*$.
Equation (1.39) has the form $\mathbf{r}^* = 2\mathbf{n}\mathbf{n} \cdot \mathbf{r} - \mathbf{r}$, whence it follows that $\mathbf{r}^* + \mathbf{r}$ has the direction of $\mathbf{n}$. Hence

$$\mathbf{n} = \frac{\mathbf{r}^* + \mathbf{r}}{|\mathbf{r}^* + \mathbf{r}|} \qquad (\varphi = \pm\pi\,;\ \mathbf{r} \cdot \mathbf{n} \neq 0)\,. \tag{1.43}$$

Now back to the general case. From (1.37) it follows that

$$(\mathbf{r}^* - \mathbf{r}) \cdot \mathbf{n} = 0\,. \tag{1.44}$$

Let $\mathsf{R}_1 = \mathsf{R}(\mathbf{n}_1, \varphi_1)$ be the tensor of a first rotation which is followed by a second rotation with the tensor $\mathsf{R}_2 = \mathsf{R}(\mathbf{n}_2, \varphi_2)$. The first rotation carries a body-fixed vector from its initial position $\mathbf{r}$ into the new position $\mathbf{r}^* = \mathsf{R}_1 \cdot \mathbf{r}$. The second rotation carries this vector $\mathbf{r}^*$ into the final position $\mathbf{r}^{**} = \mathsf{R}_2 \cdot \mathbf{r}^*$. Combination of both equations yields the formula $\mathbf{r}^{**} = \mathsf{R}_2 \cdot R_1 \cdot \mathbf{r}$. The

product $\mathsf{R}_2 \cdot R_1$ is the tensor $\mathsf{R}_{\rm res}$ of the resultant rotation $(\mathbf{n}_{\rm res}, \varphi_{\rm res})$:

$$\mathsf{R}_{\rm res} = \mathsf{R}_2 \cdot \mathsf{R}_1 \ . \tag{1.45}$$

The product depends on the order of the rotations. The product is the unit tensor, when the second rotation is the inverse of the first rotation:

$$\mathsf{R}(-\mathbf{n}, \varphi) \cdot \mathsf{R}(\mathbf{n}, \varphi) = \mathsf{I} \ . \tag{1.46}$$

Up to now coordinate-free forms of rotation tensors have been used. Applications see in Sects. 1.15.2 , 1.15.9 and 1.15.11 . Decomposition of (1.39) in basis $\underline{\mathbf{e}}^1$ results in the coordinate equation

$$\underline{r}^{*1} = \underline{R}(\mathbf{n}, \varphi)\underline{r}^1 = [\cos\varphi\, \underline{I} + (1 - \cos\varphi)\underline{n}\,\underline{n}^T + \sin\varphi\, \underline{\tilde{n}}\,]\,\underline{r}^1 \ . \tag{1.47}$$

Comparison with (1.15) shows that $\underline{R}(\mathbf{n}, \varphi)$ is the direction cosine matrix:

$$\underline{A}^{12} = \cos\varphi\, \underline{I} + (1 - \cos\varphi)\underline{n}\,\underline{n}^T + \sin\varphi\, \underline{\tilde{n}} \tag{1.48}$$

or explicitly

$$\underline{A}^{12} = \begin{bmatrix} n_1^2 + (1 - n_1^2)\cos\varphi & n_1 n_2(1 - \cos\varphi) - n_3 \sin\varphi & n_1 n_3(1 - \cos\varphi) + n_2 \sin\varphi \\ n_1 n_2(1 - \cos\varphi) + n_3 \sin\varphi & n_2^2 + (1 - n_2^2)\cos\varphi & n_2 n_3(1 - \cos\varphi) - n_1 \sin\varphi \\ n_1 n_3(1 - \cos\varphi) - n_2 \sin\varphi & n_2 n_3(1 - \cos\varphi) + n_1 \sin\varphi & n_3^2 + (1 - n_3^2)\cos\varphi \end{bmatrix} . \tag{1.49}$$

The diagonal elements can be given other forms if use is made of the constraint equation

$$n_1^2 + n_2^2 + n_3^2 = 1 \ . \tag{1.50}$$

The diagonal elements yield the first equation below, and the off-diagonal elements yield the second:

$$\cos\varphi = \frac{\operatorname{tr} \underline{A}^{12} - 1}{2} \ , \tag{1.51}$$

$$2n_i \sin\varphi = a_{kj}^{12} - a_{jk}^{12} \ \ (i, j, k = 1, 2, 3 \ \text{ cyclic}) \quad \leftrightarrow \quad 2\underline{\tilde{n}} \sin\varphi = \underline{A}^{12} - \underline{A}^{12\,T} \ . \tag{1.52}$$

The first equation is Eq.(1.21). This proves that the rotation angle φ is the angle in the eigenvalues $\lambda_{2,3} = \mathrm{e}^{\pm i\varphi}$ of the direction cosine matrix.

When the matrix $\underline{A}^{12}$ is given, the rotation parameters φ and n_1 , n_2 , n_3 can be determined in two ways. Either $\underline{n}$ is calculated from (1.22): $(\underline{A}^{12} - \underline{I})\underline{n} = \underline{0}$. Then (1.51) and (1.52) together determine φ uniquely. The alternative way is to take one of the two solutions φ satisfying (1.51) and to

calculate n_1, n_2, n_3 from (1.52). This equation for n_1, n_2, n_3 fails in the particularly simple case $\varphi = \pi$. In this case, $\underline{A}^{12}$ is the symmetric matrix (see (1.42))

$$\underline{A}^{12} = 2\underline{n}\,\underline{n}^T - \underline{I}\,. \tag{1.53}$$

It satisfies the equation $(\underline{A}^{12} - \underline{I})(\underline{A}^{12} + \underline{I}) = \underline{0}$. The trace of $\underline{A}^{12}$ is -1. From (1.20) it is known that the matrix has the real double eigenvalue $\lambda_{2,3} = -1$. Let $\underline{z}$ be the eigenvectors associated with this double eigenvalue. They are solutions of the equation $(\underline{A}^{12} + \underline{I})\underline{z} = 0$. This is the equation $\underline{n}\underline{n}^T\underline{z} = \underline{0}$, whence it follows that $\underline{n}^T\underline{z} = 0$. This means that every vector perpendicular to the rotation axis $\mathbf{n}$ is an eigenvector. Indeed, the rotation $(\mathbf{n}, \pi)$ applied to such a vector $\mathbf{z}$ results in $-\mathbf{z}$. The same displacement from $\mathbf{z}$ into $-\mathbf{z}$ occurs when the vector is reflected in the line $\mathbf{n}$.

The formulation (1.49) of the matrix $\underline{A}^{12}$ in terms of the four rotation parameters n_1, n_2, n_3 and φ is particularly useful in cases when a body is rotating about a fixed axis which is not aligned with one of the basis vectors. In this case, n_1, n_2, n_3 are constants, and only φ is a variable. Applications see in Sects. 1.15.3, 6.11 and 18.4. If one of the three coordinates n_1, n_2, n_3 is zero, the other two are defined by an angle. Example: With $n_1 = 0$, $n_2 = \sin\alpha$, $n_3 = \cos\alpha$ the matrix has the special form

$$\underline{A}^{12} = \begin{bmatrix} \cos\varphi & -\sin\varphi\cos\alpha & \sin\varphi\sin\alpha \\ \sin\varphi\cos\alpha & \cos\varphi\cos^2\alpha + \sin^2\alpha & (1-\cos\varphi)\sin\alpha\cos\alpha \\ -\sin\varphi\sin\alpha & (1-\cos\varphi)\sin\alpha\cos\alpha & \cos\varphi\sin^2\alpha + \cos^2\alpha \end{bmatrix}. \tag{1.54}$$

An application is shown in Sect. 16.2.1.

For small rotations with $|\varphi| \ll 1$ the Taylor expansion of (1.48) up to second-order terms yields the approximation

$$\underline{A}^{12} \approx \underline{I} + \varphi\,\underline{\tilde{n}} + \frac{1}{2}\varphi^2(\underline{n}\,\underline{n}^T - \underline{I})\,. \tag{1.55}$$

An application is shown in Sect. 1.15.5. The linear approximation $\underline{A}^{12} \approx \underline{I} + \varphi\,\underline{\tilde{n}}$ is known from (1.33).

In what follows, the trace $\operatorname{tr}\underline{A}^{12}$ and the vector $2\mathbf{n}\sin\varphi$ in (1.51) and (1.52) are considered again. Both are expressed in terms of unit basis vectors. For this purpose the definition of direction cosines in (1.3), $a_{ij}^{12} = \mathbf{e}_i^1 \cdot \mathbf{e}_j^2$, is used. It yields the expressions

$$\operatorname{tr}\underline{A}^{12} = \sum_{i=1}^{3} \mathbf{e}_i^1 \cdot \mathbf{e}_i^2\,, \tag{1.56}$$

$$\begin{aligned} 2n_i\sin\varphi &= \mathbf{e}_k^1 \cdot \mathbf{e}_j^2 - \mathbf{e}_j^1 \cdot \mathbf{e}_k^2 = \mathbf{e}_i^1 \times \mathbf{e}_j^1 \cdot \mathbf{e}_j^2 + \mathbf{e}_i^1 \times \mathbf{e}_k^1 \cdot \mathbf{e}_k^2 \\ &= \mathbf{e}_i^1 \cdot \left(\mathbf{e}_i^1 \times \mathbf{e}_i^2 + \mathbf{e}_j^1 \times \mathbf{e}_j^2 + \mathbf{e}_k^1 \times \mathbf{e}_k^2\right) \quad (i,j,k = 1,2,3 \text{ cyclic}) \end{aligned} \tag{1.57}$$

(in the first step $\mathbf{e}_k^1 = \mathbf{e}_i^1 \times \mathbf{e}_j^1$, $\mathbf{e}_j^1 = \mathbf{e}_k^1 \times \mathbf{e}_i^1$ and in the second step interchange of multiplication symbols and addition of a zero-term). With this expression the nonnormalized eigenvector $2\mathbf{n}\sin\varphi$ is

$$2\mathbf{n}\sin\varphi = \sum_{i=1}^{3} \mathbf{e}_i^1 \times \mathbf{e}_i^2 \,. \tag{1.58}$$

Proposition: When $\underline{A}^{12}$ is symmetric, every vector of the form

$$\mathbf{e} = \sum_{k=1}^{3} c_k(\mathbf{e}_k^1 + \mathbf{e}_k^2) \qquad (c_1,\, c_2,\, c_3 \text{ arbitr.}) \tag{1.59}$$

is an eigenvector. For a proof it suffices to show that $\mathbf{e}$ has identical coordinates in $\underline{\mathbf{e}}^1$ and in $\underline{\mathbf{e}}^2$. The coordinates are

$$\left.\begin{aligned} \mathbf{e}_i^1 \cdot \mathbf{e} &= c_i + \textstyle\sum_{k=1}^{3} c_k\big(\mathbf{e}_i^1 \cdot \mathbf{e}_k^2\big) = c_i + a_{i1}^{12}c_1 + a_{i2}^{12}c_2 + a_{i3}^{12}c_3 \,, \\ \mathbf{e}_i^2 \cdot \mathbf{e} &= c_i + \textstyle\sum_{k=1}^{3} c_k\big(\mathbf{e}_i^2 \cdot \mathbf{e}_k^1\big) = c_i + a_{i1}^{21}c_1 + a_{i2}^{21}c_2 + a_{i3}^{21}c_3 \end{aligned}\right\} (i = 1,2,3) \,. \tag{1.60}$$

Because of the symmetry $\underline{A}^{12^T} = \underline{A}^{12}$ they are, indeed, identical.

Next, (1.49) is used for expressing the complex conjugate eigenvectors associated with the eigenvalues $\cos\varphi \pm \mathrm{i}\,\sin\varphi$ of the direction cosine matrix in terms of n_1, n_2, n_3 and φ. Let $[\,m_1\;\; m_2\;\; m_3\,]^T$ be the eigenvector associated with $\cos\varphi + \mathrm{i}\,\sin\varphi$. With the abbreviations $c = \cos\varphi$, $s = \sin\varphi$ it is determined from the equations

$$\begin{bmatrix} n_1^2(1-c) - \mathrm{i}\,s & n_1n_2(1-c) - n_3 s & n_1n_3(1-c) + n_2 s \\ n_1n_2(1-c) + n_3 s & n_2^2(1-c) - \mathrm{i}\,s & n_2n_3(1-c) - n_1 s \\ n_1n_3(1-c) - n_2 s & n_2n_3(1-c) + n_1 s & n_3^2(1-c) - \mathrm{i}\,s \end{bmatrix} \begin{bmatrix} m_1 \\ m_2 \\ m_3 \end{bmatrix} = \underline{0} \,. \tag{1.61}$$

From two equations ratios such as m_1/m_3 are calculated. It turns out that they are independent of φ:

$$\left.\begin{aligned} \frac{m_1}{m_3} &= -\frac{n_1n_3 + \mathrm{i}\,n_2}{n_1^2 + n_2^2} \,, & \frac{m_2}{m_3} &= -\frac{n_2n_3 - \mathrm{i}\,n_1}{n_1^2 + n_2^2} \,, \\ \frac{m_2}{m_1} &= -\frac{n_1n_2 + \mathrm{i}\,n_3}{n_2^2 + n_3^2} \,, & \frac{m_3}{m_1} &= -\frac{n_3n_1 - \mathrm{i}\,n_2}{n_2^2 + n_3^2} \,. \end{aligned}\right\} \tag{1.62}$$

The sum of squares equals zero: $m_1^2 + m_2^2 + m_3^2 = 0$. Equating the two expressions available for m_2/m_3 yields

$$-\frac{n_2n_3 - \mathrm{i}\,n_1}{n_1^2 + n_2^2} = \frac{n_1n_2 + \mathrm{i}\,n_3}{n_3n_1 - \mathrm{i}\,n_2} \,. \tag{1.63}$$

Multiplication with $(n_1^2+n_2^2)(n_3n_1-\mathrm{i}\,n_2)(n_1n_2-\mathrm{i}\,n_3)$ results in the identity

$$-(n_1n_2-\mathrm{i}\,n_3)(n_2n_3-\mathrm{i}\,n_1)(n_3n_1-\mathrm{i}\,n_2)=(n_1^2+n_2^2)(n_1^2n_2^2+n_3^2) \tag{1.64}$$

valid for arbitrary real n_1, n_2, n_3 satisfying the constraint equation $n_1^2+n_2^2+n_3^2=1$. Since the left-hand side of the equation is invariant under a cyclic permutation of indices, also the right-hand side is:

$$(n_1^2+n_2^2)(n_1^2n_2^2+n_3^2)=(n_2^2+n_3^2)(n_2^2n_3^2+n_1^2)=(n_3^2+n_1^2)(n_3^2n_1^2+n_2^2)\,. \tag{1.65}$$

1.6 Euler-Rodrigues Parameters

Starting from (1.37) a new form is developed for the direction cosine matrix $\underline{A}^{12}$. By means of the formulas

$$1-\cos\varphi=2\sin^2\frac{\varphi}{2}\,,\qquad \sin\varphi=2\sin\frac{\varphi}{2}\cos\frac{\varphi}{2} \tag{1.66}$$

the transition to the half-angle is made. New quantities are defined as follows:

$$q_0=\cos\frac{\varphi}{2}\,,\qquad \mathbf{q}=\mathbf{n}\sin\frac{\varphi}{2}\,. \tag{1.67}$$

The vector $\mathbf{q}$ lies in the rotation axis (Fig. 1.3). Therefore, it has identical coordinates in the bases $\underline{\mathbf{e}}^1$ and $\underline{\mathbf{e}}^2$. These coordinates are denoted q_1, q_2, q_3, and the coordinate matrix is called $\underline{q}$. The four quantities $q_0,\ldots,q_3$ are referred to as *Euler-Rodrigues parameters*. They satisfy the constraint equation

$$q_0^2+\mathbf{q}^2=\sum_{i=0}^{3}q_i^2=1\,. \tag{1.68}$$

This can also be written in the forms

$$1-2\mathbf{q}^2=q_0^2-\mathbf{q}^2=2q_0^2-1\,. \tag{1.69}$$

Equations (1.67) show: A change of the signs of all four parameters means that either $\cos\varphi/2$ and $\sin\varphi/2$ change signs or $\cos\varphi/2$ and $\mathbf{n}$ change signs. The former has the effect that $(\mathbf{n},\varphi)$ is replaced by $(\mathbf{n},\varphi+2\pi)$. The latter means that $(\mathbf{n},\varphi)$ is replaced by $(-\mathbf{n},-\varphi)$. Neither one of these changes has an effect on the rotation.

Substitution of the expressions (1.66) into (1.37) produces the equation

$$\mathbf{r}^*=\mathbf{r}+2[\mathbf{q}\times(\mathbf{q}\times\mathbf{r})+q_0\mathbf{q}\times\mathbf{r}]\,. \tag{1.70}$$

Reformulation of the double cross product and application of (1.69) lead to

$$\mathbf{r}^* = (q_0^2 - \mathbf{q}^2)\mathbf{r} + 2(\mathbf{q}\mathbf{q}\cdot\mathbf{r} + q_0\mathbf{q}\times\mathbf{r}) \tag{1.71}$$

$$= [(q_0^2 - \mathbf{q}^2)\mathsf{I} + 2(\mathbf{q}\mathbf{q} + q_0\mathbf{q}\times\mathsf{I})]\cdot\mathbf{r}\,. \tag{1.72}$$

If one of the double cross products is kept, the alternative form is obtained:

$$\mathbf{r}^* = q_0^2\mathbf{r} + \mathbf{q}\mathbf{q}\cdot\mathbf{r} + \mathbf{q}\times(\mathbf{q}\times\mathbf{r}) + 2q_0\mathbf{q}\times\mathbf{r}\,. \tag{1.73}$$

Equation (1.70) yields

$$\mathbf{r}^*-\mathbf{r} = 2[\mathbf{q}\times(\mathbf{q}\times\mathbf{r})+q_0\mathbf{q}\times\mathbf{r}]\,, \qquad \mathbf{r}^*+\mathbf{r} = 2[\mathbf{r}+\mathbf{q}\times(\mathbf{q}\times\mathbf{r})+q_0\mathbf{q}\times\mathbf{r}]\,. \tag{1.74}$$

Elementary calculations show that

$$q_0(\mathbf{r}^* - \mathbf{r}) = \mathbf{q}\times(\mathbf{r}^* + \mathbf{r}) \tag{1.75}$$

or, with the so-called *Rodrigues vector*

$$\mathbf{u} = \frac{\mathbf{q}}{q_0} = \mathbf{n}\tan\frac{\varphi}{2}\,, \tag{1.76}$$

$$\mathbf{r}^* - \mathbf{r} = \mathbf{u}\times(\mathbf{r}^* + \mathbf{r})\,. \tag{1.77}$$

This relationship can also be inferred directly from Fig. 1.3. The Rodrigues vector is subject of Sects. 1.9 and 1.13 .

The coefficient of $\mathbf{r}$ in (1.72) represents a new form of the rotation tensor in (1.39): $\mathbf{r}^* = \mathsf{R}(\mathbf{n},\varphi)\cdot\mathbf{r}$. The same arguments that led to (1.48) for the direction cosine matrix $\underline{A}^{12}$ now lead to the equation

$$\underline{A}^{12} = (q_0^2 - \mathbf{q}^2)\underline{I} + 2(\underline{q}\,\underline{q}^T + q_0\underline{\tilde{q}})\,. \tag{1.78}$$

Multiplying out results in the expression

$$\underline{A}^{12} = \begin{bmatrix} q_0^2+q_1^2-q_2^2-q_3^2 & 2(q_1q_2-q_0q_3) & 2(q_1q_3+q_0q_2) \\ 2(q_1q_2+q_0q_3) & q_0^2+q_2^2-q_3^2-q_1^2 & 2(q_2q_3-q_0q_1) \\ 2(q_1q_3-q_0q_2) & 2(q_2q_3+q_0q_1) & q_0^2+q_3^2-q_1^2-q_2^2 \end{bmatrix}\,. \tag{1.79}$$

This representation of the matrix is appealing in that every element is a quadratic form of Euler-Rodrigues parameters. With (1.69) the diagonal elements have the alternative form $a_{ii}^{12} = 2(q_0^2 + q_i^2) - 1$ $(i = 1,2,3)$. Hence

$$\underline{A}^{12} = -\underline{I} + 2\begin{bmatrix} q_0^2+q_1^2 & q_1q_2-q_0q_3 & q_1q_3+q_0q_2 \\ q_1q_2+q_0q_3 & q_0^2+q_2^2 & q_2q_3-q_0q_1 \\ q_1q_3-q_0q_2 & q_2q_3+q_0q_1 & q_0^2+q_3^2 \end{bmatrix}\,. \tag{1.80}$$

The diagonal elements yield the first equation below, and the off-diagonal elements yield the second:

$$q_0 = \pm\frac{1}{2}\sqrt{1 + \operatorname{tr} \underline{A}^{12}} \qquad \text{(sign arbitrary)} , \tag{1.81}$$

$$4q_0 q_i = a_{kj}^{12} - a_{jk}^{12} \qquad (i,j,k = 1,2,3 \ \text{ cyclic}) \quad \leftrightarrow \quad 4q_0 \underline{\tilde{q}} = \underline{A}^{12} - \underline{A}^{12\,T} . \tag{1.82}$$

The equations for q_1 , q_2 , q_3 fail in the case $q_0 = 0$. This is the case $\varphi = \pi$, $\underline{q} = \underline{n}$ when $\underline{n}$ must be determined from the equation $(\underline{A}^{12} - \underline{I})\underline{n} = \underline{0}$ (see (1.51) and (1.52) in this case).

In contrast to Euler angles and to Bryan angles there is no critical case in which the Euler-Rodrigues parameters are indeterminate. Hopf [10] was the first to prove that no representation of finite rotations by three parameters is possible without singular points. Stuelpnagel [30] gave a simpler version of the proof.

The matrix $\underline{A}^{12}$ in (1.78) resulted from scalar decomposition of (1.72). If, instead, (1.73) is decomposed, the matrix has the alternative form

$$\underline{A}^{12} = q_0^2 \underline{I} + \underline{q}\,\underline{q}^T + \underline{\tilde{q}}\,\underline{\tilde{q}} + 2q_0\underline{\tilde{q}} = \underline{q}\,\underline{q}^T + (q_0\underline{I} + \underline{\tilde{q}})^2 . \tag{1.83}$$

This is the product

$$\underline{A}^{12} = \underline{G}\,\underline{H}^T \tag{1.84}$$

with the (3×4)-matrices

$$\underline{G} = [-\underline{q} \ , \ q_0\underline{I} + \underline{\tilde{q}}] , \qquad \underline{H} = [-\underline{q} \ , \ q_0\underline{I} - \underline{\tilde{q}}] . \tag{1.85}$$

The comma separates the first column from the remaining three columns. Each of these two matrices is a homogeneous linear function of Euler-Rodrigues parameters. It is an elementary task to verify that the matrices have the orthogonality properties

$$\underline{G} \begin{bmatrix} q_0 \\ \underline{q} \end{bmatrix} = \underline{H} \begin{bmatrix} q_0 \\ \underline{q} \end{bmatrix} = \underline{0} . \tag{1.86}$$

Furthermore, with the help of (1.69) the relations are verified:

$$\underline{G}\,\underline{G}^T = \underline{H}\,\underline{H}^T = \underline{q}\,\underline{q}^T + q_0^2\underline{I} - \underline{\tilde{q}}\,\underline{\tilde{q}} = \underline{I} , \tag{1.87}$$

$$\underline{G}^T\underline{G} = \underline{H}^T\underline{H} = \underline{I} - \begin{bmatrix} q_0 \\ \underline{q} \end{bmatrix} \begin{bmatrix} q_0 \\ \underline{q} \end{bmatrix}^T \qquad (\,(4 \times 4)\text{-matrices}) . \tag{1.88}$$

1.7 Relationships Between Euler-Rodrigues Parameters and Euler Angles

Expressions for Euler-Rodrigues parameters in terms of Euler angles are obtained when in (1.81) and (1.82) for $\underline{A}^{12}$ Eq.(1.28) is substituted. The diagonal elements yield

$$\begin{aligned} 1 + \operatorname{tr} \underline{A}^{12} &= 1 + c_\theta + c_\theta(c_\psi c_\phi - s_\psi s_\phi) + (c_\psi c_\phi - s_\psi s_\phi) \\ &= (1 + c_\theta)[1 + (c_\psi c_\phi - s_\psi s_\phi)] \\ &= (1 + \cos\theta)[1 + \cos(\psi + \phi)] = 4\cos^2\frac{\theta}{2}\ \cos^2\frac{\psi + \phi}{2}\ . \end{aligned} \tag{1.89}$$

Hence $q_0 = \pm\cos\theta/2\ \cos(\psi + \phi)/2$. Arbitrarily, the positive sign is chosen. From (1.82) q_1 is calculated and for this purpose

$$a_{32}^{12} - a_{23}^{12} = s_\theta(c_\psi + c_\phi) = 4\sin\frac{\theta}{2}\ \cos\frac{\theta}{2}\ \cos\frac{\psi + \phi}{2}\ \cos\frac{\psi - \phi}{2}\ . \tag{1.90}$$

This expression and the result for q_0 yield $q_1 = \sin\theta/2\ \cos(\psi - \phi)/2$. In a similar manner also q_2 and q_3 are calculated. All four formulas together read:

$$\left.\begin{aligned} q_0 &= \cos\frac{\theta}{2}\ \cos\frac{\psi + \phi}{2}\ , & q_2 &= \sin\frac{\theta}{2}\ \sin\frac{\psi - \phi}{2}\ , \\ q_1 &= \sin\frac{\theta}{2}\ \cos\frac{\psi - \phi}{2}\ , & q_3 &= \cos\frac{\theta}{2}\ \sin\frac{\psi + \phi}{2}\ . \end{aligned}\right\} \tag{1.91}$$

From these equations it follows that

$$\cos^2\frac{\theta}{2} = q_0^2 + q_3^2\ , \qquad \sin^2\frac{\theta}{2} = q_1^2 + q_2^2\ , \tag{1.92}$$

$$\cos\theta = \cos^2\frac{\theta}{2} - \sin^2\frac{\theta}{2} = q_0^2 - q_1^2 - q_2^2 + q_3^2\ , \tag{1.93}$$

$$\sin^2\theta = 4\cos^2\frac{\theta}{2}\sin^2\frac{\theta}{2}\ = 4(q_0^2 + q_3^2)(q_1^2 + q_2^2)\ , \tag{1.94}$$

$$\tan\frac{\psi + \phi}{2} = \frac{q_3}{q_0}\ , \qquad \tan\frac{\psi - \phi}{2} = \frac{q_2}{q_1}\ , \tag{1.95}$$

$$\psi = \tan^{-1}\frac{q_3}{q_0} + \tan^{-1}\frac{q_2}{q_1}\ , \qquad \phi = \tan^{-1}\frac{q_3}{q_0} - \tan^{-1}\frac{q_2}{q_1}\ . \tag{1.96}$$

Equation (1.93) is obtained more directly by equating the elements $(3,3)$ of the direction cosine matrices in (1.28) and (1.79).

1.8 Quaternions

Hamilton [8, 9] is acknowledged as inventor of quaternion algebra (in the year 1843). However, the quaternion product in connection with the composition of finite rotations was formulated first by Euler in 1748 and by Gauss in 1819 . A quaternion, abbreviated Q , is composed of a scalar u and a vector $\mathbf{v}$, i.e., of four quantities altogether. Therefore, the name quaternion. The quaternion is denoted $Q = (u, \mathbf{v})$. The product of a quaternion $(u\,,\,\mathbf{v})$ by a scalar λ is defined to be the quaternion $(\lambda u\,,\,\lambda\mathbf{v})$.

The sum and the product of two quaternions Q_1 and Q_2 are defined to be the quaternions

$$Q_1 + Q_2 = Q_2 + Q_1 = (u_1 + u_2\,,\,\mathbf{v}_1 + \mathbf{v}_2)\,, \tag{1.97}$$

$$Q_2Q_1 = (u_2\,,\,\mathbf{v}_2)(u_1\,,\,\mathbf{v}_1) = \Big(u_2u_1 - \mathbf{v}_2\cdot\mathbf{v}_1\,,\,u_2\mathbf{v}_1 + u_1\mathbf{v}_2 + \mathbf{v}_2\times\mathbf{v}_1\Big)\,. \tag{1.98}$$

Because of the term $\mathbf{v}_2\times\mathbf{v}_1$ multiplication is not commutative. It is associative, however, as can be verified by multiplying out: $Q_3Q_2Q_1 = Q_3(Q_2Q_1) = (Q_3Q_2)Q_1$.

Remark: In the mathematical literature (Blaschke [4]) a quaternion is introduced in the form

$$Q = ue_0 + v_1\mathbf{e}_1 + v_2\mathbf{e}_2 + v_3\mathbf{e}_3\,. \tag{1.99}$$

The quaternion product is defined by the multiplication rules

$$\left.\begin{aligned} &\mathbf{e}_j e_0 = \quad e_0\mathbf{e}_j = \mathbf{e}_j\,, \qquad \mathbf{e}_j\mathbf{e}_j = -e_0 \qquad (j = 1,2,3)\,,\\ &\mathbf{e}_j\mathbf{e}_k = -\mathbf{e}_k\mathbf{e}_j = \mathbf{e}_\ell \qquad (j,k,\ell = 1,2,3 \ \text{ cyclic})\,. \end{aligned}\right\} \tag{1.100}$$

End of remark.

The special quaternion $(1\,,\,\mathbf{0})$ is called unit quaternion because multiplication with an arbitrary quaternion Q yields Q , again:

$$(1\,,\,\mathbf{0})Q = Q(1\,,\,\mathbf{0}) \equiv Q\,. \tag{1.101}$$

The *conjugate* of $Q = (u, \mathbf{v})$ is defined to be the quaternion $\tilde{Q} = (u, -\mathbf{v})$. The product of a quaternion with its own conjugate is

$$Q\tilde{Q} = (u, \mathbf{v})(u, -\mathbf{v}) = (u^2 + \mathbf{v}^2\,,\,\mathbf{0}) = (u^2 + \mathbf{v}^2)(1\,,\,\mathbf{0})\,. \tag{1.102}$$

Thus, it is a nonnegative scalar multiple of the unit quaternion. The square root of this scalar is called the *norm* of Q , abbreviated

$$\|Q\| = \sqrt{u^2 + \mathbf{v}^2}\,. \tag{1.103}$$

An arbitrary quaternion Q with norm $\|Q\| \neq 0$ satisfies the equation $(\tilde{Q}/\|Q\|^2)Q = (1\,,\,\mathbf{0})$. Because of this property $\tilde{Q}/\|Q\|^2$ is called the inverse of Q .

The conjugate of the product Q_2Q_1 in (1.98) is (the vector part is multiplied by -1)

$$\widetilde{Q_2Q_1} = \Big(u_2u_1 - \mathbf{v}_2\cdot\mathbf{v}_1\,,\,-u_2\mathbf{v}_1 - u_1\mathbf{v}_2 - \mathbf{v}_2\times\mathbf{v}_1\Big)\,. \tag{1.104}$$

With the same quaternions Q_1 and Q_2 the product is calculated:

$$\begin{aligned}\tilde{Q}_1\tilde{Q}_2 &= (u_1,-\mathbf{v}_1)(u_2,-\mathbf{v}_2)\\ &= \Big(u_1u_2 - \mathbf{v}_1\cdot\mathbf{v}_2\,,\,-u_1\mathbf{v}_2 - u_2\mathbf{v}_1 + \mathbf{v}_1\times\mathbf{v}_2\Big)\,.\end{aligned} \tag{1.105}$$

Comparison reveals the formula

$$\tilde{Q}_1\tilde{Q}_2 = \widetilde{Q_2Q_1}\,. \tag{1.106}$$

With the Euler-Rodrigues parameters q_0 and $\mathbf{q}$ of Eqs.(1.67) the quaternion of a rotation is defined. It is denoted D :

$$D = (q_0,\mathbf{q}) = \Big(\cos\frac{\varphi}{2}\,,\,\mathbf{n}\sin\frac{\varphi}{2}\Big)\,. \tag{1.107}$$

It has the norm $\|D\| = \sqrt{q_0^2+\mathbf{q}^2} = 1$. Hence its inverse equals its conjugate:

$$\tilde{D} = (q_0\,,\,-\mathbf{q})\,,\qquad \tilde{D}D = (1\,,\,\mathbf{0})\,. \tag{1.108}$$

The conjugate is the quaternion of the inverse rotation. The quaternion of the null rotation $(\varphi = 0)$ is the unit quaternion $(1\,,\,\mathbf{0})$. Normalized quaternions constitute a group with respect to multiplication.

With an arbitrary vector $\mathbf{r}$ the special quaternion $(0\,,\,\mathbf{r})$ is constructed. With the vector $\mathbf{r}$ shown in Fig. 1.3 and with the quaternion D of the rotation in this figure the product is calculated:

$$D(0\,,\,\mathbf{r})\tilde{D} = (q_0,\mathbf{q})(0\,,\,\mathbf{r})(q_0,-\mathbf{q})\,. \tag{1.109}$$

The product of the last two quaternions is

$$(0\,,\,\mathbf{r})(q_0,-\mathbf{q}) = (\mathbf{r}\cdot\mathbf{q}\,,\,q_0\mathbf{r} - \mathbf{r}\times\mathbf{q})\,. \tag{1.110}$$

With this expression the scalar part of $D(0\,,\,\mathbf{r})\tilde{D}$ turns out to be

$$q_0\mathbf{r}\cdot\mathbf{q} - \mathbf{q}\cdot(q_0\mathbf{r} - \mathbf{r}\times\mathbf{q}) = 0\,. \tag{1.111}$$

The vector part is

$$\begin{aligned} & q_0(q_0\mathbf{r} - \mathbf{r}\times\mathbf{q}) + (\mathbf{r}\cdot\mathbf{q})\mathbf{q} + \mathbf{q}\times(q_0\mathbf{r} - \mathbf{r}\times\mathbf{q}) \\ &= q_0^2\mathbf{r} + q_0\mathbf{q}\times\mathbf{r} + \mathbf{q}(\mathbf{q}\cdot\mathbf{r}) + q_0\mathbf{q}\times\mathbf{r} + \mathbf{q}\times(\mathbf{q}\times\mathbf{r}) \,. \end{aligned} \tag{1.112}$$

Reformulation of the double cross product yields the expression

$$(q_0^2 - \mathbf{q}^2)\mathbf{r} + 2(\mathbf{q}\mathbf{q}\cdot\mathbf{r} + q_0\mathbf{q}\times\mathbf{r}) \,. \tag{1.113}$$

Comparison with (1.71) shows that this is the vector $\mathbf{r}^*$ of Fig. 1.3. The results are summarized in the equation

$$(0\,,\,\mathbf{r}^*) = D(0\,,\,\mathbf{r})\tilde{D} \,. \tag{1.114}$$

Next, two consecutive rotations with quaternions D_1 (first rotation) and D_2 are executed. The result of the first rotation is $(0\,,\,\mathbf{r}^*) = D_1(0\,,\,\mathbf{r})\tilde{D}_1$. The second rotation carries the vector $\mathbf{r}^*$ into the new position $\mathbf{r}^{**}$ given by the equation $(0\,,\,\mathbf{r}^{**}) = D_2(0\,,\,\mathbf{r}^*)\tilde{D}_2$. For $(0\,,\,\mathbf{r}^*)$ the expression from the previous equation is substituted. This yields the relationship $(0\,,\,\mathbf{r}^{**}) = D_2D_1(0\,,\,\mathbf{r})\tilde{D}_1\tilde{D}_2$ or, because of (1.106),

$$(0\,,\,\mathbf{r}^{**}) = (D_2D_1)(0\,,\,\mathbf{r})\widetilde{(D_2D_1)} \,. \tag{1.115}$$

This has the form (1.114). The results are summarized in

Theorem 1.4. (Euler, Gauss) *The quaternion D_{res} of the resultant of two consecutive rotations with quaternions D_1 (first rotation) and D_2 is the product*

$$\begin{aligned} D_{\text{res}} &= D_2D_1 = (q_{02}, \mathbf{q}_2)(q_{01}, \mathbf{q}_1) \\ &= \Big(\cos\frac{\varphi_2}{2}\,,\,\mathbf{n}_2\sin\frac{\varphi_2}{2}\Big)\Big(\cos\frac{\varphi_1}{2}\,,\,\mathbf{n}_1\sin\frac{\varphi_1}{2}\Big) \,. \end{aligned} \tag{1.116}$$

The multiplication rule (1.98) yields the formulas

$$\left.\begin{aligned} q_{0_{\text{res}}} &= q_{02}q_{01} - \mathbf{q}_2\cdot\mathbf{q}_1 \,, \\ \mathbf{q}_{\text{res}} &= q_{02}\mathbf{q}_1 + q_{01}\mathbf{q}_2 + \mathbf{q}_2\times\mathbf{q}_1 \,. \end{aligned}\right\} \tag{1.117}$$

More explicitly, these are formulas for the rotation angle φ_{res} and for the unit vector $\mathbf{n}_{\text{res}}$ of the resultant rotation:

$$\cos\frac{\varphi_{\text{res}}}{2} = \cos\frac{\varphi_2}{2}\cos\frac{\varphi_1}{2} - \mathbf{n}_2\cdot\mathbf{n}_1\sin\frac{\varphi_2}{2}\sin\frac{\varphi_1}{2} \,, \tag{1.118}$$

$$\begin{aligned} \mathbf{n}_{\text{res}}\sin\frac{\varphi_{\text{res}}}{2} &= \mathbf{n}_1\cos\frac{\varphi_2}{2}\sin\frac{\varphi_1}{2} + \mathbf{n}_2\cos\frac{\varphi_1}{2}\sin\frac{\varphi_2}{2} \\ &\quad + \mathbf{n}_2\times\mathbf{n}_1\sin\frac{\varphi_2}{2}\sin\frac{\varphi_1}{2} \,. \end{aligned} \tag{1.119}$$

Because of the term with $\mathbf{n}_2 \times \mathbf{n}_1$ the axis of the resultant rotation is not located in the plane of the axes of the other two rotations. Its location depends upon the order in which the rotations are executed. In contrast, the angle φ_{res} is independent of the order. Applications see in Sects. 1.15.2 and 1.15.12 .

For scalar decomposition of the vectors $\mathbf{n}_1$ and $\mathbf{n}_2$ the basis $\mathbf{e}_{1,2,3}$ shown in Fig. 1.4 is chosen. Let α be the rotation angle about $\mathbf{e}_3$ which carries $\mathbf{n}_1$ into the position $\mathbf{n}_2$. Then the vectors are

$$\mathbf{n}_{1,2} = \mathbf{e}_1 \cos\frac{\alpha}{2} \mp \mathbf{e}_2 \sin\frac{\alpha}{2} \,. \tag{1.120}$$

With these expressions (1.118) and (1.119) take the forms

$$\cos\frac{\varphi_{\text{res}}}{2} = \cos\frac{\varphi_1}{2}\cos\frac{\varphi_2}{2} - \sin\frac{\varphi_1}{2}\sin\frac{\varphi_2}{2}\,\cos\alpha \,, \tag{1.121}$$

$$\begin{aligned}\mathbf{n}_{\text{res}} \sin\frac{\varphi_{\text{res}}}{2} &= \mathbf{e}_1 \sin\frac{\varphi_1+\varphi_2}{2}\,\cos\frac{\alpha}{2} - \mathbf{e}_2 \sin\frac{\varphi_1-\varphi_2}{2}\,\sin\frac{\alpha}{2} \\ &\quad -\mathbf{e}_3 \sin\frac{\varphi_1}{2}\sin\frac{\varphi_2}{2}\,\sin\alpha \,. \end{aligned} \tag{1.122}$$

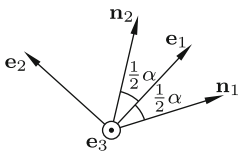

Fig. 1.4 Reference axes $\mathbf{e}_{1,2,3}$ for the vectors $\mathbf{n}_1$ and $\mathbf{n}_2$

In the case of small angles φ_1 and φ_2 the linearized Eqs.(1.118) and (1.119) have the forms

$$\cos\frac{\varphi_{\text{res}}}{2} \approx 1 \,, \qquad \mathbf{n}_{\text{res}}\varphi_{\text{res}} \approx \mathbf{n}_1\varphi_1 + \mathbf{n}_2\varphi_2 \,. \tag{1.123}$$

From the first equation it follows that also φ_{res} is small. The second equation proves that in this approximation it is possible to define rotation vectors $\boldsymbol{\varphi}_{\text{res}} = \mathbf{n}_{\text{res}}\varphi_{\text{res}}$, $\boldsymbol{\varphi}_i = \mathbf{n}_i\varphi_i$ and to calculate the resultant vector by the parallelogram rule

$$\boldsymbol{\varphi}_{\text{res}} \approx \boldsymbol{\varphi}_1 + \boldsymbol{\varphi}_2 \,. \tag{1.124}$$

The vector of a small rotation appeared already in the context of (1.33).

By squaring (1.118) and by applying theorems for circular functions it is possible to produce an equation which is free of half-angles. In contrast, no expression can be obtained for $\mathbf{n}_{\text{res}}$ which is free of half-angles and of square

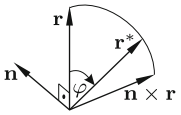

Fig. 1.5 Rotation of a vector $\mathbf{r}$ about an axis $\mathbf{n}$ normal to $\mathbf{r}$

roots. Half-angles can be avoided only in the special case when in Fig. 1.3 $\mathbf{r}$ is normal to $\mathbf{n}$. Then also $\mathbf{r}^*$ is normal to $\mathbf{n}$. This special situation is shown in Fig. 1.5. In accordance with (1.38) the vectors $\mathbf{r}^*$ and $\mathbf{r}$ satisfy the equation

$$\mathbf{r}^* = \mathbf{r}\cos\varphi + \mathbf{n}\times\mathbf{r}\sin\varphi\,. \tag{1.125}$$

The quaternion form of this equation is not only Eq.(1.114), but also the simpler equation

$$(0\,,\,\mathbf{r}^*) = (\cos\varphi\,,\,\mathbf{n}\sin\varphi)(0\,,\,\mathbf{r})\,. \tag{1.126}$$

Example: Given two consecutive rotations through identical angles φ about the $\mathbf{e}_1$-axis (first rotation) and about the $\mathbf{e}_3$-axis of a basis $\underline{\mathbf{e}}$, determine the resultant rotation $(\mathbf{n}_{\rm res},\varphi_{\rm res})$ for $\varphi = 180^\circ$ (a) and for $\varphi = 90^\circ$ (b).
Solutions are calculated from (1.117).
Problem (a): $\mathbf{n}_{\rm res} = \mathbf{e}_2\,,\quad \varphi_{\rm res} = 180^\circ\,,$
Problem (b): $\mathbf{n}_{\rm res} = (\sqrt{3}/3)(\mathbf{e}_1+\mathbf{e}_2+\mathbf{e}_3)\,,\quad \varphi_{\rm res} = 60^\circ$. End of example.

1.9 Relationships Between Three Positions of a Body

New notations: In what follows, the axial unit vector and the angle of rotation from a position i into a position $j \neq i$ are denoted $\mathbf{n}_{ij}$ and φ_{ij}, respectively. Thus, two rotations and the resultant of these two, up to now called $(\mathbf{n}_1,\varphi_1)$, $(\mathbf{n}_2,\varphi_2)$ and $(\mathbf{n}_{\rm res},\varphi_{\rm res})$, respectively, are henceforth denoted $(\mathbf{n}_{12},\varphi_{12})$, $(\mathbf{n}_{23},\varphi_{23})$ and $(\mathbf{n}_{13},\varphi_{13})$, respectively. Define $\mathbf{n}_{31} = \mathbf{n}_{13}$ and $\varphi_{31} = -\varphi_{13}$. The rotation $(\mathbf{n}_{31},\varphi_{31})$ is the inverse of the resultant rotation $(\mathbf{n}_{13},\varphi_{13})$. The three rotations $(\mathbf{n}_{12},\varphi_{12})$, $(\mathbf{n}_{23},\varphi_{23})$, $(\mathbf{n}_{31},\varphi_{31})$ executed in this order or in any order produced by cyclic permutation carry a body via two intermediate positions back into its initial position. Equations (1.118) and (1.119) establish the relationships

$$\cos\frac{\varphi_{31}}{2} = \cos\frac{\varphi_{23}}{2}\cos\frac{\varphi_{12}}{2} - \mathbf{n}_{23}\cdot\mathbf{n}_{12}\sin\frac{\varphi_{23}}{2}\sin\frac{\varphi_{12}}{2}\,, \tag{1.127}$$

$$\begin{aligned}-\mathbf{n}_{31}\sin\frac{\varphi_{31}}{2} &= \mathbf{n}_{12}\cos\frac{\varphi_{23}}{2}\sin\frac{\varphi_{12}}{2} + \mathbf{n}_{23}\cos\frac{\varphi_{12}}{2}\sin\frac{\varphi_{23}}{2}\\ &\quad + \mathbf{n}_{23}\times\mathbf{n}_{12}\sin\frac{\varphi_{23}}{2}\sin\frac{\varphi_{12}}{2}\,.\end{aligned} \tag{1.128}$$

In the first equation $\mathbf{n}_{23} \cdot \mathbf{n}_{12} = \cos\alpha_2$ is written. The index 2 of α_2 is common to both vectors. Every equation remains valid after cyclic permutation of the indices $1, 2, 3$. In the three Eqs.(1.127) the cosine law for the spherical triangle $(\mathrm{P}_{12},\mathrm{P}_{23},\mathrm{P}_{31})$ shown in Fig. 1.6 is recognized. Its vertices are the tips of the vectors $\mathbf{n}_{12}$, $\mathbf{n}_{23}$, $\mathbf{n}_{31}$. Its sides 1, 2, 3 have lengths α_1, α_2, α_3. The internal angles are semi-rotation angles. Since rotation angles differing by 2π are considered as equal, the sign convention is as follows: $\varphi_{ij}/2$ $(i, j = 1, 2, 3)$ is the internal and also the external angle from side i to side j. These results are summarized in

Theorem 1.5. *Three consecutive rotations about axes pointing from* 0 *to the vertices of a spherical triangle* $(\mathrm{P}_{12},\mathrm{P}_{23},\mathrm{P}_{31})$ *and through angles equal to twice the internal or external angles of the triangle carry a body via two intermediate positions back into its initial position. The triangle is called rotation triangle.*

The theorem is illustrated in Fig. 1.7. For the sake of simplicity, the rotation triangle $(\mathrm{P}_{12},\mathrm{P}_{23},\mathrm{P}_{31})$ is drawn as planar triangle. Consider the symmetrically located (spherical) triangle $(\mathrm{P}_{12},\mathrm{P}^*_{23},\mathrm{P}_{31})$. After the first rotation $(\mathbf{n}_{12}, \varphi_{12})$ about P_{12} it has the position $(\mathrm{P}_{12},\mathrm{P}_{23},\mathrm{P}^*_{31})$ shown by dotted lines. After the second rotation $(\mathbf{n}_{23}, \varphi_{23})$ about P_{23} it is in the position $(\mathrm{P}^*_{12},\mathrm{P}_{23},\mathrm{P}_{31})$. The same position is produced by the resultant rotation $(\mathbf{n}_{13}, \varphi_{13})$ about P_{31} with $\varphi_{13}/2$ being the external angle of the rotation triangle $(\mathrm{P}_{12},\mathrm{P}_{23},\mathrm{P}_{31})$. The internal angle at P_{31} equals $\varphi_{31}/2 = \pi - \varphi_{13}/2 = (2\pi - \varphi_{13})/2$. This is the statement made by the theorem.

Remark: In the case of nearly parallel rotation axes, the spherical triangle is a nearly planar triangle in a plane tangent to the sphere. All statements remain valid also in the limiting case of parallel rotation axes. In this case, the center 0 of the sphere is at infinity, and the triangle is a planar triangle. This special case is considered in Sect. 14.4. There, the triangle is called pole triangle.

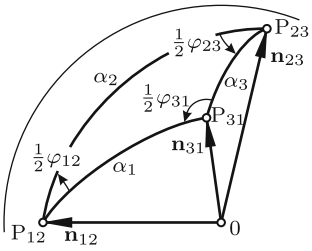

Fig. 1.6 Spherical rotation triangle

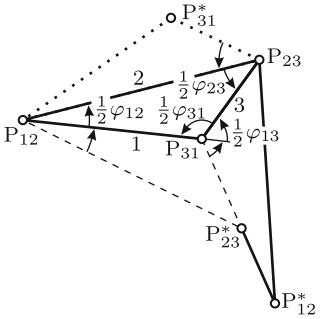

Fig. 1.7 Angles in the rotation triangle

Through (1.77) the Rodrigues vector $\mathbf{n}_{ij} \tan \varphi_{ij}/2$ of the rotation $(\mathbf{n}_{ij}, \varphi_{ij})$ was introduced. It is abbreviated $\mathbf{u}_{ij}$. Division of (1.128) through (1.127) establishes the relationship

$$\mathbf{u}_{31} = -\frac{\mathbf{u}_{12} + \mathbf{u}_{23} - \mathbf{u}_{12} \times \mathbf{u}_{23}}{1 - \mathbf{u}_{12} \cdot \mathbf{u}_{23}} \,. \tag{1.129}$$

An alternative expression for $\mathbf{u}_{31}$ is derived from the spherical triangle in Fig. 1.6. Scalar multiplication of (1.128) by $(\mathbf{n}_{23} \times \mathbf{n}_{12})$ yields

$$\mathbf{n}_{12} \times \mathbf{n}_{23} \cdot \mathbf{n}_{31} = \sin \frac{\varphi_{12}}{2} \, \sin \frac{\varphi_{23}}{2} \, \sin \frac{\varphi_{31}}{2} \, \frac{\sin^2 \alpha_2}{\sin^2 \frac{\varphi_{31}}{2}} \tag{1.130}$$

or, with the sine law

$$\frac{\sin \frac{\varphi_{12}}{2}}{\sin \alpha_3} = \frac{\sin \frac{\varphi_{23}}{2}}{\sin \alpha_1} = \frac{\sin \frac{\varphi_{31}}{2}}{\sin \alpha_2} \,, \tag{1.131}$$

$$\mathbf{n}_{12} \times \mathbf{n}_{23} \cdot \mathbf{n}_{31} = \sin \alpha_1 \, \sin \alpha_3 \, \sin \frac{\varphi_{31}}{2} \,. \tag{1.132}$$

The cosine law states that

$$\begin{aligned} &\sin \alpha_1 \, \sin \alpha_3 \, \cos \frac{\varphi_{31}}{2} = \cos \alpha_2 - \cos \alpha_1 \, \cos \alpha_3 \\ &= \mathbf{n}_{12} \cdot \mathbf{n}_{23} - (\mathbf{n}_{12} \cdot \mathbf{n}_{31})(\mathbf{n}_{23} \cdot \mathbf{n}_{31}) = (\mathbf{n}_{12} \times \mathbf{n}_{31}) \cdot (\mathbf{n}_{23} \times \mathbf{n}_{31}) \,. \end{aligned} \tag{1.133}$$

This equation in combination with (1.132) yields

$$\tan \frac{\varphi_{31}}{2} = \frac{\mathbf{n}_{12} \times \mathbf{n}_{23} \cdot \mathbf{n}_{31}}{(\mathbf{n}_{12} \times \mathbf{n}_{31}) \cdot (\mathbf{n}_{23} \times \mathbf{n}_{31})} \,. \tag{1.134}$$

Multiplication with $\mathbf{n}_{31}$ produces for the Rodrigues vector $\mathbf{u}_{31}$ the formula

$$\mathbf{n}_{31} \, \tan \frac{\varphi_{31}}{2} = \frac{(\mathbf{n}_{12} \times \mathbf{n}_{31}) \times (\mathbf{n}_{23} \times \mathbf{n}_{31})}{(\mathbf{n}_{12} \times \mathbf{n}_{31}) \cdot (\mathbf{n}_{23} \times \mathbf{n}_{31})} \,. \tag{1.135}$$

In contrast to (1.129) $\mathbf{n}_{31}$ appears on both sides of the equation. Equations (1.128) – (1.135) remain valid after cyclic permutation of the indices.

1.10 Relationships Between four Positions

Two positions determine a rotation, and three positions determine a rotation triangle. Hence four positions determine altogether six rotations and four rotation triangles. All relative positions are known if the positions 2, 3 and 4 relative to position 1 are known. These three relative positions are de-

termined by altogether nine parameters, namely, two spherical coordinates for each of the three vertices P_{1k} (identical with P_{k1}) and the rotation angles φ_{1k} $(k = 2, 3, 4)$. In each rotation triangle the axes and the semi-rotation angles are related according to Fig. 1.6. Every vertex is vertex in two triangles. The reason is that for any two triples of positions i, j, k and i, j, ℓ $(i, j, k, \ell = 1, 2, 3, 4$ different) the corresponding rotation triangles $(\mathrm{P}_{ij},\mathrm{P}_{jk},\mathrm{P}_{ki})$ and $(\mathrm{P}_{ij},\mathrm{P}_{j\ell},\mathrm{P}_{\ell i})$ are sharing the vertex P_{ij}. In both triangles the angle $\varphi_{ij}/2$ occurs at P_{ij} either as internal or as external angle. Figure 1.8a illustrates the case when it is the internal angle and Fig. 1.8b the case when it is the external angle. Equation (1.134) yields for $\tan\varphi_{ij}/2$ in the triangle $(\mathrm{P}_{ij},\mathrm{P}_{jk},\mathrm{P}_{ki})$ the first expression below and in the triangle $(\mathrm{P}_{ij},\mathrm{P}_{j\ell},\mathrm{P}_{\ell i})$ the second expression:

$$\tan\frac{\varphi_{ij}}{2} = \frac{\mathbf{n}_{ij}\cdot\mathbf{n}_{jk}\times\mathbf{n}_{ki}}{(\mathbf{n}_{ij}\times\mathbf{n}_{jk})\cdot(\mathbf{n}_{ij}\times\mathbf{n}_{ki})}\,, \qquad \tan\frac{\varphi_{ij}}{2} = \frac{\mathbf{n}_{ij}\cdot\mathbf{n}_{j\ell}\times\mathbf{n}_{\ell i}}{(\mathbf{n}_{ij}\times\mathbf{n}_{j\ell})\cdot(\mathbf{n}_{ij}\times\mathbf{n}_{\ell i})} \tag{1.136}$$

$(i, j, k, \ell = 1, 2, 3, 4$ different) . In each of the figures the vertices P_{ik}, P_{kj}, $\mathrm{P}_{j\ell}$, $\mathrm{P}_{\ell i}$ define the quadrilateral $(\mathrm{P}_{ik},\mathrm{P}_{kj},\mathrm{P}_{j\ell},\mathrm{P}_{\ell i})$. Each side of the quadrilateral connects two vertices having one index in common. Diametrically opposite vertices have no index in common. In both figures the opposite sides $\overline{\mathrm{P}_{jk}\mathrm{P}}_{ki}$ and $\overline{\mathrm{P}_{j\ell}\mathrm{P}}_{\ell i}$ of the quadrilateral are seen from P_{ij} under angles which are either equal or which add up to π. From P_{ij} also the opposite sides $\overline{\mathrm{P}_{ki}\mathrm{P}}_{\ell i}$ and $\overline{\mathrm{P}_{jk}\mathrm{P}}_{j\ell}$ are seen under angles which are either equal or which add up to π. It is a trivial statement that a side is seen from its endpoint under an arbitrary angle. Therefore, also the following is true. From every vertex of the quadrilateral each pair of opposite sides is seen under angles which are either equal or which add up to π.

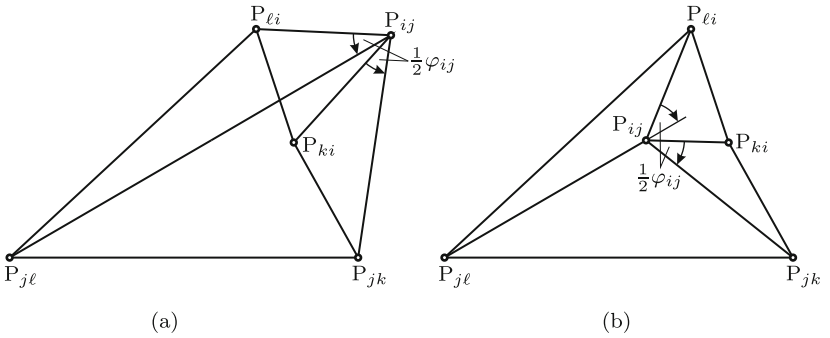

Fig. 1.8 Rotation triangles $(\mathrm{P}_{ij},\mathrm{P}_{jk},\mathrm{P}_{ki})$ and $(\mathrm{P}_{ij},\mathrm{P}_{j\ell},\mathrm{P}_{\ell i})$ and quadrilateral $(\mathrm{P}_{ik},\mathrm{P}_{kj},\mathrm{P}_{j\ell},\mathrm{P}_{\ell i})$. The vertex P_{ij} common to both triangles lies either outside **(a)** or inside **(b)** the quadrilateral

The altogether six vertices are forming three quadrilaterals, namely, $(\mathrm{P}_{12},\mathrm{P}_{23},\mathrm{P}_{34},\mathrm{P}_{41})$, $(\mathrm{P}_{13},\mathrm{P}_{32},\mathrm{P}_{24},\mathrm{P}_{41})$ and $(\mathrm{P}_{12},\mathrm{P}_{24},\mathrm{P}_{43},\mathrm{P}_{31})$. From every vertex every pair of opposite sides of every quadrilateral appears under angles which are either equal or which add up to π.

In what follows, it is assumed that of the altogether six vertices only the vertices of a single quadrilateral $(\mathrm{P}_{ik},\mathrm{P}_{kj},\mathrm{P}_{j\ell},\mathrm{P}_{\ell i})$ are given. It is natural to ask for all axial unit vectors $\mathbf{n}$ having the property that from the tip of $\mathbf{n}$ opposite sides of the given quadrilateral appear under angles which are either equal or which add up to π. The solution is found as follows. The vector $\mathbf{n}$ must satisfy the condition that the two expressions given in (1.136), but with $\mathbf{n}$ replacing $\mathbf{n}_{ij}$, are identical. This is the conditional equation

$$(\mathbf{n}\cdot\mathbf{n}_{jk}\times\mathbf{n}_{ki})[(\mathbf{n}\times\mathbf{n}_{j\ell})\cdot(\mathbf{n}\times\mathbf{n}_{\ell i})] = (\mathbf{n}\cdot\mathbf{n}_{j\ell}\times\mathbf{n}_{\ell i})[(\mathbf{n}\times\mathbf{n}_{jk})\cdot(\mathbf{n}\times\mathbf{n}_{ki})] \quad (1.137)$$

$(i,j,k,\ell = 1,2,3,4$ different$)$. It is a third-order equation for $\mathbf{n}$. All vectors $\mathbf{n}$ satisfying the equation determine a third-order cone with the apex at 0. It is called *rotation cone*. Equation (1.137) is satisfied by the four vectors $\mathbf{n}=\mathbf{n}_{jk}$, $\mathbf{n}=\mathbf{n}_{ki}$, $\mathbf{n}=\mathbf{n}_{j\ell}$ and $\mathbf{n}=\mathbf{n}_{\ell i}$. As fifth vector $\mathbf{n}_{ij}$ any generator of the rotation cone can be chosen which is not one of these four vectors. With this vector $\mathbf{n}_{ij}$ all rotation triangles on the sphere are determined and with them all rotation angles and also the sixth vector $\mathbf{n}_{k\ell}$. This vector, too, is located on the rotation cone.

The four-position theory just described is due to Roth [27]. Details see in Sects. 3.12 and 7.3. Roth' theory generalizes Burmester's planar four-position theory. This planar theory is the subject of Sect. 14.5.

1.11 Cayley-Klein Parameters

This section starts out from (1.15) relating the coordinates of a body-fixed vector in positions $\mathbf{r}$ and $\mathbf{r}^*$ which are related by a direction cosine matrix $\underline{A}^{12}$ (see Fig. 1.3). The matrix is expressed in terms of Euler-Rodrigues parameters (see (1.79)):

$$\underline{r}^* = \underline{A}^{12}\underline{r}\,, \quad (1.138)$$

$$\underline{A}^{12} = \begin{bmatrix} q_0^2+q_1^2-q_2^2-q_3^2 & 2(q_1q_2-q_0q_3) & 2(q_1q_3+q_0q_2) \\ 2(q_1q_2+q_0q_3) & q_0^2+q_2^2-q_3^2-q_1^2 & 2(q_2q_3-q_0q_1) \\ 2(q_1q_3-q_0q_2) & 2(q_2q_3+q_0q_1) & q_0^2+q_3^2-q_1^2-q_2^2 \end{bmatrix}. \quad (1.139)$$

New complex-valued parameters α and β are defined by the equations

$$\alpha = q_0 + \mathrm{i}\,q_3\,, \qquad \beta = -q_2 + \mathrm{i}\,q_1\,. \quad (1.140)$$

These parameters are referred to as *Cayley-Klein parameters*. The inverse rotation has the Euler-Rodrigues parameters q_0, $-q_1$, $-q_2$, $-q_3$ and, con-

sequently, the Cayley-Klein parameters $\bar{\alpha}$ (complex conjugate) and $-\beta$. The Cayley-Klein parameters corresponding to the null rotation ($q_0 = 1,\ q_1 = q_2 = q_3 = 0$) are $\alpha = 1,\ \beta = 0$. Equations (1.140) yield for the Euler-Rodrigues parameters the expressions

$$q_0 = \frac{1}{2}(\alpha + \bar{\alpha})\,, \quad q_3 = -\frac{\mathrm{i}}{2}(\alpha - \bar{\alpha})\,, \quad q_2 = -\frac{1}{2}(\beta + \bar{\beta})\,, \quad q_1 = -\frac{\mathrm{i}}{2}(\beta - \bar{\beta})\,. \tag{1.141}$$

With these expressions the matrix $\underline{A}^{12}$ is a function of α and β.

With the real vector coordinates r_i $(i = 1, 2, 3)$ of (1.138) new complex-valued coordinates are defined as follows:

$$\varrho_1 = r_1 + \mathrm{i}\, r_2\,, \qquad \varrho_2 = -r_1 + \mathrm{i}\, r_2\,, \qquad \varrho_3 = -r_3\,. \tag{1.142}$$

By the same equations the coordinates r_i^* $(i = 1, 2, 3)$ define new coordinates ϱ_1^*, ϱ_2^*, ϱ_3^*. The matrix forms of these definitions are

$$\underline{\varrho}^* = \underline{C}\,\underline{r}^*\,, \quad \underline{\varrho} = \underline{C}\,\underline{r}\,, \qquad \underline{C} = \begin{bmatrix} 1 & \mathrm{i} & 0 \\ -1 & \mathrm{i} & 0 \\ 0 & 0 & -1 \end{bmatrix}, \quad \underline{C}^{-1} = \frac{1}{2}\begin{bmatrix} 1 & -1 & 0 \\ -\mathrm{i} & -\mathrm{i} & 0 \\ 0 & 0 & -2 \end{bmatrix}. \tag{1.143}$$

With these expressions (1.138) becomes

$$\underline{\varrho}^* = \underline{C}\,\underline{A}^{12}\underline{C}^{-1}\underline{\varrho}\,. \tag{1.144}$$

Multiplying out results in the equation

$$\underline{\varrho}^* = \begin{bmatrix} \alpha^2 & \beta^2 & 2\alpha\beta \\ \bar{\beta}^2 & \bar{\alpha}^2 & -2\bar{\alpha}\bar{\beta} \\ -\alpha\bar{\beta} & \bar{\alpha}\beta & \alpha\bar{\alpha} - \beta\bar{\beta} \end{bmatrix} \underline{\varrho}\,. \tag{1.145}$$

This equation is simpler than its real counterpart (1.138). Of course, the coefficient matrix is not orthogonal, because ϱ_1, ϱ_2, ϱ_3 are not coordinates in a cartesian coordinate system. However, the inverse matrix is simple. It is the matrix associated with the inverse rotation which has the parameters $(\bar{\alpha}, -\beta)$ instead of (α, β).

Substitution of Eqs.(1.141) into the constraint equation $q_0^2+q_1^2+q_2^2+q_3^2 = 1$ for Euler-Rodrigues parameters yields the corresponding constraint equation for Cayley-Klein parameters:

$$\alpha\bar{\alpha} + \beta\bar{\beta} = 1\,. \tag{1.146}$$

The expression on the left-hand side is the determinant of the matrix

$$\underline{U} = \begin{bmatrix} \alpha & \beta \\ -\bar{\beta} & \bar{\alpha} \end{bmatrix}. \tag{1.147}$$

(2×2)-matrices of this form with determinant 1 constitute a group with respect to multiplication. Indeed, it is easily verified that the product of two such matrices $\underline{U}_1$ and $\underline{U}_2$ is itself an element of the group. The multiplication is associative. The unit element of the group is the unit matrix $\underline{I}$ which corresponds to the null rotation. For every element $\underline{U}$ of the group the inverse element exists, namely, the matrix associated with the inverse rotation. This is the transpose of the complex conjugate matrix. It is denoted $\bar{\underline{U}}^T$. Indeed, the product of the two equals the unit matrix:

$$\underline{U}\bar{\underline{U}}^T = \bar{\underline{U}}^T\underline{U} = \begin{bmatrix} \bar{\alpha} & -\beta \\ \bar{\beta} & \alpha \end{bmatrix} \begin{bmatrix} \alpha & \beta \\ -\bar{\beta} & \bar{\alpha} \end{bmatrix} = \underline{I}\,. \tag{1.148}$$

Matrices having these properties are called unitary matrices. The group is denoted SU(2) with U for unitary.

The definitions in Eqs.(1.140) yield for $\underline{U}$ the expression

$$\underline{U} = q_0\underline{S}_0 + q_1\underline{S}_1 + q_2\underline{S}_2 + q_3\underline{S}_3 \tag{1.149}$$

with the so-called Pauli spin matrices (see [24])

$$\underline{S}_0 = \underline{I}\,, \quad \underline{S}_1 = \begin{bmatrix} 0 & \mathrm{i} \\ \mathrm{i} & 0 \end{bmatrix}\,, \quad \underline{S}_2 = \begin{bmatrix} 0 & -1 \\ 1 & 0 \end{bmatrix}\,, \quad \underline{S}_3 = \begin{bmatrix} \mathrm{i} & 0 \\ 0 & -\mathrm{i} \end{bmatrix}\,. \tag{1.150}$$

The matrices satisfy the equations

$$\left.\begin{array}{ll} \underline{S}_j\underline{S}_0 = \quad \underline{S}_0\underline{S}_j = \underline{S}_j\,, & \underline{S}_j\underline{S}_j = -\underline{S}_0 \qquad (j = 1,2,3)\,, \\ \underline{S}_j\underline{S}_k = -\underline{S}_k\underline{S}_j = \underline{S}_\ell & (j,k,\ell = 1,2,3 \ \text{ cyclic})\,. \end{array}\right\} \tag{1.151}$$

In addition, the constraint equation is satisfied:

$$\sum_{j=0}^{3} q_j^2\underline{S}_j\underline{S}_j = \underline{I}\,. \tag{1.152}$$

Equations (1.149) and (1.151) are formally identical with (1.99) and (1.100), respectively. This identity proves

Theorem 1.6. *The resultant of two rotations with matrices $\underline{U}_1$ (first rotation) and $\underline{U}_2$ is characterized by the Cayley-Klein parameters of the unitary matrix*

$$\underline{U}_{\mathrm{res}} = \underline{U}_2\underline{U}_1\,. \tag{1.153}$$

This equation expresses in terms of complex-valued quantities what (1.116) expresses in terms of real-valued quantities. Equation (1.153) has the form (1.148) if the second rotation is the inverse of the first rotation.

In what follows, another proof of the theorem is given. Let $\underline{H}$ be the matrix $\underline{H} = r_1\underline{S}_1 + r_2\underline{S}_2 + r_3\underline{S}_3$ with the coordinates of $\underline{r}$ in (1.138). The

same formula with the coordinates of $\underline{r}^*$ defines the matrix $\underline{H}^*$. With the help of (1.150) and (1.142) the matrices are shown to be

$$\underline{H} = \begin{bmatrix} \mathrm{i}\, r_3 & \mathrm{i}\, r_1 - r_2 \\ \mathrm{i}\, r_1 + r_2 & -\mathrm{i}\, r_3 \end{bmatrix} = \mathrm{i} \begin{bmatrix} \varrho_3 & -\varrho_1 \\ \varrho_2 & -\varrho_3 \end{bmatrix} , \quad \underline{H}^* = \mathrm{i} \begin{bmatrix} \varrho_3^* & -\varrho_1^* \\ \varrho_2^* & -\varrho_3^* \end{bmatrix} . \tag{1.154}$$

These matrices satisfy the equation

$$\underline{H}^* = \underline{U}\, \underline{H}\, \bar{\underline{U}}^T \tag{1.155}$$

with the matrix $\underline{U}$ from (1.147). This is verified by multiplying out and by comparing with (1.145). Let now $\underline{U}_1$ and $\underline{U}_2$ be the matrices of two successive rotations. Then the first rotation yields $\underline{H}^* = \underline{U}_1\, \underline{H}\, \bar{\underline{U}}_1^T$. The second rotation yields

$$\underline{H}^{**} = \underline{U}_2\, \underline{H}^*\, \bar{\underline{U}}_2^T = \underline{U}_2 \Big(\underline{U}_1\, \underline{H}\, \bar{\underline{U}}_1^T \Big)\, \bar{\underline{U}}_2^T = (\underline{U}_2 \underline{U}_1)\, \underline{H}\, (\bar{\underline{U}}_2\, \bar{\underline{U}}_1)^T . \tag{1.156}$$

This proves (1.153).

In what follows, still another relationship between the vectors $\mathbf{r}$ and $\mathbf{r}^*$ is developed (Klein/Sommerfeld [12]). Without loss of generality, the vectors are assumed to be unit vectors. They are represented by points on the unit sphere centered at the origin of basis $\underline{\mathbf{e}}^1$ (Fig. 1.9). The $\mathbf{e}_1^1, \mathbf{e}_2^1$-plane is referred to as equatorial plane and the tip of $\mathbf{e}_3^1$ as north pole. Both points are projected from the north pole onto the equatorial plane by a so-called stereographic projection (see the dashed lines). Projections of points in the northern hemisphere (in the southern hemisphere) lie outside (inside) the unit circle. The projections of $\mathbf{r}$ and $\mathbf{r}^*$ are denoted z and z^*, respectively. They are interpreted as numbers $z = z_1 + \mathrm{i}\, z_2$ and $z^* = z_1^* + \mathrm{i}\, z_2^*$ in the complex equatorial plane with $\mathbf{e}_1^1$ being the real axis and with $\mathbf{e}_2^1$ being the imaginary axis[3]. From the similarity of triangles it follows that

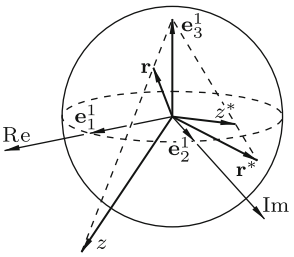

Fig. 1.9 Stereographic projection from the north pole onto the equatorial plane

$z = (r_1 + \mathrm{i}\, r_2)/(1 - r_3) = \varrho_1/(\varrho_3 + 1)$. For z also the following representation is possible. The equation $r_1^2 + r_2^2 = 1 - r_3^2$ is written in the form $(r_1 + \mathrm{i}\, r_2)(r_1 - \mathrm{i}\, r_2) = (1 + r_3)(1 - r_3)$ and, because of (1.142), in the form $\varrho_1 \varrho_2 = (\varrho_3 + 1)(\varrho_3 - 1)$. Hence $\varrho_2/(\varrho_3 - 1) = (\varrho_3 + 1)/\varrho_1 = 1/z$. The same relationships are valid for the quantities bearing the asterisk. Only the following relationships are used:

$$\varrho_1 = z(\varrho_3 + 1)\,, \qquad \varrho_2 = \frac{1}{z}\,(\varrho_3 - 1)\,, \qquad z^* = \frac{\varrho_1^*}{\varrho_3^* + 1}\,. \tag{1.157}$$

In the third equation ϱ_1^* and ϱ_3^* are replaced by the expressions from (1.145). Furthermore, the unit in the denominator is replaced by the expression $\alpha\bar{\alpha} + \beta\bar{\beta}$ (see (1.146)). This results in the equation

$$\begin{aligned} z^* &= \frac{\alpha^2\varrho_1 + \beta^2\varrho_2 + 2\alpha\beta\varrho_3}{-\alpha\bar{\beta}\varrho_1 + \bar{\alpha}\beta\varrho_2 + (\alpha\bar{\alpha} - \beta\bar{\beta})\varrho_3 + \alpha\bar{\alpha} + \beta\bar{\beta}} \\ &= \frac{\alpha[\alpha\varrho_1 + \beta(\varrho_3 + 1)] + \beta[\beta\varrho_2 + \alpha(\varrho_3 - 1)]}{\alpha[-\bar{\beta}\varrho_1 + \bar{\alpha}(\varrho_3 + 1)] + \beta[\bar{\alpha}\varrho_2 - \bar{\beta}(\varrho_3 - 1)]}\,. \end{aligned} \tag{1.158}$$

For ϱ_1 and ϱ_2 the expressions from (1.157) are substituted. This yields the final equation

$$z^* = \frac{\alpha z + \beta}{-\bar{\beta} z + \bar{\alpha}}\,. \tag{1.159}$$

Thus, z^* is a linear fractional function of z with coefficients which are the elements of the matrix $\underline{U}$. Based on this equation a new proof of (1.153) is given as follows. Let α_1 , β_1 be the Cayley-Klein parameters of the first of two successive rotations and let α_2 , β_2 be the parameters of the second rotation. Let, furthermore z^{**} be the complex number after the second rotation. Then, by these definitions,

$$z^* = \frac{\alpha_1 z + \beta_1}{-\bar{\beta}_1 z + \bar{\alpha}_1}\,, \qquad z^{**} = \frac{\alpha_2 z^* + \beta_2}{-\bar{\beta}_2 z^* + \bar{\alpha}_2}\,. \tag{1.160}$$

Substitution of the first expression into the second yields for z^{**} a linear fractional function of z with coefficients according to (1.153). End of proof.

[3] Riemann used the inverse of the stereographic projection for projecting the infinite complex plane onto the finite unit sphere. The sphere is called Riemann's sphere or sphere of complex numbers

1.12 Euler Vector. Exponential Form of the Direction Cosine Matrix

The *Euler vector* of a rotation $(\mathbf{n}, \varphi)$ is defined to be the vector $\varphi\mathbf{n}$. In the bases $\mathbf{e}^1$ and $\mathbf{e}^2$ it has identical coordinate matrices $\varphi\underline{n}$. With these coordinates the skew-symmetric matrix $\varphi\tilde{\underline{n}}$ is defined. Proposition: The direction cosine matrix is

$$\underline{A}^{12} = \mathrm{e}^{\varphi\tilde{\underline{n}}} \,. \tag{1.161}$$

Proof: According to (1.37)

$$\underline{A}^{12} = \underline{I} + \tilde{\underline{n}}\,\tilde{\underline{n}}(1 - \cos\varphi) + \tilde{\underline{n}}\sin\varphi \,. \tag{1.162}$$

The exponential function is defined by its Taylor series

$$\mathrm{e}^{\varphi\tilde{\underline{n}}} = \underline{I} + \varphi\tilde{\underline{n}} + \frac{1}{2!}\varphi^2\tilde{\underline{n}}^2 + \frac{1}{3!}\varphi^3\tilde{\underline{n}}^3 + \dots \,. \tag{1.163}$$

All terms $\tilde{\underline{n}}^k$ with $k > 2$ can be expressed either through $\tilde{\underline{n}}$ or through $\tilde{\underline{n}}^2$. This is shown as follows. The vector $\mathbf{n} \times (\mathbf{n} \times \mathbf{r})$ is $\mathbf{n}(\mathbf{n} \cdot \mathbf{r}) - \mathbf{r}$. Therefore, $\mathbf{n} \times [\mathbf{n} \times (\mathbf{n} \times \mathbf{r})] = -\mathbf{n} \times \mathbf{r}$. The coordinate form of this equation is $\tilde{\underline{n}}^3\underline{r} = -\tilde{\underline{n}}\underline{r}$. From this it follows that $\tilde{\underline{n}}^3 = -\tilde{\underline{n}}$ and by continued multiplication: $\tilde{\underline{n}}^4 = -\tilde{\underline{n}}^2$, $\tilde{\underline{n}}^5 = -\tilde{\underline{n}}^3 = \tilde{\underline{n}}$ etc. Equation (1.163) becomes

$$\begin{aligned}
\mathrm{e}^{\varphi\tilde{\underline{n}}} &= \underline{I} + \varphi\tilde{\underline{n}} + \frac{1}{2!}\varphi^2\tilde{\underline{n}}^2 - \frac{1}{3!}\varphi^3\tilde{\underline{n}} - \frac{1}{4!}\varphi^4\tilde{\underline{n}}^2 + \frac{1}{5!}\varphi^5\tilde{\underline{n}} \pm \dots \\
&= \underline{I} + \tilde{\underline{n}}\Big(\varphi - \frac{1}{3!}\varphi^3 + \frac{1}{5!}\varphi^5 \pm \dots\Big) + \tilde{\underline{n}}^2\Big[1 - \Big(1 - \frac{1}{2!}\varphi^2 + \frac{1}{4!}\varphi^4 \mp \dots\Big)\Big] \\
&= \underline{I} + \tilde{\underline{n}}\sin\varphi + \tilde{\underline{n}}\,\tilde{\underline{n}}(1 - \cos\varphi) \,.
\end{aligned} \tag{1.164}$$

This is the expression in (1.162). End of proof.
Caution: In the case of real exponents a and b the formula $\mathrm{e}^a\,\mathrm{e}^b = \mathrm{e}^{a+b}$ is valid. It is this formula which makes the exponential function useful. In the case of matrices $\underline{A}$ and $\underline{B}$ as exponents, the formula $\mathrm{e}^{\underline{A}}\,\mathrm{e}^{\underline{B}} = \mathrm{e}^{\underline{A}+\underline{B}}$ is valid if and only if $\underline{A}\,\underline{B} = \underline{B}\,\underline{A}$. Therefore, the equation

$$\mathrm{e}^{\varphi_1\tilde{\underline{n}}_1}\mathrm{e}^{\varphi_2\tilde{\underline{n}}_2} = \mathrm{e}^{\varphi_1\tilde{\underline{n}}_1 + \varphi_2\tilde{\underline{n}}_2} \tag{1.165}$$

is valid if and only if $\mathbf{n}_1 = \mathbf{n}_2$. This is the trivial case that both rotations are carried out about one and the same axis. If the equation were generally true, the resultant of two successive rotations $(\mathbf{n}_1, \varphi_1)$ and $(\mathbf{n}_2, \varphi_2)$ would be obtained by the parallelogram rule: $\mathbf{n}_{\mathrm{res}}\varphi_{\mathrm{res}} = \mathbf{n}_1\varphi_1 + \mathbf{n}_2\varphi_2$. This is known to be wrong. It is approximately valid if φ_1 and φ_2 are small.

1.13 Rodrigues Vector

Through (1.76) and (1.77) the Rodrigues vector $\mathbf{u}$ of a rotation $(\mathbf{n}, \varphi)$ was introduced:

$$\mathbf{u} = \frac{\mathbf{q}}{q_0} = \mathbf{n} \tan \frac{\varphi}{2} , \tag{1.166}$$

$$\mathbf{r}^* - \mathbf{r} = \mathbf{u} \times (\mathbf{r}^* + \mathbf{r}) . \tag{1.167}$$

The vector $\mathbf{u}$ has identical coordinates in bases $\underline{\mathbf{e}}^1$ and $\underline{\mathbf{e}}^2$. These coordinates are referred to as *Rodrigues parameters*. They are denoted u_1, u_2, u_3. The coordinate matrix is denoted $\underline{u}$, and the absolute value of the vector is denoted u. The coordinates are not subject to any constraint equation. In the critical case $\varphi = \pm\pi$, the absolute value of $\mathbf{u}$ is infinite. In this case, the direction must be given by $\mathbf{n}$. In what follows, it is assumed that $\mathbf{u}$ is finite. From (1.166) it follows that

$$q_0^2 = \cos^2 \frac{\varphi}{2} = \frac{1}{1+u^2} , \qquad \cos\varphi = \frac{1-u^2}{1+u^2} , \qquad \sin\varphi = \frac{2u}{1+u^2} . \tag{1.168}$$

Substitution into (1.40) yields for the rotation tensor the alternative expressions

$$\begin{aligned} \mathsf{R} &= \frac{(1-u^2)\mathsf{I} + 2\mathbf{u}\mathbf{u} + 2\mathbf{u}\times\mathsf{I}}{1+u^2} \\ &= -\mathsf{I} + \frac{2}{1+u^2}\left(\mathsf{I} + \mathbf{u}\mathbf{u} + \mathbf{u}\times\mathsf{I}\right) . \end{aligned} \tag{1.169}$$

Decomposition in basis $\underline{\mathbf{e}}^1$ produces for the direction cosine matrix the alternative expressions

$$\begin{aligned} \underline{A}^{12} &= \frac{1}{1+u^2} \begin{bmatrix} 1+u_1^2-u_2^2-u_3^2 & 2(u_1u_2-u_3) & 2(u_1u_3+u_2) \\ 2(u_1u_2+u_3) & 1+u_2^2-u_3^2-u_1^2 & 2(u_2u_3-u_1) \\ 2(u_1u_3-u_2) & 2(u_2u_3+u_1) & 1+u_3^2-u_1^2-u_2^2 \end{bmatrix} \\ &= -\underline{I} + \frac{2}{1+u^2} \begin{bmatrix} 1+u_1^2 & u_1u_2-u_3 & u_1u_3+u_2 \\ u_1u_2+u_3 & 1+u_2^2 & u_2u_3-u_1 \\ u_1u_3-u_2 & u_2u_3+u_1 & 1+u_3^2 \end{bmatrix} . \end{aligned} \tag{1.170}$$

If the matrix $\underline{A}^{12}$ is given, the Rodrigues parameters are obtained most easily by first calculating the Euler-Rodrigues parameters q_0, q_1, q_2, q_3 from (1.81) and (1.82) and by substituting them into (1.166):

$$\underline{\tilde{u}} = \frac{\underline{\tilde{q}}}{q_0} = \frac{\underline{A}^{12} - \underline{A}^{12^T}}{1 + \operatorname{tr} \underline{A}^{12}} . \tag{1.171}$$

The same result is obtained as follows. The diagonal elements of the matrix yield the first equation below, and the off-diagonal elements yield the second.

$$1 + \operatorname{tr} \underline{A}^{12} = \frac{4}{1+u^2} \,, \qquad \underline{A}^{12} - \underline{A}^{12^T} = \frac{4}{1+u^2}\, \tilde{\underline{u}} \,. \tag{1.172}$$

Combination of these equations yields (1.171).

Proposition: Alternative expressions for $\tilde{\underline{u}}$ are

$$\tilde{\underline{u}} = \begin{cases} (\underline{A}^{12} - \underline{I})(\underline{A}^{12} + \underline{I})^{-1} \,, \\ (\underline{A}^{12} + \underline{I})^{-1}(\underline{A}^{12} - \underline{I}) \,, \\ \underline{I} - 2(\underline{A}^{12} + \underline{I})^{-1} \,. \end{cases} \tag{1.173}$$

Proof: Decomposition of (1.167) in basis $\mathbf{e}^1$ yields, in view of (1.15), $(\underline{A}^{12} - \underline{I})\underline{r}^1 = \tilde{\underline{u}}(\underline{A}^{12} + \underline{I})\underline{r}^1$ and, consequently, the first Eq.(1.173). Using (1.10) it is shown that the matrix $\underline{A}^{12} + \underline{I}$ has the determinant $2(1 + \operatorname{tr} \underline{A}^{12})$ and the co-factors $c_{11} = c_{22} = c_{33} = 1 + \operatorname{tr} \underline{A}^{12}$, $c_{ij} = a^{12}_{ij} - a^{12}_{ji}$ $(i, j = 1, 2, 3 \,; j \neq i \,)$. Hence

$$(\underline{A}^{12} + \underline{I})^{-1} = \frac{1}{2}\left(\underline{I} - \frac{\underline{A}^{12} - \underline{A}^{12^T}}{1 + \operatorname{tr} \underline{A}^{12}}\right) = \frac{1}{2}(\underline{I} - \tilde{\underline{u}}) \,. \tag{1.174}$$

Resolving this equation for $\tilde{\underline{u}}$ results in the third Eq.(1.173). Finally, substitution into the first Eq.(1.173) produces $2\tilde{\underline{u}} = (\underline{A}^{12} - \underline{I})(\underline{I} - \tilde{\underline{u}})$. Resolving this equation for $\tilde{\underline{u}}$ results in the second Eq.(1.173) which shows that the product on the right-hand side is commutative. End of proof. For numerical evaluations (1.171) is preferable.

Multiplication of (1.174) with $(\underline{A}^{12} + \underline{I})$ reveals the formula

$$\underline{A}^{12}\underline{A}^{12} = \operatorname{tr} \underline{A}^{12}(\underline{A}^{12} - \underline{I}) + \underline{A}^{12^T} \,. \tag{1.175}$$

In contrast to the previous equations, this equation is valid also in the case $\varphi = 180^\circ$ when $\operatorname{tr} \underline{A}^{12} = -1$ and $\underline{A}^{12^T} = \underline{A}^{12}$. Through continued multiplication with $\underline{A}^{12}$ all powers $(\underline{A}^{12})^n$ $(n \geq 2)$ are expressed as linear combinations of $\underline{A}^{12}$, $\underline{A}^{12^T}$ and $\underline{I}$.

For the Rodrigues vector $\mathbf{u}_{\text{res}}$ of the resultant of two consecutive rotations with Rodrigues vectors $\mathbf{u}_1$ (first rotation) and $\mathbf{u}_2$ division of (1.119) through (1.118) yields

$$\mathbf{u}_{\text{res}} = \frac{\mathbf{u}_1 + \mathbf{u}_2 - \mathbf{u}_1 \times \mathbf{u}_2}{1 - \mathbf{u}_1 \cdot \mathbf{u}_2} \,. \tag{1.176}$$

This is known from (1.129) where $\mathbf{u}_{31}$ is $-\mathbf{u}_{\text{res}}$. In the special case of mutually orthogonal rotation axes 1 and 2 the equation is

$$\mathbf{u}_{\text{res}} = \mathbf{u}_1 + \mathbf{u}_2 - \mathbf{u}_1 \times \mathbf{u}_2 \,, \tag{1.177}$$

whence it follows that

$$\tan^2 \frac{\varphi_{\text{res}}}{2} = \tan^2 \frac{\varphi_1}{2} + \tan^2 \frac{\varphi_2}{2} + \tan^2 \frac{\varphi_1}{2} \tan^2 \frac{\varphi_2}{2} \,. \tag{1.178}$$

The quaternion Eq.(1.118) yields the simpler formula

$$\cos \frac{\varphi_{\text{res}}}{2} = \cos \frac{\varphi_1}{2} \cos \frac{\varphi_2}{2} \,. \tag{1.179}$$

Final remark: The Rodrigues vector $\mathbf{u}$ can be expressed in terms of unit basis vectors. For this purpose (1.166) is written in the form

$$\mathbf{u} = \frac{2\mathbf{n} \sin \varphi}{4 \cos^2 \varphi/2} = \frac{2\mathbf{n} \sin \varphi}{4q_0^2} = \frac{2\mathbf{n} \sin \varphi}{1 + \operatorname{tr} \underline{A}^{12}} \,. \tag{1.180}$$

Hence with (1.56) and (1.58)

$$\mathbf{u} = \frac{\sum_{i=1}^{3} \mathbf{e}_i^1 \times \mathbf{e}_i^2}{1 + \sum_{i=1}^{3} \mathbf{e}_i^1 \cdot \mathbf{e}_i^2} \,. \tag{1.181}$$

1.14 Wiener Vector

The Wiener vector $\boldsymbol{\sigma}$ of a rotation $(\mathbf{n}, \varphi)$ is a modified Rodrigues vector (see Wiener [31], Milenkovic [18]). It is defined as follows:

$$\boldsymbol{\sigma} = \mathbf{n} \tan \frac{\varphi}{4} \,. \tag{1.182}$$

It has identical coordinates in the bases $\underline{\mathbf{e}}^1$ and $\underline{\mathbf{e}}^2$. These coordinates are referred to as Wiener parameters. They are denoted σ_1, σ_2, σ_3. The coordinate matrix is denoted $\underline{\sigma}$, and the absolute value of the vector is denoted σ. The coordinates are not subject to any constraint equation. Relationships with Euler-Rodrigues parameters are expressed by the formulas

$$\left.\begin{aligned} \boldsymbol{\sigma} = \mathbf{n} \tan \frac{\varphi}{4} \quad &= \mathbf{n} \frac{\sin \frac{\varphi}{2}}{1 + \cos \frac{\varphi}{2}} = \frac{\mathbf{q}}{1 + q_0} \,, \\ q_0 = \cos \frac{\varphi}{2} \quad &= \frac{1 - \tan^2 \frac{\varphi}{4}}{1 + \tan^2 \frac{\varphi}{4}} = \frac{1 - \sigma^2}{1 + \sigma^2} \,, \\ \mathbf{q} \;= \frac{2\boldsymbol{\sigma}}{1 + \sigma^2} \,. & \end{aligned}\right\} \tag{1.183}$$

The relationship between Wiener vector and Rodrigues vector is

$$\mathbf{u} = \frac{\boldsymbol{\sigma}}{\sigma_0} , \qquad \sigma_0 = \frac{q_0}{1+q_0} = \frac{1}{2}(1-\sigma^2) . \tag{1.184}$$

The rotations $(\mathbf{n}, \varphi)$ and $(-\mathbf{n}, -\varphi + 2\pi)$ are equivalent, and the Euler-Rodrigues parameters $q_0 , \mathbf{q}$ and $-q_0 , -\mathbf{q}$ are equivalent. Hence the vector $\boldsymbol{\sigma}$ is equivalent to the vector

$$\left.\begin{aligned} \boldsymbol{\sigma}^* &= -\mathbf{n} \tan \frac{2\pi - \varphi}{4} = -\mathbf{n} \cot \frac{\varphi}{4} \\ &= \frac{-\mathbf{q}}{1-q_0} . \end{aligned}\right\} \tag{1.185}$$

The vector $\boldsymbol{\sigma}$ has its singularity at $\varphi = \pm 2\pi$ equivalent to $\varphi = 0$ when $\boldsymbol{\sigma}^*$ has its singularity.

For expressing the direction cosine matrix $\underline{A}^{12}$ in terms of Wiener parameters (1.184) is substituted into (1.170):

$$\underline{A}^{12} = \frac{1}{(1-\sigma_0)^2} \begin{bmatrix} \sigma_0^2 + \sigma_1^2 - \sigma_2^2 - \sigma_3^2 & 2(\sigma_1\sigma_2 - \sigma_0\sigma_3) & 2(\sigma_1\sigma_3 + \sigma_0\sigma_2) \\ 2(\sigma_1\sigma_2 + \sigma_0\sigma_3) & \sigma_0^2 + \sigma_2^2 - \sigma_3^2 - \sigma_1^2 & 2(\sigma_2\sigma_3 - \sigma_0\sigma_1) \\ 2(\sigma_1\sigma_3 - \sigma_0\sigma_2) & 2(\sigma_2\sigma_3 + \sigma_0\sigma_1) & \sigma_0^2 + \sigma_3^2 - \sigma_1^2 - \sigma_2^2 \end{bmatrix} \tag{1.186}$$

If the matrix $\underline{A}^{12}$ is given, the associated Wiener vectors $\boldsymbol{\sigma}$ and $\boldsymbol{\sigma}^*$ are most easily obtained by first calculating the Euler-Rodrigues parameters q_0 , q_1 , q_2 , q_3 from (1.81) and (1.82) and by substituting them into (1.183) and (1.185). The same results are obtained as follows. The diagonal elements of $\underline{A}^{12}$ yield the first equation below, and the off-diagonal elements yield the second.

$$1 + \operatorname{tr} \underline{A}^{12} = \frac{4\sigma_0^2}{(1-\sigma_0)^2} , \qquad \underline{A}^{12} - \underline{A}^{12^T} = \frac{4\sigma_0}{(1-\sigma_0)^2} \tilde{\underline{\sigma}} . \tag{1.187}$$

The first equation is a quadratic equation for σ_0. Its solutions determine $\tilde{\underline{\sigma}}$:

$$\left.\begin{aligned} \sigma_0 &= \frac{-(1 + \operatorname{tr} \underline{A}^{12}) \pm 2\sqrt{1 + \operatorname{tr} \underline{A}^{12}}}{3 - \operatorname{tr} \underline{A}^{12}} , \\ \tilde{\underline{\sigma}} &= \sigma_0 \frac{\underline{A}^{12} - \underline{A}^{12^T}}{1 + \operatorname{tr} \underline{A}^{12}} = \frac{\underline{A}^{12} - \underline{A}^{12^T}}{1 + \operatorname{tr} \underline{A}^{12} \pm 2\sqrt{1 + \operatorname{tr} \underline{A}^{12}}} . \end{aligned}\right\} \tag{1.188}$$

Equations (1.81) and (1.82) reconfirm that the last equation is

$$\tilde{\underline{\sigma}} = \frac{\pm \tilde{\underline{q}}}{1 \pm q_0} . \tag{1.189}$$

The case $\operatorname{tr} \underline{A}^{12} = 3$ occurs when $\underline{A}^{12}$ is the unit matrix. Then either $\varphi = 0$ or $\varphi = 2\pi$, i.e., either $\boldsymbol{\sigma}^* = \boldsymbol{\infty}$ or $\boldsymbol{\sigma} = \boldsymbol{\infty}$. In either case the unit vector $\mathbf{n}$ is arbitrary.

1.15 Illustrative Problems

1.15.1 Generalized Coordinates Associated with a Given Direction Cosine Matrix

For the direction cosine matrix $\underline{A}^{12} = \frac{1}{3}\begin{bmatrix} 2 & 1 & 2 \\ \frac{-11}{5} & \frac{2}{5} & 2 \\ \frac{2}{5} & \frac{-14}{5} & 1 \end{bmatrix}$ determine the associated Euler and Bryan angles, the rotation $(\mathbf{n}, \varphi)$, the Euler-Rodrigues parameters, Rodrigues parameters and Wiener parameters.

Solution: Two sets of Euler angles are determined from (1.29). With $\sigma = +1$ $\psi = 135^\circ$, $\theta = \cos^{-1}(1/3) \approx 70.5^\circ$, $\phi = \cos^{-1}(-7\sqrt{2}/10) \approx 171.9^\circ$.
Two sets of Bryan angles are determined from (1.35). With $\sigma = +1$ $\phi_1 = \sin^{-1}(-2/\sqrt{5}) \approx -63.4^\circ$, $\phi_2 = \sin^{-1}(2/3) \approx 41.8^\circ$, $\phi_3 = \sin^{-1}(-1/\sqrt{5}) \approx -26.6^\circ$.
Two identical rotations $(\mathbf{n}, \varphi)$ and $(-\mathbf{n}, -\varphi)$ are determined from (1.51) and (1.52): $\varphi = \cos^{-1}(1/15) \approx 86.2^\circ$, $[\, n_1 \; n_2 \; n_3 \,] = \sqrt{1/14}\,[\, -3 \;\; 1 \;\; -2 \,]$.
Two sets of Euler-Rodrigues parameters are determined from (1.81) and (1.82). With $q_0 = +\sqrt{8/15}$, $[\, q_1 \; q_2 \; q_3 \,] = \sqrt{1/30}\,[\, -3 \;\; 1 \;\; -2 \,]$.
Rodrigues parameters are uniquely determined from (1.171) and (1.173):
$[\, u_1 \; u_2 \; u_3 \,] = (1/4)\,[\, -3 \;\; 1 \;\; -2 \,]$.
Two sets of Wiener parameters are determined from (1.189):
$[\, \sigma_1 \; \sigma_2 \; \sigma_3 \,] = (4 \pm \sqrt{30})^{-1}\,[\, -3 \;\; 1 \;\; -2 \,]$.

1.15.2 Resultant of two 180°*-Rotations*

Given two successive 180°-rotations about axes with unit vectors $\mathbf{n}_1$ (first rotation) and $\mathbf{n}_2$ enclosing the angle $0 < \alpha < \pi$, determine the axis and the angle of the resultant rotation.

Two methods of solution are presented. The first method uses Eq.(1.45) for rotation tensors, and the second method uses Eqs.(1.118) and (1.119) for quaternions. The given rotations have the tensors $\mathsf{R}_1 = 2\mathbf{n}_1\mathbf{n}_1 - \mathsf{I}$ and $\mathsf{R}_2 = 2\mathbf{n}_2\mathbf{n}_2 - \mathsf{I}$. The unknown tensor of the resultant rotation has the form (1.40). Equation (1.45) without the subscript res has the form

$$-(1-\cos\varphi)(\mathsf{I} - \mathbf{nn}) + \sin\varphi\, \mathbf{n} \times \mathsf{I} = 4(\mathbf{n}_2 \cdot \mathbf{n}_1)\mathbf{n}_2\mathbf{n}_1 - 2\mathbf{n}_2\mathbf{n}_2 - 2\mathbf{n}_1\mathbf{n}_1 \; . \quad (1.190)$$

Scalar multiplication from the right by $\mathbf{n}$ produces the equation

$$\mathbf{0} = \mathbf{n}_2[2(\mathbf{n}_2 \cdot \mathbf{n}_1)(\mathbf{n}_1 \cdot \mathbf{n}) - (\mathbf{n}_2 \cdot \mathbf{n})] - \mathbf{n}_1(\mathbf{n}_1 \cdot \mathbf{n}) \; . \tag{1.191}$$

The coefficients of $\mathbf{n}_2$ and of $\mathbf{n}_1$ must both be zero. This requires that $\mathbf{n}_1 \cdot \mathbf{n} = 0$ and $\mathbf{n}_2 \cdot \mathbf{n} = 0$. Consequently,

$$\mathbf{n} = \frac{\pm \mathbf{n}_1 \times \mathbf{n}_2}{|\mathbf{n}_1 \times \mathbf{n}_2|} = \frac{\pm \mathbf{n}_1 \times \mathbf{n}_2}{\sin \alpha} \; . \tag{1.192}$$

Arbitrarily, the positive sign is chosen. A unique solution for the angle requires expressions for $\cos\varphi$ and for $\sin\varphi$. An equation for $\cos\varphi$ is obtained when (1.190) is scalar-multiplied from the left and from the right by $\mathbf{n}_1$. Taking into account that $\mathbf{n}_1 \cdot \mathbf{n} = 0$ this results in the equation $1 - \cos\varphi = 2[1 - (\mathbf{n}_1 \cdot \mathbf{n}_2)^2] = 2(1 - \cos^2\alpha) = 2\sin^2\alpha$, whence it follows that

$$\cos\varphi = \cos 2\alpha \; . \tag{1.193}$$

In order to get an expression for $\sin\varphi$ (1.190) is scalar-multiplied from the left by $\mathbf{n}_2$ and from the right by $\mathbf{n}_1$. On the right-hand side this yields zero. The equation reads $(1 - \cos\varphi)\mathbf{n}_2 \cdot \mathbf{n}_1 + \sin\varphi\,(\mathbf{n}_1 \times \mathbf{n}_2)^2 / \sin\alpha = 0$ or $(1 - \cos\varphi)\cos\alpha + \sin\varphi\sin\alpha = 0$ and with (1.193), finally, $\sin\alpha(\sin 2\alpha - \sin\varphi) = 0$. This together with (1.193) yields

$$\varphi = 2\alpha \; . \tag{1.194}$$

The second method of solution using quaternions is much simpler. Equations (1.118) and (1.119) are formulated with $\varphi_1 = -\pi$ (equivalent to $\varphi_1 = \pi$) and with $\varphi_2 = \pi$. This produces directly the results $\varphi_{\text{res}} = 2\alpha$, $\mathbf{n}_{\text{res}} = \mathbf{n}_1 \times \mathbf{n}_2 / |\mathbf{n}_1 \times \mathbf{n}_2| = \mathbf{n}_1 \times \mathbf{n}_2 / \sin\alpha$.

The results are summarized as follows. The resultant of two 180°-rotations about axes $\mathbf{n}_1$ (first rotation) and $\mathbf{n}_2$ enclosing the angle $0 < \alpha < \pi$ is a rotation about the axis $\mathbf{n}_1 \times \mathbf{n}_2 / |\mathbf{n}_1 \times \mathbf{n}_2|$ through the angle 2α . In Sect. 1.5 it was shown that a 180°-rotation about an axis $\mathbf{n}$ is equivalent to reflection in the line $\mathbf{n}$. Therefore, the result can also be stated as follows. The resultant of two successive reflections in lines $\mathbf{n}_1$ (first reflection) and $\mathbf{n}_2$ enclosing the angle $0 < \alpha < \pi$ is a rotation about the axis $\mathbf{n}_1 \times \mathbf{n}_2 / |\mathbf{n}_1 \times \mathbf{n}_2|$ through the angle 2α . The two 180°-rotations (reflections) are not commutative. Reversal of the order has the effect that the direction of the resultant rotation axis is reversed. The resultant rotation does not change if the pair of vectors $\mathbf{n}_1$, $\mathbf{n}_2$ is rotated in its own plane about the fixed point and with the angle α kept constant.

1.15.3 Rotations $(\mathbf{n}, \varphi)$ Resulting in Positions with the Critical Bryan Angle $\phi_2 = \pm\pi/2$

To be determined are all rotations $(\mathbf{n}, \varphi)$ resulting in positions which can be produced by Bryan angles in the critical case $\cos\phi_2 = 0$.

Solution: Equations (1.32) and (1.49) express the transformation matrix $\underline{A}^{12}$ in terms of Bryan angles and in terms of $\mathbf{n}$ and φ, respectively. Only the matrix element a_{13}^{12} is considered. The expression in (1.32) with $\cos\phi_2 = 0$ and $\sin\phi_2 = \sigma$ $(\sigma = +1$ or $-1)$ is set equal to the expression in (1.49) for the general case n_1 , n_2 , n_3 , φ . This results in the equation

$$n_1 n_3 \cos\varphi - n_2 \sin\varphi = n_1 n_3 - \sigma \qquad (\sigma = \pm 1) \; . \tag{1.195}$$

It has the form $A\cos\varphi + B\sin\varphi = C$. It has two solutions φ which are determined by
$\cos\varphi = (AC \pm BW)/N$ and $\sin\varphi = (BC \mp AW)/N$ with $N = A^2 + B^2$ and with

$$W = \sqrt{A^2 + B^2 - C^2} = \sqrt{n_1^2 n_3^2 + n_2^2 - (n_1 n_3 - \sigma)^2} = \sqrt{-(n_3 - \sigma n_1)^2} \; . \tag{1.196}$$

Real roots (a double root) exist only if $n_3 = \sigma n_1$. The results are summarized as follows. The critical case $\cos\phi_2 = 0$ occurs if the rotation $(\mathbf{n}, \varphi)$ satisfies the conditions

$$\left.\begin{aligned} & n_3 = \sigma n_1 \; , \quad n_2^2 = 1 - 2n_1^2 \; , \quad \cos\varphi = \frac{-n_1^2}{1 - n_1^2} \; , \\ & \sin\varphi = \frac{\sigma n_2}{1 - n_1^2} \quad (\sigma = \pm 1 \; , \; n_1^2 \leq 1/2 \;\; \text{arbitr.}) \; . \end{aligned}\right\} \tag{1.197}$$

1.15.4 Determine all Direction Cosine Matrices Having three Prescribed Elements

The elements $a_{11} = a$, $a_{12} = b$ and $a_{33} = c$ of a direction cosine matrix $\underline{A}$ are prescribed. To be determined are all direction cosine matrices $\underline{A}$ having these elements. Necessary and sufficient conditions for the existence of real matrices are to be formulated.

Solution: The normalizing conditions for row 1 and for column 3 yield

$$a_{13} = \sigma_1 \sqrt{1 - (a^2 + b^2)} \; , \qquad a_{23} = \sigma_2 \sqrt{a^2 + b^2 - c^2} \; , \tag{1.198}$$

where σ_1 and σ_2 are independently either $+1$ or -1 . Sufficient and necessary conditions for a_{13} and a_{23} to be real are

$$c^2 \leq a^2 + b^2 \leq 1 \,. \tag{1.199}$$

The special case $a = b = 0$: From (1.199) it follows that $c = 0$. All real solutions have the form

$$\underline{A} = \begin{bmatrix} 0 & 0 & \sigma \\ \cos\varphi & \sin\varphi & 0 \\ -\sigma\sin\varphi & \sigma\cos\varphi & 0 \end{bmatrix} \qquad (\varphi \text{ arbitr.}, \ \sigma = +1 \text{ or } -1) \,. \tag{1.200}$$

In what follows, this special case is excluded. The elements a_{21}, a_{22}, a_{31} and a_{32} are calculated from four linear equations expressing the fact that the scalar product of rows 1 and 2 equals zero, and that every diagonal element equals its own co-factor:

$$a a_{21} + b a_{22} + a_{13} a_{23} = 0 \,, \qquad a a_{22} - b a_{21} = c \,, \tag{1.201}$$

$$a c - a_{31} a_{13} = a_{22} \,, \qquad a_{22} c - a_{32} a_{23} = a \,. \tag{1.202}$$

Equations (1.201) are solved for a_{21} and a_{22}. Upon substitution of the result for a_{22} Eqs.(1.202) are uncoupled. Taking into account (1.198) the results are written in the form

$$\left.\begin{aligned} a_{21} &= -\frac{a\, a_{13} a_{23} + b\, c}{a^2 + b^2} \,, & a_{22} &= -\frac{b\, a_{13} a_{23} - a\, c}{a^2 + b^2} \,, \\ a_{31} &= -\frac{a\, c\, a_{13} - b\, a_{23}}{a^2 + b^2} \,, & a_{32} &= -\frac{b\, c\, a_{13} + a\, a_{23}}{a^2 + b^2} \,. \end{aligned}\right\} \tag{1.203}$$

Together with (1.198) these equations determine all matrices. For given numbers a, b and c satisfying conditions (1.199) and not representing the special case $a = b = c = 0$ the number of real matrices is either four or two or one depending on whether zero or one or both of the elements a_{13} and a_{23} are zero. All matrix elements are rational, if the elements in row 1 and in column 3 are rational.

Example: With $a = 2/3$, $b = 1/3$, $c = 1/3$ four matrices are calculated:

$$\begin{bmatrix} \frac{2}{3} & \frac{1}{3} & \frac{2}{3} \\ \frac{1}{3} & \frac{2}{3} & \frac{-2}{3} \\ \frac{-2}{3} & \frac{2}{3} & \frac{1}{3} \end{bmatrix}, \quad \begin{bmatrix} \frac{2}{3} & \frac{1}{3} & \frac{-2}{3} \\ \frac{1}{3} & \frac{2}{3} & \frac{2}{3} \\ \frac{2}{3} & \frac{-2}{3} & \frac{1}{3} \end{bmatrix}, \quad \begin{bmatrix} \frac{2}{3} & \frac{1}{3} & \frac{2}{3} \\ \frac{-11}{15} & \frac{2}{15} & \frac{2}{3} \\ \frac{2}{15} & \frac{-14}{15} & \frac{1}{3} \end{bmatrix}, \quad \begin{bmatrix} \frac{2}{3} & \frac{1}{3} & \frac{-2}{3} \\ \frac{-11}{15} & \frac{2}{15} & \frac{-2}{3} \\ \frac{-2}{15} & \frac{14}{15} & \frac{1}{3} \end{bmatrix} . \tag{1.204}$$

Other triples (a, b, c) resulting in rational matrix elements: $(\frac{3}{5}, \frac{4}{5}, 1)$, $(\frac{2}{7}, \frac{3}{7}, \frac{2}{7})$, $(\frac{4}{9}, \frac{7}{9}, \frac{1}{9})$, $(\frac{2}{11}, \frac{6}{11}, \frac{2}{11})$, $(\frac{3}{13}, \frac{4}{13}, \frac{3}{13})$, $(\frac{2}{15}, \frac{11}{15}, \frac{5}{15})$.
End of example.

1.15.5 Rear Axle of a Vehicle

Figure 1.10a shows the simplest design of a rigid rear axle for road vehicles (Matschinsky [15]). The axle is rigidly attached to a draw-bar which is supported in the car body by the spherical joint 0. Another spherical joint B connects the axle to a so-called sway bar or Panhard rod. The other end of this rod is supported in the car body by still another spherical joint A. The position of the axle relative to the car body is interpreted as the result of two successive rotations. Prior to the first rotation the bases $\underline{\mathbf{e}}^2$ (fixed on the axle) and $\underline{\mathbf{e}}^1$ (fixed in the car body) coincide. The first rotation about the line $\overline{\mathrm{A0}}$ (unit vector $\mathbf{n}$, rotation angle φ_1) carries the axle-fixed basis to the intermediate position $\underline{\mathbf{e}}^{2^*}$ and point B to the position B*. The second rotation is executed about the axle-fixed line $\overline{\mathrm{B^*0}}$ (unit vector $\mathbf{n}^*$, rotation angle φ_2). In Fig. 1.10b the system is shown schematically in a vertical projection in the null position $\varphi_1 = \varphi_2 = 0$. The figure shows also basis $\underline{\mathbf{e}}^1$ and the unit vectors $\mathbf{n}$ and $\mathbf{n}^*$ along the rotation axes. It is assumed that in the null position the axle, the draw-bar and the Panhard rod are coplanar. The lengths h, a, ℓ, b are given. Point B is moving along a circular path which in the figure appears as straight line. To be determined are the coordinates in $\underline{\mathbf{e}}^1$ of the wheel centers P_1 and P_2 as functions of φ_1 and φ_2.

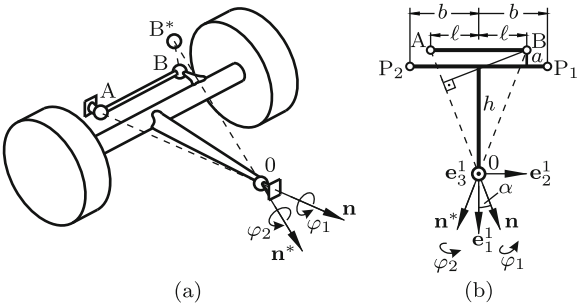

Fig. 1.10 Rear axle seen in perspective **(a)** and in vertical projection **(b)**

Solution: The lengths h, a and ℓ determine the angle α. For abbreviation the quantities $c = \cos\alpha$ and $s = \sin\alpha$ are defined. The vector $\mathbf{n}$ has in $\underline{\mathbf{e}}^1$ the coordinate matrix $[c \;\; s \;\; 0]^T$, and the vector $\mathbf{n}^*$ has in $\underline{\mathbf{e}}^{2^*}$ the coordinate matrix $[c \;\; -s \;\; 0]^T$. With the coordinates of $\mathbf{n}$ and with $\varphi = \varphi_1$ (1.49) determines the matrix $\underline{A}_1^{12}$ in the relationship $\underline{\mathbf{e}}^1 = \underline{A}_1^{12}\underline{\mathbf{e}}^{2^*}$. The same Eq.(1.49) with the coordinates of $\mathbf{n}^*$ and with $\varphi = \varphi_2$ determines the matrix $\underline{A}_2^{12}$ in the relationship $\underline{\mathbf{e}}^{2^*} = \underline{A}_2^{12}\underline{\mathbf{e}}^2$. Consequently, the matrix $\underline{A}^{12}$ in the relationship $\underline{\mathbf{e}}^1 = \underline{A}^{12}\underline{\mathbf{e}}^2$ is the product $\underline{A}^{12} = \underline{A}_1^{12}\underline{A}_2^{12}$. Springs not shown in the figure allow only small rotation angles. For this reason the second-order approximation (1.55) is used. This yields the matrix

$$\underline{A}^{12} \approx \left(\underline{I} + \frac{1}{2} \begin{bmatrix} -s^2\varphi_1^2 & cs\varphi_1^2 & 2s\varphi_1 \\ cs\varphi_1^2 & -c^2\varphi_1^2 & -2c\varphi_1 \\ -2s\varphi_1 & 2c\varphi_1 & -\varphi_1^2 \end{bmatrix} \right) \left(\underline{I} + \frac{1}{2} \begin{bmatrix} -s^2\varphi_2^2 & -cs\varphi_2^2 & -2s\varphi_2 \\ -cs\varphi_2^2 & -c^2\varphi_2^2 & -2c\varphi_2 \\ 2s\varphi_2 & 2c\varphi_2 & -\varphi_2^2 \end{bmatrix} \right)$$

$$\approx \underline{I} + \frac{1}{2} \begin{bmatrix} -s^2(\varphi_1-\varphi_2)^2 & cs(\varphi_1^2+2\varphi_1\varphi_2-\varphi_2^2) & 2s(\varphi_1-\varphi_2) \\ cs(\varphi_1^2-2\varphi_1\varphi_2-\varphi_2^2) & -c^2(\varphi_1+\varphi_2)^2 & -2c(\varphi_1+\varphi_2) \\ -2s(\varphi_1-\varphi_2) & 2c(\varphi_1+\varphi_2) & 4c^2\varphi_1\varphi_2-(\varphi_1-\varphi_2)^2 \end{bmatrix} . \quad (1.205)$$

In basis $\underline{\mathbf{e}}^2$ the wheel centers P_1 and P_2 have the constant coordinate matrices $[-h \;\; b \;\; 0]^T$ and $[-h \;\; -b \;\; 0]^T$, respectively. The desired coordinate matrices in $\underline{\mathbf{e}}^1$ are found by multiplication with $\underline{A}^{12}$. The displacements of the wheel centers in the direction of $\mathbf{e}_3^1$ are linear functions of the angles φ_1 and φ_2 whereas the displacements in the directions of $\mathbf{e}_1^1$ and $\mathbf{e}_2^1$ are second-order functions of the angles.

1.15.6 Rotation Determined from Three Positions of a Body-Fixed Point

When the body shown in Fig. 1.3 is rotated about $\mathbf{n}$ through angles φ_1, φ_2, φ_3, the body-fixed point originally positioned by the vector $\mathbf{r}$ is displaced into positions $\mathbf{r}_1$, $\mathbf{r}_2$, $\mathbf{r}_3$, respectively. If only $\mathbf{r}_1$, $\mathbf{r}_2$, $\mathbf{r}_3$ of arbitrary, but equal absolute values are given, the vector $\mathbf{n}$ and the angles $\varphi_2 - \varphi_1$ and $\varphi_3 - \varphi_1$ are determined as follows. Since $\mathbf{n}$ is orthogonal to $\mathbf{r}_1 - \mathbf{r}_2$, $\mathbf{r}_1 - \mathbf{r}_3$ and $\mathbf{r}_2 - \mathbf{r}_3$,

$$\mathbf{n} = \frac{(\mathbf{r}_1-\mathbf{r}_2)\times(\mathbf{r}_1-\mathbf{r}_3)}{|(\mathbf{r}_1-\mathbf{r}_2)\times(\mathbf{r}_1-\mathbf{r}_3)|} = \frac{\mathbf{r}_1\times\mathbf{r}_2+\mathbf{r}_2\times\mathbf{r}_3+\mathbf{r}_3\times\mathbf{r}_1}{|(\mathbf{r}_1-\mathbf{r}_2)\times(\mathbf{r}_1-\mathbf{r}_3)|} . \quad (1.206)$$

The product in the denominator can be replaced by the product of any two vector differences. According to (1.77)

$$\mathbf{r}_2-\mathbf{r}_1 = \mathbf{n}\tan\frac{\varphi_2-\varphi_1}{2}\times(\mathbf{r}_2+\mathbf{r}_1) , \qquad \mathbf{r}_3-\mathbf{r}_1 = \mathbf{n}\tan\frac{\varphi_3-\varphi_1}{2}\times(\mathbf{r}_3+\mathbf{r}_1) . \quad (1.207)$$

With the expression for $\mathbf{n}$ the products are calculated:

$$\left.\begin{aligned} \mathbf{n}\times(\mathbf{r}_2+\mathbf{r}_1) &= (\mathbf{r}_2-\mathbf{r}_1)\frac{(\mathbf{r}_1+\mathbf{r}_2)\cdot(\mathbf{r}_2-\mathbf{r}_3)}{|(\mathbf{r}_1-\mathbf{r}_2)\times(\mathbf{r}_2-\mathbf{r}_3)|} , \\ \mathbf{n}\times(\mathbf{r}_3+\mathbf{r}_1) &= (\mathbf{r}_3-\mathbf{r}_1)\frac{(\mathbf{r}_1+\mathbf{r}_3)\cdot(\mathbf{r}_2-\mathbf{r}_1)}{|(\mathbf{r}_1-\mathbf{r}_3)\times(\mathbf{r}_2-\mathbf{r}_1)|} . \end{aligned}\right\} \quad (1.208)$$

Hence

$$\left.\begin{aligned} \tan\frac{\varphi_2-\varphi_1}{2} &= \frac{|(\mathbf{r}_1-\mathbf{r}_2)\times(\mathbf{r}_2-\mathbf{r}_3)|}{(\mathbf{r}_1+\mathbf{r}_2)\cdot(\mathbf{r}_2-\mathbf{r}_3)}\,, \\ \tan\frac{\varphi_3-\varphi_1}{2} &= \frac{|(\mathbf{r}_1-\mathbf{r}_3)\times(\mathbf{r}_2-\mathbf{r}_1)|}{(\mathbf{r}_1+\mathbf{r}_3)\cdot(\mathbf{r}_2-\mathbf{r}_1)}\,. \end{aligned}\right\} \tag{1.209}$$

1.15.7 Rodrigues Vector Determined from Prescribed Point Displacements

A body with one point fixed in a reference basis $\underline{\mathbf{e}}^1$ is rotated from an initial position into a final position. Let P_1 and P_2 be two body-fixed points which together with the fixed point of the body define a triangle (thus, the three points are not collinear). In the initial position of the body P_1 and P_2 have position vectors $\mathbf{r}_1$ and $\mathbf{r}_2$ in the reference basis $\underline{\mathbf{e}}^1$. In the final position they have position vectors $\mathbf{r}_1^*$ and $\mathbf{r}_2^*$, where $|\mathbf{r}_1^*| = |\mathbf{r}_1|$ and $|\mathbf{r}_2^*| = |\mathbf{r}_2|$. The problem to be solved is the following. Given the pairs of vectors $\mathbf{r}_1$, $\mathbf{r}_2$ and $\mathbf{r}_1^*$, $\mathbf{r}_2^*$, determine the Rodrigues vector $\mathbf{u} = \mathbf{n}\tan\varphi/2$ (the axial vector $\mathbf{n}$ if $u \to \infty$) of the rotation $(\mathbf{n}, \varphi)$ carrying the body from the initial to the final position.

Solution: The rotation angle is $\varphi \neq 0$ since the two positions are not identical. Let the points be labeled such that $\mathbf{r}_1^* - \mathbf{r}_1 \neq \mathbf{0}$ and $\mathbf{r}_2^* + \mathbf{r}_2 \neq \mathbf{0}$. This is always possible since at least one difference $\mathbf{r}_i^* - \mathbf{r}_i$ and at least one sum $\mathbf{r}_i^* + \mathbf{r}_i$ $(i = 1, 2)$ is different from zero and since a difference and a sum cannot both be zero. With this labeling all denominator expressions to come are different from zero.
Starting point of the analysis are Eqs.(1.167) and (1.43):

$$\mathbf{r}_1^* - \mathbf{r}_1 = \mathbf{u}\times(\mathbf{r}_1^* + \mathbf{r}_1)\,, \qquad \mathbf{r}_2^* - \mathbf{r}_2 = \mathbf{u}\times(\mathbf{r}_2^* + \mathbf{r}_2) \qquad (\varphi \neq \pm\pi)\,. \tag{1.210}$$

$$\mathbf{n} = \frac{\mathbf{r}_2^* + \mathbf{r}_2}{|\mathbf{r}_2^* + \mathbf{r}_2|} \qquad (\varphi = \pm\pi)\,. \tag{1.211}$$

Equations (1.210) show that nonzero differences $\mathbf{r}_i^* - \mathbf{r}_i$ $(i = 1, 2)$ are orthogonal to $\mathbf{u}$. The second equation is cross-multiplied by $\mathbf{r}_1^* - \mathbf{r}_1$. Because of the said orthogonality this yields the equation

$$(\mathbf{r}_1^*-\mathbf{r}_1)\times(\mathbf{r}_2^*-\mathbf{r}_2) = (\mathbf{r}_1^*-\mathbf{r}_1)\times[\mathbf{u}\times(\mathbf{r}_2^*+\mathbf{r}_2)] = \mathbf{u}\,(\mathbf{r}_1^*-\mathbf{r}_1)\cdot(\mathbf{r}_2^*+\mathbf{r}_2)\,. \tag{1.212}$$

Two cases have to be distinguished:
Case 1) $(\mathbf{r}_1^* - \mathbf{r}_1)\times(\mathbf{r}_2^* - \mathbf{r}_2) \neq \mathbf{0}$: The desired solution is

$$\mathbf{u} = \mathbf{n}\tan\frac{\varphi}{2} = \frac{(\mathbf{r}_1^* - \mathbf{r}_1)\times(\mathbf{r}_2^* - \mathbf{r}_2)}{(\mathbf{r}_1^* - \mathbf{r}_1)\,\cdot\,(\mathbf{r}_2^* + \mathbf{r}_2)} \qquad (\mathbf{r}_1^* - \mathbf{r}_1 \text{ not orthogonal to } \mathbf{r}_2^* + \mathbf{r}_2) \tag{1.213}$$

or $\varphi = \pm\pi$ with $\mathbf{n}$ given by (1.211) else.

Case 2) $(\mathbf{r}_1^* - \mathbf{r}_1) \times (\mathbf{r}_2^* - \mathbf{r}_2) = \mathbf{0}$: In this case, there exists a scalar λ such that

$$\mathbf{r}_2^* - \mathbf{r}_2 = \lambda(\mathbf{r}_1^* - \mathbf{r}_1) \; . \tag{1.214}$$

The first Eq.(1.210) is multiplied by λ, and then the second equation is subtracted. This produces the equation

$$\mathbf{u} \times [\lambda(\mathbf{r}_1^* + \mathbf{r}_1) - (\mathbf{r}_2^* + \mathbf{r}_2)] = \mathbf{0} \tag{1.215}$$

and after combination with (1.214) the equations

$$\mathbf{u} \times (\lambda\mathbf{r}_1 - \mathbf{r}_2) = \mathbf{0} \; , \qquad \mathbf{u} \times (\lambda\mathbf{r}_1^* - \mathbf{r}_2^*) = \mathbf{0} \; . \tag{1.216}$$

The nonzero vector $(\lambda\mathbf{r}_1 - \mathbf{r}_2)$ of the first equation lies in the plane Σ spanned by $\mathbf{r}_1$ and $\mathbf{r}_2$. The vector $(\lambda\mathbf{r}_1^* - \mathbf{r}_2^*)$ of the second equation lies in the plane Σ^* spanned by $\mathbf{r}_1^*$ and $\mathbf{r}_2^*$. These two planes have either a line of intersection (case 2a) or they are identical (case 2b).

Case 2a: Equations (1.216) require that the Rodrigues vector $\mathbf{u}$ is collinear with both the vector in Σ and the vector in Σ^*. From this it follows that $\mathbf{u}$ lies in the line of intersection of the two planes, and that φ is the angle between the normals to the planes. This result is expressed as follows (note the rigid-body property $|\mathbf{r}_1 \times \mathbf{r}_2| = |\mathbf{r}_1^* \times \mathbf{r}_2^*|$) :

$$\mathbf{n} \sin\varphi = \frac{(\mathbf{r}_1 \times \mathbf{r}_2) \times (\mathbf{r}_1^* \times \mathbf{r}_2^*)}{(\mathbf{r}_1 \times \mathbf{r}_2)^2} \; , \qquad \cos\varphi = \frac{(\mathbf{r}_1 \times \mathbf{r}_2) \cdot (\mathbf{r}_1^* \times \mathbf{r}_2^*)}{(\mathbf{r}_1 \times \mathbf{r}_2)^2} \; . \tag{1.217}$$

Case 2b: The solution is $\varphi = \pm\pi$ with $\mathbf{n}$ given by (1.211).

1.15.8 Spherical Interpolation

Let $\underline{r}_1$ and $\underline{r}_2 \neq \pm\underline{r}_1$ be the coordinate matrices in basis $\underline{\mathbf{e}}^1$ of two unit vectors locating two points of a unit circle. Proposition: With the enclosed angle $\alpha = \cos^{-1}(\underline{r}_1^T \underline{r}_2)$

$$\underline{r}(\psi) = \frac{\underline{r}_1 \sin(\alpha - \psi) + \underline{r}_2 \sin\psi}{\sin\alpha} \tag{1.218}$$

is a parameter equation, with parameter ψ, of the unit circle. Proof:

$$\begin{aligned} \underline{r}^T \underline{r} \sin^2\alpha &= [\underline{r}_1^T \sin(\alpha - \psi) + \underline{r}_2^T \sin\psi][\underline{r}_1 \sin(\alpha - \psi) + \underline{r}_2 \sin\psi] \\ &= \sin(\alpha - \psi)[\sin(\alpha - \psi) + 2\cos\alpha \sin\psi] + \sin^2\psi \\ &= \sin^2\alpha \cos^2\psi - \cos^2\alpha \sin^2\psi + \sin^2\psi = \sin^2\alpha \; . \end{aligned} \tag{1.219}$$

Hence $\underline{r}^T\underline{r} \equiv 1$. End of proof.

In three-dimensional space (1.218) is the equation of the great circle passing through two points $\underline{r}_1$ and $\underline{r}_2$ on the unit sphere. The equation is used for locating points on Earth. In terms of geographical longitude λ and latitude ϕ the coordinate matrix is $\underline{r}(\psi) = [\cos\lambda\cos\phi \quad \sin\lambda\cos\phi \quad \sin\phi]^T$. With this equation ψ is converted into λ and ϕ.

In four-dimensional space the column matrix $[q_0 \ q_1 \ q_2 \ q_3]^T$ of the Euler-Rodrigues parameters associated with the angular position of a body is the unit vector $\underline{r}$. This vector $\underline{r}$ and the vector $-\underline{r}$ determine one and the same angular position. Equation (1.218) is used for the animation of motion. Two angular positions 1 and 2 determine associated vectors $\underline{r}_1$ and $\underline{r}_2$ enclosing the angle $\alpha = \cos^{-1}(\underline{r}_1^T\underline{r}_2)$. When ψ is prescribed as function of time $\psi(t)$, the Euler-Rodrigues parameters $\underline{r}(\psi(t))$ determine a tumbling motion leading the body through position 1 ($\psi = 0$) and position 2 ($\psi = \alpha$). In computer animations this tumbling motion is more attractive than the alternative possibility of rotating the body about a fixed axis from position 1 into position 2.

Equation (1.218) is not applicable to the interpolation between more than two angular positions. An ordered sequence of $m > 2$ angular positions can be interpolated as follows. The positions must be specified by rotations $(\mathbf{n}_i, \varphi_i)$ $(i = 1, \ldots, m)$. The unit vectors $\mathbf{n}_i$ define points P_i on the unit sphere with associated geographical longitudes λ_i and latitudes ϕ_i $(i = 1, \ldots, m)$. With a parameter t the three sequences of scalars λ_i, ϕ_i and φ_i $(i = 1, \ldots, m)$ are interpolated in a form $\lambda(t)$, $\phi(t)$, $\varphi(t)$ such that $\lambda(t = t_i) = \lambda_i$, $\phi(t = t_i) = \phi_i$, $\varphi(t = t_i) = \varphi_i$ $(i = 1, \ldots, m)$. The functions $\lambda(t)$ and $\phi(t)$ determine the unit vector $\mathbf{n}(t)$ of the angular position $(\mathbf{n}(t), \varphi(t))$. It is the desired interpolation.

1.15.9 Rotations Effecting a Prescribed Line Displacement

To be determined are all rotations $(\mathbf{n}, \varphi)$ about a fixed point 0 which carry a body-fixed point from a given position $\mathbf{r}_1$ into another given position $\mathbf{r}_2$. Without loss of generality, it is assumed that $\mathbf{r}_1$ and $\mathbf{r}_2$ are unit vectors. The problem can also be formulated as follows. Determine all rotations $(\mathbf{n}, \varphi)$ about a fixed point 0 which carry a body-fixed line passing through 0 from a given position $\mathbf{r}_1$ into another given position $\mathbf{r}_2$.

Solution: In the special case $\mathbf{r}_2 = -\mathbf{r}_1$, every rotation $(\mathbf{n}, \varphi = \pm\pi)$ about an axis $\mathbf{n}$ orthogonal to $\mathbf{r}_1$, $\mathbf{r}_2$ is a solution. In what follows, it is assumed that $\mathbf{r}_2 \neq -\mathbf{r}_1$. In Fig. 1.11a the vectors $\mathbf{r}_1$ and $\mathbf{r}_2$ are shown in their own plane, and in Fig. 1.11b they are shown in a projection in which they coincide. Let α be the angle which rotates $\mathbf{r}_1$ in the projection (a) into

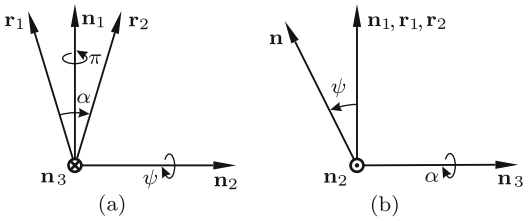

Fig. 1.11 Axes $\mathbf{n}$ of rotations carrying $\mathbf{r}_1$ into position $\mathbf{r}_2$ lie in the $\mathbf{n}_1, \mathbf{n}_3$-plane

position $\mathbf{r}_2$. Without loss of generality, it is assumed that $0 < \alpha < \pi$. Two special solutions are obvious by inspection, namely, the rotations $(\mathbf{n}_1, \pm\pi)$ and $(\mathbf{n}_3, \alpha)$ with axial unit vectors

$$\mathbf{n}_1 = \frac{\mathbf{r}_1 + \mathbf{r}_2}{2\cos\frac{\alpha}{2}}\,, \qquad \mathbf{n}_3 = \frac{\mathbf{r}_1 \times \mathbf{r}_2}{\sin\alpha}\,. \tag{1.220}$$

Together with $\mathbf{n}_2 = \mathbf{n}_3 \times \mathbf{n}_1$ these vectors define a right-handed cartesian basis. In this basis the given vectors are

$$\mathbf{r}_{1,2} = \mathbf{n}_1 \cos\frac{\alpha}{2} \mp \mathbf{n}_2 \sin\frac{\alpha}{2}\,. \tag{1.221}$$

Every rotation $(\mathbf{n}, \varphi)$ solving the problem has the property that $\mathbf{r}_1$ and $\mathbf{r}_2$ are generators of a circular cone with $\mathbf{n}$ as cone axis. From this it follows that all unit vectors $\mathbf{n}$ lie in the plane of $\mathbf{n}_1$ and $\mathbf{n}_3$. Furthermore, it is obvious that every vector in this plane is a solution $\mathbf{n}$. With a free parameter ψ it is written in the form

$$\mathbf{n}(\psi) = \mathbf{n}_1 \cos\psi - \mathbf{n}_3 \sin\psi\,. \tag{1.222}$$

As is shown in the figure, ψ is the angle from $\mathbf{n}_1$ to $\mathbf{n}$ in the positive mathematical sense around $\mathbf{n}_2$. The angles associated with the special solutions $(\mathbf{n}_1, \pm\pi)$ and $(\mathbf{n}_3, \alpha)$ are $\psi = 0$ and $\psi = -\pi/2$, respectively. The general relationship $\varphi(\psi)$ is deduced from (1.37) which, in this case, has the form

$$\mathbf{r}_2 = \mathbf{r}_1 + (1 - \cos\varphi)[(\mathbf{n}\cdot\mathbf{r}_1)\mathbf{n} - \mathbf{r}_1] + \sin\varphi\,\mathbf{n}\times\mathbf{r}_1\,. \tag{1.223}$$

Scalar multiplications by $\mathbf{r}_1$ and by $\mathbf{n}\times\mathbf{r}_1$ eliminate the expression with $\sin\varphi$ and the expression with $(1-\cos\varphi)$, respectively. For this purpose the following products are calculated from (1.221) and (1.222):

$$\left.\begin{aligned} (\mathbf{n}\cdot\mathbf{r}_1)^2 &= \cos^2\frac{\alpha}{2}\cos^2\psi\,, \\ (\mathbf{n}\times\mathbf{r}_1)^2 &= 1 - (\mathbf{n}\cdot\mathbf{r}_1)^2 = 1 - \cos^2\frac{\alpha}{2}\cos^2\psi\,, \\ (\mathbf{n}\times\mathbf{r}_1)\cdot\mathbf{r}_2 &= \mathbf{n}\cdot(\mathbf{r}_1\times\mathbf{r}_2) = -\sin\alpha\sin\psi\,. \end{aligned}\right\} \tag{1.224}$$

With these expressions the said multiplications yield the equations

$$\left.\begin{aligned} \cos\alpha &= 1 + (1-\cos\varphi)\Big(\cos^2\frac{\alpha}{2}\cos^2\psi - 1\Big)\,, \\ -\sin\alpha\sin\psi &= \sin\varphi\Big(1-\cos^2\frac{\alpha}{2}\cos^2\psi\Big) \end{aligned}\right\} \tag{1.225}$$

or

$$1-\cos\varphi = \frac{1-\cos\alpha}{1-\cos^2\frac{\alpha}{2}\cos^2\psi}\,, \qquad \sin\varphi = \frac{-\sin\alpha\sin\psi}{1-\cos^2\frac{\alpha}{2}\cos^2\psi}\,. \tag{1.226}$$

For φ and α the transition to half-angles is made everywhere. This results in the equations

$$\sin^2\frac{\varphi}{2} = \frac{\sin^2\frac{\alpha}{2}}{1-\cos^2\frac{\alpha}{2}\cos^2\psi}\,, \qquad \sin\frac{\varphi}{2}\cos\frac{\varphi}{2} = \frac{-\sin\frac{\alpha}{2}\cos\frac{\alpha}{2}\sin\psi}{1-\cos^2\frac{\alpha}{2}\cos^2\psi}\,. \tag{1.227}$$

Division of the second equation by the first produces the final equation

$$\cot\frac{\varphi}{2} = -\cot\frac{\alpha}{2}\,\sin\psi\,. \tag{1.228}$$

This equation and Eq.(1.222) for $\mathbf{n}(\psi)$ determine together the desired manifold of rotations. For the absolute value of the rotation angle the inequalities hold: $|\alpha| \le |\varphi| \le \pi$.

Example: A pair of parameter values ψ (arbitrary) and $\psi^* = \psi + \pi/2$ determines mutually orthogonal rotation axes $\mathbf{n}$ and $\mathbf{n}^*$ and rotation angles φ and φ^* satisfying the identity

$$\cot^2\frac{\varphi}{2} + \cot^2\frac{\varphi^*}{2} \equiv \cot^2\frac{\alpha}{2}\,. \tag{1.229}$$

1.15.10 Sensor Calibration

On the end-effector of a robot a basis $\underline{\mathbf{e}}^1$ is fixed. Another basis $\underline{\mathbf{e}}^2$ is fixed on a sensor which is rigidly attached to the end-effector. Let $\underline{X}$ be the unknown direction cosine matrix relating these bases: $\underline{\mathbf{e}}^1 = \underline{X}\,\underline{\mathbf{e}}^2$. The determination of $\underline{X}$ from measured data is referred to as sensor calibration. Two methods based on different measured data are described.

Method 1 : The measured data are the coordinate matrices of two arbitrarily chosen noncollinear body-fixed unit vectors $\mathbf{n}_1$ and $\mathbf{n}_2$ in both bases. They are denoted as usual: $\underline{n}_1^1$, $\underline{n}_1^2$ for $\mathbf{n}_1$ and $\underline{n}_2^1$, $\underline{n}_2^2$ for $\mathbf{n}_2$. Both pairs are related through the unknown matrix: $\underline{n}_1^1 = \underline{X}\,\underline{n}_1^2$, $\underline{n}_2^1 = \underline{X}\,\underline{n}_2^2$. The vector $\mathbf{n}_3 = \mathbf{n}_1 \times \mathbf{n}_2$ is a third linearly independent body-fixed vector the coordinate

matrices of which are related by $\underline{X}$. Its coordinate matrices are calculated from the measured data: $\underline{n}_3^1 = \tilde{\underline{n}}_1^1 \underline{n}_2^1$ and $\underline{n}_3^2 = \tilde{\underline{n}}_1^2 \underline{n}_2^2$. The altogether nine linear equations $\underline{n}_i^1 = \underline{X}\, \underline{n}_i^2$ $(i = 1, 2, 3)$ are combined in the matrix equation

$$\left[\underline{n}_1^1 \;\; \underline{n}_2^1 \;\; \underline{n}_3^1\right] = \underline{X} \left[\underline{n}_1^2 \;\; \underline{n}_2^2 \;\; \underline{n}_3^2\right] . \tag{1.230}$$

The solution is

$$\underline{X} = \left[\underline{n}_1^1 \;\; \underline{n}_2^1 \;\; \underline{n}_3^1\right] \left[\underline{n}_1^2 \;\; \underline{n}_2^2 \;\; \underline{n}_3^2\right]^{-1} . \tag{1.231}$$

In the case of orthogonal unit vectors $\mathbf{n}_1$ and $\mathbf{n}_2$ the inverse matrix equals its transpose. In the case of nonorthogonal vectors the ith row $(i = 1, 2, 3)$ of the inverse is the transpose of the coordinate matrix, in basis $\underline{\mathbf{e}}^2$, of the *reciprocal vector* (see Bronstein/Semendjajev/Musiol/Mühlig [5])

$$\mathbf{e}_i = \frac{\mathbf{n}_j \times \mathbf{n}_k}{\mathbf{n}_1 \times \mathbf{n}_2 \cdot \mathbf{n}_3} \qquad (i, j, k = 1, 2, 3 \text{ cyclic}) . \tag{1.232}$$

From $\mathbf{n}_3 = \mathbf{n}_1 \times \mathbf{n}_2$ it follows that

$$\left.\begin{aligned} \mathbf{n}_2 \times \mathbf{n}_3 \;\;\;\;\;\; &= \mathbf{n}_1 - (\mathbf{n}_1 \cdot \mathbf{n}_2)\, \mathbf{n}_2 , \\ \mathbf{n}_3 \times \mathbf{n}_1 \;\;\;\;\;\; &= \mathbf{n}_2 - (\mathbf{n}_1 \cdot \mathbf{n}_2)\, \mathbf{n}_1 , \\ \mathbf{n}_1 \times \mathbf{n}_2 \cdot \mathbf{n}_3 &= (\mathbf{n}_1 \times \mathbf{n}_2)^2 = 1 - (\mathbf{n}_1 \cdot \mathbf{n}_2)^2 . \end{aligned}\right\} \tag{1.233}$$

The measured data must satisfy the compatibility condition that $\mathbf{n}_1 \cdot \mathbf{n}_2$ is the same with both sets of coordinates.

Example: The measured data are

$$\underline{n}_1^1 = \frac{1}{15}\begin{bmatrix} 11 \\ 10 \\ 2 \end{bmatrix} , \quad \underline{n}_1^2 = \frac{1}{5}\begin{bmatrix} 4 \\ 3 \\ 0 \end{bmatrix} , \quad \underline{n}_2^1 = \frac{1}{9}\begin{bmatrix} 8 \\ 1 \\ -4 \end{bmatrix} , \quad \underline{n}_2^2 = \frac{1}{3}\begin{bmatrix} 1 \\ 2 \\ -2 \end{bmatrix} .$$

The compatibility condition is satisfied. The data determine the number $\mathbf{n}_1 \times \mathbf{n}_2 \cdot \mathbf{n}_3 = 5/9$ and the matrices

$$\left[\underline{n}_1^1 \;\; \underline{n}_2^1 \;\; \underline{n}_3^1\right] = \frac{1}{45}\begin{bmatrix} 33 & 40 & -14 \\ 30 & 5 & 20 \\ 6 & -20 & -23 \end{bmatrix} ,$$

$$\left[\underline{n}_1^2 \;\; \underline{n}_2^2 \;\; \underline{n}_3^2\right] = \frac{1}{15}\begin{bmatrix} 12 & 5 & -6 \\ 9 & 10 & 8 \\ 0 & -10 & 5 \end{bmatrix} ,$$

$$\left[\underline{n}_1^2 \;\; \underline{n}_2^2 \;\; \underline{n}_3^2\right]^{-1} = \frac{1}{25}\begin{bmatrix} 26 & 7 & 20 \\ -9 & 12 & -30 \\ -18 & 24 & 15 \end{bmatrix} ,$$

$$\underline{X} = \frac{1}{3}\begin{bmatrix} 2 & 1 & -2 \\ 1 & 2 & 2 \\ 2 & -2 & 1 \end{bmatrix} .$$

End of example.

In numerous articles published in the robotics literature the solution is attempted by the following different method. The rigid body composed of end-effector and sensor is subjected to a rotation $(\mathbf{n}, \varphi)$. This rotation carries the bases $\underline{\mathbf{e}}^1$ and $\underline{\mathbf{e}}^2$ into new positions $\underline{\mathbf{e}}^{1*}$ and $\underline{\mathbf{e}}^{2*}$, respectively. The measured data is the pair of direction cosine matrices $\underline{A}$ and $\underline{B}$ in the relationships

$$\underline{\mathbf{e}}^1 = \underline{A}\,\underline{\mathbf{e}}^{1*} \qquad \text{(a)}\,, \qquad \underline{\mathbf{e}}^2 = \underline{B}\,\underline{\mathbf{e}}^{2*} \qquad \text{(b)}\,. \tag{1.234}$$

The bases $\underline{\mathbf{e}}^1$ and $\underline{\mathbf{e}}^2$ are related through $\underline{X}$ in the initial as well as in the final position. This is expressed by the equations

$$\underline{\mathbf{e}}^1 = \underline{X}\,\underline{\mathbf{e}}^2 \qquad \text{(a)}\,, \qquad \underline{\mathbf{e}}^{1*} = \underline{X}\,\underline{\mathbf{e}}^{2*} \qquad \text{(b)}\,. \tag{1.235}$$

Applying (1.235)a, (1.234)b, (1.235)b, (1.234)a in this order results in the equation

$$\underline{\mathbf{e}}^1 = \underline{X}\,\underline{\mathbf{e}}^2 = \underline{X}\,\underline{B}\,\underline{\mathbf{e}}^{2*} = \underline{X}\,\underline{B}\,\underline{X}^T\underline{\mathbf{e}}^{1*} = \underline{X}\,\underline{B}\,\underline{X}^T\underline{A}^T\underline{\mathbf{e}}^1\,. \tag{1.236}$$

Hence $\underline{X}\,\underline{B}\,\underline{X}^T\underline{A}^T = \underline{I}$ or $\underline{A}\,\underline{X} = \underline{X}\,\underline{B}$. A single rotation does not suffice. Two rotations $(\mathbf{n}_1, \varphi_1)$ and $(\mathbf{n}_2, \varphi_2)$ about arbitrarily chosen noncollinear unit vectors $\mathbf{n}_1$, $\mathbf{n}_2$ and through arbitrary angles φ_1, φ_2 yield two equations

$$\underline{A}_i\,\underline{X} = \underline{X}\,\underline{B}_i \qquad (i = 1, 2) \tag{1.237}$$

with measured matrices $\underline{A}_i$, $\underline{B}_i$ $(i = 1, 2)$. Articles in the robotics literature were devoted to solving these equations numerically. Various complicated iterative methods were proposed for this purpose. Both equations together represent a set of eighteen homogeneous linear equations for the elements of $\underline{X}$. For having a nontrivial solution the matrices $\underline{A}_i$, $\underline{B}_i$ $(i = 1, 2)$ must be compatible. The off-diagonal elements of $\underline{A}_i, \underline{B}_i$ determine the coordinates in $\underline{\mathbf{e}}^1$ and in $\underline{\mathbf{e}}^2$, respectively, of the body-fixed vector $\mathbf{m}_i = \mathbf{n}_i \sin\varphi_i$ (see (1.52)). Compatibility requires that $\mathbf{m}_1 \cdot \mathbf{m}_1$, $\mathbf{m}_2 \cdot \mathbf{m}_2$ and $\mathbf{m}_1 \cdot \mathbf{m}_2$ be the same with both sets of coordinates.

By writing (1.237) in the form $\underline{A}_i = \underline{X}\,\underline{B}_i\,\underline{X}^T$ $\underline{A}_i$ is expressed as similarity transform of $\underline{B}_i$. Application of Theorem 1.3 (Eq.(1.24)) to this equation leads directly to (1.230).

Angeles [3] proposes a combination of both methods by formulating (1.230) not in terms of the coordinates of $\mathbf{n}_1$, $\mathbf{n}_2$ and $\mathbf{n}_1 \times \mathbf{n}_2$, but in terms of the coordinates of $\mathbf{m}_1$, $\mathbf{m}_2$ and $\mathbf{m}_1 \times \mathbf{m}_2$ calculated from measured matrices $\underline{A}_i, \underline{B}_i$ $(i = 1, 2)$.

1.15.11 Decomposition of a Rotation into three Rotations

The material of this section and of the next section was published in Wittenburg/Lilov [32]. Earlier contributions to the subject were made by Davenport [6] and Wohlhart [33]. In the nonorthogonal gimbal suspension system of Fig. 1.12 the inner axis has the direction $\mathbf{n}_1$, and the outer axis has the direction $\mathbf{n}_3$. If three rotations $(\mathbf{n}_1, \varphi_1)$, $(\mathbf{n}_2, \varphi_2)$, $(\mathbf{n}_3, \varphi_3)$ are carried out in this order, all three rotation axes $\mathbf{n}_1$, $\mathbf{n}_2$, $\mathbf{n}_3$ are given in the outer (base-fixed) reference frame. Let $(\mathbf{n}, \varphi)$ be the resultant of this sequence of rotations. Its tensor $\mathsf{R}(\mathbf{n}, \varphi)$ is the product of the tensors of the three individual rotations (see (1.45)):

$$\mathsf{R}(\mathbf{n}, \varphi) = \mathsf{R}(\mathbf{n}_3, \varphi_3) \cdot \mathsf{R}(\mathbf{n}_2, \varphi_2) \cdot \mathsf{R}(\mathbf{n}_1, \varphi_1) \,. \tag{1.238}$$

The problem to be solved is the following. The unit vector $\mathbf{n}$ and the angle φ of the resultant rotation $(\mathbf{n}, \varphi)$ and, furthermore, the unit vectors $\mathbf{n}_1$, $\mathbf{n}_2$, $\mathbf{n}_3$ of the individual rotations are given. To be determined are the angles φ_1, φ_2, φ_3. The vectors $\mathbf{n}_1$, $\mathbf{n}_2$, $\mathbf{n}_3$ are neither coplanar nor pairwise orthogonal. The relative orientation of the four vectors is specified by the six parameters

$$a_i = \mathbf{n}_j \cdot \mathbf{n}_k \,, \qquad b_i = \mathbf{n} \cdot \mathbf{n}_i \qquad (i, j, k = 1, 2, 3 \text{ different}) \,. \tag{1.239}$$

Together with a_1, a_2, a_3 also the following scalar products are given.

$$\left.\begin{aligned} a_{ii} &= (\mathbf{n}_j \times \mathbf{n}_k)^2 = 1 - a_i^2 \,, \\ a_{ij} &= (\mathbf{n}_i \times \mathbf{n}_k) \cdot (\mathbf{n}_k \times \mathbf{n}_j) = a_i a_j - a_k \,, \\ a &= \mathbf{n}_1 \cdot \mathbf{n}_2 \times \mathbf{n}_3 \,, \\ a^2 &= 1 - a_1^2 - a_2^2 - a_3^2 + 2a_1 a_2 a_3 = a_{ii} a_{jj} - a_{ij}^2 \end{aligned}\right\} \quad (i, j, k = 1, 2, 3 \text{ different}) \,. \tag{1.240}$$

The parameters b_1, b_2, b_3 represent the covariant coordinates of $\mathbf{n}$. The contravariant coordinates c_1, c_2, c_3 are defined through the equation $\mathbf{n} = c_1\mathbf{n}_1 + c_2\mathbf{n}_2 + c_3\mathbf{n}_3$. They satisfy the equations

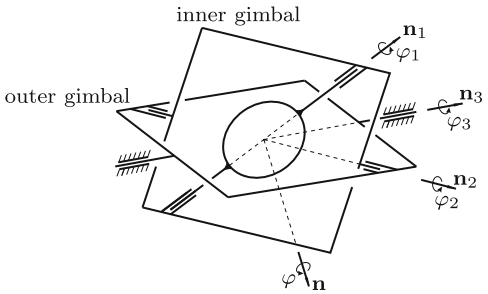

Fig. 1.12 Gimbal suspension system with nonorthogonal axes

$$\left.\begin{aligned} ac_i &= \mathbf{n}\cdot\mathbf{n}_j\times\mathbf{n}_k\ , \\ a^2c_i^2 &= (1-b_j^2)(1-b_k^2)-(b_jb_k-a_i)^2 \end{aligned}\right\} \quad (i,j,k=1,2,3 \text{ cyclic})\ . \tag{1.241}$$

Solution: Comparison of Fig. 1.12 with Fig. 1.2b shows: If $\mathbf{n}_3$, $\mathbf{n}_2$, $\mathbf{n}_1$ form a right-hand cartesian basis $\mathbf{e}_1^1$, $\mathbf{e}_2^1$, $\mathbf{e}_3^1$, the angles φ_3, φ_2, φ_1 represent, in this order, the Bryan angles ϕ_1, ϕ_2, ϕ_3, respectively. This particular case is characterized by the parameters $a_i=0$, $a=-1$ and $b_i=c_i$ $(i=1,2,3)$. The solutions $\varphi_1=\phi_3$, $\varphi_2=\phi_2$ and $\varphi_3=\phi_1$ are calculated from (1.35) with the matrix elements of (1.49) with b_i instead of n_i $(i=1,2,3)$.

In the general case, the solution is found from (1.238) as follows. Two scalar multiplications, one from the left by $\mathsf{R}(-\mathbf{n}_3,\varphi_3)$ and the other from the right by $\mathsf{R}(-\mathbf{n}_1,\varphi_1)$, produce the equation (see the identities (1.46))

$$\mathsf{R}(\mathbf{n}_2,\varphi_2)=\mathsf{R}(-\mathbf{n}_3,\varphi_3)\cdot R(\mathbf{n},\varphi)\cdot\mathsf{R}(-\mathbf{n}_1,\varphi_1)\ . \tag{1.242}$$

Scalar multiplication of this equation from the left by $\mathbf{n}_3$ eliminates φ_3, and scalar multiplication from the right by $\mathbf{n}_1$ eliminates φ_1. This follows from the identities (1.41). Thus, a scalar equation for the single unknown φ_2 is obtained by carrying out both multiplications:

$$\mathbf{n}_3\cdot\mathsf{R}(\mathbf{n}_2,\varphi_2)\cdot\mathbf{n}_1=\mathbf{n}_3\cdot\mathsf{R}(\mathbf{n},\varphi)\cdot\mathbf{n}_1\ . \tag{1.243}$$

Two coupled scalar equations for the two unknowns φ_3 and φ_2 are produced by multiplying (1.242) from the left by $\mathbf{n}_2$ and from the right by $\mathbf{n}_1$ and by multiplying from both sides by $\mathbf{n}_1$, respectively:

$$\left.\begin{aligned} \mathbf{n}_2\cdot\mathbf{n}_1 &= \mathbf{n}_2\cdot\mathsf{R}(-\mathbf{n}_3,\varphi_3)\cdot\mathsf{R}(\mathbf{n},\varphi)\cdot\mathbf{n}_1\ , \\ \mathbf{n}_1\cdot\mathsf{R}(\mathbf{n}_2,\varphi_2)\cdot\mathbf{n}_1 &= \mathbf{n}_1\cdot\mathsf{R}(-\mathbf{n}_3,\varphi_3)\cdot\mathsf{R}(\mathbf{n},\varphi)\cdot\mathbf{n}_1\ . \end{aligned}\right\} \tag{1.244}$$

Finally, two coupled scalar equations for the two unknowns φ_1 and φ_2 are produced by multiplying from the left by $\mathbf{n}_3$ and from the right by $\mathbf{n}_2$ and by multiplying from both sides by $\mathbf{n}_3$, respectively:

$$\left.\begin{aligned} \mathbf{n}_3\cdot\mathbf{n}_2 &= \mathbf{n}_3\cdot\mathsf{R}(\mathbf{n},\varphi)\cdot\mathsf{R}(-\mathbf{n}_1,\varphi_1)\cdot\mathbf{n}_2\ , \\ \mathbf{n}_3\cdot\mathsf{R}(\mathbf{n}_2,\varphi_2)\cdot\mathbf{n}_3 &= \mathbf{n}_3\cdot\mathsf{R}(\mathbf{n},\varphi)\cdot\mathsf{R}(-\mathbf{n}_1,\varphi_1)\cdot\mathbf{n}_3\ . \end{aligned}\right\} \tag{1.245}$$

These equations are obtained from (1.244) by interchanging the indices 1 and 3. Hence the solution for φ_1 is obtained from the solution for φ_3 by this interchange of indices. For this reason only (1.243) and (1.244) are considered.

The tensors are given in (1.40), for example,

$$\mathsf{R}(\mathbf{n},\varphi)=\mathbf{nn}+\cos\varphi(\mathsf{I}-\mathbf{nn})+\sin\varphi\,\mathbf{n}\times\mathsf{I} \tag{1.246}$$

and similarly $\mathsf{R}(\mathbf{n}_i,\varphi_i)$. First, the vectors are calculated:

$$\left.\begin{aligned}
\mathsf{R}(\mathbf{n}_2,\varphi_2)\cdot\mathbf{n}_1 &= a_3\mathbf{n}_2+\cos\varphi_2\,(\mathbf{n}_1-a_3\mathbf{n}_2)+\sin\varphi_2\,\mathbf{n}_2\times\mathbf{n}_1\ ,\\
\mathsf{R}(\mathbf{n},\varphi)\cdot\mathbf{n}_1 &= b_1\mathbf{n}+\cos\varphi\,(\mathbf{n}_1-b_1\mathbf{n})+\sin\varphi\,\mathbf{n}\times\mathbf{n}_1\ ,\\
\mathbf{n}_2\cdot\mathsf{R}(-\mathbf{n}_3,\varphi_3) &= a_1\mathbf{n}_3+\cos\varphi_3\,(\mathbf{n}_2-a_1\mathbf{n}_3)-\sin\varphi_3\,\mathbf{n}_2\cdot\mathbf{n}_3\times I\ ,\\
\mathbf{n}_1\cdot\mathsf{R}(-\mathbf{n}_3,\varphi_3) &= a_2\mathbf{n}_3+\cos\varphi_3\,(\mathbf{n}_1-a_2\mathbf{n}_3)-\sin\varphi_3\,\mathbf{n}_1\cdot\mathbf{n}_3\times I\ .
\end{aligned}\right\} \tag{1.247}$$

With these vectors Eq.(1.243) for φ_2 takes the form

$$a_{13}\cos\varphi_2+a\sin\varphi_2=R \tag{1.248}$$

with the given constant

$$R=a_1a_3-b_1b_3+(b_1b_3-a_2)\cos\varphi+ac_2\sin\varphi\ . \tag{1.249}$$

The equation has two solutions φ_{2_1} and φ_{2_2}. They are determined by

$$\left.\begin{aligned}
\cos\varphi_{2_k} &= \frac{a_{13}R+(-1)^k a\sqrt{a_{13}^2+a^2-R^2}}{a_{13}^2+a^2}\ ,\\
\sin\varphi_{2_k} &= \frac{aR-(-1)^k a_{13}\sqrt{a_{13}^2+a^2-R^2}}{a_{13}^2+a^2}
\end{aligned}\right\}\quad (k=1,2)\ . \tag{1.250}$$

Equations (1.244) are linear equations for $\cos\varphi_3$ and $\sin\varphi_3$

$$\left.\begin{aligned}
A_1\cos\varphi_3+B_1\sin\varphi_3&=C_1\ ,\\
A_2\cos\varphi_3+B_2\sin\varphi_3&=C_2
\end{aligned}\right\} \tag{1.251}$$

with coefficients

$$\left.\begin{aligned}
A_1&=b_1(b_2-a_1b_3)-[b_1(b_2-a_1b_3)+a_{12}]\cos\varphi+a(c_3+a_1c_2)\sin\varphi\ ,\\
B_1&=-ab_1c_1-a(1-b_1c_1)\cos\varphi+(a_3b_3-a_2b_2)\sin\varphi\ ,\\
C_1&=a_1[(b_1b_3-a_2)\cos\varphi+ac_2\sin\varphi-b_1b_3]+a_3\ ,\\
A_2&=b_1(b_1-a_2b_3)-[b_1(b_1-a_2b_3)-a_{22}]\cos\varphi+aa_2c_2\sin\varphi\ ,\\
B_2&=ab_1c_2(1-\cos\varphi)+(b_3-a_2b_1)\sin\varphi\ ,\\
C_2&=a_2[(b_1b_3-a_2)\cos\varphi+ac_2\sin\varphi-b_1b_3]+a_3^2+a_{33}\cos\varphi_2\ .
\end{aligned}\right\} \tag{1.252}$$

The coefficient C_2 is the only one which depends explicitly on φ_2. Each solution $\cos\varphi_2$ of (1.248) determines the associated solutions for $\cos\varphi_3$ and $\sin\varphi_3$. The associated solutions for $\cos\varphi_1$ and $\sin\varphi_1$ are obtained by interchanging the indices 1 and 3.

Example: Let the given resultant rotation $(\mathbf{n},\varphi)$ be the rotation $\varphi=0$. The vector $\mathbf{n}$ is unspecified. Obviously, $\varphi_1=\varphi_2=\varphi_3=0$ is a solution. Equations (1.248), (1.251) and Eqs.(1.251) with indices 1 and 3 interchanged determine two solutions. In the case $\varphi=0$, these three equations have the special forms

$$a_{jk}\cos\varphi_i + a\sin\varphi_i = a_{jk} \qquad (i,j,k = 1,2,3 \text{ different}) \,. \tag{1.253}$$

As should be expected, the parameters b_1, b_2 and b_3 do not occur. One of the solutions is, indeed, the trivial solution $\varphi_1 = \varphi_2 = \varphi_3 = 0$. Equations (1.250) yield for the second solution the formulas

$$\cos\varphi_i = \frac{a_{jk}^2 - a^2}{a_{jk}^2 + a^2} \,, \quad \sin\varphi_i = \frac{2aa_{jk}}{a_{jk}^2 + a^2} \quad (i,j,k = 1,2,3 \text{ different}) \,. \tag{1.254}$$

In the special case of mutually orthogonal vectors $\mathbf{n}_1$, $\mathbf{n}_2$, $\mathbf{n}_3$, the angles are $\varphi_1 = \varphi_2 = \varphi_3 = \pi$. End of example.

In what follows, conditions for the existence of real solutions are formulated. The solutions φ_{2_1} and φ_{2_2} determined by (1.250) are real if and only if $-\sqrt{a_{13}^2 + a^2} \le R \le \sqrt{a_{13}^2 + a^2}$. Define $x = \cos\varphi$ and $y = \sin\varphi$ so that every angle φ is represented by a point on the unit circle. The equality signs define two parallel straight lines:

$$(b_1b_3 - a_2)x + ac_2y = b_1b_3 - a_1a_3 \pm \sqrt{a_{13}^2 + a^2} \,. \tag{1.255}$$

Real solutions exist for all points of the intersection Γ of the unit circle and the strip between these lines including the lines themselves. Let r_1 and r_2 be the distances of the lines from the origin of the x, y-system. They are

$$r_{1,2} = \frac{\left| b_1b_3 - a_1a_3 \pm \sqrt{a_{13}^2 + a^2} \right|}{\sqrt{(b_1b_3 - a_2)^2 + a^2c_2^2}} \tag{1.256}$$

or with (1.240) and (1.241)

$$r_{1,2} = \frac{\left| b_1b_3 - a_1a_3 \pm \sqrt{(1 - a_1^2)(1 - a_3^2)} \right|}{\sqrt{(1 - b_1^2)(1 - b_3^2)}} \,. \tag{1.257}$$

Γ is the complete unit circle if and only if $r_{1,2} \ge 1$. In the case $a_1 = a_3 = 0$, these conditions are satisfied for arbitrary quantities b_1, b_3. In the case $b_1 = b_3 = 0$, they are satisfied if and only if $a_1 = a_3 = 0$. Because of (1.239) this means: The solutions (1.250) for φ_2 are real for *arbitrary* resultant rotations $(\mathbf{n}, \varphi)$ if and only if $\mathbf{n}_2$ is orthogonal to both $\mathbf{n}_1$ and $\mathbf{n}_3$. This is an important result. It means that the gimbal suspension system of Fig. 1.12 is capable of producing arbitrary angular orientations of the suspended body if and only if the axis between inner and outer gimbal is orthogonal to both the fixed outer gimbal axis and the axis between body and inner gimbal. Commonly used gimbal suspension systems have this property.

Indeterminacy conditions: From Euler angles as well as from Bryan angles the phenomenon of gimbal lock is known. The angles are not fully determinate

if the prescribed angular orientation of the body is characterized by gimbal lock. In the case of Euler angles, only θ and either $\psi + \phi$ or $\psi - \phi$ are determinate. In the case of Bryan angles, only ϕ_2 and either $\phi_1 + \phi_3$ or $\phi_1 - \phi_3$ are determinate. The same phenomenon occurs here. Under certain conditions for the given quantities $\mathbf{n}$, φ, $\mathbf{n}_1$, $\mathbf{n}_2$ and $\mathbf{n}_3$ the gimbals in Fig. 1.12 are locked. In this case, only φ_2 and either $\varphi_1 + \varphi_3$ or $\varphi_1 - \varphi_3$ are determinate. The derivation of these conditions is found in Wittenburg/Lilov [32]. The results can be summarized as follows. Indeterminacy occurs if the given data satisfy the conditions

$$a_3 = \sigma a_1 \,, \quad b_3 = \sigma b_1 \,, \quad \cos\varphi = \frac{\sigma a_2 - b_1^2}{a_2 - b_1^2} \,, \quad \sin\varphi = \frac{ac_2}{a_2 - b_1^2} \tag{1.258}$$

($\sigma = +1$ or -1). Equations (1.239) show that the leading two conditions are the orthogonality conditions $\mathbf{n}_2 \cdot (\mathbf{n}_1 - \sigma\mathbf{n}_3) = 0$ and $\mathbf{n} \cdot (\mathbf{n}_1 - \sigma\mathbf{n}_3) = 0$, respectively. The vectors $\mathbf{n}_1 - \mathbf{n}_3$ and $\mathbf{n}_1 + \mathbf{n}_3$ are the mutually orthogonal bisectors of the angles between $\mathbf{n}_1$ and $\mathbf{n}_3$. If the conditions (1.258) are satisfied, the angle φ_2 and the angles $\varphi_1 + \sigma\varphi_3$ are determined from the equations

$$\left.\begin{aligned} \cos\varphi_2 &= \frac{\sigma a_2 - a_1^2}{1 - a_1^2} \,, & \cos(\varphi_1 + \sigma\varphi_3) &= 1 - \frac{2a^2c_1^2}{(1 - a_1^2)(1 - b_1^2)} \,, \\ \sin\varphi_2 &= \frac{-\sigma a}{1 - a_1^2} \,, & \sin(\varphi_1 + \sigma\varphi_3) &= \frac{2ac_1(a_1b_1 - \sigma b_2)}{(1 - a_1^2)(1 - b_1^2)} \,. \end{aligned}\right\} \tag{1.259}$$

If the axes of the gimbal suspension system in Fig. 1.12 are mutually orthogonal, the conditions (1.258) are identical with (1.197).

1.15.12 Decomposition of a Rotation into three Rotations. Quaternion Formulation

In this section the problem posed in the previous section is solved by means of quaternions. Let D be the quaternion of the given resultant rotation $(\mathbf{n}, \varphi)$, and let D_1, D_2, D_3 be the quaternions of the three rotations $(\mathbf{n}_1, \varphi_1)$, $(\mathbf{n}_2, \varphi_2)$ and $(\mathbf{n}_3, \varphi_3)$, respectively. According to Theorem 1.4 (Eq.(1.116)) these quaternions satisfy the equation

$$D_3 D_2 D_1 = D \,. \tag{1.260}$$

According to (1.107)

$$D = \left(\cos\frac{\varphi}{2} \,, \mathbf{n}\sin\frac{\varphi}{2}\right) . \tag{1.261}$$

The quaternions D_1, D_2, D_3 are given by the same formula with the respective index added everywhere. For the cosines and sines of half-angles the following abbreviations are defined:

$$C_i = \cos\frac{\varphi_i}{2}\ , \quad S_i = \sin\frac{\varphi_i}{2}\ \ (i=1,2,3)\ , \quad C = \cos\frac{\varphi}{2}\ , \quad S = \sin\frac{\varphi}{2}\ . \tag{1.262}$$

With this notation the quaternions are $D_i = (C_i, \mathbf{n}_i S_i)$ $(i = 1,2,3)$ and $D = (C, \mathbf{n}S)$. Equation (1.260) becomes

$$(C_3, \mathbf{n}_3 S_3)(C_2, \mathbf{n}_2 S_2)(C_1, \mathbf{n}_1 S_1) = (C, \mathbf{n}S)\ . \tag{1.263}$$

The product is formulated in two steps. In the first step the product $(C_2, \mathbf{n}_2 S_2)(C_1, \mathbf{n}_1 S_1)$ is calculated. According to the rule (1.98) it is the quaternion

$$(C_1C_2 - \mathbf{n}_1 \cdot \mathbf{n}_2\, S_1S_2\ ,\ \mathbf{n}_1\, S_1C_2 + \mathbf{n}_2\, C_1S_2 - \mathbf{n}_1 \times \mathbf{n}_2\, S_1S_2)\ . \tag{1.264}$$

After another application of the product rule the scalar part and the vector part of (1.263) are

$$C_1C_2C_3 - (a_1C_1S_2S_3 + a_2S_1C_2S_3 + a_3S_1S_2C_3) + aS_1S_2S_3 = C\ , \tag{1.265}$$

$$\begin{aligned}&\mathbf{n}_1S_1(C_2C_3 - a_1S_2S_3) + \mathbf{n}_2S_2(C_3C_1 + a_2S_3S_1) + \mathbf{n}_3S_3(C_1C_2 - a_3S_1S_2)\\ &\quad -\mathbf{n}_1 \times \mathbf{n}_2S_1S_2C_3 - \mathbf{n}_2 \times \mathbf{n}_3C_1S_2S_3 + \mathbf{n}_3 \times \mathbf{n}_1S_1C_2S_3 = \mathbf{n}S\ .\end{aligned} \tag{1.266}$$

For the definitions of a_1, a_2, a_3 and a see (1.239) and (1.240).

Rodrigues [25] expressed the opinion that the equations cannot be solved for the unknown angles φ_1, φ_2, φ_3. As will be seen they can be solved. The vector part of the equation is scalar-multiplied by $\mathbf{n}_1$, by $\mathbf{n}_2$ and by $\mathbf{n}_3$. The scalar part and the three component equations are written as linear equations for C_1 and S_1:

$$\left.\begin{array}{lll} C_1(C_2C_3 - a_1S_2S_3) & +S_1(aS_2S_3 - a_2C_2S_3 - a_3S_2C_3) & = C\ ,\\ -C_1(aS_2S_3 - a_2C_2S_3 - a_3S_2C_3) & +S_1(C_2C_3 - a_1S_2S_3) & = b_1S\ ,\\ C_1(S_2C_3 + a_1C_2S_3) & +S_1[aC_2S_3 + a_3C_2C_3 + (a_2 - 2a_1a_3)S_2S_3] & = b_2S\ ,\\ C_1(C_2S_3 + a_1S_2C_3) & -S_1(aS_2C_3 - a_2C_2C_3 + a_3S_2S_3) & = b_3S\ . \end{array}\right\} \tag{1.267}$$

This system of equations is invariant with respect to an interchange of the indices 1 and 3. More precisely, the first as well as the third equation is individually invariant whereas the second and the fourth are invariant as a set. This invariance confirms what is known from Sect. 1.15.11. The solution for φ_1 is obtained from the solution for φ_3 by interchanging the indices 1 and 3.

The first two equations have the special forms $p\,C_1 + q\,S_1 = C$ and $-q\,C_1 + p\,S_1 = b_1S$ with coefficients p and q which are linear with respect to C_2, S_2, C_3, S_3. The sum of squares of the equations is the equation $p^2 + q^2 = C^2 + b_1^2S^2$. The right-hand side expression is a given constant.

The left-hand side expression represents the coefficient determinant of the original two equations. The equation is used in two ways. First, it is used as an equation for the unknowns φ_2 and φ_3. Second, the original two equations are solved for C_1 and S_1. Since the coefficient determinant is constant, the resulting expressions are linear with respect to C_2, S_2, C_3, S_3. These expressions are then substituted into the third and the fourth Eq.(1.267). This procedure results in two more equations for the unknowns φ_2 and φ_3. In each of the three equations the circular functions C_2, S_2, C_3, S_3 appear in products which allow the return from half-angles to full angles (the possible return to the full angle φ is postponed until later). As a result of the said algebraic manipulations the following equations are obtained:

$$\begin{aligned}
&[-a_3a_{21} + (a^2 - a_1a_{23})\cos\varphi_2 + aa_2\sin\varphi_2]\,\cos\varphi_3 \\
&+ [aa_3(\cos\varphi_2 - 1) + a_{23}\sin\varphi_2]\,\sin\varphi_3 \\
&= 2(C^2 + b_1^2S^2) + a_2(-a_1a_3 + a_{13}\cos\varphi_2 + a\sin\varphi_2) - 1\,, \qquad (1.268)
\end{aligned}$$

$$\begin{aligned}
&C[aa_3(\cos\varphi_2 - 1) + a_{23}\sin\varphi_2]\,\cos\varphi_3 \\
&- C[-a_3a_{21} + (a^2 - a_1a_{23})\cos\varphi_2 + aa_2\sin\varphi_2]\,\sin\varphi_3 \\
&= -S\{2b_3(C^2 + b_1^2S^2) + b_1[-(a_1a_3 + a_2) + a_{13}\cos\varphi_2 + a\sin\varphi_2]\}\,, \qquad (1.269)
\end{aligned}$$

$$\begin{aligned}
&[a_3b_1S + (aC - a_1b_1S)(a_1a_3 - a_{13}\cos\varphi_2 - a\sin\varphi_2) + a_{33}C\sin\varphi_2]\cos\varphi_3 \\
&+ [a_3a_{13}C + (a_1a_{33}C + ab_1S)\cos\varphi_2 - a_{13}b_1S\sin\varphi_2]\sin\varphi_3 \\
&= 2b_2S(C^2 + b_1^2S^2) + (aC - a_1b_1S)(a_1a_3 - a_{13}\cos\varphi_2 - a\sin\varphi_2) - a_3b_1S\,. \\
&\qquad (1.270)
\end{aligned}$$

The equations are linear equations for $\cos\varphi_3$ and $\sin\varphi_3$. With abbreviations $b_{k\ell}$, $c_{k\ell}$ and r_k $(k, \ell = 1, 2, 3)$ for the coefficients they have the forms

$$(b_{k1}\cos\varphi_2 + b_{k2}\sin\varphi_2 + b_{k3})\cos\varphi_3 + (c_{k1}\cos\varphi_2 + c_{k2}\sin\varphi_2 + c_{k3})\sin\varphi_3 = r_k \qquad (1.271)$$

$(k = 1, 2, 3)$. With suitable coefficients A_1, A_2, A_3 a linear combination of the three equations can be constructed which is free of the term $\cos\varphi_3$. The coefficients must satisfy the three homogeneous equations

$$A_1b_{1\ell} + A_2b_{2\ell} + A_3b_{3\ell} = 0 \qquad (\ell = 1, 2, 3)\,. \qquad (1.272)$$

These equations are solved by

$$A_1 = aa_2C^2 - b_1a_{12}SC\,, \qquad A_2 = a_{23}C - ab_1S\,, \qquad A_3 = -a_{22}C\,. \quad (1.273)$$

Similarly, coefficients are determined for a linear combination of the three equations which is free of the term $\sin\varphi_3$. These coefficients must satisfy the three Eqs.(1.272) with $c_{k\ell}$ instead of $b_{k\ell}$ $(k, \ell = 1, 2, 3)$. Surprisingly, the same coefficients A_1, A_2, A_3 of Eqs.(1.273) are found. The reason is that Eqs.(1.268) – (1.270) are three compatible equations for only two unknowns. The said linear combination eliminates φ_3. In the resulting equation φ_2 is the single unknown. As should be expected, this equation is Eq.(1.248). It has the solutions φ_{2_1} and φ_{2_2} given in (1.250). For each solution any two of the Eqs.(1.268) – (1.270) represent a system of two linear equations for the associated solutions $\cos\varphi_3$ and $\sin\varphi_3$ and after interchanging the indices 1 and 3 for the solutions $\cos\varphi_1$ and $\sin\varphi_1$. This concludes the solution of Eqs.(1.267).

In Sect. 1.15.11 it has been said that the angles φ_1 and φ_3 are individually indeterminate, if the given quantities satisfy the conditions (1.258). Under these conditions the solution is given by Eqs.(1.259). The same conditions and the same resulting equations can be deduced directly from (1.267). This is left to the reader.

1.16 Reflection in a Plane

Subject of this section are reflections of points in a plane (Fig. 1.13). The plane is referred to as reflecting plane. Points as well as the reflecting plane are defined in a reference basis $\underline{\mathbf{e}}$ with origin 0. The plane is determined by its unit normal vector $\mathbf{m}$ (sense of direction arbitrary) and by the vector $\mathbf{r}_0 = r_0\mathbf{m}$ to the foot A_0 of the perpendicular from 0 onto the plane. Let $\mathbf{r}$ be the position vector of an arbitrary point P and let, furthermore, $\mathbf{r}^*$ be the position vector of the reflection P^* of P. Reflection in a plane is defined as follows (compare the definition of reflection in a line following Eq.(1.42)). P^* is the reflection of P if
- the line $\overline{\mathrm{PP}}^*$ intersects the reflecting plane orthogonally
- the point of intersection is midpoint of $\overline{\mathrm{PP}}^*$.

Figure 1.13 shows that this definition is expressed by the equation

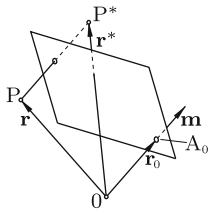

Fig. 1.13 Reflection in a plane

$$\frac{\mathbf{r}-\mathbf{r}^*}{2} = \mathbf{m}[\mathbf{m}\cdot(\mathbf{r}-\mathbf{r}_0)] \,. \tag{1.274}$$

Taking into account the identity $\mathbf{mm}\cdot\mathbf{r}_0 = \mathbf{m}r_0 = \mathbf{r}_0$ the solution for $\mathbf{r}^*$ is

$$\mathbf{r}^* = (\mathsf{I}-2\mathbf{mm})\cdot\mathbf{r} + 2\mathbf{r}_0 \tag{1.275}$$

$$= \mathsf{S}\cdot\mathbf{r} + 2\mathbf{r}_0 \,. \tag{1.276}$$

The tensor

$$\mathsf{S} = \mathsf{I} - 2\mathbf{mm} \tag{1.277}$$

is called reflection tensor. It satisfies the equation

$$\mathsf{S}\cdot\mathsf{S} = \mathsf{I} \,. \tag{1.278}$$

The tensor has the single eigenvalue $\lambda_1 = -1$ and the double eigenvalue $\lambda_2 = +1$. The eigenvector associated with the eigenvalue $\lambda_1 = -1$ is $\mathbf{m}$. Every vector $\mathbf{n}$ in the reflecting plane, i.e., normal to $\mathbf{m}$, is an eigenvector associated with the eigenvalue $\lambda_2 = +1$. This is expressed by the equations

$$(\mathsf{I}-2\mathbf{mm})\cdot\mathbf{m} = -\mathbf{m} \,, \qquad (\mathsf{I}-2\mathbf{mm})\cdot\mathbf{n} = \mathbf{n} \,. \tag{1.279}$$

Proposition 1: Reflection is involutoric (two reflections of a point P in succession in one and the same plane result in the original point P). Proof: Twofold application yields the identity:
$(\mathsf{I}-2\mathbf{mm})\cdot[(\mathsf{I}-2\mathbf{mm})\cdot\mathbf{r}+2\mathbf{r}_0]+2\mathbf{r}_0 \equiv \mathbf{r}$. End of proof.

Proposition 2: Reflections are length- as well as angle-preserving. Proof: It suffices to show that in the case $\mathbf{r}_0 = \mathbf{0}$ (point 0 is in the reflecting plane), vectors $\mathbf{r}_1$ and $\mathbf{r}_2$ from 0 to points P_1 and P_2, respectively, satisfy the equation $\mathbf{r}_1^*\cdot\mathbf{r}_2^* = \mathbf{r}_1\cdot\mathbf{r}_2$. In the special case $\mathbf{r}_1 = \mathbf{r}_2$, this equation proves that length is preserved. Equation (1.276) yields

$$\begin{aligned}\mathbf{r}_1^*\cdot\mathbf{r}_2^* &= [\mathbf{r}_1 - 2\mathbf{m}(\mathbf{m}\cdot\mathbf{r}_1)]\cdot[\mathbf{r}_2 - 2\mathbf{m}(\mathbf{m}\cdot\mathbf{r}_2)] \\ &= \mathbf{r}_1\cdot\mathbf{r}_2 + (\mathbf{m}\cdot\mathbf{r}_1)(\mathbf{m}\cdot\mathbf{r}_2)(-2-2+4) = \mathbf{r}_1\cdot\mathbf{r}_2 \,. \end{aligned} \tag{1.280}$$

End of proof.

Proposition 3: The reflection $\underline{\mathbf{e}}^*$ of a right-handed cartesian basis $\underline{\mathbf{e}}$ is a left-handed cartesian basis. Proof: Again, it suffices to consider the special case $\mathbf{r}_0 = \mathbf{0}$. Since lengths as well as right angles are preserved, it suffices to show that $\mathbf{e}_1^*\cdot\mathbf{e}_2^*\times\mathbf{e}_3^* = -1$. First, the cross product is calculated:

$$\begin{aligned}\mathbf{e}_2^*\times\mathbf{e}_3^* &= [\mathbf{e}_2 - 2\mathbf{m}(\mathbf{m}\cdot\mathbf{e}_2)]\times[\mathbf{e}_3 - 2\mathbf{m}(\mathbf{m}\cdot\mathbf{e}_3)] \\ &= \mathbf{e}_2\times\mathbf{e}_3 - 2(\mathbf{e}_2\times\mathbf{m})(\mathbf{m}\cdot\mathbf{e}_3) - 2(\mathbf{m}\times\mathbf{e}_3)(\mathbf{m}\cdot\mathbf{e}_2) \,. \end{aligned} \tag{1.281}$$

With this expression another application of (1.276) yields

$$\begin{aligned}
&\mathbf{e}_1^* \cdot \mathbf{e}_2^* \times \mathbf{e}_3^* = [\mathbf{e}_1 - 2\mathbf{m}(\mathbf{m} \cdot \mathbf{e}_1)] \cdot \mathbf{e}_2^* \times \mathbf{e}_3^* \\
&= \mathbf{e}_1 \cdot [\mathbf{e}_2 \times \mathbf{e}_3 - 2(\mathbf{e}_2 \times \mathbf{m})(\mathbf{m} \cdot \mathbf{e}_3) - 2(\mathbf{m} \times \mathbf{e}_3)(\mathbf{m} \cdot \mathbf{e}_2)] \\
&\quad -2(\mathbf{m} \cdot \mathbf{e}_2 \times \mathbf{e}_3)(\mathbf{m} \cdot \mathbf{e}_1) \\
&= \mathbf{e}_1 \cdot \mathbf{e}_2 \times \mathbf{e}_3 - 2[(\mathbf{m} \cdot \mathbf{e}_3)^2 + (\mathbf{m} \cdot \mathbf{e}_2)^2 + (\mathbf{m} \cdot \mathbf{e}_1)^2] \\
&= 1 - 2 = -1 \, . \qquad (1.282)
\end{aligned}$$

End of proof.

Example: Equation (1.275) is applied to the planar problem shown in Fig. 1.14. The vectors $\mathbf{m}$, $\mathbf{r}_0$ and $\mathbf{r}$ are in the x, y-plane of an x, y, z-system. Then also $\mathbf{r}^*$ is in this plane. This is the special case of reflection of the x, y-plane in a line located in this plane. The line is defined by the angle α measured counterclockwise from the x-axis and by the coordinate a of the point of intersection A with the x-axis. The unit vector $\mathbf{m}$ has the coordinates $[\sin\alpha \quad -\cos\alpha]^T$. Furthermore, $\mathbf{r}_0 = \mathbf{m}\, a \sin\alpha$. The coordinates of $\mathbf{r}$ and $\mathbf{r}^*$ are denoted $[x \quad y]^T$ and $[x^* \quad y^*]^T$, respectively. Equation (1.275) yields the coordinate equation

$$\begin{bmatrix} x^* \\ y^* \end{bmatrix} = \begin{bmatrix} \cos 2\alpha & \sin 2\alpha \\ \sin 2\alpha & -\cos 2\alpha \end{bmatrix} \begin{bmatrix} x \\ y \end{bmatrix} + a \begin{bmatrix} 1 - \cos 2\alpha \\ -\sin 2\alpha \end{bmatrix} \, . \qquad (1.283)$$

End of example.

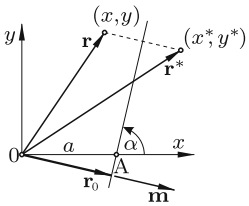

Fig. 1.14 Reflection of x, y-plane in a line located in this plane

Next, the resultant of two successive reflections in different planes is investigated. The first reflection with tensor $\mathsf{S}_1 = \mathsf{I} - 2\mathbf{m}_1\mathbf{m}_1$ and with vector $\mathbf{r}_{01}$ is followed by the reflection with tensor $\mathsf{S}_2 = \mathsf{I} - 2\mathbf{m}_2\mathbf{m}_2$ and with vector $\mathbf{r}_{02}$. A point originally located at $\mathbf{r}$ is after the first reflection in the position $\mathsf{S}_1 \cdot \mathbf{r} + 2\mathbf{r}_{01}$ and after the second reflection in the position

$$\mathbf{r}^* = \mathsf{S}_2 \cdot (\mathsf{S}_1 \cdot \mathbf{r} + 2\mathbf{r}_{01}) + 2\mathbf{r}_{02} = \mathsf{S}_2 \cdot \mathsf{S}_1 \cdot \mathbf{r} + 2(\mathsf{S}_2 \cdot \mathbf{r}_{01} + \mathbf{r}_{02}) \, . \qquad (1.284)$$

The special case of parallel planes:
This case is characterized by $\mathbf{m}_1 = \mathbf{m}_2 = \mathbf{m}$; $\mathbf{r}_{01}$ and $\mathbf{r}_{02}$ collinear; $\mathsf{S}_2 = \mathsf{S}_1 = \mathsf{I} - 2\mathbf{m}\mathbf{m}$; $\mathsf{S}_2 \cdot \mathsf{S}_1 = \mathsf{I}$ and $\mathsf{S}_2 \cdot \mathbf{r}_{01} = -\mathbf{r}_{01}$. Hence the

Theorem 1.7. *The resultant displacement* $\mathbf{r}^* - \mathbf{r}$ *caused by two successive reflections in parallel planes with collinear vectors* $\mathbf{r}_{01}$ (*first reflection*) *and* $\mathbf{r}_{02}$ *is the translation* $2(\mathbf{r}_{02} - \mathbf{r}_{01})$ *by twice the distance of the two planes in the direction normal to the planes. The translation changes sign when the order of reflections is changed.*

Next, the general case of reflections in nonparallel planes is investigated. The planes intersect in a line which, being normal to both $\mathbf{m}_1$ and $\mathbf{m}_2$, has the direction of $\mathbf{m}_1 \times \mathbf{m}_2$. Without loss of generality the origin 0 is placed on this line so that $\mathbf{r}_{01} = \mathbf{r}_{02} = \mathbf{0}$. Equation (1.284) becomes

$$\mathbf{r}^* = (\mathsf{I} - 2\mathbf{m}_2\mathbf{m}_2) \cdot (\mathsf{I} - 2\mathbf{m}_1\mathbf{m}_1) \cdot \mathbf{r} = (2\mathbf{m}_2\mathbf{m}_2 - \mathsf{I}) \cdot (2\mathbf{m}_1\mathbf{m}_1 - \mathsf{I}) \cdot \mathbf{r} \,. \quad (1.285)$$

According to (1.42) the last two tensors are the tensors of 180°-rotations about the axes $\mathbf{m}_1$ and $\mathbf{m}_2$, respectively. Hence the resultant reflection equals the resultant of two 180°-rotations about $\mathbf{m}_1$ (first rotation) and $\mathbf{m}_2$. This resultant rotation was investigated in Sect. 1.15.2. The results are summarized in

Theorem 1.8. *The resultant of two successive reflections in nonparallel planes with unit normal vectors* $\mathbf{m}_1$ (*first reflection*) *and* $\mathbf{m}_2$ *enclosing the angle* $0 < \alpha < \pi$ *is a rotation through the angle* 2α *about the axis* $\mathbf{m}_1 \times \mathbf{m}_2 / |\mathbf{m}_1 \times \mathbf{m}_2|$. *This axis is the line of intersection of the two planes. The resultant rotation does not change if the two planes are rotated about their line of intersection with the angle* α *kept constant. The sense of rotation is reversed when the order of reflections is changed. In the special case of mutually perpendicular planes* ($\alpha = \pi/2$, 180°*-rotation about the line of intersection*), *the final position is independent of the order of reflections.*

A consequence of this theorem is

Theorem 1.9. *Any sequence of an even number of reflections in planes passing through a common point* 0 *is equivalent to a rotation about an axis passing through* 0.

Indeed, each pair of consecutive reflections is equivalent to a rotation, and the resultant of an arbitrary number of rotations is equivalent to a single rotation.

References

1. Altmann S L (1986) Rotations, quaternions and double groups. Clarendon, Oxford
2. Angeles J (1988) Rational kinematics. Springer Tracts in Natural Philosophy 34, New York
3. Angeles J (2003) Fundamentals of robotic mechanical systems: Theory, methods and algorithms. 2nd ed. Springer, New York

4. Blaschke W (1960) Kinematik und Quaternionen. VEB Verl. d. Wiss., Berlin
5. Bronstein I N, Semendjajev K A, Musiol K A, Mühlig H (2008) Taschenbuch der Mathematik. 7. Aufl. Verlag Harri Deutsch
6. Davenport P B (1973) Rotations about nonorthogonal axes. AIAA J. 11:853–857
7. Geradin M, Park K C, Cardona A (1988) On the representation of finite rotations in spatial kinematics. Rep.Nr. VA-51 Univ. of Liege, Belgium
8. Hamilton W R (1853) Lectures on quaternions. Hodges & Smith, Dublin
9. Hamilton W R (1969) Elements of quaternions. 3rd ed. Chelsea, New York
10. Hopf H (1940) Systeme symmetrischer Bilinearformen und Euklidische Modelle der projektiven Räume. Naturf. Ges., Zürich:165–177
11. Klein F, Müller C (eds.) (1901-1908) Enzyklopädie der Math. Wissenschaften. v.IV: Mechanik. Teubner, Leipzig
12. Klein F, Sommerfeld A (1910) Über die Theorie des Kreisels. Teubner, Leipzig (reprint 1965)
13. Kolve D I (1993) Describing an attitude. Advances in the Astronaut. Scie. 81:289–303
14. Kuipers J. B. (1998) Quaternions and rotation sequences. Princeton Univ. Press, Princeton, New Jersey
15. Matschinsky W (1987) Die Radführungen der Strassenfahrzeuge. Analyse, Synthese, Elasto-Kinematik. TÜV Rheinland
16. Mayer A (1960) Rotations and their algebra. SIAM Review 2:77–122
17. Meyer W FR, Mohrmann H (eds.) (1921-1928) Enzyklopädie der Math. Wissenschaften. v.III: Geometrie. Teubner, Leipzig
18. Milenkovic V (1982) Coordinates suitable for angular motion synthesis in robots. Proc.Robots VI (RI of SME):407–420
19. Mises R v. (1924) Motorrechnung, ein neues Hilfsmittel der Mechanik. ZAMM 3:155–182. Engl. trans. Baker J E, Wohlhart K (1996) Motor calculus: A new theoretical device for mechanics. Institute for Mechanics, Techn. Univ. Graz
20. Müller H R (1963) Sphärische Kinematik. Deutscher Verl. d. Wissenschaften, Berlin
21. Müller H R (1963) Kinematik. Sammlung Göschen Bd.584/584a, Walter de Gruyter, Berlin
22. Müller H R (1970) Kinematische Geometrie. Jahresber. DMV 72:143–164
23. Murnaghan F D (1962) The unitary and rotation groups. Spartan books, Washington DC
24. Pauli W (1927) Zur Quantenmechanik des magnetischen Elektrons. Z.Phys. 43:601–623
25. Rodrigues O (1840) Des lois géometriques qui régissent les déplacements d'un système solide dans l'espace, et de la variation des coordonnées provenant de ces déplacement considerés indépendamment des causes qui peuvent les produire. J. Math.Pures et Appl. s.1:380–440
26. Rooney J (1977) A survey of representations of spatial rotation about a fixed point. Env. and Planning B4:185-210
27. Roth B (1967) On the screw axes and other special lines associated with spatial displacements of a rigid body. J. Eng.f.Ind. 89B:102–110
28. Schoenflies A (1886) Geometrie der Bewegung in synthetischer Darstellung. Teubner, Leipzig. reprint (2007) VDM-Verlag Dr. Müller, Saarbrücken
29. Shuster M D (1993) A survey of attitude representations. J.Astronaut.Scie.41:439–517 [with 163 lit. references]
30. Stuelpnagel J (1964) On the parametrization of the three-dimensional rotation group. Siam Rev.8:422–430
31. Wiener T F (1962) Theoretical analysis of gimballess inertial reference equipment using delta-modulated instruments. PhD thesis MIT
32. Wittenburg J, Lilov L (2003) Decomposition of a finite rotation into three rotations about given axes. Multibody System Dynamics 9:353–375
33. Wohlhart K (1992) Decomposition of a finite rotation into three consecutive rotations about given axes. 6th IFToMM Conf., Liberec:325–332

Chapter 2
Line Geometry

Line geometry was invented by Plücker. The basic idea is to consider as elements of three-dimensional space not points with point coordinates, but lines with line coordinates. A line is understood to be a straight line. In the present chapter some basic elements of line geometry are introduced.

Literature: Plücker [5, 6], Sauer [9], Sturm [11], Kruppa [3], Timerding [12], Zindler [13], Hoschek [1], Salmon [7], Salmon/Fiedler [8].

2.1 Normal Vector of a Plane. Equation of a Plane

Figure 2.1a shows a plane in a cartesian basis with origin 0. The plane does not pass through 0. Let P_0 be the foot of the perpendicular from 0 onto the plane, and let, furthermore, $d > 0$ be the length of this perpendicular. The normal vector $\mathbf{m}$ of the plane is defined to be the vector having the absolute value $|\mathbf{m}| = 1/d$ and the direction from P_0 to 0. The position vector of P_0 is $-\mathbf{m}/\mathbf{m}^2$. The vector $\mathbf{r}$ of an arbitrary point located in the plane satisfies the equation

$$\mathbf{m} \cdot \mathbf{r} = -1 \,. \tag{2.1}$$

From the coordinate form $m_x x + m_y y + m_z z = -1$ it is seen that the points of intersection of the plane with the coordinate axes have the coordinates $x = -1/m_x$, $y = -1/m_y$ and $z = -1/m_z$, respectively.

If the plane passes through 0 (Fig. 2.1b), Eq.(2.1) is replaced by

$$\mathbf{m} \cdot \mathbf{r} = 0 \,, \tag{2.2}$$

where $\mathbf{m}$ is a vector normal to the plane with arbitrary absolute value $|\mathbf{m}| \neq 0$ and with arbitrary sense of direction.

J. Wittenburg, *Kinematics*, DOI 10.1007/978-3-662-48487-6_2

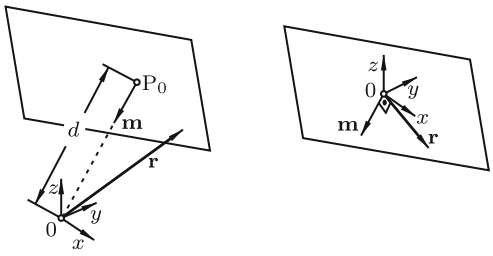

Fig. 2.1 Normal vector $\mathbf{m}$ of a plane. **(a)** The plane is not passing through the origin: $|\mathbf{m}| = 1/d$; **(b)** The plane is passing through the origin: $|\mathbf{m}|$ arbitrary

2.2 Plücker Vectors. Plücker Coordinates of a Line

Figure 2.2 shows a line in a cartesian basis with origin 0 . The line is uniquely determined by two points P and P′ with position vectors $\mathbf{r}$ and $\mathbf{r}'$, respectively. The line is also uniquely determined by the vectors

$$\mathbf{v} = \mathbf{r}' - \mathbf{r} \,, \qquad \mathbf{w} = \mathbf{r} \times \mathbf{v} = \mathbf{r} \times \mathbf{r}' \,. \tag{2.3}$$

These vectors satisfy the constraint equations

$$\mathbf{v}^2 = \text{const} \neq 0 \,, \qquad \mathbf{v} \cdot \mathbf{w} = 0 \,. \tag{2.4}$$

The vectors $\mathbf{v}$ and $\mathbf{w}$ are called first and second *Plücker vector* of the line, and their cartesian coordinates are called *Plücker coordinates* of the line. Equations (2.4) are two constraint equations for the altogether six vector coordinates. That four scalar quantities define a line is seen also as follows. Choose an arbitrary x, y, z-system in which the line has points of intersection with the x, y-plane and with the x, z-plane. Each of these points has two coordinates. In what follows, we speak of lines $(\mathbf{v}, \mathbf{w})$. The first Plücker vector $\mathbf{v}$ determines the direction of the line, and the second represents the moment of the first with respect to 0 . The line is uniquely determined by its Plücker vectors because Eqs.(2.3) yield as equation of the line

$$\mathbf{r}(\lambda) = \lambda \mathbf{v} + \frac{\mathbf{v} \times \mathbf{w}}{\mathbf{v}^2} \tag{2.5}$$

where λ is a free parameter. The perpendicular from 0 onto the line is

$$\mathbf{r}(0) = \frac{\mathbf{v} \times \mathbf{w}}{\mathbf{v}^2} \,. \tag{2.6}$$

The line passes through 0 if $\mathbf{w} = \mathbf{0}$. Multiplication of both Plücker vectors

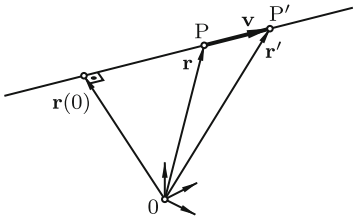

Fig. 2.2 Plücker vectors of a line

by an arbitrary common factor does not change the line. In the case $\mathbf{v}^2 = 1$, the Plücker vectors are said to be normalized.

A line $(\mathbf{v}, \mathbf{w})$ lies in a plane given by either (2.1) or (2.2) if and only if the following conditions are satisfied:

$$\mathbf{v} \cdot \mathbf{m} = 0\,, \qquad \mathbf{w} \times \mathbf{m} = \begin{cases} -\mathbf{v} & (\text{Eq.(2.1); plane not passing through } 0\,) \\ \mathbf{0} & (\text{Eq.(2.2); plane passing through } 0\,)\,. \end{cases} \tag{2.7}$$

This is seen as follows. The first equation is obviously true. Consequently,

$$\mathbf{w} \times \mathbf{m} = (\mathbf{r} \times \mathbf{v}) \times \mathbf{m} = (\mathbf{m} \cdot \mathbf{r})\mathbf{v} - (\mathbf{v} \cdot \mathbf{m})\mathbf{r} = (\mathbf{m} \cdot \mathbf{r})\mathbf{v}\,. \tag{2.8}$$

This together with (2.1) and (2.2) yields the second Eq.(2.7).

2.3 Reflection in a Line

From Sect. 1.5 it is known that reflection in a line is equivalent to 180°-rotation about the line (see (1.42)). In the present section the reflecting line is not required to pass through the origin 0 of the reference frame. The line is given by its normalized Plücker vectors $\mathbf{v}$ and $\mathbf{w}$. Equation (2.5) of the line $(\mathbf{v}, \mathbf{w})$ is

$$\mathbf{r}(\lambda) = \lambda\mathbf{v} + \mathbf{v} \times \mathbf{w}\,. \tag{2.9}$$

Let $\mathbf{z}$ be the position vector of an arbitrary point P, and let, furthermore, $\mathbf{z}^*$ be the position vector of the reflection P^* of P. By the definition of reflection in the line the vector $(\mathbf{z}^* + \mathbf{z})/2$ is position vector $\mathbf{r}_1 = \mathbf{r}(\lambda_1)$ of a point on the line. In addition, $\mathbf{z}^* - \mathbf{z}$ is normal to the line. Hence $\mathbf{z}^* = 2\mathbf{r}_1 - \mathbf{z}$ and $\mathbf{v} \cdot (\mathbf{r}_1 - \mathbf{z}) = 0$. With $\mathbf{r}_1 = \lambda_1\mathbf{v} + \mathbf{v} \times \mathbf{w}$ the latter condition yields $\lambda_1 = \mathbf{v} \cdot \mathbf{z}$ and, consequently,

$$\mathbf{z}^* = 2(\mathbf{v} \cdot \mathbf{z}\mathbf{v} + \mathbf{v} \times \mathbf{w}) - \mathbf{z} = (2\mathbf{v}\,\mathbf{v} - \mathsf{I}\,) \cdot \mathbf{z} + 2\mathbf{v} \times \mathbf{w}\,. \tag{2.10}$$

The tensor is known from (1.42). The vector $2\mathbf{v} \times \mathbf{w}$ is twice the perpendicular from 0 onto the reflecting line. With the vector $\mathbf{r}_\mathrm{A}$ of an arbitrary point A

on the line the second Plücker vector is $\mathbf{w} = \mathbf{r}_A \times \mathbf{v}$. With this expression the equation can be given the more useful form

$$\mathbf{z}^* = 2\mathbf{r}_A - \mathbf{z} + 2\mathbf{v}\,\mathbf{v} \cdot (\mathbf{z} - \mathbf{r}_A) \,. \tag{2.11}$$

2.4 Plücker Vectors of the Line of Intersection of two Planes

A line $(\mathbf{v}, \mathbf{w})$ need not be determined by two points. It may just as well be defined as intersection line of two nonparallel planes. Therefore, it is possible to express the Plücker vectors $\mathbf{v}$ and $\mathbf{w}$ in terms of the normal vectors $\mathbf{m}_1$ and $\mathbf{m}_2$ appearing in Eqs.(2.1) or (2.2) of two planes. The desired expressions are derived from (2.7). The first equation requires that $\mathbf{v}$ be orthogonal to both $\mathbf{m}_1$ and $\mathbf{m}_2$ so that $\mathbf{w} = \mathbf{r} \times \mathbf{v}$ lies in the plane of $\mathbf{m}_1$ and $\mathbf{m}_2$. An appropriate ansatz is $\mathbf{v} = \mathbf{m}_1 \times \mathbf{m}_2$, $\mathbf{w} = \mu_1 \mathbf{m}_1 + \mu_2 \mathbf{m}_2$ with unknown coefficients μ_1, μ_2. These coefficients are obtained from two equations expressing the second Eq.(2.7). Three cases have to be distinguished.
Case a: None of the two planes is passing through 0. In this case, the equations read

$$(\mu_1 \mathbf{m}_1 + \mu_2 \mathbf{m}_2) \times \mathbf{m}_i = -\mathbf{m}_1 \times \mathbf{m}_2 \qquad (i = 1, 2) \,. \tag{2.12}$$

This yields $\mu_1 = -1$, $\mu_2 = 1$. Hence the desired Plücker vectors are

$$\mathbf{v} = \mathbf{m}_1 \times \mathbf{m}_2 \,, \qquad \mathbf{w} = \mathbf{m}_2 - \mathbf{m}_1 \,. \tag{2.13}$$

Case b: Exactly one of the planes, say the plane with $\mathbf{m}_1$, passes through 0. Then (2.12) must be satisfied for $i = 2$, so that $\mu_1 = -1$, again. For plane 1 the pertinent equation is the second Eq.(2.7). It yields $\mu_2 = 0$. Thus, the solution is

$$\mathbf{v} = \mathbf{m}_1 \times \mathbf{m}_2 \,, \qquad \mathbf{w} = -\mathbf{m}_1 \,. \tag{2.14}$$

Case c: Both planes are passing through 0. Then also the line of intersection passes through 0. Hence $\mathbf{v} = \mathbf{m}_1 \times \mathbf{m}_2$, $\mathbf{w} = \mathbf{0}$.

2.5 Condition for two Lines to Intersect

Let $(\mathbf{v}_1, \mathbf{w}_1)$ and $(\mathbf{v}_2, \mathbf{w}_2)$ be two nonparallel lines, which means that $\mathbf{v}_1 \times \mathbf{v}_2 \neq \mathbf{0}$ (Fig. 2.3). No matter whether the lines intersect or not, they have a uniquely defined common perpendicular. It has the direction of $\mathbf{v}_1 \times \mathbf{v}_2$. Let $\mathbf{n}$ be the unit vector in this direction, and let, furthermore, $\mathbf{r}_1$ and $\mathbf{r}_2$ be

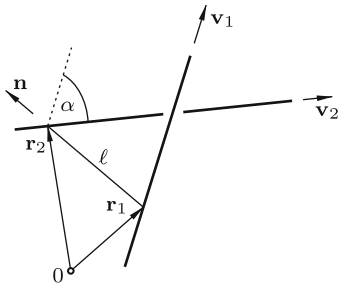

Fig. 2.3 Skew lines and common perpendicular

the vectors to the points where the perpendicular intersects the lines. With these vectors the quantities ℓ and α are defined (positive or negative):

$$\mathbf{r}_2 - \mathbf{r}_1 = \ell\mathbf{n}\,, \qquad \mathbf{v}_1 \times \mathbf{v}_2 = \mathbf{n}|\mathbf{v}_1 \times \mathbf{v}_2| = \mathbf{n}|\mathbf{v}_1||\mathbf{v}_2|\sin\alpha\,. \tag{2.15}$$

$|\ell|$ is the length of the common perpendicular, and α is the angle, right-handed about $\mathbf{n}$, which turns $\mathbf{v}_1$ into the direction of $\mathbf{v}_2$. The second Plücker vectors of the lines are $\mathbf{w}_1 = \mathbf{r}_1 \times \mathbf{v}_1$, $\mathbf{w}_2 = \mathbf{r}_2 \times \mathbf{v}_2$. With these vectors the expression is formulated:

$$\begin{aligned}\mathbf{v}_1 \cdot \mathbf{w}_2 + \mathbf{v}_2 \cdot \mathbf{w}_1 &= \mathbf{v}_1 \cdot \mathbf{r}_2 \times \mathbf{v}_2 + \mathbf{v}_2 \cdot \mathbf{r}_1 \times \mathbf{v}_1 = -\mathbf{r}_2 \cdot \mathbf{v}_1 \times \mathbf{v}_2 + \mathbf{r}_1 \cdot \mathbf{v}_1 \times \mathbf{v}_2 \\ &= (\mathbf{r}_1 - \mathbf{r}_2) \cdot \mathbf{v}_1 \times \mathbf{v}_2 = -\ell|\mathbf{v}_1 \times \mathbf{v}_2|\,. \end{aligned} \tag{2.16}$$

This is an equation for ℓ:

$$\ell = -\frac{\mathbf{v}_1 \cdot \mathbf{w}_2 + \mathbf{v}_2 \cdot \mathbf{w}_1}{|\mathbf{v}_1 \times \mathbf{v}_2|}\,. \tag{2.17}$$

Its usefulness lies in the fact that the second Plücker vector $\mathbf{w}_i = \mathbf{r}_i \times \mathbf{v}_i$ can be calculated with the vector $\mathbf{r}_i$ of an arbitrary point on the line i. The most important consequence of the equation is

Theorem 2.1. *Two lines intersect if and only if their Plücker vectors* $\mathbf{v}_1, \mathbf{w}_1$ *and* $\mathbf{v}_2, \mathbf{w}_2$ *satisfy the condition*

$$\mathbf{v}_1 \cdot \mathbf{w}_2 + \mathbf{v}_2 \cdot \mathbf{w}_1 = 0\,, \tag{2.18}$$

and the point of intersection is

$$\mathbf{r} = \frac{\mathbf{w}_1 \times \mathbf{w}_2}{\mathbf{w}_1 \cdot \mathbf{v}_2}\,. \tag{2.19}$$

The last equation is verified by substituting $\mathbf{w}_1 = \mathbf{r} \times \mathbf{v}_1$ and $\mathbf{w}_2 = \mathbf{r} \times \mathbf{v}_2$.

Example: Given four pairwise skew lines $\mathrm{g}_i = (\mathbf{v}_i, \mathbf{w}_i)$ $(i = 1, 2, 3, 4)$, determine all lines $(\mathbf{x}, \mathbf{y})$ which intersect these four given lines (the so-called

transversals of the four lines).
Proposition: The number of lines solving this problem is either two or one or zero. The following proof is due to Steiner [10] v.1:147–154. Let $\mathrm{P}(z)$ with a coordinate z along g_1 be an arbitrary point of g_1. The manifold of all lines passing through $\mathrm{P}(z)$ and intersecting g_2 defines a plane $\mathrm{E}(z)$. Let $\mathrm{Q}(z)$ be the point of intersection of g_3 with $\mathrm{E}(z)$. It can be shown that the manifold of all lines $\mathrm{g}(z) = \overline{\mathrm{P}(z)\mathrm{Q}(z)}$ for $-\infty < z < \infty$ defines a hyperboloid of one sheet, here denoted H. Thus, every point of H is passed by exactly one generator $\mathrm{g}(z)$ which intersects g_1, g_2 and g_3. The line g_4 intersects H either at two points or in a double point or not at all. The generator $\mathrm{g}(z)$ passing through such an intersection point intersects the four given lines. End of proof.

For calculating the unknown lines $(\mathbf{x}, \mathbf{y})$ all vectors are decomposed in some appropriately chosen common reference basis. The four intersection conditions $\mathbf{w}_i \cdot \mathbf{x} + \mathbf{v}_i \cdot \mathbf{y} = 0$ $(i = 1, 2, 3, 4)$ are formulated in terms of the vector coordinates. This results in a system of four homogeneous linear equations for the six unknown coordinates x_k, y_k $(k = 1, 2, 3)$. The coefficient matrix is of size (4×6). Every solution $(\mathbf{x}, \mathbf{y})$ satisfies the orthogonality condition $\mathbf{x} \cdot \mathbf{y} = 0$, i.e., $x_1y_1 + x_2y_2 + x_3y_3 = 0$, as well as the normalizing condition $x_1^2 + x_2^2 + x_3^2 = 1$. Since, by Steiner's proof, these altogether six equations have isolated solutions, the (4×6) coefficient matrix of the linear equations has rank four. From this it follows that four out of the six coordinates can be expressed as linear combinations of the remaining two. Of these two at least one is $\neq 0$ because otherwise only the trivial solution would exist. The linear combinations are substituted into the orthogonality condition $x_1y_1 + x_2y_2 + x_3y_3 = 0$. This results in a single equation for the two remaining coordinates. The equation is quadratic with respect to both coordinates. It is solved for one of them. With each of its two solutions the first four coordinates are calculated. Thus, five coordinates are expressed in terms of a single coordinate. This single coordinate may be chosen arbitrarily. For example, it may be chosen so as to satisfy the normalizing condition $x_1^2 + x_2^2 + x_3^2 = 1$. With or without normalization every 6-tuple of coordinates determines uniquely one line $(\mathbf{x}, \mathbf{y})$ solving the problem.

A concrete example: The four pairwise skew lines $(\mathbf{v}_i, \mathbf{w}_i)$ are given by the coordinates
$\mathbf{v}_1 : [\,1 \;\; 0 \;\; 3]$, $\mathbf{v}_2 : [\,1 \;\; 1 \;\; 2]$, $\mathbf{v}_3 : [\;\; 1 \;\; 2 \;\; 3]$, $\mathbf{v}_4 : [\,3 \;\; 1 \;\; -2]$,
$\mathbf{w}_1 : [\,3 \;\; -2 \;\; -1]$, $\mathbf{w}_2 : [\,1 \;\; 1 \;\; -1]$, $\mathbf{w}_3 : [\,-2 \;\; 1 \;\; 0]$, $\mathbf{w}_4 : [\,1 \;\; -3 \;\; 0]$.
The intersection conditions $\mathbf{w}_i \cdot \mathbf{x} + \mathbf{v}_i \cdot \mathbf{y} = 0$ $(i = 1, 2, 3, 4)$ are

$$\begin{bmatrix} 3 & -2 & -1 & 1 \\ 1 & 1 & -1 & 1 \\ -2 & 1 & 0 & 1 \\ 1 & -3 & 0 & 3 \end{bmatrix} \begin{bmatrix} x_1 \\ x_2 \\ x_3 \\ y_1 \end{bmatrix} = - \begin{bmatrix} 0 & 3 \\ 1 & 2 \\ 2 & 3 \\ 1 & -2 \end{bmatrix} \begin{bmatrix} y_2 \\ y_3 \end{bmatrix} .$$

Inversion of the (4×4)-matrix yields

$$\begin{bmatrix} x_1 \\ x_2 \\ x_3 \\ y_1 \end{bmatrix} = -\frac{1}{9} \begin{bmatrix} -6 & 6 & -9 & 3 \\ -7 & 7 & -6 & 2 \\ -18 & 9 & -18 & 9 \\ -5 & 5 & -3 & 4 \end{bmatrix} \begin{bmatrix} 0 & 3 \\ 1 & 2 \\ 2 & 3 \\ 1 & -2 \end{bmatrix} \begin{bmatrix} y_2 \\ y_3 \end{bmatrix} = \frac{1}{9} \begin{bmatrix} 9y_2 + & 39y_3 \\ 3y_2 + & 29y_3 \\ 18y_2 + & 108y_3 \\ -3y_2 + & 22y_3 \end{bmatrix} . \quad \text{(a)}$$

The condition $x_1y_1 + x_2y_2 + x_3y_3 = 0$ is

$\frac{1}{81}(9y_2 + 39y_3)(-3y_2 + 22y_3) + \frac{1}{9}(3y_2 + 29y_3)y_2 + \frac{1}{9}(18y_2 + 108y_3)y_3 = 0$

or $y_3(84y_2+305y_3) = 0$. This equation has two solutions $[y_2\ y_3] = [3\ \ 0]$ and $[-305\ \ 84]$ (the arbitrary factors are chosen for convenience). Substitution into (a) produces the solutions

$[x_1\ x_2\ x_3\ y_1\ y_2\ y_3] = [3\ \ 1\ \ 6\ \ -1\ \ 3\ \ 0]$ and $[59\ \ 169\ \ 398\ \ 307\ \ -305\ \ 84]$.

End of example.

2.6 Plücker Vectors of the Common Perpendicular of two Lines

In this section the lines $(\mathbf{v}_1, \mathbf{w}_1)$ and $(\mathbf{v}_2, \mathbf{w}_2)$ shown in Fig. 2.3 are considered again. The length of their common perpendicular is calculated from (2.17). To be determined are the Plücker vectors $\mathbf{v}$, $\mathbf{w}$ of the common perpendicular. Since $\mathbf{v}$ has the direction of $\mathbf{v}_1 \times \mathbf{v}_2$ the ansatz is made:

$$\mathbf{v} = \mathbf{v}_1 \times \mathbf{v}_2 , \qquad \mathbf{w} = \lambda_1 \mathbf{v}_1 \times \mathbf{w}_2 + \lambda_2 \mathbf{w}_1 \times \mathbf{v}_2 + \mu \mathbf{v}_1 \times \mathbf{v}_2 . \qquad (2.20)$$

The unknown coefficients λ_1 , λ_2 , μ are calculated from the three conditions that the common perpendicular intersects both lines, and that, furthermore, $\mathbf{v} \cdot \mathbf{w} = 0$. The intersection conditions (2.18) are $\mathbf{v} \cdot \mathbf{w}_i + \mathbf{v}_i \cdot \mathbf{w} = 0$ $(i = 1, 2)$. Substitution of (2.20) yields after elementary manipulations $\lambda_1 = \lambda_2 = 1$. The condition $\mathbf{v} \cdot \mathbf{w} = 0$ is an equation for μ :

$$(\mathbf{v}_1 \times \mathbf{v}_2) \cdot (\mathbf{v}_1 \times \mathbf{w}_2 + \mathbf{w}_1 \times \mathbf{v}_2) + \mu (\mathbf{v}_1 \times \mathbf{v}_2)^2 = 0 . \qquad (2.21)$$

Lagrange's identity for multiple products in combination with the orthogonality $\mathbf{v}_1 \cdot \mathbf{w}_1 = \mathbf{v}_2 \cdot \mathbf{w}_2 = 0$ results in

$$\mu = \frac{(\mathbf{v}_1 \cdot \mathbf{v}_2)(\mathbf{v}_1 \cdot \mathbf{w}_2 + \mathbf{v}_2 \cdot \mathbf{w}_1)}{(\mathbf{v}_1 \times \mathbf{v}_2)^2} \qquad (2.22)$$

($\mu = 0$ if the lines $(\mathbf{v}_1, \mathbf{w}_1)$ and $(\mathbf{v}_2, \mathbf{w}_2)$ intersect). With this and with $\lambda_1 = \lambda_2 = 1$ the desired Plücker vectors (2.20) are

$$\mathbf{v} = \mathbf{v}_1 \times \mathbf{v}_2 , \qquad \mathbf{w} = \mathbf{v}_1 \times \mathbf{w}_2 + \mathbf{w}_1 \times \mathbf{v}_2 + (\mathbf{v}_1 \cdot \mathbf{w}_2 + \mathbf{w}_1 \cdot \mathbf{v}_2)(\mathbf{v}_1 \cdot \mathbf{v}_2) \frac{\mathbf{v}_1 \times \mathbf{v}_2}{(\mathbf{v}_1 \times \mathbf{v}_2)^2} . \qquad (2.23)$$

The perpendicular from 0 onto the common perpendicular is the vector

$$\frac{\mathbf{v}\times\mathbf{w}}{\mathbf{v}^2}=\frac{(\mathbf{v}_1\times\mathbf{v}_2\cdot\mathbf{w}_2)\mathbf{v}_1-(\mathbf{v}_1\times\mathbf{v}_2\cdot\mathbf{w}_1)\mathbf{v}_2}{(\mathbf{v}_1\times\mathbf{v}_2)^2}\,. \tag{2.24}$$

2.7 Linear Complex

The four independent coordinates of the Plücker vectors $\mathbf{v}$ and $\mathbf{w}$ of every line in three-dimensional space may be subjected to one, to two, to three or to four independent scalar constraints. This results in line manifolds having three or two or one or zero free parameters. A manifold of lines with three free parameters (a single constraint) is called a *complex* and, in particular, a linear complex, if the constraint equation is linear. This is the case investigated in what follows. A manifold of lines with two free parameters (two constraints) is called a *congruence*, and a manifold of lines with a single free parameter (three constraints) is called a *ruled surface*. The special case of linear congruences is briefly treated in Sect. 2.8 . Ruled surfaces are the subject of Sect. 2.9 . Four independent scalar constraints determine isolated lines. Note the difference between line geometry and cartesian point geometry. Three point coordinates may be subjected to one, to two or to three independent scalar constraints. The results are surfaces, curves and points, respectively.

Let $\mathbf{a}$ and $\mathbf{b}$ be two arbitrarily prescribed, nonorthogonal vectors, i.e., $\mathbf{a}\cdot\mathbf{b}\neq 0$. Since they are nonorthogonal, they are not Plücker vectors of a line. Definition: The *linear complex* $(\mathbf{a};\mathbf{b})$ is the manifold of all lines $(\mathbf{v},\mathbf{w})$ satisfying the linear constraint equation

$$\mathbf{a}\cdot\mathbf{w}+\mathbf{b}\cdot\mathbf{v}=0\,. \tag{2.25}$$

The linear complex $(\mathbf{a};\mathbf{b})$ contains three independent coordinates. The lines $(\mathbf{v},\mathbf{w})$ are briefly called complex lines. Since (2.25) is unaffected by multiplication with an arbitrary constant, the vector $\mathbf{a}$ can be made a unit vector. In what follows, this is not assumed.

Remark: In the special case $\mathbf{a}\cdot\mathbf{b}=0$ excluded from the investigation, $\mathbf{a}$ and $\mathbf{b}$ are Plücker vectors of a line. In this case, (2.25) represents the intersection condition for the lines $(\mathbf{a},\mathbf{b})$ and $(\mathbf{v},\mathbf{w})$. It is satisfied by all lines $(\mathbf{v},\mathbf{w})$ intersecting the line $(\mathbf{a},\mathbf{b})$ at arbitrary points and in arbitrary directions. This linear complex is called a special linear complex, and the line $(\mathbf{a},\mathbf{b})$ is called its *axis*.

2.7.1 Null Point. Null Plane

Imagine that the vectors $\mathbf{a}$ and $\mathbf{b}$ start out from the origin 0 in Fig. 2.2 . The point P is an arbitrarily chosen fixed point whereas P' is a variable point.

Equations (2.3) determine the Plücker vectors of all lines passing through P. Among these lines only those are complex lines which satisfy (2.25):

$$\mathbf{a} \cdot \mathbf{r} \times \mathbf{r}' + \mathbf{b} \cdot (\mathbf{r}' - \mathbf{r}) = 0 \,. \tag{2.26}$$

This equation establishes a linear relation between the three coordinates of $\mathbf{r}'$. Hence it is the equation of a plane passing through P. All lines lying in this plane and passing through P are complex lines. Proposition: The nonnormalized vector

$$\mathbf{n} = \mathbf{a} \times \mathbf{r} + \mathbf{b} \tag{2.27}$$

is normal to the plane. Proof: Substitution of the expression for $\mathbf{n}$ into the orthogonality condition $\mathbf{n} \cdot (\mathbf{r}' - \mathbf{r}) = 0$ produces (2.26). End of proof.

For every point P (2.26) determines uniquely a plane. For reasons explained later (see Sects. 9.3 and 12.4) the point and the associated plane are called *null point* and *null plane*, respectively. Since $\mathbf{b}$ is not orthogonal to $\mathbf{a}$, the normal vector $\mathbf{n}$ is not orthogonal to $\mathbf{a}$ either. This means: No null plane contains a line parallel to $\mathbf{a}$. The vector $\mathbf{n}$ does not change if to $\mathbf{r}$ an arbitrary multiple of $\mathbf{a}$ is added. This means: Null planes passing through different null points are parallel if these null points are located on a line parallel to $\mathbf{a}$, and they are not parallel if the null points are not located on a line parallel to $\mathbf{a}$. Hence the conclusion: Every null plane has exactly one null point. In every null plane all lines passing through the null point - and these lines only - are complex lines. They form what is called a *pencil* of complex lines.

2.7.2 Axis. Pitch

For clarifying the location of the infinitely many null planes/null points in space (2.26) is rewritten by substituting $\mathbf{r} = \mathbf{r}_\mathrm{A} + \boldsymbol{\varrho}$ and $\mathbf{r}' = \mathbf{r}_\mathrm{A} + \boldsymbol{\varrho}'$ where $\mathbf{r}_\mathrm{A}$ is the position vector of an as yet unspecified point A (Fig. 2.4). This results after simple manipulations in the equation

$$\mathbf{a} \cdot \boldsymbol{\varrho} \times \boldsymbol{\varrho}' + (\mathbf{a} \times \mathbf{r}_\mathrm{A} + \mathbf{b}) \cdot (\boldsymbol{\varrho}' - \boldsymbol{\varrho}) = 0 \,. \tag{2.28}$$

For all points A on a line parallel to $\mathbf{a}$ the vectors $\mathbf{a} \times \mathbf{r}_\mathrm{A} + \mathbf{b}$ are identical (different vectors for different lines). There exists a single line parallel to $\mathbf{a}$ for the points of which $\mathbf{a} \times \mathbf{r}_\mathrm{A} + \mathbf{b}$ has the direction of $\mathbf{a}$, i.e., $\mathbf{a} \times \mathbf{r}_\mathrm{A} + \mathbf{b} = p\,\mathbf{a}$ with a scalar p of dimension length. This line is called *axis of the linear complex*. Let $\mathbf{u}$ be the particular vector $\mathbf{r}_\mathrm{A}$ which is perpendicular to the axis (see Fig. 2.4). Then also $\mathbf{a} \times \mathbf{u} + \mathbf{b} = p\,\mathbf{a}$. Cross- and dot-multiplying this equation by $\mathbf{a}$ and using the orthogonality $\mathbf{a} \cdot \mathbf{u} = 0$ one gets for $\mathbf{u}$ and for p the expressions

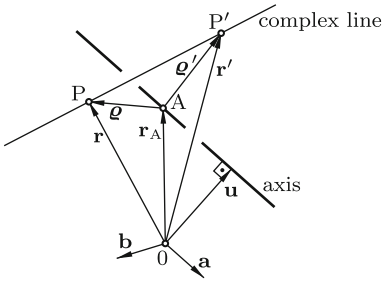

Fig. 2.4 Axis of a linear complex

$$\mathbf{u} = \frac{\mathbf{a} \times \mathbf{b}}{\mathbf{a}^2} \,, \qquad p = \frac{\mathbf{a} \cdot \mathbf{b}}{\mathbf{a}^2} \,. \tag{2.29}$$

The axis has the Plücker vectors $\mathbf{a}$ and $\mathbf{u} \times \mathbf{a} = (\mathbf{a} \times \mathbf{b}) \times \mathbf{a}/\mathbf{a}^2 = \mathbf{b} - p\,\mathbf{a}$. In a reference basis having its origin on the axis of the complex the same linear complex has the second Plücker vector $\mathbf{u} \times \mathbf{a} = \mathbf{0}$. In this reference basis the linear complex $(\mathbf{a}; \mathbf{b})$ is the complex $(\mathbf{a}; p\,\mathbf{a})$.

For better understanding the relationships between axis, constant p, null point and null plane points of a single line perpendicular to the axis are considered (Fig. 2.5). The foot of this perpendicular is chosen as origin 0 so that (2.29), (2.27) and (2.26) have the forms

$$\mathbf{u} = \mathbf{0} \,, \qquad \mathbf{b} = p\,\mathbf{a} \,, \qquad \mathbf{n} = \mathbf{a} \times \mathbf{r} + p\,\mathbf{a} \,, \tag{2.30}$$

$$\mathbf{a} \cdot [\mathbf{r} \times \mathbf{r}' + p\,(\mathbf{r}' - \mathbf{r})] = 0 \,. \tag{2.31}$$

Let P with position vector $\mathbf{r}$ be an arbitrarily chosen null point on the line. The associated null plane contains the line because (2.31) is satisfied with every position vector $\mathbf{r}'$ collinear with $\mathbf{r}$. The figure shows the pencil of complex lines in this null plane. The null plane is inclined against the axis of the complex by an angle α for which the triangle at P yields the formula (with $r = |\mathbf{r}|$)

$$\tan \alpha = \frac{p}{r} \,. \tag{2.32}$$

The angle α is the smaller, the larger the distance r of the null point from the axis.

On every line perpendicular to the axis the allocation of null planes and null points is the same. This simple allocation establishes a one-to-one relationship between a linear complex and a screw. The axis of the complex has to be interpreted as axis of a screw with pitch p. The helix of the thread at the distance r (arbitrary) from the axis progresses per revolution by $2\pi p$. Consequently, the inclination angle of this helix is the angle α in (2.32). This means: Let P be an arbitrary null point in space. The corresponding null plane is orthogonally intersected at P by the helix passing through P. In

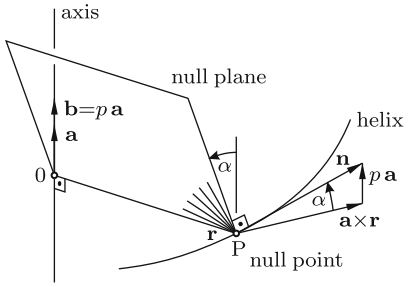

Fig. 2.5 The pencil of complex lines in the null plane with null point P is normal to the helix through P

other words: The linear complex $(\mathbf{a};\mathbf{b})$ is the manifold of all normals of all helices produced by a screw having as axis the axis of the linear complex, having the pitch p and arbitrary radius r. The pitch may be positive or negative, i.e., the screw is right-handed or left-handed.

2.7.3 Determine the Null Point if the Null Plane is Given and Vice Versa

Let $\mathbf{r}_0$ be the position vector of a null point, and let $\mathbf{m}\cdot\mathbf{r} = -1$ be Eq.(2.1) of the associated null plane. Then

$$\mathbf{m}\cdot\mathbf{r}_0 = -1\ . \tag{2.33}$$

The vector $\mathbf{a}\times\mathbf{r}_0 + \mathbf{b}$ was shown to be normal to the plane (see (2.27)). Consequently

$$\mathbf{m} = A(\mathbf{a}\times\mathbf{r}_0 + \mathbf{b}) \tag{2.34}$$

with an unknown scalar A. Cross-multiplying this equation with $\mathbf{m}$ and dot-multiplying it with $\mathbf{r}_0$ and using in either case (2.33) results in the equations

$$\mathbf{0} = -\mathbf{a} - (\mathbf{m}\cdot\mathbf{a})\mathbf{r}_0 + \mathbf{m}\times\mathbf{b}\ , \qquad -1 = A\mathbf{r}_0\cdot\mathbf{b}\ . \tag{2.35}$$

If the null plane is given, the first equation determines the null point:

$$\mathbf{r}_0 = \frac{\mathbf{m}\times\mathbf{b} - \mathbf{a}}{\mathbf{m}\cdot\mathbf{a}}\ . \tag{2.36}$$

If, instead, the null point is given, the second equation determines the null plane:

$$\mathbf{m} = \frac{\mathbf{r}_0\times\mathbf{a} - \mathbf{b}}{\mathbf{r}_0\cdot\mathbf{b}}\ . \tag{2.37}$$

2.7.4 Determine a Linear Complex from Given Complex Lines

The linear complex $(\mathbf{a}\,;\,\mathbf{b})$ is defined by Eq.(2.25): $\mathbf{a}\cdot\mathbf{w}+\mathbf{b}\cdot\mathbf{v}=0$. Given vectors $\mathbf{a}$ and $\mathbf{b}$ determine the axis and the pitch and the Plücker vectors $\mathbf{v}$ and $\mathbf{w}$ of all complex lines $(\mathbf{v}\,,\,\mathbf{w})$. The linear complex does not change if $\mathbf{a}$ and $\mathbf{b}$ are multiplied by an arbitrary constant. The vectors $\mathbf{a}$ and $\mathbf{b}$ are determined by five lines $(\mathbf{v}_i\,,\,\mathbf{w}_i)$ $(i=1,\ldots,5)$ satisfying the condition that the five equations

$$\mathbf{w}_i\cdot\mathbf{a}+\mathbf{v}_i\cdot\mathbf{b}=0 \qquad (i=1,\ldots,5) \tag{2.38}$$

are linearly independent. Applications to problems of kinematics see in Sects. 4.2.1 and 12.5. In Zindler [13] reference is made to literature on 28 different methods for determining a linear complex from given data.

2.7.5 Reciprocal Polars

In what follows, the origin 0 is again an arbitrary point, and the vector $\mathbf{a}$ need not be a unit vector. Proposition: For every line $(\mathbf{p}_1,\mathbf{q}_1)$ *not belonging* to the linear complex $(\mathbf{a};\mathbf{b})$ there exist exactly one line $(\mathbf{p}_2,\mathbf{q}_2)$ also not belonging to the linear complex and exactly one scalar $\mu\neq 0$ such that

$$\mathbf{p}_1+\mathbf{p}_2=\mu\mathbf{a}\,, \qquad \mathbf{q}_1+\mathbf{q}_2=\mu\mathbf{b}\,. \tag{2.39}$$

The lines $(\mathbf{p}_1,\mathbf{q}_1)$ and $(\mathbf{p}_2,\mathbf{q}_2)$ are called *reciprocal polars* of the linear complex.
Proof: The Plücker vectors of the two polars satisfy the equations $\mathbf{p}_1\cdot\mathbf{q}_1=\mathbf{p}_2\cdot\mathbf{q}_2=0$. Since the polar $(\mathbf{p}_1,\mathbf{q}_1)$ does not belong to the linear complex, the Plücker vectors $\mathbf{p}_1$ and $\mathbf{q}_1$ do not satisfy (2.25). Hence $\mathbf{a}\cdot\mathbf{q}_1+\mathbf{b}\cdot\mathbf{p}_1\neq 0$. With (2.39) the equation $\mathbf{p}_2\cdot\mathbf{q}_2=0$ gets the form

$$(\mu\mathbf{a}-\mathbf{p}_1)\cdot(\mu\mathbf{b}-\mathbf{q}_1)=\mu^2\mathbf{a}\cdot\mathbf{b}-\mu(\mathbf{a}\cdot\mathbf{q}_1+\mathbf{b}\cdot\mathbf{p}_1)=0\,. \tag{2.40}$$

From this it follows that there exists, indeed, a single scalar

$$\mu=\frac{\mathbf{a}\cdot\mathbf{q}_1+\mathbf{b}\cdot\mathbf{p}_1}{\mathbf{a}\cdot\mathbf{b}}\neq 0\,. \tag{2.41}$$

With this scalar the other reciprocal polar $(\mathbf{p}_2,\mathbf{q}_2)$ is uniquely determined by (2.39). Its Plücker vectors yield the identity $\mathbf{a}\cdot\mathbf{q}_2+\mathbf{b}\cdot\mathbf{p}_2=\mathbf{a}\cdot\mathbf{q}_1+\mathbf{b}\cdot\mathbf{p}_1$. This proves that also the other reciprocal polar does not belong to the linear complex. End of proof.

The polar $(\mathbf{p}_1, \mathbf{q}_1)$ remains unchanged if $\mathbf{p}_1$ and with it also $\mathbf{q}_1$ is multiplied by an arbitrary scalar. The scalar can be chosen such that (2.41) yields $\mu = 1$.

Any two reciprocal polars are skew lines. Indeed, the intersection condition (2.18) is violated:

$$\mathbf{p}_1 \cdot \mathbf{q}_2 + \mathbf{p}_2 \cdot \mathbf{q}_1 = \mathbf{p}_1 \cdot (\mu\mathbf{b} - \mathbf{q}_1) + (\mu\mathbf{a} - \mathbf{p}_1) \cdot \mathbf{q}_1 = \mu(\mathbf{a} \cdot \mathbf{q}_1 + \mathbf{b} \cdot \mathbf{p}_1) \neq 0 \,. \quad (2.42)$$

Theorem 2.2. *The common perpendicular of two reciprocal polars* $(\mathbf{p}_1, \mathbf{q}_1)$ *and* $(\mathbf{p}_2, \mathbf{q}_2)$ *intersects orthogonally the axis of the complex. In other words: The axis of the complex and the reciprocal polars have a common perpendicular.*

Proof: Let N be the common perpendicular of the axis of the complex and of the polar $(\mathbf{p}_1, \mathbf{q}_1)$. Without loss of generality the origin 0 is placed at the foot of N on the axis of the complex. Furthermore, $\mathbf{p}_1$ is assumed to be a unit vector. These assumptions have the consequence that $\mathbf{b} = p\,\mathbf{a}$, that N has the Plücker vectors $(\mathbf{p}_1 \times \mathbf{q}_1\,,\, \mathbf{0})$, and that $\mathbf{a} \cdot \mathbf{p}_1 \times \mathbf{q}_1 = 0$. The last equation expresses the orthogonality of N to the axis of the complex. It suffices to prove that N intersects the other reciprocal polar $(\mathbf{p}_2, \mathbf{q}_2)$, and that it is orthogonal to it. These are the conditions

$$\mathbf{q}_2 \cdot \mathbf{p}_1 \times \mathbf{q}_1 = 0 \,, \qquad \mathbf{p}_2 \cdot \mathbf{p}_1 \times \mathbf{q}_1 = 0 \,. \quad (2.43)$$

With $\mathbf{p}_2 = \mu\mathbf{a} - \mathbf{p}_1$ and $\mathbf{q}_2 = \mu\mathbf{b} - \mathbf{q}_1 = \mu p\,\mathbf{a} - \mathbf{q}_1$ they are, indeed, satisfied. End of proof.

Proposition: Every complex line $(\mathbf{v}, \mathbf{w})$ intersecting one out of two reciprocal polars $(\mathbf{p}_1, \mathbf{q}_1)$ and $(\mathbf{p}_2, \mathbf{q}_2)$ intersects also the other.
Proof: Suppose the intersection condition (2.18) is satisfied for the polar $(\mathbf{p}_1, \mathbf{q}_1)$, i.e., $\mathbf{v} \cdot \mathbf{q}_1 + \mathbf{w} \cdot \mathbf{p}_1 = 0$. The intersection condition for the other polar $(\mathbf{p}_2, \mathbf{q}_2)$ is

$$\begin{aligned} \mathbf{v} \cdot \mathbf{q}_2 + \mathbf{w} \cdot \mathbf{p}_2 &= \mathbf{v} \cdot (\mu\mathbf{b} - \mathbf{q}_1) + \mathbf{w} \cdot (\mu\mathbf{a} - \mathbf{p}_1) \\ &= \mu(\mathbf{a} \cdot \mathbf{w} + \mathbf{b} \cdot \mathbf{v}) - (\mathbf{v} \cdot \mathbf{q}_1 + \mathbf{w} \cdot \mathbf{p}_1) = 0 \,. \end{aligned} \quad (2.44)$$

It is satisfied because (2.25) is valid. End of proof. Conversely, if $\mathbf{v} \cdot \mathbf{q}_1 + \mathbf{w} \cdot \mathbf{p}_1 = 0$ and $\mathbf{v} \cdot \mathbf{q}_2 + \mathbf{w} \cdot \mathbf{p}_2 = 0$, then also $\mathbf{a} \cdot \mathbf{w} + \mathbf{b} \cdot \mathbf{v} = 0$, whence it follows that every line intersecting two reciprocal polars is a complex line. And furthermore: If two lines, say g and g′, have the property that every line intersecting both of them is a complex line, g and g′ are reciprocal polars.

Proposition: The two transversals of any four linearly independent complex lines $(\mathbf{v}_i, \mathbf{w}_i)$ $(i = 1, 2, 3, 4)$ of a linear complex $(\mathbf{a}; \mathbf{b})$ are reciprocal polars. Proof: Since every complex line intersecting one of two reciprocal polars intersects also the other, it suffices to show that a transversal cannot be a complex line. This is done as follows. Suppose one of the transversals is a fifth

linearly independent complex line $(\mathbf{v}_5, \mathbf{w}_5)$. Then the system of five equations $\mathbf{w}_i \cdot \mathbf{v}_5 + \mathbf{v}_i \cdot \mathbf{w}_5 = 0$ $(i = 1, 2, 3, 4, 5)$ with a coefficient matrix of rank five has the nontrivial solution $(\mathbf{v}_5, \mathbf{w}_5)$ satisfying the equation $\mathbf{v}_5 \cdot \mathbf{w}_5 = 0$. But this is not the case since linear independence of the five lines means that Eqs.(2.38), $\mathbf{w}_i \cdot \mathbf{a} + \mathbf{v}_i \cdot \mathbf{b} = 0$ $(i = 1, 2, 3, 4, 5)$, with the same coefficient matrix have the nontrivial solution $(\mathbf{a}, \mathbf{b})$ satisfying the inequality $\mathbf{a} \cdot \mathbf{b} \neq 0$. End of proof.

Let P be an arbitrary point located on one of two reciprocal polars. The manifold of all lines passing through P and intersecting the other polar represents the pencil of complex lines in the null plane which has P as null point. Figure 2.6 shows two reciprocal polars together with the pencils of complex lines in two null planes corresponding to two null points P_1 and P_2. The line connecting these null points is a complex line in both null planes. If a null point moves along one reciprocal polar, the corresponding null plane rotates about the other reciprocal polar. This has the following consequence. If the null planes are known for two null points on one reciprocal polar, the other reciprocal polar is the line of intersection of these null planes.

Two pairs of reciprocal polars determine a linear complex. According to Theorem 2.2 its axis is the common perpendicular of the common perpendiculars of the two pairs. According to Fig. 2.6 a single pair determines the null plane associated with an arbitrary null point on one of the polars. The axis, this null plane and this null point determine the radius r and the inclination angle α shown in Fig. 2.5. According to (2.32) the pitch of the linear complex is $p = r \tan \alpha$.

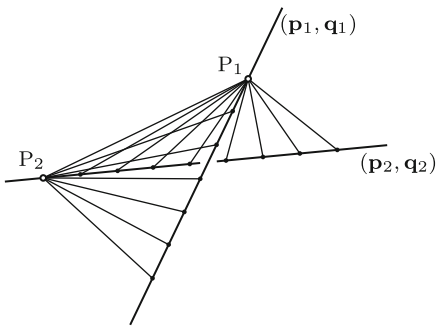

Fig. 2.6 Reciprocal polars and null planes associated with null points P_1 and P_2

2.8 Linear Congruence

A congruence is the manifold of all lines $(\mathbf{v}, \mathbf{w})$ which are subject to two constraint equations. In this section linear congruences are briefly treated. This is the special case of the intersection of two linear complexes (see (2.25)):

$$C_1 = \mathbf{a}_1 \cdot \mathbf{w} + \mathbf{b}_1 \cdot \mathbf{v} = 0\,, \qquad C_2 = \mathbf{a}_2 \cdot \mathbf{w} + \mathbf{b}_2 \cdot \mathbf{v} = 0\,. \tag{2.45}$$

The lines $(\mathbf{v}, \mathbf{w})$ of the congruence are complex lines common to both C_1 and C_2. Through every point in space a line of the congruence is passing, namely, the line of intersection of the null planes of C_1 and C_2 associated with this null point. In every plane a line of the congruence is located, namely, the line passing through the null points of C_1 and C_2 associated with this null plane. If two lines of the congruence intersect, the two null planes of C_1 and C_2 associated with this null point coincide with the plane spanned by the intersecting lines. In this case, every line in this plane and passing through this point is line of the congruence.

Equations (2.45) are equivalent to the two linear combinations (themselves linear complexes) $C_1 + \lambda_1 C_2 = 0\,,\ C_1 + \lambda_2 C_2 = 0\,,$ i.e.,

$$(\mathbf{a}_1 + \lambda_1 \mathbf{a}_2) \cdot \mathbf{w} + (\mathbf{b}_1 + \lambda_1 \mathbf{b}_2) \cdot \mathbf{v} = 0\,, \quad (\mathbf{a}_1 + \lambda_2 \mathbf{a}_2) \cdot \mathbf{w} + (\mathbf{b}_1 + \lambda_2 \mathbf{b}_2) \cdot \mathbf{v} = 0 \tag{2.46}$$

with arbitrary (real or complex) numbers λ_1 and $\lambda_2 \neq \lambda_1$. These numbers are determined such that both linear complexes are special. For this to be the case λ_1 and λ_2 must be the roots of the quadratic equation (see the remark following (2.25))

$$(\mathbf{a}_1 + \lambda \mathbf{a}_2) \cdot (\mathbf{b}_1 + \lambda \mathbf{b}_2) = 0\,. \tag{2.47}$$

Let it be assumed that the roots are different. The special linear complex with λ_i $(i = 1, 2)$ consists of all lines intersecting the line with Plücker vectors $(\mathbf{a}_1 + \lambda_i \mathbf{a}_2)$ and $(\mathbf{b}_1 + \lambda_i \mathbf{b}_2)$. The two lines thus determined are called *directrices* of the congruence. Let it be assumed that they are skew. The congruence consists of all lines intersecting both directrices. In accordance with the statements made above the following is true. Through every point in space a line exists which intersects both directrices. In every plane a line exists which intersects both directrices. If, in particular, a directrix is passing through the point or lying in the plane, the number of congruence lines through this point or in this plane is infinite. Further details see in Salmon [7] and Salmon/Fiedler [8].

2.9 Ruled Surfaces

Before investigating general ruled surfaces in Sect. 2.9.2 a special case is considered.

2.9.1 Intersection of three Linear Complexes

The intersection of three linear complexes

$$C_1 = \mathbf{a}_1 \cdot \mathbf{w} + \mathbf{b}_1 \cdot \mathbf{v} = 0\,, \quad C_2 = \mathbf{a}_2 \cdot \mathbf{w} + \mathbf{b}_2 \cdot \mathbf{v} = 0\,, \quad C_3 = \mathbf{a}_3 \cdot \mathbf{w} + \mathbf{b}_3 \cdot \mathbf{v} = 0 \tag{2.48}$$

is a one-parametric manifold of lines and hence a ruled surface F. Every generator of F belongs to the ∞^2 linear combinations (themselves linear complexes) $C = \lambda_1 C_1 + \lambda_2 C_2 + C_3 = 0$, i.e.,

$$C = (\lambda_1 \mathbf{a}_1 + \lambda_2 \mathbf{a}_2 + \mathbf{a}_3) \cdot \mathbf{w} + (\lambda_1 \mathbf{b}_1 + \lambda_2 \mathbf{b}_2 + \mathbf{b}_3) \cdot \mathbf{v} = 0 \tag{2.49}$$

with arbitrary (real or complex) parameters λ_1 and λ_2. Among these there are ∞^1 special complexes, namely, the ones satisfying the constraint equation for λ_1 and λ_2

$$(\lambda_1 \mathbf{a}_1 + \lambda_2 \mathbf{a}_2 + \mathbf{a}_3) \cdot (\lambda_1 \mathbf{b}_1 + \lambda_2 \mathbf{b}_2 + \mathbf{b}_3) = 0\,. \tag{2.50}$$

Each of these special complexes is the manifold of all lines intersecting the axis with Plücker vectors $(\lambda_1 \mathbf{a}_1 + \lambda_2 \mathbf{a}_2 + \mathbf{a}_3)$ and $(\lambda_1 \mathbf{b}_1 + \lambda_2 \mathbf{b}_2 + \mathbf{b}_3)$. Thus, a manifold of infinitely many generators of F intersect the axes of these ∞^1 special complexes. From this it follows that these axes themselves represent a second manifold of generators of F. Thus, the ruled surface F consists of two manifolds of generators, each generator of one manifold intersecting every generator of the second manifold. Consequently, the ruled surface is a quadric, i.e., in general, either a hyperboloid of one sheet or a hyperbolic paraboloid.

2.9.2 Striction Point. Distribution Parameter

A general ruled surface is a manifold of lines with a single free parameter u. It is defined through the position vector $\mathbf{r}(u)$ of a curve and the unit vector $\mathbf{e}(u)$ along the line passing through the point $\mathbf{r}(u)$. The normalized Plücker vectors of the lines are $\mathbf{e}(u)$ and $\mathbf{r}(u) \times \mathbf{e}(u)$. The lines are called *generating lines* or simply generators of the ruled surface. With an additional free parameter λ the surface has the parameter equation

$$\mathbf{x}(u,\lambda) = \mathbf{r}(u) + \lambda \mathbf{e}(u) \; . \tag{2.51}$$

Until further below three special kinds of ruled surfaces are excluded. These are
(a) general cylinders; all generators are parallel; $\mathbf{e}(u) = \text{const}$.
(b) general cones; all generators are passing through a fixed point called apex of the cone. Without loss of generality, $\mathbf{r}(u)$ is measured from the apex so that $\mathbf{r}(u)$ and $\mathbf{e}(u)$ are collinear
(c) ruled surfaces where $\mathbf{e}(u)$ is defined to be the tangent to the curve $\mathbf{r}(u)$.

In what follows, tangent planes are investigated. Derivatives with respect to u are denoted by a dot. The tangent plane at the point $\mathbf{x}(u,\lambda)$ is spanned by the vector $\dot{\mathbf{x}} = \dot{\mathbf{r}} + \lambda \dot{\mathbf{e}}$ tangent to the curve $\lambda = \text{const}$ through this point and by the vector $\mathbf{e}$ of the generator through this point. These two vectors define the unit normal vector $\mathbf{n}$ of the tangent plane at this point:

$$\mathbf{n} = \frac{(\dot{\mathbf{r}} + \lambda \dot{\mathbf{e}}) \times \mathbf{e}}{|(\dot{\mathbf{r}} + \lambda \dot{\mathbf{e}}) \times \mathbf{e}\,|} \; . \tag{2.52}$$

In what follows, statements are made about an arbitrary single generator with $u = \text{const}$. At the points $\lambda \to -\infty$ and $\lambda \to +\infty$ at infinity the unit normal vectors of the tangent planes are the mutually opposite vectors

$$\mathbf{n}_{-\infty} = \frac{\mathbf{e} \times \dot{\mathbf{e}}}{|\mathbf{e} \times \dot{\mathbf{e}}\,|} \; , \qquad \mathbf{n}_{+\infty} = -\frac{\mathbf{e} \times \dot{\mathbf{e}}}{|\mathbf{e} \times \dot{\mathbf{e}}\,|} \; . \tag{2.53}$$

The unit vector

$$\mathbf{n}_{\mathrm{S}} = \mathbf{n}_{-\infty} \times \mathbf{e} = \frac{\dot{\mathbf{e}}}{|\dot{\mathbf{e}}\,|} \tag{2.54}$$

is orthogonal to both $\mathbf{n}_{-\infty}$ and $\mathbf{n}_{+\infty}$. The particular point on the generator $u = \text{const}$ where $\mathbf{n}_{\mathrm{S}}$ is normal to the tangent plane is called *striction point* S on the generator. From (2.52) it follows that at S $[(\dot{\mathbf{r}} + \lambda_{\mathrm{S}} \dot{\mathbf{e}}) \times \mathbf{e}] \times \dot{\mathbf{e}} = \mathbf{0}$. Because of the orthogonality $\mathbf{e} \cdot \dot{\mathbf{e}} = 0$ this is the equation $(\dot{\mathbf{r}} \cdot \dot{\mathbf{e}} + \lambda_{\mathrm{S}} \dot{\mathbf{e}}^2)\mathbf{e} = \mathbf{0}$. Consequently

$$\lambda_{\mathrm{S}} = -\frac{\dot{\mathbf{r}} \cdot \dot{\mathbf{e}}}{\dot{\mathbf{e}}^2} \; . \tag{2.55}$$

With this expression (2.51) yields the position vector of the striction point:

$$\mathbf{x}_{\mathrm{S}} = \mathbf{r} + \lambda_{\mathrm{S}} \mathbf{e} = \mathbf{r} - \frac{\dot{\mathbf{r}} \cdot \dot{\mathbf{e}}}{\dot{\mathbf{e}}^2}\, \mathbf{e} \; . \tag{2.56}$$

The curve $\mathbf{x}_{\mathrm{S}}(u)$ with variable u is the locus of all striction points. It is called *striction line* of the ruled surface (in this case, line does not mean straight line).

In what follows, a single generator with $u = \text{const}$ is considered again. At the striction point S the cartesian basis with unit vectors $\mathbf{e}$, $\mathbf{n}_{\mathrm{S}}$ and

$\mathbf{n}_{-\infty} = \mathbf{e} \times \mathbf{n}_\mathrm{S}$ is defined. It is referred to as *canonical reference frame*. Let $\varphi(\lambda)$ be the angle through which the tangent plane at the point λ is rotated against the tangent plane at the striction point. Equation (2.52) for $\mathbf{n}(\lambda)$ yields $\cos\varphi = \mathbf{n}_\mathrm{S} \cdot \mathbf{n}$ and $\sin\varphi = \mathbf{n}_{-\infty} \cdot \mathbf{n}$. These are the equations (see (2.55))

$$\left.\begin{aligned} \cos\varphi &= \frac{\dot{\mathbf{e}} \cdot \dot{\mathbf{r}} \times \mathbf{e}}{|\dot{\mathbf{e}}\,|\,|(\dot{\mathbf{r}} + \lambda\dot{\mathbf{e}}) \times \mathbf{e}\,|}\,, \\ \sin\varphi &= \frac{-\dot{\mathbf{e}} \cdot \dot{\mathbf{r}} - \lambda\dot{\mathbf{e}}^2}{|\dot{\mathbf{e}}\,|\,|(\dot{\mathbf{r}} + \lambda\dot{\mathbf{e}}) \times \mathbf{e}\,|} = \frac{(\lambda_\mathrm{S} - \lambda)\dot{\mathbf{e}}^2}{|\dot{\mathbf{e}}\,|\,|(\dot{\mathbf{r}} + \lambda\dot{\mathbf{e}}) \times \mathbf{e}\,|}\,. \end{aligned}\right\} \tag{2.57}$$

This yields

$$\tan\varphi = \frac{\lambda_\mathrm{S} - \lambda}{\delta} \tag{2.58}$$

with

$$\delta = \frac{\dot{\mathbf{e}} \cdot \dot{\mathbf{r}} \times \mathbf{e}}{\dot{\mathbf{e}}^2}\,. \tag{2.59}$$

The quantity δ is constant on the generator $u = \text{const}$. It is called *distribution parameter* because it determines the distribution of the tangent planes along the generator. The rotation angle φ is an odd function of the distance $\lambda_\mathrm{S} - \lambda$ from the striction point. When traveling from the infinite point $\lambda \to -\infty$ to the infinite point $\lambda \to +\infty$, the tangent plane rotates through the angle π. At the striction point one half of this rotation is executed.

The striction point is indeterminate, and the distribution parameter is zero if $\dot{\mathbf{r}}$ is parallel to $\mathbf{e}$, i.e., if the generator $u = \text{const}$ is tangent to the curve $\mathbf{r}(u)$. This may happen at isolated points or even at all points of a curve $\mathbf{r}(u)$. Ruled surfaces where it happens at all points were excluded from consideration.

In what follows, new interpretations are given for the striction point and for the distribution parameter. Two generators associated with parameter values u and $u + \Delta u$ are considered. They are skew lines (see Fig. 2.7). Let ℓ be the length of the common perpendicular, and let α be the projected angle. The perpendicular is the axis of the screw displacement carrying one generator into the other. The quantities ℓ and α are the translatory and the angular component, respectively, of this screw displacement. For a fixed u (arbitrary) there exist in the limit $\Delta u \to 0$ a screw axis and the pitch $\lim_{\Delta u \to 0} (\ell/\alpha)$ of the screw. Propositions:

1. The screw axis has the direction of $\mathbf{n}_{-\infty}$
2. The screw axis intersects the generator $u = \text{const}$ at the striction point
3. The pitch is the distribution parameter δ.

Proof: The generators associated with u and with $u + \Delta u$ have the Plücker vectors

$$\left.\begin{aligned} \mathbf{v}_1 &= \mathbf{e}(u)\,, & \mathbf{w}_1 &= \mathbf{r}(u) \times \mathbf{e}(u)\,, \\ \mathbf{v}_2 &= \mathbf{e}(u + \Delta u)\,, & \mathbf{w}_2 &= \mathbf{r}(u + \Delta u) \times \mathbf{e}(u + \Delta u)\,. \end{aligned}\right\} \tag{2.60}$$

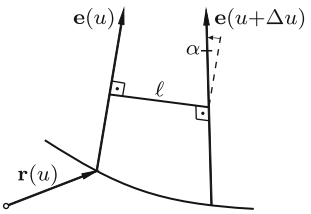

Fig. 2.7 Common perpendicular of two generators corresponding to parameter values u and $u + \Delta u$

For calculating limit values the Taylor expansions are made:

$$\left.\begin{aligned} \mathbf{v}_2 &= \mathbf{e} + \Delta u\dot{\mathbf{e}} + \tfrac{(\Delta u)^2}{2}\,\ddot{\mathbf{e}} + \dots\ , \\ \mathbf{w}_2 &= \mathbf{r}\times\mathbf{e} + \Delta u(\dot{\mathbf{r}}\times\mathbf{e} + \mathbf{r}\times\dot{\mathbf{e}}) + \tfrac{(\Delta u)^2}{2}\,(\ddot{\mathbf{r}}\times\mathbf{e} + 2\dot{\mathbf{r}}\times\dot{\mathbf{e}} + \mathbf{r}\times\ddot{\mathbf{e}}) + \dots\ . \end{aligned}\right\} \tag{2.61}$$

The first Eq.(2.23) determines the first Plücker vector of the common perpendicular: $\mathbf{v}_1\times\mathbf{v}_2 = \Delta u\,\mathbf{e}\times\dot{\mathbf{e}} + \dots$. In the limit $\Delta u \to 0$ this yields for the direction of the screw axis the vector $\mathbf{e}\times\dot{\mathbf{e}}$. This is the direction of $\mathbf{n}_{-\infty}$. Thus, proposition 1 is proved. Let $\boldsymbol{\varrho}$ be the perpendicular onto the screw axis. Equation (2.24) yields the expression

$$\boldsymbol{\varrho} = \lim_{\Delta u\to 0} \frac{(\mathbf{v}_1\times\mathbf{v}_2\cdot\mathbf{w}_2)\mathbf{v}_1 - (\mathbf{v}_1\times\mathbf{v}_2\cdot\mathbf{w}_1)\mathbf{v}_2}{(\mathbf{v}_1\times\mathbf{v}_2)^2}\ . \tag{2.62}$$

With the help of the Lagrangian identity for multiple products the following expressions are obtained (note the orthogonality $\mathbf{e}\cdot\dot{\mathbf{e}} = 0$)

$$\left.\begin{aligned} \mathbf{v}_1\times\mathbf{v}_2\cdot\mathbf{w}_2 &= \Delta u\,\mathbf{e}\times\dot{\mathbf{e}}\cdot[\,\mathbf{r}\times\mathbf{e} + \Delta u\,(\dot{\mathbf{r}}\times\mathbf{e} + \mathbf{r}\times\dot{\mathbf{e}}\,)\,] + \dots \\ &= -\Delta u\,\mathbf{r}\cdot\dot{\mathbf{e}} + (\Delta u)^2[\,-\dot{\mathbf{r}}\cdot\dot{\mathbf{e}} + (\mathbf{r}\cdot\mathbf{e}\,)\dot{\mathbf{e}}^2\,] + \dots\ , \\ \mathbf{v}_1\times\mathbf{v}_2\cdot\mathbf{w}_1 &= \Delta u\,(\mathbf{e}\times\dot{\mathbf{e}}\,)\cdot(\mathbf{r}\times\mathbf{e}\,) + \dots = -\Delta u\,\mathbf{r}\cdot\dot{\mathbf{e}} + \dots\ , \\ (\mathbf{v}_1\times\mathbf{v}_2\cdot\mathbf{w}_2)\mathbf{v}_1 &- (\mathbf{v}_1\times\mathbf{v}_2\cdot\mathbf{w}_1)\mathbf{v}_2 \\ &= (\Delta u)^2\,\dot{\mathbf{e}}^2\Big[\,(\mathbf{r}\cdot\mathbf{e})\,\mathbf{e} + (\mathbf{r}\cdot\mathbf{n}_{\mathrm{S}})\mathbf{n}_{\mathrm{S}} - \frac{\dot{\mathbf{r}}\cdot\dot{\mathbf{e}}}{\dot{\mathbf{e}}^2}\,\mathbf{e}\,\Big] + \dots \\ (\mathbf{v}_1\times\mathbf{v}_2)^2 &= (\Delta u)^2\,\dot{\mathbf{e}}^2 + \dots\ . \end{aligned}\right\} \tag{2.63}$$

This yields

$$\boldsymbol{\varrho} = (\mathbf{r}\cdot\mathbf{e})\,\mathbf{e} + (\mathbf{r}\cdot\mathbf{n}_{\mathrm{S}})\mathbf{n}_{\mathrm{S}} - \frac{\dot{\mathbf{r}}\cdot\dot{\mathbf{e}}}{\dot{\mathbf{e}}^2}\,\mathbf{e} + \dots\ . \tag{2.64}$$

The first two terms represent the components of $\mathbf{r}$ in the directions of $\mathbf{e}$ and of $\mathbf{n}_{\mathrm{S}}$, respectively. The third term is the vector $(\mathbf{r}\cdot\mathbf{n}_{-\infty})\mathbf{n}_{-\infty}$ along the screw axis. Hence the intersection point of the screw axis with the generator u is the point

$$\mathbf{r} - \frac{\dot{\mathbf{r}} \cdot \dot{\mathbf{e}}}{\dot{\mathbf{e}}^2} \mathbf{e} \,. \tag{2.65}$$

This is, indeed, the striction point S of Eq.(2.56). This ends the proof of proposition 2.

Next, the pitch $\lim_{\Delta u \to 0} (\ell/\alpha)$ of the screw is calculated. For a finite Δu Eq.(2.17) expresses $-\ell \sin\alpha$ in terms of the Plücker vectors of the two generators: $\mathbf{v}_1 \cdot \mathbf{w}_2 + \mathbf{v}_2 \cdot \mathbf{w}_1 = -\ell \sin\alpha$. Division of this equation through the equation $(\mathbf{v}_1 \times \mathbf{v}_2)^2 = \sin^2\alpha$ yields the quotient $\ell / \sin\alpha$ and in the limit $\Delta u \to 0$ the pitch:

$$\lim_{\Delta u \to 0} \frac{\ell}{\alpha} = - \lim_{\Delta u \to 0} \frac{\mathbf{v}_1 \cdot \mathbf{w}_2 + \mathbf{v}_2 \cdot \mathbf{w}_1}{(\mathbf{v}_1 \times \mathbf{v}_2)^2} \,. \tag{2.66}$$

For the denominator expression the last Eq.(2.63) is used. The same kind of expansion for the numerator expression leads to

$$\lim_{\Delta u \to 0} \frac{\ell}{\alpha} = \frac{\dot{\mathbf{r}} \cdot \mathbf{e} \times \dot{\mathbf{e}}}{\dot{\mathbf{e}}^2} \,. \tag{2.67}$$

This is, indeed, the distribution parameter δ of Eq.(2.59). End of proof.

Through (2.58) ruled surfaces become objects of kinematics. Imagine that one generator of a ruled surface F_1 and one generator of another ruled surface F_2 have identical distribution parameters δ. When the two generators, the striction points on these generators and also the tangent planes to F_1 and to F_2 at the striction points are brought into coincidence, F_1 and F_2 are in tangential contact everywhere along the common generator. This is a consequence of (2.58). Now, imagine that not only the two generators of F_1 and F_2 have identical distribution parameters, but that in every arbitrarily small neighborhood there are generators with pairwise identical distribution parameters, so that F_1 and F_2 can move relative to each other with permanent tangential contact along the actual common generator. This rotational-translational motion is called *raccording motion*. It is the subject of Sect. 9.5.

During the raccording motion the striction lines of F_1 and F_2 are permanently intersecting. The directions of their tangents at the point of intersection depend on differential-geometric quantities of higher order so that, normally, the lines are not cotangential.

Example: Determine the striction line and the distribution parameter for the hyperboloid of revolution shown in Fig. 2.8. Its equation in the x, y, z-system is given as $(x^2 + y^2)/a^2 - z^2/b^2 = 1$.
Solution: The semi-axis a is the radius of the gorge circle in the x, y-plane. This circle is chosen as curve having the position vector $\mathbf{r}(u)$. Each point $\mathbf{r}(u)$ is passed by two generators. The generators are orthogonal to $\mathbf{r}(u)$ and inclined against the x, y-plane by the angle ψ with $\tan\psi = b/a$. In the

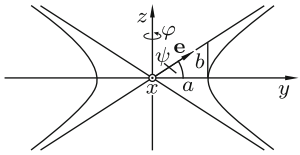

Fig. 2.8 Hyperboloid of revolution

projection in Fig. 2.8 the four generators through the points $x = \pm a$, $y = z = 0$ appear pairwise superimposed. These projected generators are the asymptotes of the contour hyperbola $y^2/a^2 - z^2/b^2 = 1$. The hyperboloid is created by rotating the generators about the z-axis. Let the parameter u be the angle φ of this rotation. Then $\dot{\mathbf{r}} = \dot{\varphi}\mathbf{e}_z \times \mathbf{r}$ and $\dot{\mathbf{e}} = \dot{\varphi}\mathbf{e}_z \times \mathbf{e}$, whence it follows that $\dot{\mathbf{r}} \cdot \dot{\mathbf{e}} = 0$, $\dot{\mathbf{e}}^2 = \dot{\varphi}^2 \cos^2 \psi$ and $\dot{\mathbf{r}} \cdot \mathbf{e} \times \dot{\mathbf{e}} = \pm\dot{\varphi}^2 a \sin\psi \cos\psi$ (the sign depends upon which of the two generators passing through $\mathbf{r}$ is considered). This together with (2.56) and (2.67) yields $\mathbf{x}_S(\varphi) \equiv \mathbf{r}(\varphi)$ and $|\delta(\varphi)| \equiv a \tan\psi = b$. Hence the striction line is the gorge circle, and the distribution parameter (identical for all generators) is the imaginary semi-axis b of the hyperboloid. Two hyperboloids of revolution with identical imaginary semi-axes can be in raccording motion. The kinematical significance of this motion is explained in Sect. 12.2. End of example.

Torses
At the beginning of this section three special kinds of ruled surfaces were excluded, namely,
(a) general cylinders; all generators are parallel; $\dot{\mathbf{e}}(u) \equiv 0$
(b) general cones; $\mathbf{r}(u)$ is measured from the apex; $\mathbf{r}(u)$ and $\mathbf{e}(u)$ are collinear for all u
(c) ruled surfaces where $\mathbf{e}(u)$ and $\dot{\mathbf{r}}(u)$ are collinear for all u.

An example for a type (c) ruled surface is the involute helicoid used as tooth flank in involute helical gears (see Sec. 16.1.8). For cylinders the distribution parameter is formally $\delta = \infty$. For cones and for type (c) ruled surfaces it is $\delta = 0$. All three types of ruled surfaces have in common that the tangent plane is the same for all points of a generator. All three of them have the property of being developable into a plane. The technical term is *torse*.

References

1. Hoschek O, Mick S (1997) Liniengeometrie. BI Hochschulskripten 713a/b, Zürich
2. Klein F, Müller C (eds.) (1901-1908) Enzyklopädie der Math. Wissenschaften. v.IV: Mechanik. Teubner, Leipzig
3. Kruppa E (1957) Analytische und konstruktive Differentialgeometrie. Springer, Wien

4. Meyer W FR, Mohrmann H (eds.) (1921-1928) Enzyklopädie der Math. Wissenschaften. v.III: Geometrie. Teubner, Leipzig
5. Plücker J (1865) On a new geometry of space. Philos.Trans. 155:725–791
6. Plücker J (1868) Neue Geometrie des Raumes gegründet auf die Betrachtung der geraden Linie als Raumelement. Teubner, Leipzig.
7. Salmon G (1914) A Treatise on the analytic geometry of three dimensions. Reprint 1958 (v.1) and 1965 (v.2), Chelsea, New York
8. Salmon G, Fiedler W (1922) Analytische Geometrie des Raumes Teil 1 (1. und 2. Lieferung): Die Elemente und die Theorie der Flächen zweiter Ordnung. (Editor Komerell, K). Teubner, Leipzig
9. Sauer R (1937) Projektive Liniengeometrie. Göschens Lehrbücherei Bd.23, de Gruyter
10. Steiner J (1881/82) Gesammelte Werke. Berlin
11. Sturm R (1892) Die Gebilde ersten und zweiten Grades der Liniengeometrie in synthetischer Behandlung. 1. Teil. Teubner, Leipzig
12. Timerding H E (1908) Geometrische Grundlegung der Mechanik eines starren Körpers. In [2]:125–189
13. Zindler K (1921) Algebraische Liniengeometrie. In [4]:973–1228

Chapter 3
Finite Screw Displacement

Subject of this chapter are relationships between two positions of a rigid body without a fixed point. These two positions, referred to as initial and final position, respectively, are assumed to be arbitrary subject only to the restriction that the final position cannot be produced from the initial position by pure translation. Motions leading from the initial to the final position are not investigated.

3.1 (4×4) Transformation Matrix

In Fig. 3.1 the most general displacement of a rigid body is shown. The body is represented by a body-fixed basis $\underline{\mathbf{e}}^2$. In the initial position $\underline{\mathbf{e}}^2$ coincides with a reference basis $\underline{\mathbf{e}}^1$ with origin 0_1. The displacement to the final position of $\underline{\mathbf{e}}^2$ with origin 0_2 is the result of a rotation $(\mathbf{n}, \varphi)$ about 0_1 followed by the translatory displacement $\mathbf{r} = \overrightarrow{0_1 0_2}$. The position of $\underline{\mathbf{e}}^2$ after the rotation and prior to translation is referred to as intermediate position (shown in dotted lines). In the final position a body-fixed point Q with position vector $\boldsymbol{\varrho}_2$ in $\underline{\mathbf{e}}^2$ has in $\underline{\mathbf{e}}^1$ the position vector

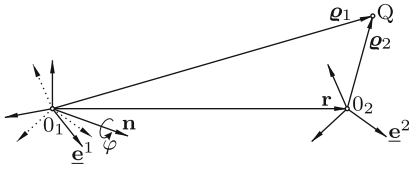

Fig. 3.1 Initial, intermediate and final positions of basis $\underline{\mathbf{e}}^2$. Position vectors of a body-fixed point Q. Rotation $(\mathbf{n}, \varphi)$ about 0_1 and translatory displacement $\mathbf{r}$

J. Wittenburg, *Kinematics*, DOI 10.1007/978-3-662-48487-6_3

$$\boldsymbol{\varrho}_1 = \boldsymbol{\varrho}_2 + \mathbf{r} \,. \tag{3.1}$$

Decomposition of this equation in $\underline{\mathbf{e}}^1$ yields the equation

$$\underline{\varrho}_1^1 = \underline{A}^{12}\underline{\varrho}_2^2 + \underline{r}^1 \,. \tag{3.2}$$

The matrix $\underline{A}^{12}$ is determined by the rotation $(\mathbf{n}, \varphi)$ about 0_1. The inverse equation is (premultiply by $\underline{A}^{21} = \underline{A}^{12^T}$ and write $\underline{r}^2 = \underline{A}^{21}\underline{r}^1$)

$$\underline{\varrho}_2^2 = \underline{A}^{21}\underline{\varrho}_1^1 - \underline{r}^2 \,. \tag{3.3}$$

It is convenient to write these equations in product form. This is achieved by adding an identity equation:

$$\begin{bmatrix} \underline{\varrho}_1^1 \\ 1 \end{bmatrix} = \begin{bmatrix} \underline{A}^{12} & \underline{r}^1 \\ \underline{0}^T & 1 \end{bmatrix} \begin{bmatrix} \underline{\varrho}_2^2 \\ 1 \end{bmatrix} \,, \quad \begin{bmatrix} \underline{\varrho}_2^2 \\ 1 \end{bmatrix} = \begin{bmatrix} \underline{A}^{21} & -\underline{r}^2 \\ \underline{0}^T & 1 \end{bmatrix} \begin{bmatrix} \underline{\varrho}_1^1 \\ 1 \end{bmatrix} \,, \quad \underline{0} = \begin{bmatrix} 0 \\ 0 \\ 0 \end{bmatrix} \,. \tag{3.4}$$

The (4×4) matrices are transformation matrices. Inversion is carried out not by transposition, but by the rule shown in Eqs.(3.4).

Example: In Fig. 3.2 a serial robot with six revolute joints is shown. Starting at the base the bodies and joints are labeled from 1 to 7 and from 1 to 6, respectively. The locations of the joint axes on the bodies are specified by body-fixed vectors $\mathbf{r}_2, \ldots, \mathbf{r}_6$ pointing from one axis to the next and by body-fixed unit vectors $\mathbf{n}_1, \ldots, \mathbf{n}_6$ along joint axes. The variable angle of rotation in joint i is called φ_i. It is the angle of body $i+1$ relative to body i. The vector $\mathbf{r}_7$ locates a specified point P on the hand of the robot. An arbitrarily chosen position of the robot is declared as null position. In this position the angles are $\varphi_1 = \varphi_2 = \ldots = \varphi_6 = 0$. On body 1 a reference basis $\underline{\mathbf{e}}^1$ is fixed with its origin 0 on the joint axis 1. On each of the bodies $i = 2, \ldots, 7$ a basis $\underline{\mathbf{e}}^i$ is fixed in such a way that in the null position all bases are oriented parallel to basis $\underline{\mathbf{e}}^1$. The given data are
- the column matrices $\underline{r}_i^i$ of the coordinates of $\mathbf{r}_i$ in $\underline{\mathbf{e}}^i \quad (i = 2, \ldots, 7)$
- the coordinates of $\mathbf{n}_i$ in $\underline{\mathbf{e}}^i$ (identical with the coordinates in $\underline{\mathbf{e}}^{i+1}$) $\quad (i = 1, \ldots, 6)$
- the angles $\varphi_i \quad (i = 1, \ldots, 6)$.

The position of the robot hand in the reference basis $\underline{\mathbf{e}}^1$ is determined by the matrix $\underline{A}^{17}$ in the equation $\underline{\mathbf{e}}^1 = \underline{A}^{17}\underline{\mathbf{e}}^7$ and by the column matrix $\underline{r}_{\mathrm{P}}^1$ of the coordinates of the position vector $\mathbf{r}_{\mathrm{P}}$ in $\underline{\mathbf{e}}^1$. To be determined are $\underline{A}^{17}$ and $\underline{r}_{\mathrm{P}}^1$ as functions of $\varphi_1, \ldots, \varphi_6$.
Solution: With the coordinates n_{i1}, n_{i2}, n_{i3} of $\mathbf{n}_i$ in $\underline{\mathbf{e}}^i$ and with φ_i Eq.(1.49) determines the matrix $\underline{A}^{i-1,i}$ in the relationship $\underline{\mathbf{e}}^{i-1} = \underline{A}^{i-1,i}\underline{\mathbf{e}}^i$. The desired matrix $\underline{A}^{17}$ is the product $\underline{A}^{12}\underline{A}^{23}\underline{A}^{34}\underline{A}^{45}\underline{A}^{56}\underline{A}^{67}$. The position vector of P is $\mathbf{r}_{\mathrm{P}} = \mathbf{r}_2 + \mathbf{r}_3 + \cdots + \mathbf{r}_7$. The desired column matrix of its coordinates in $\underline{\mathbf{e}}^1$ is the expression (to be read from right to left)

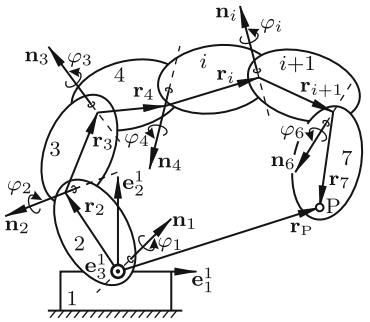

Fig. 3.2 Serial robot with six revolute joints

$$\underline{r}_{\mathrm{P}}^{1} = \underline{A}^{12}\left(\underline{r}_{2}^{2} + \underline{A}^{23}\left[\underline{r}_{3}^{3} + \underline{A}^{34}\{\underline{r}_{4}^{4} + \underline{A}^{45}[\underline{r}_{5}^{5} + \underline{A}^{56}(\underline{r}_{6}^{6} + \underline{A}^{67}\underline{r}_{7}^{7})]\}\right]\right) . \tag{3.5}$$

In terms of (4×4) matrices this equation reads

$$\begin{bmatrix} \underline{r}_{\mathrm{P}}^{1} \\ 1 \end{bmatrix} = \begin{bmatrix} \underline{A}^{12} & \underline{0} \\ \underline{0}^{T} & 1 \end{bmatrix} \begin{bmatrix} \underline{A}^{23} & \underline{r}_{2}^{2} \\ \underline{0}^{T} & 1 \end{bmatrix} \begin{bmatrix} \underline{A}^{34} & \underline{r}_{3}^{3} \\ \underline{0}^{T} & 1 \end{bmatrix} \begin{bmatrix} \underline{A}^{45} & \underline{r}_{4}^{4} \\ \underline{0}^{T} & 1 \end{bmatrix} \begin{bmatrix} \underline{A}^{56} & \underline{r}_{5}^{5} \\ \underline{0}^{T} & 1 \end{bmatrix} \begin{bmatrix} \underline{A}^{67} & \underline{r}_{6}^{6} \\ \underline{0}^{T} & 1 \end{bmatrix} \begin{bmatrix} \underline{r}_{7}^{7} \\ 1 \end{bmatrix} . \tag{3.6}$$

End of example.

3.2 Chasles' Theorem

In Fig. 3.3 the same general displacement of a rigid body is shown which was the subject of Fig. 3.1. The body is displaced from an initial position 1 to a final position 2. Let $\underline{\mathbf{e}}^2$ be a body-fixed basis which in position 1 coincides with a reference basis $\underline{\mathbf{e}}^1$ with origin 0_1 (arbitrary). In position 2 the origin of $\underline{\mathbf{e}}^2$ is at 0_2. The vector pointing from 0_1 to 0_2 is called $\mathbf{r}$. Dashed lines indicate an intermediate position $2'$ arrived at from position 1 by pure translation $\mathbf{r}$, and dotted lines indicate another intermediate position $1'$ arrived at from position 2 by pure translation $-\mathbf{r}$. The displacement from position 1 to position $1'$ is a rotation $(\mathbf{n}, \varphi)$ about 0_1, and the displacement from position $2'$ to position 2 is the same rotation $(\mathbf{n}, \varphi)$ about 0_2. Hence the conclusion: The displacement of the body from position 1 to position 2 can be interpreted in two ways, either as resultant of the rotation $(\mathbf{n}, \varphi)$ about 0_1 followed by the translation $\mathbf{r}$ or as resultant of the same translation $\mathbf{r}$ followed by the same rotation $(\mathbf{n}, \varphi)$ about 0_2.

For another origin $0_1'$ of the basis $\underline{\mathbf{e}}^1$ the rotation $(\mathbf{n}, \varphi)$ is the same because both $\underline{\mathbf{e}}^1$ and $\underline{\mathbf{e}}^2$ are oriented as before, but the translatory displacement $\mathbf{r}'$ from $0_1'$ to $0_2'$ is different. If $\boldsymbol{\varrho}$ is the vector pointing from 0_1 to

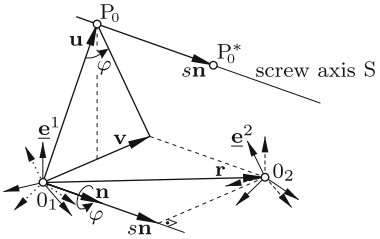

Fig. 3.3 Initial, final and two intermediate positions of a body-fixed basis $\underline{\mathbf{e}}^2$ specified by a rotation $(\mathbf{n}, \varphi)$ and a translatory displacement $\mathbf{r}$. Screw axis S and displacement $s\mathbf{n}$

$0_1'$ and $\boldsymbol{\varrho}^*$ the vector pointing from 0_2 to $0_2'$, the relationship between $\mathbf{r}'$ and $\mathbf{r}$ is $\mathbf{r}' = \mathbf{r} + \boldsymbol{\varrho}^* - \boldsymbol{\varrho}$.

Proposition: For arbitrary $\mathbf{n}$ and $\varphi \neq 0$ there exists a uniquely determined body-fixed line having the direction of $\mathbf{n}$ all points of which have identical displacements $s\mathbf{n}$ ($s = \text{const}$) in the direction along this line. More precisely, this is the statement made by

Theorem 3.1. (Chasles [8])[1] *Any not purely translatory displacement of a rigid body from an initial to a final position can be represented in a unique way as screw displacement. This screw displacement is the resultant of a rotation* $(\mathbf{n}, \varphi)$ *about a body-fixed screw axis S and a translation* $s\mathbf{n}$ *along this axis. The screw displacement is the same regardless whether the rotation or the translation is carried out first.*

Proof: Starting from $(\mathbf{n}, \varphi)$ and from the displacement $\mathbf{r}$ the screw axis and the displacement $s\mathbf{n}$ are determined as follows. Let $\boldsymbol{\varrho}$ be the body-fixed vector pointing from 0_1 to another body-fixed point P (arbitrary). After the rotation $(\mathbf{n}, \varphi)$ about 0_1 P has the position vector (see (1.37))

$$\boldsymbol{\varrho}^* = \boldsymbol{\varrho} + (1 - \cos\varphi)\,\mathbf{n} \times (\mathbf{n} \times \boldsymbol{\varrho}) + \sin\varphi\,\mathbf{n} \times \boldsymbol{\varrho}\,. \tag{3.7}$$

After the subsequent translation $\mathbf{r}$ the point has the position vector $\mathbf{r} + \boldsymbol{\varrho}^*$, so that the total displacement of P is $\mathbf{r} + \boldsymbol{\varrho}^* - \boldsymbol{\varrho}$. Points on the body-fixed screw axis, if it exists, have, prior to displacement, position vectors $\boldsymbol{\varrho} = \mathbf{u} + \lambda\mathbf{n}$ (λ arbitrary) with $\mathbf{u} \cdot \mathbf{n} = 0$. Thus, $\mathbf{u}$ is the perpendicular from 0_1 onto the screw axis. For proving the theorem it has to be shown that with these vectors $\boldsymbol{\varrho}$ the equation $\mathbf{r} + \boldsymbol{\varrho}^* - \boldsymbol{\varrho} \equiv s\mathbf{n}$ holds true independent of λ, and that, furthermore, the equation determines s and $\mathbf{u}$ uniquely. The first condition is satisfied, because λ is eliminated by the product $\mathbf{n} \times \boldsymbol{\varrho}$. The equation reads

$$\mathbf{r} - (1 - \cos\varphi)\,\mathbf{u} + \sin\varphi\,\mathbf{n} \times \mathbf{u} = s\mathbf{n}\,. \tag{3.8}$$

Scalar multiplication by $\mathbf{n}$ determines

[1] This theorem was known already to Mozzi (1765; see Giorgini [16])

$$s = \mathbf{n} \cdot \mathbf{r} \,, \tag{3.9}$$

and cross-multiplication by $\mathbf{n}$ produces the equation

$$\mathbf{n} \times \mathbf{r} - (1 - \cos\varphi)\, \mathbf{n} \times \mathbf{u} - \sin\varphi\, \mathbf{u} = \mathbf{0} \,. \tag{3.10}$$

This equation and (3.8) with $s\mathbf{n} = \mathbf{n}\mathbf{n} \cdot \mathbf{r}$ are two linear equations for $\mathbf{u}$ and for the second Plücker vector $\mathbf{u} \times \mathbf{n}$ of the screw axis:

$$\left.\begin{aligned} \sin\varphi\, \mathbf{u} - (1 - \cos\varphi)\, \mathbf{u} \times \mathbf{n} &= \mathbf{n} \times \mathbf{r} \,, \\ (1 - \cos\varphi)\, \mathbf{u} + \sin\varphi\, \mathbf{u} \times \mathbf{n} &= \mathbf{r} - \mathbf{n}\mathbf{n} \cdot \mathbf{r} = (\mathbf{n} \times \mathbf{r}) \times \mathbf{n} \,. \end{aligned}\right\} \tag{3.11}$$

With the formula $\sin\varphi/(1 - \cos\varphi) = \cot\varphi/2$ the solutions are

$$\mathbf{u} = \frac{1}{2}\Big[(\mathbf{n} \times \mathbf{r}) \times \mathbf{n} + \mathbf{n} \times \mathbf{r} \cot\frac{\varphi}{2}\Big] \,, \tag{3.12}$$

$$\mathbf{u} \times \mathbf{n} = \frac{1}{2}\Big[(\mathbf{n} \times \mathbf{r}) \times \mathbf{n} \cot\frac{\varphi}{2} - \mathbf{n} \times \mathbf{r}\Big] \,. \tag{3.13}$$

This concludes the proof. The geometrical interpretation of the formula for $\mathbf{u}$ is given in Fig. 3.3. The vector $\mathbf{r}$ is decomposed into its components $\mathbf{v}$ orthogonal to $\mathbf{n}$ and $s\mathbf{n}$ along $\mathbf{n}$, so that $s = \mathbf{n} \cdot \mathbf{r}$ in accordance with (3.9). Hence $\mathbf{r} = \mathbf{v} + s\mathbf{n}$. The screw axis is called S. It is passing through the apex P_0 of the isosceles triangle in the plane normal to $\mathbf{n}$ having $\mathbf{v}$ as base and φ as apex angle. The vector $\mathbf{u}$ is pointing from 0_1 to P_0. The first term in the expression for $\mathbf{u}$ represents the vector $\mathbf{v}/2$, and the second is the altitude of the triangle above the base. Until further below (see Sect. 3.9) the screw displacement is denoted $(\mathrm{S}, \mathbf{n}, \varphi, s)$.

In the general formula for the displacement $\mathbf{r} + \boldsymbol{\varrho}^* - \boldsymbol{\varrho}$ of arbitrary points of the body the last two terms satisfy (1.44) and (1.77):

$$(\boldsymbol{\varrho}^* - \boldsymbol{\varrho}) \cdot \mathbf{n} = 0 \,, \qquad \boldsymbol{\varrho}^* - \boldsymbol{\varrho} = \mathbf{n} \tan\frac{\varphi}{2} \times (\boldsymbol{\varrho}^* + \boldsymbol{\varrho}) \,. \tag{3.14}$$

With the first equation it is verified that the component of the displacement along the screw axis is $\mathbf{n}\mathbf{n} \cdot \mathbf{r} = s\mathbf{n}$ for all points of the body. With the second equation it is verified that the same screw axis is obtained if instead of 0_1 another point $0_1'$ is used as starting point. Let this point $0_1'$ be the point at the tip of a vector $\boldsymbol{\varrho}$ (arbitrary) from 0_1. Furthermore, let $\mathbf{u}'$ be the perpendicular from $0_1'$ onto the screw axis. It is given by (3.12) if $\mathbf{r}$ is replaced by $\mathbf{r} + \boldsymbol{\varrho}^* - \boldsymbol{\varrho}$. It has to be verified that the second Plücker vector $(\mathbf{u}' + \boldsymbol{\varrho}) \times \mathbf{n}$ of the screw axis is identical with $\mathbf{u} \times \mathbf{n}$. Because of (3.14) this is, indeed, the case:

$$
\begin{aligned}
(\mathbf{u}' + \boldsymbol{\varrho}) \times \mathbf{n} &= \frac{1}{2}\Big[(\mathbf{n} \times \mathbf{r}) \times \mathbf{n} \cot\frac{\varphi}{2} - \mathbf{n} \times \mathbf{r}\Big] \\
&+ \frac{1}{2}\Big[[\mathbf{n} \times (\varrho^* - \boldsymbol{\varrho})] \times \mathbf{n} \cot\frac{\varphi}{2} - \mathbf{n} \times (\varrho^* - \boldsymbol{\varrho})\Big] + \boldsymbol{\varrho} \times \mathbf{n} \\
&= \mathbf{u} \times \mathbf{n} + \frac{1}{2}\Big[(\varrho^* - \boldsymbol{\varrho}) \cot\frac{\varphi}{2} - \mathbf{n} \times (\varrho^* + \boldsymbol{\varrho})\Big] = \mathbf{u} \times \mathbf{n} \,. \qquad (3.15)
\end{aligned}
$$

Example: Given $\mathbf{n}$, φ, s and the position vector $\mathbf{r}_\mathrm{A}$ of a point A on the screw axis, determine the relationship between the position vectors $\mathbf{r}$ and $\mathbf{r}^*$ of an arbitrary body-fixed point before and after the screw displacement. Solution: From Fig. 1.3 it follows that the rotation is governed by (1.38) if $\mathbf{r}^*$ and $\mathbf{r}$ are replaced by $\mathbf{r}^* - \mathbf{r}_\mathrm{A}$ and $\mathbf{r} - \mathbf{r}_\mathrm{A}$, respectively. Hence the solution:

$$
\mathbf{r}^* = \mathbf{r}_\mathrm{A} + \cos\varphi\,(\mathbf{r} - \mathbf{r}_\mathrm{A}) + (1 - \cos\varphi)\mathbf{n}\mathbf{n}\cdot(\mathbf{r} - \mathbf{r}_\mathrm{A}) + \sin\varphi\,\mathbf{n} \times (\mathbf{r} - \mathbf{r}_\mathrm{A}) + s\,\mathbf{n} \,. \quad (3.16)
$$

In the special case $\varphi = \pi$, $s = 0$, the point is reflected in the screw axis:

$$
\mathbf{r}^* = 2\mathbf{r}_\mathrm{A} - \mathbf{r} + 2\mathbf{n}\,\mathbf{n} \cdot (\mathbf{r} - \mathbf{r}_\mathrm{A}) \,. \qquad (3.17)
$$

This formula is known from (2.11). End of example.

3.3 Scalar Measures of a Screw Displacement

For a screw displacement with infinitesimal quantities φ and s the quotient $p = s/\varphi$ is called pitch as is done for a machine screw. In the theory of finite screw displacements the quotient s/φ does not occur. As scalar measure of a finite screw displacement Dimentberg [12] defines the quantity

$$
p_\mathrm{D} = \frac{s}{\sin\varphi} \,. \qquad (3.18)
$$

Parkin [34] defines the quantity[2]

$$
p_\mathrm{P} = \frac{\frac{s}{2}}{\tan\frac{\varphi}{2}} \,. \qquad (3.19)
$$

These two measures are related through the equation

$$
p_\mathrm{P} = p_\mathrm{D} \cos^2\frac{\varphi}{2} \,. \qquad (3.20)
$$

[2] This measure was already used by Schönflies [32] p.1014

In the special case of an infinitesimal screw displacement both measures are identical with the pitch $p = s/\varphi$. Both measures find applications (see Huang [20] and Eqs.(3.207), (6.3), (6.23), (6.88)).

3.4 Roth' Theorem

Starting point of this section is the trivial statement: If a body is rotated about a fixed point P, every point of the body has the property that its distance from P is the same before and after the rotation. Roth [43] proved

Theorem 3.2. *Given a point* P *and two positions of a body not resulting from each other by a rotation about* P, *there exists a body-fixed plane every point of which has the property that its distance from* P *is the same in both positions.*

In what follows, not only a proof of the theorem is given. The body-fixed plane is determined as well. Let $\mathbf{r}_i$ and $\mathbf{r}'_i$ be the vectors from P to an arbitrary body-fixed point in the initial and in the final position, respectively. The condition that the distances from P be the same in both positions reads

$$\mathbf{r}_i'^2 = \mathbf{r}_i^2 \,. \tag{3.21}$$

It suffices to prove that this condition is satisfied by three noncollinear body-fixed points. Then it is satisfied by every body-fixed point in the plane spanned by these points. Four noncoplanar body-fixed points satisfying (3.21) cannot exist since otherwise the displacement of the body would be a rotation about P contrary to the assumption.

In the general case, the displacement of the body is a screw displacement. Define $(\mathbf{n}, \varphi)$ to be the rotation, $R \geq 0$ the distance of P from the screw axis, $\mathbf{e}$ a unit vector through P normal to the screw axis (in the case $R > 0$, the vector $R\mathbf{e}$ is the perpendicular from P onto the screw axis). Finally, let s be the translation along the screw axis (see Fig. 3.4). The special cases of pure translation ($s \neq 0$, $\varphi = 0$) and of pure rotation ($s = 0$, $\varphi \neq 0$) are not excluded. Three distinguished points of the unknown body-fixed plane

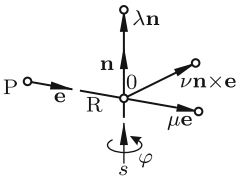

Fig. 3.4 Axes and quantities R, λ, μ, ν in the context of Roth' theorem

are its intersections with the line $\mathrm{P}\mathbf{e}$, with the screw axis and with the line perpendicular to both screw axis and line $\mathrm{P}\mathbf{e}$. The vectors $\mathbf{r}_i$ $(i = 1, 2, 3)$ from P to these points in the initial position have, with unknown quantities λ, μ and ν of dimension length, the forms

$$\mathbf{r}_1 = R\mathbf{e} + \lambda\mathbf{n}\,, \qquad \mathbf{r}_2 = (R+\mu)\mathbf{e}\,, \qquad \mathbf{r}_3 = R\mathbf{e} + \nu\mathbf{n}\times\mathbf{e}\,. \tag{3.22}$$

In the final position after the screw displacement the position vectors are found by simple inspection from Fig. 3.4:

$$\left.\begin{aligned} \mathbf{r}_1' = R\mathbf{e} + (s+\lambda)\mathbf{n}\,, \quad \mathbf{r}_2' &= s\mathbf{n} + (R+\mu\cos\varphi)\mathbf{e} + \mu\sin\varphi\;\mathbf{n}\times\mathbf{e}\,, \\ \mathbf{r}_3' &= s\mathbf{n} + (R-\nu\sin\varphi)\mathbf{e} + \nu\cos\varphi\;\mathbf{n}\times\mathbf{e}\,. \end{aligned}\right\} \tag{3.23}$$

Substitution into (3.21) yields for the unknowns the expressions

$$\lambda = -\frac{s}{2}\,, \qquad \mu = \frac{s^2}{2R(1-\cos\varphi)}\,, \qquad \nu = \frac{s^2}{2R\sin\varphi}\,. \tag{3.24}$$

Except for a single case these formulas define three points and, hence, a plane. The single case is a pure rotation about an axis not passing through P. It is characterized by $s = 0$ and $R, \varphi \neq 0$. The corresponding solutions $\lambda = \mu = \nu = 0$ define only the point 0. However, even in this case, a body-fixed plane with the required property exists. Without calculation it is obvious that the plane contains the rotation axis. In the initial position it is rotated against the line $\overline{\mathrm{P0}}$ through $-\varphi/2$ and in the final position through $+\varphi/2$. In Fig. 3.5a the points P and 0 and the two positions of the plane are shown in the projection along the rotation axis $\mathbf{n}$. Thus, it is proved that Roth' Theorem is valid without any exception. In what follows, three more special cases are considered in which the body-fixed plane is predictable without the above analysis.

1. The special case $R = 0$, $\varphi, s \neq 0$ (screw displacement with a screw axis passing through P): Without calculation it is obvious that the plane is normal to the screw axis. The perpendicular from P onto the plane is $-(s/2)\mathbf{n}$ in the initial position and $+(s/2)\mathbf{n}$ in the final position of the body (Fig. 3.5b). The plane is defined by Eqs.(3.24) which, in this case, yield $\lambda = -s/2$ and $\mu, \nu \to \infty$. A point A in this plane is displaced to A'.

2. The special case $\varphi = 0$, $s \neq 0$, R unspecified (pure translation $s\mathbf{n}$): Without calculation it is obvious that Fig. 3.5b applies also to this case. As before, Eqs.(3.24) yield $\lambda = -s/2$ and $\mu, \nu \to \infty$.

3. The special case $\varphi = \pi$, R, $s \neq 0$ (screw displacement with 180°-turn): Equations (3.24) yield $\lambda = -s/2$, $\mu = s^2/(4R)$ and $\nu \to \infty$. These results indicate that the line $\mathbf{n}\times\mathbf{e}$ is parallel to the plane. In Fig. 3.5c the two positions of the plane are shown in the projection along $\mathbf{n}\times\mathbf{e}$. The points with position vectors $\mathbf{r}_1$, $\mathbf{r}_1'$ and $\mathbf{r}_2$, $\mathbf{r}_2'$ in Eqs.(3.22) and (3.23) are marked A, A' and B, B', respectively. In this case, the solution is less

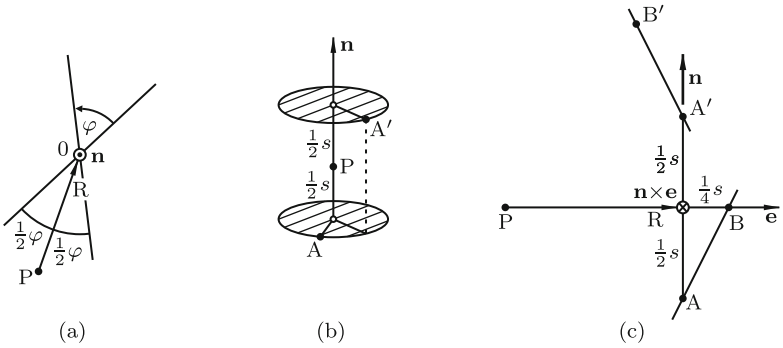

Fig. 3.5 Three special cases of Roth' theorem

obvious than in the previous cases, but it is still predictable without analysis. In all other cases λ, μ and ν are finite and different from zero.

3.5 Screw Displacement Determined from Displacements of Three Body Points

Problem: For three noncollinear body-fixed points P_1, P_2, P_3 the position vectors $\mathbf{z}_i$ before and $\mathbf{z}'_i$ after a displacement, respectively, are given $(i = 1, 2, 3)$. The three displacements $\mathbf{z}'_i - \mathbf{z}_i$ $(i = 1, 2, 3)$ are not identical. Therefore, the displacement of the body is not a translation, but a screw displacement. To be determined are the rotation $(\mathbf{n}, \varphi)$, a vector from 0 to some point on the screw axis and the translation s along the screw axis.

Solution: The rotation $(\mathbf{n}, \varphi)$ does not change if the displacement is superimposed by an arbitrary translation. Arbitrarily, the translation $-(\mathbf{z}'_3 - \mathbf{z}_3)$ is superimposed. Then the resulting displacement is the rotation $(\mathbf{n}, \varphi)$ about the fixed point P_3. The position vectors from P_3 to the body-fixed points P_1 and P_2 before and after the rotation are given by

$$\mathbf{r}_i = \mathbf{z}_i - \mathbf{z}_3 \quad \text{and} \quad \mathbf{r}^*_i = \mathbf{z}'_i - \mathbf{z}'_3 \qquad (i = 1, 2)\,, \tag{3.25}$$

respectively. These vectors determine the rotation $(\mathbf{n}, \varphi)$. Its Rodrigues vector $\mathbf{n} \tan \varphi/2$ is calculated from (1.210) – (1.217) in Sect. 1.15.7. The rotation is superimposed again by the translation $\mathbf{r} = \mathbf{z}'_3 - \mathbf{z}_3$. From the now known quantities $\mathbf{n}$, φ and $\mathbf{r}$ the translation s along the screw axis and the perpendicular $\mathbf{u}$ from P_3 onto the screw axis are calculated from (3.9) and (3.12), respectively. The desired vector from 0 to the screw axis is $\mathbf{z}_3 + \mathbf{u}$. Note: In (1.210) – (1.217) $\mathbf{u}$ is the Rodrigues vector.

3.6 Halphen's Theorem

In 1882 Halphen [17] published

Theorem 3.3. *A screw displacement* $(\mathrm{S}, \mathbf{n}, \varphi, s)$ *can be represented as resultant of two successive reflections in lines* g_1 *(first reflection) and* g_2. *The lines* g_1 *and* g_2 *intersect the screw axis* S *orthogonally. Line* g_2 *results from* g_1 *by the screw displacement* $(\mathrm{S}, \mathbf{n}, \varphi/2\,, s/2)$. *One of the two lines may be chosen arbitrarily.*

Proof: Figure 3.6 shows in two projections the screw axis S together with two lines g_1 and g_2 having the required properties. Let Q_1 be an arbitrary point of the body in the initial position prior to the first reflection. Its location relative to g_1 is specified by the quantities d and α explained in the figure. After the first reflection the body-fixed point is located at Q' and after the second reflection in g_2 it is located at Q_2. The effect of the first reflection is a rotation of the body-fixed perpendicular from Q_1 onto S through the angle 2α about S and a displacement of Q_1 by $2d$ in the direction $\mathbf{n}$. The second reflection in g_2 increases the rotation angle by $2(\varphi/2 - \alpha)$ and the displacement along S by $2(s/2 - d)$. Hence the total rotation angle is φ, and the total displacement along S is s. This proves the theorem.

In the special case $s = 0$, Halphen's theorem reduces to the statement known from Sects. 1.15.2 and 1.16 that a rotation $(\mathbf{n}, \varphi)$ can be represented as resultant of two reflections in lines which intersect $\mathbf{n}$ orthogonally and which enclose the angle $\varphi/2$. A reflection in a line and a 180°-rotation about this line result in one and the same displacement.

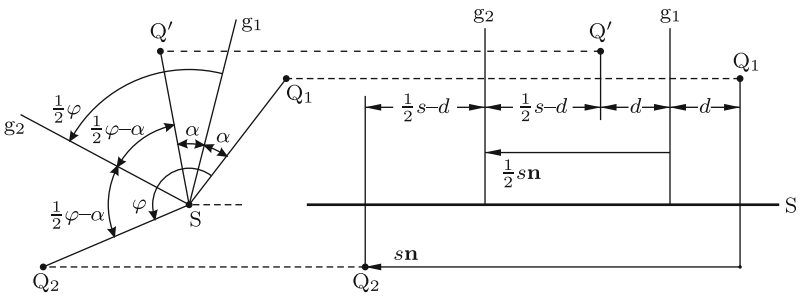

Fig. 3.6 Halphen's theorem

3.7 Resultant of two Screw Displacements. Screw Triangle

Consider now the displacement of a body which is the result of two successive screw displacements $(\mathrm{S}_1, \mathbf{n}_1, \varphi_1, s_1)$ (first screw displacement) and $(\mathrm{S}_2, \mathbf{n}_2, \varphi_2, s_2)$. According to Chasles' theorem the resultant displacement is itself a screw displacement called the resultant screw displacement $(\mathrm{S}_{\mathrm{res}}, \mathbf{n}_{\mathrm{res}}, \varphi_{\mathrm{res}}, s_{\mathrm{res}})$. This resultant is geometrically constructed by applying Halphen's theorem several times. First, the general case is considered in which the screw axes S_1 and S_2 are skew. Let g_1 be the common perpendicular of S_1 and S_2 (see Fig. 3.7). Each of the two screw displacements 1 and 2 is represented as resultant of two reflections. For the line of the second reflection of screw displacement 1 and also for the line of the first reflection of screw displacement 2 the common perpendicular g_1 is chosen. These two reflections cancel each other. Hence the resultant screw displacement is the resultant of the first reflection of screw displacement 1 and of the second reflection of screw displacement 2. The lines of these two reflections are called g_3 and g_2. According to Halphen's theorem, they are obtained by subjecting g_1 to the screw displacements $(\mathrm{S}_1, \mathbf{n}_1, -\varphi_1/2, -s_1/2)$ and $(\mathrm{S}_2, \mathbf{n}_2, \varphi_2/2, s_2/2)$, respectively. Again, according to Halphen's theorem, the resultant screw axis S_{res} is the common perpendicular of g_2 and g_3. Furthermore, $s_{\mathrm{res}}\mathbf{n}_{\mathrm{res}}/2$ is the vector along this common perpendicular shown in the figure, and $\varphi_{\mathrm{res}}/2$ is the projected angle between g_2 and g_3.

Up to now the screw axes S_1 and S_2 were assumed to be skew. Suppose now that they intersect at a point P. In this case, the common perpendicular g_1 is uniquely defined as normal through P of the plane spanned by S_1 and S_2. The length of the common perpendicular is zero.

The inverse of the resultant is the screw displacement $(\mathrm{S}_{\mathrm{res}}, \mathbf{n}_{\mathrm{res}}, -\varphi_{\mathrm{res}}, -s_{\mathrm{res}})$. It carries the body back to its initial position. The lines S_1, g_1, S_2,

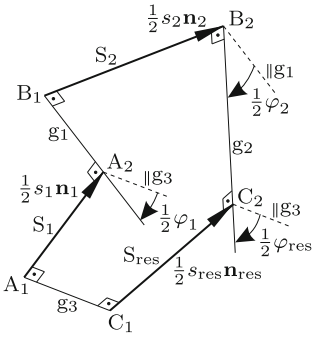

Fig. 3.7 Resultant of two screw displacements in the screw triangle

g_2, S_3, g_3 form a spatial hexagon with right angles at every corner. Three arbitrary pairwise skew lines S_1, S_2, S_3 have uniquely defined common perpendiculars g_1, g_2, g_3. Hence the three lines determine uniquely a system of three screw displacements about these lines S_1, S_2, S_3 which carry a body from an initial position via two intermediate positions back into its initial position[3]. In an arbitrarily chosen reference frame the three lines are defined by their Plücker vectors. From this it follows that the position and the shape of the hexagon are determined by twelve independent parameters. For reasons explained later the hexagon is called *spatial triangle* or *screw triangle* (Yang [51], Roth [44]). In Sects. 3.11 and 3.12 analytical relationships are developed for the screw triangle.

When in the given screw displacements 1 and 2 s_1 and s_2 are changed (all other parameters held fixed), then the lines g_2 and g_3 undergo lateral displacements. This has no effect on φ_{res} whereas all other parameters of the resultant screw displacement are effected. In Fig. 3.8 the special case $s_1 = s_2 = 0$ is shown, i.e., the resultant of two pure rotations about skew axes (S_1, $\mathbf{n}_1$, φ_1, S_2, $\mathbf{n}_2$, φ_2 and g_1 are the same as in Fig. 3.7). The points A_1 and A_2 coalesce in a single point A, and B_1 and B_2 coalesce in a single point B.

Remark: In 1848 Cayley [7],v.1 gave analytical solutions for the resultant of two successive screw displacements as well as for the inverse problem of decomposing a given screw displacement into two screw displacements with prescribed characteristics. He did not consider the special case of screw displacements with 180° rotation angles which was the subject of Halphen's paper [17] almost half a century later. Among the problems solved by Cayley are the determination of the resultant of two successive pure rotations about skew axes and the decomposition of a given screw displacement into two pure

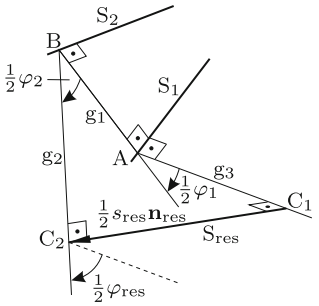

Fig. 3.8 Resultant of two rotations about skew axes

[3] The lines S_1, S_2, S_3 and their perpendiculars g_1, g_2, g_3 can change roles. Thus, the same hexagon determines three screw displacements about g_1, g_2, g_3 which carry the body from its initial position via two intermediate positions back into the initial position

rotations with prescribed characteristics. The decomposition is the subject of Cayley's

Theorem 3.4. *A given screw displacement can be represented as resultant of two subsequent pure rotations. The axis of one rotation may be prescribed arbitrarily (but not parallel to the axis of the resultant screw displacement). Then the axis of the other rotation as well as the two rotation angles are determined.*

The geometrical solution is explained in Fig. 3.8. Let it be assumed that the resultant screw displacement and the axis S_2 are prescribed as shown. The axes S_2 and S_{res} determine the common perpendicular g_2 and its endpoints B and C_2. Point C_1 is determined by s_{res}, and g_3 is determined by φ_{res}. Point A is the point of intersection of g_3 with the plane through B and perpendicular to S_2. The axis S_1 of the first rotation is the common perpendicular of g_3 and $g_1 = \overline{AB}$. Finally, $\varphi_1/2$ and $\varphi_2/2$ are the angles between g_1 and g_3 and between g_1 and g_2, respectively. An analytical solution of the problem is given in Sect. 3.11.

3.8 Dual Numbers

Let x and y be real numbers. The number $x + \varepsilon y$ is complex if $\varepsilon^2 = -1$. Clifford [10] was the first to consider the case $\varepsilon^2 = 0$. In this case, $x + \varepsilon y$ is called a *dual number* with x being its *primary part* and y its *dual part*. It must be understood that $\varepsilon^2 = 0$ does not mean that also $\varepsilon = 0$. The quantity ε is, just as $\mathrm{i} = \sqrt{-1}$, a unit, namely, the unit of the dual part. The sum and the product of two dual numbers $x_1 + \varepsilon y_1$ and $x_2 + \varepsilon y_2$ are defined by the formulas

$$\left.\begin{aligned}(x_1 + \varepsilon y_1) + (x_2 + \varepsilon y_2) &= x_1 + x_2 + \varepsilon(y_1 + y_2)\,,\\ (x_1 + \varepsilon y_1)(x_2 + \varepsilon y_2) &= x_1 x_2 + \varepsilon(x_1 y_2 + y_1 x_2)\,.\end{aligned}\right\} \tag{3.26}$$

According to these definitions, for addition as well as for multiplication the laws of commutativity, associativity and distributivity are valid. As with real numbers expressions are multiplied out term by term always keeping in mind the rule $\varepsilon^2 = 0$. Together with $\varepsilon^2 = 0$ also all higher-order terms of ε are zero: $\varepsilon^3 = \varepsilon \cdot \varepsilon^2 = 0$ etc. The difference of two dual numbers is defined uniquely via the sum. The zero dual number is the number $(0 + \varepsilon \cdot 0)$ since only this number has the property that addition to $x + \varepsilon y$ with arbitrary x, y results in $x + \varepsilon y$.

Equation (3.26) shows that the product of two dual numbers is zero not only if at least one factor is the number $(0 + \varepsilon \cdot 0)$, but also in the case $x_1 = x_2 = 0$ with arbitrary y_1, y_2. From this it follows that division by $(x + \varepsilon y)$ is not defined if $x = 0$. Indeed, multiplying both the numerator and

the denominator of $1/(x+\varepsilon y)$ by $x-\varepsilon y$ results in the expression

$$\frac{1}{x+\varepsilon y} = \frac{x-\varepsilon y}{x^2} = \frac{1}{x} + \varepsilon\,\frac{-y}{x^2} \tag{3.27}$$

which is defined only in the case $x \neq 0$.

Dual numbers $x+\varepsilon y$ and (2×2)-matrices of the form $\begin{bmatrix} x & 0 \\ y & x \end{bmatrix}$ have the same algebra as is shown by the formulas

$$\begin{bmatrix} x_1 & 0 \\ y_1 & x_1 \end{bmatrix} \begin{bmatrix} x_2 & 0 \\ y_2 & x_2 \end{bmatrix} = \begin{bmatrix} x_1x_2 & 0 \\ x_1y_2+x_2y_1 & x_1x_2 \end{bmatrix}, \quad \begin{bmatrix} x & 0 \\ y & x \end{bmatrix}^{-1} = \begin{bmatrix} 1/x & 0 \\ -y/x^2 & 1/x \end{bmatrix}. \tag{3.28}$$

Let $f(x+\varepsilon y)$ be a once differentiable function depending on the dual variable $x+\varepsilon y$ and possibly on additional parameters. The Taylor series expansion about the point x consists, because of $\varepsilon^2 = 0$, of two terms only:

$$f(x+\varepsilon y) = f(x) + \varepsilon y\,\frac{\partial f}{\partial x}\Big|_{y=0}. \tag{3.29}$$

Hence the function $f(x+\varepsilon y)$ is a dual number. Its primary part is the function of the primary part of its argument. Its dual part is the derivative of the primary part with respect to the primary part x of its argument multiplied by the dual part y of $x+\varepsilon y$. This dual part is referred to as *dual derivative*, and the process of calculating it is referred to as dual differentiation. Examples:

$$\cos(x+\varepsilon y) = \cos x - \varepsilon y \sin x\,, \quad \sin(x+\varepsilon y) = \sin x + \varepsilon y \cos x\,, \tag{3.30}$$

$$\tan(x+\varepsilon y) = \tan x + \varepsilon\,\frac{y}{\cos^2 x}\,, \quad \cot(x+\varepsilon y) = \cot x - \varepsilon\,\frac{y}{\sin^2 x}\,. \tag{3.31}$$

The product of two functions $f(x_1+\varepsilon y_1)\,g(x_2+\varepsilon y_2)$ is decomposed into primary and dual part as follows:

$$\begin{aligned} f(x_1+\varepsilon y_1)\,g(x_2+\varepsilon y_2) &= \Big(f(x_1) + \varepsilon y_1\,\frac{\partial f}{\partial x_1}\Big|_{y_1=0}\Big)\Big(g(x_2) + \varepsilon y_2\,\frac{\partial g}{\partial x_2}\Big|_{y_2=0}\Big) \\ &= f(x_1)g(x_2) + \varepsilon\Big(f(x_1)y_2\,\frac{\partial g}{\partial x_2}\Big|_{y_2=0} + y_1\,\frac{\partial f}{\partial x_1}\Big|_{y_1=0} g(x_2)\Big)\,. \end{aligned} \tag{3.32}$$

Example:

$$\sin(x_1+\varepsilon y_1)\cos(x_2+\varepsilon y_2) = \sin x_1 \cos x_2 + \varepsilon(y_1 \cos x_1 \cos x_2 - y_2 \sin x_1 \sin x_2)\,. \tag{3.33}$$

Thus, the primary part is the product of the functions of the primary parts of their variables. The rule for calculating the dual part is the product rule of dual differentiation. The dual part is linear with respect to the dual parts y_1, y_2 of the arguments of the factors f and g, respectively. With these

few rules all mathematical expressions encountered in later chapters can be decomposed into their primary and dual parts.

A MAPLE software tool developed by Sinigersky [45] has subroutines for the symbolic manipulation of dual numbers, dual vectors and dual quaternions and also for the dual differentiation of arbitrarily complex mathematical expressions.

3.9 Dual Vectors. Dual Angles

Figure 3.9 shows a *line vector* $\hat{\mathbf{v}}$ of given magnitude. This is a vector which is confined to its line. In contrast to a free vector $\mathbf{v}$ a line vector can slide along its line, but it cannot move lateral to it. A force is an example of a line vector. Its line is called line of action. Let $\mathbf{v}$ be the free vector having direction, sense of direction and magnitude in common with $\hat{\mathbf{v}}$. The line vector $\hat{\mathbf{v}}$ is uniquely determined if $\mathbf{v}$ is given and, in addition, the vector $\mathbf{r}$ from a reference point 0 to an arbitrary point of the line of $\hat{\mathbf{v}}$. The vectors $\mathbf{r}$ and $\mathbf{v}$ together define the *moment* of $\hat{\mathbf{v}}$ with respect to 0. It is abbreviated $\mathbf{w}$:

$$\mathbf{w} = \mathbf{r} \times \mathbf{v} \qquad \text{(equal for all points of the line of } \hat{\mathbf{v}}\text{)} . \tag{3.34}$$

The vectors $\mathbf{v}$ and $\mathbf{w} = \mathbf{r} \times \mathbf{v}$ represent the first and the second Plücker vectors of the line (see Sect. 2.2). They determine the line. With a free parameter λ it is given by the vector equation

$$\mathbf{r}^*(\lambda) = \lambda \mathbf{v} + \frac{\mathbf{v} \times \mathbf{w}}{\mathbf{v}^2} . \tag{3.35}$$

The Plücker vectors satisfy the conditions

$$\mathbf{v}^2 = \text{const} , \qquad \mathbf{v} \cdot \mathbf{w} = 0 . \tag{3.36}$$

Definition: The line vector $\hat{\mathbf{v}}$ is the dual vector

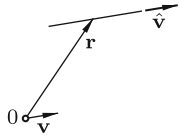

Fig. 3.9 Line vector $\hat{\mathbf{v}}$

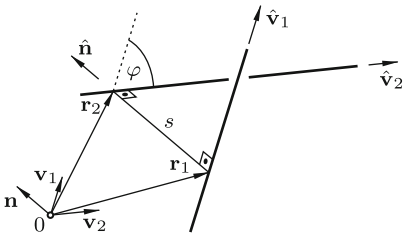

Fig. 3.10 Screw angle $\hat{\varphi} = \varphi + \varepsilon s$

$$\hat{\mathbf{v}} = \mathbf{v} + \varepsilon \mathbf{w} \,. \tag{3.37}$$

Because of (3.36) the scalar product of $\hat{\mathbf{v}}$ with itself is

$$\hat{\mathbf{v}}^2 = (\mathbf{v} + \varepsilon \mathbf{w})^2 = \mathbf{v}^2 + 2\varepsilon \mathbf{v} \cdot \mathbf{w} = \mathbf{v}^2 \,. \tag{3.38}$$

In the case $\mathbf{v}^2 = 1$, $\hat{\mathbf{v}}$ is a unit dual vector (unit line vector).

In Fig. 3.10 two unit line vectors $\hat{\mathbf{v}}_1$ and $\hat{\mathbf{v}}_2$ are shown the lines of which are skew. By assumption, $\mathbf{v}_1^2 = \mathbf{v}_2^2 = 1$. As vectors $\mathbf{r}_1$ and $\mathbf{r}_2$ the vectors to the feet of the common perpendicular of the lines are chosen. Then, by Eq.(3.37),

$$\hat{\mathbf{v}}_1 = \mathbf{v}_1 + \varepsilon \mathbf{w}_1 = \mathbf{v}_1 + \varepsilon \mathbf{r}_1 \times \mathbf{v}_1 \,, \qquad \hat{\mathbf{v}}_2 = \mathbf{v}_2 + \varepsilon \mathbf{w}_2 = \mathbf{v}_2 + \varepsilon \mathbf{r}_2 \times \mathbf{v}_2 \,. \tag{3.39}$$

These expressions are valid also when the lines are parallel. In this case, $\mathbf{r}_1$ and $\mathbf{r}_2$ are the position vectors of an arbitrary common perpendicular.
Let $\mathbf{n}$ be the unit vector in the direction of $\mathbf{r}_2 - \mathbf{r}_1$:

$$\mathbf{n} = \frac{\mathbf{r}_2 - \mathbf{r}_1}{|\mathbf{r}_2 - \mathbf{r}_1|} = \frac{\mathbf{v}_1 \times \mathbf{v}_2}{|\mathbf{v}_1 \times \mathbf{v}_2|} \,. \tag{3.40}$$

In the case of parallel lines only the first expression is useful and in the case of intersecting (not identical) lines only the second expression. Furthermore, the line vector is defined

$$\hat{\mathbf{n}} = \mathbf{n} + \varepsilon \mathbf{r}_1 \times \mathbf{n} \,. \tag{3.41}$$

It has the direction of $\mathbf{n}$, and its line is the common perpendicular.

The line vector $\hat{\mathbf{v}}_2$ can be produced from $\hat{\mathbf{v}}_1$ by a screw displacement about the screw axis $\hat{\mathbf{n}}$. The rotation angle φ and the translation s of this screw displacement (both positive, zero or negative) are determined by the equations

$$\mathbf{v}_1 \times \mathbf{v}_2 = \mathbf{n} \sin\varphi \,, \qquad \mathbf{r}_2 - \mathbf{r}_1 = \mathbf{n}\, s \,. \tag{3.42}$$

The absolute values $|s|$ and $|\varphi|$ are the distance and the projected angle, respectively, between the two lines. The special cases of parallel or intersecting lines are characterized by $\varphi = 0$ or $s = 0$, respectively.
Between the various quantities just defined the following relationships exist:

$$\mathbf{v}_1 \cdot \mathbf{v}_2 = \cos\varphi \,, \qquad (\mathbf{r}_2 - \mathbf{r}_1) \cdot (\mathbf{v}_1 \times \mathbf{v}_2) = s \sin\varphi \,. \tag{3.43}$$

Definition: The dual angle

$$\hat{\varphi} = \varphi + \varepsilon s \tag{3.44}$$

is called the *screw angle* of the screw displacement carrying $\hat{\mathbf{v}}_1$ into $\hat{\mathbf{v}}_2$. The screw displacement itself is denoted $(\hat{\mathbf{n}}, \hat{\varphi})$. This replaces the earlier notation $(\mathrm{S}, \mathbf{n}, \varphi, s)$. The pair $\mathrm{S}, \mathbf{n}$ is replaced by $\hat{\mathbf{n}}$, and the pair φ, s is replaced by $\hat{\varphi}$. The functions $\cos\hat{\varphi}$ and $\sin\hat{\varphi}$ are given in (3.30).

The definitions given for dual vectors and for dual screw angles are very useful. This is shown by calculating the dot product and the cross product of the dual unit vectors $\hat{\mathbf{v}}_1$ and $\hat{\mathbf{v}}_2$ of Fig. 3.10. With (3.39) and (3.43) the dot product is

$$\begin{aligned}
\hat{\mathbf{v}}_1 \cdot \hat{\mathbf{v}}_2 &= \mathbf{v}_1 \cdot \mathbf{v}_2 + \varepsilon(\mathbf{v}_1 \cdot \mathbf{w}_2 + \mathbf{v}_2 \cdot \mathbf{w}_1) && (3.45)\\
&= \mathbf{v}_1 \cdot \mathbf{v}_2 + \varepsilon(\mathbf{v}_1 \cdot \mathbf{r}_2 \times \mathbf{v}_2 + \mathbf{r}_1 \times \mathbf{v}_1 \cdot \mathbf{v}_2)\\
&= \mathbf{v}_1 \cdot \mathbf{v}_2 + \varepsilon(-\mathbf{r}_2 \cdot \mathbf{v}_1 \times \mathbf{v}_2 + \mathbf{r}_1 \cdot \mathbf{v}_1 \times \mathbf{v}_2)\\
&= \mathbf{v}_1 \cdot \mathbf{v}_2 - \varepsilon(\mathbf{r}_2 - \mathbf{r}_1) \cdot (\mathbf{v}_1 \times \mathbf{v}_2)\,. && (3.46)\\
&= \cos\varphi - \varepsilon s \sin\varphi && (3.47)
\end{aligned}$$

and with (3.30)

$$\hat{\mathbf{v}}_1 \cdot \hat{\mathbf{v}}_2 = \cos\hat{\varphi}\,. \tag{3.48}$$

Thus, the rule for calculating the dot product of two ordinary unit vectors is transferred to dual unit vectors.

Comparison of (3.45) and (3.47) yields $s\sin\varphi = -(\mathbf{v}_1 \cdot \mathbf{w}_2 + \mathbf{v}_2 \cdot \mathbf{w}_1)$ and the condition for two lines to intersect:

$$\mathbf{v}_1 \cdot \mathbf{w}_2 + \mathbf{v}_2 \cdot \mathbf{w}_1 = 0\,. \tag{3.49}$$

These equations repeat what is known from (2.17) and (2.18). Another important relationship is deduced from (3.46):

$$(\mathbf{r}_1 - \mathbf{r}_2) \cdot (\mathbf{v}_1 \times \mathbf{v}_2) \quad \text{is the dual derivative of} \quad \mathbf{v}_1 \cdot \mathbf{v}_2\,. \tag{3.50}$$

The usefulness of this equation is demonstrated in Sects. 5.3.1, 6.3 and 6.4.4.

Next, the cross product of the dual unit vectors $\hat{\mathbf{v}}_1$ and $\hat{\mathbf{v}}_2$ is calculated. With (3.39) it is

$$\begin{aligned}
&\hat{\mathbf{v}}_1 \times \hat{\mathbf{v}}_2 = (\mathbf{v}_1 + \varepsilon\mathbf{r}_1 \times \mathbf{v}_1) \times (\mathbf{v}_2 + \varepsilon\mathbf{r}_2 \times \mathbf{v}_2)\\
&= \mathbf{v}_1 \times \mathbf{v}_2 + \varepsilon[\mathbf{v}_1 \times (\mathbf{r}_2 \times \mathbf{v}_2) + (\mathbf{r}_1 \times \mathbf{v}_1) \times \mathbf{v}_2]\\
&= \mathbf{v}_1 \times \mathbf{v}_2 + \varepsilon[\mathbf{v}_1 \cdot \mathbf{v}_2\mathbf{r}_2 - \mathbf{v}_1 \cdot \mathbf{r}_2\mathbf{v}_2 + \mathbf{r}_1 \cdot \mathbf{v}_2\mathbf{v}_1 - \mathbf{v}_1 \cdot \mathbf{v}_2\mathbf{r}_1]\\
&= \mathbf{v}_1 \times \mathbf{v}_2 + \varepsilon[\mathbf{v}_1 \cdot \mathbf{v}_2(\mathbf{r}_2 - \mathbf{r}_1) + \mathbf{r}_1 \times (\mathbf{v}_1 \times \mathbf{v}_2)] \quad (\text{note } \mathbf{v}_1 \cdot \mathbf{r}_2 = \mathbf{v}_1 \cdot \mathbf{r}_1)\\
&= \mathbf{n}\sin\varphi + \varepsilon(\cos\varphi\,\mathbf{n}s + \mathbf{r}_1 \times \mathbf{n}\sin\varphi) \quad (\text{because of (3.43) and (3.42)})\\
&= (\mathbf{n} + \varepsilon\mathbf{r}_1 \times \mathbf{n})(\sin\varphi + \varepsilon s\cos\varphi)\,. && (3.51)
\end{aligned}$$

The correctness of the last expression is verified by multiplying out again. With (3.37) and (3.30) the final result is

$$\hat{\mathbf{v}}_1 \times \hat{\mathbf{v}}_2 = \hat{\mathbf{n}}\sin\hat{\varphi}\,. \tag{3.52}$$

Thus, also the rule for calculating the cross product of two ordinary unit vectors is transferred to dual unit vectors.

3.10 Principle of Transference

In Chap. 1 relationships were established between positions of a body before and after a rotation $(\mathbf{n}, \varphi)$ about a fixed point. Equations (3.48) and (3.52) represent the basis of the *principle of transference* first formulated by Kotelnikov [26] in 1886 and by Study [47] in 1903. It says: Given an equation relating positions of a body before and after a rotation $(\mathbf{n}, \varphi)$ about a fixed point. Replace the unit vector $\mathbf{n}$ along the axis by the dual unit vector $\hat{\mathbf{n}}$ and the rotation angle φ by the dual angle $\hat{\varphi}$. The equation thus obtained relates positions of a body before and after the screw displacement $(\hat{\mathbf{n}}, \hat{\varphi})$.

In Sects. 3.10.1 – 3.10.5 the notions of cartesian basis, direction cosine matrix, Euler angle, rotation tensor and quaternion of a rotation are *dualized*, i.e., transferred into respective dual quantities. Dualized equations relating such quantities must subsequently be split into their primary and dual parts. For this procedure it suffices to apply basic rules of (vector) algebra in combination with the rule of dual differentiation (see (3.29) – (3.33), in particular formulas (3.30) and (3.31) for trigonometric functions). These rules and formulas reveal the following facts.

1. The primary parts of dual equations contain neither second Plücker vectors $\mathbf{w}$ of screw axes nor translatory displacements s along screw axes. Thus, primary parts of equations describe a (usually nonlinear) problem of rotation about a fixed point.

2. The quantities $\mathbf{w}$ and s of screw displacements appear in the dual parts only and, moreover, in linear form only. The solution of these equations is an elementary problem. Note: First Plücker vectors $\mathbf{n}$ of screw axes and rotation angles appear in the dual parts as well. However, these quantities are known from solving the primary parts.

Due to these facts the principle of transference is a powerful tool for solving problems of very diverse nature. This is demonstrated in subsequent chapters of this book (Sects. 3.11, 3.12, 3.14 and Chaps. 5, 7, 8, 9 and 13).
Literature: Löbell [29] (applications in kinematics, statics and differential geometry), Dimentberg [12] – [14], Keler [21] – [25], Yang [51, 52, 53], Yang/Freudenstein [54], Adams [1], Roth [44], Yuan/Freudenstein/Woo [55, 56], Veldkamp [49], Hsia/Yang [19], Castelain/Flamme/Gorla/
Renaud [6], Pennock/Yang [37], Martinez/Duffy [30], Chevallier [9], Pennestri/
Stefanelli [36] and the article by Pennock/Schaaf in Erdman [15].

3.10.1 Dual Basis. Dual Direction Cosine Matrix

Using Fig. 3.11 the notion of a (right-handed, orthogonal) dual basis is introduced. Point 0 is the origin of ordinary bases $\underline{\mathbf{e}}^1$ and $\underline{\mathbf{e}}^2$. These bases are related through the direction cosine matrix (see (1.6)):

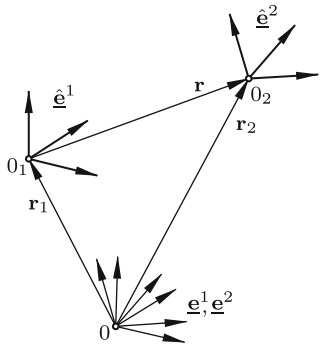

Fig. 3.11 Dual bases $\underline{\hat{\mathbf{e}}}^1$ and $\underline{\hat{\mathbf{e}}}^2$

$$\underline{\mathbf{e}}^1 = \underline{A}^{12}\underline{\mathbf{e}}^2 \,, \qquad \underline{A}^{12} = \underline{\mathbf{e}}^1 \cdot \underline{\mathbf{e}}^{2T} \,. \tag{3.53}$$

Vectors $\mathbf{r}_1$ and $\mathbf{r}_2$ locate the origins 0_1 and 0_2, respectively, of two dual bases. These dual bases are formed by the dual unit vectors $\hat{\mathbf{e}}_i^1$ and $\hat{\mathbf{e}}_i^2$ $(i = 1, 2, 3)$ which are parallel to the basis vectors of $\underline{\mathbf{e}}^1$ and $\underline{\mathbf{e}}^2$, respectively. The dual basis vectors are

$$\hat{\mathbf{e}}_i^1 = \mathbf{e}_i^1 + \varepsilon\, \mathbf{r}_1 \times \mathbf{e}_i^1 \qquad \text{and} \qquad \hat{\mathbf{e}}_i^2 = \mathbf{e}_i^2 + \varepsilon\, \mathbf{r}_2 \times \mathbf{e}_i^2 \qquad (i = 1, 2, 3) \,. \tag{3.54}$$

Let $\underline{\hat{\mathbf{e}}}^1$ and $\underline{\hat{\mathbf{e}}}^2$ denote the two dual bases as well as the column matrices of their dual basis vectors. The two sets of equations are written in the matrix forms

$$\underline{\hat{\mathbf{e}}}^1 = \underline{\mathbf{e}}^1 + \varepsilon \mathbf{r}_1 \times \underline{\mathbf{e}}^1 \,, \qquad \underline{\hat{\mathbf{e}}}^2 = \underline{\mathbf{e}}^2 + \varepsilon \mathbf{r}_2 \times \underline{\mathbf{e}}^2 \,. \tag{3.55}$$

Every dual basis vector of $\underline{\hat{\mathbf{e}}}^1$ is a linear combination of the dual basis vectors of $\underline{\hat{\mathbf{e}}}^2$. This is written in the form

$$\hat{\mathbf{e}}_i^1 = \sum_{k=1}^{3} \hat{a}_{ik}^{12}\, \hat{\mathbf{e}}_k^2 \qquad (i = 1, 2, 3) \,. \tag{3.56}$$

By scalar multiplication of this equation by $\hat{\mathbf{e}}_j^2$ and by applying (3.48) and (3.49) it is shown that the coordinates represent dual direction cosines:

$$\hat{a}_{ij}^{12} = \hat{\mathbf{e}}_i^1 \cdot \hat{\mathbf{e}}_j^2 \qquad (i, j = 1, 2, 3) \,. \tag{3.57}$$

Since the dual basis vectors intersect orthogonally, the direction cosines satisfy the conditions

$$\sum_{k=1}^{3} \hat{a}_{ik}^{12}\, \hat{a}_{jk}^{12} = \delta_{ij} \qquad (i, j = 1, 2, 3) \,. \tag{3.58}$$

Let $\hat{\underline{A}}^{12}$ be the matrix of the dual direction cosines. Dualization of (3.53) yields

$$\hat{\underline{\mathbf{e}}}^1 = \hat{\underline{A}}^{12}\hat{\underline{\mathbf{e}}}^2 , \qquad \hat{\underline{A}}^{12} = \hat{\underline{\mathbf{e}}}^1 \cdot \hat{\underline{\mathbf{e}}}^{2^T} . \tag{3.59}$$

Into the second equation the expressions (3.55) are substituted:

$$\begin{aligned} \hat{\underline{A}}^{12} &= (\underline{\mathbf{e}}^1 + \varepsilon\, \mathbf{r}_1 \times \underline{\mathbf{e}}^1) \cdot (\underline{\mathbf{e}}^2 + \varepsilon\, \mathbf{r}_2 \times \underline{\mathbf{e}}^2)^T \\ &= \underline{\mathbf{e}}^1 \cdot \underline{\mathbf{e}}^{2^T} - \varepsilon(\mathbf{r}_2 - \mathbf{r}_1) \cdot \underline{\mathbf{e}}^1 \times \underline{\mathbf{e}}^{2^T} \\ &= \underline{A}^{12} - \varepsilon\,(\mathbf{r}_2 - \mathbf{r}_1) \cdot \underline{\mathbf{e}}^1 \times \underline{\mathbf{e}}^{1^T} \underline{A}^{12} . \end{aligned} \tag{3.60}$$

Define $\mathbf{r} = \mathbf{r}_2 - \mathbf{r}_1 = \overrightarrow{0_1 0_2}$ and let r_1, r_2, r_3 be the coordinates of $\mathbf{r}$ in $\underline{\mathbf{e}}^1$. Then

$$\hat{\underline{A}}^{12} = (\underline{I} + \varepsilon\, \tilde{\underline{r}})\underline{A}^{12} , \qquad \tilde{\underline{r}} = \begin{bmatrix} 0 & -r_3 & r_2 \\ r_3 & 0 & -r_1 \\ -r_2 & r_1 & 0 \end{bmatrix} . \tag{3.61}$$

From this it follows that the product $\hat{\underline{A}}^{12}\hat{\underline{A}}^{12^T}$ is the unit matrix. Hence its inverse is also its transpose:

$$(\hat{\underline{A}}^{12})^{-1} = \hat{\underline{A}}^{12^T} . \tag{3.62}$$

The determinant of $\hat{\underline{A}}^{12}$ equals 1 (the determinant of its dual part is zero).

Let $\hat{\underline{v}}^1$ and $\hat{\underline{v}}^2$ be the dual coordinate matrices of a dual vector of the form (3.37), $\hat{\mathbf{v}} = \mathbf{v} + \varepsilon\mathbf{w}$, in the dual bases $\hat{\underline{\mathbf{e}}}^1$ and $\hat{\underline{\mathbf{e}}}^2$, respectively. The vector need not be a unit vector. The first Eq.(3.59) is proof of the transformation rule

$$\hat{\underline{v}}^1 = \hat{\underline{A}}^{12}\hat{\underline{v}}^2 . \tag{3.63}$$

This is the dualized form of the transformation rule $\underline{v}^1 = \underline{A}^{12}\underline{v}^2$ for ordinary vector coordinates.

3.10.2 Screw Axis, Screw Angle and Translation Determined from Dual Direction Cosines

From Chap. 1 on rotations about a fixed point Euler's Theorem 1.1 is known. It makes the following statements. The transformation matrix $\underline{A}^{12}$ has the eigenvalue one. In the case $\underline{A}^{12} \neq \underline{I}$, the matrix $\underline{A}^{12}$ determines uniquely a rotation $(\mathbf{n}, \varphi)$ carrying a body-fixed basis from the position $\underline{\mathbf{e}}^1$ into the position $\underline{\mathbf{e}}^2 = \underline{A}^{12^T}\underline{\mathbf{e}}^1$. The coordinate matrix $\underline{n}$ of $\mathbf{n}$, identical in both bases, is the solution of the equation

$$(\underline{A}^{12} - \underline{I})\underline{n} = \underline{0} . \tag{3.64}$$

If $\underline{A}^{12}$ is unsymmetric, φ and $\underline{n}$ are determined by (1.51) and (1.52):

$$\cos\varphi = \frac{1}{2}(\operatorname{tr}\underline{A}^{12}-1)\ , \quad 2n_i\sin\varphi = a_{kj}^{12}-a_{jk}^{12}\ \ (i,j,k=1,2,3\ \text{ cyclic})\ . \tag{3.65}$$

If $\underline{A}^{12}$ is symmetric, then $\varphi = \pm\pi$.

Transference of this theorem into dual form produces Chasles' Theorem 3.1 and the following statements. The dual transformation matrix $\hat{\underline{A}}^{12} = (\underline{I}+\varepsilon\,\underline{\tilde{r}})\underline{A}^{12}$ has the eigenvalue one. A formal proof is given further below. In the case $\underline{A}^{12} \neq \underline{I}$, the matrix $\hat{\underline{A}}^{12}$ determines uniquely a screw displacement $(\hat{\mathbf{n}},\hat{\varphi})$ carrying a body-fixed dual basis from the position $\hat{\underline{\mathbf{e}}}^1$ into the position $\hat{\underline{\mathbf{e}}}^2 = \hat{\underline{A}}^{12^T}\hat{\underline{\mathbf{e}}}^1$. As before, the dual angle $\hat{\varphi}$ and the dual unit line vector $\hat{\mathbf{n}}$ along the screw axis are written in the forms

$$\hat{\varphi} = \varphi + \varepsilon s\ , \qquad \hat{\mathbf{n}} = \mathbf{n} + \varepsilon\mathbf{w} \qquad (\mathbf{n}^2 = 1\ ,\ \mathbf{n}\cdot\mathbf{w} = 0)\ . \tag{3.66}$$

In what follows, it is shown how to determine the unknown scalars φ and s and the unknown Plücker vectors $\mathbf{n}$ and $\mathbf{w}$ if the matrix $\hat{\underline{A}}^{12}$ is given. The unknowns are determined from the equation $(\hat{\underline{A}}^{12} - \underline{I})\hat{\underline{n}} = 0$ or in detail

$$[(\underline{I}+\varepsilon\,\underline{\tilde{r}})\underline{A}^{12} - \underline{I}](\underline{n}+\varepsilon\underline{w}) = \underline{0}\ . \tag{3.67}$$

If $\underline{A}^{12}$ is unsymmetric, Eqs.(3.65) in dualized form are valid. Only the first equation is needed:

$$\cos\hat{\varphi} = \frac{1}{2}\Big\{\operatorname{tr}\,[(\underline{I}+\varepsilon\,\underline{\tilde{r}})\underline{A}^{12}] - 1\Big\}\ . \tag{3.68}$$

Equations (3.67) and (3.68) are split into their primary and dual parts. The primary parts are the original Eqs.(3.64) and (3.65) for $\underline{n}$ and φ. With the solutions for $\underline{n}$ and φ the dual parts of the equations determine $\underline{w}$ and s. The dual part of (3.67) is the equation $(\underline{A}^{12} - \underline{I})\underline{w} + \underline{\tilde{r}}\,\underline{A}^{12}\underline{n} = \underline{0}$ or, since $\underline{A}^{12}\underline{n} = \underline{n}$,

$$(\underline{A}^{12} - \underline{I})\underline{w} = -\underline{\tilde{r}}\,\underline{n}\ . \tag{3.69}$$

Since the matrix $\underline{A}^{12} - \underline{I}$ has rank two, the equation has a solution $\underline{w}$ only if the complete coefficient matrix including the right-hand side terms has rank two. This is, indeed, the case. Proof: The equation has the form $\underline{B}\,\underline{w} = -\underline{\tilde{r}}\,\underline{n}$. The homogeneous equation $\underline{B}\,\underline{w} = \underline{0}$ has the solution $\underline{w} = \mu\underline{n}$ (μ arbitrary). Because of the orthogonality of $\underline{A}^{12}$ also the equation $\underline{B}^T\,\underline{w} = \underline{0}$ has this solution. From this it follows that the rows of $\underline{B}^T$, i.e., the columns of $\underline{B}$ are in the plane orthogonal to $\underline{n}$. In this plane also the column matrix $-\underline{\tilde{r}}\,\underline{n}$ is located since it is the coordinate matrix of the vector $\mathbf{n}\times\mathbf{r}$. End of proof. Hence the inhomogeneous equation has a solution $\underline{w}_{\mathrm{p}}$. The complete solution is $\underline{w} = \mu\underline{n} + \underline{w}_{\mathrm{p}}$. From the conditions $\mathbf{n}^2 = 1$ and $\mathbf{n}\cdot\mathbf{w} = 0$ valid for Plücker

vectors it follows that $\mu = -\underline{n}^T \underline{w}_\mathrm{p}$. Thus, the final solution for $\underline{w}$ is

$$\underline{w} = (\underline{I} - \underline{n}\underline{n}^T)\underline{w}_\mathrm{p} \; . \tag{3.70}$$

The perpendicular from 0_1 onto the screw axis is the vector $\mathbf{u} = \mathbf{n} \times \mathbf{w} = \mathbf{n} \times \mathbf{w}_\mathrm{p}$. It has the coordinate matrix

$$\underline{u} = \underline{\tilde{n}}\, \underline{w}_\mathrm{p} \; . \tag{3.71}$$

These results cover also the special case when the right-hand side of (3.69) equals zero which means $\mathbf{n} \times \mathbf{r} = \mathbf{0}$. Then $\underline{w}_\mathrm{p} = \underline{0}$ and $\underline{w} = \underline{0}$. This means that the screw axis is the line connecting the origins 0_1 and 0_2. This is obvious without any analysis.

The dual part of (3.68) determines s. This equation reads (omitting the upper indices in the elements of $\underline{A}^{12}$):

$$\begin{aligned} -s \sin\varphi &= \frac{1}{2} \mathrm{tr}\,(\underline{\tilde{r}}\, \underline{A}^{12}) \\ &= \frac{1}{2}\Big[(a_{23} - a_{32})r_1 + (a_{31} - a_{13})r_2 + (a_{12} - a_{21})r_3\Big] \; . \end{aligned} \tag{3.72}$$

The three differences of matrix elements are expressed with the help of the second Eq.(3.65). This yields for s the explicit expression

$$s = n_1 r_1 + n_2 r_2 + n_3 r_3 = \underline{n}^T \underline{r}^1 \; . \tag{3.73}$$

This is identical with (3.9). For the perpendicular $\mathbf{u}$ of a screw displacement with given quantities $\mathbf{n}$, φ and $\mathbf{r}$ vector methods led to (3.12). Comparison with (3.71), $\mathbf{u} = \mathbf{n} \times \mathbf{w}_\mathrm{p}$, allows an interpretation of $\mathbf{w}_\mathrm{p}$.

In what follows, it is proved that the dual matrix $\hat{\underline{A}}^{12}$ has the eigenvalue one. The characteristic equation is $\det[(\underline{I} + \varepsilon\, \underline{\tilde{r}})\underline{A}^{12} - \lambda \underline{I}\,] = 0$. The term free of λ consists of 24 expressions which cancel each other pairwise. The remaining terms are (the upper indices in the elements of $\underline{A}^{12}$ are omitted)

$$\det(\underline{A}^{21} - \lambda \underline{I}) + \varepsilon\, \lambda \sum_{i=1}^{3} r_i \Big[\lambda(a_{jk} - a_{kj}) - (a_{ij}a_{ki} - a_{ii}a_{kj}) + (a_{ji}a_{ik} - a_{ii}a_{jk})\Big] = 0 \tag{3.74}$$

$(i, j, k = 1, 2, 3$ cyclic). From (1.10) it follows that this equation is solved with $\lambda = 1$. End of proof.

The expression (3.61) for the dual transformation matrix was obtained by applying the transference principle to the matrix $\underline{A}^{12}$ of a rotation expressed in terms of direction cosines. In Chap. 1 the matrix $\underline{A}^{12}$ has been expressed in various ways by the unit vector $\mathbf{n}$ along the axis of a rotation and by the angle φ. The most useful expressions are those in (1.49) in terms of n_1, n_2, n_3, $\sin\varphi$, $\cos\varphi$, in (1.79) in terms of Euler-Rodrigues parameters

and in (1.170) in terms of the coordinates of the Rodrigues vector. All these expressions can be transferred into dual form. Transference of (1.49) yields the expression

$$\hat{\underline{A}}^{12} = \begin{bmatrix} \hat{n}_1^2 + (1-\hat{n}_1^2)\cos\hat{\varphi} & \hat{n}_1\hat{n}_2(1-\cos\hat{\varphi}) - \hat{n}_3\sin\hat{\varphi} & \hat{n}_1\hat{n}_3(1-\cos\hat{\varphi}) + \hat{n}_2\sin\hat{\varphi} \\ \hat{n}_1\hat{n}_2(1-\cos\hat{\varphi}) + \hat{n}_3\sin\hat{\varphi} & \hat{n}_2^2 + (1-\hat{n}_2^2)\cos\hat{\varphi} & \hat{n}_2\hat{n}_3(1-\cos\hat{\varphi}) - \hat{n}_1\sin\hat{\varphi} \\ \hat{n}_1\hat{n}_3(1-\cos\hat{\varphi}) - \hat{n}_2\sin\hat{\varphi} & \hat{n}_2\hat{n}_3(1-\cos\hat{\varphi}) + \hat{n}_1\sin\hat{\varphi} & \hat{n}_3^2 + (1-\hat{n}_3^2)\cos\hat{\varphi} \end{bmatrix} . \quad (3.75)$$

Example: Determine φ, $\hat{\underline{n}} = \underline{n} + \varepsilon\underline{w}$, $\underline{u} = \tilde{\underline{n}}\,\underline{w}$, $s = \underline{n}^T\underline{r}$ and the matrix $\hat{\underline{A}}^{12}$ from the given quantities

$$\underline{A}^{12} = \begin{bmatrix} \frac{2}{3} & -\frac{11}{15} & -\frac{2}{15} \\ \frac{1}{3} & \frac{2}{15} & \frac{14}{15} \\ -\frac{2}{3} & -\frac{2}{3} & \frac{1}{3} \end{bmatrix} , \qquad \underline{r} = \frac{2}{15}\begin{bmatrix} 50 \\ 30 \\ 11 \end{bmatrix} . \quad (3.76)$$

Solution: Equation (3.65) yields $\cos\varphi = 1/15$, $\sin\varphi = 4\sqrt{14}/15$ (arbitrarily positive), $\underline{n} = (1/\sqrt{14})\,[\,-3 \;\; 1 \;\; 2\,]^T$. Equation (3.69) reads

$$\begin{bmatrix} -5 & -11 & -2 \\ 5 & -13 & 14 \\ -10 & -10 & -10 \end{bmatrix} \underline{w} = \sqrt{14}\begin{bmatrix} -7 \\ 19 \\ -20 \end{bmatrix} . \quad (3.77)$$

It has the solution $\underline{w}_\mathrm{p} = \sqrt{14}\,[\,1 \;\; 0 \;\; 1\,]^T$. In (3.70) $\underline{n}^T\underline{w}_\mathrm{p} = -1$. Furthermore,

$$\hat{\underline{n}} = \frac{1}{\sqrt{14}}\begin{bmatrix} -3+11\varepsilon \\ 1+\varepsilon \\ 2+16\varepsilon \end{bmatrix} , \quad \underline{u} = \begin{bmatrix} 1 \\ 5 \\ -1 \end{bmatrix} , \quad s = -\frac{14\sqrt{14}}{15} . \quad (3.78)$$

For $\underline{u}$ the same result is obtained from (3.13). For (3.75) the quantities are calculated:

$$\left.\begin{aligned} \cos\hat{\varphi} &= \cos\varphi - \varepsilon s\,\sin\varphi = \tfrac{1}{15^2}(15 + 28^2\varepsilon) , \\ \sin\hat{\varphi} &= \sin\varphi + \varepsilon s\,\cos\varphi = \tfrac{2\sqrt{14}}{15^2}(30 - 7\varepsilon) , \end{aligned}\right\} \quad (3.79)$$

$$\left.\begin{aligned} \hat{n}_1^2 = \tfrac{1}{14}(9-66\varepsilon) , \;\; \hat{n}_1\hat{n}_2 = \tfrac{1}{14}(-3+8\varepsilon) , \;\; \hat{n}_1\hat{n}_3 = \tfrac{1}{14}(-6-26\varepsilon), \\ \hat{n}_2^2 = \tfrac{1}{14}(1+2\varepsilon) , \quad \hat{n}_2\hat{n}_3 = \tfrac{1}{14}(2+18\varepsilon) , \\ \hat{n}_3^2 = \tfrac{1}{14}(4+64\varepsilon) . \end{aligned}\right\} \quad (3.80)$$

The desired matrix is

$$\hat{\underline{A}}^{12} = \begin{bmatrix} \frac{2}{3} & -\frac{11}{15} & -\frac{2}{15} \\ \frac{1}{3} & \frac{2}{15} & \frac{14}{15} \\ -\frac{2}{3} & -\frac{2}{3} & \frac{1}{3} \end{bmatrix} + \varepsilon\begin{bmatrix} -\frac{142}{45} & -\frac{644}{225} & -\frac{8}{225} \\ \frac{244}{45} & \frac{758}{225} & -\frac{544}{225} \\ -\frac{4}{9} & \frac{173}{45} & \frac{304}{45} \end{bmatrix} . \quad (3.81)$$

The primary part is the given matrix (3.76). End of Example.

3.10.3 Dual Euler Angles. Dual Bryan Angles

In Fig. 3.12 the dual basis $\underline{\hat{\mathbf{e}}}^2$ is produced from $\underline{\hat{\mathbf{e}}}^1$ by a screw displacement about the axis $\hat{\mathbf{e}}_1^1$ with the rotation angle ϕ_1 and the translation u_1. With $\hat{\phi}_1 = \phi_1 + \varepsilon u_1$ the dual direction cosine matrix is

$$\underline{\hat{A}}_1^{12} = \begin{bmatrix} 1 & 0 & 0 \\ 0 & \cos\hat{\phi}_1 & -\sin\hat{\phi}_1 \\ 0 & \sin\hat{\phi}_1 & \cos\hat{\phi}_1 \end{bmatrix} . \tag{3.82}$$

Formulas for $\cos\hat{\phi}$ and $\sin\hat{\phi}$ are given in (3.30). With the abbreviations $c_1 = \cos\phi_1$ and $s_1 = \sin\phi_1$ these formulas are written in the forms $\cos\hat{\phi}_1 = c_1 - \varepsilon u_1 s_1$, $\sin\hat{\phi}_1 = s_1 + \varepsilon u_1 c_1$. Hence

$$\underline{\hat{A}}_1^{12} = \begin{bmatrix} 1 & 0 & 0 \\ 0 & c_1 & -s_1 \\ 0 & s_1 & c_1 \end{bmatrix} + \varepsilon u_1 \begin{bmatrix} 0 & 0 & 0 \\ 0 & -s_1 & -c_1 \\ 0 & c_1 & -s_1 \end{bmatrix} . \tag{3.83}$$

The same result is obtained from (3.61) with $r_1 = u_1$, $r_2 = r_3 = 0$. The dual part is calculated from the primary part by the rule of dual differentiation.

In what follows, the same idea is applied to the direction cosine matrix $\underline{A}^{12}$ expressed as function of Euler angles ψ, θ and ϕ (see (1.28)). Euler angles are defined in Fig. 1.1a. They are angles of subsequent rotations about the axes $\mathbf{e}_3^1$, $\mathbf{e}_1^{2''}$ and $\mathbf{e}_3^{2'} = \mathbf{e}_3^2$. Each of these three rotations is replaced by a screw displacement about the respective axis. The three dual screw angles are denoted $\hat{\psi} = \psi + \varepsilon u_\psi$, $\hat{\theta} = \theta + \varepsilon u_\theta$ and $\hat{\phi} = \phi + \varepsilon u_\phi$, respectively. They are dual Euler angles. The dual direction cosine matrix $\underline{\hat{A}}^{12}$ is obtained from the direction cosine matrix $\underline{A}^{12}$ by the rule of dual differentiation:

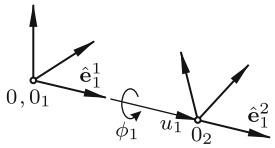

Fig. 3.12 Screw displacement $(\hat{\mathbf{e}}_1^1, \hat{\phi}_1)$ with $\hat{\phi}_1 = \phi_1 + \varepsilon u_1$

$$\hat{\underline{A}}^{12} = \begin{bmatrix} c_\psi c_\phi - s_\psi c_\theta s_\phi & -c_\psi s_\phi - s_\psi c_\theta c_\phi & s_\psi s_\theta \\ s_\psi c_\phi + c_\psi c_\theta s_\phi & -s_\psi s_\phi + c_\psi c_\theta c_\phi & -c_\psi s_\theta \\ s_\theta s_\phi & s_\theta c_\phi & c_\theta \end{bmatrix}$$

$$+\varepsilon \left(u_\psi \begin{bmatrix} -s_\psi c_\phi - c_\psi c_\theta s_\phi & s_\psi s_\phi - c_\psi c_\theta c_\phi & c_\psi s_\theta \\ c_\psi c_\phi - s_\psi c_\theta s_\phi & -c_\psi s_\phi - s_\psi c_\theta c_\phi & s_\psi s_\theta \\ 0 & 0 & 0 \end{bmatrix} \right.$$

$$+u_\theta \begin{bmatrix} s_\psi s_\theta s_\phi & s_\psi s_\theta c_\phi & s_\psi c_\theta \\ -c_\psi s_\theta s_\phi & -c_\psi s_\theta c_\phi & -c_\psi c_\theta \\ c_\theta s_\phi & c_\theta c_\phi & -s_\theta \end{bmatrix}$$

$$\left. +u_\phi \begin{bmatrix} -c_\psi s_\phi - s_\psi c_\theta c_\phi & -c_\psi c_\phi + s_\psi c_\theta s_\phi & 0 \\ -s_\psi s_\phi + c_\psi c_\theta c_\phi & -s_\psi c_\phi - c_\psi c_\theta s_\phi & 0 \\ s_\theta c_\phi & -s_\theta s_\phi & 0 \end{bmatrix} \right) . \quad (3.84)$$

The primary part is the matrix $\underline{A}^{12}$ of Eq.(1.28). Dual differentiation of the element (1,3), i.e., of the product $s_\psi s_\theta$, yields the expression $u_\psi c_\psi s_\theta + u_\theta\, s_\psi c_\theta$. These two terms are the elements (1,3) of the matrices associated with u_ψ and u_θ.

The same procedure is applied to the direction cosine matrix expressed as function of Bryan angles ϕ_1, ϕ_2 and ϕ_3 (see Fig. 1.2a and Eq.(1.32)). Each of the three subsequent rotations about the axes $\mathbf{e}_1^1$, $\mathbf{e}_2^{2''}$ and $\mathbf{e}_3^{2'} = \mathbf{e}_3^2$ is replaced by a screw displacement about the respective axis. The dual screw angles are denoted $\hat{\phi}_i = \phi_i + \varepsilon u_i \quad (i = 1, 2, 3)$. They are dual Bryan angles. The associated dual direction cosine matrix is

$$\hat{\underline{A}}^{12} = \begin{bmatrix} c_2 c_3 & -c_2 s_3 & s_2 \\ c_1 s_3 + s_1 s_2 c_3 & c_1 c_3 - s_1 s_2 s_3 & -s_1 c_2 \\ s_1 s_3 - c_1 s_2 c_3 & s_1 c_3 + c_1 s_2 s_3 & c_1 c_2 \end{bmatrix}$$

$$+\varepsilon \left(u_1 \begin{bmatrix} 0 & 0 & 0 \\ -s_1 s_3 + c_1 s_2 c_3 & -s_1 c_3 - c_1 s_2 s_3 & -c_1 c_2 \\ c_1 s_3 + s_1 s_2 c_3 & c_1 c_3 - s_1 s_2 s_3 & -s_1 c_2 \end{bmatrix} \right.$$

$$+u_2 \begin{bmatrix} -s_2 c_3 & s_2 s_3 & c_2 \\ s_1 c_2 c_3 & -s_1 c_2 s_3 & -s_1 s_2 \\ -c_1 c_2 c_3 & -c_1 c_2 s_3 & c_1 s_2 \end{bmatrix}$$

$$\left. +u_3 \begin{bmatrix} -c_2 s_3 & -c_2 c_3 & 0 \\ c_1 c_3 - s_1 s_2 s_3 & -c_1 s_3 - s_1 s_2 c_3 - c_1 s_3 & 0 \\ s_1 c_3 + c_1 s_2 s_3 & -s_1 s_3 + c_1 s_2 c_3 & 0 \end{bmatrix} \right) \quad (3.85)$$

The primary part is the matrix of Eq.(1.32). Linearization in the case of small angles yields

$$\underline{\hat{A}}^{12} \approx \begin{bmatrix} 1 & -\phi_3 & \phi_2 \\ \phi_3 & 1 & -\phi_1 \\ -\phi_2 & \phi_1 & 1 \end{bmatrix} + \varepsilon \left(u_1 \begin{bmatrix} 0 & 0 & 0 \\ \phi_2 & -\phi_1 & -1 \\ \phi_3 & 1 & -\phi_1 \end{bmatrix} + u_2 \begin{bmatrix} -\phi_2 & 0 & 1 \\ \phi_1 & 0 & 0 \\ -1 & -\phi_3 & \phi_2 \end{bmatrix} + u_3 \begin{bmatrix} -\phi_3 & -1 & 0 \\ 1 & -\phi_3 & 0 \\ \phi_1 & \phi_2 & 0 \end{bmatrix} \right) . \quad (3.86)$$

3.10.4 Dual Rodrigues Vector

The Rodrigues vector of a rotation $(\mathbf{n}, \varphi)$ is the vector $\mathbf{u} = \mathbf{n} \tan \varphi/2$. The dual Rodrigues vector of a screw displacement $(\hat{\mathbf{n}}, \hat{\varphi})$ with $\hat{\mathbf{n}} = \mathbf{n} + \varepsilon \mathbf{w}$ and $\hat{\varphi} = \varphi + \varepsilon s$ is

$$\begin{aligned} \hat{\mathbf{u}} = \hat{\mathbf{n}} \tan \frac{\hat{\varphi}}{2} &= (\mathbf{n} + \varepsilon \mathbf{w}) \Big(\tan \frac{\varphi}{2} + \varepsilon \frac{s/2}{\cos^2 \frac{\varphi}{2}} \Big) \\ &= \mathbf{n} \tan \frac{\varphi}{2} + \varepsilon \Big[\mathbf{n} \frac{s}{2} \Big(1 + \tan^2 \frac{\varphi}{2} \Big) + \mathbf{w} \tan \frac{\varphi}{2} \Big] . \end{aligned} \quad (3.87)$$

3.10.5 Dual Euler-Rodrigues Parameters. Dual Quaternions

From (1.67) the Euler-Rodrigues parameters of a rotation $(\mathbf{n}, \varphi)$ are known:

$$q_0 = \cos \frac{\varphi}{2} , \qquad \mathbf{q} = \mathbf{n} \sin \frac{\varphi}{2} . \quad (3.88)$$

They satisfy the constraint equation

$$q_0^2 + \mathbf{q}^2 = 1 . \quad (3.89)$$

According to Fig. 1.3 and to (1.70) the parameters establish between the position vectors $\boldsymbol{\varrho}$ and $\boldsymbol{\varrho}^*$ of a body-fixed point before and after the rotation the relationship

$$\boldsymbol{\varrho}^* = \boldsymbol{\varrho} + 2[\mathbf{q} \times (\mathbf{q} \times \boldsymbol{\varrho}) + q_0 \mathbf{q} \times \boldsymbol{\varrho}] . \quad (3.90)$$

The quaternion of the rotation is

$$D = (q_0 \, , \, \mathbf{q}) . \quad (3.91)$$

Corresponding dual quantities are defined for a screw displacement $(\hat{\mathbf{n}}, \hat{\varphi})$. With the quantities shown in Fig. 3.3 the dual screw angle $\hat{\varphi}$ and the dual unit vector $\hat{\mathbf{n}}$ along the screw axis are

$$\hat{\varphi} = \varphi + \varepsilon s \,, \qquad \hat{\mathbf{n}} = \mathbf{n} + \varepsilon \mathbf{u} \times \mathbf{n} \,, \qquad (\mathbf{u} \cdot \mathbf{n} = 0) \,. \tag{3.92}$$

For the translatory displacement $\mathbf{r} = \overrightarrow{0_1 0_2}$ in Fig. 3.3 Eq.(3.8) provides the expression

$$\mathbf{r} = s\mathbf{n} + \mathbf{u}(1 - \cos\varphi) + \mathbf{u} \times \mathbf{n} \sin\varphi \,. \tag{3.93}$$

The square of this vector is

$$\mathbf{r}^2 = s^2 + 2\mathbf{u}^2(1 - \cos\varphi) \,. \tag{3.94}$$

By definition, the dual Euler-Rodrigues parameters of the screw displacement are

$$\left.\begin{aligned} \hat{q}_0 &= \cos\frac{\hat{\varphi}}{2} \;\; = \cos\frac{\varphi}{2} - \varepsilon\frac{s}{2}\sin\frac{\varphi}{2} \,, \\ \hat{\mathbf{q}} &= \hat{\mathbf{n}}\sin\frac{\hat{\varphi}}{2} = (\mathbf{n} + \varepsilon\mathbf{u} \times \mathbf{n})\Big(\sin\frac{\hat{\varphi}}{2} + \varepsilon\frac{s}{2}\cos\frac{\varphi}{2}\Big) \\ &= \mathbf{n}\sin\frac{\varphi}{2} + \varepsilon\Big(\frac{s}{2}\mathbf{n}\cos\frac{\varphi}{2} + \mathbf{u} \times \mathbf{n}\sin\frac{\varphi}{2}\Big) \,. \end{aligned}\right\} \tag{3.95}$$

The dual parts are abbreviated

$$q_0' = -\frac{s}{2}\sin\frac{\varphi}{2} \,, \qquad \mathbf{q}' = \frac{s}{2}\mathbf{n}\cos\frac{\varphi}{2} + \mathbf{u} \times \mathbf{n}\sin\frac{\varphi}{2} \,. \tag{3.96}$$

With this notation

$$\hat{q}_0 = q_0 + \varepsilon q_0' \,, \qquad \hat{\mathbf{q}} = \mathbf{q} + \varepsilon\mathbf{q}' \,. \tag{3.97}$$

The dual quaternion of the screw displacement is

$$\hat{D} = (\hat{q}_0 \,, \hat{\mathbf{q}}) = D + \varepsilon D' \tag{3.98}$$

with

$$D = (q_0 \,, \mathbf{q}) \,, \qquad D' = (q_0' \,, \mathbf{q}') \,. \tag{3.99}$$

The square of the norm of D' is

$$q_0'^{\,2} + \mathbf{q}'^{\,2} = \frac{s^2}{4} + \mathbf{u}^2\sin^2\frac{\varphi}{2} = \frac{1}{4}[s^2 + 2\mathbf{u}^2(1 - \cos\varphi)] \,. \tag{3.100}$$

Comparison with (3.94) shows that

$$\mathbf{r}^2 = 4(q_0'^{\,2} + \mathbf{q}'^{\,2}) \,. \tag{3.101}$$

Next, the quaternion product $D\,\tilde{D}' = (q_0 \,, \mathbf{q})(q_0' \,, -\mathbf{q}')$ is calculated by the multiplication rule (1.98). The scalar part is

$$q_0 q_0' + \mathbf{q} \cdot \mathbf{q}' = 0 \,. \tag{3.102}$$

This equation is referred to as Study-quadric. It expresses the orthogonality of the primary and the dual part of the Euler-Rodrigues parameters. The vector part of $D\,\tilde{D}'$ is

$$\begin{aligned} -q_0\mathbf{q}' + q_0'\mathbf{q} - \mathbf{q}\times\mathbf{q}' &= -\Big[\cos\frac{\varphi}{2}\Big(\frac{s}{2}\mathbf{n}\cos\frac{\varphi}{2} + \mathbf{u}\times\mathbf{n}\sin\frac{\varphi}{2}\Big) \\ &\quad + \frac{s}{2}\sin\frac{\varphi}{2}\,\mathbf{n}\sin\frac{\varphi}{2} + \mathbf{n}\sin\frac{\varphi}{2}\times(\mathbf{u}\times\mathbf{n})\sin\frac{\varphi}{2}\Big] \\ &= -\frac{1}{2}[s\mathbf{n} + \mathbf{u}\times\mathbf{n}\sin\varphi + \mathbf{u}(1-\cos\varphi)]\,. \end{aligned} \tag{3.103}$$

Comparison with (3.93) reveals the equation

$$\mathbf{r} = 2(q_0\mathbf{q}' - q_0'\mathbf{q} + \mathbf{q}\times\mathbf{q}')\,. \tag{3.104}$$

Let $\boldsymbol{\varrho}$ and $\boldsymbol{\varrho}^*$ be the vectors from the reference point 0_1 to a body-fixed point before and after the screw displacement. According to (3.90) and (3.104) the relationship between these vectors is

$$\boldsymbol{\varrho}^* = \boldsymbol{\varrho} + 2[\mathbf{q}\times(\mathbf{q}\times\boldsymbol{\varrho}) + q_0\mathbf{q}\times\boldsymbol{\varrho}] + 2(q_0\mathbf{q}' - q_0'\mathbf{q} + \mathbf{q}\times\mathbf{q}')\,. \tag{3.105}$$

The dualized form of Theorem 1.4 is

Theorem 3.5. *The dual quaternion* $\hat{D}_{\text{res}}$ *of the resultant of two subsequent screw displacements with dual quaternions* $\hat{D}_1$ *(first screw displacement) and* $\hat{D}_2$ *is the product*

$$\hat{D}_{\text{res}} = \hat{D}_2\hat{D}_1\,. \tag{3.106}$$

Applications of the above equations see in Sect. 3.11 and in Chap. 8. Additional material see in Ravani/Roth [41].

3.11 Resultant of two Screw Displacements. Dual-Quaternion Formulation

Halphen's geometrical construction of the resultant of two screw displacements resulted in the spatial hexagon shown in Fig. 3.7. Extracting analytical expressions for the unknowns φ_{res}, s_{res} and S_{res} from this figure is difficult. Explicit solutions are most easily obtained on the basis of Theorem 3.5. The quaternion equation $D_{\text{res}} = D_2D_1$ for the resultant $(\mathbf{n}_{\text{res}}, \varphi_{\text{res}})$ of two successive rotations $(\mathbf{n}_1, \varphi_1)$ (first rotation) and $(\mathbf{n}_2, \varphi_2)$ resulted in the explicit coordinate-free Eqs.(1.118) and (1.119). Decomposition of vectors in the basis shown in Fig. 1.4 led to Eqs.(1.120) – (1.122):

$$\mathbf{n}_{1,2} = \mathbf{e}_1\cos\frac{\alpha}{2} \mp \mathbf{e}_2\sin\frac{\alpha}{2}\,, \tag{3.107}$$

$$\cos\frac{\varphi_{\text{res}}}{2} = \cos\frac{\varphi_1}{2}\cos\frac{\varphi_2}{2} - \sin\frac{\varphi_1}{2}\sin\frac{\varphi_2}{2}\cos\alpha\,, \tag{3.108}$$

$$\begin{aligned}\mathbf{n}_{\text{res}}\sin\frac{\varphi_{\text{res}}}{2} &= \mathbf{e}_1\sin\frac{\varphi_1+\varphi_2}{2}\cos\frac{\alpha}{2} - \mathbf{e}_2\sin\frac{\varphi_1-\varphi_2}{2}\sin\frac{\alpha}{2}\\ &\quad -\mathbf{e}_3\sin\frac{\varphi_1}{2}\sin\frac{\varphi_2}{2}\sin\alpha\,.\end{aligned} \tag{3.109}$$

Theorem 3.5 states that the same equations are valid when vectors $\mathbf{n}$ of rotation axes are replaced by dual vectors $\hat{\mathbf{n}} = \mathbf{n} + \varepsilon\mathbf{w}$ of screw axes and rotation angles φ by dual screw angles $\hat{\varphi} = \varphi + \varepsilon s$. The angle α between intersecting rotation axes is replaced by the dual angle $\hat{\alpha} = \alpha + \varepsilon\ell$ of the screw displacement which carries $\hat{\mathbf{n}}_1$ into $\hat{\mathbf{n}}_2$ (this means that ℓ, positive or negative, is the length of the common perpendicular of the two screw axes). For making (3.107) with $\hat{\mathbf{n}}_{1,2}$ and $\hat{\alpha}$ valid the origin 0 of the basis $\mathbf{e}_{1,2,3}$ of Fig. 1.4 must be the midpoint of the common perpendicular (see Fig. 3.13). The primary parts of the dualized equations are Eqs.(3.108) and (3.109). The dual parts are

$$\begin{aligned}s_{\text{res}}\sin\frac{\varphi_{\text{res}}}{2} = \quad & s_1\Big(\sin\frac{\varphi_1}{2}\cos\frac{\varphi_2}{2} + \cos\frac{\varphi_1}{2}\sin\frac{\varphi_2}{2}\cos\alpha\Big)\\ & +s_2\Big(\cos\frac{\varphi_1}{2}\sin\frac{\varphi_2}{2} + \sin\frac{\varphi_1}{2}\cos\frac{\varphi_2}{2}\cos\alpha\Big)\\ & -2\ell\sin\frac{\varphi_1}{2}\sin\frac{\varphi_2}{2}\sin\alpha\,,\end{aligned} \tag{3.110}$$

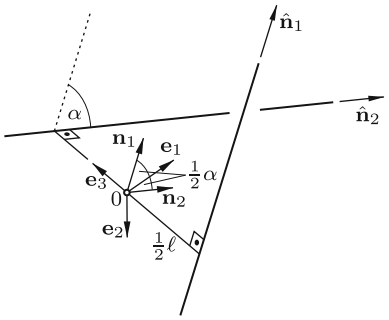

Fig. 3.13 Screw axes with reference basis $\mathbf{e}_{1,2,3}$ on the common perpendicular

$$\begin{aligned}
&\mathbf{n}_{\mathrm{res}} s_{\mathrm{res}} \cos\frac{\varphi_{\mathrm{res}}}{2} + 2\mathbf{w}_{\mathrm{res}} \sin\frac{\varphi_{\mathrm{res}}}{2} \\
&\quad = \mathbf{e}_1\Big[(s_1+s_2)\cos\frac{\varphi_1+\varphi_2}{2}\cos\frac{\alpha}{2} - \ell\sin\frac{\varphi_1+\varphi_2}{2}\sin\frac{\alpha}{2}\Big] \\
&\quad\quad -\mathbf{e}_2\Big[(s_1-s_2)\cos\frac{\varphi_1-\varphi_2}{2}\sin\frac{\alpha}{2} + \ell\sin\frac{\varphi_1-\varphi_2}{2}\cos\frac{\alpha}{2}\Big] \\
&\quad\quad -\mathbf{e}_3\Big[\Big(s_1\cos\frac{\varphi_1}{2}\sin\frac{\varphi_2}{2} + s_2\sin\frac{\varphi_1}{2}\cos\frac{\varphi_2}{2}\Big)\sin\alpha \\
&\quad\quad\quad +2\ell\sin\frac{\varphi_1}{2}\sin\frac{\varphi_2}{2}\cos\alpha\Big] . \qquad (3.111)
\end{aligned}$$

From (3.108) φ_{res} is determined (sign arbitrary), from (3.109) $\mathbf{n}_{\mathrm{res}}$, from (3.110) s_{res} and from (3.111) $\mathbf{w}_{\mathrm{res}}$. A sign change of φ_{res} results in a change of signs of all other quantities. For the screw displacement this has no effect. The quantities s_1, s_2 and s_{res} appear in linear form only.

For specifying the location of the resultant screw axis the perpendicular $\mathbf{u} = \mathbf{n}_{\mathrm{res}} \times \mathbf{w}_{\mathrm{res}}$ from point 0 onto the screw axis is needed. The cross-product of the vectors in (3.109) and (3.111) is $2\mathbf{u}\sin^2\varphi_{\mathrm{res}}/2$ where $\sin^2\varphi_{\mathrm{res}}/2$ is determined by (3.108). The result of this multiplication is[4]

$$\begin{aligned}
\mathbf{u}\sin^2\frac{\varphi_{\mathrm{res}}}{2} &= -\mathbf{e}_1\sin^2\frac{\alpha}{2}\Big[\Big(s_1\sin^2\frac{\varphi_2}{2} - s_2\sin^2\frac{\varphi_1}{2}\Big)\cos\frac{\alpha}{2} \\
&\qquad +\ell\sin\frac{\varphi_1}{2}\sin\frac{\varphi_2}{2}\sin\frac{\varphi_1-\varphi_2}{2}\sin\frac{\alpha}{2}\Big] \\
&\quad +\mathbf{e}_2\cos^2\frac{\alpha}{2}\Big[\Big(s_1\sin^2\frac{\varphi_2}{2} + s_2\sin^2\frac{\varphi_1}{2}\Big)\sin\frac{\alpha}{2} \\
&\qquad +\ell\sin\frac{\varphi_1}{2}\sin\frac{\varphi_2}{2}\sin\frac{\varphi_1+\varphi_2}{2}\cos\frac{\alpha}{2}\Big] \\
&\quad + \frac{1}{4}\mathbf{e}_3\Big[(s_2\sin\varphi_1 - s_1\sin\varphi_2)\sin\alpha + \ell(\cos\varphi_1 - \cos\varphi_2)\Big] . \qquad (3.112)
\end{aligned}$$

In accordance with Fig. 3.7 this equation shows that, in general, the resultant screw axis does not intersect the common perpendicular $\mathbf{e}_3$ of the screw axes 1 and 2. The resultant screw displacement has scalar measures p_{D} and p_{P} defined by (3.18) and (3.19). They are written in the forms

$$p_{\mathrm{D}} = \frac{s_{\mathrm{res}}}{\sin\varphi_{\mathrm{res}}} = \frac{s_{\mathrm{res}}\sin\frac{\varphi_{\mathrm{res}}}{2}}{2\sin^2\frac{\varphi_{\mathrm{res}}}{2}\cos\frac{\varphi_{\mathrm{res}}}{2}} , \qquad p_{\mathrm{P}} = p_{\mathrm{D}}\cos^2\frac{\varphi_{\mathrm{res}}}{2} . \qquad (3.113)$$

With (3.108) and (3.110) both measures are expressed in terms of s_1, φ_1, s_2, φ_2, α and ℓ. The quantities s_1 and s_2 appear only in the numerator expressions. If p_{D_i} and p_{P_i} $(i = 1, 2)$ denote the corresponding measures of

[4] Alternative forms for the factors of ℓ in (3.112):

$\sin\frac{\varphi_1}{2}\sin\frac{\varphi_2}{2}\sin\frac{\varphi_1\pm\varphi_2}{2} = \frac{1}{4}[\sin\varphi_2 \pm \sin\varphi_1 \mp \sin(\varphi_1 \pm \varphi_2)]$

the screw displacements 1 and 2, p_{D} is a linear function of p_{D_1} and p_{D_2}, and p_{P} is a linear function of p_{P_1} and p_{P_2}. The coefficients are functions of φ_1 and φ_2.

In what follows, special cases are investigated.
Special case $s_1 = s_2 = s$, $\varphi_1 = \varphi_2 = \varphi$: Equations (3.108) – (3.112) become

$$\left.\begin{aligned} \cos\frac{\varphi_{\mathrm{res}}}{2} &= \cos^2\frac{\varphi}{2} - \sin^2\frac{\varphi}{2}\,\cos\alpha\,, \\ \mathbf{n}_{\mathrm{res}}\sin\frac{\varphi_{\mathrm{res}}}{2} &= \mathbf{e}_1\sin\varphi\,\cos\frac{\alpha}{2} - \mathbf{e}_3\sin^2\frac{\varphi}{2}\,\sin\alpha\,, \\ s_{\mathrm{res}}\sin\frac{\varphi_{\mathrm{res}}}{2} &= s\,\sin\varphi(1+\cos\alpha) - \ell(1-\cos\varphi)\sin\alpha\,, \\ \mathbf{u}\,\sin^2\frac{\varphi_{\mathrm{res}}}{2} &= \mathbf{e}_2\cos^2\frac{\alpha}{2}\sin^2\frac{\varphi}{2}\Big(2s\,\sin\frac{\alpha}{2} + \ell\sin\varphi\cos\frac{\alpha}{2}\Big)\,. \end{aligned}\right\} \tag{3.114}$$

Special case $\varphi_2 = 0$: The second screw displacement is the pure translation $s_2\mathbf{n}_2$. The screw axis $\hat{\mathbf{n}}_2$, the common perpendicular of length ℓ and the origin 0 of the $\mathbf{e}_{1,2,3}$-system are not uniquely defined. Equations (3.108) – (3.112) reduce to

$$\left.\begin{aligned} &\varphi_{\mathrm{res}} = \varphi_1\,, \qquad \mathbf{n}_{\mathrm{res}} = \mathbf{n}_1\,, \qquad s_{\mathrm{res}} = s_1 + s_2\cos\alpha\,, \\ &\mathbf{u} = -\frac{1}{2}\ell\mathbf{e}_3 + \frac{1}{2}s_2\sin\alpha\Big(\mathbf{e}_1\,\sin\frac{\alpha}{2} + \mathbf{e}_2\,\cos\frac{\alpha}{2} + \mathbf{e}_3\,\cot\frac{\varphi_1}{2}\Big) \\ &\quad = -\frac{1}{2}\ell\mathbf{e}_3 + \frac{1}{2}s_2\sin\alpha\Big(\mathbf{e}_3\times\mathbf{n}_1 + \mathbf{e}_3\,\cot\frac{\varphi_1}{2}\Big)\,. \end{aligned}\right\} \tag{3.115}$$

The leading term $(-\ell/2)\mathbf{e}_3$ is the perpendicular vector from the arbitrarily chosen origin 0 onto the screw axis $\hat{\mathbf{n}}_1$. If an arbitrary point on $\hat{\mathbf{n}}_1$ is chosen as origin 0,

$$\mathbf{u} = \frac{1}{2}s_2\sin\alpha\Big(\mathbf{e}_3\times\mathbf{n}_1 + \mathbf{e}_3\,\cot\frac{\varphi_1}{2}\Big)\,. \tag{3.116}$$

The absolute value is

$$|\mathbf{u}| = \Big|\frac{\frac{s_2}{2}}{\sin\frac{\varphi_1}{2}}\,\sin\alpha\Big|\,. \tag{3.117}$$

Special case $s_1 = s_2 = 0$ (resultant of pure rotations about nonintersecting axes; see Fig. 3.8): Equations (3.108) and (3.109) remain valid without change. Equations (3.110) and (3.112) reduce to

$$s_{\mathrm{res}}\sin\frac{\varphi_{\mathrm{res}}}{2} = -2\ell\sin\frac{\varphi_1}{2}\,\sin\frac{\varphi_2}{2}\,\sin\alpha\,, \tag{3.118}$$

$$\mathbf{u}\,\sin^2\frac{\varphi_{\rm res}}{2} = \frac{\ell}{4}\Big\{ -\mathbf{e}_1\sin^3\frac{\alpha}{2}\Big[\sin\varphi_2 - \sin\varphi_1 + \sin(\varphi_1-\varphi_2)\Big] + \mathbf{e}_2\cos^3\frac{\alpha}{2}\Big[\sin\varphi_2 + \sin\varphi_1 - \sin(\varphi_1+\varphi_2)\Big] + \mathbf{e}_3(\cos\varphi_1 - \cos\varphi_2)\Big\}\,. \tag{3.119}$$

These equations govern the even more special case of the resultant of two 180°-rotations about skew axes. With $\varphi_1 = -\pi$ (equivalent to $\varphi_1 = \pi$) and with $\varphi_2 = \pi$ they yield $\varphi_{\rm res} = 2\alpha$, $s_{\rm res} = 2\ell$, $\mathbf{n}_{\rm res} = \mathbf{e}_3$, $\mathbf{u} = \mathbf{0}$. Hence the resultant is the screw displacement about the common perpendicular of the two rotation axes with rotation angle 2α and translation 2ℓ . This is the statement made by Halphen's theorem.

Example: In Theorem 3.4 the problem is posed: Decompose a screw displacement given by $s_{\rm res}$, $\varphi_{\rm res}$ and by its axis $\mathrm{S}_{\rm res}$ into two subsequent pure rotations φ_1 about S_1 (first rotation) and φ_2 about S_2 of which either only S_2 or only S_1 is given. To be determined are φ_1 , φ_2 and the axis not given.
Solution: Let S_2 be given. The unknown first rotation is the resultant of the given screw displacement followed by the inverse of the second rotation. From this it follows that (3.108) – (3.112) are valid if the following changes are made.
1. The basis $\mathbf{e}_{1,2,3}$ is placed at the midpoint of the common perpendicular g_2 of the given axes $\mathrm{S}_{\rm res}$ and S_2 . The quantities ℓ and α specify the relative location of these axes.
2. $(s_{\rm res}, \varphi_{\rm res})$, (s_1, φ_1) and (s_2, φ_2) are replaced by $(0, \varphi_1)$, $(s_{\rm res}, \varphi_{\rm res})$ and $(0, -\varphi_2)$, respectively. Following these changes (3.108), (3.109), (3.110) and (3.112) read:

$$\cos\frac{\varphi_1}{2} = \cos\frac{\varphi_{\rm res}}{2}\cos\frac{\varphi_2}{2} + \sin\frac{\varphi_{\rm res}}{2}\sin\frac{\varphi_2}{2}\cos\alpha\,, \tag{3.120}$$

$$\mathbf{n}_1\sin\frac{\varphi_1}{2} = \mathbf{e}_1\sin\frac{\varphi_{\rm res}-\varphi_2}{2}\cos\frac{\alpha}{2} - \mathbf{e}_2\sin\frac{\varphi_{\rm res}+\varphi_2}{2}\sin\frac{\alpha}{2} + \mathbf{e}_3\sin\frac{\varphi_{\rm res}}{2}\sin\frac{\varphi_2}{2}\sin\alpha\,, \tag{3.121}$$

$$0 = s_{\rm res}\Big(\sin\frac{\varphi_{\rm res}}{2}\cos\frac{\varphi_2}{2} - \cos\frac{\varphi_{\rm res}}{2}\sin\frac{\varphi_2}{2}\cos\alpha\Big) + 2\ell\sin\frac{\varphi_{\rm res}}{2}\sin\frac{\varphi_2}{2}\sin\alpha\,, \tag{3.122}$$

$$\begin{aligned}\mathbf{u}\,\sin^2\frac{\varphi_1}{2} = -\mathbf{e}_1 \sin\frac{\varphi_2}{2}\,\sin^2\frac{\alpha}{2}\Big[s_{\rm res}\sin\frac{\varphi_2}{2}\cos\frac{\alpha}{2} \\ -\ell\sin\frac{\varphi_{\rm res}}{2}\,\sin\frac{\varphi_{\rm res}+\varphi_2}{2}\,\sin\frac{\alpha}{2}\Big] \\ +\mathbf{e}_2\sin\frac{\varphi_2}{2}\,\cos^2\frac{\alpha}{2}\Big[s_{\rm res}\sin\frac{\varphi_2}{2}\sin\frac{\alpha}{2} \\ -\ell\sin\frac{\varphi_{\rm res}}{2}\,\sin\frac{\varphi_{\rm res}-\varphi_2}{2}\,\cos\frac{\alpha}{2}\Big] \\ +\frac{1}{4}\,\mathbf{e}_3\Big[s_{\rm res}\sin\varphi_2\sin\alpha+\ell(\cos\varphi_{\rm res}-\cos\varphi_2)\Big]\,. \qquad (3.123)\end{aligned}$$

Equation (3.122) determines φ_2:

$$\tan\frac{\varphi_2}{2} = \frac{s_{\rm res}}{s_{\rm res}\cot\dfrac{\varphi_{\rm res}}{2}\cos\alpha - 2\ell\sin\alpha}\,. \qquad (3.124)$$

With this angle φ_2 (3.120) and (3.121) determine $\cos\varphi_1/2$ and $\mathbf{n}_1\sin\varphi_1/2$. The vector $\mathbf{u}$ determined by (3.123) is the perpendicular from the midpoint of g_2 in Fig. 3.8 onto the first rotation axis. The equations fail in the case $\sin\alpha = 0$ (axes S_2 and $\mathrm{S}_{\rm res}$ parallel).

When instead of S_2 the axis S_1 is given, φ_1, φ_2 and S_2 are determined as follows. The unknown second rotation is the resultant of the inverse of the first rotation followed by the given screw displacement. In (3.108) – (3.112) the following changes are made.

1. The basis $\mathbf{e}_{1,2,3}$ is placed at the midpoint of the common perpendicular g_3 of the given axes $\mathrm{S}_{\rm res}$ and S_1. The quantities ℓ and α specify the relative location of these axes.
2. $(s_{\rm res}, \varphi_{\rm res})$, (s_1, φ_1) and (s_2, φ_2) are replaced by $(0, \varphi_2)$, $(0, -\varphi_1)$ and $(s_{\rm res}, \varphi_{\rm res})$, respectively. The modified Eq.(3.110) leads to

$$\tan\frac{\varphi_1}{2} = \frac{s_{\rm res}}{s_{\rm res}\cot\dfrac{\varphi_{\rm res}}{2}\cos\alpha - 2\ell\sin\alpha}\,. \qquad (3.125)$$

This is formally identical with (3.124). End of example.

Special case $\alpha = 0$ (parallel screw axes; $\mathbf{n}_1 = \mathbf{n}_2$): The case $\varphi_2 = -\varphi_1$ has to be distinguished from the general case $\varphi_2 \neq -\varphi_1$. This general case is considered first. Equations (3.108) – (3.112) reduce to

$$\varphi_{\rm res} = \varphi_1 + \varphi_2 \neq 0\,, \qquad s_{\rm res} = s_1 + s_2\,, \qquad \mathbf{n}_{\rm res} = \mathbf{n}_1 = \mathbf{n}_2\,, \qquad (3.126)$$

$$\mathbf{u}\sin\frac{\varphi_1+\varphi_2}{2} = \ell\Big(\mathbf{e}_2\sin\frac{\varphi_1}{2}\sin\frac{\varphi_2}{2} - \mathbf{e}_3\,\frac{1}{2}\sin\frac{\varphi_1-\varphi_2}{2}\Big)\,. \qquad (3.127)$$

The last equation is rewritten in the form

$$\frac{\ell}{2}\mathbf{e}_3 + \mathbf{u} = \ell\Big(\mathbf{e}_2 \sin\frac{\varphi_1}{2} + \mathbf{e}_3 \cos\frac{\varphi_1}{2}\Big)\,\frac{\sin\frac{\varphi_2}{2}}{\sin\frac{\varphi_1+\varphi_2}{2}}\,. \tag{3.128}$$

This equation proves that the parallel screw axes $\mathbf{n}_1$, $\mathbf{n}_2$ and $\mathbf{n}_{\text{res}}$, seen in projection along the axes, form the triangle (P_1,P_2,P_3) shown in Fig. 3.14a. It has internal angles $\varphi_1/2$ and $\varphi_2/2$ at P_1 and P_2, respectively, and the external angle $\varphi_{\text{res}}/2$ at P_3. The vector $(\ell/2)\mathbf{e}_3 + \mathbf{u}$ is $\overrightarrow{P_1P_3}$, and $(\mathbf{e}_2 \sin\frac{\varphi_1}{2} + \mathbf{e}_3 \cos\frac{\varphi_1}{2})$ is the unit vector in the direction of $\overrightarrow{P_1P_3}$. The equation expresses the sine law in the triangle.

In the special case $\varphi_2 = -\varphi_1$, (3.108) yields $\varphi_{\text{res}} = 0$. This indicates that the resultant of the two screw displacements is a translation. No further information is obtained from (3.109) – (3.112). Both magnitude and direction of the translation are obtained from Fig. 3.7. In the case of parallel screw axes $\mathbf{n}_1 = \mathbf{n}_2$ and with $\varphi_2 = -\varphi_1$, the lines g_2 and g_3 are parallel. In Fig. 3.14b the screw axes and the lines are shown in projection along the axes as in Fig. 3.14a. The component $(s_1+s_2)\mathbf{e}_1$ of the displacement is normal to the plane. The in-plane component is illustrated by the displacement of the point which prior to the first screw displacement is located at A. It is displaced via B to C. The total translatory displacement vector is

$$\mathbf{s}_{\text{res}} = (s_1+s_2)\mathbf{e}_1 + \overrightarrow{AC} = (s_1+s_2)\mathbf{e}_1 + \ell\,[-\sin\varphi_1\,\mathbf{e}_2 + (1-\cos\varphi_1)\mathbf{e}_3]\,. \tag{3.129}$$

Equations (3.126) – (3.129) remain valid in the case $s_1 = s_2 = 0$. In this case, the equations determine the resultant of two rotations about parallel axes. In Sects. 14.3 and 14.4 this case is investigated in more detail.

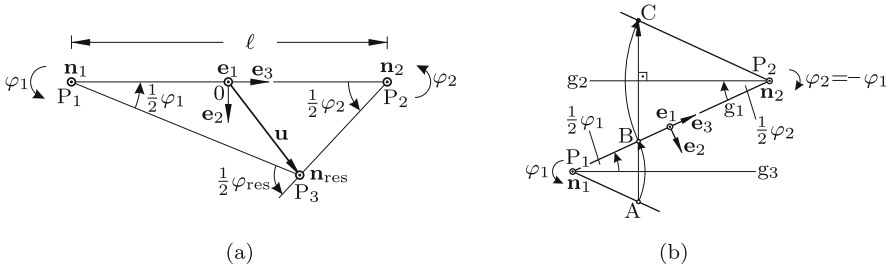

Fig. 3.14 Parallel screw axes $\mathbf{n}_1 = \mathbf{n}_2$; $\varphi_2 \neq -\varphi_1$ **(a)** and $\varphi_2 = -\varphi_1$ **(b)**

3.12 Equations for the Screw Triangle

The quaternion formulation of the resultant of two rotations led to the rotation triangle shown in Fig. 1.6. Three rotations $(\mathbf{n}_{12}, \varphi_{12})$, $(\mathbf{n}_{23}, \varphi_{23})$,

$(\mathbf{n}_{31}, \varphi_{31})$ executed in this order or in any order produced by cyclic permutation carry a body via two intermediate positions back into its initial position. Each rotation is the inverse of the resultant of the previous two. Application of the sine and cosine laws led to (1.134):

$$\tan\frac{\varphi_{31}}{2} = \frac{\mathbf{n}_{12}\times\mathbf{n}_{23}\cdot\mathbf{n}_{31}}{(\mathbf{n}_{12}\times\mathbf{n}_{31})\cdot(\mathbf{n}_{23}\times\mathbf{n}_{31})}\,. \tag{3.130}$$

Analogously, two successive screw displacements followed by the inverse of the resultant of these two carry a body via two intermediate positions back into its initial position. The figure analogous to the rotation triangle is the spatial hexagon shown in Fig. 3.7 with φ_{res} and s_{res} replaced by $-\varphi_{\text{res}}$, $-s_{\text{res}}$. This analogy explains the name screw triangle of the hexagon.

Let the three screw displacements be newly labeled 12, 23 and 31. Then, according to the principle of transference, (3.130) is valid in the form

$$\tan\frac{\hat{\varphi}_{31}}{2} = \frac{\hat{\mathbf{n}}_{12}\times\hat{\mathbf{n}}_{23}\cdot\hat{\mathbf{n}}_{31}}{(\hat{\mathbf{n}}_{12}\times\hat{\mathbf{n}}_{31})\cdot(\hat{\mathbf{n}}_{23}\times\hat{\mathbf{n}}_{31})} \tag{3.131}$$

with

$$\hat{\varphi}_{ij} = \varphi_{ij} + \varepsilon s_{ij}\,,\quad \hat{\mathbf{n}}_{ij} = \mathbf{n}_{ij} + \varepsilon\mathbf{w}_{ij}\,,\quad \mathbf{n}_{ij}^2 = 1\,,\quad \mathbf{n}_{ij}\cdot\mathbf{w}_{ij} = 0 \tag{3.132}$$

$(ij) = (12),\ (23),\ (31)$. The vectors $\mathbf{n}_{ij}$ and $\mathbf{w}_{ij}$ are the Plücker vectors of the screw axis ij in a reference frame with arbitrary origin 0. The perpendicular from 0 onto the screw axis is $\mathbf{n}_{ij}\times\mathbf{w}_{ij}$. From the dual part of the equation an expression for the translatory displacement s_{31} is developed. The dual part of the left-hand side of the equation is

$$\begin{aligned}\frac{s_{31}}{2}\frac{1}{\cos^2\frac{\varphi_{31}}{2}} &= \frac{s_{31}}{2}(1+\tan^2\frac{\varphi_{31}}{2})\\ &= \frac{s_{31}}{2}\,\frac{[(\mathbf{n}_{12}\times\mathbf{n}_{31})\cdot(\mathbf{n}_{23}\times\mathbf{n}_{31})]^2 + (\mathbf{n}_{12}\times\mathbf{n}_{23}\cdot\mathbf{n}_{31})^2}{[(\mathbf{n}_{12}\times\mathbf{n}_{31})\cdot(\mathbf{n}_{23}\times\mathbf{n}_{31})]^2}\,.\end{aligned} \tag{3.133}$$

The numerator is

$$\begin{aligned}&[(\mathbf{n}_{12}\times\mathbf{n}_{31})\cdot(\mathbf{n}_{23}\times\mathbf{n}_{31})]^2 + (\mathbf{n}_{12}\times\mathbf{n}_{23}\cdot\mathbf{n}_{31})^2\\ &= (\mathbf{n}_{12}\times\mathbf{n}_{31})^2(\mathbf{n}_{23}\times\mathbf{n}_{31})^2\,.\end{aligned} \tag{3.134}$$

This is proved as follows. With the abbreviations $\mathbf{a} = \mathbf{n}_{12}\times\mathbf{n}_{31}$ and $\mathbf{b} = \mathbf{n}_{23}\times\mathbf{n}_{31}$ and with $\beta = \sphericalangle(\mathbf{a},\mathbf{b})$ the equation reads
$\mathbf{a}^2\mathbf{b}^2\cos^2\beta + (\mathbf{n}_{12}\cdot\mathbf{b})^2 = \mathbf{a}^2\mathbf{b}^2$ or

$$\begin{aligned}&(\mathbf{n}_{12}\cdot\mathbf{b})^2 = \mathbf{a}^2\mathbf{b}^2\sin^2\beta = (\mathbf{a}\times\mathbf{b})^2 = [(\mathbf{n}_{12}\times\mathbf{n}_{31})\times\mathbf{b}]^2\\ &= [(\mathbf{n}_{12}\cdot\mathbf{b})\mathbf{n}_{31} - (\mathbf{n}_{31}\cdot\mathbf{b})\mathbf{n}_{12}]^2\,.\end{aligned} \tag{3.135}$$

This is, indeed, true since $\mathbf{n}_{31} \cdot \mathbf{b} = 0$. Thus, the dual part of the left-hand side of (3.131) is

$$\frac{s_{31}}{2} \frac{(\mathbf{n}_{12} \times \mathbf{n}_{31})^2 (\mathbf{n}_{23} \times \mathbf{n}_{31})^2}{[(\mathbf{n}_{12} \times \mathbf{n}_{31}) \cdot (\mathbf{n}_{23} \times \mathbf{n}_{31})]^2} \,. \tag{3.136}$$

The dual part of the right-hand side is calculated as follows. With Eqs.(3.132) for $\hat{\mathbf{n}}_{ij}$ the numerator has the form $N + \varepsilon N_\mathrm{d}$ with

$$\left.\begin{aligned} N &= \mathbf{n}_{12} \times \mathbf{n}_{23} \cdot \mathbf{n}_{31} \,, \\ N_\mathrm{d} &= \mathbf{n}_{23} \times \mathbf{n}_{31} \cdot \mathbf{w}_{12} + \mathbf{n}_{31} \times \mathbf{n}_{12} \cdot \mathbf{w}_{23} + \mathbf{n}_{12} \times \mathbf{n}_{23} \cdot \mathbf{w}_{31} \,. \end{aligned}\right\} \tag{3.137}$$

The denominator has the form $D + \varepsilon D_\mathrm{d}$ with

$$\left.\begin{aligned} D &= (\mathbf{n}_{12} \times \mathbf{n}_{31}) \cdot (\mathbf{n}_{23} \times \mathbf{n}_{31}) \,, \\ D_\mathrm{d} &= (\mathbf{w}_{12} \times \mathbf{n}_{31} + \mathbf{n}_{12} \times \mathbf{w}_{31}) \cdot (\mathbf{n}_{23} \times \mathbf{n}_{31}) \\ &\quad + (\mathbf{n}_{12} \times \mathbf{n}_{31}) \cdot (\mathbf{w}_{23} \times \mathbf{n}_{31} + \mathbf{n}_{23} \times \mathbf{w}_{31}) \\ &= -[(\mathbf{n}_{23} \times \mathbf{n}_{31}) \times \mathbf{n}_{31}] \cdot \mathbf{w}_{12} - [(\mathbf{n}_{12} \times \mathbf{n}_{31}) \times \mathbf{n}_{31}] \cdot \mathbf{w}_{23} \\ &\quad + [(\mathbf{n}_{23} \times \mathbf{n}_{31}) \times \mathbf{n}_{12} + (\mathbf{n}_{12} \times \mathbf{n}_{31}) \times \mathbf{n}_{23}] \cdot \mathbf{w}_{31} \,. \end{aligned}\right\} \tag{3.138}$$

In these terms the right-hand side of (3.131) is

$$\frac{N + \varepsilon N_\mathrm{d}}{D + \varepsilon D_\mathrm{d}} = \frac{N}{D} + \varepsilon \frac{DN_\mathrm{d} - ND_\mathrm{d}}{D^2} \,. \tag{3.139}$$

The dual part equals the expression in (3.136). This yields for s_{31} the expression

$$\frac{s_{31}}{2} = \frac{DN_\mathrm{d} - ND_\mathrm{d}}{(\mathbf{n}_{12} \times \mathbf{n}_{31})^2 (\mathbf{n}_{23} \times \mathbf{n}_{31})^2} \,. \tag{3.140}$$

The numerator is

$$DN_\mathrm{d} - ND_\mathrm{d} = \mathbf{v}_{12} \cdot \mathbf{w}_{12} + \mathbf{v}_{23} \cdot \mathbf{w}_{23} + \mathbf{v}_{31} \cdot \mathbf{w}_{31} \tag{3.141}$$

with vectors

$$\left.\begin{aligned} \mathbf{v}_{12} &= \Big[(\mathbf{n}_{12} \times \mathbf{n}_{31}) \cdot (\mathbf{n}_{23} \times \mathbf{n}_{31})\Big]\, \mathbf{n}_{23} \times \mathbf{n}_{31} \\ &\quad + (\mathbf{n}_{12} \times \mathbf{n}_{23} \cdot \mathbf{n}_{31}) \Big[(\mathbf{n}_{23} \times \mathbf{n}_{31}) \times \mathbf{n}_{31}\Big] \,, \\ \mathbf{v}_{23} &= -\Big[(\mathbf{n}_{12} \times \mathbf{n}_{31}) \cdot (\mathbf{n}_{23} \times \mathbf{n}_{31})\Big]\, \mathbf{n}_{12} \times \mathbf{n}_{31} \\ &\quad + (\mathbf{n}_{12} \times \mathbf{n}_{23} \cdot \mathbf{n}_{31}) \Big[(\mathbf{n}_{12} \times \mathbf{n}_{31}) \times \mathbf{n}_{31}\Big] \,, \\ \mathbf{v}_{31} &= \Big[(\mathbf{n}_{12} \times \mathbf{n}_{31}) \cdot (\mathbf{n}_{23} \times \mathbf{n}_{31})\Big]\, \mathbf{n}_{12} \times \mathbf{n}_{23} \\ &\quad - (\mathbf{n}_{12} \times \mathbf{n}_{23} \cdot \mathbf{n}_{31}) \Big[(\mathbf{n}_{23} \times \mathbf{n}_{31}) \times \mathbf{n}_{12} + (\mathbf{n}_{12} \times \mathbf{n}_{31}) \times \mathbf{n}_{23}\Big] \,. \end{aligned}\right\} \tag{3.142}$$

These vectors are simplified as follows. First, the vector $\mathbf{v}_{12}$. Obviously, $\mathbf{v}_{12} \cdot \mathbf{n}_{31} = 0$. When the multiple products are simplified, it turns out that also $\mathbf{v}_{12} \cdot \mathbf{n}_{12} = 0$. Hence $\mathbf{v}_{12}$ has the form $\mathbf{v}_{12} = A\mathbf{n}_{12} \times \mathbf{n}_{31}$ with an unknown scalar A. It is determined by dot-multiplying this equation by $(\mathbf{n}_{12} \times \mathbf{n}_{31})$. Taking into account (3.134) this results in the equation

$$\begin{aligned} A(\mathbf{n}_{12} \times \mathbf{n}_{31})^2 &= [(\mathbf{n}_{12} \times \mathbf{n}_{31}) \cdot (\mathbf{n}_{23} \times \mathbf{n}_{31})]^2 + (\mathbf{n}_{12} \times \mathbf{n}_{23} \cdot \mathbf{n}_{31})^2 \\ &= (\mathbf{n}_{12} \times \mathbf{n}_{31})^2 (\mathbf{n}_{23} \times \mathbf{n}_{31})^2 \,. \end{aligned} \tag{3.143}$$

Hence

$$\mathbf{v}_{12} = (\mathbf{n}_{23} \times \mathbf{n}_{31})^2 \, \mathbf{n}_{12} \times \mathbf{n}_{31} \,. \tag{3.144}$$

The same arguments lead to

$$\mathbf{v}_{23} = (\mathbf{n}_{12} \times \mathbf{n}_{31})^2 \, \mathbf{n}_{23} \times \mathbf{n}_{31} \,. \tag{3.145}$$

The product $\mathbf{v}_{31} \cdot \mathbf{w}_{31}$ in (3.141) eliminates the (nonzero) component of $\mathbf{v}_{31}$ in the direction of $\mathbf{n}_{31}$. For determining the relevant components the ansatz is made: $\mathbf{v}_{31} = A\mathbf{n}_{12} \times \mathbf{n}_{31} + B\mathbf{n}_{23} \times \mathbf{n}_{31} + C\mathbf{n}_{31}$. Scalar multiplication with $(\mathbf{n}_{23} \times \mathbf{n}_{31}) \times \mathbf{n}_{31}$ eliminates B and C, and scalar multiplication with $(\mathbf{n}_{12} \times \mathbf{n}_{31}) \times \mathbf{n}_{31}$ eliminates A and C. The first multiplication yields

$$\begin{aligned} A(\mathbf{n}_{12} \times \mathbf{n}_{23} \cdot \mathbf{n}_{31}) &= \Big\{ [(\mathbf{n}_{12} \cdot \mathbf{n}_{23}) - (\mathbf{n}_{12} \cdot \mathbf{n}_{31})(\mathbf{n}_{23} \cdot \mathbf{n}_{31})]\mathbf{n}_{12} \times \mathbf{n}_{23} \\ &\quad -(\mathbf{n}_{12} \times \mathbf{n}_{23} \cdot \mathbf{n}_{31})[2(\mathbf{n}_{12} \cdot \mathbf{n}_{23})\mathbf{n}_{31} - (\mathbf{n}_{12} \cdot \mathbf{n}_{31})\mathbf{n}_{23} \\ &\quad -(\mathbf{n}_{23} \cdot \mathbf{n}_{31})\mathbf{n}_{12}] \Big\} \cdot [(\mathbf{n}_{23} \cdot \mathbf{n}_{31})\mathbf{n}_{31} - \mathbf{n}_{23}] \\ &= -(\mathbf{n}_{12} \times \mathbf{n}_{23} \cdot \mathbf{n}_{31})(\mathbf{n}_{12} \cdot \mathbf{n}_{31})[1 - (\mathbf{n}_{23} \cdot \mathbf{n}_{31})^2] \\ &= -(\mathbf{n}_{12} \times \mathbf{n}_{23} \cdot \mathbf{n}_{31})(\mathbf{n}_{12} \cdot \mathbf{n}_{31})(\mathbf{n}_{23} \times \mathbf{n}_{31})^2 \,. \end{aligned} \tag{3.146}$$

Hence $A = -(\mathbf{n}_{12} \cdot \mathbf{n}_{31})(\mathbf{n}_{23} \times \mathbf{n}_{31})^2$. In the same way $B = (\mathbf{n}_{23} \cdot \mathbf{n}_{31})(\mathbf{n}_{12} \times \mathbf{n}_{31})^2$. Hence

$$\begin{aligned} \mathbf{v}_{31} = &-(\mathbf{n}_{12} \cdot \mathbf{n}_{31})(\mathbf{n}_{23} \times \mathbf{n}_{31})^2 \, \mathbf{n}_{12} \times \mathbf{n}_{31} \\ &+(\mathbf{n}_{23} \cdot \mathbf{n}_{31})(\mathbf{n}_{12} \times \mathbf{n}_{31})^2 \, \mathbf{n}_{23} \times \mathbf{n}_{31} + C\mathbf{n}_{31} \,. \end{aligned} \tag{3.147}$$

The expressions obtained for $\mathbf{v}_{12}$, $\mathbf{v}_{23}$ and $\mathbf{v}_{31}$ are substituted into (3.141). Further substitution into (3.140) yields for s_{31} the final result

$$\begin{aligned} \frac{s_{31}}{2} = &\frac{1}{(\mathbf{n}_{23} \times \mathbf{n}_{31})^2} [\mathbf{n}_{31} \cdot \mathbf{n}_{23} \times \mathbf{w}_{23} + (\mathbf{n}_{23} \cdot \mathbf{n}_{31})\mathbf{n}_{23} \cdot \mathbf{n}_{31} \times \mathbf{w}_{31}] \\ &- \frac{1}{(\mathbf{n}_{12} \times \mathbf{n}_{31})^2} [\mathbf{n}_{31} \cdot \mathbf{n}_{12} \times \mathbf{w}_{12} + (\mathbf{n}_{12} \cdot \mathbf{n}_{31})\mathbf{n}_{12} \cdot \mathbf{n}_{31} \times \mathbf{w}_{31}] \,. \end{aligned} \tag{3.148}$$

The vectors $\mathbf{n}_{12} \times \mathbf{w}_{12}$, $\mathbf{n}_{23} \times \mathbf{w}_{23}$ and $\mathbf{n}_{31} \times \mathbf{w}_{31}$ are the perpendiculars from the reference point onto the three screw axes. The scalar products of

unit vectors can be expressed through the angles α_1 and α_3 in Fig. 1.6:

$$\left.\begin{aligned} \mathbf{n}_{12}\cdot\mathbf{n}_{31} &= \cos\alpha_1\ , & (\mathbf{n}_{12}\times\mathbf{n}_{31})^2 &= \sin^2\alpha_1\ , \\ \mathbf{n}_{23}\cdot\mathbf{n}_{31} &= \cos\alpha_3\ , & (\mathbf{n}_{23}\times\mathbf{n}_{31})^2 &= \sin^2\alpha_3\ . \end{aligned}\right\} \tag{3.149}$$

Tsai and Roth [48] deduced (3.148) geometrically from Fig. 3.7. See also Bottema/Roth [5].

3.13 Resultant of two Infinitesimal Screw Displacements. Cylindroid

In this section Eqs.(3.109) – (3.112) for the resultant of two screw displacements are evaluated in the special case of infinitesimal screw displacements. Let p_1, p_2 and p_{res} be the pitches of the three screw displacements so that

$$s_i = p_i\varphi_i \quad (i=1,2)\ , \qquad s_{\text{res}} = p_{\text{res}}\varphi_{\text{res}}\ . \tag{3.150}$$

In what follows, the index res is omitted.

For Eq.(3.109) a Taylor series expansion up to 1st-order terms is made. When (3.107) is taken into account, this results in the parallelogram rule for small rotations (see Fig. 3.15):

$$\mathbf{n}\varphi = \mathbf{e}_1(\varphi_1+\varphi_2)\cos\frac{\alpha}{2} + \mathbf{e}_2(\varphi_2-\varphi_1)\sin\frac{\alpha}{2} \tag{3.151}$$

$$= \mathbf{n}_1\varphi_1 + \mathbf{n}_2\varphi_2\ . \tag{3.152}$$

In (3.110) and (3.112) $s_i = p_i\varphi_i$ $(i=1,2)$ and $s = p\varphi$ are substituted. Following this, Taylor series expansions are made up to 2nd-order terms. This results in the equations

$$p\,\varphi^2 = p_1\varphi_1^2 + p_2\varphi_2^2 + [(p_1+p_2)\cos\alpha - \ell\sin\alpha]\varphi_1\varphi_2\ , \tag{3.153}$$

$$\mathbf{u}\,\varphi^2 = \mathbf{e}_3\Big[(p_2-p_1)\varphi_1\varphi_2\sin\alpha + \frac{1}{2}\ell(\varphi_2^2-\varphi_1^2)\Big]\ . \tag{3.154}$$

From the latter equation it follows that $\mathbf{u}$ has the form $\mathbf{u} = u\mathbf{e}_3$. This means that the resultant screw axis intersects the common perpendicular $\mathbf{e}_3$ of the screw axes 1 and 2 orthogonally at the point u given by the equation

$$u\,\varphi^2 = (p_2-p_1)\varphi_1\varphi_2\sin\alpha + \frac{1}{2}\ell(\varphi_2^2-\varphi_1^2)\ . \tag{3.155}$$

Let ψ be the angle of the resultant screw axis in the $\mathbf{e}_1,\mathbf{e}_2$-plane against the $\mathbf{e}_1$-axis as shown in Fig. 3.15. The sine law applied to the triangles in this figure yields the expressions

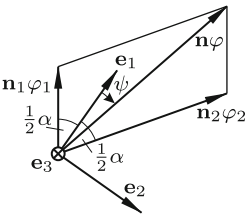

Fig. 3.15 Triangle of infinitesimal rotations

$$\varphi_1 = \varphi\,\frac{\sin\left(\dfrac{\alpha}{2}-\psi\right)}{\sin\alpha}\,, \qquad \varphi_2 = \varphi\,\frac{\sin\left(\dfrac{\alpha}{2}+\psi\right)}{\sin\alpha}\,, \tag{3.156}$$

from which it follows that

$$\left.\begin{aligned} \varphi_{1,2}^2 &= \varphi^2\,\frac{1-\cos 2\psi\cos\alpha \mp \sin 2\psi\sin\alpha}{2\sin^2\alpha}\,, \\ \varphi_1\varphi_2 &= \varphi^2\,\frac{\cos 2\psi - \cos\alpha}{2\sin^2\alpha}\,. \end{aligned}\right\} \tag{3.157}$$

Substitution into (3.153) and (3.155) results in explicit expressions for p and u:

$$p = \frac{1}{2}(p_1+p_2+\ell\cot\alpha) - \frac{\ell\cos 2\psi + (p_1-p_2)\sin 2\psi}{2\sin\alpha}\,, \tag{3.158}$$

$$u = \frac{1}{2}(p_1-p_2)\cot\alpha \qquad + \frac{\ell\sin 2\psi - (p_1-p_2)\cos 2\psi}{2\sin\alpha}\,. \tag{3.159}$$

These expressions are simpler if the transition is made to an x,y-system of principal axes which is rotated against the $\mathbf{e}_1,\mathbf{e}_2$-system through the angle ψ_0 given by

$$\cos 2\psi_0 = \frac{\ell}{\sqrt{(p_1-p_2)^2+\ell^2}}\,, \qquad \sin 2\psi_0 = \frac{p_1-p_2}{\sqrt{(p_1-p_2)^2+\ell^2}}\,. \tag{3.160}$$

More precisely, ψ_0 is the angle of the x-axis against the $\mathbf{e}_1$-axis. Then

$$\left.\begin{aligned} p &= p_0 - h\cos 2\chi\,, \\ z &= \qquad h\sin 2\chi \end{aligned}\right\} \tag{3.161}$$

with new variables

$$\chi = \psi - \psi_0\,, \qquad z = u - u_0 \tag{3.162}$$

and with constants

$$p_0 = \frac{1}{2}(p_1 + p_2 + \ell \cot\alpha) \ , \quad u_0 = \frac{1}{2}(p_1 - p_2)\cot\alpha \ , \quad h = \frac{\sqrt{(p_1 - p_2)^2 + \ell^2}}{2\sin\alpha} \ . \tag{3.163}$$

Equations (3.161) – (3.163) determine a one-parametric manifold of resultant screw displacements with the angle χ between screw axis and x-axis as parameter. In what follows, statements are made about this manifold. Elimination of χ from Eqs.(3.161) results in the equation of a circle relating p and z:

$$(p - p_0)^2 + z^2 \equiv h^2 \ . \tag{3.164}$$

Every value of z in the interval $|z| \leq |h|$ occurs at two angles χ_1 and $\chi_2 = \pi/2 - \chi_1$ which are located symmetrically with respect to $\chi = \pi/4$ as well as to $\chi = -\pi/4$. These two angles specify the directions of two screw axes which intersect at z on the $\mathbf{e}_3$-axis. The two screw axes intersecting at $z = +h$ coincide $(\chi_1 = \chi_2 = \pi/4)$. Likewise, the two screw axes intersecting at $z = -h$ coincide $(\chi_1 = \chi_2 = -\pi/4)$. The pitch associated with these screw axes is p_0.

The two screw axes intersecting at $z = 0$ are the principal x, y-axes $(\chi_1 = 0,\ \chi_2 = \pi/2)$. The associated principal pitches are the extremal pitches

$$p_{\mathrm{x}} = p_0 - h \ , \qquad p_{\mathrm{y}} = p_0 + h \ . \tag{3.165}$$

In terms of principal pitches the constants p_0 and h are

$$p_0 = \frac{1}{2}(p_{\mathrm{x}} + p_{\mathrm{y}}) \ , \qquad h = \frac{1}{2}(p_{\mathrm{y}} - p_{\mathrm{x}}) \ , \tag{3.166}$$

and Eqs.(3.161) have the forms

$$\left.\begin{aligned} p &= p_{\mathrm{x}}\cos^2\chi + p_{\mathrm{y}}\sin^2\chi \ , \\ z &= -(p_{\mathrm{x}} - p_{\mathrm{y}})\sin\chi\cos\chi \ . \end{aligned}\right\} \tag{3.167}$$

The first equation has the two forms $p - p_{\mathrm{x}} = (p_{\mathrm{y}} - p_{\mathrm{x}})\sin^2\chi$ and $p - p_{\mathrm{y}} = -(p_{\mathrm{y}} - p_{\mathrm{x}})\cos^2\chi$. Together with the second Eq.(3.167) this yields

$$\left.\begin{aligned} (p_{\mathrm{x}} - p)\cos\chi \qquad\quad + z\sin\chi &= 0 \ , \\ z\cos\chi - (p_{\mathrm{y}} - p)\sin\chi &= 0 \ . \end{aligned}\right\} \tag{3.168}$$

This is an eigenvalue problem with eigenvalue $p(z)$ and with the associated eigenvector $[\,\cos\chi(z) \quad \sin\chi(z)\,]$. The characteristic equation for p is Eq.(3.164).

Every pitch p in the interval between the extremal pitches p_{x} and p_{y} occurs at two angles $\pm\chi$. Definition: Two screws of equal pitch are called *conjugate screws*. The pair of conjugate screws at angles ± 0 coincides in the principal screw with pitch p_{x}. Likewise, the pair of conjugate screws at angles $\pm\pi$ coincides in the principal screw with pitch p_{y}. For a given pitch

p the first Eq.(3.167) and (3.164) determine the associated angles $\pm\chi$ and coordinates z . Example: For the pair of conjugate screws with pitch $p = 0$, i.e., pure rotations, the equations yield

$$\cos 2\chi_{\text{rot}} = \frac{p_0}{h} = \frac{p_\text{y} + p_\text{x}}{p_\text{y} - p_\text{x}} , \qquad z_{\text{rot}} = \pm\sqrt{h^2 - p_0^2} = \pm\sqrt{-p_\text{x}p_\text{y}} . \quad (3.169)$$

Real solutions exist only if $p_\text{x}p_\text{y} \leq 0$.

The one-parametric manifold of screw axes defines a ruled surface. With an additional parameter λ this ruled surface has the parameter representation $\mathbf{u}(\chi) + \lambda\mathbf{n}(\chi)$. Its coordinate form is

$$x = \lambda\cos\chi , \qquad y = \lambda\sin\chi , \qquad z = (p_\text{y} - p_\text{x})\sin\chi\cos\chi . \quad (3.170)$$

The parameters λ and χ are eliminated by forming $x^2 + y^2 = \lambda^2$ and $xy = \lambda^2\sin\chi\cos\chi$. Combining these equations with the third Eq.(3.170) results in the third-order equation

$$z(x^2 + y^2) = (p_\text{y} - p_\text{x})xy . \quad (3.171)$$

This ruled surface is called *cylindroid*. In the theory of ruled surfaces a line which is intersected by every generator is called *directrix*. The z-axis is a double directrix because it is intersected by two generators at every point $|z| \leq |\frac{1}{2}(p_\text{y} - p_\text{x})|$. From (2.59) the distribution parameter δ is calculated as function of χ . For this purpose the following change of notation has to be made (see (2.51)). The role of the parameter u is played by χ . The curve $\mathbf{r}(u)$ is the directrix $\mathbf{u}(\chi) = (p_\text{y} - p_\text{x})\sin\chi\cos\chi\mathbf{e}_3$, and the unit vector $\mathbf{e}(u)$ is $\mathbf{n}(\chi)$. According to (3.170) $\dot{\mathbf{n}} = \mathbf{e}_3 \times \mathbf{n}$ and $\dot{\mathbf{n}}^2 \equiv 1$. Hence with $\dot{\mathbf{u}}(\chi) = (p_\text{y} - p_\text{x})\cos 2\chi\mathbf{e}_3$ the distribution parameter is $\delta(\chi) = \dot{\mathbf{n}} \cdot \dot{\mathbf{u}} \times \mathbf{n} = (p_\text{y} - p_\text{x})\cos 2\chi$. The two pairs of coinciding generators at $z = -\frac{1}{2}(p_\text{y} - p_\text{x})$ and at $z = \frac{1}{2}(p_\text{y} - p_\text{x})$ are torsal lines $(\delta = 0)$. In Fig. 3.16 the cylindroid is represented in the x, y, z-system by an orthogonal net of lines $\chi =$ const and $\lambda =$ const. The curved lines $\lambda =$ const are kinematically insignificant. Their only purpose is to show the shape of the surface more clearly. What matters are the straight lines $\chi =$ const, i.e., the screw axes. These axes extend to $\pm\infty$. The symmetry with respect to the two planes each spanned by the directrix and by one torsal line is clearly shown.

Let $\mathbf{n}$ and $\mathbf{w}$ be the first and the second Plücker vector of the screw axis associated with the angle χ . The x, y, z-coordinates of these vectors are

$$\left.\begin{aligned} &\mathbf{n}: \ [\cos\chi \quad \sin\chi \quad 0] , \\ &\mathbf{w}: \ (p_\text{y} - p_\text{x})\sin\chi\cos\chi\,[-\sin\chi \quad \cos\chi \quad 0] . \end{aligned}\right\} \quad (3.172)$$

The results obtained so far are summarized as follows. The resultant of two arbitrarily oriented infinitesimal screw displacements with constant pa-

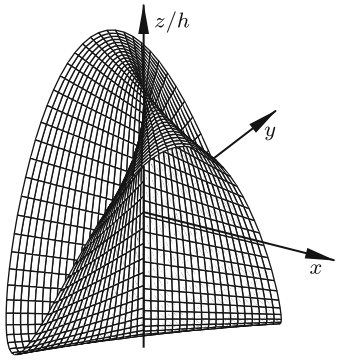

Fig. 3.16 Cylindroid

rameters α, ℓ, p_1 and p_2 and with variable parameters φ_1 and φ_2 is the manifold of screw displacements on the cylindroid defined by its axis, by u_0 and by its principal pitches p_x and p_y associated with mutually orthogonal principal axes x and y. The same manifold of screw displacements is obtained if the two principal screws are used as starting point. This is the special case $\alpha = \pi/2$ and $\ell = 0$. Equations (3.163) yield $u_0 = 0$ (this is in accordance with the statement preceding (3.165)) and $p_0 = p_\mathrm{x} + p_\mathrm{y}$, $h = p_\mathrm{y} - p_\mathrm{x}$ (as before; see Eqs.(3.165)). Every screw on the cylindroid is resultant of two principal screws about the principal axes. Also the following is true. Every screw on the cylindroid is resultant of two (arbitrary) conjugate screws. The quantities u_0 and h determining the cylindroid depend on the difference $p_1 - p_2$ only, whereas p_0 and, hence, $p(\chi)$ depend on the sum $p_1 + p_2$. If p_1 and p_2 (arbitrary) are increased by one and the same amount (arbitrary), the cylindroid remains the same, whereas $p(\chi)$ is increased by the same amount independent of χ.

The cylindroid was discovered independently by Hamilton [18] (1830), Plücker [38] (1865) (see also [39]), Battaglini [3] (1869) and Ball [2] (1900). Geometrical properties of the cylindroid see in Zindler [57]. In the present book the cylindroid is met again in the next Sect. 3.14 and in Sect. 12.6.2.

The end of the previous Sect. 3.11 on the resultant of two finite screw displacements was devoted to cases which require special considerations (Eqs.(3.118) – (3.129)). The same cases are considered here, and results are developed from the said equations. As before, the index $_\mathrm{res}$ is omitted.

Special case $\varphi_2 = 0$: Since the pitch p_2 is not defined the infinitesimal displacement s_2 is expressed in the form $s_2 = \mu\varphi_1$. As origin 0 of the $\mathbf{e}_{1,2,3}$-system an arbitrary point on the screw axis $\hat{\mathbf{n}}_1$ is chosen (see the text following (3.115)). Substituting $s_2 = \mu\varphi_1$ and $s_1 = p_1\varphi_1$ into (3.115) and (3.116) and making a Taylor series expansion for $\mathbf{u}$ results in the equations

$$\varphi = \varphi_1 \,, \quad \mathbf{n} = \mathbf{n}_1 \,, \quad p = p_1 + \mu \cos\alpha \,, \quad \mathbf{u} = \mathbf{e}_3 \mu \sin\alpha \,. \tag{3.173}$$

These equations show that the resultant screw axis has the direction of $\mathbf{n}_1$, and that it intersects the $\mathbf{e}_3$-axis orthogonally at the point $u = \mu \sin\alpha$.

Special case $\alpha = 0$ (parallel screw axes) and $\varphi_2 \neq -\varphi_1$: Equations (3.126) become (with a Taylor series expansion for $\mathbf{u}$)

$$\left.\begin{aligned} &\varphi = \varphi_1 + \varphi_2 \neq 0 \,, && p = p_1 + p_2 \,, \\ &\mathbf{n} = \mathbf{n}_1 = \mathbf{n}_2 \,, && \mathbf{u} = -\mathbf{e}_3 \frac{\ell}{2} \frac{\varphi_1 - \varphi_2}{\varphi_1 + \varphi_2} \,. \end{aligned}\right\} \tag{3.174}$$

This means that the resultant screw axis intersects the $\mathbf{e}_3$-axis orthogonally at a point u which depends on the ratio φ_2/φ_1. The points P_1, P_2 and P_3 in Fig. 3.14a are collinear.

Special case $\alpha = 0$ (parallel screw axes) and $\varphi_2 = -\varphi_1$: According to (3.129) the resultant displacement is a pure translation $\mathbf{s}$. With $s_1 = p_1\varphi_1$ and $s_2 = p_2\varphi_2 = -p_2\varphi_1$ it is

$$\mathbf{s} = [(p_1 - p_2)\mathbf{e}_1 - \ell\mathbf{e}_2]\varphi_1 \,. \tag{3.175}$$

This displacement is normal to $\mathbf{e}_3$.

3.14 Screw Displacements Effecting a Prescribed Line Displacement

In Fig. 3.17 two skew lines are defined by their unit line vectors $\hat{\mathbf{r}}_1$ and $\hat{\mathbf{r}}_2$. The line vector $\hat{\mathbf{r}}_2$ is produced from $\hat{\mathbf{r}}_1$ by the screw displacement $(\hat{\mathbf{n}}_3, \hat{\alpha})$ with the dual unit vector $\hat{\mathbf{n}}_3$ along the common perpendicular and with the dual screw angle $\hat{\alpha} = \alpha + \varepsilon\ell$ between the two lines. Without loss of generality, it is assumed that $0 < \alpha < \pi$ whereas ℓ may be positive, zero or negative. The dual unit vector $\hat{\mathbf{n}}_3$ is one of the basis vectors $\hat{\mathbf{n}}_i$ $(i = 1, 2, 3)$ of a dual basis which has its origin at the midpoint 0 of the common perpendicular. The basis vector $\hat{\mathbf{n}}_1$ is bisecting the angle α when seen in the projection along $\hat{\mathbf{n}}_3$. The line vector $\hat{\mathbf{r}}_2$ is produced from $\hat{\mathbf{r}}_1$ not only by the screw displacement $(\hat{\mathbf{n}}_3, \hat{\alpha})$, but also by the screw displacement $(\hat{\mathbf{n}}_1, \pm\pi)$. Both screw displacements carry the point A fixed on line 1 to the point B fixed on line 2. These observations stimulate an investigation of the following problems.

Problem 1: Determine the manifold of all screw displacements $(\hat{\mathbf{n}}, \hat{\varphi})$ of a rigid body which carry a body-fixed directed line from position $\hat{\mathbf{r}}_1$ into position $\hat{\mathbf{r}}_2$. In this manifold determine the submanifold of all screw displace-

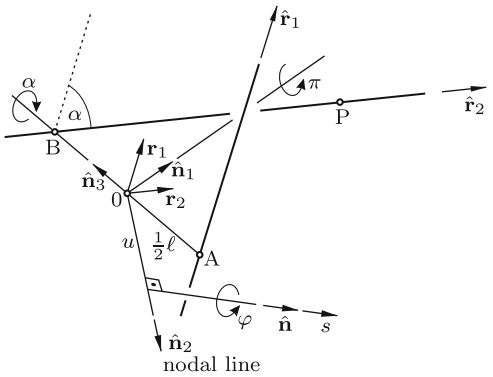

Fig. 3.17 Quantities associated with screw displacements $(\hat{\mathbf{n}}, \hat{\varphi})$ carrying the line $\hat{\mathbf{r}}_1$ into the line $\hat{\mathbf{r}}_2$

ments which are pure rotations. The problem statement does not require that point A of $\hat{\mathbf{r}}_1$ is carried to a specified point on $\hat{\mathbf{r}}_2$.

Problem 2: From the manifold of all screw displacements solving Problem 1 determine the submanifold of all screw displacements carrying point A of $\hat{\mathbf{r}}_1$ to an arbitrarily prescribed point P on $\hat{\mathbf{r}}_2$. Consider the special case P=B.

Both problems have a practical background. Let the body-fixed line be the axis of a cylindrical workpiece which is displaced by a robot from a box into the chuck of a machine. In the box the axis has position $\hat{\mathbf{r}}_1$, and in the chuck it has position $\hat{\mathbf{r}}_2$. The robot is equipped with a single cylindrical joint so that it can execute screw displacements only. The angular position of the cylindrical workpiece in the chuck is of no interest. If the depth of insertion into the chuck is not prescribed either, every screw displacement solving Problem 1 is acceptable, otherwise every screw displacement solving Problem 2.

Solution to Problem 1: The solution is deduced by means of the principle of transference from the solution to the following rotation problem solved in Sect. 1.15.9. Determine all rotations $(\mathbf{n}, \varphi)$ about a fixed point 0 which carry a body-fixed line passing through 0 from a given position $\mathbf{r}_1$ into another given position $\mathbf{r}_2$. The lines $\mathbf{r}_1$ and $\mathbf{r}_2$ and the angle α between them are shown in Fig. 1.11a. Figure 1.11b explains cartesian basis vectors $\mathbf{n}_1$, $\mathbf{n}_2$, $\mathbf{n}_3$. They are related to $\mathbf{r}_1$ and $\mathbf{r}_2$ through (1.220) and (1.221):

$$\mathbf{n}_1 = \frac{\mathbf{r}_1 + \mathbf{r}_2}{2\cos\frac{\alpha}{2}}\,, \qquad \mathbf{n}_3 = \frac{\mathbf{r}_1 \times \mathbf{r}_2}{\sin\alpha}\,, \qquad \mathbf{n}_2 = \mathbf{n}_3 \times \mathbf{n}_1\,, \tag{3.176}$$

$$\mathbf{r}_{1,2} = \mathbf{n}_1 \cos\frac{\alpha}{2} \mp \mathbf{n}_2 \sin\frac{\alpha}{2}\,. \tag{3.177}$$

The notation in Fig. 3.17 is chosen such that in the case $\ell = 0$ the dual angle $\hat{\alpha}$ is the angle α of Fig. 1.11, and that the dual vectors $\hat{\mathbf{r}}_i$ $(i = 1, 2)$ and $\hat{\mathbf{n}}_i$ $(i = 1, 2, 3)$ are the vectors $\mathbf{r}_i$ $(i = 1, 2)$ and $\mathbf{n}_i$ $(i = 1, 2, 3)$, respectively. The solution to the rotation problem of Fig. 1.11 is a one-parametric manifold of rotations $(\mathbf{n}, \varphi)$. With a free parameter ψ it is given in (1.222) and (1.228) in the form

$$\mathbf{n} = \mathbf{n}_1 \cos\psi - \mathbf{n}_3 \sin\psi \,, \qquad \cot\frac{\varphi}{2} = -\cot\frac{\alpha}{2}\,\sin\psi \,. \tag{3.178}$$

All vectors and angles are transferred into dual form by defining dual parts as follows:

$$\hat{\alpha} = \alpha + \varepsilon\ell \,, \qquad \hat{\varphi} = \varphi + \varepsilon s \,, \qquad \hat{\psi} = \psi + \varepsilon u \,, \tag{3.179}$$

$$\hat{\mathbf{n}}_i = \mathbf{n}_i \quad (i = 1, 2, 3) \,, \quad \hat{\mathbf{r}}_i = \mathbf{r}_i + \varepsilon\mathbf{w}_i \quad (i = 1, 2) \,, \quad \hat{\mathbf{n}} = \mathbf{n} + \varepsilon\mathbf{w} \,. \tag{3.180}$$

The identity $\hat{\mathbf{n}}_i = \mathbf{n}_i$ holds true because the second Plücker vectors are zero with respect to the origin 0 of the dual basis. The second Plücker vectors $\mathbf{w}_1$ and $\mathbf{w}_2$ of $\hat{\mathbf{r}}_i$ are

$$\mathbf{w}_{1,2} = \mp\frac{1}{2}\ell\mathbf{n}_3 \times \mathbf{r}_{1,2} = -\frac{1}{2}\ell\Big(\mathbf{n}_1 \sin\frac{\alpha}{2} \pm \mathbf{n}_2 \cos\frac{\alpha}{2}\Big) \,. \tag{3.181}$$

The same formulas are obtained by dual differentiation of (3.177). The quantities ψ and u are two independent parameters of the manifold of solutions. To be determined as functions of ψ and u are the dual parts s and $\mathbf{w}$ of the screw displacement. Unknown, too, is the geometrical meaning of u. The unknowns are determined as follows. Equations (3.178) are transferred into the dual forms

$$\hat{\mathbf{n}} = \mathbf{n}_1 \cos\hat{\psi} - \mathbf{n}_3 \sin\hat{\psi} \,, \qquad \cot\frac{\hat{\varphi}}{2} = -\cot\frac{\hat{\alpha}}{2}\,\sin\hat{\psi} \,. \tag{3.182}$$

The dual part of the first equation yields

$$\mathbf{w} = -u(\mathbf{n}_1 \sin\psi + \mathbf{n}_3 \cos\psi) \,. \tag{3.183}$$

This together with the first Eq.(3.178) yields for the perpendicular $\mathbf{n} \times \mathbf{w}$ from 0 onto the screw axis the expression

$$\mathbf{n} \times \mathbf{w} = u\mathbf{n}_2 \,. \tag{3.184}$$

From this it follows, first, that all screw axes intersect the line $\hat{\mathbf{n}}_2$ at right angles and, second, that the free parameter u (positive, zero or negative) represents the length of the perpendicular from 0 onto the screw axis. This is shown in Fig. 3.17. The line $\hat{\mathbf{n}}_2$ is called *nodal line* of the two lines $\hat{\mathbf{r}}_1$ and $\hat{\mathbf{r}}_2$.

The dual part of the second Eq.(3.182) is an equation for s:

$$\frac{-s/2}{\sin^2\frac{\varphi}{2}} = \frac{\ell/2}{\sin^2\frac{\alpha}{2}}\,\sin\psi - u\cot\frac{\alpha}{2}\,\cos\psi\,. \tag{3.185}$$

For $\sin^2\varphi/2$ and for other functions of φ the following expressions in terms of ψ are known from (1.227) and (1.226):

$$\sin^2\frac{\varphi}{2} = \frac{\sin^2\frac{\alpha}{2}}{1-\cos^2\frac{\alpha}{2}\cos^2\psi}\,, \qquad \sin\frac{\varphi}{2}\cos\frac{\varphi}{2} = \frac{-\sin\frac{\alpha}{2}\cos\frac{\alpha}{2}\sin\psi}{1-\cos^2\frac{\alpha}{2}\cos^2\psi}\,, \tag{3.186}$$

$$1-\cos\varphi = \frac{1-\cos\alpha}{1-\cos^2\frac{\alpha}{2}\cos^2\psi}\,, \qquad \sin\varphi = \frac{-\sin\alpha\sin\psi}{1-\cos^2\frac{\alpha}{2}\cos^2\psi}\,. \tag{3.187}$$

With the first Eq.(3.186) s becomes a function of u and ψ:

$$s = \frac{u\sin\alpha\cos\psi - \ell\sin\psi}{1-\cos^2\frac{\alpha}{2}\cos^2\psi}\,. \tag{3.188}$$

With Eqs.(3.178) for $\mathbf{n}$ and φ and with the equations for $\mathbf{w}$, $\mathbf{n}\times\mathbf{w}$ and s the two-parametric manifold of screw displacements $(\hat{\mathbf{n}},\hat{\varphi})$ solving Problem 1 is uniquely determined. The special screw displacements $(\hat{\mathbf{n}}_3,\hat{\alpha})$ and $(\hat{\mathbf{n}}_1,\pm\pi)$ shown in Fig. 3.17 belong to this manifold. The associated parameter values are $\psi=-\pi/2$, $u=0$ for the first and $\psi=0$, $u=0$ for the second.

Pure rotations satisfy the condition $s=0$, i.e.,

$$u = \frac{\ell\tan\psi}{\sin\alpha}\,. \tag{3.189}$$

This condition defines the one-parametric submanifold of rotations in the two-parametric manifold of screw displacements. The special rotation with parameter values $\psi=0$, $u=0$ belongs to this submanifold. The manifold of all rotation axes defines a ruled surface. Let x, u, z be the coordinates of points of this ruled surface along $\mathbf{n}_1$, $\mathbf{n}_2$ and $\mathbf{n}_3$, respectively. From the primary part of (3.182) and from (3.189) it follows that $z/x = -\tan\psi = -(u/\ell)\sin\alpha$ or $ux = -z\ell/\sin\alpha$. This is the equation of an equilateral hyperbolic paraboloid. In a ξ,η-system rotated through $45°$ about the $\mathbf{n}_2$-axis the transformation is $x=(\xi+\eta)\sqrt{2}/2$ and $u=(-\xi+\eta)\sqrt{2}/2$ and consequently $ux=-(\xi^2-\eta^2)/2$. Hence the principal-axes equation of the hyperbolic paraboloid is $z=(\xi^2-\eta^2)/a$ with $a=2\ell/\sin\alpha$. This ends the solution of Problem 1.

Solution to Problem 2: According to the problem statement the point A on $\hat{\mathbf{r}}_1$ at the foot of the common perpendicular is displaced to some prescribed point P on $\hat{\mathbf{r}}_2$. This displacement is achieved by a one-parametric submanifold of the screw displacements solving Problem 1. An appropriate measure

of displacement of point A is the quantity $(\mathbf{r}_P - \mathbf{r}_B)\cdot\mathbf{r}_2 = (\mathbf{r}_P - \mathbf{r}_A)\cdot\mathbf{r}_2$. The analysis to follow shows that the essential measure of displacement is the quantity $\sigma = (\mathbf{r}_P - \mathbf{r}_B)\cdot\mathbf{r}_2\cos\alpha/2$.

Further below σ is prescribed. However, before doing so, σ is determined for the screw displacements solving Problem 1 as function of ψ and u. Let $\boldsymbol{\varrho}$ be the vector leading from the point of intersection of a screw axis $\hat{\mathbf{n}}$ with the nodal line $\mathbf{n}_2$ to point A. Figure 3.17 yields the expression

$$\boldsymbol{\varrho} = -\Big(u\mathbf{n}_2 + \frac{1}{2}\ell\mathbf{n}_3\Big)\,. \tag{3.190}$$

The associated measure of displacement is

$$\sigma = \Big\{(1-\cos\varphi)[(\mathbf{n}\cdot\boldsymbol{\varrho})\mathbf{n} - \boldsymbol{\varrho}] + \sin\varphi\,\mathbf{n}\times\boldsymbol{\varrho} + s\mathbf{n}\Big\}\cdot\mathbf{r}_2\cos\frac{\alpha}{2}\,. \tag{3.191}$$

The term $s\mathbf{n}$ is due to translation, and the remaining terms are copied from (1.37). The scalar products are expressed in terms of ψ and u with the help of (3.190), (3.177) and (3.178):

$$\left.\begin{aligned} &\mathbf{n}\cdot\boldsymbol{\varrho} = \frac{1}{2}\ell\sin\psi\,, \quad \mathbf{n}\cdot\mathbf{r}_2 = \cos\frac{\alpha}{2}\cos\psi\,, \quad \boldsymbol{\varrho}\cdot\mathbf{r}_2 = -u\sin\frac{\alpha}{2}\,,\\ &\mathbf{n}\times\boldsymbol{\varrho}\cdot\mathbf{r}_2 = \frac{1}{2}\ell\sin\frac{\alpha}{2}\cos\psi - u\cos\frac{\alpha}{2}\sin\psi\,. \end{aligned}\right\} \tag{3.192}$$

For s, for $(1-\cos\varphi)$ and for $\sin\varphi$ the expressions (3.188) and (3.187), respectively, are substituted. This yields σ as function of ψ and u. The result is written in the two forms

$$\sigma = \frac{2u\sin\frac{\alpha}{2}\cos\frac{\alpha}{2} - \ell\cos^2\frac{\alpha}{2}\sin\psi\cos\psi}{1-\cos^2\frac{\alpha}{2}\cos^2\psi} = \frac{4u\sin\alpha - \ell(1+\cos\alpha)\sin 2\psi}{4-(1+\cos\alpha)(1+\cos 2\psi)}\,. \tag{3.193}$$

In what follows, the manifold of all screw displacements is determined for which σ is an arbitrarily prescribed constant $-\infty < \sigma < \infty$. Then (3.193) represents a constraint equation for ψ and u. As independent parameter ψ is chosen. The solution for u as function of ψ is written in the two forms

$$u\sin\alpha = \sigma + \cos^2\frac{\alpha}{2}\cos\psi(\ell\sin\psi - \sigma\cos\psi)\,, \tag{3.194}$$

$$u = \frac{\sigma(3-\cos\alpha)}{4\sin\alpha} + \frac{1}{4}\cot\frac{\alpha}{2}(\ell\sin 2\psi - \sigma\cos 2\psi)\,. \tag{3.195}$$

For further simplification the x,z-system of principal axes is introduced which is rotated against the $\mathbf{n}_1,\mathbf{n}_3$-axes through the angle ψ_0 defined by

$$\cos 2\psi_0 = \frac{\ell}{\sqrt{\ell^2+\sigma^2}}\,, \qquad \sin 2\psi_0 = \frac{\sigma}{\sqrt{\ell^2+\sigma^2}}\,. \tag{3.196}$$

With new variables

$$y = u - u_0 \,, \qquad \chi = \psi - \psi_0 \tag{3.197}$$

and with the constants

$$u_0 = \frac{\sigma(3 - \cos\alpha)}{4\sin\alpha} \,, \qquad h = \frac{1}{4}\cot\frac{\alpha}{2}\sqrt{\ell^2 + \sigma^2} \tag{3.198}$$

(3.195) becomes

$$y = h \sin 2\chi \,. \tag{3.199}$$

The vector $u(\chi)\mathbf{n}_2$ is the perpendicular from 0 onto the screw axis. The rotation angle φ and the translation s are determined through (3.178) and (3.188) as functions of $\psi = \chi + \psi_0$.

The one-parametric manifold of screw axes with parameter χ defines a ruled surface. With an additional free parameter λ this ruled surface has the parameter equations

$$x = \lambda\cos\chi \,, \qquad z = -\lambda\sin\chi \,, \qquad y = h\sin 2\chi \,. \tag{3.200}$$

Compare this with Eqs.(3.170). Except for an interchange of y and z both sets of equations are identical. Hence the ruled surface is a cylindroid the directrix of which is the nodal line. The parameter-free equation of the cylindroid is (cf. (3.171))

$$y(x^2 + z^2) = -2hxz \,. \tag{3.201}$$

Every prescribed value of σ determines a one-parametric manifold of screw displacements with the associated cylindroid of screw axes.

Following (3.171) some important geometrical properties of the cylindroid were listed (see Fig. 3.16). At every point y in the interval $|y| \leq |h|$ the directrix is orthogonally intersected by two screw axes. At $y = 0$ these screw axes lie in the x-axis and in the z-axis, respectively. These are the principal screw axes. At $y = -h$ and at $y = +h$ the two intersecting screw axes coincide. The angles associated with these axes are $\chi = -\pi/4$ and $\chi = +\pi/4$, respectively. These screw axes are torsal lines of the cylindroid. Each of the two planes spanned by the directrix and by a torsal line is a plane of symmetry of the cylindroid. Every pair of screw axes intersecting the directrix in one point is located symmetrically with respect to each of the planes of symmetry, i.e., under angles χ_1 and χ_2 related by the equation $\chi_2 = \pi/2 - \chi_1$. The relationship between the corresponding angles $\psi_1 = \chi_1 + \psi_0$ and $\psi_2 = \chi_2 + \psi_0$ is $\psi_2 = \pi/2 - \psi_1 + 2\psi_0$.

It was shown that the screw axes under the angles $\psi = 0$ and $\psi = -\pi/2$ belong to special screw displacements. The first one is characterized by $\varphi = \pm\pi$ and the second by $\varphi = \alpha$ and $s = \ell$. It will be seen that also the screw displacements with screw axes located symmetrically to these screw axes have special properties. The associated angles are $\psi = \pi/2 + 2\psi_0$ and $\psi = 2\psi_0$, respectively.

First, it is investigated which screw axis $\hat{\mathbf{n}}$ intersects one or the other of the two lines $\hat{\mathbf{r}}_1$ and $\hat{\mathbf{r}}_2$. The screw axis $\hat{\mathbf{n}} = \mathbf{n} + \varepsilon\mathbf{w}$ has the Plücker vectors $\mathbf{n}$ and $\mathbf{w}$ given in (3.182) and (3.183), respectively. The lines $\hat{\mathbf{r}}_i = \mathbf{r}_i + \varepsilon\mathbf{w}_i$ $(i = 1, 2)$ have the Plücker vectors $\mathbf{r}_i$ and $\mathbf{w}_i$ given in (3.177) and (3.181). The condition of intersection is $\mathbf{n} \cdot \mathbf{w}_i + \mathbf{r}_i \cdot \mathbf{w} = 0$ (see (2.18)). It turns out that this condition has for both lines the same form

$$\ell \sin\frac{\alpha}{2} \cos\psi + 2u \cos\frac{\alpha}{2} \sin\psi = 0 \,. \tag{3.202}$$

This equation is multiplied by $\sin\alpha/2$, and then $u \sin\alpha$ is replaced by the expression in (3.194). Simple reformulation produces the final form

$$(\ell \cos\psi + \sigma \sin\psi)\Big(\sin^2\frac{\alpha}{2} + \cos^2\frac{\alpha}{2}\sin^2\psi\Big) = 0 \,. \tag{3.203}$$

The results are summarized as follows. A screw axis which intersects one of the two lines intersects also the other, and there is only one such screw axis. Its angle ψ is given by $\tan\psi = -\ell/\sigma$ or, because of (3.196), by $\tan\psi = -\cot 2\psi_0$. Hence $\psi = 2\psi_0 + \pi/2$. This shows that the screw axis is the one which is located symmetrically with respect to $\chi = \pi/4$ to the screw axis associated with $\psi = 0$, $\varphi = \pi$.

Every screw axis on the cylindroid, i.e., every angle ψ or χ, respectively, is associated with a rotation angle φ and a translation s. The angle is determined by (3.178). The two screw axes along the principal axes and the two screw axes along the torsal lines are examples of pairs of mutually orthogonal screw axes (with or without intersection point). All pairs of mutually orthogonal screw axes satisfy the identity (1.229): $\cot^2(\varphi/2)+\cot^2(\varphi^*/2) \equiv \cot^2\alpha/2$.

The quantity s in the screw displacements solving Problem 2 remains to be formulated. It is obtained by substituting in (3.188) for $u \sin\alpha$ the expression from (3.194). The result is

$$s = \sigma \cos\psi - \ell \sin\psi \,. \tag{3.204}$$

Comparison with (3.195) yields the relationship

$$s(\psi) = -4 \tan\frac{\alpha}{2}\,[u(\psi/2) - u_0] \,. \tag{3.205}$$

Let s_1 and s_2 be the values of s associated with the principal axes x $(\psi = \psi_0)$ and z $(\psi = \psi_0 - \pi/2)$. With (3.196)

$$s_{1,2} = \sqrt{\frac{1}{2}\Big(\ell^2 + \sigma^2 \mp \ell\sqrt{\ell^2 + \sigma^2}\Big)} \,. \tag{3.206}$$

From (3.204) it follows that there is only a single screw displacement which is a pure rotation $(s = 0)$. The direction of its axis is determined by $\tan\psi = \sigma/\ell = \tan 2\psi_0$. Hence $\psi = 2\psi_0$. This shows that the rotation axis is the

screw axis which is located symmetrically with respect to $\chi = \pi/4$ to the screw axis associated with $\psi = -\pi/2$, $\varphi = \alpha$ and $s = \ell$.

The results developed up to this point were obtained first by Moshammer [33], Pelišek [35], Rath [40] and Lilienthal [28]. See also Bottema [4]. None of the cited papers made use of the principle of transference.

Equation (3.19) defined for screw displacements the scalar measure $p_{\text{P}} = (s/2)/\tan\varphi/2$. With the second Eq.(3.178) and with (3.204)

$$p_{\text{P}} = \frac{1}{2}\cot\frac{\alpha}{2}\sin\psi\,(\ell\sin\psi - \sigma\cos\psi) = \frac{1}{4}\cot\frac{\alpha}{2}\,[\ell(1-\cos 2\psi) - \sigma\sin 2\psi]\,. \tag{3.207}$$

The angle $\psi = 0$ is associated with $s = \sigma$ and $p_{\text{P}} = 0$. Transformation of (3.207) into the principal-axes system by means of (3.198) results in the equation

$$p_{\text{P}} = p_{\text{P}0} - h\cos 2\chi\,, \qquad p_{\text{P}0} = \frac{1}{4}\ell\cot\frac{\alpha}{2}\,. \tag{3.208}$$

The mean value $p_{\text{P}0}$ of p_{P} occurs in the torsal lines. The extremal values $p_{\text{P}0}\pm h$ have opposite signs. They occur in the principal axes. For every pair of screw axes which is located symmetrically with respect either to $\chi = \pi/4$ or to $\chi = -\pi/4$ both screw axes are associated with one and the same measure p_{P}. Equations (3.208) and (3.199) reveal the remarkable relationship

$$(p_{\text{P}} - p_{\text{P}0})^2 + y^2 \equiv h^2\,. \tag{3.209}$$

It is formally identical with (3.164).

Special case $\sigma = 0$ (A *is displaced to* B)
The formulas for $\hat{\mathbf{n}}$ and φ are independent of σ. Equations (3.195) – (3.198), (3.204) and (3.206) become

$$\left.\begin{aligned} u &= \frac{\ell}{4}\cot\frac{\alpha}{2}\sin 2\psi\,, \qquad \chi \equiv \psi\,, \qquad u_0 = 0\,, \\ s &= -\ell\sin\psi\,, \qquad s_1 = 0\,, \qquad s_2 = \ell\,. \end{aligned}\right\} \tag{3.210}$$

References

1. Adams D P (1966) Notes and comments on the application of dual numbers, dual vectors and dual quaternions in spatial kinematic analysis. NSF MIT Summer Conf.
2. Ball R S (1900) A treatise on the theory of screws. Cambridge Univ. Press
3. Battaglini B (1869) Sulle serie dei sistemi di forze. Rendiconti Acc. di Napoli VIII:87–94
4. Bottema O (1973) On a set of displacements in space. J.Eng.for Ind. 95:451–454
5. Bottema O, Roth B (1990) Theoretical kinematics. North-Holland, Dover, New York
6. Castelain J M, Flamme J M, Gorla B, Renaud M (1986) Computation of the direct and inverse geometric and differential models of robot manipulators with the aid of the hypercomplex theory, 16th I.S.I.R. Int. Symp. on Industrial Robots, Brussels

7. Cayley A (1889) The collected mathematical papers of Arthur Cayley, v.1–13. Cambridge: The Univ. Press; (1963) Johnson Reprint Co., New York
8. Chasles M (1830) Note sur les propriétés générales du système de deux corps semblables entre eux, placés d'une manière quelconque dans l'espace, et sur le déplacement fini ou infiniment petit d'un corps solide libre. Bull. Scie. Math. de Ferussac XIV:321–326
9. Chevallier D P (1996) On the transference principle: Its various forms and limitations. Mechanism Machine Theory 1:57–76
10. Clifford W K (1873) Preliminary sketch of biquaternions. Proc.London Math.Soc. IV:381–395
11. Dimentberg F M (1948) A general method for the investigation of finite displacements of spatial mechanisms and certain cases of passive constraints (Russ.) Trudy Seminara po Teorii Mashin i Mechanismov, AN SSSR 5 Nr.17:5–39; Purdue Translation No.436, Purdue Univ.
12. Dimentberg F M (1965) Screw calculus and its applications in mechanics (Russ.). Nauka, Moscow. Engl. trans. (1968) Foreign Techn. Div. WP-AFB, Ohio
13. Dimentberg F M (1978) Screw theory and its applications (Russ). Nauka, Moscow
14. Dimentberg F M (1982) Theory of spatial linkages (Russ.). Nauka, Moscow
15. Erdman A G (ed.) (1993) Modern kinematics. Developments in the last forty years. Wiley, New York (appr. 2250 literature references)
16. Giorgini G (1836) Memorie di Matematica. Soc.Ital. delle Scienze, Modena 21:1–54
17. Halphen M (1882) Sur la théorie du déplacement. Nouv. Ann. de Math. 3:296–299
18. Hamilton W R (1830) First supplement on the theory of systems of rays. Trans.Royal Irish Ac. XVI:4–62
19. Hsia L M, Yang A T (1981) On the principle of transference in three-dimensional kinematics. ASME J.of Mech. Design 103:652–656
20. Huang C (2000) On definitions of pitches and the finite screw system for displacing a line. Proc. Symp. 100th Anniversary of Ball's *A Treatise on the on the theory of screws*. Univ. of Cambridge, Trinity College
21. Keler M K (1959) Analyse und Synthese der Raumkurbelgetriebe mittels Raumliniengeometrie und dualer Grössen. Forschung Ing.-Wesen 25:26–63
22. Keler M K (1970) Die Verwendung dual-komplexer Grössen in Geometrie, Kinematik und Dynamik. Feinwerktechnik 74:31–41
23. Keler M K (1970) Analyse und Synthese räumlicher, sphärischer und ebener Getriebe in dual-komplexer Darstellung. Feinwerktechnik 74:341–351
24. Keler M K (1979) Dual vector half tangents for the representation of the finite motion of rigid bodies. Env. and Planning B 6:403–412
25. Keler M K (1998) Dual expansion of an optimal in-parallel spherical platform device into a spatial one. In: [27] 79–86
26. Kotelnikov A P (1895) Screw calculus with some of its applications in geometry and mechanics (Russ). Annals Imperial Univ. Kazan, Kazan
27. Lenarčič J, Husty M L (eds.) (1998) Advances in robot kinematics: Analysis and control, Kluwer, Dordrecht
28. Lilienthal R v. (1908) Vorlesungen über Differentialgeometrie. Bd.1: Kurventheorie, Bd.2: Flächentheorie. Teubner, Leipzig
29. Löbell F (1929) Aus der Differentialgeometrie der Schraubenscharen. Festschrift der T.H. Stuttgart zur Vollendung ihres 1. Jahrhunderts. Springer, Berlin, Wien
30. Martinez J M R, Duffy J (1993) The principle of transference: History, statement and proof. Mechanism Machine Theory 28:165–177
31. Meyer W FR, Mohrmann H (eds.) (1921-1928) Enzyklopädie der Math. Wissenschaften. v.III: Geometrie. Teubner, Leipzig
32. Meyer W F, Mohrmann H (eds.) (1921–1928) Encyklopädie der mathematischenWissenschaften mit Einschluss ihrer Anwendungen. Bd.3,Teil 2,Teilbd. A, Leipzig
33. Moshammer C (1876) Zur Geometrie der Schraubenbewegung. Wiener Sitzungsber.Math.Cl.73,Abtlg.2:143–168

34. Parkin I A (1997) Dual systems of finite displacement screws in the screw triangle. Mechanism Machine Theory 32:993–1003
35. Pelisĕk M (1889) Über den Ort der Achsen derjenigen Schraubenbewegungen, durch welche eine Strecke in eine beliebige Lage im Raum gebracht wird. Arch.Math.(2)7:1–9
36. Pennestri E, Stefanelli R (2007) Linear algebra and numerical algorithms using dual numbers, J. Multibody System Dynamics 18:323–344
37. Pennock G R, Yang A T (1985) Application of dual-number matrices to the inverse kinematics of robot manipulators. J.Mech.Trans.Auto.in Des. 107:201–208
38. Plücker J (1865) On a new geometry of space. Philos.Trans. 155:725–791
39. Plücker J (1868) Neue Geometrie des Raumes gegründet auf die Betrachtung der geraden Linie als Raumelement. Teubner, Leipzig.
40. Rath E (1907) Zur Theorie der Schraubenbewegungen. Mathem.-Naturw. Mitteilungen in Baden-Württemberg 7:9–19
41. Ravani B, Roth B (1984) Mappings in spatial kinematics. ASME J Mechanisms, Transmissions, Automation in Design 106:341–347
42. Rooney J (1978) Comparison of representations of general spatial screw displacement. Env. and Planning B5:45–88
43. Roth B (1967) The kinematics of motion through finitely separated positions. J.Appl.Mech. 34:591–598
44. Roth B (1967) On the screw axes and other special lines associated with spatial displacements of a rigid body. J. Eng.f.Ind. 89B:102–110
45. Sinigersky A (2002) Rechnerunterstützte Behandlung von dualen Grössen in der Kinematik. Studienarbeit Inst. Techn. Mech. Univ. Karlsruhe
46. Spillers W R (ed.) (1964) Basic questions of design theory. Northholland, Amsterdam
47. Study E (1903) Die Geometrie der Dynamen. Teubner, Leipzig
48. Tsai L W, Roth(1972) Design of dyads with helical, cylindrical, spherical, revolute and prismatic joints. Mechanism Machine Theory 7:85–102
49. Veldkamp G R (1976) On the use of dual numbers, vectors and matrices in instantaneous spatial kinematics. Mechanism Machine Theory 11:141–156
50. Wittenburg J (1981) Duale Quaternionen in der Kinematik räumlicher Getriebe. Eine anschauliche Darstellung. Ing.-Arch.51:17–29
51. Yang A T (1963) Application of quaternion algebra and dual numbers to the analysis of spatial mechanisms. PhD thesis Columbia Univ.
52. Yang A T (1964) Calculus of screws. In: [46]:265–281
53. Yang A T (1969) Displacement analysis of spatial five-link mechanisms using (3×3) matrices with dual-number elements. J. Eng.f.Ind. 91:152–157
54. Yang A T, Freudenstein F (1964) Application of dual-number quaternion algebra to the analysis of spatial mechanisms. Trans ASME 86E:300–308 (J.Appl.Mech.31)
55. Yuan M S C, Freudenstein F (1971) Kinematic analysis of spatial mechanisms by means of screw coordinates. Part I - Screw coordinates. J. Eng.f.Ind. 93:61–66
56. Yuan M S C, Freudenstein F, Woo L S (1971) Kinematic analysis of spatial mechanisms by means of screw coordinates. Part II - Analysis of spatial mechanisms. J. Eng.f.Ind. 93:67–73
57. Zindler K (1921) Algebraische Liniengeometrie. In [31]:973–1228

Chapter 4
Degree of Freedom of a Mechanism

A mechanism consists of rigid bodies and of joints inter-connecting the bodies. A joint is a mechanical device which introduces kinematical constraints on the motion of the two bodies relative to each other. This implies that interconnections by springs or dampers do not constitute joints since such elements do not create kinematical constraints. Two bodies cannot be connected by more than one joint. This means that the complete system of devices interconnecting two bodies is counted as a single joint. A joint does not connect more than two bodies. If, for example, $p > 2$ bodies are rotating about a single common shaft, this shaft represents $p-1$ joints each of them connecting two bodies.

A single body moving in three-dimensional space without any kinematical constraint is said to have the degree of freedom $F = 6$. This is the minimal number of generalized coordinates required for specifying its position and angular orientation relative to some reference body. Let the moving body be connected to the reference body by a joint. Kinematical constraints introduced by this joint have the effect that the body has a degree of freedom $1 \leq F \leq 5$. This number F is also called *degree of freedom* f *of the joint*. The number of independent kinematical constraints in the joint is $6 - f$. Examples: Revolute, prismatic and helical joints have $f = 1$, cylindrical and universal joints have $f = 2$, and a spherical joint has $f = 3$. The degree of freedom is $f = 4$ $(f = 5)$ if the spherical joint is free to move along a rigid line (in a rigid surface).

A mechanism is a joint-connected system of bodies. Let n be the number of bodies. One of the bodies is held fixed. In order to be connected the mechanism must have $m \geq n-1$ joints. Each joint $i = 1, \ldots, m$ has its individual degree of freedom $1 \leq f_i \leq 5$. The mechanism as a whole has a degree of freedom F. This is the minimal number of generalized coordinates required for specifying its position and angular orientation relative to the single body held fixed. The degree of freedom F depends not only on the numbers n and m and on the degrees of freedom $1 \leq f_i \leq 5$ $(i = 1, \ldots, m)$ of the

J. Wittenburg, *Kinematics*, DOI 10.1007/978-3-662-48487-6_4

individual joints, but also on the structure of the system. This dependency is the subject of the present chapter.

4.1 Grübler's Formula

A mechanism with $m = n-1$ joints is said to have *tree structure* (Fig. 4.1a). Its characteristic feature is that any two bodies are connected by a uniquely determined chain of bodies and of joints. Examples are serial robot arms without kinematical constraint of the gripper to the surrounding environment and the human body when standing on one foot and with free hands. A mechanism with $m = n$ joints contains a single closed chain or single loop. An example is shown in Fig. 4.1b. A single loop without side branches (the subsystem formed by the shaded bodies) is called *simple closed chain*. A mechanism with $m > n$ joints is called *multiloop mechanism*. It is created by adding more joints in Fig. 4.1b. In both figures the schematically indicated joints are of arbitrary nature with individual degrees of freedom $1 \le f \le 5$.

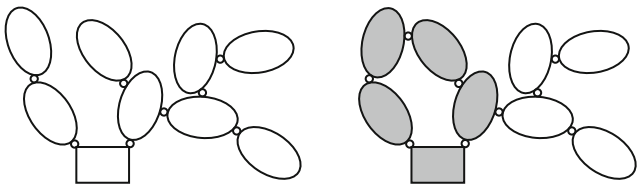

Fig. 4.1 Mechanisms with tree structure ($m = n-1$) **(a)** and with a single closed chain ($m = n$) **(b)**. Simple closed chain formed by the shaded bodies

The degree of freedom F of a mechanism is determined as follows. As a preparatory step all joints of the mechanism are removed, so that all bodies except the single body held fixed are free of kinematical constraints. In this state these $n-1$ bodies have a total degree of freedom $6(n-1)$, namely, six for each body. In joint i $(i = 1, \ldots, m)$ with joint degree of freedom $1 \le f_i \le 5$ there are $6 - f_i$ kinematical constraints. The total number of constraints of all m joints equals the sum of all numbers $(6 - f_i)$. The total number of *independent* constraints may be smaller. It is smaller by d where d (defect) denotes the number of dependent constraints. After reconstituting the removed joints the degree of freedom of the mechanism is obtained:

$$F = 6(n-1) - \Big[\sum_{i=1}^{m}(6-f_i) - d\Big] = 6(n-1-m) + d + \sum_{i=1}^{m} f_i \qquad (1 \le f_i \le 5)\,. \tag{4.1}$$

This formula is valid for all mechanisms. In theory as well as in engineering practice planar mechanisms and spherical mechanisms are important. In a planar mechanism each body is in plane motion, and the reference plane is the same for all bodies. In a spherical mechanism each body is rotating about a fixed point, and all bodies have the same fixed point. A simple example is the spherical four-bar with four bodies and four revolute joints intersecting at a single point. In planar motion as well as in spherical motion about a fixed point a single unconstrained body has the degree of freedom three. In planar as well as in spherical mechanisms an individual joint has the joint degree of freedom $1 \le f_i \le 2$ and, consequently, $3 - f_i$ constraints. In both types of mechanism the degree of freedom of the mechanism is

$$F = 3(n-1-m)+d+\sum_{i=1}^{m} f_i \quad \text{(planar and spherical mech's; } 1 \le f_i \le 2\text{)} . \quad (4.2)$$

Planar mechanisms can be seen as special cases of spherical mechanisms. The fixed point common to all bodies is at infinity.

In the literature (4.1) and (4.2) are usually written without the defect d. These formulas are due to Grübler [3]. The formulas are accompanied by the warning that false results are obtained in the case of dependent constraints. A simple example shows that false results may be obtained even if the defect is taken into account. Imagine two systems 1 and 2 which are sharing a single body 0 which is held fixed. Suppose, (4.1) yields $F_1 = -1$ for system 1 (indicating rigidity) and $F_2 = 1$ for system 2. Clearly, the entire system composed of systems 1 and 2 together has the degree of freedom $F = 1$. However, (4.1) applied to the entire system yields the wrong result $F = F_1 + F_2 = 0$ indicating rigidity. The formula $F = F_1 + F_2$ is correct if and only if $F_1, F_2 \ge 0$. The general statement is: Equations (4.1) and (4.2) applied to an entire system yield correct results if and only if, by the same equations, every subsystem of the entire system has a degree of freedom ≥ 0. Hence the conclusion: In order to get a correct result it is necessary, first, to determine the degree of freedom of subsystems. Every subsystem with a degree of freedom ≤ 0 must be counted as a single rigid body. Only then do (4.1) and (4.2) yield correct results for the entire system. Most engineering systems are so simple that the degree of freedom of subsystems is obvious without any analysis. In complex spatial multiloop systems, however, a separate analysis of subsystems may be necessary.

Equations (4.1) and (4.2) show that the degree of freedom F of a mechanism is independent of which body is chosen as fixed body.

Mechanisms with tree structure (Fig. 4.1a) are characterized by $m = n-1$ and $d = 0$. In this case, both formulas for the degree of freedom read

$$F = \sum_{i=1}^{n-1} f_i . \quad (4.3)$$

For mechanisms with a closed chain and, in particular, for the simple closed chain (Fig. 4.1b; $m = n$) (4.1) and (4.2) have the forms

$$F = \begin{cases} -6 + d + \sum_{i=1}^{n} f_i & \text{(all mechanisms; } 1 \le f_i \le 5\text{)} \\ -3 + d + \sum_{i=1}^{n} f_i & \text{(planar and spherical mech's; } 1 \le f_i \le 2\text{)}\,. \end{cases} \tag{4.4}$$

A mechanism with degree of freedom $F = 1$ is called 1-d.o.f. mechanism or mobility-one mechanism. From (4.4) follows

Theorem 4.1. *In a simple closed chain with mobility one and with independent constraints* ($F = 1$, $d = 0$) *the number of joint variables is*

$$\sum_{i=1}^{n} f_i = \begin{cases} 7 & \text{(nonspherical spatial simple closed chain)} \\ 4 & \text{(planar and spherical simple closed chains)}\,. \end{cases} \tag{4.5}$$

Applied to revolute joints ($f_i \equiv 1$) this theorem states that a simple (nonspherical) spatial closed chain must have seven revolute joints and seven bodies in order to have mobility one if all constraints are independent. For planar and for spherical simple closed chains this number of revolute joints and of bodies is four. Engineering realizations are the planar four-bar and the spherical four-bar. For both of them the first Eq.(4.4) yields the correct result $F = 1$ only if $d = 3$. Indeed, three constraints are dependent. In the planar four-bar, for example, one out of four parallel revolute joints establishes the constraint to the plane of motion. This constraint must not be counted as independent in the other three revolutes.

A mechanism is said to be *overconstrained* if it has a degree of freedom $F \ge 1$ only because of the existence of dependent constraints $(d > 0)$. Overconstrained mechanisms must be manufactured with great precision because inaccuracies result in the loss of mobility. Inhomogeneous changes of temperature may have the same effect. For these reasons most engineering mechanisms are designed such that overconstraint does not occur. Example: The ideal planar four-bar is an overconstrained mechanism. This overconstraint is avoided by giving the bearing of one axis the freedom to adjust its direction as is required.

4.2 Illustrative Examples

The determination of the defect d in Grübler's Eq.(4.1) can be a difficult problem requiring a kinematics analysis in which all mechanism parameters – link lengths and parameters specifying directions of joint axes – are involved.

In the following sections this analysis is demonstrated for seven different mechanisms.

4.2.1 Five-Point-Contact Joint

Subject of investigation is a rigid body five points of which are constrained to move in prescribed surfaces. To be determined is the degree of freedom of the body. The five surfaces constitute a single body referred to as frame. The system is a mechanism with $n = 2$ bodies and with $m = 1$ joint. The constraint of a point P_i to a surface prevents the point from moving in the direction of the unit vector $\mathbf{n}_i$ normal to the surface. There are five such constraints in the joint. If d is again the number of dependent constraints, the joint degree of freedom is $f = 6 - (5 - d) = 1 + d$. According to (4.1) this is also the degree of freedom of the mechanism and, thus, of the body.

The defect d is determined as follows. According to Chasles's Theorem 3.1 an infinitesimal displacement of a rigid body is a screw displacement with a certain screw axis and a certain pitch (this includes as special cases pure translation and pure rotation). The infinitesimal displacement of an arbitrary body-fixed point is directed along the helix through this point. Every line perpendicular to the helix is a complex line of the linear complex with this screw axis and with this pitch (see the comment on Fig. 2.5). From this it follows that the normals to the five surfaces at the points P_i $(i = 1, \ldots, 5)$ are complex lines. Let $\mathbf{r}_i$ $(i = 1, \ldots, 5)$ be the position vectors of the points P_i in a reference basis fixed on the frame. In this basis the normals have Plücker vectors $\mathbf{v}_i = \mathbf{n}_i$ and $\mathbf{w}_i = \mathbf{r}_i \times \mathbf{n}_i$ $(i = 1, \ldots, 5)$. From five *independent* complex lines the vectors $\mathbf{a}$ and $\mathbf{b}$ of a linear complex $(\mathbf{a}\,;\mathbf{b})$ are determined by Eqs.(2.38):

$$\mathbf{w}_i \cdot \mathbf{a} + \mathbf{v}_i \cdot \mathbf{b} = 0 \qquad (i = 1, \ldots, 5)\,. \tag{4.6}$$

The screw axis has the direction of $\mathbf{a}$. The location of the screw axis and the pitch are determined by (2.29):

$$\mathbf{u} = \frac{\mathbf{a} \times \mathbf{b}}{\mathbf{a}^2}\,, \qquad p = \frac{\mathbf{a} \cdot \mathbf{b}}{\mathbf{a}^2}\,. \tag{4.7}$$

From these facts it follows that the defect d of the coefficient matrix in (4.6) is the quantity determining the degree of freedom $f = 1 + d$ of the joint.

An engineering realization of the constraint of a body to five surfaces is shown in Fig. 4.2. The body, now called platform, is connected to a frame by five rods with spherical joints at both ends. Each surface is a sphere with the rod length as radius. The axes of the five rods are the complex lines. The platform on five rods finds an important engineering application in the five-point wheel suspension system for cars shown in Fig. 4.3. The platform is the

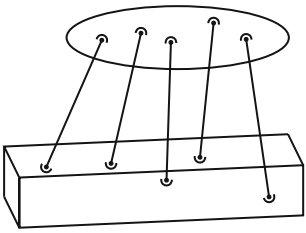

Fig. 4.2 Platform mounted on five rods with spherical joints at both ends

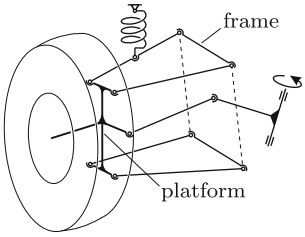

Fig. 4.3 Five-point wheel suspension system

carrier of the wheel, and the frame is the car body. A single spherical joint on the car body is operated by the steering mechanism. When the steering is held fixed, the carrier has a single degree of freedom. Springs connecting the carrier with the car body allow small carrier displacements only. These displacements are screw displacements.

The screw displacement of a platform can be made visible by the following experiment. Instead of mounting the platform on rigid rods it is suspended by five mutually skew inextensible strings in such a way that an equilibrium position exists in which the weight of the platform keeps all strings tight. A small perturbation causes the platform to oscillate about the equilibrium position. This oscillation is a screw motion about the axis and with the pitch determined by (4.6) and (4.7).

If the rods in Fig. 4.2 are counted as bodies, the entire system is composed of $n = 7$ bodies (fixed frame, platform and five rods) and of $m = 10$ spherical joints each having the joint degree of freedom $f = 3$. With these numbers Grübler's formula (4.1) yields for the degree of freedom of the mechanism the result $F' = 6(n-1-m)+d+mf = 6+d$. Since every rod has the degree of freedom of rotation about its own axis, the degree of freedom of the platform is $F = F' - 5 = 1 + d$ as before.

To a platform mounted on five rods additional rods can be added in such a way that, in the assembly position, all rods are lines of a single linear complex. In this position then, the degree of freedom of the platform is $F = 1$. In general, it is not possible to move the platform into another position. The platform is said to be *shaky* in this position. In exceptional cases a platform is mounted on more than five rods in such a way that large motions are possible. This requires an arrangement where every position in the course of motion satisfies the condition that all rods are complex lines of a single linear complex. The platform-fixed endpoint of each rod is moving on the sphere having its center at the other endpoint of the rod. In Sect. 6.8 such systems are investigated.

4.2.2 Shaky Truss

In Fig. 4.4a a planar multiloop mechanism with $n = 7$ bodies (fixed body 0 plus bodies $1, \ldots, 6$) and with $m = 9$ revolute joints is shown (the connection of bodies 2, 4 and 5 represents two joints). To be determined is the degree of freedom F.

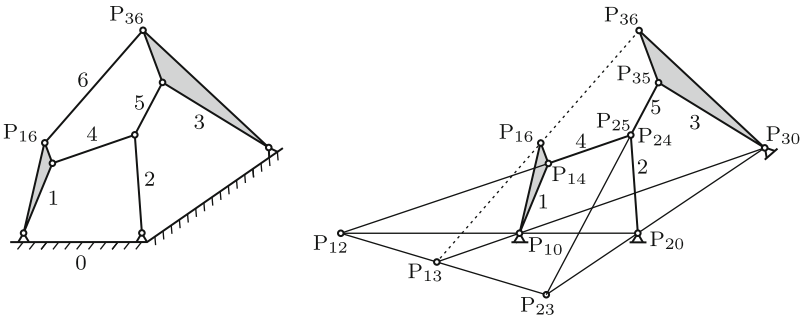

Fig. 4.4 Planar mechanism with 7 bodies and 9 revolute joints **(a)** before and **(b)** after eliminating rod 6

Solution: Equation (4.2) yields $F = d$. Hence the degree of freedom is $F > 0$ only if at least one constraint is dependent. In order to find out whether this is the case, rod 6 is eliminated and, thereby, a single constraint forcing the endpoints P_{16} and P_{36} to have identical velocity components in the direction of rod 6. The mechanism without rod 6 is shown in Fig. 4.4b. If in this system with degree of freedom $F = 1$ P_{16} and P_{36} have identical velocity components in the direction of the eliminated rod 6, this rod 6 is unnecessary which means that $d = 1$. Velocities are determined with the help of Theorem 15.3 by Kennedy and Aronhold. The condition to be satisfied is that the pole P_{13} is located on the line $\overline{P_{16}P_{36}}$. This pole P_{13} is found as intersection of the lines $\overline{P_{10}P_{30}}$ and $\overline{P_{12}P_{23}}$. The poles P_{12} and P_{23} are determined as intersections of the lines $\overline{P_{10}P_{20}}$ and $\overline{P_{14}P_{24}}$ and of the lines $\overline{P_{20}P_{30}}$ and $\overline{P_{25}P_{35}}$, respectively. In the present case, P_{13} is, indeed, located on the line $\overline{P_{16}P_{36}}$. However, this is true only in the instantaneous position of the mechanism. Hence the conclusion: In the position shown the mechanism in Fig. 4.4a has the degree of freedom $F = 1$. Neighboring positions cannot be assumed. In statics the system is called an infinitesimally mobile or shaky truss. Grübler's formula and the formula used for checking statical determinacy of trusses are directly related.

4.2.3 Closed Chain Formed by Four Planar Four-Bars

The planar system shown in Fig. 4.5 can be interpreted in different ways. For one thing, it is a multiloop system with $m = 12$ bodies (the shaded bodies plus eight rods) and with $n = 16$ revolute joints each joint having the individual degree of freedom $f = 1$. With these numbers Grübler's Eq.(4.2) yields the total degree of freedom $F = d+1$. In a much simpler interpretation each pair of rods interconnecting two shaded bodies constitutes a joint with the individual degree of freedom $f = 1$. In this interpretation the system consists of bodies 1, 2, 3, 4 and of joints 1, 2, 3, 4. With these numbers Grübler's equation yields $F = d + 1$ as before. In joint 1 the link lengths ℓ_1, r_1, a_1, r_2 represent a four-bar. Since the same is true for the other joints, the mechanism is formed by four coplanar four-bars. The link of length ℓ_1 in four-bar 1 is the fixed link. On this link the x, y reference system is fixed. The kinematics is analyzed as follows.

The links of lengths ℓ_4 and a_4 are eliminated and thereby the constraints on the x, y-coordinates of the endpoints P_1, P_2, P_3, P_4:

$$(x_2 - x_1)^2 + (y_2 - y_1)^2 - \ell_4^2 = 0\,, \qquad (x_4 - x_3)^2 + (y_4 - y_3)^2 - a_4^2 = 0\,. \quad (4.8)$$

The resulting system of four-bars 1, 2, 3 has the degree of freedom three. As independent variables the input angles φ_1, φ_2, φ_3 of these four-bars are chosen. Figure 17.1 shows that a four-bar with input angle φ_i can assume two positions with output angles ψ_{i_1} and ψ_{i_2}. Their sines and cosines are determined by (17.12) and (17.11). For four-bar 1 the equations are

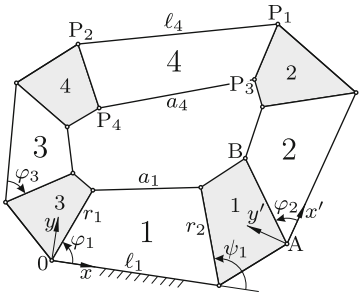

Fig. 4.5 Closed chain with planar four-bars 1, 2, 3, 4 connecting bodies 1, 2, 3, 4

$$\left.\begin{aligned} \cos\psi_{1_k} &= \frac{AC + (-1)^k B\sqrt{A^2 + B^2 - C^2}}{A^2 + B^2}\,, \\ \sin\psi_{1_k} &= \frac{BC - (-1)^k A\sqrt{A^2 + B^2 - C^2}}{A^2 + B^2} \end{aligned}\right\} \ (k = 1, 2)\,, \qquad (4.9)$$

$$\left.\begin{aligned} A &= 2r_2(\ell_1 - r_1\cos\varphi_1)\,, & B &= -2r_1r_2\sin\varphi_1\,,\\ C &= 2r_1\ell_1\cos\varphi_1 - (r_1^2+\ell_1^2+r_2^2-a_1^2)\,. \end{aligned}\right\} \tag{4.10}$$

The x,y-coordinates of the points A and B in these two positions are expressed in terms of ℓ_1, r_2, $\cos\psi_{1_k}$, $\sin\psi_{1_k}$ and of parameters specifying body 1.

The same equations, but with φ_2 as independent variable and with other parameters, determine the coordinates of P_1 and P_3 in the x',y'-system shown in the figure. As before, two different solutions exist for every angle φ_2. Transformation from the x',y'-system into the x,y-system results in expressions for the x,y-coordinates of P_1 and P_3 as functions of φ_1 and φ_2. Next, the x,y-coordinates of P_2 and P_4 are expressed as functions of φ_1 and φ_3. With minor modifications the equations are the same as for the coordinates of P_1 and P_3.

The results obtained so far are summarized as follows. Four different sets of x,y-coordinates of P_2 and P_4 are known as functions of φ_1 and φ_3, and four different sets of x,y-coordinates of P_1 and P_3 are known as functions of φ_1 and φ_2. Each of the former four sets has to be combined with each of the latter four sets. Thus, altogether sixteen combinations have to be investigated. For each combination Eqs. (4.8) are formulated. For at least one combination the degree of freedom is either $F=1$ or $F=2$. It is $F=1$ if for every φ_1 (in a certain interval) unique real solutions φ_2, φ_3 exist. It is $F=2$ if both constraint equations are identical. A combination has the degree of freedom $F=0$ if real solutions φ_2, φ_3 do not exist for any angle φ_1.

4.2.4 Trihedral Plane-Symmetric Bricard Mechanism

The mechanism shown in Fig. 4.6 is a spatial closed chain with six bodies (fixed body 0 and bodies $1,\ldots,5$) and with six revolute joints $1,\ldots,6$. The two joint axes of each body are mutually orthogonal and nonintersecting. Bodies 0, 2 and 4 are identical and bodies 1, 3 and 5 are identical. Furthermore, body 1 is a mirror image of body 0. In the position shown the bodies are inscribed in a cube with all joint axes and all common perpendiculars of adjacent joint axes aligned along edges of the cube. In this cube configuration the joint axes 1, 3, 5 form a trihedral intersecting at a single point, and the axes 2, 4, 6 form another trihedral. Furthermore, the six axes display a triple plane-symmetry. They are symmetric with respect to the plane spanned by the axes 1 and 4, to the plane spanned by the axes 2 and 5 and to the plane spanned by the axes 3 and 6.

The kinematics of the mechanism is best understood if a model is available. It can be produced from cardboard by folding bodies. The angle γ should be $30°$. From such a model it is learned that the mechanism has the

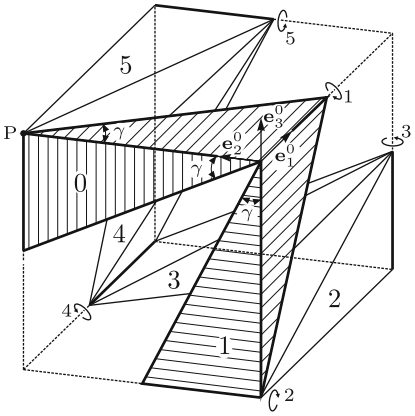

Fig. 4.6 Spatial closed chain with six bodies and six revolute joints

degree of freedom $F = 1$. Moreover, the axes 1, 3, 5 and 2, 4, 6 are permanently forming two trihedrals and also the triple plane-symmetry is preserved. These experimental results are confirmed by the following kinematics analysis (Wittenburg [7, 8]).

Equation (4.1) yields $F = d$. Hence a degree of freedom $F > 0$ exists only if at least one constraint is dependent. According to Grübler's formula there are altogether 30 constraints in the altogether six joints. It is not necessary to analyze this system of constraints. The kinematics analysis is much simpler if the joint between bodies 0 and 5 is cut. This results in a serial open chain with five joints. For this chain Grübler's formula (4.3) yields the degree of freedom $F = 5$. Reconstitution of the cut joint introduces five constraints. These are the constraints which have to be analyzed. This is done as follows. On each body i $(i = 0, \ldots, 5)$ a body-fixed basis $\underline{\mathbf{e}}^i$ is defined. In Fig. 4.6 only basis $\underline{\mathbf{e}}^0$ is shown. In the cube configuration of this figure all body-fixed bases are aligned parallel. The locations of the origins are without interest. Three of the five constraint equations express the fact that, independent of rotation angles in the joints, the chain of vectors leading from the point P on body 0 along body edges to the coincident point P on body 5 is closed. This is the vector equation

$$-\mathbf{e}_2^0 - \mathbf{e}_3^1 + \mathbf{e}_1^2 + \mathbf{e}_2^3 + \mathbf{e}_3^4 - \mathbf{e}_1^5 = \mathbf{0}\,. \tag{4.11}$$

Two more constraint equations express the fact that the vectors $\mathbf{e}_1^5$ and $\mathbf{e}_2^5$ are both orthogonal to $\mathbf{e}_3^0$:

$$\mathbf{e}_1^5 \cdot \mathbf{e}_3^0 = 0\,, \qquad \mathbf{e}_2^5 \cdot \mathbf{e}_3^0 = 0\,. \tag{4.12}$$

In order to obtain five scalar constraint equations the vectors must be decomposed in a common basis. For this purpose joint variables are defined as

follows. In joint i $(i = 1, \ldots, 5)$ φ_i is the rotation angle of body i relative to body $i-1$. Sign convention: φ_1, φ_2, φ_3 are positive and φ_4, φ_5 are negative in the case of a right-handed rotation about the basis vector in the respective joint axis. In the cube configuration all angles are zero. Let $\underline{A}_i$ be the transformation matrix for joint i defined by the equation $\underline{\mathbf{e}}^i = \underline{A}_i\, \underline{\mathbf{e}}^{i-1}$. With the abbreviations $c_i = \cos\varphi_i$, $s_i = \sin\varphi_i$ these matrices are

$$\underline{A}_1 = \begin{bmatrix} 1 & 0 & 0 \\ 0 & c_1 & s_1 \\ 0 & -s_1 & c_1 \end{bmatrix}, \quad \underline{A}_2 = \begin{bmatrix} c_2 & 0 & -s_2 \\ 0 & 1 & 0 \\ s_2 & 0 & c_2 \end{bmatrix}, \quad \underline{A}_3 = \begin{bmatrix} c_3 & s_3 & 0 \\ -s_3 & c_3 & 0 \\ 0 & 0 & 1 \end{bmatrix}, \quad \underline{A}_4 = \begin{bmatrix} 1 & 0 & 0 \\ 0 & c_4 & -s_4 \\ 0 & s_4 & c_4 \end{bmatrix}, \quad \underline{A}_5 = \begin{bmatrix} c_5 & 0 & s_5 \\ 0 & 1 & 0 \\ -s_5 & 0 & c_5 \end{bmatrix}. \tag{4.13}$$

The coordinate transformations for (4.11) and (4.12) are simplest if all vectors are decomposed either in basis $\underline{\mathbf{e}}^2$ or in $\underline{\mathbf{e}}^3$. With $\underline{\mathbf{e}}^3$ (4.11) takes the form

$$\underline{A}_3\underline{A}_2\underline{A}_1 \begin{bmatrix} 0 \\ -1 \\ 0 \end{bmatrix} + \underline{A}_3\underline{A}_2 \begin{bmatrix} 0 \\ 0 \\ -1 \end{bmatrix} + \underline{A}_3 \begin{bmatrix} 1 \\ 0 \\ 0 \end{bmatrix} + \begin{bmatrix} 0 \\ 1 \\ 0 \end{bmatrix} + \underline{A}_4^T \begin{bmatrix} 0 \\ 0 \\ 1 \end{bmatrix} + \underline{A}_4^T\,\underline{A}_5^T \begin{bmatrix} -1 \\ 0 \\ 0 \end{bmatrix} = \begin{bmatrix} 0 \\ 0 \\ 0 \end{bmatrix}. \tag{4.14}$$

These equations are

$$c_3[1 + s_2(1 - s_1)] - s_3c_1 - c_5 = 0\,, \tag{4.15}$$

$$s_3[1 + s_2(1 - s_1)] + c_3c_1 - s_4(1 - s_5) - 1 = 0\,, \tag{4.16}$$

$$c_2(1 - s_1) \qquad - c_4(1 - s_5) = 0\,. \tag{4.17}$$

Also the scalar products in (4.12) are expressed in terms of vector coordinates in $\underline{\mathbf{e}}^3$. This yields the equations

$$c_5(-c_3s_2c_1 + s_3s_1) + s_5[s_4(s_3s_2c_1 + c_3s_1) + c_4c_2c_1] = 0\,, \tag{4.18}$$

$$c_4(s_3s_2c_1 + c_3s_1) - s_4c_2c_1 \;= 0\,. \tag{4.19}$$

From experimenting with the cardboard model it is learned that in every position of the mechanism the constraint equations are satisfied:

$$\varphi_3 = \varphi_1\,, \qquad \varphi_5 = \varphi_1\,, \qquad \varphi_4 = \varphi_2\,. \tag{4.20}$$

When this is substituted, (4.15) – (4.19) become

$$\left.\begin{aligned} c_1(s_1 + s_1s_2 - s_2) &= 0\,, \\ (s_1 - 1)(s_1 + s_1s_2 - s_2) &= 0\,, \\ 0 &= 0\,, \\ c_1(1 + s_1 + s_1s_2)(s_1 + s_1s_2 - s_2) &= 0\,, \\ c_1c_2(s_1 + s_1s_2 - s_2) &= 0\,. \end{aligned}\right\} \tag{4.21}$$

These equations are satisfied if $s_1 + s_1s_2 - s_2 = 0$. This is the equation

$$\sin\varphi_2 = \frac{\sin\varphi_1}{1 - \sin\varphi_1}\,. \tag{4.22}$$

In addition to (4.20) this constitutes a fourth independent constraint equation. There are no other independent constraint equations. Hence the mechanism is overconstrained with the degree of freedom $F = 1$. As independent variable the angle φ_1 is chosen.

Remark: The constraint Eqs.(4.20) can be found without making experiments as follows. Multiply (4.16) by $c_1 c_4$, (4.17) by $-c_1 s_4$, (4.19) by $-(1 - s_1)$ and add. Simple reformulation followed by division through c_4 results in an equation relating φ_3 to φ_1:

$$(1 - s_1)c_3 = (1 - s_3)c_1 \,. \tag{4.23}$$

The equation has the solutions $\varphi_3 = \varphi_1$ and $\varphi_3 = \pi/2$. Only the first solution is useful. This is the first Eq.(4.20). Because of the equal character of all bodies and of all joints and because of the definitions of joint angles this equation holds true if the indices are increased by 1 and by 2. This yields the other two constraint equations $\varphi_4 = \varphi_2$ and $\varphi_5 = \varphi_3$. End of remark.

The relationship (4.22) is illustrated in the diagram of Fig. 4.7. Because of the conditions $|\sin\varphi_{1,2}| \leq 1$ the angles are restricted to the intervals $-210° \leq \varphi_1 \leq +30°$ and $-30° \leq \varphi_2 \leq +210°$. Motion in these intervals is possible without collision of neighboring bodies if the angle γ shown in Fig. 4.6 is $\gamma \leq 30°$. The mechanism can undergo a continuous twisting motion similar to an elastic ribbon.

Differentiation of (4.22) with respect to time yields the relationship between angular velocities:

$$\dot{\varphi}_2 = \dot{\varphi}_1 \frac{\cos\varphi_1}{(1 - \sin\varphi_1)^2 \cos\varphi_2} = \dot{\varphi}_1 \frac{\cos\varphi_1}{(1 - \sin\varphi_1)\sqrt{1 - 2\sin\varphi_1}} \,. \tag{4.24}$$

Differentiating one more time produces for the angular acceleration the expression

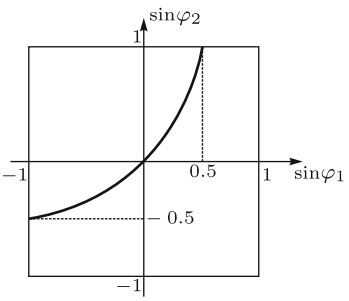

Fig. 4.7 Relationship between φ_1 and φ_2 in Fig. 4.6

$$\ddot{\varphi}_2 = \ddot{\varphi}_1 \frac{\cos\varphi_1}{(1-\sin\varphi_1)\sqrt{1-2\sin\varphi_1}} + \dot{\varphi}_1^2 \frac{2-2\sin\varphi_1-\sin^2\varphi_1}{(1-\sin\varphi_1)(1-2\sin\varphi_1)^{3/2}} \,. \quad (4.25)$$

The mechanism is highly special. A mechanism having two trihedrals of permanently intersecting axes need not be plane-symmetric, and a plane-symmetric mechanism need not be trihedral. Bricard [1] discovered a five-parametric family of trihedral mechanisms and an eight-parametric family of plane-symmetric mechanisms. These mechanisms are analyzed in Sects. 6.4.2 and 6.4.3 .

4.2.5 Line-Symmetric Bricard Mechanism

The mechanism shown in Fig. 4.8 is another spatial closed chain with six bodies (fixed body 0 and bodies $1,\ldots,5$) and with six revolute joints $1,\ldots,6$ (thick lines). The two joint axes of each body are mutually orthogonal and intersecting. In the position shown the axes are edges of a cube (dashed lines). The name of the mechanism points to the fact that the six joint axes are pairwise symmetric with respect to a line (pairs 1 and 4 , 2 and 5 , 3 and 6). In the cube configuration the line of symmetry is identified as follows. Draw in the square at the bottom of the cube the diagonal through P and give this diagonal a vertical translation by half the side length of the cube. It is obvious that a 180°-rotation about the line thus defined carries joint axis i ($i = 1,2,3$) into the position originally held by joint axis $i+3$.

A kinematics analysis is found in Pandrea [5][1]. For checking results it is helpful to have a model made of six identical pieces of cardboard.

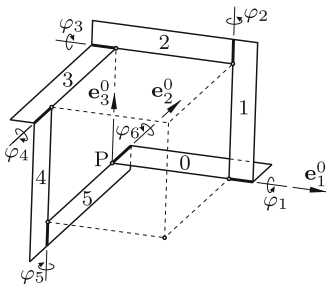

Fig. 4.8 Spatial closed chain with six bodies and six revolute joints

[1] Pandrea attributes the mechanism to Franke. In a private communication P. Dietmaier pointed out that *R. Franke: Vom Aufbau der Getriebe, v.2 (1951) Deutscher-Ingenieur-Verlag Düsseldorf* shows, without kinematics analysis, a line-symmetric mechanism in which the joint axes on the bodies are skew.

Equation (4.1) yields $F = d$. Hence a degree of freedom $F > 0$ exists only if at least one constraint is dependent. Constraint equations are formulated by a method similar to the one used in the previous section. On each body i ($i = 0, \ldots, 5$) a body-fixed basis $\underline{\mathbf{e}}^i$ is defined. In Fig. 4.8 only basis $\underline{\mathbf{e}}^0$ is shown. In the position shown in this figure all body-fixed bases are aligned parallel. Three of the five constraint equations express the fact that, independent of rotation angles in the joints, the chain of vectors leading from the point P on body 0 along body edges to the coincident point P on body 5 is closed. This is the constraint equation

$$\mathbf{e}_1^0 + \mathbf{e}_3^1 - \mathbf{e}_1^2 - \mathbf{e}_2^3 - \mathbf{e}_3^4 + \mathbf{e}_2^5 = \mathbf{0} \,. \tag{4.26}$$

Let $\underline{A}_i$ be the transformation matrix in the relationship $\underline{\mathbf{e}}^i = \underline{A}_i \underline{\mathbf{e}}^{i-1}$ ($i = 0, \ldots, 5$ cyclic). The matrices satisfy the constraint equation $\underline{A}_6 \underline{A}_5 \underline{A}_4 \underline{A}_3 \underline{A}_2 \underline{A}_1 = \underline{I}$ or

$$\underline{A}_3 \underline{A}_2 \underline{A}_1 = (\underline{A}_6 \underline{A}_5 \underline{A}_4)^T \,. \tag{4.27}$$

Every matrix $\underline{A}_i$ is a function of the rotation angle φ_i of the respective joint i. Definition: φ_i is the rotation angle of body i relative to body $i-1$ ($i = 1, \ldots, 5$) and of body 0 relative to body 5 in the case $i = 6$. Sign convention: φ_1, φ_2, φ_4 are positive and φ_3, φ_5, φ_6 are negative in the case of a right-handed rotation about the basis vector in the respective joint axis. In the configuration shown in the figure all angles are zero. With the abbreviations $c_i = \cos\varphi_i$, $s_i = \sin\varphi_i$ the matrices are

$$\left.\begin{aligned}
\underline{A}_3 &= \begin{bmatrix} 1 & 0 & 0 \\ 0 & c_3 & -s_3 \\ 0 & s_3 & c_3 \end{bmatrix}, \quad \underline{A}_2 = \begin{bmatrix} c_2 & s_2 & 0 \\ -s_2 & c_2 & 0 \\ 0 & 0 & 1 \end{bmatrix}, \quad \underline{A}_1 = \begin{bmatrix} 1 & 0 & 0 \\ 0 & c_1 & s_1 \\ 0 & -s_1 & c_1 \end{bmatrix}, \\
\underline{A}_6 &= \begin{bmatrix} c_6 & 0 & s_6 \\ 0 & 1 & 0 \\ -s_6 & 0 & c_6 \end{bmatrix}, \quad \underline{A}_5 = \begin{bmatrix} c_5 & -s_5 & 0 \\ s_5 & c_5 & 0 \\ 0 & 0 & 1 \end{bmatrix}, \quad \underline{A}_4 = \begin{bmatrix} c_4 & 0 & -s_4 \\ 0 & 1 & 0 \\ s_4 & 0 & c_4 \end{bmatrix}.
\end{aligned}\right\} \tag{4.28}$$

With these expressions (4.27) becomes

$$\begin{bmatrix} c_2 & c_1 s_2 & s_1 s_2 \\ -s_2 c_3 & c_1 c_2 c_3 + s_1 s_3 & s_1 c_2 c_3 - c_1 s_3 \\ -s_2 s_3 & c_1 c_2 s_3 - s_1 c_3 & s_1 c_2 s_3 + c_1 c_3 \end{bmatrix}$$
$$= \begin{bmatrix} c_4 c_5 c_6 + s_4 s_6 & c_4 s_5 & -c_4 c_5 s_6 + s_4 c_6 \\ -s_5 c_6 & c_5 & s_5 s_6 \\ -s_4 c_5 c_6 + c_4 s_6 & -s_4 s_5 & s_4 c_5 s_6 + c_4 c_6 \end{bmatrix} . \tag{4.29}$$

Following Pandrea the identity of matrix elements is formulated. The elements (1,2) and (2,1) yield the equations $c_1 s_2 = c_4 s_5$ and $c_3 s_2 = c_6 s_5$. They are satisfied with

$$c_4 = c_1 \,, \qquad s_5 = s_2 \,, \qquad c_6 = c_3 \,, \tag{4.30}$$

but also with $c_4 = -c_1$, $s_5 = -s_2$, $c_6 = -c_3$. In either case the signs of s_4, c_5 and s_6 are still unknown. The calculations to come reveal that the pairwise identity of all matrix elements is possible only if Eqs.(4.30) are valid in combination with

$$s_4 = -s_1 \,, \qquad c_5 = c_2 \,, \qquad s_6 = -s_3 \,. \tag{4.31}$$

Hence

$$\varphi_4 = -\varphi_1 \,, \qquad \varphi_5 = \varphi_2 \,, \qquad \varphi_6 = -\varphi_3 \,. \tag{4.32}$$

After substituting (4.30) and (4.31) into (4.29) the pairwise identity of the matrix elements (1,1) and (3,1) is formulated. This produces the equations

$$\left.\begin{array}{rl} c_1c_2c_3 & +s_1s_3 = c_2 \,, \\ s_1c_2c_3 & +(s_2 - c_1)s_3 = 0 \,. \end{array}\right\} \tag{4.33}$$

Resolving for c_3 and s_3 results in

$$c_3 = \frac{c_1 - s_2}{1 - c_1 s_2} \,, \qquad s_3 = \frac{s_1 c_2}{1 - c_1 s_2} \,. \tag{4.34}$$

By substituting these expressions the pairwise identity of all matrix elements in (4.29) is verified.

Next, (4.26) is decomposed in basis $\underline{\mathbf{e}}^3$. Using, for the moment, in (4.28) only (4.30) and (4.31) this decomposition produces the equations

$$c_2 + c_1 s_2 = 1 - s_1 \,, \tag{4.35}$$

$$c_2 - c_3 s_2 = 1 + s_3 \,, \qquad c_3 - s_2 s_3 = c_1 - s_1 s_2 \,. \tag{4.36}$$

When in (4.36) c_3 and s_3 are replaced by the expressions (4.34), these two equations are satisfied if (4.35) is satisfied. This proves the existence of a single dependent constraint. Thus, the mechanism is an overconstrained mechanism with the degree of freedom $F = 1$. Equation (4.35) has two solutions

$$\left.\begin{array}{l} c_{2_k} = \dfrac{1 - s_1 + (-1)^k c_1 \sqrt{1 + 2s_1(1 - s_1)}}{1 + c_1^2} \,, \\[2ex] s_{2_k} = \dfrac{c_1(1 - s_1) - (-1)^k \sqrt{1 + 2s_1(1 - s_1)}}{1 + c_1^2} \end{array}\right\} \quad (k = 1, 2) \,. \tag{4.37}$$

With each solution Eqs.(4.34) yield the corresponding solution φ_{3_k}. Equations (4.32) yield the remaining angles. The two pairs of solutions φ_3, φ_2 are related through the equations

$$\varphi_{3_k} = \varphi_{2_j} - \frac{\pi}{2} \qquad (k, j = 1, 2 \,;\; k \neq j) \,. \tag{4.38}$$

This is proved by substituting (4.37) into (4.34) and by verifying that $c_{3_k} = s_{2_j}$ and $s_{3_k} = -c_{2_j}$.

The square root in (4.37) is zero for $s_1 = (1 - \sqrt{3})/2$, i.e. for $\varphi_{\min} \approx -21,5°$ and for $\varphi_{\max} \approx \pi + 21,5°$. Only if φ_1 is in the interval between these bounds, the angle φ_2 is real. At the bounds the solution is $c_2 = \sqrt{3}-1$. This determines the angles $\varphi_2 \approx \pm 42,9°$. In the diagram in Fig. 4.9 φ_{2_k} and φ_{3_k} $(k = 1, 2)$ are shown as functions of φ_1. The mechanism can be assembled in two configurations. The change from one configuration to the other is achieved by opening and re-closing a single joint in such a way that body-fixed vectors along the opened joint axis have equal directions after if they have equal directions before. In Fig. 4.8 the first configuration is shown for the variable $\varphi_1 = 0$ with $\varphi_2 = \ldots = \varphi_5 = 0$. In the second configuration $\varphi_1 = 0$ is associated with $\varphi_3 = -\pi/2$, $\varphi_4 = 0$, $\varphi_2 = \varphi_5 = \varphi_6 = \pi/2$. This configuration is shown in Fig. 4.10a. It is possible to open and to re-close a single joint in such a way that the said body-fixed vectors along the joint axis reverse their relative orientation. However, this re-closing is possible in a single position only in which the system is then rigid. This position is shown in Fig. 4.10b.

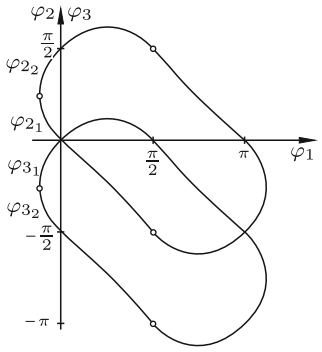

Fig. 4.9 Angles φ_{2_k} and φ_{3_k} $(k = 1, 2)$ as functions of φ_1

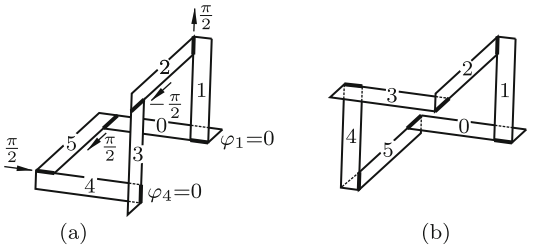

Fig. 4.10 Second mobile configuration **(a)** and rigid configuration **(b)**

Angular velocities: From (4.32) and (4.38) it follows that $\dot{\varphi}_4 = -\dot{\varphi}_1$, $\dot{\varphi}_5 = \dot{\varphi}_2$, $\dot{\varphi}_6 = -\dot{\varphi}_3$ and $\dot{\varphi}_{3_k} = \dot{\varphi}_{2_j}$ $(k, j = 1, 2;\ k \neq j)$. Therefore, it suffices to express $\dot{\varphi}_2$ in terms of $\dot{\varphi}_1$ and φ_1. Implicit differentiation of (4.35) in combination with (4.37) yields

$$\begin{aligned}\dot{\varphi}_{2_k} &= \dot{\varphi}_1 \frac{s_1 s_{2_k} - c_1}{c_1 c_{2_k} - s_{2_k}} \\ &= -\dot{\varphi}_1 \frac{(-1)^k c_1(2 - s_1) + s_1\sqrt{1 + 2s_1(1 - s_1)}}{(1 + c_1^2)\sqrt{1 + 2s_1(1 - s_1)}} \qquad (k = 1, 2). \quad (4.39)\end{aligned}$$

The mechanism is a very special case of a nine-parametric family of line-symmetric Bricard mechanisms. These mechanisms are analyzed in Sect. 6.4.1.

4.2.6 Homokinetic Shaft Coupling

The mechanism shown in Fig. 4.11 is a spatial simple closed chain $S_1R_1S_2R_2$ with an additional revolute joint R_3. The parameters are such that, in the position shown, the closed chain is symmetric with respect to the plane Σ which is bisecting the angle between links 1 and 2 (referred to as shafts 1 and 2) and containing S_1, S_2 and the point of intersection A of the revolutes R_1 and R_2 (in the figure Σ is normal to the plane of the drawing). For the entire mechanism with five bodies $0, \ldots, 4$ and with five joints Grübler's Eq.(4.4) yields the degree of freedom $F = 3$. Shaft 2 is free to change its direction in space as is indicated by arrows. In addition, shaft 1 is free to rotate about its longitudinal axis (angle of rotation φ_1). In every position of the mechanism the closed chain is symmetric with respect to the plane Σ bisecting the angle between shafts 1 and 2 and containing S_1, S_2 and A. When the direction of shaft 2 is fixed, Σ is fixed independent of φ_1. Permanent symmetry with respect to a fixed plane Σ has the consequence that both shafts have identical angular velocities: $\dot{\varphi}_2 \equiv \dot{\varphi}_1$. The results are summarized as follows. The plane-symmetric closed chain is a shaft coupling characterized by the properties

(A) the axis of shaft 2 is free to change its direction during operation

(B) $\dot{\varphi}_2/\dot{\varphi}_1 \equiv 1$ independent of φ_1 in *every* position of shaft 2 held fixed.

Shaft couplings having these two properties are called homokinetic. The combination of these properties is essential in many engineering systems. A typ-

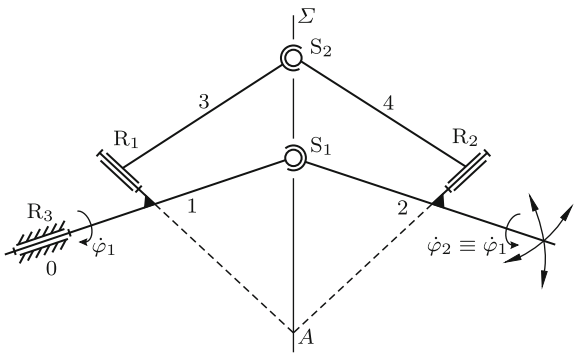

Fig. 4.11 Homokinetic shaft coupling with a plane-symmetric closed chain $S_1R_1S_2R_2$

ical example is the coupling between front wheel and drive shaft in a front-wheel driven automobile. The coupling must have property (A) since the direction of the wheel axis is changing due to steering maneuvers and to dynamic processes in the suspension system. Property (B) is necessary in order to prevent resonance vibrations in the car. The well-known Hooke's joint is a shaft coupling having property (A), but not property (B). Its ratio $\dot{\varphi}_2/\dot{\varphi}_1$ is a π-periodic function of φ_1. Only its mean value is 1. This is shown in Sect. 13.1. In the power train of a car such a source of vibrations with a frequency proportional to the speed of the car is unacceptable. It was the need for cars with front-wheel drive which triggered the development of compact and reliable homokinetic shaft couplings. See Sect. 13.4 for a more general theory.

4.2.7 Mobile Tilings

In Fig. 4.12a Q is a convex quadrilateral of arbitrary nonparallelogram-shape. By 180°-rotations about the midpoints of its sides four congruent quadrilaterals are produced. Let Q′ be one of them, and let $\mathbf{t}_1$ and $\mathbf{t}_2$ be the two diagonals as shown. By repeated translations $\mathbf{t}_1$ and $\mathbf{t}_2$ of the hexagon composed of Q and Q′ the infinite plane is filled with congruent quadrilaterals without gaps and overlaps. The individual quadrilateral is referred to as tile, and the plane-filling pattern is called tiling. The tiling is invariant with respect to periodical translations with $\mathbf{t}_1$, $\mathbf{t}_2$, $\mathbf{t}_1+\mathbf{t}_2$ and $\mathbf{t}_1-\mathbf{t}_2$. It is also invariant with respect to 180°-rotations about the midpoints of sides of quadrilaterals.

Remark: All statements made up to this point are valid also for parallelograms and for nonconvex quadrilaterals. They are also valid in the much more general case when each side of Q is replaced by an arbitrary centrally symmetric curve. More about tilings is found in Sect. 14.6.

Kokotsakis [4] recognized that a tiling made of convex quadrilaterals of arbitrary nonparallelogram-shape is a 1-d.o.f. mechanism if all quadrilaterals are rigid bodies and all sides revolute joints.

Proof (Stachel [6]): The shaded area in Fig. 4.12b is a cluster of four congruent quadrilaterals Q_1, Q_2, Q_3, Q_4 grouped around center 0_1. In what follows, it is referred to as cluster 1. When it is isolated from the surrounding quadrilaterals, it represents a spherical four-bar with constant angles α_1, α_2, α_3, α_4 and with axes along unit vectors $\mathbf{n}_1$, $\mathbf{n}_2$, $\mathbf{n}_3$, $\mathbf{n}_4$ pointing away from 0_1. Notation: α_i $(i=1,2,3,4)$ is the internal angle of Q_i at 0_1. The variable angle of rotation of Q_i relative to Q_{i-1} about $\mathbf{n}_i$ is called φ_i ($i=1,2,3,4$ cyclic; $\varphi_i=0$ in the planar position). This is the notation used in Fig. 18.1a. For a given angle φ_1 the spherical four-bar can assume two positions. Two solutions φ_4 as functions of φ_1 are determined by Eqs.(18.2),

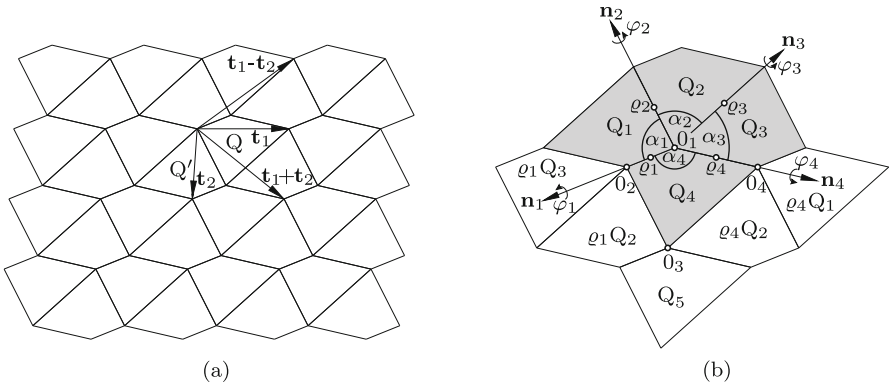

Fig. 4.12 Tiling with irregular convex quadrilaterals **(a)** and clusters of four quadrilaterals **(b)**

(18.3). With cyclic permutations of indices the same equations relate other pairs of neighboring angles so that also φ_2 and φ_3 are determined as functions of φ_1. If $(\varphi_1, \varphi_2, \varphi_3, \varphi_4)$ is a solution then, because of the symmetry to the plane, also $(-\varphi_1, -\varphi_2, -\varphi_3, -\varphi_4)$ is a solution. In what follows, $\varphi_1 > 0$ is assumed. The equations reveal the following facts. If α_4 is the largest of the four angles $\alpha_1, \alpha_2, \alpha_3, \alpha_4$, as is the case in the figure,
$\varphi_1, \varphi_2, \varphi_4 > 0$ and $\varphi_3 < 0$ in one position and
$\varphi_1, \varphi_3, \varphi_4 > 0$ and $\varphi_2 < 0$ in the other position.
These results are easily verified experimentally by folding a circular piece of paper along four radii having the directions of $\mathbf{n}_1, \mathbf{n}_2, \mathbf{n}_3, \mathbf{n}_4$ (the four sectors should be made very stiff). It is also apparent that the cluster is immobile if the quadrilateral is nonconvex.

In what follows, it is assumed that in Fig. 4.12b the shaded cluster 1 is shown deformed in one of its two possible modes $(\varphi_1, \varphi_2, \varphi_3, \varphi_4)$ with φ_1 arbitrary. Let ϱ_i denote the tensor of the 180°-rotation about the axis through the midpoint of the edge common to Q_i and Q_{i-1} which is (i) normal to $\mathbf{n}_i$ and (ii) bisecting the angle $\pi - \varphi_i$ $(i = 1, 2, 3, 4$ cyclic$)$. The rotation ϱ_i transforms Q_i into Q_{i-1} and vice versa since a 180°-rotation equals its inverse. The short-hand notation of these relationships is

$$\left.\begin{aligned} \mathrm{Q}_1 &= \varrho_1 \mathrm{Q}_4 \,, \qquad & \mathrm{Q}_4 &= \varrho_1 \mathrm{Q}_1 = \varrho_1 \varrho_2 \mathrm{Q}_2 \,, \\ \mathrm{Q}_3 &= \varrho_4 \mathrm{Q}_4 \,, \qquad & \mathrm{Q}_4 &= \varrho_4 \mathrm{Q}_3 = \varrho_4 \varrho_3 \mathrm{Q}_2 \end{aligned}\right\} \tag{4.40}$$

and, consequently,

$$\varrho_4 \varrho_3 = \varrho_1 \varrho_2 \,. \tag{4.41}$$

By applying ϱ_1 to the entire cluster 1 the overlapping congruent cluster 2 with center 0_2 and with new quadrilaterals $\varrho_1 \mathrm{Q}_2$ and $\varrho_1 \mathrm{Q}_3$ is obtained. Likewise, applying ϱ_4 to cluster 1 the overlapping congruent cluster 4 with

center 0_4 and with new quadrilaterals $\varrho_4 Q_1$ and $\varrho_4 Q_2$ is obtained. Proposition: The three quadrilaterals $\varrho_1 Q_2$, Q_4 and $\varrho_4 Q_2$ are obtained by subjecting Q_1, Q_2 and Q_3, respectively, to the rotation ϱ_2 followed by the rotation ϱ_1, i.e., $\varrho_1 Q_2 = \varrho_1 \varrho_2 Q_1$, $Q_4 = \varrho_1 \varrho_2 Q_2$, $\varrho_4 Q_2 = \varrho_1 \varrho_2 Q_3$. Proof: The first equation is true since $Q_2 = \varrho_2 Q_1$. The second equation is one of Eqs.(4.40). The third equation follows from $\varrho_4 Q_3 = \varrho_4 \varrho_3 Q_4$ in combination with (4.41). End of proof. From this it follows that the cluster 3 formed by the quadrilaterals $\varrho_1 Q_3$, Q_1, $\varrho_4 Q_3$ and Q_5 with center 0_3 is also congruent with cluster 1 and that it is the result of the said rotations. By applying the same procedure successively infinitely many clusters can be added in all directions, all clusters being congruent with cluster 1 independent of the deformation of cluster 1. This ends the proof of mobility with degree of freedom one.

Taking ϱ_1 as example, the 180°-rotations are expressed analytically as follows. It suffices to know the angle φ_1 of the rotation $(\mathbf{n}_1, \varphi_1)$ and the position vectors $\mathbf{r}_i$ $(i = 1, 2, 3)$ of the corners 0_1, 0_2, 0_3 of Q_4 in some arbitrarily chosen reference system. These data determine the midpoint $\mathbf{r}_A = (\mathbf{r}_1 + \mathbf{r}_2)/2$ on the edge and the unit vector $\mathbf{n}_1 = (\mathbf{r}_2 - \mathbf{r}_1)/|\mathbf{r}_2 - \mathbf{r}_1|$ of the rotation $(\mathbf{n}_1, \varphi_1)$. The auxiliary vector $\boldsymbol{\varrho} = \mathbf{r}_3 - \mathbf{r}_1$ determines the unit vector $\mathbf{e} = (\boldsymbol{\varrho} - \mathbf{n}_1 \, \mathbf{n}_1 \cdot \boldsymbol{\varrho})/|\boldsymbol{\varrho} - \mathbf{n}_1 \, \mathbf{n}_1 \cdot \boldsymbol{\varrho})|$ in the plane of Q_4 and normal to $\mathbf{n}_1$. The vectors $\mathbf{n}_1$ and $\mathbf{e}$ and the angle φ_1 determine the unit vector $\mathbf{n}$ along the axis of the 180°-rotation ϱ_1:

$$\mathbf{n} = \mathbf{e} \sin \frac{\varphi_1}{2} - \mathbf{n}_1 \times \mathbf{e} \cos \frac{\varphi_1}{2} \, . \tag{4.42}$$

According to (3.17) the relationship between the positions $\mathbf{r}$ and $\mathbf{r}^*$ of an arbitrary point before and after the 180°-rotation ϱ_1 is

$$\mathbf{r}^* = 2\mathbf{r}_A - \mathbf{r} + 2\mathbf{n} \, \mathbf{n} \cdot (\mathbf{r} - \mathbf{r}_A) \, . \tag{4.43}$$

Formulas for the rotations ϱ_2, ϱ_3 and ϱ_4 are obtained by cyclic permutation of indices.

References

1. Bricard R (1926/27) Leçons de cinématique. v.I.: Cinématique théorique. v.II: Cinématique appliquée. Gauthier-Villars, Paris
2. Dimentberg F M (1948) A general method for the investigation of finite displacements of spatial mechanisms and certain cases of passive constraints (Russ.) Trudy Seminara po Teorii Mashin i Mechanismov, AN SSSR 5 Nr.17:5–39; Purdue Translation No.436, Purdue Univ.
3. Grübler M (1917) Getriebelehre. Eine Theorie des Zwanglaufes und der ebenen Mechanismen. Springer, Berlin
4. Kokotsakis A (1932) Über bewegliche Polyeder. Math.Ann.107,627–647
5. Pandrea N I (2000) Elemente de mecanica solidelor in coordonate Plückeriene. Editura Acad. Romane

6. Stachel H (2009) Remarks on Miura-Ori, a Japanese folding method. Proc. Int.Conf.Eng. Graphics and Design, TU Cluc-Napoca
7. Wittenburg J (1977) Dynamics of systems of rigid bodies. Teubner Stuttgart
8. Wittenburg J (2007) Dynamics of multibody systems. Springer, Berlin Heidelberg New York

Chapter 5
Spatial Simple Closed Chains

Subject of this chapter is the kinematics of 1-d.o.f. spatial simple closed chains with axial joints. The simple closed chain is explained in Fig. 4.1b. Axial joints are the cylindrical joint (C), the revolute joint (R) and the prismatic joint (P). Overconstrained mechanisms are excluded from consideration. Then it is known from Theorem 4.1 that a 1-d.o.f. spatial simple closed chain has seven joint variables. The variable of either one revolute joint or one prismatic joint is declared independent. The problem to be solved is to determine the six dependent variables in terms of the independent variable and of constant mechanism parameters. The solution to this problem is of great engineering importance because 1-d.o.f. spatial simple closed chains are basic elements of machine mechanisms.

A simple closed chain is specified by the ordered sequence of letters C, R and P of its joints. Neither cyclic permutation of the sequence of letters nor reversal of the sequence changes the mechanism. Thus, the sequences RCPRC, CPRCR and CRPCR represent one and the same mechanism whereas the sequence CCRRP represents a different mechanism with the same set of joints. The sequence of letters does not tell which joint variable is considered as independent variable.

Let n_{C}, n_{R} and n_{P} be the numbers of cylindrical, of revolute and of prismatic joints, respectively. Important characteristic numbers are the total number n_{φ} of angular variables, the total number n_{t} of translatory variables and the total number n of joints and of bodies. These numbers are

$$n_{\varphi} = n_{\mathrm{C}} + n_{\mathrm{R}} \,, \qquad n_{\mathrm{t}} = n_{\mathrm{C}} + n_{\mathrm{P}} = 7 - n_{\varphi} \,, \qquad n = n_{\mathrm{C}} + n_{\mathrm{R}} + n_{\mathrm{P}} \,. \quad (5.1)$$

The numbers n_{C}, n_{R} and n_{P} are subject to the constraint $n_{\varphi} + n_{\mathrm{t}} = 2n_{\mathrm{C}} + n_{\mathrm{R}} + n_{\mathrm{P}} = 7$ and also to the constraint $n_{\varphi} = n_{\mathrm{C}} + n_{\mathrm{R}} > 3$ because with three or fewer rotation axes no change of angular positions is possible. An equivalent formulation is $n_{\mathrm{t}} = n_{\mathrm{C}} + n_{\mathrm{P}} \leq 3$. It expresses the fact that three is the maximum number of independent translations. Under these constraints

J. Wittenburg, *Kinematics*, DOI 10.1007/978-3-662-48487-6_5

Table 5.1 Numbers n_C, n_R, n_P, n_φ, n and associated mechanisms. Symmetrical forms printed boldface. N_φ and N_t are the numbers of configurations for a given value of the independent variable in a revolute joint and in a prismatic joint, respectively

	n_C	n_R	n_P	n_φ	n	mechanisms	N_φ	N_t
1	3	1	0	4	4	RCCC	2	–
2	2	2	1	4	5	RCPRC, CCPRR, **RCPCR**	2	4,8,8
3	1	3	2	4	6	RRRPPC, RRRPCP, RPRPCR, RPRCRP, RPRCPR	2	8
4	0	4	3	4	7	**RRPPPRR**, **RPRPRPR**, **PRRPRRP**, RRRPRPP	2	8
5	2	3	0	5	5	**RCRCR**, **CRRRC**	4*), 8	–
6	1	4	1	5	6	RRCRPR, RRCPRR, RRCRRP	8	16
7	0	5	2	5	7	**PRRRRRP**, **RPRRRPR**, **RRPRPRR**	8	16
8	1	5	0	6	6	5R-C	16	–
9	0	6	1	6	7	**6R-P**	16	16
10	0	7	0	7	7	**7R**	16	–

*) $N_\varphi = 4$ configurations exist if (i) the mechanism is $\underline{R}CRC\underline{R}$ and (ii) the independent angle is in one of the underscored revolutes. $N_\varphi = 8$ otherwise

altogether ten combinations of numbers n_C, n_R and n_P are possible. They are listed in Table 5.1 in the order of increasing numbers n_φ. For each combination the complete list of mechanisms with the respective combination is given. Whenever possible the letter sequence is shown in a form symmetrical to the central letter. Symmetrical letter sequences are printed boldface. The numbers N_φ and N_t in the last columns are results of the kinematics analysis to come. N_φ is the number of configurations which a mechanism has for a given value of the independent angular variable in a revolute joint, and N_t is the number of configurations which a mechanism has for a given value of the independent translatory variable in a prismatic joint. The planar four-bar mechanism is known to have two configurations for a given value of the input crank angle. The mechanisms in Table 5.1 have two or four or eight or sixteen configurations.

About the relationship between N_φ and N_t the following can be said without any analysis. Let the angular and the translatory variable in a cylindrical joint λ be called φ_λ and h_λ, respectively. If joint λ is a prismatic joint, φ_λ is a constant φ^*_λ and h_λ is variable. If joint λ is a revolute joint, φ_λ is variable and h_λ is a constant h^*_λ. Imagine now two mechanisms I and II with the only difference that joint λ is a prismatic joint in mechanism I and a revolute joint in mechanism II. Furthermore, it is assumed that the independent variables are chosen such that in both mechanisms $h_\lambda = h^*_\lambda$ and $\varphi_\lambda = \varphi^*_\lambda$. Then both mechanisms are identical in this position of their joint λ. Consequently, both mechanisms have the same sets of solutions for the six dependent variables. This means that N_t for mechanism I equals N_φ for mechanism II. This equality is shown in Table 5.1. By replacing in a mechanism of row 2, 3, 4, 6, 7 or 9 a prismatic joint by a revolute joint a

mechanism of row 5, 6, 7, 8, 9 or 10, respectively, is produced. The number N_t for the former equals the number N_φ for the latter.

Before starting the kinematics analysis joint variables and mechanism parameters must be defined. This is the subject of the following Sect. 5.1. Section 5.2 is devoted to coordinate transformations of relevant vectors. In Sect. 5.3 on closure conditions basic equations are formulated for the kinematics analysis. The application of these equations to the mechanisms of Table 5.1 is demonstrated in Sect. 5.4.

5.1 Joint Variables. Denavit-Hartenberg Parameters

A single-loop mechanism with n bodies has n joints ($4 \le n \le 7$). Bodies as well as joints are labeled from 1 to n in such a way that the joint axes i and $i+1$ are located on body i ($i = 1, \ldots, n$ cyclic). Figure 5.1 shows the bodies $i-1$, i and $i+1$ together with their joint axes. The most general case is assumed that the two joint axes of each body are skew. Then the two joint axes of each body i have a common normal which is fixed on the respective body i. The joint axis i is, in turn, the common normal of the thus defined common normals on bodies $i-1$ and i. On the joint axis i the dual unit line vector $\hat{\mathbf{n}}_i$ is defined, and on the common normal of the joint axes i and $i+1$, i.e., also fixed on body i, the dual unit line vector $\hat{\mathbf{a}}_i$ is defined ($i = 1, \ldots, n$).

The unit line vector $\hat{\mathbf{n}}_{i+1}$ is produced from $\hat{\mathbf{n}}_i$ by a screw displacement with $\hat{\mathbf{a}}_i$ being the screw axis. As shown in Fig. 5.1 the rotation angle about the screw axis is called α_i and the translation along the screw axis is called ℓ_i. These two constants (positive or negative) are the only kinematical parameters of body i. Together they define the constant dual screw angle

$$\hat{\alpha}_i = \alpha_i + \varepsilon \ell_i \,. \tag{5.2}$$

In the same way the unit line vector $\hat{\mathbf{a}}_i$ is produced from $\hat{\mathbf{a}}_{i-1}$ by a screw displacement with the screw axis $\hat{\mathbf{n}}_i$ and with a dual screw angle

$$\hat{\varphi}_i = \varphi_i + \varepsilon h_i \,. \tag{5.3}$$

Figure 5.1 shows also φ_i and h_i. In a cylindrical joint φ_i and h_i are joint variables. In a revolute joint h_i is a constant parameter and only φ_i is variable. In a prismatic joint φ_i is a constant parameter and h_i is variable. The constant h_i in a revolute joint is referred to as *offset*. The $4n$ quantities α_i, ℓ_i, φ_i, h_i ($i = 1, \ldots, n$) are the so-called *Denavit-Hartenberg parameters* of the mechanism (see Denavit/Hartenberg [3]). Seven among them are variables, and $4n-7$ are constant system parameters. The number of con-

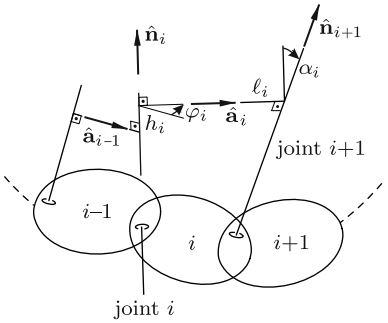

Fig. 5.1 Bodies $i-1$, i and $i+1$ with joint axes. Dual unit line vectors, body parameters and joint variables

stant system parameters ranges between nine for the mechanism RCCC and twenty-one for all mechanisms with $n = 7$.

The n line vectors $h_i\hat{\mathbf{n}}_i$ and the n line vectors $\ell_i\hat{\mathbf{a}}_i$ $(i = 1, \ldots, n)$ create a mobile spatial polygon with right angles at every corner. Analyzing the mechanism means analyzing this polygon.

The assumption that consecutive joint axes i and $i + 1$ are skew can now be dropped. If they intersect, then $\ell_i = 0$, $\hat{\alpha}_i = \alpha_i$, and the unit line vector $\hat{\mathbf{a}}_i$ is along the common normal of the joint axes through their point of intersection. If the axes of three consecutive revolutes $i - 1$, i and $i + 1$ intersect at a single point, these axes are equivalent to a spherical joint S located at this point. Example: The mechanism RRSRR is a special case of the mechanism 7R .

If two consecutive joint axes i and $i + 1$ are parallel, then $\alpha_i = 0$. The common normal to the joint axes can be placed such that either $h_i = 0$ or $h_{i+1} = 0$.

5.2 Screw Displacements. Coordinate Transformations

This section is devoted to screw displacements in the mobile spatial polygon spanned be the line vectors $h_i\hat{\mathbf{n}}_i$ and $\ell_i\hat{\mathbf{a}}_i$ $(i = 1, \ldots, n)$. The screw displacements relating $\hat{\mathbf{n}}_i$ to $\hat{\mathbf{n}}_{i+1}$ and $\hat{\mathbf{a}}_{i+1}$ to $\hat{\mathbf{a}}_i$ are described by the equations

$$\hat{\mathbf{n}}_{i+1} = \hat{\mathbf{n}}_i \cos\hat{\alpha}_i + \hat{\mathbf{a}}_i \times \hat{\mathbf{n}}_i \sin\hat{\alpha}_i \,, \qquad \hat{\mathbf{a}}_i = \hat{\mathbf{a}}_{i-1} \cos\hat{\varphi}_i + \hat{\mathbf{n}}_i \times \hat{\mathbf{a}}_{i-1} \sin\hat{\varphi}_i \,. \quad (5.4)$$

This is the dualized form of (1.125) which describes the rotation shown in Fig. 1.5 . For a more compact formulation the following abbreviations are introduced:

$$\hat{C}_i = \cos\hat{\alpha}_i\ , \qquad \hat{S}_i = \sin\hat{\alpha}_i\ , \qquad \hat{c}_i = \cos\hat{\varphi}_i\ , \qquad \hat{s}_i = \sin\hat{\varphi}_i \tag{5.5}$$

$(i = 1, \ldots, n$ cyclic) . The equations then read (in the second equation all indices are increased by one):

$$\hat{\mathbf{n}}_{i+1} = \hat{C}_i\hat{\mathbf{n}}_i + \hat{S}_i\hat{\mathbf{a}}_i \times \hat{\mathbf{n}}_i\ , \qquad \hat{\mathbf{a}}_{i+1} = \hat{c}_{i+1}\hat{\mathbf{a}}_i + \hat{s}_{i+1}\hat{\mathbf{n}}_{i+1} \times \hat{\mathbf{a}}_i \tag{5.6}$$

$(i = 1, \ldots, n$ cyclic) . On an *indeterminate* body k of the mechanism a dual cartesian basis is defined with unit basis vectors

$$\hat{\mathbf{e}}_1 = \hat{\mathbf{n}}_k\ , \qquad \hat{\mathbf{e}}_2 = \hat{\mathbf{a}}_k\ , \qquad \hat{\mathbf{e}}_3 = \hat{\mathbf{n}}_k \times \hat{\mathbf{a}}_k\ . \tag{5.7}$$

Equations (5.6) constitute two-step recursion formulas for the coordinate decomposition of all vectors $\hat{\mathbf{n}}_{k+j}$ and $\hat{\mathbf{a}}_{k+j}$ $(j = 1, 2, \ldots)$ in this basis. From $\hat{\mathbf{a}}_k$ and $\hat{\mathbf{n}}_{k+1}$

$$\begin{aligned}\hat{\mathbf{a}}_{k+1} &= \hat{c}_{k+1}\hat{\mathbf{a}}_k + \hat{s}_{k+1}(\hat{C}_k\hat{\mathbf{n}}_k + \hat{S}_k\hat{\mathbf{a}}_k \times \hat{\mathbf{n}}_k) \times \hat{\mathbf{a}}_k \\ &= \hat{s}_{k+1}\hat{S}_k\hat{\mathbf{n}}_k + \hat{c}_{k+1}\hat{\mathbf{a}}_k + \hat{s}_{k+1}\hat{C}_k\hat{\mathbf{n}}_k \times \hat{\mathbf{a}}_k\ .\end{aligned} \tag{5.8}$$

From $\hat{\mathbf{a}}_{k+1}$ and $\hat{\mathbf{n}}_{k+1}$

$$\begin{aligned}\hat{\mathbf{n}}_{k+2} &= \hat{C}_{k+1}\hat{\mathbf{n}}_{k+1} + \hat{S}_{k+1}\hat{\mathbf{a}}_{k+1} \times \hat{\mathbf{n}}_{k+1} \\ &= (\hat{C}_{k+1}\hat{C}_k - \hat{S}_{k+1}\hat{S}_k\hat{c}_{k+1})\hat{\mathbf{n}}_k + \hat{S}_{k+1}\hat{s}_{k+1}\hat{\mathbf{a}}_k \\ &\quad -(\hat{C}_{k+1}\hat{S}_k + \hat{S}_{k+1}\hat{C}_k\hat{c}_{k+1})\hat{\mathbf{n}}_k \times \hat{\mathbf{a}}_k\ .\end{aligned} \tag{5.9}$$

In the next step $\hat{\mathbf{a}}_{k+2}$ and $\hat{\mathbf{n}}_{k+3}$ are calculated by increasing in (5.8) and (5.9) all indices by one and by substituting for $\hat{\mathbf{a}}_{k+1}$ and $\hat{\mathbf{n}}_{k+2}$ the previous formulas. Formulas for $\hat{\mathbf{n}}_{k+4}$ and $\hat{\mathbf{a}}_{k+4}$ are obtained with the least effort if in the expressions for $\hat{\mathbf{n}}_{k+2}$ and $\hat{\mathbf{a}}_{k+2}$ all indices are increased by two. Example:

$$\begin{aligned}\hat{\mathbf{n}}_{k+4} = \quad & (\hat{C}_{k+3}\hat{C}_{k+2} - \hat{S}_{k+3}\hat{S}_{k+2}\hat{c}_{k+3})\hat{\mathbf{n}}_{k+2} + \hat{S}_{k+3}\hat{s}_{k+3}\hat{\mathbf{a}}_{k+2} \\ & -(\hat{C}_{k+3}\hat{S}_{k+2} + \hat{S}_{k+3}\hat{C}_{k+2}\hat{c}_{k+3})\hat{\mathbf{n}}_{k+2} \times \hat{\mathbf{a}}_{k+2}\ .\end{aligned} \tag{5.10}$$

Into this expression the previously obtained expressions for $\hat{\mathbf{n}}_{k+2}$ and $\hat{\mathbf{a}}_{k+2}$ are substituted. Every expression thus obtained is linear with respect to every sine and to every cosine involved. Products sine × cosine of one and the same angle do not appear.

From the coordinates of the vectors $\hat{\mathbf{n}}_{k+j}$ and $\hat{\mathbf{a}}_{k+j}$ (j arbitrary) in the basis (5.7) the coordinates of $\hat{\mathbf{n}}_{k-j}$ and $\hat{\mathbf{a}}_{k-j}$ are obtained by a change of symbols. This is shown as follows. Inversion of the relationships (5.4) is achieved by reversing the sign of the dual angle:

$$\hat{\mathbf{n}}_i = \hat{\mathbf{n}}_{i+1}\cos\hat{\alpha}_i - \hat{\mathbf{a}}_i \times \hat{\mathbf{n}}_{i+1}\sin\hat{\alpha}_i\ , \qquad \hat{\mathbf{a}}_{i-1} = \hat{\mathbf{a}}_i\cos\hat{\varphi}_i - \hat{\mathbf{n}}_i \times \hat{\mathbf{a}}_i\sin\hat{\varphi}_i\ . \tag{5.11}$$

With (5.5) these are the equations (in the first equation all indices are decreased by one)

$$\hat{\mathbf{n}}_{i-1} = \hat{C}_{i-1}\hat{\mathbf{n}}_i - \hat{S}_{i-1}\hat{\mathbf{a}}_{i-1} \times \hat{\mathbf{n}}_i \,, \qquad \hat{\mathbf{a}}_{i-1} = \hat{c}_i\hat{\mathbf{a}}_i - \hat{s}_i\hat{\mathbf{n}}_i \times \hat{\mathbf{a}}_i \,. \tag{5.12}$$

Comparison with (5.6) reveals: For arbitrary j the coordinates of $\hat{\mathbf{n}}_{k+j}$ in the basis (5.7) become those of $\hat{\mathbf{a}}_{k-j}$ and vice versa if (i) $\hat{\mathbf{e}}_1$ and $\hat{\mathbf{e}}_2$ are interchanged, (ii) j is replaced by $-j$ and (iii) $\hat{\alpha}$ and $\hat{\varphi}$ are interchanged.

Table 5.2 contains the coordinates of all vectors $\hat{\mathbf{n}}_{k\pm j}$ and $\hat{\mathbf{a}}_{k\pm j}$ (k arbitrary; $j = 0, 1, 2, 3$) and of $\hat{\mathbf{n}}_{k+4}$ and $\hat{\mathbf{a}}_{k-4}$. The table is used for calculating sums and products of vectors. It greatly simplifies the kinematics analysis of simple closed chains in this chapter. In Chap. 6 it is applied to overconstrained closed chains and in Chap. 7 to serial chains. When the symbol $\hat{}$ is deleted everywhere, the table gives the coordinates of first Plücker vectors $\mathbf{n}_{k\pm j}$ and $\mathbf{a}_{k\pm j}$.

Table 5.2 Vector coordinates in the dual basis with unit vectors $\hat{\mathbf{e}}_1 = \hat{\mathbf{n}}_k$, $\hat{\mathbf{e}}_2 = \hat{\mathbf{a}}_k$, $\hat{\mathbf{e}}_3 = \hat{\mathbf{n}}_k \times \hat{\mathbf{a}}_k$. The three coordinates of each vector are separated by semicolons. $\hat{C}_i = \cos\hat{\alpha}_i$, $\hat{S}_i = \sin\hat{\alpha}_i$, $\hat{c}_i = \cos\hat{\varphi}_i$, $\hat{s}_i = \sin\hat{\varphi}_i$

$\hat{\mathbf{n}}_k$	$[1 \;;\; 0 \;;\; 0]$
$\hat{\mathbf{a}}_k$	$[0 \;;\; 1 \;;\; 0]$
$\hat{\mathbf{n}}_{k+1}$	$[\hat{C}_k \;;\; 0 \;;\; -\hat{S}_k]$
$\hat{\mathbf{a}}_{k-1}$	$[0 \;;\; \hat{c}_k \;;\; -\hat{s}_k]$
$\hat{\mathbf{a}}_{k+1}$	$[\hat{s}_{k+1}\hat{S}_k \;;\; \hat{c}_{k+1} \;;\; \hat{s}_{k+1}\hat{C}_k]$
$\hat{\mathbf{n}}_{k-1}$	$[\hat{C}_{k-1} \;;\; \hat{S}_{k-1}\hat{s}_k \;;\; \hat{S}_{k-1}\hat{c}_k]$
$\hat{\mathbf{n}}_{k+2}$	$[\hat{C}_{k+1}\hat{C}_k - \hat{S}_{k+1}\hat{S}_k\hat{c}_{k+1} \;;\; \hat{S}_{k+1}\hat{s}_{k+1} \;;\; -(\hat{C}_{k+1}\hat{S}_k + \hat{S}_{k+1}\hat{C}_k\hat{c}_{k+1})]$
$\hat{\mathbf{a}}_{k-2}$	$[\hat{s}_{k-1}\hat{S}_{k-1} \;;\; \hat{c}_{k-1}\hat{c}_k - \hat{s}_{k-1}\hat{s}_k\hat{C}_{k-1} \;;\; -(\hat{c}_{k-1}\hat{s}_k + \hat{s}_{k-1}\hat{c}_k\hat{C}_{k-1})]$
$\hat{\mathbf{a}}_{k+2}$	$[\hat{c}_{k+2}\hat{s}_{k+1}\hat{S}_k + \hat{s}_{k+2}(\hat{S}_{k+1}\hat{C}_k + \hat{C}_{k+1}\hat{S}_k\hat{c}_{k+1}) \;;\; \hat{c}_{k+2}\hat{c}_{k+1} - \hat{s}_{k+2}\hat{s}_{k+1}\hat{C}_{k+1} \;;$ $\hat{c}_{k+2}\hat{s}_{k+1}\hat{C}_k - \hat{s}_{k+2}(\hat{S}_{k+1}\hat{S}_k - \hat{C}_{k+1}\hat{C}_k\hat{c}_{k+1})]$
$\hat{\mathbf{n}}_{k-2}$	$[\hat{C}_{k-2}\hat{C}_{k-1} - \hat{S}_{k-2}\hat{S}_{k-1}\hat{c}_{k-1} \;;\; \hat{C}_{k-2}\hat{S}_{k-1}\hat{s}_k + \hat{S}_{k-2}(\hat{s}_{k-1}\hat{c}_k + \hat{c}_{k-1}\hat{s}_k\hat{C}_{k-1}) \;;$ $\hat{C}_{k-2}\hat{S}_{k-1}\hat{c}_k - \hat{S}_{k-2}(\hat{s}_{k-1}\hat{s}_k - \hat{c}_{k-1}\hat{c}_k\hat{C}_{k-1})]$
$\hat{\mathbf{n}}_{k+3}$	$\Big[\; \hat{C}_{k+2}(\hat{C}_{k+1}\hat{C}_k - \hat{S}_{k+1}\hat{S}_k\hat{c}_{k+1}) + \hat{S}_{k+2}[\hat{s}_{k+2}\hat{s}_{k+1}\hat{S}_k$ $-\hat{c}_{k+2}(\hat{S}_{k+1}\hat{C}_k + \hat{C}_{k+1}\hat{S}_k\hat{c}_{k+1})] \;;$ $\hat{C}_{k+2}\hat{S}_{k+1}\hat{s}_{k+1} + \hat{S}_{k+2}(\hat{s}_{k+2}\hat{c}_{k+1} + \hat{c}_{k+2}\hat{s}_{k+1}\hat{C}_{k+1}) \;;$ $-\hat{C}_{k+2}(\hat{C}_{k+1}\hat{S}_k + \hat{S}_{k+1}\hat{C}_k\hat{c}_{k+1}) + \hat{S}_{k+2}[\hat{s}_{k+2}\hat{s}_{k+1}\hat{C}_k$ $+\hat{c}_{k+2}(\hat{S}_{k+1}\hat{S}_k - \hat{C}_{k+1}\hat{C}_k\hat{c}_{k+1})]\Big]$

Table 5.2 continued

$$
\begin{aligned}
\hat{\mathbf{a}}_{k-3}\ &\Big[\ \hat{c}_{k-2}\hat{s}_{k-1}\hat{S}_{k-1}+\hat{s}_{k-2}(\hat{S}_{k-2}\hat{C}_{k-1}+\hat{C}_{k-2}\hat{S}_{k-1}\hat{c}_{k-1})\quad;\\
&\quad\hat{c}_{k-2}(\hat{c}_{k-1}\hat{c}_k-\hat{s}_{k-1}\hat{s}_k\hat{C}_{k-1})\\
&+\hat{s}_{k-2}[\hat{S}_{k-2}\hat{S}_{k-1}\hat{s}_k-\hat{C}_{k-2}(\hat{s}_{k-1}\hat{c}_k+\hat{c}_{k-1}\hat{s}_k\hat{C}_{k-1})]\quad;\\
&-\hat{c}_{k-2}(\hat{c}_{k-1}\hat{s}_k+\hat{s}_{k-1}\hat{c}_k\hat{C}_{k-1})\\
&+\hat{s}_{k-2}[\hat{S}_{k-2}\hat{S}_{k-1}\hat{c}_k+\hat{C}_{k-2}(\hat{s}_{k-1}\hat{s}_k-\hat{c}_{k-1}\hat{c}_k\hat{C}_{k-1})]\Big]\\
\hat{\mathbf{a}}_{k+3}\ &\Big\{\ \hat{c}_{k+3}[\hat{c}_{k+2}\hat{s}_{k+1}\hat{S}_k+\hat{s}_{k+2}(\hat{S}_{k+1}\hat{C}_k+\hat{C}_{k+1}\hat{S}_k\hat{c}_{k+1})]\\
&-\hat{s}_{k+3}\Big[\hat{C}_{k+2}[\hat{s}_{k+2}\hat{s}_{k+1}\hat{S}_k-\hat{c}_{k+2}(\hat{S}_{k+1}\hat{C}_k+\hat{C}_{k+1}\hat{S}_k\hat{c}_{k+1})]\\
&-\hat{S}_{k+2}(\hat{C}_{k+1}\hat{C}_k-\hat{S}_{k+1}\hat{S}_k\hat{c}_{k+1})\Big]\ ;\\
&\quad\hat{s}_{k+3}[\hat{S}_{k+2}\hat{S}_{k+1}\hat{s}_{k+1}-\hat{C}_{k+2}(\hat{s}_{k+2}\hat{c}_{k+1}+\hat{c}_{k+2}\hat{s}_{k+1}\hat{C}_{k+1})]\\
&+\hat{c}_{k+3}(\hat{c}_{k+2}\hat{c}_{k+1}-\hat{s}_{k+2}\hat{s}_{k+1}\hat{C}_{k+1})\quad;\quad\hat{c}_{k+3}[\hat{c}_{k+2}\hat{s}_{k+1}\hat{C}_k\\
&-\hat{s}_{k+2}(\hat{S}_{k+1}\hat{S}_k-\hat{C}_{k+1}\hat{C}_k\hat{c}_{k+1})]-\hat{s}_{k+3}\Big[\hat{C}_{k+2}[\hat{s}_{k+2}\hat{s}_{k+1}\hat{C}_k\\
&+\hat{c}_{k+2}(\hat{S}_{k+1}\hat{S}_k-\hat{C}_{k+1}\hat{C}_k\hat{c}_{k+1})]+\hat{S}_{k+2}(\hat{C}_{k+1}\hat{S}_k+\hat{S}_{k+1}\hat{C}_k\hat{c}_{k+1})\Big]\Big\}\\
\hat{\mathbf{n}}_{k-3}\ &\Big\{\ \hat{S}_{k-3}[\hat{s}_{k-2}\hat{s}_{k-1}\hat{S}_{k-1}-\hat{c}_{k-2}(\hat{S}_{k-2}\hat{C}_{k-1}+\hat{C}_{k-2}\hat{S}_{k-1}\hat{c}_{k-1})]\\
&+\hat{C}_{k-3}(\hat{C}_{k-2}\hat{C}_{k-1}-\hat{S}_{k-2}\hat{S}_{k-1}\hat{c}_{k-1})\quad;\quad\hat{C}_{k-3}[\hat{C}_{k-2}\hat{S}_{k-1}\hat{s}_k\\
&+\hat{S}_{k-2}(\hat{s}_{k-1}\hat{c}_k+\hat{c}_{k-1}\hat{s}_k\hat{C}_{k-1})]-\hat{S}_{k-3}\Big[\hat{c}_{k-2}[\hat{S}_{k-2}\hat{S}_{k-1}\hat{s}_k\\
&-\hat{C}_{k-2}(\hat{s}_{k-1}\hat{c}_k+\hat{c}_{k-1}\hat{s}_k\hat{C}_{k-1})]-\hat{s}_{k-2}(\hat{c}_{k-1}\hat{c}_k-\hat{s}_{k-1}\hat{s}_k\hat{C}_{k-1})\Big]\ ;\\
&\quad\hat{C}_{k-3}[\hat{C}_{k-2}\hat{S}_{k-1}\hat{c}_k-\hat{S}_{k-2}(\hat{s}_{k-1}\hat{s}_k-\hat{c}_{k-1}\hat{c}_k\hat{C}_{k-1})]\\
&-\hat{S}_{k-3}\Big[\hat{c}_{k-2}[\hat{S}_{k-2}\hat{S}_{k-1}\hat{c}_k+\hat{C}_{k-2}(\hat{s}_{k-1}\hat{s}_k-\hat{c}_{k-1}\hat{c}_k\hat{C}_{k-1})]\\
&+\hat{s}_{k-2}(\hat{c}_{k-1}\hat{s}_k+\hat{s}_{k-1}\hat{c}_k\hat{C}_{k-1})\Big]\Big\}\\
\hline
\hat{\mathbf{n}}_{k+4}\ &\Big\{(\hat{C}_{k+3}\hat{C}_{k+2}-\hat{S}_{k+3}\hat{S}_{k+2}\hat{c}_{k+3})(\hat{C}_{k+1}\hat{C}_k-\hat{S}_{k+1}\hat{S}_k\hat{c}_{k+1})\\
&+\hat{S}_{k+3}\hat{s}_{k+3}[\hat{c}_{k+2}\hat{s}_{k+1}\hat{S}_k+\hat{s}_{k+2}(\hat{S}_{k+1}\hat{C}_k+\hat{C}_{k+1}\hat{S}_k\hat{c}_{k+1})]\\
&+(\hat{C}_{k+3}\hat{S}_{k+2}+\hat{S}_{k+3}\hat{C}_{k+2}\hat{c}_{k+3})[\hat{s}_{k+2}\hat{s}_{k+1}\hat{S}_k\\
&-\hat{c}_{k+2}(\hat{S}_{k+1}\hat{C}_k+\hat{C}_{k+1}\hat{S}_k\hat{c}_{k+1})]\ ;\\
&\quad(\hat{C}_{k+3}\hat{C}_{k+2}-\hat{S}_{k+3}\hat{S}_{k+2}\hat{c}_{k+3})\hat{S}_{k+1}\hat{s}_{k+1}\\
&+\hat{S}_{k+3}\hat{s}_{k+3}(\hat{c}_{k+2}\hat{c}_{k+1}-\hat{s}_{k+2}\hat{s}_{k+1}\hat{C}_{k+1})\\
&+(\hat{C}_{k+3}\hat{S}_{k+2}+\hat{S}_{k+3}\hat{C}_{k+2}\hat{c}_{k+3})(\hat{s}_{k+2}\hat{c}_{k+1}+\hat{c}_{k+2}\hat{s}_{k+1}\hat{C}_{k+1})\quad;\\
&-(\hat{C}_{k+3}\hat{C}_{k+2}-\hat{S}_{k+3}\hat{S}_{k+2}\hat{c}_{k+3})(\hat{C}_{k+1}\hat{S}_k+\hat{S}_{k+1}\hat{C}_k\hat{c}_{k+1})\\
&+\hat{S}_{k+3}\hat{s}_{k+3}[\hat{c}_{k+2}\hat{s}_{k+1}\hat{C}_k-\hat{s}_{k+2}(\hat{S}_{k+1}\hat{S}_k-\hat{C}_{k+1}\hat{C}_k\hat{c}_{k+1})]\\
&+(\hat{C}_{k+3}\hat{S}_{k+2}+\hat{S}_{k+3}\hat{C}_{k+2}\hat{c}_{k+3})[\hat{s}_{k+2}\hat{s}_{k+1}\hat{C}_k\\
&+\hat{c}_{k+2}(\hat{S}_{k+1}\hat{S}_k-\hat{C}_{k+1}\hat{C}_k\hat{c}_{k+1})]\Big\}\\
\hat{\mathbf{a}}_{k-4}\ &\Big\{\ (\hat{c}_{k-3}\hat{c}_{k-2}-\hat{s}_{k-3}\hat{s}_{k-2}\hat{C}_{k-3})\hat{s}_{k-1}\hat{S}_{k-1}\\
&+\hat{s}_{k-3}\hat{S}_{k-3}(\hat{C}_{k-2}\hat{C}_{k-1}-\hat{S}_{k-2}\hat{S}_{k-1}\hat{c}_{k-1})\\
&+(\hat{c}_{k-3}\hat{s}_{k-2}+\hat{s}_{k-3}\hat{c}_{k-2}\hat{C}_{k-3})(\hat{S}_{k-2}\hat{C}_{k-1}+\hat{C}_{k-2}\hat{S}_{k-1}\hat{c}_{k-1})\quad;\\
&\quad(\hat{c}_{k-3}\hat{c}_{k-2}-\hat{s}_{k-3}\hat{s}_{k-2}\hat{C}_{k-3})(\hat{c}_{k-1}\hat{c}_k-\hat{s}_{k-1}\hat{s}_k\hat{C}_{k-1})\\
&+\hat{s}_{k-3}\hat{S}_{k-3}[\hat{C}_{k-2}\hat{S}_{k-1}\hat{s}_k+\hat{S}_{k-2}(\hat{s}_{k-1}\hat{c}_k+\hat{c}_{k-1}\hat{s}_k\hat{C}_{k-1})]\\
&+(\hat{c}_{k-3}\hat{s}_{k-2}+\hat{s}_{k-3}\hat{c}_{k-2}\hat{C}_{k-3})[\hat{S}_{k-2}\hat{S}_{k-1}\hat{s}_k\\
&-\hat{C}_{k-2}(\hat{s}_{k-1}\hat{c}_k+\hat{c}_{k-1}\hat{s}_k\hat{C}_{k-1})]\quad;\\
&-(\hat{c}_{k-3}\hat{c}_{k-2}-\hat{s}_{k-3}\hat{s}_{k-2}\hat{C}_{k-3})(\hat{c}_{k-1}\hat{s}_k+\hat{s}_{k-1}\hat{c}_k\hat{C}_{k-1})\\
&+\hat{s}_{k-3}\hat{S}_{k-3}[\hat{C}_{k-2}\hat{S}_{k-1}\hat{c}_k-\hat{S}_{k-2}(\hat{s}_{k-1}\hat{s}_k-\hat{c}_{k-1}\hat{c}_k\hat{C}_{k-1})]\\
&+(\hat{c}_{k-3}\hat{s}_{k-2}+\hat{s}_{k-3}\hat{c}_{k-2}\hat{C}_{k-3})[\hat{S}_{k-2}\hat{S}_{k-1}\hat{c}_k\\
&+\hat{C}_{k-2}(\hat{s}_{k-1}\hat{s}_k-\hat{c}_{k-1}\hat{c}_k\hat{C}_{k-1})]\Big\}
\end{aligned}
$$

5.3 Closure Conditions

Having defined variables and parameters and having established basic relationships in the mobile spatial polygon of vectors $h_i\hat{\mathbf{n}}_i + \ell_i\hat{\mathbf{a}}_i \;\; (i = 1, \ldots, n)$ we can finally turn to the kinematics problem of this chapter: Determine six dependent variables of a single-loop mechanism in terms of a single independent variable. For this purpose six scalar equations relating the altogether seven variables are required. Any such equation is called closure condition because it expresses the closure of the kinematical loop. Closure conditions are highly nonlinear. Therefore, it is not useful to formulate six fully coupled equations. It is essential to formulate a set of $m < 6$ equations for m unknowns with m being as small as possible. Once these equations are solved for the m unknowns it is simple to express the remaining $6 - m$ unknowns one by one in terms of previously determined unknowns. In the literature various methods for formulating closure conditions are found:
Yang [40] – [42], Duffy [4] – [8], Duffy/Crane [9], Yuan [44], Yuan/Freudenstein/Woo [45], [46], Dukkipati/Soni [13], Dukkipati [14], Soni/Pamidi [35], Soni [36], Lee [20, 27], Lee/Liang [21] – [24], Liang/Lee/Liao [28], Woernle [39], Lee/Woernle/Hiller [26], Raghavan/Roth [32], Lee/Roth [25], Nielsen/Roth [30], Crane/Duffy [2] and others. Many more references are found in [15]. An historical overview is found in Peisach [31].

In what follows, methods developed by Woernle [39] and Lee [27] are used. They lead to a minimal set of either $m = 1$ or $m = 2$ or $m = 4$ coupled equations depending on the type of mechanism. The formulations presented appeared in Wittenburg [47].

5.3.1 Woernle-Lee Equations

Figure 5.2 shows schematically the polygon of dual-vectors of a single-loop mechanism. Actually, only the vectors associated with two specific joints labeled a and b are shown. The rest of the polygon is indicated by dashed lines. How to choose the joints a and b is explained later. These joints divide the mechanism into a *left segment* and a *right segment*. The ordinary vector $\mathbf{r}$ shown in the figure joins the axes a and b. This vector has two representations. One as a sum of vectors fixed on bodies of the left segment and one as a sum of vectors fixed on bodies of the right segment. The vectors are the primary parts of dual vectors. The two representations are

$$\mathbf{r} = \begin{cases} -(h_b\mathbf{n}_b + \ell_b\mathbf{a}_b + h_{b+1}\mathbf{n}_{b+1} + \ldots + \ell_{a-1}\mathbf{a}_{a-1}) & \text{(left segment)} \\ h_a\mathbf{n}_a + \ell_a\mathbf{a}_a + h_{a+1}\mathbf{n}_{a+1} + \ldots + \ell_{b-1}\mathbf{a}_{b-1} & \text{(right segment)} \,. \end{cases} \tag{5.13}$$

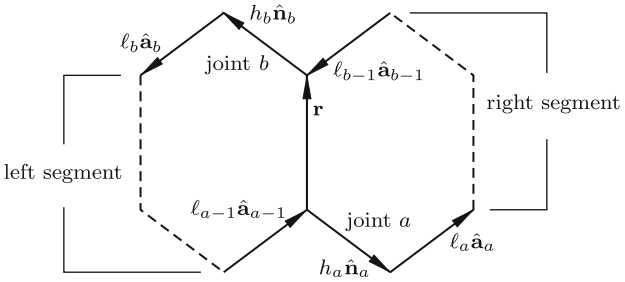

Fig. 5.2 Segments of a mechanism defined by two joints a and b

In the particular case $b = a+1$ the joints a and b are direct neighbors. In this case, the vector $\mathbf{r}$ in the right segment is $\mathbf{r} = h_a\mathbf{n}_a + \ell_a\mathbf{a}_a$. If the axes a and $a+1$ are nonparallel, then $\mathbf{a}_a = (1/S_a)(\mathbf{n}_a \times \mathbf{n}_{a+1})$ (see Fig. 5.2). In this case, (5.13) has the special form

$$\mathbf{r} = \begin{cases} -(h_{a+1}\mathbf{n}_{a+1} + \ell_{a+1}\mathbf{a}_{a+1} + \ldots + \ell_{a-1}\mathbf{a}_{a-1}) & \text{(left segment)} \\ h_a\mathbf{n}_a + \dfrac{\ell_a}{S_a}(\mathbf{n}_a \times \mathbf{n}_{a+1}) & \text{(right segment)}\,. \end{cases} \tag{5.14}$$

In terms of $\mathbf{n}_a$, $\mathbf{n}_b$ and $\mathbf{r}$ seven scalar quantities $F_1, \ldots, F_7$ are defined as follows:

$$\left.\begin{array}{ll} F_1 = \mathbf{n}_a \cdot \mathbf{n}_b\,, & F_2 = \mathbf{r} \cdot \mathbf{n}_a \times \mathbf{n}_b\,, \\ F_3 = \mathbf{n}_a \cdot \mathbf{r}\,, & F_4 = \mathbf{n}_b \cdot \mathbf{r}\,, \\ F_5 = \mathbf{r} \cdot \mathbf{n}_p \times \mathbf{n}_q & (\mathbf{r} \text{ from (5.14)};\ p \neq q \text{ arbitrary})\,, \\ F_6 = \mathbf{r}^2\,, & F_7 = \frac{1}{2}(\mathbf{n}_a \cdot \mathbf{n}_b)\mathbf{r}^2 - (\mathbf{n}_a \cdot \mathbf{r})(\mathbf{n}_b \cdot \mathbf{r}) \\ & \quad = \frac{1}{2}F_1F_6 - F_3F_4\,. \end{array}\right\} \tag{5.15}$$

The scalars F_1 and F_2 represent the primary part and the dual part, respectively, of the dual scalar product $\hat{\mathbf{n}}_a \cdot \hat{\mathbf{n}}_b$. The primary part is calculated with coordinates from Table 5.2 (without the symbol $\hat{}$). The dual part is calculated not as product $\mathbf{r}\cdot\mathbf{n}_a\times\mathbf{n}_b$, but as dual derivative of F_1 (see (3.50)). The MAPLE software tool developed by Sinigersky [34] has special routines for switching back and forth between the ordinary notation $\cos\alpha$, $\sin\alpha$, $\cos\varphi$, $\sin\varphi$ and the short-hand notation C, S, c, s. Dual differentiation is carried out automatically. By combining Table 5.2 with this tool kinematics equations for mechanisms can be formulated semi-automatically.

Each of the scalar quantities $F_1, \ldots, F_7$ is expressed in the left segment as function of variables and in the right segment as another function of variables. These functions are called F_k^ℓ and F_k^r $(k = 1, \ldots, 7)$. The equality of both scalars establishes the seven Woernle-Lee equations

$$F_k^\ell = F_k^r \qquad (k = 1, \ldots, 7)\,. \tag{5.16}$$

These equations have properties which make them useful as closure conditions. The most important properties are the following:
- the parameters φ_a and φ_b do not appear explicitly in any of the equations $F_k^\ell = F_k^r \quad (k = 1, \ldots, 7)$. This is a consequence of the fact that each of the vectors $\mathbf{n}_a$ and $\mathbf{n}_b$ is fixed on a body of the left segment and also fixed on a body of the right segment
- the parameters h_a and h_b do not appear explicitly in the equation $F_2^\ell = F_2^r$. This is a consequence of the fact that this equation is the dual derivative of the equation $F_1^\ell = F_1^r$.

From these properties the following criteria for choosing the joints a and b are derived. The joint combination ab is
- CC in mechanisms with two or three cylindrical joints (rows 1, 2, 5 of Table 5.1)
- CR in mechanisms with one cylindrical joint (rows 3, 6, 8)
- RR in all other mechanisms
- the angles φ_a and φ_b must be dependent variables.

This choice of joints has the consequence that the maximum possible number of dependent variables is eliminated from the equations. The properties of the equations $F_1^\ell = F_1^r$ and $F_2^\ell = F_2^r$ can now be stated in more detail as follows. The equation $F_1^\ell = F_1^r$ is an equation in terms of *angular* Denavit-Hartenberg parameters only. Every sine and every cosine appears in linear form only. Products sine $\times$ cosine of one and the same angle do not appear.

The independent variable is either the angle in a specific revolute joint or the translatory variable in a specific prismatic joint. Until further below *it is assumed to be an angle*. The mechanisms in Table 5.1 have a total number n_φ of angular variables in the range $4 \le n_\varphi \le 7$. With one of them being independent and with φ_a and φ_b being eliminated the equation $F_1^\ell = F_1^r$ is an equation for $1 \le n_\varphi - 3 \le 4$ unknown angular variables.

Unknowns in the equation $F_2^\ell = F_2^r$ are the same $n_\varphi - 3$ angular variables and, in addition, ν translatory variables. The number ν is the difference between the total number $n_\mathrm{t} = n_\mathrm{C} + n_\mathrm{P}$ of translatory variables and the number of cylindrical joints among the joints a and b. This formula yields $\nu = 1$ for the mechanism RCCC and $\nu = n_\mathrm{P}$ for all other mechanisms. Table 5.1 shows that ν is in the range $0 \le \nu \le 3$. The translatory variables and the sines and cosines of angular variables appear in linear form only. The mechanisms in rows 5, 8 and 10 of Table 5.1 have angular variables only $(\nu = 0)$. For these mechanisms the equation $F_2^\ell = F_2^r$ has, with other coefficients, the same form as the equation $F_1^\ell = F_1^r$.

Let b be the larger of the indices a and b so that $1 \le a < b \le n$ and $b = a + d$ with $d > 0$. Because of the cyclic repetition of the indices $1, \ldots, n$ the identity holds: $b \equiv b - n = a + d - n$. With this identity the equation $F_1^\ell = F_1^r$ is written in the form

$$\mathbf{n}_k \cdot \mathbf{n}_{k+d} = \mathbf{n}_k \cdot \mathbf{n}_{k+d-n} \qquad (k = a)\,. \tag{5.17}$$

Example: In the case $a = 3$, $b = 6$, $n = 7$, the equation is $\mathbf{n}_k \cdot \mathbf{n}_{k+3} = \mathbf{n}_k \cdot \mathbf{n}_{k-4}$ with $k = 3$. The product $\mathbf{n}_k \cdot \mathbf{n}_{k+3}$ is found in Table 5.2 as first coordinate of the vector $\mathbf{n}_{k+3}$ with $k = 3$. It is a function of φ_4 and φ_5. For the product $\mathbf{n}_k \cdot \mathbf{n}_{k-4}$ the vector $\mathbf{n}_{k-4}$ is not found in the table. The table suffices, however, because the product has the alternative form $\mathbf{n}_{k-2} \cdot \mathbf{n}_{k+2}$ with $k = 1$. It is a function of $\varphi_{k-1} = \varphi_0 \equiv \varphi_7$, $\varphi_k = \varphi_1$ and $\varphi_{k+1} = \varphi_2$. For details see the right-hand side of (5.82). End of example.

Mechanisms with $n_\varphi = 4$: Let φ_1 and φ_λ be the independent and the dependent angular variable, respectively. The equation $F_1^\ell = F_1^r$ is

$$Ac_\lambda + Bs_\lambda = R\,. \tag{5.18}$$

The coefficients A, B and R are functions of φ_1. For every value of φ_1 the equation has two (not necessarily real) solutions φ_λ. This is an important result. It means that the mechanisms in rows 1 to 4 of Table 5.1 have two different configurations for every value of the independent angular variable. This is the number N_φ shown in Table 5.1.

Dual differentiation of (5.18) produces the equation $F_2^\ell = F_2^r$:

$$(A' + h_\lambda B)c_\lambda + (B' - h_\lambda A)s_\lambda = R'\,, \tag{5.19}$$

where A', B', R' are the dual derivatives of A, of B and of R, respectively. Since φ_λ is known from (5.18), this equation is a linear equation for $\nu = 1$ or 2 or 3 translatory variables. The mechanisms in rows 1 and 2 of Table 5.1 with $\nu = 1$ are the simplest mechanisms. Equation (5.19) determines the single translatory variable. For the mechanism RCCC this is shown in detail in Sect. 5.4.1.

Mechanisms with $n_\varphi = 5$: These are the mechanisms in rows 5, 6 and 7 of Table 5.1. Let φ_λ and φ_μ be the two dependent angular variables. The equation $F_1^\ell = F_1^r$ has either the form

$$A_2c_\lambda + B_2s_\lambda = A_1c_\mu + B_1s_\mu + R_1 \tag{5.20}$$

or the form

$$\underline{A}\,[\,c_\lambda c_\mu \quad c_\lambda s_\mu \quad c_\lambda \quad s_\lambda c_\mu \quad s_\lambda s_\mu \quad s_\lambda \quad c_\mu \quad s_\mu \quad 1\,]^T = 0\,. \tag{5.21}$$

The coefficients A_1, B_1, R_1, A_2, B_2 and the row matrix $\underline{A}$ are functions of the independent variable. Equation (5.20) occurs if the joints λ and μ belong to different segments created by the cylindrical joints, and (5.21) occurs if they belong to one and the same segment.

Unknowns in the equation $F_2^\ell = F_2^r$ are the same angles φ_λ and φ_μ and, in addition, $\nu = 0$ or 1 or 2 translatory variables. For the mechanisms RCRCR and CRRRC with $\nu = 0$ the equations $F_2^\ell = F_2^r$ and $F_1^\ell = F_1^r$

have identical forms, i.e., either the form (5.20) or the form (5.21). Both equations together determine φ_λ and φ_μ. Details see in Sect. 5.4.2.

The mechanisms in rows 6 and 7 of Table 5.1: It will be seen that the equation $F_5^\ell = F_5^r$ has the form (5.21) for the same unknowns φ_λ and φ_μ. Thus, all mechanisms with $n_\varphi = 5$ are governed either by two Eqs.(5.20) or by two Eqs.(5.21). Once the two unknowns φ_λ and φ_μ are determined the equation $F_2^\ell = F_2^r$ represents a linear equation for $\nu = 1$ or $\nu = 2$ unknown translatory variables.

Mechanisms with $n_\varphi = 6$: The only mechanisms of this type are the mechanisms 5R-C and 6R-P. The joints a and b (a cylindrical and a revolute joint or two revolute joints) are chosen such that two dependent angular variables are in one segment and the third dependent angular variable together with the independent variable is in the other. Let φ_λ, φ_μ and φ_ν be the dependent variables. The matrix form of the equation $F_1^\ell = F_1^r$ is

$$\underline{A}\,[\; c_\nu \quad s_\nu \;]^T = \underline{B}\,[\; c_\lambda c_\mu \quad c_\lambda s_\mu \quad c_\lambda \quad s_\lambda c_\mu \quad s_\lambda s_\mu \quad s_\lambda \quad c_\mu \quad s_\mu \quad 1 \;]^T \,. \tag{5.22}$$

The row matrices $\underline{A}$ and $\underline{B}$ are either constant or functions of the independent variable. The equation $F_2^\ell = F_2^r$ for the mechanism 5R-C has the same form with other coefficient matrices $\underline{A}$ and $\underline{B}$.

In the equation $F_2^\ell = F_2^r$ for a mechanism 6R-P the unknown translatory variable of the prismatic joint appears in addition to the three unknown angular variables. If this translatory variable is called h_κ, the equation has the form

$$\begin{aligned} &\underline{A}\,[\; c_\nu \quad s_\nu \quad h_\kappa c_\nu \quad h_\kappa s_\nu \quad h_\kappa \;]^T \\ &= \underline{B}\,[\; c_\lambda c_\mu \quad c_\lambda s_\mu \quad c_\lambda \quad s_\lambda c_\mu \quad s_\lambda s_\mu \quad s_\lambda \quad c_\mu \quad s_\mu \quad 1 \;]^T \,. \end{aligned} \tag{5.23}$$

Mechanisms with $n_\varphi = 7$: The only mechanism of this type is the mechanism 7R. The joints a and b are chosen such that two dependent angular variables are in each segment. Let φ_7 be the independent variable. Then $a = 3$, $b = 6$ is a possible choice. The four dependent variables are φ_1, φ_2, φ_4 and φ_5. The equation $F_1^\ell = F_1^r$ is known already from the example given for Eq.(5.17). Its matrix form is

$$\begin{aligned} &\underline{A}\,[\; c_4c_5 \quad c_4s_5 \quad c_4 \quad s_4c_5 \quad s_4s_5 \quad s_4 \quad c_5 \quad s_5 \;]^T \\ &= \underline{B}\,[\; c_1c_2 \quad c_1s_2 \quad c_1 \quad s_1c_2 \quad s_1s_2 \quad s_1 \quad c_2 \quad s_2 \quad 1 \;]^T \,. \end{aligned} \tag{5.24}$$

The row matrix $\underline{A}$ is constant, and $\underline{B}$ is a function of φ_7. The equation $F_2^\ell = F_2^r$ has the same form with other coefficient matrices $\underline{A}$ and $\underline{B}$. Details see in Sect. 5.4.7.

The equations $F_3^\ell = F_3^r$ *and* $F_4^\ell = F_4^r$
Unknowns in these equations are the same $1 \le n_\varphi - 3 \le 4$ angular variables which appear in the equations $F_1^\ell = F_1^r$ and $F_2^\ell = F_2^r$ and, in addition,

all translatory variables including h_a and h_b (constant parameter or variable). In the equations for the mechanisms in rows 3, 4, 8 and 9 the total number of variables is four, so that these two equations together with the equations $F_1^\ell = F_1^r$ and $F_2^\ell = F_2^r$ represent a system of four equations for four unknowns.

The mechanisms in rows 3 and 4: The equation $F_1^\ell = F_1^r$ is Eq.(5.18). With each of its two solutions the other three equations are coupled linear equations for three unknown translatory variables.

The mechanisms 5R-C and 6R-P: Unknowns are three angular and one translatory variable. The equations $F_3^\ell = F_3^r$ and $F_4^\ell = F_4^r$ have the form (5.23), and the equations $F_1^\ell = F_1^r$ and $F_2^\ell = F_2^r$ have the form (5.22).

The mechanism 7R: The four unknowns are angular variables. The four equations $F_k^\ell = F_k^r$ $(k = 1, 2, 3, 4)$ have the form (5.24).

The equation $F_5^\ell = F_5^r$

This equation is formulated only for the mechanisms in rows 6 and 7 of Table 5.1. These mechanisms have $n_\varphi = 5$ angular variables and either $n = 6$ joints with one cylindrical and one prismatic joint or $n = 7$ joints with two prismatic joints. These joints are the only ones with translatory variables. They are chosen as joints p and q in the expression $F_5 = \mathbf{r} \cdot \mathbf{n}_p \times \mathbf{n}_q$. With (5.14) for $\mathbf{r}$ the equation $F_5^\ell = F_5^r$ is

$$\begin{aligned} &- (h_{a+1}\mathbf{n}_{a+1} + \ell_{a+1}\mathbf{a}_{a+1} + \ldots + \ell_{a-1}\mathbf{a}_{a-1} + h_a\mathbf{n}_a) \cdot (\mathbf{n}_p \times \mathbf{n}_q) \\ &= \frac{\ell_a}{S_a} (\mathbf{n}_a \times \mathbf{n}_{a+1}) \cdot (\mathbf{n}_p \times \mathbf{n}_q) \\ &= \frac{\ell_a}{S_a} [(\mathbf{n}_a \times \mathbf{n}_p) \cdot (\mathbf{n}_{a+1} \times \mathbf{n}_q) - (\mathbf{n}_a \times \mathbf{n}_q) \cdot (\mathbf{n}_{a+1} \times \mathbf{n}_p)] \,. \end{aligned} \tag{5.25}$$

The vectors $h_p\mathbf{n}_p$ and $h_q\mathbf{n}_q$ are among the vectors indicated by dots. Multiplication with $(\mathbf{n}_p \times \mathbf{n}_q)$ eliminates the variables h_p and h_q. The angular variables in the joints a and $a+1$ are eliminated as well. This means that only two dependent angular variables appear explicitly. Let them be denoted φ_λ and φ_μ. Then the equation has the form

$$\underline{A} \, [\, c_\lambda c_\mu \quad c_\lambda s_\mu \quad c_\lambda \quad s_\lambda c_\mu \quad s_\lambda s_\mu \quad s_\lambda \quad c_\mu \quad s_\mu \quad 1 \,]^T = 0 \,. \tag{5.26}$$

This is, with a different coefficient matrix $\underline{A}$, the form of the equation $F_1^\ell = F_1^r$ (see (5.21)). In both equations the unknowns φ_λ and φ_μ are the same if the joints a and $b = a+1$ are the same.

It remains to be shown how to generate the coefficient matrix $\underline{A}$ in (5.26) with the help of Table 5.2. First, the left-hand side of (5.25) is considered. It is a linear combination of products $\mathbf{n}_\ell \cdot \mathbf{n}_p \times \mathbf{n}_q$ $(\ell \neq p, q$ arbitrary) and $\mathbf{a}_\ell \cdot \mathbf{n}_p \times \mathbf{n}_q$ $(\ell \neq a$ arbitrary). Every product is evaluated as (3×3)-determinant of vector coordinates copied from Table 5.2. The goal is to formulate the determinant such that the angles φ_a and φ_{a+1} do not appear

explicitly, and that s_λ, c_λ, s_μ, c_μ appear in linear form only. This goal is achieved if the determinant is evaluated in three steps as follows.

Step 1: To those of the indices ℓ, p and q which are smaller than or equal to a the number n is added ($n = 6$ or $n = 7$). The new indices are called ℓ', p' and q'.

Step 2: The new indices ℓ', p' and q' are brought into a monotonically increasing order. One of them is the central index. To this index the name k is given. The other two indices are $k - d_1$ and $k + d_2$ with $d_1, d_2 \geq 0$.

Step 3: The rows of the (3×3)-determinant are the coordinates of the vectors with indices k, $k-d_1$ and $k+d_2$. These coordinates are copied from Table 5.2. The vector with the index k is either $\mathbf{n}_k$ with the coordinates $[1 \quad 0 \quad 0]$ or $\mathbf{a}_k$ with the coordinates $[0 \quad 1 \quad 0]$. With either one of these forms the determinant is reduced to a (2×2)-determinant. The coordinates of the vectors with indices $k - d_1$ and $k + d_2$ are linear with respect to c_λ, s_λ, c_μ and s_μ. The variables φ_a and φ_{a+1} do not appear.

Example: For a mechanism with $n = 7$ joints the product $\mathbf{a}_1 \cdot \mathbf{n}_5 \times \mathbf{n}_6$ is to be expressed such that the variables φ_a and φ_{a+1} with $a = 4$ do not appear explicitly.

Solution: The given indices are $\ell = 1 < a$, $p = 5 > a$ and $q = 6 > a$. Hence $\ell' = \ell + n = 8$, $p' = 5$, $q' = 6$. The desired form of the product is

$$\underbrace{\mathbf{a}_{k+2} \cdot \mathbf{n}_{k-1} \times \mathbf{n}_k}_{k=6}$$
$$= S_5 c_6 (c_1 c_7 - s_1 s_7 C_7) - S_5 s_6 [c_1 s_7 C_6 - s_1 (S_7 S_6 - C_7 C_6 c_7)] \,. \quad (5.27)$$

End of example.

For the left-hand side expression of (5.25) considered so far the desired form (free of φ_a and φ_{a+1} and linear in the sines and cosines of the remaining three angles) is possible no matter which angle is chosen as φ_a. For the right-hand side expression this choice is not arbitrary. For both sides the angle dictated by the right-hand side is chosen. The rule for choosing joint a is explained, first, for the mechanisms in row 6 with one prismatic joint and one cylindrical joint. Let the cylindrical joint be joint q. One of the joints a and $a+1$ must be the cylindrical joint q, and the other must be a revolute joint with a dependent angular variable. This allocation is possible no matter in which revolute joint the independent variable is located. In the case $a = q$, the right-hand side of (5.25) is

$$\frac{\ell_a}{S_a} \left(C_a \mathbf{n}_p \cdot \mathbf{n}_q - \mathbf{n}_p \cdot \mathbf{n}_{a+1} \right) . \quad (5.28)$$

In the case $a + 1 = q$, the right-hand side of (5.25) is

$$-\frac{\ell_a}{S_a}\left(C_a\mathbf{n}_p\cdot\mathbf{n}_q-\mathbf{n}_a\cdot\mathbf{n}_p\right). \tag{5.29}$$

In either case Table 5.2 yields an expression with the desired linearity properties.

Next, the mechanisms with two prismatic joints p and q are considered. The joints a and $a+1$ must be revolute joints with dependent angular variables, and one of them must be neighbor of a prismatic joint (p or q). This allocation is possible no matter in which revolute joint the independent variable is located. Since each of the two prismatic joints can be joint p, it suffices to distinguish whether joint a or joint $a+1$ is neighbor of joint p. If joint a is neighbor of joint p, then $a=p+1$ and $\mathbf{n}_a\times\mathbf{n}_p=-S_p\mathbf{a}_p$ and $\mathbf{n}_a\cdot\mathbf{n}_p=C_p$. The right-hand side of (5.25) is

$$\frac{\ell_a}{S_a}\left(-S_p\mathbf{a}_p\cdot\mathbf{n}_{a+1}\times\mathbf{n}_q-C_a\mathbf{n}_p\cdot\mathbf{n}_q+C_p\mathbf{n}_q\cdot\mathbf{n}_{a+1}\right). \tag{5.30}$$

If joint $a+1$ is neighbor of joint p, then $p=a+2$ and $\mathbf{n}_{a+1}\times\mathbf{n}_p=-S_{a+1}\mathbf{a}_{a+1}$ and $\mathbf{n}_p\cdot\mathbf{n}_{a+1}=C_{a+1}$. The right-hand side of (5.25) is

$$\frac{\ell_a}{S_a}\left(C_a\mathbf{n}_p\cdot\mathbf{n}_q-C_{a+1}\mathbf{n}_a\cdot\mathbf{n}_q+\mathbf{n}_a\times\mathbf{n}_q\cdot S_{a+1}\mathbf{a}_{a+1}\right). \tag{5.31}$$

In either case Table 5.2 yields an expression with the desired linearity properties. The products $\mathbf{a}_p\cdot\mathbf{n}_{a+1}\times\mathbf{n}_q$ and $\mathbf{n}_a\times\mathbf{n}_q\cdot\mathbf{a}_{a+1}$ are evaluated as determinants.

The equations $F_6^\ell=F_6^r$ *and* $F_7^\ell=F_7^r$
These equations are formulated only for the mechanism 7R which has angular variables only. In every scalar product appearing in the expressions for $\mathbf{r}^2$ every sine and every cosine appears in linear form only. Products sine × cosine of one and the same angle do not appear. If as joints a and b the joints 3 and 6 are chosen again, the equation $F_6^\ell=F_6^r$ has the form (5.24). Only the coefficient matrices are different.

Surprisingly, also the equation $F_7^\ell=F_7^r$ has the form (5.24) (with other coefficient matrices). In spite of the definition $F_7=\frac{1}{2}F_1F_6-F_3F_4$ the functions F_7^ℓ and F_7^r are both linear with respect to the sines and cosines of angles. For the function F_7^r this is proved as follows. With (5.13) for $\mathbf{r}$ the function F_7^r is a linear combination of products h_ih_j, $h_i\ell_j$ and $\ell_i\ell_j$ with $a\le i,j\le b$. As an example the coefficient of h_ih_j with $i\le j$ is considered. This coefficient denoted H_{ij} is

$$H_{ij}=(\mathbf{n}_a\cdot\mathbf{n}_b)(\mathbf{n}_i\cdot\mathbf{n}_j)-(\mathbf{n}_a\cdot\mathbf{n}_i)(\mathbf{n}_b\cdot\mathbf{n}_j)-(\mathbf{n}_a\cdot\mathbf{n}_j)(\mathbf{n}_b\cdot\mathbf{n}_i) \tag{5.32}$$

$$=(\mathbf{n}_a\times\mathbf{n}_i)\cdot(\mathbf{n}_b\times\mathbf{n}_j)-(\mathbf{n}_a\cdot\mathbf{n}_i)(\mathbf{n}_b\cdot\mathbf{n}_j)\qquad(a\le i\le j\le b). \tag{5.33}$$

The products $(\mathbf{n}_a\times\mathbf{n}_i)$ and $(\mathbf{n}_a\cdot\mathbf{n}_i)$ are linear with respect to the sines and cosines of angles between bodies a and i, and the products $(\mathbf{n}_b\times\mathbf{n}_j)$ and

$(\mathbf{n}_b \cdot \mathbf{n}_j)$ are linear with respect to the sines and cosines of angles between bodies b and j. From this follows the linearity of H_{ij} with respect to the sines and cosines of all angles. For other terms of F_7^r and for F_7^ℓ similar arguments hold. End of proof.

The discussion of Woernle-Lee equations is summarized as follows.

Mechanisms in rows 1 and 2 of Table 5.1: The equations with F_1 and F_2 are formulated. They have the forms (5.18) and (5.19). The first equation determines two solutions for a single unknown angle φ_λ. With each solution the second equation is a linear equation for a single translatory variable.

Mechanisms in rows 3 and 4: The equations with F_1, F_2, F_3 and F_4 are formulated. The first equation is Eq.(5.18). It determines two solutions for a single unknown angle φ_λ. With each solution the remaining three equations are linear equations for three unknown translatory variables.

Mechanisms in rows 5, 6, 7: Two equations are formulated. These are the equations with F_1 and F_2 for the mechanisms in row 5 and the equations with F_1 and F_5 for the mechanisms in rows 6 and 7. Both equations have either the form (5.20) or the form (5.21). These equations are easily decoupled. Methods of solution see in Sect. 5.4.3.

Mechanisms 5R-C, 6R-P and 7R: The four equations with F_1, F_2, F_3 and F_4 determine four unknowns. Without additional equations of another mathematical form it is impossible to decouple these equations. The necessary additional equations are the half-angle equations introduced further below.

Up to this point the independent variable was the angle of an arbitrarily chosen revolute joint. In what follows, it is the translatory variable in an arbitrarily chosen prismatic joint. This change has the effect that in each of the seven Woernle-Lee equations the number of unknown angular variables increases by one whereas the number of unknown translatory variables decreases by one. The two numbers of unknowns are $2 \leq n_\varphi - 2 \leq 4$ and $0 \leq n_\mathrm{P} - 1 \leq 2$. For the mechanisms of Table 5.1 this change has the following effect.

For the mechanisms in rows 2, 3 and 4 the same equations are formulated which are formulated for the mechanisms in rows 5, 6, 7 with an independent angular variable. These are the equations with F_1 and F_2 for the mechanisms in row 2 and the equations with F_1 and F_5 for the mechanisms in rows 3 and 4. Both equations have either the form (5.20) or the form (5.21).

For the mechanisms in rows 6, 7 and 9 the four equations with F_1, F_2, F_3 and F_4 determine four unknowns. For the mechanisms in row 6 they are the same equations which govern the mechanism 5R-C with an independent angular variable. For the mechanisms in row 7 they are the same equations which govern the mechanism 6R-P with an independent angular variable.

For the mechanism 6R-P they are the same equations which govern the mechanism 7R with an independent angular variable. These relationships were predicted when Table 5.1 was introduced.

5.3.2 Half-Angle Equations

These equations were first formulated by Lee [27]. Again, Fig. 5.2 is considered. The ordinary unit vectors $\mathbf{n}_b$, $\mathbf{a}_b$ und $\mathbf{n}_b \times \mathbf{a}_b$ form an orthogonal cartesian basis fixed on body b, and the unit vectors $\mathbf{n}_b$, $\mathbf{a}_{b-1}$, $\mathbf{n}_b \times \mathbf{a}_{b-1}$ form another basis fixed on body $b-1$. Temporarily, the abbreviations are used:

$$\mathbf{d}_b = \mathbf{n}_b \times \mathbf{a}_b \,, \qquad \mathbf{d}^*_{b-1} = \mathbf{n}_b \times \mathbf{a}_{b-1} \,. \tag{5.34}$$

The two bases are rotated against each other through the angle φ_b about the common axis $\mathbf{n}_b$. Let $\mathbf{v}$ be an arbitrary vector. Its coordinates in the two bases are related through the matrix equation

$$\begin{bmatrix} \mathbf{v}\cdot\mathbf{n}_b \\ \mathbf{v}\cdot\mathbf{a}_b \\ \mathbf{v}\cdot\mathbf{d}_b \end{bmatrix} = \begin{bmatrix} 1 & 0 & 0 \\ 0 & \cos\varphi_b & \sin\varphi_b \\ 0 & -\sin\varphi_b & \cos\varphi_b \end{bmatrix} \begin{bmatrix} \mathbf{v}\cdot\mathbf{n}_b \\ \mathbf{v}\cdot\mathbf{a}_{b-1} \\ \mathbf{v}\cdot\mathbf{d}^*_{b-1} \end{bmatrix} \,. \tag{5.35}$$

The new variable $x_b = \tan\varphi_b/2$ is defined. The expressions $\cos\varphi_b = (1 - x_b^2)/(1 + x_b^2)$ and $\sin\varphi_b = 2x_b/(1 + x_b^2)$ are substituted into (5.35). In order to avoid the quadratic term x_b^2 the equation is premultiplied by the matrix $\begin{bmatrix} 1 & 0 & 0 \\ 0 & x_b & 1 \\ 0 & 1 & -x_b \end{bmatrix}$. Following this, the identities $\sin\varphi_b - x_b\cos\varphi_b = x_b$ and $x_b\sin\varphi_b + \cos\varphi_b = 1$ are used. This results in the following equation which is linear with respect to x_b:

$$\begin{bmatrix} 1 & 0 & 0 \\ 0 & x_b & 1 \\ 0 & 1 & -x_b \end{bmatrix} \begin{bmatrix} \mathbf{v}\cdot\mathbf{n}_b \\ \mathbf{v}\cdot\mathbf{a}_b \\ \mathbf{v}\cdot\mathbf{d}_b \end{bmatrix} = \begin{bmatrix} 1 & 0 & 0 \\ 0 & -x_b & 1 \\ 0 & 1 & x_b \end{bmatrix} \begin{bmatrix} \mathbf{v}\cdot\mathbf{n}_b \\ \mathbf{v}\cdot\mathbf{a}_{b-1} \\ \mathbf{v}\cdot\mathbf{d}^*_{b-1} \end{bmatrix} \,. \tag{5.36}$$

The first equation is the identity. The other two are, in terms of the original vectors in (5.34),

$$\left.\begin{aligned} x_b\,\mathbf{v}\cdot\mathbf{a}_b + \quad \mathbf{v}\cdot\mathbf{n}_b\times\mathbf{a}_b &= -x_b\,\mathbf{v}\cdot\mathbf{a}_{b-1} + \quad \mathbf{v}\cdot\mathbf{n}_b\times\mathbf{a}_{b-1} \,, \\ \mathbf{v}\cdot\mathbf{a}_b - x_b\,\mathbf{v}\cdot\mathbf{n}_b\times\mathbf{a}_b &= \quad \mathbf{v}\cdot\mathbf{a}_{b-1} + x_b\,\mathbf{v}\cdot\mathbf{n}_b\times\mathbf{a}_{b-1} \,. \end{aligned}\right\} \tag{5.37}$$

This pair of equations is formulated with the vectors

$$\mathbf{v}_1 = \mathbf{n}_a\ , \qquad \mathbf{v}_2 = \mathbf{r}\ , \qquad \mathbf{v}_3 = \mathbf{n}_a \times \mathbf{r}\ , \qquad \mathbf{v}_4 = \frac{1}{2}\,\mathbf{r}^2\mathbf{n}_a - (\mathbf{n}_a \cdot \mathbf{r})\mathbf{r}\ . \quad (5.38)$$

The vectors $\mathbf{n}_a$ and $\mathbf{r}$ are the ones shown in Fig. 5.2 and in (5.13). In what follows, it is important that $-h_b\mathbf{n}_b$ is part of $\mathbf{r}$ in the left segment, and that $h_a\mathbf{n}_a$ is part of $\mathbf{r}$ in the right segment.

The scalar products $\mathbf{v}_i \cdot \mathbf{a}_b$ and $\mathbf{v}_i \cdot \mathbf{n}_b \times \mathbf{a}_b$ on the left-hand side of the equations are evaluated in the left segment, and the scalar products $\mathbf{v}_i \cdot \mathbf{a}_{b-1}$ and $\mathbf{v}_i \cdot \mathbf{n}_b \times \mathbf{a}_{b-1}$ on the right-hand side of the equations are evaluated in the right segment. With every vector $\mathbf{v}_i$ $(i = 1, 2, 3, 4)$ the vector products in (5.37) are linear with respect to the sines and cosines of all angles involved.

The expressions for $\mathbf{r}$ in (5.13) allow the following conclusions (note that the vector $\mathbf{n}_b \times \mathbf{a}_b$ is fixed on body b, and that the vector $\mathbf{n}_b \times \mathbf{a}_{b-1}$ is fixed on body $b-1$):

1. With all vectors $\mathbf{v}_i$ $(i = 1, 2, 3, 4)$ all scalar products are independent of both φ_a and φ_b.

2. The angle φ_b appears in every equation, however, only in the form $x_b = \tan\varphi_b/2$.

3. With $\mathbf{v}_i = \mathbf{v}_1$ only angular variables appear.

4. With $\mathbf{v}_i = \mathbf{v}_2$ all scalar products are independent of h_b. In the products on the right-hand side h_a occurs in linear form.

5. With $\mathbf{v}_i = \mathbf{v}_3$ all scalar products are independent of h_a. In the products on the left-hand side h_b occurs in linear form.

6. With $\mathbf{v}_i = \mathbf{v}_4$ both h_a and h_b occur in first and second-order terms. These equations are formulated only for the mechanism 7R in which the parameters $h_1, \ldots, h_7$ are constant.

For the evaluation of products in (5.37) Table 5.2 is used. The following facts are helpful. The vector $\mathbf{n}_b \times \mathbf{a}_b$ fixed on body b has the coordinates $[0\ 0\ 1]^T$ in the basis of body b. The vector $\mathbf{n}_b \times \mathbf{a}_{b-1}$ fixed on body $b-1$ has the coordinates $[C_{b-1}\ \ 0\ \ -S_{b-1}]^T$ in the basis of body $b-1$.

The product $\mathbf{v}_3 \cdot \mathbf{a}_b$ is formulated with $\mathbf{r} = \mathbf{r} + h_b\mathbf{n}_b - h_b\mathbf{n}_b$:

$$\mathbf{v}_3 \cdot \mathbf{a}_b = -[(\mathbf{r} + h_b\mathbf{n}_b) \times \mathbf{n}_a \cdot \mathbf{a}_b + h_b\mathbf{n}_a \cdot \mathbf{n}_b \times \mathbf{a}_b]\ . \quad (5.39)$$

In the second term the previously given coordinates of $\mathbf{n}_b \times \mathbf{a}_b$ are used. In the first term the vector $\mathbf{r} + h_b\mathbf{n}_b$ joins the dual vectors $\hat{\mathbf{n}}_a$ and $\hat{\mathbf{a}}_b$ (see Fig. 5.2). From this it follows that the first term represents the dual part of $\hat{\mathbf{n}}_a \cdot \hat{\mathbf{a}}_b$. It is calculated as dual derivative of $\mathbf{n}_a \cdot \mathbf{a}_b$. Similarly,

$$\mathbf{v}_3 \cdot \mathbf{a}_{b-1} = -\mathbf{r} \times \mathbf{n}_a \cdot \mathbf{a}_{b-1} = -(\text{dual derivative of } \mathbf{n}_a \cdot \mathbf{a}_{b-1})\ . \quad (5.40)$$

5.4 Systematic Analysis of Mechanisms

The previous section provided equations which are sufficient for the analysis of all mechanisms of Table 5.1 . In the present section methods for decoupling these equations are presented. For each type of mechanism a polynomial equation of minimal order is developed for a single unknown variable. This minimal order is the maximum number of configurations the mechanism under consideration can have for a given value of the independent variable. In these analyses all constant Denavit-Hartenberg parameters are assumed to be nonzero and arbitrary. As special cases a 7R-mechanism with three parallel joint axes and a 7R-mechanism with a spherical joint are analyzed.

5.4.1 RCCC

This is the simplest of all mechanisms listed in Table 5.1 . It has the smallest number of joints $(n = 4)$ and the smallest number of constant parameters $(4n - 7 = 9)$. Figure 5.3 shows schematically the mobile polygon with unit vectors $\mathbf{n}_i$ and $\mathbf{a}_i$ $(i = 1, 2, 3, 4)$. The vectors are uniformly directed counterclockwise. Joint 1 represents the revolute joint. The variable φ_1 in this joint is the independent variable. The six dependent variables are the quantities φ_i , h_i in the cylindrical joints $i = 2, 3, 4$. The nine constant parameters are h_1 in joint 1 and the quantities α_i , ℓ_i of bodies $i = 1, 2, 3, 4$.
General remarks on vector polygons of mechanisms: A mechanism with n joints has a polygon with $2n$ sides. It can be drawn schematically as a regular $2n$-gon with all unit vectors $\mathbf{n}_i$ and $\mathbf{a}_i$ $(i = 1, \ldots, n)$ pointing counterclockwise. A regular $2n$-gon has $2n$ axes of symmetry. Any closure condition formulated for a specific mechanism remains valid if the labels of its constant and variable Denavit-Hartenberg parameters are changed according to the

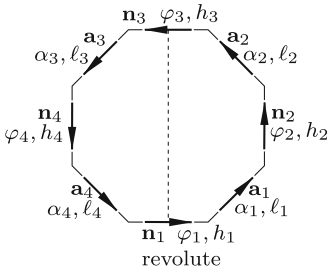

Fig. 5.3 Mechanism RCCC . Polygon with unit vectors $\mathbf{n}_i$, $\mathbf{a}_i$ and Denavit-Hartenberg parameters α_i , ℓ_i , φ_i , h_i $(i = 1, 2, 3, 4)$. Joint 1 is the revolute with the independent variable φ_1 . The dashed line of symmetry

symmetry. Symmetry is particularly useful if symmetrically located joints are of equal type, i.e., CC or RR or PP. In Fig. 5.3 this is the case for the dashed line of symmetry. Closure conditions remain valid if the quantities $(\alpha_1\,,\,\ell_1\,,\,\varphi_2\,,\,h_2\,,\,\alpha_2\,,\,\ell_2)$ are replaced by $(\alpha_4\,,\,\ell_4\,,\,\varphi_4\,,\,h_4\,,\,\alpha_3\,,\,\ell_3)$ and vice versa. Not every mechanism has such an axis of symmetry, for example not the mechanism RCPRC.

Also the following is true. Any closure condition formulated for a specific mechanism remains valid if the labels of its constant and variable Denavit-Hartenberg parameters are cyclicly increased by an arbitrary integer λ $(\pm1, \pm2, \ldots)$. This means that the two joints a and b on which the closure condition is founded are replaced by the joints $a+\lambda$ and $b+\lambda$, respectively. A cyclic rotation of labels by an integer λ is equivalent to a symmetry change of labels if the joints $a+\lambda$ and $b+\lambda$ are located symmetrically to the joints b and a, respectively. Cyclic rotation of labels and symmetry changes of labels are much simpler than re-formulations of closure conditions for new joints a and b.

Now back to the mechanism RCCC. Among the three cylindrical joints 2, 3 and 4 any two can be chosen as joints a and b. For each pair Eqs.(5.18) and (5.19) are formulated. The unknowns in these equations are the two variables of the third cylindrical joint. The first equation is the Woernle-Lee Eq.(5.17). It is given for only two joint combinations because any other combination is produced by a cyclic change of indices.

$$\left.\begin{array}{ll} \text{joint combination} & a=2\,,\,b=3: \quad \mathbf{n}_k\cdot\mathbf{n}_{k-3}=\mathbf{n}_k\cdot\mathbf{n}_{k+1} \\ \text{joint combination} & a=2\,,\,b=4: \quad \mathbf{n}_k\cdot\mathbf{n}_{k-2}=\mathbf{n}_k\cdot\mathbf{n}_{k+2} \end{array}\right\} \quad k=a\,. \tag{5.41}$$

For the joint combination $a=2\,,\,b=3$ Table 5.2 yields the equation

$$S_3[s_4 s_1 S_1 - c_4(S_4 C_1 + C_4 S_1 c_1)] + C_3(C_4 C_1 - S_4 S_1 c_1) = C_2\,. \tag{5.42}$$

This is Eq.(5.18) for φ_4:

$$Ac_4 + Bs_4 = R\,. \tag{5.43}$$

The coefficients depend on φ_1:

$$\left.\begin{array}{ll} A = -S_3(S_4 C_1 + C_4 S_1 c_1)\,, & \qquad B = S_1 S_3 s_1\,, \\ R = C_2 - C_3(C_4 C_1 - S_4 S_1 c_1)\,. & \end{array}\right\} \tag{5.44}$$

Dual differentiation of (5.43) yields Eq.(5.19) for h_4:

$$h_4(Bc_4 - As_4) = Dc_4 + Es_4 + F\,. \tag{5.45}$$

The coefficients D, E and F are the dual derivatives of $-A$, $-B$ and R, respectively:

$$\left.\begin{aligned} D = &-\ell_4 S_3(S_1S_4c_1 - C_1C_4) + \ell_1 S_3(C_1C_4c_1 - S_1S_4) \\ &+\ell_3 C_3(S_1C_4c_1 + C_1S_4) - h_1S_1S_3C_4s_1 \ , \\ F = &\ \ \ell_4 C_3(S_1C_4c_1 + C_1S_4) + \ell_1 C_3(C_1S_4c_1 + S_1C_4) \\ &-\ell_3 S_3(S_1S_4c_1 - C_1C_4) - h_1S_1C_3S_4s_1 - \ell_2 S_2 \ , \\ E = &-s_1(\ell_1 C_1S_3 + \ell_3 S_1C_3) - h_1S_1S_3c_1 \ . \end{aligned}\right\} \tag{5.46}$$

For every value of φ_1 Eq.(5.43) has two (not necessarily real) solutions φ_4. The associated solutions h_4 are determined by (5.45).

Next, equations for φ_2 and h_2 are produced. This is done by increasing all indices in (5.43) and (5.44) cyclicly by one. Equation (5.43) is replaced by the equation

$$S_4[s_1s_2S_2 - c_1(S_1C_2 + C_1S_2c_2)] + C_4(C_1C_2 - S_1S_2c_2) = C_3 \ . \tag{5.47}$$

This is the equation for φ_2:

$$A^*c_2 + B^*s_2 = R^* \ , \tag{5.48}$$

$$\left.\begin{aligned} A^* &= -S_2(S_1C_4 + C_1S_4c_1) \ , \qquad B^* = S_4S_2s_1 \ , \\ R^* &= C_3 - C_2(C_4C_1 - S_4S_1c_1) \ . \end{aligned}\right\} \tag{5.49}$$

The cyclic change of indices in (5.45) and (5.46) is left to the reader. Next, φ_3 is determined from (5.41) for the joint combination $a = 2$, $b = 4$. Table 5.2 yields the equation

$$C_3C_2 - S_3S_2c_3 = C_1C_4 - S_1S_4c_1 \ . \tag{5.50}$$

It displays the symmetry of Fig. 5.3. It determines c_3 as a linear function of c_1. Every value of φ_1 yields two solutions $\pm\varphi_3$. Dual differentiation of (5.50) produces for h_3 the formula

$$\begin{aligned} h_3S_2S_3s_3 = h_1S_1S_4s_1 &+ c_3(\ell_2C_2S_3 + \ell_3S_2C_3) + (\ell_2S_2C_3 + \ell_3C_2S_3) \\ &- c_1(\ell_1C_1S_4 + \ell_4S_1C_4) - (\ell_1S_1C_4 + \ell_4C_1S_4) \ . \end{aligned} \tag{5.51}$$

If h_3 is the solution associated with $+\varphi_3$, $-h_3$ is the solution associated with $-\varphi_3$.

The analysis is now complete except for one open problem. For every value of φ_1 there exist two solutions (φ_2, h_2), two solutions (φ_3, h_3) and two solutions (φ_4, h_4). What remains to be shown is which of the solutions φ_2, φ_4 occur together with $+\varphi_3$ and which with $-\varphi_3$. For solving this problem two closure conditions are needed relating φ_3 to φ_4 and φ_3 to φ_2, respectively. They are obtained by increasing the indices in (5.43) by two and by three, respectively. This produces the equations

$$S_1[s_2s_3S_3 - c_2(S_2C_3 + C_3S_3c_3)] + C_1(C_2C_3 - S_2S_3c_3) = C_4 \ , \tag{5.52}$$

$$S_2[s_3s_4S_4 - c_3(S_3C_4 + C_3S_4c_4)] + C_2(C_3C_4 - S_3S_4c_4) = C_1 \,. \qquad (5.53)$$

The relationship between φ_4 and φ_2 is obtained more easily from (5.50) by a cyclic increase of indices by one:

$$C_4C_3 - S_4S_3c_4 = C_2C_1 - S_2S_1c_2 \,. \qquad (5.54)$$

Any two of these equations determine whether numerically calculated angles φ_4 and φ_2 belong to $+\varphi_3$ or to $-\varphi_3$.

Special Cases: Bennett Mechanism and Spherical Four-Bar
Under certain conditions on the nine constant Denavit-Hartenberg parameters $\ell_1, \ldots, \ell_4$, $\alpha_1, \ldots, \alpha_4$ and h_1 of the mechanism RCCC the translatory variables h_2, h_3, h_4 are constant (actually identically zero) independent of the angle φ_1. This means that the mechanism has four revolute joints and, yet, a single degree of freedom. It is an overconstrained mechanism. There are two such special mechanisms. One of them is called Bennett mechanism. It is the subject of Sect. 6.2. The other is the spherical four-bar with four revolute joints the axes of which intersect at a single point. Intersection means that the Denavit-Hartenberg parameters $\ell_1, \ldots, \ell_4$ and h_1 are zero. Equations (5.46) yield $D = E = F \equiv 0$ and with this, (5.45) yields $h_4 \equiv 0$. Dual differentiation of (5.47) and (5.51) yields $h_2 \equiv 0$ and $h_3 \equiv 0$. The equations relating the angular variables $\varphi_1, \ldots, \varphi_4$ do not change (see (5.43), (5.44), (5.48), (5.49), (5.50), (5.54)). These results confirm that the spherical four-bar has a single degree of freedom.

In Fig. 5.4 a spherical four-bar is shown as quadrilateral A_0ABB_0 the links $1, 2, 3, 4$ of which are arcs of great circles on the unit sphere about the intersection point 0 of the joint axes. The unit vectors $\mathbf{n}_1, \ldots, \mathbf{n}_4$ along the axes are pointing away from 0. The unit vector $\mathbf{a}_i$ normal to both $\mathbf{n}_i$ and $\mathbf{n}_{i+1}$ has the direction of $\mathbf{n}_i \times \mathbf{n}_{i+1}$ (here and in what follows, $i = 1, \ldots, 4$ cyclic). The angle α_i is the angle about $\mathbf{a}_i$ from $\mathbf{n}_i$ to $\mathbf{n}_{i+1}$, and φ_i is the angle about $\mathbf{n}_i$ from $\mathbf{a}_{i-1}$ to $\mathbf{a}_i$ (see Fig. 5.1). The angle α_i equals the arc of link i on the unit sphere. Link i is said to have the length α_i. At this

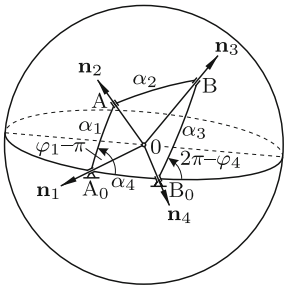

Fig. 5.4 Spherical four-bar

point the kinematics analysis is stopped. It is resumed in Chap. 18.

Final remark: The expressions in (5.42) – (5.46) are moderately complicated. For mechanisms with up to twenty-one instead of nine constant parameters much more complicated expressions are generated. In every case the generation requires only two operations. One is copying terms from Table 5.2 and the other is calculating dual derivatives. Both operations can be executed by the MAPLE software tool [34] already mentioned.

5.4.2 RCRCR and CRRRC

These mechanisms have $n = 5$ joints, $4n-7 = 13$ constant parameters, two cylindrical joints and $n_\varphi = 5$ angular variables. Figures 5.5a and b show the mobile polygons with unit vectors $\mathbf{n}_i$ and $\mathbf{a}_i$ $(i = 1, \ldots, 5)$. Each figure is structurally symmetric with respect to the dashed line.

With the cylindrical joints as joints a and b the equations $F_1^\ell = F_1^r$ and $F_2^\ell = F_2^r$ are formulated. From Sect. 5.3.1 it is known that these equations relate the angles in the three revolute joints. Two of them are unknown dependent angles. The equations have the form (5.20) if the unknowns are located in different segments created by the cylindrical joints, and they have the form (5.21) if they are located in one and the same segment. The case of location in different segments occurs if (i) the mechanism is $\underline{\mathrm{R}}\mathrm{CRC}\underline{\mathrm{R}}$ and (ii) the independent angle is in one of the underscored revolutes. This simpler case is treated first. It is the case of Fig. 5.5a with φ_1 as independent variable. The cylindrical joints are the joints 3 and 5. The equation $F_1^\ell = F_1^r$ is the equation $\mathbf{n}_k \cdot \mathbf{n}_{k+2} = \mathbf{n}_k \cdot \mathbf{n}_{k-3}$ with $k = 3$. Table 5.2 yields the explicit form

$$\begin{aligned} &C_4C_3 - S_4S_3c_4 \\ &= S_5[s_1s_2S_2 - c_1(S_1C_2 + C_1S_2c_2)] + C_5(C_1C_2 - S_1S_2c_2)\,. \end{aligned} \tag{5.55}$$

This is a special form of (5.20):

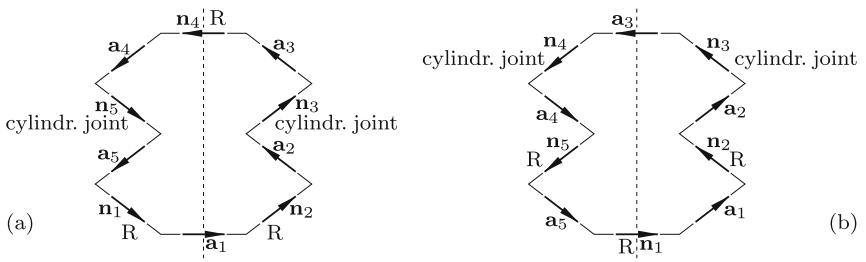

Fig. 5.5 Polygons with unit vectors for the mechanisms RCRCR **(a)** and CRRRC **(b)**

$$S_3S_4c_4 = A_1c_2 + B_1s_2 + R_1 \ . \tag{5.56}$$

The coefficients A_1, B_1 and R_1 depend on φ_1:

$$\left.\begin{array}{ll} A_1 = S_2(C_5S_1 + C_1S_5c_1) \ , & B_1 = -S_2S_5s_1 \ , \\ R_1 = C_3C_4 - C_2(C_1C_5 - S_1S_5c_1) \ . & \end{array}\right\} \tag{5.57}$$

Dual differentiation yields (5.21):

$$A_4c_4 - h_4S_3S_4s_4 = A_2c_2 + B_2s_2 + R_2 \ . \tag{5.58}$$

The coefficients are

$$A_4 = \ell_3C_3S_4 + \ell_4S_3C_4 \ , \quad A_2 = A_1' + h_2B_1 \ , \quad B_2 = B_1' - h_2A_1 \ , \quad R_2 = R_1' \tag{5.59}$$

with A_1', B_1', R_1' denoting the dual derivatives of A_1, of B_1 and of R_1, respectively.

Equations (5.56) and (5.58) are linear equations for c_4 and s_4. Substituting the solutions into the equation $c_4^2 + s_4^2 = 1$ results in an equation for φ_2 of the form

$$A\sin^2\varphi_2 + B\sin\varphi_2\cos\varphi_2 + C\sin\varphi_2 + D\cos^2\varphi_2 + E\cos\varphi_2 + F = 0 \tag{5.60}$$

with new coefficients which are functions of φ_1. The substitution $x = \tan\varphi_2/2$, $\cos\varphi_2 = (1-x^2)/(1+x^2)$, $\sin\varphi_2 = 2x/(1+x^2)$ produces for x the 4th-order equation

$$x^4(D-E+F) + 2x^3(C-B) + 2x^2(2A-D+F) + 2x(C+B) + D + E + F = 0 \ . \tag{5.61}$$

It has four (not necessarily real) solutions φ_2 for every value of φ_1. This is the number $N_\varphi = 4$ in Table 5.1. With every real solution φ_2 the associated values c_4 and s_4 and, thus, φ_4 are determined from (5.56) and (5.58).

Note: The substitution $x = \tan\varphi_2/2$ makes sense only if $\varphi_2 \neq \pi$. $\varphi_2 = \pi$ is a solution if $D - E + F = 0$ and a double solution if, in addition, also $C - B = 0$. These are the coefficients of x^4 and x^3 in the polynomial[1]. In the case $B = C = 0$, (5.60) is quadratic in $\cos\varphi_2$, and in the case $B = E = 0$, it is quadratic in $\sin\varphi_2$. In either case the substitution $x = \tan\varphi_2/2$ is unnecessary.

The variables φ_3, h_3 and φ_5, h_5 in the cylindrical joints are still unknown. The angles φ_3 and φ_5 are determined first as follows. One of the two half-angle equations (5.37) is formulated with $a = 5$, $b = 3$ and $\mathbf{v} = \mathbf{n}_5$. This is a linear equation for $x_3 = \tan\varphi_3/2$ as the only unknown. The same equation with $a = 3$, $b = 5$ and $\mathbf{v} = \mathbf{n}_3$ determines $x_5 = \tan\varphi_5/2$. Next,

[1] Example: The equation $4\sin^2\varphi + 3\sin\varphi\cos\varphi + 3\sin\varphi + 2\cos^2\varphi + \cos\varphi - 1 = 0$ has the solutions $\varphi_1 = \varphi_2 = \pi$. Equation (5.61) is $5x^2 + 6x - 1 = 0$. It has the solutions $\varphi_3 = -\pi/2$ and $\varphi_4 = -2\tan^{-1}(1/5)$

the unknowns h_3 and h_5 are expressed in terms of all other variables including the previously determined angles φ_3 and φ_5. A single linear equation for h_3 is obtained by formulating one of the half-angle equations (5.37) with $a = 5$, $b = 3$ and $\mathbf{v} = \mathbf{r}$. The same equation with $a = 3$, $b = 5$ and $\mathbf{v} = \mathbf{r}$ determines h_5. Note that the vector $\mathbf{r}$ depends upon a and b according to Fig. 5.2. This concludes the analysis of the mechanism RCRCR with φ_1 as independent variable.

Next, φ_4 is assumed to be the independent variable. In this case, both Eq.(5.55) and its dual derivative have the form (5.21). With new names for coefficients they are written in the form

$$c_1 \underbrace{(a_{i1}c_2 + a_{i2}s_2 + a_{i3})}_{A_i} + s_1 \underbrace{(b_{i1}c_2 + b_{i2}s_2 + b_{i3})}_{B_i} + \underbrace{(r_{i1}c_2 + r_{i2}s_2 + r_{i3})}_{R_i} = 0 \tag{5.62}$$

$(i = 1, 2)$. Equation (5.55) yields, for example, $a_{11} = S_5C_1S_2$, $a_{12} = 0$, $b_{11} = 0$, $b_{12} = -S_5S_2$, $r_{11} = C_5S_1S_2$, $r_{12} = 0$, $r_{13} = C_4C_3 - S_4S_3c_4 - C_5C_1C_2$. The two Eqs.(5.62) are solved as linear equations for c_1 and s_1:

$$c_1 = \frac{B_1R_2 - B_2R_1}{A_1B_2 - A_2B_1}\,, \qquad s_1 = -\frac{A_1R_2 - A_2R_1}{A_1B_2 - A_2B_1}\,. \tag{5.63}$$

The common denominator and the two numerator expressions contain zero, first and second-order terms of c_2 and s_2. Substitution into the constraint equation $c_1^2 + s_1^2 = 1$ eliminates φ_1. The resulting equation relates φ_2 to the independent variable φ_4. This is the equation $(A_1R_2 - A_2R_1)^2 + (B_1R_2 - B_2R_1)^2 - (A_1B_2 - A_2B_1)^2 = 0$. It contains zero, first, second, third and fourth-order terms of c_2 and s_2 with coefficients which are functions of φ_4:

$$A\cos^4\varphi_2 + B\cos^3\varphi_2\sin\varphi_2 + \ldots = 0\,. \tag{5.64}$$

The substitution $x = \tan\varphi_2/2$, $\cos\varphi_2 = (1-x^2)/(1+x^2)$, $\sin\varphi_2 = 2x/(1+x^2)$ produces for x an 8th-order polynomial equation[2]. For a given value of the independent variable φ_4 it has eight (not necessarily real) solutions φ_2. This is the number $N_\varphi = 8$ in Table 5.1. For every solution φ_2 the corresponding solution φ_1 is calculated from (5.63).

For the mechanism CRRRC in Fig. 5.5b the same set of Eqs.(5.62) is obtained. Only the indices of the unknown variables and the coefficients are different. The details are left to the reader. This concludes the analysis of the mechanisms RCRCR and CRRRC.

Equations (5.63) require a comment. It may happen that the common denominator and the two numerator expressions are linear functions of c_2 and s_2. This requires that in all three expressions c_2s_2 has the factor zero,

[2] $\varphi_2 = \pi$ is a root of multiplicity n if the highest-order term in the polynomial is x^{8-n}

and that c_2^2 and s_2^2 have identical factors. For the factors of $c_2 s_2$ to be zero the three conditions on the left-hand side below must be satisfied. For the factors of c_2^2 and of s_2^2 to be identical the three conditions on the right-hand side must be satisfied.

$$\left.\begin{array}{ll} a_{11}r_{22} + a_{12}r_{21} = a_{21}r_{12} + a_{22}r_{11}\,, & a_{11}r_{21} - a_{21}r_{11} = a_{12}r_{22} - a_{22}r_{12}\,, \\ b_{11}r_{22} + b_{12}r_{21} = b_{21}r_{12} + b_{22}r_{11}\,, & b_{11}r_{21} - b_{21}r_{11} = b_{12}r_{22} - b_{22}r_{12}\,, \\ a_{11}b_{22} + a_{12}b_{21} = a_{21}b_{12} + a_{22}b_{11}\,, & a_{11}b_{21} - a_{21}b_{11} = a_{12}b_{22} - a_{22}b_{12}\,. \end{array}\right\} \tag{5.65}$$

Under these conditions the equation $(A_1R_2 - A_2R_1)^2 + (B_1R_2 - B_2R_1)^2 - (A_1B_2 - A_2B_1)^2 = 0$ contains only zero, first and second-order terms of c_2 and s_2. Hence it does not have the form (5.64), but the form (5.60). This equation has four solutions for every value of the independent variable. The mechanism RRSRR analyzed in Sect. 5.5.2 is governed by a set of equations satisfying the conditions (5.65).

5.4.3 RCPRC, CCPRR and RCPCR. Independent Variable in the Prismatic Joint

These mechanisms are obtained from the previously investigated mechanisms RCRCR and CRRRC when one revolute joint is replaced by a cylindrical joint. The letter sequences are written such that the prismatic joint is joint 3. The translatory variable h_3 in this joint is the independent variable. As before, the two cylindrical joints are the joints a and b. As before, the closure conditions $F_1^\ell = F_1^r$ and $F_2^\ell = F_2^r$ are formulated and, as before, the angles φ_λ and φ_μ of two revolute joints are the only unknowns in these equations. In the mechanism RCPRC the two angles are located in different segments created by the cylindrical joints, and in the mechanisms CCPRR and RCPCR they are located in one and the same segment. For the first mechanism both equations have the form (5.20), and for the other two mechanisms they have the form (5.21). The numbers of solution are four for the former and eight for the latter. These are the numbers N_t given in Table 5.1. This concludes the analysis.

5.4.4 Mechanisms in Rows 6 and 7 of Table 5.1. Independent Variable is an Angle

It was shown that the closure condition $F_1^\ell = F_1^r$ is Eq.(5.21) with two unknowns φ_λ and φ_μ, and that the closure condition $F_5^\ell = F_5^r$ has the same form (see (5.26)). The unknowns φ_λ and φ_μ are the same in both

equations if the joints a and b are the same for both equations. The choice of these joints is dictated by the method for formulating the right-hand side of (5.26). Both equations are written in the form (5.62). For a given value of the independent variable the number of solutions is eight since the conditions (5.65) are not satisfied. This concludes the analysis.

5.4.5 5R-C

This mechanism has $n = 6$ joints, $4n-7 = 17$ constant parameters, $n_\varphi = 6$ angular variables and a single translatory variable in the cylindrical joint. Figure 5.6 shows schematically the mobile polygon with unit vectors $\mathbf{n}_i$ and $\mathbf{a}_i$ $(i = 1, \ldots, 6)$. Joint 3 is the cylindrical joint. The dashed line is an axis of structural symmetry. The vector $\mathbf{r}$ shown in the figure is

$$\mathbf{r} = \begin{cases} -(h_3\mathbf{n}_3 + \ell_3\mathbf{a}_3 + h_4\mathbf{n}_4 + \ell_4\mathbf{a}_4 + h_5\mathbf{n}_5 + \ell_5\mathbf{a}_5) & \text{(left segment)} \\ h_6\mathbf{n}_6 + \ell_6\mathbf{a}_6 + h_1\mathbf{n}_1 + \ell_1\mathbf{a}_1 + h_2\mathbf{n}_2 + \ell_2\mathbf{a}_2 & \text{(right segment)}\,. \end{cases} \tag{5.66}$$

The revolute joint 6 and the cylindrical joint 3 are chosen as joints a and b, respectively. This has the effect that every closure condition displays the symmetry.

Let φ_5 be the independent variable. Then two unknown variables φ_1 and φ_2 appear in the right segment and the single unknown variable φ_4 in the left segment. First, the closure conditions $F_1^\ell = F_1^r$ and $F_2^\ell = F_2^r$ are formulated. The former is the equation $\mathbf{n}_k \cdot \mathbf{n}_{k+3} = \mathbf{n}_k \cdot \mathbf{n}_{k-3}$ with $k = 3$. The scalar products are copied from Table 5.2:

$$\begin{aligned} &C_5(C_4C_3 - S_4S_3c_4) + S_5[s_5s_4S_3 - c_5(S_4C_3 + C_4S_3c_4)] \\ &= S_6[s_1s_2S_2 - c_1(S_1C_2 + C_1S_2c_2)] + C_6(C_1C_2 - S_1S_2c_2)\,. \end{aligned} \tag{5.67}$$

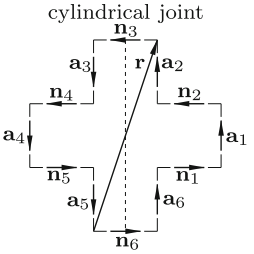

Fig. 5.6 Mechanism 5R-C. Polygon with unit vectors

This is written in the form (5.22) with $\varphi_\lambda = \varphi_1$, $\varphi_\mu = \varphi_2$ and $\varphi_\nu = \varphi_4$. The matrix $\underline{A}$ of this equation is

$$\underline{A} = [-S_3(S_4C_5 + C_4S_5c_5) \qquad S_3S_5s_5\,]^T \,. \tag{5.68}$$

The equation $F_2^\ell = F_2^r$ is the dual derivative of (5.67). It has the same form. Both equations are combined in the matrix form

$$\underline{A}_1\underline{u}_\ell = \underline{B}_1 \begin{bmatrix} \underline{u}_r \\ 1 \end{bmatrix} \,. \tag{5.69}$$

The column matrices $\underline{u}_\ell$ and $\underline{u}_r$ are

$$\underline{u}_\ell = [c_4 \quad s_4\,]^T \,, \quad \underline{u}_r = [c_1c_2 \quad c_1s_2 \quad c_1 \quad s_1c_2 \quad s_1s_2 \quad s_1 \quad c_2 \quad s_2\,]^T \,. \tag{5.70}$$

The coefficient matrices $\underline{A}_1$ and $\underline{B}_1$ are of size (2×2) and (2×9), respectively. They are functions of the independent variable φ_5 .

No other closure condition yields a third equation for the same three unknowns. The closure conditions $F_3^\ell = F_3^r$ and $F_4^\ell = F_4^r$ with $F_3 = \mathbf{n}_6 \cdot \mathbf{r}$ and $F_4 = \mathbf{n}_3 \cdot \mathbf{r}$ have the form (5.23) with $h_\kappa = h_3$. One of these equations is used later for the calculation of h_3 once φ_1 , φ_2 and φ_4 are known. For the determination of these angles the two pairs of half-angle equations (5.37) with $\mathbf{v} = \mathbf{n}_6$ and with $\mathbf{v} = \mathbf{r}$ are formulated. In the four Eqs.(5.37) the same unknown elements of $\underline{u}_\ell$ are located on the left-hand sides and the elements of $\underline{u}_r$ on the right-hand sides. All these elements occur once without and once with the factor $x_6 = \tan\varphi_6/2$. The four equations are combined in the matrix form

$$(\underline{A}_2 + x_6\underline{A}_3)\underline{u}_\ell = (\underline{B}_2 + x_6\underline{B}_3) \begin{bmatrix} \underline{u}_r \\ 1 \end{bmatrix} \,. \tag{5.71}$$

The coefficient matrices $\underline{A}_2$ and $\underline{A}_3$ are of size (4×4), and $\underline{B}_2$ and $\underline{B}_3$ are of size (4×9). They are functions of φ_5 .

The goal is now to deduce from the six Eqs.(5.69) and (5.71) a polynomial equation for a single unknown variable. Two additional equations are produced by multiplying (5.69) with x_6 . These two equations together with the two Eqs.(5.69) and the four Eqs.(5.71) represent a system of eight equations. It is written in the form

$$\underbrace{\begin{bmatrix} \underline{A}_1 & \underline{0} \\ \underline{0} & \underline{A}_1 \\ \underline{A}_2 & \underline{A}_3 \end{bmatrix}}_{\underline{A}} \underbrace{\begin{bmatrix} \underline{u}_\ell \\ x_6\underline{u}_\ell \end{bmatrix}}_{\underline{y}} = \underbrace{\begin{bmatrix} \underline{B}_1 & \underline{0} \\ \underline{0} & \underline{B}_1 \\ \underline{B}_2 & \underline{B}_3 \end{bmatrix}}_{\underline{B}} \underbrace{\begin{bmatrix} \underline{u}_r \\ 1 \\ x_6\underline{u}_r \\ x_6 \end{bmatrix}}_{\underline{z}} \qquad \text{or} \qquad \underline{A}\,\underline{y} = \underline{B}\,\underline{z} \,. \tag{5.72}$$

The coefficient matrices $\underline{A}$ and $\underline{B}$ are of size (8×4) and (8×18), respectively. Four out of these eight equations are solved for $\underline{y}$ in terms of $\underline{z}$. The

resulting expression is substituted into the last four equations. These four equations are then of the form

$$\underline{P}\,\underline{z} = \underline{0} \tag{5.73}$$

with a (4×18)-matrix $\underline{P}$. Next, two new variables $x_i = \tan\varphi_i/2$ $(i = 1, 2)$ are defined. Substituting $c_i = (1 - x_i^2)/(1 + x_i^2)$ and $s_i = 2x_i/(1 + x_i^2)$ $(i = 1, 2)$ into the submatrix $\underline{u}_r$ of $\underline{z}$ and re-arranging terms the four Eqs.(5.73) are given the forms

$$x_6(a_i x_2^2 + b_i x_2 + d_i) + (p_i x_2^2 + q_i x_2 + r_i) = 0 \qquad (i = 1, 2, 3, 4)\,. \tag{5.74}$$

The coefficients a_i, b_i, d_i, p_i, q_i, r_i themselves are second-order functions of x_1 with coefficients depending on φ_5. The four Eqs.(5.74) are multiplied with x_2. These new equations and the four Eqs.(5.74) are combined in matrix form:

$$\begin{bmatrix} a_1 & p_1 & b_1 & q_1 & d_1 & r_1 & 0 & 0 \\ a_2 & p_2 & b_2 & q_2 & d_2 & r_2 & 0 & 0 \\ a_3 & p_3 & b_3 & q_3 & d_3 & r_3 & 0 & 0 \\ a_4 & p_4 & b_4 & q_4 & d_4 & r_4 & 0 & 0 \\ 0 & 0 & a_1 & p_1 & b_1 & q_1 & d_1 & r_1 \\ 0 & 0 & a_2 & p_2 & b_2 & q_2 & d_2 & r_2 \\ 0 & 0 & a_3 & p_3 & b_3 & q_3 & d_3 & r_3 \\ 0 & 0 & a_4 & p_4 & b_4 & q_4 & d_4 & r_4 \end{bmatrix} \begin{bmatrix} x_2^3 x_6 \\ x_2^3 \\ x_2^2 x_6 \\ x_2^2 \\ x_2 x_6 \\ x_2 \\ x_6 \\ 1 \end{bmatrix} = \underline{0}\,. \tag{5.75}$$

The (8×8) coefficient matrix must satisfy two conditions.
1. For a nontrivial solution to exist the determinant Δ of the coefficient matrix must be zero.
2. The nontrivial solution must have a nonzero 8th component. This latter condition is formulated as follows. Let $\underline{K}_1$ be the (8×7)-matrix formed by the first seven columns of the coefficient matrix, and let $\underline{K}_2$ be the eighth column. Furthermore, let $\underline{\xi}$ be the column matrix

$$\underline{\xi} = [\; x_2^3 x_6 \quad x_2^3 \quad x_2^2 x_6 \quad x_2^2 \quad x_2 x_6 \quad x_2 \quad x_6 \;]^T\,. \tag{5.76}$$

Equation (5.75) has the form $\underline{K}_1\underline{\xi} = -\underline{K}_2$. Premultiplication by $\underline{K}_1^T$ produces the equation

$$\underline{K}_1^T\underline{K}_1\underline{\xi} = -\underline{K}_1^T\underline{K}_2\,. \tag{5.77}$$

This equation must have a unique solution. This is condition 2. The matrices $\underline{K}_1$ and $\underline{K}_2$ depend on x_1 which is calculated from the first condition $\Delta = 0$. This is a 16th-order equation[3] for x_1. With this equation it is proved that the mechanism 5R-C has at most sixteen different configurations for a

[3] The 16th-order polynomial is computed as interpolation-polynomial connecting sixteen numerically calculated points (x_{1_i}, Δ_i) $(i = 1, \ldots, 16)$. The general problem of *Numerical polynomial algebra* is the title of Stetter [38]

given value of the independent variable φ_5. This is the number N_φ given in Table 5.1. Lee [27] gave a numerical example with sixteen different real configurations.

Every solution x_1 determines $\varphi_1 = 2\tan^{-1} x_1$. The associated solutions x_2 and x_6, i.e., φ_2 and φ_6 are determined by (5.77). With the solutions for φ_1 and φ_2 Eqs.(5.69) are two linear equations for c_4 and s_4. They determine φ_4. The last two unknowns are the variables φ_3 and h_3 in the cylindrical joint. The equation $F_3^\ell = F_3^r$ has the form (5.23) with $h_\kappa = h_3$. It determines h_3. The angle φ_3 or rather $x_3 = \tan\varphi_3/2$, can be calculated from one half-angle equation (5.37) with $a = 6$, $b = 3$ and $\mathbf{v} = \mathbf{n}_6$. An alternative method is to formulate and to solve two linear equations for c_3 and s_3, for example, the Woernle-Lee equations $F_1^\ell = F_1^r$ with $F_1 = \mathbf{n}_4 \cdot \mathbf{n}_1$ and with $F_1 = \mathbf{n}_5 \cdot \mathbf{n}_2$. They are obtained from (5.67) by a cyclic increase of all indices by one and by two, respectively. This concludes the analysis of the mechanism 5R-C.

5.4.6 RRCRPR, RRCPRR, RRCRRP. Independent Variable in the Prismatic Joint

Each of these mechanisms can be produced from the mechanism 5R-C by replacing one revolute joint by a cylindrical joint. To be specific, the mechanism RRCRPR is investigated. Its vector polygon has the form of Fig. 5.6. The only difference as compared with the mechanism 5R-C is that joint 5 is replaced by a prismatic joint. In the previous analysis the angle φ_5 was the independent variable. Now, φ_5 is constant whereas h_5, previously constant, is the independent variable. With the joints $a = 3$ and $b = 6$ the same equations $F_1^\ell = F_1^r$ and $F_2^\ell = F_2^r$ are formulated. These are Eq.(5.67) and its dual derivative. The matrix form of these two equations is, again, Eq.(5.69). The only difference is, that now the coefficient matrix $\underline{A}_1$ is a function not of φ_5, but of h_5. Also the rest of the analysis is the same as for the mechanism 5R-C. Two pairs of half-angle equations (5.37) with $\mathbf{v} = \mathbf{n}_6$ and with $\mathbf{v} = \mathbf{r}$ result in Eqs.(5.71). Via Eqs.(5.73) - (5.75) the existence of sixteen solutions $x_1 = \tan\varphi_1/2$ for a given value of the independent variable h_5 is proved. This concludes the analysis.

5.4.7 Mechanism 7R

This mechanism has $n = 7$ joints and $4n - 7 = 21$ constant parameters. The only variables are the angles $\varphi_1, \ldots, \varphi_7$ in the revolute joints. Figure 5.7 shows schematically the polygon with unit vectors $\mathbf{n}_i$ and $\mathbf{a}_i$ $(i = 1, \ldots, 7)$.

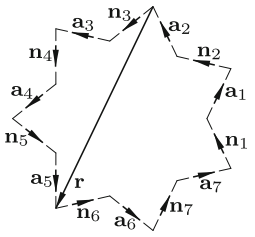

Fig. 5.7 Mechanism 7R. Polygon with unit vectors

Let φ_7 be the independent variable. Joints 3 and 6 are chosen as joints a and b for the formulation of closure conditions. The vector $\mathbf{r}$ shown in the figure is

$$\mathbf{r} = \begin{cases} h_3\mathbf{n}_3 + \ell_3\mathbf{a}_3 + h_4\mathbf{n}_4 + \ell_4\mathbf{a}_4 + h_5\mathbf{n}_5 + \ell_5\mathbf{a}_5 & \text{(left s.)} \\ -(h_6\mathbf{n}_6 + \ell_6\mathbf{a}_6 + h_7\mathbf{n}_7 + \ell_7\mathbf{a}_7 + h_1\mathbf{n}_1 + \ell_1\mathbf{a}_1 + h_2\mathbf{n}_2 + \ell_2\mathbf{a}_2) & \text{(right s.)} \end{cases} . \tag{5.78}$$

The unknown dependent variables are φ_1, φ_2 in the right segment and φ_4, φ_5 in the left segment. The four closure conditions $F_k^\ell = F_k^r$ $(k = 1, \ldots 4)$ with $F_1 = \mathbf{n}_3 \cdot \mathbf{n}_6$, $F_2 = \mathbf{r} \cdot \mathbf{n}_3 \times \mathbf{n}_6$, $F_3 = \mathbf{n}_3 \cdot \mathbf{r}$ and $F_4 = \mathbf{n}_6 \cdot \mathbf{r}$ are formulated. It was shown that all four equations have, with different coefficient matrices, the form (5.24). They are written in the matrix form

$$\underline{A}_i^* \underline{u}_\ell = \underline{B}_i^* \begin{bmatrix} \underline{u}_r \\ 1 \end{bmatrix} \qquad (i = 1, \ldots, 4) \tag{5.79}$$

with the column matrices

$$\left.\begin{aligned} \underline{u}_\ell &= [\, c_4c_5 \quad c_4s_5 \quad c_4 \quad s_4c_5 \quad s_4s_5 \quad s_4 \quad c_5 \quad s_5 \,]^T , \\ \underline{u}_r &= [\, c_1c_2 \quad c_1s_2 \quad c_1 \quad s_1c_2 \quad s_1s_2 \quad s_1 \quad c_2 \quad s_2 \,]^T . \end{aligned}\right\} \tag{5.80}$$

In order to demonstrate the usefulness of Table 5.2 the four equations are developed in detail. The equation with F_1 is written in the form (see the example following (5.17))

$$\underbrace{\mathbf{n}_k \cdot \mathbf{n}_{k+3}}_{k=3} = \underbrace{\mathbf{n}_{k-2} \cdot \mathbf{n}_{k+2}}_{k=1} . \tag{5.81}$$

With Table 5.2 this is the equation

$$\begin{aligned} & C_5\,(C_4C_3 - S_4S_3c_4) + S_5[s_5s_4S_3 - c_5(S_4C_3 + C_4S_3c_4)] \\ &= (C_6C_7 - S_6S_7c_7)(C_2C_1 - S_2S_1c_2) + [C_6S_7s_1 + S_6(s_7c_1 + c_7s_1C_7)]S_2s_2 \\ &\quad -[C_6S_7c_1 - S_6(s_7s_1 - c_7c_1C_7)](C_2S_1 + S_2C_1c_2) . \end{aligned} \tag{5.82}$$

This is the first Eq.(5.79). The coefficient matrices are

$$\left.\begin{array}{l} \underline{A}_1^* = [\,-S_3C_4S_5 \quad 0 \quad -S_3S_4C_5 \quad 0 \quad S_3S_5 \quad 0 \quad -C_3S_4S_5 \quad 0\,]\,, \\ \underline{B}_1^* = [\,-C_1S_2(C_6S_7+S_6C_7c_7) \quad S_2S_6s_7 \quad -S_1C_2(C_6S_7+S_6C_7c_7) \quad C_1S_2S_6s_7 \\ \qquad S_2(C_6S_7+S_6C_7c_7) \quad S_1C_2S_6s_7 \quad -S_1S_2(C_6C_7-S_6S_7c_7) \quad 0 \\ \qquad C_1C_2(C_6C_7-S_6S_7c_7) - C_3C_4C_5\,]\,. \end{array}\right\} \tag{5.83}$$

The second closure condition with F_2 is the dual derivative of the first equation. It is more complicated. Only the left-hand side expression is given:

$$\begin{aligned} &-\ell_5S_5(C_4C_3-S_4S_3c_4)+C_5[-\ell_4S_4C_3-\ell_3C_4S_3-(\ell_4C_4S_3+\ell_3S_4C_3)c_4+h_4S_4S_3s_4] \\ &+\ell_5C_5[s_5s_4S_3-c_5(S_4C_3+C_4S_3c_4)]+S_5\{h_5c_5s_4S_3+h_4s_5c_4S_3+\ell_3s_5s_4C_3 \\ &+h_5s_5(S_4C_3+C_4S_3c_4)-c_5[\ell_4C_4C_3-\ell_3S_4S_3+(-\ell_4S_4S_3+\ell_3C_4C_3)c_4-h_4C_4S_3s_4]\} \\ &=\ldots \quad \text{(dual derivative of the right-hand side expression of (5.82))}\,. \end{aligned} \tag{5.84}$$

The two closure conditions with $F_3 = \mathbf{n}_3 \cdot \mathbf{r}$ and $F_4 = \mathbf{n}_6 \cdot \mathbf{r}$ read

$$\begin{aligned} &h_3 + \underbrace{\mathbf{n}_k \cdot (h_4\mathbf{n}_{k+1} + \ell_4\mathbf{a}_{k+1} + h_5\mathbf{n}_{k+2} + \ell_5\mathbf{a}_{k+2})}_{k=3} \\ &= -h_6 \underbrace{\mathbf{n}_{k-2} \cdot \mathbf{n}_{k+2}}_{k=1} - \underbrace{\mathbf{n}_k \cdot (\ell_6\mathbf{a}_{k-4} + h_7\mathbf{n}_{k-3} + \ell_7\mathbf{a}_{k-3} + h_1\mathbf{n}_{k-2} + \ell_1\mathbf{a}_{k-2} + h_2\mathbf{n}_{k-1})}_{k=3}\,, \end{aligned} \tag{5.85}$$

$$\begin{aligned} &\underbrace{\mathbf{n}_k \cdot (h_3\mathbf{n}_{k-3} + \ell_3\mathbf{a}_{k-3} + h_4\mathbf{n}_{k-2} + \ell_4\mathbf{a}_{k-2} + h_5\mathbf{n}_{k-1})}_{k=6} \\ &= -h_6 - \underbrace{\mathbf{n}_k \cdot (h_7\mathbf{n}_{k+1} + \ell_7\mathbf{a}_{k+1} + h_1\mathbf{n}_{k+2} + \ell_1\mathbf{a}_{k+2} + h_2\mathbf{n}_{k+3} + \ell_2\mathbf{a}_{k+3})}_{k=6}\,. \end{aligned} \tag{5.86}$$

The scalar products are copied from Table 5.2. Simple re-arrangements result in the following equations

$$\begin{aligned} &h_3 + C_3(\ell_5s_5S_4 + h_5C_4 + h_4) + S_3s_4(\ell_5c_5 + \ell_4) + S_3c_4(\ell_5s_5C_4 - h_5S_4) \\ &= -h_2C_2 - (C_2C_1 - S_2S_1c_2)(\ell_6s_7S_7 + h_7C_7 + h_1) \\ &\quad -s_2S_2[\ell_6(c_7c_1 - s_7s_1C_7) + h_7S_7s_1 + \ell_7c_1 + \ell_1] \\ &\quad +(C_2S_1 + S_2C_1c_2)[-\ell_6(c_7s_1 + s_7c_1C_7) + h_7S_7c_1 - \ell_7s_1] \\ &\quad -h_6 \times \text{ right-hand side expression of (5.82)}\,, \end{aligned} \tag{5.87}$$

$$\begin{aligned} &h_5C_5 + (C_5C_4 - S_5S_4c_5)h_4 + S_5s_5(\ell_4 + \ell_3c_4) + (C_5S_4 + S_5C_4c_5)\ell_3s_4 \\ &+h_3 \times \text{ left-hand side expression of (5.82)} \\ &= -h_6 - h_7C_6 - \ell_7s_7S_6 - (C_6C_7 - S_6S_7c_7)(h_1 + h_2C_1 + \ell_2s_2S_1) \\ &\quad -[C_6S_7s_1 + S_6(s_7c_1 + c_7s_1C_7)](\ell_1 + \ell_2c_2) \\ &\quad -[C_6S_7c_1 - S_6(s_7s_1 - c_7c_1C_7)](-h_2S_1 + \ell_2s_2C_1)\,. \end{aligned} \tag{5.88}$$

The four Eqs.(5.82), (5.84), (5.87) and (5.88) for the unknowns φ_1, φ_2, φ_4, φ_5 are Eqs.(5.79) written in detail. Following Lee [27] the reduction to a 16th-order polynomial equation for a single unknown is achieved as

follows. First, the two Woernle-Lee Eqs.(5.16) with $F_6 = \mathbf{r}^2$ and with $F_7 = \frac{1}{2}(\mathbf{n}_3 \cdot \mathbf{n}_6)\mathbf{r}^2 - (\mathbf{n}_3 \cdot \mathbf{r})(\mathbf{n}_6 \cdot \mathbf{r})$ are formulated. These equations have, with new coefficient matrices, the form (5.79). The altogether six equations are combined in the matrix form

$$\underline{A}_1 \underline{u}_\ell = \underline{B}_1 \begin{bmatrix} \underline{u}_r \\ 1 \end{bmatrix} \tag{5.89}$$

with coefficient matrices $\underline{A}_1$ and $\underline{B}_1$ of size (6×8) and (6×9), respectively. They are functions of the independent variable φ_7.

Next, four pairs of half-angle equations (5.37) are formulated with the vectors $\mathbf{v}_1, \ldots, \mathbf{v}_4$ shown in (5.38) and with $a = 3$ and $b = 6$:

$$\left.\begin{aligned} x_6\,\mathbf{v}_i \cdot \mathbf{a}_6 + \quad \mathbf{v}_i \cdot \mathbf{n}_6 \times \mathbf{a}_6 &= -x_b\,\mathbf{v}_i \cdot \mathbf{a}_5 + \quad \mathbf{v}_i \cdot \mathbf{n}_6 \times \mathbf{a}_5 \,, \\ \mathbf{v}_i \cdot \mathbf{a}_6 - x_6\,\mathbf{v}_i \cdot \mathbf{n}_6 \times \mathbf{a}_6 &= \quad \mathbf{v}_i \cdot \mathbf{a}_5 + x_6\,\mathbf{v}_i \cdot \mathbf{n}_6 \times \mathbf{a}_5 \end{aligned}\right\} (i = 1, 2, 3, 4)\,, \tag{5.90}$$

$$\mathbf{v}_1 = \mathbf{n}_3\,, \qquad \mathbf{v}_2 = \mathbf{r}\,, \qquad \mathbf{v}_3 = \mathbf{n}_3 \times \mathbf{r}\,, \qquad \mathbf{v}_4 = \frac{1}{2}\,\mathbf{r}^2\mathbf{n}_3 - (\mathbf{n}_3 \cdot \mathbf{r})\mathbf{r}\,. \tag{5.91}$$

In each of these eight equations the elements of $\underline{u}_\ell$ appear on the left-hand side and the elements of $\underline{u}_r$ on the right-hand side. All these elements occur once without and once with the factor $x_6 = \tan\varphi_6/2$. The eight equations are combined in the matrix form

$$(\underline{A}_2 + x_6\underline{A}_3)\underline{u}_\ell = (\underline{B}_2 + x_6\underline{B}_3) \begin{bmatrix} \underline{u}_r \\ 1 \end{bmatrix} \tag{5.92}$$

with coefficient matrices $\underline{A}_2$ and $\underline{A}_3$ of size (8×8) and $\underline{B}_2$ and $\underline{B}_3$ of size (8×9). They are functions of φ_7. Another six equations are produced by multiplying (5.89) with x_6. These six equations together with the six Eqs.(5.89) and the eight Eqs.(5.92) represent a system of twenty equations. It is written in the form

$$\underbrace{\begin{bmatrix} \underline{A}_1 & \underline{0} \\ \underline{0} & \underline{A}_1 \\ \underline{A}_2 & \underline{A}_3 \end{bmatrix}}_{\underline{A}} \underbrace{\begin{bmatrix} \underline{u}_\ell \\ x_6\underline{u}_\ell \end{bmatrix}}_{\underline{y}} = \underbrace{\begin{bmatrix} \underline{B}_1 & \underline{0} \\ \underline{0} & \underline{B}_1 \\ \underline{B}_2 & \underline{B}_3 \end{bmatrix}}_{\underline{B}} \underbrace{\begin{bmatrix} \underline{u}_r \\ 1 \\ x_6\underline{u}_r \\ x_6 \end{bmatrix}}_{\underline{z}} \qquad \text{or} \qquad \underline{A}\,\underline{y} = \underline{B}\,\underline{z}\,. \tag{5.93}$$

The coefficient matrices $\underline{A}$ and $\underline{B}$ are of size (20×16) and (20×18), respectively. Sixteen out of these twenty equations are solved for $\underline{y}$ in terms of $\underline{z}$. The resulting expression is substituted into the last four equations. These four equations are then of the form

$$\underline{P}\,\underline{z} = \underline{0} \tag{5.94}$$

with a (4×18)-matrix $\underline{P}$. They are formally identical with (5.73). Also (5.74) and (5.75) and the conditions on the coefficient matrix in (5.75) are valid again (the only difference being that now φ_7 is the independent variable instead of φ_5 and that a larger number of constant Denavit-Hartenberg parameters is involved). The condition that the determinant Δ must be zero results in a 16th-order equation for $x_1 = \tan\varphi_1/2$ with coefficients depending on φ_7. Thus, it is proved that the mechanism 7R has at most sixteen configurations for a given value of the independent variable φ_7. The unknown angles φ_1, φ_2 and φ_6 are calculated as was shown following (5.77). With φ_1, φ_2 and φ_6 the column matrix $\underline{u}_r$ in the four Eqs.(5.79) is known. These equations are solved for $\underline{u}_\ell$. This solution determines the angles φ_1 and φ_2. The last unknown φ_3 is found by the method explained in the section on the mechanism 5R-C. This concludes the analysis of the mechanism 7R.

5.4.8 4R-3P. Independent Variable is an Angle

These are the mechanisms in row 4 of Table 5.1. At the end of Sect. 5.3.1 on Woernle-Lee equations it was said that the closure conditions $F_k^\ell = F_k^r$ $(k = 1, 2, 3, 4)$ are formulated not only for the mechanism 7R, but also for the mechanisms 4R-3P. These mechanisms have seven joints and, consequently, the vector polygon shown in Fig. 5.7. The mechanism 7R is converted into a mechanism 4R-3P by replacing three out of the four revolute joints 1, 2, 4 and 5 by prismatic joints. This has the effect that in the four Eqs.(5.82), (5.84), (5.87) and (5.88) three out of the variables φ_1, φ_2, φ_4 and φ_5 are (arbitrary) constants. Only one of them, say φ_j, is still a variable. For this variable (5.82) becomes an equation of the form $Ac_j + Bs_j = R$. It has two solutions for every value of the independent variable φ_7. With each solution the remaining three Eqs.(5.84), (5.87) and (5.88) become linear equations with known coefficients for the translatory variables in the three prismatic joints. This concludes the analysis of the mechanisms 4R-3P.

5.4.9 6R-P. Independent Variable is an Angle

The mechanism 6R-P has the same vector polygon the mechanism 7R has (Fig. 5.7). The mechanism 7R is converted into the mechanism 6R-P by replacing a single revolute joint by a prismatic joint. Let this be joint 5. Again, the four Eqs.(5.82), (5.84), (5.87) and (5.88) are used. As before, φ_7 is the independent variable. But now, φ_5 is a constant and h_5 is a variable. The only places where this variable appears explicitly, are the left-hand sides of (5.84), (5.87) and (5.88). These three equations have the form (5.23) with

$\lambda = 1$, $\mu = 2$, $\nu = 4$ and $\kappa = 5$. These three equations and (5.82) are combined in the matrix form

$$\underline{A}_1 \begin{bmatrix} \underline{u}_\ell \\ h_5 \underline{u}_\ell \\ h_5 \end{bmatrix} = \underline{B}_1 \begin{bmatrix} \underline{u}_r \\ 1 \end{bmatrix} \tag{5.95}$$

with the column matrices

$$\underline{u}_\ell = [c_4 \quad s_4\,]^T, \quad \underline{u}_r = [c_1c_2 \quad c_1s_2 \quad c_1 \quad s_1c_2 \quad s_1s_2 \quad s_1 \quad c_2 \quad s_2\,]^T . \tag{5.96}$$

The coefficient matrices $\underline{A}_1$ and $\underline{B}_1$ are of size (4×5) and (4×9), respectively. These four equations are supplemented by three pairs of half-angle equations (5.37) formulated with the vectors $\mathbf{v}_1$, $\mathbf{v}_2$ and $\mathbf{v}_3$ shown in (5.38). In each of these altogether six equations the column matrices of (5.95) appear once without and once with the factor $x_6 = \tan\varphi_6/2$. The six equations are combined in the matrix form

$$(\underline{A}_2 + x_6\underline{A}_3) \begin{bmatrix} \underline{u}_\ell \\ h_5 \underline{u}_\ell \\ h_5 \end{bmatrix} = (\underline{B}_2 + x_6\underline{B}_3) \begin{bmatrix} \underline{u}_r \\ 1 \end{bmatrix} . \tag{5.97}$$

The coefficient matrices $\underline{A}_2$ and $\underline{A}_3$ are of size (6×5) and $\underline{B}_2$ and $\underline{B}_3$ are of size (6×9). Another four equations are produced by multiplying (5.95) with x_6. These four equations together with the four Eqs.(5.95) and the six Eqs.(5.97) represent a system of fourteen equations. It is written in the form

$$\underbrace{\begin{bmatrix} \underline{A}_1 & \underline{0} \\ \underline{0} & \underline{A}_1 \\ \underline{A}_2 & \underline{A}_3 \end{bmatrix}}_{\underline{A}} \underbrace{\begin{bmatrix} \underline{u}_\ell \\ h_5\underline{u}_\ell \\ h_5 \\ x_6\underline{u}_\ell \\ x_6h_5\underline{u}_\ell \\ x_6h_5 \end{bmatrix}}_{\underline{y}} = \underbrace{\begin{bmatrix} \underline{B}_1 & \underline{0} \\ \underline{0} & \underline{B}_1 \\ \underline{B}_2 & \underline{B}_3 \end{bmatrix}}_{\underline{B}} \underbrace{\begin{bmatrix} \underline{u}_r \\ 1 \\ x_6\underline{u}_r \\ x_6 \end{bmatrix}}_{\underline{z}} \qquad \text{or} \qquad \underline{A}\,\underline{y} = \underline{B}\,\underline{z} . \tag{5.98}$$

The coefficient matrices $\underline{A}$ and $\underline{B}$ are of size (14×10) and (14×18), respectively. Ten out of these fourteen equations are solved for $\underline{y}$ in terms of $\underline{z}$. The resulting expression is substituted into the last four equations. These four equations are then of the form

$$\underline{P}\,\underline{z} = \underline{0} \tag{5.99}$$

with a (4×18)-matrix $\underline{P}$. They are formally identical with (5.73). The reduction to a 16th-order equation proceeds as before. Thus, it is proved that the mechanism 6R-P has at most sixteen configurations for a given value of the independent variable φ_7. The unknown angles φ_1, φ_2 and φ_6 are cal-

culated as was shown following (5.77). With these results the column matrix $\underline{z}$ in the fourteen Eqs.(5.98) is known. The ten equations already mentioned yield $\underline{y}$ and with it the variables φ_4 and h_5. The last two unknowns φ_3 and φ_6 can be determined either from half-angle equations or from Woernle-Lee equations $F_1^\ell = F_1^r$. See the sections on the mechanisms RCRCR and 5R-C. This concludes the analysis of the mechanism 6R-P when the independent variable is an angle.

5.4.10 6R-P. Independent Variable in the Prismatic Joint

Again, the vector polygon shown in Fig. 5.7 is used. This time, joint 7 is the prismatic joint. As in the analysis of the mechanism 7R the same four Eqs.(5.82), (5.84), (5.87), (5.88), the same two Woernle-Lee equations with F_6 and F_7 and the same four pairs of half-angle equations are formulated. The only difference is that in these equations φ_7 is now constant whereas h_7 is the independent variable. The only unknowns are, as before, the angles φ_1, φ_2, φ_4 and φ_5. The final result of the analysis is, again, a 16th-order polynomial equation for $x_1 = \tan\varphi_1/2$. This explains the number $N_\mathrm{t} = 16$ in Table 5.1 for this mechanism.

5.5 Mechanisms with Special Parameter Values

In the analysis of every mechanism up to now it was assumed that all constant Denavit-Hartenberg parameters are nonzero and arbitrary. The large number of parameters (between nine and twenty-one) allows for an enormous number of special cases. The Bennett mechanism and the spherical four-bar introduced in Sect. 5.4.1 are special cases of the mechanism RCCC. Table 5.2 shows that parallelity or orthogonality of the joint axes on a single body k results in substantial simplifications ($S_k = 0$, $C_k = 1$ in the former case and $S_k = 1$, $C_k = 0$ in the latter). In the following sections two special mechanisms are investigated.

5.5.1 7R with Three Parallel Joint Axes in Series

Subject of investigation is a mechanism 7R with three parallel successive joint axes, say $\mathbf{n}_2$, $\mathbf{n}_3$ and $\mathbf{n}_4$. The parallelity has the effect that the bodies 1, 2, 3 and 4 are in planar motion relative to each other. For the Denavit-

Hartenberg parameters this parallelity means $\alpha_2 = \alpha_3 = 0$ and, therefore, $S_2 = S_3 = 0$, $C_2 = C_3 = 1$. When this is substituted into (5.82), the unknowns φ_2 and φ_4 disappear. For the two remaining unknowns φ_1 and φ_5 the equation has the form

$$S_4 S_5 c_5 = A_1 c_1 + B_1 s_1 + R_1 \tag{5.100}$$

with coefficients

$$\left.\begin{aligned} A_1 &= S_1(C_6 S_7 + S_6 C_7 c_7)\,, & B_1 &= -S_1 S_6 s_7\,, \\ R_1 &= C_4 C_5 - C_1(C_6 C_7 - S_6 S_7 c_7)\,. \end{aligned}\right\} \tag{5.101}$$

Except for changes of indices (5.100) is identical with (5.56). Equation (5.84) is replaced by the dual derivative of (5.100). This equation is Eq.(5.58) with the same changes of indices. It was shown that these equations have four solutions (φ_1, φ_5) for every value of the independent variable φ_7. This ends the analysis of the special case.

5.5.2 RRSRR

The mechanism RRSRR is another special case of a mechanism 7R. The letter S stands for the spherical joint which was explained in Sect. 5.1. The polygon of vectors is shown in Fig. 5.8. Bodies 1, 2, 3, 4, 5 are coupled by revolute joints 1, 2, 3, 5 and by the spherical joint. Unit vectors $\mathbf{n}_i$ $(i = 1, 2, 3, 5)$ and $\mathbf{a}_i$ $(i = 1, 2, 5)$ are located on joint axes and on normals common to pairs of joint axes, respectively. The vectors $\ell_3\mathbf{a}_3$ and $\ell_4\mathbf{a}_4$ denote the normals from the spherical joint onto the joint axes 3 and 5, respectively. The mechanism has twelve constant parameters, namely, h_i $(i = 1, 2, 3, 5)$ in revolute joints and ℓ_i $(i = 1, \ldots, 5)$, α_i $(i = 1, 2, 5)$ on bodies. Variables are the angles φ_1, φ_2, φ_3, φ_5 in revolute joints and, in addition, three angles associated with the spherical joint. These latter ones are not considered.

The symmetry allows the same conclusions which were drawn from the symmetry of Fig. 5.3. The independent variable is either φ_5 or φ_1. Because of the symmetry only these two cases need be considered. As joints a and b in the sense of Fig. 5.2 the spherical joint and joint 3 are chosen. One of the two segments between the joints a and b has no joint variables. The other segment has the joint variables φ_1, φ_2 and φ_5. Two of these are unknowns. These two are determined from the two Woernle-Lee Eqs.(5.16) with $F_3 = \mathbf{n}_3 \cdot \mathbf{r}$ and $F_6 = \mathbf{r}^2$. The vector $\mathbf{r}$ is shown in Fig. 5.8:

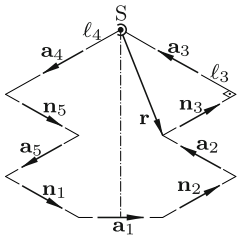

Fig. 5.8 Mechanism RRSRR with vector polygon

$$\mathbf{r} = \begin{cases} \ell_4\mathbf{a}_4 + h_5\mathbf{n}_5 + \ell_5\mathbf{a}_5 + h_1\mathbf{n}_1 + \ell_1\mathbf{a}_1 + h_2\mathbf{n}_2 + \ell_2\mathbf{a}_2 & \text{(left segment)} \\ -(h_3\mathbf{n}_3 + \ell_3\mathbf{a}_3) & \text{(right segment)} \end{cases} . \tag{5.102}$$

Taking into account the orthogonality $\mathbf{n}_3 \cdot \mathbf{a}_3 = 0$ the closure conditions are

$$\mathbf{n}_3 \cdot (\ell_4\mathbf{a}_4 + h_5\mathbf{n}_5 + \ell_5\mathbf{a}_5 + h_1\mathbf{n}_1 + \ell_1\mathbf{a}_1 + h_2\mathbf{n}_2 + \ell_2\mathbf{a}_2) = -h_3 , \tag{5.103}$$

$$(\ell_4\mathbf{a}_4 + h_5\mathbf{n}_5 + \ell_5\mathbf{a}_5 + h_1\mathbf{n}_1 + \ell_1\mathbf{a}_1 + h_2\mathbf{n}_2 + \ell_2\mathbf{a}_2)^2 = \ell_3^2 + h_3^2 . \tag{5.104}$$

In (5.104) the seven quadratic terms yield the constant $(\ell_4^2 + h_5^2 + \ldots + \ell_2^2)$. Each vector is orthogonal to its right-hand neighbor. This determines the products $\mathbf{a}_4 \cdot \mathbf{n}_5 = \mathbf{n}_5 \cdot \mathbf{a}_5 = \mathbf{a}_5 \cdot \mathbf{n}_1 = \mathbf{n}_1 \cdot \mathbf{a}_1 = \mathbf{a}_1 \cdot \mathbf{n}_2 = \mathbf{n}_2 \cdot \mathbf{a}_2 = 0$. Between each vector and its second neighbor to the right either a joint angle or a constant angle is located. This determines the five products $\mathbf{a}_4 \cdot \mathbf{a}_5 = c_5$, $\mathbf{n}_5 \cdot \mathbf{n}_1 = C_5$, $\mathbf{a}_5 \cdot \mathbf{a}_1 = c_1$, $\mathbf{n}_1 \cdot \mathbf{n}_2 = C_1$, $\mathbf{a}_1 \cdot \mathbf{a}_2 = c_2$. For calculating the remaining products the vectors are decomposed in a basis fixed on body 1. With $k = 1$ the vectors are $\mathbf{a}_4 = \mathbf{a}_{k-2}$, $\mathbf{n}_5 = \mathbf{n}_{k-1}$, $\mathbf{a}_5 = \mathbf{a}_{k-1}$, $\mathbf{n}_1 = \mathbf{n}_k$, $\mathbf{a}_1 = \mathbf{a}_k$, $\mathbf{n}_2 = \mathbf{n}_{k+1}$, $\mathbf{a}_2 = \mathbf{a}_{k+1}$, $\mathbf{n}_3 = \mathbf{n}_{k+2}$. The coordinates are copied[4] from Table 5.2 into the following Table 5.3.

Table 5.3 Coordinates of vectors in (5.103) and (5.104)

$\mathbf{a}_4$	$\mathbf{n}_5$	$\mathbf{a}_5$	$\mathbf{n}_1$	$\mathbf{a}_1$	$\mathbf{n}_2$	$\mathbf{a}_2$	$\mathbf{n}_3$
s_5S_5	C_5	0	1	0	C_1	s_2S_1	$C_2C_1 - S_2S_1c_2$
$c_5c_1 - s_5s_1C_5$	S_5s_1	c_1	0	1	0	c_2	S_2s_2
$-(c_5s_1 + s_5c_1C_5)$	S_5c_1	$-s_1$	0	0	$-S_1$	s_2C_1	$-(C_2S_1 + S_2C_1c_2)$

With these coordinates (5.103) and (5.104) take the forms

$$c_\lambda(a_{i1}c_2 + a_{i2}s_2 + a_{i3}) + s_\lambda(b_{i1}c_2 + b_{i2}s_2 + b_{i3}) + (r_{i1}c_2 + r_{i2}s_2 + r_{i3}) = 0 \tag{5.105}$$

[4] Instead of using Table 5.3 the scalar products can be obtained directly from Table 5.2. Example: $\mathbf{n}_5 \cdot \mathbf{n}_2 = \mathbf{n}_k \cdot \mathbf{n}_{k+2}$ with $k = 5$ yields $C_1C_5 - S_1S_5c_1$

$(i = 1, 2)$. The index λ equals 5 if φ_1 is the independent variable and it equals 1 if φ_5 is the independent variable. The coefficients $a_{11}, \ldots, r_{23}$ are functions of the independent variable (φ_1 or φ_5). They are given further below. The equations are identical with (5.62). The number of solutions for a given value of the independent variable is eight in the general case and four if the coefficients of c_2 and s_2 satisfy the six conditions (5.65). In the present case, these conditions are satisfied. This is shown as follows. If φ_1 is the independent variable, the auxiliary variables are defined:

$$\left.\begin{aligned} q_1 &= C_1C_5c_1 - S_1S_5 \ , \\ q_2 &= h_5S_5s_1 + \ell_5c_1 + \ell_1 \ , \\ q_3 &= h_5(C_1S_5c_1 + S_1C_5) - \ell_5C_1s_1 + h_1S_1 \ . \end{aligned}\right\} \tag{5.106}$$

In terms of these variables the coefficients of c_2 and s_2 are

$$\left.\begin{aligned} a_{11} &= \ell_2\ell_4c_1 \ , & a_{12} &= -\ell_2\ell_4C_1s_1 \ , \\ a_{21} &= S_2\ell_4C_1s_1 \ , & a_{22} &= S_2\ell_4c_1 \ , \\ b_{11} &= -\ell_2\ell_4C_5s_1 \ , & b_{12} &= -\ell_2\ell_4q_1 \ , \\ b_{21} &= S_2\ell_4q_1 \ , & b_{22} &= -S_2\ell_4C_5s_1 \ , \\ r_{11} &= \ell_2q_2 \ , & r_{12} &= \ell_2q_3 \ , \\ r_{21} &= -S_2q_3 \ , & r_{22} &= S_2q_2 \ . \end{aligned}\right\} \tag{5.107}$$

If φ_5 is the independent variable, new auxiliary variables are defined as follows:

$$q_1 = \ell_4c_5 + \ell_5 \ , \quad q_2 = \ell_4C_5s_5 - h_5S_5 \ , \quad q_3 = \ell_4S_5s_5 + h_5C_5 + h_1 \ . \tag{5.108}$$

In terms of these variables the new coefficients of c_2 and s_2 are

$$\left.\begin{aligned} a_{11} &= \ell_2q_1 \ , & a_{12} &= -\ell_2C_1q_2 \ , \\ a_{21} &= S_2C_1q_2 \ , & a_{22} &= S_2q_1 \ , \\ b_{11} &= -\ell_2q_2 \ , & b_{12} &= -\ell_2C_1q_1 \ , \\ b_{21} &= S_2C_1q_1 \ , & b_{22} &= -S_2q_2 \ , \\ r_{11} &= \ell_2\ell_1 \ , & r_{12} &= \ell_2S_1q_3 \ , \\ r_{21} &= -S_2S_1q_3 \ , & r_{22} &= S_2\ell_1 \ . \end{aligned}\right\} \tag{5.109}$$

In either case the conditions (5.65) are satisfied. The proof by inspection is elementary. This concludes the analysis of the mechanism RRSRR .

5.6 Generalized Velocities. Generalized Accelerations

The time derivatives of the seven variables φ_i and h_j are called generalized velocities $\dot{\varphi}_i$ and $\dot{h}_j$, respectively. One of them is independent and the other six are dependent. The time derivatives of six suitably chosen closure condi-

tions constitute a system of six homogeneous linear equations for the seven generalized velocities. The solution of this system expresses each of the six dependent generalized velocities as some multiple of the independent generalized velocity. Suitable closure conditions are Woernle-Lee equations which are used also for the determination of the dependent variables. In what follows, details are shown for the mechanisms RCCC and 7R.

5.6.1 RCCC

The mechanism RCCC with the labeling of joints shown in Fig. 5.3 has the seven generalized velocities $\dot{\varphi}_1$, $\dot{\varphi}_2$, $\dot{\varphi}_3$, $\dot{\varphi}_4$, $\dot{h}_2$, $\dot{h}_3$, $\dot{h}_4$. For expressing six of them as multiples of the independent velocity $\dot{\varphi}_1$ six linear equations are required. The simplest equations are the total time derivatives of (5.43), (5.45), (5.50) and (5.51) and of (5.50), (5.51) with all indices increased by one. The time derivatives of (5.43) and (5.45) are

$$\left.\begin{aligned} \dot{\varphi}_4(-As_4 + Bc_4) &= \dot{\varphi}_1(-A'c_4 - B's_4 + R') \,, \\ \dot{h}_4(Bc_4 - As_4) + \dot{\varphi}_4[h_4(-Bs_4 - Ac_4) + Ds_4 - Ec_4] &\\ = \dot{\varphi}_1[-h_4(B'c_4 - A's_4) + D'c_4 + E's_4 + F'] \,. & \end{aligned}\right\} \tag{5.110}$$

The scalars A', B', R', D', E', F' are the partial derivatives of A, B, R, D, E, F from (5.44) and (5.46) with respect to φ_1:

$$\left.\begin{aligned} A' &= S_3C_4S_1s_1 \,, \qquad B' = S_1S_3c_1 \,, \qquad R' = -C_3S_4S_1s_1 \,, \\ D' &= (\ \ell_4S_3S_1S_4 - \ell_1S_3C_1C_4 - \ell_3C_3S_1C_4)s_1 - h_1S_1S_3C_4c_1 \,, \\ F' &= (-\ell_4C_3S_1C_4 - \ell_1C_3C_1S_4 + \ell_3S_3S_1S_4)s_1 - h_1S_1C_3S_4c_1 \,, \\ E' &= -(\ell_1C_1S_3 + \ell_3S_1C_3)c_1 + h_1S_1S_3s_1 \,. \end{aligned}\right\} \tag{5.111}$$

The time derivatives of (5.50) and (5.51) are

$$\left.\begin{aligned} \dot{\varphi}_3S_3S_2s_3 &= \dot{\varphi}_1S_1S_4s_1 \,, \\ \dot{h}_3S_2S_3s_3 + \dot{\varphi}_3[h_3S_2S_3c_3 + s_3(\ell_2C_2S_3 + \ell_3S_2C_3)] &\\ = \dot{\varphi}_1[h_1S_1S_4c_1 + s_1(\ell_1C_1S_4 + \ell_4S_1C_4)] \,. & \end{aligned}\right\} \tag{5.112}$$

5.6.2 Mechanism 7R

The mechanism 7R has seven generalized velocities $\dot{\varphi}_1, \ldots, \dot{\varphi}_7$. The simplest closure condition is Eq.(5.82). Its matrix form is $\underline{A}_1^* \underline{u}_\ell = \underline{B}_1^* [\underline{u}_r^T \quad 1]^T$. The matrices $\underline{A}_1^*$, $\underline{B}_1^*$, $\underline{u}_\ell$ and $\underline{u}_r$ are given in (5.83) and (5.80). The time derivative of the equation is

$$
\begin{aligned}
&\dot\varphi_4 \underline{A}_1^*\,[\,-s_4c_5 \quad -s_4s_5 \quad -s_4 \quad c_4c_5 \quad c_4s_5 \quad c_4 \quad 0 \quad 0\,]^T\\
&+\dot\varphi_5 \underline{A}_1^*\,[\,-c_4s_5 \quad c_4c_5 \quad 0 \quad -s_4s_5 \quad s_4c_5 \quad 0 \quad -s_5 \quad c_5\,]^T\\
&=\dot\varphi_1 \underline{B}_1^*\,[\,-s_1c_2 \quad -s_1s_2 \quad -s_1 \quad c_1c_2 \quad c_1s_2 \quad c_1 \quad 0 \quad 0 \quad 0\,]^T\\
&+\dot\varphi_2 \underline{B}_1^*\,[\,-c_1s_2 \quad c_1c_2 \quad 0 \quad -s_1s_2 \quad s_1c_2 \quad 0 \quad -s_2 \quad c_2 \quad 0\,]^T\\
&+\dot\varphi_7 \underline{B}_1^{*\prime}[\quad c_1c_2 \quad c_1s_2 \quad c_1 \quad s_1c_2 \quad s_1s_2 \quad s_1 \quad c_2 \quad s_2 \quad 1\,]^T\,.
\end{aligned}
\tag{5.113}
$$

The matrix $\underline{B}_1^{*\prime}$ is the partial derivative of $\underline{B}_1^*$ with respect to φ_7:

$$
\begin{aligned}
\underline{B}_1^{*\prime} = S_6[\,&C_1S_2C_7s_7 \quad S_2c_7 \quad S_1C_2C_7s_7 \quad C_1S_2c_7\\
&-S_2C_7s_7 \quad S_1C_2c_7 \quad -S_1S_6S_7s_7 \quad 0 \quad C_1C_2S_7s_7\,]\,.
\end{aligned}
\tag{5.114}
$$

The other five equations are produced from this equation by a cyclic increase of all indices by one, by two, ..., by five (not the index 1 of $\underline{A}_1^*$ and $\underline{B}_1^*$, but all indices in $\underline{A}_1^*$ and $\underline{B}_1^*$).

It is a simple task to formulate the second time derivative. The result is a system of six linear equations for generalized accelerations $\ddot\varphi_1, \ldots, \ddot\varphi_7$. These equations contain additional terms with $\dot\varphi_i\dot\varphi_j$ $(i, j = 1, 2, 4, 5, 7)$.

5.7 Spatial Serial Robots

A spatial serial robot consists of a stationary base, a robot hand and a serial kinematical chain connecting hand and base. The serial chain is the arm of the robot. With a suitable combination of cylindrical, revolute and prismatic joints in the arm with altogether six joint variables the hand has relative to the base three rotational and three translatory degrees of freedom. The minimal number of joints is three with the joint combination 3C and the maximal number is six with the joint combination 6R. The bodies are labeled $1, \ldots, n$ with the base being body 1 and the hand being body n. The joints are labeled $1, \ldots, n-1$ beginning at the base. The problem to be solved is the following. The pose, i.e., the position and the angular orientation of the hand relative to the base, is prescribed in terms of six variables of unspecified nature, for example, by three coordinates of a single point plus three angular variables. Determine all sets of six joint variables producing this prescribed pose. The solution is found as follows. In a preparatory step the six prescribed variables are converted into another set of six variables which are defined as follows. In the prescribed pose bodies n and 1 are imagined to be connected by a revolute joint labeled n with an axis of arbitrarily chosen location and direction and with locked joint variable φ_n. The six new variables are the six Denavit-Hartenberg parameters defined by this joint, namely, α_n, ℓ_n on body n, φ_n and h_n in joint n and α_1, ℓ_1 on body 1. Together with the real joints of the robot this fictitious joint creates a spatial single-loop mechanism

with given constant Denavit-Hartenberg parameters and with a given value of the joint variable φ_n. Thus, the problem to be solved is the following. Determine six dependent joint variables of a spatial single-loop mechanism for a given value of a single independent variable φ_n. The complete solution is known from the previous sections. Table 5.4 is deduced from Table 5.1. Each of the ten rows shows the joint combination of the respective row in Table 5.1 with one revolute joint deleted. The deleted joint is the fictitious joint. The ten joint combinations represent all possible robot arms giving

Table 5.4 Serial robots with three rotational and three translatory degrees of freedom of the hand

	joint combin.	ν_r	N_φ	
1	3C	1	2	
2	2C-R-P	12	2	independent of joint sequence
3	C-2R-2P	30	2	independent of joint sequence
4	3R-3P	20	2	independent of joint sequence
5	2C-2R	6	4 8	(sequences CRCR, RCRC) (sequences CCRR, RRCC, RCCR, CRRC)
6	C-3R-P	20	8	independent of joint sequence
7	4R-2P	15	8	independent of joint sequence
8	C-4R	5	16	independent of joint sequence
9	5R-P	6	16	independent of joint sequence
10	6R	1	16	

the hand six degrees of freedom. The joints of a given joint combination can be ordered along the robot arm from base to hand in many different ways. Different sequences of letters represent different robots. Examples are the sequences (from base to hand) CRRPP, CRPRP, RRPPC etc. with the joint combination C-2R-2P. Let ν_r be the number of different robots that can be built with a given joint combination. It is calculated as follows. Let ν_C, ν_R and ν_P be the numbers of cylindrical, of revolute and of prismatic joints, respectively. The total number of joints in the arm is $\nu = \nu_C + \nu_R + \nu_P$. With these numbers the number ν_r is

$$\nu_r = \binom{\nu}{\nu_C}\binom{\nu - \nu_C}{\nu_R} . \tag{5.115}$$

The pair of numbers ν_C, ν_R in this formula can be replaced by the pair ν_C, ν_P and also by the pair ν_R, ν_P.
Example: The joint combination C-2R-2P yields $\nu_r = \binom{5}{1}\binom{4}{2} = 30$. In Table 5.4 the number ν_r is given for every joint combination.

The number N_φ is copied from Table 5.1 . It represents the number of (real or complex) six-tuples of joint variables for a given pose of the robot hand. Every real six-tuple determines an arm configuration producing the given pose. From Table 5.1 it is known that in row 5 the number N_φ is either four or eight depending on which revolute joint carries the independent angular variable. In Table 5.4 the independent variable is φ_5 in the fictitious joint 5 . This explains the correspondence between the numbers $N_\varphi = 4$ and 8 and the various joint sequences. For all other joint combinations the number N_φ is independent of the sequence of joints.

Lee [27] investigated the following problem. The hand of a 6R-robot is in pure translation with a point P of the hand moving along a given straight line. Let z be the coordinate of P along this line. The six Denavit-Hartenberg parameters α_n , ℓ_n , φ_n , h_n , α_1 , ℓ_1 of the fictitious joint are functions of z . The number of real solutions for the six joint variables, i.e., of arm configurations is a function of z , too. This function divides the z-axis into intervals with different numbers of arm configurations. With the parameter values chosen by Lee z-intervals with the maximum number $N_\varphi = 16$ were found.

References

1. Angeles J, Hommel G, Kovács P (1993) Computational kinematics. Kluwer, Dordrecht
2. Crane III C D, Duffy J (1998) Kinematic analysis of robot manipulators. Cambridge Univ. Press
3. Denavit J, Hartenberg R S (1955) A kinematic notation for lower-pair mechanisms based on matrices. J.Appl.Mech. 22:215–221
4. Duffy J (1971) An analysis of five-, six- and seven-link spatial mechanisms. Part 1: Derivation of equations for five-, six- and seven-link spatial mechanisms. Part 2: Derivation of closed-form, input-output displacement equations for the RCRRC and RPRRCR mechanisms. Proc. 3rd IFToMM Congr. v.C:83–110
5. Duffy J (1972) On the closures of spatial mechanisms. ASME Paper 72-Mech-77
6. Duffy J (1975) A foundation for a unified theory of analysis of spatial mechanisms. J. Eng.f.Ind. 97B:1159–1165
7. Duffy J (1977) Displacement analysis of seven-link 5R-2P mechanisms. J. Eng.f.Ind. 99B:692–701
8. Duffy J (1980) Analysis of mechanisms and robot manipulators. Wiley, New York
9. Duffy J, Crane C (1980) A displacement analysis of the general spatial 7-link, 7R mechanism. Mechanism Machine Theory 15:153–169
10. Duffy J, Habib-Olahi H Y (1971-2) A displacement analysis of the spatial 3R–2C mechanisms. 1. On the closures of the RCRCR mechanism. 2. Analysis of the RRCRC mechanism. J. Mechanisms 6:289–301, 463–473. 3. Analysis of the RCRRC mechanism. Mechanism Machine Theory 7:71–84
11. Duffy J, Rooney J (1974) Displacement analysis of spatial six-link, 5R-C mechanisms. J.Appl.Mech. 41:759–766
12. Duffy J, Rooney J (1974) A displacement analysis of spatial six-link 4R-P-C mechanisms. J. Eng.f.Ind. 96B:705–721
13. Dukkipati R V, Soni A (1971) Displacement analysis of RPSPR, RPSRR mechanisms. Proc.3rd World IFToMM Congr. v.D, paper D-4, 49–61

14. Dukkipati R V (1974) Closed-form displacement relationships of a class of six-link 3R+2P+1C spatial mechanisms. J. Aeronaut.Soc.India 27:159–163
15. Erdman A G (ed.) (1993) Modern kinematics. Developments in the last forty years. Wiley, New York (appr. 2250 literature references)
16. Hiller M (1981) Analytisch-numerische Verfahren zur Behandlung räumlicher Übertragungsmechanismen. VDI-Verl. 1, 76
17. Hiller M, Kekskeméthy A, Woernle C (1986) A loop-based kinematical analysis of spatial mechanisms. ASME Paper 86-DET-184
18. Kecskeméthy A, Hiller M (1992) Automatic closed-form kinematics solutions for recursive single-loop chains. ASME Mechanism Conf. Proc.:387–393
19. Kecskeméthy A (1993) On closed-form solutions of multiple-loop mechanisms. In [1]:263–274
20. Lee H-J (1984) Kinematic analysis of spatial mechanisms. M.Sc.thesis (Chin.), Beijing Univ.of Post & Telec.
21. Lee H-J, Liang C-G (1987) Displacement analysis of the spatial 7-link 6R-P linkages. Mechanism Machine Theory 22:1–11 (first presented in 2nd Chin.Nat.Conf. Taiwan 1984)
22. Lee H-J, Liang C-G (1987) Displacement analysis of the general spatial 7-link RRPRPRR mechanism. Proc.7th IFToMM Congr. Sevilla 1:223–226
23. Lee H-J, Liang C-G (1988) A new vector theory for the analysis of spatial mechanisms. Mechanism Machine Theory 23:209–217
24. Lee H-J, Liang C-G (1988) Displacement analysis of the general spatial 7-link 7R mechanism. Mechanism Machine Theory 23:219–226 (first presented in 4th Chin.Nat.Conf. Yantai 1986)
25. Lee H-J, Roth B (1993) A closed-form solution for the forward displacement analysis of a class of in-parallel mechanisms. IEEE Trans. Robotics and Automation 1:720–724
26. Lee H-J, Woernle C, Hiller M (1991) A complete solution for the inverse kinematic problem of the general 6R robot manipulator. J.Mech.Design 113:481–486
27. Li (Lee) H-J (1990) Ein Verfahren zur vollständigen Lösung der Rückwärtstransformation für Industrieroboter mit allgemeiner Geometrie, Diss. Univ.Duisburg
28. Liang C-G, Lee H-J, Liao Q Z (1988) Analysis of spatial linkages and robot mechanisms. Beijing Univ. of Post & Telec.Publ.House
29. Miura H, Arimoto S (eds.) (1990) Robotics Research. MIT Press, Cambridge, Mass.
30. Nielsen J, Roth B. (1999) On the kinematic analysis of robotic mechanisms. Int. J. Robotics Res.18:1147-1160
31. Peisach E (1991) Displacement analysis of linkages: Evolution of investigations in a historical aspect (with 82 lit. refs.). In: Hirofumi, Arimoto, Miura (eds): Robotics Research: 5th Int. Symposium. Artif. Intell. Series
32. Raghavan M, Roth B (1990) Kinematic analysis of the 6R manipulator of general geometry. 5th Int.Symp.Robotis Res. In: [29]:263–270
33. Raghavan M, Roth B (1993) Inverse kinematics of the general 6R manipulator and related linkages. ASME J. Mechanical Design 105:502–508
34. Sinigersky A (2002) Rechnerunterstützte Behandlung von dualen Grössen in der Kinematik. Studienarbeit Inst. Techn. Mech. Univ. Karlsruhe
35. Soni A H, Pamidi P R (1971) Closed-form displacement relations of a five-link R-R-C-C-R spatial mechanism. J. Eng.f.Ind. 93:221–226
36. Soni A H (1974) Mechanism synthesis and analysis. Mac-Graw Hill, New York
37. Spillers W R (ed.) (1964) Basic questions of design theory. Northholland, Amsterdam
38. Stetter H J (2004) Numerical polynomial algebra. SIAM Philad. A G (ed.) (1993)
39. Woernle C (1988) Ein systematisches Verfahren zur Aufstellung der geometrischen Schliessbedingungen in kinematischen Schleifen mit Anwendung bei der Rückwärtstransformation für Industrieroboter. Diss. Univ. Duisburg, Fortschr.-Ber.VDI R.18, Nr.59

40. Yang A T (1963) Application of quaternion algebra and dual numbers to the analysis of spatial mechanisms. PhD thesis Columbia Univ.
41. Yang A T (1964) Calculus of screws. In: [37]:265–281
42. Yang A T (1969) Displacement analysis of spatial five-link mechanisms using (3×3) matrices with dual-number elements. J. Eng.f.Ind. 91:152–157
43. Yang A T, Freudenstein F (1964) Application of dual-number quaternion algebra to the analysis of spatial mechanisms. Trans ASME 86E:300–308 (J.Appl.Mech.31)
44. Yuan M S C (1971) Displacement analysis of the RPRCRR six-link spatial mechanism. J. Eng.f.Ind. 93:1029–1035
45. Yuan M S C, Freudenstein F (1971) Kinematic analysis of spatial mechanisms by means of screw coordinates. Part I - Screw coordinates. J. Eng.f.Ind. 93:61–66
46. Yuan M S C, Freudenstein F, Woo L S (1971) Kinematic analysis of spatial mechanisms by means of screw coordinates. Part II - Analysis of spatial mechanisms. J. Eng.f.Ind. 93:67–73
47. Wittenburg J (2003) Closure conditions for spatial mechanisms. A nonrecursive formulation. Arch.Appl.Mech.72:933–948

Chapter 6
Overconstrained Mechanisms

By definition, an overconstrained mechanism is a mechanism for which Grübler's formula (4.1) yields a degree of freedom $F > 0$ only because the system of kinematic constraint equations has a sufficiently large defect $d > 0$. It is known that a simple closed kinematic chain with $n < 7$ joint variables has a degree of freedom $F > 0$ only if it is overconstrained. Sections 6.1 – 6.4 are devoted to simple closed chains with four, with five and with six revolute joints. In the remaining Sects. 6.5 – 6.11 other types of overconstrained mechanisms are analyzed.

The planar four-bar and the spherical four-bar with $n = 4$ revolute joints are among the oldest overconstrained mechanisms. Two simple overconstrained mechanisms with $n = 6$ revolute joints are shown in Figs. 6.1 and 6.2. In Fig. 6.1 the fixed frame, three shafts and the cross-shaped central bodies of two Hooke's joints are interconnected by two frame-fixed revolutes and by two more revolutes in each Hooke's joint. The mechanism shown in Fig. 6.2 was invented by Sarrus. Body 4 has the single degree of freedom of translation along the x-axis. The body is connected to the frame 1 by two dyads (bodies 2,3 and 5,6) each dyad having three parallel revolute joints

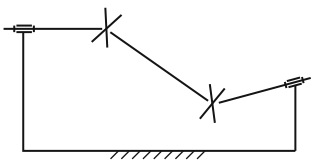

Fig. 6.1 Overconstrained mechanism composed of three shafts, two revolute and two Hooke's joints

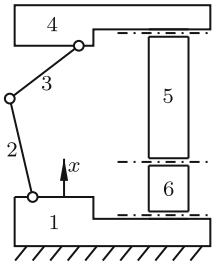

Fig. 6.2 Sarrus' overconstrained mechanism

J. Wittenburg, *Kinematics*, DOI 10.1007/978-3-662-48487-6_6

perpendicular to the x-axis (otherwise arbitrarily directed, but not all six parallel).

6.1 Bricard's Theorem on Closed Chains with Revolute Joints

The early history of the search for overconstrained mechanisms was marked by chance discoveries and by ingenuity. The first systematic investigations were made by Delassus [15, 16]. An important step forward was made by Bricard's

Theorem 6.1. *In the case of $n = 6$ revolute joints the joint axes are, in every position of the system instantaneously, lines of a linear complex. In the case of $n = 5$ revolute joints the joint axes are, in every position of the system instantaneously, lines of a linear congruence. In the case of $n = 4$ revolute joints the joint axes are, in every position of the system instantaneously, generating lines of a ruled surface of order two (a quadric).*

Proof for the case $n = 6$ (Bricard [10]): Let joint i connect bodies i and $i-1$ $(i = 1, \ldots, 6$ cyclic), and let $\omega_i(\mathbf{n}_i, \mathbf{a}_i \times \mathbf{n}_i)$ be the associated velocity screw of body i relative to body $i-1$ (see (9.33)). The vectors $\mathbf{n}_i$ and $\mathbf{a}_i \times \mathbf{n}_i$ are the Plücker vectors of joint axis i. The velocity screw of body 6 relative to itself is zero. This is the set of equations

$$\sum_{i=1}^{6} \mathbf{a}_i \times \mathbf{n}_i \omega_i = \mathbf{0} \,, \qquad \sum_{i=1}^{6} \mathbf{n}_i \omega_i = \mathbf{0} \,. \tag{6.1}$$

Decomposition in some common reference frame yields six homogeneous linear equations with a (6×6)-coefficient matrix of vector coordinates multiplied by the column matrix of angular velocities. Since these latter ones are not all zero, the coefficient matrix must be singular. More precisely, some linear combination of its rows must be zero. In vector notation this is expressed by the six equations (one for each column of the matrix)

$$\mathbf{a} \cdot \mathbf{a}_i \times \mathbf{n}_i + \mathbf{b} \cdot \mathbf{n}_i = 0 \qquad (i = 1 \ldots, 6) \tag{6.2}$$

where $\mathbf{a}$ and $\mathbf{b}$ are vectors whose altogether six coordinates are the coefficients of the said linear combination. This is Eq.(2.25) defining the lines $(\mathbf{n}_i \,, \mathbf{a}_i \times \mathbf{n}_i)$ to be lines of the linear complex $(\mathbf{a}; \mathbf{b})$. End of proof.

Proof for the case $n = 5$: The closed kinematic chain with six axes is formally reduced to a chain with five axes if the sixth axis $(\mathbf{n}_6 \,, \mathbf{a}_6 \times \mathbf{n}_6)$ has *arbitrary* location while simultaneously $\omega_6 = 0$. Equations (6.1) lead again to (6.2). Because of the arbitrariness of $\mathbf{n}_6$ and $\mathbf{a}_6 \times \mathbf{n}_6$ the said linear complex $(\mathbf{a}; \mathbf{b})$ is now subject to a linear constraint equation. This proves

that the axes $1, \ldots, 5$ are lines of a linear congruence. The proof for the case $n = 4$ repeats the same arguments. With axes 5 and 6 being arbitrary the linear complex $(\mathbf{a}; \mathbf{b})$ is subject to two linear constraint equations. This ends the proof of the theorem.

The theorem states that (in the case $n = 6$, for example) a closed kinematic chain with six joint axes is *instantaneously* mobile if in the position under investigation the six joint axes are lines of a linear complex. Motion into another position is possible only if in every intermediate position the six joint axes are lines of a linear complex. In general, this is not the case if a single assembly position of a mechanism is the result of selecting at random six lines of a linear complex as joint axes. The theorem provides a new direction to the search for overconstrained systems, namely: Find closed kinematic chains having the property that its six axes belong in *every position* to a linear complex. This search led Bricard [10] to three classes of overconstrained mechanisms which are the subjects of Sects. 6.4.1, 6.4.2 and 6.4.3. The chapter begins with the celebrated Bennett mechanism which has four revolute joints.

6.2 Bennett Mechanism

In Sect. 5.4.1 the closed kinematical chain RCCC was investigated (see Fig. 5.3 and (5.43) – (5.51)). Bennett [8] noticed that the joint variables h_2, h_3 and h_4 in the three cylindrical joints are identically zero if the parameters satisfy the conditions

$$\left.\begin{array}{llll} \alpha_3 = \alpha_1\,, & \ell_3 = \ell_1\,, & \alpha_4 = \alpha_2\,, & \ell_4 = \ell_2\,, \\ \ell_2 \sin\alpha_1 = \ell_1 \sin\alpha_2\,, & h_1 = 0\,. & & \end{array}\right\} \tag{6.3}$$

A proof is given further below. With $h_2 = h_3 = h_4 \equiv 0$ all four joints of the mechanism are revolute joints with zero offset. This mechanism is called Bennett mechanism. It is an overconstrained mechanism with the degree of freedom $F = 1$. Grübler's formula (4.1) yields $F = -2+d$. Hence the number of dependent constraint equations is $d = 3$. According to Bricard's Theorem 6.1 the joint axes are, in every position of the mechanism instantaneously, generators of a hyperboloid.

From the condition $\ell_2 \sin\alpha_1 = \ell_1 \sin\alpha_2$ it follows that $\sin\alpha_1$ and $\sin\alpha_2$ have the same sign. Arbitrarily, the positive sign is assumed, i.e., angles in the interval $0 < \alpha_1, \alpha_2 < \pi$ (angles zero and π are excluded because only spatial mechanisms are investigated). The Bennett mechanism is specified by the three parameters ℓ_1, α_1 and α_2. Together they determine ℓ_2.
Note: The alternative decision to use as parameters the quantities ℓ_1, ℓ_2 and α_1 has the disadvantage that either no real angle α_2 or two different angles α_2 satisfy the condition $\ell_2 \sin\alpha_1 = \ell_1 \sin\alpha_2$. Two mechanisms differing in

α_2 only are not representing two types of Bennett mechanism, but simply two different Bennett mechanisms.

Kinematical properties of the Bennett mechanism are deduced from the equations governing the mechanism RCCC and from the conditions (6.3). First, it is proved that $h_2 = h_3 = h_4 \equiv 0$. Equation (5.51) reduces to $h_3 = 0$. This concludes the proof for h_3. From the symmetry of Eqs.(6.3) it follows that $h_2 \equiv 0$ if $h_4 \equiv 0$. The solution $h_4 \equiv 0$ requires that the numerator expression in (5.45) be identically zero. In addition, (5.43) is valid. Therefore, it must be shown that the equations

$$Ac_4 + Bs_4 - R = 0\,, \qquad Dc_4 + Es_4 + F = 0 \tag{6.4}$$

do not contradict each other. The coefficients A, B, R, D, E, F are those given in (5.44) and (5.46). In view of (6.3) they have the forms

$$\left.\begin{array}{lll} A = -S_1(S_1C_2c_1 + S_2C_1)\,, & B = S_1^2 s_1\,, & D = \ell_1(ac_1 + b)\,, \\ R = \quad S_1(S_2C_1c_1 + S_1C_2)\,, & E = -2\ell_1 S_1C_1 s_1\,, & F = \ell_1(bc_1 + a) \end{array}\right\} \tag{6.5}$$

with constants

$$a = S_1(2C_1C_2 - S_2^2)\,, \qquad b = S_2(2C_1^2 + C_1C_2 - 1)\,. \tag{6.6}$$

With these expressions Eqs.(6.4) are two linear equations for two unknowns:

$$S_1C_2\frac{1 + c_1c_4}{s_1s_4} + C_1S_2\frac{c_1 + c_4}{s_1s_4} = S_1\,, \qquad a\,\frac{1 + c_1c_4}{s_1s_4} + b\,\frac{c_1 + c_4}{s_1s_4} = 2S_1C_1\,. \tag{6.7}$$

The solution is

$$\frac{1 + c_1c_4}{s_1s_4} = \frac{1 - C_1C_2}{C_2 - C_1}\,, \qquad \frac{c_1 + c_4}{s_1s_4} = \frac{-S_1S_2}{C_2 - C_1}\,. \tag{6.8}$$

The difference of these two equations produces on the left-hand side the expression

$$\frac{(1 - c_1)(1 - c_4)}{s_1s_4} = \tan\frac{\varphi_1}{2}\tan\frac{\varphi_4}{2} \tag{6.9}$$

and on the right-hand side the constant

$$\frac{1 - (C_1C_2 - S_1S_2)}{C_2 - C_1} = \frac{1 - \cos(\alpha_1 + \alpha_2)}{2\sin\frac{\alpha_1+\alpha_2}{2}\,\sin\frac{\alpha_1-\alpha_2}{2}} = \frac{\sin\frac{\alpha_1+\alpha_2}{2}}{\sin\frac{\alpha_1-\alpha_2}{2}}\,. \tag{6.10}$$

It can have any positive or negative value. Thus, the result for φ_4 is

$$\tan\frac{\varphi_4}{2} = p\,\cot\frac{\varphi_1}{2}\,, \qquad p = \frac{\sin\frac{\alpha_1+\alpha_2}{2}}{\sin\frac{\alpha_1-\alpha_2}{2}}\,. \tag{6.11}$$

This equation relates to every angle $0 \le \varphi_1 \le 2\pi$ a single angle φ_4 (and vice versa) for which $h_4 \equiv 0$. This concludes the proof.

The existence of a single angle φ_4 for every angle φ_1 proves that the Bennett mechanism does not have a second configuration. Full-cycle rotatability in joint 1 follows also from the fact that in (6.4) $A^2 + B^2 - R^2 = (S_1 S_2 s_1)^2 \ge 0$ and $D^2 + E^2 - F^2 = [\ell_1 S_2 (C_1 + C_2) s_1]^2 \ge 0$.

Next, the relationship between φ_2 and φ_1 is established. For the mechanism RCCC it is given by Eqs.(5.48), (5.49). With (6.3) the coefficients A^*, B^*, R^* turn out to be the coefficients A, B, R in (6.5) with α_1 and α_2 interchanged. Because of (6.11) this means that $\varphi_2 = -\varphi_4$.

Finally, the relationship between φ_3 and φ_1 is established. Equation (5.50) reduces to $\cos\varphi_3 = \cos\varphi_1$. Hence either $\varphi_3 = \varphi_1$ or $\varphi_3 = -\varphi_1$. Another equation involving φ_3 is Eq.(5.53). With (6.3) it becomes

$$S_1 C_2 (c_3 + c_4) - S_2 (s_3 s_4 - C_1 c_3 c_4) + C_1 S_2 = 0 \,. \tag{6.12}$$

Depending on whether $\varphi_3 = \varphi_1$ or $\varphi_3 = -\varphi_1$ this is one of the two equations

$$S_1 C_2 (c_1 + c_4) - S_2 (\pm s_1 s_4 - C_1 c_1 c_4) + C_1 S_2 = 0 \,. \tag{6.13}$$

For $c_1 + c_4$ and for $c_1 c_4$ expressions obtained from (6.8) are substituted. It turns out that only the equation with the minus sign is identically satisfied. This shows that $\varphi_3 = -\varphi_1$.

Next, the angular velocity $\dot\varphi_4$ and the angular acceleration $\ddot\varphi_4$ are determined by differentiating (6.11) with respect to time. The first derivative yields

$$\dot\varphi_4 = -p\,\dot\varphi_1 \frac{\cos^2\frac{\varphi_4}{2}}{\sin^2\frac{\varphi_1}{2}} = -p\,\dot\varphi_1 \frac{1}{\sin^2\frac{\varphi_1}{2}(1 + \tan^2\frac{\varphi_4}{2})} \tag{6.14}$$

$$= -p\,\dot\varphi_1 \frac{1}{\sin^2\frac{\varphi_1}{2}(1 + p^2\cot^2\frac{\varphi_1}{2})} = -p\,\dot\varphi_1 \frac{1}{\sin^2\frac{\varphi_1}{2} + p^2\cos^2\frac{\varphi_1}{2}} \tag{6.15}$$

or, finally,

$$\dot\varphi_4 = -\dot\varphi_1 \frac{2p}{1 + p^2 - (1 - p^2)\cos\varphi_1} \,. \tag{6.16}$$

The ratio $\dot\varphi_4/\dot\varphi_1$ is oscillating 2π-periodically between the extremal values $-p$ and $-1/p$. Differentiating one more time yields for the angular acceleration the expression

$$\ddot\varphi_4 = -\ddot\varphi_1 \frac{2p}{1 + p^2 - (1 - p^2)\cos\varphi_1} + \dot\varphi_1^2 \frac{2p(1 - p^2)\sin\varphi_1}{[1 + p^2 - (1 - p^2)\cos\varphi_1]^2} \,. \tag{6.17}$$

Byshgens [13] and Dimentberg/Schor [18] gave the first proofs that the Bennett mechanism, the planar four-bar and the spherical four-bar are the

only overconstrained mechanisms composed of four links and four revolute joints. See also Dietmaier [19].

In Chap. 7 chains RR are investigated. A chain RR is a chain of three bodies interconnected by two revolute joints. One of the terminal bodies is the fixed frame. The other terminal body has the degree of freedom two. Subject of investigation are positions of the moving body and trajectories of body-fixed points. In the Bennett mechanism bodies 3 and 1 are the terminal bodies of two chains RR, one with joints 1, 2 on body 2 and the other with joints 3, 4 on body 4. Equations (6.3) and the relationships $\varphi_3 = -\varphi_1$, $\varphi_4 = -\varphi_2$ show that both chains RR are congruent. Every position of body 3 and the trajectories of all points of body 3 are generated by both chains RR. In Chap. 7 these statements are arrived at by arguments different from the ones used here.

6.3 Kinematical Chains with Five Revolute Joints

The only known 5R mechanism is the Goldberg mechanism treated in Sect. 6.3.1. Whether other types exist, is an unsettled question. If so, then the fifteen constant Denavit-Hartenberg parameters ℓ_i, α_i, h_i $(i = 1, \ldots, 5)$ satisfy certain conditions. A set of sufficient conditions is formulated as follows. The unit vectors in the polygon of vectors $\ell_i \mathbf{a}_i + h_i \mathbf{n}_i$ $(i = 1, \ldots, 5)$ are shown in Fig. 5.5a in which now all five joints are understood to be revolute joints. Woernle-Lee equations eliminate two joint variables. Five equations relating φ_3, φ_1, φ_5 are based on the products $\mathbf{n}_2 \cdot \mathbf{n}_4$, $\mathbf{n}_2 \cdot \mathbf{r}$, $\mathbf{n}_4 \cdot \mathbf{r}$, $\mathbf{r}^2$ and $\mathbf{r} \cdot \mathbf{n}_2 \times \mathbf{n}_4$ with the vector $\mathbf{r}$ pointing from $\mathbf{n}_2$ to $\mathbf{n}_4$. This vector has the two representations

$$\mathbf{r} = \begin{cases} h_2\mathbf{n}_2 + \ell_2\mathbf{a}_2 + h_3\mathbf{n}_3 + \ell_3\mathbf{a}_3 & \text{(right segment)} \\ -(h_4\mathbf{n}_4 + \ell_4\mathbf{a}_4 + h_5\mathbf{n}_5 + \ell_5\mathbf{a}_5 + h_1\mathbf{n}_1 + \ell_1\mathbf{a}_1) & \text{(left segment)}\,. \end{cases} \tag{6.18}$$

The fifth equation is the dual derivative of the first equation (see (3.50)). Evaluation of the equations by means of Table 5.2 is an elementary exercise left to the reader. The first equation is $\mathbf{n}_k \cdot \mathbf{n}_{k+2} = \mathbf{n}_k \cdot \mathbf{n}_{k-3}$ with $k = 2$. The equations are

$$\left.\begin{aligned} S_2S_3c_3 \quad\quad\quad\quad\quad\quad + A_1c_5 + B_1s_5 &= R_1\,, \\ \ell_3\,S_2s_3 + A_2c_5 + B_2s_5 &= R_2\,, \\ -h_2S_2S_3c_3 \quad + \ell_2\,S_3s_3 + A_3c_5 + B_3s_5 &= R_3\,, \\ \ell_2\,\ell_3\,c_3 + h_2\ell_3\,S_2s_3 + A_4c_5 + B_4s_5 &= R_4\,, \\ (\ell_2C_2S_3 + \ell_3S_2C_3)c_3 - h_3S_2S_3s_3 + A_5c_5 + B_5s_5 &= R_5\,. \end{aligned}\right\} \tag{6.19}$$

The coefficients of $c_3 = \cos\varphi_3$ and $s_3 = \sin\varphi_3$ are constants. The coefficients A_i, B_i, R_i $(i = 1, \ldots, 5)$ are abbreviations for linear functions of $c_1 = \cos\varphi_1$

and $s_1 = \sin\varphi_1$:

$$\left.\begin{aligned}
A_1 &= -S_4(S_1C_5c_1 + C_1S_5)\,, \qquad B_1 = S_4S_1s_1\,,\\
R_1 &= \;\; C_4(S_1S_5c_1 - C_1C_5) + C_2C_3\,,\\
A_2 &= -h_4S_4(S_1C_5c_1 + C_1S_5) + \ell_4S_1s_1\,,\\
B_2 &= \ell_4(S_1C_5c_1 + C_1S_5) + h_4S_4S_1s_1\,,\\
R_2 &= (h_4C_4 + h_5)(S_1S_5c_1 - C_1C_5) - (\ell_5S_1s_1 + h_1C_1 + h_2 + h_3C_2)\,,\\
A_3 &= S_4(\ell_1C_5s_1 - h_1S_5)\,, \qquad B_3 = S_4(\ell_1c_1 + \ell_5)\,,\\
R_3 &= -[C_4(\ell_1S_5s_1 + h_1C_5 + h_5) + C_3(h_2C_2 + h_3) + h_4]\,,\\
A_4 &= -\ell_4(\ell_1c_1 + \ell_5) - h_4S_4(\ell_1C_5s_1 - h_1S_5)\,,\\
B_4 &= -h_4S_4(\ell_1c_1 + \ell_5) + \ell_4(\ell_1C_5s_1 - h_1S_5)\,,\\
R_4 &= (h_4C_4 + h_5)(\ell_1S_5s_1 + h_1C_5) + \ell_1\ell_5c_1 + h_4h_5C_4 - h_2h_3C_2\\
&\quad + \tfrac{1}{2}[\ell_1^2 + \ell_4^2 + \ell_5^2 + h_1^2 + h_4^2 + h_5^2 - (\ell_2^2 + \ell_3^2 + h_2^2 + h_3^2)]\,,\\
A_5 &= h_5B_1 + A_1'\,, \qquad B_5 = -h_5A_1 + B_1' \qquad R_5 = R_1'
\end{aligned}\right\} \tag{6.20}$$

(A_1' , B_1' , R_1' are the dual derivatives of A_1 , B_1 , R_1 , respectively).
The first four Eqs.(6.19) are solved for c_3 , s_3 , c_5 , s_5 . In terms of coefficient determinants

$$c_3 = \frac{\Delta_{c3}}{\Delta}\,, \qquad s_3 = \frac{\Delta_{s3}}{\Delta}\,, \qquad c_5 = \frac{\Delta_{c5}}{\Delta}\,, \qquad s_5 = \frac{\Delta_{s5}}{\Delta}\,. \tag{6.21}$$

Δ_{c3} and Δ_{s3} are sums of products of three functions $A_iB_jR_k$, whereas Δ_{c5} , Δ_{s5} and Δ are sums of products of only two functions (B_jR_k or A_iR_k or A_iB_j). Substitution of (6.21) into the fifth Eq.(6.19) results after multiplication with Δ in an equation in which φ_1 is the only variable. This equation must be the identity equation. The highest-order terms are c_1^3 , $c_1^2s_1$, $c_1s_1^2$ and s_1^3 . In terms of the new variable $x_1 = \tan\varphi_1/2$ it is a 6th-order equation

$$a_6x_1^6 + a_5x_1^5 + \cdots + a_1x_1 + a_0 \equiv 0\,. \tag{6.22}$$

The coefficients are functions of the fifteen parameters. Without loss of generality, the parameter ℓ_1 can be set equal to one so that $\ell_2, \ldots, \ell_5$ and $h_1, \ldots, h_5$ are determined as multiples of ℓ_1 . Hence there are only fourteen essential parameters. Equations (6.19), (6.20) remain valid when the indices of all parameters and variables are cyclicly increased by 1 , by 2 , by 3 , by 4 . Hence altogether five 6th-order identity equations with variables $x_i = \tan\varphi_i/2$ $(i = 1, \ldots, 5)$ and with coefficients depending on the fourteen essential parameters are obtained. In each identity equation the seven coefficients must be zero. In addition, the conditions $c_3^2 + s_3^2 = 1$, $c_5^2 + s_5^2 = 1$ and four more such conditions must be satisfied. Hence altogether 45 functions of the parameters must be zero.

6.3.1 Goldberg Mechanism

Goldberg [20] recognized that an overconstrained 5R mechanism can be constructed by merging two Bennett mechanisms. Both mechanisms must be identical in the parameters α_1 and ℓ_1 and different in the third parameter, i.e., α_2 in one mechanism and $\alpha_3 \neq \alpha_2$ in the other (see Fig. 6.3a). The parameters satisfy Eqs.(6.3), i.e.,

$$\ell_2 = \ell_1 \frac{\sin\alpha_2}{\sin\alpha_1}\,, \qquad \ell_3 = \ell_1 \frac{\sin\alpha_3}{\sin\alpha_1} \tag{6.23}$$

as well as the identity of pairs of opposite bodies. All joints have zero offset. Four bodies have the parameters $\ell_1\,,\ \alpha_1$. In Fig. 6.3b the mechanisms are shown in positions in which they share body 1 with parameters $\ell_1\,,\ \alpha_1$. The degree of freedom two as well as the quantities ℓ_1 and α_1 remain unchanged when body 1 is removed while preserving all six joint axes (Fig. c). Indeed, none of the original Bennett mechanisms is mobile with other than the original quantities $\ell_1\,,\ \alpha_1$. In the system of Fig. 6.3d one of the two joints bridging both mechanisms is frozen in an arbitrarily chosen position β. This results in the Goldberg mechanism with five bodies and five revolute joints. It has five constant parameters, namely, the four essential parameters $\alpha_1\,,\ \alpha_2\,,\ \alpha_3\,,\ \beta$ and the length ℓ_1 which merely determines the size.

The bodies are newly labeled as shown in Fig. 6.3d. Body i is the body of length ℓ_i $(i = 1,\ldots,5)$. Joint 3 between bodies 2 and 3 is the mobile joint bridging the two Bennett mechanisms. Body 5 with joint axes 5 and 1 is the body created by freezing the joint in the position β. The coefficients $A_i\,,\ B_i\,,\ R_i$ $(i = 1,\ldots,5)$ in (6.19) and (6.20) depend on the parameters $\ell_5\,,\ \alpha_5$ of this body 5 and on the offsets $h_5\,,\ h_1$ of its joints 5 and 1. As preparatory step these four parameters are expressed in terms of β and of the parameters $\ell_2\,,\ \alpha_2$ and $\ell_3\,,\ \alpha_3$ of the two bodies merged into body 5. These two bodies are labeled body $2'$ and body $3'$, respectively. The vector $\mathbf{r}$ pointing from axis 5 to axis 1 has the two representations

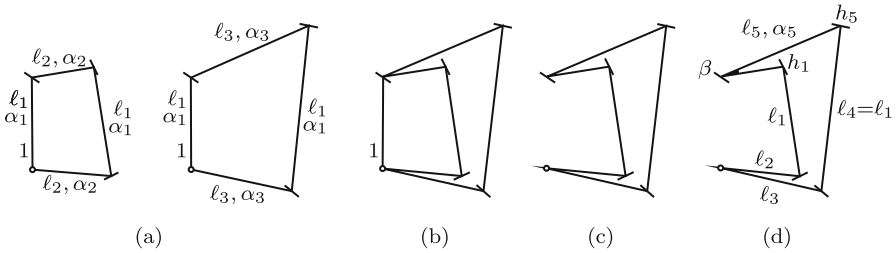

Fig. 6.3 Goldberg's creation of a 5R mechanism from two Bennett mechanisms

$$\mathbf{r} = \begin{cases} h_5\mathbf{n}_5 + \ell_5\mathbf{a}_5 + h_1\mathbf{n}_1 & \text{(right segment)} \\ \ell_2\mathbf{a}'_2 + \ell_3\mathbf{a}'_3 & \text{(left segment)} \end{cases} \tag{6.24}$$

with the notation familiar from Figs. 5.1 and 5.2. The unknown parameters are determined from five Woernle-Lee equations for the loop formed by the bodies $2'$, $3'$, 5 and by the joints 5, 1 and the frozen joint. The five equations are based on the scalar products $\mathbf{n}_5 \cdot \mathbf{n}_1$, $\mathbf{n}_5 \cdot \mathbf{r}$, $\mathbf{n}_1 \cdot \mathbf{r}$, $\mathbf{r}^2$ and $\mathbf{r} \cdot \mathbf{n}_5 \times \mathbf{n}_1$. The first four equations are obtained from Table 5.2:

$$\cos\alpha_5 = \cos\alpha_2 \cos\alpha_3 - \sin\alpha_2 \sin\alpha_3 \cos\beta \,, \tag{6.25}$$

$$h_5 + h_1 \cos\alpha_5 = \ell_2 \sin\alpha_3 \sin\beta = \ell_1 \frac{\sin\alpha_2 \sin\alpha_3 \sin\beta}{\sin\alpha_1} \,, \tag{6.26}$$

$$h_5 \cos\alpha_5 + h_1 = \ell_3 \sin\alpha_2 \sin\beta = \ell_1 \frac{\sin\alpha_2 \sin\alpha_3 \sin\beta}{\sin\alpha_1} \,, \tag{6.27}$$

$$\begin{aligned} h_5^2 + h_1^2 + 2h_5h_1 \cos\alpha_5 + \ell_5^2 &= \ell_2^2 + \ell_3^2 + 2\ell_2\ell_3 \cos\beta \\ &= \ell_1^2 \frac{\sin^2\alpha_2 + \sin^2\alpha_3 + 2\sin\alpha_2 \sin\alpha_3 \cos\beta}{\sin^2\alpha_1} \,. \end{aligned} \tag{6.28}$$

The fifth equation is the dual derivative of the first equation:

$$\begin{aligned} \ell_5 \sin\alpha_5 &= \ell_2 \sin\alpha_2 \cos\alpha_3 + \ell_3 \cos\alpha_2 \sin\alpha_3 \\ &\quad + (\ell_2 \cos\alpha_2 \sin\alpha_3 + \ell_3 \sin\alpha_2 \cos\alpha_3) \cos\beta \\ &= \ell_1 \frac{\sin^2\alpha_2 \cos\alpha_3 + \sin^2\alpha_3 \cos\alpha_2 + (\cos\alpha_2 + \cos\alpha_3) \sin\alpha_2 \sin\alpha_3 \cos\beta}{\sin\alpha_1} \,. \end{aligned} \tag{6.29}$$

From these equations the angle β is eliminated in order to express ℓ_5, h_1 and h_5 in terms of ℓ_1, α_2, α_3 and α_5 (Dietmaier [19]). Equation (6.29) with the expression for $\sin\alpha_2 \sin\alpha_3 \cos\beta$ from (6.25) yields

$$\ell_5 = \ell_1 \frac{(\cos\alpha_2 + \cos\alpha_3)}{\sin\alpha_1} \frac{(1 - \cos\alpha_5)}{\sin\alpha_5} = \ell_1 \frac{\cos\alpha_2 + \cos\alpha_3}{\sin\alpha_1} \tan\frac{\alpha_5}{2} \,. \tag{6.30}$$

The difference of (6.26) and (6.27) is

$$(h_5 - h_1)(1 - \cos\alpha_5) = 0 \,. \tag{6.31}$$

In the general case[1] $\alpha_5 \neq 0$, the equation yields $h_5 = h_1$. Equation (6.28) with ℓ_5 from (6.30) and with $\cos\beta$ from (6.25) yields

[1] Dietmaier investigates also the special cases $\alpha_5 = 0, \pi$ (axes 1 and 5 parallel). It is shown that $\alpha_5 = 0$ can occur only when the mechanism is a planar 2-d.o.f. mechanism. The case $\alpha_5 = \pi$ requires $\beta = 0$, $\alpha_2 + \alpha_3 = 0$ and $h_5 = h_1$ (arbitrary)

$$h_5 = h_1 = \ell_1 \, \frac{\sqrt{1 - \cos^2\alpha_2 - \cos^2\alpha_3 + 2\cos\alpha_2\cos\alpha_3\cos\alpha_5 - \cos^2\alpha_5}}{\sin\alpha_1(1+\cos\alpha_5)} \tag{6.32}$$

or with the identities

$$\left.\begin{aligned} &1 - \cos^2\alpha_2 - \cos^2\alpha_3 = \sin^2\alpha_2\sin^2\alpha_3 - \cos^2\alpha_2\cos^2\alpha_3 \\ &= -(\cos\alpha_2\cos\alpha_3 + \sin\alpha_2\sin\alpha_3)(\cos\alpha_2\cos\alpha_3 - \sin\alpha_2\sin\alpha_3) \\ &= -\cos(\alpha_2-\alpha_3)\cos(\alpha_2+\alpha_3)\ , \\ &2\cos\alpha_2\cos\alpha_3 = \cos(\alpha_2-\alpha_3) + \cos(\alpha_2+\alpha_3) \end{aligned}\right\} \tag{6.33}$$

$$h_5 = h_1 = \ell_1 \, \frac{\sqrt{[\cos(\alpha_2-\alpha_3) - \cos\alpha_5][\cos\alpha_5 - \cos(\alpha_2+\alpha_3)]}}{\sin\alpha_1(1+\cos\alpha_5)}\ . \tag{6.34}$$

Both ℓ_5 and h_5 are symmetric with respect to α_2 and α_3. The free parameters α_2, α_3 and α_5 are subject to the condition that h_5 must be real.

With ℓ_5 and $h_5 = h_1$ and with the parameters

$$h_2 = h_3 = h_4 = 0\ , \quad \ell_4 = \ell_1\ , \quad \alpha_4 = \alpha_1\ , \quad \ell_2 = \ell_1\frac{\sin\alpha_2}{\sin\alpha_1}\ , \quad \ell_3 = \ell_1\frac{\sin\alpha_3}{\sin\alpha_1} \tag{6.35}$$

the set of Eqs.(6.19), (6.20) and four more sets produced by cyclic permutation of all indices are formulated. In each set only the first four equations are used because the fifth equation is known to be satisfied if the first four are satisfied. Taking the first set, i.e., (6.19) and (6.20) as example three operations are carried out which are repeated with the other four sets of equations.

Operation 1: Introduction of the special parameters (6.35). The coefficients (6.20) are

$$\left.\begin{aligned} A_1 &= -S_1(S_1C_5c_1 + C_1S_5)\ , \qquad B_1 = S_1^2 s_1\ , \\ R_1 &= \ \ C_1(S_1S_5c_1 - C_1C_5) + C_2C_3\ , \\ A_2 &= \ell_1 S_1 s_1\ , \qquad B_2 = \ell_1(S_1C_5c_1 + C_1S_5)\ , \\ R_2 &= h_1[S_1S_5c_1 - C_1(1+C_5)] - \ell_5 S_1 s_1\ , \\ A_3 &= S_1(\ell_1C_5s_1 - h_1S_5)\ , \qquad B_3 = S_1(\ell_1c_1 + \ell_5)\ , \\ R_3 &= -C_1[\ell_1S_5s_1 + h_1(1+C_5)]\ , \\ A_4 &= -\ell_1(\ell_1c_1 + \ell_5)\ , \qquad B_4 = \ell_1(\ell_1C_5s_1 - h_1S_5)\ , \\ R_4 &= h_1(\ell_1S_5s_1 + h_1C_5) + \ell_1\ell_5c_1 + \tfrac{1}{2}[2\ell_1^2 + \ell_5^2 + 2h_1^2 - (\ell_2^2+\ell_3^2)]\ . \end{aligned}\right\} \tag{6.36}$$

Operation 2: From the first two Eqs.(6.19) it follows that

$$\cos\varphi_3 = \frac{R_1 - A_1c_5 - B_1s_5}{S_2S_3}\ , \qquad \sin\varphi_3 = \frac{R_2 - A_2c_5 - B_2s_5}{\ell_2S_2}\ . \tag{6.37}$$

Operation 3: Linear combinations of the equations result in two equations from which c_3 and s_3 are eliminated (note Eqs.(6.35) for h_2, ℓ_2 and ℓ_3):

$$\left.\begin{array}{rr} (\ell_1^2 A_1 - S_1^2 A_4)c_5 + & (\ell_1^2 B_1 - S_1^2 B_4)s_5 = \ell_1^2 R_1 - S_1^2 R_4 \ , \\ (A_2 - A_3)c_5 + & (B_2 - B_3)s_5 = R_2 - R_3 \ . \end{array}\right\} \tag{6.38}$$

Let in each set of four equations produced from (6.19), (6.20) by cyclic permutation of indices φ_j be the independent variable. Then the other two variables are φ_{j+2} and φ_{j-1} where φ_{j+2} is the variable associated with constant coefficients. Repetition of the same three operations result in Eqs.(6.37) of the general form

$$\left.\begin{array}{l} \cos\varphi_{j+2} = f(\varphi_j, \varphi_{j-1}) \ , \\ \sin\varphi_{j+2} = g(\varphi_j, \varphi_{j-1}) \end{array}\right\} (j = 1, 2, 3, 4, 5 \text{ cyclic}) \tag{6.39}$$

and in Eqs.(6.38) of the general form

$$\left.\begin{array}{l} u_1(\varphi_j)\cos\varphi_{j-1} + v_1(\varphi_j)\sin\varphi_{j-1} = w_1(\varphi_j) \ , \\ u_2(\varphi_j)\cos\varphi_{j-1} + v_2(\varphi_j)\sin\varphi_{j-1} = w_2(\varphi_j) \end{array}\right\} (j = 1, 2, 3, 4, 5) \ . \tag{6.40}$$

For a given angle φ_j each of these Eqs.(6.40) has two solutions φ_{j-1}. About the number of solutions common to both equations the following statement can be made. In the Goldberg mechanism two Bennett mechanisms are connected by joint 3. A single variable in a Bennett mechanism uniquely determines all other variables in the same Bennett mechanism. Hence a single common solution exists if φ_j is not φ_3. This solution is

$$\cos\varphi_{j-1} = \frac{w_1 v_2 - w_2 v_1}{u_1 v_2 - u_2 v_1} \ , \qquad \sin\varphi_{j-1} = \frac{u_1 w_2 - u_2 w_1}{u_1 v_2 - u_2 v_1} \ . \tag{6.41}$$

The associated angle φ_{j+2} is determined from (6.39).

In the case $\varphi_j = \varphi_3$ (6.19) and (6.20) are the equations

$$\left.\begin{array}{rrr} S_1 S_5 c_5 & + A_1^* c_2 + B_1^* s_2 = R_1^* \ , \\ \ell_5\, S_1 s_5 & + A_2^* c_2 + B_2^* s_2 = R_2^* \ , \\ \ell_1\, S_5 s_5 & + A_3^* c_2 + B_3^* s_2 = R_3^* \ , \\ \ell_1\, \ell_5\, c_5 & + A_4^* c_2 + B_4^* s_2 = R_4^* \end{array}\right\} \tag{6.42}$$

with the coefficients

$$\left.\begin{aligned}
A_1^* &= -S_1(C_2S_3c_3 + S_2C_3)\,, \qquad B_1^* = S_1S_3s_3\,,\\
R_1^* &= \quad C_1(S_2S_3c_3 - C_2C_3 + C_5)\,,\\
A_2^* &= \ell_1\Big[S_3s_3 - \frac{h_1}{\ell_1}\,S_1(C_2S_3c_3 + S_2C_3)\Big]\,,\\
B_2^* &= \ell_1\Big(C_2S_3c_3 + S_2C_3 + \frac{h_1}{\ell_1}\,S_1S_3s_3\Big)\,,\\
R_2^* &= \frac{\ell_1}{S_1}\Big[\frac{h_1}{\ell_1}\,S_1C_1(S_2S_3c_3 - C_2C_3 - 1) - S_2S_3s_3\Big]\,,\\
A_3^* &= \ell_1C_2S_3s_3\,, \qquad B_3^* = \ell_1(S_3c_3 + S_2)\,,\\
R_3^* &= -\frac{\ell_1}{S_1}\Big[C_1S_2S_3s_3 + \frac{h_1}{\ell_1}\,S_1(1 + C_5)\Big]\,,\\
A_4^* &= -\frac{\ell_1^2}{S_1}\Big[S_2 + S_3\Big(c_3 + \frac{h_1}{\ell_1}\,S_1C_2s_3\Big)\Big]\,,\\
B_4^* &= \frac{\ell_1^2}{S_1}\Big[C_2S_3s_3 - \frac{h_1}{\ell_1}\,S_1(S_3c_3 + S_2)\Big]\,,\\
R_4^* &= \frac{\ell_1^2}{S_1^2}\Big[S_2S_3\Big(\frac{h_1}{\ell_1}\,S_1C_1s_3 + c_3\Big) + 1 + C_2C_3 - \frac{(C_2 + C_3)^2}{1 + C_5}\Big]\,.
\end{aligned}\right\} \tag{6.43}$$

Equations (6.40) are

$$\left.\begin{aligned}
(\ell_1\ell_5A_1^* - S_1S_5A_4^*)c_2 + (\ell_1\ell_5B_1^* - S_1S_5B_4^*)s_2 &= \ell_1\ell_5R_1^* - S_1S_5R_4^*\,,\\
(\ell_1S_5A_2^* - \ell_5S_1A_3^*)c_2 + (\ell_1S_5B_2^* - \ell_5S_1B_3^*)s_2 &= \ell_1S_5R_2^* - \ell_5S_1R_3^*\,.
\end{aligned}\right\} \tag{6.44}$$

These two equations are identical, i.e., one of them is, independent of the variable φ_3, a constant multiple of the other. This is proved by verifying the identities

$$\left.\begin{aligned}
&(\ell_1\ell_5A_1^* - S_1S_5A_4^*)(\ell_1S_5B_2^* - \ell_5S_1B_3^*)\\
-\,&(\ell_1\ell_5B_1^* - S_1S_5B_4^*)(\ell_1S_5A_2^* - \ell_5S_1A_3^*) \equiv 0\,,\\
&(\ell_1\ell_5A_1^* - S_1S_5A_4^*)(\ell_1S_5R_2^* - \ell_5S_1R_3^*)\\
-\,&(\ell_1\ell_5R_1^* - S_1S_5R_4^*)(\ell_1S_5A_2^* - \ell_5S_1A_3^*) \equiv 0\,.
\end{aligned}\right\} \tag{6.45}$$

Each of them has, with different sets of constant coefficients, the form $p_1c_3^2 + p_2c_3s_3 + p_3c_3 + p_4s_3 + p_5 \equiv 0$. It is left to the reader to verify that in each of them $p_1 = p_2 = p_3 = p_4 = p_5 = 0$. Some of these proofs make use of the relationships

$$\left.\begin{aligned}
\frac{\ell_5^2}{\ell_1^2}\,S_1^2 &= \quad \frac{1 - C_5}{1 + C_5}\,(C_2 + C_3)^2\,, \qquad \frac{\ell_5}{\ell_1}\,S_1S_5 = (1 - C_5)(C_2 + C_3)\,,\\
S_5^2\Big(1 + \frac{h_1^2}{\ell_1^2}\,S_1^2\Big) &= -\frac{1 - C_5}{1 + C_5}\,(C_2 + C_3)^2 + 2(1 - C_5)(1 + C_2C_3)\,.
\end{aligned}\right\} \tag{6.46}$$

From the identity of the Eqs.(6.44) it follows that for a given angle φ_3 two sets of solutions φ_{1_k}, φ_{2_k}, φ_{4_k}, φ_{5_k} $(k = 1, 2)$ exist. For every solution φ_{2_k} $(k = 1, 2)$ the first two Eqs.(6.42) determine φ_{5_k}. Next, with $\varphi_j = \varphi_{2_k}$ (6.41) determines φ_{1_k}, and (6.39) determines φ_{4_k}. This concludes the analysis of the Goldberg mechanism.

It is unknown whether there exist 5R mechanisms other than Goldberg mechanisms. It was shown that its fourteen essential parameters must satisfy 45 conditions. Starting from the same[2] Eqs.(6.19), (6.20) Dietmaier [19] formulated a different set of 45 conditions $f_k = 0$ $(k = 1, \ldots, 45)$. A numerical search was made for zero-value minima of the function $F = \sum_{k=1}^{45} f_k^2$. Starting from a randomly picked point in the 14-dimensional parameter space the algorithm yields a certain minimum. If this minimum is not zero-valued, a new search is made with a new starting point. Among the zero-valued minima found only those are of interest which represent a new type of mechanism, i.e., neither a Goldberg mechanism nor a degenerate mechanism (planar, for example). Although Dietmaier tried 2×10^6 randomly picked starting points no new type of mechanism was found. This is not a proof, but a strong argument for the Goldberg mechanism to be the only 5R mechanism.

6.4 Kinematical Chains with Six Revolute Joints

The number of different types of overconstrained kinematic chains with six links and six revolute joints is unknown as well. Many different types are known. Simple examples are shown in Figs. 6.1 and 6.2. Systematic descriptions and analyses see in Baker [4, 7], Mavroidis/Roth [25, 26, 27] and Dietmaier [19]. Bricard [10] discovered three classes of mechanisms known as line-symmetric, plane-symmetric and trihedral mechanisms. They are the subjects of the three sections to come. Several other types of mechanisms are obtained by merging a number of Bennett mechanisms or of Goldberg mechanisms in the spirit of Goldberg's construction of the five-joint mechanism in Fig. 6.3 (Mudrov [29], Goldberg [20], Wohlhart [31, 32]). Dietmaier [19] found a new class of mechanisms by the numerical search described above. For six-link mechanisms the function to be investigated has the form $F = \sum_{k=1}^{102} f_k^2$ with functions f_k depending on eighteen Denavit-Hartenberg parameters. Dietmaier's mechanism is the subject of Sect. 6.4.4.

6.4.1 Line-Symmetric Bricard Mechanism

A mechanism having six arbitrarily skew, consecutively labeled joint axes 1, 2, 3, 4, 5, 6 is said to be symmetric with respect to a line z if the geometry is invariant to a 180°-rotation about this line. Bricard [10] recognized that such a mechanism is deformable with degree of freedom one, and that the symmetry is maintained in the course of deformation. His proof of mobility

[2] (6.19), (6.20) and Dietmaier's Eqs.(3-7) – (3-11) are identical if in the latter ones $(s_i, \theta_i, \alpha_i, a_i)$ is replaced by $(h_i, \varphi_i, \alpha_{i-1}, \ell_{i-1})$

one is as follows. Suppose that body 2 is fixed in some reference frame, and that the constraints in all joints are removed. Relative to the reference frame the line z is specified by four parameters, and the positions of bodies 1 and 3 are specified by additional twelve parameters. Through these altogether $N = 16$ parameters the positions of the other three bodies 4 , 5 and 6 are specified as well because of the symmetry with respect to z . Each revolute joint introduces five constraints. Because of the pairwise symmetry of joints the total number of independent constraints is only $3 \times 5 = 15$. The difference $N - 15 = 1$ is the degree of freedom of the mechanism. End of proof.

The line-symmetry of the mechanism finds its expression in the identities

$$\alpha_{i+3} = \alpha_i \ , \quad \ell_{i+3} = \ell_i \ , \quad \varphi_{i+3} \equiv \varphi_i \ , \quad h_{i+3} = h_i \quad (i = 1, 2, 3) \ . \tag{6.47}$$

In Fig. 6.4 the spatial polygon of vectors $h_i \mathbf{n}_i$ and $\ell_i \mathbf{a}_i$ $(i = 1, \ldots, 6)$ with these symmetrically distributed Denavit-Hartenberg parameters is shown schematically in projection along the line z . The angle φ_1 is chosen as independent variable. The angles φ_2 and φ_3 are the only dependent variables. The vector $\mathbf{r}$ joining the axes $\mathbf{n}_6$ and $\mathbf{n}_3$ has in the right and in the left segment the forms

$$\mathbf{r} = \begin{cases} \ell_3 \mathbf{a}_6 + h_1 \mathbf{n}_1 + \ell_1 \mathbf{a}_1 + h_2 \mathbf{n}_2 + \ell_2 \mathbf{a}_2 + h_3 \mathbf{n}_3 & \text{(right segment)} \\ -(\ell_3 \mathbf{a}_3 + h_1 \mathbf{n}_4 + \ell_1 \mathbf{a}_4 + h_2 \mathbf{n}_5 + \ell_2 \mathbf{a}_5 + h_3 \mathbf{n}_6) & \text{(left segment)} \ . \end{cases} \tag{6.48}$$

The Woernle-Lee equation $F_3^{\ell} = F_3^{r}$ with $F_3 = \mathbf{n}_6 \cdot \mathbf{r}$ is an equation involving only φ_1 and φ_2 . It is written in the form

$$\mathbf{n}_k \cdot \Big[\ell_3 (\mathbf{a}_k + \mathbf{a}_{k-3}) + h_1 (\mathbf{n}_{k+1} + \mathbf{n}_{k-2}) + \ell_1 (\mathbf{a}_{k+1} + \mathbf{a}_{k-2}) \\ + h_2 (\mathbf{n}_{k+2} + \mathbf{n}_{k-1}) + \ell_2 (\mathbf{a}_{k+2} + \mathbf{a}_{k-1}) + h_3 (\mathbf{n}_{k+3} + \mathbf{n}_k) \Big] = 0 \quad (k = 6) \ . \tag{6.49}$$

Copying coordinates from Table 5.2 and using (6.47) results in the equation

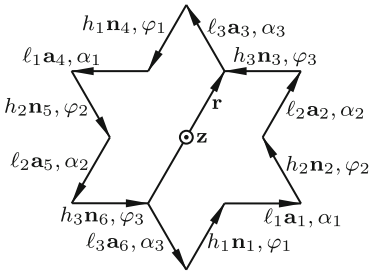

Fig. 6.4 Spatial polygon of vectors $h_i \mathbf{n}_i$ and $\ell_i \mathbf{a}_i$ of a Bricard mechanism with line of symmetry z . Vector $\mathbf{r}$ joining axes $\mathbf{n}_6$ and $\mathbf{n}_3$

$$\left.\begin{aligned}
&A_2\cos\varphi_2 + B_2\sin\varphi_2 = R_2\\
&A_2 = -h_3C_1S_2S_3\cos\varphi_1 + (\ell_2S_3 + \ell_3C_1S_2)\sin\varphi_1 - S_1S_2(h_1 + h_3C_3)\ ,\\
&B_2 = (\ell_2C_1S_3 + \ell_3S_2)\cos\varphi_1 + h_3S_2S_3\sin\varphi_1 + \ell_1S_2 + \ell_2S_1C_3\ ,\\
&R_2 = S_1S_3(h_2 + h_3C_2)\cos\varphi_1 - (\ell_1S_3 + \ell_3S_1C_2)\sin\varphi_1\\
&\qquad -h_1(C_1C_2 + C_3) - h_2(C_1C_3 + C_2) - h_3(1 + C_1C_2C_3)\ .
\end{aligned}\right\} \tag{6.50}$$

In the same way an equation for φ_3 as function of φ_1 is obtained on the basis of $F_3 = \mathbf{n}_5 \cdot \mathbf{r}$ with a vector $\mathbf{r}$ joining the axes $\mathbf{n}_5$ and $\mathbf{n}_2$. Equation (6.49) is replaced by

$$\begin{aligned}
&\mathbf{n}_k \cdot \Big[\ell_2(\mathbf{a}_k + \mathbf{a}_{k-3}) + h_3(\mathbf{n}_{k+1} + \mathbf{n}_{k-2}) + \ell_3(\mathbf{a}_{k+1} + a_{k-2})\\
&+h_1(\mathbf{n}_{k+2} + \mathbf{n}_{k-1}) + \ell_1(\mathbf{a}_{k+2} + \mathbf{a}_{k-1}) + h_2(\mathbf{n}_{k+3} + \mathbf{n}_k)\Big] = 0 \quad (k = 5)\ .
\end{aligned} \tag{6.51}$$

Evaluation results in the equation

$$\left.\begin{aligned}
&A_3\cos\varphi_3 + B_3\sin\varphi_3 = R_3\\
&A_3 = -h_2S_1S_2C_3\cos\varphi_1 + (\ell_1S_2C_3 + \ell_2S_1)\sin\varphi_1 - S_2S_3(h_1 + h_2C_1)\ ,\\
&B_3 = (\ell_1S_2 + \ell_2S_1C_3)\cos\varphi_1 + h_2S_1S_2\sin\varphi_1 + \ell_2C_1S_3 + \ell_3S_2\ ,\\
&R_3 = S_1S_3(h_2C_2 + h_3)\cos\varphi_1 - (\ell_1C_2S_3 + \ell_3S_1)\sin\varphi_1\\
&\qquad -h_1(C_1 + C_2C_3) - h_2(1 + C_1C_2C_3) - h_3(C_2 + C_1C_3)\ .
\end{aligned}\right\} \tag{6.52}$$

Each of the Eqs.(6.50) and (6.52) has two solutions $(\varphi_{2_1}, \varphi_{2_2})$ and $(\varphi_{3_1}, \varphi_{3_2})$, respectively. Their cosines and sines are

$$\left.\begin{aligned}
c_{j_k} &= \frac{A_jR_j + (-1)^kB_j\sqrt{A_j^2 + B_j^2 - R_j^2}}{A_j^2 + B_j^2}\ ,\\
s_{j_k} &= \frac{B_jR_j - (-1)^kA_j\sqrt{A_j^2 + B_j^2 - R_j^2}}{A_j^2 + B_j^2}
\end{aligned}\right\} \quad (j = 2,\,3\ ;\ k = 1,\,2)\ . \tag{6.53}$$

The square roots are identical:

$$\begin{aligned}
A_2^2 + B_2^2 - R_2^2 - (A_3^2 + B_3^2 - R_3^2) = \Big[&\ell_2^2(S_3^2 - S_1^2) + 2\ell_2S_2(\ell_3S_3C_1 - \ell_1S_1C_3)\\
&+ S_2^2(\ell_3^2 + h_3^2S_3^2 - \ell_1^2 - h_2^2S_1^2)\Big](\cos^2\varphi_1 + \sin^2\varphi_1 - 1) \equiv 0\ .
\end{aligned} \tag{6.54}$$

In order to determine which of the two solutions φ_2 belongs to which of the two solutions φ_3 an equation relating φ_2 and φ_3 is formulated by repeating the procedure once more with $F_3 = \mathbf{n}_4 \cdot \mathbf{r}$ and with a vector $\mathbf{r}$ joining the axes $\mathbf{n}_4$ and $\mathbf{n}_1$. Equation (6.49) is replaced by

$$\begin{aligned}
&\mathbf{n}_k \cdot \Big[\ell_1(\mathbf{a}_k + \mathbf{a}_{k-3}) + h_2(\mathbf{n}_{k+1} + \mathbf{n}_{k-2}) + \ell_2(\mathbf{a}_{k+1} + a_{k-2})\\
&+h_3(\mathbf{n}_{k+2} + \mathbf{n}_{k-1}) + \ell_3(\mathbf{a}_{k+2} + \mathbf{a}_{k-1}) + h_1(\mathbf{n}_{k+3} + \mathbf{n}_k)\Big] = 0 \quad (k = 4)\ .
\end{aligned} \tag{6.55}$$

Evaluation results in the equation

$$\left.\begin{aligned} &A_4\cos\varphi_3 + B_4\sin\varphi_3 = R_4 \\ &A_4 = -h_1S_1C_2S_3\cos\varphi_2 + (\ell_1C_2S_3 + \ell_3S_1)\sin\varphi_2 - S_2S_3(h_1C_1 + h_2)\ , \\ &B_4 = (\ell_1S_3 + \ell_3S_1C_2)\cos\varphi_2 + h_1S_1S_3\sin\varphi_2 + \ell_2S_3 + \ell_3C_1S_2\ , \\ &R_4 = S_1S_2(h_1C_3 + h_3)\cos\varphi_2 - (\ell_1S_2C_3 + \ell_2S_1)\sin\varphi_2 \\ &\qquad -h_1(1 + C_1C_2C_3) - h_2(C_1 + C_2C_3) - h_3(C_1C_2 + C_3)\ . \end{aligned}\right\} \tag{6.56}$$

In the example below it is shown that this equation is satisfied by the combinations $(\varphi_{2_1}, \varphi_{3_2})$ and $(\varphi_{2_2}, \varphi_{3_1})$.

Example: In Sect. 4.2.5 the special line-symmetric mechanism with parameters $\alpha_1 = \alpha_2 = \alpha_3 = \pi/2$, $\ell_1 = \ell_2 = \ell_3 = 0$ and $h_1 = h_2 = h_3 = 1$ was analyzed. With these parameters (6.50), (6.52) and (6.56) are, in this order,

$$c_2 - s_1s_2 = 1 - c_1\ , \qquad c_3 - s_1s_3 = 1 - c_1\ , \qquad c_3 - s_2s_3 = 1 - c_2\ . \tag{6.57}$$

Except for a difference in the definition of φ_1 the first equation is identical with (4.35), and the correlation between the solutions φ_2 and φ_3 has the form (4.38). Equations (6.53) are

$$\left.\begin{aligned} c_{2_{1,2}} = c_{3_{1,2}} &= \frac{1 - c_1 \pm s_1\sqrt{1 + 2c_1(1 - c_1)}}{1 + s_1^2}\ , \\ s_{2_{1,2}} = s_{3_{1,2}} &= \frac{-s_1(1 - c_1) \pm \sqrt{1 + 2c_1(1 - c_1)}}{1 + s_1^2}\ . \end{aligned}\right\} \tag{6.58}$$

By substituting these expressions it is verified that the third Eq.(6.57) is satisfied by the combinations $(\varphi_{2_1}, \varphi_{3_2})$ and $(\varphi_{2_2}, \varphi_{3_1})$. End of example.

According to Theorem 6.1 the six joint axes are, in every position of the mechanism instantaneously, lines of a linear complex. Conjecture: The axis of this linear complex intersects the line of symmetry z orthogonally. The following proof is due to Hon-Cheung [22]. It makes use of two properties of reciprocal polars which were established in Sect. 2.7.5 :
(a) The two transversals of any four independent complex lines are reciprocal polars of the linear complex.
(b) The common perpendicular of two reciprocal polars intersects orthogonally the axis of the linear complex.

Joint axes 1, 2, 3, 4 are line-symmetric to joint axes 4, 5, 6, 1 , respectively. According to (a) the two transversals of the former four axes are reciprocal polars and so are the two transversals of the latter four axes. The common perpendicular p of the former two reciprocal polars is line-symmetric to the common perpendicular p′ of the latter two reciprocal polars whence it follows that the common perpendicular of p and p′ intersects the line of symmetry z orthogonally. But according to (b) the axis of the linear complex intersects both p and p′ orthogonally, too. Therefore, this axis

and the common perpendicular of p and p′ intersecting z orthogonally are identical. End of proof.

6.4.2 Plane-Symmetric Bricard Mechanism

Another family of overconstrained mechanisms identified by Bricard [10] is referred to as plane-symmetric because of the pairwise symmetry of joint axes with respect to a plane Σ. In Fig. 6.5 the spatial polygon of vectors $h_i\mathbf{n}_i$ and $\ell_i\mathbf{a}_i$ $(i = 1, \ldots, 6)$ is shown schematically. The symmetry requires the opposite joint axes 1 and 4 to lie in Σ and to have zero offset: $h_1 = h_4 = 0$. It is left to the reader to verify that the remaining Denavit-Hartenberg parameters satisfy the conditions (for definitions see Fig. 5.1)

$$\left.\begin{array}{ll} \ell_6 = \ell_1 \,, & h_6 = h_2 \,, \\ \ell_5 = \ell_2 \,, & h_5 = h_3 \,, \\ \ell_4 = \ell_3 \,, & \end{array}\right\} \tag{6.59}$$

$$\left.\begin{array}{ll} \alpha_6 = \pi - \alpha_1 \,, & \varphi_6 \equiv -\varphi_2 \,, \\ \alpha_5 = -\alpha_2 \,, & \varphi_5 \equiv -\varphi_3 \,, \\ \alpha_4 = \pi - \alpha_3 \,. & \end{array}\right\} \tag{6.60}$$

Dissection of joints 1 and 4 produces two symmetrical twin halves of the system. Consider the twin half consisting of bodies 1, 2 and 3 and imagine body 2 to be fixed. Let body 1 be rotated relative to body 2 through an arbitrary *fixed* angle φ_2 so that joint axis 1 assumes a certain position. Likewise, let body 3 be rotated relative to body 2 through the angle φ_3 (*variable*) so that joint axis 4 generates an hyperboloid of revolution (in the case $\alpha_3 = 0$ a cylinder of radius ℓ_3 and in the case $\alpha_3 = \pi/2$ a plane every point of which outside a circle of radius ℓ_3 is located on two generators associated with different angles φ_3). The fixed axis 1 intersects

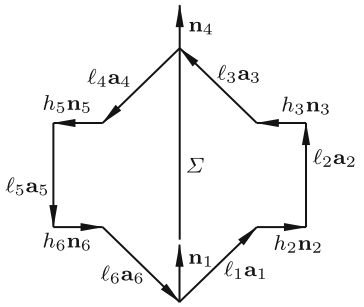

Fig. 6.5 Spatial polygon of vectors $h_i\mathbf{n}_i$ and $\ell_i\mathbf{a}_i$ of a Bricard mechanism symmetric with respect to plane Σ: $\ell_6 = \ell_1$, $h_6 = h_2$, $\ell_5 = \ell_2$, $h_5 = h_3$, $\ell_4 = \ell_3$

two generators of the hyperboloid (of the cylinder, of the plane in the said special cases) which are axes 4 coplanar with axis 1. Thus, for every φ_2 there are two angles φ_3 putting the twin half into a position with coplanar axes 1 and 4. The other twin half is mounted symmetrically thereby determining φ_1 and φ_4. Thus, not only mobility one of the mechanism is proved, but also the existence of two positions for a given independent angle φ_2. An equation relating φ_2 and φ_3 is derived from the intersection condition of the axes 1 and 4. This condition is written in the form (see Fig. 6.5)

$$\lambda\mathbf{n}_1 + \ell_1\mathbf{a}_1 + h_2\mathbf{n}_2 + \ell_2\mathbf{a}_2 + h_3\mathbf{n}_3 + \ell_3\mathbf{a}_3 + \mu\mathbf{n}_4 = \mathbf{0} \tag{6.61}$$

with unknowns λ and μ of dimension length. Decomposition of the vectors results in three equations relating λ, μ, φ_2 and φ_3. Vector coordinates are copied from Table 5.2. The simplest equations are obtained by decomposition on body 3, i.e., by evaluating the equation

$$\lambda\mathbf{n}_{k-2} + \ell_1\mathbf{a}_{k-2} + h_2\mathbf{n}_{k-1} + \ell_2\mathbf{a}_{k-1} + h_3\mathbf{n}_k + \ell_3\mathbf{a}_k + \mu\mathbf{n}_{k+1} = \mathbf{0} \tag{6.62}$$

with $k = 3$. This results in the set of equations

$$\left.\begin{aligned}
&\lambda(C_1C_2 - S_1S_2c_2) + \mu C_3 + \ell_1 s_2 S_2 + h_2 C_2 + h_3 &&= 0\,,\\
&\lambda[C_1S_2s_3 + S_1(s_2c_3 + c_2s_3C_2)] + \ell_1(c_2c_3 - s_2s_3C_2) + h_2S_2s_3 + \ell_2c_3 + \ell_3 &&= 0\,,\\
&\lambda[C_1S_2c_3 - S_1(s_2s_3 - c_2c_3C_2)] - \mu S_3 - \ell_1(c_2s_3 + s_2c_3C_2) + h_2S_2c_3 - \ell_2s_3 &&= 0\,.
\end{aligned}\right\} \tag{6.63}$$

The first two equations are solved for λ and μ. Substitution into the third equation and simple ordering of terms results in the desired equation relating φ_2 and φ_3 (terms c_2^2 and s_2^2 occuring in this process have identical coefficients; the same is true for c_3^2 and s_3^2)

$$A\cos\varphi_3 + B\sin\varphi_3 = R \tag{6.64}$$

with coefficients

$$\left.\begin{aligned}
A &= (-\ell_1C_1C_2S_3 + \ell_2S_1S_2S_3 - \ell_3S_1C_2C_3)\cos\varphi_2\\
&\quad + S_1S_3(h_2C_2 + h_3)\sin\varphi_2 + \ell_1S_1S_2S_3 - \ell_2C_1C_2S_3 - \ell_3C_1S_2C_3\,,\\
B &= S_1S_3(h_2 + h_3C_2)\cos\varphi_2 + (\ell_1C_1S_3 + \ell_3S_1C_3)\sin\varphi_2 + h_3C_1S_2S_3\,,\\
R &= (\ell_1C_1S_2C_3 + \ell_2S_1C_2C_3 - \ell_3S_1S_2S_3)\cos\varphi_2 - h_2S_1S_2C_3\sin\varphi_2\\
&\quad + \ell_1S_1C_2C_3 + \ell_2C_1S_2C_3 + \ell_3C_1C_2S_3\,.
\end{aligned}\right\} \tag{6.65}$$

The equation has two solutions φ_3 in terms of φ_2.

From the symmetry with respect to plane Σ it follows that φ_1 is uniquely determined by φ_2 and φ_3. An explicit expression for φ_1 in terms of φ_2 and φ_3 is obtained by evaluating the Woernle-Lee equation based on the product $\mathbf{n}_6 \cdot \mathbf{n}_4$. This is the equation $\mathbf{n}_k \cdot \mathbf{n}_{k-2} = \mathbf{n}_k \cdot \mathbf{n}_{k+4}$ with $k = 6$. Table 5.2 in combination with (6.60) yields the equation

$$s_1[S_3(c_2s_3 + C_2s_2c_3) + C_3S_2s_2]$$
$$= (1 - c_1)\Big[C_1S_3(s_2s_3 - C_2c_2c_3) + S_2(S_1S_3c_3 - C_1C_3c_2) - S_1C_2C_3\Big] \,, \quad (6.66)$$

whence it follows that

$$\tan\frac{\varphi_1}{2} = \frac{1 - c_1}{s_1} = \frac{S_3(c_2s_3 + C_2s_2c_3) + C_3S_2s_2}{C_1S_3(s_2s_3 - C_2c_2c_3) + S_2(S_1S_3c_3 - C_1C_3c_2) - S_1C_2C_3} \,. \quad (6.67)$$

An equation for $\tan\varphi_4/2$ is obtained in the same way by expressing the product $\mathbf{n}_3 \cdot \mathbf{n}_1$ in the two forms $\mathbf{n}_k \cdot \mathbf{n}_{k-2} = \mathbf{n}_k \cdot \mathbf{n}_{k+4}$ with $k = 3$. In view of the symmetry of Fig. 6.5 the equation is directly obtained by interchanging in (6.67) α_1 with α_3 and φ_2 with φ_3:

$$\tan\frac{\varphi_4}{2} = \frac{S_1(c_3s_2 + C_2s_3c_2) + C_1S_2s_3}{C_3S_1(s_2s_3 - C_2c_2c_3) + S_2(S_1S_3c_2 - C_1C_3c_3) - S_3C_2C_1} \,. \quad (6.68)$$

Example: The triple plane-symmetric mechanism shown in Fig. 4.6 is characterized by the parameters $\ell_1 = \ell_2 = \ell_3 = 1$, $h_2 = h_3 = 0$ and $\alpha_1 = \alpha_2 = \alpha_3 = \pi/2$. This is the special case with a single solution (φ_1, φ_3) for a given angle φ_2. Equations (6.64) and (6.67) are

$$c_2 + c_2c_3 + c_3 = 0 \,, \qquad \tan\frac{\varphi_1}{2} = \frac{c_2s_3}{c_3} \,. \quad (6.69)$$

With c_2 from the first equation the second becomes $\tan\varphi_1/2 = -s_3/(1+c_3)$ or $\varphi_1 = -\varphi_3$. Except for slightly different definitions of angles, the same results were obtained in (4.20) and (4.22). End of example.

6.4.3 Trihedral Bricard Mechanism

This mechanism was developed by Bricard [10] in search for a system having the property that in every position the six axes are lines of a special linear complex. Consider Fig. 6.6. The arbitrary spatial trihedral with lines 2, 4, 6 and with vertex A, referred to as trihedral A, is given. Furthermore, a point B is given. The perpendiculars 1, 3, 5 from B onto the three planes of trihedral A define the trihedral B. The construction implies that the lines 2, 4, 6 of trihedral A are perpendiculars of the three planes of trihedral B. With the labeling shown in Fig. 6.6 the line i ($i = 1, \ldots, 6$ cyclic) is normal to the plane of lines $i - 1$ and $i + 1$. Let P_2, P_4, P_6 and P_1, P_3, P_5 be the feet of the correspondingly labeled perpendiculars. They form the spatial polygon shown in dashed lines. The length of the side $\overline{\mathrm{P}_i\mathrm{P}_{i+1}}$ is called ℓ_i. The line segment $\overline{\mathrm{AP}_i}$ ($i = 1, 3, 5$) which is not shown is hypotenuse in the rectangular triangle (A,P_i,P_{i-1}) as well as in the rectangular triangle

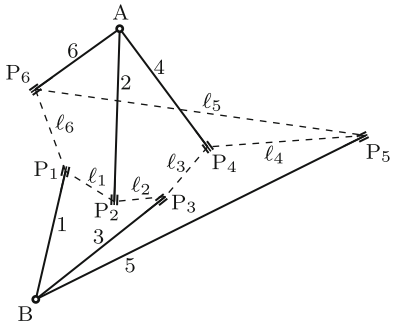

Fig. 6.6 Trihedrals A and B. Line i is normal to the plane of lines $i-1$ and $i+1$ ($i = 1, \ldots, 6$ cyclic)

(A,P_i,P_{i+1}). Consequently, $\overline{AP}_{i-1}^2 + \ell_{i-1}^2 = \overline{AP}_{i+1}^2 + \ell_i^2$ $(i = 1, 3, 5)$. This establishes the three equations

$$\ell_1^2 - \ell_6^2 = \overline{AP}_6^{\,2} - \overline{AP}_2^{\,2}\,, \quad \ell_3^2 - \ell_2^2 = \overline{AP}_2^{\,2} - \overline{AP}_4^{\,2}\,, \quad \ell_5^2 - \ell_4^2 = \overline{AP}_4^{\,2} - \overline{AP}_6^{\,2}\,. \tag{6.70}$$

Summation yields

$$\ell_1^2 + \ell_3^2 + \ell_5^2 = \ell_2^2 + \ell_4^2 + \ell_6^2\,. \tag{6.71}$$

Imagine now the lengths $\ell_1, \ldots, \ell_6$ to be rigid rods interconnected by revolute joints at the points P_i $(i = 1, \ldots, 6)$. Each joint axis has the direction of the corresponding perpendicular i. This means that each rod carries two mutually perpendicular joint axes which are also perpendicular to the rod. The axes 2, 4, 6 intersect at the single point A, and the axes 1, 3, 5 intersect at the single point B. Proposition: Every mechanism composed of six rods and of six revolute joints having these orthogonality properties and arbitrary lengths $\ell_1, \ldots, \ell_6$ satisfying (6.71) has a single degree of freedom if one body is held fixed. This is the trihedral Bricard mechanism (sometimes also referred to as orthogonal Bricard mechanism). As is the case in the Bennett mechanism each joint has zero offset. Bricard's proof of mobility one is as follows. The construction of the system requires the specification of twelve parameters, namely, three coordinates for each of the points A and B and two direction cosines for each line of trihedral A. Six out of these twelve parameters determine the dimensions of the system and the remaining six its position in space. Of interest are only the first six parameters. Their number exceeds the number of independent lengths by one. The single free parameter constitutes the single degree of freedom. End of proof. Since in every position of the mechanism the six joint axes intersect the line $\overline{AB}$, they are lines of the special linear complex with the axis $\overline{AB}$. In Fig. 4.6 the special mechanism is shown in which the six lengths $\ell_1, \ldots, \ell_6$ are identical.

A trihedral Bricard mechanism can assume so-called planar positions, i.e., positions in which the polygon of points $P_1, \ldots, P_6$ is planar. In these positions three joint axes are normal to the plane. They intersect at infinity. The other three joint axes are lying in the plane. They either intersect at a single point or are parallel. The two rods coupled by any of these three joints are collinear. From this it follows that every planar position of the mechanism creates a triangle of rods in the plane. In order to find all planar positions with collinear pairs of rods, say pairs (1,2), (3,4) and (5,6), the altogether eight combinations of sums and differences $|\ell_1 \pm \ell_2|$, $|\ell_3 \pm \ell_4|$ and $|\ell_5 \pm \ell_6|$ are calculated. Each combination is checked whether it satisfies the triangle-inequalities. In the same way all planar positions with collinear pairs of rods (2,3), (4,5) and (6,1) are determined. With at least four of the altogether sixteen combinations of sums and differences the triangle-inequalities are satisfied. The proof is left to the reader. It makes use of (6.71).

Example: The mechanism with lengths $(\ell_1, \ell_2, \ell_3, \ell_4, \ell_5, \ell_6) = (16, 3, 9, 17, 5, 8)$ has the eight planar positions shown in Figs. 6.7a-h. In Fig. 6.7d all six rods are collinear, and the intersection points of both triples of joint axes are at infinity. End of example.

The figures reveal the existence of two different types of trihedral mechanisms. In Figs. 6.7a-d the number of differences of lengths in the triangle is odd, and in Figs. 6.7e-h the number of sums of lengths is odd. According to the rules in Fig. 5.1 the following quantities are defined:
– unit vectors $\mathbf{n}_1, \ldots, \mathbf{n}_6$ along the joint axes (sense of direction arbitrary)
– vectors $\ell_i \mathbf{a}_i = \overrightarrow{P_i P_{i+1}}$ $(i = 1, \ldots, 6)$
– constant angles α_i and joint variables φ_i $(i = 1, \ldots, 6)$.
The angles $\alpha_1, \ldots, \alpha_6$ are either $+\pi/2$ or $-\pi/2$. Simple inspection reveals that, no matter how $\mathbf{n}_1, \ldots, \mathbf{n}_6$ are directed, the number of positive angles $\alpha_i = +\pi/2$ is even in Figs. 6.7a-d and odd in Figs. 6.7e-h. Wohlhart [33] who presented the first complete kinematics analysis speaks of a type 2 mechanism in the former case and of a type 1 mechanism in the latter. A type 2 mechanism is obtained from type 1 and vice versa by opening one joint and by closing it again after giving one of the neighboring bodies a 180°-rotation about a normal to the joint axis.

Let $\mathbf{n}_1, \ldots, \mathbf{n}_6$ be directed such that $\alpha_i = +\pi/2$ $(i = 1, \ldots, 6)$ in type 2, and that $\alpha_1 = \alpha_3 = \alpha_5 = +\pi/2$, $\alpha_2 = \alpha_4 = \alpha_6 = -\pi/2$ in type 1. With the usual notation $C_i = \cos\alpha_i$, $S_i = \sin\alpha_i$ this means that $C_i = 0$ $(i = 1, \ldots, 6)$ and

$$\left.\begin{array}{ll} S_i = +1 \quad (i = 1, \ldots, 6) & (\text{type } 2)\,, \\ S_1 = S_3 = S_5 = +1\,, \quad S_2 = S_4 = S_6 = -1 & (\text{type } 1)\,. \end{array}\right\} \tag{6.72}$$

The characteristic parameter specifying the type is

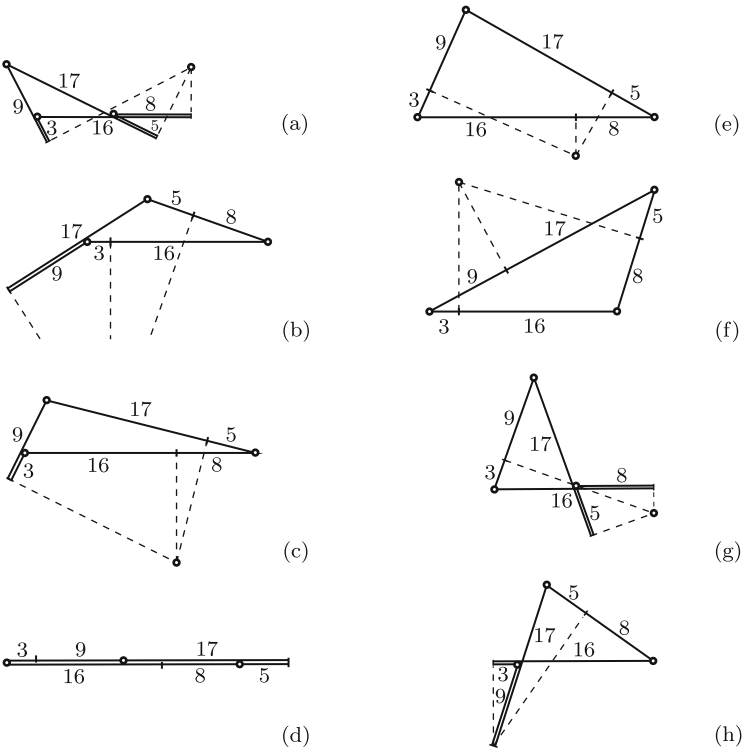

Fig. 6.7 The eight planar positions of the trihedral Bricard mechanism with lengths $(\ell_1, \ell_2, \ell_3, \ell_4, \ell_5, \ell_6) = (16, 3, 9, 17, 5, 8)$. Type 2 with odd number of differences of lengths **(Figs. a–d)** and type 1 with odd number of sums of lengths **(Figs. e–h)**

$$\lambda = S_i S_{i+1} \quad (\, i = 1, \ldots, 6 \text{ cyclic}\,) = \begin{cases} +1 & (\text{type } 2)\,, \\ -1 & (\text{type } 1)\,. \end{cases} \tag{6.73}$$

The following kinematics analysis is different from Wohlhart's. Three Woernle-Lee equations are formulated. Two equations are based on the products $\mathbf{n}_6 \cdot \mathbf{n}_4$ and $\mathbf{n}_6 \cdot \mathbf{n}_3$. They are written in the forms

$$\mathbf{n}_k \cdot \mathbf{n}_{k-2} = \mathbf{n}_k \cdot \mathbf{n}_{k+4} \qquad (k = 6)\,, \tag{6.74}$$

$$\mathbf{n}_k \cdot \mathbf{n}_{k-3} = \mathbf{n}_k \cdot \mathbf{n}_{k+3} \qquad (k = 6)\,. \tag{6.75}$$

The third equation is based on the product $\mathbf{r} \cdot \mathbf{n}_6 \times \mathbf{n}_4$ with $\mathbf{r}$ being the vector pointing from P_6 to P_4 . Since $\mathbf{r}$, $\mathbf{n}_6$ and $\mathbf{n}_4$ are coplanar, the Woernle-Lee equation splits into two equations:

$$\left.\begin{aligned} (\ell_6 \mathbf{a}_k + \ell_1 \mathbf{a}_{k+1} + \ell_2 \mathbf{a}_{k+2} + \ell_3 \mathbf{a}_{k+3}) \cdot \mathbf{n}_k \times \mathbf{n}_{k+4} &= 0\,, \\ (\ell_4 \mathbf{a}_{k-2} + \ell_5 \mathbf{a}_{k-1}) \cdot \mathbf{n}_k \times \mathbf{n}_{k-2} &= 0\,. \end{aligned}\right\} \quad (k = 6) \tag{6.76}$$

All equations are valid with indices changed cyclicly. Evaluation of (6.74) and (6.75) by means of Table 5.2 results in the equations

$$c_2 = -\frac{\lambda c_1 c_3 + c_5}{s_1 s_3}\,, \qquad s_2 = \frac{s_4 s_5}{s_1} = \frac{s_5 s_6}{s_3}\,. \tag{6.77}$$

The second expression for s_2 is the result of increasing all indices by one.

In the second Eq.(6.76) the vectors $(\ell_4\mathbf{a}_{k-2} + \ell_5\mathbf{a}_{k-1})$ and $\mathbf{n}_k \times \mathbf{n}_{k-2}$ have the coordinate matrices

$$\begin{bmatrix} \text{1st coordinate is irrelevant} \\ (\ell_4 c_5 + \ell_5)c_6 \\ -(\ell_4 c_5 + \ell_5)s_6 \end{bmatrix}\,, \quad \begin{bmatrix} 0 \\ S_4 s_5 s_6 \\ S_4 s_5 c_6 \end{bmatrix}\,, \tag{6.78}$$

respectively. Hence the second Eq.(6.76) is the identity. Not so the first equation. The vectors $(\ell_6\mathbf{a}_k + \ell_1\mathbf{a}_{k+1} + \ldots)$ and $\mathbf{n}_k \times \mathbf{n}_{k+4}$ have the coordinate matrices

$$\begin{bmatrix} \text{1st coordinate is irrelevant} \\ \ell_6 + \ell_1 c_1 + \ell_2 c_2 c_1 + \ell_3(\lambda s_3 s_1 + c_3 c_2 c_1) \\ -S_1 S_6 s_2(\ell_2 + \ell_3 c_3) \end{bmatrix}\,, \quad \begin{bmatrix} 0 \\ S_1 S_3 S_6 s_2 s_3 \\ S_3(-\lambda c_3 s_1 + s_3 c_2 c_1) \end{bmatrix}\,, \tag{6.79}$$

respectively. The scalar product allows factoring out $S_1 S_3 S_6 s_2$. The first Eq.(6.76) then is the first of the six equations below. The remaining equations are obtained by cyclic permutation of indices.

$$\left.\begin{array}{ll} 1. & (\ell_2 c_3 + \ell_3)s_1 + \lambda(\ell_1 c_1 + \ell_6)s_3 = 0\,, \\ 2. & (\ell_3 c_4 + \ell_4)s_2 + \lambda(\ell_2 c_2 + \ell_1)s_4 = 0\,, \\ 3. & (\ell_4 c_5 + \ell_5)s_3 + \lambda(\ell_3 c_3 + \ell_2)s_5 = 0\,, \\ 4. & (\ell_5 c_6 + \ell_6)s_4 + \lambda(\ell_4 c_4 + \ell_3)s_6 = 0\,, \\ 5. & (\ell_6 c_1 + \ell_1)s_5 + \lambda(\ell_5 c_5 + \ell_4)s_1 = 0\,, \\ 6. & (\ell_1 c_2 + \ell_2)s_6 + \lambda(\ell_6 c_6 + \ell_5)s_2 = 0\,. \end{array}\right\} \tag{6.80}$$

Each equation involves two variables. The first equation yields φ_3 in terms of φ_1, and the fifth equation yields φ_5 in terms of φ_1. These equations have the forms

$$A_j \cos\varphi_j + B_j \sin\varphi_j = R_j \qquad (j = 3, 5) \tag{6.81}$$

with coefficients which are functions of φ_1. Each equation has two solutions φ_{3_k} and φ_{5_k} $(k = 1, 2)$. Their cosines and sines are

$$\left.\begin{aligned} c_{j_k} &= \frac{A_j R_j + (-1)^k B_j \sqrt{A_j^2 + B_j^2 - R_j^2}}{A_j^2 + B_j^2}\,, \\ s_{j_k} &= \frac{B_j R_j - (-1)^k A_j \sqrt{A_j^2 + B_j^2 - R_j^2}}{A_j^2 + B_j^2} \end{aligned}\right\} \quad (j = 3, 5\,;\ k = 1, 2)\,. \tag{6.82}$$

By substituting coefficients it is verified that the square roots are identical: $A_3^2 + B_3^2 - R_3^2 - (A_5^2 + B_5^2 - R_5^2) = 0$ because of (6.71). Furthermore, by substituting the expressions (6.82) it is verified that the third Eq.(6.80) is satisfied by the combinations $(\varphi_{3_1}, \varphi_{5_1})$ and $(\varphi_{3_2}, \varphi_{5_2})$.

The first Eq.(6.77) determines for each of the two solutions c_3, s_3, c_5 the corresponding cosine c_2 and hence two angles $\pm\varphi_2$. The corresponding cosine c_4 is obtained by substituting the first expression $s_2 = s_4 s_5 / s_1$ into the second Eq.(6.80) and by deleting the common factor s_4. In the same way the corresponding cosine c_6 is obtained from the second expression for s_2 in combination with the sixth Eq.(6.80). The results are

$$c_4 = -\frac{\lambda s_1(\ell_2 c_2 + \ell_1) + \ell_4 s_5}{\ell_3 s_5}, \qquad c_6 = -\frac{\lambda s_3(\ell_1 c_2 + \ell_2) + \ell_5 s_5}{\ell_6 s_5}. \tag{6.83}$$

The signs of s_4 and s_6 are determined from (6.77). If s_2 changes sign, also s_4 and s_6 change signs. These results are summarized as follows. For every value of φ_1 there exist four (not necessarily real) sets of solutions $(\sigma\varphi_{2_i}, \varphi_{3_i}, \sigma\varphi_{4_i}, \varphi_{5_i}, \sigma\varphi_{6_i})$ $(i = 1, 2; \sigma = \pm 1)$. Equations (6.77) and (6.83) fail in planar positions characterized by either $s_1 = s_3 = s_5 = 0$ or by $s_2 = s_4 = s_6 = 0$. In these cases, the joint angles are determined from triangles (see Fig. 6.7).

Example: For the lengths $(\ell_1, \ell_2, \ell_3, \ell_4, \ell_5, \ell_6) = (16, 3, 9, 17, 5, 8)$ and for $\varphi_1 = 80°$ a type 1 mechanism has the solutions
$(\varphi_2, \varphi_3, \varphi_4, \varphi_5, \varphi_6) \approx (\sigma 36.8°, 142.9°, \sigma 48.4°, 127.9°, \sigma 27.3°)$ and
$(\sigma 92.8°, 67.8°, \sigma 98.3°, 83.7°, \sigma 111.5°)$ $(\sigma = \pm 1)$. End of example.

Example: The trihedral mechanism in Fig. 4.6 is a type 1 mechanism with identical lengths $\ell_i \equiv 1$ $(i = 1, \ldots, 6)$. It has four planar positions. Equations (6.80) reduce to

$$\left.\begin{array}{ll} 1. & (c_3+1)s_1 - (c_1+1)s_3 = 0, \\ 2. & (c_4+1)s_2 - (c_2+1)s_4 = 0, \\ 3. & (c_5+1)s_3 - (c_3+1)s_5 = 0, \\ 4. & (c_6+1)s_4 - (c_4+1)s_6 = 0, \\ 5. & (c_1+1)s_5 - (c_5+1)s_1 = 0, \\ 6. & (c_2+1)s_6 - (c_6+1)s_2 = 0. \end{array}\right\} \tag{6.84}$$

For a given angle φ_1 these equations and (6.77) have a single solution only, namely, $\varphi_3 = \varphi_5 = \varphi_1$, $\varphi_4 = \varphi_6 = \varphi_2$ and $c_1 + c_1 c_2 + c_2 = 0$. Except for slightly different definitions of angles, the same results were obtained in (4.20) and (4.22). Compare also the first Eq.(6.84) with (4.23). End of example.

With six rods of mutually different lengths altogether six different sequences and with each sequence both types of mechanism can be formed. In general, the numbers of planar positions are different for different sequences and for different types. Example: The sequence of lengths in Figs. 6.7a-h is

the first of the following six sequences which represent all possible mechanisms which can be formed with these lengths:

$$\left.\begin{matrix}(16,3,9,17,5,8)\\(16,8,9,17,5,3)\end{matrix}\right\}\ \text{(a)}\ ,\quad \left.\begin{matrix}(16,17,9,8,5,3)\\(16,17,9,3,5,8)\end{matrix}\right\}\ \text{(b)}\ ,\quad \left.\begin{matrix}(16,8,9,3,5,17)\\(16,3,9,8,5,17)\end{matrix}\right\}\ \text{(c)}\ .$$

It is left to the reader to verify the following statements. With each of the sequences (a) both types have four planar positions. With each of the sequences (b) both types have two planar positions. With each of the sequences (c) there are two planar positions of type 1 and three of type 2.

Condition (6.71) is $A+B+C=0$ with $A=(\ell_1-\ell_2)(\ell_1+\ell_2)$, $B=(\ell_3-\ell_4)(\ell_3+\ell_4)$, $C=(\ell_5-\ell_6)(\ell_5+\ell_6)$. Nonzero integer solutions $(\ell_1,\ell_2,\ell_3,\ell_4,\ell_5,\ell_6)$ are obtained from numbers A, B, $C=-(A+B)$ which are products of two different even or two different odd numbers. Example: $A=2\cdot 8$, $B=1\cdot 17$, $C=-1\cdot 33=-3\cdot 11$ yield $(\ell_1,\ell_2,\ell_3,\ell_4,\ell_5,\ell_6)=(5,3,9,8,16,17)$ and $(5,3,9,8,4,7)$.

Condition (6.71) is satisfied by the lengths $\ell_1=a$, $\ell_2=a+b$, $\ell_3=a+2b+c$, $\ell_4=a+c$, $\ell_5=a+b+2c$, $\ell_6=a+2b+2c$ (a,b,c arbitrary). Example: $a=b=1$, $c=2$ yield $(\ell_1,\ell_2,\ell_3,\ell_4,\ell_5,\ell_6)=(1,2,5,3,6,7)$. The mechanism with these lengths has seven planar positions (four of type 2). In one planar position of type 1 and in one of type 2 all six lengths are collinear.

6.4.4 Dietmaier's Mechanism

The ideas and results presented in this section are due to Dietmaier [19]. The analysis of the 7R mechanism in Sect. 5.4.7 resulted in a 16th-order equation for the variable $x_1=\tan\varphi_1/2$ with coefficients depending on the variable φ_7 and on constant Denavit-Hartenberg parameters. A prescribed value of φ_7 (arbitrary) determines up to sixteen real roots x_1. The 16th-order equation describes a 6R mechanism when the parameters and variables of body 7 and of joint 7 are set equal to zero: $\ell_7=h_7=0$, $\alpha_7=0$, $\varphi_7\equiv 0$ (see Fig. 5.7). This has the consequence that the coefficients of the 16th-order equation are constants. Since x_1 is variable, all seventeen coefficients must be zero. This requirement establishes seventeen conditions on the Denavit-Hartenberg parameters ℓ_i, h_i, α_i ($i=1,\ldots,6$; $\ell_1=1$ without loss of generality). The 16th-order equation remains valid when the indices of all parameters and all variables are cyclicly increased by $k=1,2,3,4,5$. Hence altogether $6\times 17=102$ conditions must be satisfied. Dietmaier's numerical search for Denavit-Hartenberg parameters satisfying these conditions led to a new family of overconstrained 6R mechanisms. The parameters must satisfy the following complicated symmetry relationships.

1. The opposite bodies 1 and 4 are identical:

$$\ell_4 = \ell_1 \,, \qquad \alpha_4 = \alpha_1 \,. \tag{6.85}$$

2. The opposite joints 2 and 5 have zero offset:

$$h_2 = 0 \,, \qquad h_5 = 0 \,. \tag{6.86}$$

3. Joints 1 and 3 and joints 4 and 6 have pairwise identical offsets:

$$h_3 = h_1 \,, \qquad h_6 = h_4 \,. \tag{6.87}$$

4. Bodies 2 and 3 and the opposite bodies 5 and 6 have pairwise identical ratios

$$\frac{\ell_2}{\sin\alpha_2} = \frac{\ell_3}{\sin\alpha_3} \,, \qquad \frac{\ell_5}{\sin\alpha_5} = \frac{\ell_6}{\sin\alpha_6} \,. \tag{6.88}$$

5. These ratios are subject to the symmetrical constraint equation

$$\frac{\ell_2}{\sin\alpha_2}(\cos\alpha_2 + \cos\alpha_3) = \frac{\ell_5}{\sin\alpha_5}(\cos\alpha_5 + \cos\alpha_6) \,. \tag{6.89}$$

The last three equations can be used for expressing ℓ_3, ℓ_5 and ℓ_6 in terms of ℓ_2, α_2, α_3, α_5 and α_6. With the usual notation $C_i = \cos\alpha_i$ and $S_i = \sin\alpha_i$

$$\ell_3 = \ell_2 \frac{S_3}{S_2} \,, \qquad \ell_5 = \ell_2 \frac{S_5(C_2 + C_3)}{S_2(C_5 + C_6)} \,, \qquad \ell_6 = \ell_2 \frac{S_6(C_2 + C_3)}{S_2(C_5 + C_6)} \,. \tag{6.90}$$

Let φ_1 be the independent variable. The associated solutions for φ_2, φ_4, φ_5, φ_6 are determined from (5.94) and (5.93) after setting $\ell_7 = h_7 = 0$, $\alpha_7 = 0$, $\varphi_7 \equiv 0$. The matrices $\underline{A}$, $\underline{B}$ and $\underline{P}$ are constants. The matrix $\underline{u}_r$ is defined in (5.80). One out of the four Eqs.(5.94) is solved for x_6. Substitution into the other equations results in three equations which are quadratic in the sines and cosines of φ_1 and φ_2. Hence they have the forms

$$A_i \sin^2\varphi_2 + B_i \sin\varphi_2 \cos\varphi_2 + C_i \sin\varphi_2 + D_i \cos^2\varphi_2 + E_i \cos\varphi_2 + F_i = 0 \tag{6.91}$$

$(i = 1, 2, 3)$ with coefficients which are functions of φ_1. The equations are fourth-order equations for the variable $x_2 = \tan\varphi_2/2$ (see (5.60)). Only those solutions x_2 which are common to all three equations determine relevant angles φ_2. Once φ_2 is known also $\varphi_6 = 2\tan^{-1} x_6$ is known and then also φ_4 and φ_5 from $\underline{y}$ (see (5.93)). Dietmaier's numerical investigations revealed that his 6R mechanism has up to four different configurations for a given value of the independent variable no matter which angle is chosen as independent variable. In this respect the mechanism is different from all other known 6R mechanisms.

6.5 Mobile Polyhedra

Euler expressed, without mathematical arguments, the conviction that all polyhedra are rigid. By this the following is meant. In a polyhedron every face is interpreted as rigid body and every edge as revolute joint. Nonrigid means that the polyhedron is a mobile mechanism. Cauchy proved that all convex polyhedra are, indeed, rigid (see Demaine/O'Rourke [17]). Bricard [10] constructed mobile nonconvex octahedra which are self-intersecting. Connelly constructed the first nonconvex polyhedron capable of moving without self-intersection. Stimulated by this achievement Steffen constructed simpler ones (see Connelly [14]). The simplest one is constructed as follows (see Fig. 6.8). Starting point is the rigid isosceles triangle $(A_1, 0, A_2)$ in the plane E with leg lengths ℓ and with vertex angle α. On the perpendicular to E through 0 the point B_1 is marked at an arbitrary distance h from 0. Rods of equal length a connect A_1 and A_2 with B_1. Two more rods of equal length b connect A_1 and A_2 with a point B_2 on the dashed bisector of the angle α. In the next step, congruent triangles (A_1,B_1,C_1) and (A_1,B_2,C_1) are constructed as follows. To B_1 a rod of length b is attached and to B_2 a rod of length a. The point C_1 connecting these rods is located on a circle in a plane normal to the line $\overline{B_1B_2}$ and with its center on this line. With a given length $\overline{A_1C_1} = c$ (arbitrary) there are two possible locations for C_1. One of them is chosen arbitrarily. Let C_1^* be the other point not chosen. Repetition of this construction produces two more triangles (A_2,B_1,C_2) and (A_2,B_2,C_2) which are congruent to the previous ones. Of the two possible locations for C_2 the one is chosen with which the dashed line $\overline{C_1C_2}$ is not parallel to $\overline{A_1A_2}$. Let C_2^* be the other point not chosen.

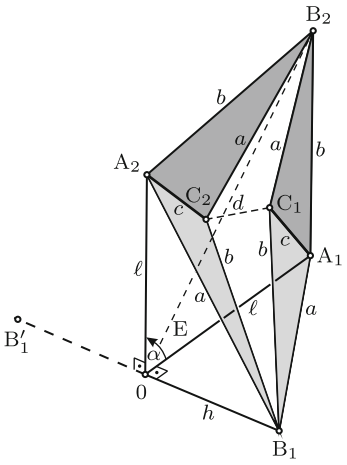

Fig. 6.8 One half of a mobile polyhedron

Now, imagine the connections of rods at the points A_1, A_2, B_1 and B_2 to be spherical joints. The system thus defined has the degree of freedom one. The rigid isosceles triangle (A_1,A_2,B_2) can rotate (in a limited angular range) about its base line $\overline{A_1A_2}$. This rotation forces C_1 and C_2 to move along certain trajectories. During this motion the distance of these two points is not constant. Now, C_1 and C_2 are connected by a rod of fixed length d. In order to restore the degree of freedom the angle α is made variable by connecting the rods $\overline{0A_1}$ and $\overline{0A_2}$ at 0 by a spherical joint.

The 1-d.o.f. system thus constructed consists of the rigid triangles $(0,A_1,B_1)$, $(0,A_2,B_1)$, (A_1,B_1,C_1), (A_1,B_2,C_1), (A_2,B_1,C_2), (A_2,B_2,C_2), (B_1,C_1,C_2) and (B_2,C_1,C_2). This system is one half of the desired polyhedron. The other half is obtained in two steps. First step: The existing halfpolyhedron - placed in the position with B_2 in E - is reflected in E. Second step: The reflections of C_1 and C_2 are replaced by the reflections of C_1^* and of C_2^*, respectively. With the reflection B_1' of B_1 the triangular faces (B_1,B_1',A_1) and (B_1,B_1',A_2) of the polyhedron are produced.

With suitably chosen lengths h, a, b, c, d B_2 is able to move along a short segment of a trajectory on either side of E without causing a collision of faces of the polyhedron. In [14] the lengths are proposed: $2h = 17$, $a = 12$, $b = 10$, $c = 5$, $d = 11$. The polyhedron can be produced by folding the symmetric figure shown in Fig. 6.9. The polyhedron has $n = 14$ faces (bodies) and $m = 21$ edges (revolute joints). With these numbers Grübler's formula (4.1) yields the degree of freedom $F = -27 + d$. Since F equals one, the system of altogether 5×21 constraint equations has the defect $d = 28$. See http://www.mathematik.com/Steffen/ for a display of the motion.

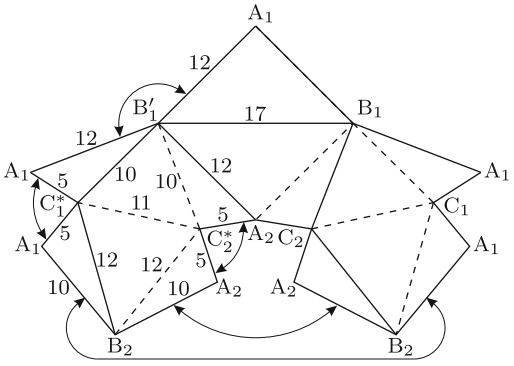

Fig. 6.9 Cutting and folding instructions for Steffen's mobile polyhedron. Valley folds in dashed lines. Mountain folds in solid lines

6.6 RRCRP Mechanism

A closed kinematic chain RRCRP has six joint variables. Hence it is rigid unless it is overconstrained. It will be seen that the special chain shown in Fig. 6.10 is overconstrained with degree of freedom one. The assembly position shown is characterized as follows. The axis of the revolute R_4 is orthogonal to the x, y-plane of the frame-fixed x, y, z-system with origin 0. The other four joint axes are in this plane (the prismatic joint P parallel to the revolute R_1 at $y = \ell = \text{const}$; the axes of the revolutes R_1 and R_2 and of the cylindrical joint C intersecting at 0; R_1 and R_2 under an angle $\alpha = \text{const}$ and R_2 and C orthogonally). After a rotation through φ_1 (arbitrary) in R_1 the unit vector $\mathbf{n}_2$ along the axis of R_2 has the coordinates $\underline{n}_2 = [\cos\alpha \quad -\sin\alpha\sin\varphi_1 \quad -\sin\alpha\cos\varphi_1]$. Dependent on φ_1 the angle φ_2 in R_2 and the translatory variable in joint C can be determined such that the vector $\mathbf{r}$ pointing to the revolute R_4 has the required coordinates $y = \ell$ and $z = 0$. Moreover, the angle φ_3 in joint C can be determined such that the axis of R_4 has the required direction orthogonal to the x, y-plane. This proves that the mechanism has the degree of freedom one, and that φ_1 can be used as independent input variable. As output the translatory variable in the prismatic joint P is chosen. Let this be the coordinate x of $\mathbf{r}$. From the orthogonality condition $\mathbf{n}_2 \cdot \mathbf{r} = 0$ it follows that

$$x = \ell \tan\alpha \sin\varphi_1 \ . \tag{6.92}$$

Rotation with constant angular velocity $\dot{\varphi}_1 = \omega$ is converted into oscillatory translation $x(t) = \ell \tan\alpha \sin\omega t$. The mechanism was used in a pneumatic saw (see *Design and development/scanning the field for ideas*, Sept.1964, p.158). See also Altmann [2, 1].

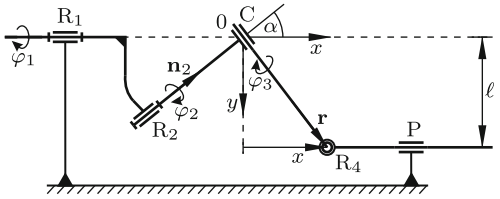

Fig. 6.10 Mechanism $R_1R_2CR_4P$ converting rotation into harmonic translation

6.7 4R-P Mechanism

In the fixed x, y, z-system of Fig. 6.11a two skew lines n_1 and n_2 are fixed. Their common perpendicular of length ℓ lies in the z-axis. This axis is intersected by n_1 at $z = \ell/2$ (point A_1) and by n_2 at $z = -\ell/2$ (point A_2). The projected angle α between the lines is bisected by the y-axis. The lines n_1 and n_2 are the axes of two cylinders 1 and 2 of equal radius r. Points denoted B_1 and B_2 are fixed on the cylinders. More precisely, B_i $(i = 1, 2)$ is fixed on cylinder i such that the line $\overline{\mathrm{A}_i\mathrm{B}_i}$ is orthogonal to both n_i and z-axis, and that, furthermore, B_1 and B_2 are, in the projection shown, on a line parallel to the y-axis and at equal distances from the x-axis. Imagine now that both cylinders are rotated about their axes through identical angles φ (arbitrary). This causes B_1 and B_2 to move on their respective circles to new positions B'_1, B'_2. The displacements in z-direction are identical, namely, $u = r \sin\varphi$, and also the displacements in x-direction are identical, namely, $r(1 - \cos\varphi)$. In the projection shown the distance between B'_1 and B'_2 is $\delta = 2r \cos\varphi \sin\alpha/2$. The generator of cylinder i passing through B'_i is called n'_i $(i = 1, 2)$. In Fig. 6.11b the essential points and lines are shown in the projection along the x-axis. In this projection, the axes and generators of the cylinders are shown as lines parallel to the y-axis. Through B'_1 and B'_2 lines $\overline{\mathrm{B}'_1\mathrm{C}_1}$ and $\overline{\mathrm{B}'_2\mathrm{C}_2}$ of equal lengths $\ell/2$ are drawn parallel to the z-axis. The line p through C_1 and C_2 is (not only in this projection) parallel to the y-axis.

Imagine now that $\overline{\mathrm{A}_1\mathrm{A}_2}$, $\overline{\mathrm{A}_1\mathrm{B}'_1}$, $\overline{\mathrm{A}_2\mathrm{B}'_2}$, $\overline{\mathrm{B}'_1\mathrm{C}_1}$ and $\overline{\mathrm{B}'_2\mathrm{C}_2}$ are rigid links which are interconnected by four revolute joints with pairwise parallel axes n_1, n'_1 and n_2, n'_2 and by a prismatic joint with the axis p. The result is a spatial overconstrained single-degree-of-freedom mechanism

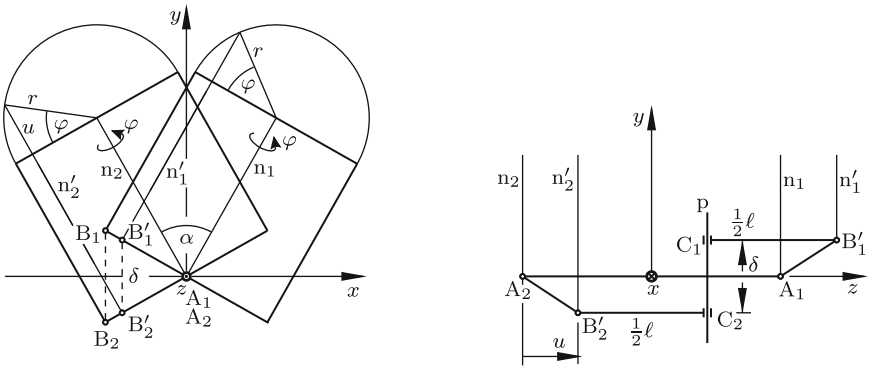

Fig. 6.11 4R-P mechanism projected along the z-axis **(a)** and along the x-axis **(b)**

4R-P with only five joint variables. The variable φ is identical in all four revolute joints. The joint variable in the prismatic joint is δ. It is independent of ℓ. This mechanism was described first by Mavroidis/Roth [27] (see also Mavroidis/Beddows [28]). The links need not have the shapes shown in the figures. Every link can be given any shape provided its two Denavit-Hartenberg parameters (length of the common perpendicular and projected angle of the two joint axes on the link) have the correct values. The link coupling the parallel axes n_1 and n_1', for example, can be placed anywhere between these axes. With this freedom of design it is possible to achieve full-cycle mobility in the revolute joints without collision of links and joint axes. The prismatic joint must be designed such that the passage through $\delta = 0$ is possible. In the special case $\alpha = 0$, the mechanism is the planar foldable four-bar in parallelogram configuration.

The mechanism is a simple means of converting the angular velocity $\dot{\varphi}$ about the fixed input axis n_1 into an identical angular velocity about the fixed skew output axis n_2 the location of which can be freely chosen by specifying the two design parameters α and ℓ. The mechanism is simpler and less expensive than a set of hypoid gears serving the same purpose. This is particularly true when ℓ is large. However, like the planar foldable four-bar the mechanism is not well suited for transmitting a large torque from the input to the output axis.

6.8 Bricard-Borel Mechanism

The system shown in Fig. 6.12a consists of two parallel circular discs 1 and 2 (radii R_1 and $r_1 \neq R_1$ arbitrary) and of $n \geq 5$ rods of equal length ℓ_1 connecting the discs. The rods are generators of a frustum of a regular cone. The system is shown in two projections. The endpoints P_i and Q_i of the rods $i = 1, \ldots, n$ are connected to the discs by spherical joints. Disc 1 is a fixed base. Disc 2 is referred to as platform. Every rod is free to rotate about its longitudinal axis. This degree of freedom is not of interest. Because of the symmetry of the arrangement it is obvious that the platform has a single degree of freedom. It is free to undergo a continuous screw motion about the vertical z-axis with an independent angular variable φ and with a translatory variable z which is a function $z(\varphi)$. This function is obtained from Fig. 6.12b which shows the vertical projection in a position φ (arbitrary). In the x, y, z-system the endpoints P_1 and Q_1 of rod 1 have the coordinates $[R_1 \;\; 0 \;\; 0]$ and $[r_1 \cos\varphi \;\; r_1 \sin\varphi \;\; z]$, respectively. The condition of constant rod length establishes between z and φ the constraint equation $(r_1 \cos\varphi - R_1)^2 + r_1^2 \sin^2\varphi + z^2 = \ell_1^2$. Hence

$$z(\varphi) = \sqrt{2R_1 r_1 \cos\varphi + \ell_1^2 - (R_1^2 + r_1^2)} \,. \tag{6.93}$$

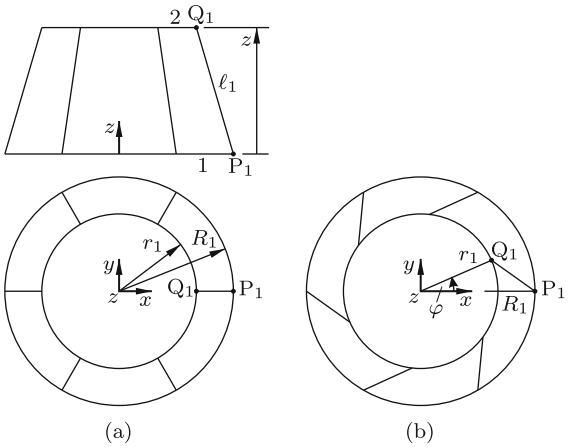

Fig. 6.12 Platform mounted on rods in positions $\varphi = 0$ **(a)** and $\varphi \neq 0$ **(b)**

The same function $z(\varphi)$ is obtained with arbitrary parameters R, r, ℓ satisfying the conditions

$$Rr = R_1 r_1 \,, \qquad \ell^2 = \ell_1^2 - (R_1^2 + r_1^2) + (R^2 + r^2) \,. \tag{6.94}$$

The same function $z(\varphi)$ is also obtained if both endpoints of a rod, i.e., the entire rod, are vertically lifted or lowered by an arbitrary amount (each rod by an individual amount). Also, because of the symmetry of the equations, it is immaterial whether the larger or the smaller radius is located on the platform. The degree of freedom one remains unchanged if an arbitrary number of rods each satisfying the said conditions is added to the system. Every point of the three-dimensional platform can be connected by a rod with a point of the base which is uniquely determined by the conditions. From this it follows that every point of the platform is moving on a base-fixed sphere. Platform-fixed points of the screw axis move on spheres with infinite radius. Conversely, every point fixed on the base moves on a platform-fixed sphere. All rods are lines of the linear complex with the given screw axis and with the pitch $p = \mathrm{d}z/\mathrm{d}\varphi$. These characteristics of the system were first discovered by Bricard [11] and Borel [9]. See also Husty/Zsombor-Murray [23].

6.9 Hyperboloid and Paraboloid Mechanisms

The hyperboloid of one sheet (Fig. 6.13a) and the hyperbolic paraboloid (Fig. 6.13b) have, in the cartesian x_1, x_2, x_3-systems shown, the equations

$$\text{hyperboloid of one sheet}: \qquad \frac{x_1^2}{a^2} + \frac{x_2^2}{b^2} - \frac{x_3^2}{c^2} = 1 \,, \tag{6.95}$$

$$\text{hyperbolic paraboloid}: \qquad \frac{x_1^2}{a^2} - \frac{x_2^2}{b^2} = x_3 \,. \tag{6.96}$$

Planes $x_1 = \text{const}$ and $x_2 = \text{const}$ intersect the hyperboloid in hyperbolas and the hyperbolic paraboloid in parabolas. Planes $x_3 = \text{const}$ intersect the hyperboloid in ellipses and the hyperbolic paraboloid in hyperbolas (in straight lines in the case $x_3 = 0$). Both surfaces are ruled surfaces, more specifically the only ruled surfaces having the property that every point is the intersection of two generating lines. The two families of generators of the hyperboloid, referred to as regulus 1 and regulus 2, have the equations (the parameters u and v are arbitrary constants; see Bronstein/Semendjajev/Musiol/Mühlig [12])

$$\left.\begin{array}{ll} \text{regulus 1}: & \dfrac{x_1}{a} + \dfrac{x_3}{c} = u\Big(1 + \dfrac{x_2}{b}\Big) \,, \quad u\Big(\dfrac{x_1}{a} - \dfrac{x_3}{c}\Big) = 1 - \dfrac{x_2}{b} \,, \\ \text{regulus 2}: & \dfrac{x_1}{a} + \dfrac{x_3}{c} = v\Big(1 - \dfrac{x_2}{b}\Big) \,, \quad v\Big(\dfrac{x_1}{a} - \dfrac{x_3}{c}\Big) = 1 + \dfrac{x_2}{b} \,. \end{array}\right\} \tag{6.97}$$

The corresponding equations for the paraboloid are

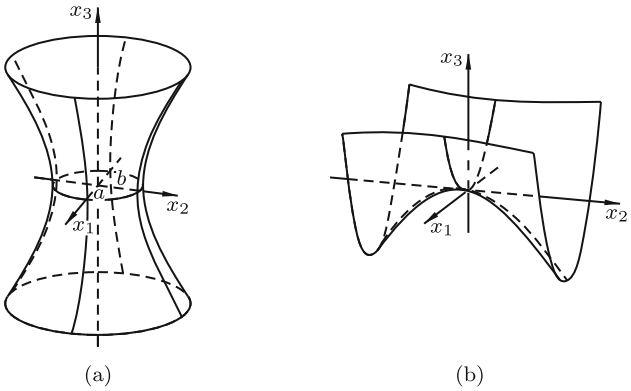

Fig. 6.13 Hyperboloid of one sheet **(a)** and hyperbolic paraboloid **(b)**

$$\left.\begin{array}{ll} \text{regulus 1}: & \dfrac{x_1}{a} + \dfrac{x_2}{b} = u \,, \quad u\Big(\dfrac{x_1}{a} - \dfrac{x_2}{b}\Big) = x_3 \,, \\ \text{regulus 2}: & \dfrac{x_1}{a} - \dfrac{x_2}{b} = v \,, \quad v\Big(\dfrac{x_1}{a} + \dfrac{x_2}{b}\Big) = x_3 \,. \end{array}\right\} \tag{6.98}$$

Hyperboloid of one Sheet

Equations (6.97) reveal the following properties of generators. Two generators belonging to one and the same regulus are skew. Every generator of

one regulus intersects all generators of the other regulus and exactly one of them at infinity. Three generators belonging to one and the same regulus are not parallel to one and the same plane. Three such generators determine a hyperboloid uniquely.

Imagine now that arbitrarily many (in the limit all) generators are rigid rods. Moreover, imagine that at every intersection point of any two such rods the respective rods are connected by a spherical joint (in the limit there is a spherical joint at every point of the hyperboloid). Proposition: The system of rods thus defined is an overconstrained mechanism having a single degree of freedom. It can move in such a way that in every position the rods are generators of a hyperboloid of one sheet. The intersections of all these hyperboloids with the plane $x_3 = 0$ are confocal ellipses.

Proof (see Bricard [10] and Hilbert/Cohn-Vossen [21]): It must be shown that the distance of any two spherical joints P and Q on an arbitrarily chosen rod is invariant under this motion. For this purpose (6.95) is written in the form

$$\sum_{i=1}^{3} \frac{x_i^2}{a_i - \lambda} = 1 \qquad (a_3 \le \lambda \le a_2 \le a_1 \quad \text{arbitr.}) \,. \tag{6.99}$$

Let p_i and q_i $(i = 1, 2, 3)$ be the coordinates of two points P and Q, respectively, on an arbitrary generator. Also the midpoint with coordinates $(p_i + q_i)/2$ $(i = 1, 2, 3)$ lies on this generator and, consequently on the surface. Hence

$$\sum_{i=1}^{3} \frac{p_i^2}{a_i - \lambda} = 1 \,, \qquad \sum_{i=1}^{3} \frac{q_i^2}{a_i - \lambda} = 1 \,, \qquad \sum_{i=1}^{3} \frac{(p_i + q_i)^2}{a_i - \lambda} = 4 \,. \tag{6.100}$$

From the third equation twice the sum of the first two equations is subtracted:

$$\sum_{i=1}^{3} \frac{(p_i - q_i)^2}{a_i - \lambda} = 0 \,. \tag{6.101}$$

Let r be the distance of the points P and Q. With (6.101)

$$r^2 = \sum_{i=1}^{3} (p_i - q_i)^2 = \sum_{i=1}^{3} (a_i - \lambda) \frac{(p_i - q_i)^2}{a_i - \lambda} = \sum_{i=1}^{3} a_i \frac{(p_i - q_i)^2}{a_i - \lambda} \,. \tag{6.102}$$

In (6.99) λ is replaced by an arbitrary λ' satisfying the conditions $a_3 \le \lambda' \le a_2$. The two hyperboloids with λ and with λ' are referred to as surface F and surface F$'$, respectively. The coordinates x_1', x_2', x_3' of points on F$'$ are generated from the coordinates x_1, x_2, x_3 of F by the affine transformation

$$x_i' = x_i \sqrt{\frac{a_i - \lambda'}{a_i - \lambda}} \qquad (i = 1, 2, 3) \,. \tag{6.103}$$

This transformation associates to the points P and Q of F points P′ and Q′, respectively, of F′ having the coordinates

$$p_i' = p_i\sqrt{\frac{a_i-\lambda'}{a_i-\lambda}}\,, \qquad q_i' = q_i\sqrt{\frac{a_i-\lambda'}{a_i-\lambda}} \qquad (i=1,2,3)\,. \tag{6.104}$$

For the distance r' of these points (6.102) is valid with the quantities bearing the prime. With (6.104)

$$r'^2 = \sum_{i=1}^{3} a_i\,\frac{(p_i'-q_i')^2}{a_i-\lambda'} = \sum_{i=1}^{3} a_i\,\frac{(p_i-q_i)^2}{a_i-\lambda} \equiv r^2\,. \tag{6.105}$$

This identity proves the invariance of the distance of points. The mechanism of rods which, in its initial position, is assembled on the hyperboloid F governed by (6.99) with given constants $a_3 \le \lambda \le a_2 \le a_1$ is able to assume a position in which it is located on a hyperboloid F′ governed by the same equation with the same constants $a_3 \le a_2 \le a_1$ and with an arbitrary $a_3 \le \lambda' \le a_2$.

The hyperboloid with the free parameter λ' intersects the plane $x_3 = 0$ in the ellipse depending on λ': $x_1^2/(a_1-\lambda') + x_2^2/(a_2-\lambda') = 1$. Its focal points are located on the x_1-axis symmetrically to the origin. Their distance is $\sqrt{(a_1-\lambda')-(a_2-\lambda')} = \sqrt{a_1-a_2}$ independent of λ'. Hence the ellipses are confocal. End of proof.

In the limit $\lambda' = a_2$ the ellipse degenerates to the line connecting the focal points. In this case, all rods lie in the x_1, x_3-plane and tangent to the hyperbola $x_1^2/(a_1-a_2) - x_3^2/(a_2-a_3) = 1$. In the limit $\lambda' = a_3$ all rods lie in the x_1, x_2-plane and tangent to the ellipse $x_1^2/(a_1-a_3) + x_2^2/(a_2-a_3) = 1$.

The hyperbolic paraboloid, too, is a 1-d.o.f. mechanism when all generators are interconnected by spherical joints at every point of intersection. By the same line of arguments it is proved that in every position the mechanism is a hyperbolic paraboloid with the equation depending on the free parameter λ:

$$\sum_{i=1}^{2} \frac{x_i^2}{a_i-\lambda} = x_3 \qquad (a_2\,,\ a_3 = \text{const}\,,\ \ a_2 \le \lambda \le a_3\,)\,. \tag{6.106}$$

Hyperbolic Mechanism for the Generation of a Plane

The minimal system of rods constituting a hyperbolic mechanism consists of five rods (see Fig. 6.14). Two skew rods g and g_1 representing generators of regulus 1 are interconnected by three rods of constant lengths (generators of regulus 2). The spherical joints on g and g_1 may be placed arbitrarily subject only to the inequality condition $\overline{P_1P_2} : \overline{P_1P_3} \neq \overline{Q_1Q_2} : \overline{Q_1Q_3}$ (in the case of equality the five lines would be generators of a hyperbolic paraboloid). Every generator of regulus 2 intersects all generators of regulus 1 and exactly one of them at infinity. Hence there exist a single generator of regulus 2 parallel

to g and a uniquely defined intersection point of this generator with g_1. Let Q be this point. When the 1-d.o.f.-mechanism is moving, each joint Q_i is moving on a sphere around P_i $(i = 1, 2, 3)$. Point Q, in particular, is moving on a sphere of infinite radius, i.e., in a plane E normal to g. Let 0 be the point where g intersects E. When E and g are held fixed as is shown in Fig. 6.14, the mechanism has the additional degree of freedom of rotation about g. Hence Q is free to move (in a certain ring-shaped region) in the fixed plane E. This generation of a plane by a mechanism having only spherical joints represents a spatial analog to the generation of a straight line by a Peaucellier inversor (see Sect. 17.13).

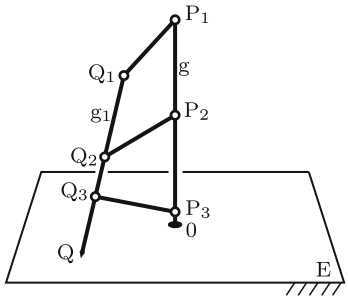

Fig. 6.14 Hyperbolic mechanism for the generation of a plane

6.10 Cam Mechanism

De la Hire is the author of

Theorem 6.2. *Mutually orthogonal tangents to an ellipse with semi axes a and b (arbitrary) intersect on the circle of radius* $\sqrt{a^2 + b^2}$ *about the center of the ellipse.*

Proof (see Fig. 6.15): In the x, y-system of principal axes the ellipse has the equation

$$\frac{x^2}{a^2} + \frac{y^2}{b^2} = 1 \tag{6.107}$$

and also the parameter equation

$$x = a\cos\psi\,, \qquad y = b\sin\psi\,. \tag{6.108}$$

The tangent t_1 at the arbitrary point $\psi = \psi_1$ has the normal form

$$x\cos\alpha + y\sin\alpha = p_1\,. \tag{6.109}$$

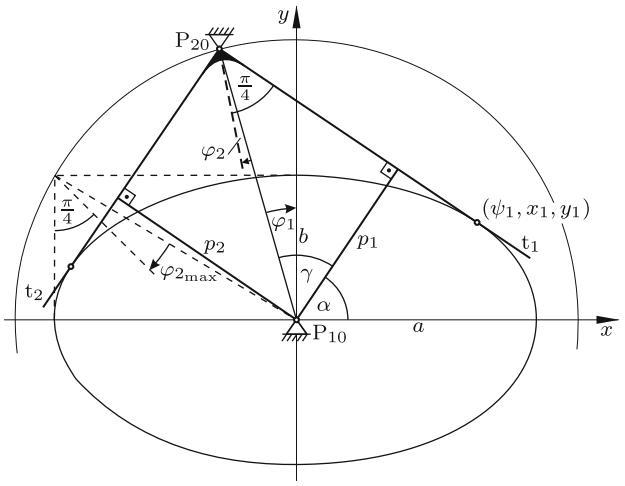

Fig. 6.15 Cam mechanism based on De la Hire's theorem on ellipses

The angle α and the length p_1 of the perpendicular from the origin onto the tangent depend on ψ_1. This dependency is investigated as follows. Through ψ_1 the new angle β is defined by the equations $\cos\psi_1 = (a/p_1)\cos\beta$, $\sin\psi_1 = (b/p_1)\sin\beta$. Together with (6.108) this yields for the coordinates x_1, y_1 associated with ψ_1 the expressions $x_1 = (a^2/p_1)\cos\beta$, $y_1 = (b^2/p_1)\sin\beta$. By assumption, these coordinates satisfy (6.107) as well as (6.109). Substitution yields the equations

$$a^2\cos^2\beta + b^2\sin^2\beta = p_1^2\,, \qquad a^2\cos\beta\cos\alpha + b^2\sin\beta\sin\alpha = p_1^2\,. \quad (6.110)$$

From them it follows that $\beta = \alpha$ and, furthermore,

$$p_1^2 = a^2\cos^2\alpha + b^2\sin^2\alpha = \frac{1}{2}(a^2+b^2) + \frac{1}{2}(a^2-b^2)\cos 2\alpha\,. \quad (6.111)$$

A tangent t_2 orthogonal to t_1 has in its normal form the parameters $\alpha \pm \pi/2$ and p_2. For this tangent (6.111) has the form $p_2^2 = a^2\sin^2\alpha + b^2\cos^2\alpha$. Hence $p_1^2 + p_2^2 = a^2 + b^2$. This concludes the proof.

The angle γ shown in the figure is determined by

$$\cos^2\gamma = \frac{p_1^2}{a^2+b^2} = \frac{1}{2} + \frac{1}{2}\,\frac{a^2-b^2}{a^2+b^2}\cos 2\alpha\,. \quad (6.112)$$

Hence

$$\cos 2\gamma = \frac{a^2-b^2}{a^2+b^2}\cos 2\alpha\,. \quad (6.113)$$

Imagine now that the ellipse is free to rotate about its center P_{10}, and that the right angle formed by t_1 and t_2 is materialized as rigid body with a fixed center at P_{20}. Then the ellipse can rotate full circle. In every position it is in tangential contact with the arms t_1 and t_2. The ellipse represents a cam, and the right angle is the follower driven by the cam. The system is mobile with degree of freedom $F = 1$. Grübler's formula (4.2) with $n = m = 3$ and $f_1 = f_2 = f_3 = 1$ yields $F = d$. This shows that the system is overconstrained with $d = 1$. Manufacturing errors result in the loss of mobility.

As angular coordinate of the cam the angle φ_1 from the frame-fixed line $\overline{P_{10}P_{20}}$ to the minor principal axis of the ellipse is chosen and as coordinate of the follower the angle φ_2 from the same frame-fixed line to the bisector of the right angle (φ_1, φ_2 positive clockwise). The figure shows that $\gamma = \varphi_2 + \pi/4$ and $\gamma - \varphi_1 + \alpha = \pi/2$. Together with (6.113) this yields

$$\varphi_1 = \varphi_2 + \alpha(\varphi_2) - \frac{\pi}{4} \qquad \text{with} \qquad \cos 2\alpha = -\frac{a^2 + b^2}{a^2 - b^2} \sin 2\varphi_2 \,. \tag{6.114}$$

This equation cannot be solved explicitly for φ_2. However, the following statements are obviously true. The angle φ_2 is an odd, π-periodic function of φ_1. It is zero for $\varphi_1 = k\pi/2$ $(k = 0, 1, 2, \cdots)$. Stationary values of φ_2 occur in positions when the principal axes of the ellipse are parallel to t_1 and to t_2 (the dashed lines in Fig. 6.15). The figure yields $\varphi_{2_{\max}} = \tan^{-1}(a/b) - \pi/4$ for $\varphi_1 = \tan^{-1}(a/b)$. Differentiation of both Eqs.(6.114) with respect to time yields the angular velocity ratio

$$\frac{\dot{\varphi}_1}{\dot{\varphi}_2} = 1 + \frac{a^2 + b^2}{a^2 - b^2} \frac{\cos 2\varphi_2}{\sin 2\alpha} \,. \tag{6.115}$$

During the quarter revolution of the ellipse from the position $\varphi_1 = \varphi_2 = 0$, $\alpha = \pi/4$ to the position $\varphi_1 = \pi/2$, $\varphi_2 = 0$, $\alpha = 3\pi/4$ this ratio changes from the extremal value $2a^2/(a^2 - b^2)$ through ∞ at $\varphi_2 = \varphi_{2_{\max}}$ to the extremal value $-2b^2/(a^2 - b^2)$. This investigation is continued in Ex. 1 of Sect. 15.1.2.

6.11 Heureka Octahedron

In Fig. 6.16a a regular octahedron is shown. It has eight faces $1, \ldots, 8$ (equilateral triangles) and six corners. Each corner is common to four faces. At each corner the four faces are grouped in two pairs of adjacent faces. The pairs are identified by the face labels separated by a komma. Examples: At the top corner pairs 1,4 and 2,3 and at the bottom corner pairs 5,8 and 6,7. Imagine the faces to be bodies pairwise interconnected by identical joints at

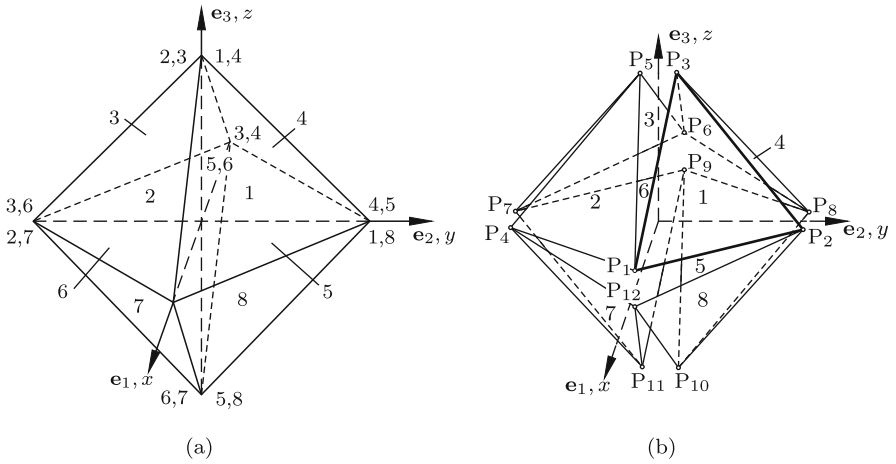

Fig. 6.16 Regular octahedron **(a)** and octahedral mechanism with twelve joints unfolded **(b)**. Front faces 1, 2, 7, 8

the corners (one joint connecting pair 1,4 and another joint connecting pair 2,3 at the top corner etc.). The resulting mechanism has $n = 8$ identical bodies and $m = 12$ identical joints. With f being the individual degree of freedom of a single joint Grübler's Eq.(4.1) yields for the total degree of freedom of the mechanism the formula $F = d + 12f - 30$. This is $F = d + 6$ in the case of spherical joints and $F = d - 6$ in the case of joints with $f = 2$ (universal joints). In Fig. 6.16b a mechanism with spherical joints is shown in a slightly unfolded position which is preserving the original symmetry. The joints are denoted $\mathrm{P}_1, \ldots, \mathrm{P}_{12}$. Example: Face 1 is connected to face 2 by joint P_1, to face 8 by joint P_2 and to face 4 by joint P_3. In what follows, it is shown that the total degree of freedom is $F = 1$ if universal joints are employed provided the two axes of rotation of the joint, each fixed on one of the connected bodies, are properly directed relative to the bodies. In 1991 a very large mechanism of this kind was a major attraction at the Scientific Exhibition HEUREKA at Zurich. Since then the mechanism is known as Heureka octahedron. Since it is $d = 7$ times overconstrained, it became the subject of scientific investigations (Stachel [30], Zsombor Murray [36], Baker [6], Wohlhart [35]). The analysis presented here is different.

The Heureka octahedron is a multiloop mechanism. This is seen from the so-called system graph shown in Fig. 6.17. Its vertices $1, \ldots, 8$ represent the bodies, and its edges $1, \ldots, 12$ (straight or curved lines) represent the joints. The appearance of a graph depends on the labeling of bodies and of joints, on the arrangement of vertices on the sheet of paper and on the shape chosen for the connecting lines. A well-drawn graph should display structural symmetries of the mechanism as clearly as possible. If possible, crossings of edges should be avoided (this is not always possible). The graph in Fig.

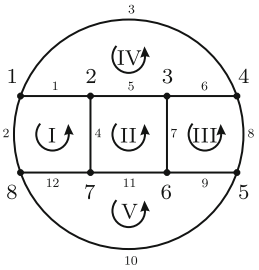

Fig. 6.17 System graph of the Heureka octahedron with elementary loops I – V

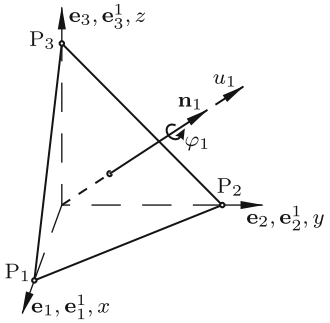

Fig. 6.18 Screw motion of face 1

6.17 is free of crossings and highly symmetric. It reveals the existence of five elementary loops I, II, III, IV and V. Each elementary loop is formed by four bodies and four joints. Other loops present in the graph are combinations of elementary loops. For proving that the Heureka octahedron has the degree of freedom $F = 1$ it suffices to prove that a single independent variable determines the kinematics of all five elementary loops. The proof is achieved as follows. First, the triangular face 1 of Fig. 6.16a is considered when it is isolated from its three neighbors. In Fig. 6.18 it is shown in the fixed reference basis $\underline{\mathbf{e}}$. The outward normal to face 1 is specified by its unit vector $\mathbf{n}_1$ with coordinates $n_1 = n_2 = n_3 = \sqrt{3}/3$. The circular cylinder with axis $\mathbf{n}_1$ which is circumscribing the triangle intersects the $\mathbf{e}_1, \mathbf{e}_2$-plane, the $\mathbf{e}_2, \mathbf{e}_3$-plane and the $\mathbf{e}_3, \mathbf{e}_1$-plane in three congruent ellipses. Clearly, it is possible to subject face 1 to a continuous screw motion with rotation φ_1 about $\mathbf{n}_1$ and with translation $u_1(\varphi_1)$ along $\mathbf{n}_1$ in such a way that P_1 moves along the ellipse in the $\mathbf{e}_3, \mathbf{e}_1$-plane, P_2 along the ellipse in the $\mathbf{e}_1, \mathbf{e}_2$-plane and P_3 along the ellipse in the $\mathbf{e}_2, \mathbf{e}_3$-plane. In what follows, the translatory displacement u_1 as well as the positions of the three points are determined as functions of φ_1. Let the position shown be the null position $\varphi_1 = 0$, $u_1 = 0$. Let, furthermore, $\underline{\mathbf{e}}^1$ be the body-fixed basis which coincides with $\underline{\mathbf{e}}$ in the null position. In $\underline{\mathbf{e}}^1$ P_1, P_2, P_3 have the coordinate matrices $\underline{R}_1^1 = [1\ 0\ 0]^T$, $\underline{R}_2^1 = [0\ 1\ 0]^T$ and $\underline{R}_3^1 = [0\ 0\ 1]^T$, respectively. This definition of unit length implies that the side length of the equilateral triangular faces is $\sqrt{2}$, and that the distance of opposite faces of the octahedron (faces 1 and 6, for example) is $4/\sqrt{3}$. Let $\underline{r}_i = [x_i\ y_i\ z_i]^T$ be the coordinate matrix of P_i $(i = 1, 2, 3)$ in $\underline{\mathbf{e}}$ after the screw displacement. It is calculated from the equation

$$\underline{r}_i = \begin{bmatrix} x_i \\ y_i \\ z_i \end{bmatrix} = \underline{A}^1 \underline{R}_i^1 + u_1 \frac{\sqrt{3}}{3} \begin{bmatrix} 1 \\ 1 \\ 1 \end{bmatrix} \qquad (i = 1, 2, 3) \qquad (6.116)$$

where $\underline{A}^1$ is the matrix in (1.49) with $n_1 = n_2 = n_3 = \sqrt{3}/3$. With the abbreviations $c = \cos\varphi_1$, $s = \sin\varphi_1$

$$\begin{bmatrix} x_i \\ y_i \\ z_i \end{bmatrix} = \frac{1}{3}\left(\begin{bmatrix} 1+2c & 1-c-s\sqrt{3} & 1-c+s\sqrt{3} \\ 1-c+s\sqrt{3} & 1+2c & 1-c-s\sqrt{3} \\ 1-c-s\sqrt{3} & 1-c+s\sqrt{3} & 1+2c \end{bmatrix} \underline{R}_i^1 + u_1\sqrt{3} \begin{bmatrix} 1 \\ 1 \\ 1 \end{bmatrix} \right) \tag{6.117}$$

$(i = 1, 2, 3)$. Each of the conditions $y_1 = z_2 = x_3 = 0$ yields

$$u_1(\varphi_1) = \frac{\sqrt{3}}{3}(\cos\varphi_1 - 1) - \sin\varphi_1 \,. \tag{6.118}$$

When this is substituted back into (6.117), the coordinates of the points are obtained:

$$\left.\begin{aligned} x_3 = y_1 = z_2 = 0 \,, \qquad & x_1 = y_2 = z_3 = \cos\varphi_1 - \frac{\sqrt{3}}{3}\sin\varphi_1 \,, \\ & z_1 = x_2 = y_3 = -\frac{2\sqrt{3}}{3}\sin\varphi_1 \,. \end{aligned}\right\} \tag{6.119}$$

These are parameter equations of the three congruent ellipses. When the position of a single point, for example x_2, y_2, is given, the angle φ_1 is determined from the equations

$$\sin\varphi_1 = -x_2\frac{\sqrt{3}}{2} \,, \qquad \cos\varphi_1 = y_2 - \frac{x_2}{2} \,. \tag{6.120}$$

Substitution into the equation $\sin^2\varphi_1 + \cos^2\varphi_1 = 1$ yields the parameter-free equation of the ellipse

$$x_2^2 + y_2^2 - x_2 y_2 = 1 \,. \tag{6.121}$$

The other two ellipses have the equations $y_3^2 + z_3^2 - y_3 z_3 = 1$ and $z_1^2 + x_1^2 - z_1 x_1 = 1$. In Fig. 6.19 the x_2, y_2-system, the y_3, z_3-system and the z_1, x_1-system are shown in a single diagram. In this diagram the three ellipses appear as a single curve. The principal-axes system ξ, η of the ellipse is rotated 45° against the coordinate axes. In this ξ, η-system the equation of the ellipse is

$$\frac{\xi^2}{2} + \frac{\eta^2}{2/3} = 1 \,. \tag{6.122}$$

The angles $\varphi_1 = -60°$ and $\varphi_1 = 30°$ mark two vertices of the ellipse. The vertices at $\varphi_1 = -60°$ and $\varphi_1 = 120°$ are the points of maximum and minimum translatory displacements $u_{1\max} = \sqrt{3}/3$ and $u_{1\min} = -\sqrt{3}$, respectively. From Fig. 6.16b it is seen that all three coordinates of P_1, P_2, P_3 as well as u_1 must be nonnegative in order to prevent interference of face 1 with other faces. Hence φ_1 is confined to the interval $-120° \le \varphi_1 \le 0$.

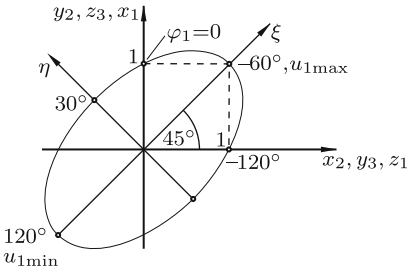

Fig. 6.19 Elliptic trajectories of P_1, P_2, P_3

At $\varphi_1 = -120°$ P_1 (P_2, P_3) is in the position initially held by P_3 (by P_1, by P_2).

Not only the isolated face 1, but every isolated face i $(i = 1, \ldots, 8)$ of the octahedron is able to execute a screw motion φ_i, u_i about its outward normal unit vector $\mathbf{n}_i$ in such a way that each of its three corners moves in one of the principal planes of basis $\underline{\mathbf{e}}$. The position shown in Fig. 6.16a is the null position $\varphi_i = 0$ $(i = 1, \ldots, 8)$. Independent of which face is chosen the three coordinates of $\mathbf{n}_i$ have identical absolute values $\sqrt{3}/3$. From this it follows that, independent of the choice of face, the circular cylinder which has $\mathbf{n}_i$ as axis and which circumscribes the triangle of face i intersects the principal planes of basis $\underline{\mathbf{e}}$ in the same three ellipses. For each of the faces $2, \ldots, 8$ the analysis differs from the one for face 1 in the signs of certain vector coordinates. In what follows, these changes are shown for face 2. The unit normal vector $\mathbf{n}_2$ has coordinates $\sqrt{3}/3[1 \;\; -1 \;\; 1]^T$. The minus sign has the effect that the transformation matrix relating bases $\underline{\mathbf{e}}$ and $\underline{\mathbf{e}}^2$ (fixed on face 2 and coinciding with $\underline{\mathbf{e}}$ in the position $\varphi_2 = 0$) is with new abbreviations $c = \cos\varphi_2$, $s = \sin\varphi_2$

$$\underline{A}^2 = \frac{1}{3}\begin{bmatrix} 1+2c & -(1-c)-s\sqrt{3} & 1-c-s\sqrt{3} \\ -(1-c)+s\sqrt{3} & 1+2c & -(1-c)-s\sqrt{3} \\ 1-c+s\sqrt{3} & -(1-c)+s\sqrt{3} & 1+2c \end{bmatrix} . \quad (6.123)$$

In basis $\underline{\mathbf{e}}^2$ P_1, P_4, P_5 have the coordinate matrices $\underline{R}_1^2 = [1 \;\; 0 \;\; 0]^T$, $\underline{R}_4^2 = [0 \;\; -1 \;\; 0]^T$ and $\underline{R}_5^2 = [0 \;\; 0 \;\; 1]^T$, respectively. In the analysis of face 1 it has already been decided that P_1 moves along the ellipse in the $\mathbf{e}_3, \mathbf{e}_1$-plane. Face 2 is connected to face 1 at P_1. The previously specified motion of P_1 in the $\mathbf{e}_3, \mathbf{e}_1$-plane is compatible with screw motion about $\mathbf{n}_2$ only if P_4 moves along the ellipse in the $\mathbf{e}_1, \mathbf{e}_2$-plane and P_5 along the ellipse in the $\mathbf{e}_2, \mathbf{e}_3$-plane. These are the only differences as compared with face 1. The same calculations which led to (6.118) and (6.119) now lead to

$$u_2(\varphi_2) = \frac{\sqrt{3}}{3}(\cos\varphi_2 - 1) + \sin\varphi_2 , \quad (6.124)$$

$$\left.\begin{aligned} y_1 = z_4 = x_5 = 0\ , \qquad & x_1 = -y_4 = z_5 = \cos\varphi_2 + \frac{\sqrt{3}}{3}\sin\varphi_2\ , \\ & z_1 = x_4 = -y_5 = \frac{2\sqrt{3}}{3}\sin\varphi_2\ . \end{aligned}\right\} \tag{6.125}$$

Face 7 is connected to face 2 at P_4. The previously specified motion of P_4 in the $\mathbf{e}_1, \mathbf{e}_2$-plane is compatible with screw motion about $\mathbf{n}_7$ only if P_{11} moves in the $\mathbf{e}_2, \mathbf{e}_3$-plane and P_{12} in the $\mathbf{e}_3, \mathbf{e}_1$-plane. The equations equivalent to (6.118) and (6.119) are

$$u_7(\varphi_7) = \frac{\sqrt{3}}{3}(\cos\varphi_7 - 1) - \sin\varphi_7\ , \tag{6.126}$$

$$\left.\begin{aligned} y_{12} = z_4 = x_{11} = 0\ , \quad & x_{12} = -y_4 = -z_{11} = \cos\varphi_7 - \frac{\sqrt{3}}{3}\sin\varphi_7\ , \\ & z_{12} = -x_4 = y_{11} = \frac{2\sqrt{3}}{3}\sin\varphi_7\ . \end{aligned}\right\} \tag{6.127}$$

Face 6 is connected to face 7 at P_{11}. The previously specified motion of P_{11} in the $\mathbf{e}_2, \mathbf{e}_3$-plane is compatible with screw motion about $\mathbf{n}_6$ only if P_9 moves in the $\mathbf{e}_3, \mathbf{e}_1$-plane and P_7 in the $\mathbf{e}_1, \mathbf{e}_2$-plane. The equations equivalent to (6.118) and (6.119) are

$$u_6(\varphi_6) = \frac{\sqrt{3}}{3}(\cos\varphi_6 - 1) + \sin\varphi_6\ , \tag{6.128}$$

$$\left.\begin{aligned} x_{11} = y_9 = z_7 = 0\ , \qquad & z_{11} = x_9 = y_7 = -\cos\varphi_6 - \frac{\sqrt{3}}{3}\sin\varphi_6\ , \\ & y_{11} = z_9 = x_7 = -\frac{2\sqrt{3}}{3}\sin\varphi_6\ . \end{aligned}\right\} \tag{6.129}$$

Face 8 is connected to face 7 at P_{12}. For this reason P_{12} is required to move in the $\mathbf{e}_3, \mathbf{e}_1$-plane. At this point it is not yet required that the loop I formed by faces 1, 2, 7 and 8 be closed at P_2. Let P_2^* be the point fixed on face 8 which coincides with P_2. The prescribed motion of P_{12} is compatible with screw motion about $\mathbf{n}_8$ only if P_2^* moves in the $\mathbf{e}_1, \mathbf{e}_2$-plane and P_{10} in the $\mathbf{e}_2, \mathbf{e}_3$-plane. The equations equivalent to (6.118) and (6.119) are

$$u_8(\varphi_8) = \frac{\sqrt{3}}{3}(\cos\varphi_8 - 1) + \sin\varphi_8\ , \tag{6.130}$$

$$\left.\begin{aligned} z_2^* = x_{10} = y_{12} = 0\ , \quad & y_2^* = -z_{10} = x_{12} = \cos\varphi_8 + \frac{\sqrt{3}}{3}\sin\varphi_8\ , \\ & x_2^* = y_{10} = -z_{12} = \frac{2\sqrt{3}}{3}\sin\varphi_8\ . \end{aligned}\right\} \tag{6.131}$$

Closure of loop I at P_2 requires that $x_2^* \equiv x_2$ and $y_2^* \equiv y_2$. This is, indeed, the case. Equations (6.131), (6.127), (6.125) and (6.119) yield $x_2^* = -z_{12} = x_4 = z_1 \equiv x_2$ and $y_2^* = x_{12} = -y_4 = x_1 \equiv y_2$.

The closure of the other four elementary loops is proved in the same way by subjecting faces 3, 4 and 5 to screw displacements about their outward normals. For reasons of symmetry this is unnecessary. Each loop is composed of four faces and four joints. In the folded position of the mechanism shown in Fig. 6.16a two of the four joints coincide in one corner of the octahedron. In loop I joints P_1 and P_{12} coincide at the front corner with coordinates $(x, y, z) = (1\ 0\ 0)$. In loop II joints P_4 and P_7 coincide at the corner $(0\ -1\ 0)$. In loop III joints P_6 and P_9 coincide at the corner $(-1\ 0\ 0)$. In loop IV joints P_3 and P_5 coincide at the top corner $(0\ 0\ 1)$, and in loop V joints P_{10} and P_{11} coincide at the bottom corner $(0\ 0\ -1)$. In every loop the geometry is the same.

Equations (6.125) and (6.119) express x_1 and z_1 once in terms of φ_1 and once in terms of φ_2. The pairwise identity of the two expressions has the form

$$\cos\varphi_2 + \frac{\sqrt{3}}{3}\sin\varphi_2 \equiv \cos\varphi_1 - \frac{\sqrt{3}}{3}\sin\varphi_1\ , \qquad \frac{2\sqrt{3}}{3}\sin\varphi_2 \equiv -\frac{2\sqrt{3}}{3}\sin\varphi_1\ . \tag{6.132}$$

Hence $\varphi_2 \equiv -\varphi_1$. Also for the coordinates of P_4, P_{11} and P_{12} two expressions in terms of two angles have been formulated. They lead to the identities $\varphi_7 \equiv -\varphi_2 \equiv \varphi_1$, $\varphi_6 \equiv -\varphi_7 \equiv \varphi_1$ and $\varphi_8 \equiv -\varphi_7 \equiv \varphi_1$. The general rule is that screw angles of any two faces coupled by a joint are of equal magnitude and opposite sign:

$$\varphi_3 \equiv \varphi_5 \equiv \varphi_7 \equiv \varphi_1\ , \qquad \varphi_2 \equiv \varphi_4 \equiv \varphi_6 \equiv \varphi_8 \equiv -\varphi_1\ . \tag{6.133}$$

These equations in combination with (6.118), (6.124), (6.126), (6.128) and (6.130) prove that all translatory displacements are identical (either all of them outward or all inward):

$$u_i(\varphi_1) \equiv u(\varphi_1) = \frac{\sqrt{3}}{3}(\cos\varphi_1 - 1) - \sin\varphi_1 \qquad (i = 1, \ldots, 8)\ . \tag{6.134}$$

Opposite faces of the octahedron have identical products screw angle times unit normal vector ($\varphi_6\mathbf{n}_6 = \varphi_1\mathbf{n}_1$, for example). From this it follows that the motion of opposite faces relative to each other is pure translation $2u(\varphi_1)$ along the common normal. For faces 1 and 6 this follows also from (6.129), (6.127), (6.125) and (6.119). In combination they state that the coordinates of opposite joints of the two faces (joints P_1 and P_9, joints P_2 and P_7, joints P_3 and P_{11}) are of equal magnitude and opposite sign: $x_9 = -x_1$, $y_9 = -y_1$, $z_9 = -z_1$ etc. In Fig. 6.16b this is shown.

Through the same Eqs.(6.129), (6.127), (6.125) and (6.119) the coordinates of all twelve points P_i $(i = 1, \ldots, 12)$ are expressed in terms of the coordi-

nates x_1 and z_1 of P_1. The coordinates are collected in Table 6.1. Column i of this table $(i = 1, \ldots, 12)$ is the coordinate matrix $\underline{r}_i = [x_i \; y_i \; z_i]^T$.

Table 6.1 Coordinates x_i, y_i, z_i of points P_i $(i = 1, \ldots, 12)$ in basis $\underline{\mathbf{e}}$

	1	2	3	4	5	6	7	8	9	10	11	12
x_i	x_1	z_1	0	z_1	0	$-x_1$	$-z_1$	$-z_1$	$-x_1$	0	0	x_1
y_i	0	x_1	z_1	$-x_1$	$-z_1$	0	$-x_1$	x_1	0	z_1	$-z_1$	0
z_i	z_1	0	x_1	0	x_1	z_1	0	0	$-z_1$	$-x_1$	$-x_1$	$-z_1$

$$x_1 = \cos\varphi_1 - \frac{\sqrt{3}}{3}\sin\varphi_1 \,, \qquad z_1 = -\frac{2\sqrt{3}}{3}\sin\varphi_1 \,.$$

At both ends of the admissible interval $-120^\circ \le \varphi_1 \le 0$ the eight faces form a closed octahedron. At $\varphi_1 = -60^\circ$ the eight faces experience the maximum outward translatory displacement $u_{\max} = \sqrt{3}/3$.

The motion of the mechanism described above is possible with twelve spherical joints. What remains to be shown is that it is possible with two-degree-of-freedom joints as well. This is done as follows. For reasons of symmetry it suffices to consider faces 1 and 2 coupled by joint P_1. Let $\boldsymbol{\Omega}_{21}$ be the angular velocity of face 2 relative to face 1 about the common point P_1. It is the difference $\boldsymbol{\Omega}_{21} = \boldsymbol{\omega}_2 - \boldsymbol{\omega}_1$ of the angular velocities of faces 2 and 1, respectively, relative to basis $\underline{\mathbf{e}}$. This difference is $\boldsymbol{\Omega}_{21} = \dot{\varphi}_2\mathbf{n}_2 - \dot{\varphi}_1\mathbf{n}_1 = -\dot{\varphi}_1(\mathbf{n}_2 + \mathbf{n}_1)$. The vectors $\mathbf{n}_1$ and $\mathbf{n}_2$ are fixed in basis $\underline{\mathbf{e}}$. The constant angle α between them is determined by $\cos\alpha = \mathbf{n}_1 \cdot \mathbf{n}_2$. The coordinates $(\sqrt{3}/3)[1 \;\; 1 \;\; 1]$ of $\mathbf{n}_1$ and $(\sqrt{3}/3)[1 \;\; -1 \;\; 1]$ of $\mathbf{n}_2$ determine $\cos\alpha = 1/3$ $(\alpha \approx 70.5^\circ)$. The vector $\mathbf{n}_2 + \mathbf{n}_1$ and, therefore, also $\boldsymbol{\Omega}_{21}$ is directed along the bisector of this angle. Hence the joint connecting faces 1 and 2 is a two-degree-of-freedom joint with an axis of rotation 1 fixed on face 1 in the direction of $\mathbf{n}_1$ and with an axis of rotation 2 fixed on face 2 in the direction of $\mathbf{n}_2$ (see Fig. 6.20). This joint is a universal joint with nonorthogonal axes intersecting at P_1.

Faces 7 and 6 are separated from face 1 by two and by three joints, respectively. Let $\boldsymbol{\Omega}_{71}$ and $\boldsymbol{\Omega}_{61}$ be their angular velocities relative to face 1. These angular velocities are $\boldsymbol{\Omega}_{71} = \dot{\varphi}_7\mathbf{n}_7 - \dot{\varphi}_1\mathbf{n}_1 = \dot{\varphi}_1(\mathbf{n}_7 - \mathbf{n}_1)$ and $\boldsymbol{\Omega}_{61} = \dot{\varphi}_6\mathbf{n}_6 - \dot{\varphi}_1\mathbf{n}_1 \equiv \mathbf{0}$. The latter formula reconfirms that face 6 is in pure translation relative to face 1. The former can be written in the alternative forms $\boldsymbol{\Omega}_{71} = \dot{\varphi}_1(\mathbf{n}_7 + \mathbf{n}_6) = \boldsymbol{\Omega}_{76}$ and $\boldsymbol{\Omega}_{71} = -\dot{\varphi}_1(\mathbf{n}_4 + \mathbf{n}_1) = -\boldsymbol{\Omega}_{41}$. These equations show that the relative angular velocities of all pairs of nonopposite faces have identical absolute values.

The Heureka octahedron at the Scientific Exhibition at Zurich would not have been a major attraction had only the identical screw motions of the eight faces relative to basis $\underline{\mathbf{e}}$ been demonstrated. Since one face of the octahedron was fixed horizontally to the ground, not the motion relative to basis $\underline{\mathbf{e}}$ was visible, but the motion of the remaining seven faces relative to the fixed face.

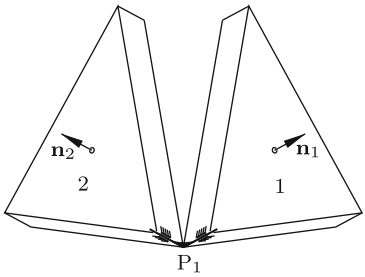

Fig. 6.20 Universal joint with nonorthogonal axes

Viewers were allowed to stand on this face while the octahedron was opening and closing around them. In what follows, it is assumed that face 1 is fixed. To be determined are the trajectories, i.e., the coordinate matrices of the points P_i $(i = 1, \ldots, 12)$ in basis $\underline{\mathbf{e}}^1$ as functions of φ_1. These matrices are denoted $\underline{R}_i^1 = [X_i\ Y_i\ Z_i]^T$. Inversion of (6.116) yields the explicit formula

$$\underline{R}_i^1 = \begin{bmatrix} X_i \\ Y_i \\ Z_i \end{bmatrix} = \underline{A}^{1\,T} \underline{r}_i - u \frac{\sqrt{3}}{3} \begin{bmatrix} 1 \\ 1 \\ 1 \end{bmatrix} \qquad (i = 1, \ldots, 12) \tag{6.135}$$

or with the abbreviations $c = \cos\varphi_1$, $s = \sin\varphi_1$ and with u from (6.134)

$$\begin{bmatrix} X_i \\ Y_i \\ Z_i \end{bmatrix} = \frac{1}{3} \left(\begin{bmatrix} 1+2c & 1-c+s\sqrt{3} & 1-c-s\sqrt{3} \\ 1-c-s\sqrt{3} & 1+2c & 1-c+s\sqrt{3} \\ 1-c+s\sqrt{3} & 1-c-s\sqrt{3} & 1+2c \end{bmatrix} \underline{r}_i + (1-c+s\sqrt{3}) \begin{bmatrix} 1 \\ 1 \\ 1 \end{bmatrix} \right) \tag{6.136}$$

$(i = 1, \ldots, 12)$. The coordinate matrices $\underline{r}_i$ in basis $\underline{\mathbf{e}}$ are known from Table 6.1. Evaluation for $i = 1, 4, 5, 7, 9, 11$ and 12 yields as functions of φ_1 the coordinates of the points fixed on faces 2, 6 and 7:

$$\left.\begin{aligned} X_1 &= 1\,, & X_4 &= \frac{2}{3}\left[s(1-4c)\frac{\sqrt{3}}{3} - c + 1\right], & X_5 &= \frac{4\sqrt{3}}{9}\, s(1-c+s\sqrt{3})\,, \\ Y_1 &= 0\,, & Y_4 &= \frac{2}{3}\left[s(1+2c)\frac{\sqrt{3}}{3} - c - 2c^2\right] + 1\,, & Y_5 &= \frac{4\sqrt{3}}{9}\, s(1+2c)\,, \\ Z_1 &= 0\,, & Z_4 &= \frac{2}{3}\left[s(1+2c)\frac{\sqrt{3}}{3} - c + 2c^2 - 1\right], & Z_5 &= \frac{4\sqrt{3}}{9}\, s(1-c-s\sqrt{3}) + 1\,, \end{aligned}\right\} \tag{6.137}$$

$$\left.\begin{aligned} X_{11} &= -\frac{2\sqrt{3}}{3}\, u\,, & X_7 &= X_{11}\,, & X_9 &= X_{11} - 1\,, & X_{12} &= Z_5\,, \\ Y_{11} &= X_{11}\,, & Y_7 &= X_{11} - 1\,, & Y_9 &= X_{11}\,, & Y_{12} &= X_5\,, \\ Z_{11} &= X_{11} - 1\,, & Z_7 &= X_{11}\,, & Z_9 &= X_{11}\,, & Z_{12} &= Y_5\,. \end{aligned}\right\} \tag{6.138}$$

Differentiation of the coordinates with respect to time yields the velocities of the points. The velocities of P_4 and P_5 are $v_4 = \frac{4}{3}\dot{\varphi}_1\sqrt{2 + (c + s\sqrt{3})^2/4} = \frac{4}{3}\dot{\varphi}_1\sqrt{2 + \cos^2(\varphi_1 - 60°)}$, $v_5 = \frac{4}{3}\dot{\varphi}_1\sqrt{2 + \cos^2\varphi_1}$.

P_4 and P_5 are both located on the sphere of radius $\sqrt{2}$ centered at P_1. Hence $(X_4-1)^2+Y_4^2+Z_4^2=2$ and $(X_5-1)^2+Y_5^2+Z_5^2=2$.
P_4 as well as P_5 is located on still another second-order surface. By substituting coordinates it is verified that

$$Y_4-Z_4+1=\tfrac{8}{3}s^2\,,\qquad Y_4+Z_4-2X_4+1=\tfrac{8}{3}\sqrt{3}\,sc\,,$$
$$X_5-Z_5+1=\tfrac{8}{3}s^2\,,\qquad X_5+Y_5+Z_5-1=\tfrac{4}{3}\sqrt{3}\,s\,.$$

Hence

$$(Y_4+Z_4-2X_4+1)^2-(1+Y_4-Z_4)[5-3(Y_4-Z_4)]=0$$

or
$$[\,X_4\;Y_4\;Z_4\,]\begin{bmatrix}2&-1&-1\\-1&2&-1\\-1&-1&2\end{bmatrix}\begin{bmatrix}X_4\\Y_4\\Z_4\end{bmatrix}-2X_4+2Z_4-2=0$$

and

$$(X_5+Y_5+Z_5-1)^2-2(X_5-Z_5+1)=0$$

or
$$[\,X_5\;Y_5\;Z_5\,]\begin{bmatrix}1&1&1\\1&1&1\\1&1&1\end{bmatrix}\begin{bmatrix}X_5\\Y_5\\Z_5\end{bmatrix}-4X_5-2Y_5-1=0\,.$$

In both equations the symmetric coefficient matrix of the second-order terms has real eigenvalues λ_1, λ_2, λ_3 and mutually orthogonal eigenvectors. Let $\underline{A}_i$ $(i=4,5)$ be the matrix with these eigenvectors as columns. The transformation $[\,X_i\;Y_i\;Z_i\,]^T=\underline{A}_i\,[\,x\;y\;z\,]^T$ results in an equation of the form $\lambda_1x^2+\lambda_2y^2+\lambda_3z^2+ax+by+cz+d=0$.

The equation for P_4:
$\lambda_1=0$, $\lambda_2=\lambda_3=3$, $\underline{A}_4=\frac{1}{6}\begin{bmatrix}2\sqrt{3}&3\sqrt{2}&\sqrt{6}\\2\sqrt{3}&-3\sqrt{2}&\sqrt{6}\\2\sqrt{3}&0&-2\sqrt{6}\end{bmatrix}$. The transformed equation is $(y-\frac{1}{6}\sqrt{2})^2+(z-\frac{1}{6}\sqrt{6})^2=\frac{8}{9}$. This is a circular cylinder. Its radius is twice the radius of the circle circumscribing the triangular face of the octahedron.

The equation for P_5:
$\lambda_1=3$, $\lambda_2=\lambda_3=0$, $\underline{A}_5=\frac{1}{6}\begin{bmatrix}-2\sqrt{3}&\sqrt{6}&-3\sqrt{2}\\-2\sqrt{3}&-2\sqrt{6}&0\\-2\sqrt{3}&\sqrt{6}&3\sqrt{2}\end{bmatrix}$. The transformed equation is $(x\sqrt{3}+1)^2+2z\sqrt{2}-2=0$. This is a cylinder with parabolic cross section in the x,z-plane.

Generalized Heureka Octahedron

The triangle shown in Fig. 6.21 in basis $\underline{\mathbf{e}}$ has its corners at points with coordinate matrices $\underline{R}_1^1=[a_1\;0\;0]^T$, $\underline{R}_2^1=[0\;a_2\;0]^T$ and $\underline{R}_3^1=[0\;0\;a_3]^T$, respectively ($a_1$, a_2, $a_3>0$ arbitrary). This triangle is face 1 of a plane-symmetric octahedron with these corners and with the opposite corners $-\underline{R}_1^1$, $-\underline{R}_2^1$ and $-\underline{R}_3^1$. The labeling of faces, the pairwise connections of faces by joints and the labeling of joints are copied from Figs. 6.16a and b. Proposition: If the joint at P_i $(i=1,\ldots,12)$ is a universal joint with joint axes along the normals of the two bodies coupled by this joint, the mechanism has the degree of freedom $F=1$. Furthermore, each face $i=1,\ldots,8$ moves in such

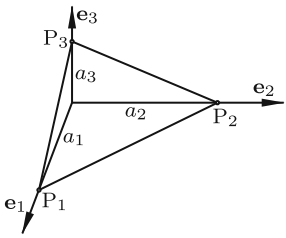

Fig. 6.21 Face 1 of a plane-symmetric octahedron

a way that (i) its normal $\mathbf{n}_i$ does not change its direction and (ii) each corner moves in an ellipse in a principle plane of basis $\underline{\mathbf{e}}$. The idea to generalize the Heureka octahedron in this way is due to Wohlhart [34]. The proof presented here is different.

For reasons of symmetry it suffices to prove the propositions for face 1. Its outward normal unit vector has the coordinates (normalized vector product $\overrightarrow{\mathrm{P_1P_2}} \times \overrightarrow{\mathrm{P_1P_3}}$)

$$n_1 = \frac{a_2 a_3}{N} \ , \quad n_2 = \frac{a_3 a_1}{N} \ , \quad n_3 = \frac{a_1 a_2}{N} \ , \quad N = \sqrt{a_1^2 a_2^2 + a_2^2 a_3^2 + a_3^2 a_1^2} \ . \tag{6.139}$$

From the analysis of the Heureka octahedron the conditions are copied that $\mathrm{P_1}$ moves in the $\mathbf{e}_3, \mathbf{e}_1$-plane, $\mathrm{P_2}$ in the $\mathbf{e}_1, \mathbf{e}_2$-plane and $\mathrm{P_3}$ in the $\mathbf{e}_2, \mathbf{e}_3$-plane. These conditions plus the stationarity condition of the unit normal vector require that the displacement of face 1 is a rotation about the unit normal vector superimposed by a translation which does not have the direction of the unit normal vector. Equation (6.116) is replaced by the equation

$$\begin{bmatrix} x_i \\ y_i \\ z_i \end{bmatrix} = \underline{A}^1 \underline{R}_i^1 + \begin{bmatrix} u_1 \\ u_2 \\ u_3 \end{bmatrix} \qquad (i = 1, 2, 3) \ , \tag{6.140}$$

where u_1, u_2, u_3 are the coordinates of the displacement in basis $\underline{\mathbf{e}}$. With the general Eq.(1.49) for $\underline{A}^1$ this equation is ($c = \cos\varphi_1$, $s = \sin\varphi_1$)

$$\begin{bmatrix} x_i \\ y_i \\ z_i \end{bmatrix} = \begin{bmatrix} n_1^2 + (1 - n_1^2)c & n_1 n_2 (1 - c) - n_3 s & n_1 n_3 (1 - c) + n_2 s \\ n_1 n_2 (1 - c) + n_3 s & n_2^2 + (1 - n_2^2)c & n_2 n_3 (1 - c) - n_1 s \\ n_1 n_3 (1 - c) - n_2 s & n_2 n_3 (1 - c) + n_1 s & n_3^2 + (1 - n_3^2)c \end{bmatrix} \underline{R}_i^1 + \begin{bmatrix} u_1 \\ u_2 \\ u_3 \end{bmatrix} \tag{6.141}$$

($i = 1, 2, 3$). For n_1, n_2, n_3 the expressions (6.139) are substituted. The conditions $y_1 = z_2 = x_3 = 0$ yield for the translatory displacements the explicit functions of φ_1:

$$\left.\begin{aligned} u_1 &= -a_3^2 a_1 \Big[\frac{a_2^2}{N^2}(1-\cos\varphi_1) + \frac{1}{N}\,\sin\varphi_1 \Big] \,, \\ u_2 &= -a_1^2 a_2 \Big[\frac{a_3^2}{N^2}(1-\cos\varphi_1) + \frac{1}{N}\,\sin\varphi_1 \Big] \,, \\ u_3 &= -a_2^2 a_3 \Big[\frac{a_1^2}{N^2}(1-\cos\varphi_1) + \frac{1}{N}\,\sin\varphi_1 \Big] \,. \end{aligned}\right\} \tag{6.142}$$

When these expressions are substituted back into (6.141), the coordinates of $\mathrm{P}_1\,,\,\mathrm{P}_2\,,\,\mathrm{P}_3$ in basis $\underline{\mathbf{e}}$ are obtained:

$$\left.\begin{aligned} x_1 &= a_1\Big(\cos\varphi_1 - \frac{a_3^2}{N}\,\sin\varphi_1 \Big) \,, \qquad & z_1 &= -\frac{a_3(a_1^2+a_2^2)}{N}\,\sin\varphi_1 \,, \\ y_2 &= a_2\Big(\cos\varphi_1 - \frac{a_1^2}{N}\,\sin\varphi_1 \Big) \,, \qquad & x_2 &= -\frac{a_1(a_2^2+a_3^2)}{N}\,\sin\varphi_1 \,, \\ z_3 &= a_3\Big(\cos\varphi_1 - \frac{a_2^2}{N}\,\sin\varphi_1 \Big) \,, \qquad & y_3 &= -\frac{a_2(a_3^2+a_1^2)}{N}\,\sin\varphi_1 \,. \end{aligned}\right\} \tag{6.143}$$

Elimination of φ_1 from the equations for x_2 and y_2 proves that the trajectory of P_2 is the ellipse

$$x_2^2\,\frac{(a_1^2+a_2^2)(a_1^2+a_3^2)}{a_1^2(a_2^2+a_3^2)^2} + \frac{y_2^2}{a_2^2} - \frac{2a_1}{a_2(a_2^2+a_3^2)}\,x_2 y_2 = 1 \,. \tag{6.144}$$

The other two ellipses are obtained by cyclic permutation of indices. In the special case $a_1 = a_2 = a_3 = 1$, which characterizes the Heureka octahedron, (6.142) – (6.144) are identical with (6.118), (6.119) and (6.121), respectively. This ends the proof that face 1 is moving in the predicted way. For reasons of symmetry the trajectories of the corners of faces $2,\ldots,8$ are congruent ellipses. For the same reason, also Eqs.(6.133) are valid: $\varphi_3 \equiv \varphi_5 \equiv \varphi_7 \equiv \varphi_1$, $\varphi_2 \equiv \varphi_4 \equiv \varphi_6 \equiv \varphi_8 \equiv -\varphi_1$. In joint P_i $(i = 1,\ldots,12)$ the relative angular velocity of the two coupled faces lies in the plane of the normals of these faces. From this it follows that joint i is a universal joint with joint axes along the normals of the two faces. The cosine of the constant angle α_i between the normals is the scalar product of the unit normal vectors. Face 1 is connected to face 2 by joint 1 (angle α_1), to face 8 by joint 2 (angle α_2) and to face 4 by joint 3 (angle α_3). The same three angles appear in the joints of each face. The four unit normal vectors involved have in basis $\underline{\mathbf{e}}$ the following coordinates: Face 1: $[n_1\ n_2\ n_3]$, face 2: $[n_1\ -n_2\ n_3]$, face 8: $[n_1\ n_2\ -n_3]$, face 4: $[-n_1\ n_2\ n_3]$. With (6.139) this yields

$$\left.\begin{aligned} \cos\alpha_1 &= \frac{a_2^2a_3^2 - a_3^2a_1^2 + a_1^2a_2^2}{a_2^2a_3^2 + a_3^2a_1^2 + a_1^2a_2^2} \,, \qquad & \cos\alpha_2 &= \frac{a_2^2a_3^2 + a_3^2a_1^2 - a_1^2a_2^2}{a_2^2a_3^2 + a_3^2a_1^2 + a_1^2a_2^2} \,, \\ \cos\alpha_3 &= \frac{-a_2^2a_3^2 + a_3^2a_1^2 + a_1^2a_2^2}{a_2^2a_3^2 + a_3^2a_1^2 + a_1^2a_2^2} \,, \qquad & \sum_i \cos\alpha_i &= 1 \,. \end{aligned}\right\} \tag{6.145}$$

References

1. Altmann F G (1954) Räumliche fünfgliedrige Koppelgetriebe. Konstruktion 6:254–259
2. Altmann F G (1954) Über räumliche sechsgliedrige Koppelgetriebe. Z. VDI 96:245–249
3. Baker J E (1979) The Bennett, Goldberg and Myard linkages-in perspective. Mechanism Machine Theory 14:239–253
4. Baker J E (1980) An analysis of the Bricard linkages. Mechanism Machine Theory 15:267–286
5. Baker J E (1984) On 5-revolute linkages with parallel adjacent joint axes. Mechanism Machine Theory 19:467–475
6. Baker J E (1993) On a network of continuously modified Bennett linkages. Proc. 6th Int.Symp. Teoria si Practica Mecanismelor, Bucharesti 2:27–34
7. Baker J E (1993) A comparative survey of the Bennett-based, 6-R revolute kinematic loops. Mechanism Machine Theory 28:83–96
8. Bennett G T (1903) A new mechanism. Engineering 76:77–78
9. Borel E (1908) Mémoire sur les déplacements a trajectoires sphériques. Mém. présenté par divers savants. Paris 2, v.33,1:1–128
10. Bricard R (1926/27) Leçons de cinématique. v.I.: Cinématique théorique. v.II: Cinématique appliquée. Gauthier-Villars, Paris
11. Bricard R (1906) Mémoire sur les déplacements à trajectoires sphériques. J. Ec. Polyt. 2, v.11:1–96
12. Bronstein I N, Semendjajev K A, Musiol K A, Mühlig H (2008) Taschenbuch der Mathematik. 7. Aufl. Verlag Harri Deutsch
13. Byshgens S S (1939) The Bennett-Berkovski mechanism (Russ). PMM v.II:513–518
14. Connelly R (1979) The rigidity of polyhedral surfaces. Mathematics Mag.52:275–283
15. Delassus E (1900) Sur les systèmes articulés gauches. Première Partie. Paris Ec.Normale Sup., Ann.Scie. 3s,XVII:445–499
16. Delassus E (1902) Sur les systèmes articulés gauches. Deuxième Partie. Paris Ec.Normale Sup., Ann.Scie. 3s,XIX:119–152
17. Demaine E D , O'Rourke J (2007) Geometric folding algorithms. Linkages, origami, polyhedra. Cambridge Univ. Press
18. Dimentberg F M, Schor Ja B (1940) The Bennett mechanism. PMM v.IV:111–118
19. Dietmaier P (1995) Einfach übergeschlossene Mechanismen mit Drehgelenken. Habil.-Schrift Graz
20. Goldberg M (1943) New five-bar and six-bar linkages in three dimensions. Trans. ASME 65:649–661
21. Hilbert D, Cohn-Vossen S (1996) Anschauliche Geometrie. 2.Aufl. Springer, Berlin. Engl. trans. (1952) Geometry and the imagination. Chelsea, New York
22. Hon-Cheung Y (1994) published in: Baker E, Wohlhart K: On the single screw reciprocal to the general line-symmetric six-screw linkage. Mechanism Machine Theory 29:169–175
23. Husty M L, Zsombor-Murray P (1994) A special type of singular Stewart–Gough platform. In: [24] 449–458
24. Lenarčič J, Ravani B (eds) (1994) Advances in robot kinematics and computational geometry. Kluwer, Dordrecht
25. Mavroidis C, Roth B (1994) Analysis and synthesis of overconstrained mechanisms. Proc. of 1994 ASME Design Techn. Conf., DE-70, Minneapolis, 115–133
26. Mavroidis C, Roth B (1995) Analysis and synthesis of overconstrained mechanisms. J. Mechanical Design 117:69–74
27. Mavroidis C, Roth B (1995) New and revised overconstrained mechanisms. J. Mechanical Design 117:75–82
28. Mavroidis C, Beddows M (1997) A spatial overconstrained mechanism that can be used in practical applications. Proc. Fifth Appl.Mechanisms

29. Mudrov P G (1976) Spatial mechanisms with revolute joints (Russ.) Isd. Kazan Univ.
30. Stachel H (1992) Zwei bemerkenswerte bewegliche Strukturen. J. Geometry 43:14–21
31. Wohlhart K (1987) A new 6R space mechanism. Proc. 7th IFToMM World Congr. 1:193–198
32. Wohlhart K (1991) Merging two general Goldberg 5R linkages to obtain a new 6R space mechanism. Mechanism Machine Theory 26:659–668
33. Wohlhart K (1993) The two types of orthogonal Bricard mechanism. Mechanism Machine Theory 28:809–817
34. Wohlhart K (1995) Das dreifach plansymmetrische Oktoid und seine Punktbahnen. Mathematica Pannonica 6:243–265
35. Wohlhart K (1995) Heureka Octahedron and Brussels folding cube as special cases of the turing tower. Proc. 6th Int.Symp. Teoria si Practica Mecanismelor, Bucharesti 2:302–311
36. Zsombor Murray P J (1992) The Brussels folding cube. Proc.3rd Int.Workshop Advances in Robot Kinematics:159–164

Chapter 7
Two-Joint Chains

Figure 7.1 shows a spatial chain of three bodies 0, 1 and 2 interconnected by two joints 1 and 2. Body 0 is referred to as frame and body 2 as terminal body. Joints are either revolute (R) or prismatic (P) or cylindric (C). Throughout Sects. 7.1 and 7.2 cylindrical joints are excluded. Chains with revolute and prismatic joints are classified by the sequence of joints (joint 1, joint 2) as RR, RP, PR, PP. Since each joint has a single joint variable, the degree of freedom of the terminal body is two. In Sect. 7.1 the work space of points fixed on the terminal body is investigated. Sect. 7.2 is devoted to the problem of synthesis of RR chains capable of producing prescribed positions of the terminal body. In Sect. 7.3 the same synthesis problem is solved for chains CC. Chains RR, PP and CC are structurally symmetric. By this is meant that the structure remains the same if body 0 becomes body 2 and vice versa.

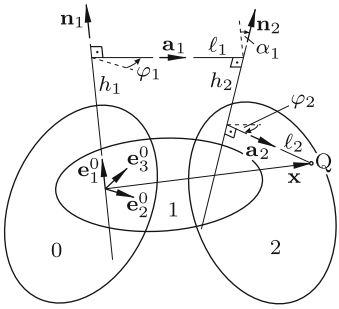

Fig. 7.1 Two-joint chain. Frame-fixed basis $\underline{\mathbf{e}}^0$. Position vector $\mathbf{x}$ of point Q fixed on body 2. Denavit-Hartenberg parameters φ_1, h_1, α_1, ℓ_1, φ_2, h_2, ℓ_2

J. Wittenburg, *Kinematics*, DOI 10.1007/978-3-662-48487-6_7

7.1 Work Space of Points of the Terminal Body

On body 0 the reference basis $\underline{\mathbf{e}}^0$ is fixed with its origin 0 at an arbitrarily chosen point on joint axis 1. The basis vector $\mathbf{e}_1^0$ is directed along this joint axis (see Fig. 7.1). Let $\mathbf{x}$ be the position vector of an arbitrary point Q fixed on the terminal body 2. The coordinates x_1, x_2, x_3 of $\mathbf{x}$ in $\underline{\mathbf{e}}^0$ are functions of the two joint variables, say q_1 and q_2, and of constant parameters of the chain. The functions define a surface in $\underline{\mathbf{e}}^0$. This surface is the work space of Q. Lines $q_1 = \text{const}$ (arbitrary) and $q_2 = \text{const}$ (arbitrary) on the surface are either circles or straight lines depending on whether the other variable not held constant is an angle in a revolute joint or a straight-line displacement in a prismatic joint. Each of the chains RR, RP, PR and PP has its own characteristic surface. The purpose of this section is to analyze, for each type of chain separately, the dependency of the surface upon the constant parameters of the chain.

Parameters and variables are the Denavit-Hartenberg parameters explained in Sect. 5.1 (see Fig. 5.1). Unambiguous definitions require a chain of mutually orthogonal lines along joint axes and lines perpendicular to joint axes. For body 1 the situation is the same as for body i in Fig. 5.1. Unit vectors along the joint axes are called $\mathbf{n}_1$ and $\mathbf{n}_2$, and the unit vector along the common perpendicular is called $\mathbf{a}_1$. Bodies 0 and 2 do not have a second joint axis. As lines perpendicular to the existing joint axes the axis $\mathbf{e}_2^0$ fixed on body 0 and the perpendicular from Q onto joint axis 2 are chosen. Let $\mathbf{a}_2$ be the unit vector pointing from the foot of this perpendicular toward Q. The lines thus specified define the Denavit-Hartenberg parameters φ_1, h_1, α_1, ℓ_1, φ_2, h_2 and ℓ_2 of the chain. If joint i ($i = 1$ or $i = 2$) is a revolute joint, φ_i is variable and h_i is constant. If joint i is a prismatic joint, φ_i is constant and h_i is variable. The position vector $\mathbf{x}$ of Q is

$$\mathbf{x} = h_1\mathbf{n}_1 + \ell_1\mathbf{a}_1 + h_2\mathbf{n}_2 + \ell_2\mathbf{a}_2 \,. \tag{7.1}$$

The coordinates of $\mathbf{n}_1$, $\mathbf{a}_1$, $\mathbf{n}_2$ and $\mathbf{a}_2$ in basis $\underline{\mathbf{e}}^0$ are taken from Table 5.2 by setting $k = 0$. The abbreviations in the table are $C_1 = \cos\alpha_1$, $S_1 = \sin\alpha_1$ and $c_k = \cos\varphi_k$, $s_k = \sin\varphi_k$ $(k = 1, 2)$. By definition (see Fig. 5.1 and Eqs.(5.6), (5.7)), basis $\underline{\mathbf{e}}^0$ is located not in joint 1 but in a joint 0 connecting body 0 to a preceding body -1. In order to adapt to the present situation the angle α_0 between joint axes 0 and 1 must, formally, be defined as zero. This means that $S_0 = 0$ and $C_0 = 1$. With these definitions Table 5.2 yields the coordinate equations

$$\begin{bmatrix} x_1 \\ x_2 \\ x_3 \end{bmatrix} = h_1 \begin{bmatrix} 1 \\ 0 \\ 0 \end{bmatrix} + \ell_1 \begin{bmatrix} 0 \\ c_1 \\ s_1 \end{bmatrix} + h_2 \begin{bmatrix} C_1 \\ S_1 s_1 \\ -S_1 c_1 \end{bmatrix} + \ell_2 \begin{bmatrix} s_2 S_1 \\ c_2 c_1 - s_2 s_1 C_1 \\ c_2 s_1 + s_2 C_1 c_1 \end{bmatrix}$$
$$= \begin{bmatrix} h_1 + h_2 C_1 + \ell_2 S_1 s_2 \\ (\ell_1 + \ell_2 c_2) c_1 - (\ell_2 C_1 s_2 - h_2 S_1) s_1 \\ (\ell_1 + \ell_2 c_2) s_1 + (\ell_2 C_1 s_2 - h_2 S_1) c_1 \end{bmatrix} . \tag{7.2}$$

These equations are the parameter equations of the surfaces to be investigated.

7.1.1 Chains RR Defining Tori

Variables in (7.2) are the angles φ_1 and φ_2. The origin of basis $\underline{\mathbf{e}}^0$ on joint axis 1 is now placed at the foot of the common perpendicular of both joint axes. This has the consequence that $h_1 = 0$. The expression $r = \sqrt{x_2^2 + x_3^2}$ depends on φ_2 only. From this it follows that the surface is a surface of revolution. It is generated by rotating a planar curve k about the axis $\mathbf{e}_1^0$, i.e., about the axis of joint 1. The generating curve has the parameter equation

$$\left.\begin{aligned} x_1(\varphi_2) &= h_2 C_1 + \ell_2 S_1 s_2 \ , \\ r(\varphi_2) \ &= \sqrt{(\ell_1 + \ell_2 c_2)^2 + (\ell_2 C_1 s_2 - h_2 S_1)^2} \ . \end{aligned}\right\} \tag{7.3}$$

The trivial case of parallel joint axes $(\alpha_1 = 0)$ is characterized by $x_1 \equiv h_2$. The workspace of Q is the ring-shaped area $|\ell_1 - \ell_2| \le r \le \ell_1 + \ell_2$ in the plane $x_1 = h_2$. In what follows, $\alpha_1 \neq 0$ is assumed.

The special case $\alpha_1 = \pi/2$, $h_2 = 0$: Equations (7.3) have the forms $x_1 = \ell_2 s_2$, $r = \ell_1 + \ell_2 c_2$. Elimination of φ_2 produces for the curve k the equation of a circle: $x_1^2 + (r - \ell_1)^2 = \ell_2^2$. The surface of revolution is the torus generated by rotating this circle about the x_1-axis. In the case $\ell_2 > \ell_1$, the circle intersects the x_1-axis. In this case, the generating curve k of the torus is moon-shaped and pointed on the axis of joint 1.

In the general case $\alpha_1 \neq 0, \pi/2$, the surface of revolution is a generalized torus with a noncircular generating curve k (see Fichter/Hunt [2]). The diversity of forms is illustrated by the two curves k_1 and k_2 shown in Fig. 7.2. Both curves have the parameters $\alpha_1 = 30°$, $h_2 = 3\sqrt{3}$ and $\ell_1 = 4$ in common. The only difference is the parameter $\ell_2 = 5$ for k_1 and $\ell_2 = 6$ for k_2. The parameters of k_1 satisfy the condition $\ell_2^2 = \ell_1^2 + h_2^2 \tan^2 \alpha_1$. Under this condition the curve is pointed on the axis of revolution at $x_1 = h_2 / C_1$.

The elimination of φ_2 from (7.3) is achieved as follows. The first Eq.(7.3) multiplied by $2\ell_1 / S_1$ is the first equation below, and the sum of squares of both Eqs.(7.3) together is the second equation.

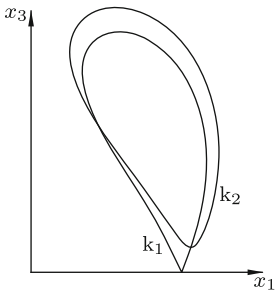

Fig. 7.2 Generating curves k_1 and k_2 of two tori

$$\frac{2\ell_1}{S_1}(x_1 - h_2C_1) = 2\ell_1\ell_2 s_2 \,, \qquad r^2 + x_1^2 - (\ell_1^2 + h_2^2 + \ell_2^2) = 2\ell_1\ell_2 c_2 \,. \quad (7.4)$$

The sum of squares of these two equations is the desired parameter-free equation of the torus:

$$\Big[r^2 + x_1^2 - (\ell_1^2 + h_2^2 + \ell_2^2)\Big]^2 + \Big(\frac{2\ell_1}{S_1}\Big)^2 (x_1 - h_2C_1)^2 = (2\ell_1\ell_2)^2 \,. \quad (7.5)$$

In terms of the original parameters α_1, ℓ_1, h_2, ℓ_2 new parameters are defined as follows:

$$p_1^2 = \ell_1^2 + h_2^2 + \ell_2^2 \,, \qquad p_2 = \frac{\ell_1}{S_1} \,, \qquad p_3 = h_2C_1 \,, \qquad p_4 = \ell_1\ell_2 \,. \quad (7.6)$$

In terms of these parameters the equation of the torus is

$$(r^2 + x_1^2 - p_1^2)^2 + 4p_2^2(x_1 - p_3)^2 = 4p_4^2 \,. \quad (7.7)$$

This yields the explicit equation

$$r(x_1) = \sqrt{p_1^2 - x_1^2 \pm 2\sqrt{p_4^2 - p_2^2(x_1 - p_3)^2}} \,. \quad (7.8)$$

From (7.6) the original parameters α_1, ℓ_1, h_2, ℓ_2 are recovered as follows. The last three equations yield

$$S_1 = \frac{\ell_1}{p_2} \,, \qquad C_1 = \sqrt{1 - \frac{\ell_1^2}{p_2^2}} \,, \qquad h_2 = \frac{p_3}{\sqrt{1 - \frac{\ell_1^2}{p_2^2}}} \,, \qquad \ell_2 = \frac{p_4}{\ell_1} \,. \quad (7.9)$$

Substitution of the expressions for h_2 and ℓ_2 into the first Eq.(7.6) results in a cubic equation for ℓ_1^2. With the abbreviation $\mu = \ell_1^2$ it reads

$$\mu^3 - (p_1^2 + p_2^2)\mu^2 + [p_2^2(p_1^2 - p_3^2) + p_4^2]\mu - p_2^2p_4^2 = 0 \,. \quad (7.10)$$

Suppose $\alpha_1\,,\ \ell_1\,,\ h_2\,,\ \ell_2$ are given. From (7.6) the associated parameters $p_1^2\,,\ p_2\,,\ p_3\,,\ p_4$ are calculated and from these, in turn, three roots $\mu_i = \ell_{1_i}^2$ $(i = 1, 2, 3)$. One of them is the prescribed quantity $\mu_1 = \ell_1^2$. Division by $(\mu - \ell_1^2)$ produces a quadratic equation. When $p_1^2\,,\ p_2\,,\ p_3\,,\ p_4$ are replaced again by the expressions (7.6), this quadratic equation is

$$\mu^2 - \Big(\frac{\ell_1^2}{S_1^2} + h_2^2 + \ell_2^2\Big)\mu + \frac{\ell_1^2\ell_2^2}{S_1^2} = 0\,. \tag{7.11}$$

The roots μ_2 and μ_3 are real and positive since their sum as well as their product is positive. The quantities $\ell_{1_2} = \sqrt{\mu_2}$ and $\ell_{1_3} = \sqrt{\mu_3}$ are parameters of two new chains RR generating the same torus which is generated by the original chain. The remaining parameters of these new chains are calculated from (7.9) and (7.6):

$$\ell_{2_{2,3}} = \frac{p_4}{\ell_{1_{2,3}}}\,,\quad S_{1_{2,3}} = \frac{\ell_{1_{2,3}}}{p_2}\,,\quad h_{2_{2,3}} = \frac{p_3}{\sqrt{1 - S_{1_{2,3}}^2}}\,,\quad C_{1_{2,3}} = C_1\,\frac{h_2}{h_{2_{2,3}}}\,. \tag{7.12}$$

The conditions $S_{1_{2,3}}^2 \le 1$ read

$$\mp\sqrt{[\ell_1^2 - S_1^2(h_2^2 + \ell_2^2)]^2 + 4S_1^2\ell_1^2h_2^2} \le \ell_1^2 - S_1^2(h_2^2 + \ell_2^2)\,. \tag{7.13}$$

The first condition is always satisfied. The second condition is satisfied only in the trivial case when $S_1\ell_1h_2 = 0$. Hence

Theorem 7.1. *Every chain* RR *with parameters* $\alpha_1\,,\ \ell_1\,,\ h_2\,,\ \ell_2$ *satisfying the condition* $\ell_1h_2\sin\alpha_1 \ne 0$ *is one out of two chains* RR *generating one and the same torus. Both chains have the first joint axis and on this joint axis the foot of the common perpendicular of joint axes 1 and 2 in common.*

The theorem is of the same nature as de la Hire's theorem on the double generation of trochoids and as the theorem of Roberts and Tschebyschev on the triple generation of coupler curves by planar four-bars (see Sects. 15.5.2 and 17.8.1). The theorem is in agreement with a statement made at the end of Sect. 6.2, namely, that in a Bennett mechanism the trajectories of all points fixed on body 3 are generated by two chains RR.

Example: The curve k_2 in Fig. 7.2 is generated by the chain RR with parameters $\alpha_1 = 30°\,,\ h_2 = 3\sqrt{3}\,,\ \ell_1 = 4$ and $\ell_2 = 6$. Equation (7.10) is $(\mu - 16)(\mu^2 - 127\mu + 48^2) = 0$. It has the roots $\mu_1 = \ell_1^2 = 16\,,\ \mu_2 \approx 21.93$ and $\mu_3 \approx 105.1$. The roots μ_2 and μ_3 yield the parameters $\ell_{1_2} \approx 4.68$ and $\ell_{1_3} \approx 10.25$. The parameters associated with $\ell_{1_2} \approx 4.68$ are $S_{1_2} \approx 0.5853$ (real angle α_{1_2}), $\ell_{2_2} \approx 5.12$ and $h_{2_2} \approx 5.55$. End of example.

7.1.2 Chains RP Defining Hyperboloids of Revolution

Variables in (7.2) are φ_1 and h_2. As before, the origin of basis $\underline{\mathbf{e}}^0$ is placed at the foot of the common perpendicular of both joint axes so that, again, $h_1 = 0$. As before, φ_1 is eliminated by forming $x_2^2 + x_3^2 = (\ell_1 + \ell_2 c_2)^2 + (\ell_2 C_1 s_2 - h_2 S_1)^2$. For h_2 the expression $h_2 = (x_1 - \ell_2 S_1 s_2)/C_1$ obtained from the first Eq.(7.2) is substituted. The resulting parameter-free equation of the surface is

$$C_1^2(x_2^2 + x_3^2) - (S_1 x_1 - \ell_2 s_2)^2 = C_1^2(\ell_1 + \ell_2 c_2)^2 \,. \tag{7.14}$$

There are two trivial cases, namely, $S_1 = 0$ (parallel joint axes 1 and 2) and $C_1 = 0$ (perpendicular joint axes). In the first case, the surface is the circular cylinder of radius $r = \sqrt{\ell_1^2 + \ell_2^2 + 2\ell_1\ell_2 c_2}$ (see (7.3)). In the second case, the surface is located in the plane $x_1 = \ell_2 s_2 = \text{const}$. The surface is the manifold of all points on or outside the circle $x_2^2 + x_3^2 = (\ell_1 + \ell_2 c_2)^2$. In the general case $S_1 C_1 \neq 0$, the surface is a hyperboloid of revolution with the x_1-axis, i.e., the axis of joint 1, as axis of revolution.

7.1.3 Chains PR Defining Elliptic Cylinders

Variables in (7.2) are h_1 and φ_2. The basis vector $\mathbf{e}_2^0$ is placed parallel to the common perpendicular of the two joint axes so that the constant angle φ_1 is zero ($c_1 = 1$, $s_1 = 0$). Then (7.2) has the form

$$\begin{bmatrix} x_1 \\ x_2 \\ x_3 \end{bmatrix} = \begin{bmatrix} h_1 + h_2 C_1 + \ell_2 S_1 s_2 \\ \ell_1 + \ell_2 c_2 \\ \ell_2 C_1 s_2 - h_2 S_1 \end{bmatrix} \,. \tag{7.15}$$

The coordinates x_2 and x_3 depend on the variable φ_2 only. With c_2 expressed through x_2 and s_2 through x_3 the equation $c_2^2 + s_2^2 = 1$ defines in the x_2, x_3-plane the ellipse

$$\Big(\frac{x_2 - \ell_1}{\ell_1}\Big)^2 + \Big(\frac{x_3 + h_2 S_1}{\ell_2 C_1}\Big)^2 = 1 \,. \tag{7.16}$$

The coordinate x_1 depends on φ_2 and, in addition, on h_1. The surface under investigation is, therefore, a cylinder with the elliptic cross section and with generating lines parallel to the axis of joint 1.

7.1.4 Chains PP Defining Planes

As in the chain PR the basis vector $\mathbf{e}_2^0$ is placed such that $\varphi_1 = 0$. Then (7.15) applies again. But now, h_1 and h_2 are the variables. The surface under investigation is the plane $x_2 = \ell_1 + \ell_2 c_2 = \text{const}$.

7.2 Chains RR Leading the Terminal Body Through Prescribed Positions

This section is devoted to chains RR. Two problems are formulated as follows.

Problem 1: Determine the constant parameters of a chain RR capable of leading the terminal body, i.e., basis $\underline{\mathbf{e}}^2$, through prescribed positions $1, 2, \ldots, m$ in basis $\underline{\mathbf{e}}^0$. In addition, the joint variables in these positions are to be determined.

Problem 2 is a relaxed form of Problem 1: Position 1 is not prescribed. Only the $m-1$ screw displacements leading from position 1 to positions $2, \ldots, m$ are prescribed.

Problem 2 has been the subject of intensive research (Roth [6, 8], Suh [10, 11], Tsai [12], Tsai/Roth [13], Huang [3], Perez Gracia/McCarthy [4]). Tsai and Roth based their analysis on the geometry of the screw triangle (Fig. 3.7). They proved that at most three positions relative to each other can be prescribed arbitrarily. The analysis led to ten coupled second-order equations for ten unknowns which were then reduced to a bicubic equation with a single real and positive root. This root proved the existence of two chains RR. It was shown that these chains form a Bennett mechanism. In view of what has been said at the end of Sect. 6.2, this result had to be expected. Perez Gracia/McCarthy [4] combined the analysis of the screw triangle with properties of the Bennett mechanism, in particular with the fact that finite displacement screws of the coupler form a cylindroid (Huang [3]). For the problem of three relative displacements a system of four coupled equations for four unknowns was obtained. These equations reproduced numerical results obtained by Tsai and Roth.

The analysis presented in what follows addresses Problem 1. The analysis is based on the principle of transference. According to this principle, first, a rotation problem is investigated. This is the case of a chain RR with intersecting joint axes. The notation of Fig. 7.1 is used again. Without loss of generality, the origins of the bases $\underline{\mathbf{e}}^0$ and $\underline{\mathbf{e}}^2$ are placed at the point of intersection of the joint axes. Furthermore, the basis vector $\mathbf{e}_2^2$ of $\underline{\mathbf{e}}^2$ is directed along the axis of joint 2. In basis $\underline{\mathbf{e}}^0$, the unit vector $\mathbf{n}_1$ along the axis of joint 1 is unknown. It is specified by two angular parameters ψ and θ defined further below. The unknown angle between joint axes 1

and 2 is now called α instead of α_1. The angles ψ, θ and α are the only constant parameters of the system. Variables are the joint angles φ_1 and φ_2. The altogether five quantities ψ, θ, α, φ_1^i and φ_2^i determine a position i of the terminal body, i.e., the transformation matrix $\underline{A}^i$ in the equation $\underline{\mathbf{e}}^2 = \underline{A}^i\,\underline{\mathbf{e}}^0$. Further below, $\underline{A}^i$ is expressed in terms of these five angles. Prescribed positions $1,\dots,m$, i.e., prescribed matrices $\underline{A}^i$ $(i = 1,\dots,m)$ are determined by $3+2m$ angles (three parameters ψ, θ, α and $2m$ joint angles φ_1^i, φ_2^i). On the other hand, a direction cosine matrix is uniquely determined by three quantities (Euler angles, for example). Hence m matrices are determined by $3m$ quantities. Thus, there are $3m$ equations for $3+2m$ unknowns. From the equality $3m = 3+2m$ it follows that at most three positions of the terminal body can be prescribed.

In what follows, $\underline{A}^i$ is expressed in terms of the angles ψ, θ, φ_1^i, α and φ_2^i of five consecutive rotations carried out in this order. In the position $\psi = \theta = \varphi_1^i = \alpha = \varphi_2^i = 0$ basis $\underline{\mathbf{e}}^2$ coincides with $\underline{\mathbf{e}}^0$. This position is referred to as initial position of $\underline{\mathbf{e}}^2$. The position after the fifth rotation is referred to as final position. Each rotation is carried out about an axis which is the result of all previous rotations. The position of $\underline{\mathbf{e}}^2$ after the kth rotation $(k = 1,2,3,4)$ is referred to as intermediate position $\underline{\mathbf{e}}^{(k)}$. As usual, a rotation is denoted by the unit vector along the axis and by the angle of rotation. The sequence of rotations and of positions of the body-fixed basis $\underline{\mathbf{e}}^2$ is as follows:

$$\left.\begin{array}{lll} & & \text{initial position} \quad \underline{\mathbf{e}}^0 \\ \text{1st rotation} & (\mathbf{e}_3^0\,,\psi) & \text{intermediate position} \quad \underline{\mathbf{e}}^{(1)} \\ \text{2nd rotation} & (\mathbf{e}_1^{(1)},\theta) & \text{intermediate position} \quad \underline{\mathbf{e}}^{(2)} \\ \text{3rd rotation} & (\mathbf{e}_2^{(2)},\varphi_1^i) & \text{intermediate position} \quad \underline{\mathbf{e}}^{(3)} \\ \text{4th rotation} & (\mathbf{e}_1^{(3)},\alpha) & \text{intermediate position} \quad \underline{\mathbf{e}}^{(4)} \\ \text{5th rotation} & (\mathbf{e}_2^{(4)},\varphi_2^i) & \text{final position} \quad \underline{\mathbf{e}}^2\,. \end{array}\right\} \tag{7.17}$$

In Fig. 7.3 all bases and angles are shown. The first two rotations position the axis of joint 1 in basis $\underline{\mathbf{e}}^0$. The axial unit vector $\mathbf{n}_1$ is $\mathbf{e}_2^{(2)}$. The fourth rotation has the effect that the joint axes $\mathbf{n}_1 = \mathbf{e}_2^{(2)}$ and $\mathbf{n}_2 = \mathbf{e}_2^{(4)}$ enclose the angle α. With self-explanatory abbreviations for the transformation matrices of the five individual rotations the prescribed matrix $\underline{A}^i$ $(i = 1,2,3)$ is the product

$$\underline{A}^i = \underline{A}_{\varphi_2^i}\underline{A}_\alpha\underline{A}_{\varphi_1^i}\underline{A}_\theta\underline{A}_\psi \qquad (i = 1,2,3)\,. \tag{7.18}$$

Hence

$$\underline{A}_{\varphi_2^i}\underline{A}_\alpha\underline{A}_{\varphi_1^i} = \underline{A}^i(\underline{A}_\theta\underline{A}_\psi)^T \qquad (i = 1,2,3)\,. \tag{7.19}$$

The following abbreviations are used:

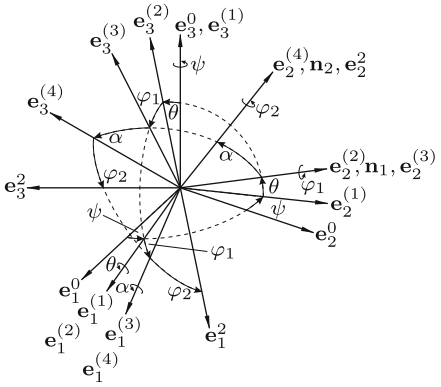

Fig. 7.3 Consecutive rotations defining the orientations of joint axes and of basis $\underline{\mathbf{e}}^2$ in basis $\underline{\mathbf{e}}^0$

$$\left.\begin{array}{llll} C_\psi = \cos\psi\,, & C_\theta = \cos\theta\,, & C_\alpha = \cos\alpha\,, & c_1^i = \cos\varphi_1^i\,, \quad c_2^i = \cos\varphi_2^i\,, \\ S_\psi = \sin\psi\,, & S_\theta = \sin\theta\,, & S_\alpha = \sin\alpha\,, & s_1^i = \sin\varphi_1^i\,, \quad s_2^i = \sin\varphi_2^i\,. \end{array}\right\} \tag{7.20}$$

With these abbreviations the matrices in (7.19) are

$$\underline{A}_{\varphi_2^i}\underline{A}_\alpha\underline{A}_{\varphi_1^i} = \begin{bmatrix} c_2^i & 0 & -s_2^i \\ 0 & 1 & 0 \\ s_2^i & 0 & c_2^i \end{bmatrix}\begin{bmatrix} 1 & 0 & 0 \\ 0 & C_\alpha & S_\alpha \\ 0 & -S_\alpha & C_\alpha \end{bmatrix}\begin{bmatrix} c_1^i & 0 & -s_1^i \\ 0 & 1 & 0 \\ s_1^i & 0 & c_1^i \end{bmatrix} \tag{7.21}$$

$$= \begin{bmatrix} c_1^i c_2^i - C_\alpha s_1^i s_2^i & S_\alpha s_2^i & -s_1^i c_2^i - C_\alpha c_1^i s_2^i \\ S_\alpha s_1^i & C_\alpha & S_\alpha c_1^i \\ c_1^i s_2^i + C_\alpha s_1^i c_2^i & -S_\alpha c_2^i & -s_1^i s_2^i + C_\alpha c_1^i c_2^i \end{bmatrix}, \tag{7.22}$$

$$\begin{aligned} \underline{A}^i(\underline{A}_\theta\underline{A}_\psi)^T &= \underline{A}^i\begin{bmatrix} C_\psi & -S_\psi & 0 \\ S_\psi & C_\psi & 0 \\ 0 & 0 & 1 \end{bmatrix}\begin{bmatrix} 1 & 0 & 0 \\ 0 & C_\theta & -S_\theta \\ 0 & S_\theta & C_\theta \end{bmatrix} \\ &= \underline{A}^i\begin{bmatrix} C_\psi & -S_\psi C_\theta & S_\psi S_\theta \\ S_\psi & C_\psi C_\theta & -C_\psi S_\theta \\ 0 & S_\theta & C_\theta \end{bmatrix}. \end{aligned} \tag{7.23}$$

The elements of the prescribed matrix $\underline{A}^i$ are denoted a_{jk}^i $(i,j,k = 1,2,3)$. Of the nine Eqs.(7.19) only the five equations for the elements with indices (2,2), (2,1), (2,3), (1,2) and (3,2) are used. In this order these equations read

$$C_\alpha = C_\theta(-a_{21}^i S_\psi + a_{22}^i C_\psi) + a_{23}^i S_\theta \qquad (i = 1,2,3)\,, \tag{7.24}$$

$$\left.\begin{aligned} S_\alpha s_1^i &= a_{21}^i C_\psi + a_{22}^i S_\psi \ , \\ S_\alpha c_1^i &= S_\theta(a_{21}^i S_\psi - a_{22}^i C_\psi) + a_{23}^i C_\theta \ , \\ S_\alpha s_2^i &= C_\theta(a_{12}^i C_\psi - a_{11}^i S_\psi) + a_{13}^i S_\theta \ , \\ -S_\alpha c_2^i &= C_\theta(a_{32}^i C_\psi - a_{31}^i S_\psi) + a_{33}^i S_\theta \end{aligned}\right\} (i = 1,2,3) \ . \tag{7.25}$$

Equations (7.24) determine ψ, θ, α. By subtracting the second equation from the first and the third equation from the second two expressions are obtained for $S_\theta / C_\theta = \tan\theta$:

$$\tan\theta = \frac{(a_{21}^1 - a_{21}^2)S_\psi - (a_{22}^1 - a_{22}^2)C_\psi}{a_{23}^1 - a_{23}^2} = \frac{(a_{21}^2 - a_{21}^3)S_\psi - (a_{22}^2 - a_{22}^3)C_\psi}{a_{23}^2 - a_{23}^3} \ . \tag{7.26}$$

This identity determines[1]

$$\tan\psi = \frac{S_\psi}{C_\psi} = \frac{(a_{22}^1 - a_{22}^2)(a_{23}^2 - a_{23}^3) - (a_{22}^2 - a_{22}^3)(a_{23}^1 - a_{23}^2)}{(a_{21}^1 - a_{21}^2)(a_{23}^2 - a_{23}^3) - (a_{21}^2 - a_{21}^3)(a_{23}^1 - a_{23}^2)} \ . \tag{7.27}$$

For arbitrarily prescribed[2] matrices $\underline{A}^1$, $\underline{A}^2$, $\underline{A}^3$ this equation has two real solutions ψ_1 and $\psi_1 + \pi$. The associated cosines and sines are C_{ψ_1}, S_{ψ_1} and $-C_{\psi_1}$, $-S_{\psi_1}$, respectively. With ψ_1 (7.26) determines two solutions θ_1 and $\theta_1 + \pi$. In the same way $\psi_1 + \pi$ determines two solutions $-\theta_1$ and $-\theta_1 + \pi$. The two pairs of solutions (ψ_1, θ_1) and $(\psi_1 + \pi, -\theta_1 + \pi)$ have to be considered as equal since they determine one and the same direction of $\mathbf{n}_1$. For the same reason the two pairs of solutions $(\psi_1, \theta_1 + \pi)$ and $(\psi_1 + \pi, -\theta_1)$ have to be considered as equal. Both of them determine the opposite direction $-\mathbf{n}_1$. In what follows, only the two pairs of solutions (ψ_1, θ_1) and $(\psi_1, \theta_1 + \pi)$ are distinguished. With the pair (ψ_1, θ_1) (7.24) determines C_α (identical for $i = 1,2,3$) and $S_\alpha = \pm\sqrt{1 - C_\alpha^2}$. This determines angles $\pm\alpha$. In the same way, the pair of solutions $(\psi_1, \theta_1 + \pi)$ determines the angles $\pm\alpha + \pi$. With each of the two triples $(\psi_1, \theta_1, \alpha)$ and $(\psi_1, \theta_1 + \pi, \alpha + \pi)$ Eqs.(7.25) determine c_1^i, s_1^i, c_2^i, s_2^i and, consequently, φ_1^i, φ_2^i $(i = 1,2,3)$. For a fixed value of i the quantities c_1^i, s_2^i, c_2^i associated with one triple are equal to those associated with the other triple, whereas the values s_1^i associated with the two triples are of opposite signs. From this it follows that the angles φ_2^i associated with the two triples are identical, whereas the angles φ_1^i associated with the two triples are of opposite sign. Since also the associated vectors $\mathbf{n}_1$ are of opposite sign, both triples represent one and the same solution. A second solution is obtained from the triple $(\psi_1, \theta_1, -\alpha)$. Both solutions are real for arbitrary prescribed positions of the terminal body.

Example: The prescribed direction cosine matrices are

---

[1] Results are invariant with respect to a change of labeling of the given matrices $\underline{A}^1$, $\underline{A}^2$, $\underline{A}^3$. One out of the three expressions for $\tan\psi$ may be $0/0$. Similarly, one out of the expressions for $\tan\theta$ may be $0/0$. If $\underline{A}^i$ is the unit matrix, then (7.24) reads $C_\alpha = C_\theta C_\psi$. This does not represent a critical case

[2] Eventually occurring degenerate cases are not investigated

$$\underline{A}^1 = \begin{bmatrix} \frac{2}{3} & \frac{1}{3} & \frac{2}{3} \\ \frac{1}{3} & \frac{2}{3} & \frac{-2}{3} \\ \frac{-2}{3} & \frac{2}{3} & \frac{1}{3} \end{bmatrix}, \quad \underline{A}^2 = \begin{bmatrix} \frac{2}{3} & \frac{1}{3} & \frac{-2}{3} \\ \frac{-11}{15} & \frac{2}{15} & \frac{-2}{3} \\ \frac{-2}{15} & \frac{14}{15} & \frac{1}{3} \end{bmatrix}, \quad \underline{A}^3 = \begin{bmatrix} \frac{-7}{9} & \frac{4}{9} & \frac{4}{9} \\ \frac{4}{9} & \frac{-1}{9} & \frac{8}{9} \\ \frac{4}{9} & \frac{8}{9} & \frac{-1}{9} \end{bmatrix}. \tag{7.28}$$

Equation (7.27) yields $\tan\psi = 1/2$, whence follow $C_\psi = 2/\sqrt{5}$ and $S_\psi = 1/\sqrt{5}$. The first expression in (7.26) is indeterminate : $0/0$. The second expression yields $\tan\theta = 3\sqrt{5}/14$, whence follow $C_\theta = 14/\sqrt{241}$ and $S_\theta = 3\sqrt{5/241}$. With ψ and θ (7.24) yields $C_\alpha = 4/\sqrt{1205}$ and $S_\alpha = \pm\sqrt{1189/1205}$. With the positive sign of S_α Eqs.(7.25) determine the sines and cosines of the variable angles φ_1 and φ_2 compiled in Table 7.1. End of example.

Table 7.1 Joint angles φ_1^i and φ_2^i associated with the matrices $\underline{A}^i$ $(i = 1, 2, 3)$

matrix $\underline{A}^i$	$s_1^i = \sin\varphi_1^i$	$c_1^i = \cos\varphi_1^i$	$s_2^i = \sin\varphi_2^i$	$c_2^i = \cos\varphi_2^i$
$\underline{A}^1$	$(4/3)\sqrt{241/1189}$	$-(37/3)\sqrt{5/1189}$	$10/\sqrt{1189}$	$-33/\sqrt{1189}$
$\underline{A}^2$	$-(4/3)\sqrt{241/1189}$	$-(37/3)\sqrt{5/1189}$	$-10/\sqrt{1189}$	$-33/\sqrt{1189}$
$\underline{A}^3$	$(7/9)\sqrt{241/1189}$	$(130/9)\sqrt{5/1189}$	$30/\sqrt{1189}$	$-17/\sqrt{1189}$

Skew Joint Axes

From the principle of transference it follows that the number of positions which can be prescribed for the terminal body of a chain with skew joint axes cannot be larger than for a chain with intersecting axes. Skew joint axes have a common perpendicular of length $\ell \neq 0$. This length ℓ and the angle α are the Denavit-Hartenberg parameters of body 1. The unit vector along the common perpendicular is called $\mathbf{a}$ (Fig 7.4). The origin 0_0 of $\underline{\mathbf{e}}^0$ is no longer located on the axis of joint 1 nor is the origin 0_2 of $\underline{\mathbf{e}}^2$ located on the axis of joint 2. The origins are defined by the vector $\mathbf{u}$ from 0_0 to the foot P_1 and by the vector $\mathbf{v}$ from the foot P_2 of the common perpendicular to 0_2. Furthermore, the bases $\underline{\mathbf{e}}^0$ and $\underline{\mathbf{e}}^2$ are fixed on their respective bodies such that they are aligned parallel in the position $\psi = \theta = \varphi_1 = \alpha = \varphi_2 = 0$. As before, the basis vector $\mathbf{e}_2^2$ is aligned parallel to the axis of joint 2, so that in position i the unit vector $\mathbf{a}$ has in $\underline{\mathbf{e}}^2$ the coordinate matrix $[\cos\varphi_2^i \;\; 0 \;\; \sin\varphi_2^i) = [c_2^i \;\; 0 \;\; s_2^i]^T$. A position i of the terminal body is prescribed by the direction cosine matrix $\underline{A}^i$ relating the bases $\underline{\mathbf{e}}^0$ and $\underline{\mathbf{e}}^2$ and by the coordinates of the vector $\mathbf{r}^i = \overrightarrow{0_0 0_2}$ in basis $\underline{\mathbf{e}}^0$. In three prescribed positions $i = 1, 2, 3$ the vector equations to be satisfied are

$$\mathbf{u} + \ell\,\mathbf{a} + \mathbf{v} = \mathbf{r}^i \qquad (i = 1, 2, 3)\,. \tag{7.29}$$

Define the column matrices $\underline{u}$ and $\underline{r}^i$ of the coordinates of $\mathbf{u}$ and $\mathbf{r}^i$, respectively, in $\underline{\mathbf{e}}^0$ and the column matrix $\underline{v}$ of the coordinates of $\mathbf{v}$ in $\underline{\mathbf{e}}^2$. With these coordinate matrices the decomposition of (7.29) in $\underline{\mathbf{e}}^0$ yields the equations

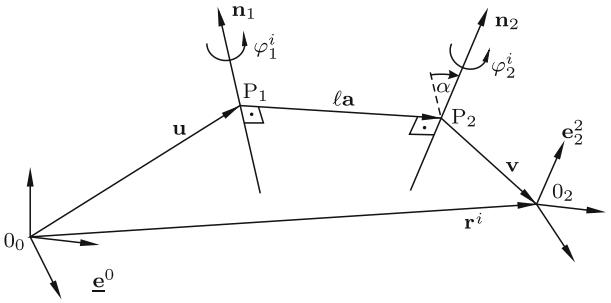

Fig. 7.4 Vectors $\mathbf{u}$, $\ell\,\mathbf{a}$, $\mathbf{v}$ and $\mathbf{r}^i$ locating the origin of basis $\underline{\mathbf{e}}^2$ in $\underline{\mathbf{e}}^0$

$$\underline{u} + \underline{A}^{iT}\left(\ell\begin{bmatrix} c_2^i \\ 0 \\ s_2^i \end{bmatrix} + \underline{v}\right) = \underline{r}^i \qquad (i = 1,2,3)\,. \tag{7.30}$$

This is a set of nine inhomogeneous linear equations for the seven unknown parameters represented by $\underline{u}$, ℓ and $\underline{v}$. The matrices $\underline{A}^i$ and $\underline{r}^i$ are prescribed, and so are c_2^i, s_2^i as solutions of (7.25). The equations do not have a solution $\underline{u}$, ℓ, $\underline{v}$. This means that Problem 1 with three prescribed positions does not have a solution. Further below the relaxed Problem 2 is investigated. Before doing so Eqs.(7.30) are derived in a different way in order to illustrate the principle of transference.

Proposition: Equations (7.30) represent the dual part of the dualized Eqs.(7.19) from which the unknown angles were obtained. Proof: Equations (7.19) are equivalent to (7.18): $\underline{A}^i = \underline{A}_{\varphi_2^i}\underline{A}_\alpha\underline{A}_{\varphi_1^i}\underline{A}_\theta\underline{A}_\psi$ $(i = 1,2,3)$. The dualization of this equation requires three operations.
Operation 1: The matrix $\underline{A}^i$ is replaced by (see the transpose in (3.61))

$$\hat{\underline{A}}^i = \underline{A}^i(\underline{I} - \varepsilon\,\tilde{\underline{r}}^i)\,, \qquad \tilde{\underline{r}}^i = \begin{bmatrix} 0 & -r_3^i & r_2^i \\ r_3^i & 0 & -r_1^i \\ -r_2^i & r_1^i & 0 \end{bmatrix}\,. \tag{7.31}$$

Operation 2: Of the five rotations on the right-hand side of the equation the rotation through the angle α is the only one which is replaced by a screw displacement. The dual screw angle is $\hat{\alpha} = \alpha + \varepsilon\ell$. This means that the matrix $\underline{A}_\alpha$ is replaced by a dual matrix $\hat{\underline{A}}_\alpha = \underline{A}_\alpha + \varepsilon\ell\underline{B}_\alpha$. For $\underline{A}_\alpha$ the expression in (7.21) is available. Dual differentiation yields

$$\underline{A}_\alpha + \varepsilon\ell\underline{B}_\alpha = \begin{bmatrix} 1 & 0 & 0 \\ 0 & C_\alpha & S_\alpha \\ 0 & -S_\alpha & C_\alpha \end{bmatrix} + \varepsilon\ell\begin{bmatrix} 0 & 0 & 0 \\ 0 & -S_\alpha & C_\alpha \\ 0 & -C_\alpha & -S_\alpha \end{bmatrix}\,. \tag{7.32}$$

Operation 3: The first rotation through the angle ψ is preceded by the translation $\mathbf{u}$, and the fifth rotation through the angle φ_2^i is followed by

the translation $\mathbf{v}$. The dual transformation matrices associated with these translations are $(\underline{I} - \varepsilon\,\underline{\tilde{u}})$ and $(\underline{I} - \varepsilon\,\underline{\tilde{v}})$, respectively (see (7.31)). The result of all three operations is the dualized form of (7.18):

$$\underline{A}^i(\underline{I} - \varepsilon\,\underline{\tilde{r}}^i) = (\underline{I} - \varepsilon\,\underline{\tilde{v}})\underline{A}_{\varphi_2^i}(\underline{A}_\alpha + \varepsilon\ell\underline{B}_\alpha)\underline{A}_{\varphi_1^i}\underline{A}_\theta\underline{A}_\psi(\underline{I} - \varepsilon\,\underline{\tilde{u}}) \tag{7.33}$$

$(i = 1, 2, 3)$. Multiplication from the right by the inverse of $\underline{A}_\theta\underline{A}_\psi(\underline{I} - \varepsilon\,\underline{\tilde{u}})$ yields

$$\underline{A}^i(\underline{I} - \varepsilon\,\underline{\tilde{r}}^i)(\underline{I} + \varepsilon\,\underline{\tilde{u}})(\underline{A}_\theta\underline{A}_\psi)^T = (\underline{I} - \varepsilon\,\underline{\tilde{v}})\underline{A}_{\varphi_2^i}(\underline{A}_\alpha + \varepsilon\ell\underline{B}_\alpha)\underline{A}_{\varphi_1^i} \tag{7.34}$$

$(i = 1, 2, 3)$. The primary parts of these equations are Eqs.(7.19). These equations determine the unknown angles ψ, θ, α and φ_1^i, φ_2^i $(i = 1, 2, 3)$. The dual parts of the equations read

$$\underline{A}^i\,(\underline{\tilde{u}} - \underline{\tilde{r}}^i)(\underline{A}_\theta\underline{A}_\psi)^T + \underline{\tilde{v}}\underline{A}_{\varphi_2^i}\underline{A}_\alpha\underline{A}_{\varphi_1^i} = \ell\underline{A}_{\varphi_2^i}\underline{B}_\alpha\underline{A}_{\varphi_1^i} \qquad (i = 1, 2, 3)\,. \tag{7.35}$$

Because of (7.19) this is identical with

$$[\underline{A}^i\,(\underline{\tilde{u}} - \underline{\tilde{r}}^i)\underline{A}^{i^T} + \underline{\tilde{v}}]\underline{A}_{\varphi_2^i}\underline{A}_\alpha\underline{A}_{\varphi_1^i} = \ell\underline{A}_{\varphi_2^i}\underline{B}_\alpha\underline{A}_{\varphi_1^i} \qquad (i = 1, 2, 3)\,. \tag{7.36}$$

Multiplication from the right by $(\underline{A}_{\varphi_2^i}\underline{A}_\alpha\underline{A}_{\varphi_1^i})^T$ yields

$$\underline{A}^i\,(\underline{\tilde{u}} - \underline{\tilde{r}}^i)\underline{A}^{i^T} + \underline{\tilde{v}} - \ell\underline{A}_{\varphi_2^i}\underline{B}_\alpha\underline{A}_\alpha^T\underline{A}_{\varphi_2^i}^T = \underline{0} \qquad (i = 1, 2, 3)\,. \tag{7.37}$$

With the matrices $\underline{A}_{\varphi_2^i}$ in (7.21) and $\underline{A}_\alpha$, $\underline{B}_\alpha$ in (7.32) this becomes

$$\underline{A}^i\,(\underline{\tilde{u}} - \underline{\tilde{r}}^i)\underline{A}^{i^T} + \underline{\tilde{v}} + \ell\begin{bmatrix} 0 & -s_2^i & 0 \\ s_2^i & 0 & -c_2^i \\ 0 & c_2^i & 0 \end{bmatrix} = \underline{0} \qquad (i = 1, 2, 3)\,. \tag{7.38}$$

The product $\underline{A}^i\,(\underline{\tilde{u}} - \underline{\tilde{r}}^i)\underline{A}^{i^T}$ expresses the similarity transformation of the tensor coordinates $(\underline{\tilde{u}} - \underline{\tilde{r}}^i)$ from basis $\underline{\mathbf{e}}^0$ into basis $\underline{\mathbf{e}}^2$ (see (1.25)). Hence the equations represent the skew-symmetric form of the equations $\underline{A}^i(\underline{u} - \underline{r}^i) + \underline{v} + \ell\,[c_2^i \;\; 0 \;\; s_2^i]^T = \underline{0}$ $(i = 1, 2, 3)$. These are Eqs.(7.30) premultiplied by $\underline{A}^i$. End of proof.

In what follows, the problem of three positions is stated in the relaxed form of Problem 2. Instead of prescribing three positions the displacement from position 1 to position 2 and the displacement from position 1 to position 3 are prescribed (and, thereby, the displacement from position 2 to position 3). Position 1 itself is not prescribed. It is part of the solution. In order to formulate the problem thus defined a second basis $\underline{\mathbf{e}}$ is rigidly attached to body 0. It has the same origin 0_0 basis $\underline{\mathbf{e}}^0$ has. The constant direction cosine matrix $\underline{A}$ in the equation $\underline{\mathbf{e}} = \underline{A}\,\underline{\mathbf{e}}^0$ is treated as unknown.

The three positions $\mathbf{r}^i$ $(i = 1, 2, 3)$ are prescribed in basis $\underline{\mathbf{e}}$. The matrices $\underline{r}^i$ $(i = 1, 2, 3)$ are now understood to be the prescribed coordinate matrices in basis $\underline{\mathbf{e}}$. This has the consequence that the coordinate matrices in $\underline{\mathbf{e}}^0$ are $\underline{A}^T\underline{r}^i$ instead of $\underline{r}^i$ $(i = 1, 2, 3)$. Hence Eqs.(7.30) are replaced by the equations

$$\underline{u} + \underline{A}^{iT}\left(\ell\begin{bmatrix} c_2^i \\ 0 \\ s_2^i \end{bmatrix} + \underline{v}\right) = \underline{A}^T\underline{r}^i \qquad (i = 1, 2, 3)\,. \tag{7.39}$$

The quantities on the left-hand side are defined as before. The matrix $\underline{A}$ introduces three new unknowns. Thus, there are nine equations for ten unknowns. The equations have, therefore, a one-parametric family of solutions.

The three unknowns in $\underline{u}$ are eliminated by formulating the differences

$$\left.\begin{aligned} (\underline{A}^1 - \underline{A}^2)^T\underline{v} + \left(\underline{A}^{1T}\begin{bmatrix} c_2^1 \\ 0 \\ s_2^1 \end{bmatrix} - \underline{A}^{2T}\begin{bmatrix} c_2^2 \\ 0 \\ s_2^2 \end{bmatrix}\right)\ell &= \underline{A}^T(\underline{r}^1 - \underline{r}^2)\,, \\ (\underline{A}^1 - \underline{A}^3)^T\underline{v} + \left(\underline{A}^{1T}\begin{bmatrix} c_2^1 \\ 0 \\ s_2^1 \end{bmatrix} - \underline{A}^{3T}\begin{bmatrix} c_2^3 \\ 0 \\ s_2^3 \end{bmatrix}\right)\ell &= \underline{A}^T(\underline{r}^1 - \underline{r}^3)\,. \end{aligned}\right\} \tag{7.40}$$

Four of these six equations are solved for the unknowns $\underline{v}$ and ℓ. Substitution of this solution into the remaining two equations results in two homogeneous linear equations for the elements of $\underline{A}$. Let $\underline{A}$ be expressed in terms of Euler-Rodrigues parameters q_0, q_1, q_2, q_3 in the form (1.79) and let, furthermore, q_0 be the independent parameter. Then the linear equations for the elements of $\underline{A}$ are second-order equations for q_1, q_2, q_3. They are supplemented by the equation $q_1^2 + q_2^2 + q_3^2 = 1 - q_0^2$. For a given value of q_0 the three second-order equations determine up to eight solutions (q_1, q_2, q_3) and associated matrices. Every solution $\underline{A}$ determines $\underline{v}$ and ℓ from (7.40), the coordinate matrices $\underline{A}^T\underline{r}^i$ in basis $\underline{\mathbf{e}}^0$ and $\underline{u}$ from (7.39).

Example: The prescribed direction cosine matrices are those in (7.28), and the prescribed coordinate matrices in basis $\underline{\mathbf{e}}$ are

$$\underline{r}^1 = \frac{\sqrt{2}}{2}\begin{bmatrix} 27 \\ 37\sqrt{2} \\ 29 \end{bmatrix}, \qquad \underline{r}^2 = \frac{\sqrt{2}}{6}\begin{bmatrix} 81 \\ 55\sqrt{2} \\ 71 \end{bmatrix}, \qquad \underline{r}^3 = \frac{\sqrt{2}}{18}\begin{bmatrix} 543 \\ 527\sqrt{2} \\ 169 \end{bmatrix}. \tag{7.41}$$

With these data and with data from Table 7.1 Eqs.(7.40) are

$$\begin{bmatrix} 0 & 16 & -8 & -120 \\ 0 & 8 & -4 & 240 \\ 20 & 0 & 0 & -560 \\ 13 & -1 & -10 & -497 \\ -1 & 7 & -2 & -211 \\ 2 & -14 & 4 & -70 \end{bmatrix}\begin{bmatrix} v_1 \\ v_2 \\ v_3 \\ \ell/\sqrt{1189} \end{bmatrix} = \begin{matrix} \underline{A}^T \\ \\ \underline{A}^T \end{matrix}\begin{bmatrix} 0 \\ 280 \\ 40\sqrt{2} \\ -150\sqrt{2} \\ -194 \\ 46\sqrt{2} \end{bmatrix}. \tag{7.42}$$

The (4×4)-submatrix of rows $1, 2, 3$ and 6 of the coefficient matrix has the inverse

$$\frac{1}{1800}\begin{bmatrix} -84 & 168 & 90 & 0 \\ -113 & -74 & 30 & -300 \\ -406 & -238 & 60 & -600 \\ -3 & 6 & 0 & 0 \end{bmatrix} .$$

With this inverse $[\, v_1 \; v_2 \; v_3 \; \ell/\sqrt{1189}\,]^T$ is expressed in terms of the elements a_{ij} of $\underline{A}$. Substitution into the remaining equations 4 and 5 results in the following homogeneous linear equations for the elements a_{ij}:

$$\left.\begin{array}{rrrr} (\,750\,a_{11} & & -2625\,a_{13}\,)\sqrt{2} \\ +4526\,a_{21} & +1288\,a_{22} & -2975\,a_{23} & \\ +(\,278\,a_{31} & +184\,a_{32} & +865\,a_{33}\,)\sqrt{2} = 0\,, \\ & (\,750\,a_{12} & +375\,a_{13}\,)\sqrt{2} & \\ +574\,a_{21} & -178\,a_{22} & +485\,a_{23} & \\ +(\,82\,a_{31} & -394\,a_{32} & -115\,a_{33}\,)\sqrt{2} = 0\,. \end{array}\right\} \tag{7.43}$$

These equations have the special solution

$$\underline{A} = \begin{bmatrix} \sqrt{2}/2 & 0 & \sqrt{2}/2 \\ 0 & 1 & 0 \\ -\sqrt{2}/2 & 0 & \sqrt{2}/2 \end{bmatrix} . \quad \text{It determines} \quad \begin{bmatrix} v_1 \\ v_2 \\ v_3 \\ \ell/\sqrt{1189} \end{bmatrix} = \begin{bmatrix} 30 \\ 9 \\ 8 \\ 1 \end{bmatrix} ,$$

$$\underline{A}^T\underline{r}^1 = \begin{bmatrix} -1 \\ 37 \\ 28 \end{bmatrix} , \quad \underline{A}^T\underline{r}^2 = \frac{1}{3}\begin{bmatrix} 5 \\ 55 \\ 76 \end{bmatrix} , \quad \underline{A}^T\underline{r}^3 = \frac{1}{9}\begin{bmatrix} 187 \\ 527 \\ 356 \end{bmatrix} , \quad \underline{u} = \begin{bmatrix} 10 \\ 20 \\ 30 \end{bmatrix} .$$

End of example.

7.3 Chains CC Leading the Terminal Body Through Prescribed Positions

This section is devoted to chains CC with skew joint axes. The problem to be solved is the same as in the previous section on chains RR. To be determined are the parameters of a chain (or of chains) leading the terminal body 2 through prescribed positions $i = 1, \ldots, m$. The positions are prescribed by
– the position vectors $\mathbf{r}_i$ $(i = 1, \ldots, m)$ of the origin of basis $\underline{\mathbf{e}}^2$ in basis $\underline{\mathbf{e}}^1$ and by
– the direction cosine matrices $\underline{A}^i$ $(i = 1, \ldots, m)$ defined by the equation $\underline{\mathbf{e}}^2 = \underline{A}^i\,\underline{\mathbf{e}}^0$.
To be determined are
– the Plücker vectors of joint axis 1 fixed in basis $\underline{\mathbf{e}}^0$
– the Plücker vectors of joint axis 2 fixed in basis $\underline{\mathbf{e}}^2$
– the Denavit-Hartenberg parameters of body 1.
What is the maximum number $m_{\max}$ of positions which can be prescribed?

These problems were solved by Roth [7]. The method of solution presented here is basically the same.

The Plücker vectors of joint axis 1 fixed in basis $\underline{\mathbf{e}}^0$ are denoted $\mathbf{n}$ (axial unit vector) and $\mathbf{w}$. The perpendicular from the origin of $\underline{\mathbf{e}}^0$ onto joint axis 1 is $\mathbf{n}\times\mathbf{w}$. The Plücker vectors of joint axis 2 fixed in basis $\underline{\mathbf{e}}^2$ are denoted $\mathbf{N}$ (axial unit vector) and $\mathbf{W}$. The perpendicular from the origin of $\underline{\mathbf{e}}^2$ onto joint axis 2 is $\mathbf{N}\times\mathbf{W}$. Since the coordinates of these vectors in $\underline{\mathbf{e}}^0$ depend on the position i of body 2, they are denoted $\mathbf{N}_i$ (axial unit vector) and $\mathbf{W}_i$. The perpendicular from the origin of $\underline{\mathbf{e}}^0$ onto joint axis 2 in position i is $\mathbf{N}_i \times (\mathbf{r}_i \times \mathbf{N}_i + \mathbf{W}_i)$. Let $\underline{N}_i$ be the coordinate matrix of $\mathbf{N}_i$ in $\underline{\mathbf{e}}^0$. Then

$$\underline{N}_i = \underline{A}^{i^T}\underline{A}^1\underline{N}_1 \qquad (i = 1,\ldots,m)\,. \tag{7.44}$$

Both joint axes are fixed on body 1. The Denavit-Hartenberg parameters α and ℓ of this body 1 are determined by the equations, independent of the position of body 2 (see (2.17)),

$$\cos\alpha \equiv \mathbf{n}\cdot\mathbf{N}_i \qquad (i = 1,\ldots,m)\,, \tag{7.45}$$

$$\ell\sin\alpha \equiv \mathbf{n}\cdot(\mathbf{r}_i\times\mathbf{N}_i + \mathbf{W}_i) + \mathbf{w}\cdot\mathbf{N}_i \qquad (i = 1,\ldots,m)\,. \tag{7.46}$$

The parameters α and ℓ are eliminated by subtracting the first equation from each of the remaining $m-1$ equations:

$$\mathbf{n}\cdot(\mathbf{N}_i - \mathbf{N}_1) = 0 \qquad (i = 2,\ldots,m)\,, \tag{7.47}$$

$$\mathbf{w}\cdot(\mathbf{N}_i - \mathbf{N}_1) = -\mathbf{n}\cdot(\mathbf{r}_i\times\mathbf{N}_i - \mathbf{r}_1\times\mathbf{N}_1 + \mathbf{W}_i - \mathbf{W}_1) \qquad (i = 2,\ldots,m)\,. \tag{7.48}$$

Three Prescribed Positions

Let joint axis 2 on body 2 be chosen arbitrarily. This means that the coordinates of $\mathbf{N}_i$ and $\mathbf{W}_i$ in $\underline{\mathbf{e}}^2$ (identical for $i = 1,2,3$) are chosen arbitrarily. The coordinates of $\mathbf{N}_i$ and $\mathbf{W}_i$ $(i = 1,2,3)$ in $\underline{\mathbf{e}}^0$ are determined by the prescribed matrices $\underline{A}^i$ $(i = 1,2,3)$. The two orthogonality conditions (7.47) determine the first Plücker vector of joint axis 1:

$$\begin{aligned}\mathbf{n} &= \frac{(\mathbf{N}_2 - \mathbf{N}_1)\times(\mathbf{N}_3 - \mathbf{N}_1)}{|(\mathbf{N}_2 - \mathbf{N}_1)\times(\mathbf{N}_3 - \mathbf{N}_1)|} \\ &= \frac{\mathbf{N}_1\times\mathbf{N}_2 + \mathbf{N}_2\times\mathbf{N}_3 + \mathbf{N}_3\times\mathbf{N}_1}{|\mathbf{N}_1\times\mathbf{N}_2 + \mathbf{N}_2\times\mathbf{N}_3 + \mathbf{N}_3\times\mathbf{N}_1|}\,.\end{aligned} \tag{7.49}$$

Since the second Plücker vector $\mathbf{w}$ is orthogonal to $\mathbf{n}$, the ansatz is made:

$$\mathbf{w} = A(\mathbf{N}_2 - \mathbf{N}_1) + B(\mathbf{N}_3 - \mathbf{N}_1)\,. \tag{7.50}$$

Substitution into (7.48) produces for A and B the scalar equations

$$\left.\begin{aligned}[A(\mathbf{N}_2-\mathbf{N}_1)+B(\mathbf{N}_3-\mathbf{N}_1)]\cdot(\mathbf{N}_2-\mathbf{N}_1)&=-\mathbf{n}\cdot(\mathbf{r}_2\times\mathbf{N}_2-\mathbf{r}_1\times\mathbf{N}_1+\mathbf{W}_2-\mathbf{W}_1)\,,\\ [A(\mathbf{N}_2-\mathbf{N}_1)+B(\mathbf{N}_3-\mathbf{N}_1)]\cdot(\mathbf{N}_3-\mathbf{N}_1)&=-\mathbf{n}\cdot(\mathbf{r}_3\times\mathbf{N}_3-\mathbf{r}_1\times\mathbf{N}_1+\mathbf{W}_3-\mathbf{W}_1)\,.\end{aligned}\right\} \tag{7.51}$$

The symmetrical coefficient matrix has the determinant

$$\begin{aligned}&(\mathbf{N}_2-\mathbf{N}_1)^2(\mathbf{N}_3-\mathbf{N}_1)^2-[(\mathbf{N}_2-\mathbf{N}_1)\cdot(\mathbf{N}_3-\mathbf{N}_1)]^2\\ &=[(\mathbf{N}_2-\mathbf{N}_1)\times(\mathbf{N}_3-\mathbf{N}_1)]^2\neq 0\,.\end{aligned} \tag{7.52}$$

With the solutions for A and B the vector $\mathbf{w}$ and also the perpendicular $\mathbf{n}\times\mathbf{w}$ from the origin of $\underline{\mathbf{e}}^0$ onto joint axis 1 is determined. Finally, (7.45) and (7.46) determine $\cos\alpha$ and $\ell\sin\alpha$. The formula for $\cos\alpha$ is

$$\cos\alpha=\frac{\mathbf{N}_1\times\mathbf{N}_2\cdot\mathbf{N}_3}{|\mathbf{N}_1\times\mathbf{N}_2+\mathbf{N}_2\times\mathbf{N}_3+\mathbf{N}_3\times\mathbf{N}_1|}\,. \tag{7.53}$$

These results are summarized as follows. If three positions of body 2 are arbitrarily prescribed, an arbitrary line on body 2 can be chosen as axis of joint 2. This axis determines uniquely the associated joint axis 1 fixed on body 0 and the Denavit-Hartenberg parameters of body 1. Because of the structural symmetry also the inverse is true: On body 0 an arbitrary line can be chosen as axis of joint 1. This line determines uniquely the associated joint axis 2 fixed on body 2 and the Denavit-Hartenberg parameters of body 1.

Four Prescribed Positions

The Plücker vector $\mathbf{n}$ must satisfy three orthogonality conditions (7.47) with vectors $(\mathbf{N}_2-\mathbf{N}_1)$, $(\mathbf{N}_3-\mathbf{N}_1)$ and $(\mathbf{N}_4-\mathbf{N}_1)$. This requires coplanarity of the three vectors:

$$(\mathbf{N}_2-\mathbf{N}_1)\cdot(\mathbf{N}_3-\mathbf{N}_1)\times(\mathbf{N}_4-\mathbf{N}_1)=0 \tag{7.54}$$

or, in terms of the coordinate matrices $\underline{N}_i$ $(i=1,2,3,4)$ in basis $\underline{\mathbf{e}}^0$,

$$\det\left[\underline{N}_2-\underline{N}_1\ ;\ \underline{N}_3-\underline{N}_1\ ;\ \underline{N}_4-\underline{N}_1\right]=0\,. \tag{7.55}$$

Because of (7.44) this equation becomes

$$\det\left[(\underline{A}^{2^T}\underline{A}^1-\underline{I})\underline{N}_1\ ;\ (\underline{A}^{3^T}\underline{A}^1-\underline{I})\underline{N}_1\ ;\ (\underline{A}^{4^T}\underline{A}^1-\underline{I})\underline{N}_1\right]=0\,. \tag{7.56}$$

This equation represents a third-order polynomial equation in terms of the coordinates of $\mathbf{N}_1$. All vectors $\mathbf{N}_1$ satisfying this equation define, if attached to the origin of $\underline{\mathbf{e}}^0$, a general cone called rotation cone. It is the cone known from Sect. 1.10. Every generator of the cone is an admissible first Plücker vector $\mathbf{N}_1$ of joint axis 2 in position 1 of the body.

Let the coordinates of $\mathbf{N}_1$ in $\underline{\mathbf{e}}^0$ be arbitrarily chosen admissible coordinates. The prescribed matrices $\underline{A}^i$ $(i=1,2,3,4)$ determine the coordinates

$\underline{A}^1\mathbf{N}_1$ in $\underline{\mathbf{e}}^2$ and the coordinates $\underline{N}_i = \underline{A}^{i\,T}\underline{A}^1\underline{N}_1$ of $\mathbf{N}_i$ $(i = 2,3,4)$ in $\underline{\mathbf{e}}^0$. The first Plücker vector $\mathbf{n}$ of joint axis 1 is determined from (7.49), and $\cos\alpha$ is determined from (7.53). The second Plücker vectors $\mathbf{w}$ and $\mathbf{W}_1$ are determined from the three Eqs.(7.48),

$$\mathbf{w}\cdot(\mathbf{N}_i - \mathbf{N}_1) = -\mathbf{n}\cdot(\mathbf{r}_i \times \mathbf{N}_i - \mathbf{r}_1 \times \mathbf{N}_1 + \mathbf{W}_i - \mathbf{W}_1) \qquad (i = 2,3,4) \quad (7.57)$$

in combination with the orthogonality relationship

$$\mathbf{w}\cdot\mathbf{n} = 0\,. \qquad (7.58)$$

The vectors are decomposed in basis $\underline{\mathbf{e}}^0$. Because of (7.44) the coordinates of $\mathbf{W}_i$ are linear functions of the coordinates of $\mathbf{W}_1$. Hence Eqs.(7.57), (7.58) represent four inhomogeneous linear equations for the coordinates of $\mathbf{w}$ with known coefficients and with right-hand side terms which are linear with respect to the coordinates of $\mathbf{W}_1$. For a solution to exist the (4×4) determinant of the complete coefficient matrix including the right-hand side terms must be zero. Because of the said properties of the matrix this equation has the form $aW_{11}+bW_{12}+cW_{13} = d$ with the coordinates W_{11}, W_{12}, W_{13} of $\mathbf{W}_1$ and with known constants a, b, c, d. The equation defines a plane E_1 in which $\mathbf{W}_1$ is located. Since $\mathbf{W}_1$ is also located in the plane E_2 normal to $\mathbf{N}_1$, the tip of $\mathbf{W}_1$ is an arbitrary point on the line of intersection of E_1 and E_2. This is expressed in the form $\mathbf{W}_1(\lambda) = \mathbf{W}_1(0) + \lambda\mathbf{e}$ (unit vector $\mathbf{e}$ having the direction of the line; perpendicular $\mathbf{W}_1(0)$ from the origin of $\underline{\mathbf{e}}^0$ onto the line; free parameter λ). For every vector $\mathbf{W}_1(\lambda)$ Eqs.(7.57) have a unique solution $\mathbf{w}(\lambda)$ satisfying also (7.58). Since this solution is linear with respect to λ, it has the form $\mathbf{w}(\lambda) = \mathbf{w}(0) + \lambda\mathbf{w}^*$ with uniquely determined vectors $\mathbf{w}(0)$ and $\mathbf{w}^*$. Equation (7.46) with $i = 1$, $\mathbf{w}(\lambda)$ and $\mathbf{W}_1(\lambda)$ determines the associated Denavit-Hartenberg parameter $\ell(\lambda)$.

The results are summarized as follows. The first Plücker vector $\mathbf{N}_1$ of joint axis 2 in position 1 is an arbitrarily chosen generator of the third-order rotation cone. This vector determines uniquely a one-parametric manifold of joint axes 2 with Plücker vectors $\mathbf{N}_1$ and $\mathbf{W}_1(\lambda)$ fixed on body 2 as well as a one-parametric manifold of joint axes 1 with Plücker vectors $\mathbf{n}$ and $\mathbf{w}(\lambda)$ fixed in $\underline{\mathbf{e}}^0$. The perpendiculars from the origin of $\underline{\mathbf{e}}^2$ onto the manifold of joint axes 2 are $\mathbf{N}_1 \times \mathbf{W}_1(\lambda)$, and the perpendiculars from the origin of $\underline{\mathbf{e}}^0$ onto the manifold of joint axes 1 are $\mathbf{n} \times \mathbf{w}(\lambda)$. From this it follows that the manifold of joint axes 2 is located in a plane fixed on body 2, and that the manifold of joint axes 1 is located in a plane fixed in $\underline{\mathbf{e}}^0$.

Five Prescribed Positions

In the case of five prescribed positions 1, 2, 3, 4, 5, positions 1, 2, 3, 4 define a rotation cone C_1, and positions 1, 2, 3, 5 define another rotation cone C_2. The first Plücker vector $\mathbf{N}_1$ of joint axis 2 in position 1 is generator of both cones. Two third-order cones having the same apex intersect in nine real or

complex straight lines. Three real lines mark the first Plücker vectors of the screw displacements leading from position 1 to position 2, from position 2 to position 3 and from position 3 to position 1, respectively. These are the eigenvectors associated with eigenvalue 1 of the prescribed matrices $\underline{A^1}^T \underline{A^2}$, $\underline{A^2}^T \underline{A^3}$ and $\underline{A^3}^T \underline{A^1}$, respectively. Since $\mathbf{N}_1$ cannot be any of these vectors, there remain either six or four or two or zero real lines representing solutions $\mathbf{N}_1$. Let $\mathbf{N}_1$ be one of these solutions. The associated vector $\mathbf{n}$ is uniquely determined from any two out of altogether four Eqs.(7.47). The associated second Plücker vectors $\mathbf{w}$ and $\mathbf{W}_1$ of joint axes 1 and 2 are determined as follows. Four positions 1, 2, 3 and 4 determine the plane E_1 described above in which $\mathbf{W}_1$ is located. By the same arguments the four positions 1, 2, 3 and 5 determine another plane E_1^* in which $\mathbf{W}_1$ is located, too. In addition, $\mathbf{W}_1$ is located in the plane E_2 normal to $\mathbf{N}_1$. Hence $\mathbf{W}_1$ is the point of intersection of E_1, E_1^* and E_2. Except for degenerate cases, this is a single point. The second Plücker vector $\mathbf{w}$ of joint axis 1 is determined by Eqs.(7.57) as before. Also this vector is uniquely determined if $\mathbf{W}_1$ is uniquely determined.

The four- and five-position theory just described is due to Roth [7]. It is the spatial generalization of Burmester's planar four- and five position theory which is the subject of Sects. 14.5 and 17.14.

References

1. Faugeras O, Giralt G (eds.) (1985) Proc. 3rd Int. Symp. Robotics Res. Cambridge MIT Press, Mass.
2. Fichter E F, Hunt K H (1975) The fecund torus, its bi-tangent circles and derived linkages, Mechanism Machine Theory 10:167–176
3. Huang C (1996) The cylindroid associated with motions of a Bennett mechanism. Proc. ASME Design Eng. Technical Conf.
4. Perez Gracia A, McCarthy J M (2002) Bennett's linkage and the cylindroid, Mechanism Machine Theory 37:1245–1260
5. Raghavan M, Roth B (1990) A general solution for the inverse kinematics of all series chains. Proc. 8th CISM-IFToMM Symp. on Robots and Manipulators:24–31
6. Roth B (1967) Finite position theory applied to mechanism synthesis: J.Appl.Mech. 34E:599–605
7. Roth B (1967) On the screw axes and other special lines associated with spatial displacements of a rigid body. J. Eng.f.Ind. 89B:102–110
8. Roth B (1968) The design of binary cranks with revolute, cylindric and prismatic joints. J. Mechanisms 3:61–72
9. Roth B (1985) Analytic design of open chains. In: [1] 281–288
10. Suh C H (1966) Synthesis and analysis of space mechanisms with use of displacement matrix. PhD thesis Berkeley
11. Suh C H (1969) On the duality in the existence of RR-links for three positions. Eng. f.Ind. 91:129–134
12. Tsai L W (1972) Design of open-loop chains for rigid-body guidance. PhD thesis Stanford

13. Tsai L W, Roth(1972) Design of dyads with helical, cylindrical, spherical, revolute and prismatic joints. Mechanism Machine Theory 7:85–102

Chapter 8
Stewart Platform

A Stewart platform (or Gough platform; Stewart [9]) is a rigid body which is connected to a supporting frame by six telescopic legs with spherical joints at both ends (Fig. 8.1). The spherical joints Q_i on the frame have position vectors $\mathbf{R}_i$ in a frame-fixed basis $\underline{\mathbf{e}}^1$, and the joints P_i on the platform have position vectors $\boldsymbol{\varrho}_i$ in a platform-fixed basis $\underline{\mathbf{e}}^2$ $(i = 1, \ldots, 6)$. Neither the six points on the platform nor those on the frame are coplanar or otherwise regularly arranged.

In a general position five legs of given constant lengths determine a linear complex (see Sect. 2.7.4) giving the platform a single degree of freedom, namely, instantaneously a screw motion about the axis of the actual linear complex. A sixth leg of constant length which is not a complex line of this linear complex connects the platform rigidly to the frame. With telescopic legs of variable lengths the degree of freedom of the platform is six. In addition, each leg has the degree of freedom of rotation about its longitudinal axis. This degree of freedom is without interest. In practice it is often suppressed by replacing one spherical joint per leg by a Hooke's joint.

Stewart platforms find applications whenever the six position variables of a body must be controllable both fast and with high accuracy. Examples are grippers of robots, carriers of vehicles in drive and flight simulators and of

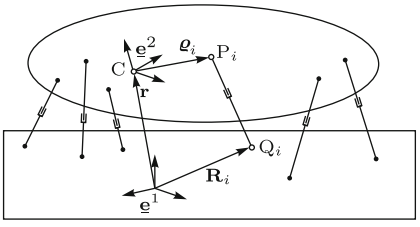

Fig. 8.1 Stewart-Gough-platform

J. Wittenburg, *Kinematics*, DOI 10.1007/978-3-662-48487-6_8

work pieces in tool machines. Stewart platforms are also found in the field of vibration control and in micro system technology. When operating a Stewart platform, positions must be avoided in which all six legs are lines of a single linear complex. In such positions the platform has at least one additional degree of freedom which cannot be controlled by actuators in the legs.

Inverse kinematics of the Stewart platform: The coordinates of the vectors $\mathbf{R}_i$ and $\boldsymbol{\varrho}_i$ $(i = 1, \ldots, 6)$ in the respective bases as well as the position of the platform, i.e., of basis $\underline{\mathbf{e}}^2$ in $\underline{\mathbf{e}}^1$ are given. To be determined are the six leg lengths ℓ_i $(i = 1, \ldots, 6)$. This is an elementary problem. The platform position determines the position of the points P_i $(i = 1, \ldots, 6)$ in $\underline{\mathbf{e}}^1$ and with them the leg lengths $\ell_i = |\overline{\mathrm{P}_i\mathrm{Q}_i}|$ $(i = 1, \ldots, 6)$.

8.1 Direct Kinematics of the General Stewart Platform

The problem of direct kinematics is considerably more difficult than inverse kinematics. It is stated as follows. Given the leg lengths ℓ_i, the vectors $\mathbf{R}_i$ in $\underline{\mathbf{e}}^1$ and the vectors $\boldsymbol{\varrho}_i$ in $\underline{\mathbf{e}}^2$ $(i = 1, \ldots, 6)$, determine all positions of $\underline{\mathbf{e}}^2$ in $\underline{\mathbf{e}}^1$. In what follows, it is assumed that the given parameters are such that the platform can assume only a finite number of positions in which the legs do not belong to a single linear complex.

Husty [2] was the first who succeeded in formulating scalar equations for the determination of all positions of a platform with arbitrarily prescribed parameters $\mathbf{R}_i$, $\boldsymbol{\varrho}_i$, ℓ_i $(i = 1, \ldots, 6)$. His coordinate formulation leads to expressions which can only be handled by an automatic formula manipulation program. The method presented here formulates the same equations in vector form. These equations are compact and simple (Wittenburg [11]).

The unknown position of $\underline{\mathbf{e}}^2$ in $\underline{\mathbf{e}}^1$ is represented as displacement from an initial position in which $\underline{\mathbf{e}}^2$ coincides with $\underline{\mathbf{e}}^1$. This displacement is described by its dual quaternion (see (3.98))

$$\hat{D} = (q_0, \mathbf{q}) + \varepsilon(q_0', \mathbf{q}') \,. \tag{8.1}$$

The unknown quantities q_0, $\mathbf{q}$, q_0' and $\mathbf{q}'$ satisfy (3.89) and (3.102)

$$q_0^2 + \mathbf{q}^2 = 1 \,, \tag{8.2}$$

$$q_0 q_0' + \mathbf{q} \cdot \mathbf{q}' = 0 \,. \tag{8.3}$$

The vector $\mathbf{r}_0 = \overrightarrow{0_1 0_2}$ joining the origins of the two bases and the square of this vector are (see (3.104) and (3.101))

$$\mathbf{r}_0 = 2(q_0\mathbf{q}' - q_0'\mathbf{q} + \mathbf{q} \times \mathbf{q}') \,, \tag{8.4}$$

$$\mathbf{r}_0^2 = 4({q_0'}^2 + \mathbf{q}'^2) \,. \tag{8.5}$$

In the initial position the platform-fixed point P_i has in $\underline{\mathbf{e}}^1$ the given position vector $\boldsymbol{\varrho}_i$. Let $\boldsymbol{\varrho}_i^*$ be its position vector in $\underline{\mathbf{e}}^1$ after the displacement. According to (3.105)

$$\boldsymbol{\varrho}_i^* = \underbrace{\boldsymbol{\varrho}_i + 2[\mathbf{q} \times (\mathbf{q} \times \boldsymbol{\varrho}_i) + q_0 \mathbf{q} \times \boldsymbol{\varrho}_i]}_{\mathbf{a}_i} + \underbrace{2(q_0 \mathbf{q}' - q_0' \mathbf{q} + \mathbf{q} \times \mathbf{q}')}_{\mathbf{r}_0} \tag{8.6}$$

$(i = 1, \ldots, 6)$. The vector $\mathbf{a}_i - \boldsymbol{\varrho}_i$ is the displacement caused by the rotation (note that $\mathbf{a}_i^2 = \boldsymbol{\varrho}_i^2$). As origin of basis $\underline{\mathbf{e}}^2$ point P_6 is chosen and as origin of $\underline{\mathbf{e}}^1$ point Q_6. The condition that the legs have prescribed lengths ℓ_i are

$$(\mathbf{R}_i - \boldsymbol{\varrho}_i^*)^2 - \ell_i^2 = 0 \qquad (i = 1, \ldots, 5) \tag{8.7}$$

and $\mathbf{r}_0^2 = \ell_6^2$. This sixth equation is, because of (8.5),

$$4({q_0'}^2 + \mathbf{q}'^2) = \ell_6^2 \,. \tag{8.8}$$

In (8.7) the term on the left-hand side is, with (8.6) and with $\mathbf{r}_0^2 = \ell_6^2$,

$$\begin{aligned} &(\mathbf{R}_i - \mathbf{a}_i - \mathbf{r}_0)^2 - \ell_i^2 \\ &= \mathbf{R}_i^2 + \ell_6^2 + \boldsymbol{\varrho}_i^2 - 2(\mathbf{R}_i - \mathbf{a}_i) \cdot \mathbf{r}_0 - 2\mathbf{R}_i \cdot (\mathbf{a}_i - \boldsymbol{\varrho}_i) - 2\mathbf{R}_i \cdot \boldsymbol{\varrho}_i - \ell_i^2 \\ &= -2(\mathbf{R}_i - \mathbf{a}_i) \cdot \mathbf{r}_0 - 4\mathbf{R}_i \cdot [\mathbf{q} \times (\mathbf{q} \times \boldsymbol{\varrho}_i) + q_0 \mathbf{q} \times \boldsymbol{\varrho}_i] \\ &\quad + (\mathbf{R}_i - \boldsymbol{\varrho}_i)^2 + \ell_6^2 - \ell_i^2 \,. \end{aligned} \tag{8.9}$$

The second term in this expression is transformed as follows:

$$\mathbf{R}_i \cdot [\mathbf{q} \times (\mathbf{q} \times \boldsymbol{\varrho}_i) + q_0 \mathbf{q} \times \boldsymbol{\varrho}_i] = (q_0 \mathbf{R}_i - \mathbf{q} \times \mathbf{R}_i) \cdot (\mathbf{q} \times \boldsymbol{\varrho}_i) \,. \tag{8.10}$$

In the first term of (8.9) the expressions from (8.6) for $\mathbf{a}_i$ and $\mathbf{r}_0$ are used. This yields

$$\begin{aligned} &(\mathbf{R}_i - \mathbf{a}_i) \cdot \mathbf{r}_0 = 2\mathbf{R}_i \cdot (q_0 \mathbf{q}' - q_0' \mathbf{q} + \mathbf{q} \times \mathbf{q}') - 2\boldsymbol{\varrho}_i \cdot (q_0 \mathbf{q}' - q_0' \mathbf{q} - \mathbf{q} \times \mathbf{q}') \\ &-4\Big\{ \boldsymbol{\varrho}_i \cdot \mathbf{q} \times \mathbf{q}' + [\mathbf{q} \times (\mathbf{q} \times \boldsymbol{\varrho}_i) + q_0 \mathbf{q} \times \boldsymbol{\varrho}_i] \cdot (q_0 \mathbf{q}' - q_0' \mathbf{q} + \mathbf{q} \times \mathbf{q}') \Big\} \,. \end{aligned} \tag{8.11}$$

The expression in curled brackets equals zero (note (8.2) and the product rule $(\mathbf{q} \times \boldsymbol{\varrho}_i) \cdot (\mathbf{q} \times \mathbf{q}') = \mathbf{q}^2(\mathbf{q}' \cdot \boldsymbol{\varrho}_i) - (\mathbf{q} \cdot \mathbf{q}')(\mathbf{q} \cdot \boldsymbol{\varrho}_i)$). Hence (8.8) takes the form

$$\begin{aligned} &\mathbf{q} \cdot (\mathbf{R}_i - \boldsymbol{\varrho}_i) q_0' + [\mathbf{q} \times (\mathbf{R}_i + \boldsymbol{\varrho}_i) - q_0 (\mathbf{R}_i - \boldsymbol{\varrho}_i)] \cdot \mathbf{q}' \\ &+ (\mathbf{q} \times \mathbf{R}_i - q_0 \mathbf{R}_i) \cdot (\mathbf{q} \times \boldsymbol{\varrho}_i) + \frac{1}{4}[(\mathbf{R}_i - \boldsymbol{\varrho}_i)^2 + \ell_6^2 - \ell_i^2] = 0 \end{aligned} \tag{8.12}$$

$(i = 1, \ldots, 5)$ and with the abbreviations

$$\mathbf{r}_i = \mathbf{R}_i - \boldsymbol{\varrho}_i \,, \qquad \mathbf{p}_i = \mathbf{R}_i + \boldsymbol{\varrho}_i \qquad (i = 1, \ldots, 5) \tag{8.13}$$

the form

$$\mathbf{q}\cdot\mathbf{r}_i q_0' + (\mathbf{q}\times\mathbf{p}_i - q_0\mathbf{r}_i)\cdot\mathbf{q}'$$
$$+(\mathbf{q}\times\mathbf{R}_i - q_0\mathbf{R}_i)\cdot(\mathbf{q}\times\boldsymbol{\varrho}_i) + \frac{1}{4}(\mathbf{r}_i^2 + \ell_6^2 - \ell_i^2) = 0 \quad (i = 1,\ldots,5)\ . \tag{8.14}$$

These five equations[1] together with (8.2), (8.3) and (8.8) determine the eight unknowns $q_{0,1,2,3}$ and $q'_{0,1,2,3}$. Before reducing them to a smaller set of equations a statement is made about the number of solutions.

Proposition: The maximum number of (real or complex) solutions is eighty. If $(q_{0,1,2,3},\, q'_{0,1,2,3})$ is a solution, also $(-q_{0,1,2,3},\, -q'_{0,1,2,3})$ is. Since these two solutions determine one and the same platform position, the maximum number of different platform positions is forty.

Proof by Wampler [10]: Define

$\underline{z}^T = [q_0\ q_1\ q_2\ q_3]$ and $\underline{z}'^T = (2/\ell_6)[q'_0\ q'_1\ q'_2\ q'_3]$. Then (8.2) and (8.3) read:

$$\underline{z}^T\underline{z} = 1\ , \qquad \underline{z}^T\underline{z}' = 0\ . \tag{8.15}$$

In (8.8) ℓ_6^2 is multiplied by $(q_0^2 + \mathbf{q}^2)$. The equation then reads

$$\frac{4}{\ell_6^2}(q_0'^2 + \mathbf{q}'^2) - (q_0^2 + \mathbf{q}^2) = 0\ . \tag{8.16}$$

This is the equation

$$\underline{z}'^T\underline{z}' - \underline{z}^T\underline{z} = 0\ . \tag{8.17}$$

Also in (8.14) the constant $(\mathbf{r}_i^2+\ell_6^2-\ell_i^2)$ is multiplied by $(q_0^2+\mathbf{q}^2)$. Following this the terms in the second row represent a quadratic form in $q_{0,1,2,3}$. It has the form $\underline{z}^T\underline{A}_i\underline{z}$ with a symmetric matrix $\underline{A}_i$. The terms in the first row are bilinear and, consequently, of the form $2\underline{z}^T\underline{B}_i\underline{z}'$. It is seen that $\underline{B}_i$ is skewsymmetric. Equations (8.14) now read

$$\underline{z}^T\underline{A}_i\underline{z} + 2\underline{z}^T\underline{B}_i\underline{z}' = 0 \qquad (i = 1,\ldots,5\,;\ \underline{A}_i^T = \underline{A}_i\ ,\ \underline{B}_i^T = -\underline{B}_i\,)\ . \tag{8.18}$$

Wampler investigates the more general equations

$$\underline{z}^T\underline{A}_i\underline{z} + 2\underline{z}^T\underline{B}_i\underline{z}' - \lambda^2\underline{z}'^T\underline{A}_i\underline{z}' = 0 \qquad (i = 1,\ldots,5\,;\ \underline{A}_i^T = \underline{A}_i\ ,\ \underline{B}_i^T = -\underline{B}_i\,) \tag{8.19}$$

in which λ is a real parameter. With new variables $\underline{x} = \underline{z} + \lambda\underline{z}'$ and $\underline{y} = \underline{z} - \lambda\underline{z}'$ the products $\underline{x}^T\underline{x}$, $\underline{y}^T\underline{y}$, $\underline{x}^T\underline{y}$ and $\underline{x}^T(\underline{A}_i - \underline{B}_i/\lambda)\underline{y}$ are formed. Using (8.15) and (8.17) as well as the symmetry of $\underline{A}_i$ and the skewsymmetry of $\underline{B}_i$ the resulting expressions are

---

[1] (8.14) can also be written in the form
$(2q_0' + \mathbf{q}\cdot\mathbf{r}_i)^2 + (2\mathbf{q}' + \mathbf{q}\times\mathbf{p}_i - q_0\mathbf{r}_i)^2 = \ell_i^2 \quad (i = 1,\ldots,5)$.
Proof: Substitute $\mathbf{p}_i = 2\mathbf{R}_i - \mathbf{r}_i$ and $\boldsymbol{\varrho}_i = \mathbf{R}_i - \mathbf{r}_i$ and use $4(q'^2_0 + \mathbf{q}'^2) = \mathbf{r}_0^2 = \ell_6^2$ and $(\mathbf{q}\cdot\mathbf{r}_i)^2 + (\mathbf{q}\times\mathbf{r}_i)^2 + q_0^2\mathbf{r}_i^2 = (\mathbf{q}^2 + q_0^2)\mathbf{r}_i^2 = \mathbf{r}_i^2$

$$\underline{x}^T\underline{x} = 1 + \lambda^2 \,, \qquad \underline{y}^T\underline{y} = 1 + \lambda^2 \,, \tag{8.20}$$

$$\underline{x}^T\underline{y} = 1 - \lambda^2 \,, \tag{8.21}$$

$$\underline{x}^T(\underline{A}_i - \frac{1}{\lambda}\underline{B}_i)\underline{y} = \underline{z}^T\underline{A}_i\underline{z} + 2\underline{z}^T\underline{B}_i\underline{z}' - \lambda^2\underline{z}'^T\underline{A}_i\underline{z}' \,. \tag{8.22}$$

According to (8.19) the expression on the right-hand side is zero. Hence

$$\underline{x}^T(\underline{A}_i - \frac{1}{\lambda}\underline{B}_i)\underline{y} = 0 \qquad (i = 1, \ldots, 5) \,. \tag{8.23}$$

The eight original equations have now been replaced by the eight new Eqs.(8.20), (8.21) and (8.23). The left-hand side expressions in both Eqs.(8.20) are homogeneous quadratic forms, and those in the altogether six Eqs.(8.21) and (8.23) are bilinear forms. About the number of solutions of such special equations a simple statement is made by Bezout's theory (see Morgan/Sommese [8]). The maximum number of solutions equals the coefficient of the term $\alpha^4\beta^4$ in the expression $(\alpha + \beta)^6(2\alpha)(2\beta)$. This coefficient is eighty. This number eighty is valid also in the case $\lambda = 0$, although (8.23) does not allow setting $\lambda = 0$. Because of the implicit function theorem every nonsingular solution in the case $\lambda = 0$ is associated with a nonsingular solution in an open set $\lambda \neq 0$. Since the maximum number of solutions is eighty in the open set, it is eighty also in the case $\lambda = 0$. This ends the proof. The proof does not answer the question whether this maximum number can actually occur. This problem was settled by Dietmaier [1]. He determined parameter values for which Husty's equations yield forty different real platform positions.

Reduction of the Equations

In what follows, the original Eqs.(8.2), (8.3), (8.8) and (8.14) for the unknowns $q_0\,, \mathbf{q}\,, q_0'$ and $\mathbf{q}'$ are considered. In several steps these equations are reduced to a system of three equations for three unknowns. Equations (8.14) and (8.3) together represent a system of linear equations for q_0' and $\mathbf{q}'$. This system is written in the form

$$c_i q_0' + \mathbf{v}_i \cdot \mathbf{q}' = b_i \qquad (i = 1, \ldots, 6) \tag{8.24}$$

with coefficients $\mathbf{v}_i\,,\ c_i\,,\ b_i$ depending on q_0 and $\mathbf{q}$:

$$\left.\begin{aligned} &\mathbf{v}_i = \mathbf{q} \times \mathbf{p}_i - q_0\mathbf{r}_i \,, \qquad c_i = \mathbf{q} \cdot \mathbf{r}_i = -\frac{1}{q_0}\mathbf{q} \cdot \mathbf{v}_i \,, \\ &b_i \;= (q_0\mathbf{R}_i - \mathbf{q} \times \mathbf{R}_i) \cdot (\mathbf{q} \times \boldsymbol{\varrho}_i) - \frac{1}{4}(\mathbf{r}_i^2 + \ell_6^2 - \ell_i^2) \end{aligned}\right\} (i = 1, \ldots, 5) \,, \tag{8.25}$$

$$c_6 = q_0 \,, \qquad \mathbf{v}_6 = \mathbf{q} \,, \qquad b_6 = 0 \,. \tag{8.26}$$

The coefficients of the sixth equation are orthogonal not only to the unknown solution $q_0', \mathbf{q}'$, but also to the coefficients of the remaining five equations:

$$c_6 c_i + \mathbf{v}_6 \cdot \mathbf{v}_i = 0 \qquad (i = 1, \ldots, 5) \; . \tag{8.27}$$

Solutions q_0' and $\mathbf{q}'$ exist if the system of equations has rank four. By assumption, this is the case. One of the four equations used must be the sixth equation because the coefficients of the other five equations belong to the three-dimensional complement of the coefficients of the sixth equation. Let it be assumed that the equations 1, 2, 3, 6 have rank four. First, the quantity q_0' is determined. It is the quotient

$$q_0' = \frac{\Delta_0}{\Delta_{1236}} \tag{8.28}$$

of the determinants[2]

$$\Delta_0 = \begin{vmatrix} b_1 & \mathbf{v}_1 \\ b_2 & \mathbf{v}_2 \\ b_3 & \mathbf{v}_3 \\ 0 & \mathbf{q} \end{vmatrix} = \mathbf{q} \cdot \sum_{i=1}^{3} b_i \mathbf{v}_j \times \mathbf{v}_k \; , \tag{8.29}$$

$$\begin{aligned} \Delta_{1236} &= -\frac{1}{q_0} \begin{vmatrix} \mathbf{q} \cdot \mathbf{v}_1 & \mathbf{v}_1 \\ \mathbf{q} \cdot \mathbf{v}_2 & \mathbf{v}_2 \\ \mathbf{q} \cdot \mathbf{v}_3 & \mathbf{v}_3 \\ -q_0^2 & \mathbf{q} \end{vmatrix} \\ &= -\frac{1}{q_0} \Big[\sum_{i=1}^{3} (\mathbf{q} \cdot \mathbf{v}_i)(\mathbf{q} \cdot \mathbf{v}_j \times \mathbf{v}_k) + q_0^2 \mathbf{v}_1 \cdot \mathbf{v}_2 \times \mathbf{v}_3 \Big] \end{aligned} \tag{8.30}$$

(here and in other sums further below $i, j, k = 1, 2, 3$ cyclic). The identity[3]

$$\sum_{i=1}^{3} (\mathbf{q} \cdot \mathbf{v}_i) \mathbf{v}_j \times \mathbf{v}_k = \mathbf{q} (\mathbf{v}_1 \cdot \mathbf{v}_2 \times \mathbf{v}_3) \tag{8.31}$$

in combination with $q_0^2 + \mathbf{q}^2 = 1$ yields

$$\Delta_{1236} = -\frac{1}{q_0} \, \mathbf{v}_1 \cdot \mathbf{v}_2 \times \mathbf{v}_3 \; . \tag{8.32}$$

With the first Eq.(8.25)

[2] The notation is unconventional. Instead of the vectors $\mathbf{v}_1, \mathbf{v}_2, \mathbf{v}_3$ and $\mathbf{q}$ the matrix contains the row matrices of the coordinates of these vectors. The corresponding (3×3) determinants are the vector products shown in (8.29) and (8.30)

[3] Verified by scalar multiplications with $\mathbf{v}_1$, $\mathbf{v}_2$, $\mathbf{v}_3$

$$\mathbf{v}_j \times \mathbf{v}_k = q_0^2 \mathbf{r}_j \times \mathbf{r}_k + q_0[(\mathbf{q}\cdot\mathbf{r}_j)\mathbf{p}_k - (\mathbf{q}\cdot\mathbf{r}_k)\mathbf{p}_j] + \mathbf{q}\,[\mathbf{q}\cdot\mathbf{p}_j \times \mathbf{p}_k + q_0(\mathbf{r}_k\cdot\mathbf{p}_j - \mathbf{r}_j\cdot\mathbf{p}_k)]\ . \tag{8.33}$$

The product $\mathbf{v}_1\cdot\mathbf{v}_2\times\mathbf{v}_3$ allows factoring out q_0. Division by $-q_0$ yields

$$\Delta_{1236} = q_0^2 \mathbf{r}_1\cdot\mathbf{r}_2\times\mathbf{r}_3 + \sum_{i=1}^{3}(\mathbf{q}\cdot\mathbf{r}_i)[\mathbf{q}\cdot\mathbf{p}_j\times\mathbf{p}_k + q_0(\mathbf{r}_k\cdot\mathbf{p}_j - \mathbf{r}_j\cdot\mathbf{p}_k)]\ . \tag{8.34}$$

The result for q_0' is written in the form

$$q_0' = \frac{\mathbf{q}\cdot\mathbf{s}}{\Delta_{1236}} \tag{8.35}$$

with the abbreviation

$$\mathbf{s} = \sum_{i=1}^{3} b_i \mathbf{v}_j \times \mathbf{v}_k\ . \tag{8.36}$$

The product $\mathbf{q}\cdot\mathbf{s}$ is of fifth degree in q_0, q_1, q_2, q_3, and Δ_{1236} is of second degree.

The vector $\mathbf{q}'$ is determined from the equations 1, 2, 3 of the system (8.24):

$$\mathbf{v}_i\cdot\mathbf{q}' = \frac{q_0'}{q_0}\,\mathbf{q}\cdot\mathbf{v}_i + b_i \qquad (i=1,2,3)\ . \tag{8.37}$$

The solution is

$$\mathbf{q}' = \frac{\displaystyle\sum_{i=1}^{3}\Big(\frac{q_0'}{q_0}\mathbf{q}\cdot\mathbf{v}_i + b_i\Big)\mathbf{v}_j\times\mathbf{v}_k}{\mathbf{v}_1\cdot\mathbf{v}_2\times\mathbf{v}_3} \tag{8.38}$$

or, with (8.35), (8.31) and (8.32),

$$\mathbf{q}' = \frac{\mathbf{q}\mathbf{q}\cdot\mathbf{s} - \mathbf{s}}{q_0\Delta_{1236}}\ . \tag{8.39}$$

The quantities q_0' and $\mathbf{q}'$ are now known as functions of q_0 and $\mathbf{q}$. In the next step q_0 and $\mathbf{q}$ are determined. For this purpose (8.8), the fourth and the fifth Eq.(8.24) and (8.2) are available. Equation (8.8) is

$$\ell_6^2 = 4({q_0'}^2 + {\mathbf{q}'}^2) = 4\,\frac{q_0^2(\mathbf{q}\cdot\mathbf{s})^2 + (\mathbf{q}\mathbf{q}\cdot\mathbf{s} - \mathbf{s})^2}{q_0^2\Delta_{1236}^2} = 4\,\frac{\mathbf{s}^2 - (\mathbf{q}\cdot\mathbf{s})^2}{q_0^2\Delta_{1236}^2}$$
$$= 4\,\frac{q_0^2\mathbf{s}^2 + (\mathbf{q}\times\mathbf{s})^2}{q_0^2\Delta_{1236}^2} \tag{8.40}$$

or

$$\mathbf{s}^2 + \left(\frac{\mathbf{q}\times\mathbf{s}}{q_0}\right)^2 = \frac{1}{4}\ell_6^2\Delta_{1236}^2 \tag{8.41}$$

and with (8.33) and (8.36)

$$\mathbf{s}^2+\left\{\mathbf{q}\times\sum_{i=1}^{3}b_i\Big[q_0\mathbf{r}_j\times\mathbf{r}_k+(\mathbf{q}\cdot\mathbf{r}_j)\mathbf{p}_k-(\mathbf{q}\cdot\mathbf{r}_k)\mathbf{p}_j\Big]\right\}^2=\frac{1}{4}\ell_6^2\Delta_{1236}^2\,. \quad (8.42)$$

This equation is of 8th order in the coordinates of $\mathbf{q}$.

With $c_\ell=-\mathbf{q}\cdot\mathbf{v}_\ell/q_0$ the fourth and the fifth Eq.(8.24) read $-\mathbf{v}_\ell\cdot\mathbf{s}/q_0=b_\ell\Delta_{1236}$ $(\ell=4,5)$ or with (8.36)

$$-\sum_{i=1}^{3}b_i\frac{\mathbf{v}_\ell\cdot\mathbf{v}_j\times\mathbf{v}_k}{q_0}=b_\ell\Delta_{1236}\qquad(\ell=4,5)\,. \quad (8.43)$$

Equation (8.32) shows that this can be written in the form

$$\sum_{i=1}^{3}b_i\Delta_{\ell jk6}=b_\ell\Delta_{1236}\quad(\ell=4,5) \quad (8.44)$$

$(i,j,k=1,2,3$ cyclic). The quantity $\Delta_{\ell jk6}$ is given in (8.34) with indices ℓ,j,k instead of $1,2,3$. It represents the coefficient determinant of the equations $\ell,j,k,6$ in the system (8.24). Equations (8.44) are of fourth order in the unknowns q_0, $\mathbf{q}$. Equations (8.35), (8.39), (8.42) and (8.44) are Husty's equations.

The equation $q_0^2+\mathbf{q}^2=1$ is used for expressing even and odd powers of q_0 in the forms $q_0^{2m}=(1-\mathbf{q}^2)^m$ and $q_0^{2m+1}=q_0(1-\mathbf{q}^2)^m$ for $m\geq 1$. With these substitutions the three Eqs.(8.42) and (8.44) have the forms $A_iq_0+B_i=0$ $(i=1,2,3)$ with coefficients A_i, B_i depending on $\mathbf{q}$ only. Substitution of $q_0=-B_3/A_3$ into the other equations results in three equations for q_1, q_2, q_3 only. These equations are

$$\left.\begin{array}{rl} A_1B_3-A_3B_1=0 & [1,3,5,7]\,,\\ A_2B_3-A_3B_2=0 & [1,3,5,7,9,11]\,,\\ (\mathbf{q}^2-1)A_3^2-B_3^2=0 & [0,2,4,6,8]\,. \end{array}\right\} \quad (8.45)$$

The numbers shown in brackets indicate the order of terms in q_1, q_2, q_3 occurring in the equations. In the first equation, for example, only terms of the orders 1, 3, 5 and 7 occur.

8.2 Triangle-Configuration of the Stewart Platform

The maximum number of platform positions is smaller than forty if the attachment points of the legs $i=1,\ldots,6$ on the platform and on the frame are in some way regularly arranged. A very special arrangement is shown

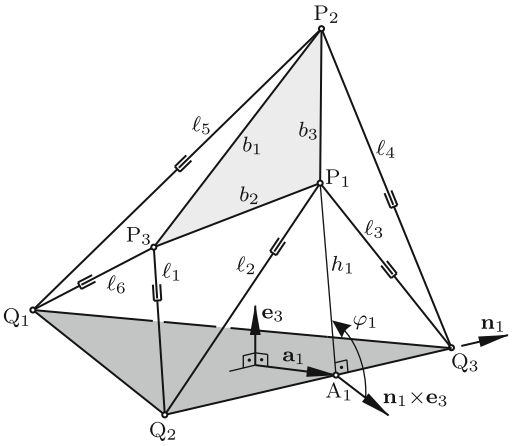

Fig. 8.2 Platform with frame triangle (Q_1,Q_2,Q_3) and platform triangle (P_1,P_2,P_3)

in Fig. 8.2. In a triangle (P_1,P_2,P_3) fixed on the platform and in another triangle (Q_1,Q_2,Q_3) fixed on the frame each corner is the attachment point of two legs. The problem of direct kinematics is to find for given forms of the triangles (P_1,P_2,P_3) and (Q_1,Q_2,Q_3) and for given leg lengths $\ell_1, \ldots, \ell_6$ all possible positions of the platform. The following method of solution is due to Merlet [4, 6, 5].

A frame-fixed reference basis is defined as follows. Its origin is an arbitrary point in the plane of the triangle (Q_1,Q_2,Q_3), and its basis vector $\mathbf{e}_3$ is normal to this plane. Furthermore, let $\mathbf{n}_i$ be the unit vector pointing from Q_j to Q_k $(i, j, k = 1, 2, 3$ cyclic). In the figure only the vector $\mathbf{n}_1$ pointing from Q_2 to Q_3 is shown. When the leg lengths are given, the triangle (Q_2,Q_3,P_1) is given, too, and so is the altitude h_1 and the foot A_1 of the perpendicular dropped from P_1 onto the line $\overline{Q_2Q_3}$. Let $\mathbf{a}_1$ be the position vector of A_1 in the reference basis and let, furthermore, φ_1 be the angle through which the altitude of length h_1 is rotated against the direction of $\mathbf{n}_1 \times \mathbf{e}_3$. Then P_1 has the position vector

$$\mathbf{r}_1 = \mathbf{a}_1 + h_1(\mathbf{n}_1 \times \mathbf{e}_3 \cos\varphi_1 + \mathbf{e}_3 \sin\varphi_1) \,. \tag{8.46}$$

In this expression the angle φ_1 is the only unknown.

What has been explained for the triangle (Q_2,Q_3,P_1) is valid, with cyclic permutation of indices, also for the triangles (Q_3,Q_1,P_2) and (Q_1,Q_2,P_3). For each of them there is an equation of the form (8.46). With the abbreviations $c_i = \cos\varphi_i$ and $s_i = \sin\varphi_i$ $(i = 1, 2, 3)$ the three equations have the forms

$$\mathbf{r}_i = \mathbf{a}_i + h_i(\mathbf{n}_i \times \mathbf{e}_3 c_i + \mathbf{e}_3 s_i) \qquad (i = 1, 2, 3) \,. \tag{8.47}$$

In Fig. 8.2 the side lengths b_1, b_2, b_3 of the platform-fixed triangle (P_1,P_2,P_3) are shown. The rigidity of the triangle requires that $b_i^2 = (\mathbf{r}_j - \mathbf{r}_k)^2$ ($i, j, k = 1, 2, 3$ cyclic). Since the vectors $\mathbf{a}_i$ and $\mathbf{n}_i$ ($i = 1, 2, 3$) are orthogonal to $\mathbf{e}_3$, these three equations have the special forms

$$\left.\begin{aligned} D_1 s_2 s_3 + E_1 c_2 c_3 + F_1 c_2 + G_1 c_3 + H_1 = 0\,, \\ D_2 s_3 s_1 + E_2 c_3 c_1 + F_2 c_3 + G_2 c_1 + H_2 = 0\,, \\ D_3 s_1 s_2 + E_3 c_1 c_2 + F_3 c_1 + G_3 c_2 + H_3 = 0 \end{aligned}\right\} \tag{8.48}$$

with constant coefficients

$$\left.\begin{aligned} D_i &= 2h_j h_k\,, \\ E_i &= 2h_j h_k \mathbf{n}_j \cdot \mathbf{n}_k\,, \\ F_i &= -2h_j \mathbf{e}_3 \cdot \mathbf{n}_j \times (\mathbf{a}_j - \mathbf{a}_k)\,, \\ G_i &= 2h_k \mathbf{e}_3 \cdot \mathbf{n}_k \times (\mathbf{a}_j - \mathbf{a}_k)\,, \\ H_i &= b_i^2 - h_j^2 - h_k^2 - (\mathbf{a}_j - \mathbf{a}_k)^2 \end{aligned}\right\} \quad (i, j, k = 1, 2, 3 \text{ cyclic})\,. \tag{8.49}$$

From these equations it is seen that if $(\varphi_1, \varphi_2, \varphi_3)$ is a solution, then also $(-\varphi_1, -\varphi_2, -\varphi_3)$ is a solution. The second solution is the reflection of the first in the plane of the frame triangle.

The third Eq.(8.48) yields

$$s_1 s_2 = -\frac{1}{D_3}(E_3 c_1 c_2 + F_3 c_1 + G_3 c_2 + H_3) \tag{8.50}$$

and after squaring

$$D_3^2 (1 - c_1^2)(1 - c_2^2) = (E_3 c_1 c_2 + F_3 c_1 + G_3 c_2 + H_3)^2\,. \tag{8.51}$$

This is a quadratic equation for c_2 with coefficients which are functions of c_1. The first two Eqs.(8.48) are resolved for s_3 and c_3. With this solution the equation $s_3^2 + c_3^2 = 1$ is formed. This is the equation

$$\begin{aligned} &[(F_1 c_2 + H_1)(E_2 c_1 + F_2) - (G_2 c_1 + H_2)(E_1 c_2 + G_1)]^2 \\ &+ [D_1 s_2 (G_2 c_1 + H_2) - D_2 s_1 (F_1 c_2 + H_1)]^2 \\ &= [D_1 s_2 (E_2 c_1 + F_2) - D_2 s_1 (E_1 c_2 + G_1)]^2\,. \end{aligned} \tag{8.52}$$

The quantities s_1 and s_2 appear only in the forms s_1^2, s_2^2 and $s_1 s_2$. The expressions s_1^2 and s_2^2 are replaced by $1 - c_1^2$ and by $1 - c_2^2$, respectively, and $s_1 s_2$ is replaced by the expression in (8.50). The resulting equation is another quadratic equation for c_2 with coefficients which are functions of c_1. With abbreviations for the said coefficients the equations are written in the forms

$$K_i c_2^2 + L_i c_2 + M_i = 0 \qquad (i = 1, 2)\,. \tag{8.53}$$

Compatibility requires that

$$\begin{vmatrix} K_1L_2 - K_2L_1 & K_1M_2 - K_2M_1 \\ K_1M_2 - K_2M_1 & L_1M_2 - L_2M_1 \end{vmatrix} = 0 \,. \tag{8.54}$$

This is an 8th-order polynomial for $c_1 = \cos\varphi_1$. Its solutions determine eight (not necessarily real) pairs of angles φ_1 and $-\varphi_1$. Merlet [4] gave a numerical example with eight different real solutions c_1 thus showing that a polynomial of degree smaller than eight cannot be found. For every solution φ_1 the two Eqs.(8.53) determine c_2 uniquely, and (8.50) determines s_2. Hence φ_2 is uniquely determined. The solutions s_3 and c_3 of the first two Eqs.(8.48) determine the angle φ_3.

References

1. Dietmaier P (1998) The Stewart-Gough platform of general geometry can have 40 real postures. In: [3]:7–16
2. Husty M L (1996) An algorithm for solving the direct kinematics of Stewart-Gough-type platforms. Mechanism Machine Theory 31:365–379 (first published in: Res.Rept. TR-CIM-94-7, Univ.McGill,1994)
3. Lenarčič J, Husty M L (eds.) (1998) Advances in robot kinematics: Analysis and control, Kluwer, Dordrecht
4. Merlet J-P (1989) Manipulateur parallèles, 4ème partie: Mode d'assemblage et cinématique directe sous forme polynomiale. Res.Rep.1135, INRIA. See also Res.Reps.646, 791, 1003, 1645, 1921, 1940
5. Merlet J-P (1990) Les robots parallèles. Hermès, Paris
6. Merlet J-P (1992) Direct kinematics and assembly modes of parallel manipulaters, Int.J.Robotics Res. 11:150–162
7. Merlet J-P (1990) Les robots parallèles. Hermès, Paris
8. Morgan A, Sommese A (1987) A homotopy for solving general polynomial systems that respects m-homogeneous structures, Appl.Math.Comp.24:101–113
9. Stewart D (1965) A platform with six degrees of freedom. Proc.Institution of Mech.Engs., London 180, Part 1:371–386
10. Wampler C W (1996) Forward displacement analysis of general six-in-parallel SPS (Stewart) platform manipulators using soma coordinates. Mechanism Machine Theory 31:331–337
11. Wittenburg J (2005) Direct kinematics of the general Stewart platform. presented at Tsinghua Univ. Beijing. (2009) Proc. Scient. Conf. BulTrans, Sozopol

Chapter 9
Angular Velocity. Angular Acceleration

This is the first chapter devoted not to position theory, but to continuous motion. The essential kinematical quantities are velocity, acceleration, angular velocity and angular acceleration.

9.1 Definitions. Basic Equations

In Fig. 9.1 an arbitrarily moving reference basis $\underline{\mathbf{e}}^1$ with origin 0 is shown. Relative to $\underline{\mathbf{e}}^1$ a body is moving. The body is represented by the basis $\underline{\mathbf{e}}^2$ rigidly attached to it. The origin A of this basis is an arbitrarily chosen point of the body. Relative to $\underline{\mathbf{e}}^2$ a point Q is moving. The position vectors of Q in the two bases are denoted $\mathbf{r}$ and $\boldsymbol{\varrho}$, respectively. The figure shows the relationship

$$\mathbf{r} = \mathbf{r}_A + \boldsymbol{\varrho} \,. \tag{9.1}$$

In general, the velocities of Q relative to the two bases are different, and also the accelerations of Q relative to the two bases are different. The velocity and the acceleration relative to $\underline{\mathbf{e}}^1$ are denoted $\mathbf{v}$ and $\mathbf{a}$, respectively. They are the first and the second time derivative, respectively, of $\mathbf{r}$ in $\underline{\mathbf{e}}^1$. The

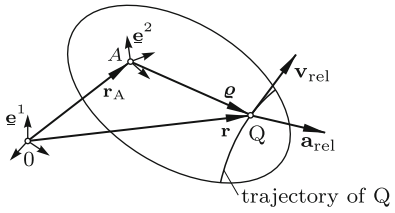

Fig. 9.1 Reference basis $\underline{\mathbf{e}}^1$, body-fixed basis $\underline{\mathbf{e}}^2$ and point Q in motion relative to $\underline{\mathbf{e}}^2$

J. Wittenburg, *Kinematics*, DOI 10.1007/978-3-662-48487-6_9

velocity and the acceleration of Q relative to $\underline{\mathbf{e}}^2$ are denoted $\mathbf{v}_{\rm rel}$ and $\mathbf{a}_{\rm rel}$, respectively. They are the first and the second time derivative, respectively, of $\boldsymbol{\varrho}$ in $\underline{\mathbf{e}}^2$. In what follows, the basis in which a vector is differentiated is denoted by an upper index set in parentheses. With this notation the said velocities and accelerations are

$$\mathbf{v} = \frac{{}^{(1)}\mathrm{d}\mathbf{r}}{\mathrm{d}t}\,, \qquad \mathbf{v}_{\rm rel} = \frac{{}^{(2)}\mathrm{d}\boldsymbol{\varrho}}{\mathrm{d}t}\,, \qquad \mathbf{a} = \frac{{}^{(1)}\mathrm{d}^2\mathbf{r}}{\mathrm{d}t^2}\,, \qquad \mathbf{a}_{\rm rel} = \frac{{}^{(2)}\mathrm{d}^2\boldsymbol{\varrho}}{\mathrm{d}t^2}\,. \quad (9.2)$$

In contrast to vectors scalar quantities have identical time derivatives in different bases. These derivatives are denoted by dots as usual. The goal of the present section is to express $\mathbf{v}$ and $\mathbf{a}$ in terms of $\boldsymbol{\varrho}$, $\mathbf{v}_{\rm rel}$ and $\mathbf{a}_{\rm rel}$ and of quantities describing the motion of $\underline{\mathbf{e}}^2$ relative to $\underline{\mathbf{e}}^1$.

The relationship between time derivatives of a vector in two bases $\underline{\mathbf{e}}^1$ and $\underline{\mathbf{e}}^2$ is met frequently and not only with position vectors. For this reason it is formulated first for a vector $\mathbf{p}$ of arbitrary physical nature. Let p_i $(i = 1, 2, 3)$ be the coordinates of $\mathbf{p}$ in $\underline{\mathbf{e}}^2$. Then

$$\begin{aligned}\frac{{}^{(1)}\mathrm{d}\mathbf{p}}{\mathrm{d}t} &= \frac{{}^{(1)}\mathrm{d}}{\mathrm{d}t}\sum_{i=1}^{3} p_i\,\mathbf{e}_i^2 = \sum_{i=1}^{3}\dot{p}_i\,\mathbf{e}_i^2 \;+\; \sum_{i=1}^{3} p_i\,\frac{{}^{(1)}\mathrm{d}}{\mathrm{d}t}\,\mathbf{e}_i^2 \\ &= \frac{{}^{(2)}\mathrm{d}\mathbf{p}}{\mathrm{d}t} \;+\; \sum_{i=1}^{3} p_i\,\frac{{}^{(1)}\mathrm{d}}{\mathrm{d}t}\,\mathbf{e}_i^2\,. \end{aligned} \quad (9.3)$$

The derivative of $\mathbf{e}_i^2$ is a vector. Let a_{ij} $(j = 1, 2, 3)$ be its unknown coordinates in $\underline{\mathbf{e}}^2$:

$$\frac{{}^{(1)}\mathrm{d}}{\mathrm{d}t}\,\mathbf{e}_i^2 = \sum_{j=1}^{3} a_{ij}\,\mathbf{e}_j^2 \qquad (i = 1, 2, 3)\,. \quad (9.4)$$

The basis vectors satisfy the orthonormality conditions $\mathbf{e}_i^2 \cdot \mathbf{e}_k^2 = \delta_{ik}$ $(i, k = 1, 2, 3)$. Differentiation of this equation in $\underline{\mathbf{e}}^1$ yields

$$\Big(\frac{{}^{(1)}\mathrm{d}}{\mathrm{d}t}\,\mathbf{e}_i^2\Big)\cdot\mathbf{e}_k^2 \;+\; \mathbf{e}_i^2\cdot\Big(\frac{{}^{(1)}\mathrm{d}}{\mathrm{d}t}\,\mathbf{e}_k^2\Big) = 0 \qquad (i, k = 1, 2, 3)\,. \quad (9.5)$$

The derivatives in parentheses are expressed by means of (9.4):

$$\Big(\sum_{j=1}^{3} a_{ij}\,\mathbf{e}_j^2\Big)\cdot\mathbf{e}_k^2 \;+\; \mathbf{e}_i^2\cdot\Big(\sum_{j=1}^{3} a_{kj}\,\mathbf{e}_j^2\Big) = 0 \qquad (i, k = 1, 2, 3)\,. \quad (9.6)$$

Because of the orthonormality conditions this reduces to $a_{ik} + a_{ki} = 0$ $(i, k = 1, 2, 3)$. Hence $a_{11} = a_{22} = a_{33} = 0$. Instead of nine unknowns a_{ij} there are only three. These are given the new names $a_{ij} = -a_{ji} = \omega_k$ $(i, j, k = 1, 2, 3$ cyclic). In these terms (9.4) gets the form

$$\frac{^{(1)}\mathrm{d}}{\mathrm{d}t}\,\mathbf{e}_i^2 = -\omega_j\,\mathbf{e}_k^2 + \omega_k\,\mathbf{e}_j^2 \qquad (i,j,k = 1,2,3 \text{ cyclic})\,. \tag{9.7}$$

The three quantities ω_i $(i = 1,2,3)$ are interpreted as coordinates of a vector $\boldsymbol{\omega}_{21}$ in $\underline{\mathbf{e}}^2$. Then

$$\frac{^{(1)}\mathrm{d}}{\mathrm{d}t}\,\mathbf{e}_i^2 = \boldsymbol{\omega}_{21} \times \mathbf{e}_i^2 \qquad (i = 1,2,3)\,. \tag{9.8}$$

The vector $\boldsymbol{\omega}_{21}$ is called *angular velocity* of the body, i.e., of basis $\underline{\mathbf{e}}^2$, relative to $\underline{\mathbf{e}}^1$. In (9.3) – (9.8) the origin A of $\underline{\mathbf{e}}^2$ does not play any role. Hence the angular velocity is independent of A. In figures the angular velocity vector may be attached to any point of the body. It is not wrong, but sometimes misleading to talk about the angular velocity *about* A. This is particularly true when the body has a fixed point different from A.

With (9.8) Eq.(9.3) gets the form

$$\frac{^{(1)}\mathrm{d}\mathbf{p}}{\mathrm{d}t} = \frac{^{(2)}\mathrm{d}\mathbf{p}}{\mathrm{d}t} + \boldsymbol{\omega}_{21}\times\mathbf{p} \quad (\boldsymbol{\omega}_{21} = \text{ angular velocity of } \underline{\mathbf{e}}^2 \text{ relative to } \underline{\mathbf{e}}^1)\,. \tag{9.9}$$

This is the desired relationship between the time derivatives of an arbitrary vector $\mathbf{p}$ in two different bases. Application to $\boldsymbol{\omega}_{21}$ itself shows that the time derivatives in both bases are identical. Therefore, the simpler notation is used:

$$\frac{^{(1)}\mathrm{d}\boldsymbol{\omega}_{21}}{\mathrm{d}t} = \frac{^{(2)}\mathrm{d}\boldsymbol{\omega}_{21}}{\mathrm{d}t} = \dot{\boldsymbol{\omega}}_{21}\,. \tag{9.10}$$

This vector is called *angular acceleration* of the body relative to $\underline{\mathbf{e}}^1$.

After these preparations the desired expressions for velocities and accelerations can be formulated. Starting point is (9.1): $\mathbf{r} = \mathbf{r}_\mathrm{A} + \boldsymbol{\varrho}$. The equation is differentiated twice with respect to time in $\underline{\mathbf{e}}^1$. The derivatives of $\mathbf{r}_\mathrm{A}$ are the velocity and the acceleration of the body-fixed point A relative to $\underline{\mathbf{e}}^1$. They are denoted $\mathbf{v}_\mathrm{A}$ and $\mathbf{a}_\mathrm{A}$, respectively. For differentiating $\boldsymbol{\varrho}$ (9.9) is used. Instead of $\boldsymbol{\omega}_{21}$ simply $\boldsymbol{\omega}$ is written. With the notation (9.2) the velocity is

$$\mathbf{v} = \mathbf{v}_\mathrm{A} + \boldsymbol{\omega} \times \boldsymbol{\varrho} + \mathbf{v}_\mathrm{rel}\,. \tag{9.11}$$

The acceleration $\mathbf{a}$ is found by differentiating one more time in $\underline{\mathbf{e}}^1$. In doing so (9.9) is applied to the second and to the third vector. Each of these vectors contributes the term $\boldsymbol{\omega} \times \mathbf{v}_\mathrm{rel}$. The resulting expression is

$$\mathbf{a} = \mathbf{a}_\mathrm{A} + \dot{\boldsymbol{\omega}} \times \boldsymbol{\varrho} + \boldsymbol{\omega} \times (\boldsymbol{\omega} \times \boldsymbol{\varrho}) + 2\boldsymbol{\omega} \times \mathbf{v}_\mathrm{rel} + \mathbf{a}_\mathrm{rel}\,. \tag{9.12}$$

In the special case $\mathbf{v}_\mathrm{rel} = \mathbf{0}$, $\mathbf{a}_\mathrm{rel} = \mathbf{0}$ (9.11) and (9.12) express the velocity and the acceleration, respectively, of the body-fixed point Q defined by the position vector $\boldsymbol{\varrho}$:

$$\mathbf{v} = \mathbf{v}_\mathrm{A} + \boldsymbol{\omega} \times \boldsymbol{\varrho} \,, \tag{9.13}$$

$$\mathbf{a} = \mathbf{a}_\mathrm{A} + \dot{\boldsymbol{\omega}} \times \boldsymbol{\varrho} + \boldsymbol{\omega} \times (\boldsymbol{\omega} \times \boldsymbol{\varrho}) \,. \tag{9.14}$$

Since these formulas are valid for all points Q of the body, they describe the velocity distribution and the acceleration distribution in the rigid body. These distributions are the subject of Sects. 9.3 and 9.8.

In (9.11) and (9.12) the rigid-body terms are called *transport velocity* $\mathbf{v}_\mathrm{t}$ and *transport acceleration* $\mathbf{a}_\mathrm{t}$ of Q. With this notation the velocity of Q is $\mathbf{v} = \mathbf{v}_\mathrm{t} + \mathbf{v}_\mathrm{rel}$, and the acceleration is $\mathbf{a} = \mathbf{a}_\mathrm{t} + 2\boldsymbol{\omega} \times \mathbf{v}_\mathrm{rel} + \mathbf{a}_\mathrm{rel}$. The term $2\boldsymbol{\omega} \times \mathbf{v}_\mathrm{rel}$ is called *Coriolis acceleration*.

In what follows, the second time derivative of $\boldsymbol{\omega}$ and the third time derivative of $\mathbf{r}$, the so-called *jerk* $\mathbf{j}$, are formulated. Also these derivatives are understood as derivatives in basis $\underline{\mathbf{e}}^1$. They are found by repeated applications of (9.9). The upper index $^{(1)}$ is omitted. The results are

$$\frac{\mathrm{d}^2\boldsymbol{\omega}}{\mathrm{d}t^2} = \boldsymbol{\gamma} + \boldsymbol{\omega} \times \dot{\boldsymbol{\omega}} \,, \tag{9.15}$$

$$\begin{aligned}
\mathbf{j} &= \frac{\mathrm{d}^3\mathbf{r}}{\mathrm{d}t^3} \\
&= \mathbf{j}_\mathrm{A} + (\boldsymbol{\gamma} + \boldsymbol{\omega} \times \dot{\boldsymbol{\omega}}) \times \boldsymbol{\varrho} + 2\dot{\boldsymbol{\omega}} \times (\boldsymbol{\omega} \times \boldsymbol{\varrho}) + \boldsymbol{\omega} \times [\dot{\boldsymbol{\omega}} \times \boldsymbol{\varrho} + \boldsymbol{\omega} \times (\boldsymbol{\omega} \times \boldsymbol{\varrho})] \\
&= \mathbf{j}_\mathrm{A} + (\boldsymbol{\gamma} - \boldsymbol{\omega}^2\boldsymbol{\omega}) \times \boldsymbol{\varrho} - 3(\dot{\boldsymbol{\omega}} \cdot \boldsymbol{\omega})\boldsymbol{\varrho} + 2(\boldsymbol{\omega} \cdot \boldsymbol{\varrho})\dot{\boldsymbol{\omega}} + (\dot{\boldsymbol{\omega}} \cdot \boldsymbol{\varrho})\boldsymbol{\omega} \,.
\end{aligned} \tag{9.16}$$

Here, $\boldsymbol{\gamma}$ is the derivative of $\dot{\boldsymbol{\omega}}$ in $\underline{\mathbf{e}}^2$, and $\mathbf{j}_\mathrm{A}$ is the jerk of the body-fixed point A relative to $\underline{\mathbf{e}}^1$.

9.2 Inverse Motion

The motion of basis $\underline{\mathbf{e}}^1$ relative to $\underline{\mathbf{e}}^2$ is called the *inverse* of the motion of $\underline{\mathbf{e}}^2$ relative to $\underline{\mathbf{e}}^1$. Let $\boldsymbol{\omega}_\mathrm{rel}$ and $\dot{\boldsymbol{\omega}}_\mathrm{rel}$ be the angular velocity and the angular acceleration, respectively, of $\underline{\mathbf{e}}^1$ relative to $\underline{\mathbf{e}}^2$. These quantities are determined as follows. Equation (9.9) is solved for the right-hand side time derivative of $\mathbf{p}$. This is achieved by interchanging the indices 1 and 2. The result is $\boldsymbol{\omega}_{12} = -\boldsymbol{\omega}_{21}$. By definition, $\boldsymbol{\omega}_{12}$ is the desired angular velocity $\boldsymbol{\omega}_\mathrm{rel}$. This yields the first equation below. The second equation follows by the argument used for (9.10) (again $\boldsymbol{\omega}$ is written instead of $\boldsymbol{\omega}_{21}$):

$$\boldsymbol{\omega}_\mathrm{rel} = -\boldsymbol{\omega} \,, \qquad \dot{\boldsymbol{\omega}}_\mathrm{rel} = -\dot{\boldsymbol{\omega}} \,. \tag{9.17}$$

Next, (9.11) is applied twice, once to an arbitrary point A fixed in $\underline{\mathbf{e}}^2$ and once to the point fixed in $\underline{\mathbf{e}}^1$ instantaneously coinciding with A. In the first case, the equation is $\mathbf{v} = \mathbf{v}_\mathrm{A}$. In the second case, $\mathbf{v} = \mathbf{0}$, and $\mathbf{v}_\mathrm{rel}$ is the desired velocity of the inverse motion. Hence in this case, $\mathbf{0} = \mathbf{v}_\mathrm{A} + \mathbf{v}_\mathrm{rel}$.

Combination of both equations yields

$$\mathbf{v}_{\mathrm{rel}} = -\mathbf{v} \,. \tag{9.18}$$

In the same way an expression for $\mathbf{a}_{\mathrm{rel}}$ is obtained from (9.12). The two applications yield the equations $\mathbf{a} = \mathbf{a}_{\mathrm{A}}$ and $\mathbf{0} = \mathbf{a}_{\mathrm{A}} + 2\boldsymbol{\omega} \times \mathbf{v}_{\mathrm{rel}} + \mathbf{a}_{\mathrm{rel}}$. Combination with (9.18) yields

$$\mathbf{a}_{\mathrm{rel}} = -\mathbf{a} + 2\boldsymbol{\omega} \times \mathbf{v} \,. \tag{9.19}$$

Again, the quantities on the left-hand side belong to the inverse motion and the ones on the right-hand side to the motion. Equations (9.17) – (9.19) are summarized in

Theorem 9.1. *The switch from motion to inverse motion has the consequence that angular velocity, angular acceleration and velocities of arbitrary points are multiplied by* (-1)*. For accelerations this rule is valid only for points satisfying the condition* $\boldsymbol{\omega} \times \mathbf{v} = \mathbf{0}$ *. These points define the instantaneous screw axis.*

9.3 Instantaneous Screw Axis. Pitch. Velocity Screw. Linear Complex of Velocity

Equations (9.1) and (9.13) describe the instantaneous velocity distribution in a rigid body at an arbitrary fixed time t . The body point at the position vector

$$\mathbf{r} = \mathbf{r}_{\mathrm{A}} + \boldsymbol{\varrho} \tag{9.20}$$

with arbitrary $\boldsymbol{\varrho}$ has the velocity

$$\mathbf{v} = \mathbf{v}_{\mathrm{A}} + \boldsymbol{\omega} \times \boldsymbol{\varrho} \,. \tag{9.21}$$

The equation is in accordance with the rigid-body property that the velocities $\mathbf{v}_1$ and $\mathbf{v}_2$ of any two body-fixed points have identical components along the line connecting these points:
$(\mathbf{v}_1 - \mathbf{v}_2) \cdot (\boldsymbol{\varrho}_1 - \boldsymbol{\varrho}_2) = [\boldsymbol{\omega} \times (\boldsymbol{\varrho}_1 - \boldsymbol{\varrho}_2)] \cdot (\boldsymbol{\varrho}_1 - \boldsymbol{\varrho}_2) = 0$.

There are two special cases, namely,
- pure translation: $\boldsymbol{\omega} = \mathbf{0}$, $\mathbf{v} \equiv \mathbf{v}_{\mathrm{A}}$ for all points of the body
- pure rotation about a point A: $\mathbf{v}_{\mathrm{A}} = \mathbf{0}$, $\mathbf{v} = \boldsymbol{\omega} \times \boldsymbol{\varrho}$.

In the general case, the velocity distribution can be interpreted as superposition of the velocity distributions of these two special motions translation with velocity $\mathbf{v}_{\mathrm{A}}$ and rotation about A with angular velocity $\boldsymbol{\omega}$.

All body-fixed points along a straight line parallel to $\boldsymbol{\omega}$ have one and the same velocity (different for different lines). In the case $\boldsymbol{\omega} \neq \mathbf{0}$, there

exists exactly one line parallel to $\boldsymbol{\omega}$ the points of which have a velocity in the direction of $\boldsymbol{\omega}$, i.e., the velocity $\mathbf{v} = p\,\boldsymbol{\omega}$ with a scalar p of dimension length. Hence for all points on this line $p\,\boldsymbol{\omega} = \mathbf{v}_{\mathrm{A}} + \boldsymbol{\omega} \times \boldsymbol{\varrho}$. Let $\mathbf{u}$ be the perpendicular from A onto this particular line. Then also

$$p\,\boldsymbol{\omega} = \mathbf{v}_{\mathrm{A}} + \boldsymbol{\omega} \times \mathbf{u} \,. \tag{9.22}$$

Cross- and dot-multiplying this equation by $\boldsymbol{\omega}$ and using the orthogonality $\boldsymbol{\omega} \cdot \mathbf{u} = 0$ one gets for $\mathbf{u}$ and for p the expressions

$$\mathbf{u} = \frac{\boldsymbol{\omega} \times \mathbf{v}_{\mathrm{A}}}{\boldsymbol{\omega}^2} \,, \qquad p = \frac{\boldsymbol{\omega} \cdot \mathbf{v}_{\mathrm{A}}}{\boldsymbol{\omega}^2} \,. \tag{9.23}$$

If in (9.21) an arbitrary point on the line determined by $\mathbf{u}$ is chosen as point A, the velocity of an arbitrary point located by the vector $\boldsymbol{\varrho}$ is

$$\mathbf{v} = p\,\boldsymbol{\omega} + \boldsymbol{\omega} \times \boldsymbol{\varrho} \,. \tag{9.24}$$

This shows that the instantaneous velocity distribution is that of a screw motion, i.e., the superposition of rotation with angular velocity $\boldsymbol{\omega}$ about this particular line and of translation with velocity $p\,\boldsymbol{\omega}$ along the line. The line is called *instantaneous screw axis* (ISA), and p is the *pitch* of the screw. The velocity $\mathbf{v}$ of an arbitrary point not located on the ISA has the direction of the helix through this point.

In the special case $p = 0$ the velocity $\mathbf{v}_{\mathrm{A}}$ and, consequently, the velocities $\mathbf{v}$ of all points of the body are in planes orthogonal to $\boldsymbol{\omega}$. This is the case of plane motion. It is the subject of Chap. 15.

In an x, y, z reference system with its origin 0 on the screw axis and with the z-axis in the direction of $\boldsymbol{\omega}$ the velocity of a body-fixed point with coordinates $[x, y, z]$ (arbitrary) has the coordinates

$$\underline{v} = \omega[\, -y \quad x \quad p\,] \tag{9.25}$$

and the absolute value $|\mathbf{v}| = \omega\sqrt{x^2 + y^2 + p^2}$. Cylinders $x^2 + y^2 = r^2$ (r arbitrary) are surfaces of equal absolute value $|\mathbf{v}|$. Lines parallel to the z-axis are lines of equal velocity $\mathbf{v}$.

Let E be the body-fixed plane parallel to the z-axis which intersects the x, y-plane in the line $y = ax + b$ (a, b arbitrary), and let, furthermore, $\mathbf{n}$ be the vector with coordinates $[\,1 \quad a \quad b/p\,]$. When attached to a point P of E this vector lies in E. From (9.25) it follows that the velocity of every point P of E is orthogonal to $\mathbf{n}$.

Next, all points of an arbitrarily located body-fixed plane E are determined which have in-plane velocities. From (9.24) it follows that no such points exist in planes orthogonal to $\boldsymbol{\omega}$. A plane E is specified by its Eq.(2.1), $\mathbf{m} \cdot \boldsymbol{\varrho} = -1$, and the in-plane condition on the velocities is $\mathbf{m} \cdot (p\,\boldsymbol{\omega} + \boldsymbol{\omega} \times \boldsymbol{\varrho}) = 0$. In terms of coordinates these two equations are

$$\left.\begin{aligned} m_x x + m_y y &= -(1 + m_z z)\,, \\ m_y x - m_x y &= -m_z p\,. \end{aligned}\right\} \tag{9.26}$$

The solution is

$$x(z) = \frac{-m_x(1 + m_z z) - m_y m_z p}{m_x^2 + m_y^2}\,, \qquad y(z) = \frac{-m_y(1 + m_z z) + m_x m_z p}{m_x^2 + m_y^2}\,. \tag{9.27}$$

This determines a straight line in E. Its Plücker vectors and the perpendicular from the origin 0 onto the line are calculated from two points of the line (see (2.3) and (2.6)). For convenience, the points $z = 0$ and $z = -1/m_z$ are chosen. Simple algebra yields the coordinates of the said three vectors (both Plücker vectors multiplied by $m_z(m_x^2 + m_y^2)$):

$$\begin{bmatrix} -m_x m_z \\ -m_y m_z \\ m_x^2 + m_y^2 \end{bmatrix}\,, \quad \begin{bmatrix} -m_y + m_x m_z p \\ m_x + m_y m_z p \\ m_z^2 p \end{bmatrix}\,, \quad \begin{bmatrix} -\dfrac{m_x}{m_x^2 + m_y^2 + m_z^2} - p\,\dfrac{m_y m_z}{m_x^2 + m_y^2} \\ -\dfrac{m_y}{m_x^2 + m_y^2 + m_z^2} + p\,\dfrac{m_x m_z}{m_x^2 + m_y^2} \\ -\dfrac{m_z}{m_x^2 + m_y^2 + m_z^2} \end{bmatrix}\,. \tag{9.28}$$

The first Plücker vector has the direction of $\mathbf{m} \times (\boldsymbol{\omega} \times \mathbf{m})$. The perpendicular onto the line is the sum of the perpendicular $-\mathbf{m}/\mathbf{m}^2$ onto the plane and an in-plane vector of absolute value $p m_z / \sqrt{m_x^2 + m_y^2}$ in the direction of $\boldsymbol{\omega} \times \mathbf{m}$.

Substitution of (9.27) into (9.25) yields the velocity as function of z. At $z = -1/m_z$ the velocity has the direction of the line and, consequently, its minimal absolute value. This minimal value is

$$|\mathbf{v}|_{\min} = p\,\omega \sqrt{1 + \frac{m_z^2}{m_x^2 + m_y^2}}\,. \tag{9.29}$$

This concludes the investigation.

In what follows, the curve defined by those body-fixed points is determined the velocities of which are directed either towards or away from a prescribed point A. Without loss of generality, A is placed on the positive x-axis with coordinates $[\,2a\,,\,0\,,\,0\,]$. With (9.25) the condition on the velocity of the point $[x, y, z]$ is

$$\frac{x - 2a}{-y} = \frac{y}{x} = \frac{z}{p}\,. \tag{9.30}$$

By eliminating the three coordinates, one at a time, the projections of the curve onto the planes of the other two coordinate axes are obtained:

$$(x - a)^2 + y^2 = a^2\,, \quad x(z) = 2a\,\frac{1}{1 + z^2/p^2}\,, \quad y(z) = 2a\,\frac{z/p}{1 + z^2/p^2}\,. \tag{9.31}$$

The curve is located on the cylinder $(x-a)^2+y^2=a^2$; it is passing through A; the z-axis is asymptote. Points on the curve on one side of A have velocities pointing away from A, and points on the other side of A have velocities pointing towards A. In terms of the polar coordinate φ in the x,y-plane ($\tan\varphi = y/x$)

$$x = a(1+\cos 2\varphi)\,, \qquad y = a\sin 2\varphi\,, \qquad z = p\,\tan\varphi\,. \tag{9.32}$$

In the case of plane motion the curve is Thales' circle $(x-a)^2+y^2=a^2$ over the diameter 0A.

Velocity Screw
The pair of vectors $(\boldsymbol{\omega}, \mathbf{v})$ in (9.24) is called velocity screw of the body[1]. By writing $\boldsymbol{\omega} = \omega\mathbf{n}$ (unit vector $\mathbf{n}$) and $\mathbf{a} = -\boldsymbol{\varrho}$ it is given the standard form

$$(\boldsymbol{\omega}, \mathbf{v}) = \omega(\mathbf{n}\,,\, \mathbf{a}\times\mathbf{n} + p\,\mathbf{n})\,. \tag{9.33}$$

The vector $\mathbf{a}$ is directed from the point having the velocity $\mathbf{v}$ to an arbitrary point of the ISA. The vectors $\mathbf{n}$ and $\mathbf{a}\times\mathbf{n}$ are the Plücker vectors of the ISA. The scalar ω is called intensity of the velocity screw. The expression in parentheses is called unit screw. There are two special cases:
The special case of plane motion ($p=0$): The unit screw is identical with the screw axis, namely, $(\mathbf{n}, \mathbf{a}\times\mathbf{n})$.
The special case of pure translation: Every point of the body has the same velocity $v\mathbf{n}$ with unit vector $\mathbf{n}$. A screw axis does not exist. The pitch is undefined ($p=\infty$ according to (9.23)). Equation (9.33) has the form

$$(\boldsymbol{\omega}, \mathbf{v}) = v(\mathbf{0}\,,\, \mathbf{n})\,. \tag{9.34}$$

In what follows, the general case is considered. The unit line vector $\hat{\mathbf{n}}$ along the ISA and the velocity screw are written as dual vectors. The former is composed of the Plücker vectors of the ISA and the latter is defined as $\hat{\boldsymbol{\omega}} = \boldsymbol{\omega} + \varepsilon\mathbf{v}$:

$$\hat{\mathbf{n}} = \mathbf{n} + \varepsilon\mathbf{a}\times\mathbf{n}\,, \tag{9.35}$$

$$\hat{\boldsymbol{\omega}} = \boldsymbol{\omega} + \varepsilon\mathbf{v} = \omega[\mathbf{n} + \varepsilon(\mathbf{a}\times\mathbf{n} + p\,\mathbf{n})]\,. \tag{9.36}$$

These dual vectors are related through the equation (to be verified by multiplying out again)

$$\hat{\boldsymbol{\omega}} = \omega(1+\varepsilon p)\hat{\mathbf{n}}\,. \tag{9.37}$$

Comparison with (2.29) shows that Eqs.(9.23) define the axis and the pitch of the linear complex $(\boldsymbol{\omega}\,;\, \mathbf{v}_{\mathrm{A}})$. It is called linear complex of velocity. From Fig. 2.5 it is known that the complex lines of this linear complex are normals of the helices, i.e., of the velocities $\mathbf{v}$. Let $\mathbf{z}$ be the first Plücker vector of

[1] The name *velocity screw* is used instead of *twist*

a complex line passing through the point with position vector $\boldsymbol{\varrho}$ and with velocity $\mathbf{v} = \mathbf{v}_A + \boldsymbol{\omega} \times \boldsymbol{\varrho}$. Orthogonality requires that $\mathbf{v} \cdot \mathbf{z} = 0$. This is the equation $(\mathbf{v}_A + \boldsymbol{\omega} \times \boldsymbol{\varrho}) \cdot \mathbf{z} = 0$ or $\boldsymbol{\omega} \cdot \boldsymbol{\varrho} \times \mathbf{z} + \mathbf{v}_A \cdot \mathbf{z} = 0$. In this equation the defining Eq.(2.25) of the linear complex $(\boldsymbol{\omega}\,;\,\mathbf{v}_A)$ is recognized. The vectors $\mathbf{z}$ and $\boldsymbol{\varrho} \times \mathbf{z}$ are the Plücker vectors of a complex line passing through the null point with position vector $\boldsymbol{\varrho}$ and with velocity $\mathbf{v} = \mathbf{v}_A + \boldsymbol{\omega} \times \boldsymbol{\varrho}$.

Theorem 9.2. *Every plane not containing a line parallel to the ISA is instantaneously intersected orthogonally by the velocity (the trajectory) of exactly one body-fixed point.*

Proof: Every such plane is a null plane. It is intersected orthogonally by a helix of the screw at its uniquely defined null point and only at this point. For a plane specified in the form $\mathbf{m} \cdot \boldsymbol{\varrho} = -1$ the null point is calculated from (2.36) which, in the present case, has the form

$$\boldsymbol{\varrho}_0 = \frac{\mathbf{m} \times p\,\boldsymbol{\omega} - \boldsymbol{\omega}}{\mathbf{m} \cdot \boldsymbol{\omega}} \,. \tag{9.38}$$

In the x, y, z-system used in (9.25) it has the coordinates $(1/m_z)[\,pm_y \quad -pm_x \quad -1\,]$. End of proof.

Theorem 9.3. *If a straight line g is at one point instantaneously normal to the velocity (the trajectory) of the coinciding body-fixed point, every point of g is instantaneously normal to the velocity of the coinciding body-fixed point.*

Proof: Orthogonality of the line g to a single trajectory means that g is a complex line of the linear complex of velocity. In the context of Fig. 2.6 it was shown that every point P of a complex line is null point of a null plane containing the line g. The null plane is intersected orthogonally by a helix at its null point P. Hence also g is intersected orthogonally. A simpler proof makes use of the rigid-body property. Body-fixed points located on g have identical velocity components along g. So, if one point has a zero velocity component, all points have. End of proof.

Theorem 9.3 explains the names null plane and null point. The null plane associated with a null point P is the locus of points which have zero velocity components toward P (see Fig. 2.5).

Imagine in Fig. 2.5 a sphere of arbitrary radius a centered at the point P with coordinates $[\,r\,,\,0\,,\,0\,]$. From Theorem 9.3 it follows that the great circle in which the null plane associated with P intersects the sphere is the locus of points on the sphere which have velocities tangent to the sphere. This is independently verified as follows. An arbitrary point $[x, y, z]$ on the sphere has the velocity coordinates (9.25), $\underline{v} = \omega[\,-y \quad x \quad p\,]$ and the local normal with coordinates $[\,x - r \quad y \quad z\,]$. The orthogonality condition is $ry + p\,z = 0$. This is the equation of the null plane associated with P.

Subject of the following investigation is the motion of a rigid body three noncollinear points P_1, P_2, P_3 of which are constrained to prescribed spatial

curves. Spatial means: The tangents to the curves at the three points are neither parallel nor are they in the plane of the points. According to Grübler's formula (4.1) the degree of freedom of the body is $F = d$. Hence without defect of the system of constraint equations the body is immobile. Let Σ_0 be the plane of the points P_1, P_2, P_3 and let, furthermore, Σ_i $(i = 1, 2, 3)$ be the plane normal to the curve at P_i.

Theorem 9.4. *The body is instantaneously mobile with degree of freedom* $F = 1$ *if the four planes* Σ_i $(i = 0, 1, 2, 3)$ *intersect at a single point.*

Proof: If the body is mobile, Σ_i $(i = 1, 2, 3)$ is the null plane corresponding to the null point P_i. Let Q_i be the point of intersection of the three planes Σ_0, Σ_j, Σ_k $(i, j, k = 1, 2, 3$ different). According to Theorem 9.3 the trajectory of the body-fixed point coinciding with Q_i intersects orthogonally both the line $\overline{\mathrm{Q}_i\mathrm{P}_j}$ and the line $\overline{\mathrm{Q}_i\mathrm{P}_k}$. Hence it intersects orthogonally also Σ_0. Consequently, Q_i is the null point of the null plane Σ_0. Since a plane has exactly one null point, motion is possible if and only if Q_1, Q_2 and Q_3 coincide in a single point Q_0. In this case, the instantaneous motion is a screw motion with degree of freedom $F = 1$. End of proof.

The instantaneous screw axis is constructed from two pairs of reciprocal polars of the linear complex (see Sect. 2.7.5). The lines $\overline{\mathrm{P}_1\mathrm{P}_2} = \mathrm{g}_3$ and $\overline{\mathrm{P}_2\mathrm{P}_3} = \mathrm{g}_1$ are not lines of the linear complex since they lie in Σ_0 without passing through the nullpoint Q_0. Since g_3 is intersected by the pencil of complex lines in Σ_1 and also by the pencil of complex lines in Σ_2, the line $\overline{\mathrm{g}}_3$ reciprocal to g_3, too, is intersected by these pencils of complex lines. Hence $\overline{\mathrm{g}}_3$ is the line of intersection of Σ_1 and Σ_2. It is passing through Q_0. For the same reason the line $\overline{\mathrm{g}}_1$ reciprocal to g_1 is the line of intersection of Σ_2 and Σ_3 also passing through Q_0. According to Theorem 2.2 the axis of the linear complex is the common perpendicular of the common perpendiculars of the pairs $\overline{\mathrm{g}}_3$, g_3 and $\overline{\mathrm{g}}_1$, g_1. The pitch of the instantaneous screw is calculated from (2.32), $p = r \tan \alpha$. The quantities r and α are explained in Fig. 2.5 where P and its nullplane are any of the pairs P_i, Σ_i $(i = 1, 2, 3)$.

The trajectories of three body-fixed points in the course of an arbitrary general motion are curves satisfying the condition stated in Theorem 9.4 not only instantaneously, but continuously.

At the beginning of Sect. 2.7.5 on reciprocal polars $(\mathbf{p}_1, \mathbf{q}_1)$ and $(\mathbf{p}_2, \mathbf{q}_2)$ of a linear complex it was shown that the absolute value of $\mathbf{p}_1$ in (2.39) can be chosen such that in (2.41) $\mu = 1$. Let this be the case. Applied to the linear complex $(\boldsymbol{\omega}\,; \mathbf{v})$ Eqs.(2.39) then read:

$$\mathbf{p}_1 + \mathbf{p}_2 = \boldsymbol{\omega}\,, \qquad \mathbf{q}_1 + \mathbf{q}_2 = \mathbf{v}\,. \tag{9.39}$$

By definition, the second Plücker vector $\mathbf{q}_i$ of a polar $(\mathbf{p}_i, \mathbf{q}_i)$ is the moment of the first vector $\mathbf{p}_i$. In the equations the kinematical relationships are recognized (note that $\mathbf{a}_i = -\boldsymbol{\varrho}_i$ $(i = 1, 2)$):

$$\boldsymbol{\omega}_1 + \boldsymbol{\omega}_2 = \boldsymbol{\omega} \,, \qquad \boldsymbol{\omega}_1 \times \boldsymbol{\varrho}_1 + \boldsymbol{\omega}_2 \times \boldsymbol{\varrho}_2 = \mathbf{v} \,. \tag{9.40}$$

These equations are proof of

Theorem 9.5. *An arbitrary velocity screw* $(\boldsymbol{\omega}, \mathbf{v})$ *with* $\boldsymbol{\omega} \neq \mathbf{0}$ *can be represented as resultant of two pure rotations. The axis of one of these rotations can be chosen arbitrarily subject to the restriction that it is not a line of the linear complex* $(\boldsymbol{\omega}; \mathbf{v})$ *. The axis of the other rotation is the uniquely determined reciprocal polar of the first axis.*

Further applications of velocity screws and linear complexes see in Chap. 12 .

9.4 Angular Velocity of a Body in Terms of Positions and Velocities of Three Points

Problem statement: In some reference basis the instantaneous position vectors $\mathbf{r}_1$, $\mathbf{r}_2$, $\mathbf{r}_3$ of three noncollinear points P_1 , P_2 , P_3 of a rigid body as well as the instantaneous velocities $\mathbf{v}_1$, $\mathbf{v}_2$, $\mathbf{v}_3$ of these points are given. To be determined is the instantaneous angular velocity $\boldsymbol{\omega}$ of the body. Since none of the three points is dominant in any way, it must be possible to find an expression for $\boldsymbol{\omega}$ which is cyclicly symmetric with respect to the indices 1, 2, 3 .

Solution: Starting point is the equation

$$\mathbf{v}_i - \mathbf{v}_j = \boldsymbol{\omega} \times (\mathbf{r}_i - \mathbf{r}_j) \qquad (i, j = 1, 2, 3) \,. \tag{9.41}$$

Using this equation the product is formed:

$$\begin{aligned} (\mathbf{v}_1 - \mathbf{v}_3) \times (\mathbf{v}_2 - \mathbf{v}_3) &= [\boldsymbol{\omega} \times (\mathbf{r}_1 - \mathbf{r}_3)] \times (\mathbf{v}_2 - \mathbf{v}_3) \\ &= \boldsymbol{\omega} \cdot (\mathbf{v}_2 - \mathbf{v}_3)\,(\mathbf{r}_1 - \mathbf{r}_3) - \boldsymbol{\omega}\,(\mathbf{r}_1 - \mathbf{r}_3) \cdot (\mathbf{v}_2 - \mathbf{v}_3) \,. \end{aligned} \tag{9.42}$$

The first scalar product is zero because of (9.41). If and only if $\boldsymbol{\omega}$ lies in the plane of the three points, again because of (9.41), also the second scalar product and, consequently, the left-hand side of the equation is zero. For the moment this special case is excluded. Then the angular velocity is

$$\boldsymbol{\omega} = \frac{(\mathbf{v}_1 - \mathbf{v}_3) \times (\mathbf{v}_2 - \mathbf{v}_3)}{(\mathbf{r}_3 - \mathbf{r}_1) \cdot (\mathbf{v}_2 - \mathbf{v}_3)} \,. \tag{9.43}$$

When multiplied out, the numerator displays the desired cyclic symmetry. Not so the denominator. Differentiation of the rigid-body property $(\mathbf{r}_3 - \mathbf{r}_1) \cdot (\mathbf{r}_2 - \mathbf{r}_3) = \text{const}$ with respect to time yields the equation

$$(\mathbf{r}_3 - \mathbf{r}_1) \cdot (\mathbf{v}_2 - \mathbf{v}_3) = -(\mathbf{v}_3 - \mathbf{v}_1) \cdot (\mathbf{r}_2 - \mathbf{r}_3) \,. \tag{9.44}$$

The left-hand side expression is the denominator of (9.43). When this expression is added one more time to both sides of the equation, the denominator takes the form

$$(\mathbf{r}_3-\mathbf{r}_1)\cdot(\mathbf{v}_2-\mathbf{v}_3)=\frac{1}{2}[(\mathbf{r}_3-\mathbf{r}_1)\cdot(\mathbf{v}_2-\mathbf{v}_3)-(\mathbf{v}_3-\mathbf{v}_1)\cdot(\mathbf{r}_2-\mathbf{r}_3)]\ . \quad (9.45)$$

This is substituted into (9.43). Then the numerator and the denominator are multiplied out. This results in two alternative forms displaying the desired symmetry (see Stojanov [11], Charlamov [4], Wittenburg [14, 15]):

$$\boldsymbol{\omega}=2\,\frac{\mathbf{v}_1\times\mathbf{v}_2+\mathbf{v}_2\times\mathbf{v}_3+\mathbf{v}_3\times\mathbf{v}_1}{\mathbf{v}_1\cdot(\mathbf{r}_2-\mathbf{r}_3)+\mathbf{v}_2\cdot(\mathbf{r}_3-\mathbf{r}_1)+\mathbf{v}_3\cdot(\mathbf{r}_1-\mathbf{r}_2)} \quad (9.46)$$

$$=-2\,\frac{\mathbf{v}_1\times\mathbf{v}_2+\mathbf{v}_2\times\mathbf{v}_3+\mathbf{v}_3\times\mathbf{v}_1}{\mathbf{r}_1\cdot(\mathbf{v}_2-\mathbf{v}_3)+\mathbf{r}_2\cdot(\mathbf{v}_3-\mathbf{v}_1)+\mathbf{r}_3\cdot(\mathbf{v}_1-\mathbf{v}_2)}\ . \quad (9.47)$$

For numerical evaluations (9.43) is preferable. With $\boldsymbol{\omega}$ and $\mathbf{v}_{\mathrm{A}}=\mathbf{v}_i$ ($i=1$ or 2 or 3) Eqs.(9.23) determine the perpendicular $\mathbf{u}_i$ from P_i onto the instantaneous screw axis and the pitch p.

If the denominator and, hence, also the numerator is zero, $\boldsymbol{\omega}$ lies in the plane of the three points. Consequently, there exist coefficients λ and μ such that

$$\boldsymbol{\omega}=\lambda(\mathbf{r}_1-\mathbf{r}_2)+\mu(\mathbf{r}_2-\mathbf{r}_3)\ . \quad (9.48)$$

This ansatz yields

$$\mathbf{v}_3-\mathbf{v}_2=\boldsymbol{\omega}\times(\mathbf{r}_3-\mathbf{r}_2)=\lambda\mathbf{n}\ ,\qquad \mathbf{v}_1-\mathbf{v}_2=\boldsymbol{\omega}\times(\mathbf{r}_1-\mathbf{r}_2)=\mu\mathbf{n}\ , \quad (9.49)$$

where $\mathbf{n}$ is the vector

$$\mathbf{n}=(\mathbf{r}_1-\mathbf{r}_2)\times(\mathbf{r}_3-\mathbf{r}_2)=-(\mathbf{r}_1\times\mathbf{r}_2+\mathbf{r}_2\times\mathbf{r}_3+\mathbf{r}_3\times\mathbf{r}_1)\ . \quad (9.50)$$

Scalar multiplication of Eqs.(9.49) by $\mathbf{n}$ yields

$$\lambda=\frac{1}{\mathbf{n}^2}\,\mathbf{n}\cdot(\mathbf{v}_3-\mathbf{v}_2)\ ,\qquad \mu=\frac{1}{\mathbf{n}^2}\,\mathbf{n}\cdot(\mathbf{v}_1-\mathbf{v}_2)\ . \quad (9.51)$$

With these expressions (9.48) has the symmetrical form

$$\boldsymbol{\omega}=\frac{1}{\mathbf{n}^2}\,\mathbf{n}\cdot\Big[\mathbf{v}_1(\mathbf{r}_2-\mathbf{r}_3)+\mathbf{v}_2(\mathbf{r}_3-\mathbf{r}_1)+\mathbf{v}_3(\mathbf{r}_1-\mathbf{r}_2)\Big]\ . \quad (9.52)$$

Special case: If P_3 is fixed, $\mathbf{r}_3=\mathbf{0}$ (arbitrarily) and $\mathbf{v}_3=\mathbf{0}$. Equations (9.43) and (9.52) are

$$\boldsymbol{\omega} = \begin{cases} -\dfrac{\mathbf{v}_1 \times \mathbf{v}_2}{\mathbf{r}_1 \cdot \mathbf{v}_2} & (\text{denominator} \neq 0) \\ \dfrac{\mathbf{r}_1 \times \mathbf{r}_2}{(\mathbf{r}_1 \times \mathbf{r}_2)^2} \cdot (\mathbf{v}_2 \mathbf{r}_1 - \mathbf{v}_1 \mathbf{r}_2) & (\text{else}) \, . \end{cases} \tag{9.53}$$

9.5 Raccording Axodes. Striction Point. Distribution Parameter

The statements made so far refer to instantaneous velocities and angular velocities at a fixed time t. In what follows, continuous motions are investigated which are neither planar motions nor motions about a fixed point. In the course of a continuous motion the ISA generates a ruled surface in the reference basis $\underline{\mathbf{e}}^1$ and another ruled surface in the body-fixed basis $\underline{\mathbf{e}}^2$. These ruled surfaces are called *fixed axode* $\mathrm{F_f}$ (fixed in $\underline{\mathbf{e}}^1$) and *moving axode* $\mathrm{F_m}$ (fixed in $\underline{\mathbf{e}}^2$).

Proposition: At every point along the common ISA the tangent planes of $\mathrm{F_f}$ and of $\mathrm{F_m}$ coincide. Proof: Let $\mathrm{k_m}$ be an arbitrary curve fixed on $\mathrm{F_m}$ which intersects the generators of $\mathrm{F_m}$. Furthermore, let P be the point which at all times t is located on both $\mathrm{k_m}$ and the ISA(t) (see Fig. 9.2). Finally, let $\mathbf{v}_{\mathrm{rel}}$ be the velocity of P along $\mathrm{k_m}$. On $\mathrm{F_f}$ P is moving along a different trajectory $\mathrm{k_f}$. Its velocity along $\mathrm{k_f}$ is, according to (9.11) and (9.24), $\mathbf{v} = p\,\boldsymbol{\omega} + \mathbf{v}_{\mathrm{rel}}$. The plane spanned by $p\,\boldsymbol{\omega}$ and $\mathbf{v}$ coincides with the plane spanned by $p\,\boldsymbol{\omega}$ and $\mathbf{v}_{\mathrm{rel}}$. Since these planes are the tangent planes of $\mathrm{F_f}$ and of $\mathrm{F_m}$, respectively, also the tangent planes coincide. End of proof. These statements are summarized in

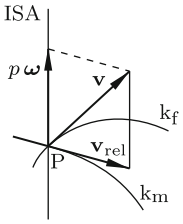

Fig. 9.2 Velocities proving that at every point of the ISA the tangent planes of the axodes coincide

Theorem 9.6. (Painlevé) *Every continuous motion of a rigid body which is neither a planar motion nor a motion about a fixed point can be interpreted as raccording motion of a body-fixed axode* $\mathrm{F_m}$ *on an axode* $\mathrm{F_f}$ *fixed in the reference basis. Both axodes are ruled surfaces which are generated by the* ISA. *The raccording motion is the superposition of translation with velocity*

$p\boldsymbol{\omega}$ along the ISA *and rotation* (*rolling motion*) *with angular velocity* $\boldsymbol{\omega}$ *about the* ISA.

In Sect. 13.2 Fenyi's joint is investigated. Its central body is executing a periodic spatial motion without a fixed point. The raccording axodes of this motion are determined in analytical form.

From Sect. 2.9 on ruled surfaces it is known that the tangent planes at all points of a generator are uniquely determined by the location of the striction point S on the generator and by the distribution parameter δ. From Theorem 9.6 it follows that both axodes have, on the common generator ISA, the same striction point and the same distribution parameter. In what follows, the pertinent formulas from Sect. 2.9 are considered again. The parameter equation of a ruled surface was written in the form (see (2.51))

$$\mathbf{x}(u,\lambda) = \mathbf{r}(u) + \lambda\mathbf{e}(u) \tag{9.54}$$

with u and λ being free parameters and with $\mathbf{e}$ being the unit vector along the generator $u = \text{const}$ (arbitrary). The striction point on the generator is determined by the value λ_{S} of λ at this point. The unit vector normal to the tangent plane at the point $\mathbf{x}(u,\lambda)$ of this generator depends on λ only. It is called $\mathbf{n}(\lambda)$, and the unit vector normal to the tangent plane at the striction point is called $\mathbf{n}_{\mathrm{S}}$. In the projection along the generator the vector $\mathbf{n}(\lambda)$ is rotated against $\mathbf{n}_{\mathrm{S}}$ through an angle $\varphi(\lambda)$. The vector $\mathbf{n}_{\mathrm{S}}$, the parameter value λ_{S}, the angle $\varphi(\lambda)$ and the distribution parameter δ are, according to (2.54), (2.55), (2.56), (2.58) and (2.59),

$$\left.\begin{aligned} \mathbf{n}_{\mathrm{S}} &= \frac{(\mathbf{e}\times\dot{\mathbf{e}})\times\mathbf{e}}{|(\mathbf{e}\times\dot{\mathbf{e}})\times\mathbf{e}|}\,, \qquad & \lambda_{\mathrm{S}} &= -\frac{\dot{\mathbf{r}}\cdot\dot{\mathbf{e}}}{\dot{\mathbf{e}}^2}\,, \\ \tan\varphi(\lambda) &= \frac{\lambda_{\mathrm{S}}-\lambda}{\delta}\,, \qquad & \delta &= \frac{\dot{\mathbf{e}}\cdot\dot{\mathbf{r}}\times\mathbf{e}}{\dot{\mathbf{e}}^2}\,. \end{aligned}\right\} \tag{9.55}$$

These formulas are not directly applicable to raccording axodes. What is needed are formulas in terms of the five kinematical quantities $\mathbf{r}_{\mathrm{A}}$, $\mathbf{v}_{\mathrm{A}}$, $\mathbf{a}_{\mathrm{A}}$, $\boldsymbol{\omega}$ and $\dot{\boldsymbol{\omega}}$. In what follows, such formulas are developed for the moving axode (Wittenburg [15]).

The parameter equation (9.54) is replaced by the equation $\mathbf{r}(t,\lambda) = \mathbf{r}_{\mathrm{A}}(t) + \mathbf{u}(t) + \lambda\mathbf{e}(t)$. Thus, the parameter u is replaced by time t, and the vector $\mathbf{r}(u)$ is replaced by the vector $\mathbf{r}_{\mathrm{A}}(t) + \mathbf{u}(t)$ to the foot of the perpendicular from A onto the ISA. The unit vector $\mathbf{e}$ along the ISA is expressed in the form $\mathbf{e} = \boldsymbol{\omega}/|\boldsymbol{\omega}|$. With this vector and with (9.23) for $\mathbf{u}$ the equation is (omitting the parameter t)

$$\mathbf{r}(\lambda) = \mathbf{r}_{\mathrm{A}} + \frac{\boldsymbol{\omega}\times\mathbf{v}_{\mathrm{A}}}{\boldsymbol{\omega}^2} + \frac{\lambda}{|\boldsymbol{\omega}|}\,\boldsymbol{\omega}\,. \tag{9.56}$$

From $\boldsymbol{\omega} = \omega\,\mathbf{e}$ and $\dot{\boldsymbol{\omega}} = \dot{\omega}\,\mathbf{e} + \omega\,\dot{\mathbf{e}}$ it follows that $(\boldsymbol{\omega}\times\dot{\boldsymbol{\omega}})\times\boldsymbol{\omega} = \omega^3\,(\mathbf{e}\times\dot{\mathbf{e}})\times\mathbf{e}$. With this equation the first Eq.(9.55) for $\mathbf{n}_{\mathrm{S}}$ is expressed in

terms of kinematical quantities:

$$\mathbf{n}_{\mathrm{S}} = \frac{(\boldsymbol{\omega} \times \dot{\boldsymbol{\omega}}) \times \boldsymbol{\omega}}{|\boldsymbol{\omega} \times \dot{\boldsymbol{\omega}}||\boldsymbol{\omega}|} \,. \tag{9.57}$$

Expressions for λ_{S}, for $\tan\varphi(\lambda)$ and for δ are found from properties of the acceleration of body-fixed points momentarily coinciding with the ISA. The point coinciding with $\mathbf{r}(\lambda)$ has the acceleration (see (9.14))

$$\mathbf{a}(\lambda) = \mathbf{a}(0) - \frac{\lambda}{|\boldsymbol{\omega}|}\, \boldsymbol{\omega} \times \dot{\boldsymbol{\omega}} \tag{9.58}$$

where $\mathbf{a}(0)$ is the acceleration of the body-fixed point at the foot of the perpendicular $\mathbf{u}$ on the ISA (see (9.23)):

$$\mathbf{a}(0) = \mathbf{a}_{\mathrm{A}} + \dot{\boldsymbol{\omega}} \times \mathbf{u} - \boldsymbol{\omega}^2 \mathbf{u} = \mathbf{a}_{\mathrm{A}} - \boldsymbol{\omega} \times \mathbf{v}_{\mathrm{A}} + \frac{\dot{\boldsymbol{\omega}} \times (\boldsymbol{\omega} \times \mathbf{v}_{\mathrm{A}})}{\boldsymbol{\omega}^2} \,. \tag{9.59}$$

Proposition: The acceleration $\mathbf{a}(\lambda)$ lies in the plane spanned by the ISA and by $\mathbf{n}(\lambda)$. Proof: The acceleration has a component along the ISA due to the translatory part of the raccording motion and a component $\mathbf{a}_{\mathrm{r}}(\lambda)$ due to the rolling motion. Consider the rolling motion alone. In Sect. 15.5.2 (Eq.(15.127)) it is shown that the body-fixed point which is in rolling contact at $\mathbf{r}(\lambda)$ is passing through a cusp of its trajectory with the normal unit vector $\mathbf{n}(\lambda)$ being, in the limit, the tangent to the trajectory. Hence $\mathbf{a}_{\mathrm{r}}(\lambda)$ has the direction of $\mathbf{n}(\lambda)$. End of proof. In particular, the acceleration $\mathbf{a}_{\mathrm{S}} = \mathbf{a}(\lambda_{\mathrm{S}})$ of the body-fixed point coinciding with the striction point lies in the plane spanned by $\boldsymbol{\omega}$ and $\mathbf{n}_{\mathrm{S}}$. From this together with (9.57) it follows that the striction point is characterized by coplanarity of the vectors $\mathbf{a}_{\mathrm{S}}$, $\boldsymbol{\omega}$ and $\dot{\boldsymbol{\omega}}$:

$$\mathbf{a}_{\mathrm{S}} \cdot \boldsymbol{\omega} \times \dot{\boldsymbol{\omega}} = 0 \,. \tag{9.60}$$

Substituting for $\mathbf{a}_{\mathrm{S}}$ the expression from (9.58) with $\lambda = \lambda_{\mathrm{S}}$ results in

$$\frac{\lambda_{\mathrm{S}}}{|\boldsymbol{\omega}|} = \frac{\mathbf{a}(0) \cdot \boldsymbol{\omega} \times \dot{\boldsymbol{\omega}}}{(\boldsymbol{\omega} \times \dot{\boldsymbol{\omega}})^2} \,. \tag{9.61}$$

Substitution of this expression into (9.56) yields the desired expression for the position vector $\mathbf{r}_{\mathrm{S}}$ of the striction point:

$$\mathbf{r}_{\mathrm{S}} = \mathbf{r}_{\mathrm{A}} + \frac{\boldsymbol{\omega} \times \mathbf{v}_{\mathrm{A}}}{\omega^2} + \frac{\mathbf{a}(0) \cdot \boldsymbol{\omega} \times \dot{\boldsymbol{\omega}}}{(\boldsymbol{\omega} \times \dot{\boldsymbol{\omega}})^2}\, \boldsymbol{\omega} \,. \tag{9.62}$$

This point S is the origin of the canonical reference frame. Unit vectors along its axes are $\mathbf{e} = \boldsymbol{\omega}/|\boldsymbol{\omega}|$, $\boldsymbol{\omega} \times \dot{\boldsymbol{\omega}}/|\boldsymbol{\omega} \times \dot{\boldsymbol{\omega}}|$ and $\mathbf{n}_{\mathrm{S}}$.

Writing (9.58) also for $\lambda = \lambda_{\mathrm{S}}$ and taking the difference results in the equation

$$\mathbf{a}(\lambda) = \mathbf{a}_\mathrm{S} + (\lambda_\mathrm{S} - \lambda)\,\frac{\boldsymbol{\omega} \times \dot{\boldsymbol{\omega}}}{|\boldsymbol{\omega}|}\,. \tag{9.63}$$

The second term is a vector normal to $\mathbf{a}_\mathrm{S}$. Hence the conclusion: The striction point is the point of minimum acceleration on the ISA: $|\mathbf{a}(\lambda)|_{\min} = |\mathbf{a}_\mathrm{S}|$.

An expression for $\tan\varphi(\lambda)$ is developed from Fig. 9.3 in which the collinear vectors $\mathbf{n}(\lambda)$ and $\mathbf{a}_\mathrm{r}(\lambda)$ are shown in the canonical reference frame. They are located in the plane spanned by $\mathbf{n}_\mathrm{S}$ and $\boldsymbol{\omega} \times \dot{\boldsymbol{\omega}}$. The angle $\varphi(\lambda)$ is determined by

$$\cos\varphi(\lambda) = \frac{\mathbf{a}_\mathrm{r}(\lambda) \cdot \mathbf{n}_\mathrm{S}}{|\mathbf{a}_\mathrm{r}(\lambda)|}\,, \qquad \sin\varphi(\lambda) = \frac{\mathbf{a}_\mathrm{r}(\lambda) \cdot \boldsymbol{\omega} \times \dot{\boldsymbol{\omega}}}{|\mathbf{a}_\mathrm{r}(\lambda)|\,|\boldsymbol{\omega} \times \dot{\boldsymbol{\omega}}|}\,. \tag{9.64}$$

The numerator expressions are with (9.57), (9.58), (9.60) and (9.63)

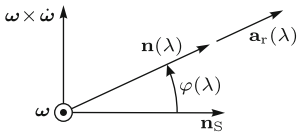

Fig. 9.3 Vectors $\mathbf{n}(\lambda)$, $\mathbf{a}_\mathrm{r}(\lambda)$ and angle $\varphi(\lambda)$ in the canonical reference frame

$$\mathbf{a}_\mathrm{r}(\lambda) \cdot \mathbf{n}_\mathrm{S} = \mathbf{a}(\lambda) \cdot \mathbf{n}_\mathrm{S} = \mathbf{a}(0) \cdot \mathbf{n}_\mathrm{S} = \frac{\mathbf{a}(0) \cdot [(\boldsymbol{\omega} \times \dot{\boldsymbol{\omega}}) \times \boldsymbol{\omega}]}{|\boldsymbol{\omega} \times \dot{\boldsymbol{\omega}}|\,|\boldsymbol{\omega}|}\,, \tag{9.65}$$

$$\mathbf{a}_\mathrm{r}(\lambda) \cdot \boldsymbol{\omega} \times \dot{\boldsymbol{\omega}} = (\lambda_\mathrm{S} - \lambda)\,\frac{(\boldsymbol{\omega} \times \dot{\boldsymbol{\omega}})^2}{|\boldsymbol{\omega}|}\,. \tag{9.66}$$

From these expressions it follows that $\tan\varphi(\lambda)$ has the desired form

$$\tan\varphi(\lambda) = \frac{\lambda_\mathrm{S} - \lambda}{\delta} \tag{9.67}$$

with the distribution parameter

$$\delta = \frac{\mathbf{a}(0) \cdot [(\boldsymbol{\omega} \times \dot{\boldsymbol{\omega}}) \times \boldsymbol{\omega}]}{(\boldsymbol{\omega} \times \dot{\boldsymbol{\omega}})^2}\,. \tag{9.68}$$

In (9.65) also $\mathbf{a}(\lambda) \cdot \mathbf{n}_\mathrm{S} = \mathbf{a}_\mathrm{S} \cdot \mathbf{n}_\mathrm{S}$ is correct. This yields the more appealing formula

$$\delta = \frac{\mathbf{a}_\mathrm{S} \cdot [(\boldsymbol{\omega} \times \dot{\boldsymbol{\omega}}) \times \boldsymbol{\omega}]}{(\boldsymbol{\omega} \times \dot{\boldsymbol{\omega}})^2}\,. \tag{9.69}$$

As has already been said, raccording motion of the moving axode and the fixed axode requires that both axodes have, at every instant of time, the same striction point $\mathbf{r}_\mathrm{S}$ and the same distribution parameter δ. The moving axode and the fixed axode exchange their roles when the change from motion

to inverse motion is made. According to Theorem 9.1 this change has the effect that $\mathbf{v}_A$, $\mathbf{a}(0)$, $\mathbf{a}_S$, $\boldsymbol{\omega}$ and $\dot{\boldsymbol{\omega}}$ are multiplied by -1. Equations (9.62) and (9.69) show, that neither $\mathbf{r}_S$ nor δ is effected by this change.

9.6 Spatial Rotation About a Fixed Point

In (9.21) the fixed point is chosen as point A. Then

$$\mathbf{v} = \boldsymbol{\omega} \times \boldsymbol{\varrho} \,. \tag{9.70}$$

The ISA is the straight line having the direction of $\boldsymbol{\omega}$ and passing through A. The translatory velocity $p\,\boldsymbol{\omega}$ of the raccording motion is zero. The raccording axodes are general cones with the common apex A. The cones are rolling one on the other without slipping. They are generated by the vector $\boldsymbol{\omega}(t)$ attached to A. They are referred to as moving cone (also *polhode cone*; fixed on the body) and as fixed cone (also *herpolhode cone*; fixed in the reference basis $\underline{\mathbf{e}}^1$). The general situation is shown in Fig. 9.4. Painlevé's general Theorem 9.6 has the special form:

Theorem 9.7. (Poinsot) *Every continuous motion of a rigid body about a fixed point can be interpreted as rolling motion of a body-fixed moving cone* (*polhode cone*) *on a cone fixed in the reference basis* $\underline{\mathbf{e}}^1$ (*herpolhode cone*). *Both cones are generated by the angular velocity vector* $\boldsymbol{\omega}(t)$.

This theorem is a direct consequence of the fact that the angular acceleration $\dot{\boldsymbol{\omega}}$ is identical in both cones and that it is tangent to both cones (Fig. 9.4).

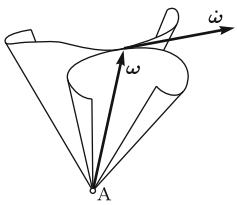

Fig. 9.4 Polhode cone and herpolhode cone

When the body has the degree of freedom one, its position is a function of a single variable, say ψ, and its angular velocity has in $\underline{\mathbf{e}}^2$ coordinates of the form $\omega_i = \dot{\psi}\, f_i(\psi)$ $(i = 1, 2, 3)$. This means that the shape of the polhode cone does not depend on the initial conditions of the motion. The same is true for the herpolhode cone. The shapes of the cones can help to detect unexpected relationships between differently defined motions. This is demonstrated by a motion defined in Sect. 10.1 and by the motion of the central cross in a Hooke's joint which is investigated in Sect. 13.1.1.

Any two bodies i and j with a common fixed point have relative to each other an angular velocity. Let $\boldsymbol{\omega}_{ij}$ be the angular velocity of body i relative to body j. Then the angular velocity of body j relative to body i (inverse motion) is

$$\boldsymbol{\omega}_{ji} = -\boldsymbol{\omega}_{ij} \,. \tag{9.71}$$

Three bodies i, j and k (arbitrary, different) with a common fixed point have relative to each other angular velocities $\boldsymbol{\omega}_{ij}$, $\boldsymbol{\omega}_{jk}$ and $\boldsymbol{\omega}_{ki}$. Repeated application of (9.8) yields the equation

$$\boldsymbol{\omega}_{ij} + \boldsymbol{\omega}_{jk} + \boldsymbol{\omega}_{ki} = \mathbf{0} \qquad (i, j, k \text{ arbitrary}) \,. \tag{9.72}$$

This shows that the instantaneous axes of rotation are coplanar and that the angular velocities form a closed planar triangle. Because of (9.71) this equation can also be written in the form

$$\boldsymbol{\omega}_{ij} + \boldsymbol{\omega}_{jk} = \boldsymbol{\omega}_{ik} \qquad (i, j, k \text{ arbitrary}) \,. \tag{9.73}$$

The equation is illustrated by the bevel gear pair shown in Fig. 9.5a. Two bevel wheels 1 and 2 are mounted in the frame 0. Their angular velocities $\boldsymbol{\omega}_{10}$ and $\boldsymbol{\omega}_{20}$ relative to the frame have the directions of the axes. The relative angular velocity $\boldsymbol{\omega}_{21}$ has the direction of the common generator of the two pitch cones. These pitch cones represent the fixed and the moving cone of the motion of one wheel relative to the other. Thus, the directions of the three angular velocities are prescribed by the design. If one of the angular velocities is prescribed, the other two are determined by (9.72). The equation requires that the vector triangle in Fig. 9.5b be closed.

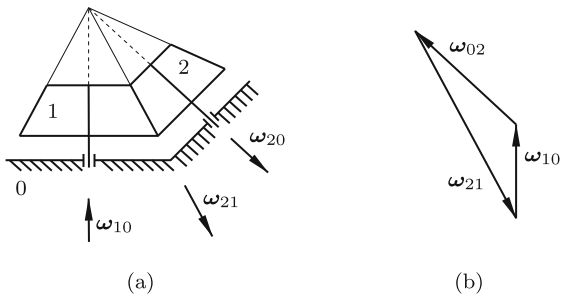

Fig. 9.5 Bevel gear pair **(a)** and angular velocity diagram **(b)**

The geometrical construction just demonstrated for two wheels is applicable to arbitrarily complicated bevel gear trains with degrees of freedom $F \geq 1$. All wheel axes as well as all generators of all pitch cones are passing through a common point. Every wheel axis and every generator common to the cones of two wheels determines the direction of a relative angular velocity.

This fact in combination with (9.71), (9.72) or (9.73) determines all angular velocities if F angular velocities are arbitrarily prescribed.

Example: In the bevel differential shown in Fig. 9.6a with bodies $0,\ldots,4$ the gear box 4 can rotate relative to the frame 0. The bevel differential has the degree of freedom $F = 2$. The lines with indices ij determine the directions of the angular velocities $\boldsymbol{\omega}_{ij}$ $(i,j = 0,\ldots,4\,;\, j \neq i)$. Any two angular velocities can be prescribed arbitrarily. Then the remaining ones are uniquely determined. In Fig. 9.6b the angular velocity diagram is shown. End of example.

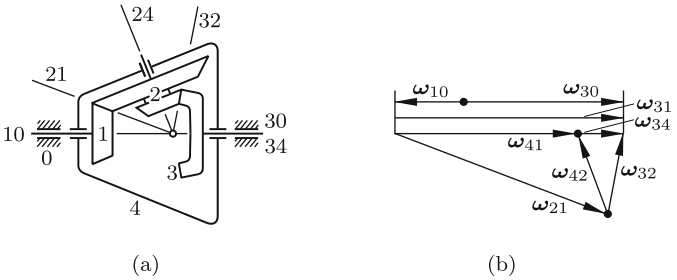

Fig. 9.6 Bevel differential **(a)** and angular velocity diagram **(b)**

9.7 The Ancient Chinese Southpointing Chariot

Subject of this section is an engineering problem. In Needham [7] it is reported that in China possibly as early as 3000 years ago and with certainty at about 200 a.C. during imperial processions two-wheel chariots were displayed on which a rotating wooden statue pointed its arm due south independent of driving maneuvers. In a rather detailed description dated 1107 a gear train connecting the wheels of the chariot to the vertical axis of the statue is described. In Fig. 9.7 the essential elements of a modern reconstruction by Lanchester [6] are shown. In the chariot (body 1) wheels 6 and 7 are rotating about vertical axes. These wheels are driven by wheel pairs 2, 4 and 3, 5, respectively. Together with the two wheels 8 wheels 6 and 7 constitute a bevel differential[2]. The statue 9 is rotated by the wheels 8. The system has only three parameters, namely, the width ℓ of the track, the radius r of the chariot wheels 2 and 3 and the angular velocity ratio

[2] In spite of its elaborate character the description of the year 1107 is not detailed enough. It does not prove the usage of a bevel differential. In Europe the bevel differential appears for the first time in the 18th century in clocks

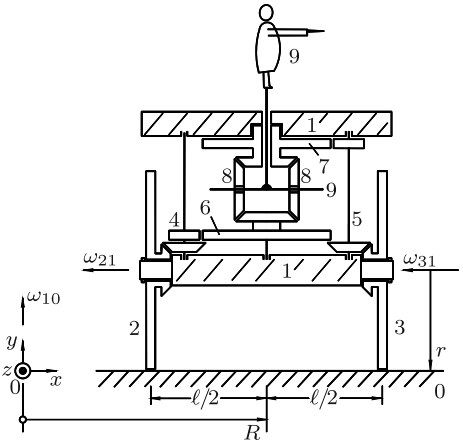

Fig. 9.7 Chinese southpointing chariot

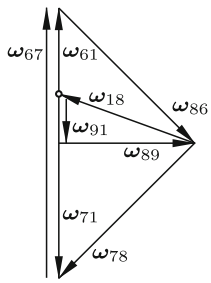

Fig. 9.8 Angular velocity diagram of the bevel differential

$|\omega_{61}/\omega_{21}| = |\omega_{71}/\omega_{31}| = i$. What are the conditions to be satisfied by these parameters in order to give the statue the desired property?
Solution: The gear train must realize the identity $\omega_{90} = \omega_{91} + \omega_{10} \equiv 0$, i.e.,

$$\omega_{91} \equiv -\omega_{10} \,. \tag{9.74}$$

As representative driving maneuver a circle with radius R about the center 0 and with angular velocity $\omega_{10} > 0$ of the chariot body is chosen. This maneuver causes angular velocities $\omega_{21} > 0$ and $\omega_{31} > 0$ in the directions shown in the figure. The points fixed on wheels 2 and 3 which are in contact with the ground have, in negative z-direction, the velocities $v_2 = \omega_{10}(R - \ell/2) - \omega_{21} r$ and $v_3 = \omega_{10}(R + \ell/2) - \omega_{31} r$, respectively. The rolling conditions require that $v_2 = v_3 = 0$. The difference of these two equations is

$$\omega_{31} - \omega_{21} = \frac{\ell}{r}\omega_{10} \,. \tag{9.75}$$

The given angular velocity ratio i yields

$$\omega_{61} = i\omega_{21} \,, \qquad \omega_{71} = -i\omega_{31} \qquad (> 0 \text{ in positive } y\text{-direction}) \,. \tag{9.76}$$

In Fig. 9.8 the angular velocity diagram of the bevel differential composed of the members 6, 7, 8 and 9 is shown. The directions of all angular velocities except $\boldsymbol{\omega}_{18}$ are prescribed by the design as shown. The magnitudes of $\boldsymbol{\omega}_{61}$ and $\boldsymbol{\omega}_{71}$ are chosen arbitrarily. They determine $\boldsymbol{\omega}_{67} = \boldsymbol{\omega}_{61} - \boldsymbol{\omega}_{71}$. First, $\boldsymbol{\omega}_{86}$ is determined from the vector equation $\boldsymbol{\omega}_{67} + \boldsymbol{\omega}_{78} + \boldsymbol{\omega}_{86} = \mathbf{0}$. Next, $\boldsymbol{\omega}_{18}$ is determined by the vector equation $\boldsymbol{\omega}_{61} + \boldsymbol{\omega}_{18} + \boldsymbol{\omega}_{86} = \mathbf{0}$. Finally, $\boldsymbol{\omega}_{91}$ and $\boldsymbol{\omega}_{89}$ are determined from the vector equation $\boldsymbol{\omega}_{91} + \boldsymbol{\omega}_{18} + \boldsymbol{\omega}_{89} = \mathbf{0}$. The angular velocity diagram reveals the relationship

$$\omega_{91} = \omega_{61} - \frac{1}{2}\omega_{67} = \omega_{61} - \frac{1}{2}(\omega_{61} - \omega_{71}) = \frac{1}{2}(\omega_{61} + \omega_{71}) \,. \tag{9.77}$$

Hence with (9.76)

$$\omega_{91} = \frac{i}{2}(\omega_{21} - \omega_{31}) \,. \tag{9.78}$$

Equations (9.74) and (9.75) yield

$$\omega_{91} = \frac{r}{\ell}(\omega_{21} - \omega_{31}) \,. \tag{9.79}$$

The identity of these two expressions is the condition to be satisfied by the system parameters:

$$i = \frac{2r}{\ell} \,. \tag{9.80}$$

The wheels shown in Fig. 9.7 do not satisfy this condition. Note: Precise functioning of the chariot requires a perfectly even terrain.

9.8 Acceleration Distribution. Instantaneous Center of Acceleration

The instantaneous acceleration distribution in a rigid body is determined by (9.14). It depends on the vectors $\mathbf{a}_\mathrm{A}$, $\boldsymbol{\omega}$ and $\dot{\boldsymbol{\omega}}$:

$$\mathbf{a} = \mathbf{a}_\mathrm{A} + \dot{\boldsymbol{\omega}} \times \boldsymbol{\varrho} + \boldsymbol{\omega} \times (\boldsymbol{\omega} \times \boldsymbol{\varrho}) \,. \tag{9.81}$$

If $\boldsymbol{\omega}$ and $\dot{\boldsymbol{\omega}}$ are not collinear, there exists a single body-fixed point G which instantaneously has zero acceleration. This point is called instantaneous *center of acceleration*. It is located on the so-called *inflection curve*. This is the geometric locus of all points characterized instantaneously by collinearity of acceleration $\mathbf{a}$ and velocity $\mathbf{v}$. The name is explained by the fact that points of inflection have this property. The condition is written in the form $\mathbf{a} = s\,\omega\,\mathbf{v}$, where s is a dimensionless parameter. Explicitly

$$\mathbf{a}_\mathrm{A} + \dot{\boldsymbol{\omega}} \times \boldsymbol{\varrho} + \boldsymbol{\omega} \times (\boldsymbol{\omega} \times \boldsymbol{\varrho}) = s\,\omega\,(\mathbf{v}_\mathrm{A} + \boldsymbol{\omega} \times \boldsymbol{\varrho}) \,. \tag{9.82}$$

This is a linear equation for $\boldsymbol{\varrho}(s)$. The center of acceleration G is the point $\boldsymbol{\varrho}_\mathrm{G} = \boldsymbol{\varrho}(s = 0)$. For $\boldsymbol{\varrho}$ the ansatz is made:

$$\boldsymbol{\varrho} = c_1 \mathbf{a}_\mathrm{A} + c_2 \dot{\boldsymbol{\omega}} + c_3 \boldsymbol{\omega} \,. \tag{9.83}$$

Substitution into (9.82) and scalar multiplications by $\mathbf{a}_\mathrm{A}$, by $\dot{\boldsymbol{\omega}}$ and by $\boldsymbol{\omega}$ result in linear equations for c_1, c_2, c_3:

$$\begin{bmatrix} (\boldsymbol{\omega}\times\mathbf{a}_{\mathrm{A}})^2 & (\boldsymbol{\omega}\times\dot{\boldsymbol{\omega}})\cdot(\boldsymbol{\omega}\times\mathbf{a}_{\mathrm{A}}+s\,\omega\mathbf{a}_{\mathrm{A}}) & \boldsymbol{\omega}\times\dot{\boldsymbol{\omega}}\cdot\mathbf{a}_{\mathrm{A}} \\ (\boldsymbol{\omega}\times\dot{\boldsymbol{\omega}})\cdot(\boldsymbol{\omega}\times\mathbf{a}_{\mathrm{A}}-s\,\omega\mathbf{a}_{\mathrm{A}}) & (\boldsymbol{\omega}\times\dot{\boldsymbol{\omega}})^2 & 0 \\ -\boldsymbol{\omega}\times\dot{\boldsymbol{\omega}}\cdot\mathbf{a}_{\mathrm{A}} & 0 & 0 \end{bmatrix} \begin{bmatrix} c_1 \\ c_2 \\ c_3 \end{bmatrix} = \begin{bmatrix} (\mathbf{a}_{\mathrm{A}}-s\,\omega\mathbf{v}_{\mathrm{A}})\cdot\mathbf{a}_{\mathrm{A}} \\ (\mathbf{a}_{\mathrm{A}}-s\,\omega\mathbf{v}_{\mathrm{A}})\cdot\dot{\boldsymbol{\omega}} \\ (\mathbf{a}_{\mathrm{A}}-s\,\omega\mathbf{v}_{\mathrm{A}})\cdot\boldsymbol{\omega} \end{bmatrix} . \quad (9.84)$$

c_1 is linear in s, c_2 is of second order in s, and c_3 is of third order.

The ansatz (9.83) fails, when A is the striction point S because $\mathbf{a}_{\mathrm{S}}$, $\dot{\boldsymbol{\omega}}$ and $\boldsymbol{\omega}$ are coplanar (see (9.60)). In this case, the vectors in (9.82) are decomposed in the canonical reference frame defined in the text following (9.62). Its basis vectors are $\mathbf{e}_1 = \boldsymbol{\omega}\times\dot{\boldsymbol{\omega}}/|\boldsymbol{\omega}\times\dot{\boldsymbol{\omega}}|$, $\mathbf{e}_2 = \mathbf{n}_{\mathrm{S}}$ (normal to the tangent plane of the raccording axodes at the striction point S) and $\mathbf{e}_3 = \boldsymbol{\omega}/|\boldsymbol{\omega}|$. The coordinate matrices of $\boldsymbol{\varrho}$, $\boldsymbol{\omega}$, $\dot{\boldsymbol{\omega}}$, $\mathbf{v}_{\mathrm{S}}$ and $\mathbf{a}_{\mathrm{S}}$ are written in the forms

$$\underline{\varrho} = \begin{bmatrix} x \\ y \\ z \end{bmatrix}, \quad \underline{\omega} = \omega \begin{bmatrix} 0 \\ 0 \\ 1 \end{bmatrix}, \quad \underline{\dot{\omega}} = \mu\omega^2 \begin{bmatrix} 0 \\ \sin\alpha \\ \cos\alpha \end{bmatrix}, \quad \underline{v}_{\mathrm{S}} = p\,\omega \begin{bmatrix} 0 \\ 0 \\ 1 \end{bmatrix}, \quad \underline{a}_{\mathrm{S}} = \ell\mu\omega^2 \begin{bmatrix} 0 \\ \sin\beta \\ \cos\beta \end{bmatrix} . \quad (9.85)$$

With this notation decomposition of (9.82) results in the equations

$$\begin{bmatrix} 1 & \mu\cos\alpha + s & -\mu\sin\alpha \\ -(\mu\cos\alpha + s) & 1 & 0 \\ \mu\sin\alpha & 0 & 0 \end{bmatrix} \begin{bmatrix} x \\ y \\ z \end{bmatrix} = \begin{bmatrix} 0 \\ \ell\,\mu\sin\beta \\ \ell\,\mu\cos\beta - sp \end{bmatrix} . \quad (9.86)$$

x is linear in s, y is of second order in s, and z is of third order. Hence the projection of the inflection curve onto the x, y-plane is a parabola and the projection onto the x, z-plane is a cubical parabola. With $s = 0$ the equations yield the coordinates of the center of acceleration G:

$$\begin{bmatrix} x_{\mathrm{G}} \\ y_{\mathrm{G}} \\ z_{\mathrm{G}} \end{bmatrix} = \frac{\ell}{\sin\alpha} \begin{bmatrix} \cos\beta \\ \mu\cos(\beta-\alpha) \\ \mu\sin(\beta-\alpha) + \dfrac{(1+\mu^2)\cos\beta}{\mu\sin\alpha} \end{bmatrix} . \quad (9.87)$$

Next, the instantaneous acceleration distribution (9.81) is considered. As point A the center of acceleration G is chosen. The acceleration is written as product of a tensor with $\boldsymbol{\varrho}$:

$$\mathbf{a} = (\dot{\boldsymbol{\omega}}\times\mathsf{I} + \boldsymbol{\omega}\,\boldsymbol{\omega} - \boldsymbol{\omega}^2\,\mathsf{I})\cdot\boldsymbol{\varrho} . \quad (9.88)$$

This equation shows that the accelerations of all body-fixed points located on a ray emanating from G have equal directions. Their magnitudes are proportional to the distance $|\boldsymbol{\varrho}|$ from G. In general, the direction is neither orthogonal to nor collinear with $\boldsymbol{\varrho}$. This gives rise to the following problems (Veldkamp [12]). Determine all straight lines passing through the center of acceleration all points of which have accelerations which are (a) orthogonal to the line or (b) collinear with the line.

Problem (a): Orthogonality means that $\mathbf{a} \cdot \boldsymbol{\varrho} = 0$, i.e.,

$$(\boldsymbol{\omega} \cdot \boldsymbol{\varrho})^2 - \boldsymbol{\omega}^2 \boldsymbol{\varrho}^2 = -(\boldsymbol{\omega} \times \boldsymbol{\varrho})^2 = 0 \,. \tag{9.89}$$

The solution is $\boldsymbol{\varrho} = \lambda_0 \boldsymbol{\omega}$ where λ_0 is an arbitrary scalar having the physical dimension length×time. This means that the only straight line passing through G which solves this problem is the line parallel to the instantaneous screw axis. The accelerations of the points on this line are $\mathbf{a} = \lambda_0 \dot{\boldsymbol{\omega}} \times \boldsymbol{\omega}$.

Problem (b): Collinearity means that $\mathbf{a}$ has the form $\mathbf{a} = \lambda \omega^2 \boldsymbol{\varrho}$ where λ is an indeterminate dimensionless scalar. With this expression (9.88) takes the form

$$[\dot{\boldsymbol{\omega}} \times \mathsf{I} + \boldsymbol{\omega}\,\boldsymbol{\omega} - \omega^2(1+\lambda)\,\mathsf{I}\,] \cdot \boldsymbol{\varrho} = \mathbf{0} \,. \tag{9.90}$$

The vectors in this equation are decomposed in the reference frame with origin G and with axes parallel to the canonical reference frame, so that $\boldsymbol{\omega}$ and $\dot{\boldsymbol{\omega}}$ have the coordinates given in (9.85). This results in the coordinate equation

$$\begin{bmatrix} -(1+\lambda) & -\mu\cos\alpha & \mu\sin\alpha \\ \mu\cos\alpha & -(1+\lambda) & 0 \\ -\mu\sin\alpha & 0 & -\lambda \end{bmatrix} \underline{\varrho} = \underline{0} \,. \tag{9.91}$$

This represents an eigenvalue problem with eigenvalues λ_i $(i = 1, 2, 3)$ and with associated eigenvectors $\underline{\varrho}_i$. The characteristic equation is

$$\lambda^3 + 2\lambda^2 + (1+\mu^2)\lambda + \mu^2 \sin^2\alpha = 0 \tag{9.92}$$

or $\lambda(\lambda+1)^2 + \mu^2(\lambda + \sin^2\alpha) = 0$. Real eigenvalues are in the interval $-\sin^2\alpha < \lambda < 0$. From this and from the equation $\mathbf{a} = \lambda\omega^2\boldsymbol{\varrho}$ it follows that the collinear vectors $\mathbf{a}$ and $\boldsymbol{\varrho}$ have opposite signs. This means that the accelerations of all points located on the straight lines determined by the eigenvectors are directed toward the center of acceleration G. The discriminant of the equation is (see Bronstein/Semendjajew/Musiol/Mühlig [3]):

$$D = \frac{\mu^2}{27}\left[\mu^4 + \frac{1}{4}\mu^2(27\cos^4\alpha - 18\cos^2\alpha - 1) + \cos^2\alpha\right] . \tag{9.93}$$

The equation $D = 0$ is a quadratic equation for μ^2 as function of $\cos\alpha$ and also a quadratic equation for $\cos^2\alpha$ as function of μ. The equation has the double root $\mu^2 = 1/3$ if $\cos\alpha = 1/3$. Real solutions exist only for $0 < \mu^2 \le 1/3$ and for $0 < |\cos\alpha| \le 1/3$. In a diagram with axes $\cos\alpha$ and μ the curve $D = 0$ separates the domain $D < 0$ with three real eigenvectors from the domain $D > 0$ with a single real eigenvector. At the point $\mu^2 = 1/3$, $\cos\alpha = 1/3$ the curve has a cusp. With these parameter values the characteristic Eq.(9.92) has the form $(\lambda + 2/3)^3 = 0$.

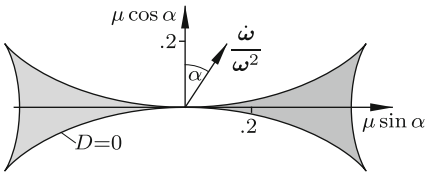

Fig. 9.9 Domains with three eigenvectors (shaded) and with a single eigenvector

The triple eigenvalue $\lambda = -2/3$ is associated with the single eigenvector $\underline{\varrho} = [\,1/\sqrt{2}\;\; 1/\sqrt{6}\;\; 1/\sqrt{3}\,]^T$.

In Fig. 9.9 the curve $D = 0$ is shown not in the $\cos\alpha, \mu$-diagram, but in a diagram with axes $\mu \sin\alpha$ and $\mu \cos\alpha$. According to (9.85) these are the coordinates of the vector $\dot{\boldsymbol{\omega}}/\boldsymbol{\omega}^2$ in the plane of $\boldsymbol{\omega}$ and $\dot{\boldsymbol{\omega}}$. The unit vector $\boldsymbol{\omega}/|\boldsymbol{\omega}|$ is directed along the $\mu \cos\alpha$-axis (see (9.85)). Three real eigenvectors exist if the vector $\dot{\boldsymbol{\omega}}/\boldsymbol{\omega}^2$ terminates in the shaded domain $D < 0$.

Three real eigenvectors are not mutually orthogonal. Let β_i be the angle between the eigenvector $\boldsymbol{\varrho}_i$ and $\boldsymbol{\omega}$. With the coordinates $\varrho_{i_1}, \varrho_{i_2}, \varrho_{i_3}$ of $\boldsymbol{\varrho}_i$

$$\cos^2\beta_i = \frac{\varrho_{i_3}^2}{\varrho_{i_1}^2 + \varrho_{i_2}^2 + \varrho_{i_3}^2} \qquad (i = 1, 2, 3)\,. \tag{9.94}$$

From the last two Eqs.(9.91) it follows that

$$\varrho_{i_2} = \varrho_{i_1} \frac{\mu \cos\alpha}{1 + \lambda_i}\,, \qquad \varrho_{i_3} = -\varrho_{i_1} \frac{\mu \sin\alpha}{\lambda_i}\,. \tag{9.95}$$

Hence

$$\begin{aligned} \cos^2\beta_i &= \frac{(1+\lambda_i)^2\mu^2 \sin^2\alpha}{\lambda_i^2(1+\lambda_i)^2 + \lambda_i^2\mu^2\cos^2\alpha + (1+\lambda_i)^2\mu^2\sin^2\alpha} \\ &= \frac{(1+\lambda_i)^2\mu^2 \sin^2\alpha}{\lambda_i[\lambda_i^3 + 2\lambda_i^2 + (1+\mu^2)\lambda_i + \mu^2\sin^2\alpha] + (1+\lambda_i)\mu^2\sin^2\alpha} \\ &= 1 + \lambda_i \end{aligned} \tag{9.96}$$

(because of (9.92)). Consequently, $\lambda_i = -\sin^2\beta_i$. The sum of the three eigenvalues equals -2 (factor 2 of λ^2 in (9.92)). Hence

$$\sum_{i=1}^{3} \cos^2\beta_i = 1\,. \tag{9.97}$$

This result is due to Bottema [1]. From $\lambda > -\sin^2\alpha$ it follows that $\sin^2\beta_i < \sin^2\alpha \quad (i = 1, 2, 3)$.

Example: With $\mu = 1/2$ and $\cos\alpha = 1/4$ (9.92) has three real roots $\lambda_1 = -3/4$, $\lambda_{2,3} = (\pm\sqrt{5} - 5)/8$. From (9.95) the associated normalized eigenvectors are calculated:

$\underline{\varrho}_1 = [\,\sqrt{15}/5 \quad \sqrt{15}/10 \quad 1/2 \quad]^T$,

$\underline{\varrho}_{2,3} = [\,\sqrt{3}/3 \quad (\sqrt{3} \mp \sqrt{15}/3)/4 \quad (\sqrt{5} \pm 1)/4\ ]^T$.

The third coordinates are the cosines in (9.97): $\cos\beta_1 = 1/2$, $\cos\beta_{2,3} = (\sqrt{5} \pm 1)/4$ ($\beta_1 = 60°$, $\beta_2 = 36°$, $\beta_3 = 72°$). End of example.

A line not passing through the center of acceleration is specified by the equation $\boldsymbol{\varrho}(\lambda) = \boldsymbol{\varrho}_0 + \lambda\mathbf{n}$ with the dimensionless unit vector $\mathbf{n}$ along the line and the perpendicular $\boldsymbol{\varrho}_0 \neq \mathbf{0}$ from the center of acceleration onto the line (hence $\boldsymbol{\varrho}_0 \cdot \mathbf{n} = 0$). The point $\boldsymbol{\varrho}(\lambda)$ has the acceleration

$$\mathbf{a}(\lambda) = \dot{\boldsymbol{\omega}} \times \boldsymbol{\varrho}_0 + \boldsymbol{\omega} \times (\boldsymbol{\omega} \times \boldsymbol{\varrho}_0) + \lambda[\dot{\boldsymbol{\omega}} \times \mathbf{n} + \boldsymbol{\omega} \times (\boldsymbol{\omega} \times \mathbf{n})] \,. \tag{9.98}$$

On every line not parallel to the ISA exactly one point has an acceleration perpendicular to the line. The pertinent value of λ is determined from the condition $\mathbf{a}(\lambda) \cdot \mathbf{n} = 0$. This is the equation

$$\dot{\boldsymbol{\omega}} \times \boldsymbol{\varrho}_0 \cdot \mathbf{n} + (\boldsymbol{\omega} \cdot \boldsymbol{\varrho}_0)(\boldsymbol{\omega} \cdot \mathbf{n}) - \lambda(\boldsymbol{\omega} \times \mathbf{n})^2 = 0 \,. \tag{9.99}$$

Next, lines and points on these lines are determined which have an acceleration along the line. The condition is $\mathbf{a}(\lambda) = \nu\mathbf{n}$ with an arbitrary scalar ν of dimension acceleration. Suppose that $\mathbf{n}$ is given. Then the equation is a linear equation for λ and for two coordinates of $\boldsymbol{\varrho}_0$ in the plane perpendicular to $\mathbf{n}$. The solutions are proportional to ν , i.e., of the form $\lambda = (\nu/\nu^*)\lambda^*$, $\boldsymbol{\varrho}_0 = (\nu/\nu^*)\boldsymbol{\varrho}_0^*$ where λ^* and $\boldsymbol{\varrho}_0^*$ are the solutions for an arbitrary reference value ν^* . They determine uniquely a straight line $(\nu/\nu^*)(\boldsymbol{\varrho}_0^* + \lambda^*\mathbf{n})$ through the center of acceleration. All points of this line, and these points only, have accelerations in the direction of $\mathbf{n}$. It remains to be shown that the coefficient matrix of λ and $\boldsymbol{\varrho}_0$ is nonsingular. Decomposition in a system in which $\mathbf{n}$ and $\boldsymbol{\varrho}_0$ have the coordinate matrices $[\,1\ 0\ 0\,]^T$ and $[\,0\ y\ z\,]^T$, respectively, results in the equation

$$\begin{bmatrix} -(\omega_2^2 + \omega_3^2) & -\dot{\omega}_3 + \omega_1\omega_2 & \dot{\omega}_2 + \omega_3\omega_1 \\ \dot{\omega}_3 + \omega_1\omega_2 & -(\omega_3^2 + \omega_1^2) & -\dot{\omega}_1 + \omega_2\omega_3 \\ -\dot{\omega}_2 + \omega_3\omega_1 & \dot{\omega}_1 + \omega_2\omega_3 & -(\omega_1^2 + \omega_2^2) \end{bmatrix} \begin{bmatrix} \lambda \\ y \\ z \end{bmatrix} = \nu \begin{bmatrix} 1 \\ 0 \\ 0 \end{bmatrix} \,. \tag{9.100}$$

It is straight-forward to show that the determinant of the coefficient matrix is $-(\dot{\boldsymbol{\omega}} \times \boldsymbol{\omega})^2 \neq 0$.

Next, (9.88) is used for determining the surface defined by all body-fixed points $\boldsymbol{\varrho}$ which have an acceleration of prescribed absolute value $|\mathbf{a}|$ (arbitrary). The vectors are again decomposed in the reference frame with origin G . With the coordinates of $\boldsymbol{\varrho}$, $\boldsymbol{\omega}$ and $\dot{\boldsymbol{\omega}}$ given in (9.85) the acceleration has the coordinates

$$\underline{a} = \omega^2[\,-x - y\mu\cos\alpha + z\mu\sin\alpha\ ,\ -y + x\mu\cos\alpha\ ,\ -x\mu\sin\alpha\,]\,. \quad (9.101)$$

On the desired surface the sum of squares equals a^2. This is the second-order equation

$$x^2(1+\mu^2)+y^2(1+\mu^2\cos^2\alpha)+z^2\mu^2\sin^2\alpha-2xz\mu\sin\alpha-2yz\mu^2\sin\alpha\cos\alpha = \frac{a^2}{\omega^4} \quad (9.102)$$

or $[\,x\ y\ z\,]\,\underline{A}\,[\,x\ y\ z\,]^T = a^2/\omega^4$ with the symmetric matrix

$$\underline{A} = \begin{bmatrix} 1+\mu^2 & 0 & -\mu\sin\alpha \\ 0 & 1+\mu^2\cos^2\alpha & -\mu^2\sin\alpha\cos\alpha \\ -\mu\sin\alpha & -\mu^2\sin\alpha\cos\alpha & \mu^2\sin^2\alpha \end{bmatrix}\,. \quad (9.103)$$

This matrix has real eigenvalues $\lambda_1\,,\,\lambda_2\,,\,\lambda_3$ and mutually perpendicular eigenvectors. In terms of the eigenvalues and in the $\overline{x},\overline{y},\overline{z}$-system of principal axes defined by the eigenvectors the equation is

$$\lambda_1\overline{x}^2 + \lambda_2\overline{y}^2 + \lambda_3\overline{z}^2 = \frac{a^2}{\omega^4}\,. \quad (9.104)$$

Both the eigenvalues and the eigenvectors are independent of a. The eigenvalues are the roots of the characteristic equation $\det(\underline{A} - \lambda\underline{I}) = 0$:

$$\lambda^3 - 2\lambda^2(1+\mu^2) + \lambda(1+\mu^2)^2 - \mu^4\sin^4\alpha = 0\,. \quad (9.105)$$

They are positive. This is seen by writing the equation in the form $\lambda[\lambda - (1+\mu^2)]^2 = \mu^4\sin^4\alpha$. Hence the surface is an ellipsoid. Vieta's theorem establishes for the eigenvalues the equations $\lambda_1+\lambda_2+\lambda_3 = 2(1+\mu^2)$ and $\lambda_1\lambda_2+\lambda_2\lambda_3+\lambda_3\lambda_1 = (1+\mu^2)^2$, whence it follows that

$$(\lambda_1+\lambda_2+\lambda_3)^2 - 4(\lambda_1\lambda_2+\lambda_2\lambda_3+\lambda_3\lambda_1) = 0 \quad (9.106)$$

or

$$\lambda_1^2+\lambda_2^2+\lambda_3^2 - 2(\lambda_1\lambda_2+\lambda_2\lambda_3+\lambda_3\lambda_1) = 0 \quad (9.107)$$

or

$$\left(\sqrt{\lambda_1}+\sqrt{\lambda_2}+\sqrt{\lambda_3}\right)\left(-\sqrt{\lambda_1}+\sqrt{\lambda_2}+\sqrt{\lambda_3}\right)\left(\sqrt{\lambda_1}-\sqrt{\lambda_2}+\sqrt{\lambda_3}\right)\left(\sqrt{\lambda_1}+\sqrt{\lambda_2}-\sqrt{\lambda_3}\right) = 0\,. \quad (9.108)$$

Let λ_1 be the largest eigenvalue. Then $\sqrt{\lambda_1} = \sqrt{\lambda_2}+\sqrt{\lambda_3}$. The ith principal semi-axis of the ellipsoid is $b_i = a/(\omega^2\sqrt{\lambda_i})$ $(i = 1,2,3)$. Hence[3] $1/b_1 = 1/b_2 + 1/b_3$ independent of a, μ and α.

[3] in [2] it is mistakenly said that b_i is proportional to $\sqrt{\lambda_i}$ and that, consequently, $b_1 = b_2 + b_3$

Example: $\mu = 2$, $\alpha = 45^\circ$ yield $\lambda_1 = 3 + 2\sqrt{2}$, $\lambda_2 = 4$, $\lambda_3 = 3 - 2\sqrt{2}$, $b_1 = (\sqrt{2} - 1)a/\omega^2$, $b_2 = \frac{1}{2}\, a/\omega^2$, $b_3 = (\sqrt{2} + 1)a/\omega^2$. This concludes the investigation.

Given a body-fixed plane E by its Eq.(2.1) , $\mathbf{m} \cdot \boldsymbol{\varrho} = -1$, determine all points $\boldsymbol{\varrho}$ of E the accelerations of which are (a) in-plane or (b) perpendicular to the plane. The same problems with *velocity* instead of *acceleration* were solved by Eqs.(9.26) – (9.28) and (9.38) for planes given in the x, y, z-system underlying these equations. In the present case, the plane is given in the reference system with origin G and with the coordinates (9.85).

Problem (a): Vectors $\boldsymbol{\varrho}$ satisfy the equations $\mathbf{m} \cdot \boldsymbol{\varrho} = -1$ and $\mathbf{m} \cdot \mathbf{a}/\omega^2 = 0$. With the coordinates (9.101) of $\mathbf{a}$ the first equation and the sum of both equations are written as linear equations for x and y in terms of z :

$$\left.\begin{array}{ll} x m_x & + y m_y = -(1 + z m_z) \,, \\ x\mu(m_y \cos\alpha - m_z \sin\alpha) & - y \mu m_x \cos\alpha = -[1 + z(\mu m_x \sin\alpha + m_z)] \,. \end{array}\right\} \tag{9.109}$$

The solution $x(z)$, $y(z)$ determines a straight line in E . No such line exists in planes with normal vectors $\mathbf{m}$ satisfying the condition that the coefficient determinant is zero. This condition is $(m_x^2 + m_y^2)\cos\alpha - m_y m_z \sin\alpha = 0$ or (see (9.28) and (9.85)) $[\mathbf{m} \times (\boldsymbol{\omega} \times \mathbf{m})] \cdot \dot{\boldsymbol{\omega}} = 0$ or $(\mathbf{m} \times \boldsymbol{\omega}) \cdot (\mathbf{m} \times \dot{\boldsymbol{\omega}}) = 0$. This shows that $\mathbf{m} = c\,\boldsymbol{\omega}$ and $\mathbf{m} = c\,\dot{\boldsymbol{\omega}}$ with $c = \text{const}$ (arbitrary) are special solutions. The general solution is obtained by writing the scalar equation in the form $m_x^2 + (m_y - \frac{1}{2} m_z \tan\alpha)^2 = (\frac{1}{2} m_z \tan\alpha)^2$. This is, with the free parameter m_z , the equation of a cone. The cone intersects the plane $m_z = \text{const}$ in a circle. Every vector $\mathbf{m}$ along a generator of the cone is a solution. The special solutions $\mathbf{m} = c\,\boldsymbol{\omega}$ and $\mathbf{m} = c\,\dot{\boldsymbol{\omega}}$ are vectors along the two generators in the plane $m_x = 0$.

Problem (b): Vectors $\boldsymbol{\varrho}$ satisfy the equations $\mathbf{m} \cdot \boldsymbol{\varrho} = -1$ and $\lambda \mathbf{m} = \mathbf{a}/\omega^2$ with an indeterminate scalar λ . Decomposition of all vectors results in four linear equations for x , y , z and λ :

$$\begin{bmatrix} 1 & \mu\cos\alpha & -\mu\sin\alpha & m_x \\ -\mu\cos\alpha & 1 & 0 & m_y \\ \mu\sin\alpha & 0 & 0 & m_z \\ m_x & m_y & m_z & 0 \end{bmatrix} \begin{bmatrix} x \\ y \\ z \\ \lambda \end{bmatrix} = \begin{bmatrix} 0 \\ 0 \\ 0 \\ -1 \end{bmatrix} \,. \tag{9.110}$$

The solution determines a single point in E . No such point exists in planes satisfying the condition that the coefficient determinant is zero. This condition is $m_z^2 + \mu^2 (m_y \sin\alpha + m_z \cos\alpha)^2 = 0$, i.e., $m_y = m_z = 0$. These planes are parallel to the plane spanned by $\boldsymbol{\omega}$ and $\dot{\boldsymbol{\omega}}$.

9.9 Angular Acceleration of a Body in Terms of Positions, Velocities and Accelerations of Three Points

Problem statement: In some reference basis the instantaneous position vectors $\mathbf{r}_1$, $\mathbf{r}_2$, $\mathbf{r}_3$ of three noncollinear points P_1, P_2, P_3 of a rigid body as well as the instantaneous velocities $\mathbf{v}_1$, $\mathbf{v}_2$, $\mathbf{v}_3$ and the instantaneous accelerations $\mathbf{a}_1$, $\mathbf{a}_2$, $\mathbf{a}_3$ of these points are given. In Sect. 9.4 the instantaneous angular velocity $\boldsymbol{\omega}$ of the body was expressed in terms of $\mathbf{r}_1$, $\mathbf{r}_2$, $\mathbf{r}_3$ and $\mathbf{v}_1$, $\mathbf{v}_2$, $\mathbf{v}_3$ (see (9.46), (9.47) and (9.52)). In the present section a cyclicly symmetric expression is developed for the angular acceleration $\dot{\boldsymbol{\omega}}$ of the body. The method of solution is similar to the one used for determining $\boldsymbol{\omega}$. Let A be an arbitrary body-fixed point and let $\boldsymbol{\varrho}_i$ be the vector pointing from A to P_i. Then $\boldsymbol{\omega} \times \boldsymbol{\varrho}_i = \mathbf{v}_i - \mathbf{v}_\mathrm{A}$. With this expression Eq.(9.81) for the acceleration $\mathbf{a}_i$ takes the form $\mathbf{a}_i = \mathbf{a}_\mathrm{A} + \dot{\boldsymbol{\omega}} \times \boldsymbol{\varrho}_i + \boldsymbol{\omega} \times (\mathbf{v}_i - \mathbf{v}_\mathrm{A})$ $(i = 1, 2, 3)$. The difference of two of these equations reads

$$\mathbf{a}_i - \mathbf{a}_j - \boldsymbol{\omega} \times (\mathbf{v}_i - \mathbf{v}_j) = \dot{\boldsymbol{\omega}} \times (\mathbf{r}_i - \mathbf{r}_j) \qquad (i, j = 1, 2, 3)\,. \tag{9.111}$$

This equation serves as starting point just as (9.41) was the starting point for formulating $\boldsymbol{\omega}$. The equivalent to (9.42) is the equation

$$\begin{aligned}[\mathbf{a}_1 - \mathbf{a}_3 - \boldsymbol{\omega} \times (\mathbf{v}_1 - \mathbf{v}_3)] \times [\mathbf{a}_2 - \mathbf{a}_3 - \boldsymbol{\omega} \times (\mathbf{v}_2 - \mathbf{v}_3)] \\ = -\dot{\boldsymbol{\omega}}\,(\mathbf{r}_1 - \mathbf{r}_3) \cdot [\mathbf{a}_2 - \mathbf{a}_3 - \boldsymbol{\omega} \times (\mathbf{v}_2 - \mathbf{v}_3)]\end{aligned} \tag{9.112}$$

If the scalar product on the right-hand side is nonzero,

$$\dot{\boldsymbol{\omega}} = \frac{[\mathbf{a}_1 - \mathbf{a}_3 - \boldsymbol{\omega} \times (\mathbf{v}_1 - \mathbf{v}_3)] \times [\mathbf{a}_2 - \mathbf{a}_3 - \boldsymbol{\omega} \times (\mathbf{v}_2 - \mathbf{v}_3)]}{(\mathbf{r}_3 - \mathbf{r}_1) \cdot [\mathbf{a}_2 - \mathbf{a}_3 - \boldsymbol{\omega} \times (\mathbf{v}_2 - \mathbf{v}_3)]}\,. \tag{9.113}$$

The numerator (abbreviated N) is multiplied out:

$$\begin{aligned}N = (\mathbf{a}_1 - \mathbf{a}_3) \times (\mathbf{a}_2 - \mathbf{a}_3) + [\boldsymbol{\omega} \times (\mathbf{v}_1 - \mathbf{v}_3)] \times [\boldsymbol{\omega} \times (\mathbf{v}_2 - \mathbf{v}_3)] \\ + [\boldsymbol{\omega} \times (\mathbf{v}_2 - \mathbf{v}_3)] \times (\mathbf{a}_1 - \mathbf{a}_3) - [\boldsymbol{\omega} \times (\mathbf{v}_1 - \mathbf{v}_3)] \times (\mathbf{a}_2 - \mathbf{a}_3)\,.\end{aligned} \tag{9.114}$$

Multiplying out further and rearranging terms results in the cyclicly symmetric expression

$$N = \sum_{i=1}^{3} \mathbf{a}_i \times [\mathbf{a}_j - \boldsymbol{\omega} \times (\mathbf{v}_j - \mathbf{v}_k)] + \boldsymbol{\omega}\boldsymbol{\omega} \cdot (\mathbf{v}_1 \times \mathbf{v}_2 + \mathbf{v}_2 \times \mathbf{v}_3 + \mathbf{v}_3 \times \mathbf{v}_1) \tag{9.115}$$

$(i, j, k = 1, 2, 3 \text{ cyclic})$. Next, the denominator in (9.113) (abbreviated D) is given a symmetric form. The equation $(\mathbf{r}_3 - \mathbf{r}_1) \cdot (\mathbf{r}_2 - \mathbf{r}_3) = \text{const}$ expressing the rigid-body property is differentiated twice with respect to time. This

yields

$$(\mathbf{r}_3-\mathbf{r}_1)\cdot(\mathbf{a}_2-\mathbf{a}_3)=-(\mathbf{a}_3-\mathbf{a}_1)\cdot(\mathbf{r}_2-\mathbf{r}_3)-2(\mathbf{v}_3-\mathbf{v}_1)\cdot(\mathbf{v}_2-\mathbf{v}_3)\ . \quad (9.116)$$

If to both sides of this equation the expression $(\mathbf{r}_3-\mathbf{r}_1)\cdot[\mathbf{a}_2-\mathbf{a}_3-2\boldsymbol{\omega}\times(\mathbf{v}_2-\mathbf{v}_3)]$ is added, the left-hand side turns out to be $2D$. Therefore,

$$\begin{aligned} D=\frac{1}{2}\Big[&(\mathbf{r}_3-\mathbf{r}_1)\cdot(\mathbf{a}_2-\mathbf{a}_3)-(\mathbf{a}_3-\mathbf{a}_1)\cdot(\mathbf{r}_2-\mathbf{r}_3)\Big]\\ &-(\mathbf{v}_3-\mathbf{v}_1)\cdot(\mathbf{v}_2-\mathbf{v}_3)-(\mathbf{r}_3-\mathbf{r}_1)\cdot\boldsymbol{\omega}\times(\mathbf{v}_2-\mathbf{v}_3)\ . \end{aligned} \quad (9.117)$$

The last two terms cancel each other (interchange the multiplication symbols and note that $(\mathbf{r}_3-\mathbf{r}_1)\times\boldsymbol{\omega}=-(\mathbf{v}_3-\mathbf{v}_1)$). The remaining terms have the desired symmetry property. Multiplying out yields the final result

$$\begin{aligned} \dot{\boldsymbol{\omega}}=2\,&\frac{\displaystyle\sum_{i=1}^{3}\mathbf{a}_i\times[\mathbf{a}_j-\boldsymbol{\omega}\times(\mathbf{v}_j-\mathbf{v}_k)]+\boldsymbol{\omega}\boldsymbol{\omega}\cdot(\mathbf{v}_1\times\mathbf{v}_2+\mathbf{v}_2\times\mathbf{v}_3+\mathbf{v}_3\times\mathbf{v}_1)}{\mathbf{a}_1\cdot(\mathbf{r}_2-\mathbf{r}_3)+\mathbf{a}_2\cdot(\mathbf{r}_3-\mathbf{r}_1)+\mathbf{a}_3\cdot(\mathbf{r}_1-\mathbf{r}_2)}\\ &(i,j,k=1,2,3\ \text{cyclic})\ . \end{aligned} \quad (9.118)$$

The angular velocity $\boldsymbol{\omega}$ is given either by (9.46) or by (9.52).

If in (9.112) the scalar product on the right-hand side is zero, also the left-hand side is zero. Because of (9.111) this means that the vectors $\dot{\boldsymbol{\omega}}\times(\mathbf{r}_1-\mathbf{r}_3)$ and $\dot{\boldsymbol{\omega}}\times(\mathbf{r}_2-\mathbf{r}_3)$ are collinear. From this it follows that $\dot{\boldsymbol{\omega}}$ is in the plane of the points P_1, P_2, P_3. Consequently, there exist coefficients λ and μ such that

$$\dot{\boldsymbol{\omega}}=\lambda(\mathbf{r}_1-\mathbf{r}_2)+\mu(\mathbf{r}_2-\mathbf{r}_3)\ . \quad (9.119)$$

This ansatz yields

$$\left.\begin{aligned} \mathbf{a}_3-\mathbf{a}_2-\boldsymbol{\omega}\times(\mathbf{v}_3-\mathbf{v}_2)&=\dot{\boldsymbol{\omega}}\times(\mathbf{r}_3-\mathbf{r}_2)=\lambda\mathbf{n}\ ,\\ \mathbf{a}_1-\mathbf{a}_2-\boldsymbol{\omega}\times(\mathbf{v}_1-\mathbf{v}_2)&=\dot{\boldsymbol{\omega}}\times(\mathbf{r}_1-\mathbf{r}_2)=\mu\mathbf{n}\ , \end{aligned}\right\} \quad (9.120)$$

where $\mathbf{n}$ is the vector

$$\mathbf{n}=(\mathbf{r}_1-\mathbf{r}_2)\times(\mathbf{r}_3-\mathbf{r}_2)=-(\mathbf{r}_1\times\mathbf{r}_2+\mathbf{r}_2\times\mathbf{r}_3+\mathbf{r}_3\times\mathbf{r}_1)\ . \quad (9.121)$$

Scalar multiplication of Eqs.(9.120) by $\mathbf{n}$ yields

$$\lambda=\frac{1}{\mathbf{n}^2}\,\mathbf{n}\cdot[\mathbf{a}_3-\mathbf{a}_2-\boldsymbol{\omega}\times(\mathbf{v}_3-\mathbf{v}_2)]\ ,\qquad \mu=\frac{1}{\mathbf{n}^2}\,\mathbf{n}\cdot[\mathbf{a}_1-\mathbf{a}_2-\boldsymbol{\omega}\times(\mathbf{v}_1-\mathbf{v}_2)]\ . \quad (9.122)$$

With these expressions (9.119) has the desired symmetrical form

$$\dot{\boldsymbol{\omega}}=\frac{1}{\mathbf{n}^2}\,\mathbf{n}\cdot\sum_{i=1}^{3}(\mathbf{a}_i-\boldsymbol{\omega}\times\mathbf{v}_i)(\mathbf{r}_j-\mathbf{r}_k)\qquad(i,j,k=1,2,3\ \text{cyclic})\ . \quad (9.123)$$

Special case: If P_3 is fixed, $\mathbf{r}_3 = \mathbf{0}$ (arbitrarily) and $\mathbf{v}_3 = \mathbf{0}$, $\mathbf{a}_3 = \mathbf{0}$. Equations (9.113) and (9.123) are

$$\dot{\boldsymbol{\omega}} = \begin{cases} -\dfrac{(\mathbf{a}_1 - \boldsymbol{\omega} \times \mathbf{v}_1) \times (\mathbf{a}_2 - \boldsymbol{\omega} \times \mathbf{v}_2)}{\mathbf{r}_1 \cdot (\mathbf{a}_2 - \boldsymbol{\omega} \times \mathbf{v}_2)} & (\text{denominator} \neq 0) \,, \\ -\dfrac{\mathbf{r}_1 \times \mathbf{r}_2}{(\mathbf{r}_1 \times \mathbf{r}_2)^2} \cdot [\mathbf{a}_1 \mathbf{r}_2 - \mathbf{a}_2 \mathbf{r}_1 - \boldsymbol{\omega} \times (\mathbf{v}_1 \mathbf{r}_2 - \mathbf{v}_2 \mathbf{r}_1)] & (\text{else}) \,. \end{cases} \tag{9.124}$$

9.10 Strapdown Inertial Navigation

The body shown in Fig. 9.10 stands for an aircraft. In an inertial reference basis $\underline{\mathbf{e}}^1$ the body-fixed point A has the position vector $\mathbf{r}(t)$. The points P_i $(i = 1, \ldots, 6)$ are six body-fixed points with position vectors $\boldsymbol{\varrho}_i = \overrightarrow{AP_i}$. Let $\mathbf{a}_i$ be the acceleration of P_i relative to $\underline{\mathbf{e}}^1$. An accelerometer positioned at P_i measures as function of time the component $\alpha_i(t)$ of this acceleration $\mathbf{a}_i$ in a body-fixed direction specified by the unit vector $\mathbf{n}_i$: $\alpha_i(t) = \mathbf{a}_i \cdot \mathbf{n}_i$ $(i = 1, \ldots, 6)$. To be determined are, as functions of time, the position $\mathbf{r}(t)$ and the direction cosine matrix $\underline{A}^{12}(t)$ relating $\underline{\mathbf{e}}^1$ to a body-fixed basis $\underline{\mathbf{e}}^2$. The characterization *strapdown* points to the fact that the accelerometers are fixed in $\underline{\mathbf{e}}^2$ rather than in an inertial platform the orientation of which relative to the reference basis $\underline{\mathbf{e}}^1$ is held constant by means of gyroscopic instruments.

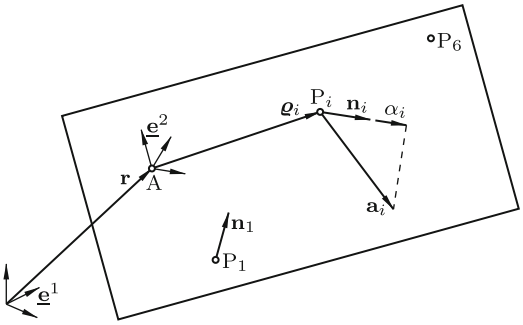

Fig. 9.10 Freely flying body with accelerometers mounted at body-fixed points $P_1, \ldots, P_6$

Solution: Starting point is the definition of $\alpha_i(t)$:

$$\mathbf{n}_i \cdot [\ddot{\mathbf{r}} + \dot{\boldsymbol{\omega}} \times \boldsymbol{\varrho}_i + \boldsymbol{\omega} \times (\boldsymbol{\omega} \times \boldsymbol{\varrho}_i)] = \alpha_i(t) \qquad (i = 1, \ldots, 6) \,. \tag{9.125}$$

This is written in the form

$$\mathbf{n}_i \cdot \ddot{\mathbf{r}} + \mathbf{c}_i \cdot \dot{\boldsymbol{\omega}} + \boldsymbol{\omega} \cdot \mathsf{D}_i \cdot \boldsymbol{\omega} = \alpha_i(t) \qquad (i = 1, \ldots, 6) \tag{9.126}$$

with vectors $\mathbf{c}_i$ and tensors D_i defined as follows:

$$\mathbf{c}_i = \boldsymbol{\varrho}_i \times \mathbf{n}_i \,, \qquad \mathsf{D}_i = \boldsymbol{\varrho}_i \mathbf{n}_i - \boldsymbol{\varrho}_i \cdot \mathbf{n}_i \mathsf{I} \qquad (i = 1, \ldots, 6) \,. \tag{9.127}$$

Let it be assumed that the vectors $\mathbf{n}_1$, $\mathbf{n}_2$ and $\mathbf{n}_3$ are linearly independent. Then the other three vectors $\mathbf{n}_4$, $\mathbf{n}_5$, $\mathbf{n}_6$ are linear combinations

$$\mathbf{n}_j = \sum_{i=1}^{3} \lambda_{ji} \mathbf{n}_i \qquad (j = 4, 5, 6) \tag{9.128}$$

with given coefficients λ_{ji}. From the jth Eq.(9.126) $(j = 4, 5, 6)$ the term $\ddot{\mathbf{r}}$ is eliminated by subtracting λ_{j1} times the first equation, λ_{j2} times the second equation and λ_{j3} times the third equation. The resulting equations are

$$\mathbf{c}_j^* \cdot \dot{\boldsymbol{\omega}} + \boldsymbol{\omega} \cdot \mathsf{D}_j^* \cdot \boldsymbol{\omega} = \alpha_j(t) - \sum_{i=1}^{3} \lambda_{ji} \alpha_i(t) \qquad (j = 4, 5, 6) \tag{9.129}$$

with

$$\mathbf{c}_j^* = \mathbf{c}_j - \sum_{i=1}^{3} \lambda_{ji} \mathbf{c}_i \,, \qquad \mathsf{D}_j^* = \mathsf{D}_j - \sum_{i=1}^{3} \lambda_{ji} \mathsf{D}_i \qquad (j = 4, 5, 6) \,. \tag{9.130}$$

Equations (9.129) are decomposed in the body-fixed basis $\underline{\mathbf{e}}^2$. In this basis the vectors $\mathbf{c}_j^*$ and the tensors D_j^* have constant coordinates. The terms involving $\dot{\boldsymbol{\omega}}$ contribute an expression of the form $\underline{C}\,\underline{\dot{\omega}}$ with a constant (3×3) matrix $\underline{C}$ the rows of which contain the coordinates of $\mathbf{c}_4^*$, $\mathbf{c}_5^*$ and $\mathbf{c}_6^*$. A necessary and sufficient condition for a solution to exist is the existence of $\underline{C}^{-1}$. Multiplication by $\underline{C}^{-1}$ produces differential equations of the form

$$\dot{\omega}_i + \sum_{j,k=1}^{3} p_{ijk} \omega_j \omega_k = f_i(t) \qquad (i = 1, 2, 3) \tag{9.131}$$

with given functions $f_i(t)$ and with given constant coefficients p_{ijk}. Numerical integration of these equations yields $\underline{\omega}(t)$. This solution is substituted into kinematic differential equations, for example, into Eq.(10.35) for Euler-Rodrigues parameters:

$$\begin{bmatrix} \dot{q}_0 \\ \underline{\dot{q}} \end{bmatrix} = \frac{1}{2} \begin{bmatrix} 0 & -\underline{\omega}^T \\ \underline{\omega} & -\tilde{\underline{\omega}} \end{bmatrix} \begin{bmatrix} q_0 \\ \underline{q} \end{bmatrix} \,. \tag{9.132}$$

From the numerical solution for $q_0(t)$, $q_1(t)$, $q_2(t)$, $q_3(t)$ the direction cosine matrix $\underline{A}^{12}(t)$ is calculated from (1.79).

In the last step, the acceleration $\ddot{\mathbf{r}}$ is calculated from the first three Eqs. (9.126). Also these equations are decomposed in the body-fixed basis $\underline{\mathbf{e}}^2$. For all vectors except $\ddot{\mathbf{r}}$ the coordinates are known by now. This yields for the coordinate matrix $\underline{\ddot{r}}^2$ in $\underline{\mathbf{e}}^2$ an equation of the form $\underline{N}\,\underline{\ddot{r}}^2 = \underline{F}(t)$ with a constant matrix $\underline{N}$. By definition, $\underline{N}^{-1}$ exists. The coordinates $\underline{\ddot{r}}^1$ of $\ddot{\mathbf{r}}$ in $\underline{\mathbf{e}}^1$ are

$$\underline{\ddot{r}}^1 = \underline{A}^{12}(t)\underline{N}^{-1}\underline{F}(t)\,. \tag{9.133}$$

Numerical integration of this equation yields $\underline{r}^1(t)$. This concludes the solution of the problem.

The equations are particularly simple if the vectors $\boldsymbol{\varrho}_i$ and $\mathbf{n}_i$ $(i = 1,\ldots,6)$ are chosen as follows (ℓ is an arbitrary reference length):

$$\left.\begin{aligned} \boldsymbol{\varrho}_1 &= -\boldsymbol{\varrho}_4 = \ell\,\mathbf{e}_2^2\,, & \mathbf{n}_1 &= -\mathbf{n}_4 = \mathbf{e}_3^2\,,\\ \boldsymbol{\varrho}_2 &= -\boldsymbol{\varrho}_5 = \ell\,\mathbf{e}_3^2\,, & \mathbf{n}_2 &= -\mathbf{n}_5 = \mathbf{e}_1^2\,,\\ \boldsymbol{\varrho}_3 &= -\boldsymbol{\varrho}_6 = \ell\,\mathbf{e}_1^2\,, & \mathbf{n}_3 &= -\mathbf{n}_6 = \mathbf{e}_2^2\,. \end{aligned}\right\} \tag{9.134}$$

In this case, the only nonzero coefficients in (9.128) are $\lambda_{41} = \lambda_{52} = \lambda_{63} = -1$. Furthermore,

$$\left.\begin{aligned} \mathbf{c}_i &= \boldsymbol{\varrho}_i \times \mathbf{n}_i = \ell\,\mathbf{e}_i^2\,, & \mathbf{c}^*_{i+3} &= 2\mathbf{c}_i & (i = 1,2,3)\\ \mathsf{D}_i &= \boldsymbol{\varrho}_i\mathbf{n}_i = \ell\,\mathbf{e}_j^2\mathbf{e}_k^2\,, & \mathsf{D}^*_{i+3} &= 2\mathsf{D}_i & (i,j,k = 1,2,3 \text{ cyclic})\,. \end{aligned}\right\} \tag{9.135}$$

This yields $\underline{C} = 2\ell\,\underline{I}$. Equations (9.131) become

$$\begin{bmatrix} \dot{\omega}_1 + \omega_2\omega_3 \\ \dot{\omega}_2 + \omega_3\omega_1 \\ \dot{\omega}_3 + \omega_1\omega_2 \end{bmatrix} = \frac{1}{2\ell}\begin{bmatrix} \alpha_1(t) + \alpha_4(t) \\ \alpha_2(t) + \alpha_5(t) \\ \alpha_3(t) + \alpha_6(t) \end{bmatrix}\,. \tag{9.136}$$

The first three Eqs.(9.126) decomposed in the body-fixed basis read

$$\begin{bmatrix} 0 & 0 & 1 \\ 1 & 0 & 0 \\ 0 & 1 & 0 \end{bmatrix}\begin{bmatrix} \ddot{r}_1^2 \\ \ddot{r}_2^2 \\ \ddot{r}_3^2 \end{bmatrix} + \ell\begin{bmatrix} \dot{\omega}_1 + \omega_2\omega_3 \\ \dot{\omega}_2 + \omega_3\omega_1 \\ \dot{\omega}_3 + \omega_1\omega_2 \end{bmatrix} = \begin{bmatrix} \alpha_1(t) \\ \alpha_2(t) \\ \alpha_3(t) \end{bmatrix}\,. \tag{9.137}$$

For the second term the right-hand side of the previous equation is substituted. Following this, the equation is multiplied by the inverse (the transpose) of the leading matrix $\underline{N}$. Transformation into the reference basis yields the final Eq.(9.133):

$$\begin{bmatrix} \ddot{r}_1^1 \\ \ddot{r}_2^1 \\ \ddot{r}_3^1 \end{bmatrix} = \frac{1}{2}\underline{A}^{12}(t)\begin{bmatrix} \alpha_2(t) - \alpha_5(t) \\ \alpha_3(t) - \alpha_6(t) \\ \alpha_1(t) - \alpha_4(t) \end{bmatrix}\,. \tag{9.138}$$

9.11 Motion on a Curved Surface

Let Σ be a continuously curved surface and let, furthermore, p and q be suitably chosen curvilinear coordinates such that every point of Σ is intersection point of two lines $p = \text{const}$ and $q = \text{const}$. The point is denoted $\mathrm{P}(p,q)$. Its position vector measured from some reference point is denoted $\mathbf{r}(p,q)$. The partial derivatives $\partial\mathbf{r}/\partial p$ and $\partial\mathbf{r}/\partial q$ are vectors tangent to the line $p = \text{const}$ and to the line $q = \text{const}$, respectively, at $\mathrm{P}(p,q)$. The unit vector $\mathbf{n}$ normal to Σ at $\mathrm{P}(p,q)$ is

$$\mathbf{n}(p,q) = \frac{\dfrac{\partial\mathbf{r}}{\partial p} \times \dfrac{\partial\mathbf{r}}{\partial q}}{\left|\dfrac{\partial\mathbf{r}}{\partial p} \times \dfrac{\partial\mathbf{r}}{\partial q}\right|} \,. \tag{9.139}$$

Example: The surface Σ is the ellipsoid $x^2/a^2+y^2/b^2+z^2/c^2 = 1$. Suitable curvilinear coordinates p and q are angles which represent geographical longitude and geographical latitude when the ellipsoid is a sphere. In the x,y,z-system the position vector $\mathbf{r}$ measured from the center, its partial derivatives and the unit normal vector $\mathbf{n}$ have the coordinates

$$\left.\begin{aligned} \mathbf{r}: &\quad [\ a\cos p\cos q \quad b\sin p\cos q \quad c\sin q\ ]\,, \\ \frac{\partial\mathbf{r}}{\partial p}: &\quad [\ -a\sin p\cos q \quad b\cos p\cos q \quad 0\ ]\,, \\ \frac{\partial\mathbf{r}}{\partial q}: &\quad [\ -a\cos p\sin q \quad -b\sin p\sin q \quad c\cos q\ ]\,, \end{aligned}\right\} \tag{9.140}$$

$$\mathbf{n}: \quad \frac{[\ bc\cos p\cos q \quad ca\sin p\cos q \quad ab\sin q\ ]}{\sqrt{(b^2\cos^2 p + a^2\sin^2 p)c^2\cos^2 q + a^2b^2\sin^2 q}} \,. \tag{9.141}$$

End of example.

Let P be a point moving on Σ. Prescribed functions $p(t)$, $q(t)$ of time t determine the trajectory $\mathbf{r}(t) = \mathbf{r}(\,p(t)\,,\,q(t)\,)$, the velocity $\dot{\mathbf{r}}(t)$ and the acceleration $\ddot{\mathbf{r}}(t)$ of P:

$$\dot{\mathbf{r}} = \frac{\partial\mathbf{r}}{\partial p}\,\dot{p} + \frac{\partial\mathbf{r}}{\partial q}\,\dot{q}\,, \qquad \ddot{\mathbf{r}} = \frac{\partial\mathbf{r}}{\partial p}\,\ddot{p} + \frac{\partial\mathbf{r}}{\partial q}\,\ddot{q} + \frac{\partial^2\mathbf{r}}{\partial p^2}\,\dot{p}^2 + \frac{\partial^2\mathbf{r}}{\partial q^2}\,\dot{q}^2 + 2\frac{\partial^2\mathbf{r}}{\partial p\partial q}\,\dot{p}\dot{q}\,. \tag{9.142}$$

Equation (9.139) with $p = p(t)$ and $q = q(t)$ determines the instantaneous unit normal vector $\mathbf{n}(t)$ at P. Its derivative with respect to time is

$$\dot{\mathbf{n}} = \frac{\partial\mathbf{n}}{\partial p}\,\dot{p} + \frac{\partial\mathbf{n}}{\partial q}\,\dot{q}\,. \tag{9.143}$$

Next, the case is considered that a plane Σ' is moving on a curved surface Σ. Let 0 be a point fixed in Σ'. The position vector of 0 is denoted $\mathbf{r}_0$. Furthermore, let $\mathbf{n}'$ and $\boldsymbol{\omega}$ be the unit normal vector and the angular velocity, respectively, of Σ'. The motion of Σ' on a curved surface Σ with coordinates p, q is called *Levi-Civita motion* (Pfister [9]) if at all times t the following constraints exist:

- Σ' is tangent to Σ
- the point of contact is 0
- the angular velocity of Σ' lies in Σ'.

These constraints are expressed through the equations

$$\mathbf{n}' \equiv \mathbf{n}(p,q)\,, \tag{9.144}$$

$$\mathbf{r}_0 \equiv \mathbf{r}(p,q)\,, \tag{9.145}$$

$$\boldsymbol{\omega} = \mathbf{n} \times \Big(\frac{\partial \mathbf{n}}{\partial p}\,\dot{p} + \frac{\partial \mathbf{n}}{\partial q}\,\dot{q} \Big)\,. \tag{9.146}$$

Proof of (9.146): The vector $\mathbf{n}'$ fixed in Σ' has the time derivative $\dot{\mathbf{n}}' = \boldsymbol{\omega} \times \mathbf{n}'$. Because of (9.144) this is the equation $\dot{\mathbf{n}} = \boldsymbol{\omega} \times \mathbf{n}$. Cross-multiplication from the left with $\mathbf{n}$ produces, because of the orthogonality of $\mathbf{n}$ and $\boldsymbol{\omega}$, the equation $\mathbf{n} \times \dot{\mathbf{n}} = \boldsymbol{\omega}$. This together with (9.143) yields (9.146). End of proof. The angular acceleration is $\dot{\boldsymbol{\omega}} = \mathbf{n} \times \ddot{\mathbf{n}}$.

Without the constraint (9.146) the system is holonomic with degree of freedom three. Suitable coordinates are the coordinates p, q of 0 on Σ and the angle between an arbitrary straight line fixed in Σ' and the tangent to the line $p = \text{const}$ at 0. Equation (9.146) is integrable in analytical form if and only if Σ is a surface with zero Gaussian curvature (for example a general cylinder). In this case, not only the position of 0, but also the angular orientation of Σ' is uniquely determined as function of p and q. If Σ is not of this special form, (9.146) is a nonholonomic constraint equation. In this case, kinematic differential equations must be formulated relating time derivatives of coordinates of the angular orientation of Σ' to $\boldsymbol{\omega}$. As coordinates Euler angles are chosen with the surface normal $\mathbf{n}$ as axis of rotation of the third angle ϕ. The constraint equation requires $\omega_3 \equiv 0$. Therefore, the kinematic differential Eqs.(10.24) have the form

$$\begin{bmatrix} \dot{\psi} \\ \dot{\theta} \\ \dot{\phi} \end{bmatrix} = \begin{bmatrix} \sin\phi/\sin\theta & \cos\phi/\sin\theta \\ \cos\phi & -\sin\phi \\ -\sin\phi\cot\theta & -\cos\phi\cot\theta \end{bmatrix} \begin{bmatrix} \omega_1 \\ \omega_2 \end{bmatrix}\,. \tag{9.147}$$

If the motion of 0 on Σ is prescribed by functions of time $p(t)$ and $q(t)$, $\mathbf{r}_0(t)$ and $\boldsymbol{\omega}(t)$ are known as functions of time. Starting from initial conditions satisfying (9.144) integration of (9.147) yields the angular orientation of Σ' as function of time.

Motion of a Curved Surface on Another Curved Surface

In Fig. 9.11a Σ_1 and Σ_2 are curved surfaces. Let p_i, q_i be the curvilinear coordinates of Σ_i $(i = 1, 2)$. Surface Σ_2 is moving relative to Σ_1 in such a way that both surfaces have, at all times t, a single (moving) point of tangential contact. Examples are the motion of a finger of a robot hand on a curved object and the single-point contact of tooth flanks in a gear train. Such motions may be holonomic or nonholonomic. In the case of pure rolling they are nonholonomic. At the instantaneous contact point P a point $\mathrm{P}_1(p_1, q_1)$ of Σ_1 coincides with a point $\mathrm{P}_2(p_2, q_2)$ of Σ_2. At P Σ_1 and Σ_2 have the same normal: $\mathbf{n}_1 \equiv \mathbf{n}_2$. The trajectories of P_1 on Σ_1 and of P_2 on Σ_2 are, in general, not cotangent. In the course of a sliding motion, for example, one trajectory may degenerate to a point while the other is a continuous curve.

The single-point contact represents a 5-d.o.f. joint. It seems natural to choose as coordinates describing the position of Σ_2 the coordinates (p_1, q_1) of P_1, the coordinates (p_2, q_2) of P_2 and, in addition, the angle between the tangents at P to the lines $p_1 = \text{const}$ and $p_2 = \text{const}$. These coordinates, originally introduced by Darboux [5], are still used in the literature. They have the disadvantage of leading to complicated expressions for the angular velocity and the angular acceleration of Σ_2.

A different set of coordinates free of this disadvantage was proposed by Neumann [8] and Richter [10] (see Pfister [9]). Following their ideas the two-body system Σ_1–Σ_2 with a 5-d.o.f.-joint is interpreted as four-body system Σ_1–Σ_1'–Σ_2'–Σ_2 with three joints (see Fig. 9.11b). Bodies Σ_1' and Σ_2' are coalescent planes which rotate relative to each other about a point 0 fixed in both planes. The angle of rotation of Σ_2' relative to Σ_1' is denoted χ. Plane Σ_1' is executing a Levi-Civita motion relative to Σ_1, and plane Σ_2' is executing another Levi-Civita motion relative to Σ_2. Point 0 is the common point of contact of the four bodies. It coincides with the moving points $\mathrm{P}_1(p_1, q_1)$ and $\mathrm{P}_2(p_2, q_2)$. The angular velocity of Σ_2 relative to Σ_1 is written in the

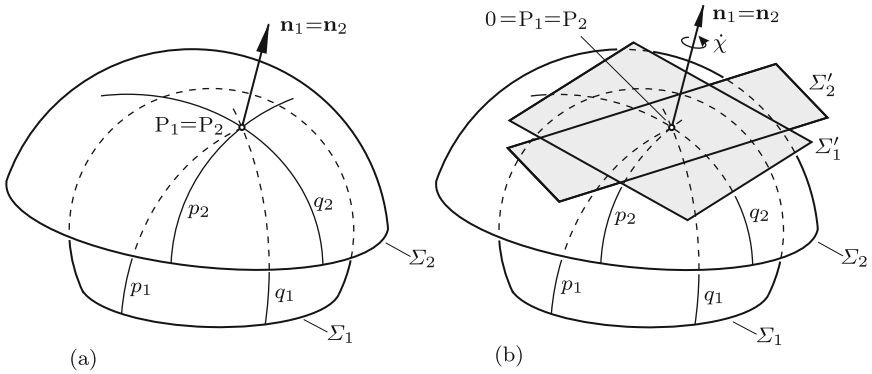

Fig. 9.11 Curved surfaces Σ_1 and Σ_2 with single-point contact **(a)** interpreted as four-body system with three joints **(b)**

form

$$\boldsymbol{\omega} = \boldsymbol{\omega}_1 + \dot{\chi}\mathbf{n}' - \boldsymbol{\omega}_2 \,, \tag{9.148}$$

where $\boldsymbol{\omega}_1$ and $\boldsymbol{\omega}_2$ are the angular velocities of Σ_1' relative to Σ_1 and of Σ_2' relative to Σ_2, respectively. Equations (9.144) – (9.146) for the two Levi-Civita motions read

$$\mathbf{n}' \equiv \mathbf{n}_1(p_1, q_1) \equiv \mathbf{n}_2(p_2, q_2) \,, \tag{9.149}$$

$$\mathbf{r}_0 \equiv \mathbf{r}_1(p_1, q_1) \equiv \mathbf{r}_2(p_2, q_2) \,, \tag{9.150}$$

$$\boldsymbol{\omega}_1 = \mathbf{n}_1 \times \left(\frac{\partial \mathbf{n}_1}{\partial p_1}\, \dot{p}_1 + \frac{\partial \mathbf{n}_1}{\partial q_1}\, \dot{q}_1 \right) , \quad \boldsymbol{\omega}_2 = \mathbf{n}_2 \times \left(\frac{\partial \mathbf{n}_2}{\partial p_2}\, \dot{p}_2 + \frac{\partial \mathbf{n}_2}{\partial q_2}\, \dot{q}_2 \right) . \tag{9.151}$$

For each Levi-Civita motion (9.147) with indices 1 or 2 attached to all variables is formulated.

9.12 Mecanum Wheel

A Swedish invention referred to as Mecanum wheel consists of a rigid wheel hub and of rigid rollers mounted on the periphery of the hub according to Fig. 9.12. Each roller can freely rotate about an axis which in radial projection makes an angle α with the axis of the wheel hub. The generating line of the rollers is formed so as to keep the hub axis at a constant distance R above ground. This distance is the outer wheel radius. When the wheel hub is rotating, the contact point on the roller moves from one end of the roller to the other, i.e., from one side of the wheel to the other. This lateral motion has interesting kinematical and dynamical effects. In a vehicle equipped with mecanum wheels the axes of the hubs are fixed on the vehicle body. Such a vehicle can rotate on the spot and translate in any direction without slipping on the ground provided a single roller per wheel has ground contact. Vehicle motion is controlled by controlling the angular velocities of wheel hubs relative to the vehicle body. Because of their maneuverability such vehicles find applications as store trolleys, assembly platforms in factories, platforms for mobile robots etc. The following kinematics analysis was published in [13].

In Fig. 9.13 the axis of the wheel hub and a single roller contacting ground are shown. The reference basis with unit basis vectors $\mathbf{e}_x\,, \mathbf{e}_y\,, \mathbf{e}_z$ is fixed on the vehicle. Its origin S is the center of the hub, $\mathbf{e}_y$ is directed along the hub axis, and $\mathbf{e}_z$ is normal to the plane on which the roller is rolling. The basis with unit basis vectors $\mathbf{e}_1\,, \mathbf{e}_2\,, \mathbf{e}_3$ is fixed on the hub. Its origin is the center S* of the roller, $\mathbf{e}_2$ is directed along the roller axis, and $\mathbf{e}_3$ is pointing towards S. Let φ be the rotation angle of the hub relative to the vehicle about $\mathbf{e}_y$ with $\varphi = 0$ in the position $\mathbf{e}_3 = \mathbf{e}_z$. The angular orientation of basis $\mathbf{e}_{1,2,3}$ with respect to basis $\mathbf{e}_{x,y,z}$ is the result of this rotation φ followed by a rotation about $\mathbf{e}_3$ through the roller inclination angle α. Hence

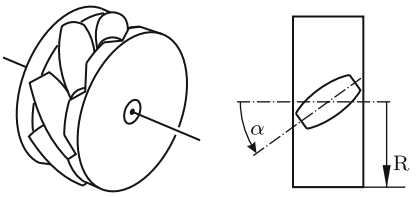

Fig. 9.12 Mecanum wheel **(a)** with parameters R and α **(b)**

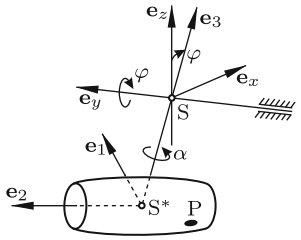

Fig. 9.13 Single roller contacting ground at P

the relationship between the two bases is

$$\begin{bmatrix}\mathbf{e}_1\\ \mathbf{e}_2\\ \mathbf{e}_3\end{bmatrix} = \begin{bmatrix}\cos\alpha & \sin\alpha & 0\\ -\sin\alpha & \cos\alpha & 0\\ 0 & 0 & 1\end{bmatrix}\begin{bmatrix}\cos\varphi & 0 & -\sin\varphi\\ 0 & 1 & 0\\ \sin\varphi & 0 & \cos\varphi\end{bmatrix}\begin{bmatrix}\mathbf{e}_x\\ \mathbf{e}_y\\ \mathbf{e}_z\end{bmatrix}$$
$$= \begin{bmatrix}\cos\alpha\cos\varphi & \sin\alpha & -\cos\alpha\sin\varphi\\ -\sin\alpha\cos\varphi & \cos\alpha & \sin\alpha\sin\varphi\\ \sin\varphi & 0 & \cos\varphi\end{bmatrix}\begin{bmatrix}\mathbf{e}_x\\ \mathbf{e}_y\\ \mathbf{e}_z\end{bmatrix} . \qquad (9.152)$$

The point P of contact between roller and ground has in basis $\mathbf{e}_{x,y,z}$ coordinates $[0\,,\,y\,,\,-R]$ with a variable $y(\varphi)$. The vertical through P intersects the roller axis. Therefore, $\boldsymbol{\varrho}_{\mathrm{SP}}$ can also be represented in the form

$$\boldsymbol{\varrho}_{\mathrm{SP}} = -r\mathbf{e}_3 + u\mathbf{e}_2 - w\mathbf{e}_z \qquad (9.153)$$

with r being the constant distance between S and S* and with variables $u(\varphi)$ and $w(\varphi)$. Decomposition of this expression in $\mathbf{e}_{x,y,z}$ with the help of (9.152) yields

$$\begin{bmatrix}-r\sin\varphi - u\sin\alpha\cos\varphi\\ u\cos\alpha\\ -r\cos\varphi + u\sin\alpha\sin\varphi - w\end{bmatrix} = \begin{bmatrix}0\\ y\\ -R\end{bmatrix} . \qquad (9.154)$$

Hence

$$y = -r\cot\alpha\tan\varphi\,, \qquad w = R - \frac{r}{\cos\varphi}\,. \qquad (9.155)$$

The velocity state of the vehicle is described by its angular velocity $\dot{\theta}\mathbf{e}_z$ and by the velocity $\mathbf{v}_{\mathrm{S}} = v_x\mathbf{e}_x + v_y\mathbf{e}_y$ of S. Let, furthermore, $\dot{\psi}\mathbf{e}_2$ be the angular velocity of the roller relative to the hub. In these terms, the contact point P of the roller has the velocity

$$\begin{aligned}\mathbf{v}_{\mathrm{P}} &= \mathbf{v}_{\mathrm{S}} + \dot\theta\mathbf{e}_z \times \boldsymbol{\varrho}_{\mathrm{SP}} + \dot\varphi\mathbf{e}_y \times \boldsymbol{\varrho}_{\mathrm{SP}} + \dot\psi\mathbf{e}_2 \times \boldsymbol{\varrho}_{\mathrm{S^*P}} \\ &= \mathbf{v}_{\mathrm{S}} + \dot\theta y\mathbf{e}_z \times \mathbf{e}_y + \dot\varphi\mathbf{e}_y \times (-R\mathbf{e}_z) + \dot\psi\mathbf{e}_2 \times (-w\mathbf{e}_z) \\ &= v_x\mathbf{e}_x + v_y\mathbf{e}_y - (\dot\theta y + \dot\varphi R)\mathbf{e}_x - \dot\psi z(\mathbf{e}_y \sin\alpha\cos\varphi + \mathbf{e}_x\cos\alpha)\,. \end{aligned} \tag{9.156}$$

The rolling condition $\mathbf{v}_{\mathrm{P}} = \mathbf{0}$ yields the equations

$$v_x - \dot\theta y - \dot\varphi R - \dot\psi w\cos\alpha = 0\,, \qquad v_y - \dot\psi w\sin\alpha\cos\varphi = 0\,. \tag{9.157}$$

For y and w the expressions (9.155) are substituted. The resulting equations are resolved for $\dot\varphi R$ and $\dot\psi$:

$$\dot\varphi R = v_x - \Big(\frac{v_y}{\cos\varphi} - \dot\theta r\tan\varphi\Big)\cot\alpha\,, \qquad \dot\psi = \frac{v_y}{(R\cos\varphi - r)\sin\alpha}\,. \tag{9.158}$$

The formula for $\dot\psi$ shows that the contacting roller does not rotate relative to the hub if $v_y = 0$. In this case, the entire wheel consisting of hub and rollers forms a single rigid body. In the position $\varphi = 0$ (contact point P vertically below S; roller axis horizontal) the first Eq.(9.158) reduces to $\dot\varphi R = v_x - v_y\cot\alpha$. From this it follows that $\dot\varphi = 0$ if the velocity $\mathbf{v}_{\mathrm{S}}$ is directed normal to the roller axis. Only the rollers are rotating. This can also be predicted from Fig. 9.12.

Equations (9.158) are valid as long as φ is in a narrow range $-\varphi_{\max} \le \varphi \le \varphi_{\max}$ assuring contact between roller and ground. When the angle φ of a roller is close to $\varphi_{\max}$, the next roller contacts ground and its angle is close to $-\varphi_{\max}$. In the case $\dot\theta \neq 0$, the two rollers require different angular velocities $\dot\varphi(\varphi_{\max})$ and $\dot\varphi(-\varphi_{\max})$. The difference is $\dot\varphi(-\varphi_{\max}) - \dot\varphi(\varphi_{\max}) = -2(r/R)\dot\theta\cot\alpha\tan\varphi_{\max}$ or, in view of (9.155), $2y_{\max}\dot\theta/R$. The quantity $2y_{\max}$ is the active width of the wheel. These results show that in phases of motion with two rollers contacting ground pure rolling is impossible if the vehicle is rotating ($\dot\theta \neq 0$). The periodical change between slipping and rolling causes vibrations of systems mounted on the vehicle. Such vibrations have been observed.

In (9.158) the angle φ is small. Assuming that also $\dot\theta$ is small the equations can be approximated as follows:

$$\dot\varphi R = v_x - v_y\cot\alpha\,, \qquad \dot\psi(R - r) = \frac{v_y}{\sin\alpha}\,. \tag{9.159}$$

Next, motions of a vehicle equipped with mecanum wheels are considered. For this purpose two new reference systems are defined in the plane of motion. One with axes X, Y is fixed on the ground. The other with basis vectors $\mathbf{e}_\xi$, $\mathbf{e}_\eta$ and origin A (arbitrary) is fixed on the vehicle. In this vehicle-fixed system a mecanum wheel is located by the vector $\mathbf{r}_{\mathrm{S}} = a\mathbf{e}_\xi + b\mathbf{e}_\eta$ of its center S and by the constant angle β between the axes $\mathbf{e}_\xi$ and $\mathbf{e}_x$. The velocity of S relative to ground is $\mathbf{v}_{\mathrm{S}} = \mathbf{v}_{\mathrm{A}} + \dot\theta\mathbf{e}_z \times \mathbf{r}_{\mathrm{S}}$. For formulating (9.159) the

coordinates in basis $\mathbf{e}_{x,y,z}$ are required. This basis is making the angle $\theta+\beta$ against the X,Y-system. Hence with $\dot{X}$ and $\dot{Y}$ denoting the coordinates of $\mathbf{v}_{\mathrm{A}}$ in the X,Y-system the desired velocities are

$$\begin{bmatrix} v_x \\ v_y \end{bmatrix} = \begin{bmatrix} \cos(\theta+\beta) & \sin(\theta+\beta) & -b \\ -\sin(\theta+\beta) & \cos(\theta+\beta) & a \end{bmatrix} \begin{bmatrix} \dot{X} \\ \dot{Y} \\ \dot{\theta} \end{bmatrix} . \tag{9.160}$$

For producing prescribed functions $X(t)\,,\, Y(t)\,,\, \theta(t)$ three controlled wheels are required. Let $a_i\,,\, b_i\,,\, \beta_i$ and $\dot{\varphi}_i$ $(i=1,2,3)$ be their position parameters and their angular velocities, respectively. The combination of (9.160) with the first Eq.(9.159) produces the equations

$$\dot{\varphi}_i = \frac{1}{R}\,[1 \quad -\cot\alpha] \begin{bmatrix} \cos(\theta+\beta_i) & \sin(\theta+\beta_i) & -b_i \\ -\sin(\theta+\beta_i) & \cos(\theta+\beta_i) & a_i \end{bmatrix} \begin{bmatrix} \dot{X} \\ \dot{Y} \\ \dot{\theta} \end{bmatrix} \tag{9.161}$$

$(i=1,2,3)$. These angular velocities $\dot{\varphi}_{1,2,3}$ produce the motion prescribed by $X(t)\,,\, Y(t)$ and $\theta(t)\,.$

Example: For a constant-velocity turn along a circular trajectory of radius r_0 and with angular velocity ω the prescribed functions are

$$\left.\begin{array}{lll} \theta = \omega t\ , & X = r_0\cos\theta\ , & Y = r_0\sin\theta\ , \\ \dot{\theta} \equiv \omega\ , & \dot{X} = -\omega r_0\sin\theta\ , & \dot{Y} = \omega r_0\cos\theta\ . \end{array}\right\} \tag{9.162}$$

On the right-hand side in (9.161) the only terms involving time-varying quantities are the terms

$$\left.\begin{aligned} \dot{X}\cos(\theta+\beta_i) + \dot{Y}\sin(\theta+\beta_i) &= \omega r_0[-\sin\theta\cos(\theta+\beta_i) + \cos\theta\sin(\theta+\beta_i)] \\ &\equiv \omega r_0\sin\beta_i\ , \\ -\dot{X}\sin(\theta+\beta_i) + \dot{Y}\cos(\theta+\beta_i) &= \omega r_0[\sin\theta\sin(\theta+\beta_i) + \cos\theta\cos(\theta+\beta_i)] \\ &\equiv \omega r_0\cos\beta_i\ . \end{aligned}\right\} \tag{9.163}$$

Since these terms are constant, also the required angular velocities $\dot{\varphi}_{1,2,3}$ are constant. End of example.

References

1. Bottema O (1965) Acceleration axes in spherical kinematics. J. Eng.f.Ind. 87B:150–154
2. Bottema O, Roth B (1990) Theoretical kinematics. North-Holland, Dover, New York
3. Bronstein I N, Semendjajev K A, Musiol K A, Mühlig H (2008) Taschenbuch der Mathematik. 7. Aufl. Verlag Harri Deutsch
4. Charlamov P V (1969) On the velocity distribution in a rigid body (Russ.). mechanika tverdovo tela 1:77–81

5. Darboux G (1972) Leçons sur la théorie générale des surfaces. v.1–4. Chelsea, New York
6. Lanchester G (1947) The yellow emperor's south-pointing chariot. China Soc. London
7. Needham J (1965) Science and Civilisation in China, vol.4.2: Mechanical Engineering, Sec.e5, Cambridge Univ.Press:297 – 303
8. Neumann C (1885) Über die rollende Bewegung eines Körpers auf einer gegebenen Horizontal-Ebene unter dem Einfluss der Schwere. Berichte über die Verhandlungen der Königlich-Sächsischen Gesellschaft der Wissenschaften zu Leipzig 37:352–378
9. Pfister F (2002) Spatial point contact kinematics and parallel transport. Proc.Instn.Mech.Engrs. 216 Part C: J. Mech.Eng.Scie.:33–45
10. Richter M (1887) Über die Bewegung eines Körpers auf einer Horizontal-Ebene. Diss. Univ. Leipzig (Metzger und Wittig)
11. Stojanov A, Nedjalkov (1956) Theoretical mechanics, part II: Kinematics, dynamics (Bulg.). Darjavno Isdat. Nauka i Iskustvo, Sofia
12. Veldkamp G R (1969) Acceleration axes and acceleration distribution in spatial motion. Eng.f.Ind 91B:147–151
13. Wampfler G, Salecker M, Wittenburg J (1988) Kinematics, dynamics and control of omnidirectional vehicles with mecanum wheels. In: Publications on multibody dynamics dedicated to Prof. R.E. Roberson on the occasion of his 65th birthday (limited edition)
14. Wittenburg J (1977) Dynamics of systems of rigid bodies. Teubner Stuttgart
15. Wittenburg J (2007) Dynamics of multibody systems. Springer, Berlin Heidelberg New York

Chapter 10
Kinematic Differential Equations

The angular velocity $\boldsymbol{\omega}$ of a body-fixed basis $\underline{\mathbf{e}}^2$ relative to a reference basis $\underline{\mathbf{e}}^1$ cannot, in general, be expressed as time derivative of some other vector. This is possible only in the special case when the direction of $\boldsymbol{\omega}$ is constant in $\underline{\mathbf{e}}^2$ and, thereby, also in $\underline{\mathbf{e}}^1$. In all other cases the relationship between variables describing the angular position of the body on the one hand and the angular velocity on the other is expressed through kinematic differential equations in which the coordinates of $\boldsymbol{\omega}$ appear as time-varying coefficients. In kinematics as well as in dynamics the relevant coordinates of $\boldsymbol{\omega}$ are those in the body-fixed basis $\underline{\mathbf{e}}^2$. In what follows, ω_1, ω_2, ω_3 are these coordinates, and the column matrix of these coordinates is denoted $\underline{\omega}$. In the sections to come kinematic differential equations are formulated for direction cosines, Euler angles, Bryan angles, Euler-Rodrigues parameters, Cayley-Klein parameters, Rodrigues parameters, Wiener parameters and for the Euler vector.

10.1 Direction Cosines

Let $\mathbf{r}$ be the position vector of an arbitrary body-fixed point. Its constant coordinate matrix $\underline{r}^2$ in $\underline{\mathbf{e}}^2$ and its time-varying coordinate matrix $\underline{r}^1(t)$ in $\underline{\mathbf{e}}^1$ are related through the equation $\underline{r}^1(t) = \underline{A}^{12}(t)\,\underline{r}^2$. Differentiation yields the velocity coordinates relative to $\underline{\mathbf{e}}^1$ and decomposed in $\underline{\mathbf{e}}^1$:

$$\underline{\dot{r}}^1 = \underline{\dot{A}}^{12}\underline{r}^2 \,. \tag{10.1}$$

In terms of $\boldsymbol{\omega}$ the velocity is $\dot{\mathbf{r}} = \boldsymbol{\omega} \times \mathbf{r}$. Its coordinate matrix in $\underline{\mathbf{e}}^2$ is $\tilde{\underline{\omega}}\,\underline{r}^2$ and in $\underline{\mathbf{e}}^1$ it is $\underline{A}^{12}\tilde{\underline{\omega}}\,\underline{r}^2$. Comparison with (10.1) yields the equation $\underline{\dot{A}}^{12}\underline{r}^2 = \underline{A}^{12}\tilde{\underline{\omega}}\,\underline{r}^2$. Since this equation is valid independent of $\underline{r}^2$, the preceding factors on both sides are equal:

J. Wittenburg, *Kinematics*, DOI 10.1007/978-3-662-48487-6_10

$$\dot{\underline{A}}^{12} = \underline{A}^{12}\tilde{\underline{\omega}} \,. \tag{10.2}$$

These are, in matrix form, the desired differential equations for direction cosines. They are called *Poisson's equations*. They are linear equations with time-varying coefficients. Equations for individual direction cosines are obtained by multiplying out:

$$\dot{a}_{11}^{12} = \omega_3 a_{12}^{12} - \omega_2 a_{13}^{12} \qquad \text{etc.} \tag{10.3}$$

Equation (10.2) yields for the trace of $\dot{\underline{A}}^{12}$ the expression

$$\operatorname{tr} \dot{\underline{A}}^{12} = -\underline{\omega}^T \underline{p} \tag{10.4}$$

with the column matrix

$$\underline{p} = \left[\, a_{32}^{12} - a_{23}^{12} \;\;,\;\; a_{13}^{12} - a_{31}^{12} \;\;,\;\; a_{21}^{12} - a_{12}^{12} \,\right]^T . \tag{10.5}$$

Its time derivative is calculated from six Eqs.(10.3):

$$\dot{\underline{p}} = \left[\left(\operatorname{tr} \underline{A}^{12} \right) \underline{I} - \underline{A}^{12^T} \right] \underline{\omega} \,. \tag{10.6}$$

The kinematic differential equations determine the direction cosines when $\omega_1(t)\,,\, \omega_2(t)\,,\, \omega_3(t)$ are known from an analytical or numerical integration of dynamics equations of motion. Frequently, dynamics equations of motion contain as unknowns not only $\omega_1\,,\, \omega_2\,,\, \omega_3$ and $\dot{\omega}_1\,,\, \dot{\omega}_2\,,\, \dot{\omega}_3$, but also the direction cosines themselves. In such cases the dynamics equations of motion and the kinematic differential equations must be integrated simultaneously.

If the direction cosine matrix is prescribed as function of time, the coordinates of $\boldsymbol{\omega}$ are calculated from the equation

$$\tilde{\underline{\omega}} = \underline{A}^{12^T} \dot{\underline{A}}^{12} \,. \tag{10.7}$$

The coordinates of $\boldsymbol{\omega}$ in basis $\underline{\mathbf{e}}^1$ define the coordinate matrix $\underline{\omega}^1$ and the skewsymmetric matrix $\tilde{\underline{\omega}}^1$. They are related to $\underline{\omega}$ and $\tilde{\underline{\omega}}$ by the transformations $\underline{\omega}^1 = \underline{A}^{12}\underline{\omega}$ and $\tilde{\underline{\omega}}^1 = \underline{A}^{12}\tilde{\underline{\omega}}\underline{A}^{12^T}$ (see (1.25)). With (10.7) the latter equation is $\tilde{\underline{\omega}}^1 = \dot{\underline{A}}^{12}\underline{A}^{12^T}$.

Example: Two points P_1 and P_2 of a body with a fixed point 0 are constrained to mutually perpendicular fixed planes E_1 and E_2, respectively. Plane E_1 is the $\mathbf{e}_1^1, \mathbf{e}_2^1$-plane of a fixed reference basis $\underline{\mathbf{e}}^1$ having 0 as origin, and E_2 is the $\mathbf{e}_1^1, \mathbf{e}_3^1$-plane of the same basis. The coordinate matrices of P_1 and P_2 in the body-fixed basis $\underline{\mathbf{e}}^2$ with origin 0 are given as $\underline{r}_1^2 = [\,1\;0\;0\,]^T$ and $\underline{r}_2^2 = [\,\cos\alpha \quad 0 \quad \sin\alpha\,]^T$, respectively $(0 < \alpha \leq \pi/2)$. The angle α is the apex angle in the isosceles triangle (P_1,0,P_2). Together with P_1 and P_2 the body-fixed lines $\overline{0\mathrm{P}}_1$ and $\overline{0\mathrm{P}}_2$ are constrained to E_1 and E_2,

respectively. The body has the degree of freedom $F = 1$. It is free to rotate such that in projection along $\mathbf{e}_1^1$ the base $\overline{\mathrm{P}_1\mathrm{P}_2}$ of the triangle is moving through all four quadrants of the $\mathbf{e}_2^1, \mathbf{e}_3^1$-plane. The kinematics is most easily described in terms of Euler angles. From (1.28) the direction cosine matrix is copied:

$$\underline{A}^{12} = \begin{bmatrix} c_\psi c_\phi - s_\psi c_\theta s_\phi & -c_\psi s_\phi - s_\psi c_\theta c_\phi & s_\psi s_\theta \\ s_\psi c_\phi + c_\psi c_\theta s_\phi & -s_\psi s_\phi + c_\psi c_\theta c_\phi & -c_\psi s_\theta \\ s_\theta s_\phi & s_\theta c_\phi & c_\theta \end{bmatrix} . \tag{10.8}$$

In $\underline{\mathbf{e}}^1$ P_1 and P_2 have the coordinate matrices $\underline{r}_1^1 = \underline{A}^{12}\underline{r}_1^2$ and $\underline{r}_2^1 = \underline{A}^{12}\underline{r}_2^2$, respectively. The third coordinate of $\underline{r}_1^1$ and the second coordinate of $\underline{r}_2^1$ are zero. This establishes the equations

$$\sin\theta\sin\phi = 0 , \qquad (\sin\psi\cos\phi + \cos\psi\cos\theta\sin\phi)\cos\alpha - \cos\psi\sin\theta\sin\alpha = 0 . \tag{10.9}$$

The solution is

$$\phi = 0 , \quad \sin\theta = \cot\alpha\tan\psi , \quad \cos\theta = \sigma\sqrt{1-\sin^2\theta} \qquad (\sigma = \pm 1) . \tag{10.10}$$

The angle ψ is chosen as independent variable. It is in the range $-\alpha \le \psi \le \alpha$. With $\sin\theta(\psi)$ and $\cos\theta(\psi)$

$$\underline{A}^{12} = \begin{bmatrix} \cos\psi & -\sin\psi\cos\theta & \sin\psi\sin\theta \\ \sin\psi & \cos\psi\cos\theta & -\cos\psi\sin\theta \\ 0 & \sin\theta & \cos\theta \end{bmatrix} . \tag{10.11}$$

Differentiation with respect to time yields

$$\dot{\underline{A}}^{12} = \dot{\psi} \begin{bmatrix} -\sin\psi & -\cos\psi\cos\theta - \sin\psi\frac{\mathrm{d}}{\mathrm{d}\psi}\cos\theta & \cos\psi\sin\theta + \sin\psi\frac{\mathrm{d}}{\mathrm{d}\psi}\sin\theta \\ \cos\psi & -\sin\psi\cos\theta + \cos\psi\frac{\mathrm{d}}{\mathrm{d}\psi}\cos\theta & \sin\psi\sin\theta - \cos\psi\frac{\mathrm{d}}{\mathrm{d}\psi}\sin\theta \\ 0 & \frac{\mathrm{d}}{\mathrm{d}\psi}\sin\theta & \frac{\mathrm{d}}{\mathrm{d}\psi}\cos\theta \end{bmatrix} \tag{10.12}$$

with

$$\left.\begin{aligned} \frac{\mathrm{d}}{\mathrm{d}\psi}\sin\theta &= \frac{\cot\alpha}{\cos^2\psi} , \\ \frac{\mathrm{d}}{\mathrm{d}\psi}\cos\theta &= \sigma\frac{\mathrm{d}}{\mathrm{d}\psi}\sqrt{1-\sin^2\theta} = -\tan\theta\frac{\mathrm{d}}{\mathrm{d}\psi}\sin\theta . \end{aligned}\right\} \tag{10.13}$$

From (10.7) the coordinates of $\boldsymbol{\omega}$ in $\underline{\mathbf{e}}^2$ are obtained:

$$\left.\begin{aligned}
\omega_1 &= \dot\psi\Big(-\sin\theta\frac{\mathrm{d}}{\mathrm{d}\psi}\cos\theta + \cos\theta\frac{\mathrm{d}}{\mathrm{d}\psi}\sin\theta\Big) \\
&= \frac{\dot\psi}{\cos\theta}\,\frac{\mathrm{d}}{\mathrm{d}\psi}\sin\theta = \sigma\dot\psi\,\frac{\cot\alpha}{\cos^2\psi\sqrt{1-\cot^2\alpha\tan^2\psi}}\,, \\
\omega_2 &= \dot\psi\sin\theta = \dot\psi\,\cot\alpha\tan\psi\,, \\
\omega_3 &= \dot\psi\cos\theta = \sigma\dot\psi\,\sqrt{1-\cot^2\alpha\tan^2\psi}\,.
\end{aligned}\right\} \tag{10.14}$$

The coordinates in $\underline{\mathbf{e}}^1$, denoted Ω_1, Ω_2, Ω_3, are obtained by the transformation $\underline{\Omega} = \underline{A}^{12}\underline{\omega}$:

$$\Omega_1 = \omega_1\cos\psi\,, \qquad \Omega_2 = \omega_1\sin\psi\,, \qquad \Omega_3 = \dot\psi\,. \tag{10.15}$$

The coordinates ω_1, ω_2, ω_3 are parameter equations of the moving polhode cone of the body, and the coordinates Ω_1, Ω_2, Ω_3 are parameter equations of the fixed herpolhode cone. The cones are best portrayed by their curves of intersection with a plane normal to $\mathbf{e}_1^2$ (the moving cone) and with a plane normal to $\mathbf{e}_1^1$ (the fixed cone), respectively. These curves have the parameter equations

$$\left.\begin{aligned}
x(\psi) &= \frac{\omega_3}{\omega_1} = \frac{\tan\alpha}{1+\tan^2\psi}\,(1-\cot^2\alpha\tan^2\psi)\,, \\
y(\psi) &= \frac{\omega_2}{\omega_1} = \frac{\tan\psi}{1+\tan^2\psi}\,\sqrt{1-\cot^2\alpha\tan^2\psi}
\end{aligned}\right\} \tag{10.16}$$

and

$$\left.\begin{aligned}
X(\psi) &= \frac{\Omega_3}{\Omega_1} = \sigma\tan\alpha\cos\psi\sqrt{1-\cot^2\alpha\tan^2\psi}\,, \\
Y(\psi) &= \frac{\Omega_2}{\Omega_1} = \tan\psi\,.
\end{aligned}\right\} \tag{10.17}$$

In both sets of equations the elimination of ψ is a simple matter. The equation for x yields

$$\tan^2\psi = \frac{\tan\alpha - x}{\cot\alpha + x}\,. \tag{10.18}$$

The resulting parameter-free equations of the curves are

$$\left.\begin{aligned}
&\text{moving cone:} && \left(\frac{x-\frac{1}{2}\tan\alpha}{\frac{1}{2}\tan\alpha}\right)^2 + \left(\frac{y}{\frac{1}{2}\sin\alpha}\right)^2 = 1\,, \\
&\text{fixed cone:} && X^2 + X^2Y^2 + Y^2 = \tan^2\alpha\,.
\end{aligned}\right\} \tag{10.19}$$

These curves are discussed in Sect. 13.1.1 where they are met again. There, it is shown that the motion of the central cross in a Hooke's joint is the inverse of the motion studied here. A plane normal to the body-fixed line $\overline{0\mathrm{P}_2}$ intersects the moving cone in the circle $(\,x = x'/\cos\alpha\,)$

$$(x' - \tfrac{1}{2}\sin\alpha)^2 + y^2 = (\tfrac{1}{2}\sin\alpha)^2\,. \tag{10.20}$$

In the case $\alpha \ll 1$ both cones are circular cones with the curves

$$(x - \tfrac{\alpha}{2})^2 + y^2 = (\tfrac{\alpha}{2})^2 \,, \qquad X^2 + Y^2 = \alpha^2 \,. \tag{10.21}$$

The smaller circle is rolling inside the fixed circle which is twice as big. These circles are met again in Sect. 15.1.2 (Fig. 15.4a). End of example.

10.2 Euler Angles

Figure 1.1a yields for the angular velocity vector $\boldsymbol{\omega}$ the expression

$$\boldsymbol{\omega} = \dot{\psi}\mathbf{e}_3^1 + \dot{\theta}\mathbf{e}_1^{2'} + \dot{\phi}\mathbf{e}_3^2 \,. \tag{10.22}$$

The vectors are decomposed in basis $\underline{\mathbf{e}}^2$. With the help of (1.26) this results in the coordinate equations

$$\begin{bmatrix} \omega_1 \\ \omega_2 \\ \omega_3 \end{bmatrix} = \begin{bmatrix} \sin\theta\sin\phi & \cos\phi & 0 \\ \sin\theta\cos\phi & -\sin\phi & 0 \\ \cos\theta & 0 & 1 \end{bmatrix} \begin{bmatrix} \dot{\psi} \\ \dot{\theta} \\ \dot{\phi} \end{bmatrix} \,. \tag{10.23}$$

Inversion yields the desired differential equations:

$$\begin{bmatrix} \dot{\psi} \\ \dot{\theta} \\ \dot{\phi} \end{bmatrix} = \begin{bmatrix} \sin\phi/\sin\theta & \cos\phi/\sin\theta & 0 \\ \cos\phi & -\sin\phi & 0 \\ -\sin\phi\cot\theta & -\cos\phi\cot\theta & 1 \end{bmatrix} \begin{bmatrix} \omega_1 \\ \omega_2 \\ \omega_3 \end{bmatrix} \,. \tag{10.24}$$

These equations are nonlinear. Numerical problems arise when θ gets close to one of the critical values $n\pi$ $(n = 0, \pm 1, \ldots)$.

10.3 Bryan Angles

Figure 1.2a yields for the angular velocity vector $\boldsymbol{\omega}$ the expression

$$\boldsymbol{\omega} = \dot{\phi}_1\mathbf{e}_1^1 + \dot{\phi}_2\mathbf{e}_2^{2'} + \dot{\phi}_3\mathbf{e}_3^2 \,. \tag{10.25}$$

The vectors are decomposed in basis $\underline{\mathbf{e}}^2$. With the help of (1.30) this results in the coordinate equations

$$\begin{bmatrix} \omega_1 \\ \omega_2 \\ \omega_3 \end{bmatrix} = \begin{bmatrix} \cos\phi_2\cos\phi_3 & \sin\phi_3 & 0 \\ -\cos\phi_2\sin\phi_3 & \cos\phi_3 & 0 \\ \sin\phi_2 & 0 & 1 \end{bmatrix} \begin{bmatrix} \dot{\phi}_1 \\ \dot{\phi}_2 \\ \dot{\phi}_3 \end{bmatrix} \,. \tag{10.26}$$

Inversion yields the desired differential equations:

$$\begin{bmatrix} \dot{\phi}_1 \\ \dot{\phi}_2 \\ \dot{\phi}_3 \end{bmatrix} = \begin{bmatrix} \cos\phi_3/\cos\phi_2 & -\sin\phi_3/\cos\phi_2 & 0 \\ \sin\phi_3 & \cos\phi_3 & 0 \\ -\cos\phi_3\tan\phi_2 & \sin\phi_3\tan\phi_2 & 1 \end{bmatrix} \begin{bmatrix} \omega_1 \\ \omega_2 \\ \omega_3 \end{bmatrix} . \qquad (10.27)$$

These equations are nonlinear. Numerical problems arise when ϕ_2 gets close to one of the critical values $\pi/2 + n\pi$ $(n = 0, \pm 1, \ldots)$.

In Sect. 1.4 it was shown that in the case of small angles ϕ_1, ϕ_2, ϕ_3 linearization of the direction cosine matrix is possible (see (1.33)). Linearization of (10.26) yields $\omega_i \approx \dot{\phi}_i$ $(i = 1, 2, 3)$. Hence the angular orientation of the body is the result of simple integration:

$$\phi_i \approx \int \omega_i \, \mathrm{d}t \qquad (|\phi_i| \ll 1 \,;\; i = 1, 2, 3) . \qquad (10.28)$$

10.4 Euler-Rodrigues Parameters

Introductory remarks: The vector $\mathbf{q} = \mathbf{n} \sin\varphi/2$ is one out of five vectors of the general form $\mathbf{z} = \mathbf{n} f(\varphi)$. The other four vectors are $\mathbf{n}$ itself, the Rodrigues vector $\mathbf{n}\tan\varphi/2$, the Wiener vector $\mathbf{n}\tan\varphi/4$ and the Euler vector $\mathbf{n}\varphi$. The vector $\mathbf{z}$ has identical coordinates in $\underline{\mathbf{e}}^1$ and in $\underline{\mathbf{e}}^2$. But its time derivatives in the two bases are different. The relationship is

$$\frac{{}^{(1)}\mathrm{d}\mathbf{z}}{\mathrm{d}t} = \frac{{}^{(2)}\mathrm{d}\mathbf{z}}{\mathrm{d}t} + \boldsymbol{\omega} \times \mathbf{z} \qquad (\mathbf{z} = \mathbf{n} f(\varphi)) . \qquad (10.29)$$

End of the introductory remarks.

Kinematic differential equations for Euler-Rodrigues parameters are established by three different methods. The first method starts out from Eqs.(1.117) for the Euler-Rodrigues parameters of the resultant of two consecutive rotations:

$$q_{0_{\mathrm{res}}} = q_{02} q_{01} - \mathbf{q}_2 \cdot \mathbf{q}_1 , \qquad \mathbf{q}_{\mathrm{res}} = q_{02}\mathbf{q}_1 + q_{01}\mathbf{q}_2 + \mathbf{q}_2 \times \mathbf{q}_1 . \qquad (10.30)$$

The parameters $(q_{01}, \mathbf{q}_1)$ are attributed to time t during a continuous motion, and the parameters $(q_{0_{\mathrm{res}}}, \mathbf{q}_{\mathrm{res}})$ are attributed to time $t + \mathrm{d}t$. The quantities $(q_{02}, \mathbf{q}_2)$ represent the Euler-Rodrigues parameters of the differential rotation $\boldsymbol{\omega}\,\mathrm{d}t = \mathbf{e}_\omega \omega \,\mathrm{d}t$ during the time interval $\mathrm{d}t$ (unit vector $\mathbf{e}_\omega$). These parameters are

$$q_{02} = \cos\left(\frac{1}{2}\omega\,\mathrm{d}t\right) = 1 , \qquad \mathbf{q}_2 = \mathbf{e}_\omega \sin\left(\frac{1}{2}\omega\,\mathrm{d}t\right) = \frac{1}{2}\boldsymbol{\omega}\,\mathrm{d}t . \qquad (10.31)$$

With these expressions Eqs.(10.30) take the forms

$$\left.\begin{aligned} q_0(t+\mathrm{d}t) &= q_0(t) - \frac{1}{2}\,\boldsymbol{\omega}\cdot\mathbf{q}(t)\,\mathrm{d}t\;, \\ \mathbf{q}(t+\mathrm{d}t) &= \mathbf{q}(t) + \frac{1}{2}\,[q_0(t)\boldsymbol{\omega} + \boldsymbol{\omega}\times\mathbf{q}(t)]\,\mathrm{d}t\;. \end{aligned}\right\} \tag{10.32}$$

Division by $\mathrm{d}t$ yields for $\dot{q}_0$ and for the derivative of $\mathbf{q}$ in $\underline{\mathbf{e}}^1$ the differential equations

$$\dot{q}_0 = -\frac{1}{2}\boldsymbol{\omega}\cdot\mathbf{q}\;, \qquad \frac{^{(1)}\,\mathrm{d}\mathbf{q}}{\mathrm{d}t} = \frac{1}{2}(q_0\boldsymbol{\omega} + \boldsymbol{\omega}\times\mathbf{q})\;. \tag{10.33}$$

Because of (10.29) the derivative in $\underline{\mathbf{e}}^2$ is

$$\frac{^{(2)}\,\mathrm{d}\mathbf{q}}{\mathrm{d}t} = \frac{1}{2}(q_0\boldsymbol{\omega} - \boldsymbol{\omega}\times\mathbf{q})\;. \tag{10.34}$$

Decomposition of these equations in $\underline{\mathbf{e}}^2$ yields the desired kinematic differential equations:

$$\begin{bmatrix} \dot{q}_0 \\ \dot{\underline{q}} \end{bmatrix} = \frac{1}{2}\begin{bmatrix} 0 & -\underline{\omega}^T \\ \underline{\omega} & -\tilde{\underline{\omega}} \end{bmatrix}\begin{bmatrix} q_0 \\ \underline{q} \end{bmatrix}\;. \tag{10.35}$$

The equations are linear with a time-varying skew-symmetric coefficient matrix.

The second method for generating these equations uses Eqs.(1.81), (1.82), (1.78) and (10.4) – (10.6) relating Euler-Rodrigues parameters to direction cosines. From (1.81), (1.82) and (10.5)

$$4q_0^2 = \operatorname{tr}\underline{A}^{12} + 1\;, \qquad 4q_0\underline{q} = \underline{p}\;. \tag{10.36}$$

Both equations are differentiated:

$$8q_0\dot{q}_0 = \operatorname{tr}\dot{\underline{A}}^{12}\;, \qquad 4q_0\dot{\underline{q}} = \dot{\underline{p}} - 4\dot{q}_0\underline{q}\;. \tag{10.37}$$

The first equation in combination with (10.4) yields $8q_0\dot{q}_0 = -\underline{\omega}^T\underline{p}$ and with the second Eq.(10.36)

$$\dot{q}_0 = -\frac{1}{2}\,\underline{\omega}^T\underline{q}\;. \tag{10.38}$$

This is the first Eq.(10.35). With this expression for $\dot{q}_0$ and with (10.6) for $\dot{\underline{p}}$ the second Eq.(10.37) becomes

$$4q_0\dot{\underline{q}} = \left[\left(\operatorname{tr}\underline{A}^{12}\right)\underline{I} - \underline{A}^{12^T} + 2\underline{q}\,\underline{q}^T\right]\underline{\omega} \tag{10.39}$$

and with (10.36) for $\operatorname{tr}\underline{A}^{12}$ and (1.78) for $\underline{A}^{12}$ $4q_0\dot{\underline{q}} = 2(q_0^2\underline{I} + q_0\tilde{\underline{q}})\underline{\omega}$. Hence

$$\dot{\underline{q}} = \frac{1}{2}(\underline{\omega}\, q_0 - \tilde{\underline{\omega}}\, \underline{q}) \; . \tag{10.40}$$

This is the second Eq.(10.35).

The third method for generating the differential equations makes use of Eqs.(1.93) and (1.96) relating Euler angles to Euler-Rodrigues parameters:

$$\cos\theta = q_0^2 - q_1^2 - q_2^2 + q_3^2 \; , \tag{10.41}$$

$$\psi = \tan^{-1}\frac{q_3}{q_0} + \tan^{-1}\frac{q_2}{q_1} \; , \qquad \phi = \tan^{-1}\frac{q_3}{q_0} - \tan^{-1}\frac{q_2}{q_1} \; . \tag{10.42}$$

Differentiation with respect to time produces the equations

$$\dot{\psi} = \frac{q_0\dot{q}_3 - q_3\dot{q}_0}{q_0^2 + q_3^2} + \frac{q_1\dot{q}_2 - q_2\dot{q}_1}{q_1^2 + q_2^2} \; , \qquad \dot{\phi} = \frac{q_0\dot{q}_3 - q_3\dot{q}_0}{q_0^2 + q_3^2} - \frac{q_1\dot{q}_2 - q_2\dot{q}_1}{q_1^2 + q_2^2} \; . \tag{10.43}$$

These expressions and the expression for $\cos\theta$ are substituted into the third differential Eq.(10.23) for Euler angles: $\omega_3 = \dot{\psi}\cos\theta + \dot{\phi}$. This results in the equation

$$\begin{aligned} \omega_3 = {} & \frac{q_0\dot{q}_3 - q_3\dot{q}_0}{q_0^2 + q_3^2} \underbrace{(q_0^2 - q_1^2 - q_2^2 + q_3^2 + 1)}_{2(q_0^2+q_3^2)} \\ & + \frac{q_1\dot{q}_2 - q_2\dot{q}_1}{q_1^2 + q_2^2} \underbrace{(q_0^2 - q_1^2 - q_2^2 + q_3^2 - 1)}_{-2(q_1^2+q_2^2)} \\ = {} & 2(q_0\dot{q}_3 - q_3\dot{q}_0 - q_1\dot{q}_2 + q_2\dot{q}_1) \; . \end{aligned} \tag{10.44}$$

Equations for ω_2 and ω_1 are obtained by cyclic permutation of the indices 1, 2 and 3. The three equations constitute rows 2, 3 and 4 of the matrix equation below. The first row represents the time derivative of the constraint equation $1 = q_0^2 + q_1^2 + q_2^2 + q_3^2$.

$$\begin{bmatrix} 0 \\ \omega_1 \\ \omega_2 \\ \omega_3 \end{bmatrix} = 2 \begin{bmatrix} q_0 & q_1 & q_2 & q_3 \\ -q_1 & q_0 & q_3 & -q_2 \\ -q_2 & -q_3 & q_0 & q_1 \\ -q_3 & q_2 & -q_1 & q_0 \end{bmatrix} \begin{bmatrix} \dot{q}_0 \\ \dot{q}_1 \\ \dot{q}_2 \\ \dot{q}_3 \end{bmatrix} \; . \tag{10.45}$$

This is the inverse of (10.35). The coefficient matrix is orthogonal (the scalar product of any two rows or columns i and j equals δ_{ij}). Consequently, its inverse equals its transpose. Hence

$$\begin{bmatrix} \dot{q}_0 \\ \dot{q}_1 \\ \dot{q}_2 \\ \dot{q}_3 \end{bmatrix} = \frac{1}{2} \begin{bmatrix} q_0 & -q_1 & -q_2 & -q_3 \\ q_1 & q_0 & -q_3 & q_2 \\ q_2 & q_3 & q_0 & -q_1 \\ q_3 & -q_2 & q_1 & q_0 \end{bmatrix} \begin{bmatrix} 0 \\ \omega_1 \\ \omega_2 \\ \omega_3 \end{bmatrix} \; . \tag{10.46}$$

Simple reordering results in (10.35).

In the course of numerical integrations of (10.35) inevitable numerical errors have the effect that computed quantities $q_i(t)$ $(i = 0, 1, 2, 3)$ do not strictly satisfy the constraint equation $q_0^2+q_1^2+q_2^2+q_3^2 = 1$. Such faulty quantities must not be used for calculating from (1.79) a direction cosine matrix for the transformation of vector coordinates. Before doing so the quantities must be replaced by corrected quantities satisfying the constraint equation. Correction formulas are developed in Sect. 10.9.

10.5 Cayley-Klein Parameters

Starting point are Eqs.(1.140) and (1.141) relating Cayley-Klein parameters to Euler-Rodrigues parameters:

$$\left.\begin{aligned} &\alpha = q_0 + \mathrm{i}\, q_3 \,, \qquad \beta = -q_2 + \mathrm{i}\, q_1 \,, \\ &q_0 = \frac{1}{2}(\alpha + \bar{\alpha}) \,, \quad q_3 = -\frac{\mathrm{i}}{2}(\alpha - \bar{\alpha}) \,, \quad q_2 = -\frac{1}{2}(\beta + \bar{\beta}) \,, \quad q_1 = -\frac{\mathrm{i}}{2}(\beta - \bar{\beta}) \,. \end{aligned}\right\} \tag{10.47}$$

The first equation yields $\dot{\alpha} = \dot{q}_0 + \mathrm{i}\,\dot{q}_3$. For $\dot{q}_0$ and for $\dot{q}_3$ the expressions from (10.46) are substituted. Following this, the parameters q_0, q_1, q_2, q_3 are again expressed in terms of α and β by substituting the expressions in (10.47). The result is

$$\dot{\alpha} = \frac{1}{2}\Big[-(q_1+\mathrm{i}\,q_2)\omega_1+(-q_2+\mathrm{i}\,q_1)\omega_2+(-q_3+\mathrm{i}\,q_0)\omega_3\Big] = \frac{1}{2}[(\mathrm{i}\,\omega_1+\omega_2)\beta+\mathrm{i}\,\omega_3\alpha] \,. \tag{10.48}$$

In the same way $\dot{\beta}$ is calculated. Both expressions are combined in matrix form as follows:

$$\begin{bmatrix} \dot{\alpha} \\ \dot{\beta} \end{bmatrix} = \frac{1}{2} \begin{bmatrix} \mathrm{i}\,\omega_3 & \mathrm{i}\,\omega_1 + \omega_2 \\ \mathrm{i}\,\omega_1 - \omega_2 & -\mathrm{i}\,\omega_3 \end{bmatrix} \begin{bmatrix} \alpha \\ \beta \end{bmatrix} \,. \tag{10.49}$$

These are the desired kinematic differential equations for Cayley-Klein parameters. They are linear. The same coefficient matrix occurs in the inverse equation

$$\begin{bmatrix} \alpha \\ \beta \end{bmatrix} = \frac{-2}{\omega_1^2 + \omega_2^2 + \omega_3^2} \begin{bmatrix} \mathrm{i}\,\omega_3 & \mathrm{i}\,\omega_1 + \omega_2 \\ \mathrm{i}\,\omega_1 - \omega_2 & -\mathrm{i}\,\omega_3 \end{bmatrix} \begin{bmatrix} \dot{\alpha} \\ \dot{\beta} \end{bmatrix} \,. \tag{10.50}$$

10.6 Rodrigues Parameters

The relationship between the Rodrigues vector $\mathbf{u}$ and the Euler-Rodrigues parameters is

$$\mathbf{u} = \frac{\mathbf{q}}{q_0} \,. \tag{10.51}$$

This in combination with the differential Eqs.(10.33) and (10.34) for Euler-Rodrigues parameters yields

$$\begin{aligned} \frac{{}^{(2)}\,\mathrm{d}\mathbf{u}}{\mathrm{d}t} &= \frac{q_0 \frac{{}^{(2)}\,\mathrm{d}\mathbf{q}}{\mathrm{d}t} - \dot{q}_0 \mathbf{q}}{q_0^2} = \frac{1}{2}\,\frac{q_0(q_0\boldsymbol{\omega} - \boldsymbol{\omega}\times\mathbf{q}) + \mathbf{q}\mathbf{q}\cdot\boldsymbol{\omega}}{q_0^2} \\ &= \frac{1}{2}(\mathsf{I} + \mathbf{u}\mathbf{u} + \mathbf{u}\times\mathsf{I})\cdot\boldsymbol{\omega} \,. \end{aligned} \tag{10.52}$$

Decomposition in $\underline{\mathbf{e}}^2$ yields the desired differential equations:

$$\dot{\underline{u}} = \frac{1}{2}(\underline{I} + \underline{u}\,\underline{u}^T + \tilde{\underline{u}})\,\underline{\omega} \,. \tag{10.53}$$

They are nonlinear.

Resolution for $\underline{\omega}$ is achieved by first resolving (10.52) for $\boldsymbol{\omega}$. With indeterminate coefficients A, B, C the ansatz $\boldsymbol{\omega} = A\mathbf{u} + B\frac{{}^{(2)}\,\mathrm{d}\mathbf{u}}{\mathrm{d}t} + C\mathbf{u}\times\frac{{}^{(2)}\,\mathrm{d}\mathbf{u}}{\mathrm{d}t}$ is made. Substitution into (10.52) results in the equation

$$\begin{aligned} 2\frac{{}^{(2)}\,\mathrm{d}\mathbf{u}}{\mathrm{d}t} &= \mathbf{u}\Big[A(1+u^2) + (B+C)\mathbf{u}\cdot\frac{{}^{(2)}\,\mathrm{d}\mathbf{u}}{\mathrm{d}t}\Big] \\ &\quad + \frac{{}^{(2)}\,\mathrm{d}\mathbf{u}}{\mathrm{d}t}\,(B - Cu^2) + \mathbf{u}\times\frac{{}^{(2)}\,\mathrm{d}\mathbf{u}}{\mathrm{d}t}\,(B+C) \,. \end{aligned} \tag{10.54}$$

Scalar multiplications with $\mathbf{u}$, with $\frac{{}^{(2)}\,\mathrm{d}\mathbf{u}}{\mathrm{d}t}$ and with $\mathbf{u}\times\frac{{}^{(2)}\,\mathrm{d}\mathbf{u}}{\mathrm{d}t}$ produce three equations for A, B and C. The third equation yields $C = -B$. The other two equations become

$$Au^2 + \Big(B - \frac{2}{1+u^2}\Big)\mathbf{u}\cdot\frac{{}^{(2)}\,\mathrm{d}\mathbf{u}}{\mathrm{d}t} = 0 \,, \quad A\mathbf{u}\cdot\frac{{}^{(2)}\,\mathrm{d}\mathbf{u}}{\mathrm{d}t} + \Big(B - \frac{2}{1+u^2}\Big)\Big(\frac{{}^{(2)}\,\mathrm{d}\mathbf{u}}{\mathrm{d}t}\Big)^2 = 0 \,. \tag{10.55}$$

The solutions are

$$A = 0 \,, \qquad B = -C = \frac{2}{1+u^2} \,. \tag{10.56}$$

This yields

$$\boldsymbol{\omega} = \frac{2}{1+u^2}\Big(\frac{{}^{(2)}\,\mathrm{d}\mathbf{u}}{\mathrm{d}t} - \mathbf{u}\times\frac{{}^{(2)}\,\mathrm{d}\mathbf{u}}{\mathrm{d}t}\Big) = \frac{2}{1+u^2}(\mathsf{I} - \mathbf{u}\times\mathsf{I})\cdot\frac{{}^{(2)}\,\mathrm{d}\mathbf{u}}{\mathrm{d}t} \,. \tag{10.57}$$

Decomposition in $\underline{\mathbf{e}}^2$ yields the final result

$$\underline{\omega} = \frac{2}{1+u^2}\,(\underline{I} - \underline{\tilde{u}})\,\underline{\dot{u}}\;. \tag{10.58}$$

10.7 Wiener Parameters

The Wiener vector $\boldsymbol{\sigma}$ is related to Euler-Rodrigues parameters through Eqs.(1.183) and (1.184):

$$\boldsymbol{\sigma} = \frac{\mathbf{q}}{1+q_0}\;, \qquad \sigma_0 = \frac{q_0}{1+q_0} = \frac{1}{2}(1-\sigma^2)\;. \tag{10.59}$$

This in combination with the differential Eqs.(10.33) and (10.34) for Euler-Rodrigues parameters yields

$$\begin{aligned}\frac{{}^{(2)}\,\mathrm{d}\boldsymbol{\sigma}}{\mathrm{d}t} &= \frac{1}{(1+q_0)^2}\Big[(1+q_0)\frac{{}^{(2)}\,\mathrm{d}\mathbf{q}}{\mathrm{d}t} - \dot{q}_0\mathbf{q}\Big] \\ &= \frac{1}{2}\Big[\frac{q_0}{1+q_0}\,\boldsymbol{\omega} + \frac{\mathbf{q}}{1+q_0}\times\boldsymbol{\omega} + \frac{\mathbf{q}\mathbf{q}\cdot\boldsymbol{\omega}}{(1+q_0)^2}\Big] \\ &= \frac{1}{2}(\sigma_0\mathsf{I} + \boldsymbol{\sigma}\boldsymbol{\sigma} + \boldsymbol{\sigma}\times\mathsf{I})\cdot\boldsymbol{\omega}\;. \end{aligned} \tag{10.60}$$

Decomposition in $\underline{\mathbf{e}}^2$ yields the desired differential equations:

$$\dot{\underline{\sigma}} = \frac{1}{2}(\sigma_0\underline{I} + \underline{\sigma}\,\underline{\sigma}^T + \underline{\tilde{\sigma}})\,\underline{\omega}\;. \tag{10.61}$$

They are nonlinear. Resolution for $\underline{\omega}$ is achieved by first resolving (10.60) for $\boldsymbol{\omega}$ by the same method which led to (10.57). This time, the ansatz $\boldsymbol{\omega} = A\boldsymbol{\sigma} + B\frac{{}^{(2)}\,\mathrm{d}\boldsymbol{\sigma}}{\mathrm{d}t} + C\boldsymbol{\sigma}\times\frac{{}^{(2)}\,\mathrm{d}\boldsymbol{\sigma}}{\mathrm{d}t}$ is made. The result is

$$\boldsymbol{\omega} = \frac{2}{(1-\sigma_0)^2}\,(\sigma_0\mathsf{I} + \boldsymbol{\sigma}\boldsymbol{\sigma} - \boldsymbol{\sigma}\times\mathsf{I})\,\frac{{}^{(2)}\,\mathrm{d}\boldsymbol{\sigma}}{\mathrm{d}t}\;. \tag{10.62}$$

Decomposition in $\underline{\mathbf{e}}^2$ yields the final result

$$\underline{\omega} = \frac{2}{(1-\sigma_0)^2}\,(\sigma_0\underline{I} + \underline{\sigma}\,\underline{\sigma}^T - \underline{\tilde{\sigma}})\,\underline{\dot{\sigma}}\;. \tag{10.63}$$

10.8 Euler Vector

The time derivative of the Euler vector $\boldsymbol{\varphi} = \mathbf{n}\varphi$ in basis $\underline{\mathbf{e}}^2$ is

$$\frac{^{(2)}\,\mathrm{d}\boldsymbol{\varphi}}{\mathrm{d}t} = \frac{^{(2)}\,\mathrm{d}\mathbf{n}}{\mathrm{d}t}\,\varphi + \mathbf{n}\dot{\varphi}\,. \tag{10.64}$$

Expressions for $\dot{\varphi}$ and for $^{(2)}\,\mathrm{d}\mathbf{n}/\,\mathrm{d}t$ in terms of $\mathbf{n}$ and $\boldsymbol{\omega}$ are derived from the definitions of Euler-Rodrigues parameters and from their kinematic differential Eqs.(10.33) and (10.34):

$$\left.\begin{aligned} q_0 &= \cos\frac{\varphi}{2} \quad (a)\,, \quad \dot{q}_0 = -\frac{1}{2}\,\boldsymbol{\omega}\cdot\mathbf{q} \quad (b)\,,\\ \mathbf{q} &= \mathbf{n}\sin\frac{\varphi}{2} \quad (c)\,, \quad \frac{^{(2)}\,\mathrm{d}\mathbf{q}}{\mathrm{d}t} = \frac{1}{2}\,(q_0\boldsymbol{\omega} + \mathbf{q}\times\boldsymbol{\omega}) \quad (d)\,. \end{aligned}\right\} \tag{10.65}$$

From (10.65)a it follows that $\dot{q}_0 = -\frac{1}{2}\dot{\varphi}\sin\varphi/2$ and from this with (10.65)b and c

$$\dot{\varphi} = \frac{\mathbf{q}\cdot\boldsymbol{\omega}}{\sin\frac{\varphi}{2}} = \mathbf{n}\cdot\boldsymbol{\omega}\,. \tag{10.66}$$

Equations (10.65)c and d yield

$$\begin{aligned} \frac{^{(2)}\,\mathrm{d}\mathbf{n}}{\mathrm{d}t} &= \frac{^{(2)}\,\mathrm{d}}{\mathrm{d}t}\Big(\frac{\mathbf{q}}{\sin\frac{\varphi}{2}}\Big) = \frac{\frac{^{(2)}\,\mathrm{d}\mathbf{q}}{\mathrm{d}t}}{\sin\frac{\varphi}{2}} - \frac{1}{2}\,\dot{\varphi}\mathbf{q}\,\frac{\cos\frac{\varphi}{2}}{\sin^2\frac{\varphi}{2}}\\ &= \frac{1}{2}\Big(\frac{\boldsymbol{\omega}\cos\frac{\varphi}{2} + \mathbf{q}\times\boldsymbol{\omega}}{\sin\frac{\varphi}{2}} - \dot{\varphi}\,\frac{\mathbf{q}}{\sin\frac{\varphi}{2}}\,\cot\frac{\varphi}{2}\Big)\\ &= \frac{1}{2}\Big(\boldsymbol{\omega}\cot\frac{\varphi}{2} + \mathbf{n}\times\boldsymbol{\omega} - \dot{\varphi}\,\mathbf{n}\cot\frac{\varphi}{2}\Big) \end{aligned} \tag{10.67}$$

and with (10.66) for $\dot{\varphi}$ and with $\cot\varphi/2 = (1+\cos\varphi)/\sin\varphi$ finally

$$\frac{^{(2)}\,\mathrm{d}\mathbf{n}}{\mathrm{d}t} = -\frac{1}{2}\Big[\frac{1+\cos\varphi}{\sin\varphi}\,(\mathbf{n}\mathbf{n} - \mathsf{I}) - \mathbf{n}\times\mathsf{I}\Big]\cdot\boldsymbol{\omega}\,. \tag{10.68}$$

With this expression and with (10.66) Eq.(10.64) takes the form

$$\frac{^{(2)}\,\mathrm{d}\boldsymbol{\varphi}}{\mathrm{d}t} = \Big\{\mathbf{n}\mathbf{n} - \frac{\varphi}{2}\Big[\frac{1+\cos\varphi}{\sin\varphi}\,(\mathbf{n}\mathbf{n} - \mathsf{I}) - \mathbf{n}\times\mathsf{I}\Big]\Big\}\cdot\boldsymbol{\omega}\,. \tag{10.69}$$

This is the desired kinematic differential equation for the Euler vector. It is nonlinear. Decomposition in $\underline{\mathbf{e}}^2$ yields the scalar differential equations

$$\underline{\dot{\varphi}} = \Big\{\underline{n}\,\underline{n}^T - \frac{\varphi}{2}\Big[\frac{1+\cos\varphi}{\sin\varphi}\,(\underline{n}\,\underline{n}^T - \underline{I}) - \tilde{\underline{n}}\Big]\Big\}\,\underline{\omega}\,. \tag{10.70}$$

Resolution for $\underline{\omega}$ is achieved by first resolving (10.69) for $\boldsymbol{\omega}$ by the same method which led to (10.57). With indeterminate coefficients $A\,,\,B\,,\,C$ the ansatz $\boldsymbol{\omega} = A\mathbf{n} + B\frac{^{(2)}\,\mathrm{d}\boldsymbol{\varphi}}{\mathrm{d}t} + C\mathbf{n}\times\frac{^{(2)}\,\mathrm{d}\boldsymbol{\varphi}}{\mathrm{d}t}$ is made. It is substituted into (10.69). With the abbreviations

$$x = \frac{\varphi}{2}\,\frac{1+\cos\varphi}{\sin\varphi}\,, \qquad y = \frac{\varphi}{2} \tag{10.71}$$

the resulting equation reads:

$$\frac{{}^{(2)}\,\mathrm{d}\boldsymbol{\varphi}}{\mathrm{d}t} = A\mathbf{n} + B\Big[(1-x)\Big(\mathbf{n}\cdot\frac{{}^{(2)}\,\mathrm{d}\boldsymbol{\varphi}}{\mathrm{d}t}\Big)\mathbf{n} + x\,\frac{{}^{(2)}\,\mathrm{d}\boldsymbol{\varphi}}{\mathrm{d}t} - y\,\mathbf{n}\times\frac{{}^{(2)}\,\mathrm{d}\boldsymbol{\varphi}}{\mathrm{d}t}\Big] + C\Big[x\,\mathbf{n}\times\frac{{}^{(2)}\,\mathrm{d}\boldsymbol{\varphi}}{\mathrm{d}t} - y\,\mathbf{n}\times\Big(\mathbf{n}\times\frac{{}^{(2)}\,\mathrm{d}\boldsymbol{\varphi}}{\mathrm{d}t}\Big)\Big]\,. \tag{10.72}$$

Scalar multiplications with $\mathbf{n}$, with $\frac{{}^{(2)}\,\mathrm{d}\boldsymbol{\varphi}}{\mathrm{d}t}$ and with $\mathbf{n}\times\frac{{}^{(2)}\,\mathrm{d}\boldsymbol{\varphi}}{\mathrm{d}t}$ produce three equations for A, B and C. The first and the third equation yield

$$A = (1-B)\mathbf{n}\cdot\frac{{}^{(2)}\,\mathrm{d}\boldsymbol{\varphi}}{\mathrm{d}t}\,, \qquad C = -B\,\frac{y}{x}\,. \tag{10.73}$$

When this is substituted, the second equation becomes an equation for B. The solutions for the three coefficients are

$$B = \frac{x}{x^2+y^2} = \frac{\sin\varphi}{\varphi}\,, \qquad A = \Big(1-\frac{\sin\varphi}{\varphi}\Big)\mathbf{n}\cdot\frac{{}^{(2)}\,\mathrm{d}\boldsymbol{\varphi}}{\mathrm{d}t}\,, \qquad C = -\frac{1-\cos\varphi}{\varphi}\,. \tag{10.74}$$

With these expressions the angular velocity is

$$\boldsymbol{\omega} = \Big[\mathbf{n}\mathbf{n} - \frac{\sin\varphi}{\varphi}\,(\mathbf{n}\mathbf{n}-\mathsf{I}) - \frac{1-\cos\varphi}{\varphi}\,\mathbf{n}\times\mathsf{I}\Big]\cdot\frac{{}^{(2)}\,\mathrm{d}\boldsymbol{\varphi}}{\mathrm{d}t}\,. \tag{10.75}$$

Decomposition in $\underline{\mathbf{e}}^2$ yields the final result

$$\underline{\omega} = \Big[\underline{n}\,\underline{n}^T - \frac{\sin\varphi}{\varphi}\,(\underline{n}\,\underline{n}^T - \underline{I}) - \frac{1-\cos\varphi}{\varphi}\,\tilde{\underline{n}}\Big]\,\dot{\underline{\varphi}}\,. \tag{10.76}$$

The kinematic differential equation for the Euler vector and the formula for $\boldsymbol{\omega}$ were established by other methods and with different notations by Stuelpnagel [5], Peres [2], Nazaroff [1], Shuster [4] and Pfister [3].

Example 1: The solutions of the various kinematic differential equations are a-priorily known if the direction cosine matrix $\underline{A}^{12}(t)$ is prescribed as function of time. As illustrative example the matrix is prescribed as follows:

$$\underline{A}^{12}(t) = \begin{bmatrix} \cos\omega t & -\sin\omega t & 0 \\ 0 & 0 & -1 \\ \sin\omega t & \cos\omega t & 0 \end{bmatrix}\,, \qquad A^{12}(0) = \begin{bmatrix} 1 & 0 & 0 \\ 0 & 0 & -1 \\ 0 & 1 & 0 \end{bmatrix}\,. \tag{10.77}$$

The initial position at $t=0$ is the result of a 90°-rotation of the body-fixed basis $\underline{\mathbf{e}}^2$ about the axis $\mathbf{e}_1^1$. From the matrix $\underline{A}^{12}(t)$ it is evident that the motion is a permanent rotation about the axis $\mathbf{e}_2^1 \equiv -\mathbf{e}_3^2$ with the angular

velocity of constant magnitude ω. This means that the vector $\boldsymbol{\omega}$ has in $\underline{\mathbf{e}}^2$ the constant coordinate matrix $\underline{\omega} = [0 \;\; 0 \;\; \omega]$. The same coordinate matrix is obtained from (10.7): $\tilde{\underline{\omega}} = \underline{A}^{12\,T}\,\underline{\dot{A}}^{12}$. The matrix $\underline{A}^{12}(t)$ determines as functions of time the corresponding Euler angles, Bryan angles and Euler-Rodrigues parameters. Equations (1.29), (1.35), (1.81) and (1.82) yield

$$\left.\begin{array}{lllll} \text{Euler angles:} & \psi \equiv 0\,, & \theta \equiv \pi/2\,, & \phi = \omega t\,, \\ \text{Bryan angles:} & \phi_1 \equiv \pi/2\,, & \phi_2 \equiv 0\,, & \phi_3 = \omega t\,, \\ \text{E.-Rodr. par's:} & q_0(t) = q_1(t) = \frac{\sqrt{2}}{2}\cos\frac{\omega t}{2}\,, & q_3(t) = \frac{\sqrt{2}}{2}\sin\frac{\omega t}{2}\,, & q_2(t) = -q_3(t)\,. \end{array}\right\} \tag{10.78}$$

The matrix $\underline{A}^{12}(t)$ also determines the eigenvector $\mathbf{n}(t) \equiv \mathbf{e}_3^2$, the Rodrigues vector $\mathbf{u}(t) = \mathbf{e}_3^2 \tan\frac{\omega t}{2}$, the Wiener vector $\boldsymbol{\sigma}(t) = \mathbf{e}_3^2 \tan\frac{\omega t}{4}$ and the Euler vector $\boldsymbol{\phi} = \mathbf{e}_3^2 \omega t$.

As illustrative examples the differential equations for Euler angles and for Euler-Rodrigues parameters are formulated. With the given angular velocity coordinates $[0 \;\; 0 \;\; \omega]$ Eqs.(10.24) for Euler angles read: $\dot{\psi} = 0$, $\dot{\theta} = 0$, $\dot{\phi} = \omega$. Together with the prescribed initial values this yields the solutions (10.78).

Equations (10.35) for Euler-Rodrigues parameters read

$$\dot{q}_0 = -\frac{\omega}{2}\,q_3\,, \qquad \dot{q}_1 = \frac{\omega}{2}\,q_2\,, \qquad \dot{q}_2 = -\frac{\omega}{2}\,q_1\,, \qquad \dot{q}_3 = \frac{\omega}{2}\,q_0\,. \tag{10.79}$$

Combining the first equation with the fourth and the second with the third results in the equations $\ddot{q}_0 = -(\omega/2)^2 q_0$ and $\ddot{q}_1 = -(\omega/2)^2 q_1$. They have the general solutions

$$q_0(t) = A_0 \cos\frac{\omega t}{2} + B_0 \sin\frac{\omega t}{2}\,, \qquad q_1(t) = A_1 \cos\frac{\omega t}{2} + B_1 \sin\frac{\omega t}{2}\,. \tag{10.80}$$

With these solutions the solutions for $q_2(t)$ and $q_3(t)$ are obtained from (10.79). The constants of integration A_0, B_0, A_1, B_1 are determined by the prescribed initial conditions $q_0(0) = q_1(0) = \sqrt{2}/2$, $q_2(0) = q_3(0) = 0$. The final results are those given in (10.78). End of example.

Example 2: The coordinates of the angular velocity $\boldsymbol{\omega}$ of a body in the body-fixed basis $\underline{\mathbf{e}}^2$ are given as functions of time in the form

$$\omega_1(t) = -\Omega \sin\omega_0 t\,, \qquad \omega_2(t) = \Omega \cos\omega_0 t\,, \qquad \omega_3(t) \equiv \mu\Omega \tag{10.81}$$

with constants μ, Ω and ω_0. They show that the body-fixed polhode cone referred to in Theorem 9.7 is a circular cone with the axis $\mathbf{e}_3^2$. The vector $\boldsymbol{\omega}$ has constant magnitude $\Omega\sqrt{1+\mu^2}$. It is rotating with the angular velocity ω_0 about the cone axis. To be determined are the herpolhode cone and the angular position of the body as functions of time.

Solution: The differential Eqs.(10.24) for Euler angles are

$$\left.\begin{aligned} \dot\psi &= \;\; \Omega\,\frac{\cos(\phi+\omega_0 t)}{\sin\theta}\;, \\ \dot\theta &= -\Omega\sin(\phi+\omega_0 t)\;, \\ \dot\phi &= -\Omega\cos(\phi+\omega_0 t)\cot\theta+\mu\Omega\;. \end{aligned}\right\} \tag{10.82}$$

Equations (10.81) are the solutions of Euler's dynamics equations of motion for a classical problem of rigid body dynamics, namely, the motion of an inertia-symmetric body about its center of mass in the absence of external torques (Wittenburg [6, 8]). The angular momentum vector of the body has constant magnitude and direction in an inertial reference basis $\underline{\mathbf{e}}^1$. This additional condition requires the Euler angles to be the special solutions

$$\left.\begin{aligned} &\phi(t) = -\omega_0 t\;, && \dot\phi \equiv -\omega_0 = \text{ const}\;, \\ &\cot\theta \equiv \mu + \frac{\omega_0}{\Omega} = \text{ const}\;, && \dot\psi \equiv \frac{\Omega}{\sin\theta} = \text{ const}\;. \end{aligned}\right\} \tag{10.83}$$

These results are interpreted as follows (see Fig. 1.1). The motion of basis $\underline{\mathbf{e}}^2$ is the superposition of two rotational motions. One is rotation with $\dot\psi =$ const about $\mathbf{e}_3^1$ in the position $\theta =$ const., and the other is rotation with $\dot\phi =$ const about $\mathbf{e}_3^2$. This means that the body-fixed axis $\mathbf{e}_3^2$ is moving on the cone with axis $\mathbf{e}_3^1$ and with semi apex angle θ. The fixed herpolhode cone generated by $\boldsymbol{\omega}$ is another circular cone also with the axis $\mathbf{e}_3^1$. The vector $\boldsymbol{\omega}$ along the line of contact of polhode and herpolhode cone is permanently in the plane spanned by $\mathbf{e}_3^2$ and $\mathbf{e}_3^1$.

The general solution $\psi(t)\,,\ \theta(t)\,,\ \phi(t)$ is obtained not from (10.82), but via Euler-Rodrigues parameters. The differential Eqs.(10.35) for these parameters are

$$\left.\begin{aligned} 2\dot q_0 &= -\Omega(-q_1\sin\omega_0 t + q_2\cos\omega_0 t + \mu q_3)\;, \\ 2\dot q_1 &= \;\;\Omega(-q_0\sin\omega_0 t - q_3\cos\omega_0 t + \mu q_2)\;, \\ 2\dot q_2 &= \;\;\Omega(-q_3\sin\omega_0 t + q_0\cos\omega_0 t - \mu q_1)\;, \\ 2\dot q_3 &= -\Omega(-q_2\sin\omega_0 t - q_1\cos\omega_0 t - \mu q_0)\;. \end{aligned}\right\} \tag{10.84}$$

Solving these equations is difficult. Solving the differential Eqs.(10.49) for the Cayley-Klein parameters $\alpha = q_0 + \mathrm{i}\,q_3$ and $\beta = -q_2 + \mathrm{i}\,q_1$ is much simpler. With $\mathrm{i}\,\omega_1(t) \pm \omega_2(t) = \pm\Omega \mathrm{e}^{\mp \mathrm{i}\,\omega_0 t}$ these equations are

$$\dot\alpha = \frac{\Omega}{2}\,\left(\mathrm{i}\,\mu\alpha + \mathrm{e}^{-\mathrm{i}\,\omega_0 t}\beta\right)\;, \qquad \dot\beta = -\frac{\Omega}{2}\,\left(\mathrm{i}\,\mu\beta + \mathrm{e}^{\mathrm{i}\,\omega_0 t}\alpha\right)\;. \tag{10.85}$$

With $D = \omega_0/\Omega$, with the dimensionless time $\tau = (\Omega/2)t$, with the chain rule $\mathrm{d}/\mathrm{d}t = (\Omega/2)\mathrm{d}/\mathrm{d}\tau$ and with the symbol $'$ denoting the derivative with respect to τ the equations are

$$\alpha' = \mathrm{i}\,\mu\alpha + \mathrm{e}^{-2\mathrm{i}\,D\tau}\beta\;, \qquad \beta' = -\left(\mathrm{i}\,\mu\beta + \mathrm{e}^{2\mathrm{i}\,D\tau}\alpha\right)\;. \tag{10.86}$$

The first equation is differentiated:

$$\alpha'' = \mathrm{i}\,\mu\alpha' + \mathrm{e}^{-2\mathrm{i}\,D\tau}(-2\mathrm{i}\,D\beta + \beta') \,. \tag{10.87}$$

By means of (10.86) the term $\mathrm{e}^{-2\mathrm{i}\,D\tau}(-2\mathrm{i}\,D\beta + \beta')$ is expressed as linear combination of α' and α. This procedure results in the second-order equation

$$\alpha'' + 2\mathrm{i}\,D\alpha' + (1 + \mu^2 + 2D\mu)\alpha = 0 \,. \tag{10.88}$$

The ansatz $\alpha = A\,\mathrm{e}^{\lambda\tau}$ leads to the equation $\lambda^2 + 2\mathrm{i}\,D\lambda + 1 + \mu^2 + 2D\mu = 0$. It has two purely imaginary solutions

$$\left.\begin{aligned} &\lambda_{1,2} = \mathrm{i}\,\nu_{1,2} \,, \qquad \nu_{1,2} = -D \pm \sqrt{1 + (D+\mu)^2} \,, \\ &\qquad\qquad \nu_1 + \nu_2 = -2\,D \,, \qquad (\nu_1 - \mu)(\nu_2 - \mu) = -1 \,. \end{aligned}\right\} \tag{10.89}$$

Hence $\alpha(\tau)$ is a linear combination of two harmonic oscillations:

$$\alpha(\tau) = A\,\mathrm{e}^{\mathrm{i}\,\nu_1\tau} + B\,\mathrm{e}^{\mathrm{i}\,\nu_2\tau} \,. \tag{10.90}$$

The first Eq.(10.86) yields

$$\begin{aligned} \beta(\tau) &= \mathrm{e}^{2\mathrm{i}\,D\tau}(\alpha' - \mathrm{i}\,\mu\alpha) \\ &= \mathrm{e}^{2\mathrm{i}\,D\tau}\left[\mathrm{i}\,(\nu_1 - \mu)A\,\mathrm{e}^{\mathrm{i}\,\nu_1\tau} + \mathrm{i}\,(\nu_2 - \mu)B\,\mathrm{e}^{\mathrm{i}\,\nu_2\tau}\right] \\ &= \mathrm{i}\,(\nu_1 - \mu)A\,\mathrm{e}^{-\mathrm{i}\,\nu_2\tau} + \mathrm{i}\,(\nu_2 - \mu)B\,\mathrm{e}^{-\mathrm{i}\,\nu_1\tau} \,. \end{aligned} \tag{10.91}$$

At this point the return from the complex Cayley-Klein parameters to the real Euler-Rodrigues parameters is made. Writing the complex constants of integration in the forms $A = A_1 + \mathrm{i}\,A_2$, $B = B_1 + \mathrm{i}\,B_2$ and expressing the exponential functions through circular functions the equations $\alpha = q_0 + \mathrm{i}\,q_3$, $\beta = -q_2 + \mathrm{i}\,q_1$ yield the explicit solutions

$$\left.\begin{aligned} q_0 &= A_1\cos\nu_1\tau - A_2\sin\nu_1\tau + B_1\cos\nu_2\tau - B_2\sin\nu_2\tau \,, \\ q_3 &= A_2\cos\nu_1\tau + A_1\sin\nu_1\tau + B_2\cos\nu_2\tau + B_1\sin\nu_2\tau \,, \\ q_2 &= (\nu_1 - \mu)(A_2\cos\nu_2\tau - A_1\sin\nu_2\tau) + (\nu_2 - \mu)(B_2\cos\nu_1\tau - B_1\sin\nu_1\tau) \,, \\ q_1 &= (\nu_1 - \mu)(A_1\cos\nu_2\tau + A_2\sin\nu_2\tau) + (\nu_2 - \mu)(B_1\cos\nu_1\tau + B_2\sin\nu_1\tau) \,. \end{aligned}\right\} \tag{10.92}$$

These are the solutions of (10.84). They determine the direction cosine matrix $\underline{A}^{12}(\tau)$ and the coordinates $\underline{\omega}^1(\tau) = \underline{A}^{12}\underline{\omega}$ of the angular velocity in basis $\underline{\mathbf{e}}^1$. These coordinates are parameter equations of the herpolhode cone.

Substitution of (10.92) into (1.92) – (1.96) yields the general solution of Eqs.(10.82) for Euler angles. Equations (1.92) are

$$\left.\begin{aligned}
&\cos^2\frac{\theta}{2} = q_0^2 + q_3^2 = A_1^2 + A_2^2 + B_1^2 + B_2^2 + f(\tau)\ ,\\
&\sin^2\frac{\theta}{2} = q_1^2 + q_2^2 = (\nu_1-\mu)^2(A_1^2+A_2^2) + (\nu_2-\mu)^2(B_1^2+B_2^2) - f(\tau)\ ,\\
&f(\tau) = 2[(A_1B_1 + A_2B_2)\cos(\nu_1-\nu_2)\tau + (A_1B_2 - A_2B_1)\sin(\nu_1-\nu_2)\tau]\ .
\end{aligned}\right\} \tag{10.93}$$

The sum of the equations is

$$[1+(\nu_1-\mu)^2](A_1^2+A_2^2) + [1+(\nu_2-\mu)^2](B_1^2+B_2^2) = 1\ . \tag{10.94}$$

This constitutes a constraint equation on the four constants of integration. The oscillatory term $f(\tau)$ with $(\nu_1-\nu_2)\tau = \sqrt{\Omega^2+(\omega_0+\omega_3)^2}\,t$ has the amplitude $2\sqrt{(A_1^2+A_2^2)(B_1^2+B_2^2)}$. The angle θ is constant if either $A_1 = A_2 = 0$ or $B_1 = B_2 = 0$. These special solutions yield

$$\cot\frac{\theta_{1,2}}{2} = \frac{1}{\nu_{1,2}-\mu} \tag{10.95}$$

and

$$\cot\theta_{1,2} = \frac{\cot^2\theta_{1,2}/2 - 1}{2\cot\theta_{1,2}/2} = \frac{1-(\nu_{1,2}-\mu)^2}{2(\nu_{1,2}-\mu)} \tag{10.96}$$

and with (10.89)

$$\cot\theta_{1,2} = \mu + D\ . \tag{10.97}$$

This is the solution (10.83). End of example.

10.9 Correction Formulas for Euler-Rodrigues Parameters

Solutions $q_k(t)$ $(k = 0,1,2,3)$ resulting from a numerical integration of the differential Eqs.(10.35) violate, because of inevitable numerical errors, the constraint Eq.(1.68)

$$f(q_0,\ldots,q_3) = \sum_{k=0}^{3} q_k^2 - 1 = 0\ . \tag{10.98}$$

The solutions must be corrected in order to be true Euler-Rodrigues parameters. In what follows, the calculated faulty quantities are denoted q_i^*, and the unknown corrected quantities are denoted q_i $(i = 0,1,2,3)$. The measure for the error of the calculated quantities is

$$\varepsilon = \sum_{k=0}^{3} q_k^{*2} - 1\ . \tag{10.99}$$

It is reasonable to determine the corrections $q_i - q_i^*$ $(i = 0, 1, 2, 3)$ such that the sum of squares is a minimum:

$$F(q_0, \ldots, q_3) = \sum_{k=0}^{3} (q_k - q_k^*)^2 = \text{ Min!} \tag{10.100}$$

The unknowns are the solutions of the equations

$$\frac{\partial}{\partial q_i}(F - \lambda f) = 0 \qquad (i = 0, 1, 2, 3) \tag{10.101}$$

where λ is the Lagrangian multiplier associated with the function f in (10.98). The equations yield $q_i = q_i^*/(1 - \lambda)$ $(i = 0, 1, 2, 3)$. Substitution into (10.98) leads to $1 - \lambda = \sqrt{1 + \varepsilon}$. The desired corrected quantities are

$$q_i = \frac{q_i^*}{\sqrt{1+\varepsilon}} = q_i^* \left(1 - \frac{\varepsilon}{2}\right) + \ldots \text{ (higher-order terms in } \varepsilon) \qquad (i = 0, 1, 2, 3) \,. \tag{10.102}$$

Normally, these correction formulas are used.

Instead of the objective function F in (10.100) some other function can be chosen in which not the differences $(q_k - q_k^*)$, but differences of geometrically significant functions of Euler-Rodrigues parameters appear explicitly. Direction cosines are significant functions. The direction cosine matrix is (see (1.80))

$$\underline{A} = [a_{ij}] = \begin{bmatrix} 2(q_0^2 + q_1^2) - 1 & 2(q_1 q_2 - q_0 q_3) & 2(q_1 q_3 + q_0 q_2) \\ 2(q_1 q_2 + q_0 q_3) & 2(q_0^2 + q_2^2) - 1 & 2(q_2 q_3 - q_0 q_1) \\ 2(q_1 q_3 - q_0 q_2) & 2(q_2 q_3 + q_0 q_1) & 2(q_0^2 + q_3^2) - 1 \end{bmatrix} \,. \tag{10.103}$$

Let $\underline{A}^* = [a_{ij}^*]$ be the matrix obtained from this equation with q_k^* instead of q_k. Equation (10.100) is replaced by (Wittenburg [7])

$$\sum_{i=1}^{3} \sum_{j=1}^{3} (a_{ij} - a_{ij}^*)^2 = \text{ Min!} \tag{10.104}$$

or

$$\sum_{i=1}^{3} \sum_{j=1}^{3} a_{ij}^2 + \sum_{i=1}^{3} \sum_{j=1}^{3} {a_{ij}^*}^2 - 2 \sum_{i=1}^{3} \sum_{j=1}^{3} a_{ij} a_{ij}^* = \text{ Min!} \tag{10.105}$$

The first double sum equals three because $\underline{A}$ is an orthogonal matrix. The second double sum is a given number. Hence the objective function is

$$F(q_0, \ldots, q_3) = \sum_{i=1}^{3} \sum_{j=1}^{3} a_{ij} a_{ij}^* = \text{ Max!} \tag{10.106}$$

With this function Eqs.(10.101) are formulated. With a_{ij} from (10.103), with f from (10.98) and with a^*_{ij} still unchanged these equations have the form

$$\begin{bmatrix} 2(a^*_{11}+a^*_{22}+a^*_{33})-\lambda & & \text{symmetric} & \\ a^*_{23}-a^*_{32} & 2a^*_{11}-\lambda & & \\ a^*_{31}-a^*_{13} & a^*_{12}+a^*_{21} & 2a^*_{22}-\lambda & \\ a^*_{12}-a^*_{21} & a^*_{13}+a^*_{31} & a^*_{23}+a^*_{32} & 2a^*_{33}-\lambda \end{bmatrix} \begin{bmatrix} q_0 \\ q_1 \\ q_2 \\ q_3 \end{bmatrix} = \underline{0}\,. \tag{10.107}$$

Next, the matrix elements a^*_{ij} are expressed by (10.103) as functions of the given quantities q^*_k. With the abbreviation $\mu = (2 - q_0^{*2} + \lambda)/4$ the system of equations is obtained:

$$\begin{bmatrix} q_0^{*2}+\varepsilon-\mu & & \text{symmetric} & \\ q_0^* q_1^* & q_1^{*2}-\mu & & \\ q_0^* q_2^* & q_1^* q_2^* & q_2^{*2}-\mu & \\ q_0^* q_3^* & q_1^* q_3^* & q_2^* q_3^* & q_3^{*2}-\mu \end{bmatrix} \begin{bmatrix} q_0 \\ q_1 \\ q_2 \\ q_3 \end{bmatrix} = \underline{0}\,. \tag{10.108}$$

This is an eigenvalue problem with eigenvalue μ. The characteristic equation is

$$\mu^2\Big[\mu^2 - (1+2\varepsilon)\mu + \varepsilon(1+\varepsilon-q_0^{*2})\Big] = 0\,. \tag{10.109}$$

The eigenvalues are

$$\mu_1 = \mu_2 = 0\,, \qquad \mu_{3,4} = \frac{1}{2}\left(1+2\varepsilon \pm \sqrt{1+4\varepsilon q_0^{*2}}\right). \tag{10.110}$$

In the case $\varepsilon = 0$ (10.108) is known to have the solutions $q_i = q_i^*$ $(i = 0,1,2,3)$. This requires $\mu = 1$. From this it follows that in the general case $\varepsilon \neq 0$ the relevant eigenvalue is

$$\mu = \frac{1}{2}\left(1+2\varepsilon+\sqrt{1+4\varepsilon q_0^{*2}}\right). \tag{10.111}$$

This is substituted into (10.108). The first equation is discarded. The remaining equations are solved for q_1, q_2 and q_3:

$$q_i = q_i^* \frac{q_0 q_0^*}{\mu - (1+\varepsilon-q_0^{*2})} \qquad (i = 1,2,3)\,. \tag{10.112}$$

With these expressions the final result for q_0 is obtained from (10.98):

$$q_0 = \left[1 + \frac{q_0^{*2}(1+\varepsilon-q_0^{*2})}{[\mu-(1+\varepsilon-q_0^{*2})]^2}\right]^{-1/2}. \tag{10.113}$$

When this is substituted back into (10.112), final results for the other three Euler-Rodrigues parameters are obtained. The first-order approximations with respect to ε are

$$\left.\begin{aligned} q_0 &= q_0^*\Big[1+\frac{1}{2}\,\varepsilon(1-2q_0^{*2})\Big]+\dots\ , \\ q_i &= q_i^*\Big[1-\frac{1}{2}\,\varepsilon(1+2q_0^{*2})\Big]+\dots \qquad (i=1,2,3)\ . \end{aligned}\right\} \tag{10.114}$$

These results differ significantly from those in (10.102).

References

1. Nazaroff G J (1979) The orientation vector differential equation. J. Guidance and Control 2:351–352
2. Peres A ((1979) Finite rotations and angular velocity. American J. Physics 48:70–71
3. Pfister F (1998) Bernoulli numbers and rotational kinematics. Trans. ASME 65:758–763
4. Shuster M D (1993) A survey of attitude representations. J.Astronaut.Scie.41:439–517 [with 163 lit. references]
5. Stuelpnagel J (1964) On the parametrization of the three-dimensional rotation group. Siam Rev.8:422–430
6. Wittenburg J (1977) Dynamics of systems of rigid bodies. Teubner Stuttgart
7. Wittenburg J (1982) A new correction formula for Euler-Rodrigues parameters. ZAMM 62:495–497
8. Wittenburg J (2007) Dynamics of multibody systems. Springer, Berlin Heidelberg New York

Chapter 11
Direct Kinematics of Tree-Structured Systems

In Fig. 11.1 a general spatial tree-structured system is shown. Its bodies $i = 0, \ldots, n$ and its joints $i = 1, \ldots, n$ are regularly labeled. By this is meant that joint i $(i = 1, \ldots, n)$ connects body i to a body $b(i) < i$. Example: In Fig. 11.1 $b(5) = 3$ and $b(1) = 0$. Regular labeling is always possible and, in general, in more than one way. The simplest tree-structure is a serial chain (a system without side branches). In a serial chain joint i $(i = 1, \ldots, n)$ connects body i to body $b(i) = i - 1$.

Body 0 is moving relative to a common reference basis $\underline{\mathbf{e}}$ according to some unspecified *prescribed* functions of time t. This general case includes the special case of a body 0 at rest. On each body i $(i = 0, \ldots, n)$ a reference basis $\underline{\mathbf{e}}^i$ is fixed. Its origin 0_i and its angular orientation on the body are chosen arbitrarily. The schematically indicated joints are of arbitrary nature with individual degrees of freedom $1 \leq f_i \leq 6$. Note: A joint with $f_i = 6$ is not a joint in the sense defined in Chap. 4 because the number of constraints is $f_i - 6 = 0$. Such a joint might have the form of a spring or damper connection. It is assumed that for each joint $i = 1, \ldots, n$ f_i joint variables $q_{i\ell}$ $(\ell = 1, \ldots, f_i)$ have been chosen which are suitable for describing the position of body i relative to body $b(i)$.

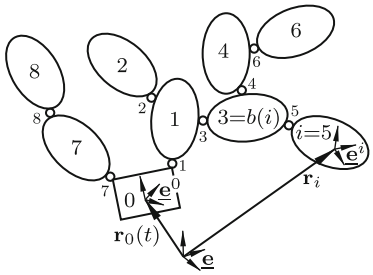

Fig. 11.1 Tree-structured system with regular labeling of bodies and of joints. Common reference basis $\underline{\mathbf{e}}$, reference basis $\underline{\mathbf{e}}^i$ fixed on body i, position vectors $\mathbf{r}_0(t)$ and $\mathbf{r}_i$

J. Wittenburg, *Kinematics*, DOI 10.1007/978-3-662-48487-6_11

The problem of direct kinematics is stated as follows. Determine as functions of joint variables and of time derivatives of joint variables for all bodies $i = 1, \ldots, n$ the position vector $\mathbf{r}_i$, the velocity $\dot{\mathbf{r}}_i$ and the acceleration $\ddot{\mathbf{r}}_i$ of 0_i relative to the common reference basis $\underline{\mathbf{e}}$, the direction cosine matrix $\underline{A}_i$ defined by the equation $\underline{\mathbf{e}} = \underline{A}_i \underline{\mathbf{e}}^i$, the angular velocity $\boldsymbol{\omega}_i$ and the angular acceleration $\dot{\boldsymbol{\omega}}_i$ relative to basis $\underline{\mathbf{e}}$. For body 0 these six quantities are, by assumption, prescribed functions of time $\mathbf{r}_0(t)$, $\dot{\mathbf{r}}_0(t)$, $\ddot{\mathbf{r}}_0(t)$, $\underline{A}_0(t)$, $\boldsymbol{\omega}_0(t)$ and $\dot{\boldsymbol{\omega}}_0(t)$. The solution to the problem is given in Sect. 11.2. It is based on the kinematics of individual joints which is treated first.

11.1 Kinematics of Individual Joints

In Fig. 11.2 a single joint i of unspecified nature connecting two bodies i and $b(i)$ is shown. The reference bases fixed on these bodies are $\underline{\mathbf{e}}^i$ and $\underline{\mathbf{e}}^{b(i)}$, respectively. Let $\underline{q}_i$ be the column matrix of joint variables $q_{i1}, \ldots, q_{if_i}$. The problem of joint kinematics is stated as follows. Determine as functions of the variables $\underline{q}_i$ and of their time derivatives the following six quantities: The position vector $\mathbf{c}_{b(i)i}$, the velocity $\mathbf{v}_i$ and the acceleration $\mathbf{a}_i$ relative to $\underline{\mathbf{e}}^{b(i)}$ of a single point P_i fixed in $\underline{\mathbf{e}}^i$, the direction cosine matrix $\underline{G}_i$ defined by the equation $\underline{\mathbf{e}}^{b(i)} = \underline{G}_i \underline{\mathbf{e}}^i$, the angular velocity $\boldsymbol{\Omega}_i$ and the angular acceleration $\boldsymbol{\varepsilon}_i$ of $\underline{\mathbf{e}}^i$ relative to $\underline{\mathbf{e}}^{b(i)}$.

The single point P_i fixed in $\underline{\mathbf{e}}^i$ is referred to as *articulation point*. How to choose this point is shown further below. The articulation point has in $\underline{\mathbf{e}}^i$ a constant position vector $\mathbf{c}_{ii}$ and in $\underline{\mathbf{e}}^{b(i)}$ a variable position vector $\mathbf{c}_{b(i)i}(\underline{q}_i)$. The first index refers to the body and the second to the joint. The velocity $\mathbf{v}_i$ and the acceleration $\mathbf{a}_i$ relative to $\underline{\mathbf{e}}^{b(i)}$ are the first and the second time derivative, respectively, of $\mathbf{c}_{b(i)i}$ in $\underline{\mathbf{e}}^{b(i)}$. For joints with holonomic constraints of arbitrary nature the six kinematical quantities have the forms

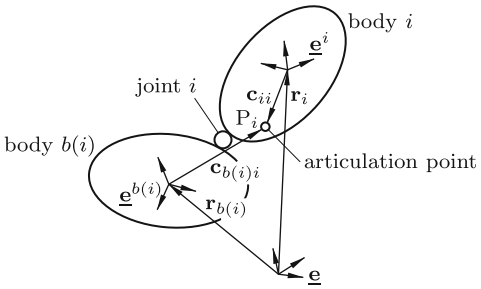

Fig. 11.2 Joint i connecting bodies i and $b(i)$. Articulation point P_i with position vectors $\mathbf{c}_{ii}$ in basis $\underline{\mathbf{e}}^i$ and $\mathbf{c}_{b(i)i}$ in basis $\underline{\mathbf{e}}^{b(i)}$. Position vectors $\mathbf{r}_i$ and $\mathbf{r}_{b(i)}$ in basis $\underline{\mathbf{e}}$

$$\left.\begin{array}{lll} \mathbf{c}_{b(i)i}(\underline{q}_i)\,, & \mathbf{v}_i = \sum_{\ell=1}^{f_i} \mathbf{k}_{i\ell}\dot{q}_{i\ell}\,, & \mathbf{a}_i = \sum_{\ell=1}^{f_i} \mathbf{k}_{i\ell}\ddot{q}_{i\ell} + \mathbf{s}_i\,, \\ \underline{G}_i(\underline{q}_i)\,, & \boldsymbol{\Omega}_i = \sum_{\ell=1}^{f_i} \mathbf{p}_{i\ell}\dot{q}_{i\ell}\,, & \boldsymbol{\varepsilon}_i = \sum_{\ell=1}^{f_i} \mathbf{p}_{i\ell}\ddot{q}_{i\ell} + \mathbf{w}_i\,. \end{array}\right\} \tag{11.1}$$

Depending on the nature of joint i, on the choice of joint variables and on the choice of the articulation point the vectors $\mathbf{k}_{i\ell}$ and $\mathbf{p}_{i\ell}$ are either fixed on body $b(i)$ or functions of joint variables. Vectors $\mathbf{s}_i \neq \mathbf{0}$ and $\mathbf{w}_i \neq \mathbf{0}$ exist only if at least one of the vectors $\mathbf{k}_{i\ell}$ or $\mathbf{p}_{i\ell}$, respectively, is not fixed on body $b(i)$. Vectors $\mathbf{s}_i$ and $\mathbf{w}_i$ are second-order functions of first time derivatives of joint variables. It is always possible to express the coordinates of $\mathbf{c}_{b(i)i}$ and of $\mathbf{v}_i$ and $\mathbf{a}_i$ in basis $\underline{\mathbf{e}}^{b(i)}$ and the coordinates of $\boldsymbol{\Omega}_i$ and $\boldsymbol{\varepsilon}_i$ in $\underline{\mathbf{e}}^{i}$ as functions of joint variables and of time derivatives of joint variables. The four velocities and accelerations are written in the forms

$$\left.\begin{array}{ll} \boldsymbol{\Omega}_i = \underline{\mathbf{p}}_i^T \dot{\underline{q}}_i\,, & \mathbf{v}_i = \underline{\mathbf{k}}_i^T \dot{\underline{q}}_i\,, \\ \boldsymbol{\varepsilon}_i = \underline{\mathbf{p}}_i^T \ddot{\underline{q}}_i + \mathbf{w}_i\,, & \mathbf{a}_i = \underline{\mathbf{k}}_i^T \ddot{\underline{q}}_i + \mathbf{s}_i \end{array}\right\} \quad (i = 1, \ldots, n) \tag{11.2}$$

with column matrices $\underline{\mathbf{p}}_i = [\mathbf{p}_{i1} \ \ldots \ \mathbf{p}_{if_i}]^T$ and $\underline{\mathbf{k}}_i = [\mathbf{k}_{i1} \ \ldots \ \mathbf{k}_{if_i}]^T$. Each of these four sets of n equations is written in matrix form. For this purpose, column matrices $\underline{\boldsymbol{\Omega}}$, $\underline{\boldsymbol{\varepsilon}}$, $\underline{\mathbf{v}}$, $\underline{\mathbf{a}}$, $\underline{\mathbf{w}}$ and $\underline{\mathbf{s}}$ of n vectors each are defined (for example $\underline{\boldsymbol{\Omega}} = [\boldsymbol{\Omega}_1 \ldots \boldsymbol{\Omega}_n]^T$). Furthermore, column matrices $\dot{\underline{q}}$ and $\ddot{\underline{q}}$ are defined which are composed of $\dot{\underline{q}}_i$ and $\ddot{\underline{q}}_i$, respectively ($i = 1, \ldots, n$). Finally, block-diagonal matrices $\underline{\mathbf{k}}$ and $\underline{\mathbf{p}}$ are defined which have the matrices $\underline{\mathbf{k}}_j$ and $\underline{\mathbf{p}}_j$, respectively, along the diagonal. In terms of these matrices the four sets of equations are

$$\left.\begin{array}{ll} \underline{\boldsymbol{\Omega}} = \underline{\mathbf{p}}^T \dot{\underline{q}}\,, & \underline{\mathbf{v}} = \underline{\mathbf{k}}^T \dot{\underline{q}}\,, \\ \underline{\boldsymbol{\varepsilon}} = \underline{\mathbf{p}}^T \ddot{\underline{q}} + \underline{\mathbf{w}}\,, & \underline{\mathbf{a}} = \underline{\mathbf{k}}^T \ddot{\underline{q}} + \underline{\mathbf{s}}\,. \end{array}\right\} \tag{11.3}$$

Examples:

1. Spherical, universal and revolute joints: The choice of the articulation point is dictated by the nature of the joint. In a spherical joint the center of the sphere is chosen. In a universal joint the point of intersection of the two axes on the central cross is chosen. In a revolute joint an arbitrary point on the joint axis is chosen. In all three cases the articulation point is fixed not only in $\underline{\mathbf{e}}^i$, but also in $\underline{\mathbf{e}}^{b(i)}$. Hence $\mathbf{c}_{b(i)i} = \text{const}$, $\mathbf{v}_i = \mathbf{0}$ and $\mathbf{a}_i = \mathbf{0}$.

2. Revolute joint: Define the unit vector $\mathbf{p}$ along the joint axis and the angle of rotation q about this axis. With these definitions $\boldsymbol{\Omega}_i = \mathbf{p}\dot{q}$ and $\boldsymbol{\varepsilon}_i = \mathbf{p}\ddot{q}$.

3. Universal joint: Define axial unit vectors $\mathbf{p}_1$ fixed on body $b(i)$ and $\mathbf{p}_2$ fixed on body i and angles of rotation q_1, q_2 about these axes. With these definitions $\boldsymbol{\Omega}_i = \mathbf{p}_1\dot{q}_1 + \mathbf{p}_2\dot{q}_2$ and $\boldsymbol{\varepsilon}_i = \mathbf{p}_1\ddot{q}_1 + \mathbf{p}_2\ddot{q}_2 + \boldsymbol{\Omega}_i \times \mathbf{p}_2\dot{q}_2$, whence it follows that $\mathbf{w}_i = \mathbf{p}_1 \times \mathbf{p}_2\dot{q}_1\dot{q}_2$.

4. Spherical joint: Three angular joint variables (Euler angles or Bryan angles) are inconvenient because they lead to unwieldy expressions for $\boldsymbol{\Omega}_i$ and $\boldsymbol{\varepsilon}_i$ and because singular positions cannot be avoided. It is preferable to use Euler-Rodrigues parameters q_0, q_1, q_2, q_3. The three rotational kinematical quantities are (see (1.79))

$$\left.\begin{aligned} \underline{G}_i &= \begin{bmatrix} q_0^2+q_1^2-q_2^2-q_3^2 & 2(q_1q_2-q_0q_3) & 2(q_1q_3+q_0q_2) \\ 2(q_1q_2+q_0q_3) & q_0^2+q_2^2-q_3^2-q_1^2 & 2(q_2q_3-q_0q_1) \\ 2(q_1q_3-q_0q_2) & 2(q_2q_3+q_0q_1) & q_0^2+q_3^2-q_1^2-q_2^2 \end{bmatrix} , \\ \boldsymbol{\Omega}_i &= \sum_{\ell=1}^{3} \mathbf{p}_{i\ell}\Omega_{i\ell} , \qquad \boldsymbol{\varepsilon}_i = \sum_{\ell=1}^{3} \mathbf{p}_{i\ell}\dot{\Omega}_{i\ell} . \end{aligned}\right\} \tag{11.4}$$

The scalars $\Omega_{i\ell}$ $(\ell = 1,2,3)$ are the coordinates of $\boldsymbol{\Omega}_i$ in basis $\underline{\mathbf{e}}^i$, and the vectors $\mathbf{p}_{i\ell}$ $(\ell = 1,2,3)$ are the basis vectors themselves. The Euler-Rodrigues parameters and the coordinates $\Omega_{i\ell}$ are related through the kinematical differential Eqs.(10.35).

5. Cylindrical joint: As articulation point an arbitrary point on the joint axis is chosen. Furthermore, the axial unit vector $\mathbf{p}$ fixed on both bodies, the cartesian coordinate q_1 along the axis and the angle of rotation q_2 about the axis are defined. With these definitions

$$\left.\begin{aligned} \mathbf{c}_{b(i)i} &= \mathbf{p}q_1 + \text{const} , & \mathbf{v}_i &= \mathbf{p}\dot{q}_1 , & \mathbf{a}_i &= \mathbf{p}\ddot{q}_1 , \\ \underline{G}_i &= \underline{G}_i(q_2) , & \boldsymbol{\Omega}_i &= \mathbf{p}\dot{q}_2 , & \boldsymbol{\varepsilon}_i &= \mathbf{p}\ddot{q}_2 . \end{aligned}\right\} \tag{11.5}$$

6. In Fig. 11.3 two cranks of a planar four-bar constitute a 1-d.o.f. joint connecting bodies i and $b(i)$. As joint variable the crank angle φ is chosen and as articulation point P_i the endpoint of this crank. The figure explains the unit vector $\mathbf{e}$ along the crank, the unit vector $\mathbf{p}$ normal to the plane and the inclination angle χ of body i. For every value of φ two (not necessarily real) angles $\chi_{1,2}$ are determined by (17.21) and (17.22):

$$A\cos\chi + B\sin\chi = C , \tag{11.6}$$

$$A = -2a(\ell - r_1\cos\varphi) , \quad B = 2r_1a\sin\varphi , \quad C = 2r_1\ell\cos\varphi - (r_1^2+\ell^2+a^2-r_2^2) . \tag{11.7}$$

Their cosines and sines are

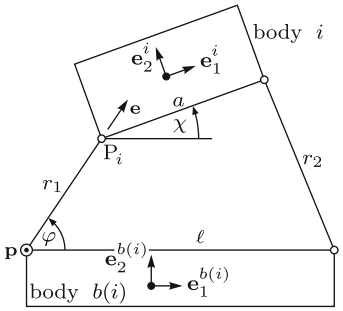

Fig. 11.3 Two cranks of a planar four-bar connecting bodies i and $b(i)$. Articulation point P_i

$$\left.\begin{aligned} \cos\chi_k &= \frac{AC - (-1)^k B\sqrt{A^2+B^2-C^2}}{A^2+B^2}\,, \\ \sin\chi_k &= \frac{BC + (-1)^k A\sqrt{A^2+B^2-C^2}}{A^2+B^2} \end{aligned}\right\} \ (k=1,2)\,. \tag{11.8}$$

The six kinematical quantities in (11.1) are

$$\left.\begin{aligned} &\mathbf{c}_{b(i)i} = r_1\mathbf{e} + \text{ const}\,, \qquad \mathbf{v}_i = \dot\varphi\mathbf{p}\times r_1\mathbf{e}\,, \qquad \mathbf{a}_i = \ddot\varphi\mathbf{p}\times r_1\mathbf{e} - \dot\varphi^2 r_1\mathbf{e}\,, \\ &\underline{G}_i = \begin{bmatrix} \cos\chi & -\sin\chi & 0 \\ \sin\chi & \cos\chi & 0 \\ 0 & 0 & 1 \end{bmatrix}\,, \quad \boldsymbol{\Omega}_i = \mathbf{p}\frac{\mathrm{d}\chi}{\mathrm{d}\varphi}\,\dot\varphi\,, \qquad \boldsymbol{\varepsilon}_i = \mathbf{p}\Big(\frac{\mathrm{d}\chi}{\mathrm{d}\varphi}\,\ddot\varphi + \frac{\mathrm{d}^2\chi}{\mathrm{d}\varphi^2}\,\dot\varphi^2\Big)\,. \end{aligned}\right\} \tag{11.9}$$

The vectors $\mathbf{a}_i$ and $\boldsymbol{\varepsilon}_i$ have the forms given in (11.1) with vectors $\mathbf{k}_{i1} = r_1\mathbf{p}\times\mathbf{e}$, $\mathbf{s}_i = -\dot\varphi^2 r_1\mathbf{e}$, $\mathbf{p}_{i1} = \mathbf{p}\,\mathrm{d}\chi/\mathrm{d}\varphi$ and $\mathbf{w}_i = \mathbf{p}\dot\varphi^2\,\mathrm{d}^2\chi/\mathrm{d}\varphi^2$. The coordinates of these vectors in basis $\underline{\mathbf{e}}^{b(i)}$ are functions of φ. Expressions for $\mathrm{d}\chi/\mathrm{d}\varphi$ and $\mathrm{d}^2\chi/\mathrm{d}\varphi^2$ are obtained by differentiating (11.6) implicitly. End of examples.

11.2 Kinematics of Entire Systems

In this section the problem of direct kinematics stated in the last paragraph prior to Sect. 11.1 is solved: Determine as functions of joint variables and of time derivatives of joint variables for all bodies $i = 1,\ldots,n$ the position vector $\mathbf{r}_i$, the velocity $\dot{\mathbf{r}}_i$ and the acceleration $\ddot{\mathbf{r}}_i$ of 0_i relative to the common reference basis $\underline{\mathbf{e}}$, the direction cosine matrix $\underline{A}_i$ defined by the equation $\underline{\mathbf{e}} = \underline{A}_i\underline{\mathbf{e}}^i$, the angular velocity $\boldsymbol{\omega}_i$ and the angular acceleration $\dot{\boldsymbol{\omega}}_i$ relative to basis $\underline{\mathbf{e}}$. Solutions are formulated in different forms for different purposes. For the purpose of minimizing computation time in numerical evaluations a

set of recursive equations is developed. For applications in analytical investigations the solutions are expressed in explicit form.

11.2.1 Recursive Solution

Figure 11.2 yields for the direction cosine matrix $\underline{A}_i$, for the angular velocity $\boldsymbol{\omega}_i$ and for the position vector $\mathbf{r}_i$ the recursion formulas

$$\left.\begin{aligned} \underline{A}_i &= \underline{A}_{b(i)}\underline{G}_i \ , \\ \boldsymbol{\omega}_i &= \boldsymbol{\omega}_{b(i)} + \boldsymbol{\Omega}_i \ , \\ \mathbf{r}_i &= \mathbf{r}_{b(i)} + \mathbf{c}_{b(i)i} - \mathbf{c}_{ii} \end{aligned}\right\} \quad (i = 1, \ldots, n) \ . \tag{11.10}$$

Recursion formulas for $\dot{\boldsymbol{\omega}}_i$, $\dot{\mathbf{r}}_i$ and $\ddot{\mathbf{r}}_i$ are obtained by differentiating $\boldsymbol{\omega}_i$ and $\mathbf{r}_i$ with respect to time. According to Eq.(9.9) in which $\underline{\mathbf{e}}^1$ and $\underline{\mathbf{e}}^2$ are now identified with $\underline{\mathbf{e}}$ and $\underline{\mathbf{e}}^{b(i)}$, respectively, the results are

$$\left.\begin{aligned} \dot{\boldsymbol{\omega}}_i &= \dot{\boldsymbol{\omega}}_{b(i)} + \boldsymbol{\varepsilon}_i + \boldsymbol{\omega}_{b(i)} \times \boldsymbol{\Omega}_i \ , \\ \dot{\mathbf{r}}_i &= \dot{\mathbf{r}}_{b(i)} + \mathbf{v}_i + \boldsymbol{\omega}_{b(i)} \times \mathbf{c}_{b(i)i} - \boldsymbol{\omega}_i \times \mathbf{c}_{ii} \ , \\ \ddot{\mathbf{r}}_i &= \ddot{\mathbf{r}}_{b(i)} + \mathbf{a}_i + \dot{\boldsymbol{\omega}}_{b(i)} \times \mathbf{c}_{b(i)i} - \dot{\boldsymbol{\omega}}_i \times \mathbf{c}_{ii} + \mathbf{h}_i \ , \\ \mathbf{h}_i &= \boldsymbol{\omega}_{b(i)} \times (\boldsymbol{\omega}_{b(i)} \times \mathbf{c}_{b(i)i}) - \boldsymbol{\omega}_i \times (\boldsymbol{\omega}_i \times \mathbf{c}_{ii}) + 2\boldsymbol{\omega}_{b(i)} \times \mathbf{v}_i \end{aligned}\right\} \tag{11.11}$$

$(i = 1, \ldots, n)$. For $\underline{G}_i$, $\boldsymbol{\Omega}_i$, $\mathbf{c}_{b(i)i}$, $\boldsymbol{\varepsilon}_i$, $\mathbf{v}_i$ and $\mathbf{a}_i$ the expressions (11.1) are substituted. The altogether six Eqs.(11.10) and (11.11) are evaluated in the given order and step by step with $i = 1, \ldots, n$. At the start with $i = 1$ the leading terms on the right-hand sides are the prescribed quantities $\underline{A}_{b(i)} = \underline{A}_0(t)$, $\boldsymbol{\omega}_{b(i)} = \boldsymbol{\omega}_0(t)$, $\mathbf{r}_{b(i)} = \mathbf{r}_0(t)$ etc. At each step i all quantities on the right-hand sides of the equations are known either from the preceding step with $b(i)$ or from a preceding equation at step i. The matrices $\underline{A}_i$ and $\underline{A}_{b(i)}$ are used for transforming vector coordinates from bases $\underline{\mathbf{e}}^i$ or $\underline{\mathbf{e}}^{b(i)}$ into basis $\underline{\mathbf{e}}$.

11.2.2 Explicit Solution

The material presented in this section is taken from Wittenburg [2, 4]. Taking angular velocities as example, it is seen from Fig. 11.1 that $\boldsymbol{\omega}_i$ $(i = 1, \ldots n$ arbitrary) is the sum of the prescribed angular velocity $\boldsymbol{\omega}_0(t)$ of body 0 and of the relative angular velocities $\boldsymbol{\Omega}_j$ of all joints on the direct path between bodies 0 and i. For this reason, numbers T_{ji} are defined as follows:

$$T_{ji} = \begin{cases} -1 & (\text{joint } j \text{ is on the direct path between bodies 0 and } i) \\ 0 & (\text{else}) \end{cases} \tag{11.12}$$

$(j, i = 1, \ldots, n)$. With these numbers the recursive Eqs.(11.10) are replaced by the explicit equations

$$\left.\begin{aligned} \underline{A}_i &= \underline{A}_0(t) \prod_{j:\, T_{ji} \neq 0} \underline{G}_j \quad (\text{indices } j \text{ monotonically increasing}) , \\ \boldsymbol{\omega}_i &= \boldsymbol{\omega}_0(t) - \sum_{j=1}^{n} T_{ji} \boldsymbol{\Omega}_j , \\ \dot{\boldsymbol{\omega}}_i &= \dot{\boldsymbol{\omega}}_0(t) - \sum_{j=1}^{n} T_{ji} (\boldsymbol{\varepsilon}_j + \boldsymbol{\omega}_{b(j)} \times \boldsymbol{\Omega}_j) , \end{aligned}\right\} \quad (i = 1, \ldots, n) . \tag{11.13}$$

$$\left.\begin{aligned} \mathbf{r}_i &= \mathbf{r}_0(t) - \sum_{j=1}^{n} T_{ji} (\mathbf{c}_{b(j)j} - \mathbf{c}_{jj}) , \\ \dot{\mathbf{r}}_i &= \dot{\mathbf{r}}_0(t) - \sum_{j=1}^{n} T_{ji} (\mathbf{v}_j + \boldsymbol{\omega}_{b(j)} \times \mathbf{c}_{b(j)j} - \boldsymbol{\omega}_j \times \mathbf{c}_{jj}) , \\ \ddot{\mathbf{r}}_i &= \ddot{\mathbf{r}}_0(t) - \sum_{j=1}^{n} T_{ji} (\mathbf{a}_j + \dot{\boldsymbol{\omega}}_{b(j)} \times \mathbf{c}_{b(j)j} - \dot{\boldsymbol{\omega}}_j \times \mathbf{c}_{jj} + \mathbf{h}_j) . \end{aligned}\right\} \quad (i = 1, \ldots, n) . \tag{11.14}$$

According to (11.1) the term $\boldsymbol{\Omega}_j$ in $\boldsymbol{\omega}_i$ and the term $\mathbf{v}_j$ in $\dot{\mathbf{r}}_i$ are linear combinations of first time derivatives $\dot{q}_{i\ell}$ of joint variables. Hence $\boldsymbol{\omega}_i$ and $\dot{\mathbf{r}}_i$ have the forms

$\boldsymbol{\omega}_i = \boldsymbol{\omega}_0(t) +$ linear combination of $\dot{q}_{i\ell}$,

$\dot{\mathbf{r}}_i = \dot{\mathbf{r}}_0(t) + \boldsymbol{\omega}_0(t) \times [\mathbf{r}_i - \mathbf{r}_0(t)] +$ linear combination of $\dot{q}_{i\ell}$.

The four sets of equations for $\boldsymbol{\omega}_i$, $\dot{\boldsymbol{\omega}}_i$, $\dot{\mathbf{r}}_i$ and $\ddot{\mathbf{r}}_i$ $(i = 1, \ldots, n)$ are written in the matrix forms

$$\left.\begin{aligned} \underline{\boldsymbol{\omega}} &= \boldsymbol{\omega}_0(t) \underline{1} + \underline{\mathbf{a}}_1 \underline{\dot{q}} , & \underline{\dot{\mathbf{r}}} &= \dot{\mathbf{r}}_0(t) \underline{1} + \boldsymbol{\omega}_0(t) \times [\underline{\mathbf{r}} - \mathbf{r}_0(t) \underline{1}] + \underline{\mathbf{a}}_2 \underline{\dot{q}} , \\ \underline{\dot{\boldsymbol{\omega}}} &= \dot{\boldsymbol{\omega}}_0(t) \underline{1} + \underline{\mathbf{a}}_1 \underline{\ddot{q}} + \underline{\mathbf{b}}_1 , & \underline{\ddot{\mathbf{r}}} &= \ddot{\mathbf{r}}_0(t) \underline{1} + \dot{\boldsymbol{\omega}}_0(t) \times [\underline{\mathbf{r}} - \mathbf{r}_0(t) \underline{1}] + \underline{\mathbf{a}}_2 \underline{\ddot{q}} + \underline{\mathbf{b}}_2 \end{aligned}\right\} \tag{11.15}$$

with column matrices $\underline{\boldsymbol{\omega}}$, $\underline{\dot{\boldsymbol{\omega}}}$, $\underline{\mathbf{r}}$, $\underline{\dot{\mathbf{r}}}$ and $\underline{\ddot{\mathbf{r}}}$ composed of n vectors each (for example $\underline{\boldsymbol{\omega}} = [\boldsymbol{\omega}_1 \ldots \boldsymbol{\omega}_n]^T$), with the column matrix $\underline{1} = [1 \ \ldots \ 1]^T$ and with the column matrices $\underline{\dot{q}}$ and $\underline{\ddot{q}}$ known from (11.3). Explicit expressions for the coefficient matrices $\underline{\mathbf{a}}_1$, $\underline{\mathbf{a}}_2$ and for the column matrices $\underline{\mathbf{b}}_1$, $\underline{\mathbf{b}}_2$ are obtained as follows. First, the $(n \times n)$ matrix $\underline{T}$ with elements T_{ji} $(j, i = 1, \ldots, n)$ and the column matrices $\underline{\mathbf{h}} = [\mathbf{h}_1 \ldots \mathbf{h}_n]^T$ and $\underline{\mathbf{f}} = [\mathbf{f}_1 \ldots \mathbf{f}_n]^T$ with elements $\mathbf{f}_j = \boldsymbol{\omega}_{b(j)} \times \boldsymbol{\Omega}_j$ are defined. Next, the difference $\mathbf{c}_{b(j)j} - \mathbf{c}_{jj}$ in Eq.(11.14) for $\mathbf{r}_i$ and the difference $\boldsymbol{\omega}_{b(j)} \times \mathbf{c}_{b(j)j} - \boldsymbol{\omega}_j \times \mathbf{c}_{jj}$ in the equation for $\dot{\mathbf{r}}_i$ are written in the forms

$$\left.\begin{aligned} \mathbf{c}_{b(j)j} - \mathbf{c}_{jj} &= \sum_{k=1}^{n} \mathbf{C}_{kj} \ , \\ -\mathbf{c}_{b(j)j} \times \boldsymbol{\omega}_{b(j)} + \mathbf{c}_{jj} \times \boldsymbol{\omega}_j &= -\sum_{k=1}^{n} \mathbf{C}_{kj} \times \boldsymbol{\omega}_k \ . \end{aligned}\right\} (j = 1, \ldots, n) \quad (11.16)$$

Through these equations the vectors are defined:

$$\mathbf{C}_{kj} = \begin{cases} -\mathbf{c}_{jj} & (\, k = j\,) \\ \mathbf{c}_{b(j)j} & (\, k = b(j)\,) \\ \mathbf{0} & (\text{else}) \end{cases} \qquad (\, k = 0, \ldots, n\,;\, j = 1, \ldots, n\,) \ . \quad (11.17)$$

With these vectors the row matrix $\underline{\mathbf{C}}_0 = [\mathbf{C}_{01} \ \ldots \ \mathbf{C}_{0n}]$ and the $(n \times n)$-matrix $\underline{\mathbf{C}}$ with elements $\mathbf{C}_{kj}$ $(k, j = 1, \ldots, n)$ are constructed. With these matrices and with other matrices known from (11.3) the five sets of Eqs.(11.13), (11.14) for $\boldsymbol{\omega}_i$, $\dot{\boldsymbol{\omega}}_i$, $\mathbf{r}_i$, $\dot{\mathbf{r}}_i$ and $\ddot{\mathbf{r}}_i$ are

$$\left.\begin{aligned} \underline{\boldsymbol{\omega}} &= \boldsymbol{\omega}_0(t)\underline{1} - \underline{T}^T \underline{\boldsymbol{\Omega}} \ , \\ \underline{\dot{\boldsymbol{\omega}}} &= \dot{\boldsymbol{\omega}}_0(t)\underline{1} - \underline{T}^T(\underline{\boldsymbol{\varepsilon}} + \underline{\mathbf{f}}) \ , \end{aligned}\right\} \quad (11.18)$$

$$\left.\begin{aligned} \underline{\mathbf{r}} &= \mathbf{r}_0(t)\underline{1} - \underline{T}^T(\underline{\mathbf{C}}_0^T + \underline{\mathbf{C}}^T\underline{1}) \ , \\ \underline{\dot{\mathbf{r}}} &= \dot{\mathbf{r}}_0(t)\underline{1} - \underline{T}^T[\boldsymbol{\omega}_0(t) \times \underline{\mathbf{C}}_0^T - \underline{\mathbf{C}}^T \times \underline{\boldsymbol{\omega}} + \underline{\mathbf{v}}] \ , \\ \underline{\ddot{\mathbf{r}}} &= \ddot{\mathbf{r}}_0(t)\underline{1} - \underline{T}^T[\dot{\boldsymbol{\omega}}_0(t) \times \underline{\mathbf{C}}_0^T - \underline{\mathbf{C}}^T \times \underline{\dot{\boldsymbol{\omega}}} + (\underline{\mathbf{a}} + \underline{\mathbf{h}})] \ . \end{aligned}\right\} \quad (11.19)$$

In (11.18) $\underline{\boldsymbol{\Omega}}$ and $\underline{\boldsymbol{\varepsilon}}$ are replaced by the expressions in (11.3). The resulting expressions for $\underline{\boldsymbol{\omega}}$ and $\underline{\dot{\boldsymbol{\omega}}}$ as well as Eqs.(11.3) for $\underline{\mathbf{v}}$ and $\underline{\mathbf{a}}$ are then substituted into the last two Eqs.(11.19). This procedure results in Eqs.(11.15) and in the desired explicit expressions for the coefficient matrices:

$$\left.\begin{aligned} \underline{\boldsymbol{\omega}} &= \boldsymbol{\omega}_0(t)\underline{1} + \underline{\mathbf{a}}_1\underline{\dot{q}} \ , \\ \underline{\dot{\boldsymbol{\omega}}} &= \dot{\boldsymbol{\omega}}_0(t)\underline{1} + \underline{\mathbf{a}}_1\underline{\ddot{q}} + \underline{\mathbf{b}}_1 \ , \\ \underline{\dot{\mathbf{r}}} &= \dot{\mathbf{r}}_0(t)\underline{1} - \boldsymbol{\omega}_0(t) \times \underline{T}^T(\underline{\mathbf{C}}_0^T + \underline{\mathbf{C}}^T\underline{1}) + \underline{\mathbf{a}}_2\underline{\dot{q}} \ , \\ \underline{\ddot{\mathbf{r}}} &= \ddot{\mathbf{r}}_0(t)\underline{1} - \dot{\boldsymbol{\omega}}_0(t) \times \underline{T}^T(\underline{\mathbf{C}}_0^T + \underline{\mathbf{C}}^T\underline{1}) + \underline{\mathbf{a}}_2\underline{\ddot{q}} + \underline{\mathbf{b}}_2 \ , \end{aligned}\right\} \quad (11.20)$$

$$\left.\begin{aligned} \underline{\mathbf{a}}_1 &= -\underline{T}^T\underline{\mathbf{p}}^T \ , & \underline{\mathbf{a}}_2 &= \underline{T}^T(\underline{\mathbf{C}}^T \times \underline{\mathbf{a}}_1 - \underline{\mathbf{k}}^T) \ , \\ \underline{\mathbf{b}}_1 &= -\underline{T}^T(\underline{\mathbf{w}} + \underline{\mathbf{f}}) \ , & \underline{\mathbf{b}}_2 &= \underline{T}^T[\,\underline{\mathbf{C}}^T \times \underline{\mathbf{b}}_1 - (\underline{\mathbf{s}} + \underline{\mathbf{h}})] \ . \end{aligned}\right\} \quad (11.21)$$

The matrices $\underline{\mathbf{a}}_1$ and $\underline{\mathbf{a}}_2$ are functions of $\underline{q}$ only, i.e., neither of $\underline{\dot{q}}$ nor of time t explicitly. The column matrices $\underline{\mathbf{b}}_1$ and $\underline{\mathbf{b}}_2$ are functions of $\underline{q}$, of $\underline{\dot{q}}$ and also of t because the vectors $\mathbf{f}_1$ and $\mathbf{h}_1$ depend on $\boldsymbol{\omega}_0(t)$. In the column matrix $\underline{\mathbf{h}}$ all centrifugal and Coriolis accelerations are collected. The

matrices $\underline{\mathbf{p}}$, $\underline{\mathbf{k}}$, $\underline{\mathbf{w}}$ and $\underline{\mathbf{s}}$ are determined by the kinematics of joints, and the matrices $\underline{T}$ and $\underline{\mathbf{C}}$ are determined by the topology of the tree.

Example: In a system with n revolute joints each joint j has a single axial unit vector $\mathbf{p}_j$ and a single rotation angle q_j around this vector. The matrix $\underline{\mathbf{p}}$ is the diagonal matrix of the vectors $\mathbf{p}_1, \ldots, \mathbf{p}_n$. As articulation points points on the joint axes are chosen. This has the consequence that not only the vectors $\mathbf{c}_{jj}$, but also the vectors $\mathbf{c}_{b(j)j}$ and, hence, all vectors in the matrices $\underline{\mathbf{C}}_0$ and $\underline{\mathbf{C}}$ are body-fixed vectors. Furthermore, $\underline{\mathbf{k}} = \underline{\mathbf{0}}$, $\underline{\mathbf{w}} = \underline{\mathbf{0}}$ and $\underline{\mathbf{s}} = \underline{\mathbf{0}}$.

A serial chain with $n = 5$ joints connecting bodies $0, \ldots, 5$ has the matrices

$$\underline{T} = -\begin{bmatrix} 1 & 1 & 1 & 1 & 1 \\ 0 & 1 & 1 & 1 & 1 \\ 0 & 0 & 1 & 1 & 1 \\ 0 & 0 & 0 & 1 & 1 \\ 0 & 0 & 0 & 0 & 1 \end{bmatrix}, \qquad \underline{\mathbf{C}} = -\begin{bmatrix} \mathbf{c}_{11} & -\mathbf{c}_{12} & \mathbf{0} & \mathbf{0} & \mathbf{0} \\ \mathbf{0} & \mathbf{c}_{22} & -\mathbf{c}_{23} & \mathbf{0} & \mathbf{0} \\ \mathbf{0} & \mathbf{0} & \mathbf{c}_{33} & -\mathbf{c}_{34} & \mathbf{0} \\ \mathbf{0} & \mathbf{0} & \mathbf{0} & \mathbf{c}_{44} & -\mathbf{c}_{45} \\ \mathbf{0} & \mathbf{0} & \mathbf{0} & \mathbf{0} & \mathbf{c}_{55} \end{bmatrix}. \tag{11.22}$$

End of Example.

From the point of view of computation time required for numerical evaluations the recursive Eqs.(11.10), (11.11) are preferable. The explicit formulation (11.20), (11.21) is useful for analytical investigations. In Chap. 19 it is applied to dynamics of mechanisms. In this application, basis $\underline{\mathbf{e}}$ is inertial space, and the origins 0_i of the body-fixed bases $\underline{\mathbf{e}}^i$ $(i = 1, \ldots, n)$ are the body centers of mass.

References

1. Sabrea Pereira M F O, Ambrósio J A C (eds.) (1989) Computer-aided analysis of rigid and flexible mechanical systems. Kluwer, Dordrecht
2. Wittenburg J (1977) Dynamics of systems of rigid bodies. Teubner Stuttgart
3. Wittenburg J (1989) Topological description of articulated systems. In [1]:159–196
4. Wittenburg J (2007) Dynamics of multibody systems. Springer, Berlin Heidelberg New York

Chapter 12
Screw Systems

In this chapter the investigation of velocity screws is resumed. Definitions see in Sect. 9.3 .

12.1 Resultant of two Velocity Screws. Cylindroid

The system shown in Fig. 12.1 has two helical joints with skew axes and with pitches p_1 and p_2 . The terminal body 2 has relative to frame 0 the degree of freedom two. The length of the common perpendicular of the joint axes is ℓ , and the projected angle is α . Unit vectors $\mathbf{n}_1$ and $\mathbf{n}_2$ having the directions of the axes are attached to the midpoint 0 of the common perpendicular. This point 0 is the origin of a frame-fixed basis $\underline{\mathbf{e}}$. The basis vector $\mathbf{e}_1$ is directed along the bisector of the angle α between $\mathbf{n}_1$ and $\mathbf{n}_2$, and $\mathbf{e}_3$ is directed along the common perpendicular. The instantaneous velocity screws of body 1 relative to frame 0 and of body 2 relative to body 1 are (see (9.33))

$$\omega_1(\mathbf{n}_1\ ,\ \mathbf{a}_1\times\mathbf{n}_1+p_1\mathbf{n}_1)\ ,\quad \omega_2(\mathbf{n}_2\ ,\ \mathbf{a}_2\times\mathbf{n}_2+p_2\mathbf{n}_2)\ ,\quad \mathbf{a}_{1,2}=\mp\frac{\ell}{2}\,\mathbf{e}_3\ . \tag{12.1}$$

Let $\omega(\mathbf{n}\ ,\ \mathbf{a}\times\mathbf{n}+p\,\mathbf{n})$ be the instantaneous velocity screw of body 2 relative to frame 0 . It is the resultant of the two velocity screws. Its unknown quantities ω , $\mathbf{n}$, $\mathbf{a}$ and p are calculated as follows. Since the superposition principle is valid for velocities the resultant velocity screw is the sum

$$\omega(\mathbf{n}\ ,\ \mathbf{a}\times\mathbf{n}+p\,\mathbf{n})=\omega_1(\mathbf{n}_1\ ,\ \mathbf{a}_1\times\mathbf{n}_1+p_1\mathbf{n}_1)+\omega_2(\mathbf{n}_2\ ,\ \mathbf{a}_2\times\mathbf{n}_2+p_2\mathbf{n}_2)\ . \tag{12.2}$$

With the above expressions for $\mathbf{a}_1$ and $\mathbf{a}_2$ this equation splits into the equations

J. Wittenburg, *Kinematics*, DOI 10.1007/978-3-662-48487-6_12

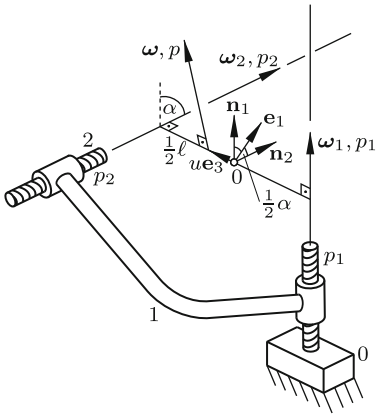

Fig. 12.1 Velocity screws with skew axes. Unit vectors $\mathbf{n}_i$ and pitches p_i $(i = 1, 2)$. Parameters α, ℓ and reference basis $\mathbf{e}_{1,2,3}$

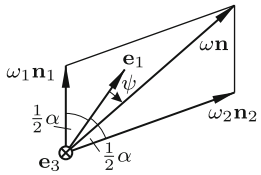

Fig. 12.2 Angular velocity triangles

$$\omega\mathbf{n} = \omega_1\mathbf{n}_1 + \omega_2\mathbf{n}_2 \,, \tag{12.3}$$

$$\omega(\mathbf{a}\times\mathbf{n} + p\,\mathbf{n}) = \omega_1\Big(-\frac{\ell}{2}\,\mathbf{e}_3\times\mathbf{n}_1 + p_1\mathbf{n}_1\Big) + \omega_2\Big(\frac{\ell}{2}\,\mathbf{e}_3\times\mathbf{n}_2 + p_2\mathbf{n}_2\Big) \,. \tag{12.4}$$

The first equation expresses the parallelogram rule for angular velocities (Fig. 12.2). It determines both magnitude and direction of $\omega\mathbf{n}$. Since $\mathbf{n}_1$ and $\mathbf{n}_2$ are normal to $\mathbf{e}_3$ also $\mathbf{n}$ is normal to $\mathbf{e}_3$. Hence

$$\mathbf{a} = u\mathbf{e}_3 \tag{12.5}$$

with an as yet unknown scalar u. This equation states that the resultant screw axis intersects the common perpendicular of the screw axes 1 and 2 orthogonally at the point $u\mathbf{e}_3$. With this expression (12.4) becomes

$$\begin{aligned}&\omega(u\mathbf{e}_3\times\mathbf{n} + p\,\mathbf{n})\\ &= \omega_1\Big(-\frac{\ell}{2}\,\mathbf{e}_3\times\mathbf{n}_1 + p_1\mathbf{n}_1\Big) + \omega_2\Big(\frac{\ell}{2}\,\mathbf{e}_3\times\mathbf{n}_2 + p_2\mathbf{n}_2\Big) \,.\end{aligned} \tag{12.6}$$

Explicit results for the unknowns p and u are obtained when this equation is dot- and cross-multiplied by $\mathbf{n}$. For this purpose the angle ψ shown in Fig. 12.2 is introduced as new parameter. It is the angle from the reference axis $\mathbf{e}_1$ to $\mathbf{n}$ (positive clockwise around $\mathbf{e}_3$). The sine law applied to the triangles in this figure yields the expressions

$$\omega_1 = \omega\,\frac{\sin\Big(\frac{\alpha}{2} - \psi\Big)}{\sin\alpha} \,, \qquad \omega_2 = \omega\,\frac{\sin\Big(\frac{\alpha}{2} + \psi\Big)}{\sin\alpha} \,. \tag{12.7}$$

Furthermore, the following products are calculated:

$$\left.\begin{aligned} \mathbf{n}\cdot\mathbf{n}_1 &= \cos\left(\frac{\alpha}{2}+\psi\right), & \mathbf{n}\times\mathbf{n}_1 &= -\,\mathbf{e}_3\sin\left(\frac{\alpha}{2}+\psi\right), \\ \mathbf{n}\cdot\mathbf{n}_2 &= \cos\left(\frac{\alpha}{2}-\psi\right), & \mathbf{n}\times\mathbf{n}_2 &= \mathbf{e}_3\sin\left(\frac{\alpha}{2}-\psi\right), \\ \mathbf{n}\cdot(\mathbf{e}_3\times\mathbf{n}_1) &= \sin\left(\frac{\alpha}{2}+\psi\right), & \mathbf{n}\times(\mathbf{e}_3\times\mathbf{n}_1) &= \mathbf{e}_3\cos\left(\frac{\alpha}{2}+\psi\right), \\ \mathbf{n}\cdot(\mathbf{e}_3\times\mathbf{n}_2) &= -\sin\left(\frac{\alpha}{2}-\psi\right), & \mathbf{n}\times(\mathbf{e}_3\times\mathbf{n}_2) &= \mathbf{e}_3\cos\left(\frac{\alpha}{2}-\psi\right). \end{aligned}\right\} \tag{12.8}$$

With these equations and with addition theorems the said multiplications of (12.6) by $\mathbf{n}$ yield the expressions

$$p = \frac{1}{2}(p_1+p_2+\ell\cot\alpha) - \frac{\ell\cos 2\psi + (p_1-p_2)\sin 2\psi}{2\sin\alpha}, \tag{12.9}$$

$$u = \frac{1}{2}(p_1-p_2)\cot\alpha \qquad + \frac{\ell\sin 2\psi - (p_1-p_2)\cos 2\psi}{2\sin\alpha}. \tag{12.10}$$

These equations are identical with Eqs.(3.158) and (3.159) governing the resultant of two infinitesimal screw displacements. Compare also Fig. 12.2 with Fig. 3.15 and Eqs.(12.7) and (3.156). The formal identity is explained by the equation $\mathrm{d}(\varphi+\varepsilon s) = (\omega+\varepsilon v)\,\mathrm{d}t$. A change of variables led to Eqs.(3.160) – (3.171) which show that the resultant screw axis is generator of a cylindroid (Fig. 3.16). The same equations and the same figure are valid for the resultant velocity screw.

Let P be an arbitrary point fixed on body 2 of Fig. 12.1. In the case $\omega_2 = 0$, P has a velocity $\mathbf{v}_1$ proportional to ω_1, and in the case $\omega_1 = 0$, P has a velocity $\mathbf{v}_2$ proportional to ω_2. Superposition determines the velocity $\mathbf{v} = \mathbf{v}_1 + \mathbf{v}_2$. If the point P is chosen at random, $\mathbf{v}_1$ and $\mathbf{v}_2$ are not collinear. Together they determine a certain plane. The direction of $\mathbf{v}$ in this plane depends on the ratio ω_1/ω_2. The question arises: Are there body-fixed points such that $\mathbf{v}_1$ and $\mathbf{v}_2$ are collinear so that the direction of $\mathbf{v}$ is independent of ω_1/ω_2? The answer is as follows. If the principal pitches of the cylindroid determined by the velocity screws (12.1) have opposite signs, there are two screws of zero pitch on the cylindroid (see (3.169)). Proposition: All body-fixed points P on the axes of these screws have the desired property. Proof: Zero pitch means that for an appropriate ratio ω_1/ω_2 such a point P has the resultant velocity $\mathbf{v} = \mathbf{v}_1 + \mathbf{v}_2 = \mathbf{0}$. This implies that $\mathbf{v}_1$ and $\mathbf{v}_2$ are collinear. Since the directions of $\mathbf{v}_1$ and $\mathbf{v}_2$ are independent of ω_1 and ω_2 also the direction of $\mathbf{v}$ is independent. End of proof.

12.2 Relative Velocity Screw. Raccording Hyperboloids

The bodies shown in Fig. 12.3 are rotating about skew axes. The length of the common perpendicular is ℓ, and the projected angle is α. Unit vectors $\mathbf{n}_1$ and $\mathbf{n}_2$ having the directions of the axes are attached to the midpoint 0 of the common perpendicular. This point 0 is the origin of a frame-fixed basis $\underline{\mathbf{e}}$. The basis vector $\mathbf{e}_1$ is directed along the bisector of the angle α between $\mathbf{n}_1$ and $\mathbf{n}_2$, and $\mathbf{e}_3$ is directed along the common perpendicular. The velocity screws of the bodies relative to the frame are

$$\omega_1(\mathbf{n}_1\ ,\ \mathbf{a}_1 \times \mathbf{n}_1)\ , \qquad \omega_2(\mathbf{n}_2\ ,\ \mathbf{a}_2 \times \mathbf{n}_2)\ , \qquad \mathbf{a}_{1,2} = \mp\frac{\ell}{2}\,\mathbf{e}_3\ . \tag{12.11}$$

Gears not shown in the figure keep the angular velocity ratio $\mu = \omega_2/\omega_1$ constant. Without loss of generality, it is assumed that $\mu > 0$. Subject of investigation is the velocity screw of body 2 relative to body 1. Let this relative velocity screw be denoted $\omega(\mathbf{n}\ ,\ \mathbf{a} \times \mathbf{n} + p\,\mathbf{n})$. It is the difference

$$\omega(\mathbf{n}\ ,\ \mathbf{a} \times \mathbf{n} + p\,\mathbf{n}) = -\omega_1(\mathbf{n}_1\ ,\ \mathbf{a}_1 \times \mathbf{n}_1) + \omega_2(\mathbf{n}_2\ ,\ \mathbf{a}_2 \times \mathbf{n}_2)\ . \tag{12.12}$$

This equation is a special case of (12.2). Equations (12.3) and (12.6) are replaced by the equations

$$\frac{\omega}{\omega_1}\mathbf{n} = -\mathbf{n}_1 + \mu\mathbf{n}_2\ , \tag{12.13}$$

$$\frac{\omega}{\omega_1}(u\mathbf{e}_3 \times \mathbf{n} + p\,\mathbf{n}) = \frac{\ell}{2}\,\mathbf{e}_3 \times (\mathbf{n}_1 + \mu\mathbf{n}_2)\ , \tag{12.14}$$

and Fig. 12.2 is replaced by Fig. 12.4. The direction of $\mathbf{n}$ relative to $\mathbf{n}_1$ and to $\mathbf{n}_2$ is described by the angles α_1 and α_2, respectively. The ratio ω/ω_1 as well as these angles are functions of μ. The cosine and sine laws yield the formulas

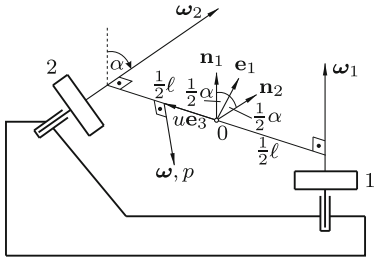

Fig. 12.3 Relative velocity screw of two rotating bodies

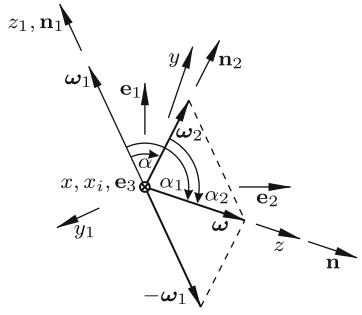

Fig. 12.4 Angular velocity triangles

$$\frac{\omega}{\omega_1} = \sqrt{1+\mu^2-2\mu\cos\alpha}\,, \tag{12.15}$$

$$\left.\begin{aligned} \sin\alpha_1 &= \frac{\omega_1}{\omega}\,\mu\sin\alpha\,, \qquad & \cos\alpha_1 &= \frac{\omega_1}{\omega}\,(\mu\cos\alpha-1)\,,\\ \sin\alpha_2 &= \frac{\omega_1}{\omega}\,\sin\alpha\,, & \cos\alpha_2 &= \frac{\omega_1}{\omega}\,(\mu-\cos\alpha)\,. \end{aligned}\right\} \tag{12.16}$$

Equation (12.14) is dot- and cross-multiplied by $\mathbf{n}$ (the same operations were performed with (12.6)):

$$\frac{\omega}{\omega_1}\,p = \frac{\ell}{2}(\sin\alpha_1+\mu\sin\alpha_2)\,, \qquad \frac{\omega}{\omega_1}\,u = \frac{\ell}{2}(\cos\alpha_1+\mu\cos\alpha_2)\,. \tag{12.17}$$

Combination with the previous equations yields for p and for u the explicit formulas

$$p = \ell\,\frac{\mu\sin\alpha}{1+\mu^2-2\mu\cos\alpha}\,, \qquad u = \frac{\ell}{2}\,\frac{\mu^2-1}{1+\mu^2-2\mu\cos\alpha}\,. \tag{12.18}$$

The resultant screw axis defined by u and $\mathbf{n}$ is fixed in basis $\underline{\mathbf{e}}$. In a basis fixed on the rotating body i $(i=1,2)$ the screw axis generates a hyperboloid of revolution. Equations describing these hyperboloids are developed as follows. Because of the rotational symmetry the hyperboloid on body i $(i=1,2)$ is described in a nonrotating cartesian x_i, y_i, z_i-system. Its origin is the intersection of the rotation axis i with the $\mathbf{e}_3$-axis. The x_i-axis is directed along $\mathbf{e}_3$, and the z_i-axis has the direction of $\mathbf{n}_i$. In this system the equation of the hyperboloid has the normal form

$$\frac{x_i^2+y_i^2}{r_i^2} - \frac{z_i^2}{b_i^2} = 1 \qquad (i=1,2) \tag{12.19}$$

with semi-axes r_i and b_i. The semi-axis r_i is the radius of the gorge circle of the hyperboloid i. These radii are

$$r_1 = \frac{\ell}{2}+u = \ell\,\frac{\mu(\mu-\cos\alpha)}{1+\mu^2-2\mu\cos\alpha}\,, \qquad r_2 = \frac{\ell}{2}-u = \ell\,\frac{1-\mu\cos\alpha}{1+\mu^2-2\mu\cos\alpha}\,. \tag{12.20}$$

In the x_1, y_1, z_1-system of body 1 the resultant screw axis lies in the plane $x_1 = r_1$, and its slope is $z_1/y_1 = \cot\alpha_1$. Similarly, in the x_2, y_2, z_2-system of body 2 the resultant screw axis lies in the plane $x_2 = -r_2$, and its slope is $z_2/y_2 = \cot\alpha_2$. Substitution of these expressions into (12.19) results in the equations $b_i^2 = r_i^2\cot^2\alpha_i$ $(i=1,2)$. For r_i and $\cot\alpha_i$ Eqs.(12.20) and (12.16) are substituted. This yields identical results $b_1 = b_2 = b$ for the imaginary semi-axes of both hyperboloids:

$$b = \left|\ell\,\frac{(\mu-\cos\alpha)(1-\mu\cos\alpha)}{\sin\alpha(1+\mu^2-2\mu\cos\alpha)}\right| = \left|\frac{r_1 r_2}{p}\right|. \tag{12.21}$$

This identity had to be expected. According to Painlevé's Theorem 9.6 the hyperboloids are in raccording motion. This is possible only if both hyperboloids have, in the common resultant screw axis, identical distribution parameters and coinciding striction points. The example at the end of Sect. 2.9 has shown that the imaginary semi-axis b is the distribution parameter, and that the striction point lies on the gorge circle.

Depending on the parameters α, ℓ and μ $|u|$ is smaller, equal or greater than $|\ell/2|$. The hyperboloid with the smaller gorge circle radius is in tangential contact either outside or inside the other hyperboloid. External contact requires that $r_1 > 0$ as well as $r_2 > 0$. Under the initial assumption $\mu > 0$ these conditions are satisfied with

$$|\cos\alpha| < \mu < \frac{1}{|\cos\alpha|} \,. \tag{12.22}$$

In addition to tangential contact along the resultant screw axis the hyperboloids may have an intersection curve. An equation for this curve is determined in the x, y, z-system whose x-axis coincides with the common perpendicular $\mathbf{e}_3$ and whose z-axis coincides with the resultant screw axis. Figure 12.4 yields the transformation relationships (abbreviations $c_i = \cos\alpha_i$, $s_i = \sin\alpha_i$ $(i = 1, 2)$)

$$x_1 = x + r_1 \,, \quad x_2 = x - r_2 \,, \quad y_i = c_i y - s_i z \,, \quad z_i = s_i y + c_i z \quad (i = 1, 2) \,. \tag{12.23}$$

With these expressions Eqs.(12.19) of the hyperboloids become

$$x^2 b^2 + y^2(b^2 c_i^2 - r_i^2 s_i^2) + z^2(b^2 s_i^2 - r_i^2 c_i^2) - (-1)^i\, 2xb^2 r_i - 2yz c_i s_i (b^2 + r_i^2) = 0 \tag{12.24}$$

$(i = 1, 2)$. The arguments leading to (12.21) showed that $r_i^2 = b^2 \tan^2\alpha_i$ $(i = 1, 2)$. From (12.16) it follows that $\tan\alpha_1 / \tan\alpha_2 < 0$ if r_1 and r_2 are both positive and > 0 otherwise. With the signs of $r_i = \pm b s_i / c_i$ chosen correctly Eqs.(12.24) become

$$x^2 c_i^2 + y^2(c_i^2 - s_i^2) + 2 s_i c_i (xb - yz) = 0 \qquad (i = 1, 2) \,. \tag{12.25}$$

These equations are identically satisfied by all points on the z-axis. The difference of the first equation multiplied by $c_2 s_2$ and the second equation multiplied by $c_1 s_1$ is the equation

$$x^2 c_1 c_2 + y^2(c_1 c_2 + s_1 s_2) = 0 \,. \tag{12.26}$$

From (12.16) it follows that

$$c_1 c_2 = \frac{(\mu\cos\alpha - 1)(\mu - \cos\alpha)}{1 + \mu^2 - 2\mu\cos\alpha} \,, \qquad c_1 c_2 + s_1 s_2 = \cos\alpha \,. \tag{12.27}$$

Hence (12.26) is solved by

$$y = \pm qx \qquad \text{with} \qquad q = \sqrt{\frac{(\mu - \cos\alpha)(1 - \mu\cos\alpha)}{\cos\alpha(1 + \mu^2 - 2\mu\cos\alpha)}} \,. \tag{12.28}$$

When this expression is substituted into one of the Eqs.(12.25), also for z a linear function of x is obtained. The first equation yields

$$z = \pm\Big[\frac{b}{q} + x\,\frac{c_1^2 + q^2(c_1^2 - s_1^2)}{2c_1 s_1 q}\Big] \,. \tag{12.29}$$

If q is real, the hyperboloids are not only in tangential contact along a common generator. In addition, they intersect in two more generators which are arranged symmetrically to the generator of tangential contact. The quantity q is real if and only if in addition to conditions (12.22) for external contact of the hyperboloids the condition $|\alpha| \le \pi/2$ is satisfied.

Equations (12.18) – (12.28) are particularly simple in the special case of two shafts rotating with identical angular velocities ($\mu = \omega_2/\omega_1 = 1$). The essential quantities are

$$\omega\mathbf{n} = \omega_1(\mathbf{n}_2 - \mathbf{n}_1) \,, \qquad p = \frac{\ell}{2}\cot\frac{\alpha}{2} \,, \qquad u = 0 \,, \tag{12.30}$$

$$r_1 = r_2 = \frac{\ell}{2} \,, \qquad b = \frac{\ell}{2}\tan\frac{\alpha}{2} \,, \qquad q = \sqrt{\frac{1 - \cos\alpha}{2\cos\alpha}} \,. \tag{12.31}$$

The result $u = 0$ tells that the screw axis intersects the common perpendicular of the two shafts orthogonally at the midpoint 0, and the result for $\omega\mathbf{n}$ tells that the screw axis $\mathbf{n}$ lies along $\mathbf{e}_2$. The two raccording hyperboloids are congruent. They are in external contact along the resultant screw axis.

12.3 Rotary Piercing of Tubes over Plug

Seamless steel tubes are hot-rolled in a so-called piercing mill by a process known as rotary piercing of tubes over plug (patent Mannesmann; see VDI-Zeitschrift Heft 25 (1890) and Fröhlich [4]). The principle is explained in Fig. 12.5. Two identical rollers 1 and 2 of radius R are rotating with equal angular velocities Ω about skew axes. The common perpendicular of the axes is the z-axis normal to the plane of the drawing. The projected angle α between the axes is bisected by the x-axis. A cylinder 3 of radius r with its axis along the x-axis is in contact with each roller at a single point on the z-axis (at $z = r$ with the top roller 1 and at $z = -r$ with the bottom roller 2). At these points the rollers have circumferential velocities $\mathbf{v}_1$ and $\mathbf{v}_2$ of equal magnitude ΩR and directions as shown. When the cylinder 3

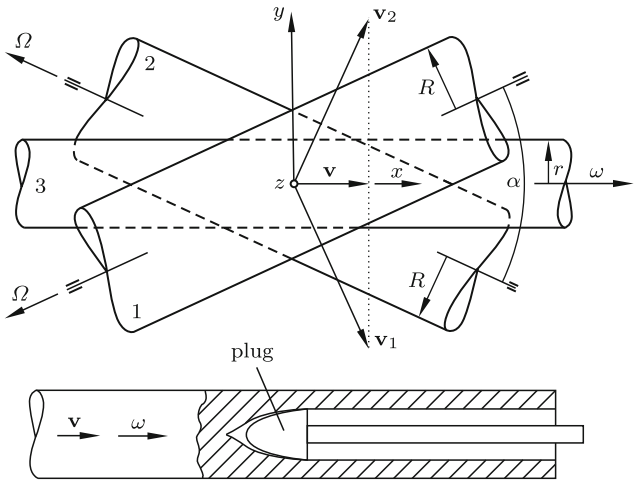

Fig. 12.5 Piercing mill

is a rigid body, it follows from the rolling conditions at the points of contact that the cylinder is in screw motion along the x-axis with translatory velocity $v = \Omega R \sin\alpha/2$ and with angular velocity $\omega = (\Omega R/r)\cos\alpha/2$. The pitch is $v/\omega = r\tan\alpha/2$. This velocity screw is neither the sum nor the difference of the velocity screws of the rollers.

Actually, the hot cylinder 3 is not rigid, but deformable. It enters the mill as a solid cylinder. It is driven by traction forces of the rollers against a conical plug (see the figure). As a result of rotation and of stress concentration in front of the plug the material is deformed into a cylindrical tube.

12.4 Analogy Between Force Screw and Velocity Screw

As is well known, an arbitrary system of forces $\mathbf{F}_1, \mathbf{F}_2, \ldots$ can be reduced to an equivalent force system consisting of a single force $\mathbf{F}$ applied to an arbitrarily chosen reduction point A and of a free torque (a couple) $\mathbf{M}_\mathrm{A}$. The force $\mathbf{F}$ is the resultant of the given forces shifted to the point A. It is independent of the location of A. The torque $\mathbf{M}_\mathrm{A}$ is the resultant moment about A of the given forces. This torque depends on the location of A. For a different reduction point Q given by the vector $\boldsymbol{\varrho} = \overrightarrow{AQ}$ the resultant torque is

$$\mathbf{M} = \mathbf{M}_\mathrm{A} + \mathbf{F} \times \boldsymbol{\varrho}\,. \tag{12.32}$$

This equation is analogous to Eq.(9.21) describing the velocity distribution in a rigid body: $\mathbf{v} = \mathbf{v}_\mathrm{A} + \boldsymbol{\omega} \times \boldsymbol{\varrho}$. Velocity is replaced by torque, and angular

velocity is replaced by force. Equation (9.21) led to the definition of an instantaneous velocity screw with pitch p and to the associated linear complex of velocity and to reciprocal polars associated with this linear complex. For every Eq.(9.21) – (9.40) the analogous equation exists for torques and forces. In what follows, this is shown in some detail. Equation (12.32) tells that for all reduction points located on a line parallel to $\mathbf{F}$ the same resultant torque is obtained (different for different lines). In the case $\mathbf{F} \neq \mathbf{0}$, there exists exactly one line parallel to $\mathbf{F}$ for the points of which the torque has the direction of $\mathbf{F}$, i.e., the torque $\mathbf{M} = p\,\mathbf{F}$ with a scalar p of dimension length. Hence for all points on this line $p\,\mathbf{F} = \mathbf{M}_{\mathrm{A}} + \mathbf{F} \times \boldsymbol{\varrho}$. Let $\mathbf{u}$ be the perpendicular from A onto this particular line. Then also

$$p\,\mathbf{F} = \mathbf{M}_{\mathrm{A}} + \mathbf{F} \times \mathbf{u}\,. \tag{12.33}$$

Cross- and dot-multiplying this equation by $\mathbf{F}$ and using the orthogonality $\mathbf{F} \cdot \mathbf{u} = 0$ one gets for $\mathbf{u}$ and for p the expressions

$$\mathbf{u} = \frac{\mathbf{F} \times \mathbf{M}_{\mathrm{A}}}{\mathbf{F}^2}\,, \qquad p = \frac{\mathbf{F} \cdot \mathbf{M}_{\mathrm{A}}}{\mathbf{F}^2}\,. \tag{12.34}$$

If as reduction point A an arbitrary point on the distinguished line thus determined is chosen, (12.32) has the form

$$\mathbf{M} = p\,\mathbf{F} + \mathbf{F} \times \boldsymbol{\varrho}\,. \tag{12.35}$$

Equations (12.33) – (12.35) are analogous to (9.22) – (9.24). The entity analogous to the velocity screw $(\boldsymbol{\omega}, \mathbf{v})$ is the *force screw*[1] $(\mathbf{F}, \mathbf{M})$. The screw axis with the direction of $\mathbf{F}$ is determined by $\mathbf{u}$. The screw has the pitch p. The resultant torque $\mathbf{M}$ with respect to a point not located on the screw axis has the direction of the tangent to the helix through this point. This point and the plane through this point and orthogonal to the helix are a null point and the associated null plane of the linear complex $(\mathbf{F}; \mathbf{M})$ associated with the force screw $(\mathbf{F}, \mathbf{M})$. The resultant torque about the null point has a zero-component along every complex line in this null plane. This is, historically, the reason for choosing the names null plane and null point[2].

Writing again $\mathbf{a} = -\boldsymbol{\varrho}$ and $\mathbf{F} = F\mathbf{n}$ the force screw has the standard form analogous to (9.33):

$$(\mathbf{F}, \mathbf{M}) = F(\mathbf{n}, \mathbf{a} \times \mathbf{n} + p\,\mathbf{n})\,. \tag{12.36}$$

The scalar F is the intensity, and the factor behind is the unit screw. There are two special cases.

---

[1] The name *force screw* is used instead of *wrench*

[2] Historically, the notion of force screw and formulas for the resultant of two force screws (Battaglini [2]) preceded the corresponding results for infinitesimal screw displacements (Ball [1])

1) Planar force system: The pitch is $p = 0$. The force screw is $F(\mathbf{n}, \mathbf{a} \times \mathbf{n})$.
2) The case $F = 0$: The force system is a free couple $\mathbf{M}$. A screw axis does not exist. The pitch is not defined ($p = \infty$ according to (12.34)). Equation (12.36) has the form (see (9.34))

$$(\mathbf{F}, \mathbf{M}) = M(\mathbf{0}, \mathbf{n}) \,. \tag{12.37}$$

The equations analogous to (9.35) – (9.37) are

$$\hat{\mathbf{n}} = \mathbf{n} + \varepsilon \mathbf{a} \times \mathbf{n} \,, \tag{12.38}$$

$$\hat{\mathbf{F}} = \mathbf{F} + \varepsilon \mathbf{M} = F[\mathbf{n} + \varepsilon(\mathbf{a} \times \mathbf{n} + p\,\mathbf{n})] \tag{12.39}$$

$$= F(1 + \varepsilon p)\hat{\mathbf{n}} \,. \tag{12.40}$$

The analogy to Theorem 9.5 is

Theorem 12.1. *An arbitrary force screw* $(\mathbf{F}, \mathbf{M})$ (*an arbitrary system of forces*) *with* $\mathbf{F} \neq \mathbf{0}$ *can be represented as resultant of two forces. The line of action of one of these forces can be chosen arbitrarily subject to the restriction that it is not a line of the linear complex* $(\mathbf{F}; \mathbf{M})$. *The line of action of the other force is the uniquely determined reciprocal polar of the first line.*

12.5 Virtual Power of a Force Screw. Reciprocal Screws

Virtual power of forces is the key to the proof of

Theorem 12.2. *If six forces* $\mathbf{F}_1, \ldots, \mathbf{F}_6$ *constitute an equilibrium system, the lines of action of these forces are complex lines of a linear complex.*

The following proof is due to Sylvester [11], v.3. Imagine that the forces are acting on a rigid body. Equilibrium requires that the virtual power of the forces calculated for a virtual velocity of the body is zero. The lines of action of five forces define the axis and the pitch of a linear complex (Eqs.(2.38), (2.29)). As virtual velocity of the body a virtual velocity screw with the same axis and the same pitch is chosen. This has the consequence that each of the five forces has individually zero virtual power since it is normal to the virtual velocity of its point of application. Since the total virtual power of all six forces must be zero also the sixth force must be normal to the virtual velocity of its point of application. Hence also the line of action of this force is a line of the same linear complex. End of proof.

Imagine that a rigid body is subject to a system of forces defined by its force screw. This force screw has either the general form $(\mathbf{F}, \mathbf{M}) = F(\mathbf{n}_1, \mathbf{a}_1 \times \mathbf{n}_1 + p_1 \mathbf{n}_1)$ or the special form $M(\mathbf{0}, \mathbf{n}_1)$ when only a free couple is acting. Imagine, furthermore, that the instantaneous state of motion of the body is given by its velocity screw. This screw has either the general form $(\boldsymbol{\omega}, \mathbf{v}) =$

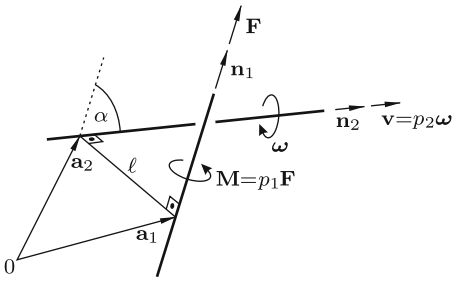

Fig. 12.6 Force screw $(\mathbf{F}, \mathbf{M}) = F(\mathbf{n}_1, \mathbf{a}_1 \times \mathbf{n}_1 + p_1\mathbf{n}_1)$ and velocity screw $(\boldsymbol{\omega}, \mathbf{v}) = \omega(\mathbf{n}_2, \mathbf{a}_2 \times \mathbf{n}_2 + p_2\mathbf{n}_2)$

$\omega(\mathbf{n}_2, \mathbf{a}_2 \times \mathbf{n}_2 + p_2\mathbf{n}_2)$ or the special form $v(\mathbf{0}, \mathbf{n}_2)$ in the case of pure translation. Virtual changes of the velocity screw are expressed in the form $\delta\omega(\mathbf{n}_2, \mathbf{a}_2 \times \mathbf{n}_2 + p_2\mathbf{n}_2)$ in the general case and in the form $\delta v(\mathbf{0}, \mathbf{n}_2)$ in the special case. In Fig. 12.6 the general case is shown with unit vectors $\mathbf{n}_1$ and $\mathbf{n}_2$ along the screw axes and with vectors $\mathbf{a}_1$ and $\mathbf{a}_2$ pointing from an arbitrary point 0 to points on the screw axes. For convenience, the points at the feet of the common perpendicular are chosen since the second Plücker vectors $\mathbf{a}_1 \times \mathbf{n}_1$ and $\mathbf{a}_2 \times \mathbf{n}_2$ are independent of which points are chosen. The virtual power δP of the force screw calculated for the virtual change of the velocity screw is

$$\delta P = \mathbf{F} \cdot \delta\mathbf{v} + \mathbf{M} \cdot \delta\boldsymbol{\omega} \,. \tag{12.41}$$

For screws of the general form

$$\delta P = \delta\omega F\Big[\mathbf{n}_1 \cdot (\mathbf{a}_2 \times \mathbf{n}_2 + p_2\mathbf{n}_2) + \mathbf{n}_2 \cdot (\mathbf{a}_1 \times \mathbf{n}_1 + p_1\mathbf{n}_1)\Big] \tag{12.42}$$

$$= \delta\omega F\Big[(\mathbf{a}_1 - \mathbf{a}_2) \cdot \mathbf{n}_1 \times \mathbf{n}_2 + (p_1 + p_2)\mathbf{n}_1 \cdot \mathbf{n}_2\Big] \,. \tag{12.43}$$

If one of the screws is general and the other is special, the virtual power is $\delta P = \delta P^* \, \mathbf{n}_1 \cdot \mathbf{n}_2$ with either $\delta P^* = \delta\omega M$ or $\delta P^* = \delta v F$. If both screws are special, then $\delta P = 0$.

Equilibrium requires that the virtual power is zero. If exactly one of the screws is special, this is the orthogonality condition $\mathbf{n}_1 \cdot \mathbf{n}_2 = 0$. In the general case, the condition is

$$(\mathbf{a}_1 - \mathbf{a}_2) \cdot \mathbf{n}_1 \times \mathbf{n}_2 + (p_1 + p_2)\mathbf{n}_1 \cdot \mathbf{n}_2 = 0 \tag{12.44}$$

and in terms of the Plücker vectors $\mathbf{n}_i$ and $\mathbf{w}_i = \mathbf{a}_i \times \mathbf{n}_i$ $(i = 1, 2)$ of the screw axes

$$\mathbf{n}_1 \cdot \mathbf{w}_2 + \mathbf{n}_2 \cdot \mathbf{w}_1 + (p_1 + p_2)\mathbf{n}_1 \cdot \mathbf{n}_2 = 0 \,. \tag{12.45}$$

The equations are symmetric with respect to the indices 1 and 2 . Two screws satisfying the condition are called *reciprocal screws*. From Fig. 12.6 it is seen

that the scalar form is

$$(p_1 + p_2)\cos\alpha - \ell \sin\alpha = 0 \,, \tag{12.46}$$

where ℓ and α (both positive or zero or negative) are the length of the common perpendicular and the projected angle between the screw axes.

Equations (12.40) and (9.37) defined the dual screws:

$$\mathbf{F} + \varepsilon\mathbf{M} = F(1+\varepsilon p_1)\hat{\mathbf{n}}_1 \,, \quad \boldsymbol{\omega} + \varepsilon\mathbf{v} = \omega(1+\varepsilon p_2)\hat{\mathbf{n}}_2 \,, \quad \hat{\mathbf{n}}_i = \mathbf{n}_i + \varepsilon\mathbf{a}_i \times \mathbf{n}_i \tag{12.47}$$

$(i = 1, 2)$. The scalar product of the dual unit screws is

$$(1+\varepsilon p_1)(1+\varepsilon p_2)\hat{\mathbf{n}}_1 \cdot \hat{\mathbf{n}}_2 = \mathbf{n}_1 \cdot \mathbf{n}_2 + \varepsilon[(\mathbf{a}_1 - \mathbf{a}_2)\cdot \mathbf{n}_1 \times \mathbf{n}_2 + (p_1+p_2)\mathbf{n}_1 \cdot \mathbf{n}_2] \,. \tag{12.48}$$

The reciprocity condition (12.44) is satisfied if the dual part of the scalar product is zero.

Example: The robot arm shown in Fig. 12.7 is mounted on a stationary frame 0. Bodies 0, 1, 2 and 3 are interconnected by a revolute joint 1, a prismatic joint 2 and a helical joint 3 with given pitch p_3. The joint axes are defined by their unit vectors $\mathbf{n}_1$, $\mathbf{n}_2$, $\mathbf{n}_3$. Joint variables are rotation angles φ_1, φ_3 in joints 1 and 3, respectively, and translatory displacements s_2 and $s_3 = p_3\varphi_3$ in joints 2 and 3, respectively. Each of these variables describes the position of the outer body relative to the inner body, and in each joint the positive direction is the direction of the axial unit vector. Two problems are stated as follows.

1. Given $\dot{\varphi}_1$, $\dot{s}_2$ and $\dot{\varphi}_3$, determine the angular velocity $\boldsymbol{\omega}_3$ of body 3 and the velocity $\mathbf{v}_\mathrm{P}$ of the given point P, both relative to the frame.

2. Body 3 is subject to a force $\mathbf{F}$ applied at P and to a torque $\mathbf{M}_\mathrm{P}$ about P. Determine the column matrix $[M_1\ F_2\ M_3]^T$ of axial joint torques and forces to be produced by motors in the joints such that the robot is in equilibrium. Formulate the conditions $M_1 = 0$, $F_2 = 0$ and $M_3 = 0$.

Solution to Problem 1: The principle of superposition yields for $\boldsymbol{\omega}_3$ and $\mathbf{v}_\mathrm{P}$ the expressions

$$\boldsymbol{\omega}_3 = \dot{\varphi}_1\mathbf{n}_1 + \dot{\varphi}_3\mathbf{n}_3 \,, \qquad \mathbf{v}_\mathrm{P} = \dot{\varphi}_1\mathbf{a}_1 \times \mathbf{n}_1 + \dot{s}_2\mathbf{n}_2 + \dot{\varphi}_3\mathbf{a}_3 \times \mathbf{n}_3 + p_3\dot{\varphi}_3\mathbf{n}_3 \tag{12.49}$$

with vectors $\mathbf{a}_1$ and $\mathbf{a}_3$ pointing from P to arbitrary points of the joint axes 1 and 3, respectively (see Fig. 12.7). The matrix form of the equations is

$$\begin{bmatrix} \boldsymbol{\omega}_3 \\ \mathbf{v}_\mathrm{P} \end{bmatrix} = \begin{bmatrix} \mathbf{n}_1 & \mathbf{0} & \mathbf{n}_3 \\ \mathbf{a}_1 \times \mathbf{n}_1 & \mathbf{n}_2 & \mathbf{a}_3 \times \mathbf{n}_3 + p_3\mathbf{n}_3 \end{bmatrix} \begin{bmatrix} \dot{\varphi}_1 \\ \dot{s}_2 \\ \dot{\varphi}_3 \end{bmatrix} \,. \tag{12.50}$$

The left-hand side is the velocity screw of body 3. The right-hand side represents the sum of the velocity screws of the three joints. Column j of the

coefficient matrix ($j = 1, 2, 3$) is the unit screw of joint j (see (9.33) and (9.34)).
Solution to Problem 2: Equilibrium requires that under virtual velocities the virtual power δP of all forces and torques acting on the system equals zero. This is the condition

$$\delta P = M_1 \delta\dot{\varphi}_1 + F_2 \delta\dot{s}_2 + M_3 \delta\dot{\varphi}_3 + \mathbf{M}_\mathrm{P} \cdot \delta\boldsymbol{\omega}_3 + \mathbf{F} \cdot \delta\mathbf{v}_\mathrm{P} = 0 \tag{12.51}$$

or written in matrix form

$$[M_1\ F_2\ M_3]\ \delta \begin{bmatrix} \dot{\varphi}_1 \\ \dot{s}_2 \\ \dot{\varphi}_3 \end{bmatrix} + [\mathbf{M}_\mathrm{P}\ \mathbf{F}] \cdot\ \delta \begin{bmatrix} \boldsymbol{\omega}_3 \\ \mathbf{v}_\mathrm{P} \end{bmatrix} = 0\ . \tag{12.52}$$

For the last column matrix the expression from (12.50) is substituted. Following this, the column matrix $\delta[\,\dot{\varphi}_1\ \dot{s}_2\ \dot{\varphi}_3\,]^T$ is factored out. Since its elements are independent and arbitrary, the factor must be zero. Transposition yields

$$\begin{bmatrix} M_1 \\ F_2 \\ M_3 \end{bmatrix} = - \begin{bmatrix} \mathbf{n}_1 & \mathbf{a}_1 \times \mathbf{n}_1 \\ \mathbf{0} & \mathbf{n}_2 \\ \mathbf{n}_3 & \mathbf{a}_3 \times \mathbf{n}_3 + p_3 \mathbf{n}_3 \end{bmatrix} \cdot \begin{bmatrix} \mathbf{M}_\mathrm{P} \\ \mathbf{F} \end{bmatrix}\ . \tag{12.53}$$

If one or more of the quantities M_1, F_2, M_3 are zero, the force screw $(\mathbf{F}, \mathbf{M}_\mathrm{P})$ is reciprocal to the respective velocity screws. The three reciprocity conditions are

$$\mathbf{n}_1 \cdot \mathbf{M}_\mathrm{P} + \mathbf{a}_1 \times \mathbf{n}_1 \cdot \mathbf{F} = 0\ , \qquad \mathbf{n}_2 \cdot \mathbf{F} = 0\ , \qquad \mathbf{n}_3 \cdot \mathbf{M}_\mathrm{P} + (\mathbf{a}_3 \times \mathbf{n}_3 + p_3 \mathbf{n}_3) \cdot \mathbf{F} = 0\ . \tag{12.54}$$

End of example.

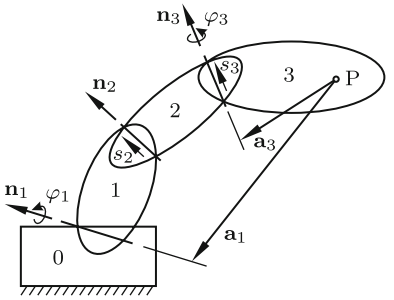

Fig. 12.7 Robot arm with frame 0, revolute joint 1, prismatic joint 2, helical joint 3

12.6 Reciprocal Screw Systems

Constraint forces in joints of a mechanism have zero virtual power. For this reason they need not be taken into account in equations expressing the principle of virtual power. This advantage of the principle, as compared with other methods, is clearly demonstrated by the equilibrium condition (12.51). It is even more important when the principle is used for formulating dynamics equations of motion of mechanisms (see Eq.(19.3)).

In what follows, constraint forces in joints of mechanisms are the subject of investigation. General statements are derived from the fact that their virtual power is zero. In abstract form this is expressed in

Theorem 12.3. *The force screw of an arbitrary system of constraint forces acting on a single body of a mechanism is reciprocal to a virtual velocity screw of the body.*

The degree of freedom of the single body under investigation is in the range $1 \le f \le 5$. Depending on the nature of the mechanism the virtual velocity screw of the body is either general or special. Only the general case is treated in detail although the simpler special case is typical for the majority of mechanisms used in engineering.

In Sect. 4.1 on Grübler's formula it was said that a body with degree of freedom f is subject to $N = 6 - f$ linearly independent constraints. The precise meaning of linear independence can now be formulated as follows. Reciprocity of a virtual velocity screw having the unit screw $(\mathbf{n},\, \mathbf{a}\times\mathbf{n}+p\,\mathbf{n})$ to N force screws having unit screws $(\mathbf{n}_i,\, \mathbf{a}_i \times \mathbf{n}_i + p_i\mathbf{n}_i)$ $(i = 1, \ldots, N)$ is expressed by N equations of the form (12.44). With the abbreviations $\mathbf{m} = \mathbf{a} \times \mathbf{n} + p\,\mathbf{n}$ and $\mathbf{m}_i = \mathbf{a}_i \times \mathbf{n}_i + p_i\mathbf{n}_i$ $(i = 1, \ldots, N)$ the equations can also be written in the form (see (12.42))

$$\mathbf{m}_i \cdot \mathbf{n} + \mathbf{n}_i \cdot \mathbf{m} = 0 \qquad (i = 1, \ldots, N)\,. \tag{12.55}$$

This is a set of N homogeneous linear equations for the coordinates of $\mathbf{n}$ and $\mathbf{m}$. The force screws are linearly independent if the $(N \times 6)$ coefficient matrix has the full rank N. In this case, the set of equations has $6 - N$ linearly independent nontrivial solutions $(\mathbf{n}\,,\ \mathbf{m})$. Any linear combination of these solutions is itself a solution. The vectors $\mathbf{n}$ and $\mathbf{m}$ of every solution determine the associated perpendicular $\mathbf{n} \times \mathbf{m}/\mathbf{n}^2$ onto the screw axis and the associated pitch $p = \mathbf{n} \cdot \mathbf{m}/\mathbf{n}^2$.

Before going into details it is pointed out again that every statement about degree of freedom, about velocity screws and about force screws is referring to an instantaneous position of the body, i.e., of the mechanism. Any generalization to continuous motions with changing relative positions of bodies requires additional arguments beyond the scope of the present investigation.

If the body under consideration has the degree of freedom $f = 1$, it is characterized by a single velocity screw and by a system of five linearly

independent reciprocal force screws. In the case $f = 2$, the number of linearly independent velocity screws is two, and the number of linearly independent force screws is four. The two linearly independent velocity screws define a cylindroid, and any resultant of the four linearly independent force screws is reciprocal to every velocity screw on the cylindroid or, shorter, reciprocal to the cylindroid. In the case $f = 3$, the number of linearly independent velocity screws as well as the number of linearly independent reciprocal force screws is three. An investigation beyond $f = 3$ is unnecessary. In the case $f = 4$, for example, the manifold of all force screws defines a cylindroid, whereas the manifold of all velocity screws are the screws reciprocal to this cylindroid. In what follows, the mutually reciprocal screw systems of order one to five are investigated. Additional material see in Timerding [12]. Hunt [5] and Phillips [8] demonstrate applications of reciprocal screws to the study of mechanisms.

12.6.1 First-Order Screw System and Reciprocal Fifth-Order System

The general form of the first-order system is a single unit screw $(\mathbf{n}, \mathbf{w} + p\,\mathbf{n})$ with Plücker vectors $\mathbf{n}$ and $\mathbf{w}$ of its axis and with pitch p. The fifth-order system reciprocal to this screw consists of all screws $(\mathbf{n}_1, \mathbf{w}_1 + p_1\mathbf{n}_1)$ satisfying the reciprocity condition (12.45):

$$\mathbf{n} \cdot \mathbf{w}_1 + [\mathbf{w} + (p + p_1)\mathbf{n}] \cdot \mathbf{n}_1 = 0\,. \tag{12.56}$$

This is Eq.(2.25), $\mathbf{a}\cdot\mathbf{w}_1 + \mathbf{b}\cdot\mathbf{n}_1 = 0$, defining the linear complex $(\mathbf{a}; \mathbf{b})$ with $\mathbf{a} = \mathbf{n}$ and $\mathbf{b} = \mathbf{w} + (p + p_1)\mathbf{n}$. Equations (2.29) yield the pitch $\mathbf{a}\cdot\mathbf{b} = p + p_1$ of this linear complex and the perpendicular onto its axis $\mathbf{u} = \mathbf{a}\times\mathbf{b} = \mathbf{n}\times\mathbf{w}$. The Plücker vectors of this axis are $\mathbf{a} = \mathbf{n}$ and $\mathbf{w}_1 = \mathbf{u} \times \mathbf{n} = \mathbf{w}$. Thus, the fifth-order screw system $(\mathbf{n}_1, \mathbf{w}_1 + p_1\mathbf{n}_1)$ reciprocal to the single screw $(\mathbf{n}, \mathbf{w} + p\,\mathbf{n})$ is the manifold of all linear complexes having the axis $(\mathbf{n}, \mathbf{w})$ of the given screw and the pitch $p + p_1$ with p_1 being a free parameter. In the special case $p_1 = -p$, there is a single reciprocal screw along the axis $(\mathbf{n}, \mathbf{w})$. All reciprocal screws of given pitch $p_1 \neq -p$ (arbitrary) passing through a given point P (arbitrary) are in the null plane associated with the null point P of the linear complex with axis $(\mathbf{n}, \mathbf{w})$ and with pitch $p + p_1$.

If a fifth-order screw system is given by five linearly independent screws $(\mathbf{n}_i, \mathbf{w}_i + p_i\mathbf{n}_i)$ $(i = 1, \ldots, 5)$, the single screw $(\mathbf{n}, \mathbf{w} + p\,\mathbf{n})$ reciprocal to all five is determined from (12.55).

Example: In Sect. 12.2 the relative motion of two wheels rotating with constant angular velocity ratio $\mu = \omega_2/\omega_1 = \text{const}$ about skew axes was shown to be a velocity screw $\omega(\mathbf{n}, \mathbf{n}\times\mathbf{r} + p\,\mathbf{n})$ (see Fig. 12.3). The direction of

the axis is determined by the parallelogram rule $\boldsymbol{\omega} = \boldsymbol{\omega}_2 - \boldsymbol{\omega}_1$ (Eq.(12.13)). The pitch $p(\mu)$ is given in the first Eq.(12.18). The second equation for $u(\mu)$ determines the point where the screw axis intersects orthogonally the common perpendicular of the two wheel axes. Imagine the two wheels to be a pair of gears with any kind of teeth appropriate for keeping the relative velocity screw constant. Let P be an arbitrary point at which, in the course of meshing, two tooth flanks are in tangential contact, and let $\mathbf{n}_1$ be the common unit normal vector at P. The normal contact force $F\mathbf{n}_1$ exerted at P by one tooth flank on the other is a force screw $F(\mathbf{n}_1, \mathbf{n}_1 \times \mathbf{r} + p_1\mathbf{n}_1)$ with pitch $p_1 = 0$. Being a constraint force with zero virtual power the force screw is reciprocal to the relative velocity screw. Hence the conclusion (Phillips [9]): Whatever tooth shapes are chosen and wherever tangential contact is established in the course of meshing the common normal at the point of contact must belong to the linear complex having the axis and the pitch p of the relative velocity screw. This statement is an expression of the fact that the relative sliding velocity at the point of contact, $\mathbf{v}_{21} = \omega(\mathbf{n} \times \boldsymbol{\rho} + p\,\mathbf{n})$ with $\boldsymbol{\rho}$ being the vector from an arbitrary point on the screw axis to the contact point, has the direction of the helix through the contact point. If one tooth flank is prescribed, the other, so-called conjugate flank is determined by this condition. In Sect. 16.2 this is shown in more detail. End of example.

12.6.2 Second-Order Screw System and Reciprocal Fourth-Order System

The general form of the second-order system is the screw system on a cylindroid. Some of its properties are known from Eqs.(3.150) – (3.172) and from Fig. 3.16. The third-order Eq.(3.171) of the cylindroid is

$$z(x^2 + y^2) = 2hxy\,, \qquad 2h = p_{\mathrm{y}} - p_{\mathrm{x}}\,. \tag{12.57}$$

The z-axis is the directrix. The principal screws along x-axis and y-axis have the principal pitches p_{x} and p_{y}, respectively. In the context of reciprocity conjugate screws (screws of equal pitch) play an important role. For simplification the expression 'two screws intersect' means that 'the axes of the two screws intersect'. From (12.46) it follows that a screw along the z-axis with arbitrary pitch including $p = \infty$ (pure translation) is reciprocal to the cylindroid, because all screws on the cylindroid are intersected perpendicularly by the z-axis. Another consequence of Eq.(12.46) is

Theorem 12.4. *Let σ and $\overline{\sigma}$ be two conjugate screws of pitch p (arbitrary) on the cylindroid. Any screw τ intersecting both σ and $\overline{\sigma}$ (the two points of intersection being arbitrary) and having the pitch $-p$ is reciprocal to both*

σ and $\overline{\sigma}$ and, hence, to the cylindroid since every screw on the cylindroid is a linear combination of the two conjugate screws.

Special reciprocal screws identified by this theorem are the screw along the x-axis with pitch $-p_{\mathrm{x}}$ and the screw along the y-axis with pitch $-p_{\mathrm{y}}$. Indeed, either one of them is reciprocal to both principal screws and, hence, to the cylindroid.

From the third-order Eq.(12.57) of the cylindroid it follows that any line neither parallel nor orthogonal to the z-axis intersects the cylindroid in three points located on three screws (two of which may coalesce or be imaginary). In particular

Theorem 12.5. *A screw τ intersecting two conjugate screws σ and $\overline{\sigma}$ of pitch p intersects a third screw σ^* on the cylindroid perpendicularly. And conversely: If a screw τ intersects one screw σ^* perpendicularly, it intersects, in addition, two conjugate screws (which may coalesce or be imaginary).*

The first statement is proved as follows. By Theorem 12.4 the screw with pitch $-p$ is reciprocal to σ^* since σ^* is a linear combination of the two conjugate screws with pitch p. However, the pitch of σ^* is different from p since not more than two screws on the cylindroid have identical pitches. Therefore, reciprocity of τ and σ^* requires, because of (12.46), that τ and σ^* intersect perpendicularly. This ends the proof of the first statement. The converse is true since it follows from (12.57) that none of the other two screws intersected by τ is intersected perpendicularly. Therefore, reciprocity to τ requires that both have the same pitch. End of proof.

In what follows, analytical methods are used for proving that there are no reciprocal screws other than those covered by Theorem 12.4. The analysis will show that every point not lying on the z-axis is apex of a second-order cone all generators of which are axes of reciprocal screws. The cylindroid is represented by a pair of conjugate screws σ and $\overline{\sigma}$ with angles χ and $-\chi$ (arbitrary). Their common pitch is given by (3.167),

$$p_{1,2} = p_{\mathrm{x}} \cos^2 \chi + p_{\mathrm{y}} \sin^2 \chi \,, \tag{12.58}$$

and their first and second normalized Plücker vectors, denoted $\mathbf{n}_1$, $\mathbf{w}_1$ and $\mathbf{n}_2$, $\mathbf{w}_2$, have the x, y, z-coordinates (see (3.172))

$$\mathbf{n}_{1,2}: \; [\cos\chi \;\; \pm\sin\chi \;\; 0] \,, \quad \mathbf{w}_{1,2}: \; (p_{\mathrm{y}} - p_{\mathrm{x}}) \sin\chi \cos\chi \, [-\sin\chi \;\; \pm\cos\chi \;\; 0] \,. \tag{12.59}$$

Let τ be the unknown reciprocal screw with normalized Plücker vectors $\mathbf{n}$ and $\mathbf{w}$ and with pitch p. The coordinates of $\mathbf{n}$ are denoted $[n_{\mathrm{x}} \; n_{\mathrm{y}} \; n_{\mathrm{z}}]$. Let x, y, z be the coordinates of a point on the screw axis. The second Plücker vector $\mathbf{w}$ has the coordinates $[-zn_{\mathrm{y}} + yn_{\mathrm{z}} \;\; zn_{\mathrm{x}} - xn_{\mathrm{z}} \;\; -yn_{\mathrm{x}} + xn_{\mathrm{y}}]$. The screw τ must satisfy the two reciprocity conditions (12.45):

$$\mathbf{n}\cdot\mathbf{w}_i+\mathbf{n}_i\cdot\mathbf{w}+(p+p_i)\mathbf{n}\cdot\mathbf{n}_i=0 \qquad (i=1,2)\ . \tag{12.60}$$

These equations are

$$\begin{aligned}&(p_{\mathrm{y}}-p_{\mathrm{x}})\sin\chi\cos\chi(-\sin\chi n_{\mathrm{x}}\pm\cos\chi n_{\mathrm{y}})\\ &+\cos\chi(-zn_{\mathrm{y}}+yn_{\mathrm{z}})\pm\sin\chi(zn_{\mathrm{x}}-xn_{\mathrm{z}})\\ &+(p+p_{\mathrm{x}}\cos^2\chi+p_{\mathrm{y}}\sin^2\chi)(\cos\chi n_{\mathrm{x}}\pm\sin\chi n_{\mathrm{y}})=0\ .\end{aligned} \tag{12.61}$$

The sum and the difference of the equations are

$$\left.\begin{aligned}(p_{\mathrm{x}}+p)n_{\mathrm{x}}-zn_{\mathrm{y}}+yn_{\mathrm{z}}=0\ ,\\ zn_{\mathrm{x}}+(p_{\mathrm{y}}+p)n_{\mathrm{y}}-xn_{\mathrm{z}}=0\ .\end{aligned}\right\} \tag{12.62}$$

Solving for p yields the equivalent expressions

$$p=\frac{zn_{\mathrm{y}}-yn_{\mathrm{z}}}{n_{\mathrm{x}}}-p_{\mathrm{x}}=\frac{xn_{\mathrm{z}}-zn_{\mathrm{x}}}{n_{\mathrm{y}}}-p_{\mathrm{y}}\ . \tag{12.63}$$

Elimination of p results in the equation

$$(xn_{\mathrm{x}}+yn_{\mathrm{y}})n_{\mathrm{z}}-z(n_{\mathrm{x}}^2+n_{\mathrm{y}}^2)-(p_{\mathrm{y}}-p_{\mathrm{x}})n_{\mathrm{x}}n_{\mathrm{y}}=0\ . \tag{12.64}$$

Let x_0, y_0, z_0 be the coordinates of an arbitrary point P not lying on the z-axis. A reciprocal screw τ passing through P has direction cosines n_{x}, n_{y}, n_{z} which are proportional to $(x-x_0)$, $(y-y_0)$, $(z-z_0)$, respectively. Hence the reciprocal screws passing through P are defined by the equation ($p_{\mathrm{y}}-p_{\mathrm{x}}=2h$)

$$[x(x-x_0)+y(y-y_0)](z-z_0)-z[(x-x_0)^2+(y-y_0)^2]-2h(x-x_0)(y-y_0)=0\ . \tag{12.65}$$

This is the equation of a second-order cone with apex P. The cone is referred to as *reciprocal cone*. Its properties are revealed by investigating the curves of intersection with planes $z=\text{const}$ and with the cylindroid.

The cone has a generator parallel to the z-axis (the equation is satisfied by $x=x_0$, $y=y_0$ and z arbitrary). At a point called A this generator intersects a single screw of the cylindroid (perpendicularly). Let σ_0 be this screw. Its angle χ_0 against the x-axis is $\chi_0=\tan^{-1}(y_0/x_0)$. The conjugate screw $\overline{\sigma}_0$ lies under the angle $-\chi_0$ against the x-axis. These two screws lie in the planes $z=h\sin 2\chi_0$ and $z=-h\sin 2\chi_0$, respectively. In Fig. 12.8a the screws σ_0 and $\overline{\sigma}_0$ are shown in the projection along the z-axis (briefly called vertical projection). The points P and A are projected into the point called P_0. Among all planes $z=\text{const}$ the plane $z=-z_0$ is the one for which Eq.(12.65) is simplest, namely,

$$z_0(x^2+y^2-x_0^2-y_0^2)+2h(x-x_0)(y-y_0)=0\ . \tag{12.66}$$

Let this conic section be denoted e_1. It is passing through P_0 with the slope $-x_0/y_0$, i.e., perpendicularly to σ_0. Its principal axes are rotated 45° against the x, y-directions. This rotation is accomplished by the substitution

$$x = \frac{\xi - \eta}{\sqrt{2}} , \qquad y = \frac{\xi + \eta}{\sqrt{2}} . \tag{12.67}$$

It results in the equation

$$\xi^2(z_0+h)+\eta^2(z_0-h)-\sqrt{2}\,h[\xi(x_0+y_0)+\eta(x_0-y_0)]-z_0(x_0^2+y_0^2)+2hx_0y_0 = 0 . \tag{12.68}$$

Its standard form is

$$\begin{aligned}(z_0+h)\left[\xi - \frac{h}{\sqrt{2}}\,\frac{x_0+y_0}{z_0+h}\right]^2 + (z_0-h)\left[\eta - \frac{h}{\sqrt{2}}\,\frac{x_0-y_0}{z_0-h}\right]^2 \\ = \frac{z_0^2}{z_0^2-h^2}\,[z_0(x_0^2+y_0^2) - 2hx_0y_0] .\end{aligned} \tag{12.69}$$

The conic section is either elliptic or parabolic or hyperbolic depending on whether $|z_0| - |h|$ is positive or zero or negative, respectively. The ellipse e_1 shown in Fig. 12.8a is associated with the parameters $x_0 = 4$, $y_0 = 3$, $z_0 = 2$, $h = 1$. It is used for illustrating relationships which, in modified form, are valid in the parabolic and in the hyperbolic case, as well.

In the vertical projection every generator of the reciprocal cone intersects e_1 at P_0 and at a second point G. The coordinates x, y and $z = -z_0$ of G determine the direction cosines

$$\left.\begin{aligned} n_{\mathrm{x}} &= \frac{x-x_0}{N} , \qquad n_{\mathrm{y}} = \frac{y-y_0}{N} , \qquad n_{\mathrm{z}} = \frac{-2z_0}{N} , \\ N &= \sqrt{(x-x_0)^2+(y-y_0)^2+4z_0^2} \end{aligned}\right\} \tag{12.70}$$

of this generator and, with (12.63), the associated pitch p. With this pitch, the screw τ having the generator $\overline{\mathrm{PG}}$ as axis is reciprocal to the cylindroid. The pitch associated with the generator parallel to the z-axis is ∞ since $n_{\mathrm{z}}/n_{\mathrm{x}}$ and $n_{\mathrm{z}}/n_{\mathrm{y}}$ tend towards ∞ when G tends towards P_0.

Equation (12.65) of the cone as well as Eq.(12.57) of the cylindroid is linear in z. Elimination of z results in an equation for the curve of intersection of cone and cylindroid in the vertical projection. Collecting the terms involving z (12.65) has the form

$$-z_0[x(x-x_0)+y(y-y_0)]-2h(x-x_0)(y-y_0)+z[x_0(x-x_0)+y_0(y-y_0)] = 0 . \tag{12.71}$$

Substituting for z the expression $z = 2hxy/(x^2+y^2)$ from (12.57) and multiplying with (x^2+y^2) results in the equation

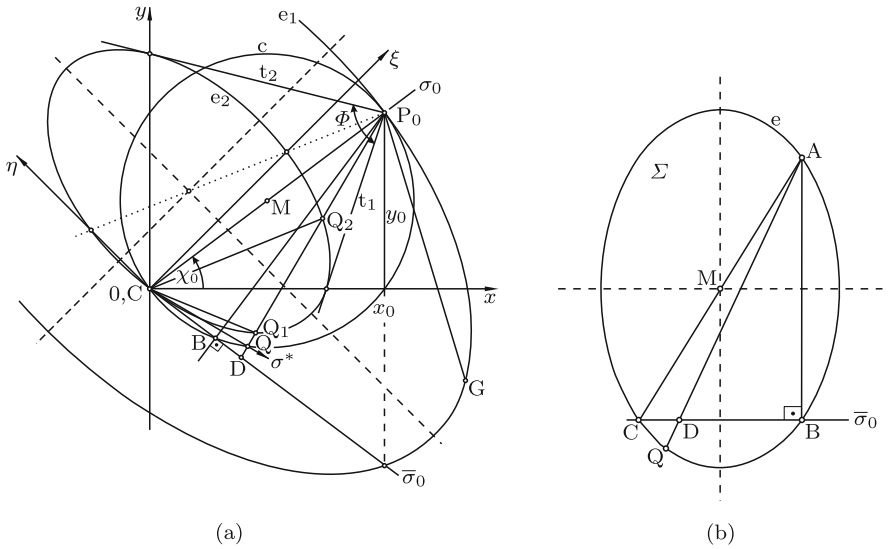

Fig. 12.8 a) Projection along the z-axis of the curves e_1, e_2 and c in which the reciprocal cone with apex P intersects the plane $z = -z_0$ and the cylindroid. Conjugate screws σ_0 and $\overline{\sigma}_0$. **b)** Plane Σ spanned by A and $\overline{\sigma}_0$ intersects the cylindroid in the line $\overline{\sigma}_0$ and an ellipse e. Line $\overline{\mathrm{AD}}$ intersects in Q a third screw σ^* orthogonally

$$(x^2+y^2)\Big\{-z_0[x(x-x_0)+y(y-y_0)]-2h(x-x_0)(y-y_0)\Big\}$$
$$+\,2hxy[x_0(x-x_0)+y_0(y-y_0)]=0\,. \qquad (12.72)$$

It is identical with

$$\Big[x(x-x_0)+y(y-y_0)\Big]\Big[z_0(x^2+y^2)+2h(xy-xy_0-yx_0)\Big]=0\,. \qquad (12.73)$$

This shows that the cone and the cylindroid intersect in curves which, in vertical projection, are a circle and another second-order curve e_2 with principal axes rotated 45° against the x, y-system. The circle called c is shown in Fig. 12.8a. It is independent of z_0. It is passing through the origin 0 and through P_0, and its center M is midpoint between these points. The other second-order curve e_2 is passing through the origin 0 with the slope $-y_0/x_0$, which means that at 0 it is tangent to $\overline{\sigma}_0$. The transformation (12.67) results in the equation

$$\xi^2(z_0+h)+\eta^2(z_0-h)-\sqrt{2}\,h[\xi(x_0+y_0)+\eta(x_0-y_0)]=0\,. \qquad (12.74)$$

Its standard form is

$$(z_0+h)\left[\xi-\frac{h}{\sqrt{2}}\,\frac{x_0+y_0}{z_0+h}\right]^2+(z_0-h)\left[\eta-\frac{h}{\sqrt{2}}\,\frac{x_0-y_0}{z_0-h}\right]^2$$
$$=\frac{h^2}{z_0^2-h^2}\left[z_0(x_0^2+y_0^2)-2hx_0y_0\right]. \tag{12.75}$$

Comparison with (12.69) shows that e_2 and e_1 are concentric and similar the size ratio being z_0/h. In Fig. 12.8a both ellipses are shown. The conic section e_2 intersects the x-axis (the y-axis) at $x=2hy_0/z_0$ (at $y=2hx_0/z_0$). Equation (12.73) yields the slope of the tangents t_1 and t_2 to e_2 at these points. It is easily verified that both tangents are passing through P_0. The sector formed by the two tangents including the tangents themselves is denoted Φ. Since e_2 is section of a cone it is located in a plane. In general, a plane intersects the third-order cylindroid in a third-order curve. In the present case, this curve splits into the conic section e_2 and a straight line. This straight line is the tangent $\overline{\sigma}_0$ of e_2.

The reciprocal cone and its intersections with the cylindroid are interpreted geometrically as follows. Let Σ be the plane spanned by the point A on σ_0 and by the conjugate screw $\overline{\sigma}_0$. For reasons explained above plane Σ intersects the cylindroid in the straight line $\overline{\sigma}_0$ and in a second-order curve. Since the cylindroid is confined to the interval $|z|\le|h|$, the curve must be an ellipse e. For reasons explained later it is the ellipse which in the vertical projection appears as circle c. Thus, $\overline{\sigma}_0$ is common to the two planes in which the cylindroid is intersected by the reciprocal cone. The ellipse e intersects the line $\overline{\sigma}_0$ at the point C on the z-axis and at the point B at the foot of the perpendicular from A (the angle at B is right also in vertical projection). The vertical distance between A and B is $z_\mathrm{A}-z_\mathrm{B}=2h\sin 2\chi_0$. The projected distance is $2r\sin 2\chi_0$ where r is the radius of circle c. Hence the angle of inclination α of plane Σ is determined by $\tan\alpha=h/r$. Since the ellipse extends from $z=-h$ to $z=h$ the semi-major axis of the ellipse is

$$a=\frac{h}{\sin\alpha}=h\frac{\sqrt{1+\tan^2\alpha}}{\tan\alpha}=\sqrt{h^2+r^2}\,. \tag{12.76}$$

These results establish as by-product

Theorem 12.6. *A circular cylinder of radius r having the directrix as generator intersects the cylindroid in an ellipse with semi-axes r and $\sqrt{h^2+r^2}$.*

Figure 12.8b shows the screw $\overline{\sigma}_0$ and the ellipse e with points A, B and C in their own plane Σ. Let D be an arbitrary point on the screw $\overline{\sigma}_0$. From Theorem 12.5 it follows that at the point of intersection Q with e the line $\overline{\mathrm{AD}}$ intersects a third screw σ^* orthogonally. When D is point C the third screw σ^* is the only other screw which, together with $\overline{\sigma}_0$, intersects the z-axis at this point C. When D is point B the third screw σ^* coalesces with $\overline{\sigma}_0$ expressing the fact that plane Σ is tangent to the cylindroid at B. This explains why the ellipse e is passing through B and C.

The line $\overline{\mathrm{AQ}}$ and the associated orthogonal screw σ^* are shown also in the projection of Fig. 12.8a. In this projection the orthogonality is nothing but Thales' theorem on the circle c. The screw σ^* is orthogonal not only to the line $\overline{\mathrm{AQ}}$, but also to the generator $\overline{\mathrm{PQ}}$ of the reciprocal cone. From the second part of Theorem 12.5 it follows that the generator $\overline{\mathrm{PQ}}$ intersects the cylindroid in two conjugate screws, i.e., at two points. In the projection of Fig. 12.8a these are the points Q_1 and Q_2 on e_2. They are real if the line $\overline{\mathrm{P}_0\mathrm{Q}}$ belongs to Φ. In this case, the lines $\overline{0\mathrm{Q}_1}$ and $\overline{0\mathrm{Q}_2}$ are the projections of the two conjugate screws. With their angle against the x-axis (12.58) determines the pitch, say p'. The screw $\overline{\mathrm{PQ}}$ with pitch $-p'$ is reciprocal to the cylindroid. Screws on the cylindroid have pitches p' in the interval $p_\mathrm{x} \le p' \le p_\mathrm{y}$ (assuming arbitrarily that $p_\mathrm{x} < p_\mathrm{y}$). Hence the conclusion: Reciprocal screws $\overline{\mathrm{PQ}}$ with projections $\overline{\mathrm{P}_0\mathrm{Q}}$ belonging to Φ have pitches $-p_\mathrm{y} \le -p' \le -p_\mathrm{x}$. All other reciprocal screws on the cone have pitches outside this range. The reciprocal screws with pitches $-p_\mathrm{x}$ and $-p_\mathrm{y}$ have axes which are, in the vertical projection, the tangents t_1 and t_2, respectively. It is easily verified, that the points of intersection of e_2 with the ξ,η-axes are located on the line passing through P_0 and through the center of e_2. From this it follows that the reciprocal screw having, in the vertical projection, this axis has the pitch $-\frac{1}{2}(p_\mathrm{x} + p_\mathrm{y})$.

Except for one special case, this ends the geometrical interpretation of the reciprocal cone. The special case is the one when the apex P is on the cylindroid, i.e., P=A. In this case, the cone breaks up into two planes. One of them is plane Σ. According to Theorem 12.4 every screw in Σ passing through A and having the pitch $-p$ (p being the pitch of σ_0 and $\overline{\sigma}_0$) is reciprocal to the cylindroid. The second plane Σ' is the one normal to σ_0 and passing[3] through A. According to Theorem 12.5 every line in this plane and passing through A intersects two (not necessarily real) conjugate screws having an associated pitch p'. Therefore, the screw having this line as axis and the pitch $-p'$ is reciprocal to the cylindroid. This ends the analysis of the fourth-order screw system reciprocal to a given cylindroid.

In what follows, the inverse problem is solved: Determine the cylindroid reciprocal to a given fourth-order screw system represented by four independent screws labeled 1, 2, 3, 4. The method of solution is due to Ball [1]. Let the four given screws be ordered such that their pitches are $p_1 < p_2 < p_3 < p_4$. Screws 1 and 3 define the cylindroid $(1,3)$, and screws 2 and 4 define the cylindroid $(2,4)$. Choose a pitch p such that $p_2 < p < p_3$. On each of the cylindroids $(1,3)$ and $(2,4)$ there are two real conjugate screws having this pitch p. These altogether four screws have two transversals. Let σ and τ be the two screws having these transversals as axes and the pitch $-p$. By

[3] Plane Σ' intersects the cylindroid in a third-order curve. In the x',y',z'-system defined by the transformation $x = x'\cos\chi_0 - y'\sin\chi_0$, $y = x'\sin\chi_0 + y'\cos\chi_0$, $z = z' + h\sin 2\chi_0$ Σ' is the plane $x' = 2r$. Substitution into (12.57) yields the desired equation: $z'(4r^2 + y'^2) + 2hy'(y'\sin 2\chi_0 - 2r\cos 2\chi_0) = 0$

Theorem 12.4 the cylindroid determined by σ and τ is reciprocal to the four screws 1, 2, 3, 4. Thus, the problem is solved.

This section is closed by the demonstration of still another property of the cylindroid. Proposition: For every screw 1 on the cylindroid specified by its angle χ_1, by its coordinate $z_1 = h\sin 2\chi_1$ and by its pitch $p_1 = p_0 - h\cos 2\chi_1$ there exists one other screw 2 on the cylindroid with an angle χ_2, with the coordinate $z_2 = h\sin 2\chi_2$ and with the pitch $p_2 = p_0 - h\cos 2\chi_2$ such that the screws 1 and 2 are reciprocal to each other. Proof: As condition for reciprocity Eq.(12.46) is used: $(p_1 + p_2)\cos\alpha - \ell\sin\alpha = 0$. Substitution of $p_1 + p_2 = 2p_0 - h(\cos 2\chi_1 + \cos 2\chi_2)$, $\ell = h(\sin 2\chi_2 - \sin 2\chi_1)$ and $\alpha = \chi_2 - \chi_1$ yields

$$2p_0\cos(\chi_2 - \chi_1) - h\Big[(\cos 2\chi_1 + \cos 2\chi_2)\cos(\chi_2 - \chi_1) + (\sin 2\chi_2 - \sin 2\chi_1)\sin(\chi_2 - \chi_1)\Big] = 0\,. \quad (12.77)$$

The factor of h being $2\cos(\chi_2 + \chi_1)$ this becomes

$$\tan\chi_1\tan\chi_2 = -\frac{p_0 - h}{p_0 + h} = -\frac{p_\mathrm{x}}{p_\mathrm{y}}\,. \quad (12.78)$$

This equation determines for every angle χ_1 two angles χ_2 and $\chi_2 + \pi$ belonging to one and the same screw 2. This ends the proof. Proposition: The pitches p_1 and p_2 associated with any such pair of reciprocal screws on the cylindroid satisfy the identity

$$\frac{1}{p_1} + \frac{1}{p_2} \equiv \frac{1}{p_\mathrm{x}} + \frac{1}{p_\mathrm{y}} \qquad \text{or} \qquad \frac{p_1 p_2}{p_1 + p_2} \equiv \frac{p_\mathrm{x} p_\mathrm{y}}{p_\mathrm{x} + p_\mathrm{y}}\,. \quad (12.79)$$

Proof: In terms of tangents the pitches are (see (3.167))

$$p_i = \frac{p_\mathrm{x} + p_\mathrm{y}\tan^2\chi_i}{1 + \tan^2\chi_i} \qquad (i = 1, 2)\,. \quad (12.80)$$

These expressions are substituted into the equation $p_1 p_2(p_\mathrm{x} + p_\mathrm{y}) = (p_1 + p_2)p_\mathrm{x}p_\mathrm{y}$. Upon multiplying out $(\tan\chi_1\tan\chi_2)^2$ is replaced by $(p_\mathrm{x}/p_\mathrm{y})^2$. This proves the identity.

12.6.3 Third-Order Screw System and Reciprocal Third-Order System

In a body with degree of freedom three some body-fixed basis with origin 0 and with unit basis vectors $\mathbf{e}_x$, $\mathbf{e}_y$, $\mathbf{e}_z$ is instantaneously free to move with

three velocity screws having the basis vectors as screw axes. These screws have the standard form $\omega_x(\,\mathbf{e}_x\,,\,p_x\mathbf{e}_x\,)\,,\ \omega_y(\,\mathbf{e}_y\,,\,p_y\mathbf{e}_y\,)\,,\ \omega_z(\,\mathbf{e}_z\,,\,p_z\mathbf{e}_z\,)$ with fixed pitches $p_x\,,\ p_y\,,\ p_z$ and with variable intensities $\omega_x\,,\ \omega_y\,,\ \omega_z\,.$ The resultant velocity screw has the standard form

$$(\boldsymbol{\omega}\,,\,\mathbf{a}\times\boldsymbol{\omega}\,+p\,\boldsymbol{\omega}\,)=\omega\,(\mathbf{n}\,,\,\mathbf{a}\times\mathbf{n}\,+p\,\mathbf{n}\,) \tag{12.81}$$

with intensity ω and with normalized Plücker vectors $\mathbf{n}$ and $\mathbf{a}\times\mathbf{n}$ of the screw axis. The unknowns are determined from the equations

$$\omega\,\mathbf{n}=\omega_x\mathbf{e}_x+\omega_y\mathbf{e}_y+\omega_z\mathbf{e}_z\ , \tag{12.82}$$

$$\omega\,(\mathbf{a}\times\mathbf{n}\,+p\,\mathbf{n})=\omega_x p_x\mathbf{e}_x+\omega_y p_y\mathbf{e}_y+\omega_z p_z\mathbf{e}_z \tag{12.83}$$

From the first equation it follows that $\omega_x=\omega n_x$ etc. Hence the second equation becomes

$$\mathbf{a}\times\mathbf{n}\,+p\,\mathbf{n}=p_x n_x\mathbf{e}_x+p_y n_y\mathbf{e}_y+p_z n_z\mathbf{e}_z\ . \tag{12.84}$$

Scalar multiplication by $\mathbf{n}$ yields for the pitch

$$p=p_x n_x^2+p_y n_y^2+p_z n_z^2\ . \tag{12.85}$$

The vector $\mathbf{a}$ is position vector of an arbitrary point on the screw axis. Its coordinates are denoted $[\,x\ y\ z\,]$. Decomposition of (12.84) yields the eigenvalue problem

$$\left.\begin{aligned}(p_x-p)n_x\ &+z n_y\ &-y n_z=0\ ,\\ -z n_x\ &+(p_y-p)n_y\ &+x n_z=0\ ,\\ y n_x\ &-x n_y\ &+(p_z-p)n_z=0\end{aligned}\right\} \tag{12.86}$$

with eigenvalue p and eigenvector $\mathbf{n}$. The characteristic equation is

$$(p_x-p)x^2+(p_y-p)y^2+(p_z-p)z^2=-(p_x-p)(p_y-p)(p_z-p) \tag{12.87}$$

or

$$\begin{aligned}p^3-(p_x+p_y+p_z)p^2+(x^2+y^2+z^2+p_xp_y+p_yp_z+p_zp_x)p\\ -\,(p_xx^2+p_yy^2+p_zz^2+p_xp_yp_z)=0\ .\end{aligned} \tag{12.88}$$

For any given point $[\,x\ y\ z\,]$ this third-order equation has three (real or complex) roots $p_1\,,\ p_2\,,\ p_3\,.$ By Vieta's theorem, $p_1+p_2+p_3=p_x+p_y+p_z=\text{const}$ (coefficient of $-p^2$). The number of real roots depends upon the discriminant D (see Bronstein/Semendjajev/Musiol/Mühlig [3]). The equation $D=0$ defines a surface of sixth order in $x\,,\ y$ and z separating two domains $D<0$ and $D>0\,.$ Through each point $[\,x\ y\ z\,]$ in the domain $D<0$ three screw axes with different real pitches $p_1\,,\ p_2\,,\ p_3$ are passing, and

through each point in the domain $D > 0$ a single screw axis with real pitch is passing. The coordinates n_x, n_y, n_z of the unit eigenvector associated with an eigenvalue p_i of multiplicity one are determined by two of the Eqs.(12.86) in combination with the condition $n_x^2 + n_y^2 + n_z^2 = 1$. In what follows, it is assumed that

$$p_z < p_y < p_x \tag{12.89}$$

thereby excluding the special cases $p_z = p_y < p_x$, $p_z < p_y = p_x$ and $p_z = p_y = p_x$. For $p = \text{const}$ Eq.(12.87) is the equation of a real hyperboloid of one sheet if p is in the interval $p_z \le p \le p_x$. The axes of all screws with given pitch p are generators belonging to one and the same regulus of the respective hyperboloid. All screws having pitch $-p$ and screw axes belonging to the other regulus are reciprocal to the first ones because every generator of one regulus intersects all generators of the other regulus. All hyperboloids have the x, y, z-axes as principal axes. The following five cases have to be distinguished

1. $p_z < p < p_y$: Hyperboloid $x^2/a^2 + y^2/b^2 - z^2/c^2 = 1$; elliptical cross section with semi-axes
$a = \sqrt{(p_y - p)(p - p_z)} < b = \sqrt{(p_x - p)(p - p_z)}$ in the x, y-plane; $c = \sqrt{(p_x - p)(p_y - p)}$

2. $p_y < p < p_x$: Hyperboloid $-x^2/a^2 + y^2/b^2 + z^2/c^2 = 1$; elliptical cross section with semi-axes
$b = \sqrt{(p_x - p)(p - p_z)} > c = \sqrt{(p_x - p)(p - p_y)}$ in the y, z-plane; $a = \sqrt{(p - p_y)(p - p_z)}$

3. $p = p_z$: $x = y = 0$, z arbitrary; the hyperboloid degenerates to the z-axis

4. $p = p_y$: The hyperboloid degenerates to the pair of planes $x = \pm z\sqrt{(p_y - p_z)/(p_x - p_y)}$, y arbitrary

5. $p = p_x$: $y = z = 0$, x arbitrary; the hyperboloid degenerates to the x-axis.

The hyperboloid associated with $p = 0$ (real only if p_z and p_x are of different sign) is referred to as *pitch quadric*. It has the equation

$$\frac{x^2}{p_y p_z} + \frac{y^2}{p_z p_x} + \frac{z^2}{p_x p_y} = -1 \,. \tag{12.90}$$

Zero-pitch screws about generators of one regulus are reciprocal to zero-pitch screws about generators of the other regulus. Hence

Theorem 12.7. *Pure rotation of an hyperboloid about a generator of regulus 1 has the effect that every point* P *of the hyperboloid has a velocity normal to the generator of regulus 2 through* P

The practical significance of this theorem is illustrated in Fig. 12.9 . The body with a spherical head is the terminal body of a chain with three revolute joints along skew axes n_1 , n_2 and n_3 . In the absence of the support of the spherical head the body is free to move instantaneously with independent angular velocities (zero-pitch velocity screws) about the three lines. Through these lines a hyperboloid is determined on which the lines belong to one regulus (regulus 1). The other regulus 2 is the manifold of all transversals t_1 , t_2 , t_3 etc. of the three lines. Forces (zero-pitch force screws) along these lines are reciprocal to zero-pitch velocity screws along lines of regulus 1 . The rigid support of the spherical head is causing such a force along the line t_1 . Neither this force nor constraint forces along other transversals have any effect on the instantaneous mobility of the body. The hyperboloid is the pitch quadric of the two mutually reciprocal zero-pitch screw systems.

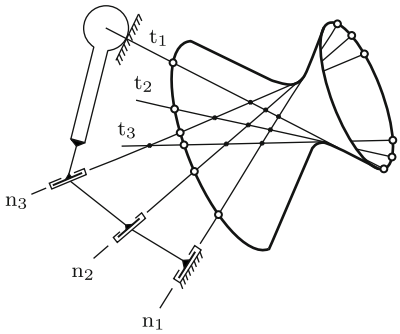

Fig. 12.9 Pitch quadric defined by three lines n_1 , n_2 , n_3 . Body moving instantaneously with independent angular velocities (zero-pitch velocity screws) about these lines regardless of constraint forces (zero-pitch force screws) along transversals

References

1. Ball R S (1900) A treatise on the theory of screws. Cambridge Univ. Press
2. Battaglini B (1869) Sulle serie dei sistemi di forze. Rendiconti Acc. di Napoli VIII:87–94
3. Bronstein I N, Semendjajev K A, Musiol K A, Mühlig H (2008) Taschenbuch der Mathematik. 7. Aufl. Verlag Harri Deutsch
4. Fröhlich I (1892) Kinematika (theory of motion) (Hung.). Magyar Tudományos Akadémia
5. Hunt K H (1959) Mechanisms and motion. English Universities Press, London
6. Hunt K H (1990) Kinematic geometry of mechanisms. Clarendon Press, Oxford
7. Klein F, Müller C (eds.) (1901-1908) Enzyklopädie der Math. Wissenschaften. v.IV: Mechanik. Teubner, Leipzig
8. Phillips J (1984/88) Freedom in machinary. vol.1,2. Cambridge Univ. Press, Cambridge, New York et al.

9. Phillips J (2003) General spatial involute gearing. Springer, Berlin, Heidelberg, New York
10. Schell W (1879) Theorie der Bewegung und der Kräfte. Teubner, Leipzig
11. Sylvester J J (1904/08/09/12) The collected mathematical papers of James Joseph Sylvester, v.1–4. Chelsea, New York
12. Timerding H E (1908) Geometrische Grundlegung der Mechanik eines starren Körpers. In [7]:125–189

Chapter 13
Shaft Couplings

A shaft coupling is, in the broadest sense, a mechanical device transmitting rotational motion from a shaft 1 to another shaft 2. In addition, a shaft coupling may serve the purpose of keeping one shaft in position relative to the other. Example: If both shafts are mounted in bearings in a common frame, a pair of gears having the transmission ratio one (spur gears, bevel gears or hypoid gears depending on the relative location of the shafts) is a shaft coupling transmitting rotational motion in such a way that $\omega_1 = \text{const}$ in shaft 1 causes $\omega_2 \equiv \omega_1 = \text{const}$ in shaft 2. If both shafts are mounted in parallel and sufficiently close together, an Oldham coupling is serving the same purpose. The Oldham coupling is functioning properly even in the case when the distance between the shafts is changing during operation. Neither gears nor Oldham couplings serve the purpose of keeping one shaft in position relative to the other. Another example: Only shaft 1 is mounted in fixed bearings. Shaft 2 is required to intersect shaft 1 at a given point 0 whereas its direction is free to change. Bevel gears are not applicable in this case. A common Hooke's joint (also called universal joint) is a possible shaft coupling. Its cross-shaped central body serves the purpose of keeping the shafts intersecting at 0. In addition, rotational motion is transmitted from shaft 1 to shaft 2. However, as will be seen in the following section, $\omega_1 = \text{const}$ in shaft 1 does not cause $\omega_2 \equiv \omega_1 = \text{const}$ in shaft 2. Shaft couplings allowing changes of relative position while maintaining the identity $\omega_2 \equiv \omega_1$ are called homokinetic. The general theory of homokinetic couplings is the subject of Sect. 13.4. The engineering importance and a simple example were explained in Sect. 4.2.6.

J. Wittenburg, *Kinematics*, DOI 10.1007/978-3-662-48487-6_13

13.1 Hooke's Joint

In the plane of Fig. 13.1 two shafts 1 and 2 are mounted in bearings such that the shaft axes intersect at point 0 under a constant angle α. The shafts are coupled by a Hooke's joint. Its essential element is a cross-shaped central body. Each shaft is connected to this body by a revolute joint the axis of which is normal to the shaft. On the central body the two joint axes intersect orthogonally at 0. In the figure the system is shown in a position in which one axis of the central body is in the plane of the drawing, while the other axis is perpendicular to it. The central body and the two revolute joints together constitute Hooke's joint. The angle α is a free parameter which in Fig. 13.1 is prescribed by the other two revolute joints connecting the shafts to a frame. The entire system composed of frame, shafts, central body and of four revolute joints represents a spherical four-bar with center 0. From Chap. 4 it is known that the degree of freedom is one. Thus, Hooke's joint transmits a rotation from shaft 1 to shaft 2. Let φ_1 and φ_2 be the angles of rotation of shaft 1 and of shaft 2, respectively, relative to the frame. They are related by a constraint equation $f(\varphi_1, \varphi_2) = 0$. In what follows, this equation is formulated. Subsequently, various other kinematical relationships are derived from this equation.

In Fig. 13.1 $\underline{\mathbf{e}}^1$ and $\underline{\mathbf{e}}^2$ are two reference bases fixed on the frame. Their common basis vectors $\mathbf{e}_3^1 = \mathbf{e}_3^2$ are normal to the plane of the two shafts, and $\mathbf{e}_1^1$ and $\mathbf{e}_1^2$ are directed along the respective shaft axes. The bases are related by the constant transformation matrix

$$\underline{A}^{12} = \begin{bmatrix} \cos\alpha & -\sin\alpha & 0 \\ \sin\alpha & \cos\alpha & 0 \\ 0 & 0 & 1 \end{bmatrix} . \tag{13.1}$$

Let $\mathbf{n}_1$ and $\mathbf{n}_2$ be unit vectors fixed on the central body along the joint axes. In the position shown in Fig. 13.1 $\mathbf{n}_1 = \mathbf{e}_2^1$. Let this be the position $\varphi_1 = 0$ of shaft 1 and the position $\varphi_2 = -\pi/2$ of shaft 2. This means that $\varphi_2 = 0$ is the position when $\mathbf{n}_2 = \mathbf{e}_2^2$. In a position φ_1 (arbitrary) $\mathbf{n}_1$ has

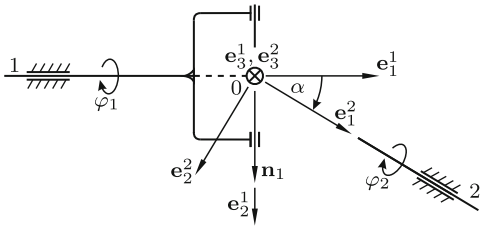

Fig. 13.1 Hooke's joint with frame-fixed bases $\underline{\mathbf{e}}^1$, $\underline{\mathbf{e}}^2$ in position $\varphi_1 = 0$, $\varphi_2 = -\pi/2$

in basis $\underline{\mathbf{e}}^1$ the coordinate matrix $\underline{n}_1^1 = [0 \;\; \cos\varphi_1 \;\; \sin\varphi_1]^T$. Similarly, in a position φ_2 (arbitrary) $\mathbf{n}_2$ has in $\underline{\mathbf{e}}^2$ the coordinate matrix

$$\underline{n}_2^2 = [0 \;\; \cos\varphi_2 \;\; \sin\varphi_2]^T \,. \tag{13.2}$$

Transformation yields the coordinate matrix $\underline{n}_2^1 = \underline{A}^{12}\underline{n}_2^2$ in basis $\underline{\mathbf{e}}^1$. The coordinate matrices $\underline{n}_1^1$ and $\underline{n}_2^1$ determine the coordinate matrix $\underline{n}_3^1 = \tilde{n}_1^1 \underline{n}_2^1$ of the vector $\mathbf{n}_3 = \mathbf{n}_1 \times \mathbf{n}_2$. The three coordinate matrices are

$$\underline{n}_1^1 = \begin{bmatrix} 0 \\ \cos\varphi_1 \\ \sin\varphi_1 \end{bmatrix}, \quad \underline{n}_2^1 = \begin{bmatrix} -\sin\alpha\cos\varphi_2 \\ \cos\alpha\cos\varphi_2 \\ \sin\varphi_2 \end{bmatrix}, \quad \underline{n}_3^1 = \begin{bmatrix} -\cos\alpha\sin\varphi_1\cos\varphi_2 + \cos\varphi_1\sin\varphi_2 \\ -\sin\alpha\sin\varphi_1\cos\varphi_2 \\ \sin\alpha\cos\varphi_1\cos\varphi_2 \end{bmatrix}. \tag{13.3}$$

From the first two matrices the desired relationship $f(\varphi_1, \varphi_2) = 0$ is obtained. Orthogonality of the vectors $\mathbf{n}_1$ and $\mathbf{n}_2$ requires that $\mathbf{n}_1 \cdot \mathbf{n}_2 = 0$. This is the equation $f(\varphi_1, \varphi_2) = \cos\varphi_1\cos\alpha\cos\varphi_2 + \sin\varphi_1\sin\varphi_2 = 0$ or

$$\tan\varphi_2 \tan\varphi_1 = -\cos\alpha \,. \tag{13.4}$$

This relationship was first published in 1824 by Jean Victor Poncelét (1788-1867) (see also Poncelét [15]). The output angle φ_2 is an odd, π-periodic function of the input angle φ_1. It is independent of the sign of α. In view of Fig. 13.1 this had to be expected. The equation yields the expressions

$$\left.\begin{aligned} \cos\varphi_2 &= \frac{1}{\sqrt{1+\tan^2\varphi_2}} = \frac{\sin\varphi_1}{\sqrt{1-\sin^2\alpha\cos^2\varphi_1}} \,, \\ \sin\varphi_2 &= \frac{-\cos\alpha\cos\varphi_1}{\sqrt{1-\sin^2\alpha\cos^2\varphi_1}} \,. \end{aligned}\right\} \tag{13.5}$$

Differentiation of (13.4) with respect to time results in the equation $(\dot{\varphi}_2/\cos^2\varphi_2)\tan\varphi_1 + (\dot{\varphi}_1/\cos^2\varphi_1)\tan\varphi_2 = 0$. This yields for the angular velocity ratio the expression

$$\frac{\dot{\varphi}_2}{\dot{\varphi}_1} = -\frac{\sin\varphi_2\cos\varphi_2}{\sin\varphi_1\cos\varphi_1} \,. \tag{13.6}$$

Elimination of φ_2 by means of (13.5) leads to the final formula

$$\frac{\dot{\varphi}_2}{\dot{\varphi}_1} = \frac{\cos\alpha}{1-\sin^2\alpha\cos^2\varphi_1} \,. \tag{13.7}$$

This is an even π-periodic function of φ_1. In the case $\dot{\varphi}_1 = \text{const}$, the angular velocity $\dot{\varphi}_2$ is oscillating π-periodically between the extremal values $\dot{\varphi}_1\cos\alpha$ and $\dot{\varphi}_1/\cos\alpha$.

One more differentiation with respect to time yields for the angular acceleration $\ddot{\varphi}_2$ the expression (valid for $\dot{\varphi}_1 = \text{const}$)

$$\ddot{\varphi}_2 = -\dot{\varphi}_1^2 \frac{\sin^2\alpha\cos\alpha\sin 2\varphi_1}{(1-\sin^2\alpha\cos^2\varphi_1)^2}\ , \quad \ddot{\varphi}_2 \approx -\dot{\varphi}_1^2\alpha^2\sin 2\varphi_1 \quad (\alpha \ll 1)\ . \tag{13.8}$$

The difference $\chi(\varphi_1) = \varphi_2 - \varphi_1 + \pi/2$ is an odd π-periodic function of φ_1 (note that $\varphi_2 = -\pi/2$ when $\varphi_1 = 0$). Its maxima and minima of equal absolute value occur in positions when $\dot{\varphi}_2 = \dot{\varphi}_1$. According to (13.7) this is the case when $\cos^2\varphi_1 = 1/(1+\cos\alpha)$. From this it follows that $\sin^2\varphi_1 = \cos\alpha/(1+\cos\alpha)$ and $\tan\varphi_1 = \sqrt{\cos\alpha}$. Furthermore, according to (13.4), $\tan\varphi_2 = -\sqrt{\cos\alpha}$. This yields for the maximum of χ the formula

$$\begin{aligned}\tan\left(\chi_{\max} - \frac{\pi}{2}\right) &= -\cot\chi_{\max} = \tan(\varphi_2 - \varphi_1) \\ &= \frac{\tan\varphi_2 - \tan\varphi_1}{1+\tan\varphi_2\tan\varphi_1} = \frac{-2\sqrt{\cos\alpha}}{1-\cos\alpha}\ .\end{aligned} \tag{13.9}$$

Hence

$$\chi_{\max} = \tan^{-1}\frac{1-\cos\alpha}{2\sqrt{\cos\alpha}}\ . \tag{13.10}$$

Example: $\chi_{\max} \approx 4.1^\circ$ at $\varphi_1 \approx 42.9^\circ$ for $\alpha = 30^\circ$. The Taylor formula for small angles α is $\chi_{\max} \approx \alpha^2/4$. End of example.

13.1.1 Polhode and Herpolhode Cones of the Central Cross

The cross-shaped central body is executing a periodic motion about a fixed point. For this reason, both the polhode cone and the herpolhode cone are closed cones. In what follows, these cones are determined[1]. Let $\dot{\psi}_1\mathbf{n}_1$ and $\dot{\psi}_2\mathbf{n}_2$ be the angular velocities of the cross relative to the two shafts so that the angular velocity $\boldsymbol{\omega}$ of the cross relative to the frame has the alternative forms

$$\boldsymbol{\omega} = \dot{\varphi}_1\mathbf{e}_1^1 + \dot{\psi}_1\mathbf{n}_1 = \dot{\varphi}_2\mathbf{e}_1^2 + \dot{\psi}_2\mathbf{n}_2\ . \tag{13.11}$$

In the reference basis with basis vectors $\mathbf{n}_1$, $\mathbf{n}_2$, $\mathbf{n}_3 = \mathbf{n}_1 \times \mathbf{n}_2$ fixed on the cross $\boldsymbol{\omega}$ has the coordinates

$$\omega_1 = \dot{\psi}_1 = \dot{\varphi}_2\mathbf{e}_1^2\cdot\mathbf{n}_1\ , \qquad \omega_2 = \dot{\psi}_2 = \dot{\varphi}_1\mathbf{e}_1^1\cdot\mathbf{n}_2\ , \qquad \omega_3 = \dot{\varphi}_1\mathbf{e}_1^1\cdot\mathbf{n}_3\ . \tag{13.12}$$

[1] In Wittenburg/Roberson [18] the cones are determined for a Hooke's joint with a nonorthogonal central cross

The scalar products are read from (13.2) and (13.3). For $\cos\varphi_2$, $\sin\varphi_2$ and $\dot\varphi_2$ the expressions (13.5) and (13.7) are substituted. This results in

$$\left.\begin{aligned} \omega_1 = \dot\psi_1 = \dot\varphi_1 \frac{\sin\alpha\cos\alpha\cos\varphi_1}{1-\sin^2\alpha\cos^2\varphi_1}\,, \qquad \omega_2 = -\dot\varphi_1 \frac{\sin\alpha\sin\varphi_1}{\sqrt{1-\sin^2\alpha\cos^2\varphi_1}}\,, \\ \omega_3 = \dot\varphi_1 \frac{-\cos\alpha}{\sqrt{1-\sin^2\alpha\cos^2\varphi_1}}\,. \end{aligned}\right\} \tag{13.13}$$

These equations are parameter equations of the polhode cone (the moving cone) with φ_1 as parameter. The cone is best portrayed by its curve of intersection with a plane parallel to the $\mathbf{n}_1,\mathbf{n}_2$-plane. This curve has the parameter equations

$$x(\varphi_1) = \frac{\omega_1}{\omega_3} = \frac{-\sin\alpha\cos\varphi_1}{\sqrt{1-\sin^2\alpha\cos^2\varphi_1}}\,, \quad y(\varphi_1) = \frac{\omega_2}{\omega_3} = \tan\alpha\sin\varphi_1\,. \tag{13.14}$$

Squaring both equations leads to expressions for $\cos^2\varphi_1$ and for $\sin^2\varphi_1$. Their sum equals one. This is the parameter-free equation

$$x^2 + x^2y^2 + y^2 = \tan^2\alpha\,. \tag{13.15}$$

In Fig. 13.2 curves are shown for various angles α. The ellipse is explained later. An investigation of the curvature shows that the transition from convex to nonconvex curves occurs at $\alpha = 60°$. The smaller α the better is the approximation of a circle of radius α. In joints used in engineering angles up to approximately $\alpha = 35°$ are realizable. At the points of symmetry of the curve marked by $|x| = |y|$ (13.15) yields $y^2 = 1/\cos\alpha - 1$. Equation (13.14) yields for the associated angle φ_1 the expression $\sin\varphi_1 = \sqrt{\cos\alpha/(1+\cos\alpha)}$. This is the angle associated with the maximum difference $\chi_{\max}$.

The herpolhode cone (the fixed cone) is determined by the coordinates of $\boldsymbol{\omega}$ in basis $\underline{\mathbf{e}}^1$. Let these coordinates be denoted Ω_1, Ω_2, Ω_3. Equation (13.11) in combination with (13.3) and with $\dot\psi_1$ from (13.13) results in

$$\left.\begin{aligned} \Omega_1 = \dot\varphi_1\,, \qquad \Omega_2 = \dot\psi_1\mathbf{n}_1\cdot\mathbf{e}_2^1 = \dot\varphi_1\frac{\sin\alpha\cos\alpha\cos^2\varphi_1}{1-\sin^2\alpha\cos^2\varphi_1}\,, \\ \Omega_3 = \dot\psi_1\mathbf{n}_1\cdot\mathbf{e}_3^1 = \dot\varphi_1\frac{\sin\alpha\cos\alpha\sin\varphi_1\cos\varphi_1}{1-\sin^2\alpha\cos^2\varphi_1}\,. \end{aligned}\right\} \tag{13.16}$$

This yields the ratios

$$\left.\begin{aligned} X(\varphi_1) = \frac{\Omega_2}{\Omega_1} = \frac{\sin\alpha\cos\alpha\cos^2\varphi_1}{1-\sin^2\alpha\cos^2\varphi_1}\,, \\ Y(\varphi_1) = \frac{\Omega_3}{\Omega_1} = \frac{\sin\alpha\cos\alpha\sin\varphi_1\cos\varphi_1}{1-\sin^2\alpha\cos^2\varphi_1}\,. \end{aligned}\right\} \tag{13.17}$$

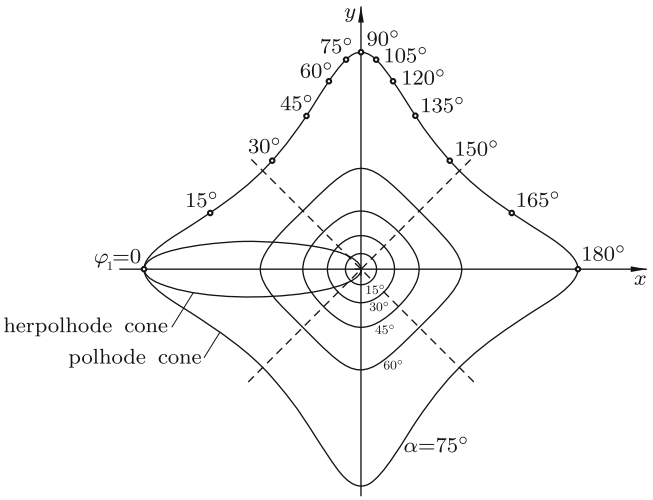

Fig. 13.2 Intersection curves of polhode cones of the cross-shaped central body with a plane parallel to the $\mathbf{n}_1, \mathbf{n}_2$-plane for Hooke's joints with various angles α. The ellipse represents the herpolhode cone associated with $\alpha = 75°$ in the position $\varphi_1 = 0$

They are parameter equations of the intersection curve of the herpolhode cone with a plane normal to the shaft axis $\mathbf{e}_1^1$. The parameter φ_1 is eliminated by calculating $\tan\varphi_1 = Y/X$ and hence $\cos^2\varphi_1 = X^2/(X^2+Y^2)$. This expression is substituted back into the equation for $X(\varphi_1)$. The result is the ellipse

$$\left(\frac{X - \frac{1}{2}\tan\alpha}{\frac{1}{2}\tan\alpha}\right)^2 + \left(\frac{Y}{\frac{1}{2}\sin\alpha}\right)^2 = 1\,. \tag{13.18}$$

Figure 13.3 shows the location of the herpolhode cone and of this ellipse relative to the two shafts. Both shaft axes are generators of the cone. The projection of the ellipse along the axis of shaft 2 is a circle. In the position $\varphi_1 = 0$ the planes of intersection of the cones coincide, and the common generator $\boldsymbol{\omega}$ lies in the shaft axis 2. In Fig. 13.2 the ellipse associated with $\alpha = 75°$ is shown in this position. For arbitrary α and in every position φ_1 the fixed cone lies entirely inside the moving cone so that rolling of one cone on the other is possible without collision. Per revolution of shaft 1 the vector

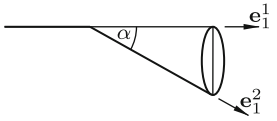

Fig. 13.3 Herpolhode cone with elliptic cross section between the shaft axes

$\boldsymbol{\omega}$ is sweeping out the fixed cone twice and the moving cone once. This means that the moving cone is rolling around the fixed cone twice per revolution of shaft 1.

The cones are known from Sect. 10.1. The motion studied there is the inverse of the motion of the central cross. The moving cone of one motion is the fixed cone of the other and vice versa (compare (13.15) and (13.18) with (10.19)).

In preparation for Sect. 13.2.1 the angle of rotation ψ_1 of the cross relative to shaft 1 is determined as function of φ_1. Arbitrarily, $\psi_1 = 0$ is associated with $\varphi_1 = 0$. From (13.12) and (13.13) it follows that

$$\frac{\mathrm{d}\psi_1}{\mathrm{d}\varphi_1} = \frac{\sin\alpha\cos\alpha\cos\varphi_1}{1-\sin^2\alpha\cos^2\varphi_1} \,. \tag{13.19}$$

With the new variable $z = \tan\varphi_1/2$ and with the constant $k^2 = (1-\sin\alpha)/(1+\sin\alpha)$ this takes the form

$$\begin{aligned}\psi_1 &= 2\tan\alpha \int \frac{1-z^2}{(1+k^2z^2)(1+z^2/k^2)}\,\mathrm{d}z \\ &= \frac{2\tan\alpha}{k^2-1}\Big[k^2\int\frac{\mathrm{d}z}{1+k^2z^2} - \int\frac{\mathrm{d}z}{1+z^2/k^2}\Big] \\ &= \tan^{-1}(z/k) - \tan^{-1}(kz) = \tan^{-1}(\tan\alpha\sin\varphi_1)\,. \end{aligned} \tag{13.20}$$

Hence

$$\tan\psi_1 = \tan\alpha\sin\varphi_1 \,. \tag{13.21}$$

This equation is the second Eq.(10.10).

13.2 Fenyi's Joint

Figure 13.4 is the exploded view of a shaft coupling brought to the author's attention by Fenyi[2]. The coupled shafts 1 and 2 are skew. They are mounted in frame-fixed bearings not shown in the figure. Let $\hat{\mathbf{e}}_2^1$ and $\hat{\mathbf{e}}_2^2$ be dual unit vectors along the shaft axes, and let, furthermore, $\hat{\alpha} = \alpha + \varepsilon\ell$ be the constant dual screw angle displacing $\hat{\mathbf{e}}_2^1$ into the position $\hat{\mathbf{e}}_2^2$. The projected angle α and the length ℓ of the common perpendicular of the two shaft axes are the only parameters of the joint. To each shaft and at right angles to the shaft two collinear trunnions are rigidly attached. These trunnions are moving in bearings of the central ring-shaped body. The axes of these bearings intersect at a right angle at M. In the assembled state the ring transmits the rotational motion of shaft 1 to shaft 2. Relative to each pair

[2] Stanislo Fenyi, Forschungszentrum Karlsruhe

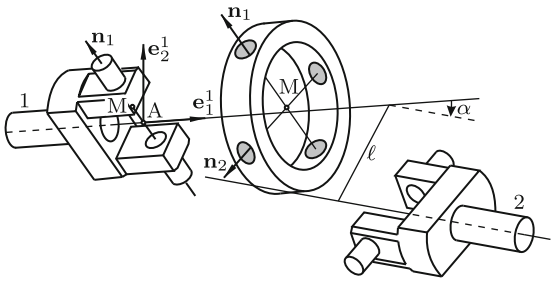

Fig. 13.4 Exploded view of Fenyi's joint

of trunnions the ring executes a screw motion. It is assumed that shaft 1 is in pure rotation relative to the frame (angle of rotation φ_1). In order to function properly the bearings of shaft 2 must allow shaft 2 to execute a screw motion composed of a rotation φ_2 and a translation z. In the special case $\alpha = 0$, the joint is the Oldham coupling shown in Fig. 15.6. In the special case $\ell = 0$, the joint is Hooke's joint shown in Fig. 13.1, and all screw displacements are pure rotations.

The following kinematics investigation is based on the principle of transference. The rotational part of the problem is identical with that of a Hooke's joint with parameter α. The principle of transference is applied to Eq.(13.4):

$$\tan\varphi_2 \tan\varphi_1 = -\cos\alpha \,. \tag{13.22}$$

The angle α is replaced by $\hat{\alpha} = \alpha + \varepsilon\ell$, and the angle φ_2 is replaced by $\hat{\varphi}_2 = \varphi_2 + \varepsilon z$. The angle φ_1 is not effected because shaft 1 is, by assumption, in pure rotation. Thus, the dual form of (13.22) is $\tan\hat{\varphi}_2 \tan\varphi_1 = -\cos\hat{\alpha}$. This is the equation (see (3.31))

$$\left(\tan\varphi_2 + \varepsilon\frac{z}{\cos^2\varphi_2}\right)\tan\varphi_1 = -(\cos\alpha - \varepsilon\ell\sin\alpha) \,. \tag{13.23}$$

The primary part of this equation is Eq.(13.22). The dual part is $(z/\cos^2\varphi_2)\tan\varphi_1 = \ell\sin\alpha$. Writing $1/\cos^2\varphi_2 = 1 + \tan^2\varphi_2$ and using (13.22) this yields for the translatory displacement of shaft 2 the expression

$$z = \ell\,\frac{\sin\alpha\sin\varphi_1\cos\varphi_1}{1 - \sin^2\alpha\cos^2\varphi_1} \,. \tag{13.24}$$

This is an odd, π-periodic function of φ_1. Its maxima and minima of equal absolute value occur when $\mathrm{d}z/\mathrm{d}\varphi_1 = 0$. This equation leads to $\cos^2\varphi_1 = 1/(1+\cos^2\alpha)$, $\sin^2\varphi_1 = \cos^2\alpha/(1+\cos^2\alpha)$ and $\sin\varphi_1\cos\varphi_1 = \cos\alpha/(1+\cos^2\alpha)$. When this is substituted into (13.24), the maximum range of the translatory displacement of shaft 2 is found to be

$$z_{\max} - z_{\min} = 2z_{\max} = \ell \tan\alpha \,. \tag{13.25}$$

13.2.1 Raccording Axodes of the Central Ring

The central ring is executing a periodic spatial motion without a fixed point. The periodically moving instantaneous screw axis is the generator of two closed raccording axodes. In what follows, parameter equations with φ_1 as parameter are developed for these axodes. On the frame the basis $\underline{\mathbf{e}}^1$ known from Fig. 13.1 is fixed. Its origin A is the point where the axis of shaft 1 intersects the first axis of the ring. On the ring the basis $\underline{\mathbf{n}}$ with basis vectors $\mathbf{n}_1$, $\mathbf{n}_2$, $\mathbf{n}_3$ known from Fig. 13.1 is defined. It has its origin at the point of intersection M of the two ring axes. By writing the vector from A to M in the form $z_1\mathbf{n}_1$ the coordinate $z_1 = z_1(\varphi_1)$ is defined. Let $\mathbf{u}(\varphi_1)$ be the perpendicular from A onto the instantaneous screw axis (ISA) of the ring, and let, furthermore, $\boldsymbol{\omega}(\varphi_1)$ be the angular velocity of the ring relative to the frame. With a dimensionless parameter λ the vectors from A and from M to an arbitrary point P(λ) on the ISA are

$$\left.\begin{aligned} \mathbf{r}_{\mathrm{AP}}(\varphi_1,\lambda) &= \mathbf{u}(\varphi_1) + \frac{\lambda\ell}{\dot\varphi_1}\boldsymbol{\omega}(\varphi_1) \,, \\ \mathbf{r}_{\mathrm{MP}}(\varphi_1,\lambda) &= \mathbf{u}(\varphi_1) + \frac{\lambda\ell}{\dot\varphi_1}\boldsymbol{\omega}(\varphi_1) - z_1(\varphi_1)\mathbf{n}_1 \,. \end{aligned}\right\} \tag{13.26}$$

The coordinates of $\mathbf{r}_{\mathrm{AP}}$ in basis $\underline{\mathbf{e}}^1$ and the coordinates of $\mathbf{r}_{\mathrm{MP}}$ in basis $\underline{\mathbf{n}}$ are the desired parameter equations of the fixed axode and of the moving axode, respectively. With increasing $|\lambda|$ the equations of the axodes approach asymptotically those of the herpolhode cone and of the polhode cone, respectively, of the cross-shaped central body in Hooke's joint (see Figs. 13.2 and 13.3).

The perpendicular $\mathbf{u}$ from A onto the ISA is, according to (9.23),

$$\mathbf{u} = \frac{\boldsymbol{\omega} \times \mathbf{v}_{\mathrm{A}}}{\boldsymbol{\omega}^2} \tag{13.27}$$

with $\mathbf{v}_{\mathrm{A}}$ being the velocity of the ring-fixed point coinciding with A. This velocity is $\mathbf{v}_{\mathrm{A}} = \dot z_1 \mathbf{n}_1$. Expressions for z_1 and for $\dot z_1$ are obtained by transferring Eq.(13.21) into dual form: $\tan(\psi_1 + \varepsilon z_1) = \tan(\alpha + \varepsilon\ell)\sin\varphi_1$. Its dual part is the expression for z_1 given below. Differentiation[3] yields $\dot z_1$. With the abbreviations $C = \cos\alpha$, $S = \sin\alpha$, $c = \cos\varphi_1$, $s = \sin\varphi_1$ the expressions are

[3] $\dot z_1$ is also the dual part of the dualized expression for $\dot\psi_1$ given in the first Eq.(13.29)

$$z_1 = \ell \, \frac{s}{1 - S^2 c^2} \, , \qquad \dot{z}_1 = \dot{\varphi}_1 \ell \, \frac{c(C^2 - S^2 s^2)}{(1 - S^2 c^2)^2} \, . \tag{13.28}$$

The angular velocity $\boldsymbol{\omega}$ of the ring is identical with the angular velocity of the cross-shaped body in Hooke's joint. From (13.11), (13.12) and (13.13) the following expressions are copied:

$$\left.\begin{aligned} \dot{\psi}_1 &= \dot{\varphi}_1 \, \frac{SCc}{1 - S^2 c^2} \, , \qquad \boldsymbol{\omega} = \dot{\varphi}_1 \mathbf{e}_1^1 + \dot{\psi}_1 \mathbf{n}_1 \, , \\ \boldsymbol{\omega}^2 &= \dot{\varphi}_1^2 + \dot{\psi}_1^2 = \dot{\varphi}_1^2 \, \frac{1 - S^2 c^2 (1 + S^2 s^2)}{(1 - S^2 c^2)^2} \, . \end{aligned}\right\} \tag{13.29}$$

With these expressions and with $\mathbf{v}_{\mathrm{A}} = \dot{z}_1 \mathbf{n}_1$ (13.27) yields

$$\mathbf{u} = \ell \, \frac{c(C^2 - S^2 s^2)}{1 - S^2 c^2 (1 + S^2 s^2)} \, (-s \, \mathbf{e}_2^1 + c \, \mathbf{e}_3^1) \, . \tag{13.30}$$

This expression and the expressions for $\boldsymbol{\omega}$ and for z_1 are substituted into (13.26). The coordinates of $\boldsymbol{\omega}$ in the bases $\underline{\mathbf{e}}^1$ and $\underline{\mathbf{n}}$ are known from (13.16) and (13.13), respectively. The coordinates of $\mathbf{e}_2^1$ and of $\mathbf{e}_3^1$ in $\underline{\mathbf{n}}$ are calculated from (13.3) and (13.5). Substitution of all these expressions results in the desired parameter equations for the axodes:

Fixed axode in basis $\mathbf{e}_{1,2,3}^1$: moving axode in basis $\mathbf{n}_{1,2,3}$:

$$\ell \begin{bmatrix} \lambda \\ \dfrac{-cs(C^2 - S^2 s^2)}{1 - S^2 c^2 (1 + S^2 s^2)} + \lambda \dfrac{CSc^2}{1 - S^2 c^2} \\ \dfrac{c^2 (C^2 - S^2 s^2)}{1 - S^2 c^2 (1 + S^2 s^2)} + \lambda \dfrac{CScs}{1 - S^2 c^2} \end{bmatrix} \, , \quad \ell \begin{bmatrix} \dfrac{-s + \lambda CSc}{1 - S^2 c^2} \\ \dfrac{-1}{\sqrt{1 - S^2 c^2}} \left[\dfrac{Cc(C^2 - S^2 s^2)}{1 - S^2 c^2 (1 + S^2 s^2)} + \lambda Ss \right] \\ \dfrac{1}{\sqrt{1 - S^2 c^2}} \left[\dfrac{Scs(C^2 - S^2 s^2)}{1 - S^2 c^2 (1 + S^2 s^2)} - \lambda C \right] \end{bmatrix} \, . \tag{13.31}$$

In Fig. 13.5 the axodes for the parameter value $\alpha = 60°$ are shown (the fixed axode dark, the white moving axode in a single position). Each axode is represented by a net of lines $\lambda = \text{const}$ $(-2 \le \lambda \le 2)$ and $\varphi_1 = \text{const}$. The moving axode is raccording around the fixed axode twice per revolution of shaft 1. For showing the moving axode in a single position $\varphi_1 = \phi$ together with the fixed axode the coordinates in the column matrix on the right-hand side of (13.31) are transformed into basis $\underline{\mathbf{e}}^1$. The transformation matrix for this purpose is composed of the three columns shown in (13.3) with $\varphi_1 = \phi$. To the resulting coordinates the coordinates of the vector $\mathbf{r}_{\mathrm{AM}}(\phi) = z_1(\phi) \mathbf{n}_1(\phi)$ are added (see (13.26)). The raccording motion is made visible by showing the moving axode in a sequence of pictures over the full range of values $0 \le \phi \le 2\pi$.

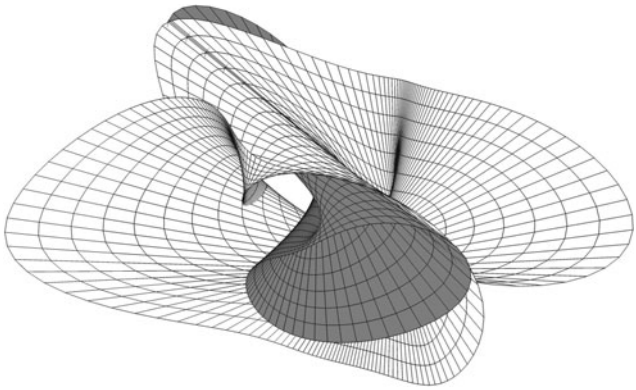

Fig. 13.5 Raccording axodes of the central ring for $\alpha = 60°$ (fixed axode dark)

13.3 Series-Connected Hooke's Joints

Equation (13.7) has shown that the output angular velocity of Hooke's joint is oscillating if the input angular velocity is constant. For this reason the single Hooke's joint has a limited range of engineering applications. The present section is devoted to the following problem. A chain of shafts $1, \ldots, n$ is interconnected by Hooke's joints $1, \ldots, n-1$. The shafts labeled 1 and n are referred to as input shaft and as output shaft, respectively. The entire system between these two shafts represents a single joint. To be formulated are necessary and sufficient conditions guaranteeing the angular velocity ratio $\dot{\varphi}_n/\dot{\varphi}_1 \equiv 1$.

First, the case $n = 3$ is investigated, i.e., the case of Hooke's joints 1 and 2 coupling shafts 1, 2 and 3. The parameter α of Fig. 13.1 associated with Hooke's joint 1 is now called α_1. The parameter α_2 associated with Hooke's joint 2 is the constant angle between shafts 2 and 3. Until further below it is assumed that shafts 1, 2 and 3 are coplanar. Since they are coplanar, only two configurations are possible in which shafts 1 and 3 intersect at an angle which is either $\alpha_1 + \alpha_2$ or $\alpha_1 - \alpha_2$. The cross of each of the two Hooke's joints is rotating relative to shaft 2 about an axis which is perpendicular to shaft 2. Let β_2 be the constant angle between these two perpendiculars. It is a third parameter in addition to α_1 and α_2. The sign of β_2 is specified by the definition that $\varphi_2 - \beta_2$ is the input angle of the second Hooke's joint. Applying (13.4) to both joints results in the relationships

$$\tan\varphi_2 \tan\varphi_1 = -\cos\alpha_1 \,, \qquad \tan\varphi_3 \tan(\varphi_2 - \beta_2) = -\cos\alpha_2 \,. \tag{13.32}$$

In what follows, only the special cases $\beta_2 = 0$ and $\beta_2 = \pi/2$ are considered. With the identity $\tan\psi = -\cot(\psi - \pi/2)$ the second Eq.(13.32) is given the form

$$\left.\begin{aligned} \beta_2 = 0: &\qquad \cot(\varphi_3 - \tfrac{\pi}{2}) \tan\varphi_2 = \cos\alpha_2 \ , \\ \beta_2 = \tfrac{\pi}{2}: &\qquad \tan\varphi_3 \cot\varphi_2 = \cos\alpha_2 \ . \end{aligned}\right\} \tag{13.33}$$

Combination with the first Eq.(13.32) eliminates φ_2. The result is the desired input-output relationship

$$\left.\begin{aligned} \beta_2 = 0: &\qquad \tan(\varphi_3 - \tfrac{\pi}{2}) \tan\varphi_1 = -\cos\alpha_1 / \cos\alpha_2 \ , \\ \beta_2 = \tfrac{\pi}{2}: &\qquad \tan\varphi_3 \tan\varphi_1 = -\cos\alpha_1 \cos\alpha_2 \ . \end{aligned}\right\} \tag{13.34}$$

This is written in the form

$$\tan(\varphi_3 - \gamma_3) \tan\varphi_1 = -a_3 \ , \qquad a_3 = \begin{cases} \cos\alpha_1 / \cos\alpha_2 & (\beta_2 = 0) \\ \cos\alpha_1 \cos\alpha_2 & (\beta_2 = \frac{\pi}{2}) \end{cases} \tag{13.35}$$

with either $\gamma_3 = \pi/2$ or $\gamma_3 = 0$.

The generalization to chains with $n-1$ Hooke's joints coupling shafts $1, \ldots, n$ is straight-forward. Again, the shafts are assumed to be coplanar. With each new shaft i a new shaft parameter β_{i-1} (either $\beta_{i-1} = 0$ or $\beta_{i-1} = \pi/2$) and a new joint parameter α_{i-1} are introduced and with them a new equation of the general form (13.33) with indices i and $i-1$ instead of 3 and 2. The angle φ_{i-1} is eliminated by combining this equation with the previous equation of the general form (13.35). The final result for the input-output relationship for a chain of $n-1$ Hooke's joints coupling shafts $1, \ldots, n$ has the form

$$\tan(\varphi_n - \gamma_n) \tan\varphi_1 = -a_n \tag{13.36}$$

with constants γ_n and a_n. The latter is

$$a_n = \cos\alpha_1 \prod_{i=2}^{n-1} (\cos\alpha_i)^{\nu_i} \ , \qquad \nu_i = \begin{cases} +1 & (\beta_i = \frac{\pi}{2}) \\ -1 & (\beta_i = 0) \end{cases} \qquad (n \geq 3) \ . \tag{13.37}$$

Differentiation with respect to time yields the angular velocity ratio (compare the transition from (13.4) to (13.7))

$$\frac{\dot\varphi_n}{\dot\varphi_1} = \frac{a_n}{1 - (1 - a_n^2) \cos^2\varphi_1} \ . \tag{13.38}$$

The desired angular velocity ratio $\dot\varphi_n / \dot\varphi_1 \equiv 1$ is achieved with $a_n = 1$. This is a condition on the joint parameters $\alpha_1, \ldots, \alpha_{n-1}$ and on the shaft parameters $\beta_2, \ldots, \beta_{n-1}$.

Example $n = 3$: Equation (13.35) shows that $a_3 = 1$ requires $\beta_2 = 0$ and, in addition, $\cos\alpha_1 / \cos\alpha_2 = 1$, i.e., $|\alpha_1| = |\alpha_2|$. This result was to be expected. In Figs. 13.6a and b the two possible arrangements with coplanar shafts 1, 2 and 3 are shown.

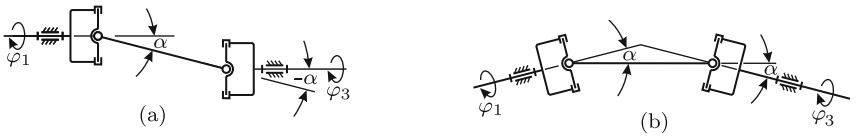

Fig. 13.6 The two possible couplings of coplanar shafts 1, 2, 3 by two Hooke's joints resulting in $\dot{\varphi}_3 \equiv \dot{\varphi}_1$

At this point the condition of coplanarity of the three shafts is abandoned. Obviously, the property $\dot{\varphi}_3 \equiv \dot{\varphi}_1$ is preserved if the planar system (for example, the one in Fig. 13.6a) is subjected to the following three-step operation:
Step 1: In an arbitrary position shaft 2 is cut thus splitting the entire system into a left part 1 and a right part 2
Step 2: Part 2 including joint 2 and the bearing of shaft 3 is rotated as one single rigid body about the axis of shaft 2 through an arbitrary angle ψ
Step 3: In the new position ψ the two parts of shaft 2 are rigidly joined together.

In the special case $\psi = \pi$, the new position is the position shown in Fig. 13.6b. If $\psi \neq \pi$, the axes of shafts 1 and 3 are skew in the new position.

Example $n = 4$: Equation (13.37) shows that the condition $a_4 = 1$ is satisfied in each of the following three cases.
Case a: $(\beta_2, \beta_3) = (\frac{\pi}{2}, 0)$ and $\cos\alpha_1 \cos\alpha_2 = \cos\alpha_3$
Case b: $(\beta_2, \beta_3) = (0, 0)$ and $\cos\alpha_2 \cos\alpha_3 = \cos\alpha_1$
Case c: $(\beta_2, \beta_3) = (0, \frac{\pi}{2})$ and $\cos\alpha_3 \cos\alpha_1 = \cos\alpha_2$.

In Fig. 13.7 case (c) is illustrated by a system of coplanar axes with $\alpha_3 = \alpha_1 = 20°$ and $\cos\alpha_2 = \cos^2 20°$ $(\alpha_2 \approx 28°)$. This example shows that geometrical symmetry of the coupling of shafts 1 and 4 is not a necessary condition for the identity of input and output angular velocity.

Example $n = 5$: The condition $a_5 = 1$ is satisfied by altogether seven different combinations $(\beta_2, \beta_3, \beta_4)$ and by associated conditions on $\alpha_1, \ldots, \alpha_4$. The details are left to the reader. See also Duditza [4, 7]. In Fig. 13.8 a simple example with five coplanar axes is shown. It is the combination of two systems of the type shown in Fig. 13.6b. The parameters are $\beta_2 = \beta_3 = \beta_4 = 0$ and $\alpha_1 = \alpha_2 = \alpha_3 = \alpha_4 = \alpha$. Shafts 1, 3 and 5 have identical angular velocities $\dot{\varphi}_5 \equiv \dot{\varphi}_3 \equiv \dot{\varphi}_1$.

In every system with coplanar axes $i = 1, \ldots, n$ the property $\dot{\varphi}_n \equiv \dot{\varphi}_1$ is preserved if the three-step operation explained for the case $n = 3$ is applied analogously, i.e., by cutting an arbitrary intermediate shaft $j = 2, \ldots, n-1$ and by a rigid-body rotation of the part located beyond the cut shaft. This operation may even be performed repeatedly with different intermediate shafts.

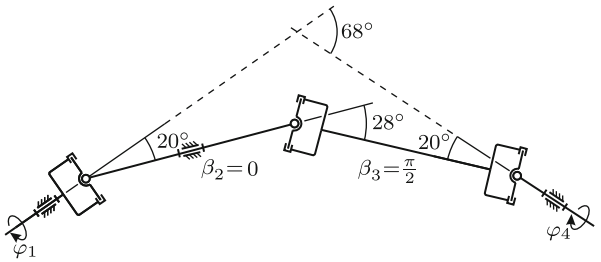

Fig. 13.7 Unsymmetrical coupling of coplanar shafts 1 , 2 , 3 , 4 by three Hooke's joints resulting in $\dot{\varphi}_4 \equiv \dot{\varphi}_1$

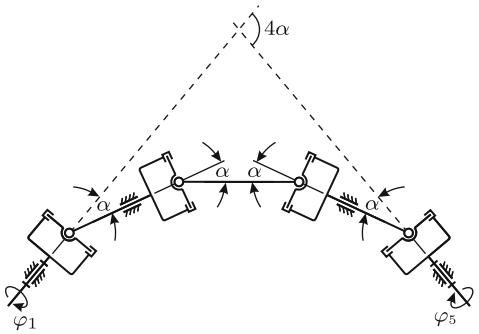

Fig. 13.8 Coupling of coplanar shafts 1 , 2 , 3 , 4 , 5 by four Hooke's joints resulting in $\dot{\varphi}_5 \equiv \dot{\varphi}_3 \equiv \dot{\varphi}_1$

13.4 Homokinetic Shaft Couplings

By definition, the coupling of two shafts is homokinetic if it satisfies the conditions

(A) the axes of the shafts are free to change their relative position and direction during operation

(B) the angular velocities are identical in *every* relative position and direction held fixed.

The homokinetic coupling is the mechanism required for positioning and directing the axis of shaft 2 relative to shaft 1 . If both location and direction of this axis are variable, the mechanism must have the degree of freedom $F = 5$ (three coordinates of a single point plus two direction cosines). Couplings of simpler nature, namely, with degree of freedom $F = 2$, are required for shafts the axes of which are permanently intersecting at a fixed point. In engineering these simpler solutions are fully sufficient. Such coupling cannot be a serial chain because it would have to be a chain of two intersecting revolute joints. However, this is Hooke's joint which is known to violate condition (B). This means that homokinetic couplings must be closed kinematic chains.

13.4.1 Couplings With a Spherical Joint

Permanent intersection of the axes of shafts 1 and 2 is most easily achieved by means of a spherical joint. According to Grübler's Eq.(4.4) a simple closed chain with a spherical joint must have five additional joint variables in order to have the degree of freedom $F = 2$. Let Σ be the plane which is (i) bisecting the angle between the two shafts and (ii) normal to the plane spanned by the shafts. Conditions (A) and (B) are both satisfied if in every relative position of the shafts the closed chain is both structurally and dimensionally symmetric with respect to Σ. If only revolute joints R, prismatic joints P and combinations of these two (cylindrical joints C, spherical joints S and planar joints E) are used, altogether eight five-variable chains can be formed which are structurally symmetric with respect to a central joint. These are the chains RR**R**RR, RR**P**RR, PR**R**RP, RP**R**PR, R**S**R, P**S**P, C**R**C and R**E**R. The central joint is indicated by a boldface letter. If the central joint is a revolute R, its axis must lie in Σ. If it is a prismatic joint P, it must be perpendicular to Σ. If it is a planar joint E, the plane E must be normal to Σ. Every one of the eight mechanisms has been used in patented shaft couplings. Detailed documentations see in Kutzbach [10, 11], Duditza [5] and Seherr-Thoss/Schmelz/Aucktor [17]. In most engineering realizations adjacent joint axes are either parallel or at right angles. This is not a necessary condition. The only necessary condition, in addition to symmetry, is that the shafts must have the freedom to rotate full cycle.

A homokinetic coupling based on the chain R**S**R was shown in Fig. 4.11. A coupling based on the chain CRC is shown schematically in Fig. 13.9a. It was known to Koenigs [9] already. The patented engineering realization is known as Hebson coupling. A single chain CRC suffices. The second chain CRC is added in order to diminish dynamical unbalance (total balance is achieved when shafts 1 and 2 are collinear). In a Hebson coupling a larger number of chains is evenly distributed around the cylinders. The joints R in these chains may be replaced by spherical joints since the additional degrees of freedom thus introduced are passive. With this coupling inclination angles up to 90° are possible.

The so-called Tracta coupling shown schematically in Fig. 13.9b is based on the chain RER. The chain is encapsulated in two concentric spherical shells which together represent the spherical joint connecting shafts 1 and 2. The axes of both revolutes R are in the plane E. Each revolute axis intersects one shaft axis orthogonally. Rotations in these revolutes keep plane E normal to plane Σ independent of the angular position φ of the shafts. In the figure plane E is shown in the positions $\varphi = 0, \pi$ and $\varphi = \pm\pi/2$. The Tracta coupling is widely used in the automotive field because of the following properties: Inclination angles up to 50°; compact form; simple assembly; no loss of lubrication; large wear-resistant contact surfaces.

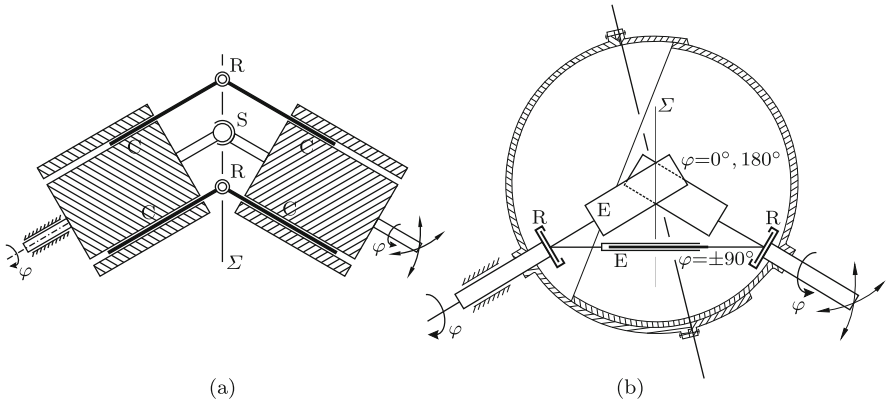

Fig. 13.9 Hebson coupling **(a)** and Tracta coupling **(b)**

In the homokinetic coupling shown in Fig. 13.10 two revolutes on either side of plane Σ constitute the central cross of a Hooke's joint each connecting one shaft to the intermediate body 3. For this reason the coupling is referred to as bicardanic coupling. Body 3 is a cylinder with the axis 0_1-0_2 inside of which centrally placed rings 4 provide a planar joint in plane Σ for the smaller circular disc 5. Normal to this disc another hollow cylinder 6 is rigidly connected. This cylinder is guide for two spherical bodies fixed at the ends of shafts 1 and 2 at equal distances from 0_1 and from 0_2, respectively. The entire mechanism connecting shafts 1 and 2 is homokinetic. The point of intersection of the shafts is not fixed on the shafts, but constrained to lie in Σ. This type of coupling finds applications in low-speed vehicles such as agricultural machines. For high-speed vehicles it is not suitable because the nonuniform motion of the coupling mechanism is a source of vibrations.

Duditza [4, 5] and Kutzbach [10] describe various other forms of bicardanic homokinetic couplings.

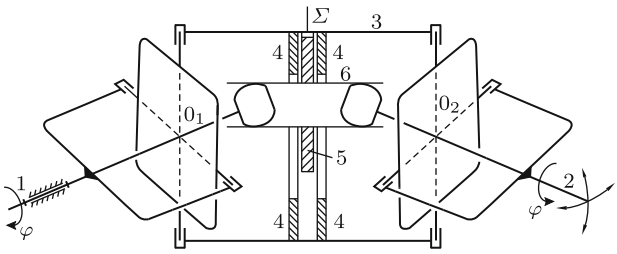

Fig. 13.10 Bicardanic homokinetic coupling

13.4.2 Couplings With Three Parallel Serial Chains

In the shaft couplings described in the previous section permanent symmetry of a five-d.o.f. chain with respect to plane Σ is achieved by a central spherical joint S closing the chain. The same constraints that are exerted by the spherical joint S can be exerted by placing two additional five-d.o.f. chains parallel to the first one. For reasons of dynamic balancing and of simplicity of design three identical chains are placed at intervals of 120°. The so-called Clemens coupling shown schematically in Fig. 13.11 is derived from Fig. 4.11. The serial chain $R_1S_2R_2$ of this coupling is placed three times in parallel. On each shaft the three revolute axes fixed on the shaft are placed 120° apart. The three spherical joints are permanently in the bisecting plane Σ.

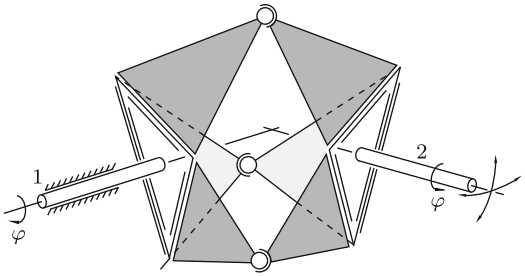

Fig. 13.11 Clemens coupling with three identical parallel chains RSR

The shafts 1 and 2 in Fig. 13.12 are connected to the sides of the rigid isosceles triangle (0_1,C,0_2) of base length 2ℓ and apex angle 2β by two pairs of revolutes R_1, R_2 and R_3, R_4. At 0_1 the axis of R_1 intersects both shaft 1 and R_2 orthogonally, and at 0_2 the axis of R_4 intersects both shaft 2 and R_3 orthogonally. In the figure the symmetrical position is shown in which the shafts intersect in the bisecting plane Σ normal to $\overline{0_1 0_2}$ and passing through C. When the shafts are held fixed in this position, rotation of the triangle about the line $\overline{0_1 0_2}$ causes both shafts to rotate through identical angles φ. The chain $R_1R_2R_3R_4$ is one out of three identical chains sharing the line $\overline{0_1 0_2}$ and the plane Σ. The entire shaft coupling thus described is known as Unitru coupling. It is homokinetic because it allows changing the direction of shaft 2 while maintaining symmetry with respect to Σ.

In what follows, it is shown under which condition on the design parameter β, for a given inclination angle α of the shafts, the triangle and the shafts are free to rotate full cycle. Definition: The angle of rotation φ of the shafts and the angle of rotation ψ of the triangle are zero when the shafts as well as the triangle are in the plane of the drawing (the frame-fixed x, y-plane). In this position the revolutes R_1 and R_4 are parallel to the z-axis. The point P on the axis of R_4 at the distance ℓ from 0_2 is an auxiliary point. With

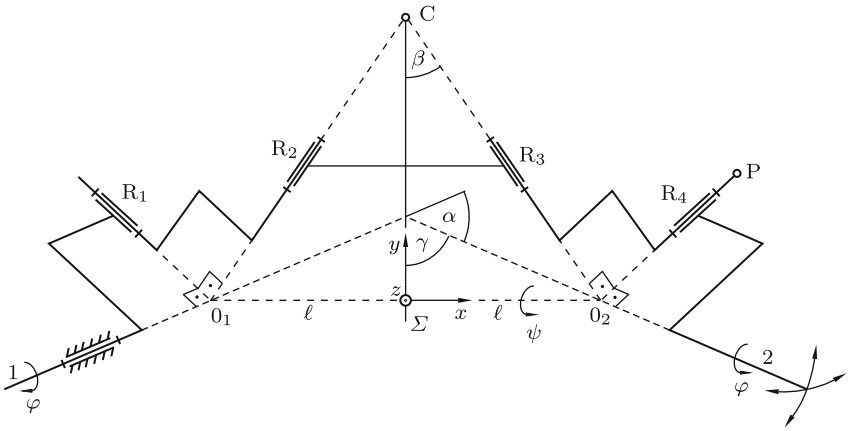

Fig. 13.12 Single serial chain of a Unitru coupling

the altitude $\ell \cot \beta$ of the triangle the x, y, z-coordinates of C and P are

$$\left.\begin{array}{lll} C(\psi,\beta): & \ell[0 & \cos\psi\cot\beta \quad \sin\psi\cot\beta]\,, \\ P(\varphi,\gamma): & \ell[1-\sin\varphi\cos\gamma & -\sin\varphi\sin\gamma \quad \cos\varphi\,]\,. \end{array}\right\} \tag{13.39}$$

The distance between C and P is $\ell\sqrt{2+\cot^2\beta}$ independent of ψ and φ. This condition yields the equation

$$\cos\psi\sin\varphi\sin\gamma - \sin\psi\cos\varphi = \tan\beta\sin\varphi\cos\gamma\,. \tag{13.40}$$

It has the form $A\cos\psi + B\sin\psi = R$. The triangle can rotate full cycle if $A^2 + B^2 - R^2 \geq 0$ for $0 \leq \varphi \leq 2\pi$. This is the condition

$$1 - \frac{\cos^2\gamma}{\cos^2\beta}\sin^2\varphi \geq 0\,. \tag{13.41}$$

This requires $\cos\beta \geq \cos\gamma$ or $\beta \leq \gamma \leq \pi/2$. The inclination angle between the two shafts is $\alpha = \pi - 2\gamma$. Thus, the condition is $2\beta \leq \pi - \alpha$. With $2\beta = 90°$ inclination angles α up to 90° are possible.

13.4.3 Ball-in-Track Joints

The symmetrical five-d.o.f. chains essential for all previously described shaft couplings have the disadvantage of being structurally complex. Much simpler realizations are shown in Figs. 13.13a and b. The shafts in Fig. 13.13a are connected by a spherical joint. The shafts as well as the symmetrical curves

of arbitrary shape drawn in thick lines are in the plane of the drawing. Imagine these curves to be rigid and rigidly attached to the shafts. Due to the symmetry the point of contact is in the bisecting plane Σ. Both symmetry with respect to and contact in the bisecting plane are maintained when the inclination angle α between the shafts is changed and also, when both shafts are rotated through arbitrary identical angles into positions in which the two curves are no longer coplanar. The sliding point contact of two curves constitutes a five-d.o.f. joint. The symmetrical closed chain formed by this joint in parallel to the spherical joint represents a homokinetic coupling of shafts 1 and 2. However, since point contact is transmitting force from one shaft to the other in only one sense of direction of rotation, a second pair of rigid curves for the opposite sense of direction is necessary. This is the pair drawn in dashed lines in the same plane. Repeating the arguments at the beginning of the previous section the shaft coupling continues to be homokinetic if the central spherical joint is replaced by two additional sets of curves in planes placed at intervals of $120°$. Engineering realizations see in Kutzbach [10]. The contacting curves are edges of bodies.

Single-point contact of curves is unsatisfactory. A much better design is the so-called ball-in-track joint shown in Fig. 13.13b. The role of the contact point is played by the center C of a spherical ball of arbitrary diameter. Motion of C relative to the shafts along prescribed symmetric curves is realized by appropriately curved shallow grooves referred to as tracks in which the ball is constrained to move. Each track is rigidly attached to one of the shafts. The element composed of a ball enclosed between two crossing tracks is called ball-in-track joint. It is a five-d.o.f. joint. Homokinetic shaft couplings with ball-in-track joints have many advantages such as small size, small dynamic unbalance and distribution of contact forces among a large number of balls. However, there are disadvantages, too. Problems arise from the fact that the motion of balls in crossing tracks is not rolling, but sliding and boring with the possibility of jamming due to friction. This aspect of kinematics see in Phillips/Winter [14].

The so-called Devos coupling shown schematically in Fig. 13.14 has two balls-in-tracks in parallel to a spherical joint S. The tracks are symmetrically located cylinders. In order to keep the centers of the balls in the bisecting plane Σ the balls are also constrained to move along the cylindrical pin 3 which is rigidly attached to the sphere of the joint S. This implies that the sphere of the joint S cannot be rigidly connected to any of the two shafts. Details of design not shown in the figure allow the shaft coupling to be assembled under prestress in such a way that its elements are firmly held together.

Figure 13.15 shows the essential elements of a shaft coupling without central spherical joint and with balls in torus-shaped tracks in the particular position when the circular lines of contact between ball and both tori (indi-

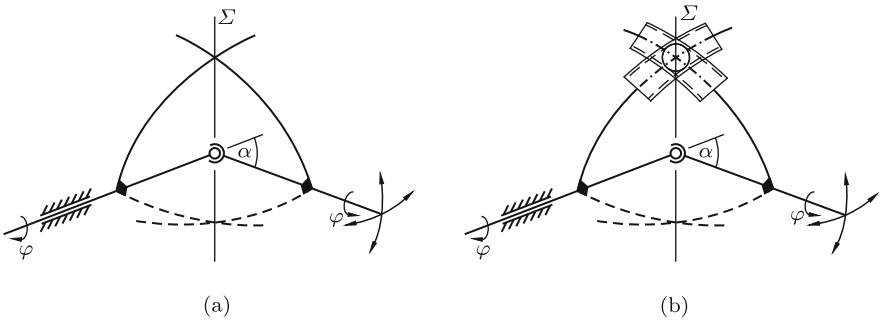

Fig. 13.13 Homokinetic coupling with contacting symmetrical curves **(a)** and with a ball-in-track joint **(b)**

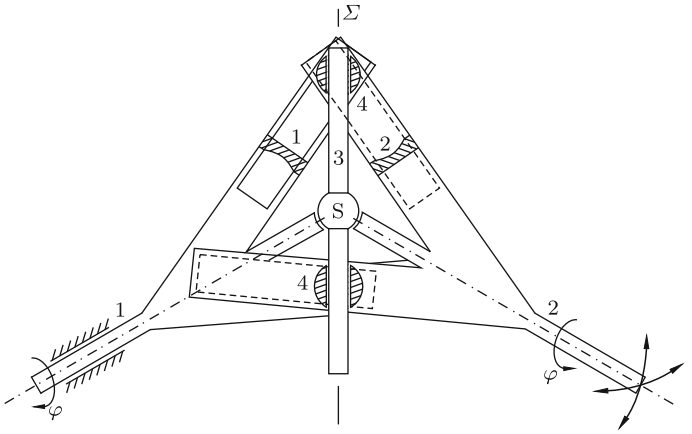

Fig. 13.14 Devos coupling with balls in cylindrical tracks

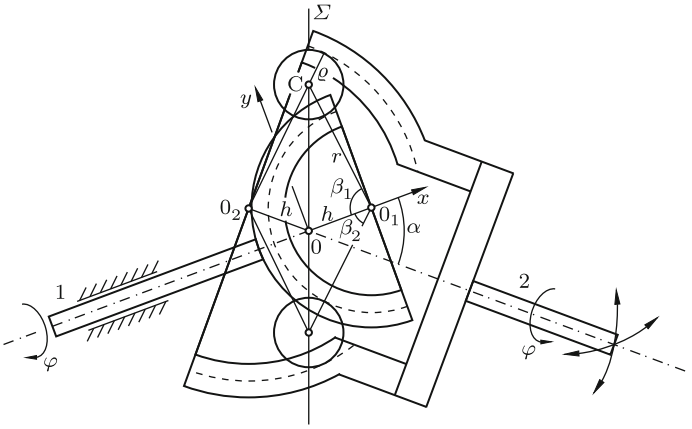

Fig. 13.15 Homokinetic shaft coupling with balls in torus-shaped tracks

cated by the dashed circles) are in the plane of the drawing[4]. Let this be the position $\varphi = 0$ of the shafts. The radii r_1 and r_2 of these circles satisfy the condition $r_2 - r_1 = 2\rho$ where ρ is the radius of the balls. This has the effect that the trajectory of the center C of the ball relative to shaft 1 is the circle of radius $r = r_1 + \rho$ about 0_1 and that the trajectory of C relative to shaft 2 is the circle of the same radius r about 0_2. In the position $\varphi = 0$ these circles are symmetric with respect to and intersecting in the bisecting plane Σ. The pair of balls shown in the figure is one out of three or more pairs moving in tracks which are placed at equal angular intervals. After what has been said in the context of Figs. 13.13a,b the symmetry properties prove that the shaft coupling is homokinetic. Not only in the position $\varphi = 0$, but in arbitrary positions $\varphi \neq 0$ point C is in the plane Σ at equal distances r from 0_1 and from 0_2. Hence the trajectory of C relative to the frame is a circle in Σ with the center at the midpoint between 0_1 and 0_2. The radius of this circle depends on α.

The position of C in the tracks is described by the angle $\beta = \sphericalangle(00_1\mathrm{C})$. It is a function φ. The extremal values β_1 and β_2 are obtained from the condition that the x, y-coordinates of C satisfy the equation $x = y \tan \alpha/2$. This is the set of equations

$$h - r\cos\beta_{1,2} = \pm r \sin\beta_{1,2} \tan\frac{\alpha}{2} \,. \tag{13.42}$$

Solving for $\sin\beta_{1,2}$ results in the formulas

$$\sin\beta_{1,2} = \frac{(h/r)\tan\alpha/2 \pm \sqrt{1 + \tan^2\alpha/2 - (h/r)^2}}{1 + \tan^2\alpha/2} \,. \tag{13.43}$$

An animation of the motion is on display in *Wikipedia Homokinetisches Gelenk*.

13.4.4 Tripod Joint

The tripod joint shown in Fig. 13.16 is another ball-in-track coupling. Its kinematics was investigated by Roethlisberger/Aldrich [16], Duditza [5], Duditza/Diaconescu [6], Durum [8], Orain [12, 13] and Akbil/Lee [1, 2]. In what follows, an elementary analysis is presented. Imagine that in the fixed cartesian x_1, y_1, z_1-system of Fig. 13.17 the shaft labeled 1 is rotating about the z_1-axis. The rotation angle is φ. A point Q fixed on the shaft at radius a is moving on a circle. In the position φ of the shaft Q has the coordinates $x_1(\varphi) = a\cos\varphi$, $y_1(\varphi) = a\sin\varphi$. The circle and this point Q(φ) are

[4] The dimensions chosen in the figure are unrealistic because they allow only small variations of the angle α

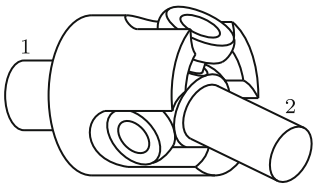

Fig. 13.16 Tripod joint. Balls sliding on the rays of the star-shaped tripod 2 are guided in tracks fixed on shaft 1

projected parallel to the z_1-axis onto the x, y-plane of another fixed x, y, z-system which is inclined against the x_1, y_1, z_1-system by an angle α about the x_1-axis. The projection of the circle is the ellipse with semi-axes a and $b = a/\cos\alpha$. Point $\mathrm{Q}(\varphi)$ is projected into the point $\mathrm{P}(\varphi)$ with coordinates

$$x(\varphi) = a\cos\varphi\ , \qquad y(\varphi) = b\sin\varphi\ . \tag{13.44}$$

Let, in the same x, y-plane, $x_0(\varphi)$ and $y_0(\varphi)$ be the coordinates of another point $\mathrm{P}_0(\varphi)$, i.e., of another curve. To be determined are all curves $\mathrm{P}_0(\varphi)$ having the property that the angle between the line $\overline{\mathrm{P}_0(\varphi)\mathrm{P}}(\varphi)$ and the x-axis is identical with φ. This is the condition

$$\frac{b\sin\varphi - y_0(\varphi)}{a\cos\varphi - x_0(\varphi)} \equiv \tan\varphi\ . \tag{13.45}$$

The ansatz

$$x_0(\varphi) = \xi(\varphi)\cos\varphi\ , \qquad y_0(\varphi) = \eta(\varphi)\sin\varphi \tag{13.46}$$

results in the condition

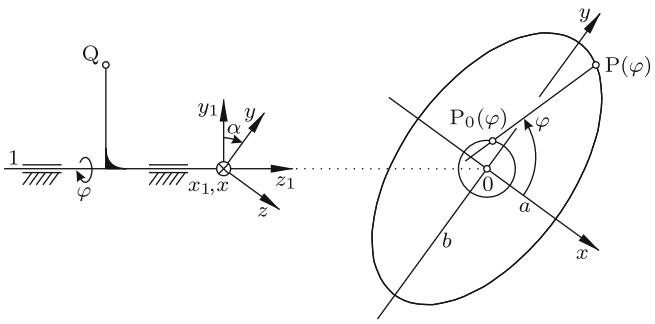

Fig. 13.17 Point Q fixed at radius a on the rotating shaft 1 (rotation angle φ) is projected parallel to the z_1-axis into the point $\mathrm{P}(\varphi)$ in the fixed x, y-plane. Another point $\mathrm{P}_0(\varphi)$ in the x, y-plane

$$\eta(\varphi) - \xi(\varphi) \equiv b - a \,. \tag{13.47}$$

This condition is satisfied by infinitely many functions, for example, by the family of functions $\xi(\varphi) = -r(\cos^2\varphi + c_1)$, $\eta(\varphi) = r(\sin^2\varphi + c_2)$ with constants r , c_1 , c_2 satisfying the constraint equation $r(1+c_1+c_2) = b-a$. In the special case $c_1 = c_2 = -3/4$, $r = -2(b-a)$, Eqs.(13.46) are

$$\left.\begin{aligned} x_0(\varphi) &= \varrho\cos 3\varphi \,, \qquad y_0(\varphi) = \varrho\sin 3\varphi \,, \\ \varrho &= -\frac{r}{4} = \frac{b-a}{2} = a\,\frac{1-\cos\alpha}{2\cos\alpha} \,. \end{aligned}\right\} \tag{13.48}$$

When shaft 1 is rotating with angular velocity $\dot\varphi$, $\mathrm{P}_0(\varphi)$ is moving with angular velocity $3\dot\varphi$ on the circle with radius ϱ about 0 , and the line $\overline{\mathrm{P}_0(\varphi)\mathrm{P}(\varphi)}$ is rotating with angular velocity $\dot\varphi$. Examples: $\varrho \approx 0.08a$ for $\alpha = 30^\circ$, $\varrho \approx 0.21a$ for $\alpha = 45^\circ$, $\varrho = 0.5a$ for $\alpha = 60^\circ$. The Taylor formula is $\varrho/a \approx \alpha^2/4$.

Imagine that on the circle of radius a fixed on shaft 1 not a single point Q , but three points Q_1 , Q_2 , Q_3 are marked 120° apart. The projections of these points are three points $\mathrm{P}_i(\varphi)$ $(i = 1, 2, 3)$ on the ellipse. For each one of these points (13.48) yields the same point $\mathrm{P}_0(\varphi)$ since $3 \cdot 120^\circ = 2\pi$. From this it follows that the rays $\overline{\mathrm{P}_0(\varphi)\mathrm{P}_i(\varphi)}$ $(i = 1, 2, 3)$ emanating from $\mathrm{P}_0(\varphi)$ form a rigid 120°-star with the center at P_0 . This star is rotating with angular velocity $\dot\varphi$ while its center P_0 is moving on the circle of radius ϱ with angular velocity $3\dot\varphi$. The lines $\overline{\mathrm{Q}_i(\varphi)\mathrm{P}_i(\varphi)}$ $(i = 1, 2, 3)$ are parallel to the axis of shaft 1 and fixed on shaft 1 . In the tripod joint shown in Fig. 13.16 the star, the three lines $\overline{\mathrm{Q}_i(\varphi)\mathrm{P}_i(\varphi)}$ $(i = 1, 2, 3)$ and the permanent intersection of each ray with the associated line at P_i are materially realized. Each ray is guide for a ball which is free to move along the ray. The associated line fixed on shaft 1 is the axis of a cylinder in which the ball is also free to move. Orthogonal to the star and through its center P_0 a shaft 2 is rigidly attached to the star. The star and this shaft together constitute the tripod giving the joint its name. The tripod has the same angular velocity $\dot\varphi$ shaft 1 has independent of the direction of shaft 2 relative to shaft 1 . It has the additional degree of freedom of translation along the axis of shaft 1 . In spite of these properties the tripod joint is not homokinetic because shaft 2 cannot be held fixed due to its motion on a cylinder of radius ϱ . By means of an Oldham coupling the motion of shaft 2 can be transmitted to a shaft 3 the axis of which is the z-axis. This combination tripod joint – Oldham coupling is a homokinetic coupling of shafts 1 and 3 .

If a point fixed on shaft 2 at a distance $\ell \gg a$ from P_0 is coupled to the z-axis by a spherical joint S , the kinematics of the tripod is slightly changed. An analysis made by Duditza and Diaconescu [5, 6] leads to the following first-order approximation. Three times per revolution of shaft 1 the axis of shaft 2 is moving on a circular cone with the apex at S and with the semi-

vertex angle $\varrho/\ell \ll 1$, and the angular velocity of the tripod about shaft 2 is approximately $\dot{\varphi}(1 - A\cos 3\varphi)$ with $A = \frac{3}{2}(a/\ell)\tan\alpha\,\tan^2\alpha/2 \ll 1$.

References

1. Akbil E, Lee T W (1983) Kinematic structure and functional analysis of shaft couplings involving pode joints. J. Mechanisms,Transm.,Automation in Design 105:672–681
2. Akbil E, Lee T W (1984) On the motion characteristics of tripode joints. Part 1: General case. Part 2: Applications. J. Mechanisms,Transm.,Automation in Design, 106:228–234 and 235–245
3. Balken J (1981) Systematische Entwicklung von Gleichlaufgelenken. Diss. TU München
4. Duditza F (1973) Kardangelenkgetriebe und ihre Anwendungen. VDI-Verl., Düsseldorf
5. Duditza F (1974) Cuplaje mobile homocinetice. Tehnica, Bucarest
6. Duditza F, Diaconescu D (1975) Zur Kinematik und Dynamik von Tripode-Gelenkgetrieben. Konstruktion 27:335–341
7. Duditza F, Diaconescu D, Böhm C, Saulescu R (2003) Transmisii cardanice. Editura Transilvania Expres 2003
8. Durum M M (1975) Kinematic properties of tripode joints. J.Eng.Ind.97B:708–713
9. Koenigs G (1897) Leçons de cinématique. Avec des notes par G. Darboux, E. et F. Cosserat. Hermann, Paris
10. Kutzbach K (1937) Quer- und winkelbewegliche Wellenkupplungen. Kraftfahrtechnische Forschungsarbeiten 6:1–25
11. Kutzbach K (1937) Quer- und winkelbewegliche Gleichganggelenke für Wellenleitungen. VDI-Zeitschr. 81:889–892
12. Orain M (1976) Contribution à l'étude des joints de transmission tripodes. Diss. Univ. Pièrre et Marie Curie, Paris
13. Orain M (1977) Allgemeine Theorie und experimentelle Forschung der Gleichlaufgelenke. Glaenzer Spicer,Poissy, France
14. Phillips J R , Winter H (1968) Über die Frage des Gleitens in Kugel-Gleichganggelenken. VDI Z.110:228–233
15. Poncelét J V (1836) Cours de mécanique appliquée aux machines, deuxième section: Du joint brisé ou universel. Gauthiers-Villars 1836 et 1874. German trans.: Leske (1845, 1848) Lehrbuch der Anwendung der Mechanik auf Maschinen. Darmstadt
16. Roethlisberger J M, Aldrich F C (1967) The Tripot universal joint. SAE paper No.690257
17. Graf v. Seherr-Thoss H-C, Schmelz F, Aucktor E (2002) Gelenke und Gelenkwellen 2nd ed. Springer, Berlin, Heidelberg, New York
18. Wittenburg J, Roberson R E (1982) Polhode and herpolhode cones in a generalized Hooke's joint. ZAMM 62:589–598

Chapter 14
Displacements in a Plane

Subject of this chapter are relationships between positions of a plane Σ in a reference plane Σ_0. Motions leading from one position to another are not considered. Displacements in a plane are translation, rotation, reflection and resultants of these three. All of them are special cases of the spatial displacements investigated in Chaps. 1 and 3. Consequently, theorems governing the latter remain valid, normally in simplified form. In addition, special theorems exist which are valid for planar displacements only.
Literature: Koenigs [10, 11], Schoenflies/Grübler [15], Bereis [1], Blaschke /Müller [2], Wunderlich [16].

14.1 Complex Numbers in Planar Kinematics

In planar kinematics vector equations can be replaced by equations written in terms of complex numbers. In what follows, these two formulations are compared. The complex plane is the $\mathbf{e}_1, \mathbf{e}_2$-plane of a cartesian $\mathbf{e}_1, \mathbf{e}_2, \mathbf{e}_3$-system with origin 0. The real axis is the $\mathbf{e}_1$-axis. Let a and b be the cartesian coordinates of a point P in the plane (Fig. 14.1). The position vector of this point is denoted $\mathbf{r} = a\mathbf{e}_1 + b\mathbf{e}_2$. The complex number representing the point is denoted $z = a + \mathrm{i}\, b$. It can be interpreted as directed object pointing from 0 to P. In contrast to $\mathbf{r}$ it is not a vector. The conjugate of z is defined to be $\overline{z} = a - \mathrm{i}\, b$. It is easy to verify the following correspondences between vectors and complex numbers:

$$\mathbf{r}^2 = a^2 + b^2\,, \qquad z\overline{z} = a^2 + b^2\,, \tag{14.1}$$

$$\mathbf{r}_1 + \mathbf{r}_2 = (a_1 + a_2)\mathbf{e}_1 + (b_1 + b_2)\mathbf{e}_2\,, \qquad z_1 + z_2 = (a_1 + a_2) + \mathrm{i}\,(b_1 + b_2)\,, \tag{14.2}$$

$$\mathbf{r}_1 \cdot \mathbf{r}_2 = a_1a_2 + b_1b_2\,, \qquad \tfrac{1}{2}(\overline{z}_1 z_2 + z_1\overline{z}_2) = a_1a_2 + b_1b_2\,, \tag{14.3}$$

$$\mathbf{r}_1 \times \mathbf{r}_2 = (a_1b_2 - a_2b_1)\mathbf{e}_3\,, \qquad \tfrac{1}{2}(\overline{z}_1 z_2 - z_1\overline{z}_2) = \mathrm{i}\,(a_1b_2 - a_2b_1)\,. \tag{14.4}$$

J. Wittenburg, *Kinematics*, DOI 10.1007/978-3-662-48487-6_14

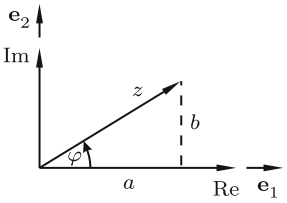

Fig. 14.1 Complex number

From the last two correspondences the following statements are deduced.

$$\left.\begin{array}{r} z_1 \text{ and } z_2 \text{ are mutually orthogonal if } z_1\overline{z}_2 = -\overline{z}_1 z_2 \\ z_1 \text{ and } z_2 \text{ are collinear (equal or opposite direction) if } z_1\overline{z}_2 = \overline{z}_1 z_2\ . \end{array}\right\} \tag{14.5}$$

These conditions can also be formulated as follows:

$$\left.\begin{array}{r} z_1 \text{ and } z_2 \text{ are mutually orthogonal if } \operatorname{Re}(\overline{z}_1 z_2) = 0 \\ z_1 \text{ and } z_2 \text{ are collinear (equal or opposite direction) if } \operatorname{Im}(\overline{z}_1 z_2) = 0\ . \end{array}\right\} \tag{14.6}$$

In conclusion it can be said that all vector algebraic operations can be expressed in terms of complex numbers. Complex numbers have additional advantages which make them more powerful than vectors. For one thing, division is possible:

$$\frac{z_1}{z_2} = \frac{z_1\overline{z}_2}{z_2\overline{z}_2} = \frac{z_1\overline{z}_2}{a_2^2 + b_2^2}\ . \tag{14.7}$$

The most important advantage is that a complex number $z = a + \mathrm{i}\,b$ can be expressed in exponential form as $z = |z|e^{\mathrm{i}\varphi}$ where $|z| = \sqrt{a^2 + b^2}$ and φ are polar coordinates (see Fig. 14.1). The angle is also referred to as argument of z: $\varphi = \operatorname{Arg} z$. The conversion from one form to the other is achieved by Euler's formula for a complex number of absolute value 1:

$$e^{\mathrm{i}\,\varphi} = \cos\varphi + \mathrm{i}\,\sin\varphi\ . \tag{14.8}$$

The exponential form is used for multiplication and for division:

$$z_1 z_2 = |z_1||z_2|e^{\mathrm{i}\,(\varphi_1+\varphi_2)}\ . \tag{14.9}$$

This formula shows that multiplication has the effect of stretch-rotation. The absolute values are multiplied, and the angles are summed. The conjugate of $z = |z|e^{\mathrm{i}\,\varphi}$ is $\overline{z} = |z|e^{-\mathrm{i}\,\varphi}$. From this it follows that $z/\overline{z} = e^{\mathrm{i}\,2\varphi}$ and hence

$$\varphi = \frac{1}{2\mathrm{i}} \ln \frac{z}{\overline{z}}\ . \tag{14.10}$$

Example 1: In Fig. 14.2 the vector $\mathbf{r}_\mathrm{B}$ is uniquely determined by the coordinates $x = 4$, $y = 3$ of the vector $\mathbf{r}_\mathrm{A}$, by the angle α and by the absolute value $|\mathbf{r}_\mathrm{B}| = 7$. The calculation of the coordinates of $\mathbf{r}_\mathrm{B}$ by methods of vector algebra is cumbersome. In terms of the complex numbers r_A and r_B the solution is much simpler:

$$\begin{aligned} r_\mathrm{B} &= \frac{7}{5}\, e^{\mathrm{i}\alpha}\, r_\mathrm{A} = \frac{7}{5}(\cos\alpha + \mathrm{i}\,\sin\alpha)(4 + 3\mathrm{i}) \\ &= \frac{7}{5}(4\cos\alpha - 3\sin\alpha) \;+\; \mathrm{i}\,\frac{7}{5}(3\cos\alpha + 4\sin\alpha)\;. \end{aligned} \tag{14.11}$$

End of example.

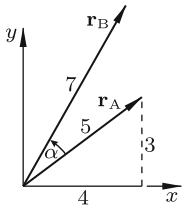

Fig. 14.2 Determination of $\mathbf{r}_\mathrm{B}$ from x, y, α and $|\mathbf{r}_\mathrm{B}|$

Example 2: Let $r_i = x_i + \mathrm{i}\,y_i \;\; (i = 1, 2)$ be two complex numbers. Under what condition does a counterclockwise rotation of r_1 through the angle α produce a complex number parallel to r_2?
Solution: The condition is $\mathrm{Im}(e^{\mathrm{i}\,\alpha} r_1 \overline{r}_2) = 0$ or

$$\begin{aligned} &\mathrm{Im}\left[(\cos\alpha + \mathrm{i}\sin\alpha)(x_1 + \mathrm{i}\,y_1)(x_2 - \mathrm{i}\,y_2)\right] \\ &= (x_1 x_2 + y_1 y_2)\sin\alpha - (x_1 y_2 - y_1 x_2)\cos\alpha = 0\;. \end{aligned} \tag{14.12}$$

End of example.

Example 3: $z(t) = r(t)e^{\mathrm{i}\,\varphi(t)}$ with real functions $r(t) \geq 0$ and $\varphi(t)$ is the time-dependent complex number representing a point in planar motion along a trajectory in the complex plane. The quantities $r(t)$ and $\varphi(t)$ are polar coordinates. The first and the second time derivatives yield for the velocity and for the acceleration the expressions $v(t) = \dot{z} = (\dot{r} + \mathrm{i}\,\dot{\varphi} r)e^{\mathrm{i}\,\varphi(t)}$ and $a(t) = \ddot{z} = [\ddot{r} - \dot{\varphi}^2 r + \mathrm{i}\,(\ddot{\varphi} r + 2\dot{\varphi}\dot{r})]e^{\mathrm{i}\,\varphi(t)}$, respectively. The development of the corresponding vector equations is more complicated. These equations read $\mathbf{v}(t) = \dot{r}\mathbf{e}_\mathrm{r} + \dot{\varphi} r \mathbf{e}_\mathrm{t}$ and $\mathbf{a}(t) = (\ddot{r} - \dot{\varphi}^2 r)\mathbf{e}_\mathrm{r} + (\ddot{\varphi} r + 2\dot{\varphi}\dot{r})\mathbf{e}_\mathrm{t}$ with unit vectors $\mathbf{e}_\mathrm{r}$ (radial) and $\mathbf{e}_\mathrm{t}$ (tangential). End of example.

14.1.1 Curvature of a Plane Curve

Let $r(t)$ be the complex representation of a plane curve. The real parameter t is time if $r(t)$ is the trajectory of a moving point. What follows, is valid, however, also for curves which have nothing to do with motion such as geometrical ornaments. In such cases t does not represent time. The derivative with respect to t is denoted $r' = \mathrm{d}r/\mathrm{d}t$.

The chord $r(t+\Delta t) - r(t)$ divided by Δt converges in the limit $\Delta t \to 0$ towards the complex number r' having the direction of the tangent. Let $n(t)$ be the normal to the curve at the point $r(t)$. It has the direction of $r'\mathrm{i}$. With a real parameter λ this normal has the complex form

$$\zeta = r + \lambda r'\mathrm{i} \,. \tag{14.13}$$

From this equation and from the conjugate complex equation $\bar{\zeta} = \bar{r} - \lambda \bar{r}'\mathrm{i}$ the parameter λ is eliminated. This produces for the normal $n(t)$ of the curve the parameter-free representation

$$(\zeta - r)\bar{r}' + (\bar{\zeta} - \bar{r})r' = 0 \,. \tag{14.14}$$

In Fig. 14.3 the normals $n(t)$ and $n(t+\Delta t)$ are shown. In the limit $\Delta t \to 0$ their point of intersection converges toward the center of curvature M of the curve for the point $r(t)$. Hence M is at the intersection of n and n'. The equation of n' is obtained by differentiating (14.14):

$$(\zeta - r)\bar{r}'' + (\bar{\zeta} - \bar{r})r'' = 2r'\bar{r}' \,. \tag{14.15}$$

Let ζ_{M} be the complex number pointing to the center of curvature. It is obtained by multiplying (14.14) by r'', (14.15) by r' and by taking the difference:

$$\zeta_{\mathrm{M}} = r + 2r' \, \frac{r'\bar{r}'}{r'\bar{r}'' - \bar{r}'r''} \,. \tag{14.16}$$

The absolute value of the second term represents the radius of the circle of curvature of the curve at the point $r(t)$. Its inverse is the curvature κ. The curvature is (note the factor i in (14.13) and the equation $|r'| = (r'\bar{r}')^{1/2}$)

$$\kappa = \frac{1}{2\mathrm{i}} \, \frac{\bar{r}'r'' - r'\bar{r}''}{(r'\bar{r}')^{3/2}} \,. \tag{14.17}$$

The same expression can also be found as follows. According to (14.10) the angle $\mathrm{Arg}(r')$ of the tangent r' against the real axis is

$$\mathrm{Arg}(r') = \frac{1}{2\mathrm{i}} \ln \frac{r'}{\bar{r}'} \,. \tag{14.18}$$

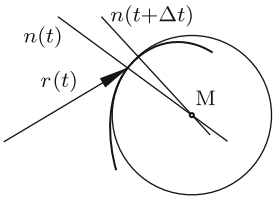

Fig. 14.3 Normals $n(t)$ and $n(t+\Delta t)$ of a curve and center of curvature M

The curvature is the derivative of this angle with respect to the arc length s of the curve:

$$\kappa = \frac{\mathrm{d}}{\mathrm{d}s}\,\mathrm{Arg}(r') = \frac{1}{2\mathrm{i}}\,\frac{\mathrm{d}}{\mathrm{d}s}\left(\ln\frac{r'}{\overline{r}'}\right). \tag{14.19}$$

The arc element $\mathrm{d}s$ satisfies the equation

$$(\mathrm{d}s)^2 = |\mathrm{d}r|^2 = |r'\mathrm{d}t|^2 = r'\overline{r}'(\mathrm{d}t)^2\,. \tag{14.20}$$

This yields the formula

$$\frac{\mathrm{d}}{\mathrm{d}s} = \frac{\mathrm{d}}{\mathrm{d}t}\,\frac{\mathrm{d}t}{\mathrm{d}s} = \frac{1}{(r'\,\overline{r}')^{1/2}}\,\frac{\mathrm{d}}{\mathrm{d}t}\,. \tag{14.21}$$

Application to (14.19) yields for the curvature again the expression (14.17).

A point of stationary curvature of a curve is called vertex. An ellipse, for example, has four vertices. Every point of a circle is a vertex. The vertex condition $\mathrm{d}\kappa/\mathrm{d}t = 0$ is the equation

$$2r'\overline{r}'(\overline{r}'r''' - r'\overline{r}''') - 3(\overline{r}'r'' - r'\overline{r}'')(\overline{r}'r'' + r'\overline{r}'') = 0\,. \tag{14.22}$$

14.2 Elementary Displacements

The plane Σ positions of which are investigated is represented by a triangle fixed in Σ. In Fig. 14.4 this triangle is shown in three positions $(\mathrm{A}_1,\mathrm{A}_2,\mathrm{A}_3)$, $(\mathrm{A}'_1,\mathrm{A}'_2,\mathrm{A}'_3)$ and $(\mathrm{A}''_1,\mathrm{A}''_2,\mathrm{A}''_3)$ in the reference plane Σ_0. Every position can be produced from every other position by a displacement. Arrows indicate the *sense* of the triangles (clockwise or counterclockwise). The sense of the triangle $(\mathrm{A}'_1,\mathrm{A}'_2,\mathrm{A}'_3)$ is equal to that of the triangle $(\mathrm{A}_1,\mathrm{A}_2,\mathrm{A}_3)$, whereas the sense of the triangle $(\mathrm{A}''_1,\mathrm{A}''_2,\mathrm{A}''_3)$ is opposite. This shows that there are displacements preserving the sense and others reversing the sense.

We begin by defining three elementary displacements called *translation*, *rotation* and *reflection*. During a translation, abbreviated T, every point experiences the same translatory displacement t. A rotation, abbreviated C, is carried out about a fixed point called *pole* P through an angle φ (positive

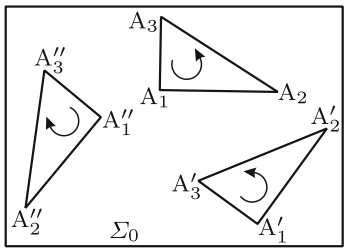

Fig. 14.4 Triangle in three positions in the reference plane Σ_0. Arrows indicate the sense (clockwise or counterclockwise)

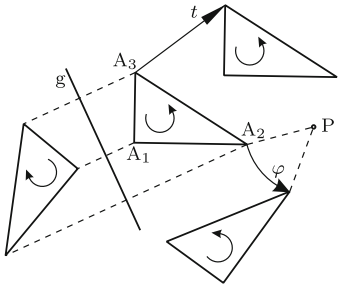

Fig. 14.5 Triangle in its original position (A_1,A_2,A_3) and following a translatory displacement t, a rotation about P and reflection in the line g

counterclockwise). A reflection in a line g, abbreviated S, produces a mirror image the line g being the mirror. The triangle (A_1,A_2,A_3) in Fig. 14.5 is used for demonstrating a translatory displacement t, rotation about a pole P and reflection in a line g. Translation and rotation are both sense-preserving displacements. From Sect. 1.16 it is known that reflection is a sense-reversing displacement.

The three elementary displacements are formulated analytically as follows. The reference plane Σ_0 is interpreted as complex plane. Let z be the complex number representing an arbitrary point of Σ prior to the displacement, and let z' be the complex number representing the same point in its position after the displacement. The equivalent vectors are $\mathbf{z}$ and $\mathbf{z}'$ (so, the symbol $'$ does not indicate differentiation). Relationships between z' and z for the three elementary displacements are deduced from Figs. 14.6a,b,c.

Translation T: Let t be the complex number representing the translatory displacement as is shown in Fig. 14.6a. Then

$$z' = z + t\,. \tag{14.23}$$

The equivalent vector equation is

$$\mathbf{z}' = \mathbf{z} + \mathbf{t}\,. \tag{14.24}$$

The inverse of the translation $\mathbf{t}$ is the translation $-\mathbf{t}$.

Rotation C: Let p be the complex number locating the pole P as is shown in Fig. 14.6b. Then $z' - p = \mathrm{e}^{\mathrm{i}\,\varphi}(z - p)$ and, consequently,

$$z' = p + w(z - p) \qquad \text{with} \quad w = \mathrm{e}^{\mathrm{i}\,\varphi} = \cos\varphi + \mathrm{i}\,\sin\varphi\,. \tag{14.25}$$

The trivial case $\varphi = 0$ is characterized by $w = 1$ and the case $\varphi = \pi$ by $w = -1$. The general expression for w yields

$$1 - w = 2\sin\frac{\varphi}{2}\Big(\sin\frac{\varphi}{2} - \mathrm{i}\cos\frac{\varphi}{2}\Big) = 2\sin\frac{\varphi}{2}\exp\Big[\mathrm{i}\,(\frac{\varphi}{2} - \frac{\pi}{2})\Big]\,, \qquad (14.26)$$

$$\frac{1}{1-w} = \frac{1}{2}\Big(1 + \mathrm{i}\cot\frac{\varphi}{2}\Big)\,, \qquad \frac{w}{1-w} = \frac{1}{2}\Big(-1 + \mathrm{i}\cot\frac{\varphi}{2}\Big)\,. \qquad (14.27)$$

The inverse of the rotation with pole P and with rotation angle φ is the rotation about the same pole P with the rotation angle $-\varphi$.

Reflection S: As is shown in Fig. 14.6c the reflecting line is represented in the form $a+\lambda b$ with complex numbers a and b and with the real parameter λ. Proposition: The desired relationship between z' and z is

$$z' = a + \frac{b}{\overline{b}}\,(\overline{z} - \overline{a})\,. \qquad (14.28)$$

Proof: First, the reflecting line $a + \lambda b$ is mapped onto the real axis by the translation $-a$ followed by the rotation associated with multiplication by $\overline{b}$. Through these operations the points z and z' are mapped into the points $\overline{b}(z-a)$ and $\overline{b}(z'-a)$, respectively. These new points are reflections of each other in the real axis. From this it follows that $\overline{b}(z'-a)$ is the complex conjugate of $\overline{b}(z-a)$. This establishes the equation $\overline{b}(z'-a) = b(\overline{z} - \overline{a})$. Resolution for z' produces (14.28). End of proof. The equivalent vector equation is Eq.(1.276):

$$\mathbf{z}' = (\mathsf{I} - 2\mathbf{m}\mathbf{m})\cdot\mathbf{z} + 2\mathbf{r}_0 \qquad (14.29)$$

with the unit vector $\mathbf{m}$ normal to the reflecting line (sense of direction arbitrary) and with the perpendicular $\mathbf{r}_0$ from the origin onto the reflecting line. The inverse of the reflection in a line is this reflection itself. Thus, reflections are involutoric.

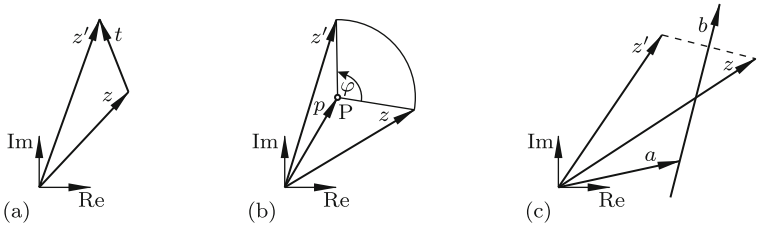

Fig. 14.6 Complex numbers z and z' before and after translation **(a)**, rotation **(b)** and reflection **(c)**

14.3 Resultant Displacements. Commutativity Conditions

Resultants of two displacements are written as products, for example $\mathrm{T_2T_1}$ as resultant of a translation $\mathrm{T_1}$ followed by another translation $\mathrm{T_2}$ and TC as resultant of a rotation C followed by a translation T. Altogether nine resultants have to be investigated, namely, $\mathrm{T_2T_1}$, $\mathrm{C_2C_1}$, $\mathrm{S_2S_1}$, TS, ST, SC, CS, TC, CT. From the fact that S is the only sense-reversing elementary displacement it follows that TS, ST, SC and CS are sense-reversing whereas $\mathrm{T_2T_1}$, $\mathrm{C_2C_1}$, $\mathrm{S_2S_1}$, TC and CT are sense-preserving. The investigation to come reveals, among other things, conditions for products to be commutative, for example conditions for the equality $\mathrm{TS} = \mathrm{ST}$.

The resultant $\mathrm{T_2T_1}$: The equivalent Eqs.(14.23) and (14.24) make the statement

$$z' = z + t_1 + t_2 \,, \qquad \mathbf{z}' = \mathbf{z} + \mathbf{t}_1 + \mathbf{t}_2 \,. \tag{14.30}$$

The resultant is a translation which is calculated by the parallelogram rule. The resultant is unconditionally commutative: $\mathrm{T_2T_1} = \mathrm{T_1T_2}$. Moreover, translations form a group. Indeed, the resultant is itself a translation; the associative law is valid; the unit element exists, namely, the translation $\mathbf{t} = \mathbf{0}$, and the inverse element exists, namely, the translation $-\mathbf{t}$.

The resultant $\mathrm{S_2S_1}$: For reflections the vector formulation (14.29) is more convenient than the complex formulation (14.28). In Sect. 1.16 the same formulation was used for reflections in an arbitrarily oriented plane. In the present planar case, reflecting planes are orthogonal to the plane Σ_0. Their intersections with Σ_0 are the reflecting lines. Theorems 1.8 and 1.7 on the resultant $\mathrm{S_2S_1}$ remain valid in the following simplified forms.

Theorem 14.1. *The resultant of two successive reflections in nonparallel lines with unit normal vectors* $\mathbf{m}_1$ (*first reflection*) *and* $\mathbf{m}_2$ *enclosing the angle* $0 < \varphi < \pi$ *is a rotation through the angle* 2φ *about the axis* $\mathbf{m}_1 \times \mathbf{m}_2 / |\mathbf{m}_1 \times \mathbf{m}_2|$ *normal to* Σ_0 *through the point* P *of intersection of the two reflecting lines. The resultant rotation does not change when the two lines are rotated about their point of intersection with the angle* φ *kept constant. The sense of rotation is reversed when the order of reflections is changed. In the special case of mutually perpendicular lines* ($\varphi = \pi/2$, 180°-*rotation*), *the final position is independent of the order of reflections.*

Theorem 14.2. *The resultant displacement* $\mathbf{z}' - \mathbf{z}$ *caused by two successive reflections in parallel lines with normal vectors* $\mathbf{r}_{01} = r_{01}\mathbf{m}$ (*first reflection*) *and* $\mathbf{r}_{02} = r_{02}\mathbf{m}$ *is the translation* $2(\mathbf{r}_{02} - \mathbf{r}_{01})$ *by twice the distance of the two lines in the direction normal to the lines. The translation changes sign when the order of reflections is changed.*

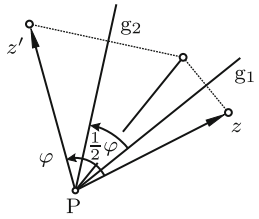

Fig. 14.7 Generation of z' from z by two successive reflections in lines g_1 (first reflection) and g_2 and the resulting rotation about the pole P

The two successive reflections and the rotation about P referred to in Theorem 14.1 are shown in Fig. 14.7. According to the last sentence in this theorem two successive reflections are commutative if and only if the reflecting lines g_1 and g_2 are orthogonal.

The resultants TS and ST: Let $\mathbf{e}$ be the unit vector in the direction of the reflecting line (sense of direction arbitrary). The translation is

$$\mathbf{t} = \mathbf{mm}\cdot\mathbf{t} + \mathbf{ee}\cdot\mathbf{t} \qquad (\,\mathbf{m}\cdot\mathbf{m} = \mathbf{e}\cdot\mathbf{e} = 1\,,\ \mathbf{m}\cdot\mathbf{e} = 0\,)\,. \tag{14.31}$$

For the two resultant displacements the relationships between the final position $\mathbf{z}'$ and the initial position $\mathbf{z}$ are according to (14.29)

$$\left.\begin{aligned} \mathrm{TS}\ :\quad & \mathbf{z}' = (\mathsf{I} - 2\mathbf{mm})\cdot\mathbf{z} + 2\mathbf{r}_0 + \mathbf{t}\,, \\ \mathrm{ST}\ :\quad & \mathbf{z}' = (\mathsf{I} - 2\mathbf{mm})\cdot(\mathbf{z} + \mathbf{t}) + 2\mathbf{r}_0\,. \end{aligned}\right\} \tag{14.32}$$

With (14.31) these relationships become

$$\left.\begin{aligned} \mathrm{TS}\ :\quad & \mathbf{z}' = (\mathsf{I} - 2\mathbf{mm})\cdot\mathbf{z} + 2(\mathbf{r}_0 + \tfrac{1}{2}\,\mathbf{mm}\cdot\mathbf{t}) + \mathbf{ee}\cdot\mathbf{t}\,, \\ \mathrm{ST}\ :\quad & \mathbf{z}' = (\mathsf{I} - 2\mathbf{mm})\cdot\mathbf{z} + 2(\mathbf{r}_0 - \tfrac{1}{2}\,\mathbf{mm}\cdot\mathbf{t}) + \mathbf{ee}\cdot\mathbf{t}\,. \end{aligned}\right\} \tag{14.33}$$

Let g denote the reflecting line specified by the perpendicular $\mathbf{r}_0$. The vectors $(\mathbf{r}_0 + \frac{1}{2}\,\mathbf{mm}\cdot\mathbf{t})$ and $(\mathbf{r}_0 - \frac{1}{2}\,\mathbf{mm}\cdot\mathbf{t})$ have both the direction of $\mathbf{r}_0$. They are the perpendiculars from the origin onto two lines parallel to and at equal distances from g. Comparison with the first Eq.(14.32) for the resultant TS shows that each equation expresses the resultant of a reflection about a line parallel to g followed by the translation $\mathbf{ee}\cdot\mathbf{t}$ along g.

Definition: The special resultant displacement TS of a reflection followed by a translation along the reflecting line is called *glide reflection*. The results obtained are summarized as follows. The resultants TS and ST are different glide reflections. The difference is that their reflecting lines are parallel to and at equal distances from g. Their translatory displacements along the reflecting lines are equal. Identity of the two resultants, i.e., commutativity $\mathrm{TS} = \mathrm{ST}$, requires that $\mathbf{m}\cdot\mathbf{t} = 0$.

A glide reflection is the same independent of whether the reflection is carried out before or after the translation. It has the property that the midpoint $(\mathbf{z}+\mathbf{z}')/2$ of the displacement lies on the reflecting line, and that the translation (positive in the direction of $\mathbf{e}$) is $\mathbf{t} = \mathbf{e}\cdot(\mathbf{z}'-\mathbf{z})$. A glide reflection is a screw displacement with rotation angle π. For this reason the analytical methods developed in Chap. 3 are applicable. In the theory of planar displacements glide reflections are as important as translations and rotations.

Theorem 14.3. *Every sense-reversing displacement is either a reflection or a glide reflection. Every sense-preserving displacement is either a translation or a rotation.*

Proof: Let $\mathbf{z}_i$ $(i = 1,2,3)$ be the initial positions of the corner points of a triangle, and let $\mathbf{z}_i'$ $(i = 1,2,3)$ be the final positions. First, the case is considered that the displacement is sense-reversing. In this case, two out of the three midpoints $(\mathbf{z}_i + \mathbf{z}_i')/2$, say $(\mathbf{z}_1 + \mathbf{z}_1')/2$ and $(\mathbf{z}_2 + \mathbf{z}_2')/2$, are different. They define a line g. It is an elementary task to prove that also $(\mathbf{z}_3 + \mathbf{z}_3')/2$ is located on g. Hint: Consider, first, the special triangle the third corner $\mathbf{z}_3$ of which is located on g at the midpoint $(\mathbf{z}_1 + \mathbf{z}_1')/2$. Then it follows from the rigid-body property that also $\mathbf{z}_3'$ is located on g, and that, furthermore, the three translations $\mathbf{e}\cdot(\mathbf{z}_i' - \mathbf{z}_i)$ $(i = 1,2,3)$ are equal. Next, a triangle with an arbitrarily located corner $\mathbf{z}_3$ is considered which is rigidly connected to the previously considered special triangle. Using, again, the rigid-body property and elementary geometry it is shown that also in this case the midpoint $(\mathbf{z}_3 + \mathbf{z}_3')/2$ is located on g, and that, furthermore, the translation $\mathbf{e}\cdot(\mathbf{z}_3' - \mathbf{z}_3)$ is the same as before. If the identical translations $\mathbf{e}\cdot(\mathbf{z}_i' - \mathbf{z}_i)$ $(i = 1,2,3)$ are zero, the displacement is a reflection in g. This ends the proof of the first part of the theorem.

Next, the case is considered that the displacement is sense-preserving. In this case, the three midpoints $(\mathbf{z}_i+\mathbf{z}_i')/2$ $(i = 1,2,3)$ are not collinear, so that the displacement is not a glide reflection. If the three displacements $\mathbf{z}_i' - \mathbf{z}_i$ $(i = 1,2,3)$ are identical, the displacement is a translation by this vector difference. Otherwise it is a rotation. In this case, the initial and final positions of two points suffice for determining the pole and the angle of the rotation. In complex formulation these are the quantities z_i and z_i' $(i = 1,2)$. The points are denoted A_i in the initial position and A_i' in the final position. The first Eq.(14.25) applied to both points yields two equations for the unknowns p and w:

$$z_1' = p + w(z_1 - p)\,, \qquad z_2' = p + w(z_2 - p)\,. \tag{14.34}$$

The solutions are

$$w = \frac{z_2' - z_1'}{z_2 - z_1}\,, \qquad p = \frac{1}{1-w}\,z_i' - \frac{w}{1-w}\,z_i \qquad (i = 1,2)\,. \tag{14.35}$$

The rigid-body property $|z_2' - z_1'| = |z_2 - z_1| =$ has the consequence that $|w| = 1$. Therefore and with (14.27) the solutions determine the angle φ

and the pole:

$$w = \mathrm{e}^{\mathrm{i}\,\varphi} = \frac{z_2' - z_1'}{z_2 - z_1}\,, \qquad p = \frac{1}{2}\Big[(z_i' + z_i) + \mathrm{i}\,(z_i' - z_i)\cot\frac{\varphi}{2}\Big] \qquad (i = 1, 2)\,. \tag{14.36}$$

In Fig. 14.8a these results are interpreted geometrically. The expression for w determines uniquely (except for 2π) the angle φ between the dashed lines $\overline{\mathrm{A_1A_2}}$ and $\overline{\mathrm{A_1'A_2'}}$. The formulas for p express the fact that the pole P is the intersection point of the midnormals of $\overline{\mathrm{A_1A_1'}}$ and $\overline{\mathrm{A_2A_2'}}$. The angle φ is the angle at P in the isosceles triangles $(\mathrm{A_1,P,A_1'})$ and $(\mathrm{A_2,P,A_2'})$. The triangle $(\mathrm{P,A_1,A_2})$ fixed in Σ is rotated about P into the position $(\mathrm{P,A_1',A_2'})$. In Fig. 14.8b $\overline{\mathrm{A_1A_1'}}$ and $\overline{\mathrm{A_2A_2'}}$ are parallel. In this case, P is the intersection of the lines $\overline{\mathrm{A_1A_2}}$ and $\overline{\mathrm{A_1'A_2'}}$. In Fig. 14.8c all four points $\mathrm{A_1}$, $\mathrm{A_1'}$, $\mathrm{A_2}$, $\mathrm{A_2'}$ are collinear. In this case, $\varphi = \pi$, and the pole P is midpoint between $\mathrm{A_1}$ and $\mathrm{A_1'}$ and also midpoint between $\mathrm{A_2}$ and $\mathrm{A_2'}$. End of proof.

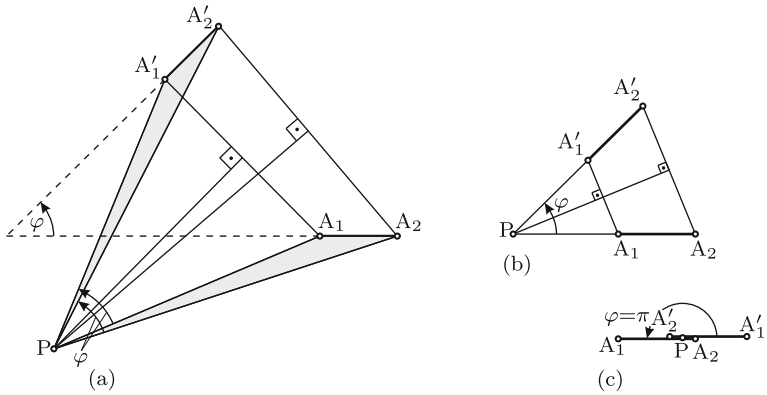

Fig. 14.8 Geometric construction of pole P and rotation angle φ from the positions of two points before and after a rotation. P lies on the midnormals of $\overline{\mathrm{A_1A_1'}}$ and of $\overline{\mathrm{A_2A_2'}}$. Fig. **a**: The midnormals do not coincide. Fig. **b**: The midnormals coincide. P lies on the lines $\overline{\mathrm{A_1A_2}}$ and $\overline{\mathrm{A_1'A_2'}}$. Fig. **c**: Special case $\varphi = \pi$: P is midpoint of $\overline{\mathrm{A_1A_1'}}$ and of $\overline{\mathrm{A_2A_2'}}$

The resultants SC and CS: Both resultants are glide reflections. For both resultants the line of reflection and the translation along this line are constructed geometrically by displacing an isosceles triangle from an initial position 1 via an intermediate position 2 into the final position 3. This geometrical approach is simpler than the analytical approach by means of complex numbers. First, the resultant SC is considered. In Fig. 14.9a the point P is the pole of the rotation C, and g is the reflecting line of the subsequent reflection S. Let φ be the angle of the rotation C (positive counterclockwise). In the intermediate position 2 following the rotation the triangle has the apex P, the apex angle φ and the base on g. From this position 2

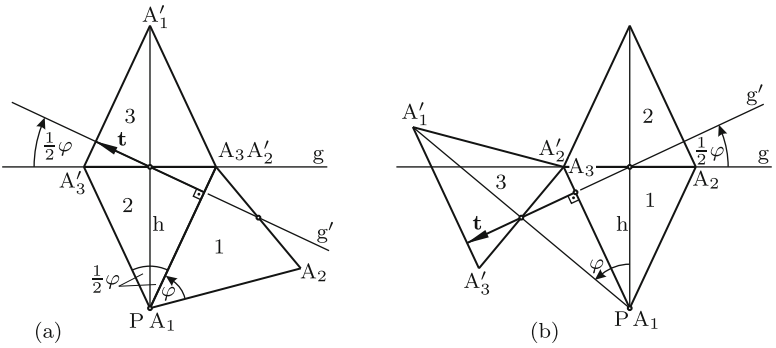

Fig. 14.9 Resultants SC **(a)** and CS **(b)**. Pole P and angle φ of the rotation C, line of reflection g, line g′ and translation $\mathbf{t}$ of the resultant glide reflection

the initial position 1 is obtained by the inverse of the rotation C, i.e., by clockwise rotation through φ about P. The final position 3 is the result of reflecting position 2 in the line g. In position 1 the corner points of the triangle are denoted A_1, A_2, A_3 as shown. In position 3 these points assume the positions A'_1, A'_2, A'_3. The desired line g′ of the glide reflection is the line passing through the midpoints between A_i and A'_i $(i = 1, 2, 3)$. Two of these midpoints coincide. The line g′ makes the angle $\varphi/2$ with g. It is orthogonal to the lines $\overline{A_1A'_2}$ and $\overline{A'_1A'_3}$. Hence the distance between these two lines is the translation of the glide reflection along g′. In terms of the distance h of P from g this translation $\mathbf{t}$ is $2h \sin \varphi/2$ in the direction shown by the arrow.

Next, the resultant CS is considered (Fig. 14.9b). The pole P and the angle φ of the rotation C as well as the line g of the reflection S are as before. Positions 1 and 2 of the triangle before and after the reflection and the final position 3 after the rotation are as shown. The points initially located at A_1, A_2, A_3 assume the final positions A'_1, A'_2, A'_3. The line g′ of the glide reflection is determined as before. Again, two of the midpoints between A_i and A'_i $(i = 1, 2, 3)$ coincide. The line g′ makes the angle $\varphi/2$ with g, but this time to the other side. As before, the translation $\mathbf{t}$ of the glide reflection along g′ is $2h \sin \varphi/2$ in the direction shown by the arrow.

The resultants SC and CS are commutative if and only if P is located on g ($h = 0$) and if, in addition, $\varphi = \pi$. Under these conditions the lines g′ of both resultants are the perpendicular to g through P, and the translation is zero. This means that the resultant is a reflection.

The resultants TC and CT: The complex formulations (14.23) and (14.25) are used. For the two resultants the relationships between the final position z' and the initial position z are

$$\left.\begin{array}{ll} \mathrm{TC}: & z' = p + w(z-p) + t\,, \\ \mathrm{CT}: & z' = p + w(z+t-p) \end{array}\right\} \qquad w = \mathrm{e}^{\mathrm{i}\,\varphi}\,. \tag{14.37}$$

The equations can be written in the forms

$$\left.\begin{array}{lll} \mathrm{TC}: & z' = p^* + w(z-p^*) & \text{with} \quad p^* = p + \dfrac{t}{1-w} = p + \dfrac{t}{2}\left(1 + \mathrm{i}\cot\dfrac{\varphi}{2}\right), \\ \mathrm{CT}: & z' = p^{**} + w(z-p^{**}) & \text{with} \quad p^{**} = p + t\,\dfrac{w}{1-w} = p - \dfrac{t}{2}\left(1 - \mathrm{i}\cot\dfrac{\varphi}{2}\right). \end{array}\right\} \tag{14.38}$$

Both resultants are rotations through the angle φ of the rotation C about different poles located by p^* and p^{**}, respectively. For geometrical interpretations see Fig. 14.10 which shows P, φ and t, and, prior to displacements, two lines 0 and 1 which are fixed in Σ. For the resultant TC only line 1 is of interest. After the rotation C it is in position 2, and after the subsequent translation T it is in the final position 3. The same final position is the result of the rotation through φ about P^*. The difference $p^* - p$ has the components $t/2$ and $(t/2)\cot\varphi/2$. The pole P^* is the apex of the isosceles triangle with base t and with the angle φ at P^*. For the resultant CT only line 0 is of interest. After the translation T it is in position 1, and after the subsequent rotation C it is in the final position 2. The same final position is the result of the rotation through φ about P^{**}. These results show that the resultant TC is never commutative.

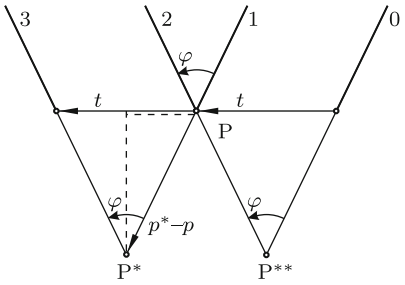

Fig. 14.10 Resultants TC and CT are rotations about different poles P^* and P^{**}

The resultant $\mathrm{C_2C_1}$: At the end of Sect. 3.11 the resultant of two screw displacements with parallel screw axes was derived from dual quaternion equations. The results were summarized in (3.126) – (3.129) and in Figs. 3.14a,b. The resultant $\mathrm{C_2C_1}$ of two rotations about parallel axes is the special case $s_1 = s_2 = 0$. In what follows, these results are derived from the complex formulations (14.25) – (14.27). Let p_1, φ_1 be the pole location and the angle, respectively, of the first rotation $\mathrm{C_1}$ and p_2, φ_2 those of the second rotation $\mathrm{C_2}$. Equation (14.23) yields the relationship between the final position z' and the initial position z in the form

$$z' = p_2 + w_2[p_1 + w_1(z - p_1) - p_2] \,, \qquad w_i = \mathrm{e}^{\mathrm{i}\,\varphi_i} \quad (i = 1, 2) \,. \tag{14.39}$$

In the special case $\varphi_2 = -\varphi_1$, which means $w_1 w_2 = 1$, the resultant is a translation, because the equation then reads

$$z' = z + t \qquad \text{with} \quad t = (1 - w_2)(p_2 - p_1) = (1 - \cos\varphi_1 + \mathrm{i}\,\sin\varphi_1)(p_2 - p_1) \,. \tag{14.40}$$

This is, with a different notation, the special case $s_1 = s_2 = 0$ of (3.129). The translation t is the complex number equivalent to the vector $\overrightarrow{\mathrm{AC}}$ in Fig. 3.14b.

In the general case $\varphi_2 \neq -\varphi_1$, the resultant $\mathrm{C_2C_1}$ is a rotation. Equation (14.39) has the form

$$z' = p + w_1 w_2 (z - p) \qquad \text{with} \quad p = p_1 + (p_2 - p_1)\frac{1 - w_2}{1 - w_1 w_2} \,. \tag{14.41}$$

The factor $w_2 w_1$ shows that the angle of the resultant rotation is

$$\varphi_{\mathrm{res}} = \varphi_1 + \varphi_2 \,. \tag{14.42}$$

From the formula for p and from (14.26) it follows that

$$p - p_1 = (p_2 - p_1)\,\exp\Big(-\mathrm{i}\,\frac{\varphi_1}{2}\Big)\,\frac{\sin\frac{\varphi_2}{2}}{\sin\frac{\varphi_1+\varphi_2}{2}} \,. \tag{14.43}$$

Except for differences of notation, the last two equations are identical with (3.126) and (3.128). The geometrical interpretation was given in Fig. 3.14a. The poles identified by p_1, p_2 and p define a triangle ($\mathrm{P_1}$,$\mathrm{P_2}$,$\mathrm{P_3}$) with internal angles $\varphi_1/2$ and $\varphi_2/2$ at $\mathrm{P_1}$ and $\mathrm{P_2}$, respectively, and with the external angle $\varphi_{\mathrm{res}}/2$ at $\mathrm{P_3}$.

Equations (14.39) and (14.43) show that the resultant displacement $\mathrm{C_2C_1}$ is commutative only in the case when the poles $\mathrm{P_1}$ and $\mathrm{P_2}$ coincide. Table 14.1 summarizes the commutativity conditions found for the various resultant displacements. The resultant $\mathrm{T_2T_1}$ is the only resultant which is unconditionally commutative, and reflection is the only displacement which can be commutative in the product with all three elementary displacements.

Table 14.1 Commutativity conditions for elementary displacements

$\mathrm{T_2T_1}$	always commutative; forms a group
TS	commutative if translation parallel to reflecting line (glide reflection)
CS	commutative if rotation angle $= \pi$ and pole on reflecting line
$\mathrm{S_2S_1}$	commutative if the reflecting lines are orthogonal
$\mathrm{C_2C_1}$	commutative if both poles identical
CT	never commutative

14.4 Relationships Between Three Positions

With a new notation this section continues the investigation of the *pole triangle* defined by (14.42) and (14.43). The pole and the angle of a rotation from a position i into a position j are denoted P_{ij} and φ_{ij}, respectively. The pole and the angle of the inverse rotation from position j into position i are

$$\mathrm{P}_{ji} = \mathrm{P}_{ij} , \qquad \varphi_{ji} = -\varphi_{ij} . \tag{14.44}$$

The first rotation about the pole P_{12} through the angle φ_{12} carries the plane Σ from a position 1 into a position 2, and the second rotation about the pole P_{23} through the angle φ_{23} into a position 3. The resultant of the two rotations is the rotation through the angle $\varphi_{13} = \varphi_{12} + \varphi_{23}$ or, what is the same, through $\varphi_{13} = 2\pi + \varphi_{12} + \varphi_{23}$, about P_{13}. The inverse rotation through the angle $\varphi_{31} = -\varphi_{13}$ about the same pole carries Σ back into its initial position. Hence with (14.44)

$$\frac{1}{2}(\varphi_{12} + \varphi_{23} + \varphi_{31}) = \pi . \tag{14.45}$$

According to this equation $\varphi_{12}/2$, $\varphi_{23}/2$ and $\varphi_{31}/2$ are the internal angles of the pole triangle $(\mathrm{P}_{12},\mathrm{P}_{23},\mathrm{P}_{31})$ (see Fig. 14.11). Every side of the triangle is labeled by the index common to the two poles on this side. Since rotation angles differing by 2π are considered as equal, the angle $\varphi_{ij}/2$ is the internal and also the external angle leading from side i to side j. The results are summarized in

Theorem 14.4. *Three consecutive rotations about the poles of a pole triangle through angles which are twice the internal or external angles of the triangle carry the plane via two intermediate positions back into its initial position.*

This theorem represents a special case of Theorem 1.5 on three rotations about non-coplanar axes intersecting at a single point (see the spherical triangle in Fig. 1.7). If the intersection point moves to infinity, the spherical triangle degenerates to the planar pole triangle.
Let Q be an arbitrary point fixed in Σ and let Q_1, Q_2 and Q_3 be the points in the reference plane Σ_0 where Q is located in the positions 1, 2 and 3 of Σ. These points are called homologous points of Q. At every pole the two sides of the triangle and the enclosed semi-rotation angle create the situation shown in Fig. 14.7. Every two of the points Q_1, Q_2 and Q_3 are carried into each other by a sequence of two reflections in sides of the triangle. The altogether six reflections are sharing one and the same *reflection point* Q'. In Fig. 14.11 this reflection point is shown in the triangle $(\mathrm{Q}_1,\mathrm{Q}_2,\mathrm{Q}_3)$. The circumcircle of this triangle and its center Q_0 are shown as well. The homologous points Q_1, Q_2, Q_3 are now simply called circle points. In what follows, relationships between circle points, poles and the points Q' and Q_0

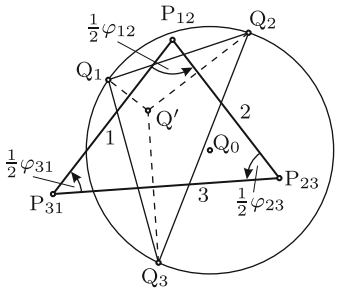

Fig. 14.11 Pole triangle (P_{12},P_{23},P_{31}) with sides 1 , 2 , 3 and with internal angles $\varphi_{12}/2$, $\varphi_{23}/2$, $\varphi_{31}/2$. Three homologous points Q_1 , Q_2 , Q_3 with reflection point Q' , circumcircle and center Q_0

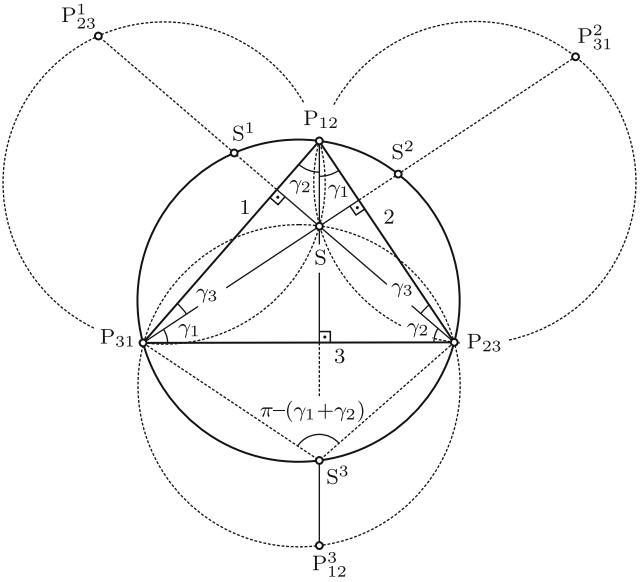

Fig. 14.12 Reflections of poles, orthocenter S and circumcircle

are developed, first by geometrical and then by analytical methods. In Sect. 17.14 these relationships are used for the design of mechanisms leading a plane through prescribed positions. As a preparatory step some new points and circles are defined in the pole triangle (P_{12},P_{23},P_{31}) (see Fig. 14.12). The reflection of P_{ij} in the opposite side of the triangle is called the *reflected pole* P_{ij}^k $(i, j, k = 1, 2, 3$ different). Every reflected pole lies on the perpendicular from the pole onto the opposite side of the pole triangle. The point of concurrency of these perpendiculars (the orthocenter of the triangle) is denoted S . The reflection of S in the triangle side $\overline{P_{ij}P_{jk}}$ (twice the index j) is denoted S^j $(j = 1, 2, 3)$. Proposition: The three points S^j $(j = 1, 2, 3)$ are

located on the circumcircle of the pole triangle. Proof: The altitudes of the pole triangle create pairs of similar right-angled triangles so that angles γ_1, γ_2 and γ_3 appear twice each as shown. The angles subtended by the line segment $\overline{\mathrm{P}_{jk}\mathrm{P}}_{ki}$ are $\gamma_i+\gamma_j$ at P_{ij} and $180°-(\gamma_i+\gamma_j)$ at S^k. From this it follows that both points are located on the circle. End of proof. Consequently, the three reflections of the circumcircle in the sides of the triangle (dashed lines) intersect at S.

Next, relationships are formulated between the center Q_0, the reflection point Q', the circle points Q_1, Q_2, Q_3 and the poles. The point Q_0 is the intersection point of the midperpendiculars of the triangle (Q_1,Q_2,Q_3), and every midperpendicular passes through one pole. The midperpendiculars are shown in Fig. 14.13. As an example, consider the perpendicular bisector passing through P_{12}. At P_{12} the angles satisfy the equation $\sphericalangle(\mathrm{P}_{31}\mathrm{P}_{12}\mathrm{P}_{23}) = \varphi_{12}/2$ as well as the equation $\sphericalangle(\mathrm{Q}_1\mathrm{P}_{12}\mathrm{Q}_0) = \frac{1}{2}\sphericalangle(\mathrm{Q}_1\mathrm{P}_{12}\mathrm{Q}_2) = \varphi_{12}/2$. Since the angles $\sphericalangle(\mathrm{Q}_1\mathrm{P}_{12}\mathrm{P}_{31})$ and $\sphericalangle(\mathrm{P}_{31}\mathrm{P}_{12}\mathrm{Q}')$ are equal, they are also equal to the angle $\sphericalangle(\mathrm{Q}_0\mathrm{P}_{12}\mathrm{P}_{23})$. In Fig. 14.13 these angles are denoted β_{12}. By the same arguments angles β_{23} and β_{13} appear twice each at the other poles of the pole triangle. As is shown in the figure each angle is measured from two sides of the triangle with opposite signs. Through these relationships the point Q' is determined if Q_0 is given and vice versa. If Q_0 (if Q') is not located in a pole, Q' (or Q_0) is uniquely determined. The circle points Q_1, Q_2, Q_3 are obtained by reflecting Q' in the sides of the pole triangle. Obviously, the following statement is true: The center Q_0 and the reflection

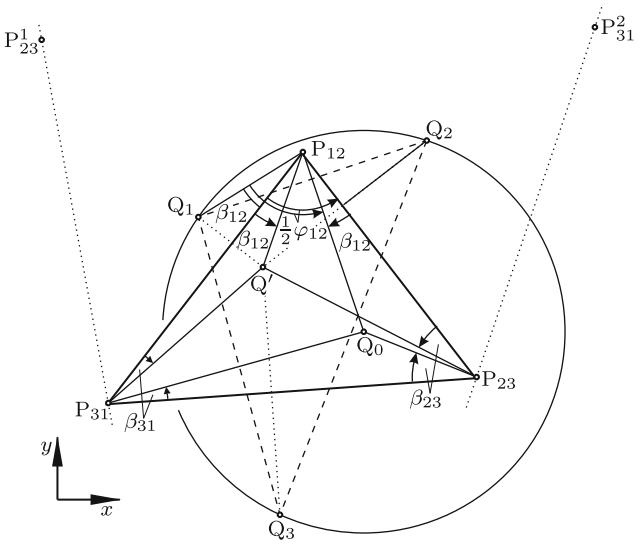

Fig. 14.13 Relationships between circle points, reflection point Q' and center Q_0

point Q' can be interchanged. If Q_0 is made the reflection point of three homologous points, Q' is their center point (Burmester [4]). The two points can be inside, on the perimeter or outside the triangle. It is left to the reader to prove that the radii of the circle about Q_0 and of the circle about Q' as center are equal.

Special case (a): Q_0 coincides with a pole, for example with P_{12}: In this case, $Q'=Q_3$ is an undetermined point on the line $\overline{P_{23}P_{31}}$; Q_1 lies on the dotted line $\overline{P_{31}P_{23}^1}$, and Q_2 lies on the line $\overline{P_{23}P_{31}^2}$.

Special case (b): Q' coincides with a pole, for example with P_{12}: In this case, $Q_1=Q_2=Q'=P_{12}$; $Q_3=P_{12}^3$; Q_0 is an undetermined point on the line $\overline{P_{23}P_{31}}$.

Infinitely Distant Center Point

With a center point Q_0 at infinity the circle points Q_1, Q_2, Q_3 are on a straight line. Its location is explained by Fig. 14.14. Let Q_0 be prescribed as intersection of two arbitrarily directed parallel lines passing through P_{12} and P_{23}, respectively. In this case, the angles β_{12} and β_{23} explained in Fig. 14.13 are identical: $\beta_{12}=\beta_{23}=\beta$. This has the consequence that Q' lies on the circumcircle of the pole triangle (equal angles β subtended by the chord $\overline{P_{31}Q'}$). Since Q_1, Q_2, Q_3 are the reflections of Q' in the sides of the triangle, each point lies on the reflection of the circumcircle in one side of the triangle. Since these reflected circles are concurrent in S, the line $\overline{Q_1Q_2Q_3}$ passes through S.

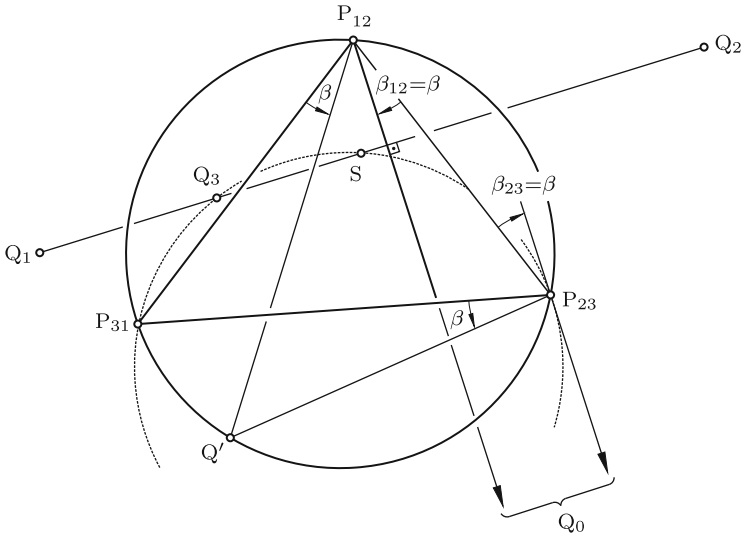

Fig. 14.14 Collinear points Q_1, Q_2, Q_3 and S. Center Q_0 at infinity

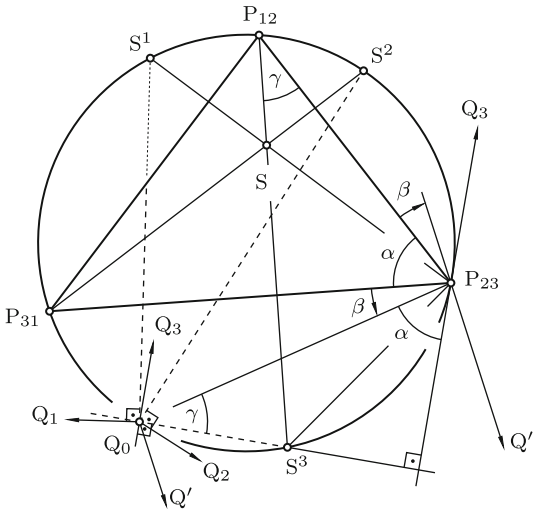

Fig. 14.15 Reflection point Q' and circle points at infinity. Center Q_0 on circumcircle of pole triangle

Infinitely Distant Circle Points

The interchangeability of center point Q_0 and reflection point Q' has the consequence: If Q_0 is an arbitrarily prescribed point on the circumcircle of the pole triangle, the corresponding reflection point Q' and the corresponding circle points Q_1, Q_2, Q_3 are at infinity. The direction toward the reflection point Q' is determined by the angle β against the triangle side $\overline{P_{23}P_{31}}$ (Fig. 14.15). Proposition: The direction toward the circle point Q_i $(i = 1, 2, 3)$ is normal to the line $\overline{Q_0 S^i}$. The proof is given for the case $i = 3$: The lines leading from P_{23} toward Q' and Q_3, respectively, must be symmetric with respect to the line $\overline{P_{23}P_{31}}$. This is, indeed, the case since not only the two angles β are equal, but also the two angles denoted α are equal. The reason is that $\gamma = 90° - \alpha$ is the angle subtended by the chord $\overline{S^3 P_{23}}$. End of proof.

Sense of Triangle of Circle Points

In Fig. 14.16 the pole triangle of Fig. 14.13 is shown again. Its sides 1, 2 and 3 define the *sense of the pole triangle*. In the figure the sense is clockwise. In what follows, the side i of the pole triangle continued to infinity in both directions is referred to as line i $(i = 1, 2, 3)$. The lines 1, 2 and 3 divide the infinite plane into seven domains (the lines themselves do not belong to any of these domains). If the center point Q_0 is inside the pole triangle, also Q' is inside, and the triangle of circle points Q_1, Q_2, Q_3 has the same sense the pole triangle has. Every time Q_0 crosses one of the lines 1, 2, 3 the sense of the triangle of circle points is reversed. Hence both triangles have the same sense if Q_0 is located in one of the four domains marked $=$, and they have

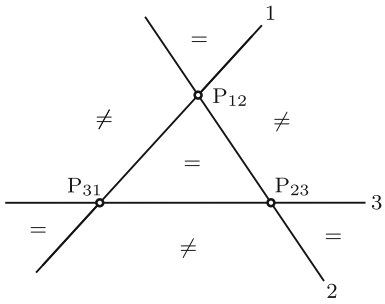

Fig. 14.16 The seven domains in the plane of the pole triangle and the sense of the triangle of circle points Q_1, Q_2, Q_3. Symbols $=$ and $\neq$ indicate that the sense is equal or opposite, respectively, to the sense of the pole triangle if Q_0 is located in the domain under consideration

opposite senses if Q_0 is located in one of the three domains marked $\neq$. If Q_0 is located on one of the lines 1, 2, 3, but not in a pole, two circle points coincide (see the special case (b) above). In this case, there is no unique sense of the triangle of circle points. If Q_0 is located in a pole, Q' is an arbitrary point of the opposite line (see the special case (a) above). In this case, the sense of the triangle of circle points depends upon whether Q' is located on a side of the pole triangle or on one of the continuations of this side. In the former case, the sense equals the sense of the pole triangle, and in the latter it is opposite to it.

Analytical Relationships

In what follows, the geometrical relationships described so far are expressed in analytical form. First, the relationship between center point Q_0 and reflection point Q' is expressed in terms of so-called normal coordinates. In Fig. 14.17 the normal coordinates u_1, u_2, u_3 of Q_0 are shown. Definition: u_i is the distance from the line i. All three normal coordinates are positive if Q_0 is inside the triangle. Since a point of a plane has only two independent coordinates, the three coordinates are subject to a constraint equation. It expresses the fact that the areas of the three triangles created by the segments connecting Q_0 with the poles add up to the total area A of the triangle. In terms of the side lengths s_1, s_2, s_3 this is the constraint equation

$$s_1u_1 + s_2u_2 + s_3u_3 = 2A\,. \tag{14.46}$$

Let u'_1, u'_2, u'_3 be the correspondingly defined normal coordinates of the reflection point Q'. The two-fold symmetrical occurrence of the angle β_{31} has the consequence that $u_1 : u_3 = u'_3 : u'_1$. From this and from two more such equations it follows that the desired analytical relationship between Q_0 and Q' has the form

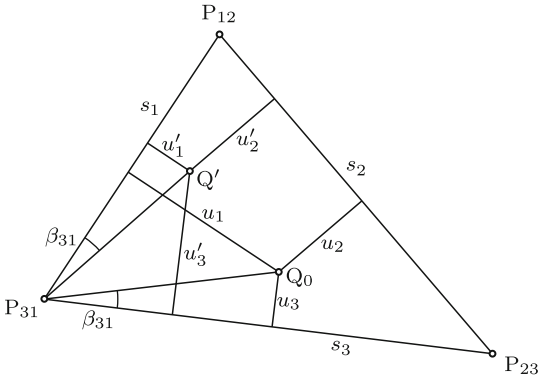

Fig. 14.17 Normal coordinates of center Q_0 and of reflection point Q'

$$u_1 : u_2 : u_3 = \frac{1}{u'_1} : \frac{1}{u'_2} : \frac{1}{u'_3} \,. \tag{14.47}$$

It is quadratic-involutoric. Further applications of normal coordinates to the study of positions of a plane are found in Blaschke [3] p.165 .

In what follows, analytical relationships are developed between the circle points Q_1 , Q_2 , Q_3 and the center point Q_0 . In an arbitrary cartesian coordinate system fixed in Σ_0 the coordinates of a point are interpreted as real part and as imaginary part of a complex number. This number is given the name of the point itself. Examples are the numbers Q_1 and P_{12} in Fig. 14.13 . In this figure, the example $i = 1$, $j = 2$ illustrates the fact that for arbitrary combinations of indices i and $j \neq i$ the difference $\mathrm{Q}_0 - \mathrm{P}_{ij}$ is rotated against the difference $\mathrm{Q}_i - \mathrm{P}_{ij}$ through the angle $\varphi_{ij}/2$. This means that the numbers $\mathrm{e}^{\mathrm{i}\,\varphi_{ij}/2}(\mathrm{Q}_i - \mathrm{P}_{ij})$ and $(\mathrm{Q}_0 - \mathrm{P}_{ij})$ have equal directions $(i, j = 1, 2, 3\,;\ i \neq j\,)$. According to (14.6) this is expressed in the form

$$\mathrm{Im}\Big[\Big(\cos\frac{\varphi_{ij}}{2} + \mathrm{i}\,\sin\frac{\varphi_{ij}}{2}\Big)(\mathrm{Q}_i - \mathrm{P}_{ij})(\bar{\mathrm{Q}}_0 - \bar{\mathrm{P}}_{ij})\Big] = 0 \qquad (i, j = 1, 2, 3\,;\ i \neq j\,) \,. \tag{14.48}$$

Let the coordinates of the points be denoted as follows:

$$\mathrm{Q}_i = \xi_i + \mathrm{i}\,\eta_i \,, \qquad \mathrm{Q}_0 = x + \mathrm{i}\,y \,, \qquad \mathrm{P}_{ij} = u_{ij} + \mathrm{i}\,v_{ij} \qquad (i, j = 1, 2, 3\,;\ i \neq j\,) \,. \tag{14.49}$$

Substitution of these expressions results in equations which are linear with respect to ξ_i , η_i , x and y . If the center point is known and the circle points are unknown, the equations are written in the form (abbreviations $s_{ij} = \sin\varphi_{ij}/2$, $c_{ij} = \cos\varphi_{ij}/2$):

$$\begin{aligned} &\xi_i\big[(x - u_{ij})s_{ij} - (y - v_{ij})c_{ij}\big] + \eta_i\big[(x - u_{ij})c_{ij} + (y - v_{ij})s_{ij}\big] \\ &= x(u_{ij}s_{ij} + v_{ij}c_{ij}) - y(u_{ij}c_{ij} - v_{ij}s_{ij}) - s_{ij}(u_{ij}^2 + v_{ij}^2) \end{aligned} \tag{14.50}$$

$(i, j = 1, 2, 3;\ i \neq j)$. For a fixed value of i $(i = 1, 2, 3)$ these are two equations for ξ_i and η_i. Equation (14.48) shows that no unique solution exists if Q_0 is located in a pole. This is the special case (a) explained above.

If the coordinates (ξ_i, η_i) of a single circle point are given, the equations are resolved for the coordinates (x, y) of the center point. For $i = 1, 2$ and 3 one and the same coordinates (x, y) are obtained. Formally, this resolution is achieved by reversing the sign of φ_{ij} and by interchanging (ξ_i, η_i) and (x, y). The reason is that the resulting equations express the fact that the numbers $\mathrm{e}^{-\mathrm{i}\,\varphi_{ij}/2}(\mathrm{Q}_0 - \mathrm{P}_{ij})$ and $(\mathrm{Q}_i - \mathrm{P}_{ij})$ have equal directions. The solution is not unique if Q_i is located in a pole. This is the special case (b) explained above.

14.5 Relationships Between Four Positions. Pole Curve

Two positions of a plane determine a pole and a rotation angle, and three positions determine a pole triangle. Hence four positions determine altogether six poles and four pole triangles. In Fig. 14.18 the four positions are defined by the points A_i, B_i $(i = 1, 2, 3, 4)$. The poles are constructed according to the rules of Fig. 14.7. In what follows, it is assumed that no pole is at infinity and that no two poles coincide. All relative positions are known if the positions 2, 3 and 4 relative to position 1 are known. These three relative positions are determined by altogether nine parameters. These are two coordinates for each of the three poles P_{1k} and the rotation angles φ_{1k} $(k = 2, 3, 4)$. Between the poles and the semi-rotation angles of every pole triangle exist the relationships shown in Fig. 14.11 and in (14.45). Every pole is pole in two triangles. The reason is that for any two triples of positions i, j, k and i, j, ℓ $(i, j, k, \ell = 1, 2, 3, 4$ different) the corresponding pole triangles $(\mathrm{P}_{ij}, \mathrm{P}_{jk}, \mathrm{P}_{ki})$ and $(\mathrm{P}_{ij}, \mathrm{P}_{j\ell}, \mathrm{P}_{\ell i})$ are sharing the pole P_{ij}. In both triangles the angle $\varphi_{ij}/2$ is either internal or external angle at P_{ij}. As an example, consider the pole P_{12} common to the pole triangles $(\mathrm{P}_{12}, \mathrm{P}_{23}, \mathrm{P}_{13})$ and $(\mathrm{P}_{12}, \mathrm{P}_{24}, \mathrm{P}_{14})$. From P_{12} the sides $\overline{\mathrm{P}_{23}\mathrm{P}_{13}}$ and $\overline{\mathrm{P}_{24}\mathrm{P}_{14}}$ are seen under one and the same angle $\varphi_{12}/2$. Also the sides $\overline{\mathrm{P}_{23}\mathrm{P}_{24}}$ and $\overline{\mathrm{P}_{13}\mathrm{P}_{14}}$ are seen from P_{12} under one and the same angle (different from $\varphi_{12}/2$). The two pairs of sides represent pairs of *opposite sides* of the *pole quadrilateral* $(\mathrm{P}_{13}, \mathrm{P}_{32}, \mathrm{P}_{24}, \mathrm{P}_{41})$. This notation indicates the sequence of poles. Every side connects two poles having one index in common. Poles in opposite corners, so-called *opposite poles*, have no index in common.

Opposite sides of this pole quadrilateral are seen also from P_{34} under one and the same angle (different for each pair) and, finally, they are seen under one and the same angle from any pole of the pole quadrilateral itself. The reason is that a side seen from one of its endpoints appears under an arbitrary angle.

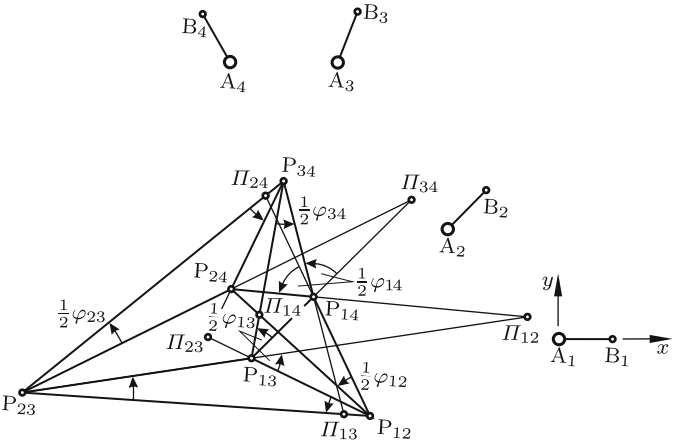

Fig. 14.18 Poles P_{ij} and points Π_{ij} corresponding to four positions $\overline{\mathrm{A}_i\mathrm{B}_i}$ $(i = 1,\dots,4)$. In the x,y-system in which A_1 and B_1 have coordinates $(0;0)$ and $(1;0)$, respectively, A_2, A_3, A_4 have the coordinates $(-2;2)$, $(-4;5)$ and $(-6;5)$, respectively. The angles from $\overline{\mathrm{A}_1\mathrm{B}_1}$ to $\overline{\mathrm{A}_i\mathrm{B}_i}$ $(i = 2,3,4)$ are $45°$, $70°$ and $120°$, respectively

The quadrilateral just considered is one of altogether three pole quadrilaterals of the general form $(\mathrm{P}_{ij},\mathrm{P}_{jk},\mathrm{P}_{k\ell},\mathrm{P}_{\ell i})$ $(i,j,k,\ell = 1,2,3,4$ different). The other two are $(\mathrm{P}_{12},\mathrm{P}_{23},\mathrm{P}_{34},\mathrm{P}_{41})$ and $(\mathrm{P}_{12},\mathrm{P}_{24},\mathrm{P}_{43},\mathrm{P}_{31})$. For all pole quadrilaterals the following is true: From every pole any pair of opposite sides is seen under angles which are either equal or which add up to π. Example: From P_{13} the opposite sides $\overline{\mathrm{P}_{12}\mathrm{P}_{23}}$ and $\overline{\mathrm{P}_{34}\mathrm{P}_{41}}$ are seen under the angles $\pi - \varphi_{13}/2$ and $\varphi_{13}/2$, respectively. These angles have equal tangents. In what follows, it is assumed that of the altogether six poles only the poles of a single quadrilateral $(\mathrm{P}_{ij},\mathrm{P}_{jk},\mathrm{P}_{k\ell},\mathrm{P}_{\ell i})$ are given. It is natural to ask for all points P having the property that from P opposite sides of the given quadrilateral appear under angles which are either equal or which add up to π. The solution is found as follows. The pole quadrilateral $(\mathrm{P}_{ij},\mathrm{P}_{jk},\mathrm{P}_{k\ell},\mathrm{P}_{\ell i})$ is shown in Fig. 14.19. let $\mathbf{r}_{ij}$, $\mathbf{r}_{jk}$, $\mathbf{r}_{k\ell}$ and $\mathbf{r}_{\ell i}$ be the vectors pointing from P to the four poles. Furthermore, let $\mathbf{e}$ be the unit vector normal to the plane. Equality of tangents of angles is expressed as follows:

$$\frac{\mathbf{e}\cdot\mathbf{r}_{ij}\times\mathbf{r}_{jk}}{\mathbf{r}_{ij}\cdot\mathbf{r}_{jk}} = \frac{\mathbf{e}\cdot\mathbf{r}_{\ell i}\times\mathbf{r}_{k\ell}}{\mathbf{r}_{k\ell}\cdot\mathbf{r}_{\ell i}} \qquad (i,j,k,\ell = 1,2,3,4 \text{ different}) . \qquad (14.51)$$

The relationships just described for pole triangles are identical with those for spherical triangles associated with four positions of a rigid body with a fixed point (see Fig. 1.8a,b and (1.137)). It was shown that in the spherical case, (1.137) defines a third-order cone of rotation axes. In the present planar case, (14.51) defines a third-order *pole curve* (Burmester [4]). The curve is uniquely defined by a single pole quadrilateral, i.e., by eight parameters. On

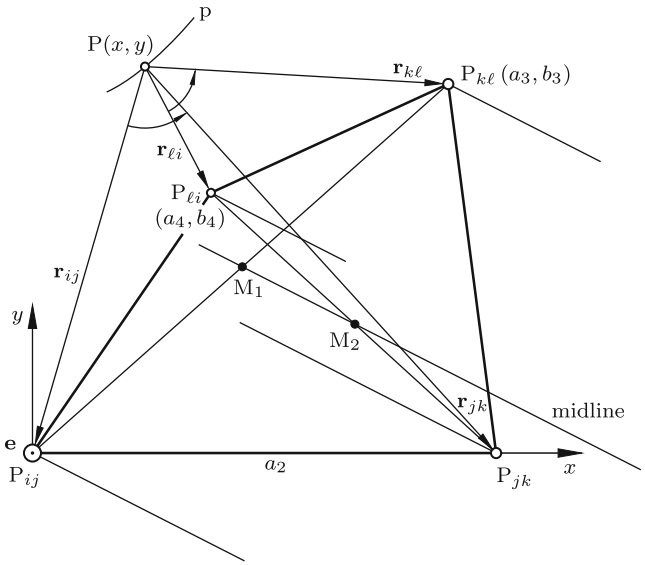

Fig. 14.19 Pole quadrilateral with vectors defining the pole curve p. Midline $\overline{\mathrm{M_1M_2}}$

this curve a fifth pole can be chosen arbitrarily. Its location determines the ninth parameter and, hence, also the sixth pole. Also this sixth pole lies on the pole curve.

In Sect. 17.14 the pole curve plays a central role in the synthesis of linkages leading a plane through prescribed positions. In what follows, the curve is abbreviated p. It has many remarkable properties. Its equation in a cartesian x, y-system is deduced from (14.51). As shown in Fig. 14.19 the axes are chosen such that P_{ij} is the origin and that P_{jk} lies on the x-axis. The coordinates of the poles are denoted $(a_2, 0)$, (a_3, b_3) and (a_4, b_4) as shown. With (x, y) being the coordinates of the point P the vectors in (14.51) have the coordinates
$\mathbf{r}_{ij} : (-x, -y)$, $\mathbf{r}_{jk} : (a_2 - x, -y)$, $\mathbf{r}_{k\ell} : (a_3 - x, b_3 - y)$, $\mathbf{r}_{\ell i} : (a_4 - x, b_4 - y)$. Equation (14.51) takes the form

$$\frac{a_2 y}{x^2 + y^2 - a_2 x} = \frac{(b_4 - b_3)x + (a_3 - a_4)y + a_4 b_3 - a_3 b_4}{x^2 + y^2 - (a_3 + a_4)x - (b_3 + b_4)y + a_3 a_4 + b_3 b_4} \,. \quad (14.52)$$

Re-ordering of terms produces the following equation which is cubic in x as well as in y:

$$(\lambda x + \mu y + A)(x^2 + y^2) + B(y^2 - x^2) + 2Cxy + Dx + Ey = 0 \,, \quad (14.53)$$

$$\left.\begin{array}{lll} \lambda = b_4 - b_3\,, & \mu = a_3 - a_2 - a_4\,, & A = b_3(a_2 + a_4) - a_3 b_4\,, \\ B = a_2 b_4\,, \quad C = a_2 a_4\,, & D = a_2(a_3 b_4 - a_4 b_3)\,, & E = -a_2(a_3 a_4 + b_3 b_4)\,. \end{array}\right\} \tag{14.54}$$

In the case $\lambda = \mu = 0$, the pole quadrilateral is a parallelogram, and p is an equilateral hyperbola. In what follows, this special case is excluded. It is treated in Luck/Modler [13].

Propositions: 1) The curve p has an asymptote which is parallel to what is called the *midline* of the pole quadrilateral. This is the line connecting the midpoints of its diagonals.

2) In the x, y-system the asymptote has the slope $-\lambda/\mu$.

Proof for (1): In Fig. 14.19 the midpoints of the diagonals are denoted M_1 and M_2. Through the four poles lines parallel to the midline $\overline{\mathrm{M}_1\mathrm{M}_2}$ are drawn. The projections of opposite sides of the pole quadrilateral along $\overline{\mathrm{M}_1\mathrm{M}_2}$ are equally long. From this it follows that from the infinitely distant intersection points of these parallel lines pairs of opposite sides are seen under equal angles. This proves proposition (1). In the x, y-system M_1 and M_2 have the coordinates $x_1 = a_3/2$, $y_1 = b_3/2$ and $x_2 = (a_2 + a_4)/2$, $y_2 = b_4/2$. This yields for the slope of $\overline{\mathrm{M}_1\mathrm{M}_2}$ the expression $(y_2 - y_1)/(x_2 - x_1) = (b_3 - b_4)/(a_3 - a_2 - a_4)$. According to (14.54) this is $-\lambda/\mu$. End of proof.

The cubical nature of p has the consequence that every (straight) line not parallel to the asymptote intersects p at three points two of which might be imaginary. Lines parallel to the asymptote intersect p at two – real or imaginary – points. The asymptote itself intersects p at a single real point.

In Fig. 14.20 the same pole quadrilateral is shown. Each side is denoted by the index common to the poles at its endpoints. Let Π_{ik} be the intersection point of the opposite sides j and ℓ and let $\Pi_{j\ell}$ be the intersection point of the opposite sides i and k. From Π_{ik} and from $\Pi_{j\ell}$ opposite sides are seen under equal angles β_{ik} and $\beta_{j\ell}$, respectively. Hence both points belong to p. The altogether three pole quadrilaterals define six points Π_{ij} $(i, j = 1, 2, 3, 4\,;\ i \neq j)$. In Fig. 14.18 these points are shown.

In Fig. 14.20 circles k_i and k_k with the peripheral angle β_{ik} subtended by the opposite sides i and k, respectively, are drawn. They intersect at Π_{ik} and at one more point which, because of the equality of the two angles, also belongs to p. By the same argument the circles k_j and k_ℓ with the peripheral angle $\beta_{j\ell}$ subtended by the opposite sides j and ℓ, respectively, intersect at $\Pi_{j\ell}$ and at one more point belonging to p. The figure shows that the four circles intersect at a single point Φ. This is proved as follows. To begin with, let Φ be the intersection of k_j and k_k only. Also k_i is passing through Φ if the peripheral angles $\alpha - \beta_{j\ell}$ at Φ and γ at $\mathrm{P}_{\ell i}$ are equal. This is, indeed, the case since α appears as peripheral angle in the circle k_k also at $\mathrm{P}_{k\ell}$, and from the triangle $(\mathrm{P}_{\ell i}, \mathrm{P}_{k\ell}, \Pi_{j\ell})$ it follows that $\gamma = \alpha - \beta_{j\ell}$. In the same way it is shown that also the circle k_ℓ is passing through Φ.

The curve p intersects the four circles at Φ, Π_{ik}, $\Pi_{j\ell}$, at the poles of the pole quadrilateral and at no other point. Indeed, if there were to be another

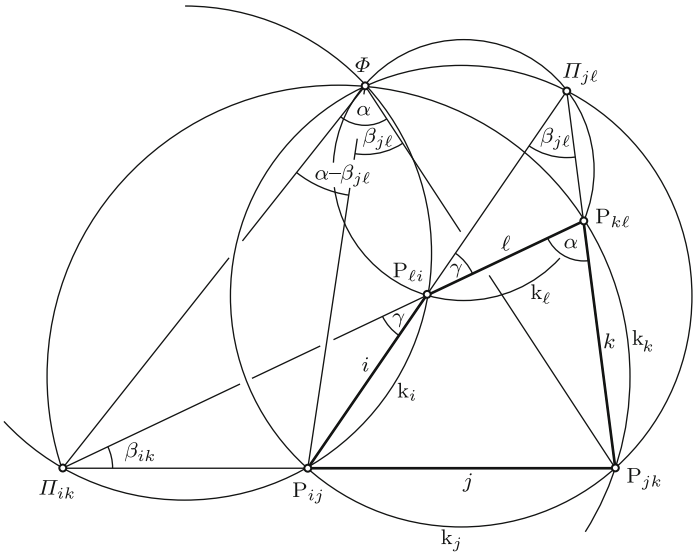

Fig. 14.20 Π-points of a pole quadrilateral and focus Φ

intersection point, say with the circle k_j, the side j would be seen from this point under the angle $\beta_{j\ell}$ and the opposite side ℓ under a different angle.

For each of the three pole quadrilaterals there exists an intersection point Φ of four associated circumcircles of triangles. All three intersection points coincide. Indeed, if they were different points, the curve p could not interconnect these three points, the six poles and the six Π-points without intersecting at least one of the twelve circles at one more point. The significant point Φ is called the *focus* of p.

Of the asymptote so far only its direction parallel to the midline of the pole quadrilateral is known. The focus Φ determines also its location. In Fig. 14.20 the following is seen. If, with the pair of opposite poles P_{ij} and $\mathrm{P}_{k\ell}$ being fixed, the pole $\mathrm{P}_{\ell i}$ tends on p towards Φ, the pole P_{jk} tends towards infinity on the asymptote. From this it follows that the asymptote is on the same side of Φ as the midline and at twice the distance. Another consequence is that the midlines of all three pole quadrilaterals coincide.

Another significant point on p is defined by the circumcircles of the four pole triangles (see Fig. 14.21). The circumcircles intersect at a single point U. This is proved as follows. First, only the circumcircles of the triangles $(\mathrm{P}_{12},\mathrm{P}_{24},\mathrm{P}_{41})$ and $(\mathrm{P}_{13},\mathrm{P}_{34},\mathrm{P}_{41})$ are considered. They intersect at P_{41} and at U. At P_{41} the peripheral angle subtended by $\overline{\mathrm{P}_{12}\mathrm{P}_{24}}$ in the one circle and the peripheral angle subtended by $\overline{\mathrm{P}_{13}\mathrm{P}_{34}}$ in the other circle are equal. Hence also at U the peripheral angles subtended by these sides are equal. Since these sides are opposite sides of a pole quadrilateral, U belongs to p. From no other point of the circle except P_{41} and U the two opposite sides are

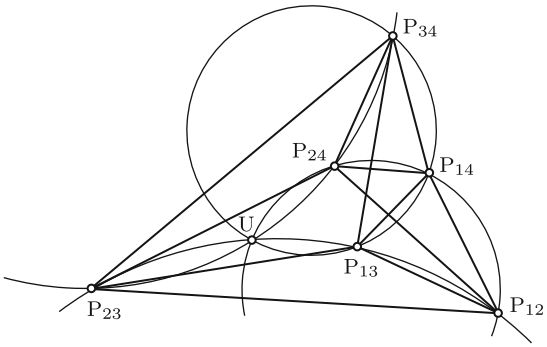

Fig. 14.21 Poles of Fig. 14.18 with circumcircles of four pole triangles intersecting at U

seen under equal angles. The same statements are valid for the circumcircles of any two of the four pole triangles. From this it follows that, first, all four circles intersect at U and that, second, the curve p intersects these four circumcircles at no points other than U and the poles.

In what follows, a property of the six Π-points is revealed. Let the curve p be given and on it an arbitrary point P together with two straight lines passing through P. These lines intersect p at two more points each. The four intersection points thus defined constitute a pole quadrilateral one Π-point of which is the given point P. Now, choose as point P the pole $\mathrm{P}_{\ell i}$ in Fig. 14.20 and through $\mathrm{P}_{\ell i}$ the lines $\overline{\mathrm{P}_{\ell i}\mathrm{P}_{ij}}$ and $\overline{\mathrm{P}_{\ell i}\mathrm{P}_{k\ell}}$. These lines create the pole quadrilateral $(\mathrm{P}_{ij}, \Pi_{j\ell}, \mathrm{P}_{k\ell}, \Pi_{ik})$ in which $\Pi_{j\ell}$ and Π_{ik} are opposite poles. The six Π-points constitute three pairs of opposite poles. Consequently, they represent the poles belonging to four positions of the plane with which the same pole curve p is associated. The Π-points of these poles are poles again etc. Starting from the six original poles this procedure produces an infinite sequence of six-tuples of poles all lying on p. On a computer screen a graph of p is most easily generated by calculating a sufficiently large number of six-tuples of poles. In Fig. 14.22 the pole curve for the six poles of Fig. 14.18 is shown together with its focus and its asymptote. The point of intersection of the asymptote with p is called *cardinal point* H of p.

Next, Eq.(14.53) of the pole curve p is considered again. New coordinates ξ, η are defined through the transformation equations

$$x = \frac{\mu(\xi - \xi_0) + \lambda(\eta - \eta_0)}{\sqrt{\lambda^2 + \mu^2}}\,, \qquad y = \frac{-\lambda(\xi - \xi_0) + \mu(\eta - \eta_0)}{\sqrt{\lambda^2 + \mu^2}} \tag{14.55}$$

where ξ_0 and η_0 are as yet unspecified constants. This transformation has the effect that the ξ-axis is parallel to the asymptote of p. Substitution into (14.53) produces an equation of the form

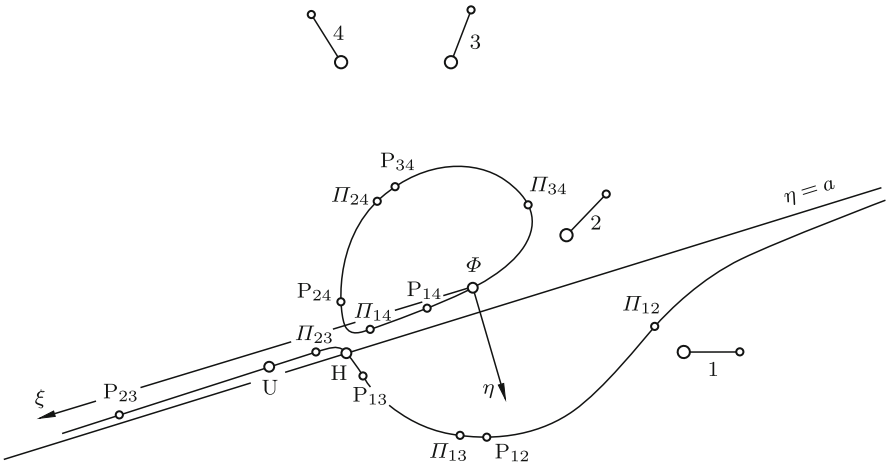

Fig. 14.22 Pole curve for the poles of Fig. 14.18 with significant points and lines

$$\left[\sqrt{\lambda^2+\mu^2}(\eta-\eta_0)+A'\right](\xi^2+\eta^2)+B'(\eta^2-\xi^2)+2C'\xi\eta+D'\xi+E'\eta+F=0\,. \tag{14.56}$$

The coefficients $A', \ldots, F$ are functions of λ, μ, $A, \ldots, E$ and of ξ_0, η_0. The constants ξ_0 and η_0 are chosen such that $B'=0$ and $C'=0$:

$$\xi_0 = -\frac{2B\lambda\mu + C(\lambda^2-\mu^2)}{(\lambda^2+\mu^2)^{3/2}}\,, \qquad \eta_0 = \frac{2C\lambda\mu - B(\lambda^2-\mu^2)}{(\lambda^2+\mu^2)^{3/2}}\,. \tag{14.57}$$

Further below it is proved that the origin of the ξ,η-system is the focus Φ. The x,y-coordinates of the origin are obtained from (14.55):

$$x_\Phi = \frac{B\lambda - C\mu}{\lambda^2+\mu^2}\,, \qquad y_\Phi = -\frac{B\mu + C\lambda}{\lambda^2+\mu^2}\,. \tag{14.58}$$

From the fact that the origin Φ lies on p it follows that also $F=0$. With new abbreviations a, d and e Eq.(14.56) of the curve gets its normal form

$$(\eta-a)(\xi^2+\eta^2)+d\,\xi+e\eta=0\,. \tag{14.59}$$

The formula for a is

$$a = 2\eta_0 - \frac{A}{\sqrt{\lambda^2+\mu^2}}\,. \tag{14.60}$$

For proving that Φ is the origin it suffices to show that the coordinates x_Φ, y_Φ satisfy the equations of the circles k_i and k_j of Fig. 14.20. The equation of a circle passing through three points (x_i, y_i) $(i=1,2,3)$ is

$$\begin{vmatrix} x^2+y^2 & x & y & 1 \\ x_1^2+y_1^2 & x_1 & y_1 & 1 \\ x_2^2+y_2^2 & x_2 & y_2 & 1 \\ x_3^2+y_3^2 & x_3 & y_3 & 1 \end{vmatrix} = 0 \, .$$

The points P_{ij}, $\mathrm{P}_{\ell i}$, $\mathit{\Pi}_{ik}$ on k_i have the coordinates $(0,0)$, (a_4, b_4) and $(a_2^*, 0)$, and the points P_{ij}, $\mathit{\Pi}_{j\ell}$, P_{jk} on k_j have the coordinates $(0,0)$, (a_4^*, b_4^*) and $(a_2, 0)$ with

$$a_2^* = a_4 - b_4 \frac{a_3 - a_4}{b_3 - b_4} \, , \qquad a_4^* = \frac{a_4 a_2 b_3}{b_3 a_4 - b_4 (a_3 - a_2)} \, , \qquad b_4^* = \frac{b_4}{a_4} \, a_4^* \, . \tag{14.61}$$

With these coordinates the equations of k_i and k_j are

$$\left.\begin{aligned} -(x^2+y^2) + x a_2^* + y \left[\frac{a_4}{b_4} (a_4 - a_2^*) + b_4 \right] &= 0 \, , \\ -(x^2+y^2) + x a_2 + y \left[\frac{a_4}{b_4} (a_4^* - a_2) + b_4^* \right] &= 0 \, . \end{aligned}\right\} \tag{14.62}$$

Both equations are, indeed, satisfied with (14.58) in combination with (14.54). End of proof.

Resolution of (14.59) for $\eta - a$ yields an expression which tends to zero for $\xi \to \pm\infty$. Consequently, the asymptote of p in the ξ, η-system has the equation $\eta = a$. Its intersection with p, i.e., the cardinal point H in Fig. 14.22, has the coordinates $\eta_{\mathrm{H}} = a$ and $\xi_{\mathrm{H}} = -ae/d$. The midline of all three pole quadrilaterals has the equation $\eta = a/2$. This follows from previous comments on Fig. 14.20.

Further properties of the pole curve are revealed by introducing in (14.59) for $\xi^2 + \eta^2$ the abbreviation r^2 and by resolving the equation for η. This results in the equations

$$\xi^2 + \eta^2 = r^2, \qquad \eta = a \, \frac{r^2 - \xi d/a}{r^2 + e} = \eta_{\mathrm{H}} \, \frac{r^2 + e\, \xi/\xi_{\mathrm{H}}}{r^2 + e} \, . \tag{14.63}$$

They are parameter equations with parameter r of a family of concentric circles centered at $\mathit{\Phi}$ and of a family of lines passing through the cardinal point H. The pole curve p is the geometric locus of all intersection points of the family of circles and the family of lines (for each value of r one circle and one line). The circle and the line for $r = 0$ intersect at the double point $\mathit{\Phi}$. From this it follows that the tangent to p in $\mathit{\Phi}$ passes through H. This follows more directly from the derivative of (14.59). At $\mathit{\Phi}$ it is $\eta' = -d/e = \eta_{\mathrm{H}}/\xi_{\mathrm{H}}$.

Proposition: A pole curve with parameters

$$a = 2\eta_{\mathrm{D}} \, , \qquad d = 2\xi_{\mathrm{D}} \eta_{\mathrm{D}} \, , \qquad e = \eta_{\mathrm{D}}^2 - \xi_{\mathrm{D}}^2 \tag{14.64}$$

has the double point $(\xi_{\mathrm{D}}, \eta_{\mathrm{D}})$ and at this point the derivatives

$$\xi'_{1,2} = \frac{\mathrm{d}\xi}{\mathrm{d}\eta}\Big|_{1,2} = \frac{\xi_\mathrm{D}}{\eta_\mathrm{D}} \pm \sqrt{1 + \left(\frac{\xi_\mathrm{D}}{\eta_\mathrm{D}}\right)^2} \,. \tag{14.65}$$

From the relationship $\xi'_2 = -1/\xi'_1$ it follows that the crossing at the double point is at right angles (Fig. 14.23).

Proof: In (14.59) a, d and e are replaced by the expressions in (14.64). In addition, the transformation $\xi = x + \xi_\mathrm{D}$, $\eta = y + \eta_\mathrm{D}$ to a parallel x, y-system with origin $(\xi_\mathrm{D}, \eta_\mathrm{D})$ is made. The resulting equation is quadratic in x:

$$x^2(y - \eta_\mathrm{D}) + 2xy\xi_\mathrm{D} + y^2(y + \eta_\mathrm{D}) = 0 \,. \tag{14.66}$$

It is satisfied by $x = y = 0$. The Taylor formula for the solutions in the neighborhood of the origin is $x_{1,2} = y\xi'_{1,2}$ with the expressions (14.65). End of proof.

The equation

$$e = \frac{a^2}{4} - \frac{d^2}{a^2} \tag{14.67}$$

resulting from (14.64) is a necessary condition for the existence of a double point. Because of the squaring of a and d it is not a sufficient condition.

A pole curve without double point is either bicursal (Fig. 14.22) or unicursal (the solid line in Fig. 14.23). Of which type it is can be seen directly from Fig. 14.18. An arbitrarily chosen quadrilateral (P_{ij},P_{jk},$\mathrm{P}_{k\ell}$,$\mathrm{P}_{\ell i}$)

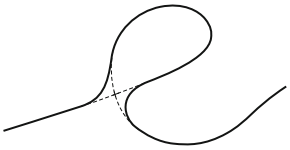

Fig. 14.23 Pole curve unicursal (solid line) and with double point (dashed line)

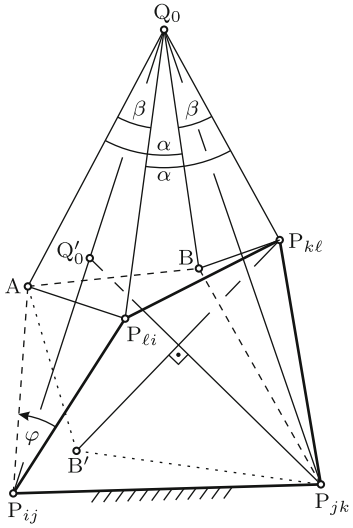

Fig. 14.24 Pole curve generated by a pole quadrilateral interpreted as four-bar

$(i, j, k, \ell = 1, 2, 3, 4$ different) is interpreted as mobile four-bar with two arbitrarily chosen neighboring poles, say P_{ij} and P_{jk}, serving as frame (Fig. 14.24). Following a rotation φ of the left crank (or rocker) the coupler $\overline{P_{\ell i}P_{k\ell}}$ is either in the position $\overline{AB}$ or in the position $\overline{AB'}$. The midnormal of $\overline{P_{\ell i}A}$ is intersected by the midnormal of $\overline{P_{k\ell}B}$ at Q_0 and by the midnormal of $\overline{P_{k\ell}B'}$ at Q_0'. Proposition: Q_0 and Q_0' are located on p.
Proof for Q_0: The triangles (Q_0,A,B) and (Q_0,$P_{\ell i}$, $P_{k\ell}$) have all three side lengths and, hence, also the angle α in common. Therefore, also the angles denoted β are equal. From Q_0 opposite sides of the quadrilateral are seen under identical angles ($\overline{P_{ij}P_{jk}}$ and $\overline{P_{\ell i}P_{k\ell}}$ under the angle α and $\overline{P_{ij}P_{\ell i}}$ and $\overline{P_{jk}P_{k\ell}}$ under the angle $\beta/2$). This ends the proof for Q_0. The proof for Q_0' is based on the congruence of the triangles (Q_0',A,B′) and (Q_0',$P_{\ell i}$,$P_{k\ell}$). End of proof.

The pole curve is composed of the trajectories of Q_0 and Q_0' generated when the shortest link of the four-bar is rotated through its entire angular range. Depending on the link lengths this range is either 2π (case I; fully rotating link) or $< 2\pi$ (case II). Conditions see in Grashof's Theorem 17.1 (Eq. (17.4)). In case I, the trajectories of Q_0 and Q_0' are isolated from each other which means that the pole curve is bicursal. In case II, the pole curve is unicursal. The curve has a double point if the four-bar is foldable.

14.6 Tilings

Tiles are congruent plane figures which, if properly arranged, fill the infinite plane without gaps and overlaps. The resulting pattern is called tiling. Every tile of a tiling can be made to coincide with any other tile of the same tiling by translation or rotation or reflection or glide reflection. The problem of finding all possible forms of tiles is an open problem (see Grünbaum/Shephard [6]). The present section is devoted to important contributions made by Heesch [8]. Without showing details of the theory his final results are presented because they have great aesthetical appeal as well as great economical and engineering importance. If the infinitely extended tiling as a whole coincides with itself after a rotation about a pole P_0 through an angle $2\pi/n$ (n integer), it coincides with itself also after a rotation about P_0 through any of the angles $2k\pi/n$ $(k = 1, \ldots, n)$. The tilings under consideration have the property that periodical translations in one or more directions $1, 2, \ldots$ with associated minimal period lengths $t_1, t_2, \ldots$ result in self-coincidence. Let t be the smallest of these period lengths. Translation by t carries the said rotation pole P_0 to a point P_1 at the distance t, and the translation by $-t$ carries it in the opposite direction to a point P_{-1} so that P_{-1}, P_0 and P_1 are collinear with equal distances t. Rotation about P_0 through the angle $2k\pi/n$ carries P_1 into a point $P(k, n)$. This point may coincide with P_{-1}. If it does not

coincide, however, then, by assumption, its distance from P_{-1} cannot be smaller than t. It is easily proved that this condition can be satisfied for all $k = 1, \ldots, n$ only with $n = 1, 2, 3, 4$ and 6. In the case $n = 5$, for example, it is not satisfied with $k = 2$. Thus, the only possible rotation angles are $2\pi/n$ with $n = 2, 3, 4$ and 6.

Heesch gives a list of 28 basic types of tiles. The boundary of a tile consists of at least two pairs and of at most five pairs of congruent segments. In each pair of segments one segment can be *arbitrarily prescribed* (continuously curved or with corners). The associated second segment is produced from this first one either by translation or by rotation or by glide reflection. In the case of rotation, one of the endpoints of the first segment is the pole, and the rotation angle is $2\pi/n$ with $n = 6, 4, 3$ or 2. A pair of segments with rotation angle $2\pi/n$ $(n = 6, 4, 3)$ is abbreviated C_nC_n, and a pair of segments with rotation angle $180°$ (i.e., a centrally symmetric line) is simply abbreviated C (instead of C_2C_2). Figures 14.25a and b show as examples a pair C_6C_6 and a line C.

Each segment in a pair of translated segments is abbreviated T, and each segment in a pair of glide-reflected segments is abbreviated G. A pair T···T must be disconnected (no intersections; no common endpoints). An example is shown in Fig. 14.25c. A pair of glide-reflected segments is either disconnected (G···G in Fig. 14.25d) or one endpoint of one segment coincides with the image of the other endpoint (GG in Fig. 14.25e).

A basic type of tile is identified as follows. With an arbitrarily chosen sense along the boundary the segments are sequentially listed by the symbols denoting the corresponding displacements (C_n, C, T or G). The complete sequence of symbols serves as identifier of the basic type. If the boundary contains two pairs of glide-reflected segments, these pairs are denoted $G_1 \cdots G_1$ and $G_2 \cdots G_2$. Likewise, two pairs of translated segments are denoted $T_1 \cdots T_1$ and $T_2 \cdots T_2$. If a boundary contains several pairs of rotated segments with identical rotation angles, the pairs are placed in brackets, for example $(C_4C_4)(C_4C_4)$. In this case, one segment C_4 of the first pair and one segment C_4 of the second pair can be prescribed independently and arbitrarily. In the case of two or more lines C all lines are independent.

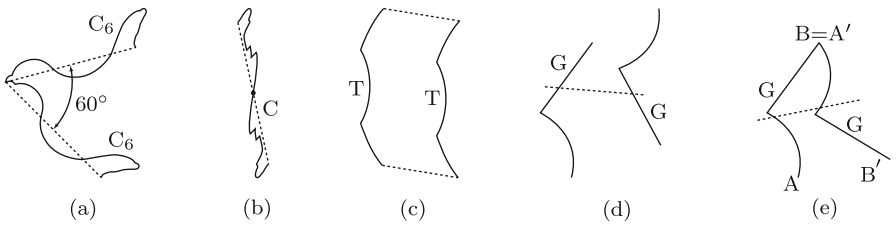

Fig. 14.25 Segment-pair C_6C_6 **(a)**, centrally symmetric curve C **(b)**, segment-pair T···T **(c)**, glide-reflected segment-pairs G···G **(d)** and GG **(e)**

The altogether 28 basic types are grouped in Table 14.2 as follows[1]. Numbers 1 and 2 involve translations only (T), numbers 3 and 4 glide reflections only (G), numbers 5 - 15 rotations only (C or C_n), numbers 16, 17, 18 T and C only, numbers 19, 20, 21 T and G only, numbers 22 - 26 C and G only and numbers 27 and 28 T, C and G.

Table 14.2 Basic types of tiles

1	$T_1T_2T_1T_2$	11	$(C_4C_4)(C_4C_4)$	21	$TG_1G_2TG_2G_1$ [2)]
2	$T_1T_2T_3T_1T_2T_3$	12	$(C_3C_3)(C_3C_3)(C_3C_3)$	22	CGG
3	$G_1G_1G_2G_2$	13	$C_3C_3C_6C_6$	23	CCGG
4	$G_1G_2G_1G_2$ [1)]	14	$C(C_4C_4)(C_4C_4)$	24	CGCG
5	CCC	15	$CC_3C_3C_6C_6$	25	$CG_1G_2G_1G_2$ [3)]
6	CCCC	16	TCTC	26	$CG_1CG_2G_1G_2$ [3)]
7	CC_3C_3	17	TCTCC	27	TCTGG
8	CC_4C_4	18	TCCTCC	28	TCCTGG
9	CC_6C_6	19	TGTG		
10	$(C_3C_3)(C_3C_3)$	20	$TG_1G_1TG_2G_2$		

[1)] The endpoints of the segments form a rectangle
[2)] The axes of both glide reflections are orthogonal to the translation of the pair $T\cdots T$
[3)] The axes of both glide reflections are orthogonal to each other

Remarks: The footnotes 1), 2) and 3) of the Table are conditions. In what follows, some geometrical properties are listed which do not represent conditions, but consequences of two general conventions. The first general convention requires that the boundary of each basic type is closed and free of double points. This implies that the freedom in choosing one segment per pair is not unlimited. The second general convention requires that in basic types with several pairs of the form C_nC_n in each pair the sense of direction of rotation (from the first segment to the second segment) be the same. These conventions have the following consequences which are not obvious immediately.
Basic type No. 3: The axes of both glide reflections are parallel.
Basic type No. 10: The four endpoints of the segments form a rhombus.
Basic type No. 11: The four endpoints of the segments form a square.
Basic type No. 12: The three poles form an equilateral triangle.
Basic type No. 13: The pole of the pair C_3C_3 lies outside the equilateral triangle formed by the pair C_6C_6.
Basic type No. 19: The axis of glide reflection is orthogonal to the translation of the pair $T\cdots T$. Begin by drawing the pair $T\cdots T$.
Basic types No. 20, 27, 28: All glide reflection axes are parallel to the translation of the pair $T\cdots T$. Begin by drawing the pair $T\cdots T$.

[1] From a mathematical point of view a different arrangement in a (6×10)-matrix is necessary in which rows correspond to displacement groups and columns to line nets. See Heesch [8]

The nine basic types No. 2, 12, 14, 15, 18, 20, 21, 26 and 28 represent principal types from which all other basic types can be produced by shrinking pairs of segments to zero. The following examples demonstrate the freedom of choice in the design of tiles.

Basic type No. 12 $(C_3C_3)(C_3C_3)(C_3C_3)$: In Fig. 14.26a the points A, B and P as well as the segment C_3 from A to B and the segment C_3 from A to P are freely chosen. 120°-rotations of these segments about B and P, respectively, produce the points A′ and A″. The pole D of the third pair C_3C_3 and the poles B and P form an equilateral triangle. The freely chosen segment C_3 from D to A′ is rotated through 120° about D. In Fig. 14.26b the tiling is shown. The salamander is a modification of a form originally drawn by the artist Escher. In a preface to one of Escher's books Heesch expresses his respect for Escher's intuitive grasp of the basic type $(C_3C_3)(C_3C_3)(C_3C_3)$. See also Coxeter's comments on Escher's work in Locher [12].

Basic type No. 15 $CC_3C_3C_6C_6$: In Fig. 14.27a the points A, B and D as well as the segment C_6 from A to B and the segment C_3 from A to D are freely chosen. Rotations about B through 60° and about D through 120° produce the points A′ and A″. These points are connected by a freely chosen centrally symmetric line C. In Fig. 14.27b the tiling is shown (published in 1985 in [5] p.56 and the same year as frontcover of the June issue of *mathe-plus. Duden-Zeitschrift für Schüler*).

Basic type No. 26 $CG_1CG_2G_1G_2$: In Fig. 14.28a the points A, B and A″ as well as the segment G_1 from A to B and the segment G_2 from B to A″ are freely chosen. The segment G_1 from A to B is glide-reflected to A′B′ (axis 1-1 of glide reflection and translation along the axis arbitrary). The segment G_2 from B to A″ is glide-reflected to B″A (condition: Axis

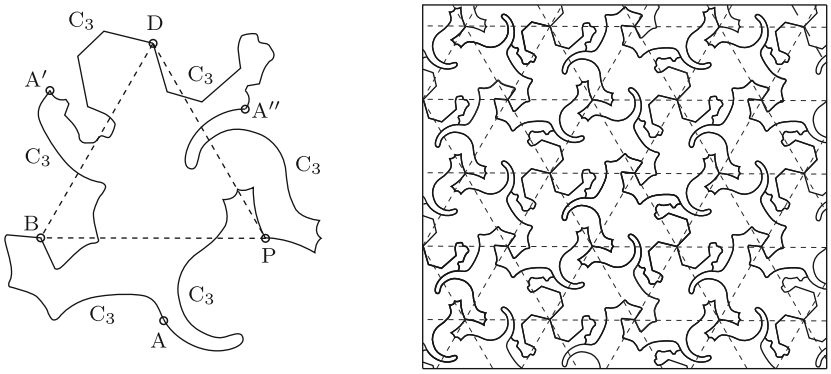

Fig. 14.26 Basic type $(C_3C_3)(C_3C_3)(C_3C_3)$ **(a)** and the resulting tiling **(b)**. No corner occurs at A so that this point is concealed

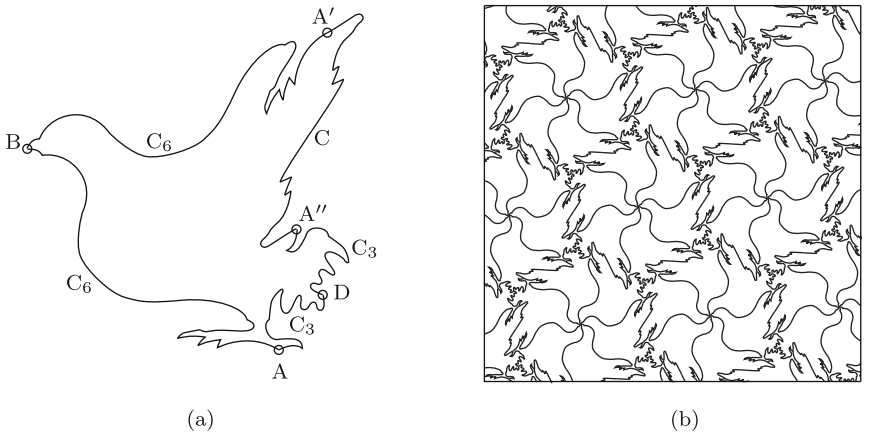

Fig. 14.27 Basic type $CC_3C_3C_6C_6$ **(a)** and the resulting tiling **(b)**. No corner occurs at A′ so that this point is concealed

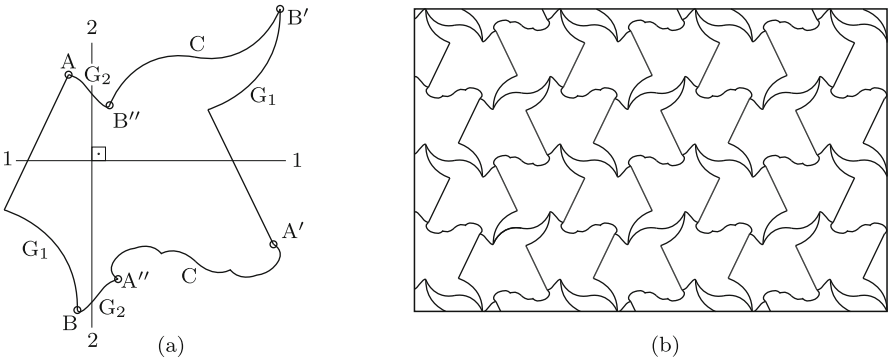

Fig. 14.28 Basic type $CG_1CG_2G_1G_2$ with mutually orthogonal glide-reflection axes **(a)** and the resulting tiling **(b)**

2-2 orthogonal to axis 1-1). Points A′ and A″ as well as B′ and B″ are connected by freely chosen centrally symmetric lines C . In Fig. 14.28b the tiling is shown.

Heesch's results have (quote Heesch) *two important fields of application: For one thing, they represent a basis for teaching all branches of art design with surfaces; on the other hand, they constitute a rationalization principle for the mass production of semi-finished products.* Mass-produced parts made of sheet metal for certain engineering purposes can often, without loss of functionality, be slightly changed in shape so as to become tiles. The production of sheet metal parts having this property reduces sheet metal waste, produc-

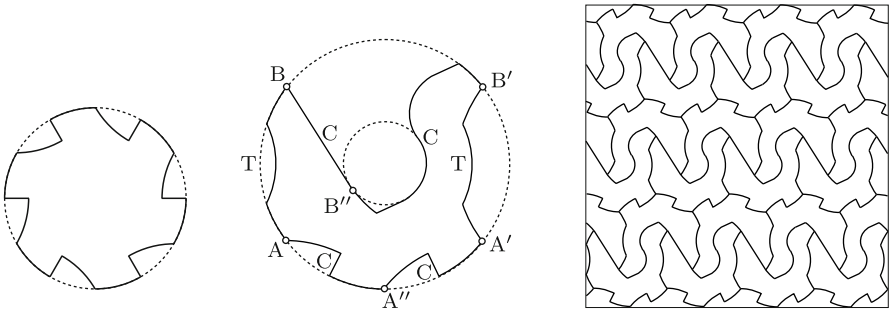

Fig. 14.29 Tile of type $(C_3C_3)(C_3C_3)(C_3C_3)$ fitting into a circle **(a)** and tile of type TCCTCC fitting into a circular ring the inner radius of which is one third of the outer radius **(b)**. The resulting tiling **(c)**

tion time per piece as well as wear of tools. In Figs. 14.29a,b two tiles are shown which fit into a circle. The tile in Fig. 14.29b leaves room for a central circular object. The tiling with this shape is shown in Fig. 14.29c.

Heesch's theory does not require symmetry of individual tiles. However, both axially symmetric tiles and centrally symmetric tiles can be obtained from many basic types by a proper choice of segments. To give an example, the basic type No. 2, $T_1T_2T_3T_1T_2T_3$, is a centrally symmetric hexagon if as segments T_1, T_2 and T_3 straight lines are chosen (lengths and directions arbitrary). Other important results obtained from Table 14.2 are the following.

Every triangle is a tile of the basic type CCC.

Every quadrilateral (convex or nonconvex) is a tile of the basic type CCCC.

Table 14.2 does not solve the problem for pentagons and hexagons completely, but it provides important contributions to the solution. For being a tile it is not necessary, but sufficient that two or more congruent polygons properly joined together represent a basic type. In Heesch/Kienzle [7] ten different sets of sufficient conditions are listed for pentagons and thirty for hexagons. Some of these sets of conditions are as follows.

Pentagons

1. A pentagon with two parallel sides is a tile. Two congruent pentagons of such a shape produce the basic type $T_1T_2T_3T_1T_2T_3$ (Figs. 14.30a,b). Special cases: Figure a with two or three or four or five sides of the pentagon equal in length.

2. A pentagon (convex or nonconvex) is a tile if it has two right angles with pairwise identical leg lengths (the thick lines in Fig. 14.31). As is shown in the same figure four congruent pentagons of such a shape produce the basic type $T_1T_2T_1T_2$. Special cases: Convex pentagons with three or four or five sides equal in length.

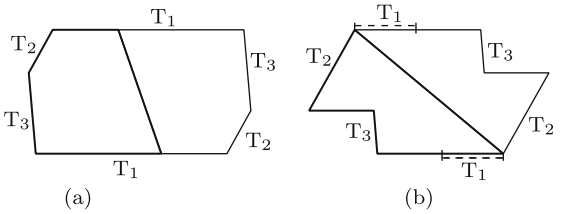

Fig. 14.30 Basic types $T_1T_2T_3T_1T_2T_3$ with two congruent pentagons (convex and nonconvex) with two parallel sides

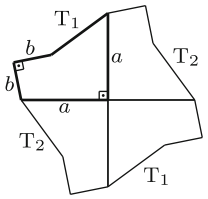

Fig. 14.31 Basic type $T_1T_2T_1T_2$ with four congruent pentagons

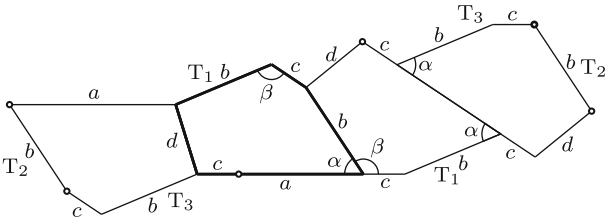

Fig. 14.32 Basic type $T_1T_2T_3T_1T_2T_3$ produced from four congruent pentagons having two non-adjacent sides of equal lengths b and angles $\alpha + \beta = 180°$. Segments T_1, T_2, T_3 of the boundary are marked by small circles

3. A pentagon is a tile if it has two nonadjacent sides of equal length b and angles $\alpha + \beta = 180°$ (the thick lines in Fig. 14.32). As is shown in the same figure four congruent pentagons of such a shape produce the basic type $T_1T_2T_3T_1T_2T_3$. The same is true if the condition $\alpha+\beta = 180°$ is replaced by the condition $\alpha + \beta = 360°$. Special cases: Three or four or five sides of the pentagon equal in length.

Hexagons: Let the sides of the hexagon be sequentially labeled 1 to 6.
1. A hexagon is a tile if (i) sides 1 and 3 are parallel and (ii) sides 4 and 6 are parallel (Fig. 14.33 a or b)
2. A hexagon is a tile if sides 1, 3 and 5 are parallel (Fig. 14.33c)
3. A hexagon is a tile if either sides 1 and 3 or sides 1 and 4 are (i) parallel and (ii) equal in length (Fig. 14.33d or e).

It is left to the reader to produce from each of the Figs. 14.33a–e a basic type by joining several congruent hexagons together.

It was said that the conditions on pentagons and hexagons given by Heesch/Kienzle are sufficient, but not necessary. For the following statements the reader is referred to Schattschneider [14] and Grünbaum/Shephard [6]. 1. The number of different types of convex pentagonal tiles is unknown. Many types are known, including types not satisfying the conditions given by Heesch/Kienzle.
2. The number of different types of convex hexagonal tiles is known to be three.

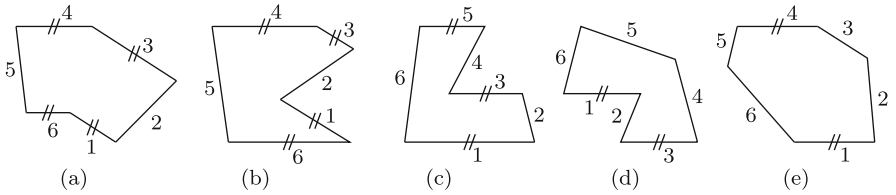

Fig. 14.33 Hexagonal tiles. **(a)** and **(b)** Sides 1 and 3 parallel, and sides 4 and 6 parallel; **(c)** Sides 1 , 3 and 5 parallel; **(d)** Sides 1 and 3 parallel and equal in length; **(e)** Sides 1 and 4 parallel and equal in length

3. Convex polygonal tiles with seven or more corners do not exist.
4. With many polygonal tiles more than one tiling is possible. Example: In the case $a = b$ the pentagon in Fig. 14.31 admits the tiling shown in Fig. 14.32. A more remarkable example is the equilateral pentagon with internal angles $140°$, $60°$, $160°$, $80°$, $100°$ (in this order) found by Rice (see Schattschneider [14]). Since there are eleven ways in which these angles can be combined to make $360°$, several different tilings are possible, including two which display rotational and no other form of symmetry. This pentagon is composed of a rhomb and an equilateral triangle. It is a special case of the type shown in Fig. 14.30a .

References

1. Bereis R (1951) Aufbau einer Theorie der ebenen Bewegung mit Verwendung komplexer Zahlen. Österr.Ing.-Arch. 5:246–266
2. Blaschke W, Müller H R (1956) Ebene Kinematik. Oldenbourg, München
3. Blaschke W (1985) Gesammelte Werke, v.2: Works of W. Blaschke on Kinematics (18 titles; pp.33–209). Thales, Essen
4. Burmester L (1888) Lehrbuch der Kinematik. Felix,Leipzig
5. Chatterji S D, Fenyö I, Kulisch U (1985) Jahrbuch Überblicke Mathematik (Mathematical Surveys) 18, B.I. Wissenschaftsverlag
6. Grünbaum B, Shephard G C (1987) Tilings and patterns. Freeman and Co.
7. Heesch H, Kienzle O (1963) Flächenschluss. System der Formen lückenlos aneinanderschliessender Flachteile. Springer, Berlin
8. Heesch H (1968) Reguläres Parkettierungsproblem. Westdeutscher Verl., Köln, Opladen
9. Klein F, Müller C (eds.) (1901-1908) Enzyklopädie der Math. Wissenschaften. v.IV: Mechanik. Teubner, Leipzig
10. Koenigs G (1897) Leçons de cinématique. Avec des notes par G. Darboux, E. et F. Cosserat. Hermann, Paris
11. Koenigs G (1905) Introduction à une théorie nouvelle des méchanismes. Hermann, Paris
12. Locher J L (1971) Die Welten des M.C. Escher. Meulenhoff International Amsterdam. German trans. Manfred Pawlak Verl.-Ges. mbH, Herrsching
13. Luck K, Modler K-H (1990) Getriebetechnik. Analyse, Synthese, Optimierung. Springer, Berlin, Heidelberg, New York

14. Schattschneider D (1982) Tiling the plane with congruent pentagons. Mathematics Magazine 51, No.1:29–44
15. Schoenflies A, Grübler M (1908) Kinematik. In: [9]:190–278
16. Wunderlich W (1970) Ebene Kinematik. BI-Verl. Mannheim

Chapter 15
Plane Motion

The present chapter is devoted to theorems on centrodes, to curvature theory, to properties of trochoids with applications and to related problems. Literature: Koenigs [20, 21], Schoenflies/Grübler [26], Bereis [1], Blaschke /Müller [3], Geronimus [11], Wunderlich [30].

15.1 Instantaneous Center of Rotation. Centrodes

According to (9.13) the instantaneous velocity distribution in a rigid body in an arbitrary state of motion is determined by the velocity $\mathbf{v}_A$ of a single point A and by the angular velocity $\boldsymbol{\omega}$:

$$\mathbf{v} = \mathbf{v}_A + \boldsymbol{\omega} \times \boldsymbol{\varrho} \,. \tag{15.1}$$

If the velocity $\mathbf{v}_A(t)$ of the single point A is, independent of t, in a fixed plane Σ_A, and if, in addition, $\boldsymbol{\omega}(t)$ is, independent of t, orthogonal to Σ_A, the velocity $\mathbf{v}(t)$ of every point of the body and, consequently, also its trajectory, is in a plane parallel to Σ_A. This state of motion of the body is called plane motion. In the special case $\boldsymbol{\omega}(t) \equiv \mathbf{0}$, plane motion is pure translation with velocity $\mathbf{v}_A(t)$. In what follows, $\boldsymbol{\omega}(t) \neq \mathbf{0}$ is assumed. In this general case, the screw axis (ISA) has the constant direction of $\boldsymbol{\omega}(t)$, and the pitch is $p \equiv 0$ (see (9.23)). The perpendicular from A onto the screw axis is *instantaneously*

$$\mathbf{u} = \frac{\boldsymbol{\omega} \times \mathbf{v}_A}{\boldsymbol{\omega}^2} \,. \tag{15.2}$$

If as point A a point on the instantaneous screw axis is chosen, (15.1) becomes

$$\mathbf{v} = \boldsymbol{\omega} \times \boldsymbol{\varrho} \,. \tag{15.3}$$

J. Wittenburg, *Kinematics*, DOI 10.1007/978-3-662-48487-6_15

This equation shows that the instantaneous velocity distribution is that of a rotation with $\boldsymbol{\omega}$ about what is called *instantaneous axis of rotation*.

In what follows, the body is represented by a single body-fixed plane Σ_2 which is moving in a reference plane Σ_1. The body-fixed point A, its velocity $\mathbf{v}_A$ and the vector $\mathbf{u}$ are located in Σ_2 as well as in Σ_1. The point at the tip of $\mathbf{u}$ is the point of intersection of the instantaneous axis of rotation with both planes. This point is referred to as *instantaneous center of rotation* P because Σ_2 is instantaneously rotating about P. During a *continuous plane motion* which is not a rotation about a fixed axis the instantaneous center P is neither fixed in Σ_2 nor fixed in Σ_1. Its trajectory in Σ_2 is called *moving centrode* $\mathrm{k_m}$. It is determined by the time-varying vector $\mathbf{u}(t)$ given by (15.2). The trajectory of P in Σ_1 is called *fixed centrode* $\mathrm{k_f}$. At every time t both centrodes have point P in common and, at this point, zero relative velocity. Let $\mathbf{v}_{\mathrm{rel}}$ be the velocity of P along the moving centrode. Then its velocity along the fixed centrode is, according to (9.11), $\mathbf{v} = \mathbf{v}_A + \boldsymbol{\omega} \times \mathbf{u} + \mathbf{v}_{\mathrm{rel}} = \mathbf{v}_{\mathrm{rel}}$. Hence the tangents of the centrodes at P coincide (see Fig. 15.1). These results are summarized in

Theorem 15.1. *During a continuous plane motion of a body the moving centrode* $\mathrm{k_m}$ (*fixed in* Σ_2) *is rolling without slipping on the fixed centrode* $\mathrm{k_f}$ (*fixed in* Σ_1).

This theorem is a special case of Painlevé's Theorem 9.6 on the raccording motion of two axodes which are generated by the instantaneous screw axis in general spatial motion of a rigid body. In plane motion the screw axis is the instantaneous axis of rotation. Both axodes are general cylinders. The raccording motion is pure rolling. The centrodes are the intersections of the cylinders with the planes Σ_1 and Σ_2.

Inverse motion: The inverse of the motion of Σ_2 relative to Σ_1 is the motion of Σ_1 relative to Σ_2. Both motion and inverse motion have the same instantaneous center of rotation P and the same centrodes in Σ_1 and in Σ_2. What the fixed centrode is for the inverse motion is the moving centrode

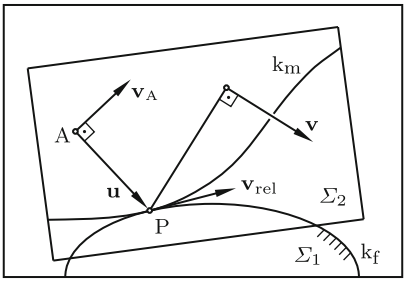

Fig. 15.1 Fixed centrode $\mathrm{k_f}$ in reference plane Σ_1, moving centrode $\mathrm{k_m}$ in body-fixed plane Σ_2, instantaneous center of rotation P and vector $\mathbf{u}$

for the motion and vice versa. In both motion and inverse motion P moves along the centrodes with equal velocities.

15.1.1 Theorems of Burmester and Kennedy/Aronhold

Equation (15.2) determines the location of the instantaneous center P. In Sect. 15.2.1 a simpler equation in terms of complex numbers is formulated. For most practical purposes the following geometric method of construction is preferable. According to (15.3) the vector from the center P to an arbitrary point of the body is orthogonal to the velocity $\mathbf{v}$ of this point. From this it follows that P lies on the normal of $\mathbf{v}$ through the body point under consideration. Two nonparallel normals determine P uniquely. Consequently, P is known if for two body points with nonparallel velocities the directions of these velocities are known. Neither the magnitudes nor the senses of direction need be known. If the velocities are parallel, also their magnitudes must be known. There are two special cases.
1. Permanent rotation about an axis fixed in Σ_1 and, consequently, also fixed in Σ_2. In this case, the point P on this axis is not only instantaneous, but permanent center of rotation. Centrodes do not exist.
2. Pure translation: All points of Σ_2 have identical velocities. The angular velocity is $\boldsymbol{\omega} = \mathbf{0}$. Equation (15.2) states that the center P is the infinitely distant intersection of the normals to these velocities.

In Fig. 15.2 a body is shown together with the instantaneous center P. The velocity $\mathbf{v}_i$ of an arbitrary body-fixed point P_i is proportional to the radius $\overline{\mathrm{PP}}_i$. Let the *rotated velocity* $\mathbf{v}_i^*$ be the vector $\mathbf{v}_i$ rotated counterclockwise through $\pi/2$. It is pointing towards P. Elementary geometry yields Burmester's

Theorem 15.2. *The polygon connecting the tips of the rotated velocities* $\mathbf{v}_i^*$ *of points* P_i $(i = 1, 2, \dots)$ *is both similar and directed parallel to the polygon* $\mathrm{P}_1, \mathrm{P}_2, \dots$.

This theorem is valid independent of the scale chosen for the velocity vectors. If, in particular, the scale is chosen such that all vectors $\mathbf{v}_i^*$ terminate at P, the similar polygon degenerates to the point P.

If three bodies i, j and k are in plane motion relative to each other, there exist, at any time t, three instantaneous centers P_{ij}, P_{jk}, P_{ki} and three relative angular velocities $\boldsymbol{\omega}_{ij}$, $\boldsymbol{\omega}_{jk}$, $\boldsymbol{\omega}_{ki}$. Definition: $\boldsymbol{\omega}_{ij}$ is the angular velocity of body i (first index) relative to body j. Then

$$\boldsymbol{\omega}_{ji} = -\boldsymbol{\omega}_{ij} \,. \tag{15.4}$$

In addition, $\boldsymbol{\omega}_{ik} = \boldsymbol{\omega}_{ij} + \boldsymbol{\omega}_{jk}$ is valid and, consequently,

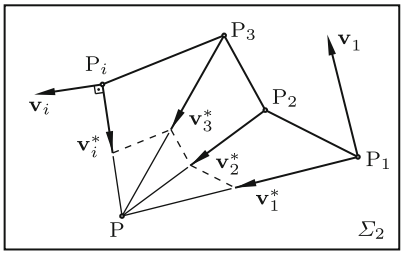

Fig. 15.2 Velocities $\mathbf{v}_i$ and rotated velocities $\mathbf{v}_i^*$ of body-fixed points P_i

$$\boldsymbol{\omega}_{ij} + \boldsymbol{\omega}_{jk} + \boldsymbol{\omega}_{ki} = \mathbf{0} \,. \tag{15.5}$$

In multi-link mechanisms it frequently happens that for less than two points of some link the directions of the velocities are known. In such cases, the geometric construction of the instantaneous center requires

Theorem 15.3. (Kennedy/Aronhold)[1] *The instantaneous centers* P_{ij} , P_{jk} *and* P_{ki} *of three bodies* i , j , k *in plane motion relative to each other are collinear.*

Proof: Suppose the centers P_{ik} and P_{jk} are known (Fig. 15.3). The center P_{ij} is the point at which body i and body j have equal velocities $\mathbf{v}$ relative to body k. This establishes the equation $\boldsymbol{\omega}_{ik} \times \boldsymbol{\varrho}_{\mathrm{P}_{ik}\mathrm{P}_{ij}} = \boldsymbol{\omega}_{jk} \times \boldsymbol{\varrho}_{\mathrm{P}_{jk}\mathrm{P}_{ij}}$. The two vector products are collinear only if $\boldsymbol{\varrho}_{\mathrm{P}_{ik}\mathrm{P}_{ij}}$ and $\boldsymbol{\varrho}_{\mathrm{P}_{jk}\mathrm{P}_{ij}}$ are collinear. This ends the proof already. In addition, the equation requires the two vector products to be equal in magnitude and in sense of direction. If $\boldsymbol{\varrho}_{\mathrm{P}_{ik}\mathrm{P}_{ij}}$ and $\boldsymbol{\varrho}_{\mathrm{P}_{jk}\mathrm{P}_{ij}}$ have equal directions (opposite directions), also $\boldsymbol{\omega}_{ik}$ and $\boldsymbol{\omega}_{jk}$ have equal directions (opposite directions). Hence the scalar magnitudes satisfy

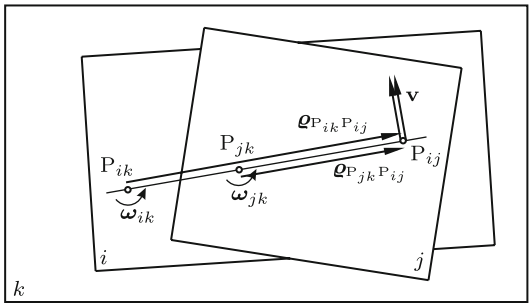

Fig. 15.3 Theorem of Kennedy and Aronhold

[1] Aronhold 1882, Kennedy 1886. See Kennedy [18]

the equation

$$\frac{\omega_{ik}}{\omega_{jk}} = \frac{\varrho_{\mathrm{P}_{jk}\mathrm{P}_{ij}}}{\varrho_{\mathrm{P}_{ik}\mathrm{P}_{ij}}} \,. \tag{15.6}$$

The theorem of Kennedy and Aronhold is a special case of the theorem stating that three instantaneous screw axes associated with spatial motions of three bodies relative to each other have a common perpendicular (see Sect. 12.1).

15.1.2 Illustrative Examples

In this section the importance of instantaneous centers and of centrodes for the solution of practical problems is illustrated by eight examples.

Example 1 : Cam mechanism
The cam mechanism of Fig. 6.15 is investigated again. The missing instantaneous center P_{12} is determined from (15.6) by setting $k = 0\,,\ i = 1\,,\ j = 2\,,$ $\omega_{10} = \dot{\varphi}_1$ and $\omega_{20} = \dot{\varphi}_2$. The distance between P_{10} and P_{20} is the constant $\sqrt{a^2 + b^2}$. Hence $\varrho_{\mathrm{P}_{20}\mathrm{P}_{12}} = \varrho_{\mathrm{P}_{10}\mathrm{P}_{12}} - \sqrt{a^2 + b^2}$. Therefore, with the abbreviation $\varrho_{\mathrm{P}_{10}\mathrm{P}_{12}} = \varrho\,,\ \dot{\varphi}_1/\dot{\varphi}_2 = (\varrho - \sqrt{a^2 + b^2})/\varrho$ or

$$\varrho = \frac{\sqrt{a^2 + b^2}}{1 - \dot{\varphi}_1/\dot{\varphi}_2} \,. \tag{15.7}$$

In the rotating x, y-system P_{12} has the coordinates $x = -\varrho\cos\varphi_1\ ,\ y = \varrho\sin\varphi_1$. The ratio $\dot{\varphi}_1/\dot{\varphi}_2$ and the angle φ_1 are known functions of φ_2 (see (6.114) and (6.115)). The coordinates $x(\varphi_2)\,,\ y(\varphi_2)$ determine the centrode fixed on the cam. It was shown that during the quarter revolution of the ellipse from the position $\varphi_1 = \varphi_2 = 0\ ,\ \alpha = \pi/4$ to the position $\varphi_1 = \pi/2\ ,\ \varphi_2 = 0\ ,\ \alpha = 3\pi/4$ the ratio $\dot{\varphi}_1/\dot{\varphi}_2$ changes from the extremal value $2a^2/(a^2 - b^2)$ through ∞ at $\varphi_2 = \varphi_{2_{\max}}$ to the extremal value $-2b^2/(a^2 - b^2)$. The associated points of the centrode have the coordinates $[\,x = 0\,,\ y = -(a^2 - b^2)/\sqrt{a^2 + b^2}\,]\ ,\ [\,x = 0\,, y = 0\,]$ and $[\,x = (a^2 - b^2)/\sqrt{a^2 + b^2}\ ,\ y = 0\,]$, respectively. The entire centrode is obtained by reflecting the curved segment connecting these three points in the x-axis and in the y-axis. The centrode has the form of a rosette with four leaves of equal length (one pair of leaves different in shape from the other). Similar arguments lead to equations for the centrode fixed on the follower. This centrode is an oval with a single axis of symmetry along the bisector of the right angle.

Example 2 : Elliptic trammel
In Fig. 15.4a a rod of length ℓ is shown the endpoints A and B of which move along mutually orthogonal guides. These guides define the plane Σ_1 . The rod is part of the infinitely extended plane Σ_2 . The instantaneous center P is the intersection point of the perpendiculars drawn as dashed lines. In

every position of the rod its distances from M and from the midpoint C of the rod are ℓ and $\ell/2$, respectively. From this it follows that the circles shown in the figure are the centrodes. Theorem 15.1 says that the small circle k_2 fixed on the rod rolls in the big circle k_1 fixed in Σ_1.

Remark: In Sect. 10.1 the motion of a body with a fixed point 0 was investigated two points P_1 and P_2 of which are constrained to two mutually orthogonal fixed planes E_1 and E_2, respectively. In the projection along the line of intersection of E_1 and E_2 these planes are mutually orthogonal guides for the projections of P_1 and P_2. When the apex angle α in the triangle $(P_1,0,P_2)$ is very small, the polhode cone and the herpolhode cone have the circular cross sections described by Eqs.(10.21). These are the circles shown in Fig. 15.4a where the two points are called A and B. End of remark.

Obviously, not only the points A and B on the circumference of k_2, but every point on this circumference moves along a straight line through M. Hence two wheels having the diameter ratio $1:2$ can be used for guiding the endpoints of a rod along two lines under an arbitrary angle α (see Fig. 15.4b). If ℓ is again the rod length, the radius of the small wheel is $\ell/(2\sin\alpha)$. This follows from the theorem that in the small circle the central angle subtended by the chord ℓ equals 2α.

During two full revolutions of k_2 the rod moves through all four quadrants of k_1. From an engineering point of view the generation of this motion by means of two toothed wheels is better than by sliding two points along straight guides. The simplest possible forms of toothed wheels are shown in Fig. 15.5. On the small wheel cylinders of arbitrary diameter are fixed with their centers on the circumference of k_2. Every cylinder is moving in a slot cut into the big wheel. The cylinders and the slots are the flanks of the teeth. The minimum number of teeth is two. Pins, as the cylinders are called, are the historically oldest forms of teeth. See also Sec. 16.1.5.

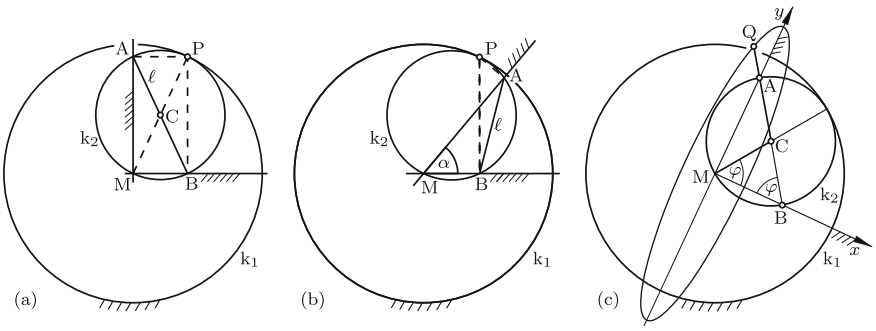

Fig. 15.4 Orthogonal **(a)** and nonorthogonal **(b)** guides for points A and B. Fixed centrode k_1 and moving centrode k_2. Elliptical trajectory of Q fixed in Σ_2 **(c)**

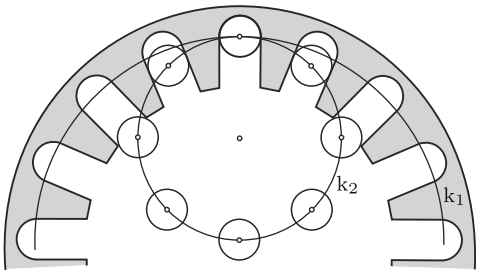

Fig. 15.5 Pinion with eight cylindric pins. Circles k_1 and k_2 of Fig. 15.4a

In what follows, the trajectory of an arbitrary point Q fixed in Σ_2 is investigated. The straight line passing through Q and C intersects k_2 at two points A and B (see Fig. 15.4c). After what has been said these points move along mutually orthogonal straight lines passing through M. These lines fixed in Σ_1 constitute the x, y-system best suited for the description of the trajectory of Q. With r denoting the radius of the small circle and with the distance R of Q from C the x, y-coordinates of Q are

$$x = (r - R)\cos\varphi\,, \qquad y = (r + R)\sin\varphi\,. \tag{15.8}$$

In the special cases $R = r$ and $R = -r$, these are the equations of the straight lines $x \equiv 0$ and $y \equiv 0$, respectively. In all other cases, the constraint equation $\cos^2\varphi + \sin^2\varphi = 1$ produces the equation of an ellipse:

$$\frac{x^2}{(r-R)^2} + \frac{y^2}{(r+R)^2} = 1\,. \tag{15.9}$$

The semi-axes $|r - R|$ and $|r + R|$ are the distances of Q from A and from B, respectively. Hence the conclusion: A rod with endpoints moving along straight guides as well as a set of gear wheels having the diameter ratio $1 : 2$ is capable of generating elliptical trajectories with arbitrary ratio of principal axes. For this reason both systems are referred to as *elliptic trammel*.

Darboux Motion

Before continuing with plane motion a harmonic translation along the axial z-axis is superimposed on the rolling motion. Let $z(\varphi) = a\sin\varphi$ with arbitrary amplitude a be the displacement when the radius $\overline{\mathrm{MC}}$ is under the angle φ against the x-axis as shown in Fig. 15.4c. In this so-called Darboux motion the circles k_1 and k_2 are the cross sections of raccording cylinders.

Proposition: The trajectory of every body-fixed point is located in a plane (every point in its own plane) and, furthermore, these trajectories are either ellipses or straight-line segments.

Proof: As representative point the point is chosen which has in the position $\varphi = 0$ the coordinates $x = (r - R)\cos\varphi_0$, $y = (r + R)\sin\varphi_0$, $z = z_0$

with arbitrary constants R, φ_0, z_0. In the position $\varphi \neq 0$ (arbitrary) it has the coordinates $x(\varphi) = (r - R)\cos(\varphi + \varphi_0)$, $y(\varphi) = (r + R)\sin(\varphi + \varphi_0)$, $z(\varphi) = a\sin\varphi + z_0$. The trajectory is in a plane if these coordinates are linearly dependent, i.e., if there are constants F, G, K such that $Fx(\varphi) + Gy(\varphi) + z(\varphi) + K \equiv 0$. This is the condition

$$\begin{aligned} &\sin\varphi\,[-F(r-R)\sin\varphi_0 + G(r+R)\cos\varphi_0 + a] \\ &+\cos\varphi\,[\ F(r-R)\cos\varphi_0 + G(r+R)\sin\varphi_0] \quad + K + z_0 \equiv 0\,. \end{aligned} \tag{15.10}$$

It is satisfied by

$$F = \frac{a\sin\varphi_0}{r-R} \qquad G = -\frac{a\cos\varphi_0}{r+R} \qquad K = -z_0\,. \tag{15.11}$$

This proves that the trajectory is planar. That it is either an ellipse or a straight-line segment follows from the fact that its projection onto the x, y-plane is described by (15.9). End of proof. Darboux [7] showed that this special motion is the only nonplanar motion (planar in the narrower sense defined following (15.1)) having the property that every body-fixed point is moving in a plane (see also Bottema/Roth [4]).

After this digression the plane motion shown in Fig. 15.4a is considered again. In what follows, the inverse motion is investigated. This means that the small circle k_2 is stationary. The large circle k_1 is rolling on k_2. Every diameter of k_1 is sliding through a fixed point on k_2. This is shown in Fig. 15.6a. The two mutually perpendicular diameters of k_1 which up to now were fixed guides for moving points A and B are now moving lines g_1 and g_2 which are guided through fixed points A and B, respectively. An engineering realization is the Oldham coupling of which an exploded view is shown in Fig. 15.6b. The fixed points A and B are located on the axes of two parallel shafts with discs 1 and 2. Grooves on these discs are guides for the lines g_1 and g_2 which are materialized as rails on the central disc 3. The Oldham coupling transmits the angular velocity of one shaft to the other.

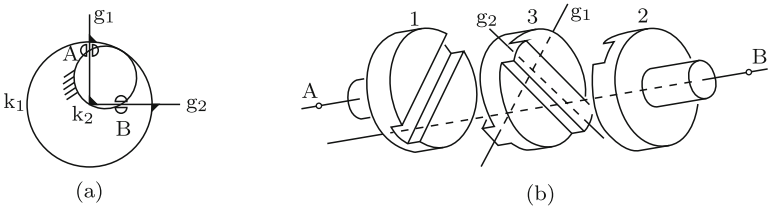

Fig. 15.6 Mutually perpendicular lines g_1 and g_2 guided through fixed points A and B **(a)** and exploded view of Oldham coupling **(b)**

Figure 15.7a shows the circle k_1 rolling on the fixed circle k_2. As in Fig. 15.4a the radii are denoted ℓ for k_1 and $\ell/2$ for k_2. Also the notations P and M for the instantaneous center of rotation and for the center of k_1 are the same. To be investigated is the trajectory of an arbitrary point Q fixed on k_1 at the radius R ($R<\ell$ or $R=\ell$ or $R>\ell$). This point Q determines two mutually perpendicular diameters fixed on k_1 which are sliding through fixed points A and B on the circumference of k_2. The trajectory of Q, from now on abbreviated q, is most easily described in the x,y-system with origin A and with the x-axis along the diameter $\overline{AB}$ of k_2. The polar coordinates r and φ of Q are related through the equation[2]

$$r(\varphi) = \ell\cos\varphi + R \tag{15.12}$$

(right-angled triangle (M,A,B)). The x,y-coordinates are

$$\left.\begin{aligned} x(\varphi) &= r\cos\varphi = (\ell\cos\varphi + R)\cos\varphi\ , \\ y(\varphi) &= r\sin\varphi\ = (\ell\cos\varphi + R)\sin\varphi\ . \end{aligned}\right\} \tag{15.13}$$

Elimination of φ yields the implicit equation

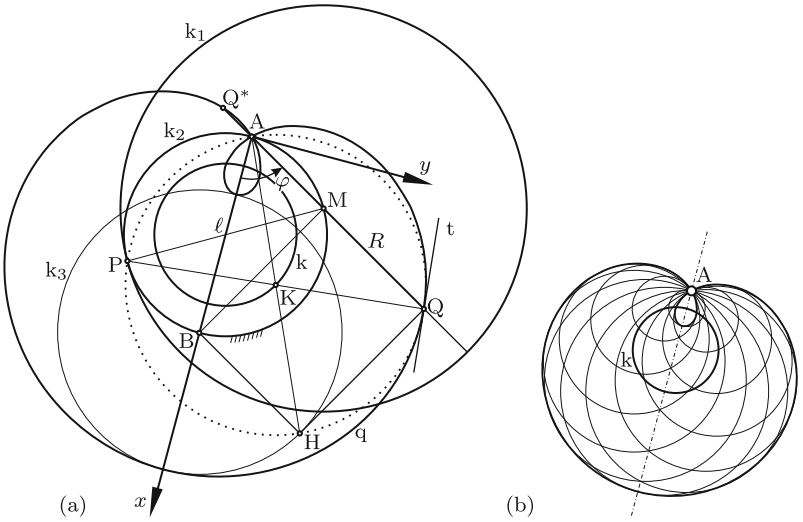

Fig. 15.7 Fig. **a:** Fixed circle k_2 of radius $\ell/2$ and rolling circle k_1 of radius ℓ. Mutually perpendicular diameters of k_1 sliding through fixed points A and B. Limaçon of Pascal q traced by Q. Fig. **b:** Limaçon of Pascal enveloped by circles centered on the circle k and passing through A

[2] A curve having the polar-coordinate equation $r(\varphi) = f(\varphi)+$ const is said to be a *conchoid* of the curve with the polar-coordinate equation $r(\varphi) = f(\varphi)$. By this definition, the limaçon of Pascal is a conchoid of the circle k_2

$$(x^2 + y^2 - \ell x)^2 = R^2(x^2 + y^2) \,. \tag{15.14}$$

In terms of the dimensionless quantities $\xi = x/\ell$, $\eta = y/\ell$ and $\varrho = R/\ell$ the equation is

$$(\xi^2 + \eta^2 - \xi)^2 = \varrho^2(\xi^2 + \eta^2) \,. \tag{15.15}$$

These curves are called limaçons of Pascal (after Etienne Pascal, father of Blaise Pascal).

Equation (15.14) shows that the x-axis is an axis of symmetry of q. The equation does not change if R is replaced by $-R$. Hence two points Q and Q^* located symmetrically to M trace one and the same limaçon of Pascal. The reason is that the center M of k_1 circles k_2 twice per revolution of k_1. After half a revolution M is in its initial position, while Q is in the position Q^* opposite M. Other properties of limaçons of Pascal are explained geometrically as follows. In Fig. 15.7a the line $\overline{QH}$ perpendicular to the line $\overline{AQ}$ is drawn. It is tangent to the circle k_3 with radius R and with fixed center B. From this it follows that the limaçon of Pascal q is the *pedal curve* of this circle. The pedal curve of an arbitrary curve c is defined as follows. From a fixed point A perpendiculars are dropped to all tangents of c. The curve connecting the feet of these perpendiculars is the pedal curve of c. From this it follows that q is tangent to k_3 at the points of intersection with the x-axis.

The tangent t of q in Q is perpendicular to $\overline{PQ}$ since P is instantaneous center. The midpoint K of $\overline{PQ}$ is also midpoint of $\overline{AH}$. Thales' circle over $\overline{PQ}$ (the dotted circle) passes through the fixed point A (also through H). At Q it is tangent to q. Points H and K vary with φ. Their cartesian coordinates x_H, y_H and x_K, y_K are related through the equations $x_H = 2x_K$ and $y_H = 2y_K$. Since H lies on the fixed circle $(x_H - \ell)^2 + y_H^2 = R^2$, point K lies on the fixed circle $(x_K - \ell/2)^2 + y_K^2 = (R/2)^2$. This is the circle k shown in Fig. 15.7a. It is concentric with k_2, and its radius is $R/2$. These facts are summarized in the statement that q is enveloped by all circles centered on k and passing through A. This is demonstrated in Fig. 15.7b in which A and the circle k are copied from Fig. 15.7a.

Next, the polar-coordinate equation (15.12) is considered again: $r(\varphi) = \ell\cos\varphi + R$. In the case $R < \ell$, the function $r(\varphi)$ has two roots. They are associated with the double point A of q (Fig. 15.8a). In the case $R = \ell$, $r(\varphi)$ has a double root. In this case, q has a cusp at A (Fig. 15.8b). This curve is called *cardioid*. In the case $\ell < R < 2\ell$, shapes with inflection points result (Fig. 15.8c), and in the case $R > 2\ell$, shapes without inflection points (Fig. 15.8d). In the case $R > \ell$, the fixed point A is an isolated point which is not part of the trajectory traced by Q. Equation (15.14) is satisfied by the coordinates $x = y = 0$ of A independent of R, whereas the polar-coordinate equation $r(\varphi) = \ell\cos\varphi + R$ shows that $r = 0$ is possible if and only if $R \le \ell$.

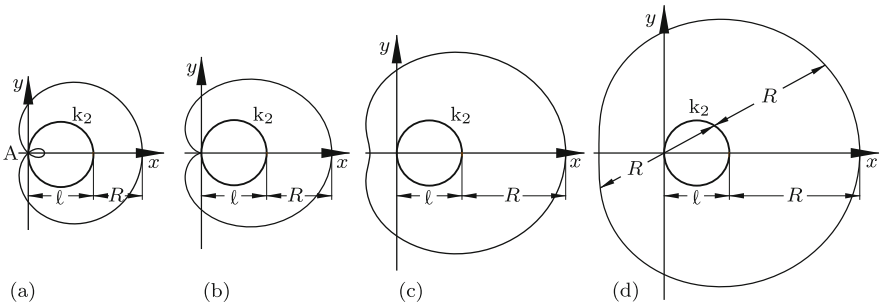

Fig. 15.8 Limaçons of Pascal with double point A **(a)**, with a cusp (cardioid **(b)**), with inflection points **(c)** and without inflection points **(d)**

The generation of ellipses and of limaçons of Pascal by means of an elliptic trammel is made use of in many engineering apparatuses (examples see in Wunderlich [30]).

Example 3: Body with one line passing through a fixed point and with one point moving along a fixed line

In Fig. 15.9 the x, y-system is the fixed frame Σ_1, and the ξ, η-system is the moving body Σ_2. The body-fixed η-axis is constrained to pass through point A fixed in the frame at $x = a$, and point B fixed on the body at $\xi = b$ is constrained to move along the frame-fixed y-axis. To be determined are the equations of the fixed centrode $\mathrm{k_f}$ in the x, y-system and of the moving centrode $\mathrm{k_m}$ in the ξ, η-system. In addition, equations are to be formulated for the trajectory of the body-fixed point Q with coordinates $\xi = v$, $\eta = u$ (arbitrary).

Solution: Motion and inverse motion (motion of Σ_1 relative to Σ_2) are of identical nature. Equations for the centrode $\mathrm{k_f}$ in the x, y-system are transformed into equations for $\mathrm{k_m}$ in the ξ, η-system by replacing (x, y, a, b) by (ξ, η, b, a). This is seen by reflecting the figure in the line $y = x$.

Fixed centrode $\mathrm{k_f}$: The instantaneous center P is the intersection of the normal to the η-axis at A and the normal to the y-axis at B. The x, y-coordinates of P are expressed in terms of the angle φ:

$$x = a + y\tan\varphi\,, \qquad y = a\tan\varphi + \frac{b}{\cos\varphi} = a\tan\varphi + b\sqrt{1+\tan^2\varphi}\,. \quad (15.16)$$

Elimination of $\tan\varphi$ results in the equation

$$y^2 - a(x-a) = b\sqrt{y^2 + (x-a)^2}\,. \quad (15.17)$$

In the special case $b = 0$, this is the parabola $y^2 = a(x-a)$. In the special case $b = a$, it is the parabola $y^2 = a(2x-a)$. In this case, Fig. 15.9 is symmetric. The pole P is equidistant from the fixed point A and from the

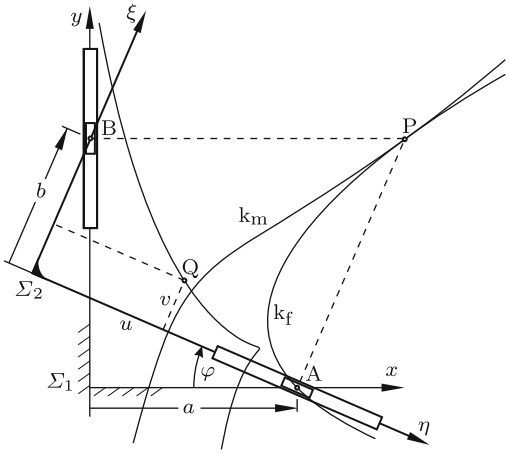

Fig. 15.9 The body-fixed η-axis is constrained to pass through the frame-fixed point A, and the body-fixed point B is constrained to move along the frame-fixed y-axis. Fixed centrode $\mathrm{k_f}$, moving centrode $\mathrm{k_m}$ and trajectory of body-fixed point Q

fixed y-axis. Hence A is the focus, and the y-axis is the directrix of the parabola. The moving centrode is the congruent parabola $\eta^2 = a(2\xi - a)$ with focus B and with the η-axis as directrix.

In the general case $b \neq 0\,,\ a\,,$ squaring of (15.17) produces a quadratic equation for $x - a$ with the solutions

$$x - a = \frac{y}{a^2 - b^2}\left(ya \pm b\sqrt{y^2 + a^2 - b^2}\right)\,. \tag{15.18}$$

This equation is satisfied by the coordinates $x = a\,,\ y = 0$ of A. This does not mean that $\mathrm{k_f}$ is unconditionally passing through A. This happens when B is at the origin of the x, y-system. This is possible only if $a^2 > b^2$. Likewise, $\mathrm{k_m}$ is passing through B only if $b^2 > a^2$.

Trajectory of Q: In terms of φ the x, y-coordinates of Q are

$$\left.\begin{aligned} x &= u\cos\varphi + (v - b)\sin\varphi\,, \\ y &= (\eta_\mathrm{A} - u)\sin\varphi + v\cos\varphi \\ &= -u\sin\varphi + v\cos\varphi + (a + b\sin\varphi)\tan\varphi\,. \end{aligned}\right\} \tag{15.19}$$

The velocity and the acceleration of Q are determined by the time derivatives $\dot{x}\,,\ \dot{y}$ and $\ddot{x}\,,\ \ddot{y}\,,$ respectively. For eliminating φ the second equation is written in the form

$$y\cos\varphi = -u\sin\varphi\cos\varphi + v(1 - \sin^2\varphi) + a\sin\varphi + b\sin^2\varphi\,. \tag{15.20}$$

Solving for $\cos\varphi$ yields the expression

$$\cos\varphi = \frac{v + a\sin\varphi + (b-v)\sin^2\varphi}{y + u\sin\varphi} \,. \tag{15.21}$$

Substitution into the first Eq.(15.19) produces a linear equation for $\sin\varphi$ with the solution

$$\sin\varphi = \frac{uv - xy}{u(x-a) + y(b-v)} \,. \tag{15.22}$$

With this expression the first Eq.(15.19) yields

$$\cos\varphi = \frac{x(x-a) + v(b-v)}{u(x-a) + y(b-v)} \,. \tag{15.23}$$

The parameter-free equation $\sin^2\varphi + \cos^2\varphi = 1$ is quadratic in y:

$$\begin{aligned} &y^2[x^2 - (b-v)^2] - 2yu[bx - a(b-v)] \\ &= u^2[(x-a)^2 - v^2] - [x(x-a) + v(b-v)]^2 \,. \end{aligned} \tag{15.24}$$

In the case $u = 0$, (15.22) follows directly from the first Eq.(15.19).

If Q is located on $\mathrm{k_m}$, the trajectory has a cusp on $\mathrm{k_f}$ in the position when Q is the pole P. The condition for Q to be located on $\mathrm{k_m}$ is obtained from (15.17) by replacing $(x\,,\,y\,,\,a\,,\,b)$ by $(v\,,\,u\,,\,b\,,\,a)$:
$u^2 - b(v-b) = a\sqrt{u^2 + (v-b)^2}$.

Example 4: Rod moving tangent to a circle and with one point along a straight line

The rod $\overline{\mathrm{AB}}$ in Figs. 15.10a,b is constrained to move tangentially to a unit circle and with its endpoint A along a straight line. In Fig. 15.10a this line is a diameter of the circle and in Fig. 15.10b it is a tangent to the circle. To be determined are in either case the equations of the fixed centrode $\mathrm{k_f}$ in the x, y-system with origin 0 and of the moving centrode $\mathrm{k_m}$ in the ξ, η-system with origin A.

Solution: In both figures the instantaneous center P is the intersection of the normal to the circle at the point of contact and of the normal to the straight line at A. The coordinates x, y and ξ, η of P as functions of the angle α are obtained from triangles. First, Fig. 15.10a is analyzed. The coordinates of P are

$$\left.\begin{aligned} x &= \frac{1}{\cos\alpha} \,, & y &= x\tan\alpha = \frac{\sin\alpha}{\cos^2\alpha} \,, \\ \xi &= \tan\alpha \,, & \eta &= y\sin\alpha \;= \tan^2\alpha \,. \end{aligned}\right\} \tag{15.25}$$

Elimination of α yields for $\mathrm{k_f}$ and $\mathrm{k_m}$ the equations

$$\mathrm{k_f}: \quad y^2 = \frac{\sin^2\alpha}{\cos^4\alpha} = \frac{1}{\cos^4\alpha} - \frac{1}{\cos^2\alpha} = x^2(x^2-1) \,, \qquad \mathrm{k_m}: \quad \eta = \xi^2 \,. \tag{15.26}$$

In Fig. 15.10b P has the coordinates

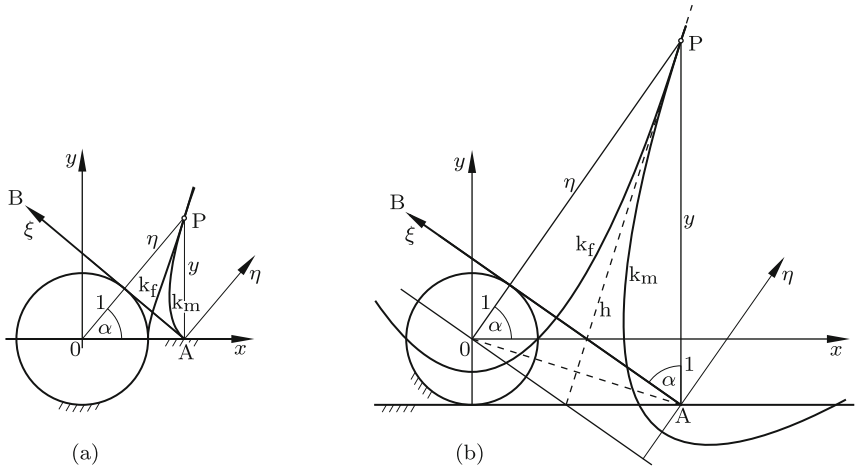

Fig. 15.10 Rod $\overline{\mathrm{AB}}$ moving tangentially to a unit circle. The endpoint A is moving along a diameter of the circle **(a)** or along a tangent to the circle **(b)**. Fixed centrodes $\mathrm{k_f}$ and moving centrodes $\mathrm{k_m}$

$$\left.\begin{aligned} x &= \frac{1}{\cos\alpha} + \tan\alpha = \frac{1+\sin\alpha}{\cos\alpha}\,, \qquad y = x\tan\alpha = \frac{\sin\alpha}{1-\sin\alpha}\,, \\ \xi &= (1+y)\cos\alpha = \frac{\cos\alpha}{1-\sin\alpha} \equiv x\,, \quad \eta = (1+y)\sin\alpha = \frac{\sin\alpha}{1-\sin\alpha} \equiv y\,. \end{aligned}\right\} \tag{15.27}$$

The first two equations yield $x^2 = (1+\sin\alpha)/(1-\sin\alpha) = 1+2\sin\alpha/(1-\sin\alpha) = 1+2y$. Hence the centrodes are the congruent parabolas $x^2 = 2y+1$ and $\xi^2 = 2\eta+1$. These parabolas are shown in Fig. 15.10b. The foci are 0 and A, respectively, and the directrices are the line $y = -1$ and the line $\eta = -1$, respectively. Through a comparison of angles it is verified that (0,A,P) is an isosceles triangle. From this it follows that the parabolas are located symmetrically with respect to the altitude h of the triangle, and that this altitude is the common tangent at P.

The motions shown in Figs. 15.10a and b can be interpreted in a different way as follows. The body-fixed line $\eta = -1$ is moving through the fixed point 0, and the body-fixed point A is moving along a fixed line $y = \text{const}$ ($y = 0$ in Fig. 15.10a and $y = -1$ in Fig. 15.10b). With this interpretation both motions turn out to be special cases of Fig. 15.9. The notation is different, however. Figure 15.10a is the special case $b = 0$, and Fig. 15.10b is the special case $a = b = 1$. From (15.17) it was deduced that in the former case one of the centrodes is a parabola, and that in the latter case both centrodes are congruent parabolas.

Example 5: Centrodes of couplers in four-bar mechanisms
The quadrilateral $\mathrm{A_0ABB_0}$ shown in Fig. 15.11 is a foldable four-bar mecha-

nism in antiparallelogram configuration. The fixed link A_0B_0 and the coupler AB have equal length ℓ, and the crossed cranks A_0A and B_0B have equal length $r > \ell$. In the instantaneous position shown the line t–t is a line of symmetry. To be determined are the fixed centrode k_f and the moving centrode k_m of the coupler.

Solution: The instantaneous center P is the point of intersection of the cranks. Since its distance from B equals its distance from A_0, the sum of the distances PA and PB is the constant length $A_0A = r$. From this it follows that the moving centrode k_m is the ellipse having A and B as foci and passing through P. For reasons of symmetry the fixed centrode k_f is the ellipse having A_0 and B_0 as foci. The line t–t is the instantaneous tangent. The semi principal axes of the ellipses are $a = r/2$ and $b = 1/2\sqrt{r^2 - \ell^2} < a$. This is seen by drawing the four-bar and the ellipses in the two positions in which $\overline{AB}$ is parallel to $\overline{A_0B_0}$.

In what follows, the same four-bar is considered, but this time the longer link BB_0 is the fixed link. The moving coupler is the link AA_0. In this case, P^* is the instantaneous center of the coupler. Since its distance from B equals its distance from A_0, the difference of the distances P^*A and P^*A_0 is the constant length $AB = \ell$. From this it follows that the moving centrode k_m^* is the hyperbola having A and A_0 as foci and passing through P^*. For reasons of symmetry the fixed centrode k_f^* is the hyperbola having B and B_0 as foci. The line t–t is the instantaneous tangent. The semi principal axes of the hyperbolas are $a = \ell/2$ (real axis) and $b = 1/2\sqrt{r^2 - \ell^2}$. This concludes the investigation.

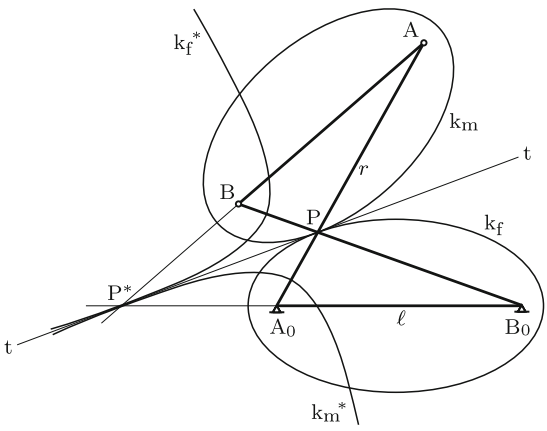

Fig. 15.11 Foldable four-bar mechanism in antiparallelogram configuration. The centrodes of the coupler are ellipses when the coupler is the shorter link and hyperbolas otherwise

In the foldable four-bar considered next, not opposite links, but adjacent links have pairwise identical lengths. The left crank A_0A and the coupler AB have length a, and the fixed link A_0B_0 and the right crank B_0B have length $\ell > a$. The four-bar should be drawn in a position in which the crank angle $\varphi = \sphericalangle(B_0A_0A)$ is in the range $0 < \varphi < \pi/2$. The line $\overline{AB_0}$ is a line of symmetry. As before, the pole P of the coupler is the point of intersection of the cranks. Its polar coordinates in the fixed frame are φ and $r = A_0P$. Let R be the distance of P from B_0. The law of cosines states that $R^2 = \ell^2 + r^2 + 2\ell r \cos\varphi$. Auxiliary lines and points are defined as follows. The line through B parallel to the line of symmetry intersects the line $\overline{A_0B_0}$ at a point C at the distance ℓ from B_0 (similar triangles). The line through B_0 parallel to the coupler intersects the auxiliary line $\overline{BC}$ at a point D. Finally, let P^* be the reflection of P in the line of symmetry. The similarity of the triangles (B,P^*,C) and (D,B_0,C) establishes the equation $(R+\ell)/r = \ell/a$. Hence $R = \ell(r/a - 1)$. Setting the square of this expression equal to the previous expression for R^2 results in the polar-coordinate equation for the fixed centrode k_f:

$$r = \frac{2\ell a}{\ell^2 - a^2}\,(\ell + a\cos\varphi)\,. \tag{15.28}$$

Comparison with (15.12) shows that k_f is a limaçon of Pascal and, because of $\ell > a$, one without double point. Its line of symmetry is $\overline{A_0B_0}$. The constant coefficients depending on ℓ and a determine the quantities ℓ and R of Fig. 15.8.

An equation for the moving centrode k_m is obtained as follows. In the coupler-fixed system the pole P has the polar coordinates $\varphi = \sphericalangle(ABB_0)$ and $r' = BP = \ell - R$ and with the above expression for R $r' = \ell(2 - r/a)$. Hence $r = a(2 - r'/\ell)$. Substitution into (15.28) results in the desired equation for k_m:

$$r' = \frac{2\ell a}{a^2 - \ell^2}\,(a + \ell\cos\varphi)\,. \tag{15.29}$$

This is a limaçon of Pascal with the double point B and with the line of symmetry $\overline{BA}$. The equation is obtained directly from (15.28) by interchanging ℓ and a.

Example 6: Door mechanism

In Fig. 15.12 the labeled six-body linkage of an airplane door is shown in the position door closed. The body of the airplane is the frame 0, and the door is body 5. All revolute joints are instantaneous centers with labels as shown. The joints of bodies 0, 1, 2, 3 form a parallelogram 1, and the joints of bodies 5, 3, 2, 4 form another parallelogram 2. Both parallelograms share bodies 2 and 3 and the joint P_{23}. About which point P_{50} does the door rotate relative to the frame in the position shown? Where is P_{50} located in other positions of the door? In doors of modern furniture the same linkage is used with link lengths on the order of 1 cm.

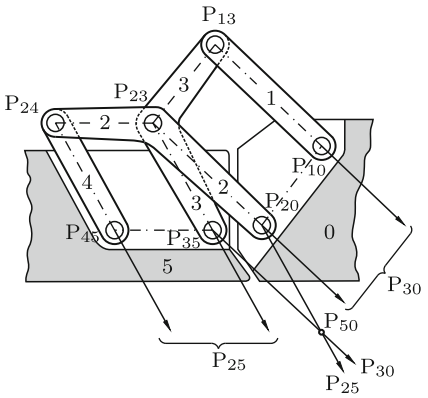

Fig. 15.12 Six-link door mechanism with permanent center of rotation P_{50}

Solution: In a parallelogram parallel sides rotate relative to each other about an infinitely distant instantaneous center. According to the theorem of Kennedy/Aronhold this center is the intersection of the other pair of parallel sides of the same parallelogram. Examples: P_{30} is the intersection of the lines $\overline{P_{13}P_{10}}$ and $\overline{P_{23}P_{20}}$, and P_{25} is the intersection of the lines $\overline{P_{23}P_{35}}$ and $\overline{P_{24}P_{45}}$. This determines the desired center P_{50} as intersection of the lines $\overline{P_{20}P_{25}}$ and $\overline{P_{30}P_{35}}$. The instantaneous centers P_{50}, P_{20}, P_{23} and P_{35} form a parallelogram.

During large motions of the door body 3 is in translatory motion relative to body 0. The parallelogram 2 produces constraints forcing also body 4 to be in translatory motion relative to body 0. During a translatory motion of a body the difference of the position vectors of two body-fixed points A and B is constant: $\mathbf{r}_A - \mathbf{r}_B = \text{const}$. Applied to body 3 this means: The two joints connecting body 3 with body 5 and with body 2, respectively, have a constant difference of position vectors. Since the latter joint is moving on a circle around P_{20}, the former is moving on a circle around P_{50}. The same argument applies to body 4. The joints connecting this body with body 5 and with body 2, respectively, have a constant difference of position vectors. Since the latter joint is moving on a circle around P_{20}, the former is moving on a circle around P_{50}. Hence two points of body 5 move on circles about P_{50}. This proves that P_{50} is not only instantaneously, but permanently center of rotation of the door.

Example 7: Instantaneous centers of an eight-link mechanism
In this example, the theorem of Kennedy and Aronhold alone does not suffice for constructing instantaneous centers of rotation. In addition, also Burmester's theorem 15.2 must be applied. The planar linkage in Fig. 15.13 consists of the frame 0 and of moving bodies $1, \ldots, 7$ which are interconnected by the ten revolute joints A, B, C, D, E, B′, C′, D′, E′, F. Ac-

cording to Grübler's Eq.(4.2) the degree of freedom of the linkage is one. To be determined are the instantaneous centers $P_{i0}\ \ (i = 1, \ldots, 7)$ and P_{23}.

Solution: All revolute joints are centers of rotation with the respective labels as shown. Examples are P_{10}=A and P_{12}=B. The system does not contain any four-bar linkage so that no pair of straight lines is available which, by the theorem of Kennedy and Aronhold, might yield an additional instantaneous center. In the following applications of Burmester's theorem 15.2 *velocity* always means velocity relative to frame 0. In Fig. 15.13 the rotated velocities of the points B and B′ are drawn to scale as vectors $\mathbf{v}^*_{\mathrm{B}}$ and $\mathbf{v}^*_{\mathrm{B}'}$, respectively, terminating at the center P_{10} =A. Theorem 15.2 applied to body 2 states that the tip of the rotated velocity $\mathbf{v}^*_{\mathrm{E}}$ of point E on rod 2 lies on the line h parallel to rod 2. The tip of the rotated velocity $\mathbf{v}^*_{\mathrm{D}}$ of D lies on the line $\overline{\mathrm{CD}}$ since rod 4 rotates about the center P_{40} =C. Next, theorem 15.2 is applied to body 6. The tips of the rotated velocities $\mathbf{v}^*_{\mathrm{D}}$, $\mathbf{v}^*_{\mathrm{E}}$ and $\mathbf{v}^*_{\mathrm{F}}$ form a triangle which is both similar and parallel to the triangle (D,E,F). It is the triangle (D_1,E_1,F_1) if the tip of $\mathbf{v}^*_{\mathrm{E}}$ is located at E_1, and it degenerates to point M (intersection of h and $\overline{\mathrm{CD}}$) if the tip of $\mathbf{v}^*_{\mathrm{E}}$ is located at M. Since the tip of $\mathbf{v}^*_{\mathrm{E}}$ is an as yet unknown point on h, the tip of $\mathbf{v}^*_{\mathrm{F}}$ is an as yet unknown point on the line g=$\overline{\mathrm{MF}}_1$.

By the same arguments applied to the right-hand side of the system, i.e., to bodies 1, 3, 5 and 7, the tip of $\mathbf{v}^*_{\mathrm{F}}$ is located also on the line g′=$\overline{\mathrm{M'F'}}_1$. Hence the tip of $\mathbf{v}^*_{\mathrm{F}}$ lies at the intersection Q of g and g′. This determines the instantaneous center P_{60} as intersection of the velocity normals $\mathbf{v}^*_{\mathrm{D}}$ and $\mathbf{v}^*_{\mathrm{F}}$ and the instantaneous center P_{70} as intersection of $\mathbf{v}^*_{\mathrm{D}'}$ and $\mathbf{v}^*_{\mathrm{F}}$.

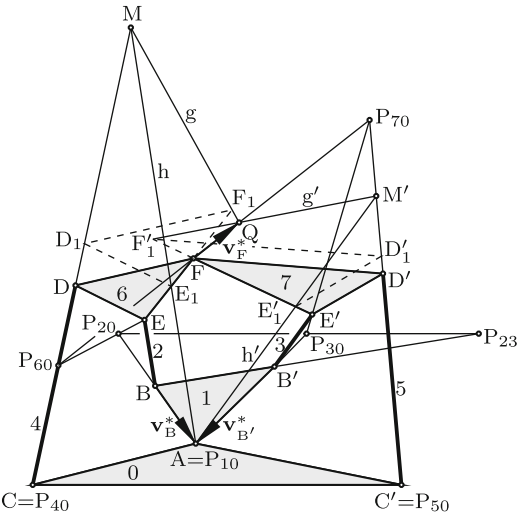

Fig. 15.13 Mechanism with eight links and ten revolute joints. The geometric construction of P_{60} and P_{70} rests on Burmester's theorem 15.2

All other instantaneous centers are found with the help of the theorem of Kennedy and Aronhold. Examples: The center P_{20} is the intersection of the lines $\overline{P_{62}P_{60}} = \overline{EP_{60}}$ and $\overline{P_{10}P_{21}} = \overline{AB}$. The center P_{30} is the intersection of the lines $\overline{E'P_{70}}$ and $\overline{AB'}$. The center P_{23} is the intersection of the lines $\overline{P_{20}P_{30}}$ and $\overline{P_{21}P_{31}} = \overline{BB'}$.

Example 8: Kutzbach's angular velocity diagram for spur gears
In spur gears all bodies move in one common plane. All axes of gear wheels and also all pitch points are instantaneous centers of rotation. Since the distances of these points are constant, also all angular velocity ratios are constant. The planetary gear shown in Fig. 15.14a is used as illustrative example for explaining Kutzbach's general-purpose method for determining angular velocities [22]. The gear consists of the stationary frame 0, the pinion cage 1 and gear wheels 2, 3 and 4. The degree of freedom is one. A single, arbitrary angular velocity is prescribed, for example, ω_{10} (pinion cage 1 relative to the frame). To be determined are all angular velocities ω_{ij} $(i, j = 0, \ldots, 4;\ i \neq j)$.

Solution: The instantaneous centers P_{30}, P_{32} and P_{24} in Fig. 15.14a are pitch points, and the centers P_{31}, P_{21}, P_{10} and P_{40} are located on wheel axes. From these centers lines parallel to the axes are drawn thus creating the r, v-velocity diagram in Fig. 15.14b. This velocity diagram consists of straight lines $i = 0, \ldots, 4$. Definition: The line i is the graph of the function $v_i(r)$. This function determines the velocity (relative to body 0) of the point fixed on body i at the radius r from the center line. The line 0 for the frame and the line $v_1(r) = \omega_{10} r$ for the pinion cage 1 are given by the problem statement. These lines are drawn first (with arbitrary scale). Wheel 3 has at the radius of P_{30} the same velocity body 0 has, and at the radius of P_{31} the same velocity body 1 has. Through these two points the line 3

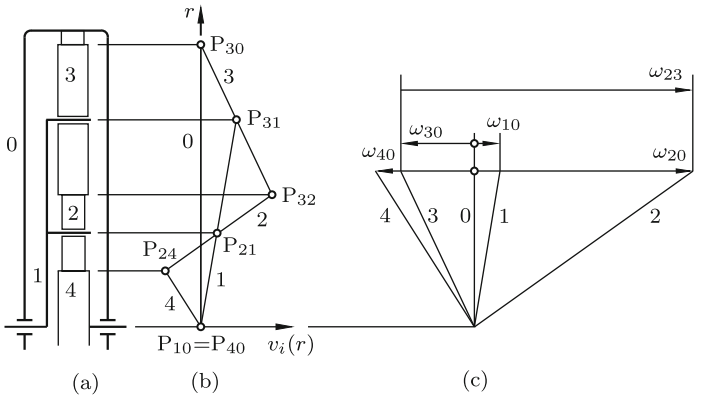

Fig. 15.14 Planetary gear **(a)**, velocity diagram **(b)** and angular velocity diagram **(c)**

is determined. Subsequently, the lines 2 and 4 are determined in the same way.

The diagram in Fig. 15.14c is the angular velocity diagram. It is constructed by drawing, from a point on the center line, lines parallel to all lines in the velocity diagram. These lines have the equations $v_i(r) = \omega_{i0} r$. The function values at an arbitrarily chosen radius $r = r_0$ are $\omega_{i0} r_0$. Thus, these values together with the scale chosen for the prescribed angular velocity ω_{10} determine the directions and magnitudes of all other angular velocities ω_{i0} $(i = 1 \ldots, 4)$. With these velocities also all relative angular velocities $\omega_{ij} = \omega_{i0} - \omega_{j0}$ $(i, j = 1, \ldots, 4;\ i \neq j)$ are determined. For demonstration ω_{23} is shown.

15.2 Velocity and Acceleration in Complex Formulation

In the case of plane motion, complex formulations of position, velocity and acceleration of points are more convenient than vector formulations. In Fig. 15.15 the planes Σ_1 and Σ_2 of Fig. 15.1 are shown again. To Σ_1 the real and the imaginary axis of a complex plane are attached. In this plane complex numbers representing positions, velocities and accelerations are formulated. Let $\varphi(t)$ be the time-dependent angle of rotation of Σ_2 relative to Σ_1. It is the angle of an arbitrarily chosen line fixed in Σ_2 against the real axis fixed in Σ_1 (positive counterclockwise). The angular velocity and the angular acceleration of Σ_2 are $\dot{\varphi}$ and $\ddot{\varphi}$, respectively. It is assumed that $\dot{\varphi} \neq 0$. Points A and Q are arbitrarily chosen points fixed in Σ_2. Let r_A and r be the complex numbers specifying their positions in Σ_1. The relationship between the two is expressed in the form

$$r = r_\mathrm{A} + \varrho \mathrm{e}^{\mathrm{i}\,\varphi} \qquad (\varrho = \text{ complex const}) \,. \tag{15.30}$$

Differentiation with respect to time yields expressions for velocity and ac-

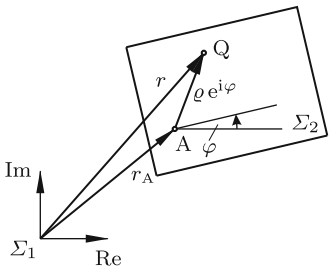

Fig. 15.15 Complex numbers r_A and r specifying the positions in Σ_1 of two points A and Q fixed in Σ_2. ϱ is a complex constant

celeration. With the abbreviations $\dot{r} = v$, $\dot{r}_{\mathrm{A}} = v_{\mathrm{A}}$, $\ddot{r} = a$ and $\ddot{r}_{\mathrm{A}} = a_{\mathrm{A}}$ these expressions are

$$v = v_{\mathrm{A}} + \mathrm{i}\,\dot{\varphi}\varrho \mathrm{e}^{\mathrm{i}\,\varphi} = v_{\mathrm{A}} + \mathrm{i}\,\dot{\varphi}(r - r_{\mathrm{A}}) \,, \tag{15.31}$$

$$a = a_{\mathrm{A}} + \mathrm{i}\,\ddot{\varphi}(r - r_{\mathrm{A}}) + \mathrm{i}\,\dot{\varphi}(v - v_{\mathrm{A}}) = a_{\mathrm{A}} + (\mathrm{i}\,\ddot{\varphi} - \dot{\varphi}^2)(r - r_{\mathrm{A}}) \,. \tag{15.32}$$

These equations are the complex formulations of the vector Eqs.(9.13) and (9.81) in the case of planar motion. At time $t = \text{const}$ (arbitrary) v and a are linear functions of r with constant coefficients. From this fact Burmester derived two theorems:

Theorem 15.4. *The tips of the complex velocities* v_i *of arbitrary points* Q_i *of* Σ_2 $(i = 1, 2, \dots)$ *produce a figure similar to the figure produced by the points* Q_i *.*

Theorem 15.5. *The tips of the complex accelerations* a_i *of arbitrary points* Q_i *of* Σ_2 $(i = 1, 2, \dots)$ *produce a figure similar to the figure produced by the points* Q_i *.*

Theorem 15.4 is the complex formulation of Theorem 15.2 on rotated velocities.

15.2.1 Instantaneous Center of Rotation

Let r_{P} be the complex number representing the instantaneous center of rotation P. Equation (15.31) with $r = r_{\mathrm{P}}$ and $v = 0$ yields the expression

$$r_{\mathrm{P}} = r_{\mathrm{A}} + \frac{\mathrm{i}\,v_{\mathrm{A}}}{\dot{\varphi}} \,. \tag{15.33}$$

This is the complex formulation of (15.2). In the special case A=P and $v_{\mathrm{P}} = 0$, (15.31) becomes

$$v = \mathrm{i}\,\dot{\varphi}(r - r_{\mathrm{P}}) \,. \tag{15.34}$$

This is the complex formulation of (15.3). Two complex velocities v_{A} and v of arbitrary points positioned at r_{A} and r, respectively, determine the instantaneous center of rotation r_{P} uniquely. Equation (15.34) is written also with r_{A} and v_{A}: $v_{\mathrm{A}} = \mathrm{i}\,\dot{\varphi}(r_{\mathrm{A}} - r_{\mathrm{P}})$. Multiplying this equation by v, (15.34) by v_{A} and taking the difference results in

$$r_{\mathrm{P}} = \frac{v r_{\mathrm{A}} - v_{\mathrm{A}} r}{v - v_{\mathrm{A}}} \,. \tag{15.35}$$

This is the complex formulation of the geometric construction of P as point of intersection of the normals to the velocities of two points. Solving the equation for v yields the expression

$$v = v_{\mathrm{A}} \frac{r - r_{\mathrm{P}}}{r_{\mathrm{A}} - r_{\mathrm{P}}} \,. \tag{15.36}$$

15.2.2 Instantaneous Center of Acceleration

Equation (15.32) shows that there exists a point in Σ_2 which has, instantaneously, the acceleration $a = 0$. This point is called instantaneous center of acceleration G. Actually, every body-fixed point on the line through G and normal to Σ_2 has zero acceleration. The complex position r_{G} of G is

$$r_{\mathrm{G}} = r_{\mathrm{A}} - \frac{a_{\mathrm{A}}}{\mathrm{i}\,\ddot{\varphi} - \dot{\varphi}^2} \,. \tag{15.37}$$

In the special case A=G and $a_{\mathrm{G}} = 0$, (15.32) becomes

$$a = (\mathrm{i}\,\ddot{\varphi} - \dot{\varphi}^2)(r - r_{\mathrm{G}}) \,. \tag{15.38}$$

Two complex accelerations a_{A} and a of arbitrary points positioned at r_{A} and r, respectively, determine the instantaneous center of acceleration r_{G} uniquely. Equation (15.38) is written also with r_{A} and a_{A}: $a_{\mathrm{A}} = (\mathrm{i}\,\ddot{\varphi} - \dot{\varphi}^2)(r_{\mathrm{A}} - r_{\mathrm{G}})$. Multiplying this equation by a, (15.38) by a_{A} and taking the difference results in

$$r_{\mathrm{G}} = \frac{a r_{\mathrm{A}} - a_{\mathrm{A}} r}{a - a_{\mathrm{A}}} \,. \tag{15.39}$$

Solving this equation for a yields the expression

$$a = a_{\mathrm{A}} \frac{r - r_{\mathrm{G}}}{r_{\mathrm{A}} - r_{\mathrm{G}}} \,. \tag{15.40}$$

Equations (15.37) – (15.40) correspond to (15.33) – (15.36).

In (15.38) the factor $(\mathrm{i}\,\ddot{\varphi} - \dot{\varphi}^2)$ is the same for all points of Σ_2. This factor has the effect of stretch rotation of $r - r_{\mathrm{G}}$. Let α be the angle of this stretch rotation. The angle is $\pi/2$ in the special case $\dot{\varphi} = 0$, and it is π in the special case $\ddot{\varphi} = 0$. Figure 15.16 shows the general case with the center of acceleration G and with the accelerations a_1 and a_2 of two points Q_1 and Q_2, respectively. By attaching to Q_1 not only a_1, but also a_2 and the acceleration zero of G the triangle $(\mathrm{P}_1,\mathrm{P}_2^*,\mathrm{Q}_1)$ is obtained. From (15.38) it follows that the triangles $(\mathrm{G},\mathrm{Q}_1,\mathrm{P}_1)$ and $(\mathrm{G},\mathrm{Q}_2,\mathrm{P}_2)$ are similar, and from Theorem 15.5 it follows that the triangles $(\mathrm{P}_1,\mathrm{P}_2^*,\mathrm{Q}_1)$ and $(\mathrm{Q}_1,\mathrm{Q}_2,\mathrm{G})$ are similar. These two similarities are the geometrical interpretations of (15.40) and (15.39). They determine a_2 if only G and the acceleration a_1 are given, and they determine G if only a_1 and a_2 are given.

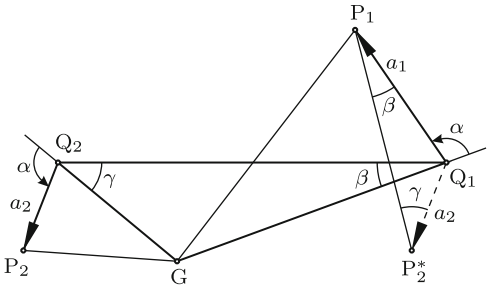

Fig. 15.16 Center of acceleration G and accelerations a_1, a_2 of points Q_1, Q_2

15.2.3 Inflection Circle. Bresse Circles

Subject of investigation is again the instantaneous state of plane motion at some fixed time t. Up to now the locations of the real axis and the imaginary axis of the complex plane in Σ_1 were unspecified. Now, the instantaneous center of rotation P is chosen as origin. Furthermore, the imaginary axis is given the (positive or negative) direction of the acceleration of the point of Σ_2 coinciding with P. This has the consequence that the center of rotation has position $r_P = 0$, velocity $v_P = 0$ and acceleration $a_P = \mathrm{i}\, a_0$ with a positive or negative scalar a_0. The position in Σ_1 of a point fixed in Σ_2 is written in the form $r = x + \mathrm{i}\, y$. This means that x and y are cartesian coordinates along the real and the imaginary axis. In these terms Eqs.(15.31) and (15.32) for velocity and acceleration of the point r have the forms

$$\left.\begin{aligned} v &= \mathrm{i}\,\dot\varphi(x + \mathrm{i}\, y) & a &= \mathrm{i}\, a_0 + (\mathrm{i}\,\ddot\varphi - \dot\varphi^2)(x + \mathrm{i}y) \\ &= -\dot\varphi y + \mathrm{i}\,\dot\varphi x\,, & &= -\dot\varphi^2 x - \ddot\varphi y + \mathrm{i}\,(a_0 - \dot\varphi^2 y + \ddot\varphi x)\,. \end{aligned}\right\} \qquad (15.41)$$

The following problems are solved.
1. Determine all points of Σ_2 characterized by collinearity of acceleration a and velocity v.
2. Determine all points of Σ_2 characterized by mutual orthogonality of acceleration a and velocity v.

The center of acceleration G as well as the center of rotation P are singular points satisfying both conditions. The first condition is satisfied by points the trajectories of which have zero curvature. In other words: The point is either on a straight trajectory or it is instantaneously inflection point of its trajectory. The second condition is satisfied by points the acceleration of which is instantaneously pointing through P (either toward P or away from P). In other words: These points have, instantaneously, no acceleration component along their trajectory. According to (14.6) a and v are collinear if the imaginary part of $a\overline{v}$ is zero, and they are mutually orthogonal if the

real part is zero. With (15.41)

$$a\overline{v} = \dot{\varphi}\{\ddot{\varphi}(x^2 + y^2) + a_0 x + \mathrm{i}\,[\dot{\varphi}^2(x^2 + y^2) - a_0 y]\}\ . \tag{15.42}$$

Both conditions result in the equation of a circle. The first circle is called *inflection circle* (geometric locus of all instantaneous inflection points). Both circles are also referred to as Bresse circles [6]. Their equations are

$$\text{inflection circle:} \qquad \dot{\varphi}^2(x^2 + y^2) - a_0 y = 0\ , \tag{15.43}$$

$$\text{second Bresse circle:} \qquad \ddot{\varphi}\,(x^2 + y^2) + a_0 x = 0\ . \tag{15.44}$$

In Fig. 15.17 both circles are drawn in solid lines. With the coordinate

$$y_2 = \frac{a_0}{\dot{\varphi}^2} \tag{15.45}$$

of the point denoted P_2 the inflection circle has the equation

$$x^2 + y^2 - y_2 y = 0\ . \tag{15.46}$$

From the figure it is seen that at points of inflection tangents to trajectories are passing through P_2. At the origin P and at the center of acceleration G both circles intersect orthogonally. The coordinates of G are

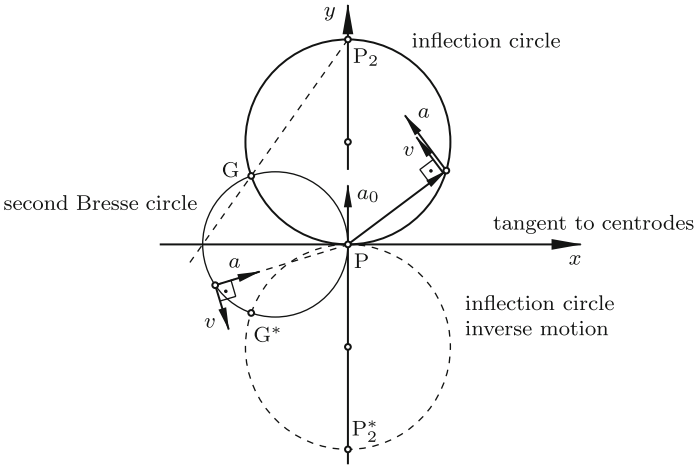

Fig. 15.17 Center of acceleration G at the intersection of the Bresse circles (solid lines). Inflection circle (dashed line) and center of acceleration G^* of the inverse motion

$$x_{\mathrm{G}} = -y_2\,\frac{\ddot{\varphi}/\dot{\varphi}^2}{1 + (\ddot{\varphi}/\dot{\varphi}^2)^2}\ , \qquad y_{\mathrm{G}} = y_2\,\frac{1}{1 + (\ddot{\varphi}/\dot{\varphi}^2)^2}\ . \tag{15.47}$$

The line passing through P_2 and G passes also through the second point of intersection of the second Bresse circle with the x-axis. In the case $\ddot{\varphi} = 0$, the second Bresse circle degenerates to the line $x = 0$, and the center of acceleration G is located at P_2.

Next, the motion of Σ_2 is again interpreted as rolling motion of the centrode fixed in Σ_2 on the centrode fixed in Σ_1. The point of rolling contact is P. The point of Σ_2 coinciding with P has, instantaneously, zero velocity and the acceleration a_0 in y-direction. From this it follows that its trajectory has a cusp in P. The trajectory into and out of P is tangent to the y-axis. This means that the y-axis is the common normal of both centrodes, and the x-axis is the common tangent.

Example: In the elliptic trammel shown in Fig. 15.4a the circle k_2 is the moving centrode. It was shown that all points of k_2 move on straight lines. From this it follows that k_2 is also the inflection circle. The second Bresse circle has its center on the tangent to the inflection circle in P. Its radius depends on $\ddot{\varphi}$. End of example.

15.2.4 Center of Acceleration and Bresse Circles of the Inverse Motion

The inverse of the motion of Σ_2 relative to Σ_1 is the motion of Σ_1 relative to Σ_2. For angular velocity and angular acceleration of Σ_1 and for velocities and accelerations of points fixed in Σ_1 (9.17), (9.18) and (9.19) are valid for general spatial motion:

$$\boldsymbol{\omega}_{\mathrm{rel}} = -\boldsymbol{\omega}\,, \quad \dot{\boldsymbol{\omega}}_{\mathrm{rel}} = -\dot{\boldsymbol{\omega}}\,, \quad \mathbf{v}_{\mathrm{rel}} = -\mathbf{v}\,, \quad \mathbf{a}_{\mathrm{rel}} = -\mathbf{a} + 2\boldsymbol{\omega} \times \mathbf{v}\,. \tag{15.48}$$

The quantities carrying the index rel are associated with the inverse motion, and the ones without this index are associated with the motion. In the special case of planar motion, the equations have the forms

$$\dot{\varphi}_{\mathrm{rel}} = -\dot{\varphi}\,, \qquad \ddot{\varphi}_{\mathrm{rel}} = -\ddot{\varphi}\,, \qquad v_{\mathrm{rel}} = -v\,, \qquad a_{\mathrm{rel}} = -a + 2\mathrm{i}\,\dot{\varphi} v\,. \tag{15.49}$$

Let G^* be the center of acceleration of the inverse motion. Its location r_{G^*} is obtained in two steps. First, in (15.37) for the location r_G of G the index rel is attached to all quantities. In the second step all quantities carrying the index are replaced by the respective expressions in (15.49). The result is

$$r_{G^*} = r_A + \frac{2\mathrm{i}\,\dot{\varphi} v_A - a_A}{\mathrm{i}\,\ddot{\varphi} + \dot{\varphi}^2}\,. \tag{15.50}$$

The same procedure applied to (15.43) and (15.44) yields for the Bresse circles of the inverse motion the equations

$$\text{inflection circle:} \qquad \dot{\varphi}^2(x^2+y^2)+a_0 y=0\,, \tag{15.51}$$

$$\text{second Bresse circle:} \qquad \ddot{\varphi}\,(x^2+y^2)+a_0 x=0\,. \tag{15.52}$$

Thus, the second Bresse circles of motion and inverse motion are identical, whereas the inflection circle of the inverse motion is the reflection of the inflection circle of the motion in the tangent to the centrodes. Also the center of acceleration G^* is the reflection of the center of acceleration G. In Fig. 15.17 all centers and circles are shown.

15.3 Curvature of Plane Trajectories

15.3.1 Normal Poles

As before, an arbitrary continuous motion of a plane Σ_2 relative to a reference plane Σ_1 is considered. In the present section curvatures of trajectories of points of Σ_2 are investigated. Curvature is a differential-geometric property which is determined by the shape of the trajectory independent of the motion generating the trajectory. For this reason, the complex representation known from (15.30) is used with φ as independent variable:

$$r(\varphi)=r_{\mathrm{A}}(\varphi)+\varrho \mathrm{e}^{\mathrm{i}\,\varphi} \qquad (\varrho=\text{ const})\,. \tag{15.53}$$

As before, $\dot{\varphi}\neq 0$ is assumed which means that the instantaneous center of rotation exists.

The nth derivative of r with respect to φ is denoted $r^{(n)}$. For the derivatives with $n=1$, 2 and 3 also the notations r', r'' and r''' are used. The nth derivative is (see (15.31) and (15.32))

$$r^{(n)}=r_{\mathrm{A}}^{(n)}+\mathrm{i}^n\varrho \mathrm{e}^{\mathrm{i}\,\varphi}=r_{\mathrm{A}}^{(n)}+\mathrm{i}^n(r-r_{\mathrm{A}}) \qquad (n=1,2,\ldots)\,. \tag{15.54}$$

Definition: The *normal pole* of nth order, denoted P_n, is the particular point of Σ_2 for which the nth derivative is zero. Let r_{P_n} be the complex number representing P_n. Then, by definition,

$$0=r_{\mathrm{A}}^{(n)}+\mathrm{i}^n(r_{\mathrm{P}_n}-r_{\mathrm{A}}) \qquad (n=1,2,\ldots)\,, \tag{15.55}$$

whence it follows that

$$r_{\mathrm{P}_n}=r_{\mathrm{A}}-\mathrm{i}^{-n}r_{\mathrm{A}}^{(n)} \qquad (n=1,2,\ldots)\,. \tag{15.56}$$

The expression on the right-hand side is independent of ϱ. Since A is an arbitrary point of Σ_2, r_{A} can be replaced by r. Hence

$$r_{\mathrm{P}_n} = r - \mathrm{i}^{-n} r^{(n)} \qquad (n = 1, 2, \ldots) \,. \tag{15.57}$$

For $n = 1, \ldots, 4$ the formula yields

$$r_{\mathrm{P}_1} = r + \mathrm{i}\, r' \,, \quad r_{\mathrm{P}_2} = r + r'' \,, \quad r_{\mathrm{P}_3} = r - \mathrm{i}\, r''' \,, \quad r_{\mathrm{P}_4} = r - r^{(4)} \,. \tag{15.58}$$

In continuing this sequence the factors $+\mathrm{i}$, $+1$, $-\mathrm{i}$, -1 of the nth derivative are periodically repeated. Equation (15.57) yields

$$r^{(n)} = \mathrm{i}^n (r - r_{\mathrm{P}_n}) \qquad (n = 1, 2, \ldots) \,. \tag{15.59}$$

Thus, $r^{(n)}$ is known for all points of Σ_2 if P_n is known. Writing (15.57) also for $r_{\mathrm{P}_{n+1}}$ and taking the difference results in the equation

$$\mathrm{i}^n (r_{\mathrm{P}_{n+1}} - r_{\mathrm{P}_n}) = r^{(n)} + \mathrm{i}\, r^{(n+1)} \qquad (n = 1, 2, \ldots) \tag{15.60}$$

and with the first Eq.(15.58)

$$r_{\mathrm{P}_1}^{(n)} = \mathrm{i}^n (r_{\mathrm{P}_{n+1}} - r_{\mathrm{P}_n}) \qquad (n = 1, 2, \ldots) \,. \tag{15.61}$$

The relationship $\mathrm{d}r/\mathrm{d}t = \dot{\varphi}\, \mathrm{d}r/\mathrm{d}\varphi$ shows that P_1 is identical with the instantaneous center of velocity. In the special case of motion with $\dot{\varphi} = \text{const}$, $\mathrm{d}^n r/\mathrm{d}t^n = \dot{\varphi}^n\, r^{(n)}$ and, in particular, $\mathrm{d}^2 r/\mathrm{d}t^2 = \dot{\varphi}^2\, r''$. From this it follows that in the special case $\dot{\varphi} = \text{const}$, P_2 is identical with the instantaneous center of acceleration G. Already in Fig. 15.17 this point was denoted P_2. In the x, y-system of this figure the normal poles are, in the instantaneous position shown,

$$r_{\mathrm{P}_1} = 0 \,, \qquad r_{\mathrm{P}_2} = \mathrm{i}\, y_2 \,, \qquad r_{\mathrm{P}_n} = x_n + \mathrm{i}\, y_n \qquad (n > 2) \,. \tag{15.62}$$

The coordinates y_2, x_n and y_n $(n > 2)$ are determined by the motion of plane Σ_2.

Example: In Figs. 15.26 and 15.27 the rolling motion of a planetary wheel 1 on or inside a fixed sun wheel 0 is shown. The planetary wheel is the moving plane Σ_2, and the sun wheel is plane Σ_1. The point denoted P_{10} is the normal pole P_1. As points A and Q in the sense of Fig. 15.15 the wheel center P_{12} and the wheel-fixed point C are chosen. Their complex numbers r_{A} and r are given in (15.119) in terms of constant parameters r_0, r_1, b and of the variables φ_1 and φ_2 explained in the figures: $r_{\mathrm{A}} = (r_1 - r_0)\mathrm{e}^{\mathrm{i}\,\varphi_2}$, $r = (r_1 - r_0)\mathrm{e}^{\mathrm{i}\,\varphi_2} + b\mathrm{e}^{\mathrm{i}\,\varphi_1}$. The angle φ_1 is the angle φ of Eq.(15.53). From (15.120) the relationship $\varphi_2 = \lambda\varphi$ with $\lambda = r_1/(r_1 - r_0)$ is copied. With the additional abbreviation $r_1 - r_0 = a$ the complex numbers are

$$r_{\mathrm{A}} = a\mathrm{e}^{\mathrm{i}\,\lambda\varphi} \,, \qquad r = a\mathrm{e}^{\mathrm{i}\,\lambda\varphi} + b\mathrm{e}^{\mathrm{i}\,\varphi} \,. \tag{15.63}$$

The nth derivative of r is

$$r^{(n)} = \mathrm{i}^n(\lambda^n a\mathrm{e}^{\mathrm{i}\,\lambda\varphi} + b\mathrm{e}^{\mathrm{i}\,\varphi}) = \mathrm{i}^n[r - a(1-\lambda^n)\mathrm{e}^{\mathrm{i}\,\lambda\varphi}] \,. \tag{15.64}$$

With this expression Eq.(15.57) for the normal pole P_n becomes

$$r_{\mathrm{P}_n} = a(1-\lambda^n)\mathrm{e}^{\mathrm{i}\,\lambda\varphi} = (1-\lambda^n)r_{\mathrm{A}} \qquad (n \geq 1) \,. \tag{15.65}$$

Hence $r_{\mathrm{P}_n} - r_{\mathrm{A}} = -\lambda^n r_{\mathrm{A}}$. This shows that the normal poles are located on the normal to the centrodes, and that their distances from the center of the planetary wheel form a geometric series. The elliptic trammel in Fig. 15.4 is the planetary gear with $\lambda = -1$. In this special case, the normal poles coalesce alternatingly with P_1 and with the center of the planetary wheel. End of example.

15.3.2 Normal Poles of the Inverse Motion

Let P_n^* be the nth-order normal pole of the inverse motion (motion of Σ_1 relative to Σ_2). From Sect. 15.1 it is known that $\mathrm{P}_1^* = \mathrm{P}_1$. Furthermore, from Fig. 15.17 it is known that P_2^* and P_2 are located symmetrically to P_1 on the normal to the centrode. With (15.53) P_n^* ($n \geq 1$ arbitrary) is expressed in terms of $\mathrm{P}_1, \ldots, \mathrm{P}_n$ as follows. In the inverse motion r is constant while $r_{\mathrm{A}}(\varphi)$ and $\varrho(\varphi)$ are variable. The derivatives of order $n = 0$ to $n = 3$ yield the equations

$$\left.\begin{aligned}
n = 0: \quad & r = r_{\mathrm{A}} + \varrho\mathrm{e}^{\mathrm{i}\,\varphi} \,, \\
n = 1: \quad & 0 = r'_{\mathrm{A}} + \mathrm{i}\,\varrho\mathrm{e}^{\mathrm{i}\,\varphi} + \varrho'\mathrm{e}^{\mathrm{i}\,\varphi} \\
& \;\; = r'_{\mathrm{A}} + \mathrm{i}\,(r - r_{\mathrm{A}}) + \varrho'\mathrm{e}^{\mathrm{i}\,\varphi} \,, \\
n = 2: \quad & 0 = r''_{\mathrm{A}} - \mathrm{i}\,r'_{\mathrm{A}} + \mathrm{i}\,\varrho'\mathrm{e}^{\mathrm{i}\,\varphi} + \varrho''\mathrm{e}^{\mathrm{i}\,\varphi} \\
& \;\; = r''_{\mathrm{A}} - 2\mathrm{i}\,r'_{\mathrm{A}} + (r - r_{\mathrm{A}}) + \varrho''\mathrm{e}^{\mathrm{i}\,\varphi} \,, \\
n = 3: \quad & 0 = r'''_{\mathrm{A}} - 2\mathrm{i}\,r''_{\mathrm{A}} - r'_{\mathrm{A}} + \mathrm{i}\,\varrho''\mathrm{e}^{\mathrm{i}\,\varphi} + \varrho'''\mathrm{e}^{\mathrm{i}\,\varphi} \\
& \;\; = r'''_{\mathrm{A}} - 3\mathrm{i}\,r''_{\mathrm{A}} - 3r'_{\mathrm{A}} - \mathrm{i}\,(r - r_{\mathrm{A}}) + \varrho'''\mathrm{e}^{\mathrm{i}\,\varphi} \,.
\end{aligned}\right\} \tag{15.66}$$

According to (15.55) $r_{\mathrm{A}}^{(n)} = -\mathrm{i}^n(r_{\mathrm{P}_n} - r_{\mathrm{A}})$ ($n = 1, 2, \ldots$). Furthermore, by definition $r = r_{\mathrm{P}_n^*}$ when $\varrho^{(n)} = 0$. When this is substituted, the equations are

$$\left.\begin{aligned}
& n = 1: \;\; 0 = -\mathrm{i}\,(r_{\mathrm{P}_1} - r_{\mathrm{A}}) + \mathrm{i}\,(r_{\mathrm{P}_1^*} - r_{\mathrm{A}}) \qquad \text{or} \quad r_{\mathrm{P}_1^*} = r_{\mathrm{P}_1} \,, \\
& n = 2: \;\; 0 = (r_{\mathrm{P}_2} - r_{\mathrm{A}}) - 2(r_{\mathrm{P}_1} - r_{\mathrm{A}}) + (r_{\mathrm{P}_2^*} - r_{\mathrm{A}}) \quad \text{or} \quad r_{\mathrm{P}_1} = \tfrac{1}{2}(r_{\mathrm{P}_2^*} + r_{\mathrm{P}_2}) \,, \\
& n = 3: \;\; 0 = \mathrm{i}\,(r_{\mathrm{P}_3} - r_{\mathrm{A}}) - 3\mathrm{i}\,(r_{\mathrm{P}_2} - r_{\mathrm{A}}) + 3\mathrm{i}\,(r_{\mathrm{P}_1} - r_{\mathrm{A}}) - \mathrm{i}\,(r_{\mathrm{P}_3^*} - r_{\mathrm{A}}) \quad \text{or} \\
& \qquad\quad r_{\mathrm{P}_3^*} - r_{\mathrm{P}_3} = 3(r_{\mathrm{P}_1} - r_{\mathrm{P}_2}) \,.
\end{aligned}\right\} \tag{15.67}$$

The results for $n = 1$ and for $n = 2$ reconfirm what is already known. The result for $n = 3$ states that the two pairs of poles P_1 , P_2 and P_3^* , P_3 are the

parallel sides of a trapezoid and that the ratio of the lengths of these sides is $1:3$. From the sequence of Eqs.(15.67) continued for $n>3$ the following explicit expression for $r_{\mathrm{P}_n^*}$ is deduced:

$$r_{\mathrm{P}_n^*} = \sum_{k=1}^{n} \binom{n}{k} (-1)^{k-1} r_{\mathrm{P}_k} \,. \tag{15.68}$$

The proof by induction is left to the reader.

15.3.3 Euler-Savary Equation

In this section the curvature of trajectories is investigated. An important role is played by the inflection circle shown in Fig. 15.18. As is known from Fig. 15.17 the circle is determined by the normal poles P_1 and P_2. It is the geometric locus of all points of Σ_2 the trajectories of which have, instantaneously, an inflection point and a tangent passing through the normal pole P_2 which has the coordinate (see (15.45)) $y_2 = a_0/\dot{\varphi}^2$, a_0 being the acceleration of the point of Σ_2 coinciding with P_1. For simplifying the figure the case $y_2<0$ is illustrated.The tangent to the inflection circle in P_1 is also the tangent to the centrodes which are in rolling contact at P_1. The vector $\mathbf{e}$ in the figure is the unit vector along an arbitrarily directed line through P_1. In what follows, this line is referred to as line $\mathbf{e}$. It is specified by the angle α against the x-axis. Let Q with position vector $r\mathbf{e}$ be an arbitrary point fixed in Σ_2 on the line $\mathbf{e}$. Furthermore, let W be the second intersection point of the line $\mathbf{e}$ with the inflection circle. Its position vector is denoted $r_{\mathrm{W}}\mathbf{e}$, so that α and r_{W} are the polar coordinates of the circle. To be determined is the instantaneous center of curvature M of the trajectory of Q. The position vector of M is denoted $R\mathbf{e}$. The coordinates r, r_{W} and R are positive, zero or negative. Finally, let ϱ be the radius of curvature of the trajectory of Q (not to be confused with the complex number ϱ in (15.53)). Its definition is

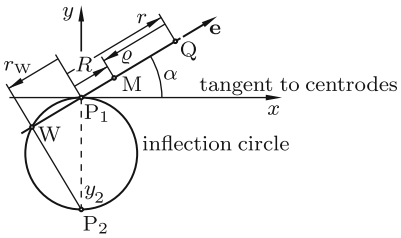

Fig. 15.18 Inflection circle with normal poles P_1 and P_2. On a line $\mathbf{e}$ a point Q fixed in Σ_2, the center of curvature M of the trajectory of Q and the second point of intersection W with the inflection circle

$$\varrho = R - r \,. \tag{15.69}$$

In the case shown in the figure, $\varrho < 0$.

The desired relationship between M and Q, i.e., between R and r is found as follows. The velocity $\mathbf{v}$ of Q has the magnitude $v = r\dot{\varphi}$. The normal component of the acceleration of Q which is directed toward M is denoted $a_{\mathrm{n}}\mathbf{e}$. Its magnitude a_{n} (positive or negative) is a function of the radius of curvature:

$$a_{\mathrm{n}} = \frac{v^2}{\varrho} = \frac{r^2\dot{\varphi}^2}{R-r} \,. \tag{15.70}$$

With (9.81) a_{n} is expressed through the acceleration $\mathbf{a}_0$ of the point of Σ_2 instantaneously coinciding with P_1:

$$a_{\mathrm{n}} = \mathbf{a}_0 \cdot \mathbf{e} - r\dot{\varphi}^2 \,. \tag{15.71}$$

Hence

$$\mathbf{a}_0 \cdot \mathbf{e} - r\dot{\varphi}^2 = \frac{r^2\dot{\varphi}^2}{R-r} \tag{15.72}$$

or, after simple re-formulation,

$$\frac{1}{r} - \frac{1}{R} = \frac{1}{s} \tag{15.73}$$

with the abbreviation

$$s = \frac{\mathbf{a}_0 \cdot \mathbf{e}}{\dot{\varphi}^2} = \frac{a_0}{\dot{\varphi}^2} \sin\alpha = y_2 \sin\alpha \,. \tag{15.74}$$

The quantity s is a constant on the line $\mathbf{e}$. Equation (15.73) is called Euler-Savary equation[3]. The derivation shown here is due to Fayet [9]. An alternative form is

$$\left(\frac{1}{r} - \frac{1}{R}\right) \sin\alpha = \frac{1}{y_2} = \text{ const} \,. \tag{15.75}$$

From the unconditionally valid three-angle equation[4]

---

[3] Euler 1765, Savary 1845

[4] When $\pi/2$ is added to all three angles or to α_1 and α_2 only or to α_1 only, the alternative equations are obtained:
$\cos\alpha_1 \sin(\alpha_2 - \alpha_3) + \cos\alpha_2 \sin(\alpha_3 - \alpha_1) + \cos\alpha_3 \sin(\alpha_1 - \alpha_2) = 0$,
$\cos\alpha_1 \cos(\alpha_2 - \alpha_3) - \cos\alpha_2 \cos(\alpha_3 - \alpha_1) + \sin\alpha_3 \sin(\alpha_1 - \alpha_2) = 0$,
$\cos\alpha_1 \sin(\alpha_2 - \alpha_3) - \sin\alpha_2 \cos(\alpha_3 - \alpha_1) + \sin\alpha_3 \cos(\alpha_1 - \alpha_2) = 0$.
The corresponding equations for hyperbolic functions are
$\sinh x_1 \sinh(x_2 - x_3) + \sinh x_2 \sinh(x_3 - x_1) + \sinh x_3 \sinh(x_1 - x_2) = 0$,
$\cosh x_1 \sinh(x_2 - x_3) + \cosh x_2 \sinh(x_3 - x_1) + \cosh x_3 \sinh(x_1 - x_2) = 0$,
$\cosh x_1 \cosh(x_2 - x_3) - \cosh x_2 \cosh(x_3 - x_1) - \sinh x_3 \sinh(x_1 - x_2) = 0$,
$\cosh x_1 \sinh(x_2 - x_3) - \sinh x_2 \cosh(x_3 - x_1) + \sinh x_3 \cosh(x_1 - x_2) = 0$.
These formulas are not found in any collection of formulas known to the author including the rich collection Skanavi [27]

$$\sin\alpha_1 \sin(\alpha_2 - \alpha_3) + \sin\alpha_2 \sin(\alpha_3 - \alpha_1) + \sin\alpha_3 \sin(\alpha_1 - \alpha_2) = 0 \quad (15.76)$$

in combination with (15.74) it follows that

$$s_1 \sin(\alpha_2 - \alpha_3) + s_2 \sin(\alpha_3 - \alpha_1) + s_3 \sin(\alpha_1 - \alpha_2) = 0\,. \quad (15.77)$$

Given the constants s_1 and s_2 on two lines $\mathbf{e}_1$, $\mathbf{e}_2$ and the direction of a third line $\mathbf{e}_3$ relative to these two, the equation determines the constant s_3 on line $\mathbf{e}_3$. The tangent to the centrodes as line of reference is not needed for this purpose. The equation was first formulated by Fayet [9] without, however, explicitly referring to (15.76).

From the right-angled triangle $(\mathrm{P}_1,\mathrm{W},\mathrm{P}_2)$ in Fig. 15.18 it follows that $r_\mathrm{W} = y_2 \sin\alpha$. This proves the identity of s with the polar coordinate r_W:

$$s = r_\mathrm{W}\,. \quad (15.78)$$

This follows also directly from (15.73). At the inflection point W the center of curvature is at infinity. Hence $R = \infty$ and $s = r_\mathrm{W}$.

Euler-Savary Equation of the Inverse Motion
In the inverse motion, trajectories in Σ_2 produced by points Q fixed in Σ_1 are considered. Let M^* be the center of curvature with the position vector $R^*\mathbf{e}$. In the inverse motion $\mathbf{a}_0$ is replaced by $-\mathbf{a}_0$ (see Theorem 9.1; $\mathbf{a}_0$ is the acceleration of the point coinciding with P_1). From (15.74) it follows that s is replaced by $-s$. Thus, the Euler-Savary equation of the inverse motion is

$$\frac{1}{r} - \frac{1}{R^*} = -\frac{1}{s}\,. \quad (15.79)$$

Now back to the motion. The trajectory of the point Q coinciding with P_1 ($r = 0$) has a cusp at P_1. About the curvature at the cusp no statement is made by the Euler-Savary equation.

On the tangent to the centrodes, i.e., on the line characterized by $\alpha = 0$, (15.75) requires that $R = 0$ independent of r. This means: For all points Q on this line, with the exception of Q=P_1, the associated center of curvature M is located at P_1.

A single pair of points $\mathrm{Q}_1, \mathrm{M}_1$ and its quantities r_1, R_1 determine a line $\mathbf{e}_1$ and, through (15.73), the constant s_1 on this line. The same equation then determines for every point Q on this line the associated point M. Likewise, a second pair of points $\mathrm{Q}_2, \mathrm{M}_2$ on another line $\mathbf{e}_2$ determines s_2 on this line and then for every point Q on this line the associated point M. Subsequently, Fayet's Eq.(15.77) determines the constant s_3 on any third line $\mathbf{e}_3$ specified by the angular difference $\alpha_3 - \alpha_1$ and, consequently, the center of curvature M for every point Q on this line.

Example: These analytical methods find an important application in the theory of the four-bar mechanism (see the four-bar $\mathrm{M}_1\mathrm{Q}_1\mathrm{Q}_2\mathrm{M}_2$ in Fig. 15.19).

The moving plane Σ_2 under investigation is the plane fixed to the coupler $\overline{Q_1Q_2}$. When the four-bar is moving, every point Q fixed in Σ_2 moves along a trajectory referred to as coupler curve. Properties of coupler curves are the subject of Sect. 17.8. The Euler-Savary equation determines the center of curvature of the coupler curve in an instantaneous position of Q.

The pole P_1 of Σ_2 lies at the intersection of the cranks. On the lines $\mathbf{e}_1$ and $\mathbf{e}_2$ the fixed points M_1 and M_2 are the centers of curvature associated with Q_1 and Q_2, respectively. The figure provides the quantities r_1, R_1, r_2, R_2 and $\alpha_2 - \alpha_1$ from which s_1 and s_2 and everything else is calculated. The points W_1 and W_2 have the polar coordinates s_1 and s_2, respectively. The pole P_2 is the point of intersection of the perpendiculars to the lines $\mathbf{e}_1$ and $\mathbf{e}_2$ at W_1 and W_2, respectively. In the auxiliary ξ, η-system with origin P_1 and with the ξ-axis along $\mathbf{e}_1$ these perpendiculars have the equations $\xi = s_1$ and $\xi\cos(\alpha_2 - \alpha_1) + \eta\sin(\alpha_2 - \alpha_1) = s_2$, respectively. Hence P_2 has the coordinates $\xi_2 = s_1$, $\eta_2 = [s_2 - s_1\cos(\alpha_2 - \alpha_1)]/\sin(\alpha_2 - \alpha_1)$. The tangent to the centrodes has the equation $\eta = -\xi\xi_2/\eta_2$. The significance of the angles β_1, β_2 is explained later. End of example.

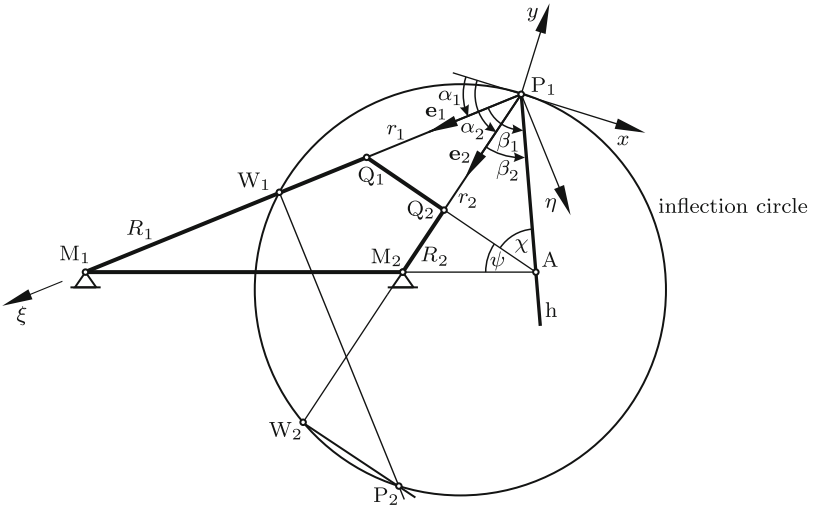

Fig. 15.19 Four-bar $M_1Q_1Q_2M_2$, inflection circle of the coupler-fixed plane and angles $\alpha_1 = \beta_2$, $\alpha_2 = \beta_1$ of Bobillier's theorem

The analytical methods explained above have geometrical interpretations which are useful for graphical constructions. Graphical constructions have the advantage of making things visible. But they have the disadvantage of relying on intersections of lines which, frequently, are either almost parallel or intersecting outside the available sheet of paper.

First, a method known as *sawtooth construction* is explained. As preparatory step, the Euler-Savary Eq.(15.73) in combination with (15.69), $R = \varrho + r$, and with (15.78), $s = r_{\mathrm{W}}$, is written in the form

$$\varrho(r_{\mathrm{W}} - r) = r^2 \,. \tag{15.80}$$

Consider Fig. 15.20 which is in part a copy of Fig.15.18. The relationships between the points P_1, Q, M and W on a line $\mathbf{e}$ can be expressed geometrically as follows. Let P^* be an arbitrarily chosen auxiliary point. Lines $\overline{\mathrm{P}^*\mathrm{M}}$ and $\overline{\mathrm{P}^*\mathrm{P}_1}$ are drawn and parallel to these lines the lines g_1 through P_1 and g_2 through W. Proposition: The point of intersection W^* of g_1 and g_2 lies on the line $\overline{\mathrm{P}^*\mathrm{Q}}$.
Proof: The triangles $(\mathrm{Q},\mathrm{M},\mathrm{P}^*)$ and $(\mathrm{Q},\mathrm{P}_1,\mathrm{W}^*)$ are similar, and the triangles $(\mathrm{Q},\mathrm{P}_1,\mathrm{P}^*)$ and $(\mathrm{Q},\mathrm{W},\mathrm{W}^*)$ are similar. Therefore, $\overline{\mathrm{QP}^*} : \overline{\mathrm{QW}^*}$ equals $\varrho : r$ as well as $r : (r_{\mathrm{W}} - r)$. Hence $\varrho(r_{\mathrm{W}} - r) = r^2$. This is Eq.(15.80). End of proof.

The name sawtooth construction refers to the shape of the figure. If P_1 and any two of the points Q, M and W are given, the missing third point is determined.

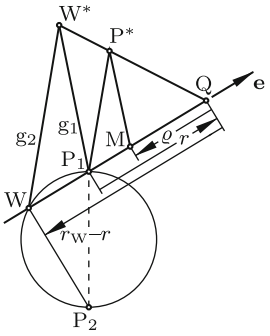

Fig. 15.20 Sawtooth construction

Example: In Fig. 15.19 the points $\mathrm{W}_1, \mathrm{W}_2$ can be constructed by two sawtooth constructions applied to the lines $\mathbf{e}_1$ and $\mathbf{e}_2$ (preferably, both with one and the same auxiliary point P^*). Following this, the normal pole P_2 is constructed graphically as point of intersection of two perpendiculars. Any third line $\mathbf{e}_3$ intersects the circle in a point W_3. For an arbitrary point Q on this line the associated point M can be constructed by one more sawtooth construction. End of example.

Bobillier showed that the tangent to the centrodes (the x-axis) can be constructed without constructing the inflection circle (see Fig. 15.19). It suffices to draw the line h through P_1 and the point A at the intersection of the

lines $\overline{M_1M_2}$ and $\overline{Q_1Q_2}$ (when the quadrilateral $M_1Q_1Q_2M_2$ is interpreted as four-bar, A is the instantaneous center of rotation of the two cranks relative to each other). The lines $\mathbf{e}_1$, $\mathbf{e}_2$ and h define the angles β_1 and β_2. Bobillier is author of

Theorem 15.6.

$$\alpha_1 = \beta_2 , \qquad \alpha_2 = \beta_1 . \tag{15.81}$$

Proof (Husty[17]): According to (15.75)

$$\left(\frac{1}{r_1} - \frac{1}{R_1}\right) \sin\alpha_1 = \left(\frac{1}{r_2} - \frac{1}{R_2}\right) \sin\alpha_2 . \tag{15.82}$$

Consider the triangles (A,P_1,M_1) and (A,P_1,Q_1) located to the right of line $\mathbf{e}_1$. The difference of the areas equals the area of the triangle (A,Q_1,M_1). This is expressed in the form

$$\overline{AP}_1\,\overline{AM}_1\,\sin(\psi+\chi) - \overline{AP}_1\,\overline{AQ}_1\,\sin\chi = \overline{AQ}_1\,\overline{AM}_1\,\sin\psi \tag{15.83}$$

or, after division through $\overline{AP}_1\,\overline{AM}_1\,\overline{AQ}_1\,\sin\chi\sin(\psi+\chi)$,

$$\frac{1}{\overline{AQ}_1\,\sin\chi} - \frac{1}{\overline{AM}_1\,\sin(\psi+\chi)} = \frac{\sin\psi}{\overline{AP}_1\,\sin\chi\sin(\psi+\chi)} . \tag{15.84}$$

The sine law applied to the triangles (A,P_1,Q_1) and (A,P_1,M_1) yields

$$\overline{AQ}_1\,\sin\chi = r_1\sin\beta_1 , \qquad \overline{AM}_1\,\sin(\psi+\chi) = R_1\sin\beta_1 . \tag{15.85}$$

Hence the previous equation becomes

$$\left(\frac{1}{r_1} - \frac{1}{R_1}\right)\frac{1}{\sin\beta_1} = \frac{\sin\psi}{\overline{AP}_1\,\sin\chi\sin(\psi+\chi)} . \tag{15.86}$$

The same arguments applied to the triangles located to the right of line $\mathbf{e}_2$ result in the equation

$$\left(\frac{1}{r_2} - \frac{1}{R_2}\right)\frac{1}{\sin\beta_2} = \frac{\sin\psi}{\overline{AP}_1\,\sin\chi\sin(\psi+\chi)} \tag{15.87}$$

with the same expression on the right-hand side. Hence

$$\left(\frac{1}{r_1} - \frac{1}{R_1}\right)\sin\beta_2 = \left(\frac{1}{r_2} - \frac{1}{R_2}\right)\sin\beta_1 . \tag{15.88}$$

Comparison with (15.82) shows that $\alpha_1 = \beta_2$ and $\alpha_2 = \beta_1$. End of proof.

Once the tangent to the centrodes is known, the theorem can be used for constructing the center of curvature M_3 associated with an arbitrarily chosen point Q_3. This is done in the following steps.

1. Draw the line h' through P_1 under the angle α_1 (known by now) against the line $\overline{\mathrm{P}_1\mathrm{Q}_3}$.
2. Construct the point A' as point of intersection of h' with the line $\overline{\mathrm{Q}_1\mathrm{Q}_3}$.
3. The desired point M_3 is the point of intersection of the lines $\overline{\mathrm{M}_1\mathrm{A}'}$ and $\overline{\mathrm{P}_1\mathrm{Q}_3}$.

15.3.4 Radii of Curvatures of Centrodes

In Fig. 15.21 the points Q and M on an arbitrary line $\mathbf{e}$ are those of Fig. 15.18. In the figure also the centrode k_2 fixed in Σ_2 and the centrode k_1 fixed in Σ_1 together with their point P_1 of rolling contact are shown. The centers of curvature of the centrodes at P_1 are denoted $\mathrm{M}_1^{\mathrm{p}}$ and $\mathrm{M}_2^{\mathrm{p}}$, respectively. They are located on the common normal to the centrodes. Let $\mathbf{e}_{\mathrm{n}}$ be the unit vector directed from P_1 toward $\mathrm{M}_2^{\mathrm{p}}$. The radii of curvature ϱ_1 and ϱ_2 are defined by expressing the vector from P_1 to $\mathrm{M}_i^{\mathrm{p}}$ $(i = 1, 2)$ in the form $\varrho_i \mathbf{e}_{\mathrm{n}}$. This means that always $\varrho_2 > 0$, whereas ϱ_1 is positive or negative depending on whether the two centrodes are curved toward the same side or toward opposite sides. From (15.46) it is known that the acceleration $\mathbf{a}_0$ of the point fixed in Σ_2 and coinciding with P_1 has the direction of $\mathbf{e}_{\mathrm{n}}$. This acceleration remains unchanged if the centrodes are replaced by their instantaneous circles of curvature. The reason is that acceleration as well as curvature depend on first- and second-order derivatives of position vectors only, whereas the difference between curve and circle of curvature depends on higher-order derivatives. Thus, $\mathbf{a}_0$ is the acceleration produced by the rolling motion of the circle of curvature of k_2 on the circle of curvature of k_1. This acceleration is taken from (15.127) in the chapter on cycloids. For the present purpose the notation has to be changed as follows. The radius r_0 must be replaced by ϱ_1, r_1 by ϱ_2 and the angular velocity $\dot{\varphi}_1$ by $\dot{\varphi}$. The

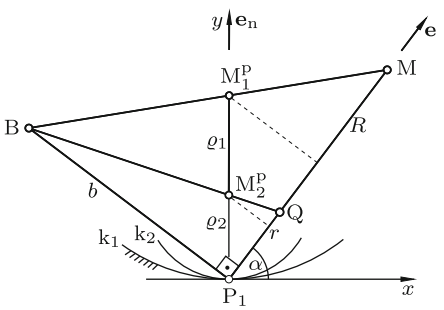

Fig. 15.21 Points Q and M on a line $\mathbf{e}$ and centrodes k_1, k_2 together with their centers of curvature $\mathrm{M}_1^{\mathrm{p}}$, $\mathrm{M}_2^{\mathrm{p}}$

sign conventions remain unchanged. The positive real axis of Fig. 15.36 has the direction of $\mathbf{e}_\mathrm{n}$. With this change of notation

$$\frac{1}{\varrho_2} - \frac{1}{\varrho_1} = \frac{\dot{\varphi}^2}{a_0} = \frac{1}{y_2} \,. \tag{15.89}$$

Comparison with (15.73) and (15.74) shows that the relationship between M_1^p and M_2^p is the same as the relationship between associated points M and Q on the line $\mathbf{e}_\mathrm{n}$. Equation (15.75) establishes between ϱ_1, ϱ_2 and the radii R, r of any pair of associated points M and Q the relationship

$$\left(\frac{1}{r} - \frac{1}{R}\right) \sin\alpha = \frac{1}{\varrho_2} - \frac{1}{\varrho_1} \,. \tag{15.90}$$

When ϱ_1 and ϱ_2 are known, this equation determines the center of curvature M for every point Q in the entire plane. Euler showed that this analytical solution is equivalent to the following geometrical solution. Construct in Fig. 15.21 the point B as point of intersection of the line $\overline{\mathrm{QM}_2^\mathrm{p}}$ with the perpendicular to $\mathbf{e}$ through P_1. Proposition: The center of curvature M lies at the intersection of $\mathbf{e}$ and $\overline{\mathrm{BM}_1^\mathrm{p}}$. Proof: As auxiliary quantity the length $b = \overline{\mathrm{BP}}_1$ is introduced. Similar triangles yield

$$\frac{R}{b} = \frac{R - \varrho_1 \sin\alpha}{\varrho_1 \cos\alpha} \,, \qquad \frac{r}{b} = \frac{r - \varrho_2 \sin\alpha}{\varrho_2 \cos\alpha} \,. \tag{15.91}$$

Elimination of b produces (15.90). End of proof. Note: Unlike (15.90), the geometrical construction fails when Q and M are located on the normal $\mathbf{e}_\mathrm{n}$.

Example: Equation (15.90) and the alternative geometrical construction of M are of particular interest in the case when the centrode k_2 is materialized as circular wheel rolling on the inside or outside of another circular wheel k_1. Trajectories of points Q fixed in the plane of k_2 are called trochoids. They are the subject of Sect. 15.5. For every position of Q the associated center of curvature is determined. Consider, for example, the special case when k_1 is a straight line (a wheel of infinite radius ϱ_1) and when Q is a point on the circumference of k_2. The trajectory is the cusped cycloid b shown in Fig. 15.38 where the points Q and P_1 are denoted C and P, respectively. In this case, the rule of construction in Fig. 15.21 shows that P is the midpoint between the generating point C and the center of curvature M. End of example.

Equation (15.89) shows that the normal poles P_1 and P_2 do not suffice for determining ϱ_1 and ϱ_2. In addition, also P_3 must be known. An expression for ϱ_1 in terms of the coordinates of these three poles is found as follows. The circle of curvature with radius ϱ_1 has the equation $x^2 + y^2 - 2\varrho_1 y = 0$. Hence $\varrho_1 \equiv (x^2 + y^2)/(2y)$ and

$$\varrho_1 = \lim_{x\to 0} \frac{x^2}{2y} \,. \tag{15.92}$$

For determining this limit value it is sufficient to formulate the Taylor expansion of the centrode k_1, i.e., of the trajectory of P_1, in the neighborhood of the origin. In complex notation this is the curve $r_{\mathrm{P}_1}(\varphi)$. For convenience, it is assumed that $r_{\mathrm{P}_1}(0)$ is the origin. Hence

$$r_{\mathrm{P}_1}(\varphi) = r_{\mathrm{P}_1}(0) + \varphi\, r'_{\mathrm{P}_1}(0) + \frac{1}{2}\,\varphi^2\, r''_{\mathrm{P}_1}(0) + \dots \,. \tag{15.93}$$

The derivatives of r_{P_1} are expressed by means of (15.61) in terms of normal poles:

$$r_{\mathrm{P}_1}(\varphi) = r_{\mathrm{P}_1}(0) + \mathrm{i}\,\varphi\big[r_{\mathrm{P}_2}(0) - r_{\mathrm{P}_1}(0)\big] - \frac{1}{2}\,\varphi^2\big[r_{\mathrm{P}_3}(0) - r_{\mathrm{P}_2}(0)\big] + \cdots \tag{15.94}$$

and with the coordinates (15.62) of the normal poles

$$r_{\mathrm{P}_1}(\varphi) = \Big[- y_2\varphi - \frac{1}{2}\, x_3\varphi^2 + \cdots \Big] + \mathrm{i}\,\Big[\frac{1}{2}(y_2 - y_3)\varphi^2 + \cdots \Big] \,. \tag{15.95}$$

The expressions in square brackets are in the limit $\varphi \to 0$ the functions x and y required for (15.92). This yields for ϱ_1 the first equation below. Equation (15.89) then determines ϱ_2:

$$\varrho_1 = \frac{y_2^2}{y_2 - y_3} \,, \qquad \varrho_2 = \frac{y_2^2}{2y_2 - y_3} \,. \tag{15.96}$$

15.3.5 Cubic of Stationary Curvature. Directrix

In Sect. 14.1.1 the curvature κ of a curve and vertices of a curve were defined. The vertex condition $\mathrm{d}\kappa/\mathrm{d}\varphi = 0$ is Eq.(14.22):

$$2r'\overline{r}'(\overline{r}'r''' - r'\overline{r}''') - 3(\overline{r}'r'' - r'\overline{r}'')(\overline{r}'r'' + r'\overline{r}'') = 0 \,. \tag{15.97}$$

This equation determines all points r of a moving plane Σ_2 which are momentarily at a vertex of their respective trajectories. Let x and y be the coordinates of r in the x, y-system of Fig. 15.17: $r = x + \mathrm{i}\,y$. For the derivatives r', r'' and r''' Eqs.(15.59) are used: $r^{(n)} = i^n(r - r_{\mathrm{P}_n})$ $(n = 1, 2, 3)$. For r_{P_n} $(n = 1, 2, 3)$ Eqs.(15.62) are substituted. This results in the expressions

$$r' = \mathrm{i}\,(x + \mathrm{i}\,y) \,, \qquad r'' = -x - \mathrm{i}\,(y - y_2) \,, \qquad r''' = y - y_3 - \mathrm{i}\,(x - x_3) \tag{15.98}$$

and

$$\left.\begin{aligned} r'\overline{r}' = x^2 + y^2 \,, \qquad \overline{r}'r'' = y_2 x + \mathrm{i}\,(x^2 + y^2 - y_2 y) \,, \\ \overline{r}'r''' = -(x^2 + y^2) + x_3 x + y_3 y + \mathrm{i}\,(y_3 x - x_3 y) \,. \end{aligned}\right\} \tag{15.99}$$

With these expressions (15.97) takes the form

$$[(3y_2 - y_3)x + x_3 y](x^2 + y^2) - 3y_2^2 xy = 0 \tag{15.100}$$

or

$$(\lambda x + \mu y)(x^2 + y^2) - xy = 0 \tag{15.101}$$

with two parameters

$$\lambda = \frac{3y_2 - y_3}{3y_2^2} \,, \qquad \mu = \frac{x_3}{3y_2^2} \,. \tag{15.102}$$

Because of the third-order terms the curve is referred to as *cubic of stationary curvature*. The equation is simplest in terms of polar coordinates $r\,,\ \alpha\,.$ Substitution of $x = r\cos\alpha\,,\ y = r\sin\alpha$ results in the explicit equation

$$r = \frac{\cos\alpha \sin\alpha}{\lambda\cos\alpha + \mu\sin\alpha} \,. \tag{15.103}$$

The stationarity condition $\mathrm{d}r/\mathrm{d}\alpha = 0$ is $\tan^3\alpha = \lambda/\mu$, and the stationary value is $r_{\mathrm{stat}} = (1/\mu)[1 + (\lambda/\mu)^{2/3}]^{-3/2} = (1/\lambda)[1 + (\mu/\lambda)^{2/3}]^{-3/2}$.

If the x, y-coordinates of two vertices are known, λ and μ are determined by two linear Eqs.(15.101). Then also the coordinates of the normal pole P_3 and the radii of curvature of the centrodes are known. Equations (15.102) and (15.96) yield the expressions

$$x_3 = 3y_2^2\mu \,, \qquad y_3 = 3y_2(1 - y_2\lambda) \,, \tag{15.104}$$

$$\varrho_1 = \frac{y_2}{3\lambda y_2 - 2} \,, \qquad \varrho_2 = \frac{y_2}{3\lambda y_2 - 1} \,. \tag{15.105}$$

Taylor expansion of (15.101) about the origin starts with the second-order term $-xy$. From this it follows that the curve has a double point at the origin, and that at the origin both the x-axis and the y-axis are tangents.

In the special case $\lambda = 0\,,\ \mu \neq 0$, the curve has the equation $y[\mu(x^2 + y^2) - x] = 0$. It splits into the x-axis and a circle. Likewise, in the special case $\mu = 0\,,\ \lambda \neq 0$, the curve has the equation $x[\lambda(x^2 + y^2) - y] = 0$. It splits into the y-axis and a circle. The two circles with their centers at $(\,x = 1/(2\mu)\,,\ y = 0\,)$ and $(\,x = 0\,,\ y = 1/(2\lambda)\,)$, respectively, are the circles of curvature of the curve at the double point.

Equation (15.101) of the curve is a special case of Eq.(14.53) defining Burmester's pole curve. The geometrical reason is the following. Burmester's pole curve is the expression of relationships between centers of rotation defined by four discrete positions of a plane. The cubic of stationary curvature

is the expression of relationships between instantaneous centers of rotation defined by four infinitesimally neighboring positions of a plane (at a vertex a trajectory is contacting the curve in – at least – four infinitesimally close neighboring points; it is contacting its circle of curvature in at least three points). In Sect. 14.5 properties of Burmester's pole curve were investigated (see (14.53) – (14.63)). The curve has an asymptote. The asymptote has the slope $-\lambda/\mu$. It intersects the curve at a single point H called cardinal point. Another characteristic point is the focus Φ. The tangent to the curve in Φ passes through H. For the cubic of stationary curvature with Eq.(15.101) the following special formulas are obtained[5]. The equation of the asymptote parallel to the line $\lambda x + \mu y = 0$ is

$$\lambda x + \mu y + \frac{\lambda\mu}{\lambda^2 + \mu^2} = 0 \,. \tag{15.106}$$

The cardinal point H and the focus Φ have the coordinates

$$\left.\begin{aligned} x_{\mathrm{H}} &= -\lambda \frac{\lambda\mu}{\lambda^4 - \mu^4} \,, \qquad & y_{\mathrm{H}} &= \mu \frac{\lambda\mu}{\lambda^4 - \mu^4} \,, \\ x_{\Phi} &= \frac{\mu}{2(\lambda^2 + \mu^2)} \,, \qquad & y_{\Phi} &= \frac{\lambda}{2(\lambda^2 + \mu^2)} \,. \end{aligned}\right\} \tag{15.107}$$

From these equations it follows that P_1 lies halfway between the asymptote and the line parallel to the asymptote and passing through Φ.

Example: The coupler of the four-bar mechanism shown in Fig. 15.19 is considered again. The points Q_1 and Q_2 are both vertices because every point of a circular trajectory is a vertex. Hence the x, y-coordinates of these points determine the parameters λ and μ, the cubic of stationary curvature, its asymptote, the normal pole P_3, the radii of curvature of the centrodes and the points H and Φ of the coupler in the instantaneous position shown. In Fig. 15.22 the cubic of stationary curvature, its asymptote and the points H and Φ are shown together with various other lines and points which are explained later. End of example.

Directrix of the Cubic of Stationary Curvature

In Fig. 15.23 the x, y-system with origin P_1 is the same as in previous figures. Let $\hat{\mathrm{Q}}$ be an arbitrary point (not yet confined to the straight line referred to as directrix). The diagonal in the rectangle defined by the axes and by the lines parallel to the axes and the perpendicular from the origin onto this diagonal define the point Q. Through this construction every point $\hat{\mathrm{Q}}$ is

[5] The transformation (14.55), (14.57) determines the normal form (14.59) $(\eta - a)(\xi^2 + \eta^2) + d\,\xi + e\eta = 0$. Its parameters are

$a = \frac{-2\lambda\mu}{(\lambda^2+\mu^2)^{3/2}}$, $\quad d = \frac{-\lambda\mu(\lambda^2-\mu^2)}{(\lambda^2+\mu^2)^3}$, $\quad e = \frac{-(\lambda^4-6\lambda^2\mu^2+\mu^4)}{4(\lambda^2+\mu^2)^3}$.

These parameters satisfy the condition (14.67) for the existence of a double point: $e = a^2/4 - d^2/a^2$

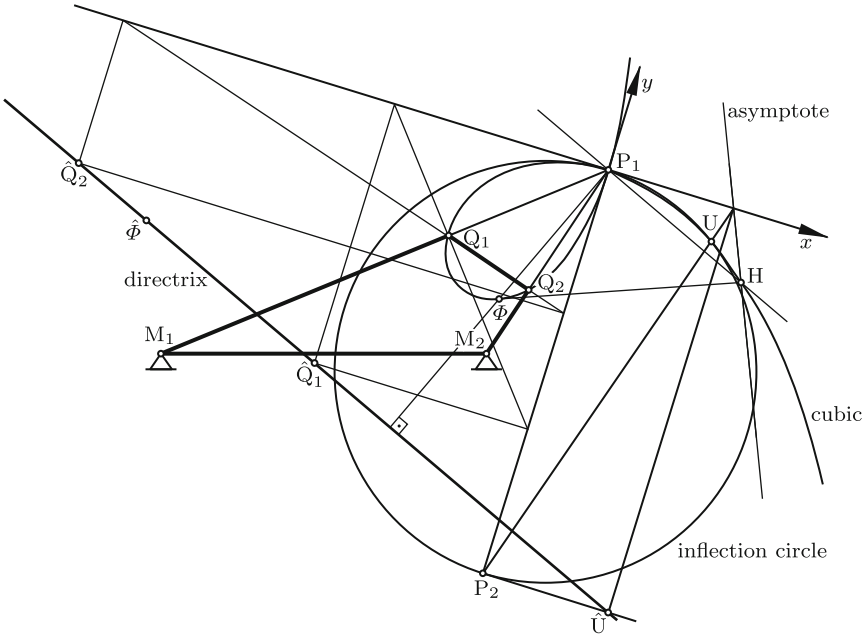

Fig. 15.22 Four-bar of Fig. 15.19 with inflection circle, cubic of stationary curvature, directrix, asymptote, focus Φ, cardinal point H and Ball's point U of the coupler

mapped into a uniquely defined point Q. Points $\hat{\mathrm{Q}}$ on the x-axis and/or on the y-axis are mapped into the origin P_1. The inverse mapping of Q into $\hat{\mathrm{Q}}$ is determined by drawing through Q the perpendicular to the line joining Q with P_1. This rule of construction fails if Q is a point on the x-axis and/or on the y-axis. The geometrical rules for constructing Q from $\hat{\mathrm{Q}}$ and vice versa are expressed analytically as follows. Let $\hat{x}$ and $\hat{y}$ be the coordinates of $\hat{\mathrm{Q}}$ and x and y be the coordinates of Q. The two lines intersecting at Q have the equations $y/\hat{y} + x/\hat{x} = 1$ and $y/x = \hat{x}/\hat{y}$. Resolving once for x and y and once for $\hat{x}$ and $\hat{y}$ results in the equations

$$x = \hat{y}\,\frac{\hat{x}\hat{y}}{\hat{x}^2 + \hat{y}^2}\,, \qquad y = \hat{x}\,\frac{\hat{x}\hat{y}}{\hat{x}^2 + \hat{y}^2}\,, \tag{15.108}$$

$$\hat{x} = \frac{x^2 + y^2}{x}\,, \qquad \hat{y} = \frac{x^2 + y^2}{y}\,. \tag{15.109}$$

Through these equations it is reconfirmed that every point $\hat{\mathrm{Q}}$ is mapped into a uniquely defined point Q, and that the inverse mapping from Q into $\hat{\mathrm{Q}}$ is uniquely defined for all points Q except points on the x-axis and/or on the y-axis. From (15.108) it follows that

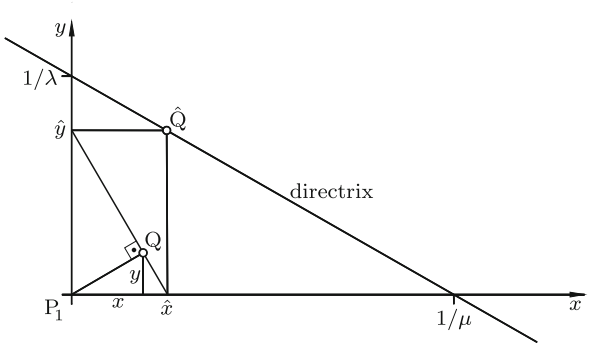

Fig. 15.23 Geometric construction of Q from $\hat{\mathrm{Q}}$ and vice versa

$$\left.\begin{aligned} \lambda x + \mu y &= (\lambda\hat{y} + \mu\hat{x})\frac{\hat{x}\hat{y}}{\hat{x}^2+\hat{y}^2}\,, \\ x^2 + y^2 &= \frac{\hat{x}^2\hat{y}^2}{\hat{x}^2+\hat{y}^2}\,, \qquad xy = \frac{\hat{x}^3\hat{y}^3}{(\hat{x}^2+\hat{y}^2)^2} \end{aligned}\right\} \tag{15.110}$$

and, hence

$$(\lambda x + \mu y)(x^2+y^2) - xy = (\mu\hat{x} + \lambda\hat{y} - 1)\frac{\hat{x}^3\hat{y}^3}{(\hat{x}^2+\hat{y}^2)^2}\,. \tag{15.111}$$

Hence the conclusion: If $\hat{\mathrm{Q}}$ is located on the line $\mu\hat{x} + \lambda\hat{y} - 1 = 0$, Q is located on the cubic of stationary curvature. Thus, this line is mapped into the cubic of stationary curvature by means of the construction shown in Fig. 15.23 and also by means of (15.108). The line is called *directrix* of the cubic of stationary curvature. It intersects the x-axis at $x = 1/\mu$ and the y-axis at $y = 1/\lambda$. These two points of intersection are mapped into the double point $x = y = 0$ of the cubic of stationary curvature.

From Eqs.(15.107) for the coordinates of H and Φ it follows that the line $\overline{\mathrm{P_1H}}$ is parallel to the directrix and that, furthermore, Φ is the midpoint of the perpendicular from the origin $\mathrm{P_1}$ onto the directrix. Equations (15.109) map H and Φ into points $\hat{\mathrm{H}}$ and $\hat{\Phi}$, respectively, on the directrix. These points have the coordinates

$$\hat{x}_{\mathrm{H}} = \frac{-\mu}{\lambda^2-\mu^2}\,, \qquad \hat{y}_{\mathrm{H}} = \frac{\lambda}{\lambda^2-\mu^2}\,, \qquad \hat{x}_{\Phi} = \frac{1}{2\mu}\,, \qquad \hat{y}_{\Phi} = \frac{1}{2\lambda}\,. \tag{15.112}$$

Point $\hat{\Phi}$ is the midpoint between the points of intersection of the directrix with the x- and y-axes. In Fig. 15.22 $\hat{\Phi}$ and lines for the construction of $\hat{\mathrm{Q}}_1$ and $\hat{\mathrm{Q}}_2$ from Q_1 and Q_2, respectively, according to Fig. 15.23 are shown.

15.3.6 Ball's Point

The cubic of stationary curvature intersects the inflection circle at the pole P_1 and at one more point. This point is called *Ball's point*, denoted U. The trajectory of the point of Σ_2 coinciding with U has at this point not only zero curvature, but also zero rate of change of curvature. It is, therefore, a good straight-line approximation of its tangent $\overline{UP}_2$. The coordinates of U are determined as follows. The inflection circle has the equation (see (15.46))

$$x^2 + y^2 - y_2 y = 0 \,. \tag{15.113}$$

Combination with (15.100) for the cubic of stationary curvature produces the equation $y_2 y(-y_3 x + x_3 y) = 0$. The solution $y = 0$ belongs to the pole P_1. The second solution yields for the coordinates of U the ratio $y_U/x_U = y_3/x_3$. This shows that U is located on the line $\overline{P_1 P_3}$. Substitution of $y_U = x_U y_3/x_3$ into (15.113) yields an expression for x_U. The coordinates are

$$x_U = x_3 \frac{y_2 y_3}{x_3^2 + y_3^2} \,, \qquad y_U = y_3 \frac{y_2 y_3}{x_3^2 + y_3^2} \,. \tag{15.114}$$

By substituting for x_3 and y_3 the expressions (15.104) the coordinates are expressed in terms of y_2, λ and μ:

$$x_U = y_2 \frac{\mu y_2 (1 - \lambda y_2)}{(1 - \lambda y_2)^2 + \mu^2 y_2^2} \,, \qquad y_U = y_2 \frac{(1 - \lambda y_2)^2}{(1 - \lambda y_2)^2 + \mu^2 y_2^2} \,. \tag{15.115}$$

With the expressions (15.114) Eqs.(15.109) determine the coordinates of the associated point $\hat{U}$ on the directrix. It turns out that $\hat{y}_U = y_2$. This means that $\hat{U}$ is the point of intersection of the directrix with the tangent to the inflection circle at the pole P_2. From this point $\hat{U}$ Ball's point U can be constructed following the rules of Fig. 15.23. In Fig. 15.22 $\hat{U}$ and U and the geometrical construction are shown. Remark: That the asymptote intersects the x-axis at the point $x = x_{\hat{U}}$ is a peculiarity of this example. Normally, this is not the case.

At the beginning it was said that the trajectory of the point of Σ_2 coinciding with Ball's point U is a good straight-line approximation of its tangent $\overline{UP}_2$. In engineering, straight-line approximations are required for many purposes. So-called level-luffing jib cranes, for example, are large-size four-bars maneuvering the load-lifting hook. The pulley for the hook-carrying rope is attached to the coupler at a point which is Ball's point when the crane is halfway between its extremal positions. The parameters of the four-bar are chosen such that the almost straight trajectory is horizontal. This arrangement has the effect that a load is carried in good approximation horizontally when the crane is operating with constant length of the rope. Details see in Dijksman [8].

15.4 Holditch's Theorem

In a reference plane Σ a closed curve k is given (Fig. 15.24a). The curve may be either convex or nonconvex. It is free of double points. It may have straight-line segments and a finite number of corners. A rod (a line segment) of length 2ℓ is guided with its endpoints C_1 and C_2 on k. Provided ℓ is sufficiently small a periodic motion is possible such that per period the rod is rotated through 2π counterclockwise (this sense of rotation is arbitrarily chosen) and that at the end of the period C_1 and C_2 are back in their initial positions. In the course of this motion both C_1 and C_2 trace the entire curve k. In what follows, this motion is investigated. Taking the nonconvex curve and the rod in Fig. 15.24a as example, the following statements can be made. The periodic motion is, in general, not possible without reversing several times (more precisely an even number of times)

- the sense of direction of motion of C_1 and C_2 along k
- the sense of rotation of the rod.

Uniform sense of rotation is possible if and only if k is convex. Uniform sense of direction of motion of C_1 and C_2 is, in general, impossible even if k is convex.

Let $\mathbf{r}_C$ be the vector pointing from some reference point 0 fixed in Σ to the midpoint C of the rod and let, furthermore, $\boldsymbol{\varrho}$ be the vector from C to C_1. Then $\mathbf{r}(t) = \mathbf{r}_C(t) + \lambda\boldsymbol{\varrho}(t)$ (λ arbitrary) is the time-dependent position vector of the point denoted $P(\lambda)$ on the line passing through C_1 and C_2. In the course of the said periodic motion every point $P(\lambda)$ traces a closed trajectory. In Fig. 15.24b the trajectories of P(0) (point C) and of $P(\lambda = \sqrt{2})$ are shown. The curve k itself is the trajectory of both $P(1) = C_1$ and of $P(-1) = C_2$.

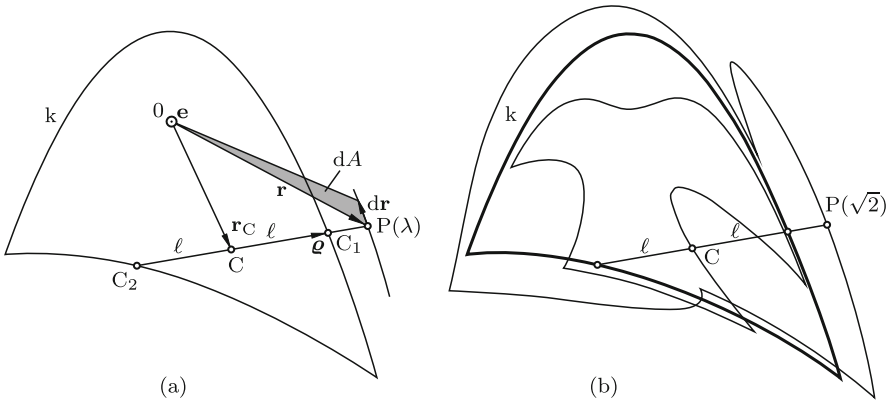

Fig. 15.24 Curve k with guided rod $\overline{C_1C_2}$. Areal element dA of the trajectory of $P(\lambda)$ **(a)** and trajectories of points $P(0) = C$ and $P(\lambda = \sqrt{2})$ **(b)**

In Fig. 15.24a the shaded areal element $\mathrm{d}A$ enclosed by the position vector $\mathbf{r}$ and by the path element $\mathrm{d}\mathbf{r}$ is shown. It is expressed in the form $\mathrm{d}A = \frac{1}{2}\,\mathbf{e}\cdot\mathbf{r}\times\mathrm{d}\mathbf{r}$ where $\mathbf{e}$ is the unit vector normal to the plane (sense of direction as indicated). Areal elements can be positive, zero or negative. Let $A(\lambda)$ be the area enclosed by the trajectory of $\mathrm{P}(\lambda)$. It is the line integral over the closed trajectory:

$$A(\lambda) = \frac{1}{2}\,\mathbf{e}\cdot\oint \mathbf{r}\times\mathrm{d}\mathbf{r} = \frac{1}{2}\,\mathbf{e}\cdot\Big[\oint \mathbf{r}_\mathrm{C}\times\mathrm{d}\mathbf{r}_\mathrm{C} + \lambda\Big(\oint \mathbf{r}_\mathrm{C}\times\mathrm{d}\boldsymbol{\varrho} + \oint \boldsymbol{\varrho}\times\mathrm{d}\mathbf{r}_\mathrm{C}\Big) + \lambda^2\oint \boldsymbol{\varrho}\times\mathrm{d}\boldsymbol{\varrho}\Big]\,. \tag{15.116}$$

The term free of λ represents the area $A(0)$ enclosed by the trajectory of C. The coefficient of λ^2 is the area $\pi\ell^2$ of the circle having the rod length 2ℓ as diameter. The coefficient of λ is the difference $\frac{1}{2}[A(1)-A(-1)]$. It is zero because $A(1)$ as well as $A(-1)$ is the area enclosed by k. Hence

$$A(\lambda) = A(0) + \lambda^2\pi\ell^2\,. \tag{15.117}$$

Subtraction of the same equation for the special case $\lambda = 1$ results in

$$A(\lambda) - A(1) = (\lambda^2 - 1)\pi\ell^2\,. \tag{15.118}$$

This equation is Holditch's [15] famous[6]

Theorem 15.7. *The difference of the areas enclosed by the trajectory of* $\mathrm{P}(\lambda)$ *and by* k *is, independent of the shape of* k, (λ^2-1) *times the area* $\pi\ell^2$ *of the circle having the rod length* 2ℓ *as diameter.*

Example: For the trajectories with $\lambda = 0$ and $\lambda = \sqrt{2}$ shown Fig. 15.24b the difference of areas is the same, namely, $\pi\ell^2$.

If k is convex, trajectories of points with $|\lambda| < 1$ are inside of k or on k, and trajectories of points with $|\lambda| > 1$ are outside of k or on k.

If the shape of k is such that in some section of motion C_1 and C_2 are guided on nonparallel straight lines, the trajectories of all points $\mathrm{P}(\lambda)$ in this section are segments of ellipses (see the elliptic trammel in Sect. 15.1.2). This case is illustrated in Fig. 15.25a. The curve k is an equilateral triangle, and the length 2ℓ of the rod is smaller than the altitude of the triangle. The trajectory of the midpoint C=P(0) is composed of three congruent elliptic segments and of three straight-line segments. Arrows indicate the sense of

[6] Holditch's brief communication (less than a single page) seems to indicate that only convex curves k and points with $|\lambda| \le 1$ are considered. These restrictions are unnecessary. The theorem is one out of very few global statements about curves (global in contrast to local statements of differential geometry). For this reason Giering [12] speaks of a *jewel of geometry*. Generalizations of the theorem see in Schoenflies/Grübler [26], Hoschek [16], Hering [13] and Feldhoff [10]

direction of motion of P(0). These arrows show that the area $A(0)$ enclosed by the trajectory of P(0) is calculated from the partial areas denoted A_1, A_2 and A_3 according to the formula $A(0) = A_3 - A_2 - 2A_1$.

The vertices of the triangle are the centers of the ellipses. Point C is at a vertex of an ellipse when the rod is either parallel to or orthogonal to an altitude of the triangle. These two positions yield for the semi major axes a and b of the ellipses the formulas $a = \frac{3}{4}Lc$, $b = a/3$ where L is the side length of the triangle and c (arbitrary) is the ratio $c = 2\ell/h$ (rod length divided by the altitude of the triangle).

In Fig. 15.25b the curve k is the same triangle. The rod length equals the altitude of the triangle ($c = 1$). This is the maximum possible length. At the points of contact the elliptic segments have equal tangents and equal curvature. The rod may be guided along k such that P(0) traces the trajectory in the way shown in Fig. 15.25a. However, the rod may also be guided such that its endpoints C_1 and C_2 move along k without reversing the sense of direction. In this case, P(0) is tracing twice per period the oval formed by the three elliptic segments (see the arrows). From this it follows that the two areas denoted A_2 and A_3 are identical and that, furthermore, $A(0) = -2A_1 = A(1) - \pi\ell^2$. With the side length L of the triangle $A(1) = L^2\sqrt{3}/4$ and $\ell = L\sqrt{3}/4$. Hence the area of the oval is $A_1 = \frac{1}{32}L^2(3\pi - 4\sqrt{3})$.

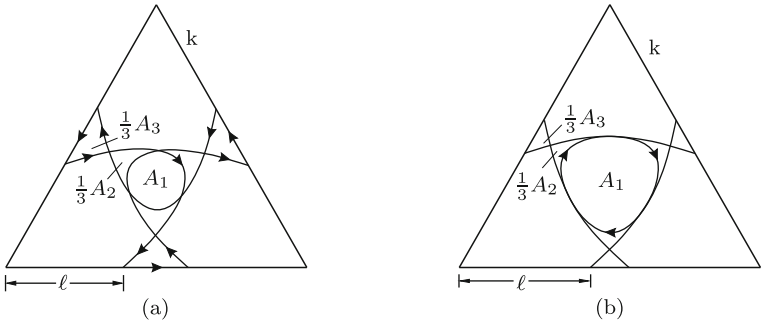

Fig. 15.25 Trajectory of the midpoint P(0) when k is an equilateral triangle. In **(a)** the rod length 2ℓ is smaller than the altitude of the triangle, and in **(b)** it equals the altitude

15.5 Trochoids

Trochoids are trajectories of points C fixed on a *planetary wheel* 1 which is rolling on a stationary *sunwheel* 0. In Figs. 15.26 and 15.27 all possible arrangements of wheels are shown. In Fig. 15.26 the wheels are touching each

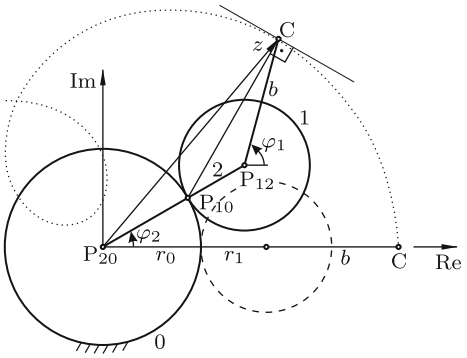

Fig. 15.26 Wheels touching each other from the outside. For the straight-line position shown the parameters are $r_0 = -3$, $r_1 = 2$, $b = 4$

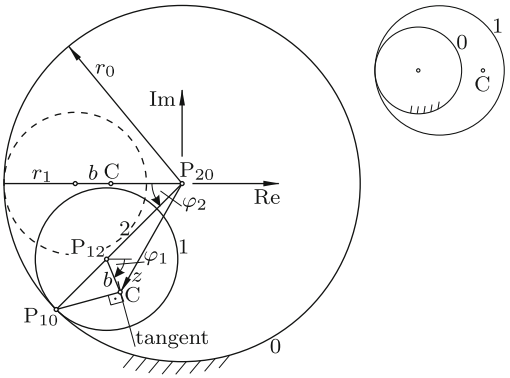

Fig. 15.27 Wheel 1 inside wheel 0. For the straight-line position shown the parameters are $r_0 = 5$, $r_1 = 2$, $b = 1$. In the small figure wheel 0 is inside wheel 1

other from the outside, and in Fig. 15.27 one wheel is inside the other. The one inside may be either wheel 1 or wheel 0 (see the small figure). The point C fixed on wheel 1 is located at a radius which is either smaller than or equal to or larger than the radius of wheel 1. Depending on the arrangement of the wheels and on the location of C on wheel 1 trochoids come in many different shapes. This makes them interesting for engineering applications. Mathematical investigations of trochoids started very early because of their role in the explanation of orbits of solar planets by cycles and epicycles (de la Hire [14], J. Bernoulli). The crank 2 connecting the centers of the wheels has no influence on the shape of trochoids. Its only purpose is to keep the wheels in touch and to make wheel 1 rolling.

The curvature of trochoids was the subject of the example illustrating Fig. 15.21.

From the elliptic trammel in Fig. 15.4 the following results are known about wheels having the ratio $1:2$ of radii with the small wheel being inside the larger wheel. If the small wheel is the planetary wheel 1, trochoids are diameters of wheel 0 if C is located on the circumference of wheel 1 and ellipses otherwise. If the large wheel is the planetary wheel 1, trochoids are limaçons of Pascal (Fig. 15.8).

15.5.1 Basic Equations in Complex Notation

Three parameters suffice if the radii r_0 and r_1 of the wheels and the radius b of point C on wheel 1 are defined as quantities which may be positive or negative. These definitions are given next. In Figs. 15.26 and 15.27 the poles P_{20}, P_{12} and P_{10} are shown. The tangent to the trochoid is the normal to the line $\overline{P_{10}C}$. The position of C is specified by the complex number z in the complex plane with origin P_{20}. A system has several, possibly even infinitely many so-called straight-line positions. In these positions the three poles and the point C are located on a single line. The real axis of the complex plane is placed along the line of an arbitrarily chosen straight-line position. In the chosen position the signs of the scalar parameters r_0, r_1 and b are defined as follows:

$r_0 > 0$ ($r_0 < 0$) if P_{20} lies to the right (to the left) of P_{10},
$r_1 > 0$ ($r_1 < 0$) if P_{12} lies to the right (to the left) of P_{10},
$b > 0$ ($b < 0$) if C lies to the right (to the left) of P_{12}.

The rotation angles φ_1 of wheel 1 and φ_2 of crank 2 relative to frame 0 are zero in the straight-line position and positive counterclockwise. The parameters belonging to Figs. 15.26 and 15.27 are given in the figure headings. With parameters and variables thus defined the complex number z representing C is always

$$z = (r_1 - r_0)\mathrm{e}^{\mathrm{i}\,\varphi_2} + b\mathrm{e}^{\mathrm{i}\,\varphi_1} \,. \tag{15.119}$$

The angular ratio φ_1/φ_2 is constant and, consequently, identical with the angular velocity ratio $\dot{\varphi}_1/\dot{\varphi}_2$. According to (15.6) the ratio is

$$\frac{\varphi_1}{\varphi_2} = \frac{\dot{\varphi}_1}{\dot{\varphi}_2} = \frac{r_1 - r_0}{r_1} \,. \tag{15.120}$$

The angular velocities themselves need not be constant. Trochoids are closed (nonclosed) curves if the ratio $\varphi_1/\varphi_2 = (r_1 - r_0)/r_1$ is a rational number (an irrational number, respectively). In gears with teeth the ratio is rational.

Equation (15.119) is differentiated twice with respect to time. In combination with (15.120) this yields for the velocity and the acceleration of the generating point C the complex expressions

$$\dot{z} = \mathrm{i}\,\dot{\varphi}_1\left(r_1 \mathrm{e}^{\mathrm{i}\,\varphi_2} + b\mathrm{e}^{\mathrm{i}\,\varphi_1}\right), \tag{15.121}$$

$$\ddot{z} = \mathrm{i}\,\ddot{\varphi}_1\left(r_1 \mathrm{e}^{\mathrm{i}\,\varphi_2} + b\mathrm{e}^{\mathrm{i}\,\varphi_1}\right) - \dot{\varphi}_1^2\left(\frac{r_1^2}{r_1 - r_0}\mathrm{e}^{\mathrm{i}\,\varphi_2} + b\mathrm{e}^{\mathrm{i}\,\varphi_1}\right). \tag{15.122}$$

Imagine that in the mechanism of Figs. 15.26 or 15.27 the crank is making a single 2π-rotation so that its final position coincides with its initial position. Then also the circle of wheel 1 is the same in the final and in the initial position. However, wheel 1 is rotated in this process through the angle $\Delta\varphi_1 = 2\pi(r_1 - r_0)/r_1$. If $(r_1 - r_0)/r_1$ is not an integer number, C assumes a new position C_1. From this it follows that two points of wheel 1 on the same radius b and displaced by the angle $\Delta\varphi_1$ trace one and the same trochoid. For the same reason all points C_1, C_2 etc. with equal angular displacements $\Delta\varphi_1$ trace one and the same trochoid. For a closed trochoid there exists a minimal integer number ν such that $\nu\Delta\varphi_1$ is an integer multiple of 2π. The points $\mathrm{C}, \mathrm{C}_1, \ldots, \mathrm{C}_\nu$ on wheel 1 form a regular polygon all vertices of which trace one and the same trochoid. This fact is made use of in the Wankel engine (see Fig. 15.28). The mechanism in this figure has the parameters $r_0 = 2$ and $r_1 = 3$. They yield $\Delta\varphi_1 = \frac{1}{3}\,2\pi$. The polygon is an equilateral triangle. This triangle represents the rotating piston. Between piston and trochoid three chambers are created the volumes of which are periodically changing when the crank is rotating. The trochoid itself depends on the additional free parameter b. In Fig. 15.28 $b = 9$ is chosen. In a Wankel engine the three sides of the piston are not straight lines, but curves shaped in such a way that the ratio of minimum and maximum chamber volumes is as small as possible. The optimal curve is described by Wunderlich [30].

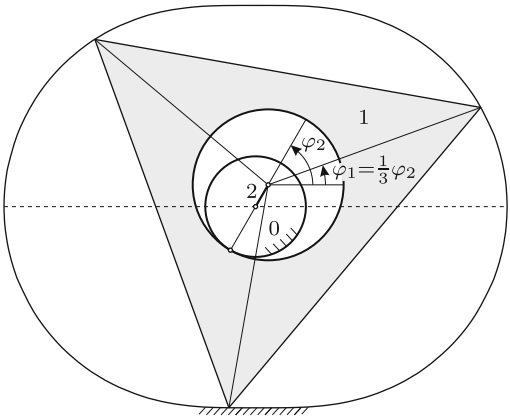

Fig. 15.28 The equilateral triangle is the rotating piston of a Wankel engine. Its vertices trace the trochoid with parameters $r_0 = 2$, $r_1 = 3$, $b = 9$

15.5.2 Double Generation of Trochoids

The trochoid of a mechanism with parameters $r_0\,, r_1\,, b$ is generated by another mechanism having the same center P_{20}, but different parameters $r_0^*\,,\ r_1^*$ and b^* (Philippe de la Hire [14]). This double generation has interesting engineering applications. The complex number z in (15.119) remains unchanged if the new parameters satisfy the conditions

$$r_1^* - r_0^* = b\,, \qquad b^* = r_1 - r_0\,, \qquad \varphi_2^* = \varphi_1\,, \qquad \varphi_1^* = \varphi_2\,. \tag{15.123}$$

From the last two conditions it follows that $\varphi_2^*/\varphi_1^* = \varphi_1/\varphi_2$ and with this from (15.120) $r_1^*/(r_1^* - r_0^*) = (r_1 - r_0)/r_1$ or after simple reformulation

$$\frac{r_1}{r_0} + \frac{r_1^*}{r_0^*} = 1\,. \tag{15.124}$$

This equation and the first two Eqs.(15.123) together determine $r_0^*\,,\ r_1^*$ and b^*:

$$r_0^* = -\frac{b}{r_1}\,r_0\,, \qquad r_1^* = \frac{b}{r_1}(r_1 - r_0)\,, \qquad b^* = r_1 - r_0\,. \tag{15.125}$$

These formulas lead to the statement:

$$\text{if} \quad \left|\frac{b}{r_1}\right| \gtreqless 1\,, \qquad \text{then} \quad \left|\frac{b^*}{r_1^*}\right| \lesseqgtr 1 \quad \text{and} \quad \left|\frac{r_0^*}{r_0}\right| \gtreqless 1\,. \tag{15.126}$$

In Figs. 15.29 and 15.30 the solid lines show again the mechanisms of Figs. 15.26 and 15.27, respectively. The second mechanism is found graphically as follows (see Fig. 15.29). The centers P_{20}^* of wheel 0^* and P_{20} of wheel 0 coalesce. The dashed lines parallel to the lines $\overline{\mathrm{P}_{20}\mathrm{P}_{12}}$ and $\overline{\mathrm{P}_{12}\mathrm{C}}$ form the parallelogram with the corner P_{12}^* opposite P_{12}. The point P_{12}^* is the center of wheel 1^*. The pole P_{10}^* is determined by the fact that it is on the line $\overline{\mathrm{P}_{12}^*\mathrm{P}_{20}}$ as well as on the normal $\overline{\mathrm{P}_{10}\mathrm{C}}$ to the tangent of the trochoid. The poles $\mathrm{P}_{20}\,,\ \mathrm{P}_{10}^*$ and P_{12}^* determine the positions of the wheels 0^* and 1^*. The parallelogram is seen to accomplish the interchange of angles as is prescribed by the last two Eqs.(15.123). In the case of opposite signs of φ_2 and φ_1 (Fig. 15.30), interchanging the angles has the effect that the cranks of the two generating mechanisms must be rotated in opposite directions in order to trace the trochoid in the same sense.

The two generating mechanisms have some properties in common. By other properties they can be distinguished. First, a distinguishing property. If P_{20} is outside the circle of wheel 1 in one generation, P_{20} is inside the circle of wheel 1 in the other generation (see Figs. 15.29 and 15.30). By convention, the generation with P_{20} outside the circle of wheel 1 is called first generation. Next, a property common to both generating mechanisms. Wheel 0 is

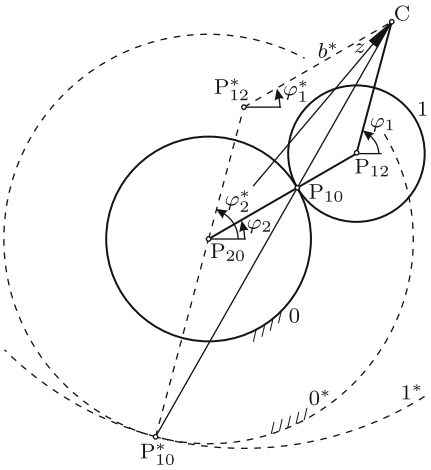

Fig. 15.29 First and second generation of the trochoid of Fig. 15.26. Parameters $r_0 = -3$, $r_1 = 2$, $b = 4$ (first generation; solid lines) and $r_0^* = 6$, $r_1^* = 10$, $b^* = 5$ (second generation; dashed lines)

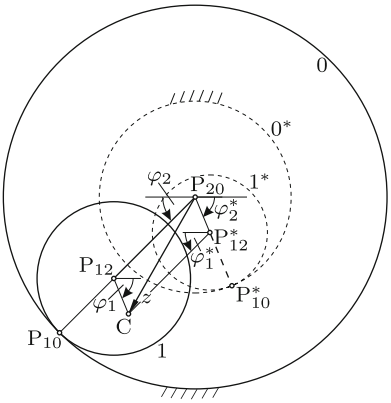

Fig. 15.30 First and second generation of the trochoid of Fig. 15.27. Parameters $r_0 = 5$, $r_1 = 2$, $b = 1$ (first generation) and $r_0^* = -5/2$, $r_1^* = -3/2$, $b^* = -3$ (second generation)

touched by wheel 1 either in both mechanisms from the outside (Fig. 15.29) or in both mechanisms from the inside (Fig. 15.30). Trochoids generated by mechanisms of the former type are called epitrochoids, and trochoids generated by mechanisms of the latter type are called hypotrochoids. Epitrochoids and hypotrochoids alike are divided into three families:

1. Trochoids have double points if in the first generation the generating point C is outside the circle of wheel 1, i.e., if $|b/r_1| > 1$. Such trochoids are called curtate trochoids (Fig. 15.26 and the limaçon of Pascal in Fig. 15.8a).
2. Trochoids have cusps on the circumference of wheel 1 if the generating point C is located on the circumference of wheel 1 (in both generations; $|b/r_1| = 1$). Such trochoids are called *cycloids* (either epicycloids or hypocycloids).
3. Trochoids have neither double points nor cusps if in the first generation point C is inside of wheel 1, i.e., if $|b/r_1| < 1$. Such trochoids are called prolate trochoids (Fig. 15.28 and the limaçons of Pascal in Figs. 15.8c,d).

Example: In the system shown in Fig. 15.31 with parameters $r_0 > r_1 > 0$ the trajectory of C is a hypocycloid. Wheel 1 is rotating with angular velocity $\dot{\varphi}_1 = \text{const}$. Determine in the position shown (C in the cusp of the cycloid) the acceleration a_0 of C and for an arbitrary position the velocity v.

Solution: In (15.121) and (15.122) the substitution $b = -r_1$ is made. In the position $\varphi_1 = \varphi_2 = 0$ the acceleration is

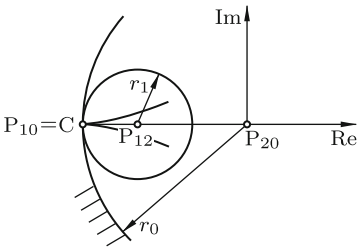

Fig. 15.31

$$a_0 = \ddot{z} = \frac{\dot{\varphi}_1^2}{1/r_1 - 1/r_0} \quad \text{in the direction of the positive real axis .} \tag{15.127}$$

For the velocity v (15.121) yields

$$\begin{aligned} v^2 = |\dot{z}|^2 &= \dot{\varphi}_1^2 r_1^2 [(\cos\varphi_2 - \cos\varphi_1)^2 + (\sin\varphi_2 - \sin\varphi_1)^2] \\ &= 2\dot{\varphi}_1^2 r_1^2 \Big[1 - (\cos\varphi_2 \cos\varphi_1 + \sin\varphi_2 \sin\varphi_1)\Big] = 2\dot{\varphi}_1^2 r_1^2 [1 - \cos(\varphi_1 - \varphi_2)] \\ &= 4\dot{\varphi}_1^2 r_1^2 \sin^2 \frac{\varphi_1 - \varphi_2}{2} \, . \end{aligned} \tag{15.128}$$

This complicated calculation is of course unnecessary. In the resulting formula $v = \dot{\varphi}_1 2r_1 \sin\frac{1}{2}(\varphi_1 - \varphi_2)$ the factor of $\dot{\varphi}_1$ is the distance of C from the instantaneous center of velocity P_{10}. The maximum velocity occurs in the vertices of the trajectory: $v_{\max} = 2r_1\dot{\varphi}_1$. End of example.

15.5.3 Cycloids

Both generating mechanisms of a cycloid share the same sunwheel 0 and, furthermore, cusps occur on the sunwheel. An example is the cardioid shown in Fig. 15.8b. It is an epitrochoid with the two generations according to Fig. 15.32. Hypocycloids of particular interest are *Steiner's hypocycloid* in Fig. 15.33b and the *astroid* in Fig. 15.33c. A special case belonging to this family is the system shown in Fig. 15.33a. It is known from the elliptic trammel. This particular hypocycloid is a diameter of the sunwheel.

Equation (15.119) for the astroid is simplest when as straight-line position $\varphi_1 = \varphi_2 = 0$ not the position shown in Fig. 15.33c is chosen, but the position when P_{10} is a cusp of the astroid. Then $r_1 = \frac{1}{4}r_0$, $b = -\frac{1}{4}r_0$ and

$$\begin{aligned} z &= -\frac{3}{4}r_0 (\cos\varphi_2 + \mathrm{i}\sin\varphi_2) - \frac{1}{4}r_0 (\cos 3\varphi_2 - \mathrm{i}\sin 3\varphi_2) \\ &= -r_0 (\cos^3\varphi_2 + \mathrm{i}\sin^3\varphi_2) \, . \end{aligned} \tag{15.129}$$

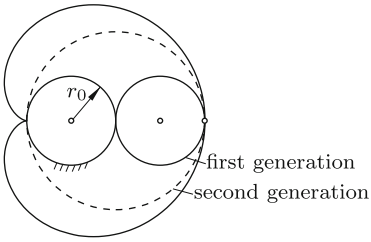

Fig. 15.32 Cardioid. First generation with $r_1 = -r_0$; second generation with $r_1^* = 2r_0$

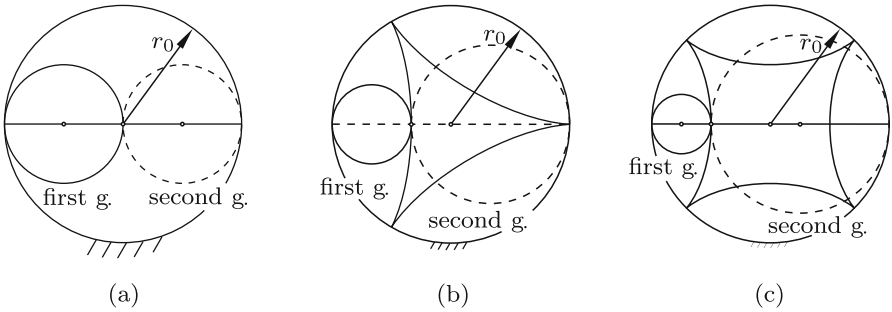

Fig. 15.33 First and second generation of the rectilinear hypocycloid ($r_1 = \frac{1}{2}r_0$ **(a)**), Steiner's hypocycloid ($r_1 = \frac{1}{3}r_0$ **(b)**), astroid ($r_1 = \frac{1}{4}r_0$ **(c)**)

In Fig. 15.34a three circles 1, s_1 and s_2 with radii r, nr and $(n+1)r$, respectively, ($n \geq 2$ integer) are one inside the other with a common contact point Q. In the example shown, $n = 3$. Circle s_2 is held fixed. When circle 1 rolls inside s_1, an arbitrarily chosen point P on the circumference traces a hypocycloid z_1 with n cusps on s_1. Similarly, when circle 1 rolls inside s_2, the same point P traces a hypocycloid z_2 with $n+1$ cusps on s_2 (in the example shown, z_1 is Steiner's hypocycloid and z_2 is an astroid). The hypocycloid z_2 is fixed on the fixed circle s_2. Both cycloids have the common tangent t normal to $\overline{QP}$. According to (15.125) the second generation of z_2 has the same sunwheel s_2 and an inner planetary wheel with radius nr. This is the radius of s_1. Thus, the rolling of s_1 inside s_2 represents the second generation of z_2. In this second generation of z_2 all cusps of z_1 move along z_2, and in every position z_1 and z_2 are co-tangential at one point. The centers 0_1 of s_1 and 0_2 of s_2, at the distance r from each other, are the poles P_{12} and P_{20}, respectively, of crank 2. Equation (15.120) yields $\dot{\varphi}_1/\dot{\varphi}_2 = 1/n$.

In Fig. 15.34b the special case $n = 2$ is shown. In this case, the hypocycloid z_1 is a diameter of s_1 having the length $4r$, and z_2 is Steiner's hypocycloid with radius $3r$ of the sunwheel s_2. In the second generation of z_2 (s_1 rolling inside s_2) the endpoints of the diameter move along z_2. During this

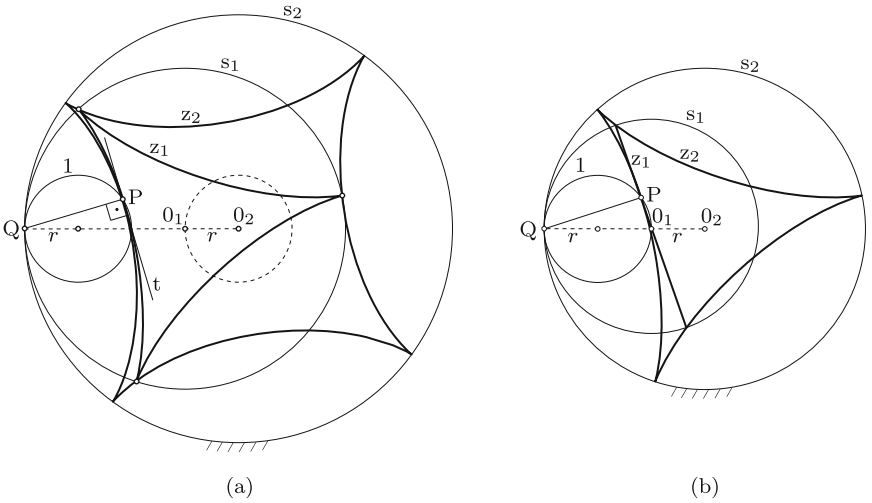

Fig. 15.34 Rolling of circle 1 (radius r) inside circles s_1 (radius nr) and s_2 (radius $(n+1)r$) produces hypocycloids z_1 and z_2, respectively. When s_1 rolls in s_2, the cusps of z_1 are guided along z_2, and both hypocycloids are continuously in tangential contact. Cases $n = 3$ **(a)** and $n = 2$ **(b)**

motion the diameter is always in tangential contact with z_2 and, consequently, inside z_2. In other words: The diameter of length $4r$ can be rotated full circle inside Steiner's hypocycloid with a sunwheel of radius $3r$. For a long time it was believed that this hypocycloid represents the smallest area inside of which a line segment of length $4r$ can be rotated full circle. Besicovitch [2] showed, however, that this is possible inside arbitrarily small areas. These areas consist of intricately branching subdomains.

The area enclosed by Steiner's hypocycloid is calculated from Holditch's Eq.(15.117), $A(\lambda) = A(0) + \lambda^2\pi\ell^2$, with $\ell = 2r$ and $\lambda = 1$ and with the area $A(0)$ enclosed by the midpoint of the line segment. The trajectory of this midpoint is the circle of radius r inscribed in Steiner's hypocycloid. When the line segment is rotating once counterclockwise, the midpoint traces this circle twice clockwise. Therefore, $A(0) = -2\pi r^2$. Hence the area enclosed by the cycloid is $A(1) = 2\pi r^2$, i.e., twice the area of the inscribed circle. Every point fixed on the line segment traces a trochoid. With the pertinent value of λ the formula yields the area enclosed by this trochoid.

Now back to the general case with $n > 2$. The motion of cycloid z_1 inside z_2 is creating n chambers of periodically changing volumes. This phenomenon has found engineering applications. If the crank is driven by a motor, the chambers can be used for pumping fluid. By controlling the pressure inside the chambers by means of a rotating distribution valve z_1, the crank can be driven (the crank rotating n times as fast as z_1). The

systems shown in Figs. 15.34a and b are special cases of cycloidal gearings. For additional material on this subject see Sec. 16.1.2.

Consider the cycloid z_1 in Fig. 15.35. It is the trajectory of the point C fixed on wheel 1 rolling on wheel 0. This generating system is referred to as system r_0, r_1. As straight-line position with angles $\varphi_1 = \varphi_2 = 0$ the position is chosen when C is located at the vertex C_0 of z_1. Then the parameters are $r_0 < 0$ and $r_1 > 0$. The circle on which C_0 is located is called *circle of vertices*. Its radius is $2r_1 - r_0$. The line $\overline{P_{10}C}$ is the normal n to z_1 at C. The tangent t passes through the point P_{12}^* common to wheel 1 and to the circle of vertices (wheel 1 is Thales' circle in the right-angled triangle (P_{10},C,P_{12}^*)). The rotation angle φ_1 of wheel 1 is (see (15.120))

$$\varphi_1 = \frac{r_1 - r_0}{r_1}\,\varphi_2\,. \tag{15.130}$$

The angle $\sphericalangle(CP_{12}P_{12}^*)$ is seen to be $\varphi_1 - \varphi_2$, whence it follows that $\sphericalangle(CP_{10}P_{12}^*) = \frac{1}{2}(\varphi_1 - \varphi_2)$ (theorem on angles subtended by the chord $\overline{CP}_{12}^*$). The angle of rotation of the normal n as well as of the tangent t from their positions in the straight-line position is $\alpha = \frac{1}{2}(\varphi_1 - \varphi_2) + \varphi_2 = \frac{1}{2}(\varphi_1 + \varphi_2)$ or, with (15.130),

$$\alpha = \frac{2r_1 - r_0}{2r_1}\,\varphi_2\,. \tag{15.131}$$

Comparison with (15.130) shows that this is the rotation angle of a wheel with radius $2r_1$ instead of r_1 rolling on the same sunwheel 0. In the figure this wheel is shown in the position α as dashed line. The tangent t is a diameter fixed on this wheel. These results are summarized in

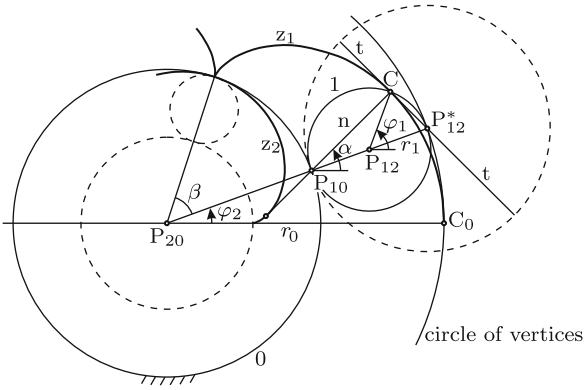

Fig. 15.35 Cycloid z_1 enveloped by the diameter of a rolling wheel and evolute z_2

Theorem 15.8. *A cycloid generated as point trajectory in a system* r_0, r_1 *is enveloped by a diameter fixed on the planetary wheel in the system* $r_0, 2r_1$

Consider the special case $r_0 = -2r_1$ shown in Fig. 15.36. The circle of vertices has the radius $R = 2|r_0|$. The epicycloid has two cusps. From Fig. 15.35 the general formula $\beta = \sphericalangle(\mathrm{P}_{10}\mathrm{P}^*_{12}\mathrm{C}) = \frac{1}{2}\pi - \frac{1}{2}(\varphi_1 - \varphi_2)$ is known. In the special case under consideration, this becomes $\beta = \frac{1}{2}\pi - \varphi_2$. In Fig. 15.36 it is seen that β is also the angle between the line $\overline{\mathrm{P}_{20}P^*_{12}}$ and the perpendicular s to the line $\overline{\mathrm{P}_{20}C_0}$. A light beam having the direction of s is reflected on the circle of vertices in the direction of the tangent to the cycloid. This explains a phenomenon which can be observed in a cup of coffee in early-morning sunshine. Parallel sun rays are reflected on the inner wall of the cup (circle of vertices of radius R). The reflected rays envelope an epicycloid with two cusps on the circle of radius $R/2$. In the vicinity of one cusp the cycloid is clearly visible.

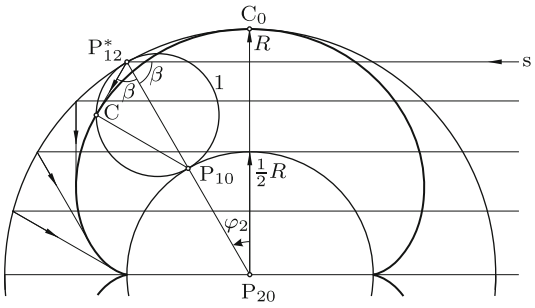

Fig. 15.36 Generation of a two-cusped epicycloid by means of reflected light

As another special case Steiner's hypocycloid of Fig. 15.33b is considered. The first generating system is the system $r_0, \frac{1}{3}r_0$. According to the theorem the cycloid is enveloped by a diameter fixed on the planetary wheel in the system $r_0, \frac{2}{3}r_0$. This system is also the second generating system of the same cycloid. In other words: The endpoints of the enveloping diameter of the planetary wheel in the second generation are tracing the cycloid. This property is known already from Fig. 15.34b. Steiner's hypocycloid is the only hypocycloid having this property.

Next, the evolute of the cycloid z_1 in Fig. 15.35 is determined. Let it be called z_2. By definition, z_2 is the curve which is enveloped by the normal n of z_1. The following facts are obvious:

1. n is tangent to z_2; n is passing through P_{10} which is located on the circle with radius r_0
2. t is tangent to z_1; t is passing through P^*_{12} which is located on the circle with radius $2r_1 - r_0$

3. $\overline{\mathrm{P}_{20}\mathrm{P}_{10}}$ is collinear with $\overline{\mathrm{P}_{20}\mathrm{P}_{12}^{*}}$; both n and t are rotating with $\dot{\alpha}$; n is orthogonal to t .

A direct consequence of these facts is

Theorem 15.9. (Bernoulli, de la Hire)[7] *The evolute of a cycloid* z_1 *in the system* r_0, r_1 *is another similar cycloid* z_2 *, which is the trajectory of a point in the new system* pr_0, pr_1 *with* $p = r_0/(2r_1 - r_0)$ *. The circle of vertices in the new system is identical with the circle of the sunwheel in the initial system. The vertices of the evolute* z_2 *coalesce with the cusps of* z_1 *.*

Figure 15.35 shows the evolute z_2 and in dashed lines the wheels of the new system. Further properties of cycloids and of trochoids in general are found in Wunderlich [30] and Strubecker [28]. Higher-order trochoids were investigated by Wunderlich [29].

15.5.4 Ordinary Cycloids

An ordinary cycloid[8] is the trajectory of an arbitrary point (not just a circumferential point) fixed on a circular wheel which is rolling along a straight line. This is the situation when in Fig. 15.26 r_0 is infinite. In what follows, the notation shown in Fig. 15.37 is used. The radii of the circle and of point C are denoted r and b respectively ($r, b > 0$). The angle of roll of the circle is φ (positive clockwise). The position $\varphi = 0$ is defined to be the position when the center as well as point C is on the imaginary axis with C being below the center of the circle. In this position these two points have the complex numbers $\mathrm{i}\,r$ and $z = \mathrm{i}\,(r - b)$, respectively. In the position φ (arbitrary) the numbers are $r\varphi + \mathrm{i}\,r$ and

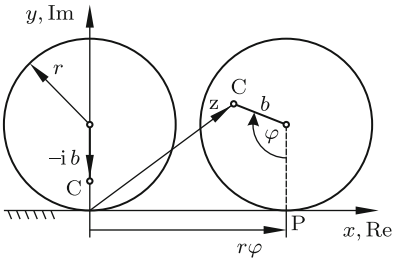

Fig. 15.37 Ordinary cycloid

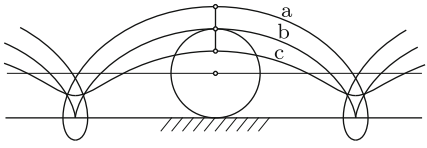

Fig. 15.38 Ordinary cycloids: Curtate **(a)** , cusped **(b)** , prolate **(c)**

[7] J. Bernoulli 1692, de la Hire 1694

[8] Leibniz [23] quotes Cardinal de Susa (1454) to be the first to mention this curve

$$z = r\varphi + \mathrm{i}\, r - \mathrm{i}\, b\mathrm{e}^{-\mathrm{i}\,\varphi} \,, \tag{15.132}$$

respectively. This yields for the x, y-coordinates of C and for their time derivatives the expressions

$$\left.\begin{aligned} x &= r\varphi - b\sin\varphi \,, & y &= r - b\cos\varphi \,, \\ \dot{x} &= \dot{\varphi}(r - b\cos\varphi) \,, & \dot{y} &= \dot{\varphi} b \sin\varphi \,, \\ \ddot{x} &= \ddot{\varphi}(r - b\cos\varphi) + \dot{\varphi}^2 b \sin\varphi \,, & \ddot{y} &= b(\ddot{\varphi}\sin\varphi + \dot{\varphi}^2\cos\varphi) \,. \end{aligned}\right\} \tag{15.133}$$

Depending on whether $b < r$ or $b = r$ or $b > r$ ordinary cycloids are either curtate or cusped or prolate (Fig. 15.38). By the conventions of Sect. 15.5.2 only the cusped cycloids should be called cycloids. The indiscriminate name *ordinary cycloid* is much older than this convention. The cusped ordinary cycloid has in the cusps the acceleration coordinates

$$\ddot{x} = 0 \,, \qquad \ddot{y} = r\dot{\varphi}^2 \,. \tag{15.134}$$

Another property was shown in the example illustrating Fig. 15.21: In every position φ the point of rolling P is midpoint between the generating point C and the center of curvature M.

15.5.5 Involute of a Circle

The inverse motion of a circle rolling along a straight line is the rolling of a straight line g on a fixed circle k of radius r_0. This is the situation when in Fig. 15.26 r_1 is infinite. In Fig. 15.39 the line g is tangent to k at point A. To be investigated are the trajectories traced by the point B fixed on g and by the point P rigidly attached to g at the distance h on the perpendicular

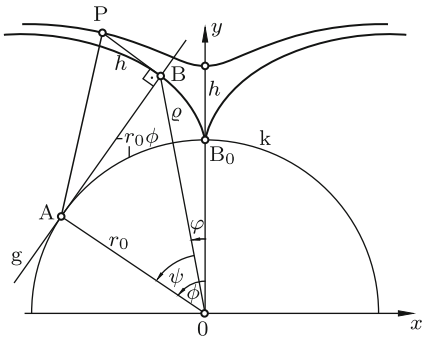

Fig. 15.39 Involute of base circle k generated by B and epitrochoid traced by P

through B. In the case $h < 0$, P is located on the other side of g, i.e., on the side toward the circle k.

First, the trajectory of B. It is an epicycloid. Point A is the instantaneous center of rotation of g and, therefore, the center of curvature of the trajectory of B. The trajectory is, therefore, the involute of k, and k is called base circle of the involute. The segment $\overline{\mathrm{AB}}$ may be interpreted as part of a string which is winding off the circle k. Figure 15.39 shows that the following facts are true

- every normal to the involute is tangent to k and vice versa
- the involute has a cusp B_0 on k. It is symmetric with respect to the diameter of k through B_0
- the line segment $\overline{\mathrm{AB}}$ which is the radius of curvature of the involute at B equals the length of the arc AB_0 of k. It is $r_0\phi$. The element of the arc length of the involute is, therefore, $\mathrm{d}s = r_0\phi\,\mathrm{d}\phi$ and the arc length itself is $s = r_0\phi^2/2$ ($s = 0$ at B_0)
- in terms of the angle ψ as parameter B has the polar coordinates (note that $\varphi + \psi = \phi = \tan\psi$)

$$\rho(\psi) = \frac{r_0}{\cos\psi}\,, \qquad \varphi(\psi) = \operatorname{inv}\psi \tag{15.135}$$

with the *involute function* defined as

$$\operatorname{inv}\psi = \tan\psi - \psi \tag{15.136}$$

- involutes of base circles with different radii r_0 are geometrically similar
- involutes on one and the same base circle, i.e., trajectories of different points $\mathrm{B}_1, \mathrm{B}_2, \ldots$ fixed on g are parallel curves.

Next, the trajectory of P is investigated. It is an epitrochoid. This time, cartesian coordinates in the special x, y-system shown and polar coordinates ρ, φ are expressed not as functions of the angle ψ, but of ϕ. With $\overline{\mathrm{AB}} = r_0\phi$ the coordinates are

$$\left.\begin{aligned} x &= -(r_0 + h)\sin\phi + r_0\phi\cos\phi\,, \quad & \rho &= \sqrt{x^2 + y^2} = \sqrt{(r_0 + h)^2 + r_0^2\phi^2}\,, \\ y &= (r_0 + h)\cos\phi + r_0\phi\sin\phi\,, \quad & \tan\varphi &= \frac{x}{y}\,. \end{aligned}\right\} \tag{15.137}$$

The coordinate $x(\phi)$ is an odd function of ϕ, and $y(\phi)$ is an even function of ϕ. From this it follows that the y-axis is an axis of symmetry. The tangent to the trajectory at P is normal to the line $\overline{\mathrm{AP}}$. In the special case $h = 0$, the curve is the involute with the polar coordinates (15.135). Another special case is $h = -r_0$ (P is at the center 0 of the circle in the position $\phi = 0$). In this case, the equations are $\rho = r_0\phi$ and $\varphi = \phi - \pi/2$. These are the equations of Archimedes' spiral.

The coordinate x is zero if ϕ satisfies the equation $\phi = [(r_0 + h)/r_0]\tan\phi$. This equation has the solution $\phi = 0$ and one more solution if $h < 0$. These

curves have a double point on the axis of symmetry. They are curtate, and those with $h > 0$ (without double point) are prolate.

15.5.6 Dwell Mechanisms Based on Cycloids

In the mechanism shown in Fig. 15.40 the crank 2 causes the planetary wheel 1 (radius r) to roll inside the sunwheel 0 (radius R). In the position $\varphi = 0$ point A lies on the x-axis at $x_A = R - 2r$. Rod 3 (length ℓ) connects A to the slider 4. The figure shows the case $R/r = 3$. In what follows, the general case $R/r = n$ ($n \geq 3$; integer) is investigated. In the interval $-\varphi_0 \leq \varphi \leq +\varphi_0$ with $\varphi_0 = \pi/n$ the hypocycloid traced by A is a rather good approximation of a circular arc. For this reason it is possible to render the ratio $\xi(\lambda, \varphi) = x_B(\lambda, \varphi)/r$ in the interval $-\varphi_0 \leq \varphi \leq +\varphi_0$ approximately constant provided the ratio $\lambda = \ell/r$ is chosen appropriately. The mechanism can then be used as dwell mechanism with a single dwell per revolution of crank 2. An appropriate value λ_1 is obtained if ℓ is the radius of curvature ϱ of the hypocycloid at the point $\varphi = 0$. Another appropriate value λ_2 is obtained from the condition $\xi(\lambda_2, 0) = \xi(\lambda_2, \varphi_0)$. To be determined are λ_1 and λ_2 as functions of n. The optimal value λ_0 is obtained from the condition that the difference between the absolute maximum and the absolute minimum of the function $\xi(\lambda, \varphi)$ in the interval $-\varphi_0 \leq \varphi \leq +\varphi_0$ is minimal. This is Tshebychev's criterion of optimality. Determine λ_0 and the minimal difference in the cases $n = 3$ and $n = 4$.

Solution: Figure 15.40 shows the poles P_{10}, P_{20} and P_{12}. With these poles (15.6) yields the angular velocity ratio $\omega_{10}/\omega_{20} = -(n-1)$. This is Eq.(15.120). This ratio yields for the angle of rotation α of wheel 1 rel-

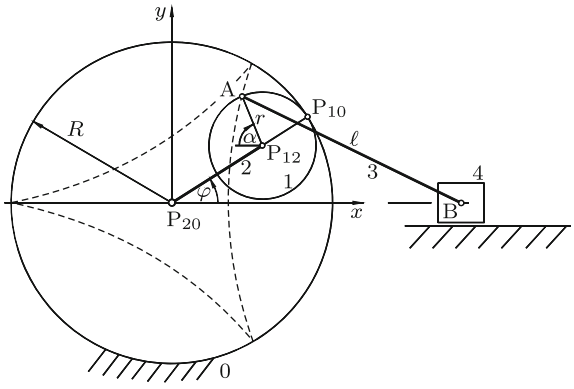

Fig. 15.40 Dwell mechanism

ative to the x, y-system the expression $\alpha = (n-1)\varphi$ (positive clockwise; see the figure). This determines the coordinates of A and B:

$$\left.\begin{aligned} x_{\mathrm{A}} &= r[(n-1)\cos\varphi - \cos(n-1)\varphi]\,, \\ y_{\mathrm{A}} &= r[(n-1)\sin\varphi + \sin(n-1)\varphi]\,, \end{aligned}\right\} \tag{15.138}$$

$$\xi(\lambda,\varphi) = \frac{x_{\mathrm{B}}}{r} = \frac{1}{r}\Big(x_{\mathrm{A}} + \sqrt{\ell^2 - y_{\mathrm{A}}^2}\,\Big) = (n-1)\cos\varphi - \cos(n-1)\varphi + \sqrt{\lambda^2 - [(n-1)\sin\varphi + \sin(n-1)\varphi]^2}\,. \tag{15.139}$$

The curvature κ of a curve with parameter equations $x(\varphi)$, $y(\varphi)$ is

$$\kappa = \frac{x'y'' - y'x''}{(x'^2 + y'^2)^{3/2}} \qquad (' = \mathrm{d}/\mathrm{d}\varphi)\,. \tag{15.140}$$

The radius of curvature is $\varrho = 1/\kappa$. For the radius of curvature of the trajectory of A Eqs.(15.138) yield

$$\left.\begin{aligned} x'_{\mathrm{A}} &= r(n-1)[-\sin\varphi + \sin(n-1)\varphi]\,, \quad & x''_{\mathrm{A}} &= r(n-1)[-\cos\varphi + (n-1)\cos(n-1)\varphi]\,, \\ y'_{\mathrm{A}} &= r(n-1)[\cos\varphi + \cos(n-1)\varphi]\,, & y''_{\mathrm{A}} &= -r(n-1)[\sin\varphi + (n-1)\sin(n-1)\varphi]\,. \end{aligned}\right\} \tag{15.141}$$

From the values for $\varphi = 0$ the desired ratio λ_1 is found:

$$\lambda_1 = \frac{1}{r|\kappa(0)|} = 4\,\frac{n-1}{n-2}\,. \tag{15.142}$$

For determining λ_2 the relations are used

$$\sin(n-1)\varphi_0 = \sin(\pi - \pi/n) = \sin\varphi_0\,, \qquad \cos(n-1)\varphi_0 = -\cos\varphi_0\,. \tag{15.143}$$

With these relations the conditional equation $\xi(\lambda_2, 0) = \xi(\lambda_2, \varphi_0)$ for λ_2 takes the form

$$n - 2 + \lambda_2 = n\cos\varphi_0 + \sqrt{\lambda_2^2 - n^2\sin^2\varphi_0}\,. \tag{15.144}$$

Squaring produces a linear equation with the solution

$$\lambda_2 = \frac{1 + n(n-2)\sin^2\varphi_0/2}{1 - n\sin^2\varphi_0/2}\,. \tag{15.145}$$

Next, the optimal ratio λ_0 is determined and for this purpose the absolute maximum and the absolute minimum of the function $\xi(\lambda,\varphi)$ in the interval $0 \le \varphi \le \varphi_0$ with λ being a constant parameter. First, all angles φ in the interval $0 \le \varphi \le \varphi_0$ are determined for which $\xi(\lambda,\varphi)$ attains stationary values. These angles are the roots of the equation $\partial\xi/\partial\varphi = 0$. With (15.139) this is the equation

$$\Big[\sin(n-1)\varphi - \sin\varphi\Big]\sqrt{\lambda^2 - [(n-1)\sin\varphi + \sin(n-1)\varphi]^2}$$
$$- \Big[(n-1)\sin\varphi + \sin(n-1)\varphi\Big]\Big[\cos\varphi + \cos(n-1)\varphi\Big] = 0\,. \qquad (15.146)$$

It has the root $\varphi_1 = 0$ and also the root $\varphi_2 = \varphi_0$ since because of (15.143) the first and the second term in brackets are both zero for $\varphi = \varphi_0$. From this it follows that for $\lambda = \text{const}$ (arbitrary) the function $\xi(\lambda, \varphi)$ has stationary values at $\varphi = 0$ and at $\varphi = \varphi_0$. These stationary values as functions of λ are denoted $\xi_{s1}(\lambda)$ and $\xi_{s2}(\lambda)$. Equation (15.144) yields

$$\xi_{s1}(\lambda) = n - 2 + \lambda\,, \qquad \xi_{s2}(\lambda) = n\cos\varphi_0 + \sqrt{\lambda^2 - n^2\sin^2\varphi_0}\,. \qquad (15.147)$$

For $\lambda = \lambda_2$ these stationary values are identical, namely,

$$\xi_{s1}(\lambda_2) = \xi_{s2}(\lambda_2) = \frac{n-1}{1 - n\sin^2\varphi_0/2}\,. \qquad (15.148)$$

From this identity it follows that (15.146) has at least one more root in the interval $0 \le \varphi \le \varphi_0$ provided λ satisfies certain conditions. Further progress at this point is possible only if the integer n is specified.

Special case $n = 3$ ($\varphi_0 = 60°$): Equations (15.142) and (15.145) yield $\lambda_1 = 8$ and $\lambda_2 = 7$. With the formulas

$$\left.\begin{aligned} \sin 2\varphi - \sin\varphi &= 2\sin\varphi(\cos\varphi - \tfrac{1}{2})\,, \\ 2\sin\varphi + \sin 2\varphi &= 2\sin\varphi(\cos\varphi + 1)\,, \\ \cos\varphi + \cos 2\varphi &= 2(\cos\varphi - \tfrac{1}{2})(\cos\varphi + 1) \end{aligned}\right\} \qquad (15.149)$$

Equation (15.146) becomes

$$\sin\varphi\,\Big(\cos\varphi - \frac{1}{2}\Big)\Big[\sqrt{\lambda^2 - 4\sin^2\varphi(\cos\varphi+1)^2} - 2(\cos\varphi+1)^2\Big] = 0\,. \quad (15.150)$$

This equation has, in addition to the roots $\varphi_1 = 0$ and $\varphi_2 = \varphi_0 = 60°$, a third root φ_3. Squaring and simple reformulations yield the explicit result

$$\cos[\varphi_3(\lambda)] = \frac{1}{2}\,\lambda^{2/3} - 1\,. \qquad (15.151)$$

This root is in the interval $0 \le \varphi_3 \le \varphi_0$ if $\sqrt{27} \le \lambda \le 8 = \lambda_1$. Let $\xi_{s3}(\lambda)$ be the associated third stationary value. It is calculated with $\cos[\varphi_3(\lambda)]$ from (15.139). The altogether three stationary values are (see (15.147))

$$\xi_{s1}(\lambda) = 1 + \lambda\,, \quad \xi_{s2}(\lambda) = \frac{3}{2} + \sqrt{\lambda^2 - \frac{27}{4}}\,, \quad \xi_{s3}(\lambda) = 3(\lambda^{2/3} - 1)\,. \quad (15.152)$$

For $\lambda = \lambda_2 = 7$ they are two identical maxima and a single minimum:

$$\xi_{s1}(7) = \xi_{s2}(7) = 8\,, \qquad \xi_{s3}(7) \approx 7.9779\,. \tag{15.153}$$

In the neighborhood of $\lambda = 7$ $\xi_{s1}(\lambda)$ and $\xi_{s2}(\lambda)$ are nonidentical maxima, and $\xi_{s3}(\lambda)$ is a minimum. Define the two differences maximum minus minimum:

$$f_{13}(\lambda) = \xi_{s1}(\lambda) - \xi_{s3}(\lambda)\,, \qquad f_{23}(\lambda) = \xi_{s2}(\lambda) - \xi_{s3}(\lambda)\,. \tag{15.154}$$

Their derivatives with respect to λ at the point $\lambda = 7$ are $f'_{13}(7) < 0$ and $f'_{23}(7) > 0$. This together with (15.153) allows the conclusion that the desired optimal parameter is $\lambda_0 = \lambda_2 = 7$. Figure 15.41 shows the graphs of the function $\xi(\lambda, \varphi) - \xi(\lambda, 0)$ for $\lambda = 7$ and for $\lambda = 8$ in the interval $-80° \le \varphi \le 80°$. Notice the scale. The differences between maximum and minimum are

$$\Delta\xi(7) = \xi_{s2}(7) - \xi_{s3}(7) \approx 0.022\,, \quad \Delta\xi(8) = \xi_{s2}(8) - \xi_{s1}(8) \approx 0.066\,. \tag{15.155}$$

The quality of dwell is much better with $\lambda_0 = \lambda_2 = 7$ than with $\lambda_1 = 8$ obtained from the condition on curvature. Equation (15.151) determines the angle $\varphi_3(7) \approx 33.9°$.

In Fig. 15.41 the upper limit of the interval of dwell is denoted φ_4. It is defined through the equation $\xi(7, \varphi_4) = \xi_{s3}(7)$ or explicitly

$$2\cos\varphi_4 - 2\cos^2\varphi_4 + 1 + \sqrt{49 - 4(1 - \cos^2\varphi_4)(\cos\varphi_4 + 1)^2} = 3(7^{2/3} - 1)\,. \tag{15.156}$$

Solving for the root and squaring results in a cubic equation for $\cos\varphi_4$. Since this equation has the double root $\cos\varphi_4 = \cos[\varphi_3(7)] = \frac{1}{2}\,7^{2/3} - 1$, a linear equation is obtained. This equation has the solution $\cos\varphi_4 = \frac{1}{4}(5 - 7^{2/3})$, $\varphi_4 \approx 70.4°$. Thus, the dwell has the length of approximately $141°$ per revolution of the crank.

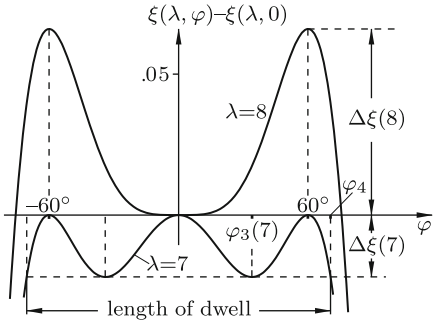

Fig. 15.41 Graphs of functions $\xi(\lambda, \varphi) - \xi(\lambda, 0)$ for $\lambda = 7$ and for $\lambda = 8$

Special case $n = 4$ ($\varphi_0 = 45°$): Equations (15.142) and (15.145) yield $\lambda_1 = 6$ and $\lambda_2 = 1 + 3\sqrt{2}$. With the formulas

$$\left.\begin{aligned} \sin 3\varphi - \sin\varphi &= 4\sin\varphi(\cos^2\varphi - \tfrac{1}{2}) \,, \\ 3\sin\varphi + \sin 3\varphi &= 4\sin\varphi(\cos^2\varphi + \tfrac{1}{2}) \,, \\ \cos\varphi + \cos 3\varphi &= 4\cos\varphi(\cos^2\varphi - \tfrac{1}{2}) \end{aligned}\right\} \tag{15.157}$$

Equation (15.146) becomes

$$\sin\varphi\left(\cos^2\varphi - \frac{1}{2}\right)\left[\sqrt{\lambda^2 - 16\sin^2\varphi\left(\cos^2\varphi + \frac{1}{2}\right)^2} - 4\cos\varphi\left(\cos^2\varphi + \frac{1}{2}\right)\right] = 0 \,. \tag{15.158}$$

It has the roots $\varphi_1 = 0$, $\varphi_2 = \varphi_0 = 45°$ and $\cos[\varphi_3(\lambda)] = \frac{1}{2}\sqrt{\lambda - 2}$. The associated stationary values are

$$\xi_{s1}(\lambda) = 2 + \lambda \,, \qquad \xi_{s2}(\lambda) = 2\sqrt{2} + \sqrt{\lambda^2 - 8} \,, \qquad \xi_{s3}(\lambda) = 4\sqrt{\lambda - 2} \,. \tag{15.159}$$

As in the case $n = 3$, the optimal ratio λ_0 is identical with λ_2. The smallest difference between the maximum and the minimum of $\xi(\lambda, \varphi)$ is $\xi_{s2}(\lambda_0) - \xi_{s3}(\lambda_0) \approx 0.040$.

What follows next, is valid again for the general case with $n \geq 3$ (integer). The pole P_{10} in Fig. 15.40 lies on the line $\overline{AB}$ if the points A, B and P_{10} satisfy the condition $(x_B - x_A)(y_{10} - y_A) + y_A(x_{10} - x_A) = 0$. The coordinates in this equation are $x_{10} = nr\cos\varphi$, $y_{10} = nr\sin\varphi$ and x_A, y_A, $x_B = r\xi$ from (15.138) and (15.139). Substitution of these expressions yields, surprisingly, Eq.(15.146) again. This identity has to be interpreted as follows. At $\varphi = 0$ and also at $\varphi = \varphi_0$ P_{10} lies on the line $\overline{AB}$ independent of the value of λ. In the interval $-\varphi_0 \leq \varphi \leq +\varphi_0$ P_{10} lies on the line $\overline{AB}$ independent of φ if λ has the optimal value λ_0. Outside the interval $-\varphi_0 \leq \varphi \leq +\varphi_0$ P_{10} does not lie, in general, on the line $\overline{AB}$.

15.6 Rectangle Moving Between two Lines and a Point

Figures 15.42a and b illustrate a problem encountered when moving a piece of furniture. The rectangle of unit length is to be displaced from position I to position II in the space formed by the angle α between straight lines g_1 and g_2 and by the point P_0. Given α and the coordinates x_0, y_0 of P_0 in the x, y-system shown in the figures, determine whether the prescribed displacement is possible and if so, what is the maximum admissible width B_{max} of the rectangle?

In the literature only the special case $\alpha = \pi/2$ is treated analytically (Miller [24], Husty/Karger/Sachs/Steinhilper [17], Moretti [25], Boute [5]).

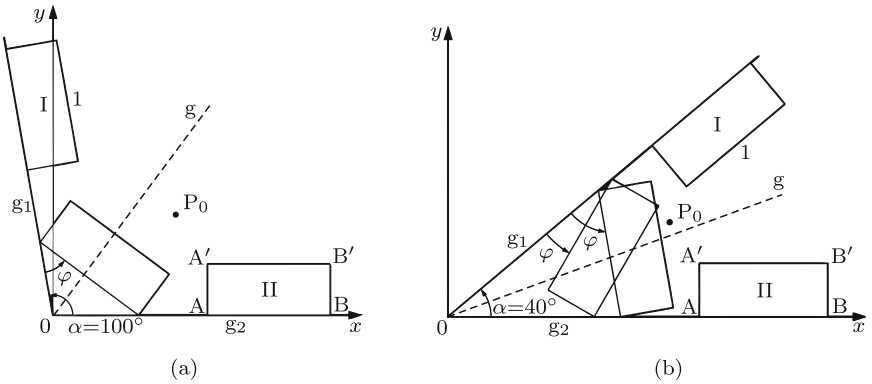

Fig. 15.42 Rectangle of unit length in a space defined by α and P_0 in cases $\alpha > \pi/2$ **(a)** and $\alpha < \pi/2$ **(b)**. Initial position I, intermediate positions with position angle φ and final position II

In all four references the maximum length of the rectangle for a given width is determined. This statement of the problem results in a sixth-order polynomial equation for the unknown length. In the present section the problem is stated differently. The length of the rectangle is given. The maximum possible width is the unknown. This approach leads to a fourth-order polynomial in the case $\alpha \geq \pi/2$ and to a sixth-order polynomial in the case $\alpha < \pi/2$.

For achieving the maximum possible width corner points of the rectangle must be guided along g_1 and g_2. In the case $\alpha \geq \pi/2$ shown in Fig. 15.42a, the motion of the rectangle consists of three phases, namely, of translation along g_1 until B is at 0, of a motion with the position variable φ in the interval $0 \leq \varphi \leq \pi - \alpha$ and of translation along g_2. These phases are numbered 1, 3 and 5. In the case $\alpha < \pi/2$ shown in Fig. 15.42b, phase 3 is restricted to the interval $\pi/2 - \alpha \leq \varphi \leq \pi/2$. In the interval $0 \leq \varphi \leq \pi/2 - \alpha$ between phases 1 and 3 a phase 2 occurs with A moving along g_1 and with B′ moving along g_2. Between phases 3 and 5 a phase 4 occurs with A′ moving on g_1 and with B on g_2. The translatory motions in phases 1 and 5 are trivial. The other motions in phases 2, 3 and 4 are known from the elliptic trammel in Sect. 15.1.2. They are called elliptic motions because trajectories of body-fixed points are ellipses. The inverse motion is known, too. For an observer fixed on the moving rectangle P_0 is moving on a limaçon of Pascal.

The solution to the problem is simplified by the fact that the trajectory of every point of the rectangle is symmetric with respect to the bisector g of the angle α. Phase 1 is symmetric to phase 5, phase 2 is symmetric to phase 4, and phase 3 is symmetric with respect to its midpoint in the position $\varphi = (\pi - \alpha)/2$. For two positions of P_0 which are symmetric with respect to g the maximum possible width is the same. For this reason it suffices to

investigate the case when P_0 is below the symmetry axis g or on g. Thus, the maximum possible width is determined in phases 3 (second half only), 4 and 5.

Method of Solution
The width b of the rectangle is treated as a free parameter. For each phase i of motion $(i = 1, \ldots, 5)$ a one-parametric family of curves $E_i(b)$ is defined as follows. For a given value of b $E_i(b)$ is the curve on which P_0 must be located such that in phase i a rectangle of width b has a degree of freedom when it is in contact with P_0.

Let $f_i(x, y, b) = 0$ be the equation describing $E_i(b)$. Furthermore, let the domain Γ_i be the set of all points (x, y) in the sector between g_1 and g_2 for which the equation $f_i(x_0, y_0, b) = 0$ has (at least) one real solution b. With this definition the maximum width $B_{\max}$ for a given location (x_0, y_0) of P_0 is the minimum $b_{\min}$ of all solutions b of the equations $f_i(x_0, y_0, b) = 0$ $(i = 1, 3, 5$ if $\alpha \geq \pi/2$ and $i = 1, \ldots, 5$ if $\alpha < \pi/2)$. In the case $b_{\min} < 0$, the displacement from position I to position II is not possible.

It will be seen that each pair of domains Γ_i and Γ_j $(j \neq i)$ has a nonempty intersection. Let Γ_i' $(i = 1, \ldots, 5)$ be the subdomain of Γ_i in which P_0 must be located so that $b_{\min}$ is a solution of $f_i(x_0, y_0, b) = 0$. If the domains Γ_i' $(i = 1, \ldots, 5)$ are known, the solution for $B_{\max}$ is found in two steps. First, it is determined in which domain Γ_k' P_0 is located. Then, the single equation $f_k(x_0, y_0, b) = 0$ is solved. Its smallest root is $B_{\max}$.

The domains Γ_i' $(i = 1, \ldots, 5)$ are determined by their boundaries. Let $G_{ij} = G_{ji}$ $(i, j = 1, \ldots, 5;\ i \neq j)$ be the boundary between Γ_i' and Γ_j'. By definition, for every point (x, y) on G_{ij} there exists a real value of b satisfying the equations $f_i(x, y, b) = 0$ and $f_j(x, y, b) = 0$. Elimination of b from these equations yields an equation for G_{ij}.

15.6.1 Obtuse-Angled Corner

This is the case $\alpha \geq \pi/2$. Figure 15.42a shows that the curve $E_5(b)$ in phase 5 is the line $y \equiv b$ for $x \geq 0$. The curve $E_1(b)$ is the reflection of $E_5(b)$ in g. It is the line parallel to g_1 at the distance b. Its equation is

$$x \sin\alpha - y \cos\alpha - b = 0 \qquad (x \cos\alpha + y \sin\alpha \geq 0)\,. \tag{15.160}$$

From this it follows that the domain Γ_5 is the first quadrant of the x, y-plane, and that Γ_1 is the reflection of Γ_5 on g. Furthermore, the symmetry axis g is the boundary G_{15} between the domains Γ_1' and Γ_5'.

Next, a parametric equation is given for the curve $E_3(b)$ in phase 3 of the motion. Figure 15.43 shows a rectangle of width b in phase 3. The instantaneous center of rotation P (or pole P) is the intersection of the

normals to g_1 at A and to g_2 at B. It has the coordinates $x_P = \sin\varphi/\sin\alpha$ and $y_P = \cos\varphi/\sin\alpha$. Its distance from 0 is $1/\sin\alpha$ independent of φ. Thus, the pole is moving on the circle with radius $1/\sin\alpha$ about 0. Let $n(\varphi)$ be the normal to $\overline{AB}$ through P. In the figure the quantities φ and b and the location of P_0 are chosen such that the following conditions are satisfied:
a) P_0 lies on $\overline{A'B'}$
b) P_0 lies on $n(\varphi)$. When these conditions are satisfied, P_0 lies between A′ and B′. The point of the rectangle coinciding with P_0 has zero velocity in the direction of $n(\varphi)$. In this position the rectangle has a degree of freedom. With a larger width b motion is impossible. From this it follows that $E_3(b)$ is the envelope of all lines $\overline{A'B'}$ in the interval $0 \le \varphi \le \pi - \alpha$. This implies that curves $E_3(b_1)$ and $E_3(b_2)$ are parallel curves with the distance $|b_1 - b_2|$ between them. The envelope $E_3(b)$ is determined as follows. The normal form of $\overline{A'B'}$ with φ and b as free parameters is $x\cos\beta + y\sin\beta - (p + b) = 0$. With the length $p = x_P\cos\beta$ of the perpendicular from 0 onto the line $\overline{AB}$ and with $\beta = \varphi + \alpha - \pi/2$ this becomes

$$\left(x - \frac{\sin\varphi}{\sin\alpha}\right)\sin(\varphi + \alpha) - y\cos(\varphi + \alpha) - b = 0\,. \tag{15.161}$$

On $E_3(b)$ this equation as well as its partial derivative with respect to φ is satisfied:

$$x\cos(\varphi + \alpha) + y\sin(\varphi + \alpha) - \frac{\sin(2\varphi + \alpha)}{\sin\alpha} = 0\,. \tag{15.162}$$

The solutions of these two equations for x and y are parameter equations of $E_3(b)$:

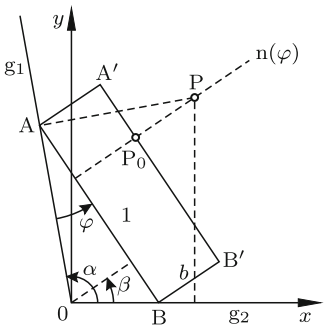

Fig. 15.43 Rectangle in a position φ with instantaneous center of rotation P and with P_0 on the edge $\overline{A'B'}$

$$\left.\begin{aligned} x(\varphi,b) &= \quad b\sin(\varphi+\alpha)+\frac{\sin\varphi+\cos\varphi\sin(\varphi+\alpha)\cos(\varphi+\alpha)}{\sin\alpha}\,,\\ y(\varphi,b) &= -b\cos(\varphi+\alpha)+\frac{\cos\varphi\sin^2(\varphi+\alpha)}{\sin\alpha}\end{aligned}\right\}\ (0<\varphi<\pi-\alpha)\,. \tag{15.163}$$

Figure 15.44 shows parallel curves $\mathrm{E}_3(b)$ for several values $b \geq 0$ in the case $\alpha = 110°$. The lines n_1 and n_2 are the normals $\mathrm{n}(\varphi = 0)$ and $\mathrm{n}(\varphi = \pi - \alpha)$, respectively. The curves $\mathrm{E}_3(b)$ are symmetric with respect to g. The endpoints for $\varphi = 0$ and for $\varphi = \pi - \alpha$ are located on n_1 and n_2, respectively. The endpoint on n_2 has the coordinates $x = 1$, $y = b$. The curve $\mathrm{E}_3(b = 0)$ is the envelope of all lines $\overline{\mathrm{AB}}$. When P_0 is located on $\mathrm{E}_3(0)$, the maximum admissible width of the rectangle is $B_{\max} = 0$. For points P_0 in the domain between g_1, g_2 and $\mathrm{E}_3(0)$ no rectangle can be moved from position I to position II.

For parameter values b in a certain, as yet unknown interval the curves $\mathrm{E}_3(b)$ have cusps. Let K be the curve connecting all cusps. It is the evolute of all $\mathrm{E}_3(b)$ and also the envelope of the normals $\mathrm{n}(\varphi)$. The equation of $\mathrm{n}(\varphi)$ is Eq.(15.162). On K this equation as well as its partial derivative with respect to φ is satisfied:

$$-x\sin(\varphi+\alpha)+y\cos(\varphi+\alpha)-\frac{2\cos(2\varphi+\alpha)}{\sin\alpha}=0\,. \tag{15.164}$$

The solutions of these two equations for x and y are parameter equations of K:

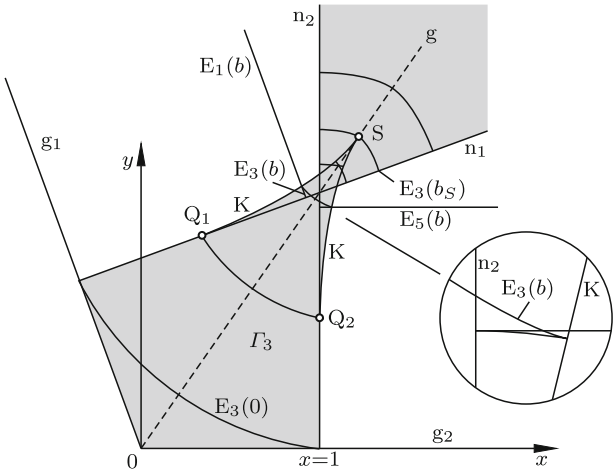

Fig. 15.44 Domain Γ_3 (shaded), evolute K and curves $\mathrm{E}_3(b)$ for several values of b in the case $\alpha = 110°$. Curves $\mathrm{E}_3(b)$ with $-2\cot\alpha < b < b_\mathrm{S}$ have cusps on K

$$\left.\begin{aligned} x(\varphi) &= \frac{3\sin\varphi - \sin(3\varphi + 2\alpha)}{2\sin\alpha} \\ y(\varphi) &= \frac{3\cos\varphi + \cos(3\varphi + 2\alpha)}{2\sin\alpha} \end{aligned}\right\} \quad (0 < \varphi < \pi - \alpha)\,. \tag{15.165}$$

In Fig. 15.44 the evolute K is shown. It is symmetric with respect to g. Its endpoints associated with $\varphi = 0$ and with $\varphi = \pi - \alpha$ are the points Q_1 on n_1 and Q_2 on n_2, respectively. At these points K merges tangentially with n_1 (with n_2). The point Q_2 has the coordinate $y = -2\cot\alpha$. The tip S of K belonging to the central value $\varphi = (\pi - \alpha)/2$ has the coordinates $x_S = 1/\sin(\alpha/2)$, $y_S = 1/\cos(\alpha/2)$. Its distance from 0 is $2/\sin\alpha$, i.e., twice the radius of the pole circle. The width $b = b_S$ associated with the special curve $E_3(b)$ through S is obtained from the first Eq.(15.161) with $x = x_S$ and $\varphi = (\pi - \alpha)/2$. It is $b_S = (3 - \cos\alpha)/(2\sin\alpha)$. From this it follows that the curve $E_3(b)$ has cusps if b is in the interval $-2\cot\alpha \le b \le b_S$.

The domain Γ_3 of definition of curves $E_3(b)$ is the shaded domain in Fig. 15.44. In what follows, the boundary G_{35} between the domains Γ_3' and Γ_5' is determined. By definition, every point of G_{35} is the intersection point of two curves $E_3(b)$ and $E_5(b)$ with identical b. Since both curves have the point with coordinates $x = 1$, $y = b$ in common, the normal n_2 is part of G_{35}. Figure 15.44 shows that a curve $E_3(b)$ with cusps and the line $E_5(b)$ for the same value of b have a second point of intersection located between the lines n_2 and K (in the small figure this is shown schematically). Also this point is part of G_{35}. A parameter equation for G_{35} is found as follows. For $E_3(b)$ Eqs.(15.161) and (15.162) are used (in the interval $(\pi - \alpha)/2 \le \varphi \le \pi - \alpha$ describing the branch below the symmetry line g). In both equations b is replaced by y because $E_5(b)$ has the equation $y = b$. This results in two linear equations for x and y:

$$\left.\begin{aligned} x\sin(\varphi + \alpha) - y[1 + \cos(\varphi + \alpha)] &= \frac{\sin\varphi\sin(\varphi + \alpha)}{\sin\alpha}\,, \\ x\cos(\varphi + \alpha) + y\sin(\varphi + \alpha) &= \frac{\sin(2\varphi + \alpha)}{\sin\alpha} \end{aligned}\right\} \quad \left(\frac{\pi - \alpha}{2} \le \varphi < \pi - \alpha\right). \tag{15.166}$$

The coefficient determinant is $1 + \cos(\pi + \alpha)$. In the solutions for x and y this determinant appears not only as denominator, but also as factor in both numerators. From this it follows that both x and y are indeterminate in the case $\varphi = \pi - \alpha$. The solution associated with this indeterminacy is the line n_2 which was shown to be part of G_{35}. The other branch of G_{35} is described by the solutions for x and y after canceling out the factor $1 + \cos(\pi + \alpha)$. These are the equations

$$\left.\begin{aligned} x(\varphi) &= \frac{\sin\varphi + \cos\varphi\sin(\varphi + \alpha)}{\sin\alpha} \\ y(\varphi) &= \frac{[1 - \cos(\varphi + \alpha)]\cos\varphi}{\sin\alpha} \end{aligned}\right\} \quad \left(\frac{\pi - \alpha}{2} \le \varphi < \pi - \alpha\right). \tag{15.167}$$

Let S^* be the endpoint associated with $\varphi = (\pi - \alpha)/2$. It is located on g. Its coordinates are

$$x^* = \frac{1+\sin\frac{\alpha}{2}}{2\sin\frac{\alpha}{2}}\,, \qquad y^* = \frac{1+\sin\frac{\alpha}{2}}{2\cos\frac{\alpha}{2}} = \frac{1}{2}\tan\frac{\pi+\alpha}{4}\,. \tag{15.168}$$

The other endpoint associated with $\varphi = \pi - \alpha$ is the point Q_2 on n_2. In Fig. 15.45 this branch of the boundary G_{35} is shown. The results are summarized as follows. The domain Γ_3' has the symmetry axis g. The part below g is bounded by the section $0 \le x \le 1$ of the x-axis, by the section of n_2 between the points $(x = 1\,,\ y = 0)$ and Q_2 and by the section of G_{35} between Q_2 and S^*. That the section of n_2 above Q_2 does not play a role is seen in Fig. 15.44 from the curves $\mathrm{E}_3(b)$ and $\mathrm{E}_5(b)$ terminating on this section of n_2. Figure 15.45 shows also the domains Γ_1', Γ_3' and Γ_5', the line g and the curve $\mathrm{E}_3(0)$. The three domains have the point S^* in common. If P_0 is located at S^*, all three motion phases 1, 3 and 5 yield one and the same maximum width $B_{\max}$. This implies that S^* has equal distances from g_1, from g_2 and from the curve $\mathrm{E}_3(0)$. The maximum width is $B_{\max} = y^*$ with y^* from (15.168).

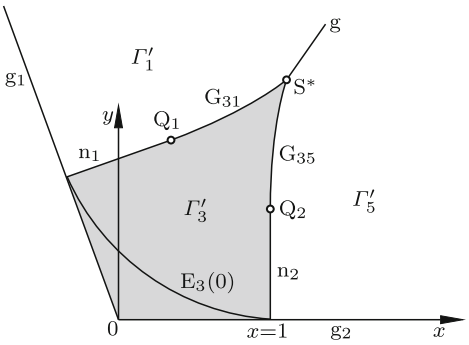

Fig. 15.45 Domains Γ_1', Γ_5' and Γ_3' (shaded) for $\alpha = 110°$

Next, equations determining $B_{\max}$ are formulated for the three domains Γ_1', Γ_3' and Γ_5'. At the beginning it was said that the equation describing the curve $\mathrm{E}_i(b)$ becomes an equation for b if, first, P_0 is located in Γ_i' and if, second, for x and y the coordinates x_0 and y_0 of P_0 are substituted. The maximum admissible width $B_{\max}$ is the smallest of the roots b. The three cases are:

P_0 is located in Γ_1': The equation of $\mathrm{E}_1(b)$ is Eq.(15.160). With $x = x_0\,,\ y = y_0$ the explicit result is obtained: $B_{\max} = x_0 \sin\alpha - y_0 \cos\alpha$.

P_0 is located in Γ_5': The equation of $\mathrm{E}_3(b)$ is $y = b$. Hence $B_{\max} = y_0$.

P_0 is located in Γ_3': $\mathrm{E}_3(b)$ is represented by (15.161) and (15.162). With $x = x_0\,,\ y = y_0$ these equations are

$$\left.\begin{aligned} b(\varphi) &= \Big(x_0 - \frac{\sin\varphi}{\sin\alpha}\Big)\sin(\varphi+\alpha) - y_0\cos(\varphi+\alpha)\,, \\ x_0\cos(\varphi+\alpha) &+ y_0\sin(\varphi+\alpha) - \frac{\sin(2\varphi+\alpha)}{\sin\alpha} = 0 \end{aligned}\right\} \qquad (0<\varphi<\pi-\alpha)\,. \tag{15.169}$$

For every root φ of the second equation the associated solution $b(\varphi)$ is calculated from the first equation. On the number of solutions the following statement can be made. Consider in Fig. 15.44 the curve $\mathrm{E}_3(b)$ with the cusp shown in the enlarged inset. A neighboring curve $\mathrm{E}_3(b+\Delta b)$ with a sufficiently small Δb intersects the curve $\mathrm{E}_3(b)$ at two points, one of them located between G_{31} and n_1 and the other between G_{35} and n_2. Hence the conclusion: Two solutions b exist if P_0 is located either between G_{31} and n_1 or between G_{35} and n_2. A single solution exists if P_0 is located elsewhere in Γ_3'.

For solving the second Eq.(15.169) the terms $\cos(\varphi+\alpha)$, $\sin(\varphi+\alpha)$ and $\sin(2\varphi+\alpha)$ are expressed in terms of functions of individual angles by means of addition theorems. In the resulting equation the variable $u=\tan\varphi/2$ is introduced by substituting the expressions $\cos\varphi=(1-u^2)/(1+u^2)$ and $\sin\varphi=2u/(1+u^2)$. After multiplication with $(1+u^2)^2$ a fourth-order equation for u is obtained. With the abbreviations $s=\sin\alpha$, $c=\cos\alpha$ it reads

$$\left.\begin{aligned} &a_4u^4+a_3u^3+a_2u^2+a_1u+a_0=0\,, \\ &a_4 = 1+cx_0+sy_0\,, \quad a_3 = 2(sx_0-cy_0-2c/s)\,, \\ &a_0 = 1-cx_0-sy_0\,, \quad a_1 = 2(sx_0-cy_0+2c/s)\,, \quad a_2=-6\,. \end{aligned}\right\} \tag{15.170}$$

The degree four has the following explanation. For an observer fixed on the moving rectangle P_0 is moving on a limaçon of Pascal. Solutions b are distances between the line $\overline{\mathrm{AB}}$ which is now fixed and all tangents to the limaçon which are parallel to $\overline{\mathrm{AB}}$. Figures 15.8a – d show that the maximum number of parallel tangents is four.

15.6.2 Right-Angled Corner

This is the special case $\alpha=\pi/2$. The parametric equation (15.163) of the curve $\mathrm{E}_3(0)$ is $x=\sin^3\varphi$, $y=\cos^3\varphi$. This is the equation of an astroid (see (15.129)). The parameter-free form is $x^{2/3}+y^{2/3}=1$. The parametric equation (15.165) of the evolute K is $x=\sin\varphi(1+2\cos^2\varphi)$, $y=\cos\varphi(1+2\sin^2\varphi)$. In a ξ,η-system rotated though $\pi/4$ against the x,y-system the coordinates are $\xi=(y+x)/\sqrt{2}=(\cos\varphi+\sin\varphi)(1+\sin2\varphi)/\sqrt{2}$, $\eta=(y-x)/\sqrt{2}=(\cos\varphi-\sin\varphi)(1-\sin2\varphi)/\sqrt{2}$. With ψ defined by $\varphi=\psi-\pi/4$ this becomes $\xi=2\sin^3\psi$, $\eta=2\cos^3\psi$. This represents the astroid $\mathrm{E}_3(0)$

rotated through $\pi/4$ and multiplied by 2. This result is a special case of Theorem 15.9 stating that the evolute of a cycloid is a similar cycloid.

The parametric equation (15.167) of the curve G_{35} is $x = \sin\varphi + \cos^2\varphi$ (1), $y = \cos\varphi(1+\sin\varphi)$ (2). From (1) $1-\cos^2\varphi = (x-\cos^2\varphi)^2$ (3) and from (2) in combination with (1) $y^2 = \cos^2\varphi\,(2x + 2 - 3\cos^2\varphi)$. Elimination of $\cos^4\varphi$ from the last two equations yields $\cos^2\varphi = (y^2 - 3x^2 + 3)/(5 - 4x)$. Substitution of this expression into (3) results in a parameter-free equation for G_{35}:
$(x^2 + y^2)^2 + y^2(11 - 14x) + 2x(x^2 - 1) - 1 = 0$ and resolved for y^2
$y^2 = -\frac{1}{2}[(5 - 4x)^{3/2} + 2x^2 - 14x + 11]$.
Equation (15.170) reads $(1 + y_0)u^4 + 2x_0u^3 - 6u^2 + 2x_0u + (1 - y_0) = 0$.

15.6.3 Acute-Angled Corner

This is the case $\alpha < \pi/2$. Both domains Γ_1 and Γ_5 cover the entire sector between g_1 and g_2. The curves $E_1(b)$ and $E_5(b)$ have the same equations as before.

Phase 3 of the motion is restricted to the interval $\pi/2-\alpha \le \varphi \le \pi/2$. In this interval all previous results remain valid, i.e., Eqs.(15.161) – (15.163) for the curves $E_3(b)$, Eq.(15.165) for K and Eq.(15.167) for the curved section of G_{35}. In the center $\varphi = (\pi - \alpha)/2$ of the interval all curves intersect the symmetry axis g.

Figure 15.46 shows for $\alpha = 40°$ the curve K, the curved section of G_{35} and curves $E_3(b)$ for several values $b \ge 0$. At the final angle $\varphi = \pi/2$ the curve K and all curves $E_3(b)$ terminate on the line $y = 1$. In particular, $E_3(0)$ terminates at the point Q_0 with the coordinate $x = \cot\alpha$, and K terminates at the point Q_3 with the coordinate $x = 2\cot\alpha$. The curved section of G_{35} starts at the point S^* (see Fig. 15.45 and (15.168)), and it terminates with $\varphi = \pi/2$ at the intersection of g_2 and $E_3(0)$. Reflection of G_{35} on g produces G_{31}. The domain Γ_3 is the shaded area of the sector between g_1 and g_2.

Phase 2: Figure 15.47 shows a rectangle and a point P_0 in positions satisfying the conditions (a) and (b). For the center of rotation P the dashed auxiliary lines yield the x-coordinates $x_P = (\sin\varphi + b\cos\varphi)/\sin\alpha$, $y_P = (\cos\varphi - b\sin\varphi)/\sin\alpha$. Elimination of φ yields $x_P^2 + y_P^2 = (1 + b^2)/\sin^2\alpha$.

The normal $n(\varphi)$ intersects the line $\overline{A'B'}$ between A' and B' only if $x_P \ge x_A$. With the angle ψ shown in the figure this condition is $\varphi \ge \pi/2 - \alpha - \psi$ or $\sin\varphi \ge \sin(\pi/2 - \alpha - \psi)$. With $\sin\psi = b/\sqrt{1 + b^2}$, $\cos\psi = 1/\sqrt{1 + b^2}$ the condition becomes $\sin\varphi \ge (\cos\alpha - b\sin\alpha)/\sqrt{1 + b^2}$. From this it follows that in equations for the curves $E_2(b)$ the variable φ is subject to the condition $\varphi_0 \le \varphi \le \pi/2 - \alpha$ with

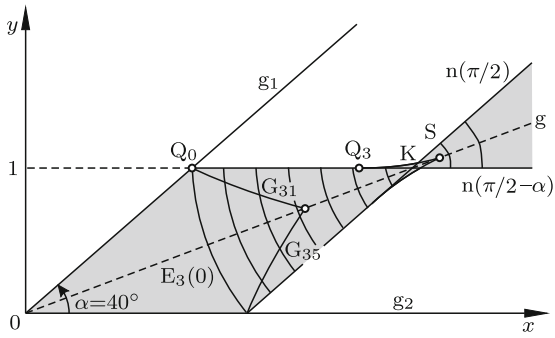

Fig. 15.46 Curves, points and domains of Figs. 15.44 and 15.45 for $\alpha = 40°$

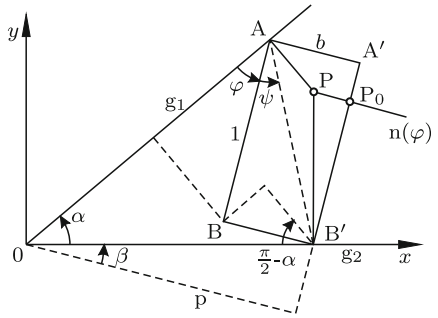

Fig. 15.47 Phase 2 with center of rotation P and with P_0 on the edge $\overline{A'B'}$

$$\left.\begin{array}{lll} \sin\varphi_0 = \dfrac{\cos\alpha - b\sin\alpha}{\sqrt{1+b^2}}\,, & \cos\varphi_0 = \dfrac{\sin\alpha + b\cos\alpha}{\sqrt{1+b^2}} & (b \le \cot\alpha) \\ \varphi_0 = 0 & & (b \ge \cot\alpha)\,. \end{array}\right\} \tag{15.171}$$

The normal form of the equation for the line $\overline{A'B'}$ is determined by the angle $\beta = \pi/2 - (\varphi + \alpha)$ and by the length $p = x_P \cos\beta$ of the perpendicular. The equation is

$$x\sin(\varphi+\alpha) - y\cos(\varphi+\alpha) - \frac{(\sin\varphi + b\cos\varphi)\sin(\varphi+\alpha)}{\sin\alpha} = 0\,. \tag{15.172}$$

On $E_2(b)$ this equation as well as its partial derivative with respect to φ is satisfied:

$$x\cos(\varphi+\alpha) + y\sin(\varphi+\alpha) - \frac{\sin(2\varphi+\alpha) + b\cos(2\varphi+\alpha)}{\sin\alpha} = 0\,. \tag{15.173}$$

The solutions of these two equations for x and y are parameter equations of $E_2(b)$:

$$\left.\begin{aligned} x(\varphi,b) &= \frac{\sin\varphi + b\cos\varphi + (\cos\varphi - b\sin\varphi)\sin(\varphi+\alpha)\cos(\varphi+\alpha)}{\sin\alpha}\,, \\ y(\varphi,b) &= \frac{(\cos\varphi - b\sin\varphi)\sin^2(\varphi+\alpha)}{\sin\alpha} \end{aligned}\right\} (\varphi_0 \le \varphi \le \pi/2-\alpha)\,. \tag{15.174}$$

Figure 15.48 shows for $\alpha = 40°$ curves $\mathrm{E}_2(b)$ for several values $b \ge 0$. At the end of the interval, i.e., for $\varphi = \pi/2 - \alpha$, all curves terminate on the normal to g_1 through the point Q_0 known from Fig. 15.46. The interval starts with $\varphi = \varphi_0$ given by (15.171). All curves $\mathrm{E}_2(b)$ with $b \ge \cot\alpha$ start on the line $y = \sin\alpha$. In particular, $\mathrm{E}_2(b = \cot\alpha)$ starts at the point R_0 with the coordinate $x = (1 + 1/\sin^2\alpha)\cos\alpha$. The curve $\mathrm{E}_2(b)$ with $b \le \cot\alpha$ (arbitrary) starts at the point with the coordinates

$$x(b) = \sqrt{1+b^2}\,\cot\alpha + \frac{b}{\sqrt{1+b^2}}\,, \qquad y(b) = \frac{1}{\sqrt{1+b^2}} \qquad (0 \le b \le \cot\alpha)\,. \tag{15.175}$$

These coordinates are obtained from (15.174) by substituting for $\sin\varphi$ and $\cos\varphi$ the expressions $\sin\varphi_0$ and $\cos\varphi_0$, respectively, of (15.171). Equation (15.175) is a parametric equation of the curve called e_1. It starts with $b = 0$ at the point Q_0 and it terminates with $b = \cot\alpha$ at the point R_0. Elimination of the parameter b yields the explicit equation $x = \sqrt{1-y^2} + (1/y)\cot\alpha$ (valid for $\sin\alpha \le y \le 1$).

The domain Γ_2 is the shaded area in Fig. 15.48. Of its boundary only the small section is still unknown on which the curves $\mathrm{E}_2(b)$ have cusps. This section is called e_2. For a given value of b (arbitrary) all normals $\mathrm{n}(\varphi)$ envelope a curve $\mathrm{K}(b)$. This curve $\mathrm{K}(b)$ is found by the same method that was used for the curve K of Fig. 15.44. Starting point is Eq.(15.173) of the normal $\mathrm{n}(\varphi)$. On $\mathrm{K}(b)$ this equation as well as its partial derivative with respect to φ is satisfied:

$$-x\sin(\varphi+\alpha) + y\cos(\varphi+\alpha) - 2\,\frac{\cos(2\varphi+\alpha) - b\sin(2\varphi+\alpha)}{\sin\alpha} = 0\,. \tag{15.176}$$

At the cusp of $\mathrm{E}_2(b)$ Eqs.(15.172), (15.173) and (15.176) have the quantities b, x, y and φ in common. Summation of (15.172) and (15.176) eliminates x and y. The resulting equation is solved for b:

$$b = \frac{3\cos(\varphi+\alpha)\cos\varphi - \cos\alpha}{3\cos(\varphi+\alpha)\sin\varphi + \sin\alpha}\,. \tag{15.177}$$

Substitution of this expression into (15.174) results in the desired parametric equation for e_2:

$$\left.\begin{aligned} x(\varphi) &= \frac{[2+\sin^2(\varphi+\alpha)]\cos(\varphi+\alpha)}{\sin\alpha[3\cos(\varphi+\alpha)\sin\varphi + \sin\alpha]} \\ y(\varphi) &= \frac{\sin^3(\varphi+\alpha)}{\sin\alpha[3\cos(\varphi+\alpha)\sin\varphi + \sin\alpha]} \end{aligned}\right\} (0 \le \varphi \le \pi/2-\alpha)\,. \tag{15.178}$$

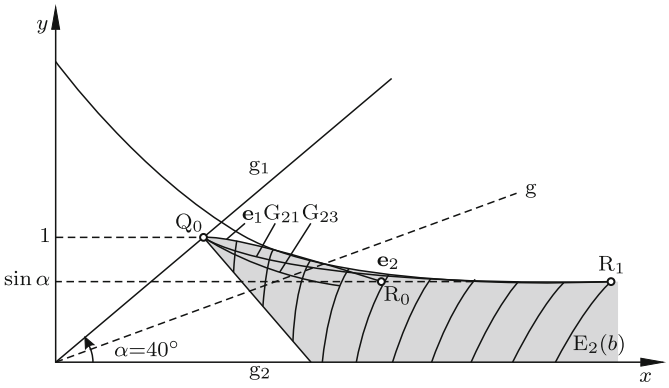

Fig. 15.48 Curves, points and domains associated with phase 2 of the motion for $\alpha = 40°$

In Fig. 15.48 this curve is shown. With $\varphi = 0$ it starts at the point R_1 with coordinates $x = (1 + 2/\sin^2\alpha)\cos\alpha$, $y = \sin\alpha$. At this point the curve e_2 merges tangentially with the line $y = \sin\alpha$. With $\varphi = \pi/2 - \alpha$ the curve terminates at the point $x = 0$, $y = 1/\sin^2\alpha$. No explicit formulas have been found for the point of tangential contact between e_2 and e_1. The section of e_2 to the right of this point is part of the boundary of Γ_2.

In what follows, the curves G_{21} and G_{23} are determined. First, the curve G_{21}. It is the geometric locus of the intersection points of $E_2(b)$ and $E_1(b)$. The expressions (15.174) are substituted into (15.160). The resulting equation is solved for b:

$$b = \frac{(1+\cos\varphi)\cos(\varphi+\alpha)}{(1+\cos\varphi)\sin(\varphi+\alpha) - \sin\alpha} \,. \tag{15.179}$$

When this is substituted back into (15.174), the parametric equation for G_{21} is obtained:

$$\left.\begin{aligned} x(\varphi) &= \frac{\cos\alpha + [1+\sin\alpha\sin(\varphi+\alpha)]\cos(\varphi+\alpha)}{\sin\alpha[(1+\cos\varphi)\sin(\varphi+\alpha) - \sin\alpha]} \\ y(\varphi) &= \frac{\sin^2(\varphi+\alpha)}{(1+\cos\varphi)\sin(\varphi+\alpha) - \sin\alpha} \end{aligned}\right\} \quad (0 \le \varphi \le \pi/2 - \alpha) \,. \tag{15.180}$$

Figure 15.48 shows the curve G_{21}. With $\varphi = 0$ it starts at the same point R_1 as e_2. With $\varphi = \pi/2 - \alpha$ it terminates at Q_0.

Next, the curve G_{23} is determined. Since neither for $E_2(b)$ nor for $E_3(b)$ an equation free of the parameter φ is known, the curve G_{23} cannot be found by the method used for G_{21}. For $E_2(b)$ (15.172) and (15.173) are used and for $E_3(b)$ (15.161) and (15.162). At the intersection point the equations are identical in x and y, but the parameters φ are not the same for $E_2(b)$ and $E_3(b)$. The angles are called φ_2 for $E_2(b)$ and φ_3 for $E_3(b)$. The equations are written as linear equations for x, y and b with coefficients depending

on φ_2 and φ_3:

$$\begin{bmatrix} \sin(\varphi_2+\alpha) & -\cos(\varphi_2+\alpha) & -\cos\varphi_2\sin(\varphi_2+\alpha)/\sin\alpha \\ \cos(\varphi_2+\alpha) & \sin(\varphi_2+\alpha) & -\cos(2\varphi_2+\alpha)/\sin\alpha \\ \sin(\varphi_3+\alpha) & -\cos(\varphi_3+\alpha) & -1 \\ \cos(\varphi_3+\alpha) & \sin(\varphi_3+\alpha) & 0 \end{bmatrix} \begin{bmatrix} x \\ y \\ b \end{bmatrix}$$

$$= \frac{1}{\sin\alpha} \begin{bmatrix} \sin\varphi_2\sin(\varphi_2+\alpha) \\ \sin(2\varphi_2+\alpha) \\ \sin\varphi_3\sin(\varphi_3+\alpha) \\ \sin(2\varphi_3+\alpha) \end{bmatrix} . \tag{15.181}$$

A necessary condition for the existence of solutions x, y, b is the vanishing of the (4×4)-determinant of the coefficients including the right-hand side expressions. The third and the fourth columns are multiplied by $\sin\alpha$. Then, using addition theorems, the terms $\cos(2\varphi_i+\alpha)$ and $\sin(2\varphi_i+\alpha)$ are expressed as functions of φ_i and of $(\varphi_i+\alpha)$ $(i=2,3)$. Finally, the abbreviations are introduced: $s=\sin\alpha$, $c=\cos\alpha$, $s_i=\sin\varphi_i$, $c_i=\cos\varphi_i$, $S_i=\sin(\varphi_i+\alpha)$, $C_i=\cos(\varphi_i+\alpha)$ $(i=2,3)$. The resulting equation has the form

$$\begin{vmatrix} S_2 & -C_2 & -c_2S_2 & s_2S_2 \\ C_2 & S_2 & -c_2C_2+s_2S_2 & s_2C_2+c_2S_2 \\ S_3 & -C_3 & -s & s_3S_3 \\ C_3 & S_3 & 0 & s_3C_3+c_3S_3 \end{vmatrix} = 0 . \tag{15.182}$$

Linear combinations of rows 1 and 2 with coefficients S_2 and C_2 and of rows 3 and 4 with coefficients S_3 and C_3 result in the equation

$$\begin{vmatrix} 1 & 0 & -c_2+s_2C_2S_2 & s_2+c_2C_2S_2 \\ 0 & 1 & s_2S_2^2 & c_2S_2^2 \\ 1 & 0 & -S_3s & s_3+c_3C_3S_3 \\ 0 & 1 & C_3s & c_3S_3^2 \end{vmatrix} = 0 . \tag{15.183}$$

Expansion of this determinant leads to the equation

$$\begin{aligned} &(s_2S_2^2-sC_3)(s_3+c_3C_3S_3)+S_2^2(sc_2S_3-1) \\ &+c_3S_3^2(c_2-s_2C_2S_2-sS_3)+sC_3(s_2+c_2C_2S_2-sS_3)=0 . \end{aligned} \tag{15.184}$$

Finally, the expressions $S_i=s_ic+c_is$ and $C_i=c_ic-s_is$ are introduced $(i=2,3)$. This results in an equation for φ_2 and φ_3. Its highest-order term is $\cos^3\varphi_2\cos^4\varphi_3$. The solution for, say φ_2, must be calculated numerically. For reasons of symmetry it suffices to consider the interval $\pi/2-\alpha \le \varphi_3 \le (\pi-\alpha)/2$. For every pair of values (φ_2,φ_3) the corresponding quantities x, y and b are calculated from (15.181). From b the angle φ_0 of Eq.(15.171) is calculated. If the condition $\varphi_0 \le \varphi_2 \le \pi/2-\alpha$ is satisfied, x and y

are the coordinates of a point of G_{23}. Figure 15.48 shows the curve G_{23} calculated for the angle $\alpha = 40°$.

Reflection of G_{21} and G_{23} on g produces G_{45} and G_{43}, respectively. Figure 15.49 displays the curves G_{ij} $(i, j = 1, \ldots, 5; j \neq i)$. Together with g_1 and g_2 they divide the sector between g_1 and g_2 into the domains $\Gamma'_1, \ldots \Gamma'_5$. The domain boundaries G_{31} and G_{35} shown as dashed lines are irrelevant.

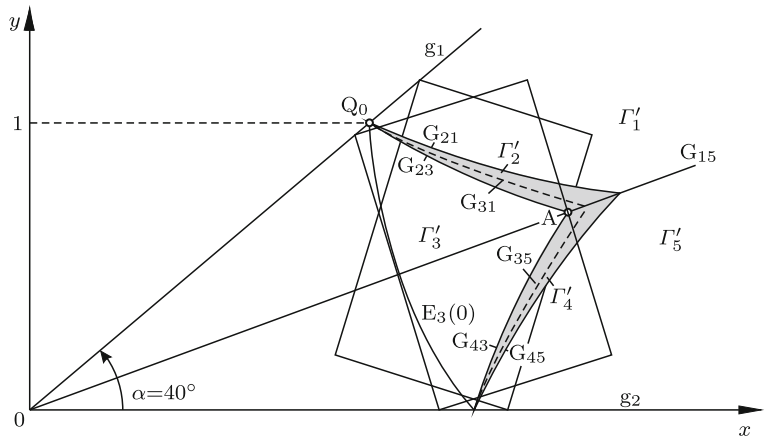

Fig. 15.49 Domains $\Gamma'_1, \ldots \Gamma'_5$ (Γ'_2, Γ'_4 shaded) for $\alpha = 40°$. When P_0 is point A, the rectangle of maximum width is in contact with P_0 in three positions occurring in phases 2, 3 and 4. Two positions are shown

Finally, an equation determining $b_{\min}$ is formulated for the case when P_0 is located in Γ'_2. Equations (15.174) determine b and φ if $x = x_0$ and $y = y_0$ is substituted. The second equation is solved for b and then this expression is substituted into the first equation. This results in the equations

$$b(\varphi) = \cot\varphi - y_0 \frac{\sin\alpha}{\sin\varphi \sin^2(\varphi + \alpha)} , \tag{15.185}$$

$$\left(x_0 \sin\varphi - \frac{1}{\sin\alpha}\right) \sin^2(\varphi + \alpha) + y_0[\cos\varphi - \sin\varphi \sin(\varphi + \alpha)\cos(\varphi + \alpha)] = 0 . \tag{15.186}$$

The last equation is an equation for φ. As was done with (15.169), the variable $u = \tan\varphi/2$ is introduced. The result is the 6th-order equation for u (with abbreviations $s = \sin\alpha$, $c = \cos\alpha$)

$$\left.\begin{array}{ll} b_6u^6+b_5u^5+b_4u^4+b_3u^3+b_2u^2+b_1u+b_0=0\,, & \\ b_6=-(y_0+s)\,, & b_5=\ 2s(sx_0-cy_0)+4c\,, \\ b_0=\ \ y_0-s\,, & b_1=\ 2s(sx_0-cy_0)-4c\,, \\ b_4=-8s(cx_0+sy_0)+3y_0+5s-4/s\,, & b_3=12c(cx_0+sy_0)-4x_0\,, \\ b_2=\ \ 8s(cx_0+sy_0)-3y_0+5s-4/s\,. & \end{array}\right\} \tag{15.187}$$

Every real solution u determines an angle $\varphi = 2\tan^{-1}u$. If this angle satisfies the condition $\varphi_0 \le \varphi \le \pi/2-\alpha$, the corresponding width $b(\varphi)$ is calculated from (15.185). The smallest of all widths thus determined is the desired solution $B_{\max}$.

In Fig. 15.49 point A belongs to the three domains Γ_2', Γ_3' and Γ_4'. When P_0 is at A, the rectangle of maximum width is in contact with P_0 in three positions. The two positions in phases 2 and 3 are shown. The coordinates of A, the associated maximum width b and the associated angle φ in phase 2 are determined as follows. The coordinates in phase 2 as functions of b and φ are given in (15.174). The coordinates in phase 3 are (see Fig. 15.49)

$$x = y\cot\frac{\alpha}{2} = \cos\frac{\alpha}{2}\left(\frac{1}{2}\cot\frac{\alpha}{2}+b\right)\,, \qquad y=\frac{1}{2}\cos\frac{\alpha}{2}+b\sin\frac{\alpha}{2}\,. \tag{15.188}$$

Equating the two yields two equations for the unknowns b and φ. Elimination of b leads to an equation for φ. It can only be solved numerically since it contains as highest-order term $\cos^3\varphi$.

References

1. Bereis R (1951) Aufbau einer Theorie der ebenen Bewegung mit Verwendung komplexer Zahlen. Österr.Ing.-Arch. 5:246–266
2. Besicovitch A S (1928) On Kakeya's problem and a similar one. Mathematische Zeitschrift 27:312–320
3. Blaschke W, Müller H R (1956) Ebene Kinematik. Oldenbourg, München
4. Bottema O, Roth B (1990) Theoretical kinematics. North-Holland, Dover, New York
5. Boute R T (2004) Moving a rectangle around a corner – geometrically. Am.Math.Monthly 111:435–437
6. Bresse J A C (1853) Sur un théorème nouveau concernant les mouvements plan, et sur l'application de la cinématique a la détermination des rayons de courbure. J.Ec.Polyt.Paris 35:89–115
7. Darboux G (1881) Sur le déplacement d'une figure invariable. Comptes Rendus Acad. Scie. XCII:118–121
8. Dijksman E A (1976) Motion geometry of mechanisms. Cambridge Univ. Press,
9. Fayet M (1988) Une nouvelle formule relative aux courbures dans un mouvement plan; nous proposons de l'appeler "Formule de Bobillier". Mechanism Machine Theory 23:135–139
10. Feldhoff H-J (1984) Periodische Bewegungsvorgänge zweidimensionaler Riemannscher Mannigfaltigkeiten und die Analoga der Sätze von Holditch und Woolhouse in zweidimensionalen Räumen konstanter Krümmung. Diss. Köln Univ.

11. Geronimus Ya. L. (1962) Geometric apparatus of the theory of synthesis of planar mechanisms (russ.). Gos. Isd. Physico-Math. Lit. Moscow
12. Giering O (1997) Perlen der Geometrie. Beispiele aus drei Jahrtausenden. TU München, Fak. Math., Report TUM M9710
13. Hering L (1981) Holditch-Sätze für Regelflächen und deren Übertragungen auf ebene und sphärische Kurven. Diss. TH Darmstadt
14. Hire P de la (1706) Traité des roulettes. Mém.Math.Phys.Acad.Royale Scie.,Paris
15. Holditch H (1858) Geometrical theorem. Quat.J.Pure and Appl.Math.2:38. See also Lady's and gentleman's diary for the year 1858
16. Hoschek J (1975) Eine Verallgemeinerung des Satzes von Holditch. Monatshefte Math.80:93-99
17. Husty M L, Karger A, Sachs S, Steinhilper W (1997) Kinematik und Robotik. Springer, Berlin, Heidelberg, New York
18. Kennedy A B W (1886) The mechanics of machinary. Macmillan, London
19. Klein F, Müller C (eds.) (1901-1908) Enzyklopädie der Math. Wissenschaften. v.IV: Mechanik. Teubner, Leipzig
20. Koenigs G (1897) Leçons de cinématique. Avec des notes par G. Darboux, E. et F. Cosserat. Hermann, Paris
21. Koenigs G (1905) Introduction à une théorie nouvelle des méchanismes. Hermann, Paris
22. Kutzbach K (1927) Mehrgliedrige Radgetriebe und ihre Gesetze. Maschinenbau - Gestaltung, Betrieb, Wirtschaft. VDI-Verl. Berlin 6:1080–1083
23. Leibniz G W (1768) Opera Omnia, Genf, v.III:95. reprint (1989) Olms-Verl., Hildesheim
24. Miller N (1949) The problem of a non-vanishing girder rounding a corner. Am.Math.Monthly 56:177–179
25. Moretti C (2002) Moving a couch around a corner. College Math.J.33:196–200
26. Schoenflies A, Grübler M (1908) Kinematik. In: [19]:190–278
27. Skanavi M I (Ed.) Sbornik sadach po matematike dlya postupajushchich vo vtusy. Kn.1 Algebra [Collection of mathematical problems of entrance examinations at technical universities. Book 1 Algebra]
28. Strubecker K (1964) Differentialgeometrie I. Kurventheorie der Ebene und des Raumes. Sammlung Göschen Bd.113/1113a, Walter de Gruyter, Berlin
29. Wunderlich W (1946) Höhere Radlinien. Österr.Ing.Arch.1:277–296
30. Wunderlich W (1970) Ebene Kinematik. BI-Verl. Mannheim

Chapter 16
Theory of Gearing

Gears are wheels with teeth shaped so as to transmit rotational motion from one wheel to another. One of the wheels may be a rack (a wheel of infinite radius). In this case, rotational motion of a wheel is transformed into translatory motion of the rack or vice versa. The present chapter is restricted to gears transforming uniform motion of one wheel into uniform motion of the other wheel or rack. This restriction eliminates from investigation specialties such as elliptical wheels, Geneva wheels etc.

Gear pairs are classified by the relative location of the wheel axes and by the shapes of teeth. Wheel axes are either parallel or intersecting or skew. In all three cases there is a choice between external gearing (both wheels carrying the teeth externally and contacting each other externally) and internal gearing (one wheel with external teeth inside the other wheel with internal teeth). In all these cases an infinite variety of tooth shapes exists for transmitting uniform motion into uniform motion. For practical reasons only a small number of shapes is actually used. Criteria for making the choice between external and internal gearing and for selecting particular tooth shapes are among others (not necessarily in the given order and not unrelated)
– the power to be transmitted
– the gear ratio ω_2/ω_1 to be produced
– the volume required
– magnitude and direction of load imposed on shaft bearings
– the amount of sliding of contacting teeth (heat development, wear, lubrication)
– the kind of contact (convex-convex or convex-concave; along a line; at a single point)
– the sensitivity to manufacturing errors
– the amount of noise produced
– manufacturing costs.

Gearing technology has reached a high standard of precision. Of its many aspects only some elements of kinematics are treated in the present

J. Wittenburg, *Kinematics*, DOI 10.1007/978-3-662-48487-6_16

chapter. For more information the reader is referred to Schoenflies/Grübler [17], Disteli[3, 4] and to the handbooks by Bonfiglioli Riduttori S.p.A. [1], Townsend [18], Litvin [12], Dudley [5, 6], K. Roth [15, 16] and to the rich literature cited therein. For the history of gearing see Matschoss [13].

Let ω_1 and ω_2 be the scalar magnitudes (both positive) of the angular velocities of a pair of gears relative to the frame in which the gear axes are mounted, and let n_1 and n_2 be the numbers of teeth of the two gears. The gear ratio is

$$\mu = \frac{\omega_2}{\omega_1} = \frac{n_1}{n_2} \tag{16.1}$$

for external as well as for internal gears and with parallel or intersecting or skew gear axes.

16.1 Parallel Axes

Transmission of rotation from one shaft to another parallel shaft is possible by means of two cylindrical friction wheels which are rolling one on the other without slipping. In Figs. 16.1a and b cross sections of the two possible arrangements of wheels are shown. The radii are r_1 and r_2. The circles p_1 and p_2 rolling one on the other are the centrodes of the wheels. The point of rolling is the center of relative rotation P_{12}. In the theory of gearing the centrodes are referred to as *pitch circles* and P_{12} as *pitch point*. The wheels in Fig. 16.1a are rotating relative to the fixed frame with opposite senses of direction whereas those in Fig. 16.1b are rotating with equal senses of direction. If in both cases ω_1 and ω_2 are the magnitudes of the angular velocities relative to the frame, in both cases the rolling condition is $\omega_1 r_1 = \omega_2 r_2$ or

$$\mu = \frac{\omega_2}{\omega_1} = \frac{r_1}{r_2} \,. \tag{16.2}$$

If the wheels are gears, the centrodes exist only virtually. As is indicated in the figures on parts of the circumferences the centrodes are replaced by teeth. These teeth must have shapes which ensure that the gear ratio ω_2/ω_1 is constant throughout the motion. Necessary conditions are formulated further below. In Fig. 16.1a both wheels have external gearing whereas in Fig. 16.1b the larger external wheel has internal gearing. Equations (16.1) and (16.2) establish between angular velocities, radii of pitch circles and numbers of teeth the relationship

$$\mu = \frac{\omega_2}{\omega_1} = \frac{r_1}{r_2} = \frac{n_1}{n_2} \,. \tag{16.3}$$

A cylindrical gear – with external or internal gearing – is called *spur gear* if the teeth are parallel to the gear axis. Such gears are treated first. Spur gears have line contact. This has the consequence that unavoidable misalignment

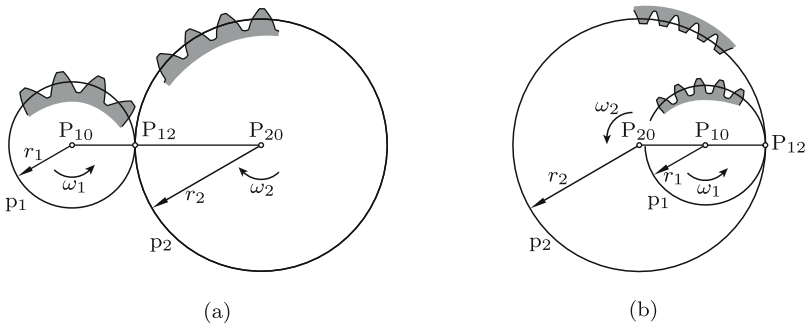

Fig. 16.1 Cylindrical friction wheels in rolling contact with opposite **(a)** and with equal senses of rotation **(b)**

of wheel axes results in edge contact leading to rapid destruction of teeth. In order to prevent this kind of failure the tooth flanks on the wheel with fewer teeth are given a minute crowning so that point contact is guaranteed. In what follows, the kinematics of ideal spur gears without crowning is investigated.

From Fig. 16.2 a necessary condition on the shapes of teeth ensuring constant gear ratio ω_2/ω_1 is deduced. The figure shows two tooth flanks which are instantaneously in contact at B. They belong to two wheels which are rotating about fixed centers P_{10} and P_{20} with *instantaneous* angular velocities ω_1 and ω_2, respectively. Note that at this point pitch circles do not yet exist. According to the theorem of Kennedy and Aronhold the instantaneous center P_{12} of relative rotation of the wheels is the point of intersection of the common normal at B with the line $\overline{\mathrm{P}_{10}\mathrm{P}_{20}}$. The vectors $\mathbf{a} = \overrightarrow{\mathrm{P}_{10}\mathrm{P}_{20}}$ and $\mathbf{b} = \overrightarrow{\mathrm{P}_{12}\mathrm{P}_{10}}$ determine the instantaneous gear ratio (see (15.6))

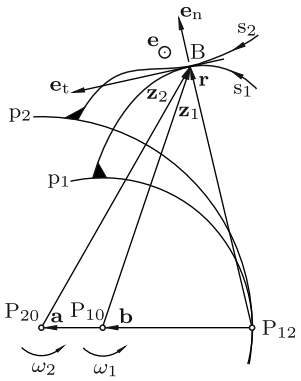

Fig. 16.2 Wheels 1 and 2 in planar motion with fixed centers P_{10}, P_{20} and with tangential contact of tooth flanks at B. Vectors $\mathbf{z}_1$, $\mathbf{z}_2$, $\mathbf{r}$, $\mathbf{a} = \mathbf{z}_1 - \mathbf{z}_2$, $\mathbf{b} = \mathbf{r} - \mathbf{z}_1$ and unit vectors $\mathbf{e}$, $\mathbf{e}_\mathrm{n}$, $\mathbf{e}_\mathrm{t}$. Arc lengths s_1 and s_2 of tooth flanks

$$\mu = \frac{\omega_2}{\omega_1} = \frac{b}{a+b} \tag{16.4}$$

where a and b are the magnitudes of $\mathbf{a}$ and $\mathbf{b}$, respectively (both positive if $\mathbf{a}$ and $\mathbf{b}$ are pointing in the same direction; the figure shows the case of internal gearing; in the case of external gearing the vectors $\mathbf{a}$ and $\mathbf{b}$ have opposite directions). In the case of arbitrarily shaped tooth flanks, the center P_{12} is not fixed, and μ is a function of the angle of rotation of wheel 1. Hence the

Theorem 16.1. *A constant gear ratio $\mu = \omega_2/\omega_1$ requires mating tooth flanks to be shaped such that throughout the period of tangential contact the common normal at the point of contact passes through a fixed point on the line $\overline{\mathrm{P}_{10}\mathrm{P}_{20}}$. Then this point is the pitch point P_{12} of two virtual pitch circles p_1, p_2. Tooth flanks satisfying this condition are said to be conjugate.*

The condition stated in this theorem is necessary, but not sufficient. Another necessary condition is that before a pair of meshing teeth is separating the subsequent pair of teeth must have started meshing already. In the following section Theorem 16.1 is used for formulating a relationship between the curvatures of conjugate tooth flanks at the point of contact.

With certain restrictions one out of two meshing tooth flanks, say flank f_1, can be chosen arbitrarily. The conjugate flank f_2 is then uniquely determined. In Sec. 16.1.4 Theorem 16.1 is used for determining parameter equations of f_2 from given parameter equations of f_1.

An altogether different way of determining the unknown flank f_2 from a given flank f_1 is based on the fact that f_2 is enveloped by f_1 when the wheels are rotating with the prescribed gear ratio. This is true not only for spur gears, but for all kinds of gears. In engineering practice, this fact is the basis of manufacturing methods. A cutting or milling tool 1 having the shape of f_1 is brought in contact with a cylindrical blank 2. Tool 1 and blank 2 are rotating with the prescribed gear ratio. In addition, tool 1 is slowly moved into blank 2 thereby removing material in such a way that at every stage the shape of 2 is enveloped by the shape of 1. This process is continued until tool 1 and the finished wheel 2 have reached the desired relative position. A survey of manufacturing methods see in K. Roth [16].

16.1.1 Curvature Relationship of Meshing Tooth Flanks

As is shown in Fig. 16.2 the fixed vectors $\mathbf{a} = \overrightarrow{\mathrm{P}_{10}\mathrm{P}_{20}}$ and $\mathbf{b} = \overrightarrow{\mathrm{P}_{12}\mathrm{P}_{10}}$ are expressed in terms of instantaneous vectors $\mathbf{z}_1$, $\mathbf{z}_2$ and $\mathbf{r}$: $\mathbf{a} = \mathbf{z}_1 - \mathbf{z}_2$, $\mathbf{b} = \mathbf{r} - \mathbf{z}_1$. In addition, the mutually orthogonal unit vectors $\mathbf{e}$ (axis of rotation), $\mathbf{e}_\mathrm{n}$ (normal) and $\mathbf{e}_\mathrm{t} = \mathbf{e} \times \mathbf{e}_\mathrm{n}$ (tangent) are used. In terms of these

vectors $\boldsymbol{\omega}_i = \omega_i \mathbf{e}$ $(i = 1, 2)$ and $\mathbf{r} = r\mathbf{e}_\mathrm{n}$. At B the tooth flanks are sliding relative to each other. The relative velocity is expressed in two ways. In terms of relative rotation about P_{12} it is

$$\mathbf{v}_{12} = (\boldsymbol{\omega}_1 - \boldsymbol{\omega}_2) \times \mathbf{r} = \omega_1 r(1-\mu)\mathbf{e}_\mathrm{t} \,. \tag{16.5}$$

Expressed as difference of the velocities of the two body-fixed points coinciding with B it is

$$\mathbf{v}_{12} = \boldsymbol{\omega}_1 \times \mathbf{z}_1 - \boldsymbol{\omega}_2 \times \mathbf{z}_2 \,. \tag{16.6}$$

Let s_1 and s_2 be the arc lengths of the flanks at B with directions as shown in the figure. The velocities of B relative to the two flanks are $\dot{s}_1\mathbf{e}_\mathrm{t}$ and $\dot{s}_2\mathbf{e}_\mathrm{t}$, respectively. The curvatures of the contacting flanks at B are denoted κ_1 and κ_2. The sign conventions are such that the angular velocity of $\mathbf{e}_\mathrm{n}$ is given by the formula $(\kappa_1\dot{s}_1 + \omega_1)\mathbf{e}$ as well as by the formula $(\kappa_2\dot{s}_2 + \omega_2)\mathbf{e}$ (in Fig. 16.2 $\kappa_1 > 0$ and $\kappa_2 < 0$). From the equality of these two expressions it follows that

$$\kappa_1\dot{s}_1 - \kappa_2\dot{s}_2 = -\omega_1(1-\mu) \,. \tag{16.7}$$

Furthermore,

$$\dot{\mathbf{e}}_\mathrm{n} = (\kappa_1\dot{s}_1 + \omega_1)\mathbf{e}_\mathrm{t} \,. \tag{16.8}$$

From the identity $\mathbf{z}_1 - \mathbf{z}_2 \equiv \mathbf{a} = \text{const}$ it follows that

$$\dot{\mathbf{z}}_2 \equiv \dot{\mathbf{z}}_1 = \dot{s}_1\mathbf{e}_\mathrm{t} + \boldsymbol{\omega}_1 \times \mathbf{z}_1 = \dot{s}_2\mathbf{e}_\mathrm{t} + \boldsymbol{\omega}_2 \times \mathbf{z}_2 \tag{16.9}$$

and from this in combination with (16.5)

$$\dot{s}_1 - \dot{s}_2 = -\omega_1 r(1-\mu) \,. \tag{16.10}$$

In order to bring angular accelerations into play the orthogonality relationship $\mathbf{v}_{12} \cdot \mathbf{e}_\mathrm{n} = 0$ is differentiated with respect to time:

$$\dot{\mathbf{v}}_{12} \cdot \mathbf{e}_\mathrm{n} + \mathbf{v}_{12} \cdot \dot{\mathbf{e}}_\mathrm{n} = 0 \,. \tag{16.11}$$

Equation (16.6) yields

$$\dot{\mathbf{v}}_{12} = \dot{\boldsymbol{\omega}}_1 \times \mathbf{z}_1 + \boldsymbol{\omega}_1 \times \dot{\mathbf{z}}_1 - (\dot{\boldsymbol{\omega}}_2 \times \mathbf{z}_2 + \boldsymbol{\omega}_2 \times \dot{\mathbf{z}}_2) \,. \tag{16.12}$$

The condition $\mu = \text{const}$ means that $\dot{\boldsymbol{\omega}}_2 = \mathbf{0}$ if $\dot{\boldsymbol{\omega}}_1 = \mathbf{0}$. Therefore, the equation must be valid for $\dot{\boldsymbol{\omega}}_1 = \dot{\boldsymbol{\omega}}_2 \equiv \mathbf{0}$. Hence, with (16.9),

$$\begin{aligned} \dot{\mathbf{v}}_{12} &= (\boldsymbol{\omega}_1 - \boldsymbol{\omega}_2) \times \dot{\mathbf{z}}_1 = (1-\mu)\boldsymbol{\omega}_1 \times (\dot{s}_1\mathbf{e}_\mathrm{t} + \boldsymbol{\omega}_1 \times \mathbf{z}_1) \\ &= -\omega_1(1-\mu)(\dot{s}_1\mathbf{e}_\mathrm{n} + \omega_1\mathbf{z}_1) \,. \end{aligned} \tag{16.13}$$

With this expression and with (16.5) and (16.8) Eq.(16.11) becomes

$$(\kappa_1\dot{s}_1 + \omega_1)r - (\dot{s}_1 + \omega_1\mathbf{e}_\mathrm{n} \cdot \mathbf{z}_1) = 0 \tag{16.14}$$

The coefficient of ω_1 is $r - \mathbf{e}_n \cdot \mathbf{z}_1 = \mathbf{e}_n \cdot (\mathbf{r} - \mathbf{z}_1) = \mathbf{e}_n \cdot \mathbf{b}$. Thus, the equation yields

$$\dot{s}_1 = \omega_1 \frac{\mathbf{e}_n \cdot \mathbf{b}}{1 - \kappa_1 r} \,. \tag{16.15}$$

From (16.10) an expression for $\dot{s}_2$ is obtained. Substitution of these two expressions into (16.7) results in the desired condition on curvatures of conjugate flanks. It has the symmetrical form

$$\mathbf{e}_n \cdot \mathbf{b}(\kappa_1 - \kappa_2) + (1 - \mu)(1 - \kappa_1 r)(1 - \kappa_2 r) \equiv 0 \,. \tag{16.16}$$

In terms of radii of curvature $\varrho_i = 1/\kappa_i$ $(i = 1, 2)$ it has the form

$$\mathbf{e}_n \cdot \mathbf{b}\,(\varrho_2 - \varrho_1) + (1 - \mu)(\varrho_1 - r)(\varrho_2 - r) \equiv 0 \,. \tag{16.17}$$

Equations (16.4) through (16.17) remain valid in the limit case $a \to \infty$, i.e., $\omega_2 \to 0$ and $\mu \to 0$. In this case, body 2 in Fig. 16.2 is a rack in translatory motion with velocity $v = \omega_1 r_1$. Equations (16.16) and (16.17) are used not only in kinematics, but also for calculations of Hertzian pressures from curvatures at points of contact.

16.1.2 Camus' Theorem

In Fig. 16.3 p_1 and p_2 are the pitch circles of two wheels with pitch point P_{12}. Let q be an arbitrary smooth curve which is fixed in a plane Σ and which is in tangential contact with p_1 and p_2 at P_{12}. Furthermore, let Q be an arbitrary point fixed in Σ, i.e., rigidly connected to q. The curve q is rolled once on p_1 and once on p_2. Point Q generates in the first process a trajectory f_1 on wheel 1 and in the second process a trajectory f_2 on wheel 2. Camus[1] proved

Theorem 16.2. *The trajectories* f_1 *and* f_2 *are conjugate tooth flanks.*

Proof: In the figure the rotations of p_1 and p_2 about their centers with rolling contact at P_{12} and the rolling of q on both pitch circles occur simultaneously in such a way that q is permanently in contact with p_1 and with p_2 at P_{12}. For an observer fixed on p_1 Q is moving along f_1 and for an observer fixed on p_2 Q is moving along f_2. In this process Q is permanently contact point of f_1 and f_2, and the line $\overline{\mathrm{P}_{12}\mathrm{Q}}$ is permanently the common normal of f_1 and f_2 at this contact point Q. Hence, by Theorem 16.1, f_1 and f_2 are conjugate tooth flanks. These arguments are valid for external as well as for internal gearing. End of Proof.

[1] Ch.E.L. Camus (1699 – 1768), Theorem of 1733

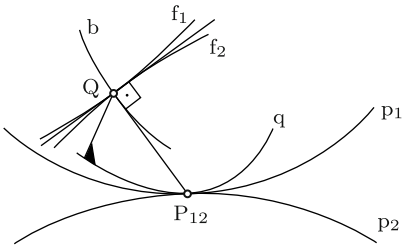

Fig. 16.3 Pitch circles p_1, p_2, curve q and point Q rigidly connected to q. During simultaneous rolling contact at P_{12} point Q is generating conjugate tooth flanks f_1 and f_2 and the frame-fixed line of contact b

The trajectory of the contact point Q in a frame-fixed reference system (line b in the figure) is referred to as *line of contact*. At Q the line $\overline{P_{12}Q}$ is tangent to b.

16.1.3 Cycloidal Gearing

Camus' theorem provides a simple explanation of de la Hire's classical theory of cycloidal gearing[2]. In Fig. 16.4 the case of external gearing is demonstrated. The curve q is a circle touching p_1 from the inside and p_2 from the outside, and Q is a point fixed on q. When the circle q is rolled inside p_1, Q generates a hypocycloid f_1 fixed on p_1, and when q is rolled on p_2, Q generates an epicycloid f_2 fixed on p_2. The two cycloids are conjugate flanks. More precisely, f_1 is the bottom part of a tooth on p_1, and f_2 is the top part of a tooth on p_2. The missing parts of the teeth are generated by means of another circle q′ which is rolled on the outside of p_1 and on the inside of p_2. This circle generates the epicycloid f_1' on p_1 and the hypocycloid f_2' on p_2. In Fig. 16.4 the circles q and q′ have equal diameters. This is not necessary, though.
Remark: One of the pitch circles, say p_1, may be a rack, i.e., a circle of infinite radius. In this case, f_1 and f_1' are ordinary cycloids generated by rolling q and q′ on the straight pitch line p_1.

A given gear ratio $\omega_2/\omega_1 = n_1/n_2 = r_1/r_2$ requires that each wheel is equipped with equally spaced identical teeth, n_1 on wheel 1 and n_2 on wheel 2. The length of arc of the pitch circle available per tooth is identical for both pitch circles. It is called *circular pitch* t:

$$t = \frac{2\pi r_1}{n_1} = \frac{2\pi r_2}{n_2} \,. \tag{16.18}$$

[2] de la Hire (1694)

In Fig. 16.4 the numbers are $n_1 = 9$ and $n_2 = 12$. The height of a tooth above the pitch circle, the so-called *addendum* a, is limited by the condition that teeth must not be pointed. The maximum possible addendum is dictated by the epicycloids on the smaller wheel. On both wheels the cycloidal tooth flanks have the same height a above and the same depth a below the pitch circle, so that the active height of the teeth is $2a$. The feet of neighboring teeth are separated by a smooth curve called fillet the purpose of which is (i) to reduce the notch effect, (ii) to prevent contact with the tips of opposite teeth and (iii) to provide room for lubricating fluids.

In the course of meshing the point of contact is moving along the dotted line of contact A_1-P_{12}-A_2 with endpoints A_1 and A_2 on the dashed addendum circles. It is seen that the gearing satisfies another necessary condition, namely, that before one pair of meshing teeth is loosing contact another pair is already meshing. The relative sliding velocity at a contact point B anywhere on the line of contact is given by (16.5). It is proportional to the distance $r = \overline{\mathrm{BP}}_{12}$. It is maximal at A_1 and at A_2 and it is zero when P_{12} is the point of contact.

In well-lubricated gears (no friction force in the common tangent plane) the force transmitted by one tooth on the other has the direction of the contact normal $\overline{\mathrm{BP}}_{12}$. The periodical change of this direction is a disadvantage of cycloidal gears. Another weakness, from the point of view of bending stiffness and bending stresses, is the concave shape of the bottom parts of teeth. A favorable characteristic is the concave–convex contact of teeth which reduces contact pressure as well as wear. For all these reasons cycloidal gears are used in fine precision mechanics exclusively. An example is the watch gear shown in Fig. 16.5. In this particular example, the hypocycloids inside the pitch circles are straight lines passing through the respective centers. This indicates that the radius of the circle q equals $r_1/2$, and that the radius of the circle q′ equals $r_2/2$. The large backlash of this gearing does not cause

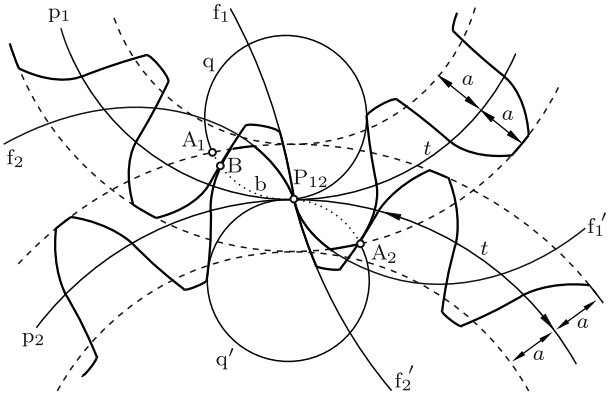

Fig. 16.4 Generation of cycloidal tooth flanks by rolling circles q and q′ on p_1 and p_2

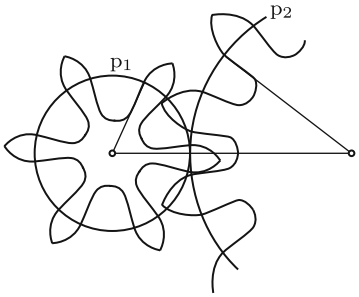

Fig. 16.5 Watch gearing with straight-line tooth flanks inside the pitch circles

problems because in watch gearings the sense of rotation does not change.

Remark: All kinds of gears require a small backlash preventing teeth from having contact on both flanks simultaneously. For the manufacturing of teeth this means that on the pitch circle the arc length of a tooth is a little smaller than half the circular pitch t, and that the width between teeth is a little larger than $t/2$. In the remainder of this chapter this is not mentioned again.

16.1.4 Construction of Conjugate Flanks

Reuleaux showed how to use Theorem 16.1 for constructing conjugate tooth flanks. In Fig. 16.6 his method is demonstrated in the case of external gearing. The figure shows pitch circles p_1 and p_2 with fixed centers P_{10} and P_{20} and the pitch point P_{12}. Let flank f_1 on wheel 1 be some arbitrarily prescribed smooth curve subject only to the condition that the normal to f_1 at the point B_1 (arbitrary) intersects p_1. Let N_1 be this wheel-fixed point of intersection. In Fig. 16.6 f_1 is shown when wheels 1 and 2 are in some arbitrarily chosen

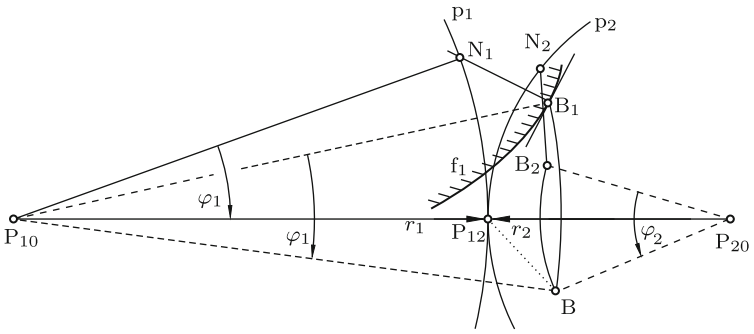

Fig. 16.6 Reuleaux's construction of flank f_2 conjugate to a given flank f_1

initial position. To each pair (point B_1, normal $\overline{B_1N_1}$) a conjugate pair (point B_2, normal $\overline{B_2N_2}$) of flank f_2 in the initial position of f_2 is constructed as follows. Conjugate means that (B_1, $\overline{B_1N_1}$) and (B_2, $\overline{B_2N_2}$) are the points and normals which coincide in the course of meshing at a certain point B. Let $\varphi_1 = \sphericalangle(B_1P_{10}B)$ be the unknown angle of rotation of wheel 1 carrying B_1 to B. According to Theorem 16.1 the common normal to the flanks at B is the dotted line passing through P_{12}. This means that the rotation through φ_1 carries the wheel-fixed point N_1 to P_{12}. Hence $\varphi_1 = \sphericalangle(N_1P_{10}P_{12})$. When wheel 1 rotates through φ_1, wheel 2 rotates in the opposite direction through $\varphi_2 = \mu\varphi_1$. Hence, the initial positions of B_2 and $\overline{B_2N_2}$ are determined by rotating wheel 2 from the meshing position (B, $\overline{BP_{12}}$) through the angle $-\varphi_2$. In this way the contact point B and the initial positions of B_2 and $\overline{B_2N_2}$ of flank f_2 are determined for each pair (B_1, $\overline{B_1N_1}$) of flank f_1. It may happen that flank f_1 is intersecting f_2 at some point while it is in contact at another point. This phenomenon is called undercutting. It restricts the freedom in choosing flank f_1. The geometric locus of all contact points B is the line of contact (see the example in Fig. 16.4 where the line of contact is the arc sequence A_1-P_{12}-A_2).

Analytically, the condition in Theorem 16.1 is formulated as follows. The x_0, y_0-system shown in Fig. 16.7a is frame-fixed. Against this x_0, y_0-system the x, y-system fixed on wheel 1 and the ξ, η-system fixed on wheel 2 are rotated through the angles φ_1 (arbitrary) counterclockwise and $\varphi_2 = \mu\varphi_1 = (n_2/n_1)\varphi_1$ clockwise, respectively. The following transformation equations are deduced from the figure:

$$\left.\begin{aligned} x_0 &= x\cos\varphi_1 - y\sin\varphi_1 - r_1\ , \\ y_0 &= x\sin\varphi_1 + y\cos\varphi_1\ , \end{aligned}\right\} \tag{16.19}$$

$$\left.\begin{aligned} \xi &= -x\cos(\varphi_1+\varphi_2) + y\sin(\varphi_1+\varphi_2) + (r_1+r_2)\cos\varphi_2\ , \\ \eta &= \ \ x\sin(\varphi_1+\varphi_2) + y\cos(\varphi_1+\varphi_2) - (r_1+r_2)\sin\varphi_2\ . \end{aligned}\right\} \tag{16.20}$$

Flank f_1 is assumed to be given in the x, y-system in the form $x(u)$, $y(u)$ with a parameter u. To be determined are, in parameter form as functions of u, the line of contact in the frame-fixed x_0, y_0-system and the conjugate flank f_2 in the ξ, η-system. The solution is found as follows. The transformation (16.19) of $x(u)$, $y(u)$ into the x_0, y_0-system yields for flank f_1 as functions of φ_1 the coordinates

$$x_0(u) = x(u)\cos\varphi_1 - y(u)\sin\varphi_1 - r_1\ , \qquad y_0(u) = x(u)\sin\varphi_1 + y(u)\cos\varphi_1\ . \tag{16.21}$$

Let the partial derivative with respect to u be denoted by the symbol prime. The normal to f_1 has the slope $-x_0'(u)/y_0'(u)$. The condition that in the position φ_1 the normal at the point $x_0(u)$, $y_0(u)$ passes through P_{12} has the form $y_0(u)/x_0(u) = -x_0'(u)/y_0'(u)$ or $x_0(u)x_0'(u) + y_0(u)y_0'(u) = 0$.

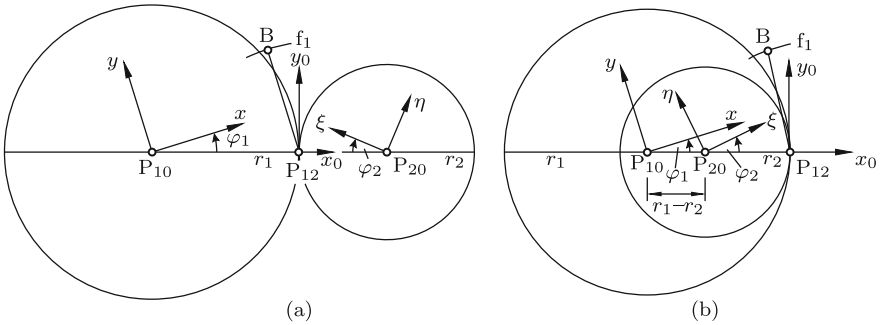

Fig. 16.7 Frame-fixed x_0, y_0-system and wheel-fixed x, y- and ξ, η-systems for external gearing **(a)** and for internal gearing **(b)**. Flank f_1 with coordinates $x(u)$, $y(u)$. Contact point B with normal passing through P_{12}

With (16.21) this is the equation

$$\begin{aligned}&[x(u)\cos\varphi_1 - y(u)\sin\varphi_1 - r_1][x'(u)\cos\varphi_1 - y'(u)\sin\varphi_1]\\ +\,&[x(u)\sin\varphi_1 + y(u)\cos\varphi_1][x'(u)\sin\varphi_1 + y'(u)\cos\varphi_1] = 0\end{aligned} \quad (16.22)$$

or

$$\left.\begin{aligned}&A\cos\varphi_1 + B\sin\varphi_1 = C\ ,\\ &A = r_1 x'(u)\ , \qquad B = -r_1 y'(u)\ , \quad C = x(u)x'(u) + y(u)y'(u)\ .\end{aligned}\right\} \quad (16.23)$$

The equation has two solutions φ_1 given by

$$\cos\varphi_1(u) = \frac{AC \mp B\sqrt{A^2+B^2-C^2}}{A^2+B^2}\ , \quad \sin\varphi_1(u) = \frac{BC \pm A\sqrt{A^2+B^2-C^2}}{A^2+B^2}\ . \quad (16.24)$$

Each solution determines the angle $\varphi_1(u)$, i.e., the position of wheel 1, for which the point $x_0(u)$, $y_0(u)$ determined by (16.21) is a point of contact (point B of Fig. 16.6). From this it follows that the line of contact has, in the frame-fixed x_0, y_0-system, the parameter equations

$$\left.\begin{aligned}x_{0_\mathrm{B}}(u) &= x(u)\cos\varphi_1(u) - y(u)\sin\varphi_1(u) - r_1\ ,\\ y_{0_\mathrm{B}}(u) &= x(u)\sin\varphi_1(u) + y(u)\cos\varphi_1(u)\ .\end{aligned}\right\} \quad (16.25)$$

Equations (16.20) determine the ξ, η-coordinates of flank f_2:

$$\left.\begin{aligned}\xi(u) &= -x(u)\cos[\varphi_1(u)+\varphi_2(u)] + y(u)\sin[\varphi_1(u)+\varphi_2(u)] + (r_1+r_2)\cos\varphi_2(u)\ ,\\ \eta(u) &= \ \ x(u)\sin[\varphi_1(u)+\varphi_2(u)] + y(u)\cos[\varphi_1(u)+\varphi_2(u)] - (r_1+r_2)\sin\varphi_2(u)\ .\end{aligned}\right\} \quad (16.26)$$

These equations represent a mapping of flank f_1 into flank f_2. This ends the solution of the problem for external gearing.

In the case of internal gearing, Fig. 16.7b replaces Fig. 16.7a. Deliberately, the inner wheel is given the label 2 in contrast to the labeling in Figs. 16.1b and 16.2. The x_0, y_0-system and the x, y-system are located as before. This has the consequence that (16.19) and (16.22) – (16.25) remain valid. The line of contact is the same for external and for internal gearing. Equations (16.26) for flank f_2 are replaced by

$$\left.\begin{aligned} \xi(u) = \;\; & x(u)\cos[\varphi_2(u)-\varphi_1(u)] + y(u)\sin[\varphi_2(u)-\varphi_1(u)] - (r_1-r_2)\cos\varphi_2(u)\,, \\ \eta(u) = -& x(u)\sin[\varphi_2(u)-\varphi_1(u)] + y(u)\cos[\varphi_2(u)-\varphi_1(u)] + (r_1-r_2)\sin\varphi_2(u)\,. \end{aligned}\right\} \tag{16.27}$$

Here and in (16.26)

$$\varphi_2(u) = \frac{n_1}{n_2}\,\varphi_1(u)\,, \qquad r_2 = \frac{n_2}{n_1}\,r_1\,. \tag{16.28}$$

Remark: Sometimes it is simpler to solve (16.23) for $u(\varphi_1)$ than for $\varphi_1(u)$. In such cases, the free parameter in (16.25) – (16.28) is φ_1.

16.1.5 Pin Gears

The teeth of a pin gear are circular cylinders mounted between two circular discs. Manufacture is inexpensive since no cutting of teeth is necessary. For this reason the larger of the two wheels is made the pin wheel. Pin gears of small size are used in watches and of large size in reducers of cranes and other heavy-duty machinery.

Figure 16.8 shows a case of external gearing. On the larger wheel pins of radius ρ are placed with their centers on the pitch circle p_1. Consider the pin centered at the pitch point P_{12}. Let this position be the position $\varphi_1 = \varphi_2 = 0$ of the wheels. The circular contour of the pin is the given flank f_1. When the pitch circles are rotating with rolling contact at P_{12}, the center

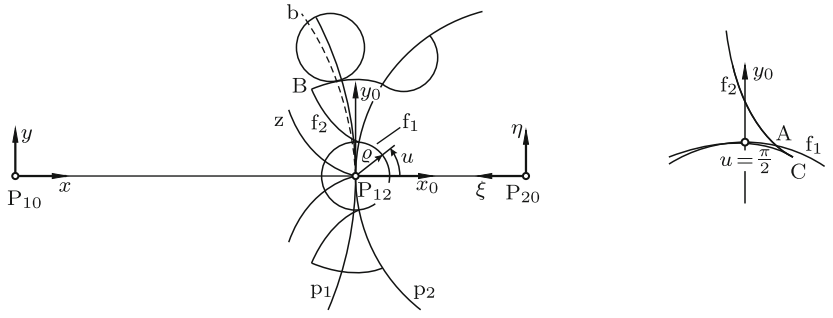

Fig. 16.8 External pin gearing with $r_1 = 2r_2$, $\rho = 0.2r_2$. Circle f_1, conjugate flank f_2, cycloid z traced by the center of the pin, line of contact b

of the pin traces an epicycloid z fixed on p_2. In the same process the circle f_1 fixed on p_1 sweeps over an area of wheel 2 which is enveloped by two curves which are parallel to z at the distance ρ. These parallel curves are the flanks f_2 conjugate to f_1. With the angle u as parameter the equations of the circle f_1 are

$$x(u) = r_1 + \rho\cos u\ , \qquad y(u) = \rho\sin u\ . \tag{16.29}$$

Hence $x'(u) = -\rho\sin u$, $y'(u) = \rho\cos u$. Equation (16.23) has the form

$$\sin(u + \varphi_1) = \sin u\ . \tag{16.30}$$

The solutions are

$$\left.\begin{array}{ll} \varphi_1 = 0\ : & u \text{ arbitrary}\ , \\ \varphi_1 \neq 0\ : & \varphi_1 = \pm\pi - 2u\ . \end{array}\right\} \tag{16.31}$$

The solution in the case $\varphi_1 = 0$ expresses the fact that in the position shown in the figure the normal at every point of the circle passes through P_{12}. The solutions $\varphi_1 = \pm\pi - 2u$ represent identical positions of wheel 1. Therefore, it suffices to consider the solution $\varphi_1 = \pi - 2u$. The position shown in the figure is characterized by $\varphi_1 = 0$, i.e., by $u = \pi/2$. This means that in the position shown flank f_2 is in contact with the pin at this point. Substituting (16.29) and the solution $\varphi_1 = \pi - 2u$ into (16.25) results in the equations for the line of contact:

$$\left.\begin{array}{l} x_{0_B}(u) = -r_1(1 + \cos 2u) - \rho\cos u = -(2r_1\cos u + \rho)\cos u\ , \\ y_{0_B}(u) = \quad r_1\sin 2u\ + \rho\sin u = \quad (2r_1\cos u + \rho)\sin u\ . \end{array}\right\} \tag{16.32}$$

Comparison with (15.13) shows that the line of contact is a limaçon of Pascal. Substitution of (16.29) into (16.26) yields for f_2 the equations

$$\left.\begin{array}{l} \xi(u) = -\rho\cos[u + \varphi_1(u) + \varphi_2(u)]\ - r_1\cos[\varphi_1(u) + \varphi_2(u)]\ + (r_1 + r_2)\cos\varphi_2(u)\ , \\ \eta(u) = \quad \rho\sin[u + \varphi_1(u) + \varphi_2(u)]\ + r_1\sin[\varphi_1(u) + \varphi_2(u)]\ - (r_1 + r_2)\sin\varphi_2(u) \end{array}\right\} \tag{16.33}$$

with

$$\varphi_1(u) = \pi - 2u\ , \qquad \varphi_2(u) = \frac{n_1}{n_2}\,\varphi_1(u)\ , \qquad r_1 = \frac{n_1}{n_2}\,r_2\ . \tag{16.34}$$

Example: In Fig. 16.8 the parameters are $n_1 = 16$, $n_2 = 8$ (implying $r_1 = 2r_2$) and $\rho = 0.2r_2$. Equations (16.32) and (16.33) are

$$\left.\begin{array}{ll} x_{0_B}(u) = -r_2(4\cos u + 0.2)\cos u\ , & \xi(u) = r_2\,(0.2\cos 5u + 2\cos 6u + 3\cos 4u)\ , \\ y_{0_B}(u) = \quad r_2(4\cos u + 0.2)\sin u\ , & \eta(u) = r_2\,(0.2\sin 5u\ + 2\sin 6u + \ 3\sin 4u)\ . \end{array}\right\} \tag{16.35}$$

The line of contact is the dotted line denoted b. The functions $\xi(u)$, $\eta(u)$ without the terms $\cos 5u$ and $\sin 5u$ describe the cycloid z traced by the center of the pin. These lines b and z as well as the flank f_2 display the

symmetry shown in the figure. The following discussion of f_2 is concerned with the branch $\eta > 0$. The small figure shows, enlarged and schematically, the curves f_1 and f_2 in the vicinity of tangential contact at the point $u = \pi/2$. At this point f_2 is passing, with increasing u, from the outside to the inside of f_1. After passing through a cusp C it crosses f_1 at another point A. With the given parameters the cusp C is the point $u \approx 92.4°$, $\xi \approx 0.9792 r_2$, $\eta \approx 0.1986 r_2$, and A is the point $u \approx 93.2°$, $\xi \approx 0.9816 r_2$, $\eta \approx 0.1992 r_2$. This means that A lies at approximately 0.09ρ to the right of the y_0-axis. The tip B of the tooth shown in the large figure is the point of intersection of f_2 with the line $\eta = \frac{\pi}{8}\xi$. It is associated with $u \approx 103.5°$. In conclusion: The arc A–B of f_2 has contact with f_1 in the narrow interval $93.2° < u < 103.5°$ of f_1. To the right of A the tooth flank must be given a form avoiding contact with the pin. The arc A–C of f_2 interferes with the pin. This problem of interference does not occur when the centers of the pins are placed on a circle of radius $< r_1$, for then the cycloid z and the parallel curve f_2 do not have cusps. End of example.

Example: In Fig. 16.9 a case of internal gearing is shown. The outer wheel 1 has $n_1 = 10$ pins, and the inner wheel 2 has $n_2 = 9$ teeth, so that $r_2/r_1 = n_2/n_1 = 9/10$. The centers of the pins of radius ρ are placed on a circle of radius λr_1 with $\lambda > 1$. With the angle u shown in the figure the flank f_1 of the pin having its center on the x-axis is given by the equations

$$x(u) = \lambda r_1 - \rho \cos u \,, \qquad y(u) = -\rho \sin u \,. \tag{16.36}$$

Equation (16.23) is

$$\sin(u + \varphi_1) = \lambda \sin u \,. \tag{16.37}$$

The solution for u as function of φ_1 is

$$u(\varphi_1) = \tan^{-1} \frac{\sin \varphi_1}{\lambda - \cos \varphi_1} \,. \tag{16.38}$$

With this expression Eqs.(16.25) for the line of contact and Eqs.(16.27) for the conjugate flank f_2 are equations with φ_1 as parameter. For the specific numerical example $\lambda = 2$, $\rho = 0.2 r_1$ flank f_2 has the equations

$$\left.\begin{aligned} \xi(\varphi_1) &= \quad r_1 \Big[2\cos \tfrac{1}{9}\varphi_1 - \tfrac{1}{10} \cos \tfrac{10}{9}\varphi_1 - \tfrac{1}{5} \cos\big(\tfrac{1}{9}\varphi_1 - u(\varphi_1)\big) \Big] \,, \\ \eta(\varphi_1) &= -r_1 \Big[2\sin \tfrac{1}{9}\varphi_1 - \tfrac{1}{10} \sin \tfrac{10}{9}\varphi_1 - \tfrac{1}{5} \sin\big(\tfrac{1}{9}\varphi_1 - u(\varphi_1)\big) \Big] \,. \end{aligned}\right\} \tag{16.39}$$

Flank f_2 is the curve parallel to the trajectory traced by the center of the pins. The latter one is the prolate epitrochoid e described by the functions without the terms with factor $\rho = 1/5$. Flank f_2 is generating nine teeth which are meshing with the ten pins on wheel 1. All pins are meshing simultaneously. At every contact point the contact normal is passing through the pitch point

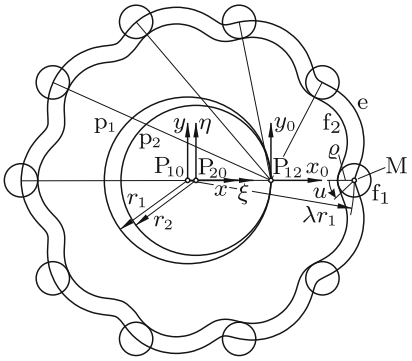

Fig. 16.9 Internal pin gearing with ten pins on the larger wheel 1 and with nine teeth on wheel 2. Epitrochoid e traced by the center of the pin and parallel tooth flank f_2

P_{12}. The line of contact itself is not shown. It is not passing through P_{12}. This means that there is sliding at every contact point in every position of the wheels. End of example.

In Fig. 15.5 the geometrically simplest case of internal pin gearing is illustrated. It is the case with the inner pitch circle being half the size of the outer and with pins located on the inner wheel. The cycloids traced by the centers of the pins are straight lines and so are the parallel curves, i.e., the tooth flanks on the outer wheel. It is easy to show that also in this case the line of contact is a limaçon of Pascal.

16.1.6 External Involute Spur Gears

In well-lubricated gears (no friction force in the common tangent plane) the force transmitted by one tooth on the other has the direction of the contact normal (line $\overline{BP}_{12}$ in Fig. 16.6). When the transmitted torque is constant, both magnitude and direction of this force should also be constant in order to prevent periodic excitations. These conditions are satisfied if and only if the line of contact is a straight line in which case it is also the line of action of the contact force. Another desirable property of gears is the following. Conjugate flanks of two wheels should be geometrically similar in order to be able to use one and the same manufacturing tool for both wheels. In what follows, it is shown that the *involute* of a circle is the curve having these desired properties. This was first shown by Euler [7]. For properties of involutes see Sect. 15.5.4. In Fig. 16.10 the pitch circles of two wheels with centers P_{10} and P_{20} and with pitch point P_{12} are shown again. Through P_{12} a straight line $\overline{A_1A_2}$ is drawn under an arbitrary angle α. This line is tangent to two so-called *base circles* c_1 about P_{10} and c_2 about P_{20}. Their radii are

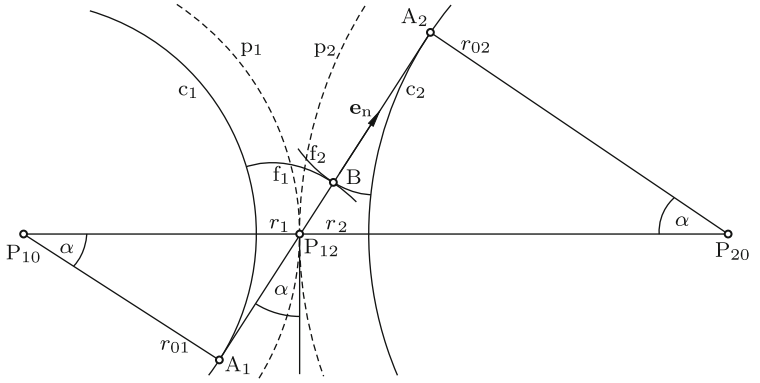

Fig. 16.10 Spur gears with involute tooth flanks

$$r_{0i} = r_i \cos\alpha \qquad (i = 1, 2) \; . \tag{16.40}$$

The ratio is $r_{01}/r_{02} = r_1/r_2$. The base circles c_1 and c_2 are rigidly attached to the respective wheels. Imagine the straight line $\overline{\mathrm{A}_1\mathrm{A}_2}$ to be part of a string which is wound off circle c_1 and rolled up by circle c_2 when the wheels are rotating. Consider a point B fixed on the string in its motion from A_1 to A_2 . Seen from an observer fixed on c_1 the trajectory of B is the involute f_1 , and seen from an observer fixed on c_2 the trajectory of B is the involute f_2 . At B the two involutes are in tangential contact. The common normal is the line $\overline{\mathrm{BP}}_{12}$. This proves the two properties of involute gearing stated in the beginning: Involutes are, indeed, tooth flanks producing a constant gear ratio $\omega_2/\omega_1 = r_1/r_2$. Both flanks are geometrically similar, and the line of contact is a straight line, namely, the line $\overline{\mathrm{A}_1\mathrm{A}_2}$. This frame-fixed line is the line of action of the contact force. In addition, involute tooth flanks have the important property to remain conjugate, i.e., to be meshing correctly, when the distance between the centers of the two base circles is changed. Involute tooth flanks are the only ones having this property[3]. With changing distance the angle α as well as the radii r_1 and r_2 of the pitch circles change in such a way that the ratio r_1/r_2 remains unchanged.

That the two involutes are conjugate tooth flanks is confirmed by (16.17). In the present case, the quantities a and b as well ϱ_1 and ϱ_2 have pairwise opposite signs. With the definitions given in Fig. 16.2 the various quantities are $a = r_1 + r_2$, $b = -r_1$, $\mu = b/(a+b) = -r_1/r_2$, $\mathbf{e}_\mathrm{n} \cdot \mathbf{b} = -r_1 \sin\alpha$, $\varrho_1 - r = r_1 \sin\alpha$, $\varrho_2 - r = -r_2 \sin\alpha$ and $\varrho_2 - \varrho_1 = -(r_1 + r_2)\sin\alpha$. With these quantities (16.17) is, indeed, satisfied.

The angle α is called *angle of pressure*. If for a given angle of pressure the radius r_{01} is made larger and larger, the meshing segment of flank f_1 is curved less and less. In the limit $r_{01} \to \infty$ a rack with straight-line tooth

[3] For proofs see Bricard [2] and Fayet [8]

flanks is obtained. Hence the conclusion: A wheel 2 with involute gearing and a rack 1 with straight line tooth flanks and with equal angle of pressure α satisfy the condition that a constant angular velocity ω_2 of the wheel produces a constant translatory velocity $r_2\omega_2$ of the rack.

Remark: It is unnecessary to prove by means of (16.22) – (16.26) that the flank f_2 conjugate to an involute flank f_1 on the base circle c_1 is an involute on the base circle c_2. As is seen in Fig. 16.10 the definition of the involute implies that the line $\overline{\mathrm{A}_1\mathrm{A}_2}$ is the line of contact. Therefore, the following formulation of (16.22) and (16.25) is done simply as an exercise. Parameter equations of the involute on the base circle c_1 of radius $r_1\cos\alpha$ are copied from (15.137) with $h = 0$ and with u instead of ϕ:

$$\left.\begin{aligned} x(u) &= r_1\cos\alpha(-\sin u + u\cos u)\ , & x'(u) &= -r_1\cos\alpha\ u\sin u\ , \\ y(u) &= r_1\cos\alpha(\cos u + u\sin u)\ , & y'(u) &= \ \ r_1\cos\alpha\ u\cos u\ . \end{aligned}\right\} \tag{16.41}$$

Equation (16.22) has the form

$$u[\cos\alpha + \sin(u+\varphi_1)] = 0 \tag{16.42}$$

or $\sin(u+\varphi_1) = -\cos\alpha = -\sin(\alpha+\pi/2)$. Hence $\varphi_1 = -(u+\alpha+\pi/2)$ and

$$\cos\varphi_1 = -\sin(u+\alpha)\ , \qquad \sin\varphi_1 = -\cos(u+\alpha)\ . \tag{16.43}$$

With these expressions Eqs.(16.25) for the line of contact are

$$\left.\begin{aligned} x_{0_\mathrm{B}}(u) &= -r_1\sin\alpha\,(\sin\alpha + u\cos\alpha)\ , \\ y_{0_\mathrm{B}}(u) &= -r_1\cos\alpha\,(\sin\alpha + u\cos\alpha)\ . \end{aligned}\right\} \tag{16.44}$$

Hence $y_{0_\mathrm{B}}(u) = x_{0_\mathrm{B}}(u)\cot\alpha$. This is, indeed, the equation of the line $\overline{\mathrm{A}_1\mathrm{A}_2}$ in Fig. 16.10. The transformation of Eqs.(16.26) into the standard form of an involute is tedious. End of remark.

For a single wheel the radius r of the pitch circle, the angle of pressure α and the number n of teeth determine the radius $r_0 = r\cos\alpha$ of the base circle and the circular pitch

$$t = \frac{2\pi r}{n}\ . \tag{16.45}$$

Two mating wheels have the same circular pitch t since $r_1/n_1 = r_2/n_2$. Following (16.18) the addendum a and the active height $2a$ of teeth were defined. In the theory of involute gearing these quantities are expressed in terms of the so-called *module* m which is defined by the equation

$$m = \frac{2r}{n} = \frac{t}{\pi}\ . \tag{16.46}$$

Two mating wheels have the same module m. By industrial standard a normal tooth has height m above and depth $(6/5)m$ below the pitch circle.

These two measures are referred to as *addendum* and *dedendum*, respectively. With appropriate tools the involute is cut between the circle with radius $r_\mathrm{i} = r - m$ and the *addendum circle* with radius $r_\mathrm{a} = r + m$. The difference $r_\mathrm{a} - r_\mathrm{i} = 2m$ is the active height of the teeth. The clearance of radial width $m/5$ at the foot of teeth is the room for the fillet which was explained following (16.18). The definition (16.46) is chosen such that the tooth thickness $d(r_\mathrm{a})$ at the tip of the tooth is reasonable for any number n of teeth. Reasonable means not unnecessarily large and always positive. A formula for $d(r_\mathrm{a})$ is given in (16.66).

Figure 16.11 shows the contact line $\overline{\mathrm{A_1A_2}}$ of Fig. 16.10. Tooth contact is confined to the segment $\overline{\mathrm{B_1B_2}}$ inside the addendum circles with radii $r_{\mathrm{a}1}$ and $r_{\mathrm{a}2}$. These radii determine the angles γ_1 and γ_2 and the length ℓ of the segment $\overline{\mathrm{B_1B_2}}$:

$$\ell = r_{01}(\tan\gamma_1 - \tan\alpha) + r_{02}(\tan\gamma_2 - \tan\alpha)\,, \qquad \cos\gamma_i = \frac{r_{0i}}{r_{\mathrm{a}i}} \quad (i = 1, 2)\,. \tag{16.47}$$

Before one pair of teeth goes out of meshing the next pair must be meshing already. On the line of contact the distance between points of meshing of subsequent teeth is $\delta = 2\pi r_{01}/n_1 = 2\pi r_{02}/n_2$ (since involutes are parallel curves the distance δ equals the arc length on the base circle). The ratio $\varepsilon = \ell/\delta$ is called *contact ratio*. It must be larger than 1. The formulas yield the expression

$$\varepsilon = \frac{\ell}{\delta} = \frac{1}{2\pi}\left[n_1(\tan\gamma_1 - \tan\alpha) + n_2(\tan\gamma_2 - \tan\alpha)\right]\,, \quad \cos\gamma_i = \frac{r_{0i}}{r_{\mathrm{a}i}} \quad (i = 1, 2)\,. \tag{16.48}$$

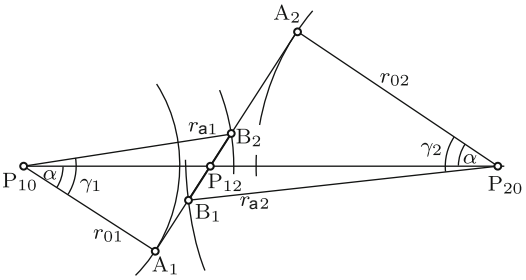

Fig. 16.11 Segment $\overline{\mathrm{B_1B_2}}$ of tooth contact on the line of contact $\overline{\mathrm{A_1A_2}}$

One out of many ways of cutting teeth of the desired shape into a cylindrical blank of radius $r_\mathrm{a} = r + m$ is by means of a *rack cutter*. This is a modified rack which is capable of meshing with the wheel to be cut. Its teeth are cutting blades. The motion of work piece and rack cutter relative to each other

is the intended rolling of the pitch circle p on the pitch line Π of the rack cutter superimposed by a reciprocating translatory motion in the direction normal to the plane of rolling (Fig. 16.12a). In the space of width m above and m below the pitch line Π the tooth of the rack cutter has straight-line flanks under the angle of pressure α. Industrial standard is $\alpha = 20°$. The distance between adjacent teeth on the pitch line equals the circular pitch $t = \pi m$ of the wheel. The straight-line section of the tooth is cutting the involute. The tip of radial extension $m/5$ consists of a straight-line segment parallel to Π and of a circular arc which is cutting the fillet.

Figure 16.12a shows the line of contact passing through the pitch point P_{12} under the angle α and touching the base circle c of the involute at A (compare with Fig. 16.10). The segment $\overline{P_{12}A}$ has length $r \sin\alpha$. Hence the distance of A from the line Π is $r \sin^2\alpha$. In order to avoid undercutting the condition $m \le r \sin^2\alpha$ must be satisfied. In view of (16.46) this is a condition on the number of teeth of the wheel:

$$n > \frac{2}{\sin^2\alpha} \approx 17.1 \qquad (\text{for } \alpha = 20°)\,. \tag{16.49}$$

In practice $n = 17$ is acceptable.

Addendum Modification

In order to allow for numbers of teeth $n < 18$ without undercutting the rack cutter is laterally shifted away from the wheel. In Fig. 16.12b this so-called rack shift or *addendum modification* is denoted e. Note that the pitch line Π is not shifted because it is, by definition, the tangent to the pitch circle. Only the teeth of the rack are shifted. Consequently, the condition $m \le r \sin^2\alpha$ is replaced by $m - e \le r \sin^2\alpha$ or

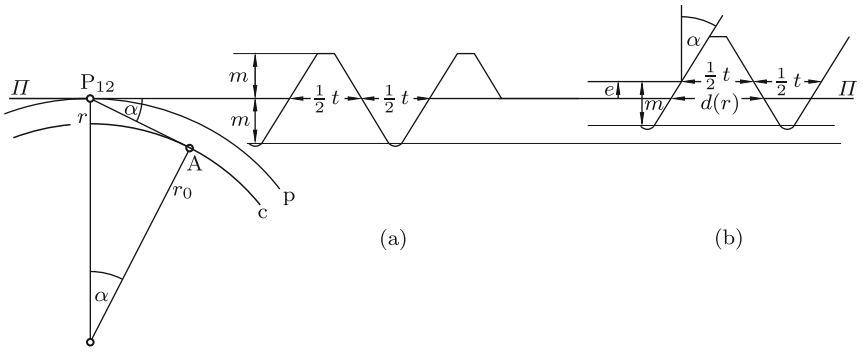

Fig. 16.12 Gear and rack cutter in normal position **(a)** and with addendum modification $e > 0$ **(b)**. Pitch circle p and pitch line Π are the same in both cases

$$m\left(1 - \frac{e}{m}\right) \le r \sin^2\alpha\,. \tag{16.50}$$

With $m = 2r/n$ this is a condition on e/m as function of n:

$$\frac{e}{m} \geq 1 - \frac{n}{2}\sin^2\alpha \,. \tag{16.51}$$

Example: $n = 13$ yields $e/m \geq 0.24$, and $n = 8$ yields $e/m \geq 0.53$. End of example.

In what follows, the effects of addendum modification on the geometry of teeth are investigated. The inner radius of the involute tooth flank is $r_\mathrm{i} = r + e - m$. Definition: The tooth thickness $d(\rho)$ at an arbitrary radius $\rho \geq r_\mathrm{i}$ is the arc length of the circle of radius ρ between the flanks of the tooth (see Fig. 16.13). The thickness $d(r)$ on the pitch circle equals the space width between the tooth flanks of the rack cutter on the line II. Figure 16.12b shows that this is

$$d(r) = \frac{t}{2} + 2e\tan\alpha = r\Big(\frac{\pi}{n} + \frac{4}{n}\,\frac{e}{m}\tan\alpha\Big) \,. \tag{16.52}$$

The factor of r is the angle under which $d(r)$ is seen from the wheel center. The thickness $d(\rho)$ at the radius ρ is seen under an angle which is larger by $2[\mathrm{inv}\,\alpha - \mathrm{inv}\,\psi(\rho)]$ (see Figs. 16.13 and 15.39). The angles in this expression are (see (15.135) and (15.136)):

$$\begin{aligned} &\mathrm{inv}\,\alpha = \tan\alpha - \alpha \,, \qquad \mathrm{inv}\,\psi(\rho) = \tan\psi(\rho) - \psi(\rho) \\ &\text{with} \qquad \cos\psi(\rho) = \frac{r_0}{\rho} = \frac{r}{\rho}\cos\alpha \,. \end{aligned} \tag{16.53}$$

With these angles the thickness $d(\rho)$ is determined by the equation

$$d(\rho) = \rho\left[\frac{\pi}{n} + \frac{4}{n}\,\frac{e}{m}\tan\alpha + 2[\mathrm{inv}\,\alpha - \mathrm{inv}\,\psi(\rho)]\right] \,. \tag{16.54}$$

It is seen that an addendum modification $e > 0$ has the effect of increasing the tooth thickness. The foot of the involute on the base circle is characterized by $\mathrm{inv}\,\psi(\rho) = 0$. Consequently, the angle χ between the cusps of the involute

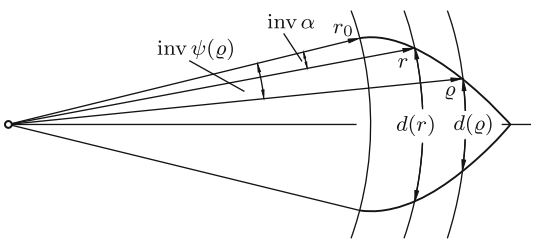

Fig. 16.13 Tooth thickness $d(\rho)$ at radius ρ (arbitrary), thickness $d(r)$ on the pitch circle of radius r and associated angles. See also Fig. 15.39

tooth flanks on the base circle is

$$\chi = \frac{\pi}{n} + 2\left[\left(1 + \frac{2}{n}\,\frac{e}{m}\right)\tan\alpha - \alpha\right] . \tag{16.55}$$

Let ρ_{p} be the radius at which the tooth thickness is zero (the index p stands for *pointed* tooth). Equations (16.53) and (16.54) yield the formulas

$$\operatorname{inv}\psi_{\mathrm{p}} = \frac{\chi}{2} , \qquad \rho_{\mathrm{p}} = r\,\frac{\cos\alpha}{\cos\psi_{\mathrm{p}}} . \tag{16.56}$$

Solving an equation $\operatorname{inv}\psi = c = \text{const}$, i.e., $f = \tan\psi - \psi - c = 0$, for ψ is done by the Newton-Raphson iteration formula $\psi_{i+1} = \psi_i - f(\psi_i)/f'(\psi_i)$. This is the equation

$$\psi_{i+1} = \psi_i - \frac{\tan\psi_i - \psi_i - c}{\tan^2\psi_i} . \tag{16.57}$$

A good starting value is (taken from Townsend [18], Chap.6)

$$\psi_0 = \begin{cases} 1.441c^{1/3} - 0.366c & (c \le 0.5) \\ 0.243\pi + 0.471\tan^{-1} c & (c > 0.5) . \end{cases} \tag{16.58}$$

Example: The given constant is $c = \operatorname{inv} 85^\circ$ which means that the exact solution is $\psi = 85^\circ$. The formulas yield $\psi_0 \approx 83.4^\circ$, $\psi_1 \approx 85.5^\circ$, $\psi_2 \approx 85.05^\circ$, $\psi_3 \approx 85.0005^\circ$. End of example.

In what follows, the meshing of two wheels with addendum modifications e_1 and e_2 is investigated. Without addendum modifications the geometry is as shown in Fig. 16.10 . Because of increased tooth thickness it is necessary to increase the distance $r_1 + r_2$ between the wheel centers in order to avoid interference of teeth. It has already been said that proper meshing of two involute flanks is possible with arbitrary distances. Let D' be the unknown distance. It determines the radii r_1' and r_2' of new pitch circles and a new angle of pressure α' such that

$$r_1' + r_2' = D' , \qquad \frac{r_2'}{r_1'} = \frac{r_2}{r_1} = \frac{n_2}{n_1} , \qquad \cos\alpha' = \frac{r_{01}}{r_1'} = \frac{r_{02}}{r_2'} . \tag{16.59}$$

The distance D' is determined by the condition that on these new pitch circles the tooth thickness $d(r_1')$ on wheel 1 equals the space width $w(r_2')$ between neighboring teeth on wheel 2 (and vice versa). The tooth thickness is given by (16.54) with $\psi(r_1') = \alpha'$:

$$d(r_1') = r_1'\left[\frac{\pi}{n_1} + \frac{4}{n_1}\,\frac{e_1}{m}\tan\alpha + 2(\operatorname{inv}\alpha - \operatorname{inv}\alpha')\right] . \tag{16.60}$$

The space width is

$$w(r_2') = r_2' \left[\frac{\pi}{n_2} - \frac{4}{n_2} \frac{e_2}{m} \tan\alpha - 2(\mathrm{inv}\,\alpha - \mathrm{inv}\,\alpha') \right] . \tag{16.61}$$

The change of signs is explained by the fact that the sum of the angles subtended by tooth thickness and space width equals $2\pi/n_2$. Equating both expressions and making use of the second Eq.(16.59) results in an equation for α':

$$\mathrm{inv}\,\alpha' = \left[1 + \frac{2(e_1+e_2)}{m(n_1+n_2)} \right] \tan\alpha - \alpha . \tag{16.62}$$

With the angle α' thus determined the distance D' is calculated from (16.59):

$$D' = \frac{r_{01}+r_{02}}{\cos\alpha'} = (r_1+r_2)\frac{\cos\alpha}{\cos\alpha'} . \tag{16.63}$$

Next, the radii r_{ai} $(i=1,2)$ of the addendum circles at the tips of teeth are determined. The inner radii of the involute flanks are known to be $r_{ii} = r_i + e_i - m$ $(i=1,2)$. The active height $h = r_{a1} - r_{i1} = r_{a2} - r_{i2}$ of the teeth is the difference

$$\begin{aligned} h &= D' - (r_{i1}+r_{i2}) = D' - [(r_1+e_1-m)+(r_2+e_2-m)] \\ &= 2m - \left[e_1+e_2-(r_1+r_2)\left(\frac{\cos\alpha}{\cos\alpha'} - 1 \right) \right] . \end{aligned} \tag{16.64}$$

Without addendum modification (also in the more general case $e_1+e_2=0$) this formula yields the normal active height $2m$. It can be shown that $h < 2m$ if $e_1+e_2 > 0$. The desired radii of the addendum circles are

$$r_{ai} = r_{ii} + h = r_i + e_i - m + h \qquad (i=1,2) . \tag{16.65}$$

With these radii Eq.(16.48) for the contact ratio remains valid provided α is replaced by α'.

Example: For a pair of wheels the data are given: $n_1 = 8$, $e_1/m = 0.56$; $n_2 = 13$, $e_2/m = 0.24$. To be determined are the angles χ_i and the radii ρ_{pi} $(i=1,2)$ of the teeth, the distance D', the active height h, the radii r_{ai} $(i=1,2)$ and the contact ratio ε. All lengths are to be expressed as multiples of r_1.
Solution: Equations (16.55) – (16.65) and (16.48) yield
$\chi_1 \approx 30.05°$, $\psi_{p1} \approx 47.50°$, $\rho_{p1} \approx 1.391\,r_1$, $\chi_2 \approx 17.22°$, $\psi_{p2} \approx 40.73°$, $\rho_{p2} \approx 2.015\,r_1$, $\alpha' \approx 27.92°$, $D' \approx 2.792\,r_1$, $h \approx 0.467\,r_1$, $r_{a1} \approx 1.357\,r_1$, $r_{a2} \approx 1.902\,r_1$, $\gamma_1 \approx 46.17°$, $\gamma_2 \approx 36.60°$, $\varepsilon \approx 1.09$.
End of example.

In this example, the purpose of addendum modification is to prevent undercutting. The same goal is achieved without addendum modification by

increasing the tooth numbers $n_1 = 8$, $n_2 = 13$ to $n_1 = 24$, $n_2 = 39$. Addendum modification is used not only for the prevention of undercutting. Another purpose is to achieve a desired distance D' of the wheel axes or a desired change of tooth thickness (possibly with addendum modification $e_1 + e_2 < 0$). If, for example, D' is prescribed, (16.63) and (16.62) determine α' and $e_1 + e_2$.

This section is closed with a formula for the tooth thickness $d(r_a)$ at the tip of a tooth in the case of zero addendum modification. With (16.46) the tip radius is $r_a = r + m = r(1 + 2/n)$. Hence with (16.53) and (16.54)

$$d(r_a) = r\left(1 + \frac{2}{n}\right)\left[\frac{\pi}{n} + 2(\operatorname{inv}\alpha - \operatorname{inv}\psi)\right], \qquad \cos\psi = \frac{\cos\alpha}{1 + \frac{2}{n}}. \quad (16.66)$$

With $\alpha = 20°$ this formula yields $d(r_a) \approx 0.076r$ for $n = 18$ and $d(r_a) \approx 0.032r$ for $n = 48$. These very reasonable figures show that the engineering standard addendum is well chosen.

16.1.7 Internal Involute Spur Gears

Figure 16.14 differs from Fig. 16.10 in that the pitch circle p_1 of wheel 1 with radius r_1 is inside wheel 2. The outer wheel has internal gearing, whereas the inner wheel has external gearing as before. As in Fig. 16.10 the common normal $\mathbf{e}_n$ to the involutes f_1 and f_2 at the point of contact B is tangent to the base circles c_1 and c_2. Equation (16.17) is satisfied with $a = r_2 - r_1$, $b = r_1$, $\mu = b/(a+b) = r_1/r_2$, $\mathbf{e}_n \cdot \mathbf{b} = -r_1 \sin\alpha$, $\varrho_2 - \varrho_1 = \overline{A_1 A_2} = (r_2 - r_1)\sin\alpha$, $\varrho_1 - r = r_1 \sin\alpha$ and $\varrho_2 - r = r_2 \sin\alpha$. This suffices as proof for the involutes being conjugate tooth flanks.

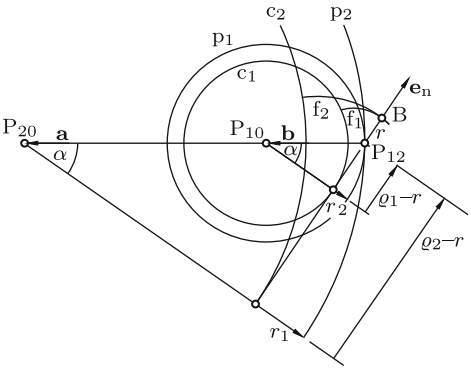

Fig. 16.14 Wheel 2 with internal gearing meshing with wheel 1 with external gearing

In comparison with the pairing of two wheels with external gearing the pairing internal / external gearing has the following advantages:
– the internal teeth have the shape of the free space between external involute teeth. Consequently,
– the teeth are stronger because they are thicker at the base
– since the internal teeth have concave flanks, the Hertzian pressure is smaller
– both shafts have the same sense of rotation; this has the consequence that
– the sliding velocity of tooth flanks relative to each other is proportional not to $|\omega_1| + |\omega_2|$, but to $|\omega_1| - |\omega_2|$
– the design is more compact because it has the size of the outer wheel
– in a given volume more power can be transmitted
– the inner wheel and the contact zone are shielded by the outer wheel.

A disadvantage is that many manufacturing methods available for external gears cannot be used for internal gears.

Problems of undercutting occur when the difference $n_2 - n_1$ of the numbers of teeth is too small. From experience it is known that no undercutting occurs if $n_2 - n_1 > 10$. Differences smaller than 10 are possible with a reduced tooth height of the internal teeth.

Equations (16.62) and (16.63) for the angle of pressure α' and for the distance D' of wheel centers as function of addendum modification is replaced by the equations

$$\operatorname{inv}\alpha' = \left[1 + \frac{2(e_2 - e_1)}{m(n_2 - n_1)}\right] \tan\alpha - \alpha \,, \qquad D' = (r_2 - r_1)\frac{\cos\alpha}{\cos\alpha'} \,. \quad (16.67)$$

The equation for α' results from the condition that the tooth thickness $d(r_1')$ given by (16.60) equals the space width $w(r_2')$ between neighboring teeth on wheel 2 and that the latter is given by (16.60) with the index 1 replaced by 2 .

16.1.8 Involute Helical Gearing

The pitch circles p_1 , p_2 and the base circles c_1 , c_2 (radii r_{01} , r_{02}) shown in Fig. 16.10 and the string $\overline{\mathrm{A}_1\mathrm{A}_2}$ wound around the base circles are the front views (cross sections) of pitch cylinders, of base cylinders c_1 , c_2 and of a belt wound around the base cylinders. Figure 16.15 is a perspective view. In the frame-fixed x, y, z-system the moving planar section E of the belt is defined by the pressure angle α . The following statements repeat what has been said in the context of Fig. 16.10 . Seen from an observer fixed on c_1 the trajectory of a belt-fixed point B is an involute in the plane $z = \text{const}$ in which B is located and seen from an observer fixed on c_2 the trajectory of B is another involute. At B the involutes are in tangential contact the

common tangent being normal to E. With points B located on a belt-fixed straight line parallel to the z-axis two conjugate involute tooth flanks of spur wheels with straight-line teeth are generated. In Fig. 16.15 the belt-fixed points B are located on a belt-fixed straight line e which is making an angle β_0 against lines parallel to the z-axis. The involutes are shown for only two points on this line. The conjugate tooth flanks formed by the manifold of involutes for all points of the line are surfaces h_1 and h_2 called *involute helicoids*. Both helicoids are instantaneously in tangential contact along the generating line e. The common tangent plane intersects E orthogonally. This means that a helicoid is a ruled surface of the special kind called torse (distribution parameter $\delta = 0$ on every generator; see the end of Sec. 2.9.2). In wrapping around the base cylinders the belt-fixed line e is forming on each base cylinder c_i $(i = 1, 2)$ a *base helix* H_i having the slope $\cot \beta_0$. From this it follows that every generator of the helicoid h_i is tangent to H_i. The base helices on the two base cylinders have opposite hands.

The unit vector $\mathbf{n}$ normal to the common tangent plane of h_1 and h_2 is located in E and normal to e. In the x, y, z-system it has the constant coordinates

$$\left.\begin{aligned} n_x &= \sin\alpha \cos\beta_0 \ , \\ n_y &= \cos\alpha \cos\beta_0 \ , \\ n_z &= -\sin\beta_0 \ . \end{aligned}\right\} \tag{16.68}$$

Points fixed on h_1 and h_2 have, in the contact position and in the direction of $\mathbf{n}$, velocities of magnitude

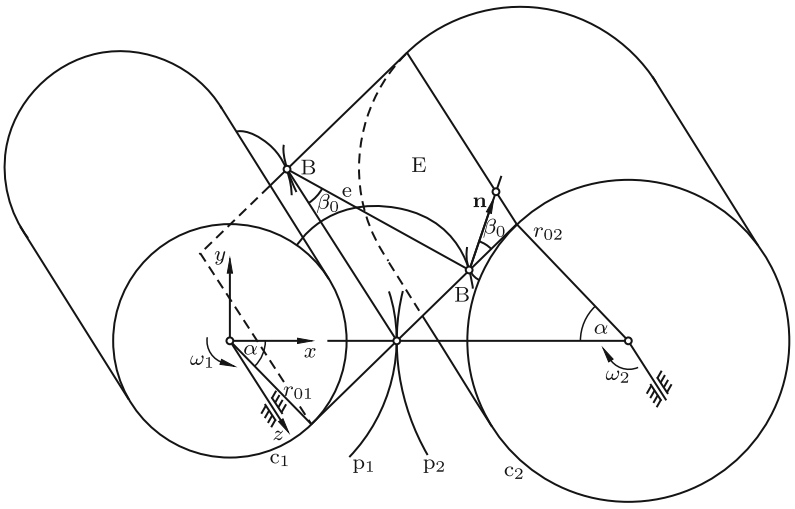

Fig. 16.15 Involutes generated by all points B of line e are forming involute helicoids contacting along the line with common normal $\mathbf{n}$.

$$v_i = \omega_i r_{0i} \cos\beta_0 \qquad (i = 1, 2) \,. \tag{16.69}$$

From the kinematical constraint $v_1 = v_2$ it follows that

$$\frac{\omega_2}{\omega_1} = \frac{n_1}{n_2} = \frac{r_{01}}{r_{02}} \,. \tag{16.70}$$

In the absence of friction the resultant contact force has the frame-fixed direction of $\mathbf{n}$. Let F be the magnitude of this force. Its torque about the axis of wheel i $(i = 1, 2)$ has magnitude $Fr_{0i}\cos\beta_0$. Equilibrium in the state of constant angular velocities requires $M_i - Fr_{0i}\cos\beta_0 = 0$ with M_i being the external torque about the axis of wheel i. Thus, both direction and magnitude of the resultant contact force are constant:

$$\mathbf{F} = \frac{M_i}{r_{0i}\cos\beta_0}\,\mathbf{n} = \text{ const} \qquad (i = 1 \text{ or } 2) \,. \tag{16.71}$$

In axial direction the force has the component $F\sin\beta_0 = (M_1/r_{01})\tan\beta_0$. Each wheel must be supported in a bearing capable of carrying this axial load. The axial component is zero if each wheel is composed of two symmetrical sections, one with left-turning and the other with right-turning helicoids (so-called double helical gearing).

An involute helical gear with base helix angle β_0 can be cut by an ordinary rack cutter used for cutting straight involute teeth. As in Fig. 16.12a the pitch cylinder of the gear is in rolling contact with the pitch plane Π of the rack cutter (in Fig. 16.12a the pitch line Π is the side view of the pitch plane). The only difference is that the teeth t – t of the rack cutter must make an angle β with the z-axis as is shown in Fig. 16.16. This angle β is the helix angle not on the base cylinder, but on the larger pitch cylinder of radius r. The helix on this cylinder has the smaller slope

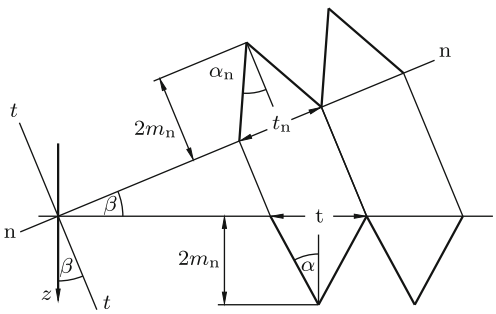

Fig. 16.16 Rack cutter and pitch cylinder positioned for involute helicoidal tooth flanks. Cross sections normal to teeth and normal to the axis of the pitch cylinder

$$\cot\beta = \frac{r_0}{r}\cot\beta_0 = \cos\alpha\cot\beta_0 \ . \tag{16.72}$$

The rack cutter in Fig. 16.12a is specified by the pressure angle $\alpha = 20°$, by the distance t which equals the circular pitch and by the addendum $m = t/\pi$ (the active tooth height is $2m$). In what follows, these quantities are given the new names $\alpha_\mathrm{n} = 20°$, t_n and $m_\mathrm{n} = t_\mathrm{n}/\pi$, respectively. The index n points to the fact that these parameters are measured in the plane n – n normal to the teeth of the rack cutter. In Fig. 16.16 the involute is cut in the plane normal to the gear axis. The tooth height is in both planes the same, i.e., $m_\mathrm{n} = t_\mathrm{n}/\pi$. The circular pitch and the pressure angle are different, however. They are now called t and α. The figure shows that

$$t = \frac{t_\mathrm{n}}{\cos\beta} \ , \qquad \tan\alpha = \frac{\tan\alpha_\mathrm{n}}{\cos\beta} \ . \tag{16.73}$$

Formally, (16.46) yields the associated module

$$m = \frac{t}{\pi} = \frac{m_\mathrm{n}}{\cos\beta} \ . \tag{16.74}$$

This is not the tooth height. The circular pitch t, the numbers n_1, n_2 of teeth and the angle α determine the radii of the pitch cylinders and of the base cylinders:

$$r_i = \frac{t_\mathrm{n} n_i}{2\pi\cos\beta} = \frac{m n_i}{2} \ , \qquad r_{0i} = r_i\cos\alpha \qquad (i = 1, 2) \ . \tag{16.75}$$

From Fig. 16.10 it is known that involute tooth flanks of spur gears have the property to remain conjugate when the distance between the gear axes is changed. It is this property which led to Eqs.(16.50) – (16.65) relating addendum modification to changes of tooth thickness and to changes of distance between gear axes. Involute helical gears with parallel axes, too, remain conjugate when the distance between the gear axes is changed. The reason is that in every cross section $z{=}\,\mathrm{const}$ two involute tooth flanks are meshing. Consequently, Eqs. (16.50) – (16.65) are valid also for helical involute gears if the following rules are observed. Everywhere, t and α are the quantities defined in (16.73). In (16.50), (16.64) and (16.65) the quantity m is the tooth height m_n. In contrast, in (16.52) m is introduced via (16.74). It is, therefore, the quantity defined by this equation. This is true also for (16.54), (16.55), (16.60) and (16.61) which are derived from (16.52).

Example: In condition (16.50) for non-undercutting,

$$m\left(1 - \frac{e}{m}\right) \le r\sin^2\alpha \ , \tag{16.76}$$

m is the tooth height m_n, and r and α are the quantities given in (16.75) and (16.73), respectively. Hence the condition is

$$\frac{e}{m_\mathrm{n}} \geq 1 - \frac{n}{2}\frac{\sin^2\alpha}{\cos\beta} = 1 - \frac{n}{2}\frac{\tan^2\alpha_\mathrm{n}}{\cos\beta(\cos^2\beta + \tan^2\alpha_\mathrm{n})} \tag{16.77}$$

and in the case $e = 0$ (zero addendum modification)

$$n \geq \frac{2\cos\beta(\cos^2\beta + \tan^2\alpha_\mathrm{n})}{\tan^2\alpha_\mathrm{n}} \,. \tag{16.78}$$

In Table 16.1 this dependency on β is shown for helical gears produced by a standard rack cutter with $\alpha_\mathrm{n} = 20°$. The table shows that an increase of β

Table 16.1 Condition (16.78) for helical gears produced by a rack cutter with $\alpha_\mathrm{n} = 20°$

β	0°	10°	20°	30°	40°	45°
$n \geq$	18	17	15	12	9	7

is an effective means against undercutting. This is one of many advantages of involute helical gears as compared with involute spur gears. Another advantage is that the contact ratio can be made $\gg 1$ by increasing β. Another advantage is that gears with helical teeth develop less noise because the inset of meshing is gradual rather than abrupt along the entire length of teeth. End of example.

Up to now the case of external helical gearing has been considered. However, two gears with equal base helix angles β_0 are meshing correctly also in the case, when the larger wheel has internal gearing. As in the case of internal straight involute teeth, the problem of undercutting requires special investigations. And so does the problem of assembly in the case when the difference $n_1 - n_2$ is small.

Involute Helicoid Analytically
Let $x_0(\phi)$ and $y_0(\phi)$ be the coordinates of a curve with the free parameter ϕ in the plane $z = 0$ of an x, y, z-system. A surface called helicoid is generated by subjecting this curve to a continuous screw displacement with axis z, angle of rotation ψ and pitch p. The helicoid has the coordinates

$$\left.\begin{aligned} x(\phi,\psi) &= x_0(\phi)\cos\psi - y_0(\phi)\sin\psi \,, \\ y(\phi,\psi) &= x_0(\phi)\sin\psi + y_0(\phi)\cos\psi \,, \\ z(\psi) \quad &= p\psi \,. \end{aligned}\right\} \tag{16.79}$$

The helicoid is an involute helicoid on the base cylinder of radius r_0 and with a base helix of slope $\cot\beta_0$ if the generating curve is the involute on the base circle of radius r_0 and if the pitch is $p = r_0\cot\beta_0$. The coordinates

of the involute are copied from (15.137) with $h = 0$:

$$x_0(\phi) = r_0(-\sin\phi + \phi\cos\phi)\ , \qquad y_0(\phi) = r_0(\ \cos\phi + \phi\sin\phi)\ . \tag{16.80}$$

Substitution into (16.79) yields for the involute helicoid the parameter equations

$$\left.\begin{aligned} x(\phi,\psi) &= r_0[-\sin(\phi+\psi) + \phi\cos(\phi+\psi)]\ , \\ y(\phi,\psi) &= r_0[\ \ \cos(\phi+\psi) + \phi\sin(\phi+\psi)]\ , \\ z(\psi) \ \ &= r_0\psi\cot\beta_0 \end{aligned}\right\} \tag{16.81}$$

or, in terms of the parameters ϕ and $\alpha = \phi + \psi$ instead of ϕ and ψ,

$$\left.\begin{aligned} x(\phi,\alpha) &= r_0(-\sin\alpha + \phi\cos\alpha)\ , \\ y(\phi,\alpha) &= r_0(\ \ \cos\alpha + \phi\sin\alpha)\ , \\ z(\phi,\alpha) &= r_0(\alpha-\phi)\cot\beta_0\ . \end{aligned}\right\} \tag{16.82}$$

The line $\psi = \text{const}$ (arbitrary) is the involute rotated through ψ in the plane $z = r_0\psi\cot\beta_0$. The line $\phi = \text{const}$ (arbitrary) is a helix on the cylinder of radius $\sqrt{x^2+y^2} = r_0\sqrt{1+\phi^2}$. The line $\phi = 0$, in particular, is the base helix with coordinates $x(\psi) = -r_0\sin\psi$, $y(\psi) = r_0\cos\psi$, $z(\psi) = r_0\psi\cot\beta_0$. Lines $\alpha = \text{const}$ are straight lines because each of the three coordinates is a linear function of ϕ with constant coefficients. These lines are swept through by the line e of Fig. 16.15. In Fig. 16.17 the involute helicoid is shown. Figure 15.39 explains why it consists of two surfaces emerging from the base helix on the base cylinder. On each surface lines α=const tangent to the base helix are shown. The surfaces extend to infinity. In the figure they are truncated by lines ϕ=const. The unit vector $\mathbf{n}$ normal to the helicoid is

$$\mathbf{n} = \frac{\dfrac{\partial\boldsymbol{\rho}}{\partial\phi}\times\dfrac{\partial\boldsymbol{\rho}}{\partial\alpha}}{\left|\dfrac{\partial\boldsymbol{\rho}}{\partial\phi}\times\dfrac{\partial\boldsymbol{\rho}}{\partial\alpha}\right|}\ . \tag{16.83}$$

With (16.82) this formula yields the coordinates

$$\left.\begin{aligned} n_x &= \cos\alpha\cos\beta_0\ , \\ n_y &= \sin\alpha\cos\beta_0\ , \\ n_z &= \sin\beta_0\ . \end{aligned}\right\} \tag{16.84}$$

The vector is constant on every line $\alpha = \text{const}$. The coordinates are identical with those in (16.68) if α is replaced by $\pi/2 - \alpha$ and β_0 by $-\beta_0$.

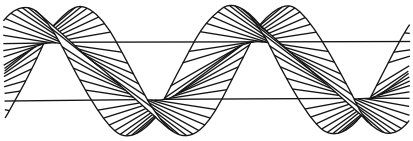

Fig. 16.17 Base helix and involute helicoid on base cylinder

16.2 Skew Axes

In Sect. 12.2 the relative motion of two wheels rotating with constant angular velocity ratio $\mu = \omega_2/\omega_1 = \text{const}$ about skew axes was shown to be a velocity screw. Its axis has the direction of the relative angular velocity $\boldsymbol{\omega}_2 - \boldsymbol{\omega}_1$ (Eq.(12.13)). The axis intersects orthogonally the common perpendicular of the two wheel axes at a point determined by $u(\mu)$. This scalar as well as the pitch $p(\mu)$ of the screw are given in (12.18). Seen by an observer fixed on wheel i $(i = 1, 2)$ the screw axis is sweeping out an hyperboloid of revolution with a gorge circle of radius r_i given in (12.20). Both hyperboloids have one and the same imaginary semi-axis b given in (12.21). The hyperboloids are in raccording motion sharing the frame-fixed screw axis, the striction point on the common perpendicular of the wheel axes and also the distribution parameter which is identical with b. The example given in Sect. 12.6.1 revealed the following reciprocity relationship which is now stated as

Theorem 16.3. *A constant gear ratio ω_2/ω_1 requires tooth flanks to be shaped such that wherever tangential contact of tooth flanks is established the common normal at the point of contact belongs to the linear complex having the axis and the pitch of the relative velocity screw.*

This theorem is the spatial generalization of Theorem 16.1 for plane motions of spur gears. In Sect. 16.1.4 Reuleaux's construction of conjugate tooth flanks for spur gears was explained (see Fig. 16.6). The spatial generalization of this method is explained in the next section. For simplifying the comparison of both methods the same notation for points, lines and angles is used.

16.2.1 Construction of Conjugate Flanks

In Fig. 16.18 P_{10} and P_{20} are the endpoints of the common perpendicular of the axes of the raccording hyperboloids 1 and 2. At P_{12} the axis of the relative velocity screw is shown normal to the plane of the drawing (unit vector $\mathbf{n}$). The axes of the hyperboloids (unit vectors $\mathbf{n}_1$ and $\mathbf{n}_2$) are tilted against $\mathbf{n}$ through the angles α_1 and α_2, respectively, defined in Fig. 12.4 and in (12.16). The absolute values of the vectors $\mathbf{r}_1$ and $\mathbf{r}_2$ are the radii of the gorge circles of the hyperboloids. Let flank f_1 on wheel 1 be some

arbitrarily prescribed smooth surface subject only to the condition that the normal to f_1 at B_1 (arbitrary) intersects the hyperboloid 1. Let N_1 be this wheel-fixed point of intersection. In Fig. 16.18 f_1 is shown when wheels 1 and 2 are in some arbitrarily chosen *initial position*. To each pair (point B_1, normal $\overline{B_1N_1}$) a conjugate pair (point B_2, normal $\overline{B_2N_2}$) of flank f_2 in the initial position of f_2 is constructed as follows. Conjugate means that (B_1, $\overline{B_1N_1}$) and (B_2, $\overline{B_2N_2}$) are the points and normals which coincide in the course of meshing at a certain point B. This point B is determined by Theorem 16.3. In contrast to the planar case in Fig. 16.6, it cannot be constructed graphically. Analytically it is determined as follows. From (2.25) it is known that a line with Plücker vectors $(\mathbf{v}_1, \mathbf{w}_1)$ belongs to a linear complex $(\mathbf{a}; \mathbf{b})$ if

$$\mathbf{a} \cdot \mathbf{w}_1 + \mathbf{b} \cdot \mathbf{v}_1 = 0 \,. \tag{16.85}$$

The vectors are represented in the x, y, z-system shown in Fig. 12.4 which has the origin at P_{12}, the x-axis along $\mathbf{r}_1$ and the z-axis along the axis of the relative velocity screw. In this reference frame the vectors of the linear complex are $\mathbf{a} = \mathbf{n}$ and $\mathbf{b} = p\,\mathbf{n}$ (see the text following (2.29)). The displacement from B_1 to B is a rotation through an unknown angle φ_1 about $\mathbf{n}_1$. Let $\mathbf{z}_1(0)$ be the given position vector of B_1 and $\mathbf{z}_1(\varphi_1)$ the position vector of B. With the rotation tensor $\mathsf{R}(\mathbf{n}_1, \varphi_1)$ defined in (1.40)

$$\mathbf{z}_1(\varphi_1) = \mathbf{r}_1 + \mathsf{R}(\mathbf{n}_1, \varphi_1) \cdot (\mathbf{z}_1(0) - \mathbf{r}_1) \,. \tag{16.86}$$

Let $\mathbf{v}_1(0)$ be the given unit vector along the normal $\overline{B_1N_1}$. By the same rotation this vector is carried into the position

$$\mathbf{v}_1(\varphi_1) = \mathsf{R}(\mathbf{n}_1, \varphi_1) \cdot \mathbf{v}_1(0) \,. \tag{16.87}$$

This is the first Plücker vector of the normal to the tooth flanks at point B. The second Plücker vector is $\mathbf{w}_1(\varphi_1) = \mathbf{z}_1(\varphi_1) \times \mathbf{v}_1(\varphi_1)$. Since the vectors $(\mathbf{z}_1(\varphi_1) - \mathbf{r}_1)$ and $\mathbf{v}_1(\varphi_1)$ and, consequently, also their vector cross product are fixed on wheel 1, this is

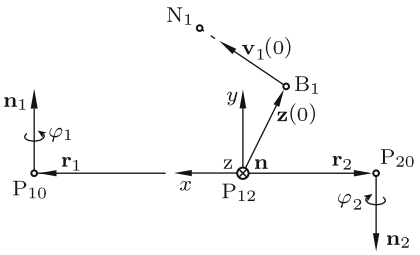

Fig. 16.18 Construction of flank f_2 conjugate to a given flank f_1

$$\mathbf{w}_1(\varphi_1) = \mathbf{r}_1 \times \mathsf{R}(\mathbf{n}_1, \varphi_1) \cdot \mathbf{v}_1(0) + \mathsf{R}(\mathbf{n}_1, \varphi_1) \cdot (\mathbf{z}_1(0) - \mathbf{r}_1) \times \mathbf{v}_1(0) \,. \quad (16.88)$$

The vectors $\mathbf{v}_1(\varphi_1)$, $\mathbf{w}_1(\varphi_1)$, $\mathbf{a} = \mathbf{n}$ and $\mathbf{b} = p\,\mathbf{n}$ are substituted into (16.85). The equation is then decomposed in the x, y, z-system. The vectors $\mathbf{r}_1$ and $\mathbf{n}$ have the coordinate matrices $[\,r_1\ 0\ 0\,]^T$ and $[\,0\ 0\ 1\,]^T$, respectively. The tensor $\mathsf{R}(\mathbf{n}_1, \varphi_1)$ has the coordinate matrix $\underline{A}^{12}$ given in (1.54) with $\sin\alpha_1$ and $\cos\alpha_1$ from (12.16). The resulting equation for the unknown angle φ_1 has the form $A\cos\varphi_1 + B\sin\varphi_1 = C$ with coefficients A, B, C satisfying the condition $A^2 + B^2 - C^2 > 0$ for the existence of real solutions. For comparison: The equivalent Eq.(16.23) for the planar case has the same form. With the pertinent solution φ_1 the position vector $\mathbf{z}_2(0)$ of B_2 and the unit normal vector $\mathbf{v}_2(0)$ at B_2 are determined by subjecting $\mathbf{z}_1(\varphi_1)$ and $\mathbf{v}_1(\varphi_1)$ to the rotation $\varphi_2 = -(n_1/n_2)\varphi_1$ about $\mathbf{n}_2$. This is done by Eqs.(16.86) and (16.87) with indices changed accordingly.

16.2.2 General Spatial Involute Gearing

Let h_1 and h_2 be two involute helicoids on skew axes. Each helicoid h_i $(i = 1, 2)$ has its own base cylinder c_i of radius r_{0i}, its own base helix angle β_{0i} and its own angle α_i which determines the radius $r_i = r_{0i}/\cos\alpha_i$ of the pitch cylinder p_i (see Fig. 16.15). The pitch cylinder is rolling on the pitch plane of the rack cutter used for producing the helicoid. Let h_1 be the helicoid on gear 1 in Fig. 16.15. The axis of h_2 intersects the x-axis orthogonally at a point $x = d \geq r_1 + r_2$. The projected angle between the two axes is called λ (rotation about the x-axis in the positive mathematical sense). Thus, the x-axis is the common perpendicular of the axes, and d is the minimal distance. The situation shown in Fig. 16.15 is the special case $\beta_{01} = \beta_{02} = \beta_0$, $\alpha_1 = \alpha_2 = \alpha$, $d = r_1 + r_2$, $\lambda = 0$.

Following Giovannozzi [9, 10] and without reference to Theorem 16.3 it is shown that under certain conditions h_1 and h_2 are conjugate tooth flanks. In particular, it is shown that the distance d has no influence on any of the angular relationships which follow. The reason is that involute helicoids are torses. On every generator the tangent plane is the same for all points of this generator.

Let P be a point of contact. For each of the two helicoids h_i $(i = 1, 2)$ the statements made in the context of Fig. 16.15 are valid, namely: The contact point P is located on a generator e_i of h_i in a plane E_i which is tangent to the base cylinder c_i and defined by the angle α_i. The generator e_i is making the base helix angle β_{0i} with lines parallel to the axis of c_i. The contact normal at P lies in E_1 as well as in E_2 and it is normal to e_1 as well as to e_2. From the skewness of the axes it follows that h_1 and h_2 have single-point contact and that the frame-fixed line of intersection of E_1 and

E_2, referred to as g, is the common contact normal. According to (16.69) the point fixed on h_i which is coinciding with P has, in the direction of g, a velocity component of magnitude $v_i = \omega_i r_{0i} \cos\beta_{0i}$ $(i = 1, 2)$. From the kinematical constraint $v_1 = v_2$ it follows that

$$\frac{\omega_2}{\omega_1} = \frac{n_1}{n_2} = \frac{r_{01}\cos\beta_{01}}{r_{02}\cos\beta_{02}} \,. \tag{16.89}$$

When the helicoids rotating with this angular velocity ratio remain in contact, the contact point P moves along g. Hence the frame-fixed line g is the line of contact. Being normal to h_1 and to h_2 it is the line of action of the normal contact force which, therefore, is frame-fixed, too. Another consequence of (16.89) is that, depending on β_{01} and β_{02}, the wheel having the smaller number of teeth may have the larger radius.

Tangential contact requires that at the point of contact the unit normal vectors $\mathbf{n}_1$ of h_1 and $\mathbf{n}_2$ of h_2 satisfy the equation $\mathbf{n}_2 = -\mathbf{n}_1$. The x, y, z-coordinates of $\mathbf{n}_1$ are known from (16.68):

$$\left.\begin{aligned} n_{1x} &= \sin\alpha_1 \cos\beta_{01} \,, \\ n_{1y} &= \cos\alpha_1 \cos\beta_{01} \,, \\ n_{1z} &= -\sin\beta_{01} \,. \end{aligned}\right\} \tag{16.90}$$

The vector $\mathbf{n}_2$ has, prior to the rotation through λ, coordinates

$$\left.\begin{aligned} &-\sin\alpha_2 \cos\beta_{02} \,, \\ &-\cos\alpha_2 \cos\beta_{02} \,, \\ &\sin\beta_{02} \,. \end{aligned}\right\} \tag{16.91}$$

Following this rotation it has the coordinates

$$\left.\begin{aligned} n_{2x} &= -\sin\alpha_2 \cos\beta_{02} \,, \\ n_{2y} &= -\cos\alpha_2 \cos\beta_{02} \cos\lambda - \sin\beta_{02} \sin\lambda \,, \\ n_{2z} &= -\cos\alpha_2 \cos\beta_{02} \sin\lambda + \sin\beta_{02} \cos\lambda \,. \end{aligned}\right\} \tag{16.92}$$

The contact condition $\mathbf{n}_2 = -\mathbf{n}_1$ is the set of equations

$$\left.\begin{aligned} \sin\alpha_2 \cos\beta_{02} &= \sin\alpha_1 \cos\beta_{01} \,, \\ \cos\alpha_2 \cos\beta_{02} \cos\lambda + \sin\beta_{02} \sin\lambda &= \cos\alpha_1 \cos\beta_{01} \,, \\ \cos\alpha_2 \cos\beta_{02} \sin\lambda - \sin\beta_{02} \cos\lambda &= -\sin\beta_{01} \,. \end{aligned}\right\} \tag{16.93}$$

These equations are solved by

$$\cos\alpha_1 = \frac{\sin\beta_{02} - \sin\beta_{01}\cos\lambda}{\cos\beta_{01}\sin\lambda} \,, \quad \cos\alpha_2 = -\frac{\sin\beta_{01} - \sin\beta_{02}\cos\lambda}{\cos\beta_{02}\sin\lambda} \,. \tag{16.94}$$

The helices on the pitch cylinders have the slopes (see (16.72))

$$\left.\begin{aligned}\cot\beta_1 &= \cos\alpha_1 \cot\beta_{01} = \frac{1}{\sin\lambda}\left(\frac{\sin\beta_{02}}{\sin\beta_{01}} - \cos\lambda\right) ,\\ \cot\beta_2 &= \cos\alpha_2 \cot\beta_{02} = \frac{-1}{\sin\lambda}\left(\frac{\sin\beta_{01}}{\sin\beta_{02}} - \cos\lambda\right) .\end{aligned}\right\} \tag{16.95}$$

From these equations it follows that

$$\cot(\beta_2 - \beta_1) = \frac{1 + \cot\beta_1 \cot\beta_2}{\cot\beta_1 - \cot\beta_2} = \cot\lambda . \tag{16.96}$$

Hence

$$\beta_2 - \beta_1 = \lambda \tag{16.97}$$

(the second solution $\beta_2 - \beta_1 = \lambda + \pi$ must be dismissed because it is not valid in the case $\beta_2 = \beta_1$, $\lambda = 0$). Equations (16.95) also yield

$$1 + \cot^2\beta_i = \frac{1}{\sin^2\beta_{0i}} \frac{\sin^2\beta_{01} + \sin^2\beta_{02} - 2\sin\beta_{01}\sin\beta_{02}\cos\lambda}{\sin^2\lambda} \tag{16.98}$$

$(i = 1, 2)$. This in combination with $r_i = r_{0i}/\cos\alpha_i$ and with (16.89) proves that

$$\begin{aligned}\frac{r_1\cos\beta_1}{r_2\cos\beta_2} &= \frac{r_1\cot\beta_1}{r_2\cot\beta_2}\sqrt{\frac{1+\cot^2\beta_2}{1+\cot^2\beta_1}}\\ &= \frac{r_{01}\cos\beta_{01}}{r_{02}\cos\beta_{02}} = \frac{\omega_2}{\omega_1} .\end{aligned} \tag{16.99}$$

The equations up to this point were first formulated by Giovannozzi [9].

In (16.94) the substitutions are made:

$$\left.\begin{aligned}\sin\beta_{0i} &= \frac{1}{\sqrt{1+\cot^2\beta_{0i}}} = \frac{1}{\sqrt{1+\cot^2\beta_i/\cos^2\alpha_i}} ,\\ \cos\beta_{0i} &= \frac{\cot\beta_{0i}}{\sqrt{1+\cot^2\beta_{0i}}} = \frac{\cot\beta_i/\cos\alpha_i}{\sqrt{1+\cot^2\beta_i/\cos^2\alpha_i}}\end{aligned}\right\} \quad (i = 1, 2) . \tag{16.100}$$

Following this substitution the equations are squared. This results in

$$\left.\begin{aligned}&\cos^2\alpha_1(\cos^2\alpha_2 + \cot^2\beta_2)(\cos\lambda + \sin\lambda\cot\beta_1)^2\\ &= \cos^2\alpha_2(\cos^2\alpha_1 + \cot^2\beta_1) ,\\ &\cos^2\alpha_2(\cos^2\alpha_1 + \cot^2\beta_1)(\cos\lambda - \sin\lambda\cot\beta_2)^2\\ &= \cos^2\alpha_1(\cos^2\alpha_2 + \cot^2\beta_2) .\end{aligned}\right\} \tag{16.101}$$

When λ is replaced by $\beta_2 - \beta_1$, both equations become

$$(\tan\alpha_2\cos\beta_2)^2 = (\tan\alpha_1\cos\beta_1)^2 \tag{16.102}$$

or, with (16.73),

$$\tan^2 \alpha_{n_2} = \tan^2 \alpha_{n_1} \ . \tag{16.103}$$

This equation shows that both gears must be cut by rack cutters with identical normal pressure angles α_n. This condition and (16.97) together constitute necessary and sufficient conditions for the two helicoids to be conjugate tooth flanks. If the crossing angle λ of the gear axes is prescribed, β_1 and β_2 may be chosen positive, zero or negative subject only to (16.97). In the case $\beta_i = 0$, gear i is a spur gear. The angles β_1, β_2 and α_n determine the angles α_1 and α_2. Equations (16.89) – (16.103) are the rules governing general spatial involute gearing (title of Phillips' book [14]). The equations are independent of the shortest distance d of the wheel axes. So is the direction of the line of contact g. Only the location of g in the x, y, z-system depends on d. The line is laterally displaced when d is changed (all other parameters held constant). In general, g does not intersect the x-axis. The helicoids remain conjugate when the shortest distance d is changed. This requires, of course, a change of tooth thickness.

In engineering the special case $d = r_1 + r_2$ is standard for gears with zero addendum modification. In this case, the pitch cylinders are in (sliding) contact on the x-axis at the point $x = r_1$. In what follows, this point is called P_0. The line g is passing through this point. Figure 16.19 shows in projection along the x-axis the angular velocities $\boldsymbol{\omega}_1$ and $\boldsymbol{\omega}_2$ of the pitch cylinders under the angle λ. The point P_0 is in the plane of the drawing. The cylinder c_1 is below and the cylinder c_2 is above this plane. The line t – t stands for the coinciding teeth of two imaginary rack cutters, one in mesh with gear 1 and the other in mesh with gear 2. The figure is a generalization of Fig. 16.16 which shows the special case $\lambda = 0$. As in this figure the line t – t is making the angle β_i with the axis of gear i $(i = 1, 2)$. At P_0 the pitch cylinders and the pitch planes of the associated rack cutters have the velocities $\mathbf{v}_i$ of magnitude $r_i\omega_i$ $(i = 1, 2)$ in the directions shown. The relative velocity $\mathbf{v}_2 - \mathbf{v}_1$ has the direction t – t of the teeth if β_1 and β_2 are

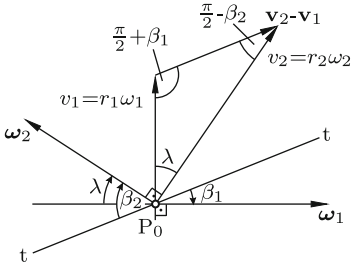

Fig. 16.19 Coinciding rack cutters with teeth t – t under helix angles β_1 and β_2 against the axes of pitch cylinders c_1 and c_2. Velocity triangle of pitch cylinders and rack cutters

satisfying (16.97). Indeed, the sine law applied to the velocity triangle with the angles λ, $\pi/2+\beta_1$ and $\pi/2-\beta_2$ states that $r_2\omega_2/\cos\beta_1 = r_1\omega_1/\cos\beta_2$. This is Eq.(16.99). By the figure it is confirmed that the initially coinciding teeth of both rack cutters are permanently coinciding and that the two gears are permanently meshing. For the sliding velocity $\mathbf{v}_2 - \mathbf{v}_1$ the cosine law yields the formula

$$|\mathbf{v}_2 - \mathbf{v}_1| = \omega_1 r_1 \sqrt{1 + \left(\frac{\omega_2 r_2}{\omega_1 r_1}\right)^2 - 2\,\frac{\omega_2 r_2}{\omega_1 r_1}\cos\lambda}\,. \tag{16.104}$$

From (16.97) it follows that $\cos\beta_1 = \cos\beta_2\cos\lambda + \sin\beta_2\sin\lambda$. Substitution into (16.99) yields for β_1 and β_2 the formulas

$$\tan\beta_2 = \frac{\frac{\omega_2}{\omega_1}\,\frac{r_2}{r_1} - \cos\lambda}{\sin\lambda}\,, \qquad \beta_1 = \beta_2 - \lambda\,. \tag{16.105}$$

The three quantities λ, ω_2/ω_1 and r_2/r_1 are free design parameters. If, for example, λ and ω_2/ω_1 are prescribed, the third parameter r_2/r_1 can be chosen such that the sliding velocity in (16.104) is below an acceptable level.

Gear i $(i = 1, 2)$ has an addendum cylinder of radius $r_{ai} = r_i + m_n$. The contact line g passing through P_0 intersects the cylinder 1 at a point P_1 and the cylinder 2 at a point P_2. The gears must have axial lengths ℓ_1 and ℓ_2 and positions on their shafts such that in the course of meshing of two tooth flanks the contact point can move all the way from P_1 to P_2. Lengths larger than ℓ_1 and ℓ_2 are unnecessary.

In (16.48) the contact ratio was given for spur gears with involute teeth. It is left to the reader to show that in the case of skew axes the contact ratio is

$$\varepsilon = \frac{1}{2\pi}\left[n_1\frac{\tan\gamma_1 - \tan\alpha_1/\cos\beta_1}{\cos^2\beta_1} + n_2\frac{\tan\gamma_2 - \tan\alpha_2/\cos\beta_2}{\cos^2\beta_2}\right]$$
$$\text{with} \quad \cos\gamma_i = \frac{r_{0i}}{r_{ai}} \quad (i = 1, 2)\,. \tag{16.106}$$

References

1. Bonfiglioli Riduttori S.p.A. (Eds.) (1995) Gear Motor Handbook. Springer, Berlin Heidelberg New York
2. Bricard R (1926/27) Leçons de cinématique. v.I.: Cinématique théorique. v.II: Cinématique appliquée. Gauthier-Villars, Paris
3. Disteli M (1908) Über einige Sätze der kinematischen Geometrie, welche der Verzahnungslehre zylindrischer und konischer Räder zugrunde liegen. Z.Math.Phys. 56:233–257
4. Disteli M (1911) Über die Verzahnung der Hyperboloidräder mit geradlinigem Eingriff. Z.Math.Phys. 59:244–298

5. Dudley D W (1962) Gear Handbook. The design, manufacture and application of gears. McGraw-Hill, New York
6. Dudley D W (1984) Handbook of practical gear design. McGraw-Hill, New York
7. Euler L (1767) Supplementum de figura dentium rotarum. Novi Commentarii Acad.Sci.Imper.Petropolitanae, v.II, St.Petersburg
8. Fayet M (2002) On the reverse of one property of involute gears. ASME J. Mech. Des. 124:330–333
9. Giovannozzi R (1947) Intorno alla trasmissione del moto fra assi sghembi mediante ruote elicoidale. Lincei - Rend. Sc. fis. mat. e nat. II:586–595
10. Giovannozzi R (1980) Costruzioni di Macchine, v.II, 5th ed., Patron Bologna
11. Klein F, Müller C (eds.) (1901-1908) Enzyklopädie der Math. Wissenschaften. v.IV: Mechanik. Teubner, Leipzig
12. Litvin F L (1994) Gear geometry and applied theory. Prentice Hall, Englewood Cliffs, New Jersey
13. Matschoss C (1940) Geschichte des Zahnrades. Appendix: Kutzbach K.: Nebst Bemerkungen zur Entwicklung der Verzahnung. VDI-Verlag Berlin
14. Phillips J (2003) General spatial involute gearing. Springer, Berlin, Heidelberg, New York
15. Roth K (2001) Zahnradtechnik. Stirnrad-Evolventenverzahnungen. Geometrische Grundlagen, Profilverschiebungen, Toleranzen, Festigkeit. 2nd ed. Springer Berlin, Heidelberg, New York
16. Roth K (1998) Zahnradtechnik. Evolventenverzahnungen zur Getriebeverbesserung. Evoloid-, Komplement-, Keilschräg-, konische-, Konus-, Kronenrad-, Torus-, Wälzkolbenverzahnungen, Zahnrad-Erzeugungsverfahren. Springer Berlin, Heidelberg
17. Schoenflies A, Grübler M (1908) Kinematik. In: [11]:190–278
18. Townsend D P (Ed.) (1992) Dudley's Gear Handbook. McGraw-Hill, New York

Chapter 17
Planar Four-Bar Mechanism

The solid lines in Fig. 17.1 are the links of a planar four-bar mechanism or briefly planar four-bar. The link lengths ℓ (base or fixed link), r_1 (input link), r_2 (output link) and a (coupler) are free parameters. They determine, whether individual links can rotate relative to others full cycle (i.e., unlimited) or through an angle smaller than 2π. The link lengths also determine the so-called transfer function relating the output angle ψ to the input angle φ. The time derivative of this function yields the *transmission ratio* $i = \dot{\varphi}/\dot{\psi}$ as function of φ. The transfer function and the transmission ratio depend on three parameters only, namely, on r_1/ℓ, r_2/ℓ and a/ℓ. Points fixed in the plane of the coupler move along *coupler curves*. The shapes of these curves depend on six parameters, namely, on the four link lengths and, in addition, on two coordinates of the coupler-fixed point in the coupler plane. The coupler plane as a whole undergoes a translatory-rotatory motion through a continuum of positions which depends on the four link lengths. The said dependencies which are the subject of the following sections are highly complicated. It is this complexity in combination with simplicity of design which makes the planar four-bar the most important linkage in engineering.

Literature on four-bars and on other linkages: Erdman (Ed.) [11], Artobolevski [1], Geronimus [16], Dijksman [10].

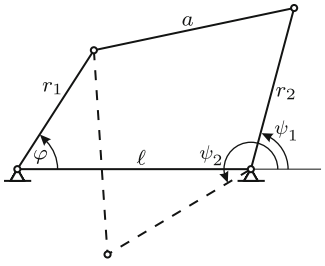

Fig. 17.1 Planar four-bar in the two positions existing for a given input angle φ

J. Wittenburg, *Kinematics*, DOI 10.1007/978-3-662-48487-6_17

In many machines a certain desired property is achieved by combining a four-bar with additional elements. A typical example is shown in Fig. 17.2. Without the motor-driven crank mechanism MDB drawn with dashed lines the mechanism is a four-bar A_0ABB_0 with base A_0B_0. None of its links is able to rotate full cycle relative to the base. When this four-bar is moving through its entire range, the coupler-fixed point C traces the dotted coupler curve. A section of this curve is a very good straight-line approximation. The combination of the four-bar A_0ABB_0 with the crank mechanism MDB results in a machine in which C is moving periodically back and forth the straight section when the crank is rotating. Point C can be used as guide for the piston of the pump at an oil-well.

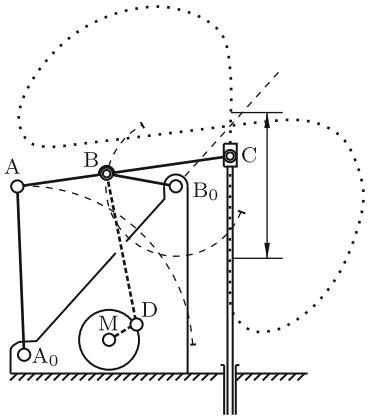

Fig. 17.2 Combination of four-bar and crank mechanism in a pump

17.1 Grashof Condition

In this section answers are given to the following questions. Through which angle can two neighboring links of a four-bar rotate relative to each other? Under which condition is this angle unlimited? In this case, one link is said to be fully rotating relative to the other. For every possible angle φ between two neighboring links there exist two positions of the four-bar (see Fig. 17.1). In some four-bars the transition from one of these positions into the other can be achieved by a continuous motion. In others the transition is possible only by disconnecting and reassembling the four-bar. Under which conditions is disconnection and reassembly necessary? The properties addressed by these questions do not depend on which link is chosen as fixed link and which as input link. Arbitrarily, the angle φ of the link of length r_1 against the

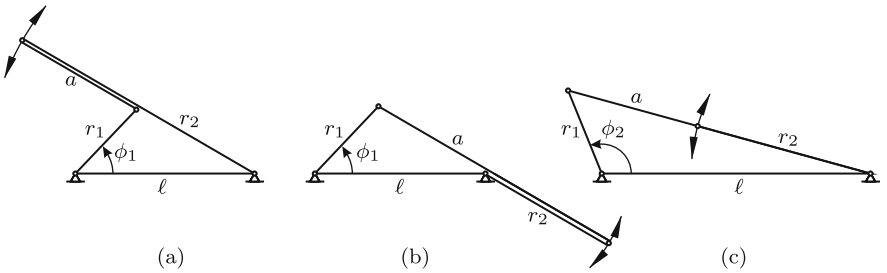

Fig. 17.3 Limit positions of a four-bar

link of length ℓ is investigated. Extremal values of φ in limit positions are denoted ϕ. In Figs. 17.3a,b,c all possible configurations in limit positions are shown. All of them are characterized by collinearity of the other two links of the four-bar. For the extremal angles ϕ_1 and ϕ_2 the cosine law yields the expressions

$$\cos\phi_{1,2} = \frac{r_1^2 + \ell^2 - (r_2 \mp a)^2}{2r_1\ell} \,. \tag{17.1}$$

The links are fully rotating relative to each other if $\cos\phi_1 \geq +1$ as well as $\cos\phi_2 \leq -1$. These conditions are

$$\text{a)} \quad |r_1 - \ell| \geq |r_2 - a| \,, \qquad \text{b)} \quad r_1 + \ell \leq r_2 + a \,. \tag{17.2}$$

In the special case of four identical link lengths $\ell = r_1 = r_2 = a \quad \phi_1 = 0$, $\phi_2 = \pi$. This means that neighboring links can rotate full cycle relative to each other.

In what follows, it is assumed that at least two link lengths are different. Let $\ell_{\min}$ and $\ell_{\max} \neq \ell_{\min}$ be the smallest and the largest, respectively, of the four link lengths, and let ℓ' and ℓ'' ($\ell' < \ell''$ or $\ell' = \ell''$ or $\ell' > \ell''$) be the other two link lengths so that

$$\ell_{\min} \leq \ell' \,,\; \ell'' \leq \ell_{\max} \qquad (\ell_{\max} \neq \ell_{\min}) \,. \tag{17.3}$$

Grashof[1] [17] is the author of

Theorem 17.1. *The link of length $\ell_{\min}$ is fully rotating relative to all other links if and only if the condition*

$$\ell_{\min} + \ell_{\max} \leq \ell' + \ell'' \tag{17.4}$$

[1] F. Grashof 1826-1893, professor at the *Polytechnische Schule Karlsruhe*, now Karlsruhe Institute of Technology (KIT); one of the founders and first chairman of *Verein Deutscher Ingenieure* (VDI)

is satisfied. Then these other links are fully rotating relative to the link with $\ell_{\min}$ *, but they are not fully rotating relative to each other. If condition (17.4) is not satisfied, no link is fully rotating relative to any other link.*

Proof: The following statements are easily verified if not obvious.
I. Equations (17.1) as well as conditions (17.2a,b) are invariant with respect to an interchange of r_1 and ℓ and also of r_2 and a.
II. If neither r_1 nor ℓ is $\ell_{\min}$, one of the conditions (17.2a), (17.2b) is violated.
III. If either (r_1, ℓ) or (ℓ, r_1) is the pair $(\ell_{\min}, \ell_{\max})$, condition (17.2a) is satisfied, and condition (17.2b) is condition (17.4).
IV. If either (r_1, ℓ) or (ℓ, r_1) is the pair $(\ell_{\min}, \ell')$, condition (17.2b) is satisfied, and condition (17.2a) is condition (17.4).
The combination of statements I to IV proves Grashof's theorem. According to this theorem four-bars are divided into

- four-bars satisfying Grashof's condition; these four-bars are further subdivided
  - general case: $\ell_{\min} + \ell_{\max} < \ell' + \ell''$
  - special case: $\ell_{\min} + \ell_{\max} = \ell' + \ell''$
- four-bars not satisfying Grashof's condition, i.e., four-bars with $\ell_{\min} + \ell_{\max} > \ell' + \ell''$.

Matters are even more complicated due to the fact that in engineering practice a particular link of a four-bar is declared to be the fixed link. A neighboring link (input link or output link) is referred to as *crank* or as *rocker* depending on whether or not it is fully rotating relative to the fixed link. Depending on the behavior of input link and output link a four-bar is either a *double-crank* or a *crank-rocker* or a *double-rocker*. It is obvious that a four-bar not satisfying Grashof's condition is a double-rocker. On the other hand, a four-bar satisfying Grashof's condition may be either a *double-crank* or a *crank-rocker* or a *double-rocker*. Details are worked out in what follows.

Four-Bars Satisfying Grashof's Inequality Condition $\ell_{\min} + \ell_{\max} < \ell' + \ell''$. For demonstration the link lengths $(3, 5, 6, 7)$ are used which satisfy Grashof's condition $(3 + 7 < 5 + 6)$. In Fig. 17.4a the fixed link is the shortest link. This link (and only this link) is fully rotating relative to all other links. In other words: The input link, the output link and the coupler are fully rotating relative to the fixed link. Hence the four-bar is a *double-crank*. For a single input angle the two existing positions of the four-bar are shown (one of them with dashed lines).

In Fig. 17.4b the input link is the shortest link. Only this link is fully rotating relative to all other links. Hence the four-bar is a *crank-rocker*. The four-bar is shown in all four limit positions of the rocker. The angular range of the rocker consists of two sectors $< 180°$ which are arranged symmetrically to the base line. The base line is outside these sectors. For a single input angle the two existing positions of the four-bar are shown (one of them with

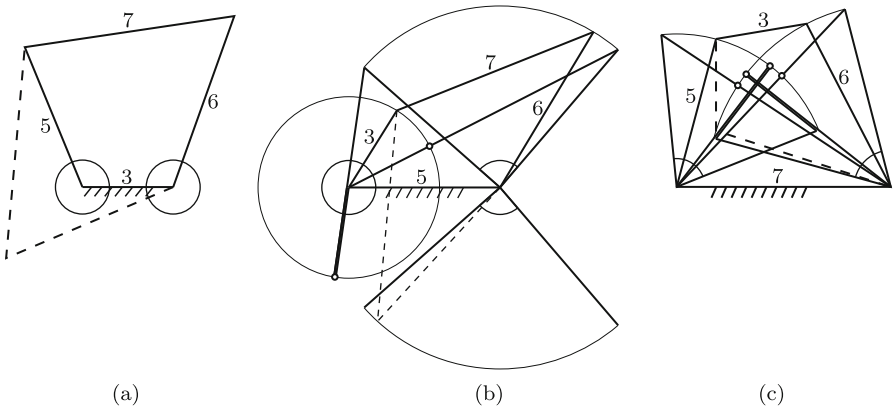

Fig. 17.4 Four-bars with different distributions of the link lengths (3, 5, 6, 7). Double-crank (**a**) with all links fully rotating. Crank-rocker (**b**) with fully rotating input crank. Double-rocker of first kind with fully rotating coupler (**c**)

dashed lines). In these two positions the output link is located on opposite sides of the base line.

Figure 17.4c differs from Fig. 17.4a in that the fixed link and the coupler are interchanged. The coupler is the shortest link. Only the coupler is fully rotating relative to all other links. The four-bar is referred to as *double-rocker of first kind*. The figure shows the limit positions of both rockers. The angular range of each rocker is a single sector. The sectors of both rockers are on one and the same side of the base line. For a single input angle the two existing positions of the four-bar are shown (one of them with dashed lines). In these two positions the output link is located on one and the same side of the base line.

In Figs. 17.4a , b and c reflection of every possible position in the base line is another possible position.

Four-Bars not Satisfying Grashof's Condition
For demonstration the link lengths (4, 5, 6, 8) are used which do not satisfy Grashof's condition $(4+8 > 5+6)$. Not a single link is fully rotating relative to the fixed link. These four-bars are referred to as *double-rockers of second kind*. Figure 17.5a shows the limit positions of both rockers. The angular range of each rocker is a single sector which is symmetrical to the base line. For a single input angle the two existing positions of the four-bar are shown (one of them with dashed lines). In Figs. 17.5a,b,c the four given lengths are given to different links of the four-bar. It is seen that depending on this distribution the fixed link is inside the angular range of either both rockers (Fig. 17.5a) or of a single rocker (Fig. 17.5b) or of no rocker (Fig. 17.5c).

Foldable Four-Bars Satisfying Grashof's Equality Condition $\ell_{\min} + \ell_{\max} = \ell' + \ell''$.

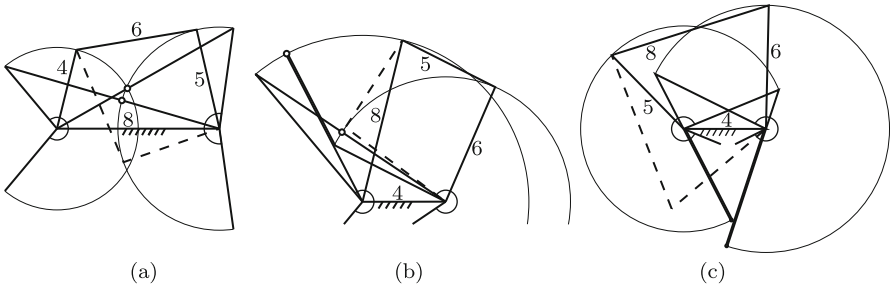

Fig. 17.5 Three double-rockers of second kind with different distributions of the link lengths (4, 5, 6, 8). No link is fully rotating

For demonstration the link lengths (1, 3, 4, 6) are used which satisfy the condition that $1+6=3+4$. Depending on whether the shortest link is the fixed link or the input link or the coupler the four-bar is either a double-crank or a crank-rocker or a double-rocker of first kind, respectively (compare Figs. 17.4a, b, c). In this respect there is no difference to the general case of four-bars satisfying the inequality condition $\ell_{\min}+\ell_{\max}<\ell'+\ell''$. The equality $\ell_{\min}+\ell_{\max}=\ell'+\ell''$ has the consequence that the four-bar is *foldable*. In a folded position all four links are collinear. Two different kinds of foldable four-bars have to be distinguished:
- first kind: $r_1+a=r_2+\ell$ (Fig. 17.6a)
- second kind: $r_1+r_2=a+\ell$ (Fig. 17.6b).
With link lengths (1, 3, 4, 6) the following foldable four-bars (ℓ, r_1, a, r_2) can be formed:
Foldable four-bars of first kind: Two double-cranks (1, 3, 4, 6), (1, 4, 3, 6);
four crank-rockers (4, 1, 6, 3), (3, 1, 6, 4), (6, 1, 4, 3), (6, 1, 3, 4);
two double-rockers of first kind (4, 6, 1, 3), (3, 6, 1, 4) ;
Foldable four-bars of second kind: One double-crank (1, 3, 6, 4);
two crank-rockers (3, 1, 4, 6), (4, 1, 3, 6);
one double-rocker of first kind (6, 4, 1, 3).

Example: The foldable four-bar of first kind in Fig. 17.6a is the double-rocker with $(\ell, r_1, a, r_2)=(4,6,1,3)$, and the foldable four-bar of second kind in Fig. 17.6b is the double-rocker with $(\ell, r_1, a, r_2)=(6,4,1,3)$. For a single angle φ of the input link the two associated positions of coupler and output link are shown. The points P_1 and P_2 are the instantaneous centers of rotation of the coupler in these positions. Let x be the coordinate of P_1 or P_2. In positions sufficiently close to the folded position ($\varphi=\psi=0$ in Fig. 17.6a and $\varphi=\pi-\psi=0$ in Fig. 17.6b) the following approximations are valid:

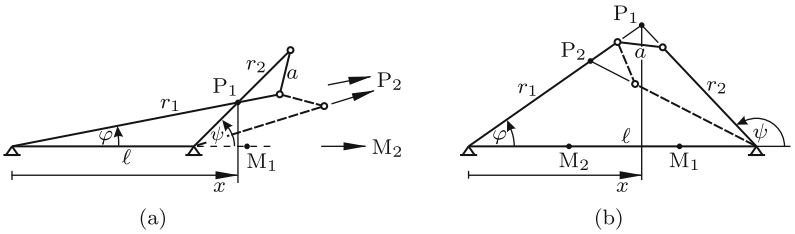

Fig. 17.6 **(a)** Foldable four-bar of first kind: $r_1+a=r_2+\ell$ $(\ell=4,\ r_1=6,\ a=1,\ r_2=3)$. **(b)** Foldable four-bar of second kind: $r_1+r_2=a+\ell$ $(\ell=6,\ r_1=4,\ a=1,\ r_2=3)$. Instantaneous centers of rotation P_1 and P_2 of the coupler tend toward M_1 and M_2 when the four-bar is folding

$$x\tan\varphi\approx\begin{cases}(x-\ell)\tan\psi & \text{(foldable four-bars of first kind)}\\ (\ell-x)\tan(\pi-\psi) & \text{(foldable four-bars of second kind).}\end{cases}\tag{17.5}$$

In Sect. 17.2 these approximations are used for determining instantaneous centers of rotation of the coupler in folded positions when intersection points P_1 and P_2 do not exist. End of example.

In the folded position motion is possible in two ways with either $\dot\psi/\dot\varphi>0$ or $\dot\psi/\dot\varphi<0$. In engineering applications of foldable four-bars provisions must be made either to avoid the folded position or to pass through it with prescribed sense of rotation.

Consider again Figs. 17.3a,b,c. When the input link of length r_1 is moving away from its limit position, the joint connecting coupler and output link is free to move in two different directions as is indicated by arrows. From this the following conclusion is drawn. Two positions of a four-bar which are associated with an arbitrarily given angle of a *rocker* can be reached one from the other by a continuous motion. The four-bars in Figs. 17.4a,c as well as those in Figs. 17.5a,b,c have this property. In contrast, two positions of a four-bar which are associated with an arbitrarily given angle of a *crank* cannot be reached one from the other by a continuous motion, but only by disconnection and reassembly (Figs. 17.4b,c). Exception: Foldable four-bars. Transition from one position to the other is possible via the folded position.

17.2 Transfer Function

From Figs. 17.5 and 17.4 it is known that to every position $(\varphi,\ \psi)$ of the four-bar the position symmetrical to the base line $\overline{A_0B_0}$ with angles $(-\varphi,\ -\psi)$ exists. This symmetry is found in all subsequent equations. The transfer function determines ψ as function of φ. First, implicit forms $f(\varphi,\psi)=0$ of the transfer function are formulated. Starting point are the coordinates of

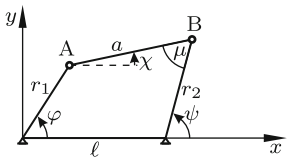

Fig. 17.7 Four-bar with input angle φ, output angle ψ, inclination angle χ of the coupler, transmission angle μ

the points A and B in the x, y-system shown in Fig. 17.7:

$$\left.\begin{aligned} x_{\mathrm{A}} &= r_1 \cos\varphi\,, & x_{\mathrm{B}} &= \ell + r_2 \cos\psi\,, \\ y_{\mathrm{A}} &= r_1 \sin\varphi\,, & y_{\mathrm{B}} &= \quad r_2 \sin\psi\,. \end{aligned}\right\} \tag{17.6}$$

The constant length a of the coupler requires that $(x_{\mathrm{B}}-x_{\mathrm{A}})^2+(y_{\mathrm{B}}-y_{\mathrm{A}})^2 = a^2$ or explicitly

$$(\ell + r_2\cos\psi - r_1\cos\varphi)^2 + (r_2\sin\psi - r_1\sin\varphi)^2 - a^2 = 0\,. \tag{17.7}$$

This is already the desired equation $f(\varphi,\psi) = 0$. Reformulation gives it the form

$$f = 2r_2(\ell - r_1\cos\varphi)\cos\psi - 2r_1 r_2 \sin\varphi\sin\psi - 2\ell r_1\cos\varphi + r_1^2 + \ell^2 + r_2^2 - a^2 = 0 \tag{17.8}$$

or alternatively

$$f = 2\ell r_2\cos\psi - 2\ell r_1\cos\varphi - 2r_1 r_2\cos(\varphi-\psi) + r_1^2 + \ell^2 + r_2^2 - a^2 = 0\,. \tag{17.9}$$

Equation (17.8) has the form

$$A(\varphi)\cos\psi + B(\varphi)\sin\psi = C(\varphi) \tag{17.10}$$

with coefficients

$$A = 2r_2(\ell - r_1\cos\varphi),\quad B = -2r_1 r_2\sin\varphi\,,\quad C = 2r_1\ell\cos\varphi - (r_1^2+\ell^2+r_2^2-a^2)\,. \tag{17.11}$$

For every angle φ there exist two solutions ψ_1 and ψ_2. They are determined through their sines and cosines:

$$\left.\begin{aligned} \cos\psi_k &= \frac{AC + (-1)^k B\sqrt{A^2+B^2-C^2}}{A^2+B^2}\,, \\ \sin\psi_k &= \frac{BC - (-1)^k A\sqrt{A^2+B^2-C^2}}{A^2+B^2} \end{aligned}\right\} \quad (k = 1,2)\,. \tag{17.12}$$

These expressions depend on three parameters only, namely, on r_1/ℓ, r_2/ℓ and a/ℓ. Equations (17.11) yield

$$A^2 + B^2 = 4r_2^2(\ell^2 + r_1^2 - 2r_1\ell\cos\varphi) = -4r_2^2(C + r_2^2 - a^2)\ , \tag{17.13}$$

$$\begin{aligned} A^2 + B^2 - C^2 &= 4r_2^2a^2 - (C + 2r_2^2)^2 \\ &= -[C + 2r_2(a + r_2)][C - 2r_2(a - r_2)] \qquad (17.14) \\ &= -[2r_1\ell\cos\varphi - (r_1^2 + \ell^2) + (r_2 + a)^2] \\ &\quad \times[2r_1\ell\cos\varphi - (r_1^2 + \ell^2) + (r_2 - a)^2]\ . \qquad (17.15) \end{aligned}$$

The angles ψ_1 and ψ_2 are real for all angles φ satisfying the condition $A^2 + B^2 - C^2 \geq 0$. Let ϕ denote all angles φ for which the equality sign is valid. From (17.15) the cosines of these angles are obtained:

$$\cos\phi_{1,2} = \frac{r_1^2 + \ell^2 - (r_2 \mp a)^2}{2r_1\ell}\ . \tag{17.16}$$

These are the Eqs.(17.1). The angles are the limit angles of the input link known from Figs. 17.3a,b,c.

This section is closed with an application of (17.9) to foldable four-bars (see Figs. 17.6a,b). In the process of folding the instantaneous centers of rotation P_1 and P_2 of the coupler tend toward points M_1 and M_2 on the base line. These points are determined by combining (17.5) and (17.9). First, foldable four-bars of first kind are considered. In the limit $\varphi \to 0$, $\psi \to 0$ (17.5) yields $x/(x - \ell) = \psi/\varphi$. With $\ell = r_1 - r_2 + a$ (17.9) becomes

$$r_1(r_1{+}a){+}r_2(r_2{-}a){-}r_1r_2[1{+}\cos(\varphi{-}\psi)]{-}(r_1{-}r_2{+}a)(r_1\cos\varphi{-}r_2\cos\psi) = 0\ . \tag{17.17}$$

Taylor expansion up to second-order terms and division through φ^2 produces for $\lambda = \psi/\varphi = x/(x - \ell)$ the quadratic equation $\lambda^2 r_2(r_2 - a) - 2r_1r_2\lambda = -r_1(r_1 + a)$. The solutions $\lambda_{1,2}$ and the associated coordinates $x_{1,2}$ of M_1 and M_2 are

$$\lambda_{1,2} = \frac{r_1r_2 \pm \sqrt{r_1r_2a\ell}}{r_2(r_2 - a)}\ , \qquad x_{1,2} = \frac{\lambda_{1,2}}{\lambda_{1,2} - 1}\,\ell\ . \tag{17.18}$$

The solution for foldable four-bars of second kind is obtained in a similar way. In (17.9) the substitutions $\psi = \pi - \alpha$ and $\ell = r_1 + r_2 - a$ are made. Following this, a Taylor expansion up to second-order terms is made. The result is a quadratic equation for $\lambda = \alpha/\varphi = x/(\ell - x)$. The solutions $\lambda_{1,2}$ are identical with those in (17.18):

$$\lambda_{1,2} = \frac{r_1r_2 \pm \sqrt{r_1r_2a\ell}}{r_2(r_2 - a)}\ , \qquad x_{1,2} = \frac{\lambda_{1,2}}{\lambda_{1,2} + 1}\,\ell\ . \tag{17.19}$$

Examples: The link lengths of Fig. 17.6a yield $x_1 \approx 5.17$, $x_2 \approx 10.8$ and those of Fig. 17.6b yield $x_1 \approx 4.64$, $x_2 \approx 2.21$. These are the points M_1 and M_2 shown in the figure. End of examples.

17.3 Interchange of Input Link and Fixed Link

In Fig. 17.8 the four-bar A_0ABB_0 with link lengths ℓ, r_1, a, r_2 is called four-bar F. Dashed lines parallel to the fixed link and to the input link define the point P. The quadrilateral B_0PAB is drawn one more time in dotted lines. The dotted quadrilateral is called four-bar F*. Its fixed link has length r_1, and its input link has length ℓ. Both four-bars have the same coupler and the same output link. If F is a foldable four-bar, also F* is foldable. If F is a double-rocker of first kind (of second kind), also F* is a double-rocker of first kind (of second kind). If F is a double-crank, F* is either a double-crank or a crank-rocker. If F is a crank-rocker, F* is either a double-crank (if fixed link and crank are interchanged) or a crank-rocker (if fixed link and rocker are interchanged). Example: Let F be the crank-rocker in Fig. 17.4b. Interchange of fixed link and crank produces the double-crank of Fig. 17.4a.

In Fig. 17.8 F and F* have one and the same input angle φ. The relation between the output angles ψ and ψ^* is seen to be

$$\psi + \psi^* \equiv \varphi + \pi \,. \tag{17.20}$$

For a given angle φ Eqs.(17.12) determine in the four-bar F two angles ψ_1 and ψ_2 and in the four-bar F* with coefficients $A^* = 2r_2(r_1 - \ell\cos\varphi)$, $B^* = -2\ell r_2 \sin\varphi$, $C^* = C$ two angles ψ_1^* and ψ_2^*. The coordination of the pairs of angles is as follows: $\psi_1 + \psi_2^* \equiv \varphi + \pi$. This is verified by substituting

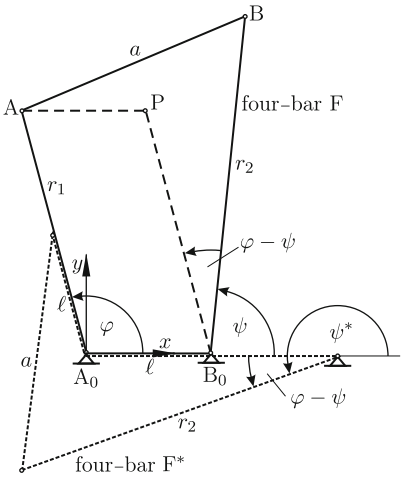

Fig. 17.8 Four-bar F and the associated four-bar F* with link lengths r_1 and ℓ interchanged

A, B, C and A^*, B^*, C^* into the equation $\cos\psi_1\cos\psi_2^* - \sin\psi_1\sin\psi_2^* \equiv -\cos\varphi$.

17.4 Inclination Angle of the Coupler. Transmission Angle

Figure 17.7 defines the inclination angle χ of the coupler against the base line. Its dependency on φ is found by the same method that was used for ψ. Point B has coordinates $x_B = r_1\cos\varphi + a\cos\chi$ and $y_B = r_1\sin\varphi + a\sin\chi$. These expressions are substituted into the constraint equation $(x_B - \ell)^2 + y_B^2 = r_2^2$. This results in the equation

$$\bar{A}\cos\chi + \bar{B}\sin\chi = \bar{C}\,, \tag{17.21}$$

$$\bar{A} = -2a(\ell - r_1\cos\varphi)\,, \quad \bar{B} = 2r_1 a\sin\varphi\,, \quad \bar{C} = 2r_1\ell\cos\varphi - (r_1^2 + \ell^2 + a^2 - r_2^2)\,. \tag{17.22}$$

These coefficients are obtained from those in (17.11) by interchanging r_2 and $-a$. The equation has the solutions

$$\left.\begin{aligned} \cos\chi_k &= \frac{\bar{A}\bar{C} - (-1)^k\bar{B}\sqrt{\bar{A}^2 + \bar{B}^2 - \bar{C}^2}}{\bar{A}^2 + \bar{B}^2}\,, \\ \sin\chi_k &= \frac{\bar{B}\bar{C} + (-1)^k\bar{A}\sqrt{\bar{A}^2 + \bar{B}^2 - \bar{C}^2}}{\bar{A}^2 + \bar{B}^2} \end{aligned}\right\} \ (k = 1, 2). \tag{17.23}$$

The exponent k in this equation must be the same as in (17.12). Only then the constraint equation $r_1\cos\varphi + a\cos\chi = \ell + r_2\cos\psi$ is satisfied.

The angle χ reaches a stationary value (maximum or minimum) when the angular velocity $\dot{\chi}$ of the coupler is zero. This is the case when the instantaneous center of rotation P_{30}, i.e., the intersection of input link and output link, is at infinity. Figure 17.9 shows that this is possible in two positions. Let $\varphi = \varphi_\infty$ and χ_{stat} be the associated angles. One position is characterized by $\psi = \varphi_\infty$ and the other by $\psi = \varphi_\infty + \pi$. Equation (17.10) yields for $\cos\varphi_\infty$ the two expressions given below. Expressions for the associated stationary angles χ_{stat} are obtained from the cosine law applied to the triangles shown in Fig. 17.9:

$$\cos\varphi_\infty = \frac{\ell^2 - a^2 + (r_1 \mp r_2)^2}{2\ell(r_1 \mp r_2)}\,, \quad \cos\chi_{\text{stat}} = \frac{\ell^2 + a^2 - (r_1 \mp r_2)^2}{2a\ell}\,. \tag{17.24}$$

The angles φ_∞ have a kinematical interpretation. They determine the directions of asymptotes of the fixed centrode of the coupler. The centrode has no asymptotes if both cosines have absolute values > 1, i.e., if the conditions $(\ell - a)^2 > (r_1 - r_2)^2$ and $(\ell + a)^2 < (r_1 + r_2)^2$ are satisfied. This is the

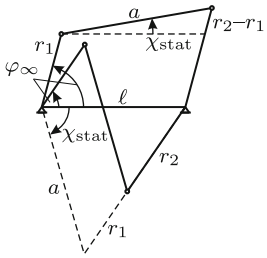

Fig. 17.9 Stationary values of the angle χ occur when the cranks are parallel

case if and only if the coupler is fully rotating. These four-bars are either double-cranks (Fig. 17.4a) or double-rockers of first kind (Fig. 17.4c). In Ex. 6 of Sect. 15.1.2 centrodes of couplers of four-bars with special link lengths were investigated.

In Fig. 17.7 the transmission angle μ of a four-bar is defined. Its dependency on φ is obtained as follows. The length of the diagonal starting from A is expressed by means of the cosine law once in terms of $\cos\varphi$ and once in terms of $\cos\mu$. The identity of these expressions results in

$$\cos\mu = \frac{2r_1\ell\cos\varphi - (r_1^2+\ell^2) + r_2^2 + a^2}{2r_2a} \,. \tag{17.25}$$

Extremal values of μ are obtained from (17.1) by interchanging (r_1, ℓ) and (r_2, a):

$$\cos\mu_{\text{stat}} = \frac{r_2^2 + a^2 - (\ell \mp r_1)^2}{2r_2a} \,. \tag{17.26}$$

In positions with these extremal values the input link and the fixed link are collinear (see Fig. 17.3). In phases of motion in which the coupler is required to transmit a large torque to the output link the transmission angle μ should differ from $\pi/2$ as little as possible. In other words: $|\cos\mu|$ should be as small as possible.

17.5 Transmission Ratio. Angular Acceleration of Output Link

The angular velocity ratio $i = \dot\varphi/\dot\psi$ is called *transmission ratio* of the four-bar. In what follows, the inverse value $1/i = \dot\psi/\dot\varphi$ is represented in geometric and in analytical form. The geometric form is obtained from (15.6). Let the fixed link, the input link and the output link be links 0, 1 and 2, respectively, so that $\omega_{10} = \dot\varphi$ and $\omega_{20} = \dot\psi$ (see Fig. 17.10). Equation (15.6) with $i = 2$, $j = 1$, $k = 0$ yields the expression

$$\frac{1}{i} = \frac{\dot\psi}{\dot\varphi} = \frac{\varrho_{P_{10}P_{12}}}{\varrho_{P_{20}P_{12}}} = \frac{x_{12}}{x_{12}-\ell} = \frac{\xi}{\xi-1} \qquad \left(\xi = \frac{x_{12}}{\ell}\right) . \tag{17.27}$$

Here, $x_{12}(\varphi)$ is the coordinate of the instantaneous center P_{12} along the base line. The dimensionless quantity ξ is zero at the center P_{10} and it equals one at the center P_{20}. Over the ξ-axis thus defined the ratio $1/i$ is plotted at the center P_{12}.

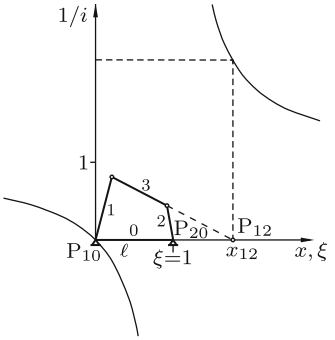

Fig. 17.10 Dimensionless coordinate $\xi = x_{12}/\ell$ of the instantaneous center P_{12} and inverse transmission ratio $1/i$ as function of ξ

An analytical expression for the ratio $1/i$ is found by differentiating the transfer function $f(\varphi,\psi) = 0$ with respect to time:

$$\dot\varphi\,\frac{\partial f}{\partial \varphi} + \dot\psi\,\frac{\partial f}{\partial \psi} = 0 . \tag{17.28}$$

Hence

$$\frac{1}{i} = \frac{\dot\psi}{\dot\varphi} = -\frac{\partial f}{\partial \varphi}\Big/\frac{\partial f}{\partial \psi} . \tag{17.29}$$

Equation (17.9) yields

$$\frac{\partial f}{\partial \varphi} = 2\ell r_1 \sin\varphi + 2r_1 r_2 \sin(\varphi-\psi) , \qquad \frac{\partial f}{\partial \psi} = -2\ell r_2 \sin\psi - 2r_1 r_2 \sin(\varphi-\psi) . \tag{17.30}$$

Hence

$$\frac{1}{i} = \frac{r_1}{r_2}\;\frac{\ell\sin\varphi + r_2\sin(\varphi-\psi)}{\ell\sin\psi + r_1\sin(\varphi-\psi)} = \frac{r_1}{r_2}\;\frac{\ell\sin\varphi + r_2(\sin\varphi\cos\psi - \cos\varphi\sin\psi)}{\ell\sin\psi + r_1(\sin\varphi\cos\psi - \cos\varphi\sin\psi)} . \tag{17.31}$$

Temporarily, this is abbreviated as $r_1 N/(r_2 D)$ (numerator N, denominator D). Equations (17.12) yield the expressions

$$N(A^2+B^2) = \ell(A^2+B^2)\sin\varphi + r_2\Big[(A\sin\varphi - B\cos\varphi)C \mp (B\sin\varphi + A\cos\varphi)\sqrt{A^2+B^2-C^2}\Big]\,, \tag{17.32}$$

$$D(A^2+B^2) = \ell\Big(BC \pm A\sqrt{A^2+B^2-C^2}\Big) + r_1\Big[(A\sin\varphi - B\cos\varphi)C \mp (B\sin\varphi + A\cos\varphi)\sqrt{A^2+B^2-C^2}\Big]\,. \tag{17.33}$$

From (17.11) it follows that

$$\left.\begin{aligned} &A\sin\varphi - B\cos\varphi = 2r_2\ell\sin\varphi\,,\\ &B\sin\varphi + A\cos\varphi = 2r_2(\ell\cos\varphi - r_1)\,,\\ &\ell B + r_1(A\sin\varphi - B\cos\varphi) = 0\,. \end{aligned}\right\} \tag{17.34}$$

These equations in combination with (17.13) and (17.14) yield the formula

$$\frac{2}{i} = \frac{\cos\varphi - p_1}{\cos\varphi - p_2} \pm \frac{(\cos\varphi - p_3)\sin\varphi}{(\cos\varphi - p_2)\sqrt{\lambda^2 - (\cos\varphi - p_4)^2}} \tag{17.35}$$

with dimensionless constants

$$\left.\begin{aligned} &\lambda = \frac{r_2 a}{r_1\ell}\,, \qquad p_1 = \frac{r_1}{\ell}\,, \qquad p_2 = \frac{r_1^2+\ell^2}{2r_1\ell} = \frac{1}{2}\Big(p_1 + \frac{1}{p_1}\Big) \geq 1\,,\\ &p_3 = p_2 - \frac{r_2^2 - a^2}{2r_1\ell}\,, \qquad p_4 = p_2 - \frac{r_2^2 + a^2}{2r_1\ell}\,. \end{aligned}\right\} \tag{17.36}$$

These constants are related as follows:

$$p_2^2 - 1 = (p_1 - p_2)^2\,, \qquad (p_4 - p_2)^2 - \lambda^2 = (p_3 - p_2)^2\,. \tag{17.37}$$

The expression $\cos\varphi - p_2$ in (17.35) is zero only if the conditions $\varphi = 0$ and $r_1 = \ell$ are satisfied which imply that also $r_2 = a$. The square root in (17.35) is zero for angles $\varphi = \phi_{1,2}$ satisfying one of the equations $\cos\phi_{1,2} - p_4 = \pm\lambda$. This is Eq.(17.1) defining the angles shown in Figs. 17.3a,b,c .

With the exception of p_1 all constants in (17.36) are invariant with respect to an interchange of base length ℓ and input link length r_1. Because of the first Eq.(17.37) this is true also for $(p_1 - p_2)^2$. A relation between the ratios $1/i$ and $1/i^*$ of the two four-bars with interchanged link lengths is obtained by differentiating the identity Eq.(17.20) with respect to time:

$$\frac{1}{i} + \frac{1}{i^*} = \frac{\dot\psi}{\dot\varphi} + \frac{\dot\psi^*}{\dot\varphi} \equiv 1\,. \tag{17.38}$$

The total time derivative of (17.28) yields the transfer characteristics on the acceleration level:

$$\ddot{\varphi}\,\frac{\partial f}{\partial \varphi} + \ddot{\psi}\,\frac{\partial f}{\partial \psi} + \dot{\varphi}^2\,\frac{\partial^2 f}{\partial \varphi^2} + 2\dot{\varphi}\dot{\psi}\,\frac{\partial^2 f}{\partial \varphi \partial \psi} + \dot{\psi}^2\,\frac{\partial^2 f}{\partial \psi^2} = 0\,. \tag{17.39}$$

Furthermore, $\dot{\psi} = \dot{\varphi}/i$ with (17.29) for $1/i$. This together with the derivatives in (17.30) yields for $\ddot{\psi}$ the expression

$$\ddot{\psi} = i\ddot{\varphi} + \dot{\varphi}^2\,\frac{r_1\ell\cos\varphi - (r_2\ell/i^2)\cos\psi + r_1 r_2(1-1/i)^2\cos(\varphi-\psi)}{r_2\ell\sin\psi + r_1 r_2\sin(\varphi-\psi)}\,. \tag{17.40}$$

17.6 Stationary Values of the Transmission Ratio

In this section geometrical and analytical methods are used for determining those input angles φ for which the ratio $1/i$ in (17.35) and hence the transmission ratio i itself attains stationary values. Starting from Fig. 17.10 Freudenstein [14] discovered the following geometrical relationship. Imagine that the input link is moving with $\dot{\varphi} > 0$ through its entire angular range. In the course of this motion the instantaneous center P_{12} moves along the ξ-axis. Whenever it has zero velocity, the ratio $1/i$ attains a stationary value. This is a consequence of the monotonicity property of the function $1/i(\xi)$ shown in the figure. The velocity of P_{12} is zero if and only if the coupler-fixed point momentarily coinciding with P_{12} has a velocity in the direction of the coupler (labeled body 3). Then the center P_{30} of the coupler lies on the normal to the coupler erected in P_{12}. In other words: In positions of the four-bar with a stationary value of $1/i$ the lines $\overline{\mathrm{P}_{12}\mathrm{P}_{30}}$ and $\overline{\mathrm{P}_{31}\mathrm{P}_{32}}$ are mutually orthogonal[2]. Figure 17.11 shows two different four-bars in such positions.

If a stationary value occurs at $\varphi = 0$ or at $\varphi = \pi$, P_{12} and P_{30} are located on the base line, and the coupler is orthogonal to the base line. Then the parameters satisfy the condition

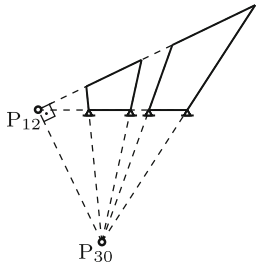

Fig. 17.11 Two four-bars in positions when $\overline{\mathrm{P}_{12}\mathrm{P}_{30}}$ is orthogonal to the coupler

[2] In Bobillier's Theorem 15.6 the line $\overline{\mathrm{P}_{12}\mathrm{P}_{30}}$ was shown to play another important role (line h in Fig. 15.19)

$$\left.\begin{aligned} &\text{stationary value at } \varphi = 0: && (\ell - r_1)^2 + a^2 = r_2^2\,, \\ &\text{stationary value at } \varphi = \pi: && (\ell + r_1)^2 + a^2 = r_2^2\,. \end{aligned}\right\} \tag{17.41}$$

In the vicinity of an angle φ for which $1/i$ has a stationary value the angle between the lines $\overline{\mathrm{P}_{12}\mathrm{P}_{30}}$ and $\overline{\mathrm{P}_{31}\mathrm{P}_{32}}$ is very sensitive to changes of φ. The desired angle φ can, therefore, be determined graphically rather precisely by checking the orthogonality. In order to determine for a given four-bar all positions with a stationary value of $1/i$ the four-bar and the center P_{12} must be drawn for a number of (monotonically increasing) angles φ over the entire possible range $\phi_1 \le \varphi \le \phi_2$. A stationary value of $1/i$ is passed every time the moving center P_{12} changes its sense of direction along the ξ-axis (jumps from ∞ to $-\infty$ do not count as changes of sense of direction). Once a position is known approximately it can be improved by checking the angle between the lines $\overline{\mathrm{P}_{12}\mathrm{P}_{30}}$ and $\overline{\mathrm{P}_{31}\mathrm{P}_{32}}$.

Example: For the double-crank in Fig. 17.4a this investigation reveals that stationary values of $1/i$ occur in the two positions shown in Fig. 17.12a with $\varphi \approx 9°$ and with $\varphi \approx 95°$. With the coordinate of P_{12} (17.27) yields for the position $\varphi \approx 9°$ a maximum $(1/i)_{\max} \approx 2.7$ and for the position $\varphi \approx 95°$ a minimum $(1/i)_{\min} \approx 0.42$.

For the crank-rocker of Fig. 17.4b the same investigation can be made. This is unnecessary, however, because this four-bar is obtained from the previously investigated one by interchanging the fixed link and the input link. From (17.38) it follows that two four-bars thus related have stationary values of $1/i$ for one and the same angles φ. Furthermore, these stationary values add up to one. If the stationary value is a maximum in one of the four-bars, it is a minimum in the other and vice versa. Hence the crank-rocker of Fig. 17.4b has at $\varphi \approx 9°$ a minimum $(1/i)_{\min} \approx -1.7$ and at $\varphi \approx 95°$ a maximum $(1/i)_{\max} \approx 0.58$. Figure 17.12b shows the crank-rocker in these positions. End of example.

In what follows, two analytical methods for determining stationary values of $1/i$ are described. Method 1 is a direct method based on (17.35). With the abbreviation $x = \cos\varphi$ it is written in the form

$$\left.\begin{aligned} &\frac{2}{i(x)} = \frac{x - p_1}{x - p_2} \pm \frac{(x - p_3)Q}{(x - p_2)P}\,, \\ &P = \sqrt{\lambda^2 - (x - p_4)^2}\,, \qquad Q = \sqrt{1 - x^2}\,. \end{aligned}\right\} \tag{17.42}$$

The stationarity condition $\mathrm{d}(1/i)/\mathrm{d}x = 0$ has the form (the prime denotes the derivative with respect to x)

$$\mp(p_1 - p_2)P^2 = (p_3 - p_2)PQ + (x - p_2)(x - p_3)(PQ' - QP')\,. \tag{17.43}$$

Now, $P' = -(x - p_4)/P$ and $Q' = -x/Q$ are substituted. The resulting equation is multiplied by PQ. This eliminates the case $\sin\varphi = 0$. Whether

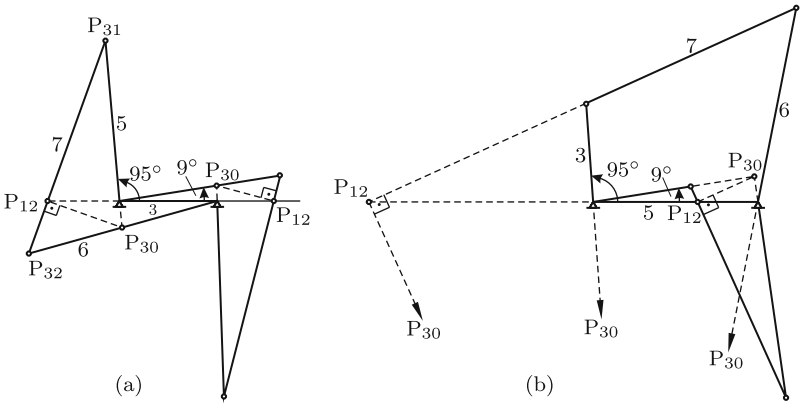

Fig. 17.12 The double-crank of Fig. 17.4a **(a)** and the crank-rocker of Fig. 17.4b **(b)** in the two positions with stationary values of $1/i$

this is a solution is checked with (17.41). After this multiplication the equation has the form

$$\begin{aligned}
&\pm (p_1 - p_2)[(x - p_4)^2 - \lambda^2]\sqrt{(x^2 - 1)[(x - p_4)^2 - \lambda^2]} \\
&= (p_3 - p_2)(x^2 - 1)[(x - p_4)^2 - \lambda^2] \\
&\quad -(x - p_2)(x - p_3)[p_4(1 + x^2) + x(\lambda^2 - p_4^2 - 1)] \,. \qquad (17.44)
\end{aligned}$$

The special case $r_1 = \ell$ is characterized by $p_1 = p_2 = 1$ and, therefore, by the third-order equation

$$(p_3{-}1)(1{+}x)[\lambda^2{-}(x{-}p_4)^2]{+}(x{-}p_3)[p_4(1{+}x^2){+}x(\lambda^2{-}p_4^2{-}1)] = 0 \,. \quad (17.45)$$

The equation is quadratic if, in addition, also $a = \ell$.

In the general case $r_1 \neq \ell$, (17.44) is squared. The squared equation is invariant with respect to the interchange of r_1 and ℓ (see the comments following (17.36) and (17.37)). Because of the sign $\pm$ no extraneous roots are introduced by squaring. Equation (17.44) with the positive sign has the meaningless root $x = p_2 > 1$. This is verified with the help of (17.37). From this it follows that the squared equation is divisible by $(x - p_2)^2$. Following this division it is a sixth-order equation. The division is performed in two steps. Squaring results in the equation

$$\begin{aligned}
&(\ x^2 - 1)[(x - p_4)^2 - \lambda^2]^2\Big\{(p_1 - p_2)^2[(x - p_4)^2 - \lambda^2] - (p_3 - p_2)^2(x^2 - 1)\Big\} \\
&= (x - p_2)F(x)\Big\{(x - p_2)F(x) - 2(p_3 - p_2)(x^2 - 1)[(x - p_4)^2 - \lambda^2]\Big\} \quad (17.46)
\end{aligned}$$

with the third-order polynomial

$$F(x) = (x - p_3)[p_4(1 + x^2) + x(\lambda^2 - p_4^2 - 1)] \,. \tag{17.47}$$

Taking into account (17.37) the expression in curled brackets on the left-hand side is written in the form $(x - p_2)(Ax + B)$ with constants

$$A = (p_1 - p_2)^2 - (p_3 - p_2)^2 \,, \qquad B = p_2 A - 2p_4(p_1 - p_2)^2 \,. \tag{17.48}$$

Division of (17.46) by $(x - p_2)$ produces the equation

$$\begin{aligned}(x^2 - 1)[(x - p_4)^2 - \lambda^2]\Big\{[(x - p_4)^2 - \lambda^2](Ax + B) + 2(p_3 - p_2)F(x)\Big\} \\ = (x - p_2)[F(x)]^2 \,.\end{aligned} \tag{17.49}$$

The expression in curled brackets is a third-order polynomial $K_3x^3 + K_2x^2 + K_1x + K_0$ with coefficients

$$\left.\begin{aligned} K_3 &= A + 2p_4(p_3 - p_2) \,, \\ K_2 &= B - 2p_4A + 2(p_3 - p_2)(\lambda^2 - p_4^2 - 1 - p_3p_4) \,, \\ K_1 &= -2p_4B + A(p_4^2 - \lambda^2) + 2(p_3 - p_2)[p_4 - p_3(\lambda^2 - p_4^2 - 1)] \,. \end{aligned}\right\} \tag{17.50}$$

Division by $(x - p_2)$ produces the second-order polynomial $K_3x^2 + (x + p_2)(K_2 + p_2K_3) + K_1$. With this expression (17.49) yields the desired sixth-order equation

$$(x^2-1)[(x-p_4)^2-\lambda^2][K_3x^2+(x+p_2)(K_2+p_2K_3)+K_1]-[F(x)]^2 = 0 \,. \tag{17.51}$$

The coefficient of x^6 is

$$K_3 - p_4^2 = (p_1 - p_2)^2 - (p_3 - p_2 - p_4)^2 = \frac{(\ell^2 - a^2)(a^2 - r_1^2)}{(r_1\ell)^2} \,. \tag{17.52}$$

The equation is of fifth order if $a = \ell$ and/or $a = r_1$. Only real roots $|x| \le 1$ are significant. For every such root it is checked to which sign in (17.44) the root belongs. With the same sign (17.42) and (17.12) determine the corresponding stationary value of $1/i$ and the angle ψ.

Example: With the parameters of the double-crank in Fig. 17.4a as well as with those of the crank-rocker in Fig. 17.4b (17.51) has the four real roots $x = \cos\varphi \approx -0.084$, 0.9882, 1.11 and 4.02. The first two roots determine the angles $\varphi \approx 94.8°$ and $\varphi \approx 8.8°$, respectively. These are the angles shown in Figs. 17.12a and b. End of example.

The second (historically the first) analytical method for determining stationary values of $1/i$ is due to Freudenstein [14]. Also this method leads to a sixth-order equation. The method starts out from Fig. 17.10 and from the coupler curve traced by a point C fixed on the coupler line $\overline{P_{31}P_{32}}$. Let $\eta = \text{const}$ be the coordinate of this point along the coupler line ($\eta = 0$, when

C is at P_{31} and $\eta > 0$, when C and P_{32} are on the same side of P_{31}). In Sect. 17.8.3 the equation of the coupler curve in the x, y-system of Fig. 17.7 is given. In what follows, only the coordinates of the intersection points of the curve with the x-axis are needed. They are the roots of Eq.(17.100) which is cubic with respect to x and to η:

$$(\eta - a)(x - \ell)(x^2 + \eta^2 - r_1^2) - \eta x[(x - \ell)^2 + (\eta - a)^2 - r_2^2] = 0\,. \quad (17.53)$$

The corresponding angle φ is determined by the cosine law:

$$\cos\varphi = \frac{x^2 + r_1^2 - \eta^2}{2r_1 x}\,. \quad (17.54)$$

In Sect. 17.8.4 it is pointed out that not every real root x of (17.53) represents an intersection point of the coupler-curve with the x-axis. A root represents a singular point without kinematical significance if it is associated with values $|\cos\varphi| > 1$. In what follows, only those roots are of interest which yield values $|\cos\varphi| \le 1$.

Let now C be the coupler-fixed point which coincides with P_{12} when the four-bar is in a position with a stationary value of $1/i$. In Fig. 17.13 this situation is shown. The coordinate η of this point is associated with a solution x of (17.53) which is equal to the stationary value of the coordinate x_{12} of the center P_{12}. Although x_{12} and x have different definitions, x as function of η has the same stationary value. From this it follows that the implicit derivative of (17.53) with respect to η is valid with $\mathrm{d}x/\mathrm{d}\eta = 0$. This is the equation

$$(x - \ell)(x^2 + \eta^2 - r_1^2) - x[(x - \ell)^2 + (\eta - a)^2 - r_2^2] - 2\ell\eta(\eta - a) = 0\,. \quad (17.55)$$

This equation and (17.53) together determine the unknowns x and η. De-

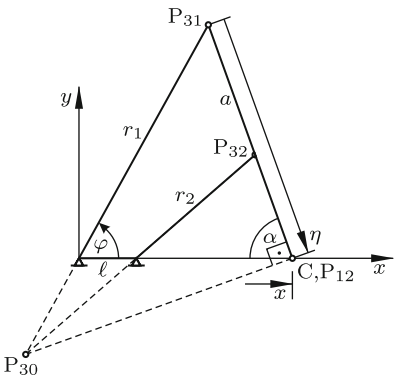

Fig. 17.13 Four-bar in a position with stationary value of $1/i$. The coupler point C momentarily coinciding with P_{12} has coordinates x and η

coupling leads to the desired sixth-order equation. This decoupling is achieved in several steps. First, (17.55) is multiplied by η and then (17.53) is subtracted. This results in the equation

$$a(x-\ell)(x^2+\eta^2-r_1^2)-2\ell\eta^2(\eta-a)=0\,. \tag{17.56}$$

This equation and (17.55) are rewritten by introducing the dimensionless variable $\xi = x/\ell$ already known and the new dimensionless variable $\nu = \eta/a$. The new equations for the unknowns ξ and ν are

$$\ell^2\xi^2-\xi(\ell^2+a^2+r_1^2-r_2^2)+r_1^2+a^2[-3\nu^2+2\nu(1+\xi)]=0\,, \tag{17.57}$$

$$\ell^2(\xi^3-\xi^2)+r_1^2(1-\xi)+a^2[-2\nu^3+\nu^2(1+\xi)]=0\,. \tag{17.58}$$

In order to get a linear equation for ν (17.57) is multiplied by $(\lambda_1+\lambda_2\nu)$ and then added to (17.58). The free coefficients λ_1 and λ_2 are then determined such that the coefficients of ν^3 and ν^2 equal zero. This yields two linear equations for λ_1 and λ_2. Their solutions are $\lambda_1 = -(1+\xi)/9$, $\lambda_2 = -2/3$. The resulting linear equation for ν has the solution

$$\nu=\frac{8(\ell^2\xi^3+r_1^2)+\xi^2(r_1^2-9\ell^2+a^2-r_2^2)+\xi(\ell^2-9r_1^2+a^2-r_2^2)}{2\{\xi^2(a^2+3\ell^2)-\xi[3(\ell^2+r_1^2-r_2^2)+a^2]+a^2+3r_1^2\}}\,. \tag{17.59}$$

This expression is substituted back into (17.57). The result of this procedure is the desired sixth-order equation for ξ:

$$C_6\xi^6+C_5\xi^5+C_4\xi^4+C_3\xi^3+C_2\xi^2+C_1\xi+C_0=0\,. \tag{17.60}$$

The coefficients[3] are

$$\left.\begin{aligned}
C_6 &= 4\ell^2(\ell^2-a^2)^2\,,\\
C_5 &= 4\ell^2[(r_2^2-r_1^2)(3\ell^2+5a^2)-3(\ell^2-a^2)^2]\,,\\
C_4 &= (a^2+12\ell^2)[(\ell^2-a^2)^2+(r_1^2-r_2^2)^2-2\ell^2(r_1^2+r_2^2)]\\
&\quad -2a^4(r_1^2+r_2^2)+20\ell^2[3r_1^2(\ell^2+a^2)+a^2(r_1^2-r_2^2)]\,,\\
C_3 &= -2\Big[2(\ell^6+r_1^6)+18\ell^2r_1^2(\ell^2+r_1^2)-3(\ell^4+r_1^4)(a^2+2r_2^2)\\
&\quad +2\ell^2r_1^2(29a^2-12r_2^2)+2r_2^2(\ell^2+r_1^2)(3r_2^2-a^2)\\
&\quad +(a^2-2r_2^2)(a^2-r_2^2)^2\Big]\,.
\end{aligned}\right\} \tag{17.61}$$

C_0, C_1 and C_2 are obtained from C_6, C_5 and C_4, respectively, by interchanging ℓ and r_1, and C_3 is symmetric with respect to ℓ and r_1. To every real solution ξ the corresponding ν is calculated from (17.59). With

[3] In [14] the symmetry with respect to ℓ and r_1 is not shown. The coefficient of x^5 is misprinted. The correct coefficient is $d[32b^2(a^2-c^2)-12(d^2-b^2)n]$. Another misprint occurs in Eq.(30) which must begin with $(x-d)$ instead of with $(x-d)^2$

$x = \ell\xi$ and $\eta = a\nu$ (17.54) determines the corresponding angle φ. The corresponding stationary value of $1/i$ is given by (17.27): $1/i = \xi/(\xi - 1)$.

Consider again two four-bars resulting one from the other by interchanging the link lengths r_1 and ℓ. Let (17.60) be the conditional equation for one of these four-bars. The equation for the other four-bar is $C_0\xi^6 + C_1\xi^5 + C_2\xi^4 + C_3\xi^3 + C_4\xi^2 + C_5\xi + C_6 = 0$. If ξ is a root of one equation, $1/\xi$ is root of the other equation. With both roots (17.59) and (17.54) determine one and the same angle φ. For both roots the corresponding quantities $1/i$ are calculated from (17.27). These two quantities add up to one.

It is seen that $C_6 = 0$ if $a = \ell$ and that $C_0 = 0$ if $a = r_1$. In either case (17.60) is of fifth order. Under the same conditions also the previous method resulted in a fifth-order equation (see (17.52)). In the case $r_1 = \ell$, the previous method resulted in the third-order Eq.(17.45). With the present method this case yields the identities $C_6 = C_0$, $C_5 = C_1$ and $C_4 = C_2$. Equation (17.60) then has the form

$$C_0\xi^6 + C_1\xi^5 + C_2\xi^4 + C_3\xi^3 + C_2\xi^2 + C_1\xi + C_0 = 0 . \tag{17.62}$$

If ξ is a root, also $1/\xi$ is a root. Also the quadratic equation $\xi^2 + b\xi + 1 = 0$ has this property. Hence there exist coefficients b_1, b_2, b_3 such that (17.62) has the form

$$C_0(\xi^2 + b_1\xi + 1)(\xi^2 + b_2\xi + 1)(\xi^2 + b_3\xi + 1) = 0 . \tag{17.63}$$

The determination of b_1, b_2, b_3 by comparison of coefficients requires solving a cubic equation.

17.7 Transmission of Forces and Torques

Transmission of motion is not the only purpose of mechanisms. Equally important is transmission of forces and torques. In what follows, the state of equilibrium of an arbitrary planar or spatial single-degree-of-freedom mechanism is investigated. The planar four-bar is just an example. For every mechanism the input variable is called φ, and the output variable is called ψ. Let, furthermore, M_1 be the driving torque applied to the input link, and let M_2 be the counteracting torque applied to the output link. Thus, a torque $M_1 > 0$ is accelerating the mechanism and a torque $M_2 > 0$ is decelerating it. In a state of equilibrium the ratio M_2/M_1 has a certain value. It is determined from the equilibrium condition. According to the principle of virtual power this is the equation

$$M_1\delta\dot{\varphi} + (-M_2)\delta\dot{\psi} = 0 . \tag{17.64}$$

From the definition of the transmission ratio $i = \dot{\varphi}/\dot{\psi}$ it follows that $\delta\dot{\psi} = \delta\dot{\varphi}/i$. Therefore, the equilibrium condition is $(M_1 - M_2/i)\delta\dot{\varphi} = 0$. Hence

$$\frac{M_2}{M_1} = i \,. \tag{17.65}$$

This equation is valid in the more general sense that φ and ψ are generalized coordinates (for example, angles or cartesian coordinates), and that M_1, M_2 are the associated generalized forces (torques or forces).

In a mechanism for the generation of large forces or torques the transmission ratio i should be as large as possible. Typical examples are shears, prongs and clamping devices of various kinds. In what follows, the shears shown in Figs. 17.14a – d are investigated. Each of them is a four-bar. The input and output variables are the opening widths x_1 and x_2 between the points of application of the hand forces F_1 and the cutting forces F_2, respectively. In each case the equilibrium condition (17.65) is

$$\frac{F_2}{F_1} = \frac{\dot{x}_1}{\dot{x}_2} \,. \tag{17.66}$$

In each case the ratio of forces is to be expressed in terms of the lengths given in the figures.

Solution: Since x_1 and x_2 describe relative positions, it is unnecessary to declare any particular link as fixed link. In Table 17.1 the velocities $\dot{x}_1$ and $\dot{x}_2$ are expressed in terms of relative angular velocities (positive counterclockwise). These expressions are obvious from the figures. In each expression

Table 17.1 Ratio F_2/F_1 in terms of angular velocities

shears	(a)	(b)	(c)	(d)
$\frac{F_2}{F_1} = \frac{\dot{x}_1}{\dot{x}_2}$	$\frac{\ell_1}{\ell_4}\,\frac{\omega_{10}}{\omega_{23}}$	$\frac{\ell_1+\ell_2}{\ell_4}\,\frac{\omega_{10}}{\omega_{20}}$	$\frac{\ell_1+\ell_2}{\ell_2+\ell_3+\ell_4}\,\frac{\omega_{10}}{\omega_{23}}$	$\frac{\ell_1}{\ell_4}\,\frac{\omega_{10}}{\omega_{23}}$

the two relative angular velocities are related through a constraint equation. These equations have the following forms.

(a) $\dot{x}_3 = -\ell_2\omega_{10} = -\ell_3\omega_{23}$,

(b) The constraint $\dot{x}_3 = 0$ means that $\ell_2\omega_{10} - (\ell_2 + \ell_3)\omega_{20} = 0$,

(c) $\dot{x}_3 = -\ell_3\omega_{10} = -(\ell_2 + \ell_3)\omega_{23}$,

(d) In Fig. 17.14d instantaneous centers are shown. From (15.6) it follows that $\omega_{10}/\omega_{30} = L_4/L_3$ and $\omega_{23}/\omega_{30} = L_1/L_2$ and, consequently, $\omega_{10}/\omega_{23} = L_2L_4/(L_1L_3)$.

With these constraint equations the final results shown in Table 17.2 are obtained.

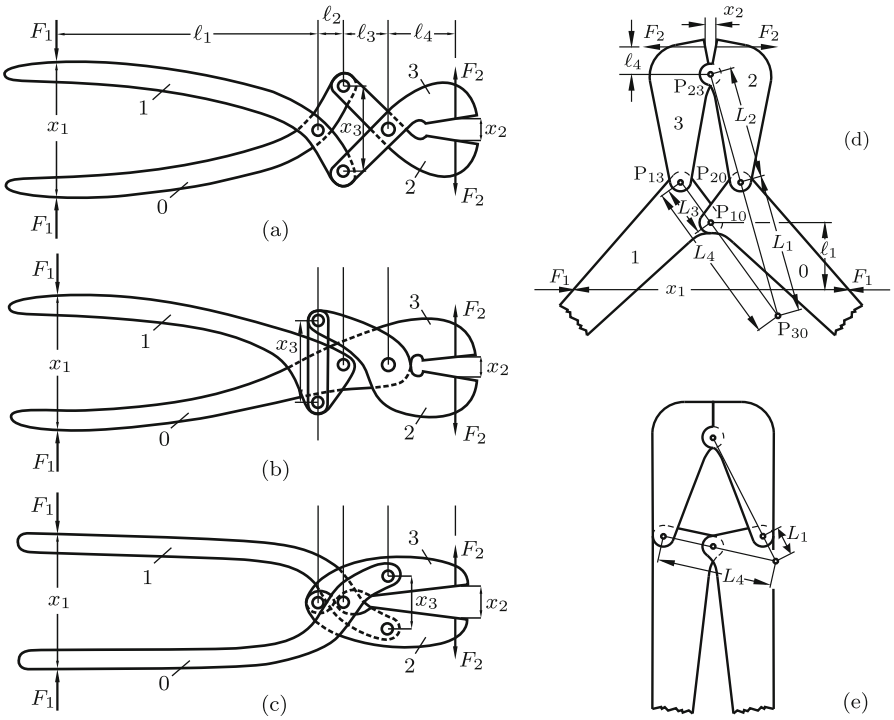

Fig. 17.14 Shears (**a**), (**b**), (**c**) with parameters $\ell_1, \ldots, \ell_4$ and shears (**d**) with instantaneous centers of rotation open and closed (**e**)

Table 17.2 Ratio F_2/F_1 in terms of link lengths

shears	(a)	(b)	(c)	(d)
$\frac{F_2}{F_1}$	$\frac{\ell_1\ell_3}{\ell_2\ell_4}$	$\frac{(\ell_1+\ell_2)(\ell_2+\ell_3)}{\ell_2\ell_4}$	$\frac{(\ell_1+\ell_2)(\ell_2+\ell_3)}{\ell_3(\ell_2+\ell_3+\ell_4)}$	$\frac{\ell_1 L_2}{\ell_4 L_3}\,\frac{L_4}{L_1}$

Comparative evaluation: Figures 17.14a,b,c are drawn with identical lengths $\ell_1 = 35$, $\ell_2 = 3.5$, $\ell_3 = 6$, $\ell_4 = 9$. With these lengths $F_2/F_1 \approx 6.7$ for the shears (a), $F_2/F_1 \approx 11.6$ for the shears (b) and $F_2/F_1 \approx 3.3$ for the shears (c). Shears (c) are the only ones in which the object to be cut can be placed in the position $\ell_4 = 0$. Then, $F_2/F_1 \approx 6.4$. With parameters of commercially available pruning-shears of this kind a ratio $F_2/F_1 = 15$ is possible. Compared with all other devices these shears have the advantage that for a given width of the object to be cut the opening angle between the shearing blades is the smallest.

In shears (d) the lengths L_2 and L_3 are constant. The lengths L_4 and L_1 depend very much on the opening angle. Both of them decrease monotonically in the process of closing the blades. Figure 17.14e shows the blades fully closed. The dimensions should be chosen such that in this position the instantaneous centers P_{13}, P_{10} and P_{20} are almost collinear as shown. In this case, the ratio L_4/L_1 is > 1 in every position, and it increases monotonically when the blades are closing. With shears of this kind reinforcement steel rods of 15 mm diameter can be cut by hand.

17.8 Coupler Curves

Every point fixed in the plane of the coupler traces a *coupler curve* when the four-bar is moving through its entire range. It is the complexity of these curves to which the four-bar owes much of its importance in engineering (see Fig. 17.2). In the following sections properties of coupler curves are investigated. The curvature of coupler curves was the subject of Sect. 15.3.3 (see Fig. 15.19).

17.8.1 Roberts/Tschebychev Theorem. Cognate Four-Bars

Figure 17.15 is started by drawing the four-bar $\mathrm{A_0A_1B_1B_0}$ and a point C fixed in the plane of the coupler $\mathrm{A_1B_1}$. This plane is represented by the *coupler triangle* ($\mathrm{A_1}$,$\mathrm{B_1}$,C). Subject of investigation is the coupler curve generated by C. To this basic figure lines $\mathrm{A_0A_2C}$ and $\mathrm{B_0A_3C}$ are added thus creating two parallelograms. In the next step, triangles similar to the coupler triangle are drawn as shown with bases $\mathrm{A_2C}$ and $\mathrm{A_3C}$. This results in points $\mathrm{B_2}$ and $\mathrm{B_3}$. Finally, another parallelogram defining the point $\mathrm{C_0}$ is drawn. Point $\mathrm{A_0}$ is made the origin of a complex plane. In this complex plane arbitrary points such as $\mathrm{B_1}$, for example, are interpreted as complex numbers. The number is given the name of the point itself. For the addition of complex numbers the parallelogram rule is valid. This means, for example, that the number C_0 is the sum

$$C_0 = A_2 + (B_2 - A_2) + (C_0 - B_2) \,. \tag{17.67}$$

The coupler triangle ($\mathrm{A_1}$,$\mathrm{B_1}$,C) defines the complex number

$$z = \frac{|C - A_1|}{|B_1 - A_1|} \, \mathrm{e}^{\mathrm{i}\,\alpha} \,. \tag{17.68}$$

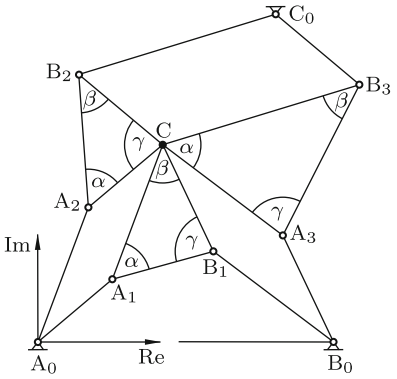

Fig. 17.15 Roberts/Tschebychev theorem

The definition is such that

$$C - A_1 = (B_1 - A_1)z \; . \tag{17.69}$$

For the three terms in (17.67) the figure yields the expressions

$$A_2 = C - A_1 = (B_1 - A_1)z \; , \qquad B_2 - A_2 = (C - A_2)z = A_1 z \; , \tag{17.70}$$

$$C_0 - B_2 = B_3 - C = (A_3 - C)z = (B_0 - B_1)z \; . \tag{17.71}$$

Substitution into (17.67) reveals that

$$C_0 = (B_1 - A_1 + A_1 + B_0 - B_1)z = B_0 z = \text{ const} \; . \tag{17.72}$$

Thus, C_0 remains fixed independent of the motion of the four-bar $A_0A_1B_1B_0$. From this follows

Theorem 17.2. (Roberts[4]/Tschebychev[5]) *For every four-bar* $A_0A_1B_1B_0$ *with a coupler point* C *there exist two additional four-bars* $A_0A_2B_2C_0$ *and* $B_0A_3B_3C_0$ *the coupler points* C *of which trace one and the same coupler curve. Because of this property the three four-bars are said to be cognate.*

The coupler triangles of the three four-bars are similar, but in each triangle another angle is opposite the coupler. Equation (17.72) shows that also the triangle (A_0,B_0,C_0) is similar to the coupler triangle (A_1,B_1,C). For B_2 the sum of the two Eqs.(17.70) yields

$$B_2 = B_1 z \; . \tag{17.73}$$

[4] Samuel Roberts (1827-1913); published 1875

[5] Pavnuty Lvovic Tschebychev (1821-1894); he considers a basic figure with arbitrary coupler triangle, but with identical link lengths $r_1 = r_2$, and he constructs geometrically one other four-bar ([40] p.273 published in 1878)

Hence also the triangle (A_0,B_1,B_2) is similar to the coupler triangle and with the same argument also the triangle (B_0,A_1,B_3).

Imagine that the three four-bars are physically connected at C, and that B_0 and C_0 are free to move. The resulting mechanism is deformable subject to the constraints that (i) links and coupler triangles remain undeformed, and that (ii) parallelograms remain parallelograms. In Fig. 17.16 a position is shown in which the links of four-bar $A_0A_1B_1B_0$ are stretched out in the line $A_0\tilde{A}_1\tilde{B}_1\tilde{B}_0$. The new positions of the remaining points (denoted by the symbol tilde) are determined by the three parallelograms not shaded and by the three similar coupler triangles (shaded). In this position all three four-bars have their links stretched out. The triangle $(A_0\tilde{B}_0\tilde{C}_0)$ is similar to the coupler triangles. It is this figure from which all lengths of the other two four-bars are most easily obtained.

Figure 17.15 is particularly simple if the coupler point C in the four-bar $A_0A_1B_1B_0$ is located on the line $\overline{A_1B_1}$ of the coupler. This case is characterized by $\alpha = 0$ or π and z real. From this it follows that in all three four-bars C is located on the coupler line. The positions of C_0, A_2, B_2, A_3 and B_3 are determined by the equations $C_0 = B_0 z$, $A_2 = (B_1 - A_1)z$, $B_2 = B_1 z$, $B_3 = C + (B_0 - A_1)z$ with real z. Figure 17.17 explains how to proceed geometrically when the four-bar $A_0A_1B_1B_0$ and point C on the coupler are given. As in Fig. 17.15 A_2 and A_3 are constructed by drawing the parallelograms $A_0A_1CA_2$ and $B_0B_1CA_3$. Next, B_2 and B_3 are constructed, the former as point of intersection of the lines $\overline{A_0B_1}$ and $\overline{CA_2}$ and the latter as point of intersection of the lines $\overline{B_0A_1}$ and $\overline{CA_3}$. Finally, C_0 is constructed as in Fig. 17.15 by drawing the parallelogram $B_2CB_3C_0$.

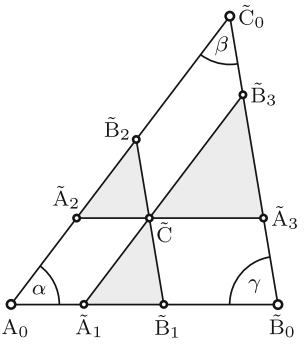

Fig. 17.16 Cognate four-bars of Fig. 17.15 deformed

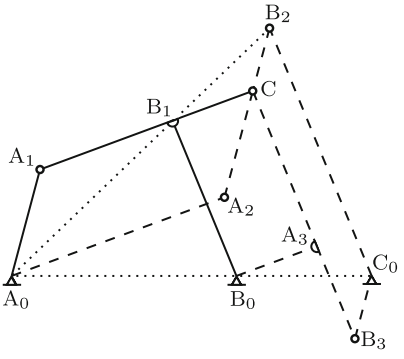

Fig. 17.17 Cognate four-bars with coupler point C on the coupler line

In what follows, the general case shown in Fig. 17.15 is considered again. The parallelity of lines in parallelograms in combination with the rigidity of coupler triangles has the consequences: If one of the links $\overline{A_0A_1}$, $\overline{A_2B_2}$ and

$\overline{C_0B_3}$ is fully rotating, all three of them are fully rotating, and if any one of them is not fully rotating, none of them is fully rotating. The same statements apply to the links $\overline{B_0B_1}$, $\overline{A_3B_3}$ and $\overline{C_0B_2}$. The combination of these arguments leads to the following statements:

1. If four-bar $A_0A_1B_1B_0$ is a double-rocker of second kind, the other two four-bars are double-rockers of second kind as well.
2. If four-bar $A_0A_1B_1B_0$ is a double-crank, the other two four-bars are double-cranks as well.
3. If four-bar $A_0A_1B_1B_0$ is a crank-rocker with crank $\overline{A_0A_1}$, four-bar $A_0A_2B_2C_0$ is double-rocker of first kind, and four-bar $B_0A_3B_3C_0$ is a crank-rocker with crank $\overline{C_0B_3}$.
4. If four-bar $A_0A_1B_1B_0$ is a double-rocker of first kind, the other two four-bars are crank-rockers with cranks $\overline{A_0A_2}$ and $\overline{B_0A_3}$, respectively.

The Roberts-Tschebychev theorem has important engineering applications. If the generation of some particular coupler curve is required and if there is not enough space for the chosen four-bar, the same coupler curve is generated by two other four-bars which are located somewhere else and which are different in size. The same curve can be generated by still other linkages. Equation (17.71), $C_0 - B_2 = (B_0 - B_1)z$, shows that the links $\overline{C_0B_2}$ and $\overline{B_0B_1}$ have identical angular velocities when the four-bars are moving. Identical angular velocities are produced also by means of three gears with centers fixed in the base according to Fig. 17.18a. The two outer gears have arbitrary, but equal diameters, and each of them is rigidly connected with one of the two links. The central gear has arbitrary diameter and arbitrary location. When the central gear is set into motion, C is generating the same coupler curve that is generated by the three four-bars.

The linkage shown in Fig. 17.18b is composed of some of the links in Fig. 17.15. The degree of freedom is two. The parallelogram is free to rotate as rigid body about A_0. It may also deform. Hence it is possible to guide B_1 along an arbitrarily prescribed curve (within a certain workspace). From (17.73), $B_2 = B_1 z$, it follows that B_2 generates the same curve rotated through the angle α and multiplied by the factor $|z| = \overline{A_1C}/\overline{A_1B_1}$. This linkage is called Sylvester's plagiograph [38], v.3.

If, in particular, B_1 is guided along a straight line f_1 (arbitrary), B_2 is moving along a straight line f_2 which is rotated counter-clockwise against f_1 through α. The links $A_0A_1B_1$ with B_1 guided along f_1 constitute a slider-crank mechanism, and the links $A_0A_2B_2$ with B_2 guided along f_2 constitute another slider-crank mechanism. With both mechanisms the coupler-fixed point C traces one and the same coupler curve. Thus, the existence of two cognate slider-crank mechanisms is proved. The figure explains how to construct one from the other.

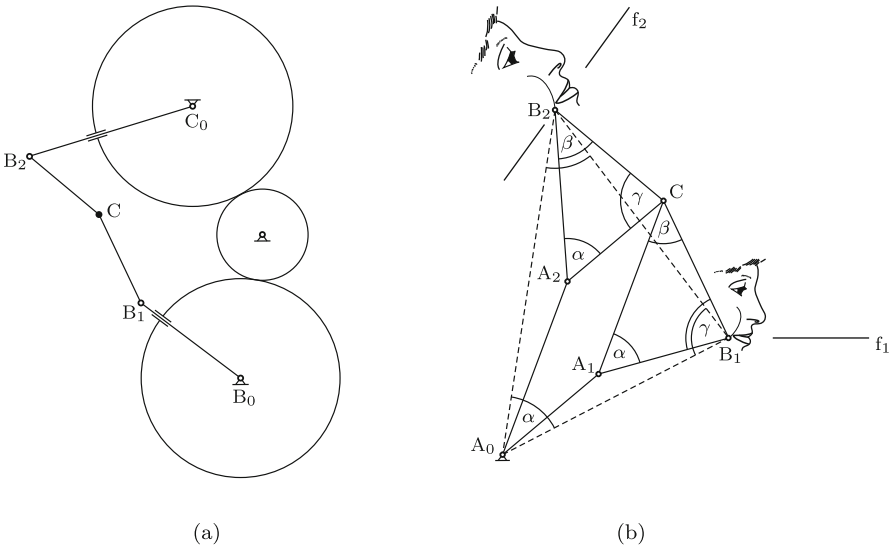

Fig. 17.18 **Fig. a:** The trajectory of C is identical with the coupler curve generated in Fig. 17.15. **Fig. b:** Sylvester's plagiograph. Cognate slider-crank mechanisms defined by f_1 and f_2

17.8.2 Parameter Equations for Coupler Curves

For the graphical display of coupler curves a parameter representation of the curve is required which determines, in the x, y-system of Fig. 17.19, the coordinates x and y of the coupler point C as functions of the input angle φ. Constant parameters in these functions are ℓ, r_1, r_2, a and the coordinates η and ζ of C in the coupler plane. Using the inclination angle

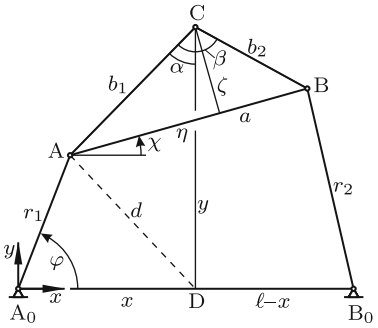

Fig. 17.19 Constant parameters η, ζ, b_1, b_2, β and variable coordinates x, y of the coupler point C

χ of the coupler as auxiliary variable the coordinates of C are

$$x = r_1 \cos\varphi + \eta \cos\chi - \zeta \sin\chi \,, \qquad y = r_1 \sin\varphi + \eta \sin\chi + \zeta \cos\chi \,. \quad (17.74)$$

This is the desired parameter representation of the coupler curve. For $\cos\chi$ and $\sin\chi$ the expressions from (17.23) are substituted:

$$\left.\begin{aligned} \cos\chi_k &= \frac{\bar{A}\bar{C} - (-1)^k \bar{B}\sqrt{\bar{A}^2 + \bar{B}^2 - \bar{C}^2}}{\bar{A}^2 + \bar{B}^2} \,, \\ \sin\chi_k &= \frac{\bar{B}\bar{C} + (-1)^k \bar{A}\sqrt{\bar{A}^2 + \bar{B}^2 - \bar{C}^2}}{\bar{A}^2 + \bar{B}^2} \,, \end{aligned}\right\} \; (k = 1, 2) \,, \qquad (17.75)$$

$$\bar{A} = -2a(\ell - r_1 \cos\varphi) \,, \quad \bar{B} = 2r_1 a \sin\varphi \,, \quad \bar{C} = 2r_1 \ell \cos\varphi - (r_1^2 + \ell^2 + a^2 - r_2^2) \,. \qquad (17.76)$$

Every input angle φ determines two positions of the four-bar and, hence, two positions of the coupler point C. From Sect. 17.1 it is known that double-rockers of first kind (Fig. 17.4c) and of second kind (Figs. 17.5a,b,c) have the property that the two positions can be reached one from the other by a continuous motion. Hence these four-bars have the property that the coupler curve is unicursal (a single closed curve). In contrast, double-cranks and crank-rockers have the property that the two positions associated with a single input angle cannot be reached one from the other by a continuous motion, but only by disconnection and reassembly (see Figs. 17.4a and b). This has the consequence that coupler curves of such four-bars are bicursal (two closed branches). The transition from unicursal to bicursal coupler curves occurs in foldable four-bars. In this case, the two closed branches of a bicursal curve create a singular point. The three coupler curves in Fig. 17.20 demonstrate the transition from unicursal to bicursal curves. Except for r_1 the sets of parameters $(\ell\,,\, r_1\,,\, r_2\,,\, a\,,\, \eta\,,\, \zeta)$ are the same for all three curves. The circle is explained following Eq.(17.87).

17.8.3 Implicit Equation for Coupler Curves

Figure 17.19 is considered again. This time, the location of the coupler point C in the coupler plane is specified not by the parameters $a\,,\, \eta\,,\, \zeta$, but by the parameters $b_1\,,\, b_2\,,\, \beta$. The transformation equations between these two sets of parameters are

$$\left.\begin{aligned} b_1 &= \sqrt{\eta^2 + \zeta^2} \,, \qquad b_2 = \sqrt{(a-\eta)^2 + \zeta^2} \,, \qquad \cos\beta = \frac{b_1^2 + b_2^2 - a^2}{2b_1 b_2} \,, \\ a &= \sqrt{b_1^2 + b_2^2 - 2b_1 b_2 \cos\beta} \,, \quad \eta = \frac{b_1(b_1 - b_2\cos\beta)}{a} \,, \quad \zeta = \frac{b_1 b_2 \sin\beta}{a} \,. \end{aligned}\right\} \qquad (17.77)$$

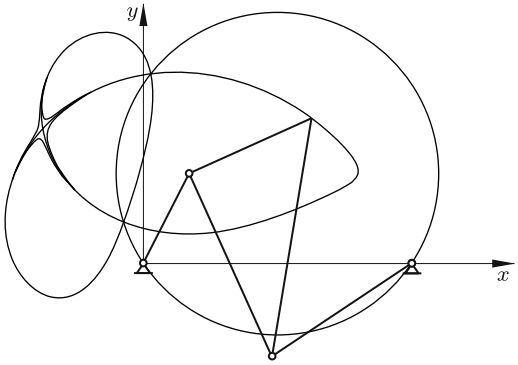

Fig. 17.20 Coupler curves of a double-rocker of second kind with $r_1 = 3.01$ (unicursal), of a foldable four-bar with $r_1 = 3$ and of a crank-rocker with $r_1 = 2.99$ (bicursal). The other parameters $\ell = 8$, $r_2 = 5$, $a = 6$, $\eta = 0$ and $\zeta = 4$ are the same in all three cases. For the circle see (17.87)

For making statements about properties of coupler curves the parameters b_1, b_2, β are more suitable. First statements are the following.
In the case $b_1 = 0$ (in the case $b_2 = 0$), coupler curves are circles or arcs of circles with radius r_1 about A_0 (with radius r_2 about B_0). Coupler curves are confined to the area bounded by the concentric circles about A_0 with radii $|r_1 - b_1|$ and $r_1 + b_1$ and by the concentric circles about B_0 with radii $|r_2 - b_2|$ and $r_2 + b_2$. In the case $b_1, b_2 \gg \ell, a, r_1, r_2$, coupler curves are approximately circles or arcs of circles.

The goal of the following analysis is an implicit equation of the coupler curve in the form $f(x, y, \ell, r_1, r_2, b_1, b_2, \beta) = 0$. In developing this equation the auxiliary variables α and d shown in Fig. 17.19 are used temporarily. From the figure it is seen that

$$x = r_1 \cos\varphi + b_1 \sin\alpha \,. \tag{17.78}$$

The cosine law applied to the triangles (A,D,A_0) and (A,D,C) yields two expressions for d^2. The identity of these expressions is the equation

$$r_1^2 + x^2 - 2xr_1 \cos\varphi = b_1^2 + y^2 - 2b_1 y \cos\alpha \,. \tag{17.79}$$

For $r_1 \cos\varphi$ the expression from (17.78) is substituted. This results in the following equation which is linear with respect to both $\sin\alpha$ and $\cos\alpha$:

$$2b_1(x \sin\alpha + y \cos\alpha) = x^2 + y^2 + b_1^2 - r_1^2 \,. \tag{17.80}$$

The same equations are formulated for the triangles (B,D,C) and (B,D,B_0). They are obtained by replacing in the above equations x, r_1, b_1, α by $\ell - x$, r_2, b_2, $\beta - \alpha$, respectively. To $\sin(\beta - \alpha)$ and to $\cos(\beta - \alpha)$ addition

theorems are applied. The equation equivalent to (17.80) then reads

$$2b_2\Big\{[(x-\ell)\cos\beta + y\sin\beta]\sin\alpha - [(x-\ell)\sin\beta - y\cos\beta]\cos\alpha\Big\}$$
$$= (x-\ell)^2 + y^2 + b_2^2 - r_2^2\,. \tag{17.81}$$

These two equations are solved for $\sin\alpha$ and $\cos\alpha$. Let Δ be the coefficient determinant. It is

$$\Delta = -4b_1b_2[(x^2+y^2)\sin\beta - \ell(x\sin\beta + y\cos\beta)]\,. \tag{17.82}$$

The solutions are

$$\left.\begin{aligned}
\cos\alpha &= \frac{-2}{\Delta}\Big\{b_2(x^2+y^2+b_1^2-r_1^2)[(x-\ell)\cos\beta + y\sin\beta] \\
&\qquad - b_1x[(x-\ell)^2 + y^2 + b_2^2 - r_2^2]\Big\}\,, \\
\sin\alpha &= \frac{-2}{\Delta}\Big\{b_2(x^2+y^2+b_1^2-r_1^2)[(x-\ell)\sin\beta - y\cos\beta] \\
&\qquad + b_1y[(x-\ell)^2 + y^2 + b_2^2 - r_2^2]\Big\}\,.
\end{aligned}\right\} \tag{17.83}$$

Substitution of these expressions into the constraint equation $\cos^2\alpha + \sin^2\alpha = 1$ eliminates the auxiliary variable α. The resulting equation is the desired implicit equation of the coupler curve:

$$\begin{aligned}
&\Big\{b_2(x^2+y^2+b_1^2-r_1^2)[(x-\ell)\sin\beta - y\cos\beta] \\
&\qquad + b_1y[(x-\ell)^2 + y^2 + b_2^2 - r_2^2]\Big\}^2 \\
&+ \Big\{b_2(x^2+y^2+b_1^2-r_1^2)[(x-\ell)\cos\beta + y\sin\beta] \\
&\qquad - b_1x[(x-\ell)^2 + y^2 + b_2^2 - r_2^2]\Big\}^2 \\
&= 4b_1^2b_2^2\Big[(x^2+y^2)\sin\beta - \ell(x\sin\beta + y\cos\beta)\Big]^2\,.
\end{aligned} \tag{17.84}$$

In multiplying out the factor (x^2+y^2) is encountered repeatedly. The equation has the form

$$\begin{aligned}
&p_1(x^2+y^2)^3 + (x^2+y^2)^2(p_2x + p_3y) + (x^2+y^2)(p_4x^2 + p_5xy + p_6y^2 \\
&+p_7x + p_8y) + p_9x^2 + p_{10}xy + p_{11}y^2 + p_{12}x + p_{13}y + p_{14} = 0\,.
\end{aligned} \tag{17.85}$$

With the abbreviations $p = b_1^2 - r_1^2$, $q = \ell^2 + b_2^2 - r_2^2$, $\lambda = 2b_1b_2\cos\beta = b_1^2 + b_2^2 - a^2$, $a\eta = b_1b_2\sin\beta$ and $a\zeta = b_1(b_1 - b_2\cos\beta)$ (see (17.77)) the coefficients are

$$
\left.
\begin{aligned}
p_1 &= a^2 \,, & p_8 &= 2\ell a\zeta(\lambda + r_1^2 + r_2^2 - \ell^2 - a^2) \,, \\
p_2 &= -2\ell a(a+\eta) \,, & p_9 &= Z - 2\ell^2(2a^2\zeta^2 + \lambda p) \,, \\
p_3 &= -2\ell a\zeta \,, & p_{10} &= 4\ell^2 a\zeta(p - \lambda) \,, \\
p_4 &= p_6 + 4\ell^2 a\eta \,, & p_{11} &= Z - \ell^2\lambda^2 \,, \\
p_5 &= 4\ell^2 a\zeta \,, & p_{12} &= \ell p(\lambda q - 2b_2^2 p) \,, \\
p_6 &= \ell^2 b_2^2 + p(b_2^2 - b_1^2 - a^2) + 2a(q\eta - 2a\zeta^2) \,, & p_{13} &= -2\ell a\zeta pq \,, \\
p_7 &= \ell\,[\lambda(3p+q) + 8a^2\zeta^2 - 4(b_2^2 p + b_1^2 q)] \,, & p_{14} &= \ell^2 b_2^2 p^2 \,, \\
& & Z &= p(2\ell^2 b_2^2 - \lambda q) + b_2^2 p^2 + b_1^2 q^2 \,.
\end{aligned}
\right\} \tag{17.86}
$$

The highest-order term $p_1(x^2+y^2)^3$ shows that on each of the imaginary lines $y = +\mathrm{i}x$ and $y = -\mathrm{i}x$ the coupler curve has a triple-root at infinity. The curve is a tricircular sextic.

Proposition: An arbitrary circle with center point coordinates x_0, y_0 and with radius r intersects the coupler curve in six (not necessarily real) points. The following proof provides a method for calculating the intersection points. With a parameter γ the circle has the parameter equations $x = x_0 + r\cos\gamma$, $y = y_0 + r\sin\gamma$. This yields $x^2 + y^2 = r^2 + x_0^2 + y_0^2 + 2r(x_0\cos\gamma + y_0\sin\gamma)$. These expressions are substituted into (17.85). The result is an equation of third order in $\cos\gamma$ and $\sin\gamma$. The substitution $z = \tan\gamma/2$ leads to a 6th-order polynomial equation for z. End of proof.

The existence of six intersection points of a coupler curve and a circle can be expressed in the following alternative form. Given three circles a, b, c and a triangle (A,B,C), there exist six (not necessarily real) positions of the triangle in which A lies on a, B on b and C on c. This result is important for Sect. 17.10 on planar robots.

The equation $\Delta = 0$ can be written in the form

$$
\left(x - \frac{\ell}{2}\right)^2 + \left(y - \frac{\ell}{2}\cot\beta\right)^2 = \left(\frac{\ell}{2\sin\beta}\right)^2 . \tag{17.87}
$$

It is the equation of the circle shown in Fig. 17.21. The circle passes through A_0 and B_0. It has the central semi-angle β and, hence, the peripheral angle β. It was shown that β is also the angle at C_0 in the triangle (A_0,B_0,C_0) of Fig. 17.15. Therefore, also C_0 is located on the circle. From this fact Roberts concluded Theorem 17.2 on the existence of three cognate four-bars generating one and the same coupler curve. The three centers A_0, B_0 and C_0 are referred to as singular foci, and the circle itself is called *circle of singular foci*. Since Δ equals zero on the circle, $\cos\alpha$ and $\sin\alpha$ are indeterminate if the coupler point is located on the circle. Indeterminate means that at least two different positions of the four-bar generate one and the same point of the coupler curve. In other words: The coupler curve intersects the circle at this point at least twice.

Figure 17.22 proves the inverse statement: If the coupler point C is at one and the same point in two (or more) positions of the four-bar, this multiple point lies on the circle. The coupler triangle is (A_1,B_1,C) in one position

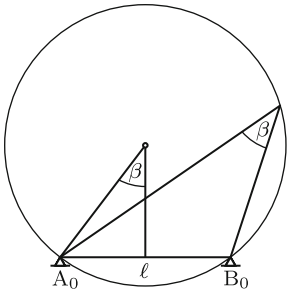

Fig. 17.21 Circle of singular foci

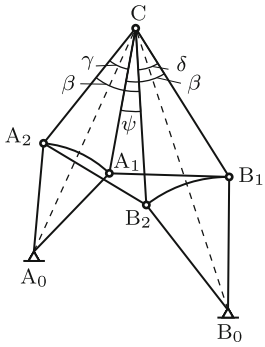

Fig. 17.22 Proof that double points of the coupler curve lie on the circle of singular foci

and (A$_2$,B$_2$,C) in the other. It must be shown that $\sphericalangle$(A$_0$,C,B$_0$) equals the angle β in the coupler triangle. The dashed lines $\overline{\mathrm{A_0C}}$ and $\overline{\mathrm{B_0C}}$ bisect the auxiliary angles γ and δ. With ψ as auxiliary angle $\beta = \gamma + \psi = \delta + \psi$ and, consequently, $\delta = \gamma$. Hence $\sphericalangle$(A$_0$,C,B$_0$)$= \gamma/2 + \psi + \delta/2 = \beta$. End of proof.

There is only a single type of double point of a coupler curve which, in general, is not located on the circle (17.87). This is the singular point on the coupler curve of a foldable four-bar associated with the folded position. It is a point belonging to two branches of the curve and to a single position of the four-bar. Example: The four-bar with parameters $\ell = 8$, $r_1 = 3$, $r_2 = 5$, $a = 6$ is a foldable four-bar. The coupler point $\eta = 0$, $\zeta = 4$ generates the coupler curve shown in Fig. 17.20 which has two ordinary double points on the circle (17.87) and the singular double point related to the folded position.

Conditions for the singular double point to lie on the circle of singular foci are formulated as follows. Let the parameters of the foldable four-bar satisfy the condition $\ell + r_1 = a + r_2$. In the folded position the coupler point C has the coordinates $x = \eta - r_1$, $y = \zeta$. The condition to lie on the circle $\Delta = 0$ is, according to (17.82),

$$[b_1^2 + r_1^2 + r_1\ell - \eta(2r_1 + \ell)]\sin\beta - \zeta\ell\cos\beta = 0 \tag{17.88}$$

and with η and ζ from (17.77)

$$a(b_1^2 + r_1^2 + r_1\ell) - b_1^2(2r_1 + \ell) + 2r_1b_1b_2\cos\beta = 0 \tag{17.89}$$

and with $\cos\beta$ from (17.77)

$$(\ell + r_1 - a)(r_1a - b_1^2) + r_1b_2^2 = 0\,. \tag{17.90}$$

With $\ell + r_1 - a = r_2$ this is the first equation below. Both equations together constitute the desired conditions.

$$a = \frac{b_1^2}{r_1} - \frac{b_2^2}{r_2} , \qquad \ell = a + r_2 - r_1 . \tag{17.91}$$

In terms of dimensionless parameters μ_1, μ_2 the conditions are

$$\left.\begin{aligned} b_1 &= \mu_1 r_1 , & b_2 &= \mu_2 r_2 , \\ a &= \mu_1^2 r_1 - \mu_2^2 r_2 , & \ell &= (\mu_1^2 - 1) r_1 - (\mu_2^2 - 1) r_2 . \end{aligned}\right\} \tag{17.92}$$

The parameters μ_1, r_1, μ_2, r_2 can be chosen arbitrarily subject to the conditions that (i) $a > 0$, (ii) a, b_1, b_2 satisfy the triangle inequalities and (iii) $\ell > 0$.

In what follows, four-bars are considered which are not foldable. Like any other circle the circle of singular foci (17.87) intersects a coupler curve at not more than six real points. Hence a coupler curve can have at most three double points. In Fig. 17.23 a coupler curve with three double points is shown. It is generated by a double-rocker with parameters $\ell = 10$, $r_1 = 4$, $a = 4$, $r_2 = 9$, $\eta = 2$, $\zeta = 4$. Two double points may coincide in a quadruple point. An example is shown in Fig. 17.28.

A double point degenerates into a cusp if the loop associated with the double point contracts into a single point. From this it follows that also cusps lie on the circle (17.87), and that the maximum number of cusps is three. The condition for a cusp to exist is that the coupler point C is located on the moving centrode of the coupler. In the course of rolling of the moving centrode on the fixed centrode the point C generates the cusp when it is the point of contact, i.e., the instantaneous center of rotation of the coupler and, hence, the intersection point of the input and the output link of the four-bar.

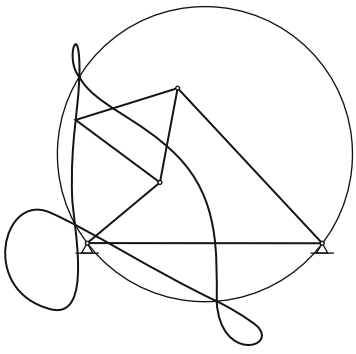

Fig. 17.23 Coupler curve with three double points on the circle with Eq.(17.87). Double-rocker with parameters $\ell = 10$, $r_1 = 4$, $a = 4$, $r_2 = 9$, $\eta = 2$, $\zeta = 4$

Figure 17.24 demonstrates that this may happen in altogether four different configurations. The common feature is that the segments of lengths (r_1, b_1) and (r_2, b_2) are pairwise collinear. In any such configuration the base $\overline{A_0B_0}$ is seen from C either under the angle β or under the angle $\pi - \beta$. This proves again that cusps lie on the circle (17.87). In the four-bar A_0ABB_0 drawn with thick lines the cosine law applied to the triangles (A_0,B_0,C) and (A,B,C) yields the equations

$$\left.\begin{aligned} \ell^2 &= (r_1 + b_1)^2 + (r_2 + b_2)^2 - 2(r_1 + b_1)(r_2 + b_2)\cos\beta \,, \\ a^2 &= b_1^2 + b_2^2 - 2b_1 b_2 \cos\beta \,. \end{aligned}\right\} \tag{17.93}$$

Elimination of $\cos\beta$ results in a condition for the existence of cusps:

$$b_1 b_2[(r_1+b_1)^2+(r_2+b_2)^2-\ell^2]-(r_1+b_1)(r_2+b_2)(b_1^2+b_2^2-a^2) = 0 \,. \tag{17.94}$$

With reference to Fig. 17.24 (b_1, b_2) can be replaced by $(-b_1, b_2)$, $(b_1, -b_2)$ and $(-b_1, -b_2)$.

Example: To be determined are parameters of coupler curves of foldable four-bars of the kind $\ell + r_1 = a + r_2$ which have not only the singular double point, but also a cusp on the circle of singular foci.
Solution: The parameters must satisfy (17.92) as well as (17.94). Substitution of the expressions (17.92) into (17.94) results in
$(\mu_1 + \mu_2 - 1)[\mu_1(1 + \mu_1)r_1 - \mu_2(1 + \mu_2)r_2]^2 = 0$, i.e.,

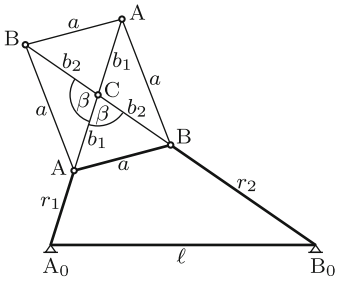

Fig. 17.24 Four different four-bars A_0ABB_0 in positions in which the coupler point C coincides with the instantaneous center of rotation of the coupler thereby passing through a cusp of its coupler curve

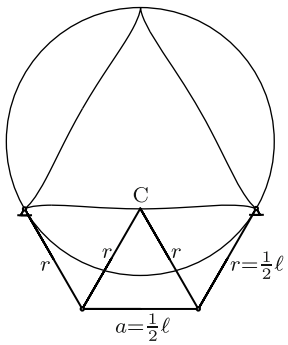

Fig. 17.25 Coupler curve with three cusps on the circle with Eq.(17.87). Symmetrical double-rocker with parameters $r_1 = a = r_2 = b_1 = b_2 = .5\ell$

$$\left.\begin{array}{lll} \text{either} \quad \mu_2 = 1 - \mu_1 & (\,\mu_1\,,\, r_1\,,\, r_2 \text{ arbitrary}) & \text{(a)} \\ \text{or} \quad r_2 = \dfrac{\mu_1(1+\mu_1)}{\mu_2(1+\mu_2)} r_1 & (\,\mu_1\,,\, \mu_2,\, r_1 \text{ arbitrary}) & \text{(b)}\,. \end{array}\right\} \tag{17.95}$$

As is the case in (17.94) $(\,\mu_1\,,\,\mu_2\,)$ may be replaced by $(\,-\mu_1\,,\,\mu_2\,)$, $(\,\mu_1\,,\,-\mu_2\,)$ and $(\,-\mu_1\,,\,-\mu_2\,)$. Parameters of coupler curves having the desired properties are determined either from (a) or from (b). Condition (b) is a special case. Substitution of this expression for r_2 and of $b_1 = \mu_1 r_1$, $b_2 = \mu_2 r_2$ into the second Eq.(17.93) shows that $\cos\beta = 1$. This means that the generating point of the coupler curve lies on the coupler. End of example.

Figure 17.25 is proof of the existence of coupler curves with three cusps. A coupler curve has three cusps if in one of the three positions both A and B are located on the circle with the diameter A_0–B_0 (Cayley [6] v.9:551–580, Mayer [27]). Let the position drawn in thick lines in Fig. 17.24 be modified so as to satisfy this condition. The angles in the coupler triangle are denoted β, $\sphericalangle(\mathrm{CBA}) = \alpha$ and $\sphericalangle(\mathrm{CAB}) = \gamma$. Proposition: The triangles (C,A_0,B_0) and (C,A,B) are congruent with $\sphericalangle(\mathrm{CA_0B_0}) = \alpha$ and $\sphericalangle(\mathrm{CB_0A_0}) = \gamma$. Proof: It suffices to prove the first identity. This is done in three steps.
1. $\sphericalangle(\mathrm{CA_0B}) = \pi/2 - \beta$ (right-angled triangle).
2. The center 0 of the said circle is the apex of the three isosceles triangles (A_0,0,A), (A,0,B) and (B,0,B_0). The second triangle has the apex angle $\sphericalangle(\mathrm{A0B}) = \pi - 2\beta$ (twice the angle subtended by A–B). Hence $\sphericalangle(\mathrm{BA0}) = \sphericalangle(\mathrm{AB0}) = \beta$.
3. The angles $\sphericalangle(\mathrm{CA_0B_0}) = \sphericalangle(\mathrm{A_0}A0)$ and $\sphericalangle(\mathrm{CBA}) = \alpha$ are both equal to $\pi - \beta - \gamma$. End of proof. The bisected isosceles triangles establish for the internal angles of the triangles the formulas

$$\cos\alpha = \pm\frac{r_1}{\ell}\,, \qquad \cos\beta = \frac{a}{\ell}\,, \qquad \cos\gamma = \pm\frac{r_2}{\ell}\,, \qquad \alpha+\beta+\gamma = \pi\,. \tag{17.96}$$

The signs $\pm$ take into account that, formally, the sign of r_1 and/or r_2 can be reversed. The cosines of the internal angles $\beta_{1,2,3}$ of an arbitrary triangle satisfy the equation[6]

$$\sum_{i=1}^{3} \cos^2\beta_i + 2\prod_{i=1}^{3}\cos\beta_i = 1\,. \tag{17.97}$$

Hence Eqs.(17.96) are equivalent to

$$\frac{a^2 + r_1^2 + r_2^2}{\ell^2} \pm 2\,\frac{a r_1 r_2}{\ell^3} = 1\,. \tag{17.98}$$

This equation shows that ℓ is the largest link length. If two of the three ratios r_1/ℓ, r_2/ℓ, a/ℓ are given, the equation is a quadratic equation for

[6] Proved by substituting $\beta_3 = \pi - (\beta_1 + \beta_2)$

the third. The ratios determine the angles in the coupler triangle, the side lengths $b_1 = a \sin\alpha / \sin\beta$, $b_2 = a \sin\gamma / \sin\beta$ and the position of the cusp. This cusp is referred to as principal cusp because it is the only one in which both endpoints of the coupler are located on the circle with the diameter A_0–B_0. In the other two positions only one of them is on this circle. More precisely, in the second position the endpoint originally at A has moved to the reflection A' of A in the line $\overline{A_0B_0}$, and the cusp is on the line $\overline{A_0A'}$ at the distance $|r_1 - b_1|$ from A_0. Similarly, in the third position the endpoint originally at B has moved to the reflection B' of B in the line $\overline{A_0B_0}$, and the cusp is on the line $\overline{B_0B'}$ at the distance $|r_2 - b_2|$ from B_0. Simple algebra reveals that the distances of the second and of the third cusp from the principal cusp are $\ell \sin 2\alpha / \sin\beta$ and $\ell \sin 2\gamma / \sin\beta$, respectively. These expressions resemble those for b_1 and b_2. According to the Roberts-Tschebychev Theorem three cusps are generated by three cognate four-bars. Each cusp is the principal cusp for one of these four-bars. In Fig. 17.25 the three cognate four-bars are congruent.

The conditions (17.96) are particularly simple in the case of foldable four-bars. Example: Foldable four-bars of the kind $a + r_2 = \ell + r_1$. With (17.96) this equation is $\cos\beta + \cos\gamma = 1 + \cos\alpha = 1 - \cos(\beta + \gamma)$ or

$$(1 + \cos\beta)\cos\gamma - \sin\beta\sin\gamma = 1 - \cos\beta \,. \tag{17.99}$$

This is an equation for γ in terms of β. It has real roots γ for angles β satisfying the condition $\cos\beta \geq 2 - \sqrt{5}$ ($\beta < 104°$ approximately).

Additional material on coupler curves is found in Mayer [27] and Müller [28, 30, 31].

17.8.4 Symmetrical Coupler Curves

Coupler curves which are symmetrical with respect to the base line $\overline{A_0B_0}$ have an Eq.(17.84) in which y appears in terms of even orders only. For this it is necessary that $\sin\beta = 0$. This means that the generating coupler point C lies on the coupler line $\overline{AB}$ (not necessarily between the points A and B). The coupler curve in Fig. 17.2 is an example. According to the Roberts-Tschebychev theorem every such coupler curve is generated by two more four-bars. Also in these four-bars the coupler point lies on the coupler line.

In Eq.(17.84) for symmetrical coupler curves with $\sin\beta = 0$ the parameters are $b_1 = \eta$ and $b_2 = \eta - a$ where η is the parameter used in Fig. 17.19. Of particular interest are intersection points of the coupler curve with the axis of symmetry. With $y = 0$ the following equation is obtained for these points which is of third order in x and in η:

$$(\eta - a)(x - \ell)(x^2 + \eta^2 - r_1^2) - \eta x[(x - \ell)^2 + (\eta - a)^2 - r_2^2] = 0\,. \quad (17.100)$$

For given parameters the equation has either one or three real roots x. For this reason one does not expect coupler curves which do not intersect the x-axis. Such coupler curves do exist, however. Example: If $\eta = 2a$ and $r_2 = a$, the equation has the roots $x_1 = \ell$ and $x_{2,3} = \ell \pm \sqrt{4a^2 + \ell^2 - r_1^2}$. For the parameter values $\ell = 1$, $a = 1.3$ and $r_1 = 0.4$ the three roots are real. Yet, the coupler curve does not intersect the x-axis. In Fig. 17.38 the branch of this curve above the x-axis is shown. The three real roots are marked B_0, P_1 and P_2. They represent singular points of the coupler curve. In order to understand this phenomenon (17.80) and (17.81) must be formulated for the special case $b_1 = \eta$, $b_2 = \eta - a$, $\beta = 0$, $y = 0$:

$$x^2 + \eta^2 - 2x\eta \sin\alpha = r_1^2\,, \qquad (x - \ell)^2 + (\eta - a)^2 - 2(x - \ell)(\eta - a)\sin\alpha = r_2^2\,. \quad (17.101)$$

Each equation expresses the cosine law for one of the triangles of Fig. 17.13. The elimination of $\sin\alpha$ is possible without imposing the constraint equation $\cos^2\alpha + \sin^2\alpha = 1$. Simple linear combination of the equations results in (17.100). Only those real solutions of this equation are admissible solutions for which Eqs.(17.101) yield $|\sin\alpha| \le 1$.

Symmetrical coupler curves of a different nature are generated if the four-bar and the coupler triangle satisfy the symmetry conditions $r_1 = r_2 = r$ and $b_1 = b_2 = b$, respectively. Fig. 17.26 shows the system in its symmetrical trapezoidal position. The coupler curve of point C is symmetrical with respect to the midnormal of the base $\overline{\mathrm{A_0B_0}}$. The figure shows also one of the cognate four-bars which, according to the Roberts-Tschebychev theorem, generate the same coupler curve. The third four-bar is the reflection of the second in the midnormal of the base $\overline{\mathrm{A_0B_0}}$. The parameters of the second four-bar are denoted r_1', a', r_2', b_1', b_2'. They satisfy the condition $r_2' = b_2' = a'$. Hence also this is a sufficient condition for the coupler curve to be symmetric. The symmetry axis passes through C_0, and its inclination angle against the base line $\overline{\mathrm{C_0A_0}}$ is $\beta/2$. The angle at C is $\beta' = \pi/2 - \beta/2$.

In Fig. 17.27 this kind of four-bar $\mathrm{A_0A_1B_1B_0}$ with coupler point C is shown again, but this time with the usual notation, i.e., $r_2 = b_2 = a$ instead of $r_2' = b_2' = a'$ and β instead of β'. The length of the input link is r. The symmetry axis of the coupler curve passes through B_0 under the angle $\pi/2 - \beta$ against the base line. The symmetry axis is made the y-axis of an x, y-system with origin B_0. At B_1 the transmission angle 2α is shown. It is convenient to use α as independent variable for the x, y-coordinates of C. From isosceles triangles with the apex B_1 the auxiliary quantities ϱ and d are obtained:

$$\varrho = 2a\cos(\alpha - \beta)\,, \qquad d = 2a\sin\alpha\,. \quad (17.102)$$

The angle δ appears also in the triangle $(\mathrm{A_0,B_0,A_1})$. The cosine law $r^2 = d^2 + \ell^2 - 2d\ell\cos\delta$ yields

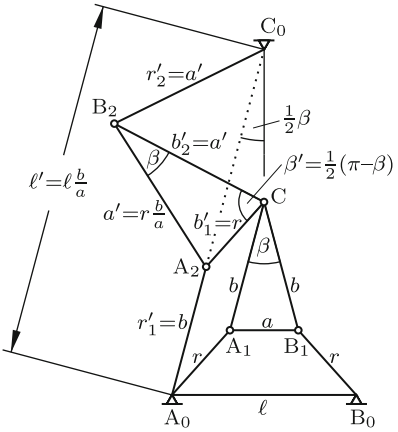

Fig. 17.26 Cognate four-bars generating a symmetrical coupler curve

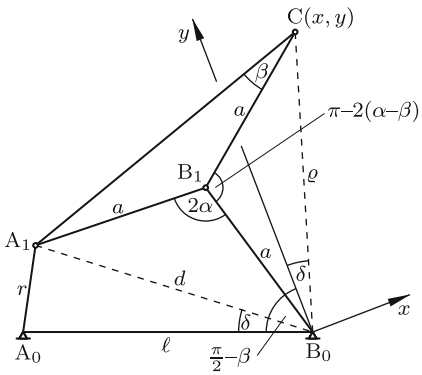

Fig. 17.27 Four-bar generating a coupler curve with symmetry axis y

$$\cos\delta = \frac{4a^2\sin^2\alpha + \ell^2 - r^2}{4a\ell\sin\alpha} \tag{17.103}$$

With these expressions the coordinates of C are

$$\begin{aligned} y = \varrho\cos\delta &= \frac{4a^2\sin^2\alpha + \ell^2 - r^2}{2\ell\sin\alpha}\,\cos(\alpha-\beta) \\ &= \frac{1}{2\ell}\Big[4a^2(\cos\beta\sin\alpha\cos\alpha + \sin\beta\sin^2\alpha) \\ &\qquad +(\ell^2-r^2)(\sin\beta+\cos\beta\cot\alpha)\Big]\,, \end{aligned} \tag{17.104}$$

$$\begin{aligned} x &= \pm\varrho\sin\delta = \pm\sqrt{\varrho^2 - y^2} \\ &= \pm\sqrt{4a^2\cos^2(\alpha-\beta) - y^2}\,. \end{aligned} \tag{17.105}$$

These equations find an application in Sect. 17.12.3.

From the figure it is seen that intersection points of the coupler curve with the symmetry axis are characterized by $\delta = 0$. In such positions A_1 lies on the base line. Then either $d = \ell - r$ or $d = \ell + r$ and $y = \varrho$. Equations (17.102) yield the associated angles α and the stationary values y:

$$\sin\alpha = \frac{\ell \mp r}{2a}\,, \qquad y = 2a\cos(\alpha-\beta)\,. \tag{17.106}$$

The position $d = \ell - r$ is always possible, the position $d = \ell + r$ only if the four-bar is a crank-rocker. It is left to the reader to show that the positions $d = \ell - r$ and $d = \ell + r$ of a crank-rocker yield identical values of y if the parameters satisfy the condition $r^2 + \ell^2\cot^2\beta = 4a^2\cos^2\beta$. In this case,

the coupler curve has a quadruple point on the circle of singular foci. In Fig. 17.28 these conditions are satisfied.

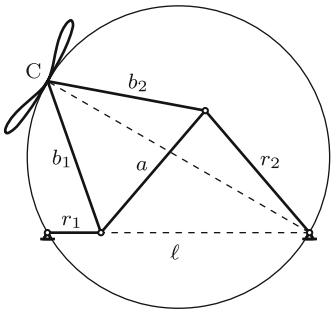

Fig. 17.28 Symmetrical coupler curve with quadruple point on the circle of singular foci. Crank-rocker with parameters $\ell = 2\sqrt{6}$, $r_1 = 1$, $r_2 = a = b_1 = b_2 = 3$

17.9 Slider-Crank. Inverted Slider-Crank

The slider-crank mechanism shown in Fig. 17.29a is derived from the four-bar in Fig. 17.19 by moving the point B_0 in y-direction to $-\infty$. This has the effect that the endpoint B of the coupler of length a is guided along the straight line $y = h = \text{const}$. In the inverted slider-crank mechanism of Fig. 17.29b the coupler of length a has become the fixed link, while the fixed link with the parameter h has become the moving coupler. The parameter h can be positive or zero or negative. Arbitrarily, it is considered as positive in both figures. In both figures the crank angle φ is the input variable, and the inclination angle χ of the coupler and the position s of the slider are output variables. Every value of φ is associated with two positions of the mechanism. In Fig. 17.29a the two values of χ and s are determined by the equations

$$\sin\chi_{1,2} = \frac{h - r\sin\varphi}{a}\,, \qquad s_{1,2} = r\cos\varphi \pm \sqrt{a^2 - (h - r\sin\varphi)^2}\,. \quad (17.107)$$

In Fig. 17.29b the output variables are obtained from two equations expressing the fact that the slider has the coordinates $x = a$ and $y = 0$:

$$r\cos\varphi + h\cos\chi + s\sin\chi = a\,, \qquad r\sin\varphi + h\sin\chi - s\cos\chi = 0\,. \quad (17.108)$$

Decoupling produces the equations

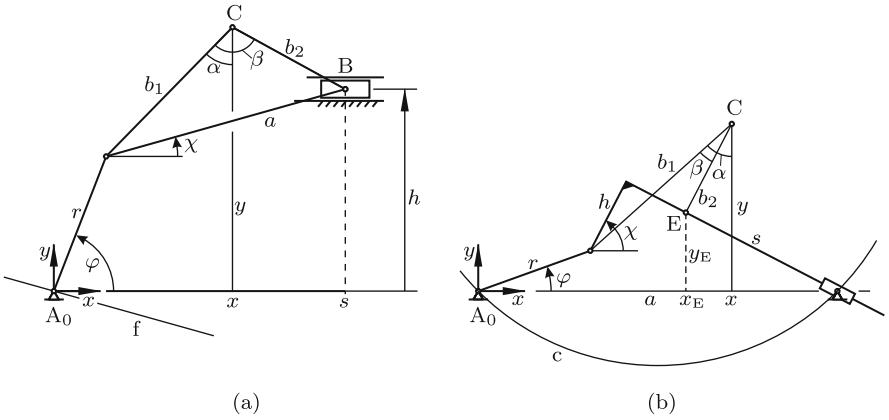

Fig. 17.29 Slider-crank **(a)** and inverted slider-crank **(b)**

$$\left.\begin{aligned}(r\cos\varphi - a)\cos\chi + r\sin\varphi\sin\chi &= -h\ ,\\ s = r\sin\varphi\cos\chi - (r\cos\varphi - a)\sin\chi\ .&\end{aligned}\right\} \tag{17.109}$$

The first equation has two solutions $\cos\chi_{1,2}$ and $\sin\chi_{1,2}$. The associated solutions $s_{1,2}$ are obtained from the second equation. In both figures the equivalent to Grashof's Theorem 17.1 is

Theorem 17.3. *The link with the shorter of the two lengths a and r is fully rotating relative to all other links if*

$$h^2 \le (a-r)^2\ . \tag{17.110}$$

Coupler curves: In both figures the coupler-fixed point C is specified by constant parameters b_1, b_2 and β. In Fig. 17.29a the notation is the same as in Fig. 17.19, whereas in Fig. 17.29b b_2 and β are defined differently. Implicit equations for coupler curves in the form $f(x, y, r, b_1, b_2, \beta) = 0$ are obtained from two linear equations for the sine and cosine of the auxiliary variable angle α. For both figures (17.78) and (17.79) are valid. Hence also the resulting Eq.(17.80) is valid:

$$2b_1(x\sin\alpha + y\cos\alpha) = x^2 + y^2 + b_1^2 - r^2\ . \tag{17.111}$$

In Fig. 17.29a the second linear equation for $\cos\alpha$ and $\sin\alpha$ is

$$y = h + b_2\cos(\beta - \alpha)\ . \tag{17.112}$$

In Fig. 17.29b the coordinates of point E satisfy the three equations

$$x_E = x - b_2\sin(\alpha-\beta)\ ,\quad y_E = y - b_2\cos(\alpha-\beta)\ ,\quad x_E = a - y_E\cot(\alpha-\beta)\ . \tag{17.113}$$

Elimination of x_E and y_E produces the desired second linear equation:

$$(x-a)\sin(\alpha-\beta)+y\cos(\alpha-\beta)=b_2\ . \tag{17.114}$$

To this equation and to (17.112) addition theorems are applied. Following this, the two sets of equations, one for Fig. 17.29a and one for Fig. 17.29b, are solved for $\cos\alpha$ and $\sin\alpha$. As in Eqs.(17.83) for the four-bar these solutions have the forms $\cos\alpha = U/\Delta$ and $\sin\alpha = V/\Delta$ with the pertinent coefficient determinants U, V and Δ. The desired implicit equations of the coupler curves are the equations $\cos^2\alpha+\sin^2\alpha=1$, i.e., $U^2+V^2=\Delta^2$. The equation $\Delta=0$ determines the locus of double points and cusps of coupler curves. Omitting elementary intermediate steps only the final equations are documented.

Figure 17.29a: The equation of the coupler curve is the quartic

$$\begin{aligned}&\Big[b_2(x^2+y^2+b_1^2-r^2)\sin\beta-2b_1x(y-h)\Big]^2\\ &+\Big[b_2(x^2+y^2+b_1^2-r^2)\cos\beta-2b_1y(y-h)\Big]^2\\ &=4b_1^2b_2^2(x\cos\beta-y\sin\beta)^2\ .\end{aligned} \tag{17.115}$$

The equation $\Delta=0$ defines the straight line (line f in Fig. 17.29a)

$$y=x\cot\beta\ . \tag{17.116}$$

Since a straight line intersects a quartic in at most four real points, the maximum number of double points and of cusps is two. In the context of Fig. 17.18b the existence of two cognate slider-crank mechanisms producing one and the same coupler curve has been proved.

Figure 17.29b: The equation of the coupler curve is the tricircular sextic

$$\begin{aligned}&\Big\{(x^2+y^2+b_1^2-r^2)[y\sin\beta+(x-a)\cos\beta]-2b_1b_2x\Big\}^2\\ &+\Big\{(x^2+y^2+b_1^2-r^2)[y\cos\beta-(x-a)\sin\beta]-2b_1b_2y\Big\}^2\\ &=4b_1^2\Big\{x[y\cos\beta-(x-a)\sin\beta]-y[y\sin\beta+(x-a)\cos\beta]\Big\}^2\ .\end{aligned} \tag{17.117}$$

The equation $\Delta=0$ defines the circle of singular foci (circle c in Fig. 17.29b)

$$\Big(x-\frac{a}{2}\Big)^2+\Big(y-\frac{a}{2}\cot\beta\Big)^2=\Big(\frac{a}{2\sin\beta}\Big)^2\ . \tag{17.118}$$

This equation is formally identical with Eq.(17.87) for the four-bar. Both a and ℓ denote the length of the fixed link. The definitions of β are different,

however. The maximum number of double points and of cusps of coupler curves on the circle is three. It can be shown that the third singular focus coincides with the singular focus A_0. This has the consequence that there are no cognate inverted slider-crank mechanisms.

17.10 Planar Parallel Robot

The triangular platform (A,B,C) of the planar parallel robot in Fig. 17.30 is positioned by means of three telescopic arms with controllable lengths r_i ($i = 1, 2, 3$) which are pivoted at A_0, B_0, C_0. The platform serves as carrier of tools or of work pieces[7]. The characterization as *parallel* points to the fact that the platform is positioned by arms in a parallel arrangement in contrast to a *serial* robot where it is positioned by a single arm with a series of links and joints (see Sect. 5.7). Parallel robots are able to manipulate heavier loads than serial robots, and they position them with higher accuracy and with greater stiffness.

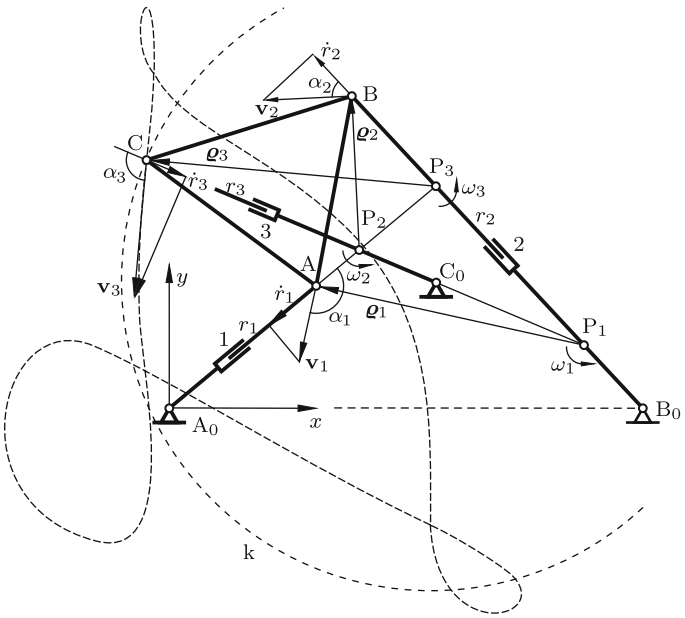

Fig. 17.30 Planar parallel robot. Four-bar A_0ABB_0 with coupler curve generated by C. The rate of change $\dot{r}_3$ of the leg length r_3 causes the platform to rotate with angular velocity $\omega_3 = \dot{r}_3/(\varrho_3 \cos\alpha_3)$ about P_3

[7] Other types of three-legged planar robots see in Hayes/Husty [21]

The planar parallel robot poses the following kinematics problem. Altogether nine parameters are given. These are three quantities specifying the triangle (A,B,C), the arm lengths r_i $(i = 1, 2, 3)$ and, in the x, y-system shown, the x-coordinate of B_0 and the x, y-coordinates of C_0. To be determined are all possible positions of the triangle (A,B,C).

Solution: Imagine that joint C connecting the platform with arm 3 is eliminated. Point C is located on the coupler curve generated by C fixed to the four-bar A_0ABB_0 and also on the circle k of radius r_3 about C_0. The four-bar and the coupler curve in Fig. 17.30 are copied from Fig. 17.23. The circle k intersects the coupler curve at six points. This is the maximum possible number of points. How to calculate these points was explained following (17.85). Each point determines a possible position of the robot. This concludes the position analysis.

Next, the velocity state is analyzed. Imagine that the telescopic joint in arm 3 is a passive joint so that this arm adapts itself freely to motions of the four-bar A_0ABB_0 with fixed lengths r_1 and r_2. The platform (A,B,C) has relative to the base the instantaneous center P_3 at the intersection of arms 1 and 2. Let $\boldsymbol{\omega}_3$ be the angular velocity of the coupler ($\omega_3 > 0$ counterclockwise). The velocity of C is $\mathbf{v}_3 = \boldsymbol{\omega}_3 \times \boldsymbol{\varrho}_3$. It is tangent to the coupler curve. As is shown α_3 denotes the angle between $\mathbf{r}_3$ and $\mathbf{v}_3$ in the case $\omega_3 > 0$. Arm 3 changes its length with the velocity $\dot{r}_3 = \omega_3 \varrho_3 \cos\alpha_3$. Conversely, if $\dot{r}_3$ is prescribed, $\omega_3 = \dot{r}_3/(\varrho_3 \cos\alpha_3)$. This angular velocity and the instantaneous center P_3 determine the velocities of A, B and C. The formula for ω_3 shows that $\dot{r}_3 \neq 0$ is possible only if in the position under investigation the coupler curve and the circle k are not in tangential contact. The quantities ϱ_3 and $\cos\alpha_3$ are calculated from the triangle (C_0,P_3,C).

Similar statements are valid when in the position under investigation arm 1 only or arm 2 only experiences a rate of change of length $\dot{r}_1$ or $\dot{r}_2$, respectively. In Fig. 17.30 also the instantaneous centers P_1, P_2 together with the associated quantities $\boldsymbol{\varrho}_1$, α_1 and $\boldsymbol{\varrho}_2$, α_2 are shown. When the three rates of change $\dot{r}_1$, $\dot{r}_2$, $\dot{r}_3$ occur simultaneously, the superposition principle yields the resultant angular velocity

$$\omega = \sum_{i=1}^{3} \frac{\dot{r}_i}{\varrho_i \cos\alpha_i} \,. \tag{17.119}$$

The velocity of each of the points A, B, C is the sum of three velocities two of which are collinear. The instantaneous center of the platform is the intersection point of the normals of the velocities of A, B and C.

17.11 Four-Bars with Prescribed Transmission Characteristics

The transmission characteristic is the relation between input angle φ and output angle ψ. In what follows, the implicit form (17.9) is used:

$$-\ell r_1 \cos\varphi + \ell r_2 \cos\psi = r_1 r_2 \cos(\varphi - \psi) + \frac{1}{2}[a^2 - (r_1^2 + \ell^2 + r_2^2)] \,. \quad (17.120)$$

It depends upon the three parameters r_1/ℓ, r_2/ℓ and a/ℓ where ℓ is a given unit length. In some engineering applications it is required that a four-bar produces prescribed pairs of input and output angles (φ_k, ψ_k) $(k = 1, 2, \ldots)$. In other applications it is required that some prescribed function $\psi = f(\varphi)$ be optimally approximated over a certain interval $0 \le \varphi \le \varphi_{\max}$. These and related problems have been treated extensively in the literature (see, for example, Lichtenheldt/Luck [26], Hain [18, 19], Soni [36]). In what follows, a few problems are discussed in detail.

17.11.1 Prescribed Pairs of Input-Output Angles

First, the case is treated that three pairs of angles (φ_k, ψ_k) $(k = 1, 2, 3)$ are prescribed. Equation (17.120) yields the three equations

$$-\ell r_1 \cos\varphi_k + \ell r_2 \cos\psi_k = r_1 r_2 \cos(\varphi_k - \psi_k) + \frac{1}{2}[a^2 - (r_1^2 + \ell^2 + r_2^2)] \quad (17.121)$$

$(k = 1, 2, 3)$. The differences first minus second and second minus third equation have the general forms

$$A_1 \ell r_1 + B_1 \ell r_2 = C_1 r_1 r_2 \,, \qquad A_2 \ell r_1 + B_2 \ell r_2 = C_2 r_1 r_2 \qquad (17.122)$$

with given constants A_i, B_i, C_i $(i = 1, 2)$. Division by $r_1 r_2$ results in two linear equations for ℓ/r_1 and ℓ/r_2 with uniquely determined real solutions. These solutions are substituted into one of the Eqs.(17.121). This equation then determines a^2/ℓ^2. The solution thus obtained is useful only if, first, $r_1 > 0$, $r_2 > 0$, $a^2/\ell^2 > 0$ and, second, the four-bar with these link lengths is capable of producing the prescribed pairs of angles in the desired order and without disconnection and reassembly.

In most engineering applications it is not required that the four-bar produces prescribed pairs of angles (φ_k, ψ_k) $(k = 1, 2, \ldots)$. Instead, pairs of angular differences $(\varphi_k - \varphi_0, \psi_k - \psi_0)$ $(k = 1, 2, \ldots)$ are prescribed where the pair (φ_0, ψ_0) is an *unspecified initial position* of the four-bar. The angles φ_0 and ψ_0 are free parameters so that the total number of free parameters

is five. In this formulation of the problem (17.120) must be satisfied for the pair (φ_0, ψ_0) and for up to four pairs $(\varphi_0+\varphi_k, \psi_0+\psi_k)$ $(k = 1, 2, 3, 4)$. The previous discussion has shown that results may be useless for various reasons (negative or imaginary link lengths, wrong order etc.). Therefore, only three pairs $(\varphi_0 + \varphi_k, \psi_0 + \psi_k)$ $(k = 1, 2, 3)$ are prescribed. This has the consequence, that the solutions for ψ_0, r_1, r_2 and a are functions of φ_0. This initial angle φ_0 is a free parameter which is chosen later so as to arrive at a useful solution. The altogether four equations are

$$-\ell r_1 \cos\varphi_0 + \ell r_2 \cos\psi_0 = r_1 r_2 \cos(\varphi_0 - \psi_0) + \frac{1}{2}[a^2 - (r_1^2 + \ell^2 + r_2^2)] \,, \quad (17.123)$$

$$\begin{aligned} -\ell r_1 \cos(\varphi_0 + \varphi_k) + \ell r_2 \cos(\psi_0 + \psi_k) &= r_1 r_2 \cos(\varphi_0 + \varphi_k - \psi_k - \psi_0) \\ &+ \frac{1}{2}[a^2 - (r_1^2 + \ell^2 + r_2^2)] \qquad (k = 1, 2, 3) \,. \end{aligned} \quad (17.124)$$

The first equation is subtracted from each of the remaining three equations. The differences are then divided by $r_1 r_2$. This results in the equations

$$\begin{aligned} &\frac{\ell}{r_2}[\cos(\varphi_0 + \varphi_k) - \cos\varphi_0] - \frac{\ell}{r_1}[\cos(\psi_0 + \psi_k) - \cos\psi_0] \\ &= \cos(\varphi_0 - \psi_0) - \cos(\varphi_0 + \varphi_k - \psi_k - \psi_0) \qquad (k = 1, 2, 3) \,. \end{aligned} \quad (17.125)$$

These are three linear inhomogeneous equations for ℓ/r_1 and ℓ/r_2. For a solution to exist it is necessary that the (3×3)-coefficient determinant including the right-hand side terms be zero. This condition results in an equation in which φ_0 and ψ_0 are the only unknowns. In order to be able to express ψ_0 as function of φ_0 Eqs.(17.125) are rewritten with the help of addition theorems in such a way that $\cos\psi_0$ and $\sin\psi_0$ are isolated. The equations thus rewritten are

$$\left.\begin{array}{ll} a_k \frac{\ell}{r_2} + (b_k \cos\psi_0 + c_k \sin\psi_0)\frac{\ell}{r_1} = d_k \cos\psi_0 + f_k \sin\psi_0 \,, & \\ a_k = \cos(\varphi_0 + \varphi_k) - \cos\varphi_0 \,, & d_k = \cos\varphi_0 - \cos(\varphi_0 + \varphi_k - \psi_k) \,, \\ b_k = 1 - \cos\psi_k \,, & f_k = \sin\varphi_0 - \sin(\varphi_0 + \varphi_k - \psi_k) \,, \\ c_k = \sin\psi_k & \end{array}\right\} \quad (17.126)$$

$(k = 1, 2, 3)$. The condition is

$$\begin{vmatrix} a_1 & b_1\cos\psi_0 + c_1\sin\psi_0 & d_1\cos\psi_0 + f_1\sin\psi_0 \\ a_2 & b_2\cos\psi_0 + c_2\sin\psi_0 & d_2\cos\psi_0 + f_2\sin\psi_0 \\ a_3 & b_3\cos\psi_0 + c_3\sin\psi_0 & d_3\cos\psi_0 + f_3\sin\psi_0 \end{vmatrix} = 0 \quad (17.127)$$

or explicitly

$$A\cos^2\psi_0 + B\sin^2\psi_0 + 2C\cos\psi_0\sin\psi_0 = 0\ , \tag{17.128}$$

$$\left.\begin{aligned} A &= a_1(b_2d_3 - b_3d_2) + a_2(b_3d_1 - b_1d_3) + a_3(b_1d_2 - b_2d_1)\ , \\ B &= a_1(c_2f_3 - c_3f_2) + a_2(c_3f_1 - c_1f_3) + a_3(c_1f_2 - c_2f_1)\ , \\ C &= \tfrac{1}{2}[a_1(b_2f_3 - b_3f_2) + a_2(b_3f_1 - b_1f_3) + a_3(b_1f_2 - b_2f_1) \\ &\quad + a_1(c_2d_3 - c_3d_2) + a_2(c_3d_1 - c_1d_3) + a_3(c_1d_2 - c_2d_1)]\ . \end{aligned}\right\} \tag{17.129}$$

In the special case $A = B \neq 0$, the solutions are $\psi_0 = -\frac{1}{2}\sin^{-1}(A/C)$ and $\psi_0 = \pi - \frac{1}{2}\sin^{-1}(A/C)$. In the special case $A \neq 0$, $B = 0$, the solutions are $\psi_0 = \pm\pi/2$ and $\psi_0 = -\frac{1}{2}\tan^{-1}A/(2C)$ and $\psi_0 = \pi - \frac{1}{2}\tan^{-1}A/(2C)$. In all other cases division by $\cos^2\psi_0$ results in the quadratic equation $B\tan^2\psi_0 + 2C\tan\psi_0 + A = 0$. Each solution $\tan\psi_0$ determines two angles ψ_0 which differ by $180°$. With each real solution ψ_0 two out of the three Eqs.(17.126) determine r_1/ℓ and r_2/ℓ. With these solutions r_1/ℓ and r_2/ℓ (17.123) determines a^2/ℓ^2. At this point the desired formulation of the unknowns ψ_0, r_1, r_2 and a as functions of the free parameter φ_0 is accomplished. The variation of φ_0 in search of a useful solution must be done numerically.

17.11.2 Prescribed Transmission Ratios

In this section four-bars are determined which produce two prescribed pairs of angles (φ_k, ψ_k) $(k = 1, 2)$ and, in the second position (φ_2, ψ_2), a prescribed value i_2 of the transmission ratio $i = \dot\varphi/\dot\psi$. The first two conditions yield the equations (see (17.121))

$$-\ell r_1\cos\varphi_k + \ell r_2\cos\psi_k = r_1r_2\cos(\varphi_k - \psi_k) + \frac{1}{2}[a^2 - (r_1^2 + \ell^2 + r_2^2)] \tag{17.130}$$

$(k = 1, 2)$. As before, the difference of these two equations produces the first Eq.(17.122). For the transmission ratio (17.31) is used. This yields an equation of the same type:

$$-\ell r_1\sin\varphi_2 + \frac{\ell r_2}{i_2}\sin\psi_2 = r_1r_2\Big(1 - \frac{1}{i_2}\Big)\sin(\varphi_2 - \psi_2)\ . \tag{17.131}$$

This is the second Eq.(17.122). The further steps of solution are as before.

The method of solution for five parameters (see (17.123), (17.124)) remains the same if one or two of the Eqs.(17.124) are replaced by the requirement that the transmission ratio is prescribed for one or two of the remaining pairs of angles.

17.11.3 Jeantaud's Steering Mechanism

In an automobile the steering mechanism causes the axes of the front wheels to turn about points A_0 and B_0 fixed in the car body. In Fig. 17.31 the axes are shown in a vertical projection during a left turn. With an ideal steering mechanism the turning angles α and β are coordinated such that the two front axes and the rear axis of the car have, independent of the radius R of the curve, a common intersection point. The lengths ℓ and h are constant parameters. From triangles the equations are obtained: $h = (R - \ell/2)\tan\alpha$, $h = (R + \ell/2)\tan\beta$. Elimination of the variable R results in

$$\cot\beta - \cot\alpha = \frac{\ell}{h} . \tag{17.132}$$

This equation defines the function $\beta(\alpha)$. It is an odd function. The curve denoted k in Fig. 17.32 is the graph of this function for the specific parameter value $\ell/h = 0.5$ in the interval of interest up to the maximum steering angles $(\alpha_{\max}, \beta_{\max})$. If, for example, $\alpha_{\max} = 40°$, (17.132) yields $\beta_{\max} \approx 30.6°$.

Jeantaud invented the steering mechanism shown in Fig. 17.33. It is a symmetrical four-bar approximating (17.132). The input link and the output link of equal length r are rotating about A_0 and B_0, respectively. They are rigidly connected with the front axes. The figure shows the mechanism in the symmetrical trapezoidal position (front axes not turned) and in a

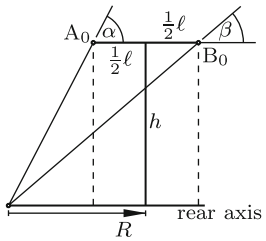

Fig. 17.31 Ideal turning angles α and β of the front axes of a car during a turn

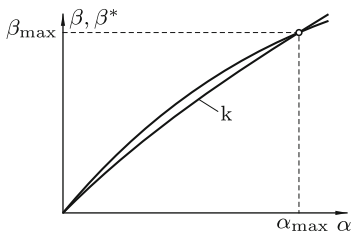

Fig. 17.32 Graph of the function $\beta = f(\alpha)$ for $\ell/h = 0.5$ (curve k) and approximation by a Jeantaud mechanism with nonoptimal parameters (ϱ, γ)

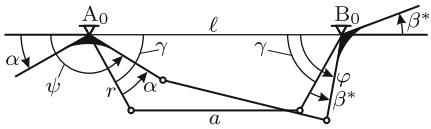

Fig. 17.33 Jeantaud mechanism

position effecting a left turn. The link lengths are ℓ, r and a. Suitable dimensionless parameters are $\varrho = r/\ell$ and the angle γ. The figure shows that $a = \ell - 2r\cos\gamma$. Hence

$$2r^2 + \ell^2 - a^2 = 2r^2 + 4r\ell(1 - \varrho\cos\gamma)\cos\gamma = 2r\ell(2\cos\gamma - \varrho\cos 2\gamma) \ . \quad (17.133)$$

The turning angle of the left front axis is α. The angle of the right axis is called not β, but β^* because it is an approximation of β. The figure shows angles ψ and φ. When this figure is rotated $180\,^\circ$, it has the form and the notation of Fig. 17.7. Equation (17.9) relating φ and ψ is

$$2r\ell(\cos\psi - \cos\varphi) - 2r^2\cos(\varphi - \psi) + 2r^2 + \ell^2 - a^2 = 0 \ . \quad (17.134)$$

For $2r^2 + \ell^2 - a^2$ the expression in (17.133) is substituted. Figure 17.33 shows that $\varphi = \gamma + \beta^*$ and $\psi = \pi + \alpha - \gamma$. Also these substitutions are made. When the resulting equation is divided by $2r\ell$, it has the form

$$\cos(\gamma + \beta^*) + \cos(\gamma - \alpha) - \varrho\cos(2\gamma + \beta^* - \alpha) = 2\cos\gamma - \varrho\cos 2\gamma \ . \quad (17.135)$$

After applying the addition theorem for the cosine function this takes the form

$$A\cos\beta^* + B\sin\beta^* = C \ , \quad (17.136)$$

$$\left.\begin{aligned} A &= \cos\gamma - \varrho\cos(2\gamma - \alpha) \ , \quad C = 2\cos\gamma - \varrho\cos 2\gamma - \cos(\gamma - \alpha) \ , \\ B &= -\sin\gamma + \varrho\sin(2\gamma - \alpha) \ . \end{aligned}\right\} \quad (17.137)$$

The equation has two solutions β^*. Their sines are

$$\sin\beta^* = \frac{BC \pm A\sqrt{A^2 + B^2 - C^2}}{A^2 + B^2} \ . \quad (17.138)$$

The pertinent solution is the one which has the same sign that α has. This solution defines a two-parametric manifold of functions $\beta^*(\alpha, \varrho, \gamma)$ with parameters ϱ and γ. Every parameter combination (ϱ, γ) determines a curve $\beta^*(\alpha)$ in the diagram of Fig. 17.32. It is reasonable to require that the curve passes through the point $\alpha = \alpha_{\max}$, $\beta^* = \beta_{\max}$. This means that (17.135) is satisfied with $\alpha = \alpha_{\max}$ and $\beta^* = \beta_{\max}$. This equation determines for every value of γ the associated value of ϱ. Thus, a one-parametric manifold of curves with parameter γ is left. In Fig. 17.32 a single nonoptimal curve is shown. The optimal value of γ is determined from the criterion that the maximum of the deviation $|\beta^*(\alpha) - \beta(\alpha)|$ in the interval $0 \le \alpha \le \alpha_{\max}$ be minimal. It turns out that this criterion yields two solutions $\gamma_1 > 0$ and $\gamma_2 < 0$. Example: With $\ell/h = 0.5$, $\alpha_{\max} = 40^\circ$ and $\beta_{\max} \approx 30.6^\circ$ the solutions are $\gamma_1 \approx 67^\circ$, $\varrho_1 \approx 0.25$ and $\gamma_2 \approx -121^\circ$, $\varrho_2 \approx 0.25$. The four-bar with γ_2 is located in front of the front axis. The four-bar with γ_1 is the one shown in Fig. 17.33. It is located behind the front axis (Brossard [4]).

17.12 Coupler Curves with Prescribed Properties

A problem frequently encountered in engineering is the design of a four-bar for the generation of a coupler curve having certain prescribed properties. If the four-bar has to be a crank-rocker, a suitable design may be found in the book by Hrones/Nelson [22]. It is a compilation of 7300 coupler curves. In each diagram a single crank-rocker is shown together with coupler curves for a variety of coupler-fixed points. A different ordering principle of coupler curves is found in Volmer [41]. Each diagram is a compilation of four-bars (not only crank-rockers) and of coupler curves having the same singular foci and the same double points on the circle of singular foci (17.87). In what follows, some mathematical problems and methods of solution are discussed which are encountered in the generation of coupler curves with prescribed properties.

17.12.1 Coupler Curves Passing Through Prescribed Points

The parameter representation of the coupler curve in the form of Eqs.(17.74) – (17.76) contains the six constant parameters ℓ, r_1, r_2, a, η, ζ and as seventh parameter the variable φ. These equations describe the coupler curve in the special x, y-system of Fig. 17.19. Three additional constant parameters determine the location of this x, y-system in an x', y'-reference system.

In a typical problem statement it is required that a coupler curve passes through prescribed points in the x', y'-system. Also the order in which these points are passed is prescribed. Let m be the number of prescribed points. The $2m$ prescribed coordinates result in $2m$ conditional equations. These equations contain $9 + m$ free parameters, namely, the nine constant parameters listed above and for every prescribed point the associated crank angle. From the equality $2m = 9 + m$ it follows that up to nine points can be prescribed. To be sure, not for every set of nine prescribed points real solutions exist and if they are real, the nine points are, in general, not passed in the prescribed order. It may happen that the calculated coupler curve is bicursal with some of the nine points on each branch.

The number m of points that can be prescribed is smaller than nine if the additional requirement exists that the angle $\varphi_k - \varphi_1$ of rotation of the input crank associated with the passage from point P_1 to point P_k is prescribed for $k = 2, \ldots, m$. The only free angle is φ_1. This means that altogether ten free parameters exist while the number of equations to be satisfied is $2m$ as before. From the equality $2m = 10$ it follows that at most five points can be prescribed. Methods for solving this problem see in Freudenstein [15] and Dijksman [8].

17.12.2 Straight-Line Approximations

Coupler curves with approximately straight-line segments have important engineering applications (see Fig. 17.2). The earliest straight-line approximation was invented by Watt[8] for the purpose of guiding the piston in his steam engine. His four-bar is a symmetrical double-rocker of second kind with link lengths ℓ, r_1, a, r_2 satisfying the conditions $r_1 = r_2 = r$ and $\ell = 2\sqrt{r^2 + (a/2)^2}$. The ratio a/r is a free parameter. In Fig. 17.34a the four-bar with link lengths $r = 35$, $a = 24$ and $\ell = 74$ is shown in four positions. The figure-eight-shaped coupler curve generated by the midpoint C of the coupler is symmetric to both the base line $\overline{A_0B_0}$ and the midnormal of this base line. The maximum distance from the base line (in position 4 of point C) is $\sqrt{a(\ell - a)/2}$.

Watt was unaware of cognate four-bars since the Roberts-Tchebychev theorem had not yet been discovered. So was Evans who invented the so-called *grashopper linkage* shown in Fig. 17.34b. It is a cognate of Watt's mechanism. Positions 1, 2, 3, 4 of the coupler point C are the same as in Fig. 17.34a. Evans' linkage has the advantage of being half the size of Watt's mechanism for one and the same coupler curve.

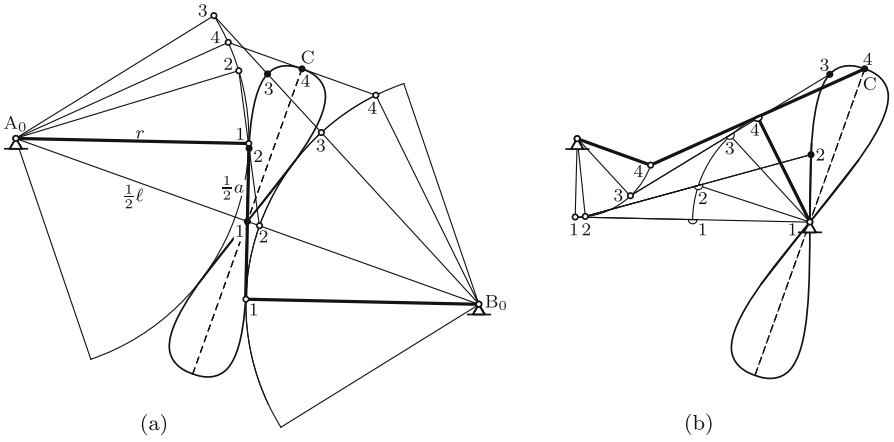

Fig. 17.34 Watt's straight-line approximation by a double-rocker with $r = 35$, $a = 24$, $\ell = 74$ **(a)** and Evans' grashopper linkage **(b)**, a cognate of Watt's mechanism

[8] James Watt (1736-1819) nowadays primarily known for the invention of steam engines wrote: "Though I am not over anxious after fame, yet I am more proud of the parallel motion than of any other mechanical invention I have ever made"

Roberts[9] is the inventor of another straight-line approximation (see Fig. 17.35). The coupler curve is symmetric with respect to the midnormal of the base. In the symmetry position shown the coupler point C is on the base line (coupler length $a = \ell/2$, coupler triangle with $b_1 = b_2 = r$). The three congruent triangles are determined by the single parameter $\varrho = r/\ell$. In the figure the case $\varrho = .6$ is shown. The coupler curve has a cusp and double points at A_0 and B_0.

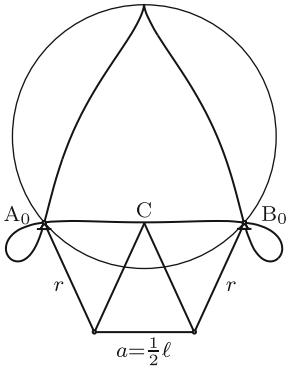

Fig. 17.35 Roberts' straight-line approximation by the double-rocker with $r/\ell = .6$

Remark on the influence of the parameter ϱ: With $\varrho = 1/2$ the coupler curve has three cusps. This curve is shown in Fig. 17.25. With every $\varrho > 1/2$ the coupler curve has a single cusp and double points at A_0 and B_0. The midpoint between A_0 and B_0 is a minimum. The maximum deviation $\Delta_{\max}$ from the straight line between A_0 and B_0 occurs at two symmetrically located maxima. With increasing ϱ this $\Delta_{\max}$ tends monotonically toward zero[10]. In the same process the straight-line approximation becomes increasingly better in an increasingly longer interval extending beyond the points A_0 and B_0. With $\varrho = 3/4$ the four-bar is foldable. With $\varrho > 3/4$ the coupler is fully rotating. From an engineering point of view large values of ϱ are impractical.

Watt's, Evans' and Roberts' straight-line approximations were found by engineering intuition. A more systematic approach was explained in Sect. 15.3.6. The coupler curve of the point which, in a position under investigation, is Ball's point of the coupler is a good straight-line approximation, because it has at this point zero curvature and zero rate of change of curvature. A textbook entirely devoted to straight-line approximations (by means of four-bars and of other linkages) is Kraus [25]. Straight-line approximations by means of inverted slider-crank mechanisms see also in Wunderlich [46]. By

[9] Richard Roberts (1789-1864), not to be confused with Samuel Roberts (1827-1913) of the Roberts/Tschebychev theorem

[10] $\Delta_{\max}/\ell \approx .0154$ for $\varrho = .5$, $\Delta_{\max}/\ell \approx .0068$ for $\varrho = .6$, $\Delta_{\max}/\ell \approx .0029$ for $\varrho = .75$

far the best straight-line approximations by coupler curves of four-bars were obtained by Tschebychev [39, 40] who used this problem for demonstrating the power of a new and widely applicable approximation theory invented by him. His method is the subject of the next section.

17.12.3 Tschebychev's Straight-Line Approximations

The general problem solved by Tschebychev is the following. In a given interval $x_a \le x \le x_b$ a given function $F(x)$ is to be approximated by another function of the form

$$P_n(x, p_0, \ldots, p_n) = p_0 f_0(x) + \ldots + p_n f_n(x) \tag{17.139}$$

with free parameters $p_0, \ldots, p_n$ and with *given* linearly independent functions $f_0(x), \ldots, f_n(x)$. Tschebychev proved

Theorem 17.4. *If the function $P_n(x, p_0, \ldots, p_n)$ has at most n real roots in the interval $x_a \le x \le x_b$, uniquely determined parameters $p_0, \ldots, p_n$ exist such that the maximum of the absolute value of the approximation error $\Delta_n(x, p_0, \ldots, p_n) = P_n(x, p_0, \ldots, p_n) - F(x)$ in the interval $x_a \le x \le x_b$ is minimal:*

$$|\Delta_n(x, p_0, \ldots, p_n)|_{\max} = Min! \qquad (x_a \le x \le x_b)\,. \tag{17.140}$$

Moreover, if D is this maximum, the optimal function $\Delta_n(x, p_0, \ldots, p_n)$ attains in the interval $x_a \le x \le x_b$ alternatingly not less than $(n+2)$ times extremal values D and $-D$.

For a proof of the theorem see Tschebychev [39] (p.111 and 273), Watson [45] and Powell [34]. Figure 17.36 shows schematically the graph of the optimal function Δ_n in the case $n = 2$. At the boundaries x_a and x_b and at unspecified points x in the interval $x_a \le x \le x_b$ the maximum D and the minimum $-D$ are attained not less than four times. Points x of extremal values in the interval are double roots of one of the two equations

$$\Delta_n(x, p_0, \ldots, p_n) \pm D = 0\,. \tag{17.141}$$

Extrema at the boundaries x_a and x_b of the interval are either simple roots or double roots of (17.141). Double roots satisfy also the equation

$$\Delta_n'(x, p_0, \ldots, p_n) = 0\,. \tag{17.142}$$

The $n+2$ Eqs.(17.141) and the n Eqs.(17.142) for double roots x in the interior of the interval represent altogether $2n+2$ equations. This equals the

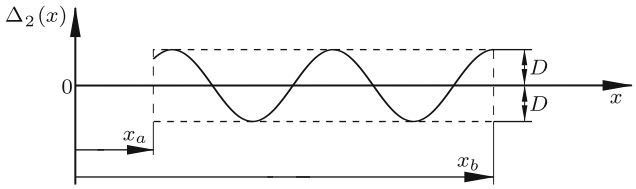

Fig. 17.36 Optimal function $\Delta_2(x, p_0, p_1, p_2)$ with extrema D and $-D$ inside and on the boundaries of the interval $x_a \le x \le x_b$

number of unknowns. Unknown are D, $p_0, \ldots, p_n$ and the n double roots x in the interior of the interval. Thus, it is possible to express all unknowns in terms of x_a and x_b. The equations are linear with respect to D, p_0, $\ldots$, p_n and they are nonlinear with respect to the double roots x in the interior of the interval.

Remarks: 1. The set of Eqs.(17.141) does not change if D is replaced by $-D$. For this reason D is redefined as either maximum or minimum of the function.

2. If in (17.140) the function Δ_n is replaced by $\lambda\Delta_n$ with an arbitrary constant λ, the solutions for p_0, $\ldots$, p_n, x_1, $\ldots$, x_{n+2} remain unaltered, but D is replaced by λD.

Now back to straight-line approximations. In [40] p.51 Tschebychev investigated the family of coupler curves which are symmetric with respect to the midnormal of the base $\overline{A_0B_0}$ and among these coupler curves those which approximate a straight line parallel to the base. Roberts' coupler curve belongs to this family. Watt's does not. For the family of symmetric coupler curves the parameter Eqs.(17.104), (17.105) based on Fig. 17.27 are used[11]:

$$\left.\begin{aligned} y(\alpha) &= \frac{1}{2\ell}\Big[4a^2(\cos\beta\sin\alpha\cos\alpha + \sin\beta\sin^2\alpha) \\ &\qquad + (\ell^2 - r^2)(\sin\beta + \cos\beta\cot\alpha)\Big]\,, \\ x(\alpha) &= \pm\sqrt{4a^2\cos^2(\alpha-\beta) - y^2}\,. \end{aligned}\right\} \tag{17.143}$$

The symmetry-axis is the y-axis. The constant parameters of the four-bar are ℓ, r, a, β, and the free parameter is the angle α. Intersection points of the coupler curve with the y-axis are associated with one of the angles (see (17.106))

$$\sin\alpha = \frac{\ell \mp r}{2a}\,. \tag{17.144}$$

[11] The four-bar analyzed in [40] p.51 is the one with symmetries $r_1 = r_2$ and $b_1 = b_2$. Only later Tschebychev [40] p.273 discovered what is now known as Roberts/Tschebychev theorem. The formulation presented here follows the exposition in Artobolevski/Levitski/Cherkudinov [2] without, however, making the substitution $z = \sin^2\alpha$

Tschebychev determined parameters ℓ, r, a, β such that the coupler curve is the optimal approximation to a straight line $y = y_0 = \text{const}$. The difference $y(\alpha) - y_0$ or rather a constant multiple of it is the function $\Delta_n = P_n - F$. With $n = 2$ it is written in the form

$$\Delta_2 = \frac{2\ell}{(\ell^2 - r^2)\cos\beta}\,[y(\alpha) - y_0] = p_0 f_0(\alpha) + p_1 f_1(\alpha) + p_2 f_2(\alpha) - F(\alpha) \tag{17.145}$$

with the following functions and coefficients

$$f_0(\alpha) = 1\,, \quad f_1(\alpha) = \sin\alpha\cos\alpha\,, \quad f_2(\alpha) = \sin^2\alpha\,, \quad F(\alpha) = -\cot\alpha\,, \tag{17.146}$$

$$p_0 = \tan\beta - \frac{2y_0\ell}{(\ell^2 - r^2)\cos\beta}\,, \qquad p_1 = \frac{4a^2}{\ell^2 - r^2}\,, \qquad p_2 = \frac{4a^2\tan\beta}{\ell^2 - r^2}\,. \tag{17.147}$$

In this formulation the problem appears as approximation of the function $F(\alpha) = -\cot\alpha$ by $P_2 = p_0 f_0 + p_1 f_1 + p_2 f_2$. In the interval $0 \le \alpha \le \pi$ the function P_2 has at most two real roots. In the segment of the coupler curve which is of interest the inequality $0 < \alpha < \pi/2$ holds. Thus, the conditions for the applicability of Tschebychev's theorem are satisfied. Equations (17.141) read:

$$p_0 + p_1\sin\alpha\cos\alpha + p_2\sin^2\alpha + \cot\alpha \pm D = 0\,. \tag{17.148}$$

According to the theorem each equation has (at least) one simple root and one double root in the interval $0 < \alpha < \pi/2$. This is, indeed, the case. The equations can be written in the forms

$$\left.\begin{aligned}\sin(\alpha - \alpha_1)\sin^2(\alpha - \alpha_3) = 0\,,\\ \sin(\alpha - \alpha_4)\sin^2(\alpha - \alpha_2) = 0\end{aligned}\right\} \tag{17.149}$$

with constants $0 < \alpha_1\,, \ldots, \alpha_4 < \pi/2$. For the first equation this is shown as follows. With an addition theorem and after division through $\sin\alpha\sin\alpha_1\sin^2\alpha_3$ the equation has the form

$$(\cot\alpha_1 - \cot\alpha)[1 + (\cot^2\alpha_3 - 1)\sin^2\alpha - 2\cot\alpha_3\sin\alpha\cos\alpha] = 0\,. \tag{17.150}$$

Multiplying out further leads to

$$\begin{aligned}\cot\alpha_1 + 2\cot\alpha_3 + (1 - 2\cot\alpha_1\cot\alpha_3 - \cot^2\alpha_3)\sin\alpha\cos\alpha\\ + [(\cot^2\alpha_3 - 1)\cot\alpha_1 - 2\cot\alpha_3]\sin^2\alpha - \cot\alpha = 0\,.\end{aligned} \tag{17.151}$$

This is indeed Eq.(17.148). In the case $+D$, comparison of coefficients yields

$$p_0 = -\cot\alpha_1 - 2\cot\alpha_3 - D\,, \tag{17.152}$$

$$\left.\begin{aligned} p_1 &= \cot^2\alpha_3 + 2\cot\alpha_1\cot\alpha_3 - 1 = \frac{2\sin(\alpha_1+2\alpha_3)}{(1-\cos 2\alpha_3)\sin\alpha_1}\,, \\ p_2 &= 2\cot\alpha_3 + (1-\cot^2\alpha_3)\cot\alpha_1 = -\frac{2\cos(\alpha_1+2\alpha_3)}{(1-\cos 2\alpha_3)\sin\alpha_1}\,. \end{aligned}\right\} \tag{17.153}$$

In the same way the second Eq.(17.149) and Eq.(17.148) with $-D$ yield

$$p_0 = -\cot\alpha_4 - 2\cot\alpha_2 + D\,, \tag{17.154}$$

$$p_1 = \frac{2\sin(\alpha_4+2\alpha_2)}{(1-\cos 2\alpha_2)\sin\alpha_4}\,, \qquad p_2 = -\frac{2\cos(\alpha_4+2\alpha_2)}{(1-\cos 2\alpha_2)\sin\alpha_4}\,. \tag{17.155}$$

The results obtained so far are summarized as follows. Each of the equations $\Delta_2 = \pm D$ has in the interval $0 < \alpha < \pi/2$ a simple root (α_1 or α_4) and a double root (α_2 or α_3). Suppose that $\alpha_1 < \alpha_4$. The graph of the optimal function Δ_2 is as shown in Fig. 17.36 with α instead of x. The roots α_1 and α_4 are the boundaries of the approximation interval.

The six Eqs.(17.152) – (17.155) suffice for determining the unknowns D, p_0, p_1, p_2, α_2 and α_3 as functions of α_1 and α_4. The two Eqs.(17.142), which are valid for $x = \alpha_2$ and for $x = \alpha_3$, are not needed because Eqs.(17.148) are available in the explicit form (17.149). Solutions for the unknowns are obtained as follows. Equations (17.152) and (17.154) yield

$$p_0 = -\frac{1}{2}(\cot\alpha_4 + \cot\alpha_1) - (\cot\alpha_3 + \cot\alpha_2)\,, \tag{17.156}$$

$$D = \frac{1}{2}(\cot\alpha_1 - \cot\alpha_4) + (\cot\alpha_3 - \cot\alpha_2)\,. \tag{17.157}$$

With (17.153) and (17.155)

$$\frac{p_1}{p_2} = -\tan(\alpha_1+2\alpha_3) = -\tan(\alpha_4+2\alpha_2)\,. \tag{17.158}$$

From this it follows that either

$$\alpha_1 + 2\alpha_3 = \alpha_4 + 2\alpha_2 \tag{17.159}$$

or $\alpha_1 + 2\alpha_3 = \alpha_4 + 2\alpha_2 + \pi$. From these two equations and from (17.153) and (17.155) it follows that either

$$(1-\cos 2\alpha_3)\sin\alpha_1 = (1-\cos 2\alpha_2)\sin\alpha_4 \tag{17.160}$$

or $(1-\cos 2\alpha_3)\sin\alpha_1 = -(1-\cos 2\alpha_2)\sin\alpha_4$. Because of the restriction $0 < \alpha_1, \alpha_4 < \pi/2$ only (17.159) together with (17.160) is useful. Equation (17.159) yields

$$\alpha_3 = \alpha_2 + \frac{1}{2}(\alpha_4 - \alpha_1)\,. \tag{17.161}$$

With the corresponding expression $\cos 2\alpha_3 = \cos 2\alpha_2 \cos(\alpha_4 - \alpha_1) - \sin 2\alpha_2 \sin(\alpha_4 - \alpha_1)$ Eq.(17.160) becomes an equation for α_2:

$$[\sin\alpha_4 - \sin\alpha_1 \cos(\alpha_4 - \alpha_1)] \cos 2\alpha_2 + \sin\alpha_1 \sin(\alpha_4 - \alpha_1) \sin 2\alpha_2 = \sin\alpha_4 - \sin\alpha_1 \ . \tag{17.162}$$

Of its two solutions for α_2 only one is located between α_1 and α_4. Only this solution is useful. The associated angle α_3 is calculated from (17.161). Following this, Eqs.(17.155) – (17.157) determine p_0, p_1, p_2 and D as functions of α_1 and α_4.

The three Eqs.(17.147) relate the seven quantities α_1, α_4, ℓ, y_0, r, a and β. These relations are expressed as follows. Equating the two expressions for p_0 in (17.147) and (17.156) yields for y_0 the expression shown below. Similarly, equating the two expressions for p_1 in (17.147) and (17.153) yields for a^2 the expression shown below. Finally, equating the expressions for p_2/p_1 in (17.147) and (17.158) yields for $\tan\beta$ the two expressions shown below.

$$y_0 = \frac{\ell^2 - r^2}{2\ell} \cos\beta \Big[\tan\beta + \frac{1}{2}(\cot\alpha_4 + \cot\alpha_1) + (\cot\alpha_3 + \cot\alpha_2) \Big] \ , \tag{17.163}$$

$$a^2 = (\ell^2 - r^2) \, \frac{\sin(\alpha_1 + 2\alpha_3)}{2(1 - \cos 2\alpha_3) \sin\alpha_1} \ , \tag{17.164}$$

$$\tan\beta = -\cot(\alpha_1 + 2\alpha_3) = -\cot(\alpha_4 + 2\alpha_2) \ . \tag{17.165}$$

Four out of the seven quantities α_1, α_4, ℓ, y_0, r, a and β can (within certain limits) be prescribed arbitrarily. The base length ℓ is prescribed as unit length. The interval boundaries α_1 and α_4 are associated with certain points (x_1, y_1) and (x_4, y_4), respectively, of the coupler curve which are determined by (17.143). It is the segment of the coupler curve between these points which is approximated to the straight line $y = y_0$. Now, it is decided that one of these points, say (x_1, y_1), is located on the symmetry axis. Because of the symmetry this has the consequence that the coupler curve is approximated in the segment of double length between the points $(-x_4, y_4)$ and (x_4, y_4). According to (17.144) the condition $x_1 = 0$ has one of the forms $\sin\alpha_1 = (\ell \mp r)/(2a)$. By an investigation which is omitted here it can be shown that a better approximation of the straight line $y = y_0$ is achieved when the plus sign is chosen:

$$\sin\alpha_1 = \frac{\ell + r}{2a} \ . \tag{17.166}$$

The angle α_1 is real only if the four-bar to be determined is a crank-rocker. Whether the results satisfy this condition remains to be seen.

The third quantity we prescribe is $\beta = 0$. This means that the coupler point lies on the coupler line. Having made these decisions on ℓ, α_1 and β

a one-parametric manifold of four-bars is left. As parameter the ratio

$$\varrho = \frac{r}{\ell} \tag{17.167}$$

is chosen. It should be noted that Roberts' four-bar is a double-rocker with an angle $\beta \neq 0$. Thus, the straight-line approximations to be determined are of a different nature[12].

The next task is to express the quantities y_0 and a in (17.163) and (17.164) in terms of ℓ and ϱ. In addition, two new quantities are defined which are measures of quality of the approximation. These are the relative length $L/\ell = 2x_4/\ell = 2x(\alpha_4)/\ell$ of the approximately straight segment and the relative width $B/L = 2(y - y_0)_{\max}/L$ of the error in this segment. These quantities are expressed in terms of ϱ. This is done first for B/ℓ. Equations (17.145) and (17.157) yield the preliminary expression

$$\begin{aligned} \frac{B}{\ell} &= \frac{2(y - y_0)_{\max}}{\ell} = \frac{\ell^2 - r^2}{\ell^2} D \\ &= (1 - \varrho^2)\Big[\frac{1}{2}(\cot\alpha_1 - \cot\alpha_4) + (\cot\alpha_3 - \cot\alpha_2)\Big] . \end{aligned} \tag{17.168}$$

With $\beta = 0$ Eqs.(17.165) take the simple forms

$$2\alpha_3 = \frac{\pi}{2} - \alpha_1 , \qquad 2\alpha_2 = \frac{\pi}{2} - \alpha_4 . \tag{17.169}$$

With these expressions (17.160) becomes
$(1 - \sin\alpha_1)\sin\alpha_1 = (1 - \sin\alpha_4)\sin\alpha_4$.
This has the trivial solution $\alpha_4 = \alpha_1$ and the significant solution

$$\sin\alpha_4 = 1 - \sin\alpha_1 . \tag{17.170}$$

The first Eq.(17.169) yields $\sin(\alpha_1 + 2\alpha_3) = 1$ and $\cos 2\alpha_3 = \sin\alpha_1$ or with (17.166) $\cos 2\alpha_3 = (\ell + r)/(2a)$. Substitution of these expressions into (17.164) leads to

$$a = \frac{\ell}{2}(3 - \varrho) . \tag{17.171}$$

The parameter ϱ is free subject to the condition that the four-bar is a crank-rocker. For this to be the case, $r = \varrho\ell$ must be the shortest link. In addition, Grashof's inequality (17.4), $\ell_{\min} + \ell_{\max} \leq \ell' + \ell''$, must be satisfied. Both conditions are satisfied if and only if $0 < \varrho \leq 1$.

The expression obtained for a is substituted back into (17.166). With this equation and with (17.169) and (17.170) the formulas are obtained:

[12] Tschebychev [40] (p.273, p.285, p.301 and p.495) investigated also the case $\beta \neq 0$. Also for this case he gave explicit formulas for a one-parametric family of four-bars. In [40] p.495 the approximation of a circle is investigated

$$\left.\begin{aligned} \sin\alpha_1 &= \frac{1+\varrho}{3-\varrho}\,, \quad \cos\alpha_1 = \frac{2\sqrt{2(1-\varrho)}}{3-\varrho}\,, \quad \cot\alpha_3 = \frac{1+\sin\alpha_1}{\cos\alpha_1}\,, \\ \sin\alpha_4 &= 2\frac{1-\varrho}{3-\varrho}\,, \quad \cos\alpha_4 = \frac{\sqrt{(5-3\varrho)(1+\varrho)}}{3-\varrho}\,, \quad \cot\alpha_2 = \frac{1+\sin\alpha_4}{\cos\alpha_4}\,. \end{aligned}\right\} \tag{17.172}$$

With these expressions (17.163) and (17.168) yield for the location y_0 of the straight line and for the measure of quality B/ℓ the formulas

$$\frac{y_0}{\ell} = \sqrt{2(1-\varrho)} + \frac{1}{8}(5-3\varrho)\sqrt{(5-3\varrho)(1+\varrho)}\,, \tag{17.173}$$

$$\frac{B}{\ell} = 2\sqrt{2(1-\varrho)} - \frac{1}{4}(5-3\varrho)\sqrt{(5-3\varrho)(1+\varrho)}\,. \tag{17.174}$$

For the ratio L/ℓ Eqs.(17.143) yield

$$\begin{aligned} y_4 &= \frac{1}{2\ell}\cot\alpha_4[(3\ell-r)^2\sin^2\alpha_4 + \ell^2 - r^2] \\ &= \frac{\ell}{4}(5-3\varrho)\sqrt{(5-3\varrho)(1+\varrho)}\,, \end{aligned} \tag{17.175}$$

$$\begin{aligned} \frac{L}{\ell} &= \frac{2x_4}{\ell} = \frac{2}{\ell}\sqrt{(3\ell-r)^2\cos^2\alpha_4 - y_4^2} \\ &= \frac{1}{2}\sqrt{3(5-3\varrho)(1+\varrho)(3-\varrho)(3\varrho-1)}\,. \end{aligned} \tag{17.176}$$

From L/ℓ and B/ℓ the second measure of quality B/L is calculated.

$L > 0$ requires that $\varrho > 1/3$. The diagram in Fig. 17.37 shows as functions of ϱ the ratios L/ℓ and $|B/L|$ characterizing the quality of the straight-line approximation. The former should be large and the latter very small. These goals are achieved with values of ϱ close to $1/3$.

Example: With $\varrho = r/\ell = .4$ (17.171), (17.173), (17.176) and (17.174), determine the coupler length $a = 1.3\ell$, the length $y_0 \approx 2.19\ell$ and the measures of quality $L/\ell \approx 1.44$ and $|B/L| \approx .00020$. This is an excellent straight-line approximation. The entire coupler curve is shown in Fig. 17.38. The four-bar is drawn in solid lines. Dashed lines show the cognate four-bar generating the same coupler curve. For the significance of the points B_0, P_1 and P_2 see the comment following (17.100). For comparison: The straight-line approximations by Watt / Evans (Fig. 17.34a,b) and by Roberts (Fig. 17.35) are not nearly as good. The measures of quality for Roberts' approximation are $L/\ell \approx 1$ and $|B/L| \approx .0068$. From Fig. 17.37 it is seen that with increasing ϱ the measure of quality L/ℓ improves while the essential measure of quality $|B/L|$ deteriorates. For $\varrho = r/\ell = .5$, for example, the measures are $L/\ell \approx 2.22$ and $|B/L| \approx .0022$. This is still a very good straight-line approximation. End of example.

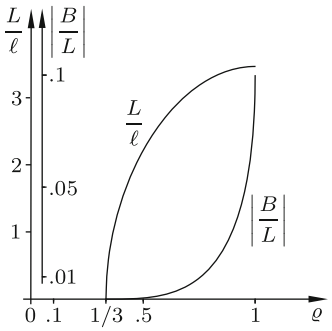

Fig. 17.37 Measures of quality L/ℓ and $|B/L|$ of Tschebychev's straight-line approximations as functions of $\varrho = r/\ell$

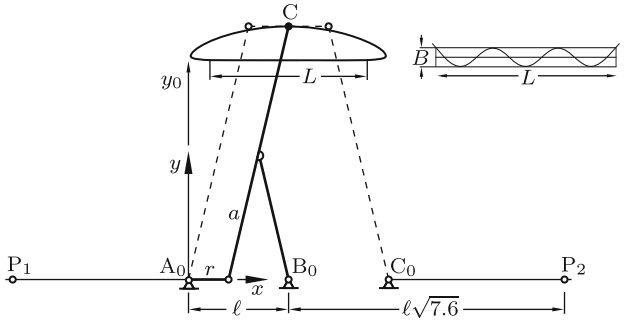

Fig. 17.38 Tschebyschev's straight-line approximation. Solid lines: Crank-rocker with $r = .4\ell$, $a = 1.3\ell$. Approximation of the line $y_0 \approx 2,19\ell$. Measures of quality $L/\ell \approx 1.44$, $|B/L| \approx .00020$. In dashed lines the cognate four-bar generating the same coupler curve. For P_1 and P_2 see the text following (17.100)

17.13 Peaucellier Inversor

Until after Tschebychev's work on straight-line approximations it was taken for granted that no plane mechanism consisting of rigid links with rotary joints could possibly generate an exact straight line. It caused, therefore, quite a sensation when in 1864 Peaucellier [33] invented a simple mechanism achieving just this[13]. The mechanism which became known as Peaucellier inversor is shown in Fig. 17.39 . It has two fixed points 0 and A a distance a apart. A crank of length ϱ connects A to the point called P . This point P is connected to 0 via two rods of equal length b and four rods of equal length $c < b$. The trajectory of P is the circle k with the equation

$$(x - a)^2 + y^2 = \varrho^2 \ . \tag{17.177}$$

[13] The history of this invention see in Sylvester [38], v.3

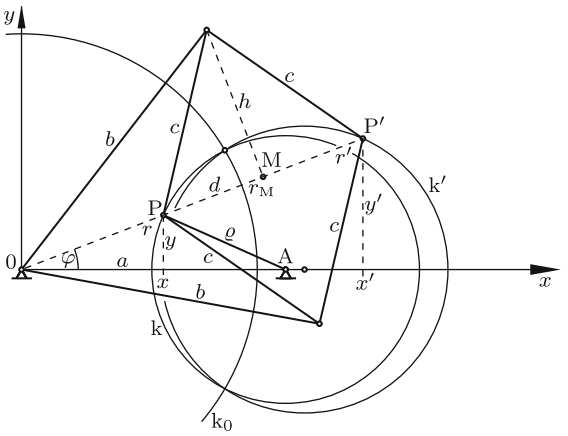

Fig. 17.39 Peaucellier inversor. Coordinates r, φ, x, y, r', x', y'. Circles $\mathrm{k}, \mathrm{k}_0, \mathrm{k}'$

In what follows, the trajectory of P' is investigated. First, relationships between the polar coordinates of P and P' are established. Both points have equal polar coordinates φ, but different polar coordinates r and r'. The relationship between r and r' is established as follows. In terms of r_{M} (polar coordinate of M) and of auxiliary lengths d and h the polar coordinates are $r = r_{\mathrm{M}} - d$ and $r' = r_{\mathrm{M}} + d$. Hence $rr' = r_{\mathrm{M}}^2 - d^2$. Also $r_{\mathrm{M}}^2 = b^2 - h^2$ and $d^2 = c^2 - h^2$. Therefore, finally,

$$rr' = R^2 \qquad (R^2 = b^2 - c^2 = \text{const} > 0) \,. \tag{17.178}$$

The transformation of P into P' or vice versa according to this equation is called *inversion in the circle*

$$x^2 + y^2 = R^2 \,. \tag{17.179}$$

The circle itself is called inversion circle k_0. Every point of k_0 is transformed into itself. The trajectory of P' is the inverse of the circle k in k_0. Its equation is obtained as follows. Let (x, y) and (x', y') be the cartesian coordinates of P and P', respectively. The two sets of coordinates are related by the equations

$$x = x' \frac{r}{r'} = x' \frac{R^2}{r'^2} = \frac{x' R^2}{x'^2 + y'^2} \,, \qquad y = \frac{y' R^2}{x'^2 + y'^2} \,. \tag{17.180}$$

Substitution of these expressions into (17.177) results in the desired equation of the trajectory of P':

$$\left(x' - a \frac{R^2}{a^2 - \varrho^2}\right)^2 + y'^2 = \left(\varrho \frac{R^2}{a^2 - \varrho^2}\right)^2 . \tag{17.181}$$

This is another circle centered on the x-axis. It is called the inverted circle k'. Depending on R, a and ϱ the circles k and k_0 may or may not intersect in real points. If they intersect, k' intersects the circle k_0 in the same points because every point of k_0 is transformed into itself. In Fig. 17.39 the circles intersect in two points. Let ξ be the x-coordinate of these points. Equations (17.177) and (17.179) yield

$$\xi = \frac{R^2 + a^2 - \varrho^2}{2a} \,. \tag{17.182}$$

The circle k' intersects the x-axis at the points

$$x_1 = \frac{R^2}{a + \varrho} \,, \qquad x_2 = \frac{R^2}{a - \varrho} \,. \tag{17.183}$$

In the limit $\varrho \to a$ the circle k' degenerates. Its radius, its center point coordinate as well as the point x_2 of intersection with the x-axis tend toward infinity. In contrast, the other point of intersection tends toward the finite point $x_1 = R^2/(2a)$. The point ξ tends toward the same point. Thus, the circle k' degenerates to the straight line $x = R^2/(2a)$ and to a point at infinity. In Fig. 17.40 the limiting case $\varrho = a$ is shown. Point P is moving on the circle k passing through 0, while P' is moving along the straight line $x = R^2/(2a)$. In the example shown the circles k and k_0 do not intersect. If they intersect, also the trajectory of P' passes through the points of intersection. If ϱ and a are different, but almost identical, k' is a circle of very large radius which intersects the x-axis at a point very close to $x_1 = R^2/(2a)$. In engineering such circular trajectories are as interesting as straight-line trajectories. Peaucellier's discovery inspired Hart [20], Sylvester [38] and Kempe [23] to invent other mechanisms with rotary joints which generate straight lines (see also Schoenflies/Grübler [35], Dijksman [9], Pavlin/Wohlhart [32], Demaine/O'Rourke [7]).

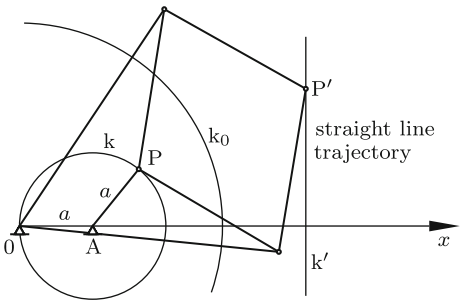

Fig. 17.40 Straight-line trajectory of P' in the special case $\varrho = a$

17.14 Four-Bars Producing Prescribed Positions of the Coupler Plane. Burmester Theory

The purpose of many linkages is to carry a planar object, i.e., a plane Σ, through an ordered set of prescribed positions $1, \ldots, n$ relative to a reference plane Σ_0. If the number n is sufficiently small, this task can be achieved by making Σ the coupler plane and Σ_0 the frame of a four-bar (as will be seen the condition is $n \leq 5$). The moving four-bar carries the plane Σ through a continuum of positions, to which the prescribed positions belong if the free design parameters are chosen properly. The complete solution to this problem which is due to Burmester [5] is the subject of this chapter. Extensive use is made of Sect. 14.5 in which fundamental concepts of Burmester were introduced. See the definitions of homologous points of points of Σ, of pole triangle, pole quadrilateral and pole curve. Burmester's basic idea is the following. The two Σ-fixed endpoints of the coupler move on circles about frame-fixed endpoints of two cranks (or rockers). Hence the problem can be stated as follows. Determine all n-tuples of homologous points $Q_1, \ldots, Q_n$ which are located on a circle and for each such n-tuple the center Q_0 of the circle. The line segments $\overline{Q_0 Q_i}$ $(i = 1, \ldots, n)$ defined by each such n-tuple represent the positions of a suitable crank in the positions $\Sigma_1, \ldots, \Sigma_n$ of the coupler plane Σ. Two arbitrarily chosen n-tuples of this kind define two suitable cranks and, thus, a four-bar. Whether a four-bar thus determined produces the prescribed positions in the prescribed order remains to be seen. The problem of order is the subject of Sect. 17.14.4.

In what follows, n homologous points on a circle are called circle points, and the center of the circle is called center point. The slider-crank mechanism in Fig. 17.29a is a degenerate four-bar in that one center point Q_0 is at infinity. The circle is a straight line. The elliptic trammel in Fig. 15.4 has two sliders. In the inverted slider-crank mechanism in Fig. 17.29b and in the inverted elliptic trammel the sliders are pivoted at center points Q_0 fixed in Σ_0. The associated circle points $Q_1, \ldots, Q_n$ are at infinity. In the mechanism shown in Fig.15.9 one slider is pivoted in the frame Σ_0 and the other in the coupler Σ. This mechanism equals its inverse.

17.14.1 Three Prescribed Positions

Three prescribed positions can be generated by four-bars of all types including the previously listed degenerate forms. Three prescribed positions determine a pole triangle (P_{12}, P_{23}, P_{31}). Since three points are always located on a circle, one out of three circle points Q_1, Q_2, Q_3 can be chosen arbitrarily. The other two circle points are then found as is shown in Fig. 14.11 by

reflections in the sides of the pole triangle. The center point Q_0 is the center of the circumcircle of the triangle (Q_1,Q_2,Q_3).

Instead of a single circle point the center point Q_0 can be chosen arbitrarily. The associated circle points Q_1, Q_2, Q_3 are determined either geometrically by the pole triangle (Fig. 14.13) or analytically from (14.50). Following Fig. 14.13 special cases (a) and (b) were explained when a pole is chosen either as center point or as circle point.

Figure 14.14 explains how to determine solutions with a center point Q_0 at infinity and with circle points Q_1, Q_2, Q_3 along a straight line. The straight line is passing through the orthocenter S of the pole triangle. If the line is prescribed, the circle points are determined, and if a single circle point is prescribed, the line and the other two circle points are determined.

Figure 14.15 explains how to determine solutions with circle points lying at infinity. As center point Q_0 an arbitrary point on the circumcircle of the pole triangle can be chosen. The chosen point determines the directions $\overline{Q_0Q_i}$ $(i = 1, 2, 3)$ in the three positions. They are the normals to the lines $\overline{Q_0S^i}$. Instead of Q_0 the direction towards a single infinitely distant circle point, say Q_3, can be chosen. It determines the line $\overline{Q_0S^3}$ and, consequently, Q_0 and the other two directions.

17.14.2 Four Prescribed Positions. Center Point Curve. Circle Point Curves

Four prescribed positions of the coupler plane determine six poles, four pole triangles, three pole quadrilaterals and the associated pole curve p (see Figs. 14.18 and 14.22). The pole curve is the geometric locus of all points from which opposite sides of a pole quadrilateral are seen under angles which are either identical or which add up to π. The present problem is to determine all four-tuples of homologous points Q_1, Q_2, Q_3, Q_4 which are located on a circle and for each circle the center point Q_0. Following Burmester the geometric locus of all center points thus defined is called *center point curve*. Proposition: The center point curve is the pole curve. Proof: Figure 17.41 shows four homologous points Q_1, Q_2, Q_3, Q_4 on a circle with center Q_0. Homologous means that the poles of the pole quadrilateral (P_{12},P_{23},P_{34},P_{41}) are located somewhere on the dashed bisectors of the angles of rotation $\varphi_{ij} = \sphericalangle(Q_iP_{ij}Q_j)$ $(i, j = 1, 2, 3, 4$ different). From Q_0 the opposite sides $\overline{P_{12}P_{23}}$ and $\overline{P_{34}P_{41}}$ are seen under the angles $\frac{1}{2}(\beta_{12} + \beta_{23})$ and $\frac{1}{2}(\beta_{34} + \beta_{41})$, respectively. Since $\beta_{12} + \beta_{23} + \beta_{34} + \beta_{41} = 2\pi$, these angles add up to π. If a pole, say P_{41}, is located on the other side of Q_0, the two opposite sides of the pole quadrilateral are seen under identical angles. End of proof.

Thus, both cranks of any four-bar capable of leading the coupler plane through four prescribed positions must be centered on the pole curve. The

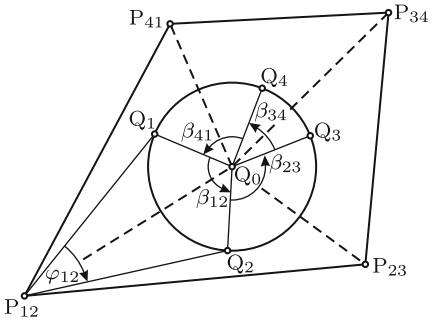

Fig. 17.41 Pole quadrilateral with four circle points and center point Q_0

problem of determining circle points associated with a chosen center point or of determining the center point associated with a chosen circle point is reduced to the previously solved problem with three prescribed positions since a solution satisfying four prescribed positions $1, 2, 3, 4$ satisfies any three positions, for example, positions $1, 2, 3$ and positions $1, 2, 4$. Hence circle points associated with a chosen center point Q_0 are determined either geometrically from pole triangles (Fig. 14.13) or analytically from Eqs.(14.50) which are now valid for the larger set of indices $i, j = 1, 2, 3, 4$ ($i \neq j$).

Special case: As center point Q_0 a pole is chosen, for example, Q_0=P_{12}. From the text following Fig. 14.13 (special case (a)) it is known that in the pole triangle associated with positions $1, 2, 3$ Q_3 is an undetermined point on the line $\overline{P_{23}P_{31}}$. For the same reason, Q_3 is an undetermined point on the line $\overline{P_{34}P_{41}}$ in the pole triangle associated with positions $1, 3, 4$. Hence Q_3 is the point of intersection of these two lines.

There is only a single solution with a center point Q_0 at infinity and with circle points Q_1, Q_2, Q_3, Q_4 along a straight line. The center point Q_0 is the infinitely distant point on the asymptote of the pole curve. The straight line is orthogonal to the asymptote. Since it is passing through the orthocenters, of all four pole triangles (see Fig. 14.14) collinearity of these orthocenters is proved.

Likewise, there is only a single solution with circle points Q_1, Q_2, Q_3, Q_4 at infinity. From Fig.14.15 it is known that the center point Q_0 is located on the circumcircles of all four pole triangles. These circles have a single point of intersection U (Fig. 14.22). As in the case of three positions, the directions $\overline{Q_0Q_i}$ $(i = 1, 2, 3, 4)$ toward the infinitely distant circle points are determined from pole triangles (Fig. 14.15). A center point Q_0 on p close to U is associated with a very long crank with very distant circle points.

Circle point curves: The geometric locus of the circle point Q_i is called *circle point curve* k_i $(i = 1, 2, 3, 4)$. If a single circle point curve, say k_1, is known, the other three curves are obtained by rotating k_1 about poles. From Fig. 14.13 and Eq.(14.50) it is known that Q_1 and Q_0 switch roles if

the angles φ_{12} and φ_{13} are replaced by $-\varphi_{12}$ and $-\varphi_{13}$, respectively. This means that the pole P_{23} is replaced by its reflection P_{23}^1 in the side $\overline{P_{12}P_{31}}$ of the pole triangle (see Fig. 14.12). With other indices the same is true for the other two pole triangles (P_{12},P_{24},P_{41}) and (P_{13},P_{34},P_{41}) associated with Q_1. In these triangles P_{24} and P_{34} are replaced by the reflected poles P_{24}^1 and P_{34}^1, respectively. Hence the conclusion: The circle point curve k_1 is the center point curve (pole curve) associated with the six poles P_{12}, P_{13}, P_{14}, P_{23}^1, P_{24}^1, P_{34}^1. The curve passes through these six poles. It does not pass through the poles P_{23}, P_{24}, P_{34}. With indices properly changed the same is true for the circle point curves k_2, k_3 and k_4.

17.14.3 Five Prescribed Positions

Center points Q_0 are located on the center point curve associated with the four positions 1 , 2 , 3 , 4 as well as on the center point curve associated with the four positions 1 , 2 , 3 , 5. Two third-order curves have nine (real or imaginary) points of intersection. Since the curves are circular, there exist two imaginary points of intersection at infinity. This leaves seven points of intersection. Each of the two curves passes through the poles P_{12}, P_{23} und P_{31}. That these points cannot be center points Q_0 is proved by taking P_{12} as example. According to statements made earlier positions 1 , 2 , 3 , 4 require Q_3 to be the point of intersection of the lines $\overline{P_{23}P_{31}}$ and $\overline{P_{34}P_{41}}$. For the same reason, positions 1 , 2 , 3 , 5 require Q_3 to be the point of intersection of the lines $\overline{P_{23}P_{31}}$ and $\overline{P_{35}P_{51}}$. This is impossible. End of proof.

Hence either zero or two or four real points of intersection are candidates as center point Q_0, namely, those real points which are different from P_{12}, P_{23} and P_{31}. These points are called *Burmester points*. For methods of construction of these points see Müller [29]. No four-bar producing five prescribed positions exists if the number of Burmester points is zero. A single four-bar exists if the number is two and six if the number is four. This completes the solution of Burmester's problem in the case of five prescribed positions. More than five positions cannot, in general, be prescribed.

17.14.4 Crank-Rockers Producing Four Prescribed Positions in Prescribed Order

A Burmester solution for four prescribed positions is inadmissible if the four-bar produces the prescribed positions either in a wrong order or in two different configurations of the four-bar. The problem of identifying admissible solutions was first investigated by Filemon [12, 13] and since then by many re-

searchers. A list of 170 references is given in Balli/Chand [3]. In what follows, Filemon's method of identifying all admissible crank-rockers is described.

A crank-rocker is producing four prescribed positions in the prescribed order 1 , 2 , 3 , 4 if the circle points on the crank circle are arranged in the order Q_1 , Q_2 , Q_3 , Q_4 either clockwise or counterclockwise. For this to be the case, the three triangles of circle points (Q_1,Q_2,Q_3), (Q_2,Q_3,Q_4) and (Q_3,Q_4,Q_1) must have one and the same sense. For the definition of sense of a triangle see Fig. 14.16 and the accompanying text. The sense is determined by the location of the center point Q_0 relative to the three lines of the corresponding pole triangle. Four pole triangles have altogether twelve lines dividing the infinite plane into domains. From Fig. 14.22 the following properties of the center point curve are known. The curve is intersected by lines at the six poles P_{ij} , at the six points Π_{ij} $(i, j = 1, 2, 3, 4$ different) and at no other point. From this and from Fig. 14.16 the following conclusions are drawn. When Q_0 travels on p through a pole P_{ij} $(i, j = 1, 2, 3, 4$ different), two lines belonging to one and the same pole triangle are crossed. This crossing has no effect on the sense of any triangle of circle points. In contrast, when Q_0 travels through a point Π_{ij} $(i, j = 1, 2, 3, 4$ different), two lines belonging to different pole triangles are crossed. This has the consequence that two triangles of circle points change sense. The six points Π_{ij} $(i, j = 1, 2, 3, 4$ different) divide the curve into seven sections (no matter whether the curve is unicursal or bicursal). The senses of circle point triangles do not change as long as Q_0 stays in one and the same section of the curve. Identical senses of all three circle point triangles are achieved with a set of points Q_0 which is either a single section or the union of several nonneighboring sections. In what follows, the set is denoted σ_c.

Example: In Fig. 14.22 the sense of the three circle point triangles is clockwise for points Q_0 in the unbounded section to the right of Π_{12} and in the section Π_{14}-Φ-Π_{34}. It is counterclockwise in the unbounded section to the left of Π_{23}. Thus, the set σ_c of admissible crank centers is the union of these three sections.

From Fig. 17.4b the following properties of crank-rockers are known. A four-bar is a crank-rocker if
(a) Grashof's inequality condition $\ell_{\min} + \ell_{\max} \leq \ell' + \ell''$ is satisfied and if, in addition,
(b) the crank has the minimal length $\ell_{\min}$.
The angular range of a rocker consists of two disconnected sectors $< 180°$ which are arranged symmetrically with respect to the base line. For being an admissible crank-rocker a Burmester solution must satisfy condition
(c) all four circle points of the rocker must be on one and the same side of the base line, for otherwise the four prescribed positions could not be produced without disconnecting and reassembling the crank-rocker.

An algorithm determining, for a given center point curve p, all admissible crank-rockers can now be formulated as follows.

Choose an arbitrary point Q_{0r} of p and an arbitrary point Q_{0c} of the set σ_c (the indices r and c stand for rocker and crank, respectively). Determine the circle point Q_{1r} associated with Q_{0r} and the circle point Q_{1c} associated with Q_{0c}. These four points determine a four-bar in the prescribed position 1. If this four-bar does not satisfy conditions (a) and (b), choose another point Q_{0c} of the set σ_c and repeat. Otherwise, determine also the circle points Q_{2r}, Q_{3r}, Q_{4r} associated with Q_{0r} and check whether condition (c) is satisfied. If not, choose another point Q_{0c} of the set σ_c and repeat. Otherwise, Q_{0r} and Q_{0c} are centers of the rocker and of the crank of an admissible crank-rocker. The sequence of decisions thus described has to be made for every point Q_{0r} of p in combination with every point Q_{0c} of the set σ_c.

17.15 Trajectory of the Center of Mass of a Four-Bar

In Fig. 17.42a r_0, r_1, r_2, r_3 represent differences of complex numbers in the complex plane. All of them have constant absolute values. They form a quadrilateral. The relation between the four is

$$r_2 = r_1 + r_3 - r_0 \,. \tag{17.184}$$

Let it be assumed that r_0 has constant direction. Then the differences of complex numbers form a mobile four-bar with base r_0. For any coupler-fixed point C a complex constant z exists such that

$$\overline{A_1C} = zr_3 \,. \tag{17.185}$$

When the four-bar is moving, the tip of the complex number

$$r_C = r_1 + zr_3 \tag{17.186}$$

traces the coupler curve generated by C.

The moving links $i = 1, 2, 3$ have masses m_i and centers of mass S_i (Fig. 17.42b). The positions of the centers of mass on the bodies are expressed in the form

$$\varrho_i = z_i r_i \qquad (i = 1, 2, 3) \tag{17.187}$$

with complex constants z_i. Let r_S be the complex number representing the composite system center of mass S of the four-bar (the moving parts only). It is determined by the formula

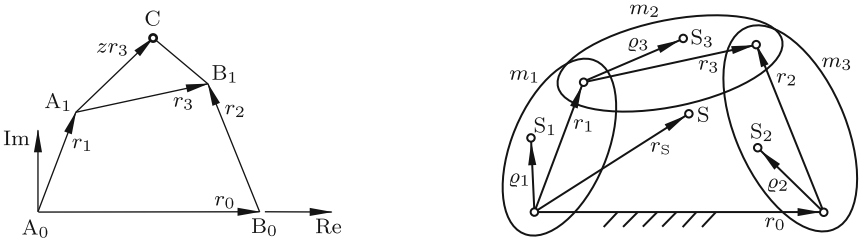

(a) (b)

Fig. 17.42 Four-bar with coupler point C **(a)** and with centers of mass **(b)**

$$
\begin{aligned}
r_S &= \frac{m_1\varrho_1 + m_3(r_1+\varrho_3) + m_2(r_0+\varrho_2)}{m_1+m_2+m_3} \\
&= \frac{m_1 z_1 r_1 + m_3(r_1+z_3 r_3) + m_2[r_0 + z_2(r_1+r_3-r_0)]}{m_1+m_2+m_3} \\
&= \frac{(m_1 z_1 + m_2 z_2 + m_3) r_1 + (m_2 z_2 + m_3 z_3) r_3 + m_2(1-z_2) r_0}{m_1+m_2+m_3} \,. \qquad (17.188)
\end{aligned}
$$

In the general case $m_1 z_1 + m_2 z_2 + m_3 \neq 0$,

$$
r_S = \frac{m_1 z_1 + m_2 z_2 + m_3}{m_1+m_2+m_3}\left(r_1 + \frac{m_2 z_2 + m_3 z_3}{m_1 z_1 + m_2 z_2 + m_3}\, r_3\right) + \frac{m_2(1-z_2) r_0}{m_1+m_2+m_3} \,. \qquad (17.189)
$$

The term in parentheses has the form (17.186) with

$$
z = \frac{m_2 z_2 + m_3 z_3}{m_1 z_1 + m_2 z_2 + m_3} \,. \qquad (17.190)
$$

The complex number r_C moves along the coupler curve of the coupler-fixed point C specified by this constant z. The constant complex factor in front has the effect of a stretch-rotation of this coupler curve and the constant behind has the effect of a translatory displacement. Hence the trajectory of the composite center of mass of a moving four-bar is similar to a uniquely determined coupler curve of the four-bar.

The acceleration of the composite center of mass determines the resultant inertia force acting on the base of the four-bar. The resultant force is zero throughout the motion if (17.188) yields $r_S = \text{const}$. This is the case under the weak conditions

$$
m_1 z_1 + m_2 z_2 + m_3 = 0 \,, \qquad m_2 z_2 + m_3 z_3 = 0 \,. \qquad (17.191)
$$

In these conditions the link lengths do not appear. The four link lengths, the three masses and, in addition, the position of the center of mass on a single link, for example, the number z_3, can be chosen arbitrarily. Both

conditions are satisfied if the centers of mass on the other two bodies satisfy the conditions

$$z_1 = \frac{m_3}{m_1}\,(z_3 - 1)\,, \qquad z_2 = -\,\frac{m_3}{m_2}\,z_3\,. \tag{17.192}$$

Note that for producing the time-varying angular acceleration of the coupler a torque is required. Even if the conditions (17.191) are satisfied this torque causes time-varying forces of equal magnitude and opposite directions acting on the base in the crank bearings.

References

1. Artobolevski I I (1964) Mechanisms for the generation of plane curves. Pergamon Press, Oxford
2. Artobolevski I I, Levitski N I, Cherkudinov S A (1959) Synthesis of plane mechanisms (Russ.). Isdat.Phys.-Mat. Lit., Moscow
3. Balli S S, Chand S (2002) Defects in link mechanisms and solution rectification. Mechanism Machine Theory 37:851–876
4. Brossard J P (2006) Dynamique du véhicule - Modélisation des systèmes complexes, Presses Polytechniques et universitaires Romandes
5. Burmester L (1888) Lehrbuch der Kinematik. Felix,Leipzig
6. Cayley A (1889) The collected mathematical papers of Arthur Cayley, v.1–13. Cambridge: The Univ. Press; (1963) Johnson Reprint Co., New York
7. Demaine E D , O'Rourke J (2007) Geometric folding algorithms. Linkages, origami, polyhedra. Cambridge Univ. Press
8. Dijksman E A (1969) Coordination of coupler-point positions and crank rotations in connection with Roberts' configuration. Trans ASME 91B:55–65
9. Dijksman E A (1975) Kempe's linkages and their derivations. J. Eng. Ind. 97B:801–808
10. Dijksman E A (1976) Motion geometry of mechanisms. Cambridge Univ. Press,
11. Erdman A G (ed.) (1993) Modern kinematics. Developments in the last forty years. Wiley, New York (appr. 2250 literature references)
12. Filemon E: Marking points for crank-rocker linkage on the centerpoint curve. Periodika Polytechnica XV:287–291
13. Filemon E (1972) Useful ranges of centerpoint curves for design of crank-and-rocker linkages. Mechanism Machine Theory 7:47–53
14. Freudenstein F (1956) On the maximum and minimum velocities and the accelerations in four-link mechanisms. Trans. ASME 78:779–787
15. Freudenstein F (1959) Structural error analysis in plane kinematics synthesis. Trans ASME 81B:15–22
16. Geronimus Ya. L. (1962) Geometric apparatus of the theory of synthesis of planar mechanisms (russ.). Gos. Isd. Physico-Math. Lit. Moscow
17. Grashof F (1883) Theoretische Maschinenlehre v.2. (1875 v.1, 1890 v.3). Voss, Leipzig
18. Hain K (1967) Atlas für Getriebe-Konstruktionen Bd.1,2. Vieweg, Braunschweig
19. Hain K (1961) Angewandte Getriebelehre. VDI-Verl., Düsseldorf. Engl. trans. (1968) Applied kinematics. 2nd ed. McGraw Hill, New York
20. Hart H (1875) A parallel motion. Proc.London Math.Soc.6:137–139
21. Hayes M J O, Husty M L (2003) On the kinematic constraint surfaces of general three-legged planar robot platforms. Mechanism Machine Theory 38:379–394
22. Hrones J A, Nelson G L (1951) Analysis of the four-bar linkage. Wiley, New York
23. Kempe A B (1875) On a general method of producing exact rectilinear motion by linkworks. Proc.Roy.Soc.London 23:565–577

24. Klein F, Müller C (eds.) (1901-1908) Enzyklopädie der Math. Wissenschaften. v.IV: Mechanik. Teubner, Leipzig
25. Kraus R (1956) Geradführungen durch das Gelenkviereck. VDI-Verl., Düsseldorf
26. Lichtenheldt W, Luck K (1979) Konstruktionslehre der Getriebe. Akademie-Verl., Berlin
27. Mayer A E (1938) Koppelkurven mit drei Spitzen und spezielle Koppelkurvenbüschel. Mathematische Zeitschrift 43:389–445
28. Müller R (1891) Über die Doppelpunkte der Koppelkurve. Z. Mathematik Physik 36:65–70. Engl.Transl. (1962) On the double points of coupler curves. Kansas State Univ. Bull. 46, Special Report 21:14–22
29. Müller R (1892) Konstruktion der Burmesterschen Punkte für ein ebenes Gelenkviereck. Z. Mathematik Physik 37:213–217 and (1893) 38:129–147
30. Müller R (1897) Beiträge zur Theorie des ebenen Gelenkvierecks. Z. Mathematik Physik 42:247–271. Engl.Transl. (1962) Contributions to the theory of the planar four-bar. Kansas State Univ. Bull. 46, Special Report 21:135–168
31. Müller R (1901) Die Koppelkurve mit sechspunktig berührender Tangente. Z. Mathematik Physik 46:330–342. Engl.Transl. (1962) The coupler curve with six-point osculating tangent. Kansas State Univ. Bull. 46, Special Report 21:178–194
32. Pavlin G, Wohlhart K (1992) On straigh-line space mechanisms. Proc. 6th Int. IFToMM Conf.:241–246
33. Peaucellier N (1874) Transformation du mouvement circulaire en mouvement rectiligne. Revue Scientif.4:499
34. Powell M J D (1981) Approximation theory and methods. Cambridge Univ.Press
35. Schoenflies A, Grübler M (1908) Kinematik. In: [24]:190–278
36. Soni A H (1974) Mechanism synthesis and analysis. Mac-Graw Hill, New York
37. Suh C H (1967) Design of space mechanisms for function generation. J. Eng.f.Ind. 89B:507–512
38. Sylvester J J (1904/08/09/12) The collected mathematical papers of James Joseph Sylvester, v.1–4. Chelsea, New York
39. Tschebychev P L (1961) Oeuvres de P.L. Tchebychef, v.I. Dover, New York. Théorie des mécanismes connus sous le nom de parallélogrammes. pp.111–143. Sur les questions de minima qui se rattachent à la représentation approximative des fonctions. pp.273–378.
40. Tschebychev P L (1962) Oeuvres de P.L. Tchebychef, v.II. Chelsea, New York. Sur un mécanisme. pp.51-57. Les plus simples systèmes de tiges articulées. pp.273–281. Sur les parallélogrammes composés de trois éléments et symétriques par rapport à un axe. pp.285–297. Sur les parallèlogrammes composés de trois éléments quelconques. pp.301–331. Sur le système articulé le plus simple donnant des mouvements symétriques par rapport à un axe. pp.495–540
41. Volmer J (1956/57) Ein Beitrag zur Erzeugung von Koppelkurven. Wiss.Z.Dresden 6:491–510
42. Volmer J (ed.) (1976) Autorenkollektiv: Getriebetechnik – Lehrbuch VEB, Berlin
43. Volmer J (ed.) (1979) Getriebetechnik-Koppelgetriebe. VEB, Berlin
44. Volmer J (ed.) (1992) Getriebetechnik-Grundlagen. Verl. Technik, Berlin
45. Watson G A (1980) Approximation theory and numerical methods. Wiley, New York
46. Wunderlich W (1970) Ebene Kinematik. BI-Verl. Mannheim

Chapter 18
Spherical Four-Bar Mechanism

From Sect. 5.4.1 it is known that the spherical four-bar mechanism or briefly spherical four-bar is a special mechanism RCCC. Figure 18.1a is a copy of Fig. 5.4. The four-bar has four revolute joints the axes of which intersect in a single point 0. The links are shown as arcs of great circles on the unit sphere about 0. Constant parameters $\alpha_i > 0$, joint variables φ_i and associated unit vectors $\mathbf{n}_i$ and $\mathbf{a}_i$ $(i = 1, \ldots, 4)$ were defined as follows. The unit vectors $\mathbf{n}_1, \ldots, \mathbf{n}_4$ along the joint axes are pointing away from 0. The unit vector $\mathbf{a}_i$ has the direction of $\mathbf{n}_i \times \mathbf{n}_{i+1}$ (here and in what follows, $i = 1, \ldots, 4$ cyclic). The angle α_i is the angle about $\mathbf{a}_i$ from $\mathbf{n}_i$ to $\mathbf{n}_{i+1}$. This angle is the arc length (link length) of link i. Throughout this chapter it is assumed that $\alpha_i \leq \pi$. The joint variable φ_i is the angle about $\mathbf{n}_i$ from $\mathbf{a}_{i-1}$ to $\mathbf{a}_i$. In what follows, link 4 is considered as frame, link 1 as input link, link 2 as coupler and link 3 as output link. This means that the angles φ_1 and φ_4 represent the input angle and the output angle, respectively. Since the spherical four-bar is a special mechanism RCCC, it is governed by the same

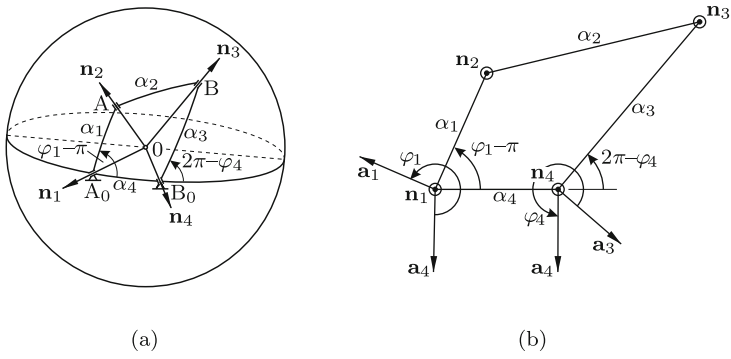

Fig. 18.1 Spherical four-bar mechanism. General case **(a)** and planar case **(b)**

J. Wittenburg, *Kinematics*, DOI 10.1007/978-3-662-48487-6_18

equations relating joint variables $\varphi_1, \ldots, \varphi_4$ and parameters $\alpha_1, \ldots, \alpha_4$. On the other hand, the spherical four-bar shares many characteristics with the planar four-bar. In the limit $\alpha_i \to 0$ $(i = 1, 2, 3, 4)$ it is a planar four-bar in a plane tangent to the sphere (Fig. 18.1b).

18.1 Transfer Function

The transfer function relating the angles φ_1 and φ_4 is known from the analysis of the mechanism RCCC. It is copied from (5.43) and (5.44):

$$A \cos\varphi_4 + B \sin\varphi_4 = R \tag{18.1}$$

with coefficients (abbreviations $C_i = \cos\alpha_i$ and $S_i = \sin\alpha_i$)

$$\left.\begin{aligned} A &= -S_3(S_4C_1 + C_4S_1\cos\varphi_1)\,, \qquad B = S_1S_3\sin\varphi_1\,, \\ R &= C_2 - C_3(C_4C_1 - S_4S_1\cos\varphi_1)\,. \end{aligned}\right\} \tag{18.2}$$

The equation has two solutions φ_4 which are determined by their sines and cosines:

$$\left.\begin{aligned} \cos\varphi_{4_k} &= \frac{AR + (-1)^k B\sqrt{A^2 + B^2 - R^2}}{A^2 + B^2}\,, \\ \sin\varphi_{4_k} &= \frac{BR - (-1)^k A\sqrt{A^2 + B^2 - R^2}}{A^2 + B^2} \end{aligned}\right\} \ (k = 1, 2)\,. \tag{18.3}$$

In the case $\alpha_i \ll 1$ $(i = 1, 2, 3, 4)$, when the spherical four-bar approximates a planar four-bar in a plane tangent to the sphere the coefficients A, B, R are represented by their second-order approximations

$$\left.\begin{aligned} A &\approx -\alpha_3(\alpha_1\cos\varphi_1 + \alpha_4)\,, \quad B \approx \alpha_1\alpha_3\sin\varphi_1\,, \\ R &\approx \alpha_1\alpha_4\cos\varphi_1 - \tfrac{1}{2}(\alpha_2^2 - \alpha_1^2 - \alpha_3^2 - \alpha_4^2)\,. \end{aligned}\right\} \tag{18.4}$$

Compare this with the transfer function of the planar four-bar given in (17.10) and (17.11). In these equations the following changes of notation are necessary (see Fig. 18.1b). The input angle φ of the planar four-bar is identified with $\varphi_1 - \pi$ and the output angle ψ with $2\pi - \varphi_4$. The link lengths r_1, a, r_2, ℓ of the planar four-bar are given the new names α_1, α_2, α_3, α_4, respectively. Following these changes (17.10) and (17.11) are identical with (18.1), (18.4).

18.2 Grashof Type Conditions

Grashof's conditions for the planar four-bar were deduced from Figs. 17.1a,b,c which show limit positions of the input link. These positions are characterized by collinearity of coupler and output link. In the case of the spherical four-bar, the equivalence to collinearity of coupler and output link is the coincidence of the great circles of coupler and output link. If, for convenience, great-circle arcs are drawn as straight lines, the Figs. 18.2a,b,c are equivalent to Figs. 17.1a,b,c. The triangles are spherical triangles. The angles ϕ_1 and ϕ_2 are limit values of the input angle φ_1. The cosine law for spherical triangles yields the equations

$$\cos(\alpha_3 \pm \alpha_2) = \cos\alpha_1 \cos\alpha_4 + \sin\alpha_1 \sin\alpha_4 \cos(\phi_{1,2} - \pi) \; . \tag{18.5}$$

Hence

$$\cos\phi_{1,2} = \frac{\cos\alpha_1 \cos\alpha_4 - \cos(\alpha_3 \pm \alpha_2)}{\sin\alpha_1 \sin\alpha_4} \; . \tag{18.6}$$

The same expressions are obtained from the condition that in (18.3) $A^2 + B^2 - R^2 = 0$. Equations (18.2) yield (with the abbreviations $c_1 = \cos\varphi_1$ and $s_1 = \sin\varphi_1$)

$$\begin{aligned} A^2 + B^2 - R^2 = \; & S_1^2[c_1^2(S_3^2C_4^2 - S_4^2C_3^2) + s_1^2S_3^2] + 2c_1S_1S_4(C_1C_4 - C_2C_3) \\ & + C_1^2(S_3^2S_4^2 - C_3^2C_4^2) + C_2(2C_1C_3C_4 - C_2) \; . \end{aligned} \tag{18.7}$$

Substituting $S_3^2 = 1 - C_3^2$, $S_4^2 = 1 - C_4^2$ and $s_1^2 = 1 - c_1^2$ this is rewritten in the form

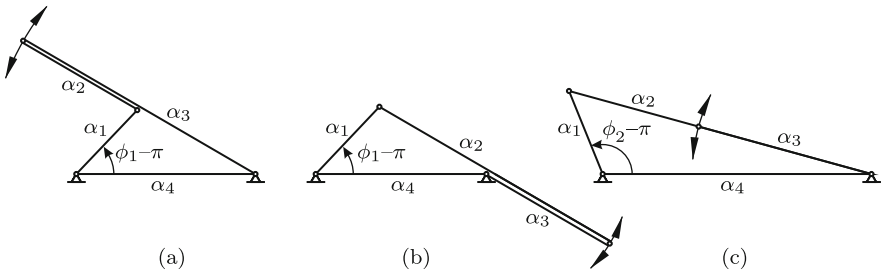

Fig. 18.2 Spherical four-bar in limit positions of the input link

$$
\begin{aligned}
&S_1^2[(1-C_3^2)-c_1^2(1-C_4^2)]+2c_1S_1S_4(C_1C_4-C_2C_3)+C_1^2[(1-C_3^2)-C_4^2]\\
&+C_2(2C_1C_3C_4-C_2)\\
&=-S_1^2S_4^2c_1^2+2c_1S_1S_4(C_1C_4-C_2C_3)+S_3^2-C_1^2C_4^2+C_2(2C_1C_3C_4-C_2)\\
&=-[S_1S_4c_1-(C_1C_4-C_2C_3)]^2\\
&+(C_1C_4-C_2C_3)^2+S_3^2-C_1^2C_4^2+C_2(2C_1C_3C_4-C_2)\\
&=-[S_1S_4c_1-(C_1C_4-C_2C_3)]^2+S_2^2S_3^2\\
&=-[(C_2C_3+S_2S_3)-(C_1C_4-S_1S_4c_1)]\\
&\times[(C_2C_3-S_2S_3)-(C_1C_4-S_1S_4c_1)]\,. \qquad (18.8)
\end{aligned}
$$

The roots c_1 of this expression are, indeed, the quantities in (18.6).

The input link is fully rotating relative to the base if Eqs.(18.5) yield $\cos(\phi_1-\pi)\geq+1$ as well as $\cos(\phi_2-\pi)\leq-1$. These are the conditions

$$
\cos(\alpha_4+\alpha_1)\geq\cos(\alpha_3+\alpha_2)\,,\qquad \cos(\alpha_3-\alpha_2)\geq\cos(\alpha_4-\alpha_1)\,. \qquad (18.9)
$$

The special case of four identical link lengths $\alpha_1=\alpha_2=\alpha_3=\alpha_4$ is treated first. Equations (18.5) yield $\phi_1-\pi=0$, $\phi_2-\pi=\pi$. This means that the input link can rotate full circle relative to the base.

In what follows, it is assumed that at least two link lengths are different. Let $\alpha_{\min}$ and $\alpha_{\max}\neq\alpha_{\min}$ be the smallest and the largest link length, respectively, and let α' and α'' be the other link lengths so that $\alpha_{\min}\leq\alpha'$, $\alpha''\leq\alpha_{\max}$. Because of the assumption $0<\alpha_i\leq\pi$ $(i=1,2,3,4)$ the second condition (18.9) is equivalent to

$$
|\alpha_3-\alpha_2|\leq|\alpha_4-\alpha_1|\,. \qquad (18.10)
$$

The first condition is satisfied if

$$
\left.\begin{array}{ll}\text{either} & \alpha_4+\alpha_1\leq\alpha_3+\alpha_2\leq2\pi-(\alpha_4+\alpha_1)\\ \text{or} & 2\pi-(\alpha_4+\alpha_1)\leq\alpha_3+\alpha_2\leq\alpha_4+\alpha_1\,.\end{array}\right\} \qquad (18.11)
$$

Condition (18.10) and the first condition (18.11) are satisfied if and only if

$$
\left.\begin{array}{ll}\alpha_1+\alpha_4\leq\pi\,, & \alpha_1+\alpha_2+\alpha_3+\alpha_4\leq2\pi\,,\\ \alpha_1=\alpha_{\min}\quad\text{or}\quad\alpha_4=\alpha_{\min}\,, & \alpha_{\min}+\alpha_{\max}\leq\alpha'+\alpha''\,.\end{array}\right\} \qquad (18.12)
$$

Condition (18.10) and the second condition (18.11) are satisfied if and only if

$$
\left.\begin{array}{ll}\alpha_1+\alpha_4\geq\pi\,, & \alpha_1+\alpha_2+\alpha_3+\alpha_4\geq2\pi\,,\\ \alpha_1=\alpha_{\max}\quad\text{or}\quad\alpha_4=\alpha_{\max}\,, & \alpha_{\min}+\alpha_{\max}\geq\alpha'+\alpha''\,.\end{array}\right\} \qquad (18.13)
$$

In conclusion, link 1 is a fully rotating crank if either the set of conditions (18.12) or the set of conditions (18.13) is satisfied. The last two of the con-

ditions (18.12) are formally identical with Grashof's condition for the planar four-bar. Conditions (18.13) are different. Examples: Conditions (18.12) are satisfied by the set of parameters $\alpha_1 = 50°$, $\alpha_2 = 100°$, $\alpha_3 = 120°$, $\alpha_4 = 80°$, and conditions (18.13) are satisfied by the set of parameters $\alpha_1 = 120°$, $\alpha_2 = 70°$, $\alpha_3 = 100°$, $\alpha_4 = 160°$. The above results apply also to the mechanism RCCC.

Like planar four-bars also spherical four-bars fall into the categories of crank-rockers, double-cranks, double-rockers and foldable four-bars. A spherical four-bar is foldable if $\alpha_{\min} + \alpha_{\max} = \alpha' + \alpha''$.

18.3 Coupler Curves

Every point C fixed on the coupler of a moving spherical four-bar traces a coupler curve which is located on a sphere. Without loss of generality the point C is chosen on the unit sphere. Together with the endpoints A and B of the coupler the point C creates a coupler-fixed spherical triangle (A,B,C). In Fig. 18.3 arcs of great circles are schematically represented by straight lines. As parameters of the coupler triangle the angles α_5, α_6 and α_7 are chosen. They are equivalent to the parameters b_1, b_2 and β of the coupler triangle of the planar four-bar in Fig. 17.19. As coordinates of the coupler point C its geographical longitude u and its geographical latitude v are used (A_0 and B_0 lie in the equatorial plane; $u = 0$ at A_0). The meridian passing through C defines the point D on the equator.

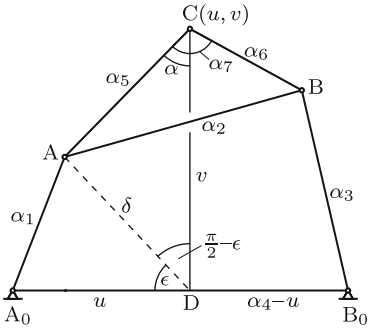

Fig. 18.3 Spherical four-bar with coupler point C in the coupler triangle (A,B,C). Schematic view with great-circle arcs shown as straight lines. All lengths are angles. Geographical coordinates u, v. Auxiliary angles α, ε, δ

18.3.1 Implicit Equation for Coupler Curves

To be determined is an implicit equation of the coupler curve in the form $f(u, v, \alpha_1, \alpha_3, \alpha_4, \alpha_5, \alpha_6, \alpha_7) = 0$. The following derivation is due to Dobrovolski [1]. It is analogous to the development for the planar four-bar (see Fig. 17.19 and Eqs.(17.78) – (17.84)). Temporarily, the auxiliary variables α, ε and δ are used. Spherical cosine and sine laws applied to the triangle (A,D,C) and the spherical cosine law applied to the triangle (A,D,A_0) yield the equations

$$\cos\alpha = \frac{\cos\delta - C_5\cos v}{S_5\sin v}\,, \qquad \cos\varepsilon = S_5\frac{\sin\alpha}{\sin\delta}\,, \qquad \cos\varepsilon = \frac{C_1 - \cos\delta\cos u}{\sin\delta\sin u}\,. \tag{18.14}$$

From the identity of the last two expressions it follows that

$$\cos\delta = \frac{C_1 - S_5\sin\alpha\sin u}{\cos u}\,. \tag{18.15}$$

Substitution of this expression into the first Eq.(18.14) results in the following equation which is linear with respect to both $\sin\alpha$ and $\cos\alpha$:

$$S_5(\sin u\sin\alpha + \cos u\sin v\cos\alpha) = C_1 - C_5\cos u\cos v\,. \tag{18.16}$$

The same equations are formulated for the triangles (B,D,C) and (B,D,B_0). They are obtained by replacing in the above equations u, α_1, α_5, α by $\alpha_4 - u$, α_3, α_6, $\alpha_7 - \alpha$, respectively. To $\sin(\alpha_7 - \alpha)$ and to $\cos(\alpha_7 - \alpha)$ addition theorems are applied. The equation equivalent to (18.16) then reads

$$\begin{aligned} S_6\Big\{&[S_7\sin v\cos(\alpha_4 - u) - C_7\sin(\alpha_4 - u)]\sin\alpha + [C_7\sin v\cos(\alpha_4 - u) \\ &+S_7\sin(\alpha_4 - u)]\cos\alpha\Big\} = C_3 - C_6\cos(\alpha_4 - u)\cos v\,. \end{aligned} \tag{18.17}$$

These two equations are solved for $\sin\alpha$ and $\cos\alpha$. Let Δ be the coefficient determinant. It is a simple expression if also $\sin(\alpha_4 - u)$ and $\cos(\alpha_4 - u)$ are developed:

$$\Delta = S_5S_6[S_4C_7\sin v - C_4S_7 + S_7\cos^2 v\cos u(S_4\sin u + C_4\cos u)]\,. \tag{18.18}$$

In the numerator determinants for $\sin\alpha$ and for $\cos\alpha$ the expressions $\sin(\alpha_4 - u)$ and $\cos(\alpha_4 - u)$ are kept unchanged. The resulting expressions are

$$\sin\alpha = \frac{1}{\Delta}\Big\{ S_6(C_1 - C_5\cos u\cos v)[C_7\sin v\cos(\alpha_4 - u) + S_7\sin(\alpha_4 - u)] - S_5[C_3 - C_6\cos(\alpha_4 - u)\cos v]\cos u\sin v\Big\}\,, \tag{18.19}$$

$$\cos\alpha = \frac{1}{\Delta}\Big\{ S_5[C_3 - C_6\cos(\alpha_4 - u)\cos v]\sin u - S_6(C_1 - C_5\cos u\cos v) \times [S_7\sin v\cos(\alpha_4 - u) - C_7\sin(\alpha_4 - u)]\Big\}\,. \tag{18.20}$$

Substitution into the constraint equation $\cos^2\alpha + \sin^2\alpha = 1$ eliminates the auxiliary variable α. The resulting equation is the desired implicit equation of the coupler curve:

$$\begin{aligned} &\Big\{ S_6(C_1 - C_5\cos u\cos v)[C_7\sin v\cos(\alpha_4 - u) + S_7\sin(\alpha_4 - u)] - S_5[C_3 \\ &-C_6\cos(\alpha_4 - u)\cos v]\cos u\sin v\Big\}^2 + \Big\{ S_5[C_3 - C_6\cos(\alpha_4 - u)\cos v]\sin u \\ &-S_6(C_1 - C_5\cos u\cos v)[S_7\sin v\cos(\alpha_4 - u) - C_7\sin(\alpha_4 - u)]\Big\}^2 \\ &= \Delta^2\,. \end{aligned} \tag{18.21}$$

When this is multiplied out, the function $\sin(\alpha_4 - u)$ disappears. Only the term $\cos(\alpha_4 - u) = S_4\sin u + C_4\cos u$ is left. The final form of the equation reads

$$\begin{aligned} &S_6^2(C_1 - C_5\cos u\cos v)^2[1 - \cos^2 v(S_4\sin u + C_4\cos u)^2] \\ &+ S_5^2[C_3 - C_6\cos v(S_4\sin u + C_4\cos u)]^2(1 - \cos^2 u\cos^2 v) \\ &- 2S_5S_6(C_1 - C_5\cos u\cos v)[C_3 - C_6\cos v(S_4\sin u + C_4\cos u)] \\ &\times [S_4S_7\sin v + C_4C_7 - C_7\cos^2 v\cos u(S_4\sin u + C_4\cos u)] \\ &= S_5^2S_6^2[S_4C_7\sin v - C_4S_7 + S_7\cos^2 v\cos u(S_4\sin u + C_4\cos u)]^2\,. \end{aligned} \tag{18.22}$$

The condition for the coupler curve to pass through the north pole (the south pole) of the sphere is that the equation is satisfied with $v = \pi/2$ (with $v = -\pi/2$). These conditions are

$$S_6^2C_1^2 + S_5^2C_3^2 - 2S_5S_6C_1C_3(C_7C_4 \pm S_7S_4) = S_5^2S_6^2(\pm S_4C_7 - C_4S_7)^2 \tag{18.23}$$

or

$$[S_5S_6\cos(\alpha_7 \mp \alpha_4) - C_1C_3]^2 = (S_5^2 - C_1^2)(S_6^2 - C_3^2)\,. \tag{18.24}$$

Equation (18.22) can be written in a simpler form when the transition is made to cartesian coordinates in an x, y, z-system defined as follows[1]. The origin is the center 0 of the sphere, the z, x-plane is the equatorial plane, the

[1] This idea was conceived in 2005 by Andrey Shutovich (St. Peterburg), then undergraduate student in Karlsruhe

z-axis passes through A_0, and the y-axis passes through the north pole. The point on the sphere with geographical coordinates u, v has the cartesian coordinates

$$x = \sin u \cos v \,, \qquad y = \sin v \,, \qquad z = \cos u \cos v \,. \tag{18.25}$$

Every expression in (18.22) is an algebraic function of x, y and z. The variable x occurs only in the form $p = S_4 x + C_4 z$. With this abbreviation the equation becomes

$$\begin{aligned} & S_6^2 (C_1 - C_5 z)^2 (1 - p^2) + S_5^2 (C_3 - C_6 p)^2 (1 - z^2) \\ & - 2 S_5 S_6 (C_1 - C_5 z)(C_3 - C_6 p)[S_4 S_7 y + C_7 (C_4 - z p)] \\ & = S_5^2 S_6^2 [S_4 C_7 y - S_7 (C_4 - z p)]^2 \qquad (p = S_4 x + C_4 z) \,. \end{aligned} \tag{18.26}$$

This fourth-order polynomial equation defines a surface. Curves of intersection with planes $z = \text{const}$ are conic sections. The coupler curve is the intersection of the surface with the unit sphere

$$x^2 + y^2 + z^2 = 1 \,. \tag{18.27}$$

Proposition: An arbitrary circle on the sphere intersects the coupler curve in eight (not necessarily real) points. This can also be expressed in the following form. Given three circles a, b, c on a sphere and a spherical triangle (A,B,C), there exist eight (not necessarily real) positions of the triangle in which A lies on a, B on b and C on c. In Chap.17.8.3 on triangles and circles in a plane the number of positions was found to be six (see the text following (17.86)).

Proof: Intersection points are located on the fourth-order surface, on the second-order sphere and in the plane of intersection of the circle with the sphere. Let $y = ax + bz + c$ be the equation of the plane. Substitution into (18.27) and (18.26) results in the equation of an ellipse and in a fourth-order equation with circularity zero, respectively. These two equations have eight solutions (x, z). End of proof. In Sect. 18.3.6 other forms of proof are given.

18.3.2 Symmetrical Coupler Curves

From the planar four-bar it is known that points on the coupler line, and only these points, generate coupler curves which are symmetrical with respect to the base line. In the case of the spherical four-bar, the equivalence to symmetry with respect to the base line is symmetry with respect to the x, z-plane (the base plane). This symmetry exists if in (18.26) the variable y either disappears altogether or appears in quadratic form only. The latter happens if $S_7 = 0$ ($\alpha_7 = 0$ or $\pi/2$). This is the case when the point generating the

coupler curve is located on the great circle of the coupler. This represents a direct analogy to the planar four-bar.

The variable y disappears altogether if either $\alpha_4 = \pi$ or $\alpha_3 = \alpha_6 = \alpha_7 = \pi/2$ or $\alpha_1 = \alpha_5 = \alpha_7 = \pi/2$. The case $\alpha_4 = \pi$ is the geometrically trivial case that the input axis $\mathbf{n}_1$ and the output axis $\mathbf{n}_4$ are directed along one and the same diameter of the sphere. In (18.26) not only y, but also x disappears. After division through $(1 - z^2)$ a quadratic equation for z is left. Its solutions define two planes $z \equiv z_1$ and $z \equiv z_2$. These planes intersect the unit sphere (18.27) in two circles which represent the coupler curve. Equation (18.1) has the form $\cos(\varphi_1 - \varphi_4) = (C_2 + C_1C_3)/(S_1S_3) = \text{const}$.

The case $\alpha_3 = \alpha_6 = \alpha_7 = \pi/2$ is not trivial. Equation (18.26) has the form $F(x, z) = 0$. It defines a cylinder the generators of which are parallel to the y-axis. The coupler curve is the line of intersection of this cylinder with the sphere. From the identity $\alpha_6 = \alpha_7 = \pi/2$ it follows that also the length α_2 of the coupler equals $\pi/2$. Thus, the coupler triangle is isosceles with two right angles. The case $\alpha_1 = \alpha_5 = \alpha_7 = \pi/2$ differs from the case $\alpha_3 = \alpha_6 = \alpha_7 = \pi/2$ only in that input link and output link change their roles.

From the planar four-bar it is known that coupler curves are symmetrical with respect to the midnormal of the base if the four-bar and the coupler triangle satisfy the symmetry conditions $r_1 = r_2$ and $b_1 = b_2$, respectively (see Fig. 17.26). The equivalent statement for the spherical four-bar is the following. If the four-bar and the coupler triangle satisfy the symmetry conditions $\alpha_3 = \alpha_1$ and $\alpha_6 = \alpha_5$, respectively, the coupler curve is symmetrical with respect to the plane spanned by the y-axis and the bisector of the angle α_4. With $C_3 = C_1$, $S_3 = S_1$, $C_6 = C_5$, $S_6 = S_5$ Eq.(18.26) takes, after simple re-arrangements of terms, the form

$$\begin{aligned} &2[C_1^2 - C_5^2 z^2 p^2 - C_1C_5(z + p)(1 - zp)] + (C_5^2 - C_1^2)(z^2 + p^2) \\ &- 2[C_1^2 + C_5^2 zp - C_1C_5(z + p)][S_4S_7y + C_7(C_4 - zp)] \\ &= S_5^2[S_4C_7y - S_7(C_4 - zp)]^2 \,. \end{aligned} \tag{18.28}$$

The bisector of α_4 is made the $\bar{z}$-axis of a new cartesian $\bar{x}, y, \bar{z}$-system. The transformation equations are

$$x = \bar{x}\cos\frac{\alpha_4}{2} + \bar{z}\sin\frac{\alpha_4}{2}\,, \quad z = -\bar{x}\sin\frac{\alpha_4}{2} + \bar{z}\cos\frac{\alpha_4}{2}\,, \quad p = \bar{x}\sin\frac{\alpha_4}{2} + \bar{z}\cos\frac{\alpha_4}{2}\,. \tag{18.29}$$

The only variable terms in (18.28) are y, $z^2 + p^2$, zp and $z + p$. For the latter ones the expressions are obtained:

$$\left.\begin{aligned} z^2 + p^2 &= (1 + C_4)\bar{z}^2 + (1 - C_4)\bar{x}^2 \,, \\ 2zp &= (1 + C_4)\bar{z}^2 - (1 - C_4)\bar{x}^2 \,, \\ z + p &= 2\bar{z}\cos\frac{\alpha_4}{2} \,. \end{aligned}\right\} \tag{18.30}$$

When this is substituted into (18.28), $\bar{x}$ occurs only in the forms $\bar{x}^2$ and $\bar{x}^4$. This confirms the symmetry. For $\bar{x}^2$ the expression $1 - y^2 - \bar{z}^2$ obtained from the equation of the sphere is substituted. The resulting equation is the functional equation of the projection of the coupler curve onto the plane of symmetry. The equation is of fourth order in both y and $\bar{z}$.

18.3.3 Geometrical Locus of Double Points

The linear Eqs.(18.16) and (18.17) for $\sin\alpha$ and $\cos\alpha$ do not have a unique solution when the determinant Δ in (18.18) equals zero:

$$S_4 C_7 \sin v - C_4 S_7 + S_7 \cos^2 v \cos u (S_4 \sin u + C_4 \cos u) = 0 \,. \tag{18.31}$$

This equation defines a curve τ on the unit sphere. The determinant appears also on the right-hand side of (18.26). Thus, the equation $\Delta = 0$ has the alternative form

$$S_4 C_7 y - C_4 S_7 + S_7 z (S_4 x + C_4 z) = 0 \,. \tag{18.32}$$

This equation defines a surface in the x, y, z-system. The curve τ is the intersection of the surface with the unit sphere.

Indeterminacy of $\sin\alpha$ and $\cos\alpha$ means that a position of the coupler point C on τ is produced by (at least) two positions of the four-bar with different angles α. This means that a point C on τ is a multiple point of the coupler curve. For comparison: In the case of the planar four-bar, the condition $\Delta = 0$ defines the circle of singular foci with Eq.(17.87). Figure 17.22 was used for proving that the inverse statement is true: If the coupler point C is at one and the same point in two (or more) different positions of the four-bar, this multiple point lies on the circle. Following Dobrovolski [2] the same Fig. 17.22 is now used for proving that this statement holds true for spherical four-bars if the word *circle* is replaced by *curve* τ. The straight lines in the figure are interpreted as arcs of great circles on the unit sphere and the angle β in the coupler triangle has the new name α_7. Repeating the old arguments it is shown that the angle $\sphericalangle(\mathrm{A_0CB_0})$ equals the angle α_7 of the coupler triangle. In other words this means: The curve τ described by (18.31) and (18.32) is the geometric locus of all points on the sphere from which the base $\overline{\mathrm{A_0B_0}}$ is seen under the angle α_7. In the plane this property defines the circle of singular foci (17.87). Like this circle also the curve τ

is uniquely determined by the base length α_4 and by the angle α_7 in the coupler triangle.

In what follows, more properties of the curve τ are revealed. Special points located on τ are the base points A_0 and B_0 and the points diametrically opposed to these two. This can be verified by substituting the coordinates (u, v) of these points into (18.31). The coordinates are $(u, v) = (0, 0)$, $(0, \pi)$, $(\alpha_4, 0)$ and (α_4, π), respectively. Another proof uses the geometric argument that from each of the four points the base $\overline{A_0B_0}$ is seen under an arbitrary angle and, thus, under the angle α_7.

Symmetry properties of the curve τ are revealed when (18.32) is transformed into the $\bar{x}, y, \bar{z}$-system by substituting for x and z the expressions from (18.29). This produces the equation

$$S_4C_7y - C_4S_7 + \frac{1}{2}S_7[(1 + C_4)\bar{z}^2 - (1 - C_4)\bar{x}^2] = 0 \,. \tag{18.33}$$

It is the principal-axes equation of a hyperbolic paraboloid. The curve τ is the intersection of the paraboloid with the sphere. The curve is symmetrical with respect to the $\bar{x}, y$-plane and also to the $y, \bar{z}$-plane. The same symmetry properties are revealed by (18.31). With a new variable w defined through the equation $u = w + \alpha_4/2$ the two planes of symmetry are the planes $w = 0$ and $w = \pi/2$. In terms of w the last term in (18.31) is

$$\begin{aligned} &\cos u(S_4 \sin u + C_4 \cos u) = \cos(w + \alpha_4/2)\cos(w - \alpha_4/2) \\ &= \frac{1}{2}(C_4 + \cos 2w) \end{aligned} \tag{18.34}$$

so that (18.31) becomes

$$S_4C_7 \sin v - C_4S_7 + \frac{1}{2}S_7 \cos^2 v(C_4 + \cos 2w) = 0 \,. \tag{18.35}$$

Equation (18.33) and the equation of the sphere are now used for formulating equations for the projections of τ onto the two planes of symmetry. The equations are obtained by making in (18.33) the substitutions $\bar{x}^2 = 1 - y^2 - \bar{z}^2$ and $\bar{z}^2 = 1 - y^2 - \bar{x}^2$, respectively. The projections turn out to be the ellipses

$$\frac{\bar{z}^2}{\frac{S_4^2}{2S_7^2(1-C_4)}} + \left[\frac{y + \frac{C_7S_4}{S_7(1-C_4)}}{\frac{S_4}{S_7(1-C_4)}}\right]^2 = 1 \,, \qquad \frac{\bar{x}^2}{\frac{S_4^2}{2S_7^2(1+C_4)}} + \left[\frac{y - \frac{C_7S_4}{S_7(1+C_4)}}{\frac{S_4}{S_7(1+C_4)}}\right]^2 = 1 \,. \tag{18.36}$$

In Fig. 18.4 these ellipses are shown for the three sets of parameters $(\alpha_4, \alpha_7) = (60°, 30°)$, $(60°, 60°)$ and $(60°, 90°)$. The circles represent the projections of the unit sphere. Only the elliptic sections inside the circles belong to curves τ.

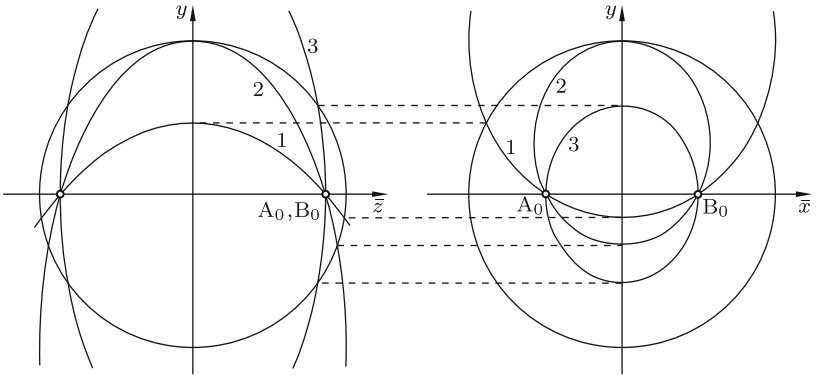

Fig. 18.4 Projections of the unit sphere and of three curves τ onto the planes of symmetry $w = \pi/2$ ($\bar{z}, y$-plane) and $w = 0$ ($\bar{x}, y$-plane). Ellipses 1 , 2 , 3 for the sets of parameters $(\alpha_4, \alpha_7) = (60°, 30°)$, $(60°, 60°)$ and $(60°, 90°)$, respectively

From the properties of the curve τ it follows that two spherical four-bars have one and the same curve τ only if they have the same base points A_0 and B_0 and the same angle α_7 . From this it follows that for spherical four-bars there is no theorem equivalent to the Roberts-Tschebyschev Theorem 17.2. This is the most significant qualitative difference between planar and spherical four-bars.

In both projections in Fig. 18.4 the ellipse belonging to the parameters $(60°, 60°)$ is passing through the north pole. Hence, also the curve τ is passing through the north pole. The general condition for a curve τ to pass through a pole is that (18.35) be satisfied by $v = \pi/2$ (north pole) or by $v = -\pi/2$ (south pole). This is the case if the parameters α_4 and α_7 satisfy the condition $\sin(\alpha_4 - \alpha_7) = 0$ (north pole) or $\sin(\alpha_4 + \alpha_7) = 0$ (south pole). Under these conditions (18.35) has the special forms (upper sign for north pole)

$$\cos 2w = \cos\alpha_4 \, \frac{1 \mp \sin v}{1 \pm \sin v} \qquad \leftrightarrow \qquad \sin v = \mp \frac{\cos 2w - \cos\alpha_4}{\cos 2w + \cos\alpha_4} \, . \tag{18.37}$$

These equations display the following properties. The curve has a double point at the respective pole. At the double point the curve is tangent to the two great circles $w = \alpha_4$ and $w = -\alpha_4$. The entire curve is located between these two great circles. It intersects the equator at the points $w = \alpha_4/2$ and $w = -\alpha_4/2$ (these are the base points A_0 and B_0). At $w = 0$ the curve reaches its extremal geographical latitude $v = \mp \sin^{-1}[(1 - \cos\alpha_4)/(1 + \cos\alpha_4)]$. The curve τ is unicursal in the case $|\tan\alpha_7| < |\tan\alpha_4|$ and it is bicursal in the case $|\tan\alpha_7| > |\tan\alpha_4|$.

18.3.4 Stereographic Projection

From the previous section it is known that double points of coupler curves are located on the curve τ if these points are associated with two different positions of the spherical four-bar[2]. For making statements about the number of double points algebraic equations in terms of two variables are needed for the coupler curve and for the curve τ. Such equations are obtained by a suitable projection. Parallel projections are not suitable because they may produce double points to which no double point on the sphere corresponds. Following Primrose/Freudenstein [7] a stereographic projection from a central point Q located on the sphere onto the plane tangent to the sphere at the point opposite Q is used. As central point Q the point opposite the base point A_0 is chosen. In contrast to Primrose/Freudenstein, not (18.22) written in terms of geographical coordinates is used, but (18.26) written in terms of the cartesian coordinates x, y, z. In the x, y, z-system the central point Q has the coordinates $(0, 0, -1)$, and the plane of projection has the equation $z = 1$. Let P be an arbitrary point on the sphere with coordinates (x, y, z), and let P′ with coordinates $(\xi, \eta, 1)$ be the stereographic projection of P. Because of the collinearity of Q, P and P′

$$\frac{\xi}{x} = \frac{\eta}{y} = \frac{2}{z+1} \,. \tag{18.38}$$

Also $x^2 + y^2 + z^2 = 1$. Resolution of these equations for ξ and η yields

$$\xi = \frac{2x}{z+1} \,, \qquad \eta = \frac{2y}{z+1} \,. \tag{18.39}$$

Conversely, resolution for x, y and z yields

$$x = \frac{4\xi}{\xi^2+\eta^2+4} \,, \qquad y = \frac{4\eta}{\xi^2+\eta^2+4} \,, \qquad z = \frac{4-\xi^2-\eta^2}{\xi^2+\eta^2+4} \,. \tag{18.40}$$

These expressions are substituted into (18.26). After multiplication with the common denominator $(\xi^2 + \eta^2 + 4)^4$ the following equation is obtained for the stereographic projection of the coupler curve:

[2] The double point produced by a foldable spherical four-bar in the folding position belongs to two different branches of the coupler curve and to a single position of the four-bar. Therefore, this double point may or may not be located on τ

$$
\begin{aligned}
&S_6^2[(\xi^2+\eta^2)(C_1+C_5)+4(C_1-C_5)]^2\\
&\times[S_4^2(\xi^2+\eta^2)^2+8(\xi^2+\eta^2)(C_4S_4\xi+1+C_4^2)+16S_4(-S_4\xi^2-2C_4\xi+S_4)]\\
&+16S_5^2(\xi^2+\eta^2)[(\xi^2+\eta^2)(C_3+C_4C_6)-4(S_4C_6\xi-C_3+C_4C_6)]^2\\
&-8S_5S_6[(\xi^2+\eta^2)(C_1+C_5)+4(C_1-C_5)]\\
&\times[(\xi^2+\eta^2)(C_3+C_4C_6)-4(S_4C_6\xi-C_3+C_4C_6)]\\
&\times\{(\xi^2+\eta^2)[S_4(C_7\xi+S_7\eta)+4C_4C_7]+4S_4(-C_7\xi+S_7\eta)\}\\
&=16S_5^2S_6^2\{(\xi^2+\eta^2)[S_4(-S_7\xi+C_7\eta)-4C_4S_7]+4S_4(S_7\xi+C_7\eta)\}^2\ . \qquad (18.41)
\end{aligned}
$$

In multiplying out the factor $(\xi^2+\eta^2)$ is encountered repeatedly. Separation of terms of orders eight, seven, six, five and lower results in an equation of the form

$$
\begin{aligned}
p_1(\xi^2+\eta^2)^4+(\xi^2+\eta^2)^3(p_2\xi+p_3\eta)+(\xi^2+\eta^2)^2(p_4\xi^2+p_5\xi\eta+p_6\eta^2\\
+p_7\xi+p_8\eta)+\ldots\,\text{(fourth- and lower-order terms)}=0\ . \qquad (18.42)
\end{aligned}
$$

The constant coefficients $p_1\,, p_2\,, \ldots$ are complicated functions of the system parameters $\alpha_1\,, \ldots, \alpha_7$. The simplest coefficient is $p_1=[S_4S_6(C_1+C_5)]^2$. The curve is of order eight with circularity four.

Equation (18.42) provides the basis for another proof of the theorem that a coupler curve intersects a circle on the unit sphere in eight points. First, it is proved that the stereographic projection of an arbitrary circle on the sphere is itself a circle. This is done as follows. A circle on the unit sphere is defined by a point fixed on the sphere and by an angle α. If (x_0, y_0, z_0) and (x, y, z) denote the coordinates of the fixed point and of a point on the circle, respectively, the equation of the circle is $xx_0+yy_0+zz_0=\cos\alpha$. Substitution of the expressions (18.40) yields the equation of the stereographic projection of the circle:

$$
(\xi^2+\eta^2)(z_0+\cos\alpha)-4(x_0\xi+y_0\eta+\cos\alpha)=0\ . \qquad (18.43)
$$

This, is indeed, the equation of a circle. Let now ξ_0, η_0 be the coordinates of the center of this circle, and let r be its radius. The circle has the parameter representation $\xi=\xi_0+r\cos\gamma$, $\eta=\eta_0+r\sin\gamma$. This yields $\xi^2+\eta^2=r^2+\xi_0^2+\eta_0^2+2r(\xi_0\cos\gamma+\eta_0\sin\gamma)$. These expressions are substituted into (18.42). The resulting equation is of fourth order in $\cos\gamma$ and $\sin\gamma$. The substitution $z=\tan\gamma/2$ leads to an 8th-order polynomial equation for z. This ends the proof.

The proof can also be formulated as follows. The stereographic projection of the coupler curve results in an 8th-order equation independent of which point on the sphere is chosen as central point of the projection. The central point can be chosen such that the given circle to be intersected by the coupler

curve is projected into a straight line. This line intersects the 8th-order curve at eight points.

Next, the curve τ is subjected to the stereographic projection. Let τ' be this projection. On τ' the right-hand side expression of (18.41) is zero. This is the desired equation of τ'. It is necessary to distinguish between the general case $\alpha_7 \neq \pi/2$ and the special case $\alpha_7 = \pi/2$. The two equations describing τ' read:

$$\alpha_7 \neq \frac{\pi}{2}: \quad (\xi^2+\eta^2)(\eta-\lambda\xi-\mu)+4(\eta+\lambda\xi)=0 \quad (\lambda=\tan\alpha_7\ ,\ \mu=4\lambda\cot\alpha_4)\ , \tag{18.44}$$

$$\alpha_7 = \frac{\pi}{2}: \quad \eta = \pm\sqrt{\frac{4\xi}{\xi+\cot\alpha_4}-\xi^2}\ . \tag{18.45}$$

Equation (18.44) defines a curve of third order with circularity one. It is of the same type as Burmester's center point curve (see (14.53)). The factor of $(\xi^2+\eta^2)$ yields the equation for the asymptote of the curve: $\eta=\lambda\xi+\mu$. The existence of an asymptote is due to the fact that the curve τ on the sphere passes through the central point Q of the stereographic projection. Both the origin and the point of intersection of the asymptote with the line $\eta+\lambda\xi=0$ lie on τ'. The line $\eta+\lambda\xi=0$ is tangent to τ' at the origin. From Eqs.(18.36) it is known under which conditions τ' is unicursal, bicursal and double-point curve, respectively. Furthermore, it is known that a double point is either the north pole or the south pole. The projections of these points are the points $\xi=0$, $\eta=2$ and $\xi=0$, $\eta=-2$, respectively.

Equations (18.42) and (18.44) for the projections of the coupler curve and of the curve τ, respectively, determine the number of double points of coupler curves. The orders eight and three, respectively, and the circularities four and one, respectively, tell that the two curves have a total of sixteen points of intersection. Thus, there is a total of eight double points. Two double points lie at infinity on the imaginary lines $\xi=\pm i\eta$. Proposition: Two more double points are the imaginary points with the coordinates[3] $\xi=-2C_4/S_4$, $\eta=\pm 2\mathrm{i}/S_4$. Proof: Substitution of these coordinates yields $\xi^2+\eta^2=-4$. Three terms appearing in (18.41) are individually zero. These are the terms

$$\left.\begin{aligned} &S_4^2(\xi^2+\eta^2)^2+8(\xi^2+\eta^2)(C_4S_4\xi+1+C_4^2)\\ &\quad +16S_4(-S_4\xi^2-2C_4\xi+S_4)=0\ ,\\ &(\xi^2+\eta^2)(C_3+C_4C_6)-4(S_4C_6\xi-C_3+C_4C_6)=0\ ,\\ &(\xi^2+\eta^2)[S_4(-S_7\xi+C_7\eta)-4C_4S_7]+4S_4(S_7\xi+C_7\eta)=0\ . \end{aligned}\right\} \tag{18.46}$$

This shows that both sides of the equation are individually zero. Thus, the points are located not only on the projection of the coupler curve, but also on the curve τ'. End of proof.

[3] The coordinates reported in [7] are incorrect due to a sign error in the formula for $\tan u$

This leaves, finally, a maximum number of four real double points. That this number can actually occur in a unicursal coupler curve is demonstrated by Fig. 18.5 . It shows in stereographic projection the coupler curve and the curve τ for the set of parameters $\alpha_1 = 85°$, $\alpha_2 = 82°$, $\alpha_3 = 100°$, $\alpha_4 = 90°$, $\alpha_5 = \alpha_6 = 50°$ (α_2 , α_5 and α_6 determine $\alpha_7 \approx 117.8°$). Note: In this figure the central point of the stereographic projection is the north pole (the point $y = 1$). This has the advantage that the projection of the curve τ is symmetric[4].

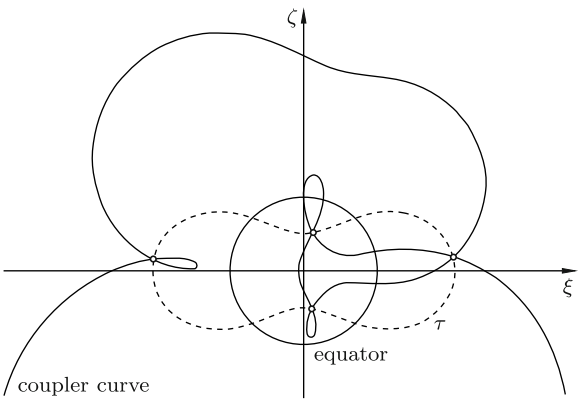

Fig. 18.5 Unicursal coupler curve with four double points on the curve τ in stereographic projection from the north pole. Parameters $\alpha_1 = 85°$, $\alpha_2 = 82°$, $\alpha_3 = 100°$, $\alpha_4 = 90°$, $\alpha_5 = \alpha_6 = 50°$, $\alpha_7 \approx 117.8°$

18.3.5 Cusps

As is known from the planar four-bar double points may degenerate into cusps. Conditions for the occurrence of cusps are developed as follows (compare with the formulation of condition (17.94) for the planar four-bar and with Fig. 17.24). The coupler point C is located in a cusp when the coupler is momentarily rotating about the axis $\overline{0C}$. Then A_0 , A and C lie on a great circle, and B_0 , B and C lie on another great circle. This can happen in altogether four different configurations. The common feature is that the

[4] Equation (18.33) is the principal-axes equation of τ . The pertinent transformation equations are

$$\bar{x} = \frac{4\xi}{\xi^2+\zeta^2+4}, \qquad y = \frac{\xi^2+\zeta^2-4}{\xi^2+\zeta^2+4}, \qquad \bar{z} = \frac{4\zeta}{\xi^2+\zeta^2+4}.$$

This projection produces the principal-axes equation of the curve shown in Fig. 18.5:

$$(\xi^2+\zeta^2)^2 \sin(\alpha_4-\alpha_7) - 8(\xi^2-\zeta^2)\sin\alpha_7 - 16\sin(\alpha_4+\alpha_7) = 0$$

great-circle arcs of lengths α_1, α_5 and of α_3, α_6 are pairwise co-tangent. In any such configuration the base $\overline{A_0B_0}$ is seen from C either under the angle α_7 or under the angle $\pi - \alpha_7$. This proves again that cusps lie on the curve τ. The four configurations are shown by Fig. 17.24 if the straight lines are interpreted as great-circle arcs and if the notations are changed according to Fig. 18.3. The cosine law applied to the spherical triangles (A_0,B_0,C) and (A,B,C) yields the equations

$$\left.\begin{aligned} C_4 &= \cos(\alpha_1+\alpha_5)\cos(\alpha_3+\alpha_6) + \sin(\alpha_1+\alpha_5)\sin(\alpha_3+\alpha_6)C_7\,, \\ C_2 &= C_5C_6 + S_5S_6C_7\,. \end{aligned}\right\} \quad (18.47)$$

Elimination of $C_7 = \cos\alpha_7$ results in a condition for the existence of cusps. With the help of addition theorems it can be given the form

$$\begin{aligned} &C_1S_3S_5(C_5 - C_2C_6) + S_1C_3S_6(C_6 - C_2C_5) \\ &+ S_1S_3(C_5^2 + C_6^2 - C_2C_5C_6 - 1) + S_5S_6(C_4 - C_1C_2C_3) = 0\,. \end{aligned} \quad (18.48)$$

With reference to Fig. 17.24 the combination (S_1, S_3) can be replaced by any of the combinations $(-S_1, S_3)$, $(S_1, -S_3)$ and $(-S_1, -S_3)$. In Primrose/Freudenstein [7] the numerical example is given: $\alpha_1 = \alpha_3 = \alpha_4 = 90°$, $\alpha_5 = \alpha_6 = 30°$, $\alpha_2 = \cos^{-1}\frac{2}{3}$. With these parameters both the four-bar and the coupler triangle are symmetric. Condition (18.48) is satisfied with all four combinations (S_1, S_3), $(-S_1, S_3)$, $(S_1, -S_3)$ and $(-S_1, -S_3)$. Equation (18.47) yields $C_7 = -1/3$. The coupler curve with these parameters is bicursal with two cusps in each branch. It is shown in Fig. 18.6 together with the curve τ in the same stereographic projection that was used in Fig. 18.5.

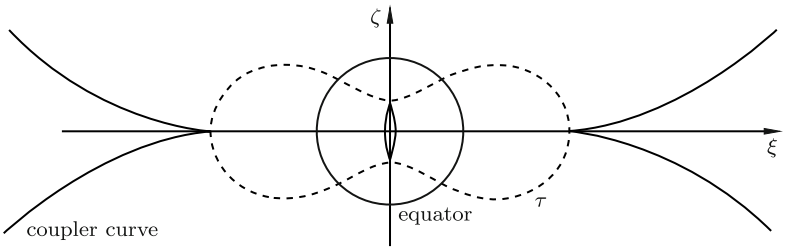

Fig. 18.6 Bicursal coupler curve with four cusps on the curve τ in stereographic projection from the north pole. Parameters $\alpha_1 = \alpha_3 = \alpha_4 = 90°$, $\alpha_5 = \alpha_6 = 30°$, $\alpha_2 = \cos^{-1}\frac{2}{3}$, $\alpha_7 = \cos^{-1}\left(\frac{-1}{3}\right)$

18.3.6 Parameter Equations for Coupler Curves

In Fig. 18.7 a spherical four-bar with coupler triangle and with coordinate systems x, y, z and x^*, y, z^* is shown. The parameters $\alpha_1, \ldots, \alpha_7$, the variables φ_1, φ_4 and the axial unit vectors $\mathbf{n}_1$, $\mathbf{n}_2$, $\mathbf{n}_3$, $\mathbf{n}_4$ are those of Fig. 18.1a. The x, y, z-system with unit basis vectors $\mathbf{e}_x$, $\mathbf{e}_y$, $\mathbf{e}_z$ is defined in the text preceding (18.25). The x^*, y, z^*-system is rotated against the x, y, z-system through the angle α_4 about the y-axis. The transformation is

$$\begin{bmatrix} x \\ y \\ z \end{bmatrix} = \begin{bmatrix} C_4 & 0 & S_4 \\ 0 & 1 & 0 \\ -S_4 & 0 & C_4 \end{bmatrix} \begin{bmatrix} x^* \\ y \\ z^* \end{bmatrix} . \tag{18.49}$$

The coupler triangle is defined as usual by the parameters α_5, α_6, α_7. In addition, angular parameters η, ζ of the coupler point C and the auxiliary angle χ are introduced. The parameters η, ζ are equivalent to the parameters of equal name in the coupler triangle of the planar four-bar in Fig. 17.19. Cosine and sine laws establish the equations

$$\left.\begin{aligned} &C_2 = C_5 C_6 + S_5 S_6 C_7 , \quad C_5 = \cos\eta \cos\zeta , \quad C_6 = \cos(\alpha_2 - \eta)\cos\zeta , \\ &\sin\zeta = S_5 \sin\chi , \qquad \cos\chi = \frac{C_6 - C_5 C_2}{S_5 S_2} . \end{aligned}\right\} \tag{18.50}$$

The goal of the following analysis is to express the coordinates x, y, z of the coupler point C as functions of the single variable φ_1. Such parameter equations are the basis of graphical displays of coupler curves. Together with the x, y, z-coordinates the geographical coordinates u, v determined by (18.25) and the stereographic coordinates ξ, η determined by (18.39) become functions of φ_1. The desired functions are obtained by expressing the position

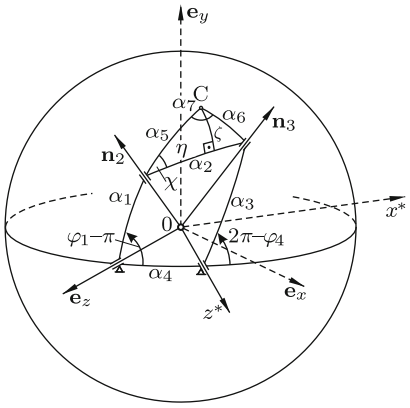

Fig. 18.7 Parameters η, ζ and α_5, α_6, α_7 in the coupler triangle. Coordinate systems

vector $\overrightarrow{0C}$ of the coupler point C in two forms:

$$\overrightarrow{0C} = x\mathbf{e}_x + y\mathbf{e}_y + z\mathbf{e}_z \,, \qquad \overrightarrow{0C} = z_1\mathbf{n}_2 + z_2\mathbf{n}_3 + z_3\mathbf{n}_2 \times \mathbf{n}_3 \,. \tag{18.51}$$

This identity is written in the form

$$[\mathbf{e}_x\ \mathbf{e}_y\ \mathbf{e}_z] \begin{bmatrix} x \\ y \\ z \end{bmatrix} = [\mathbf{n}_2 \quad \mathbf{n}_3 \quad \mathbf{n}_2 \times \mathbf{n}_3] \begin{bmatrix} z_1 \\ z_2 \\ z_3 \end{bmatrix} \,. \tag{18.52}$$

The expression on the right-hand side is transformed in two steps. In Step 1, the constants z_1, z_2, z_3 are expressed in terms of the parameters of the coupler triangle. In Step 2, the vectors $\mathbf{n}_2$, $\mathbf{n}_3$ and $\mathbf{n}_2 \times \mathbf{n}_3$ are expressed as linear combinations of $\mathbf{e}_x$, $\mathbf{e}_y$, $\mathbf{e}_z$ with variable coefficients.
Step 1: Scalar multiplications of the second Eq.(18.51) by $\mathbf{n}_2$, $\mathbf{n}_3$ and $\mathbf{n}_2 \times \mathbf{n}_3$ result in the equations (see Fig. 18.7)
$C_5 = z_1 + C_2 z_2$, $C_6 = C_2 z_1 + z_2$, $\sin\zeta = S_2 z_3$, whence it follows that

$$\begin{bmatrix} z_1 \\ z_2 \\ z_3 \end{bmatrix} = \frac{1}{S_2^2} \begin{bmatrix} C_5 - C_2C_6 \\ C_6 - C_2C_5 \\ S_2 \sin\zeta \end{bmatrix} \,. \tag{18.53}$$

Using (18.50) alternative expressions in terms of α_5, α_6, α_7 only or in terms of α_2, η, ζ only can be obtained, for example

$$C_5 - C_2C_6 = S_6(C_5S_6 - S_5C_6C_7) \,, \qquad S_2^2 = 1 - (C_5C_6 + S_5S_6C_7)^2 \,,$$
$$(C_5 - C_2C_6)/S_2^2 = \sin(\alpha_2 - \eta)\cos\zeta/S_2 \,, \qquad (C_6 - C_2C_5)/S_2^2 = \sin\eta\,\cos\zeta/S_2 \,.$$

Step 2: Figure 18.7 shows that $\mathbf{n}_2$ has in the x, y, z-system the coordinates (with the abbreviations $c_i = \cos\varphi_i$, $s_i = \sin\varphi_i$) $[-S_1c_1 \quad -S_1s_1 \quad C_1]$.
Similarly, in the x^*, y, z^*-system $\mathbf{n}_3$ has the coordinates $[S_3c_4 \quad -S_3s_4 \quad C_3]$.
The transformation (18.49) yields the coordinates in the x, y, z-system:
$[C_3S_4 + S_3C_4c_4 \quad -S_3s_4 \quad C_3C_4 - S_3S_4c_4]$. The x, y, z-coordinates of $\mathbf{n}_2$ and $\mathbf{n}_3$ constitute the first and the second column of the matrix below. Together they determine the coordinates of $\mathbf{n}_2 \times \mathbf{n}_3$ in column 3.

$$\underline{A} = \begin{bmatrix} -S_1c_1 & C_3S_4 + S_3C_4c_4 & C_1S_3s_4 - S_1s_1(C_3C_4 - S_3S_4c_4) \\ -S_1s_1 & -S_3s_4 & C_1(C_3S_4 + S_3C_4c_4) + S_1c_1(C_3C_4 - S_3S_4c_4) \\ C_1 & C_3C_4 - S_3S_4c_4 & S_1[s_1(C_3S_4 + S_3C_4c_4) + S_3c_1s_4] \end{bmatrix} \,. \tag{18.54}$$

For c_4 and s_4 the expressions (18.3) are substituted. The matrix $\underline{A}$ is then a function of φ_1. The matrix establishes the relation

$$[\mathbf{n}_2 \quad \mathbf{n}_3 \quad \mathbf{n}_2 \times \mathbf{n}_3] = [\mathbf{e}_x\ \mathbf{e}_y\ \mathbf{e}_z]\,\underline{A}(\varphi_1) \,. \tag{18.55}$$

Substitution of (18.55) and (18.53) into (18.52) results in the desired parameter equations for the coupler curve:

$$\begin{bmatrix} x \\ y \\ z \end{bmatrix} = \frac{1}{S_2^2} \underline{A}(\varphi_1) \begin{bmatrix} C_5 - C_2 C_6 \\ C_6 - C_2 C_5 \\ S_2 \sin\zeta \end{bmatrix} . \tag{18.56}$$

18.4 Spherical Parallel Robot

The spherical linkage with center 0 shown in Fig. 18.8 is a parallel robot. The position of its triangular platform (A,B,C) is controlled by the angles of rotation α_i about fixed (not necessarily orthogonal) axes. The kinematics has been investigated by Gosselin, Sefriou and Richard [3, 4]. The problem

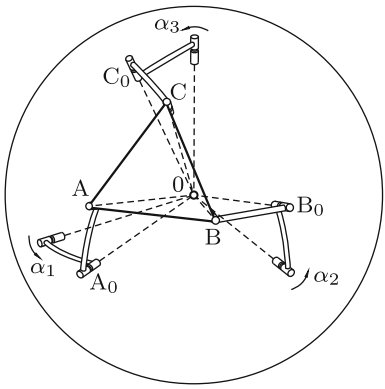

Fig. 18.8 Spherical parallel robot

of direct kinematics is to determine all positions of the platform when the angles α_i $(i = 1, 2, 3)$ are given. The solution to this problem is found in Sects. 18.3.1 and 18.3.4 . When the angles are given, the points A_0 , B_0 and C_0 are fixed. Imagine that in this position the connection C between the binary link C_0C and the triangle (A,B,C) is opened. The binary link is then free to lead its point C on a circle about C_0 , and the spherical four-bar A_0ABB_0 is free to lead its coupler-fixed point C along a coupler curve. Hence C is a point of intersection of this circle and this coupler curve. The maximum number of real points of intersection was shown to be eight. The calculation of these points is based either on Eqs.(18.26) and (18.27) or on Eq.(18.42).

Gosselin and Gagne [5] investigated the special case when all angular system parameters equal $\pi/2$. In what follows, their analysis is presented in a modified form. In Fig. 18.9 the mutually orthogonal rotation axes $\mathbf{e}_1^1$, $\mathbf{e}_2^1$, $\mathbf{e}_3^1$ are directed along the edges of the fixed cube 1 . The platform-fixed axes $\overline{0A}$, $\overline{0B}$, $\overline{0C}$ are the axes $\mathbf{e}_1^2$, $\mathbf{e}_2^2$, $\mathbf{e}_3^2$ along the edges of another cube 2 representing the platform. Each pair of binary links connects an axis on cube

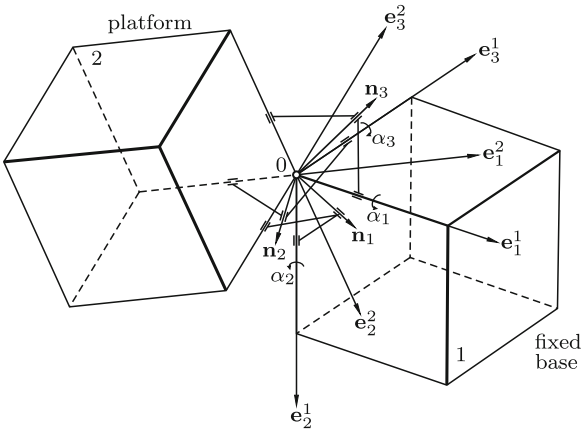

Fig. 18.9 Special spherical parallel robot

1 to an axis on cube 2. The labeling of axes and of pairs of binary links is as follows. The pair connected to the axis $\mathbf{e}_i^1$ which is operated by the angle α_i is referred to as pair i. It connects $\mathbf{e}_i^1$ to $\mathbf{e}_{i+1}^2$ via the internal axis $\mathbf{n}_{i-1}$ ($i = 1, 2, 3$ cyclic). The orthogonality of axes of binary links is expressed by the equations

$$\mathbf{n}_1 \cdot \mathbf{e}_2^1 = 0\,, \qquad \mathbf{n}_2 \cdot \mathbf{e}_3^1 = 0\,, \qquad \mathbf{n}_3 \cdot \mathbf{e}_1^1 = 0\,, \tag{18.57}$$

$$\mathbf{n}_1 \cdot \mathbf{e}_3^2 = 0\,, \qquad \mathbf{n}_2 \cdot \mathbf{e}_1^2 = 0\,, \qquad \mathbf{n}_3 \cdot \mathbf{e}_2^2 = 0\,. \tag{18.58}$$

Let the null position $\alpha_1 = \alpha_2 = \alpha_3 = 0$ be the one in which for $i = 1, 2, 3$ the triple of vectors $\mathbf{e}_i^1$, $\mathbf{e}_i^2$ and $\mathbf{n}_i$ coalesces. With this definition, the vectors $\mathbf{n}_1$, $\mathbf{n}_2$, $\mathbf{n}_3$ have in basis $\underline{\mathbf{e}}^1$ the coordinates (with abbreviations $C_i = \cos\alpha_i$, $S_i = \sin\alpha_i$)

$$\underline{n}_1 = [\, C_2 \quad 0 \quad -S_2 \,]^T\,, \quad \underline{n}_2 = [\, -S_3 \quad C_3 \quad 0 \,]^T\,, \quad \underline{n}_3 = [\, 0 \quad -S_1 \quad C_1 \,]^T\,. \tag{18.59}$$

With these coordinates and with the direction cosine matrix $\underline{A}$ defined by the equation $\underline{\mathbf{e}}^1 = \underline{A}\,\underline{\mathbf{e}}^2$ the orthogonality conditions (18.58) have the forms

$$-S_3 a_{11} + C_3 a_{21} = 0\,, \quad -S_1 a_{22} + C_1 a_{32} = 0\,, \quad C_2 a_{13} - S_2 a_{33} = 0\,. \tag{18.60}$$

The problem of direct kinematics is to solve these equations for the direction cosines when the angles α_i ($i = 1, 2, 3$) are given. It is known that with three angular position variables critical cases occur. Here, a critical case occurs when a single angle equals $\pi/2$ or $-\pi/2$. Example: From Fig. 18.9 it is seen that $\alpha_1 = \pi/2$ is possible only in combination with $\alpha_3 = 0$ and with $\mathbf{n}_1 = \mathbf{e}_2^1 = \mathbf{e}_3^2$. In this position the platform is free to rotate about $\mathbf{n}_1$, and α_2 is arbitrary independent of this rotation. Hence the platform position is

not controllable if $\alpha_1 = \pi/2$. With a cyclic change of indices the same is true for $\alpha_2 = \pi/2$ and for $\alpha_3 = \pi/2$. In order to avoid critical positions the robot must be operated in the range $-\pi/2 < \alpha_i < \pi/2$ $(i = 1, 2, 3)$.

Solving Eqs.(18.60) is difficult because of second-order constraint equations for direction cosines. The solution is simpler when the matrix is expressed in terms of Bryan angles. Following [5] the sequence of rotations is defined as follows (this differs from the sequence chosen in Sect. 1.4). The first rotation is the one with angle ϕ_3 about the axis $\mathbf{e}_3^1$. Then follows the rotation with angle ϕ_2 about the actual position of $\mathbf{e}_2^2$ and then the rotation with angle ϕ_1 about the actual position of $\mathbf{e}_1^2$. With this sequence of rotations the direction cosine matrix is (with abbreviations $c_i = \cos\phi_i$, $s_i = \sin\phi_i$)

$$\underline{A} = \begin{bmatrix} c_2c_3 & -c_1s_3 + s_1s_2c_3 & s_1s_3 + c_1s_2c_3 \\ c_2s_3 & c_1c_3 + s_1s_2s_3 & -s_1c_3 + c_1s_2s_3 \\ -s_2 & s_1c_2 & c_1c_2 \end{bmatrix} . \tag{18.61}$$

With direction cosines expressed in this form Eqs.(18.60) become

$$\left.\begin{array}{ll} c_2\sin(\phi_3 - \alpha_3) = 0 \ , & \\ c_1S_1c_3 & +s_1(S_1s_3s_2 - C_1c_2) = 0 \ , \\ c_1(C_2c_3s_2 - S_2c_2) & +s_1C_2s_3 \qquad\quad = 0 \ . \end{array}\right\} \tag{18.62}$$

The first equation has the solutions

$$\phi_{3_1} = \alpha_3 \ , \qquad \phi_{3_2} = \alpha_3 + \pi \tag{18.63}$$

and the irrelevant solution $c_2 = 0$ independent of α_1, α_2, α_3 which marks the critical case for Bryan angles.

The second and the third equation are homogeneous linear equations for c_1 and s_1. Nontrivial solutions exist if the determinant of the coefficients is zero. This condition is

$$c_2[c_2(C_1S_2 - S_1C_2s_3c_3) - s_2(C_1C_2c_3 + S_1S_2s_3)] = 0 \ . \tag{18.64}$$

As before, the solution $c_2 = 0$ is of no interest. The remaining term yields

$$\tan\phi_2 = \frac{s_2}{c_2} = \frac{C_1S_2 - S_1C_2s_3c_3}{C_1C_2c_3 + S_1S_2s_3} \ . \tag{18.65}$$

The third Eq.(18.62) yields

$$\tan\phi_1 = \frac{s_1}{c_1} = \frac{S_2c_2 - C_2c_3s_2}{C_2s_3} \ . \tag{18.66}$$

For each of the two solutions ϕ_3 (18.65) determines two solutions ϕ_2 also differing by π, and for each of these two solutions (18.66) determines two solutions ϕ_1 also differing by π. Hence there are altogether eight sets of solutions ϕ_1, ϕ_2, ϕ_3. The associated sines and cosines are substituted into the matrix (18.61). It turns out that the four matrices associated with ϕ_{3_2} are identical with those associated with ϕ_{3_1}. Hence there are only four different platform positions.

Example: Given the angles $\alpha_1 = 30°$, $\alpha_2 = 45°$ and $\alpha_3 = 60°$. With the solution $\phi_3 = \alpha_3 = 60°$ Eq.(18.65) yields $\tan\phi_2 = 3/4$. Consequently, $c_2 = \pm 4/5$ and $s_2 = \pm 3/5$. With the plus sign (18.66) yields $\tan\phi_1 = \sqrt{1/3}$, i.e., $\phi_1 = 30°$ and $\phi_1 = 210°$. End of example.

In what follows, the direction cosine matrix $\underline{A}$ of Eq.(18.61) is expressed not in terms of Bryan angles, but in the form (1.49) through the angle φ and the direction of a single rotation. The coordinates of the unit vector along the axis of rotation are denoted $a_{1,2,3}$ since $n_{1,2,3}$ have already been used. With the abbreviations $c = \cos\varphi$ and $s = \sin\varphi$ the matrix is

$$\underline{A}^{12} = \begin{bmatrix} a_1^2(1-c)+c & a_1a_2(1-c)-a_3s & a_1a_3(1-c)+a_2s \\ a_1a_2(1-c)+a_3s & a_2^2(1-c)+c & a_2a_3(1-c)-a_1s \\ a_1a_3(1-c)-a_2s & a_2a_3(1-c)+a_1s & a_3^2(1-c)+c \end{bmatrix} . \tag{18.67}$$

With these expressions for the direction cosines the orthogonality conditions (18.60) are

$$C_i[a_ja_k(1-c)+a_is]-S_i[a_j^2(1-c)+c] = 0 \qquad (i,j,k = 1,2,3 \text{ cyclic}) . \tag{18.68}$$

The resolution for c, s and $a_{1,2,3}$ in terms of given values of C_i, S_i $(i = 1,2,3)$ is difficult. The only simple case is the special case of identical angles $\alpha_i \equiv \alpha$ $(C_i \equiv C,\ S_i \equiv S)$. For reasons of symmetry it can be predicted that $a_1 = a_2 = a_3 = \sqrt{1/3}$ is a solution. With these simplifications the three Eqs.(18.68) are identical. With the abbreviation $T = \tan\alpha = S/C$ they have the form

$$(1+2T)\cos\varphi - \sqrt{3}\sin\varphi + T - 1 = 0 . \tag{18.69}$$

This equation has the irrelevant root $\varphi = 240°$ independent of T and the relevant root

$$\cos\varphi = \frac{2+2T-T^2}{2(1+T+T^2)} , \qquad \sin\varphi = \frac{T(T+2)\sqrt{3}}{2(1+T+T^2)} . \tag{18.70}$$

Final remark: The realization of a spherical joint 0 of the platform by means of six binary links and nine joints is complicated. It is unnecessarily complicated if only two degrees of freedom are required as is the case when

a platform is used for pointing a light-beam or a camera. In such cases, it suffices to mount the platform on a Hooke's joint.

References

1. Dobrovolski V V (1940) A new theory of spherical mechanisms (Russ.). Trudy MSII, Sb.VI
2. Dobrovolski V V (1944) On spherical coupler curves (Russ.). PMM v.8:475–477
3. Gosselin C M, Séfriou J, Richard M J (1994) On the direct kinematics of spherical three-degree-of-freedom parallel manipulators with a coplanar platform. ASME J. Mech.Des. 116:587–593
4. Gosselin C M, Séfriou J, Richard M J (1994) On the direct kinematics of spherical three-degree-of-freedom parallel manipulators of general architecture. ASME J. Mech.Des. 116:594–598
5. Gosselin C M, Gagne M (1995) A closed-form solution for the direct kinematics of a special three-degree-of-freedom parallel manipulator. In: [6]:231–240
6. Merlet J-P, Ravani B (eds.) (1995) Computational kinematics '95. Kluwer, Dordrecht
7. Primrose E J F, Freudenstein F (1969) Spatial motions. I. Point paths of mechanisms with four or fewer links. J. Eng.f.Ind. 91B:103–114

Chapter 19
Dynamics of Mechanisms

For numerical investigations into the dynamics of mechanisms nonlinear differential equations must be formulated. The formulation given in this chapter allows writing a general-purpose software tool applicable to arbitrary mechanisms. The change from one mechanism to another is accomplished by changing readily available input data. More information see in Wittenburg [4].

19.1 Conservative Single-Degree-of-Freedom Mechanisms

Subject of this introductory section is the following rather special yet frequently arising problem of dynamics. Imagine an arbitrary single-degree-of-freedom mechanism with an input shaft and an output shaft. Both shafts are rotating about frame-fixed axes. Simple examples: Hooke's joint, the planar four-bar, the spherical four-bar and the Bennett mechanism. The transmission ratio of a single-degree-of-freedom mechanism is the ratio $i = \dot{\varphi}_1/\dot{\varphi}_2$ (input angular velocity / output angular velocity). For the four illustrative examples the transmission ratio is known as function of the input angle φ_1. For Hooke's joint the function is (see (13.7)) $i(\varphi_1) = (1 - \sin^2\alpha\cos^2\varphi_1)/\cos\alpha$. For the planar four-bar the function is given in (17.35), and for the Bennett mechanism it is given in (6.16).

In what follows, only those mechanisms are considered which satisfy the condition $i(\varphi_1) \neq 0$. In words: If $\dot{\varphi}_2 \neq 0$, then $\dot{\varphi}_1 \neq 0$ independent of φ_1. Imagine that in a single-degree-of-freedom mechanism with a known function $i(\varphi_1) \neq 0$ a rotor with moment of inertia J_1 is mounted on the input shaft and that another rotor with moment of inertia J_2 is mounted on the output shaft. Compared with these rotors the masses and moments of inertia of both shafts and of the coupling mechanism are assumed to be negligible. Furthermore, it is assumed that no external torques are applied to

J. Wittenburg, *Kinematics*, DOI 10.1007/978-3-662-48487-6_19

the shafts and that no springs and dampers are present in the entire system. Under these conditions the mechanism is idling with time-varying angular velocities $\dot{\varphi}_1$ and $\dot{\varphi}_2$. The law of conservation of kinetic energy requires that $J_1\dot{\varphi}_1^2 + J_2\dot{\varphi}_2^2 \equiv 2T = \text{const}$. The constant is given by the initial condition on $\dot{\varphi}_1$. The solution for $\dot{\varphi}_1$ is $\dot{\varphi}_1 = \sqrt{2T/[J_1 + J_2/i^2(\varphi_1)]}$. With the dimensionless parameter $\lambda^2 = J_2/J_1$ and with the constant angular velocity ω_0 defined through the equation $2T = (J_1 + J_2)\omega_0^2$ the solution is

$$\dot{\varphi}_1 = \omega_0 \sqrt{\frac{1+\lambda^2}{1+\lambda^2/i^2(\varphi_1)}} \,. \tag{19.1}$$

The graph of this function in a $\varphi_1, \dot{\varphi}_1$-diagram is called phase curve of the motion. Except for the special case $i(\varphi_1) = \text{const}$ which is typical for gear trains the angular velocity $\dot{\varphi}_1$ is not constant.

19.2 The General Problem of Dynamics

Subject of investigation for the rest of this chapter are joint-connected spatial mechanisms without dry friction in the joints. The system structure is arbitrary (serial chain, tree structure, single-loop or multiloop systems). Holonomic joints of arbitrary nature are taken into consideration. Most systems are joint-connected to a frame which is fixed in inertial space. In this chapter the more general case is considered that the system is joint-connected to a *carrier body* labeled body 0 which is moving relative to inertial space according to *prescribed* functions of time. Since this motion is prescribed, neither the center of mass nor the mass nor moments of inertia of body 0 are of concern. The body is represented by a moving basis $\underline{\mathbf{e}}^0$. The prescribed functions of time for body 0 are the position vector $\mathbf{r}_0(t)$, the velocity $\dot{\mathbf{r}}_0(t)$ and the acceleration $\ddot{\mathbf{r}}_0(t)$ of the origin of basis $\underline{\mathbf{e}}^0$ relative to an inertial basis $\underline{\mathbf{e}}$, the direction cosine matrix $\underline{A}_0(t)$ defined by the equation $\underline{\mathbf{e}} = \underline{A}_0\underline{\mathbf{e}}^0$, the angular velocity $\boldsymbol{\omega}_0(t)$ and the angular acceleration $\dot{\boldsymbol{\omega}}_0(t)$ relative to basis $\underline{\mathbf{e}}$. Since the motion of $\underline{\mathbf{e}}^0$ is prescribed, virtual displacements and virtual changes of velocity are zero. In the special case that body 0 is at rest the matrix $\underline{A}_0(t)$ is the unit matrix and the other five vectorial quantities are identically zero. This means that $\underline{\mathbf{e}}^0$ permanently coincides with $\underline{\mathbf{e}}$.

The general system under consideration is subject to arbitrary external forces and torques as well as to arbitrary internal forces and torques caused by springs, dampers or actuators (active elements) connecting bodies of the system. Let $F \geq 1$ (arbitrary) be the total degree of freedom so that the position of the system in basis $\underline{\mathbf{e}}$ is specified by F independent variables (generalized coordinates). Let $\underline{q} = [q_1 \ \ldots \ q_F]^T$ be the column matrix of suitably chosen variables. At this point it is unnecessary to specify whether

the variables are joint variables or variables specifying positions of bodies relative to basis $\underline{\mathbf{e}}$. Large motions of the system are governed by F nonlinear differential equations for the chosen variables $\underline{q}$. The goal of this chapter is to write these equations in the standard matrix form

$$\underline{A}\,\underline{\ddot{q}} = \underline{B}\,. \tag{19.2}$$

Because of the nonlinearity of the system the matrix $\underline{A}$ depends on the variables $\underline{q}$. It will be shown that $\underline{A}$ is symmetric and positive definite. The column matrix $\underline{B}$ depends on $\underline{q}$, on $\underline{\dot{q}}$ and, because of the prescribed motion of body 0, explicitly on time t. Explicit expressions for $\underline{A}$ and $\underline{B}$ are derived from the principle of virtual power which is the subject of the following section.

There are systems which are moving without kinematical constraints to inertial space. Typical examples are freely falling systems and systems orbiting Earth. The motion of the composite system center of mass C is governed by Newton's law $M\ddot{\mathbf{r}}_{\mathrm{C}} = \mathbf{F}_{\mathrm{res}}$ (total system mass M, resultant external force $\mathbf{F}_{\mathrm{res}}$). This vector equation – equivalent to three scalar equations – can be used for reducing the F scalar Eqs.(19.2) to a smaller set of $F-3$ equations. How to do this is shown in Sect. 19.4.1.

19.3 Principle of Virtual Power

The principle of virtual power is written in the Lagrangian form

$$\sum_{i=1}^{n} \int_{m_i} \delta\dot{\mathbf{r}} \cdot (\ddot{\mathbf{r}}\,\mathrm{d}m - \mathrm{d}\mathbf{F}) = 0\,. \tag{19.3}$$

The integral is taken over the mass m_i of body i, and the sum is taken over all bodies $i = 1, \ldots, n$. The vector $\mathbf{r}$ denotes the radius vector of a mass element $\mathrm{d}m$ of body i in the inertial basis $\underline{\mathbf{e}}$, $\ddot{\mathbf{r}}$ its absolute acceleration and $\delta\dot{\mathbf{r}}$ a virtual change of its velocity. Body 0 does not contribute to the sum because of $\delta\dot{\mathbf{r}} = \mathbf{0}$. The force $\mathrm{d}\mathbf{F}$ is the total force applied to $\mathrm{d}m$. It may be the infinitesimal weight $\mathbf{g}\,\mathrm{d}m$ of $\mathrm{d}m$. It may also be a finite force applied to $\mathrm{d}m$. Constraint forces caused by ideal kinematical constraints in joints do not contribute to virtual power because for every pair of constraint forces $\mathbf{F}_1 = +\mathbf{F}$ and $\mathbf{F}_2 = -\mathbf{F}$ (actio = reactio) the term $\delta\dot{\mathbf{r}}_1 \cdot \mathbf{F}_1 + \delta\dot{\mathbf{r}}_2 \cdot \mathbf{F}_2$ is equal to zero.

First, the contribution of a single rigid body i to the sum in (19.3) is formulated. Let $\mathbf{r}_i$ be the radius vector of the body center of mass C_i in $\underline{\mathbf{e}}$ and let, furthermore, $\boldsymbol{\varrho}$ be the body-fixed vector from C_i to the mass element $\mathrm{d}m$ (see Fig. 19.1). These definitions establish the three kinematics equations below. The last equation expresses the fact that C_i is the body

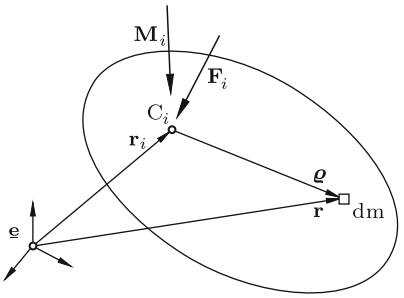

Fig. 19.1 Vectors $\mathbf{r}_i$ and $\boldsymbol{\varrho}$ locating the body i center of mass and a mass element $\mathrm{d}m$

center of mass.

$$\mathbf{r} = \mathbf{r}_i + \boldsymbol{\varrho}\,, \qquad \delta\dot{\mathbf{r}} = \delta\dot{\mathbf{r}}_i + \delta\boldsymbol{\omega}_i \times \boldsymbol{\varrho}\,, \qquad \ddot{\mathbf{r}} = \ddot{\mathbf{r}}_i + \ddot{\boldsymbol{\varrho}}\,, \qquad \int_{m_i} \boldsymbol{\varrho}\,\mathrm{d}m = \mathbf{0}\,. \tag{19.4}$$

With these equations a single integral in (19.3) is

$$\begin{aligned}\int_{m_i} \delta\dot{\mathbf{r}} \cdot (\ddot{\mathbf{r}}\,\mathrm{d}m - \mathrm{d}\mathbf{F}) &= \int_{m_i} (\delta\dot{\mathbf{r}}_i + \delta\boldsymbol{\omega}_i \times \boldsymbol{\varrho}) \cdot [(\ddot{\mathbf{r}}_i + \ddot{\boldsymbol{\varrho}})\,\mathrm{d}m - \mathrm{d}\mathbf{F}] \\ = \delta\dot{\mathbf{r}}_i \cdot (\ddot{\mathbf{r}}_i m_i - \mathbf{F}_i) &+ \delta\boldsymbol{\omega}_i \cdot \Big(\int_{m_i} \boldsymbol{\varrho} \times \ddot{\boldsymbol{\varrho}}\,\mathrm{d}m - \int_{m_i} \boldsymbol{\varrho} \times \mathrm{d}\mathbf{F} \Big)\,. \end{aligned} \tag{19.5}$$

The force $\mathbf{F}_i$ is the resultant applied force on body i. Its line of action passes through the body center of mass C_i. The last integral is the resultant applied torque $\mathbf{M}_i$ about the center of mass. The first integral is

$$\int_{m_i} \boldsymbol{\varrho} \times \ddot{\boldsymbol{\varrho}}\,\mathrm{d}m = \frac{\mathrm{d}}{\mathrm{d}t} \int_{m_i} \boldsymbol{\varrho} \times \dot{\boldsymbol{\varrho}}\,\mathrm{d}m\,. \tag{19.6}$$

The term $\dot{\boldsymbol{\varrho}}\,\mathrm{d}m$ under the integral on the right-hand side is the *momentum* of the mass element $\mathrm{d}m$. The integral is the *moment of momentum*, also called *angular momentum* of the entire body about the body center of mass. The formula $\dot{\boldsymbol{\varrho}} = \boldsymbol{\omega}_i \times \boldsymbol{\varrho}$ yields $\boldsymbol{\varrho} \times \dot{\boldsymbol{\varrho}} = \boldsymbol{\varrho} \times (\boldsymbol{\omega}_i \times \boldsymbol{\varrho}) = (\boldsymbol{\varrho}^2 \mathsf{I} - \boldsymbol{\varrho}\boldsymbol{\varrho}) \cdot \boldsymbol{\omega}_i$ and

$$\int_{m_i} \boldsymbol{\varrho} \times \dot{\boldsymbol{\varrho}}\,\mathrm{d}m = \int_{m_i} (\boldsymbol{\varrho}^2 \mathsf{I} - \boldsymbol{\varrho}\boldsymbol{\varrho})\,\mathrm{d}m \cdot \boldsymbol{\omega}_i = \mathsf{J}_i \cdot \boldsymbol{\omega}_i\,. \tag{19.7}$$

This equation defines the central *inertia tensor* J_i of the body:

$$\mathsf{J}_i = \int_{m_i} (\boldsymbol{\varrho}^2 \mathsf{I} - \boldsymbol{\varrho}\boldsymbol{\varrho})\,\mathrm{d}m\,. \tag{19.8}$$

The integral in (19.6) and (19.5) is the absolute time derivative of $\mathsf{J}_i \cdot \boldsymbol{\omega}_i$. This is (see (9.9)) $\mathsf{J}_i \cdot \dot{\boldsymbol{\omega}}_i + \boldsymbol{\omega}_i \times \mathsf{J}_i \cdot \boldsymbol{\omega}_i$. Thus, Eq.(19.3) for the entire system finally becomes

$$\sum_{i=1}^{n} \Big[\delta\dot{\mathbf{r}}_i \cdot (m_i \ddot{\mathbf{r}}_i - \mathbf{F}_i) + \delta\boldsymbol{\omega}_i \cdot (\mathsf{J}_i \cdot \dot{\boldsymbol{\omega}}_i + \boldsymbol{\omega}_i \times \mathsf{J}_i \cdot \boldsymbol{\omega}_i - \mathbf{M}_i) \Big] = 0 \,. \qquad (19.9)$$

The quantities $\delta\dot{\mathbf{r}}_i$, $\delta\boldsymbol{\omega}_i$, $\ddot{\mathbf{r}}_i$ and $\dot{\boldsymbol{\omega}}_i$ appear in linear form. For this reason the equation is written in the matrix form

$$\delta\dot{\underline{\mathbf{r}}}^T \cdot (\underline{m}\, \ddot{\underline{\mathbf{r}}} - \underline{\mathbf{F}}) + \delta\underline{\boldsymbol{\omega}}^T \cdot (\underline{\mathsf{J}} \cdot \dot{\underline{\boldsymbol{\omega}}} - \underline{\mathbf{M}}^*) = 0 \,. \qquad (19.10)$$

Here, $\underline{\mathbf{r}}$, $\underline{\mathbf{F}}$, $\underline{\boldsymbol{\omega}}$ and $\underline{\mathbf{M}}^*$ are column matrices of n vectors each, for example, $\underline{\mathbf{r}} = [\mathbf{r}_1 \ \ldots \mathbf{r}_n]^T$. The column matrix $\underline{\mathbf{M}}^*$ is introduced for abbreviation. Its elements are the vectors

$$\mathbf{M}_i^* = \mathbf{M}_i - \boldsymbol{\omega}_i \times \mathsf{J}_i \cdot \boldsymbol{\omega}_i \qquad (i = 1, \ldots, n) \,. \qquad (19.11)$$

Finally, $\underline{m}$ and $\underline{\mathsf{J}}$ are diagonal $(n \times n)$-matrices with masses $m_1, \ldots, m_n$ and inertia tensors $\mathsf{J}_1, \ldots, \mathsf{J}_n$, respectively, along the diagonal.

Following (19.2) the need for a special investigation into systems without kinematical constraints to inertial space was pointed out. In this investigation the composite system center of mass C plays an important role. Let $\mathbf{r}_\mathrm{C}$ be the radius vector of C in the inertial basis $\underline{\mathbf{e}}$, and let $\mathbf{R}_i$ be the vector pointing from the composite system center of mass C to the body i center of mass. From these definitions it follows that

$$\mathbf{r}_i = \mathbf{r}_\mathrm{C} + \mathbf{R}_i \,, \qquad \ddot{\mathbf{r}}_i = \ddot{\mathbf{r}}_\mathrm{C} + \ddot{\mathbf{R}}_i \quad (i = 1, \ldots, n) \,, \qquad \sum_{i=1}^{n} \mathbf{R}_i m_i = \mathbf{0} \,. \quad (19.12)$$

The expressions for $\mathbf{r}_i$ and $\ddot{\mathbf{r}}_i$ are substituted into (19.9). Multiplying out and using the last Eq.(19.12) results in the equation (M is the total system mass $M = m_1 + \ldots + m_n$)

$$\delta\dot{\mathbf{r}}_\mathrm{C} \cdot \Big(M\ddot{\mathbf{r}}_\mathrm{C} - \sum_{i=1}^{n} \mathbf{F}_i \Big) + \sum_{i=1}^{n} \Big[\delta\dot{\mathbf{R}}_i \cdot (m_i \ddot{\mathbf{R}}_i - \mathbf{F}_i) + \delta\boldsymbol{\omega}_i \cdot (\mathsf{J}_i \cdot \dot{\boldsymbol{\omega}}_i - \mathbf{M}_i^*) \Big] = 0 \,. \quad (19.13)$$

The absence of constraints to inertial space has the consequence that $\delta\dot{\mathbf{r}}_\mathrm{C}$ is independent. Hence the factor behind is zero. This is Newton's law for the composite system center of mass:

$$M\ddot{\mathbf{r}}_\mathrm{C} = \sum_{i=1}^{n} \mathbf{F}_i \,. \qquad (19.14)$$

The rest of the equation is written in the matrix form

$$\delta\dot{\underline{\mathbf{R}}}^T \cdot (\underline{m}\,\ddot{\underline{\mathbf{R}}} - \underline{\mathbf{F}}) + \delta\underline{\boldsymbol{\omega}}^T \cdot (\underline{\mathbf{J}} \cdot \dot{\underline{\boldsymbol{\omega}}} - \underline{\mathbf{M}}^*) = 0\ . \tag{19.15}$$

The formal difference between this equation and Eq.(19.10) for arbitrary systems is that $\underline{\mathbf{R}}$ replaces $\underline{\mathbf{r}}$. Between $\underline{\mathbf{R}}$ and $\underline{\mathbf{r}}$ exists a simple relationship. By definition, the radius vector of the composite system center of mass is

$$\mathbf{r}_{\mathrm{C}} = \frac{1}{M}\sum_{j=1}^{n} m_j \mathbf{r}_j\ . \tag{19.16}$$

Substitution into the first Eq.(19.12) yields

$$\mathbf{R}_i = \sum_{j=1}^{n} \Big(\delta_{ij} - \frac{m_j}{M}\Big)\mathbf{r}_j \qquad (i = 1, \ldots, n)\ . \tag{19.17}$$

Let $\underline{\mu}$ be the dimensionless constant matrix with elements

$$\mu_{ij} = \delta_{ij} - \frac{m_i}{M} \qquad (i, j = 1, \ldots, n)\ . \tag{19.18}$$

Then the matrix form of all n Eqs.(19.17) is

$$\underline{\mathbf{R}} = \underline{\mu}^T \underline{\mathbf{r}}\ . \tag{19.19}$$

The matrix $\underline{\mu}$ has remarkable properties. It satisfies the three equations

$$\underline{\mu}^T \underline{1} = \underline{0}\ , \qquad \underline{\mu}\,\underline{\mu} = \underline{\mu}\ , \qquad \underline{\mu}\,\underline{m} = \underline{m}\,\underline{\mu}^T = \underline{\mu}\,\underline{m}\,\underline{\mu}^T\ . \tag{19.20}$$

The first equation states that the sum of all rows is a row of zeros which means that $\underline{\mu}$ is singular. Hence (19.19) cannot be resolved for $\underline{\mathbf{r}}$. This is obvious for physical reasons. The positions $\underline{\mathbf{r}}$ of the body centers of mass in inertial space cannot be determined if only the positions relative to the composite system center of mass are known. For a proof of the other two equations it must be shown that $(\underline{\mu}\,\underline{\mu})_{ij} = \mu_{ij}$ and that $(\underline{\mu}\,\underline{m}\,\underline{\mu}^T)_{ij} = (\underline{\mu}\,\underline{m})_{ij} = \mu_{ij} m_j$. These two matrix elements are

$$\left.\begin{aligned} (\underline{\mu}\,\underline{\mu})_{ij} &= \sum_{k=1}^{n} \mu_{ik}\mu_{kj} \quad = \sum_{k=1}^{n} \mu_{ik}\Big(\delta_{kj} - \frac{m_k}{M}\Big) \quad = \mu_{ij} - \frac{1}{M}\sum_{k=1}^{n} \mu_{ik} m_k\ , \\ (\underline{\mu}\,\underline{m}\,\underline{\mu}^T)_{ij} &= \sum_{k=1}^{n} \mu_{ik} m_k \mu_{jk} = \sum_{k=1}^{n} \mu_{ik} m_k \Big(\delta_{jk} - \frac{m_j}{M}\Big) = \mu_{ij} m_j - \frac{m_j}{M}\sum_{k=1}^{n} \mu_{ik} m_k\ . \end{aligned}\right\} \tag{19.21}$$

The sum $\sum_{k=1}^{n} \mu_{ik} m_k$ appearing in both equations equals zero. End of proof.

19.4 Equations of Motion

The formulation of equations of motion is simplest for systems with tree structure. This is the subject of Sect. 19.4.1 . In Sect. 19.4.3 the procedure for systems with closed kinematic chains is explained.

19.4.1 Systems with Tree Structure

In Sect. 11.2.2 the kinematics analysis of tree-structured systems in terms of joint variables resulted in Eqs.(11.20) and (11.21):

$$\left.\begin{aligned}
\underline{\boldsymbol{\omega}} &= \boldsymbol{\omega}_0(t)\underline{1} + \underline{\mathbf{a}}_1\dot{\underline{q}} \,, \\
\dot{\underline{\boldsymbol{\omega}}} &= \dot{\boldsymbol{\omega}}_0(t)\underline{1} + \underline{\mathbf{a}}_1\ddot{\underline{q}} + \underline{\mathbf{b}}_1 \,, \\
\dot{\underline{\mathbf{r}}} &= \dot{\mathbf{r}}_0(t)\underline{1} - \boldsymbol{\omega}_0(t) \times \underline{T}^T(\underline{\mathbf{C}}_0^T + \underline{\mathbf{C}}^T\underline{1}) + \underline{\mathbf{a}}_2\dot{\underline{q}} \,, \\
\ddot{\underline{\mathbf{r}}} &= \ddot{\mathbf{r}}_0(t)\underline{1} - \dot{\boldsymbol{\omega}}_0(t) \times \underline{T}^T(\underline{\mathbf{C}}_0^T + \underline{\mathbf{C}}^T\underline{1}) + \underline{\mathbf{a}}_2\ddot{\underline{q}} + \underline{\mathbf{b}}_2 \,,
\end{aligned}\right\} \tag{19.22}$$

$$\left.\begin{aligned}
\underline{\mathbf{a}}_1 &= -\underline{T}^T\underline{\mathbf{p}}^T \,, & \underline{\mathbf{a}}_2 &= \underline{T}^T(\underline{\mathbf{C}}^T \times \underline{\mathbf{a}}_1 - \underline{\mathbf{k}}^T) \,, \\
\underline{\mathbf{b}}_1 &= -\underline{T}^T(\underline{\mathbf{w}} + \underline{\mathbf{f}}) \,, & \underline{\mathbf{b}}_2 &= \underline{T}^T[\underline{\mathbf{C}}^T \times \underline{\mathbf{b}}_1 - (\underline{\mathbf{s}} + \underline{\mathbf{h}})] \,.
\end{aligned}\right\} \tag{19.23}$$

For the definitions of the various matrices see the equations prior to (11.20). For abbreviation the acceleration terms $\dot{\underline{\boldsymbol{\omega}}}$ and $\ddot{\underline{\mathbf{r}}}$ are written in the forms

$$\left.\begin{aligned}
\dot{\underline{\boldsymbol{\omega}}} &= \underline{\mathbf{a}}_1\ddot{\underline{q}} + \underline{\mathbf{b}}_1^* \,, \\
\ddot{\underline{\mathbf{r}}} &= \underline{\mathbf{a}}_2\ddot{\underline{q}} + \underline{\mathbf{b}}_2^*
\end{aligned}\right\} \tag{19.24}$$

with

$$\underline{\mathbf{b}}_1^* = \underline{\mathbf{b}}_1 + \dot{\boldsymbol{\omega}}_0(t)\underline{1} \,, \qquad \underline{\mathbf{b}}_2^* = \underline{\mathbf{b}}_2 + \ddot{\mathbf{r}}_0(t)\underline{1} - \dot{\boldsymbol{\omega}}_0(t) \times \underline{T}^T(\underline{\mathbf{C}}_0^T + \underline{\mathbf{C}}^T\underline{1}) \,. \tag{19.25}$$

In Sect. 11.2.2 the vector $\mathbf{r}_i$ was by definition the position vector of the unspecified origin 0_i of a basis $\underline{\mathbf{e}}^i$ fixed on body i in some unspecified common reference basis $\underline{\mathbf{e}}$. In the present section the origin 0_i of $\underline{\mathbf{e}}^i$ is the body i center of mass, and the common reference basis $\underline{\mathbf{e}}$ is fixed in inertial space. With these definitions, $\ddot{\underline{\mathbf{r}}}$ and $\dot{\underline{\boldsymbol{\omega}}}$ are the quantities required for (19.10). The virtual velocity changes are

$$\left.\begin{aligned}
\delta\underline{\boldsymbol{\omega}} &= \underline{\mathbf{a}}_1\,\delta\dot{\underline{q}} \,, \\
\delta\dot{\underline{\mathbf{r}}} &= \underline{\mathbf{a}}_2\,\delta\dot{\underline{q}} \,.
\end{aligned}\right\} \tag{19.26}$$

Substitution of (19.24) and (19.26) into (19.10) results in the equation

$$\delta\underline{\dot{q}}^T\left\{(\underline{\mathbf{a}}_2^T\cdot\underline{m}\,\underline{\mathbf{a}}_2+\underline{\mathbf{a}}_1^T\cdot\underline{\mathsf{J}}\cdot\underline{\mathbf{a}}_1)\underline{\ddot{q}}-[\underline{\mathbf{a}}_2^T\cdot(\underline{\mathbf{F}}-\underline{m}\,\underline{\mathbf{b}}_2^*)+\underline{\mathbf{a}}_1^T\cdot(\underline{\mathbf{M}}^*-\underline{\mathsf{J}}\cdot\underline{\mathbf{b}}_1^*)]\right\}=0\ . \quad (19.27)$$

The elements of $\delta\underline{\dot{q}}$ are independent. From this it follows that the factor behind equals zero. This yields the desired equations of motion for joint variables:

$$\underline{A}\,\underline{\ddot{q}}=\underline{B}\ , \quad (19.28)$$

$$\underline{A}=\underline{\mathbf{a}}_2^T\cdot\underline{m}\,\underline{\mathbf{a}}_2+\underline{\mathbf{a}}_1^T\cdot\underline{\mathsf{J}}\cdot\underline{\mathbf{a}}_1\ , \qquad \underline{B}=\underline{\mathbf{a}}_2^T\cdot(\underline{\mathbf{F}}-\underline{m}\,\underline{\mathbf{b}}_2^*)+\underline{\mathbf{a}}_1^T\cdot(\underline{\mathbf{M}}^*-\underline{\mathsf{J}}\cdot\underline{\mathbf{b}}_1^*)\ . \quad (19.29)$$

As predicted, the inertia matrix $\underline{A}$ is symmetric. It is also positive definite. The proof is given for a system in which body 0 is inertial space. Twice the total kinetic energy T of such a system is

$$\begin{aligned}2T&=\sum_1^n(m_i\dot{\mathbf{r}}_i^2+\boldsymbol{\omega}_i\cdot\mathsf{J}_i\cdot\boldsymbol{\omega}_i)=\underline{\dot{\mathbf{r}}}^T\cdot\underline{m}\,\underline{\dot{\mathbf{r}}}+\underline{\boldsymbol{\omega}}^T\cdot\underline{\mathsf{J}}\cdot\underline{\boldsymbol{\omega}}\\&=\underline{\dot{q}}^T(\underline{\mathbf{a}}_2^T\cdot\underline{m}\,\underline{\mathbf{a}}_2+\underline{\mathbf{a}}_1^T\cdot\underline{J}\cdot\underline{\mathbf{a}}_1)\underline{\dot{q}}=\underline{\dot{q}}^T\underline{A}\underline{\dot{q}}\ .\end{aligned} \quad (19.30)$$

Thus, the matrix $\underline{A}$ is the coefficient matrix of the total kinetic energy. Since the kinetic energy is positive definite, also the matrix $\underline{A}$ is.

Next, tree-structured systems without kinematical constraints to inertial space are considered. In this case, body 0 is inertial space. Equations of motion are formulated from Eqs.(19.19) and (19.15). Equations (19.24) and (19.26) yield

$$\left.\begin{aligned}\underline{\boldsymbol{\omega}}&=\underline{\mathbf{a}}_1\underline{\ddot{q}}+\underline{\mathbf{b}}_1^*\ , & \underline{\ddot{\mathbf{R}}}&=\underline{\mu}^T(\underline{\mathbf{a}}_2\underline{\ddot{q}}+\underline{\mathbf{b}}_2^*)\ ,\\ \delta\underline{\boldsymbol{\omega}}&=\underline{\mathbf{a}}_1\,\delta\underline{\dot{q}}\ , & \delta\underline{\dot{\mathbf{R}}}&=\underline{\mu}^T\underline{\mathbf{a}}_2\,\delta\underline{\dot{q}}\ .\end{aligned}\right\} \quad (19.31)$$

Substitution into (19.15) results in the equation

$$\delta\underline{\dot{q}}^T\left\{(\underline{\mathbf{a}}_2^T\underline{\mu}\cdot\underline{m}\,\underline{\mu}^T\underline{\mathbf{a}}_2+\underline{\mathbf{a}}_1^T\cdot\underline{\mathsf{J}}\cdot\underline{\mathbf{a}}_1)\underline{\ddot{q}}-[\underline{\mathbf{a}}_2^T\underline{\mu}\cdot(\underline{\mathbf{F}}-\underline{m}\,\underline{\mu}^T\underline{\mathbf{b}}_2^*)+\underline{\mathbf{a}}_1^T\cdot(\underline{\mathbf{M}}^*-\underline{\mathsf{J}}\cdot\underline{\mathbf{b}}_1^*)]\right\}=0\ . \quad (19.32)$$

As before, the elements of $\delta\underline{\dot{q}}$ are independent. The equations of motion are

$$\underline{\hat{A}}\,\underline{\ddot{q}}=\underline{\hat{B}}\ , \quad (19.33)$$

$$\left.\begin{aligned}\underline{\hat{A}}&=\underline{\mathbf{a}}_2^T\underline{\mu}\cdot\underline{m}\,\underline{\mu}^T\underline{\mathbf{a}}_2+\underline{\mathbf{a}}_1^T\cdot\underline{\mathsf{J}}\cdot\underline{\mathbf{a}}_1\ ,\\ \underline{\hat{B}}&=\underline{\mathbf{a}}_2^T\underline{\mu}\cdot(\underline{\mathbf{F}}-\underline{m}\,\underline{\mu}^T\underline{\mathbf{b}}_2^*)+\underline{\mathbf{a}}_1^T\cdot(\underline{\mathbf{M}}^*-\underline{\mathsf{J}}\cdot\underline{\mathbf{b}}_1^*)\ .\end{aligned}\right\} \quad (19.34)$$

During numerical evaluations the matrices $\underline{\mathbf{a}}_1$, $\underline{\mathbf{b}}_1^*$, $\underline{\mathbf{a}}_2$, $\underline{\mathbf{b}}_2^*$ are not calculated from (19.23) and (19.25), but directly from (19.24) in combination with the recursive Eqs.(11.11). The formulation (19.23) is useful for nonnumerical investigations. The expressions for $\underline{\mathbf{a}}_2$ and $\underline{\mathbf{b}}_2$ show that in (19.29) and (19.34) the products $(\underline{\mathbf{C}}\,\underline{T})^T$ and $(\underline{\mathbf{C}}\,\underline{T}\,\underline{\mu})^T$ play a prominent role. If all joints of a system are spherical joints, the elements of these matrices can be

interpreted as body-fixed vectors. In terms of these vectors certain problems of analytical mechanics can be formulated very elegantly (see Wittenburg [4]).

19.4.2 Constraint Forces and Torques in Joints

In a joint with kinematical constraints the coupled bodies are in contact either at individual points or along certain lines or in a certain surface. Constraint forces are, therefore, distributed forces. Since the bodies are assumed rigid, it is impossible to determine the distribution of constraint forces. Only an equivalent force system can be determined which consists of a single force and a single torque. The torque depends upon the choice of the point at which the single force is thought to be acting. It is natural to choose for each joint i the articulation point located on body i. Let $\mathbf{X}_i$ and $\mathbf{Y}_i$ be the constraint force and the constraint torque, respectively, thus defined for joint i. More precisely, $+\mathbf{X}_i$ and $+\mathbf{Y}_i$ are acting on body $b(i)$, and $-\mathbf{X}_i$ and $-\mathbf{Y}_i$ are acting on body i (see Fig. 11.2). In order to express whether a given constraint force is applied to a given body with positive or with negative sign or not at all numbers S_{ji} are defined as follows:

$$S_{ji} = \begin{cases} -1 & \text{(j=i)} \\ +1 & \text{(j=b(i))} \\ 0 & \text{(else)} \end{cases} \quad (j, i = 1, \ldots, n) \,. \tag{19.35}$$

The first index refers to a body and the second to a joint. With this definition the resultant of all constraint forces and the resultant of all constraint torques applied to body j (arbitrary) are the sums (summation over all joints)

$$\sum_{i=1}^{n} S_{ji}\mathbf{X}_i \,, \qquad \sum_{i=1}^{n} S_{ji}(\mathbf{c}_{ji} \times \mathbf{X}_i + \mathbf{Y}_i) \qquad (j = 1, \ldots, n) \,. \tag{19.36}$$

By assumption, there are no dry friction forces. If, as before, $\mathbf{F}_j$ and $\mathbf{M}_j$ denote the external resultant force and the external resultant torque, respectively, Newton's and Euler's equations for the isolated body j have the forms

$$\left.\begin{aligned} m_j\ddot{\mathbf{r}}_j &= \mathbf{F}_j + \sum_{i=1}^{n} S_{ji}\mathbf{X}_i \,, \\ \mathsf{J}_j \cdot \dot{\boldsymbol{\omega}}_j + \boldsymbol{\omega}_j \times \mathsf{J}_j \cdot \boldsymbol{\omega}_j &= \mathbf{M}_j + \sum_{i=1}^{n} S_{ji}\mathbf{c}_{ji} \times \mathbf{X}_i + \sum_{i=1}^{n} S_{ji}\mathbf{Y}_i \end{aligned}\right\} (j = 1, \ldots, n) \,. \tag{19.37}$$

The vector $S_{ji}\mathbf{c}_{ji}$ is the vector $\mathbf{C}_{ji}$ known from (11.17). With this abbreviation and with the $(n \times n)$-matrix $\underline{S}$ with elements S_{ji} the two sets of

equations are written as follows:

$$\underline{m}\,\ddot{\underline{\mathbf{r}}} = \underline{\mathbf{F}} + \underline{S}\,\underline{\mathbf{X}}\,, \qquad \underline{\mathsf{J}}\cdot\dot{\underline{\boldsymbol{\omega}}} = \underline{\mathbf{M}}^{*} + \underline{\mathbf{C}}\times\underline{\mathbf{X}} + \underline{S}\,\underline{\mathbf{Y}}\,. \tag{19.38}$$

The various quantities in these equations are known from previous equations (see (19.29)). Further progress relies on

Theorem 19.1. *The matrix* $\underline{S}$ *is the inverse of* $\underline{T}$*.*

Proof: From the definition in (19.35) it follows that the product $\underline{T}\,\underline{S}$ has the elements

$$(\underline{T}\,\underline{S})_{ji} = \sum_{k=1}^{n} T_{jk}S_{ki} = T_{ji}S_{ii} + T_{jb(i)}S_{b(i)i} = -T_{ji} + T_{jb(i)} \qquad (j,i = 1,\ldots,n)\,. \tag{19.39}$$

Two cases have to be distinguished. In the case $j = i$, (11.12) yields $T_{ii} = -1$ and $T_{ib(i)} = 0$ whence follows $(\underline{T}\,\underline{S})_{ii} = 1$. In the case $j \neq i$, joint j satisfies one of the following two conditions. a) Joint j is on the direct path between bodies 0 and i and also on the direct path between bodies 0 and $b(i)$. b) Joint j is neither on the direct path between bodies 0 and i nor on the direct path between bodies 0 and $b(i)$. If the former is true, then $T_{ji} = T_{jb(i)} = -1$ and if the latter is true, then $T_{ji} = T_{jb(i)} = 0$. In either case, $(\underline{T}\,\underline{S})_{ji} = 0$. End of proof[1].

With this theorem Eqs.(19.38) can be solved explicitly for the constraint forces and constraint torques. Premultiplication by $\underline{T}$ yields

$$\underline{\mathbf{X}} = \underline{T}(\underline{m}\,\ddot{\underline{\mathbf{r}}} - \underline{\mathbf{F}})\,, \qquad \underline{\mathbf{Y}} = \underline{T}(\underline{\mathsf{J}}\cdot\dot{\underline{\boldsymbol{\omega}}} - \underline{\mathbf{M}}^{*} - \underline{\mathbf{C}}\times\underline{\mathbf{X}})\,. \tag{19.40}$$

The expression for $\underline{\mathbf{X}}$ is substituted into the equation for $\underline{\mathbf{Y}}$. The numerical evaluation of these equations is done in parallel with the numerical integration of the equations of motion.

19.4.3 Systems with Closed Kinematical Chains

From Chap. 4 it is known that the joint variables of a closed kinematical chain are subject to kinematical constraints. As illustrative example the trihedral Bricard mechanism shown in Fig. 4.6 is used. It is a simple closed chain with six joints. For the kinematics analysis see Eqs.(4.12) – (4.25). The analysis started with the removal of joint 6 thus creating a serial chain with five

[1] In graph theory the matrices $\underline{T}$ and $\underline{S}$ are referred to as path matrix and incidence matrix, respectively. The matrix $\underline{\mathbf{C}}$ represents a weighted incidence matrix. Whereas the path matrix is defined for tree-structured systems only, the definition of incidence matrix can be generalized to include multiloop systems. Details see in Wittenburg [3, 4]

joint variables $\varphi_1, \ldots, \varphi_5$. Closure of the removed sixth joint resulted in four independent constraint Eqs.(4.20) and (4.22):

$$\varphi_3 = \varphi_1 \,, \qquad \varphi_5 = \varphi_1 \,, \qquad \varphi_4 = \varphi_2 \,, \qquad \sin\varphi_2 = \frac{\sin\varphi_1}{1-\sin\varphi_1} \,. \tag{19.41}$$

The total degree of freedom is $F = 1$. Hence the mechanism is governed by a single differential equation for a single independent variable. Which of the variables is chosen as independent, is a matter of taste. The equations suggest to choose φ_1. A single differential equation for φ_1 is developed as follows. First, equations of motion are formulated for the system without joint 6. This system is a particularly simple tree-structured system with regularly labeled bodies $0, \ldots, 5$ and joints $i = 1, \ldots, 5$. Equations of motion for the variables $\underline{q} = [\varphi_1\ \varphi_2\ \varphi_3\ \varphi_4\ \varphi_5]^T$ have the form (19.28):

$$\underline{A}\,\underline{\ddot{q}} = \underline{B} \,, \tag{19.42}$$

$$\underline{A} = \mathbf{a}_2^T \cdot \underline{m}\,\mathbf{a}_2 + \mathbf{a}_1^T \cdot \underline{\mathsf{J}} \cdot \mathbf{a}_1 \,, \qquad \underline{B} = \mathbf{a}_2^T \cdot (\mathbf{F} - \underline{m}\,\mathbf{b}_2^*) + \mathbf{a}_1^T \cdot (\mathbf{M}^* - \underline{\mathsf{J}} \cdot \mathbf{b}_1^*) \,. \tag{19.43}$$

In the present case, the equations are particularly simple since body 0 is at rest and since all joints are revolute joints. For what follows, not Eq.(19.28), but the preceding Eq.(19.27) is used:

$$\delta\underline{\dot{q}}^T(\underline{A}\underline{\ddot{q}} - \underline{B}) = 0 \,. \tag{19.44}$$

The constraint Eqs.(19.41) have the effect that the elements of $\delta\underline{\dot{q}}$ are not independent. The elements of $\underline{\ddot{q}}$ are not independent, either. The necessary relationships are obtained by differentiating the constraint equations with respect to time. The first and the second time derivatives are known from (4.24) and (4.25):

$$\left.\begin{aligned} \dot\varphi_5 = \dot\varphi_3 = \dot\varphi_1 \,, \quad \dot\varphi_4 = \dot\varphi_2 &= \dot\varphi_1 \frac{\cos\varphi_1}{(1-\sin\varphi_1)\sqrt{1-2\sin\varphi_1}} \,, \\ \ddot\varphi_5 = \ddot\varphi_3 = \ddot\varphi_1 \,, \quad \ddot\varphi_4 = \ddot\varphi_2 &= \ddot\varphi_1 \frac{\cos\varphi_1}{(1-\sin\varphi_1)\sqrt{1-2\sin\varphi_1}} \\ &\quad + \dot\varphi_1^2 \frac{2-2\sin\varphi_1-\sin^2\varphi_1}{(1-\sin\varphi_1)(1-2\sin\varphi_1)^{3/2}} \,. \end{aligned}\right\} \tag{19.45}$$

With the abbreviations

$$g = \frac{\cos\varphi_1}{(1-\sin\varphi_1)\sqrt{1-2\sin\varphi_1}} \,, \qquad h = \dot\varphi_1^2 \frac{2-2\sin\varphi_1-\sin^2\varphi_1}{(1-\sin\varphi_1)(1-2\sin\varphi_1)^{3/2}} \tag{19.46}$$

the two sets of equations establish relationships of the form

$$\underline{\dot q} = \underline{G}\,\dot q_1 \,, \qquad \delta\underline{\dot q} = \underline{G}\,\delta\dot q_1 \,, \qquad \underline{\ddot q} = \underline{G}\,\ddot q_1 + \underline{H} \tag{19.47}$$

with column matrices

$$\underline{G} = \begin{bmatrix} 1 \\ g \\ 1 \\ g \\ 1 \end{bmatrix} , \qquad \underline{H} = \begin{bmatrix} 0 \\ h \\ 0 \\ h \\ 0 \end{bmatrix} . \tag{19.48}$$

The expressions for $\delta\underline{\dot{q}}$ and for $\underline{\ddot{q}}$ are substituted into (19.44). This results in the equation

$$\delta\dot{q}_1 \underline{G}^T [\underline{A}(\underline{G}\,\ddot{q}_1 + \underline{H}) - \underline{B}] = 0 . \tag{19.49}$$

Since $\delta\dot{q}_1$ is independent, the factor behind is zero. This is the desired single differential equation for the independent variable q_1:

$$(\underline{G}^T \underline{A}\,\underline{G})\,\ddot{q}_1 = \underline{G}^T (\underline{B} - \underline{A}\,\underline{H}) . \tag{19.50}$$

The matrices $\underline{A}$ and $\underline{B}$ depend explicitly on $q_1, \ldots, q_5$ and $\dot{q}_1, \ldots, \dot{q}_5$. The dependent quantities $q_2, \ldots, q_5$ and $\dot{q}_2, \ldots, \dot{q}_5$ are expressed in terms of q_1 and $\dot{q}_1$ with the help of (19.41) and (19.45).

The method just described for the trihedral Bricard mechanism is applicable to arbitrary multiloop systems. A multiloop system is converted into a system with tree structure by deleting suitably chosen joints. Optimal strategies are described in Möller [1]. The resulting tree-structured system has a certain degree of freedom F and an equal number of joint variables $\underline{q} = [q_1 \ \ldots \ q_F]^T$. For this system Eq.(19.44) is established. Restoration of the deleted joints results in a set of constraint equations (loop-closure conditions) for the variables $\underline{q}$. Let ν be the total number of independent constraint equations. Then the total degree of freedom of the multiloop system is $F - \nu$. An equal number of equations of motion has to be formulated. In general, constraint equations are not available in explicit form like Eqs.(19.41), but in the implicit form

$$f_i(q_1, \ldots, q_F) = 0 \qquad (i = 1, \ldots, \nu) . \tag{19.51}$$

Examples of such loop-closure conditions for a single loop are known from Chap. 5. $F - \nu$ of the variables are independent, and the remaining ν variables are dependent. Which of the variables are considered as independent is a matter of choice. Often, this choice is dictated by the equations. As was the case with the Bricard mechanism, the constraint equations are differentiated twice with respect to time. This results in the equations

$$\dot{f}_i = \sum_{j=1}^{F} \frac{\partial f_i}{\partial q_j}\,\dot{q}_j = 0 , \quad \ddot{f}_i = \sum_{j=1}^{F} \frac{\partial f_i}{\partial q_j}\,\ddot{q}_j + \sum_{j=1}^{F}\sum_{k=1}^{F} \frac{\partial^2 f_i}{\partial q_j \partial q_k}\,\dot{q}_j \dot{q}_k = 0 \tag{19.52}$$

$(i = 1, \ldots, \nu)$. These are two sets of ν linear equations, one for the ν dependent velocities and the other for the ν dependent accelerations. Each

set of equations is solved for these ν quantities. Let $\underline{q}^*$ be the column matrix of the $F-\nu$ independent variables. The solutions for the dependent quantities combined with identities for the independent quantities result in equations of the forms

$$\underline{\dot{q}} = \underline{G}\,\underline{\dot{q}}^* \,, \qquad \delta\underline{\dot{q}} = \underline{G}\,\delta\underline{\dot{q}}^* \,, \qquad \underline{\ddot{q}} = \underline{G}\,\underline{\ddot{q}}^* + \underline{H} \,. \tag{19.53}$$

This is a generalization of Eqs.(19.47). The matrix $\underline{G}$ is of size $F \times (F-\nu)$, and $\underline{H}$ is a column matrix. The expressions for $\delta\underline{\dot{q}}$ and for $\underline{\ddot{q}}$ are substituted into (19.44). This results in the equation

$$\delta\underline{\dot{q}}^{*T}\underline{G}^T[\underline{A}(\underline{G}\,\underline{\ddot{q}}^* + \underline{H}) - \underline{B}] = 0 \,. \tag{19.54}$$

By definition, the elements of $\delta\underline{\dot{q}}^*$ are independent. This yields the desired $F-\nu$ equations of motion for the independent variables:

$$(\underline{G}^T\,\underline{A}\,\underline{G})\,\underline{\ddot{q}}^* = \underline{G}^T(\underline{B} - \underline{A}\,\underline{H}) \,. \tag{19.55}$$

The $(F-\nu)\times(F-\nu)$-coefficient matrix is symmetric. The matrices $\underline{G}$ and $\underline{A}$ depend explicitly on all F variables $q_1, \ldots, q_F$. The matrices $\underline{B}$ and $\underline{H}$ depend on $q_1, \ldots, q_F$ and, in addition, on $\dot{q}_1, \ldots, \dot{q}_F$. For the dependent velocities explicit expressions are available. Not so for the dependent variables. This means that in the course of numerical integration for every evaluation of the matrices the nonlinear constraint equations (19.51) must be solved for the dependent variables. For two reasons this is not a very time-consuming task. First, the Jacobian $\underline{G}$ is available so that a Newton-Raphson method can be applied. Second, the previous solution for time t is a good approximation for the actual solution at time $t + \Delta t$. It is more difficult to determine initial values satisfying the constraint equations.

References

1. Möller M (1992) Ein Verfahren zur automatischen Analyse der Kinematik mehrschleifiger räumlicher Mechanismen. Diss. Univ. Stuttgart
2. Sabrea Pereira M F O, Ambrósio J A C (eds.) (1989) Computer-aided analysis of rigid and flexible mechanical systems. Kluwer, Dordrecht
3. Wittenburg J (1989) Topological description of articulated systems. In [2]:159–196
4. Wittenburg J (2007) Dynamics of multibody systems. Springer, Berlin Heidelberg New York

References to Additional Literature

1. Angeles J (1982) Spatial kinematic chains, analysis, synthesis, optimisation. Springer, New York
2. Angeles J (1988) Rational kinematics. Springer Tracts in Natural Philosophy 34, New York
3. Angeles J, Hommel G, Kovács P (1993) Computational kinematics. Kluwer, Dordrecht
4. Angeles J (2003) Fundamentals of robotic mechanical systems: Theory, methods and algorithms. 2nd ed. Springer, New York
5. Artobolevski I I (1986) Mechanisms in modern engineering design. v.1–3, Mir, Moscow
6. Beggs J S (1966) Advanced mechanism. Macmillan, New York
7. Beggs J S (1983) Kinematics. Springer, Berlin, Heidelberg, New York
8. Beyer R (1931) Technische Kinematik. Barth, Leipzig
9. Beyer R (1953) Kinematische Getriebesynthese. Springer, Berlin (Engl. trans. Kuenzel H (1963) The kinematic synthesis of linkages. Chapman and Hall, London)
10. Beyer R (1963) Technische Raumkinematik. Springer, Berlin
11. Bogolyubov A N (1967) Razvitie problem mekhaniki mashin (Bibliografiya) [Development of problems of mechanics in machines (Bibliography)], Naukova Dumka, Kiev
12. Crelier L (1911) Systèmes cinématiques. Gauthier-Villars, Paris
13. de Groot J (Ed.) (1970) Bibliography on kinematics. v.1,2. Eindhoven Univ. of Techn.
14. Dizioğlu B (1965,1967) Getriebelehre v.1: Grundlagen, v.2: Massbestimmung. Vieweg, Braunschweig
15. Dresig H, Naake S, Rockhausen L (1994) Vollständiger und harmonischer Ausgleich ebener Mechanismen. Fortschritt-Berichte VDI, Reihe 18, 155,71 pp. Düsseldorf
16. Dresig H, Schönherr J, Peisach E E (2000) Typ- und Masssynthese von ebenen Koppelgetrieben mit höheren Gliedergruppen. Abschlussbericht DFG-Forschungsvorhaben Dr234/7-2, Bonn
17. Giering O, Hoschek J (eds.) (1994) Geometrie und ihre Anwendungen. Hanser, München
18. Hall A S (1966) Kinematics and linkage design. Prentice-Hall, Englewood Cliffs, New Jersey
19. Heun K (1906) Lehrbuch der Mechanik. Teil 1: Kinematik. Göschen, Leipzig
20. Jones F D, Horton H L, Newell J A (eds.) (1968) Ingenious mechanisms for designers and inventers, vol.1,2,3,4 Industrial Press, New York
21. Julia G (1936) Cours de cinématique (rédigé par J. Dieudonné). 2nd. ed. Gauthier-Villars, Paris
22. Klein F, Müller C (eds.) (1901-1908) Enzyklopädie der Math. Wissenschaften. v.IV: Mechanik. Teubner, Leipzig

J. Wittenburg, *Kinematics*, DOI 10.1007/978-3-662-48487-6

23. Koenigs G (1905) Introduction à une théorie nouvelle des méchanismes. Hermann, Paris
24. Lebedev P A (1966) Kinematics of spatial mechanisms (Russ.). Isdat. Maschinostr., Moscow (with references to 115 Russian titles)
25. Lenarčič J, Ravani B (eds) (1994) Advances in robot kinematics and computational geometry. Kluwer, Dordrecht
26. Lenarčič J, Parenti-Castelli V (eds.) (1996) Advances in robot kinematics. Kluwer, Dordrecht
27. Lenarčič J, Husty M L (eds.) (1998) Advances in robot kinematics: Analysis and control, Kluwer, Dordrecht
28. Miura H, Arimoto S (eds.) (1990) Robotics Research. MIT Press, Cambridge, Mass.
29. Müller R (1932) Einführung in die theoretische Kinematik. Springer, Berlin
30. Pandrea N I (2000) Elemente de mecanica solidelor in coordonate Plückeriene. Editura Acad. Romane
31. Pennock G R (ed.) (1994) Mechanism, synthesis and analysis. v.DE-70, ASME
32. Pottmann H (1994) Kinematische Geometrie (with 363 literature ref.). In: [17]
33. Prudhomme R, Lemasson G (1955) Cinématique. Dunod, Paris
34. Reuleaux F (1900) Theoretische Kinematik v.2. Vieweg, Braunschweig.
35. Sandor G N, Erdman A G (1984) v.I: Mechanism Design. Analysis and synthesis. v.II: Advanced Mechanism Design. Analysis and synthesis. Prentice Hall, Englewood Cliffs, New York
36. Schoenflies A (1886) Geometrie der Bewegung in synthetischer Darstellung. Teubner, Leipzig. reprint (2007) VDM-Verlag Dr. Müller, Saarbrücken
37. Schoenflies A, Grübler M (1908) Kinematik. In: [22]:190–278
38. Spillers W R (ed.) (1964) Basic questions of design theory. Northholland, Amsterdam
39. Suh C H, Radcliff W (1978) Kinematics and mechanism design. Wiley, New York

Index

J. Wittenburg, *Kinematics*, DOI 10.1007/978-3-662-48487-6